

HANDBOOK OF APPLIED SURFACE AND COLLOID CHEMISTRY

Volume 1

Edited by

Krister Holmberg

*Chalmers University of Technology,
Göteborg, Sweden*

Associate Editors

Dinesh O. Shah

*University of Florida,
USA*

Milan J. Schwuger

*Forschungszentrum Jülich GmbH,
Germany*



JOHN WILEY & SONS, LTD

Copyright © 2002 by John Wiley & Sons Ltd,
Baffins Lane, Chichester,
West Sussex PO19 1UD, England

National 01243 779777
International (+44) 1243 779777
e-mail (for orders and customer service enquiries): cs-books@wiley.co.uk
Visit our Home Page on <http://www.wiley.co.uk>
or <http://www.wiley.com>

All Rights Reserved. No part of this publication may be reproduced, stored in a retrieval system, or transmitted, in any form or by any means, electronic, mechanical, photocopying, recording, scanning or otherwise, except under the terms of the Copyright, Designs and Patents Act 1988 or under the terms of a licence issued by the Copyright Licensing Agency Ltd, 90 Tottenham Court Road, London, UK W1P 0LP, without the permission in writing of the publisher and the copyright holder.

Other Wiley Editorial Offices

John Wiley & Sons, Inc., 605 Third Avenue,
New York, NY 10158-0012, USA

Wiley-VCH GmbH, Pappelallee 3,
D-69469 Weinheim, Germany

John Wiley & Sons Australia Ltd, 33 Park Road, Milton,
Queensland 4064, Australia

John Wiley & Sons (Asia) Pte Ltd, 2 Clementi Loop #02-01,
Jin Xing Distripark, Singapore 0512

John Wiley & Sons (Canada) Ltd, 22 Worcester Road,
Rexdale, Ontario M9W 1L1, Canada

Library of Congress Cataloging-in-Publication Data

Handbook of applied surface and colloid chemistry / edited by Krister Holmberg.
p.cm.

Includes bibliographical references and index.

ISBN 0-471-49083-0 (alk. paper)

1. Chemistry, Technical. 2. Surface chemistry. 3. Colloids. I. Holmberg, Krister, 1946-

TP149 .H283 2001
660 – dc21

2001024347

British Library Cataloguing in Publication Data

A catalogue record for this book is available from the British Library

ISBN 0-471-49083-0

Typeset in 9/11pt Times Roman by Laser Words Pvt. Ltd., Chennai, India.

Printed and bound in Great Britain by Antony Rowe Ltd. Chippenham, Wiltshire.

This book is printed on acid-free paper responsibly manufactured from sustainable forestry, in which at least two trees are planted for each one used for paper production.

Contents – Volume 1

Contributors List	ix	CHAPTER 7 Surface Chemistry of Paper	123
Foreword <i>Brian Vincent</i>	xiii	<i>Fredrik Tiberg, John Daicic and Johan Fröberg</i>	
Preface	xv	CHAPTER 8 Surface Chemistry in the Polymerization of Emulsion	175
PART 1 Surface Chemistry in Important Technologies	1	<i>Klaus Tauer</i>	
CHAPTER 1 Surface Chemistry in Pharmacy	3	CHAPTER 9 Colloidal Processing of Ceramics	201
<i>Martin Malmsten</i>		<i>Lennart Bergström</i>	
CHAPTER 2 Surface Chemistry in Food and Feed	39	CHAPTER 10 Surface Chemistry in Dispersion, Flocculation and Flotation	219
<i>Björn Bergenståhl</i>		<i>Brij M. Moudgil, Pankaj K. Singh and Joshua J. Adler</i>	
CHAPTER 3 Surface Chemistry in Detergency	53	CHAPTER 11 Surface Chemistry in the Petroleum Industry	251
<i>Wolfgang von Rybinski</i>		<i>James R. Kanicky, Juan-Carlos Lopez-Montilla, Samir Pandey and Dinesh O. Shah</i>	
CHAPTER 4 Surface Chemistry in Agriculture	73	PART 2 Surfactants	269
<i>Tharwat F. Tadros</i>		CHAPTER 12 Anionic Surfactants	271
CHAPTER 5 Surface and Colloid Chemistry in Photographic Technology	85	<i>Antje Schmalstieg and Guenther W. Wasow</i>	
<i>John Texter</i>		CHAPTER 13 Nonionic Surfactants	293
CHAPTER 6 Surface Chemistry in Paints	105	<i>Michael F. Cox</i>	
<i>Krister Holmberg</i>		CHAPTER 14 Cationic Surfactants	309
		<i>Dale S. Steichen</i>	

CHAPTER 15 Zwitterionic and Amphoteric Surfactants 349 <i>David T. Floyd, Christoph Schunicht and Burghard Gruening</i>	CHAPTER 21 Surfactant Liquid Crystals . . . 465 <i>Syed Hassan, William Rowe and Gordon J. T. Tiddy</i>
CHAPTER 16 Polymeric Surfactants 373 <i>Tharwat F. Tadros</i>	CHAPTER 22 Environmental Aspects of Surfactants 509 <i>Lothar Huber and Lutz Nitschke</i>
CHAPTER 17 Speciality Surfactants 385 <i>Krister Holmberg</i>	CHAPTER 23 Molecular Dynamics Computer Simulations of Surfactants . . . 537 <i>Hubert Kuhn and Heinz Rehage</i>
CHAPTER 18 Hydrotropes 407 <i>Anna Matero</i>	Index – Volume 1 551
CHAPTER 19 Physico-Chemical Properties of Surfactants 421 <i>Björn Lindman</i>	Index – Volume 2 563
CHAPTER 20 Surfactant–Polymer Systems 445 <i>Björn Lindman</i>	Cumulative Index 573

Contents – Volume 2

Contributors List	ix	PART 4	Phenomena in Surface Chemistry	117
Foreword <i>Brian Vincent</i>	xiii	CHAPTER 7	Wetting, Spreading and Penetration	119
Preface	xv		<i>Karina Grundke</i>	
PART 3	Colloidal Systems and Layer Structures at Surfaces	CHAPTER 8	Foam Breaking in Aqueous Systems	143
	1		<i>Robert J. Pugh</i>	
CHAPTER 1	Solid Dispersions	CHAPTER 9	Solubilization	159
	<i>Staffan Wall</i>		<i>Thomas Zemb and Fabienne Testard</i>	
	3	CHAPTER 10	Rheological Effects in Surfactant Phases	189
CHAPTER 2	Foams and Foaming		<i>Heinz Hoffmann and Werner Ulbricht</i>	
	<i>Robert J. Pugh</i>	PART 5	Analysis and Characterization in Surface Chemistry	215
	23			
CHAPTER 3	Vesicles	CHAPTER 11	Measuring Equilibrium Surface Tensions	217
	<i>Brian H. Robinson and Madeleine Rogerson</i>		<i>Michael Mulqueen and Paul D. T. Huibers</i>	
	45	CHAPTER 12	Measuring Dynamic Surface Tensions	225
CHAPTER 4	Microemulsions		<i>Reinhard Miller, Valentin B. Fainerman, Alexander V. Makievski, Michele Ferrari and Giuseppe Loglio</i>	
	<i>Klaus Wormuth, Oliver Lade, Markus Lade and Reinhard Schomäcker</i>			
	55			
CHAPTER 5	Langmuir–Blodgett Films			
	<i>Hubert Motschmann and Helmuth Möhwald</i>			
	79			
CHAPTER 6	Self-Assembling Monolayers: Alkane Thiols on Gold			
	<i>Dennis S. Everhart</i>			
	99			

CHAPTER 13 Determining Critical Micelle Concentration 239 <i>Alexander Patist</i>	CHAPTER 18 Measuring Particle Size by Light Scattering 357 <i>Michal Borkovec</i>
CHAPTER 14 Measuring Contact Angle 251 <i>C. N. Catherine Lam, James J. Lu and A. Wilhelm Neumann</i>	CHAPTER 19 Measurement of Electrokinetic Phenomena in Surface Chemistry 371 <i>Norman L. Burns</i>
CHAPTER 15 Measuring Micelle Size and Shape 281 <i>Magnus Nydén</i>	CHAPTER 20 Measuring Interactions between Surfaces 383 <i>Per M. Claesson and Mark W. Rutland</i>
CHAPTER 16 Identification of Lyotropic Liquid Crystalline Mesophases 299 <i>Stephen T. Hyde</i>	CHAPTER 21 Measuring the Forces and Stability of Thin-Liquid Films 415 <i>Vance Bergeron</i>
CHAPTER 17 Characterization of Microemulsion Structure 333 <i>Ulf Olsson</i>	CHAPTER 22 Measuring Adsorption 435 <i>Bengt Kronberg</i>

Contributors List

Joshua J. Adler

Department of Materials Science and Engineering, and Engineering Research Center for Particle Science and Technology, PO Box 116135, University of Florida, Gainesville, FL-32611, USA

Björn Bergenståhl

Department of Food Technology, Center for Chemistry and Chemical Engineering, Lund University, PO Box 124, SE-221 00 Lund, Sweden

Vance Bergeron

Ecole Normale Supérieure, Laboratoire de Physique Statistique, 24 Rue Lhomond 75231, Paris CEDEX 05, France

Lennart Bergström

Institute for Surface Chemistry, PO Box 5607, SE-114 86 Stockholm, Sweden

Michal Borkovec

Department of Inorganic, Analytical and Applied Chemistry, CABE, University of Geneva, Sciences II, 30 quai Ernest Ansermet, CH-1211 Geneva 4, Switzerland

Norman L. Burns

Amersham Pharmacia Biotech, 928 East Arques Avenue, Sunnyvale, CA 94085-4520, USA

Per M. Claesson

Department of Chemistry, Surface Chemistry, Royal Institute of Technology, SE-100 44 Stockholm, Sweden *and* Institute for Surface Chemistry, PO Box 5607, SE-114 86 Stockholm, Sweden

Michael F. Cox

Sasol North America, Inc., PO Box 200135, 12024 Vista Parke Drive, Austin, TX-78726, USA

John Daicic

Institute for Surface Chemistry, PO Box 5607, SE-114 86 Stockholm, Sweden

Dennis S. Everhart

Kimberly Clark Corporation, 1400, Holcombe Bridge Road, Roswell, GA-30076-2199, USA

Valentin B. Fainerman

International Medical Physicochemical Centre, Donetsk Medical University, 16 Ilych Avenue, Donetsk 340003, Ukraine

Michele Ferrari

CNR – Istituto di Chimica Fisica Applicata dei Materiali, Via De Marini 6, I-16149 Genova, Italy

David T. Floyd

Degussa-Goldschmidt Care Specialties, PO Box 1299, 914, East Randolph Road, Hopewell, VA-23860, USA

Johan Fröberg

Institute for Surface Chemistry, PO Box 5607, SE-114 86 Stockholm, Sweden

Burghard Gruening

Degussa-Goldschmidt Care Specialties, Goldschmidtstrasse 100, D-45127 Essen, Germany

Karina Grundke

Institute of Polymer Research Dresden, Hohe Strasse 6, D-01069 Dresden, Germany

Syed Hassan

Department of Chemical Engineering, UMIST, PO Box 88, Manchester, M60 1QD, UK

Heinz Hoffmann

Lehrstuhl für Physikalische Chemie I der Universität Bayreuth, Universitätsstrasse 30, D-95447 Bayreuth, Germany

Krister Holmberg

Department of Applied Surface Chemistry, Chalmers University of Technology, SE-412 96 Göteborg, Sweden

Lothar Huber

Adam Bergstrasse 1B, D-81735 München, Germany

Paul D. T. Huibers

Department of Chemical Engineering, Massachusetts Institute of Technology, Cambridge, MA 02139-4307, USA

Stephen T. Hyde

Applied Mathematics Department, Research School of Physical Sciences, Australia National University, Canberra 0200, Australia

James R. Kanicky

Center for Surface Science and Engineering, Departments of Chemical Engineering and Anesthesiology, PO Box 116005, University of Florida, Gainesville, FL-32611, USA

Bengt Kronberg

Institute for Surface Chemistry, PO Box 5607, SE-114 86 Stockholm, Sweden

Hubert Kuhn

Department of Physical Chemistry, University of Essen, Universitaetsstrasse 3-5, D-45141 Essen, Germany

Markus Lade

Institute for Technical Chemistry, Technical University of Berlin, Sekr. TC 8, Strasse der 17 Juni 124, D-10623 Berlin, Germany

Oliver Lade

Institute for Physical Chemistry, University of Cologne, Luxemburger Strasse 116, D-50939 Cologne, Germany

C. N. Catherine Lam

Department of Mechanical and Industrial Engineering, University of Toronto, 5 King's College Road, M5S 3G8 Toronto, Ontario, Canada

Björn Lindman

Department of Physical Chemistry 1, Chemical Center, Lund University, PO Box 124, SE-221 00 Lund, Sweden

Giuseppe Loglio

Department of Organic Chemistry, University of Florence, Via G. Capponi 9, 50121 Florence, Italy

James J. Lu

Department of Mechanical and Industrial Engineering, University of Toronto, 5 King's College Road, M5S 3G8 Toronto, Ontario, Canada

Alexander V. Makievski

International Medical Physicochemical Centre, Donetsk Medical University, 16 Ilych Avenue, Donetsk 340003, Ukraine

Martin Malmsten

Institute for Surface Chemistry and Royal Institute of Technology, PO Box 5607, SE-114 86 Stockholm, Sweden

Anna Matero

Institute for Surface Chemistry, PO Box 5607, SE-114 86 Stockholm, Sweden

Reinhard Miller

Max-Planck-Institute of Colloids and Interfaces, Am Mühlenberg, D-14476 Golm, Germany

Helmuth Möhwald

Max-Planck-Institute of Colloids and Interfaces, Am Mühlenberg, D-14476 Golm, Germany

Juan-Carlos Lopez-Montilla

Center for Surface Science and Engineering, Departments of Chemical Engineering and Anesthesiology, PO Box 116005, University of Florida, Gainesville, FL-32611, USA

Hubert Motschmann

Max-Planck-Institute of Colloids and Interfaces, Am Mühlenberg, D-14476 Golm, Germany

Brij M. Moudgil

Department of Materials Science and Engineering, and Engineering Research Center for Particle Science and Technology, PO Box 116135, University of Florida, Gainesville, FL-32611, USA

Michael Mulqueen

Department of Chemical Engineering, Massachusetts Institute of Technology, Cambridge, MA 02139-4307, USA

A. Wilhelm Neumann

Department of Mechanical and Industrial Engineering, University of Toronto, 5 King's College Road, M5S 3G8 Toronto, Ontario, Canada

Lutz Nitschke

Karwendelstrasse 47, D-85560 Ebersberg, Germany

Magnus Nydén

Department of Applied Surface Chemistry, Chalmers University of Technology, SE-412 96 Göteborg, Sweden

Ulf Olsson

Department of Physical Chemistry 1, Center for Chemistry and Chemical Engineering, PO Box 124, S-221 00 Lund, Sweden

Samir Pandey

Center for Surface Science and Engineering, Departments of Chemical Engineering and Anesthesiology, PO Box 116005, University of Florida, Gainesville, FL-32611, USA

Alexander Patist

Cargill Inc., Central Research, 2301 Crosby Road, Wayzata, MN-55391, USA

Robert J. Pugh

Institute for Surface Chemistry, PO Box 5607, SE-114 86 Stockholm, Sweden

Heinz Rehage

Department of Physical Chemistry, University of Essen, Universitaetsstrasse 3-5, D-45141 Essen, Germany

Brian H. Robinson

School of Chemical Sciences, University of East Anglia, Norwich, Norfolk, NR4 7TJ, UK

Madeleine Rogerson

School of Chemical Sciences, University of East Anglia, Norwich, Norfolk, NR4 7TJ, UK

William Rowe

Department of Chemical Engineering, UMIST, PO Box 88, Manchester, M60 1QD, UK

Mark W. Rutland

Department of Chemistry, Surface Chemistry, Royal Institute of Technology, SE-100 44 Stockholm, Sweden *and* Institute for Surface Chemistry, PO Box 5607, SE-114 86 Stockholm, Sweden

Wolfgang von Rybinski

Henkel KgaA, Henkelstrasse 67, D-40191 Düsseldorf, Germany

Antje Schmalstieg

Thaerstrasse 23, D-10249 Berlin, Germany

Reinhard Schomäcker

Institute for Technical Chemistry, Technical University of Berlin, Sekr. TC 8, Strasse des 17 Juni 124, D-10623 Berlin, Germany

Christoph Schunicht

Degussa-Goldschmidt Care Specialties, Goldschmidstrasse 100, D-45127 Essen, Germany

Dinesh O. Shah

Center for Surface Science and Engineering, Departments of Chemical Engineering and Anesthesiology, PO Box 116005, University of Florida, Gainesville, FL-32611, USA

Pankaj K. Singh

Department of Materials Science and Engineering, and Engineering Research Center for Particle Science and Technology, PO Box 116135, University of Florida, Gainesville, FL-32611, USA

Dale S. Steichen

Akzo Nobel Surface Chemistry AB, SE-444 85 Stenungsund, Sweden

Tharwat F. Tadros

89, Nash Grove Lane, Wokingham, Berkshire, RG40 4HE, UK

Klaus Tauer

Max Planck Institute of Colloids and Interfaces, D-14424 Golm, Germany

Fabienne Testard

Service de Chemie Moléculaire, CE Saclay, Batelle 125, F-999 91 Gif-sur-Yvette, France

John Texter

Strider Research Corporation, 265 Clover Street,
Rochester, NY 14610-2246, USA

Fredrik Tiberg

Institute for Surface Chemistry, PO Box 5607, SE-114
86 Stockholm, Sweden

Gordon J. T. Tiddy

Department of Chemical Engineering, UMIST, PO Box
88, Manchester, M60 1QD, UK

Werner Ulbricht

Lehrstuhl für Physikalische Chemie I der Universität
Bayreuth, Universitätsstrasse 30, D-95447 Bayreuth,
Germany

Staffan Wall

Department of Chemistry, Physical Chemistry, Göteborg
Universitet, SE-412 96 Göteborg, Sweden

Guenther W. Wasow

Karl-Marx-Alle 133, D-10243 Berlin, Germany

Klaus Wormuth

Institute for Technical Chemistry, Technical University
of Berlin, Sekr. TC 8, Strasse des 17 Juni 124, D-10623
Berlin, Germany

Thomas Zemb

Service de Chimie Moléculaire, CE Saclay, Batelle 125,
F-999 91 Gif-sur-Yvette, France

Foreword

I am delighted to have been given the opportunity to write a *Foreword* for this important, landmark book in Surface and Colloid Chemistry. It is the first major book of its kind to review, in such a wide-ranging and comprehensive manner, the more technical, applied aspects of the subject. Yet it does not skip the fundamentals. It would have been wrong to have done so. After all, chemical technology is the application of chemical knowledge to produce new products and processes, and to control better existing ones. One cannot achieve these objectives without a thorough understanding of the relevant fundamentals. An attractive feature of this book is that the author of each chapter has been given the freedom to present, as he/she sees fit, the spectrum of the relevant science, from pure to applied, in his/her particular topic. Of course this approach inevitably leads to some overlap and repetition in different chapters, but that does not necessarily matter. Fortunately, the editor has not taken a “hard-line” on this. This arrangement should be extremely useful to the reader (even if it makes the book look longer), since one does not have to search around in different chapters for various bits of related information. Furthermore, any author will naturally have his own views on, and approach to, a specific topic, moulded by his own experience. It is often useful for someone else, particularly a newcomer, wanting to research a particular topic, to have different approaches presented to them. (There is no absolute truth in science, only commonly accepted wisdom!). For example, someone primarily interested in learning about the roles that surfactants or polymers play in formulating a pharmaceutical product, might well gain from also reading about this in a chapter of agrochemicals, or food detergents. Alternatively, someone wishing to learn about paper making technology might also benefit from delving into the chapter on paints. It is very useful to have all this information together in one source. Of course, there are, inevitably, some gaps. The editor himself points out the absence of a comprehensive chapter on emulsions, for example, but to have covered every nook and cranny of this field would be an impossible task, and have taken

forever to achieve! A refreshing feature of this book is its timeliness.

The book will be of tremendous use, not only to those working on industrial research and development, over a whole range of different technologies which are concerned with surface and colloid chemistry, but also to academic scientists in the field, a major proportion of whom interact very strongly with their industrial colleagues. It will compliment very well, existing textbooks in surface and colloid science, which, in general, take the more traditional approach of reviewing systematically the fundamental (pure) aspects of the subject, and add in a few examples of applications, by a way of illustration.

I personally will find this book an extremely useful teaching aid, and I am certain many of my colleagues and universities (particularly at post-graduate level), but also to an activity more and more of us in the field are becoming involved in, namely presenting various aspects of surface and colloid science to industrialists, at a specialist schools, workshops, awareness forums, etc.

I believe that Krister Holmberg was the ideal choice to have edited this book. Not only does he have a wide experience of different aspects of the field, but he has successively worked in Industry, been Director of an internationally recognised research institute (The Ytkemiska Institutet – The Institute for Surface Chemistry – in Stockholm), and is now heading up the Department of Applied Surface Chemistry at Chalmers University of Technology. He has done an outstanding job in putting this book together, and has produced an extremely valuable reference source for all of us working with surfaces and colloids.

Brian Vincent

*Leverhulme Professor of Physical Chemistry and
Director of The Bristol Colloid Centre
School of Chemistry, University of Bristol
BS8 1TS, UK*

Preface

This book is intended as a comprehensive reference work on surface and colloid chemistry. Its title, "Handbook of Applied Surface and Colloid Chemistry", implies that the book is practically oriented rather than theoretical. However, most chapters treat the topic in a rather thorough manner and commercial aspects, related to specific products, etc. are normally not included. All chapters are up-to-date and all have been written for the specific purpose of being chapters in the "Handbook". As will be apparent to the user, the many topics of the book have been covered in a comprehensive way. Taken together, the chapters constitute an enormous wealth of surface and colloid chemistry knowledge and the book should be regarded as a rich source of information, arranged in a way that I hope the reader will find useful.

When it comes to the important but difficult issues of scope and limitations, there is one clear-cut borderline. The "Handbook" covers "wet" but not "dry" surface chemistry. This means that important applications of dry surface chemistry, such as heterogeneous catalysis involving gases, and important vacuum analysis techniques, such as Electron Spectroscopy for Chemical Analysis (ESCA) and Selected-Ion Mass Spectrometry (SIMS), are not included. Within the domain of wet surface chemistry, on the other hand, the aim has been to have the most important applications, phenomena and analytical techniques included.

The book contains 45 chapters. The intention has been to cover all practical aspects of surface and colloid chemistry. For convenience the content material is divided into five parts.

Part One, *Surface Chemistry in Important Technologies*, deals with a selected number of applications of surface chemistry. The 11 chapters cover a broad range of industrial and household uses, from life-science-related applications such as pharmaceuticals and food, via detergency, agriculture, photography and paints, to industrial processes such as paper-making, emulsion polymerization, ceramics processing, mineral processing, and oil production. There are several more areas in which surface chemistry plays a role and many more chapters

could have been added. The number of pages are limited, however, and the present topics were deemed to be the most important. Other editors may have made a different choice.

Part Two, *Surfactants*, contains chapters on the four major classes of surfactants, i.e. anionics, nonionics, cationics and zwitterionics, as well as chapters on polymeric surfactants, hydrotropes and novel surfactants. The physico-chemical properties of surfactants and properties of liquid crystalline phases are the topics of two comprehensive chapters. The industrially important areas of surfactant-polymer systems and environmental aspects of surfactants are treated in some detail. Finally, one chapter is devoted to computer simulations of surfactant systems.

Part Three, *Colloidal Systems and Layer Structures at Surfaces*, treats four important colloidal systems, i.e. solid dispersions (suspensions), foams, vesicles and liposomes, and microemulsions. A chapter on emulsions should also have been included here but was never written. However, Chapter 8, *Surface Chemistry in the Polymerization of Emulsion*, gives a rather thorough treatment of emulsions in general, while Chapter 24, *Solid Dispersions*, provides a good background to colloidal stability, which to a large part is also relevant to emulsions. Taken together, these two chapters can be used as a reference to the field of emulsions. Part Three also contains chapters on two important layer systems, i.e. Langmuir-Blodgett films and self-assembled monolayers.

Part Four, *Phenomena in Surface Chemistry*, consists of extensive reviews of the important phenomena of foam breaking, solubilization, rheological effects of surfactants, and wetting, spreading and penetration.

Part Five, *Analysis and Characterization in Surface Chemistry*, concerns a selected number of experimental techniques. As with the selection of topics that make up Part One, this list of 12 chapters could have been longer and another editor may have made a different choice of topics within the given number of chapters. However, the experimental methods chosen are all important and I hope that the way this part is organized will prove useful.

Most books related to analysis and characterization are divided into chapters on different techniques, such as “Fluorescence” or “Self-diffusion NMR”, i.e. the division is by method. By contrast, the division here is by problem. As an example, when the reader wants to find out how to best measure micelle size he (or she) does not need to know from the beginning which methods to consider. The reader can go directly to Chapter 38, *Measuring Micelle Shape and Size*, where the relevant information is collected.

All 45 chapters can be regarded as overview articles. They all cover the area in a broad way and in addition they often give in-depth information on specific sub-areas which the author has considered particularly important. Each chapter also gives references to literature sources for those who need deeper penetration into the area. Each of the chapters is written as a separate entity, meant to stand on its own. This means that each chapter can be read separately. However, those knowledgeable in the field know that the topics of the “Handbook” chapters are not isolated. For example, there are obviously many connections between Chapter 25, *Foams and Foaming*, and Chapter 31, *Foam Breaking in Aqueous Systems*, Chapter 27, *Microemulsions*, has much in common with both Chapter 32, *Solubilization*, and Chapter 40, *Characterization of Microemulsion Structure*, while Chapter 19, *Physico-chemical Properties of Surfactants*, deals among many other things with *lyotropic liquid crystals* which is the topic of Chapter 21 and which has strong links to Chapter 39, *Identification of Lyotropic Liquid Crystalline Mesophases*. Such connections will lead to some overlap. However, this is natural and should not present any problem. First, a certain overlap is unavoidable if each chapter is to be an independent entity. Secondly, different authors will treat a particular topic differently and these different views can often complement each other. Since both of these aspects are helpful to the reader, small overlaps have not been a concern for the editor.

The “Handbook of Applied Surface and Colloid Chemistry” is unique in scope and the only work of its kind in the field of surface and colloid chemistry. There exist comprehensive and up-to-date books lean-

ing towards the fundamental side of surface chemistry, with Hans Lyklema’s “Fundamentals of Interface and Colloid Science” being one good example. There are excellent books on surfactants and there are good textbooks on surface chemistry in general, such as “The Colloidal Domain” by Fennell Evans and Håkan Wennerström and “Surfactants and Interfacial Phenomena” by Milton Rosen. However, there exists no substantial work like the “Handbook of Applied Surface and Colloid Chemistry” which covers applied surface chemistry in a broad sense. Against this background, one may say that the book fills a gap. I hope therefore that the “Handbook” will soon establish itself as an important reference work for researchers both in industry and in academia.

I am grateful to my co-editors, Milan Schwuger of Forschungszentrum Jülich and Dinesh O. Shah from the University of Florida for helping me to identify the chapter authors. We, the editors, are extremely pleased that we have managed to raise such an interest for the project within the surface chemistry community. Almost all of those that we approached expressed a willingness to contribute and the result has been that the contributors of the “Handbook” are all leading experts in their respective fields. This is the best guarantee for a balanced treatment of the topic and for an up-to-date content.

On behalf of the entire editorial team, I would like to thank all those who contributed as chapter authors. Four persons, Björn Lindman, Robert Pugh, Tharwat Tadros and Krister Holmberg, have written two chapters each. The rest of the 45 chapters have been written by different individual authors. In total 70 individuals from 10 countries contributed to the work. I hope that when they see the “Handbook” in print they will regard the result to be worth the effort. Finally, I would like to thank Dr David Hughes at Wiley (Chichester, UK) for his constant encouragement and patience.

Krister Holmberg

Chalmers University of Technology
Sweden

Göteborg, January 2001

PART 1

**SURFACE CHEMISTRY IN
IMPORTANT TECHNOLOGIES**

CHAPTER 1

Surface Chemistry in Pharmacy

Martin Malmsten

Institute for Surface Chemistry and Royal Institute of Technology, Stockholm, Sweden

1	Introduction	3	5	Drug Delivery through Thermodynamically Stable Systems	15
2	Surface Activity of Drugs	4	5.1	Micellar solutions	15
3	Effects of Drug Surface Activity on Formulation Structure and Stability	6	5.2	Cyclodextrin solutions	16
4	Drug Delivery through Dispersed Colloidal Systems	8	5.3	Microemulsions	17
4.1	Emulsions	8	5.3.1	Oral administration	18
4.2	Liposomes	9	5.3.2	Topical administration	18
4.2.1	Parenteral administration	9	5.3.3	Parenteral administration	19
4.2.2	Targeting of liposomes	10	5.4	Liquid crystalline phases	20
4.2.3	Topical administration	11	5.5	Gels	21
4.2.4	Liposomes in gene therapy	11	6	Responsive Systems	24
4.3	Dispersed lipid particles	12	6.1	Temperature-responsive systems	24
4.3.1	Dispersed liquid crystalline phases	12	6.2	Electrostatic and pH-responsive systems	25
4.3.2	Dispersed solid lipid particles	12	7	Biodegradable Systems	26
4.4	Dispersed polymer particles	13	7.1	Solid systems	27
4.5	Aerosols	15	7.2	Polymer gels	29
			7.3	Surface coatings	29
			8	Acknowledgements	30
			9	References	30

1 INTRODUCTION

Issues related to surface chemistry are quite abundant in drug delivery, but are frequently not recognized as such. The primary reason for this is that surface and colloid chemistry has only during the last few decades matured into a broad research area, and researchers active in adjacent research areas, such as galenic pharmacy in academia and industry, have only recently started to pay interest to surface chemistry and recognized its importance, e.g. for the understanding of particularly more

advanced drug delivery formulations. Such formulations play an important role in modern drug delivery, since the demands on delivery vehicles have increased, e.g. regarding drug release rate, drug solubilization capacity, minimization of drug degradation, reduction of drug toxicity, taste masking, etc., but also since the vehicle as such may be used to control the drug uptake and biological response. As will be discussed in some detail below, this is the case, e.g. in parenteral administration of colloidal drug carriers, topical formulations and oral vaccination.

In this present chapter, different types of colloidal drug carriers will be discussed from a surface and colloid

chemistry point of view. This will include discussions of dispersed systems such as emulsions, liposomes, dispersed solid particles, dispersed liquid crystalline phases etc. Furthermore, thermodynamically stable systems, such as micellar solutions, microemulsions, liquid crystalline phases and gels will be covered, as will biodegradable and responsive carrier systems. Frequently, the surface activity of the active substance in itself affects the structure and stability of such carriers, which must therefore be taken into account when designing the drug delivery system. Moreover, the surface chemistry of the carrier in itself is sometimes of direct importance for the performance of the formulation, as will be exemplified below.

Clearly, there are also numerous other areas which could be included in a chapter devoted to the application of surface and colloid chemistry in pharmacy, in particular relating to the surface properties of dry formulations, such as spray or freeze-dried powders, wettability of drug crystals, etc. However, in order to harmonize with the scope of the volume as a whole, these aspects of surface chemistry in pharmacy will not be covered here. Furthermore, even with the restriction of covering only "wet" systems, the aim of the present chapter is to illustrate important and general effects, rather than to provide a complete coverage of this vast field.

2 SURFACE ACTIVITY OF DRUGS

Even small drug molecules are frequently amphiphilic, and therefore also generally surface active. This means that the drug tends to accumulate at or close to an interface, be it a gas/liquid, solid/liquid or liquid/liquid interface. This surface activity frequently depends on the balance between electrostatic, hydrophobic and van der Waals forces, as well as on the drug solubility. Since the former balance depends on the degree of charging and screening, the surface activity, and frequently also the solubility of the drug, it often depends on the pH and the excess electrolyte concentration. As an example of this, Figure 1.1 shows the adsorption of benzocaine at nylon particles and the corresponding drug dissociation curve (1). As can be seen, the two curves overlap perfectly, indicating that the surface activity in this case is almost entirely dictated by the pH-dependent drug solubility. Thus, with decreasing solubility, accumulation at the surface, resulting in a reduction of the number of drug-water contacts, becomes relatively more favourable.

Considering the surface activity of drugs, as well as its consequences, e.g. for the interaction between the

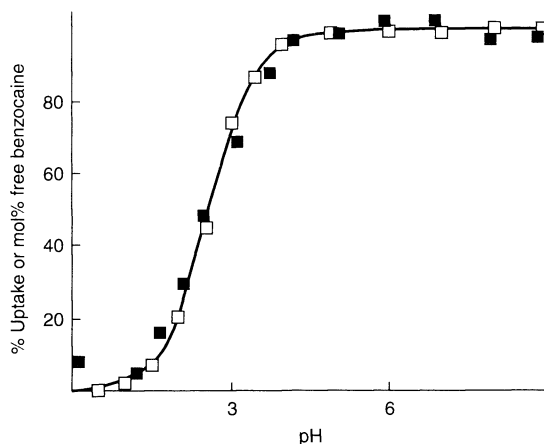


Figure 1.1. Adsorption of benzocaine on nylon 6 powder versus pH at an ionic strength of 0.5 M and a temperature of 30°C (filled symbols). The drug dissociation curve (open symbols) is also shown (data from ref. (1))

drugs and lipid membranes and other supermolecular structures, one could expect that the action of the drug could be at least partly attributed to its surface activity. During the past few years, there have been several attempts to correlate the biological effects of drugs with their surface activities. At least in some cases, such a correlation seems to exist. For example, Seeman and Baily investigated the surface activity of a series of neuroleptic phenothiazines, and found a correlation with the clinical effects of these substances (2). Similarly, the surface activities of local anesthetics have been found to correlate to the biological activities of these substances (3). For example, Figure 1.2 show results by Abe *et al.* on this (3a). In general, however, the surface activities of drugs may contribute to their biological action, although the relationship between surface activity and biological effect is less straightforward.

Although even small drug molecules may be strongly surface active, the general trend is that provided that the substance is readily soluble, i.e. forming a one-phase solution, this surface activity is typically rather limited. With increasing size of the drug molecule, e.g. on going to oligopeptide or other macromolecular drugs, the surface activity of the drug generally increases as a result of the decreasing mixing entropy loss on adsorption. The adsorption of oligopeptides at a surface depends on a delicate balance of a number of factors, including the molecular weight, the solvency (solubility) of the peptide, and the interactions between the peptide and the surface, just to mention

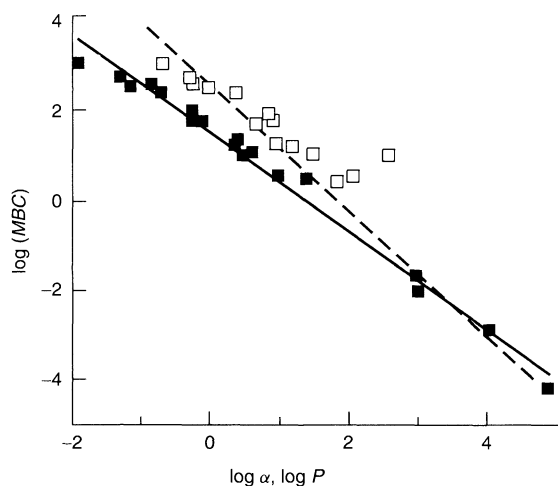


Figure 1.2. Correlation between the biological potency of local anaesthetics, given as the minimum blocking concentration (*MBC*), and activated carbon adsorption (α , filled squares) or octanol–water partition coefficient P (open squares) (data from ref. (3a))

a few. For example, Malmsten and co-workers investigated the adsorption of oligopeptides of the type [AlaTrpTrpPro] $_n$ (T_n), [AlaTrpTrpAspPro] $_n$ (N_n) and [AlaTrpTrpLysPro] $_n$ (P_n) ($1 \leq n \leq 3$) at methylated silica and found that the adsorption of these peptides increases with the length of the peptides in all cases, but more strongly so for the positively charged P_n peptides than for the T_n and N_n peptides (4, 5). This is a result of the electrostatic attractive interaction between the lysine positive charges and the negatively charged methylated silica surface. The importance of the amino acid composition for the surface activity of oligopeptide drugs was also demonstrated by Arnebrant and Ericsson, who investigated the adsorption properties of arginine vasopressin (AVP), a peptide hormone involved, e.g. in blood pressure regulation and kidney function, and desamino-8-D-arginine vasopressin (dDAVP), a commercial analogue, at the silica/water and air/water interfaces (6). It was found that the adsorption in this case was also dominated by electrostatic interactions, and that both peptides are highly surface active. Furthermore, analogously to the results discussed above, the adsorption was found to depend quite strongly on the rather minor variation in structure for the two substances. These and other issues on the interfacial behaviour of biomolecules have been discussed more extensively elsewhere (7, 8).

For the same reason that oligopeptide drugs tend to be more surface active than small-molecule drugs,

proteins and other macromolecular drugs are frequently more surface active than oligopeptide drugs. Again, however, the surface activity is dictated by a delicate balance of contributions, such as the protein size and conformational stability, protein–solvent, protein–protein, and protein–surface interactions, etc. As an example of this, Figure 1.3 shows the adsorption of insulin at hydrophilic chromium surfaces as a function of concentration of Zn^{2+} , which is known to induce formation of hexamers (9, 10). With an increasing concentration of Zn^{2+} , the surface activity was also found to increase, clearly as a result of protein aggregation. In fact, at certain conditions only the oligomers adsorb, whereas the unimers do not (8). This makes monomeric forms, in which amino acid substitutions preventing the oligomerization are made, interesting, e.g. for preventing the adsorption in storage vials, which otherwise could result in problems relating to material loss and hence in a change in the amount of drug administered.

An interesting way to reduce the surface activity of both small and large drugs is to couple the drug molecules to chains of poly(ethylene oxide) (PEO) (11, 12). Through the introduction of the PEO chains, a repulsive steric interaction between the modified drug and a surface is introduced at the same time as the attractive interactions of van der Waals, hydrophobic or electrostatic nature are reduced. Naturally, this is analogous to modifying surfaces with PEO chains in order to make them protein-rejecting, as discussed in detail previously (8, 13–16). By reducing the surface activity of the drug through PEO modification, numerous other positive

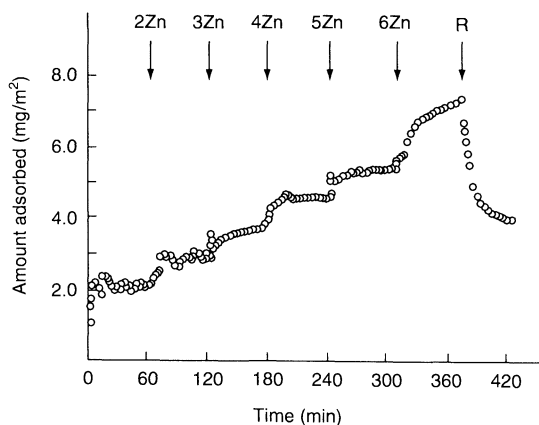


Figure 1.3. Amount of insulin adsorbed on chromium versus time at stepwise additions of Zn^{2+} (number of Zn^{2+} /hexamer) to an initially zinc-free human insulin solution (data from ref. (9))

effects can also be achieved, e.g. relating to increased circulation time, reduced immunicity and antigenicity after parenteral administration, reduced enzymatic degradation and proteolysis, increased solubility, stability towards aggregation, and reduced toxicity (11). For example, analogous to PEO-modified colloidal drug carriers (discussed below), the bloodstream circulation time of intravenously administered peptide and protein drugs may be significantly enhanced through coupling of PEO chains to the protein/peptide (11). The reason for this is probably that the PEO chains form a steric protective layer, analogous to that formed for PEO-modified colloids, which in turn reduces short-range specific interactions (e.g. immuno-recognition). Also analogous to PEO-modified colloidal drug carriers is that the reduced interaction with serum proteins also causes reduced immunicity and antigenicity (11). Furthermore, due to the PEO modification, close proximity between the drug and enzyme is precluded, which in turn may enhance the drug chemical stability. As an illustration of this, Table 1.1 shows the effect of proteolysis on the remaining activity for a number of proteins. As can be seen, a significantly higher remaining activity is found for the PEO-modified proteins in most cases. PEO-modification may also be used in order to increase the solubility of both hydrophobic and strongly crystallizing substances, etc. These and other aspects of PEO-modifications of both macromolecular and low-molecular-weight drugs have been discussed in detail previously (11–14).

Due to the surface activities of drugs, as well as the influence of interfacial interactions on the structure and stability of colloidal and self-assembled systems, the presence of the drug is frequently found to affect both the types of structure formed and their stabilities. This is of great importance, since it means that the properties of the drug must be considered in the design of the drug carrier, irrespective of the carrier being an emulsion, a microemulsion, a micellar solution, a liquid crystalline

phase, etc. This will be discussed and illustrated in more detail below.

3 EFFECTS OF DRUG SURFACE ACTIVITY ON FORMULATION STRUCTURE AND STABILITY

As outlined briefly above, particularly surface-active drugs, but also hydrophobic and charged hydrophilic ones, frequently affect the performance of drug carrier systems. In particular, surfactant-containing systems, such as micellar solutions, microemulsions and liquid crystalline phases, are quite sensitive to the presence of drugs. In order to understand the effect of the drug on the structure and stability of these systems, it is helpful to consider the packing aspects of these surfactant structures. Thus, the structures formed by such systems depend to a large extent on the favoured packing of the surfactant molecules. This, in turn, depends on the surfactant charge, the screening of the charge, the surfactant chain length, the bulkiness of the hydrophobic chain, etc. For example, for charged surfactants with not too long a hydrocarbon tail at low salt concentrations, structures strongly curved towards the oil phase are generally preferred due to the repulsive electrostatic head-group interaction and the small volume of the hydrophobic tail, thus resulting in small spherical micelles. On increasing the excess salt concentration or the addition of intermediate or long-chain cosurfactants (e.g. alcohols), etc., the balance is shifted, and less curved aggregates (e.g. hexagonal or lamellar liquid crystalline phases) are formed. These and numerous other effects relating to the packing of surfactant in self-assembled structures have been discussed extensively earlier (17–20).

On addition of a drug molecule to such a system, this will distribute according to its hydrophobicity/hydrophilicity and surface activity. Thus, while small and hydrophobic drug molecules will be solubilized in the hydrophobic domains, hydrophilic and strongly charged ones tend to become localized in the aqueous solution, and surface-active ones to at least some extent at the interface between these regions. The effect of the incorporation of the drug molecules in different domains of self-assembled surfactant systems can be understood from simple packing considerations. Thus, if a hydrophobic drug molecule is incorporated in the hydrophobic domains, the volume of the latter increases, which results in a decreased curvature toward the oil (in oil-in-water (o/w) structures) or an increased curvature towards the water (in reversed water-in-oil (w/o)

Table 1.1. Enzymatic activity, relative to that of the native enzyme, after extensive degradation with trypsin, as well as the effect of PEO-modification of the enzymes on the proteolysis by trypsin (from ref. (11))

Protein	% Activity (native)	% Activity (PEO-modified)
Catalase	0	95
Asparaginase	12	80
Streptokinase	50	50
β -glucuronidase	16	83
Phenylalanine- ammonia-lyase	17	34

structures). This tends to lead to micellar growth (o/w systems), transition between liquid crystalline phases (e.g. from micellar to hexagonal, hexagonal to lamellar (o/w systems) or lamellar to reversed hexagonal (w/o systems)), etc., or a change in microemulsion structure (e.g. from o/w to bicontinuous, or from bicontinuous to w/o). If the drug is distributed towards the aqueous compartment, the effect of the solubilization depends to some extent on its charge, at least for ionic surfactant systems. Therefore, the drug can act as an electrolyte, thus screening the electrostatic interactions in the self-assembled system, and thereby promoting structures less curved towards the oil phase (o/w) or more pronounced towards the water phase (w/o). For uncharged water-soluble drugs, on the other hand, electrostatic effects are minor. For amphiphilic drugs, finally, the situation is somewhat more complex, as the final outcome of the drug incorporation will depend on a balance of these factors, and will hence be dependent on the charge of the molecule (and frequently also on pH), the length and bulkiness of its hydrophobic part, the excess electrolyte concentration, etc.

As an example of the effects of an amphiphilic drug on the structure of surfactant self-assemblies, Figure 1.4 shows part of the phase diagram of monoolein, water, lidocaine base and lidocaine-HCl (21). As can be seen, the cubic phase (c) formed by the monoolein-water system transforms into a lamellar liquid crystalline phase on addition of lidocaine-HCl, whereas it transforms into a reversed hexagonal or reversed micellar phase on addition of the lidocaine base. Based on X-ray data, it was inferred that the cubic phase of the monoolein-water system had a slightly reversed curvature (critical packing parameter about 1.2). Thus, on addition of the

charged lidocaine-HCl, this molecule is incorporated into the lipid layer, and due to the repulsive electrostatic interaction between the charges, the curvature towards water decreases. On the other hand, the addition of the hydrophobic lidocaine base causes the hydrophobic volume to increase, thereby resulting in a transition in the other direction.

Moreover, the stability and structure of microemulsions have been found to depend on the properties of solubilized drugs. In particular, the stability is generally strongly affected by surface-active drugs. For example, sodium salicylate has been found to significantly alter the stability region of microemulsions prepared from lecithin, and specifically to increase the extension of the microemulsion region (22). Furthermore, Carlfors *et al.* studied microemulsions formed by water, isopropyl myristate and nonionic surfactant mixtures, as well as their solubilization of lidocaine, and found that the surface active but lipophilic lidocaine lowered the phase inversion temperature (PIT) (23). This is what would be expected from simple packing considerations, since increasing the effective oil volume favours a decrease in the curvature towards the oil, as well as the formation of reversed structures. Thus, this behaviour is analogous to that of the monoolein/water/lidocaine system discussed above.

Furthermore, Corswant and Thorén investigated the effects of drugs on the structure and stability of lecithin-based microemulsions (24). It was found that felodipine, being practically insoluble in water and slightly soluble in the oil-phase used, acted like a non-penetrating oil. Thus, with increasing felodipine concentration the surfactant film curves towards the water, resulting in expulsion of the latter from the microemulsion and oil

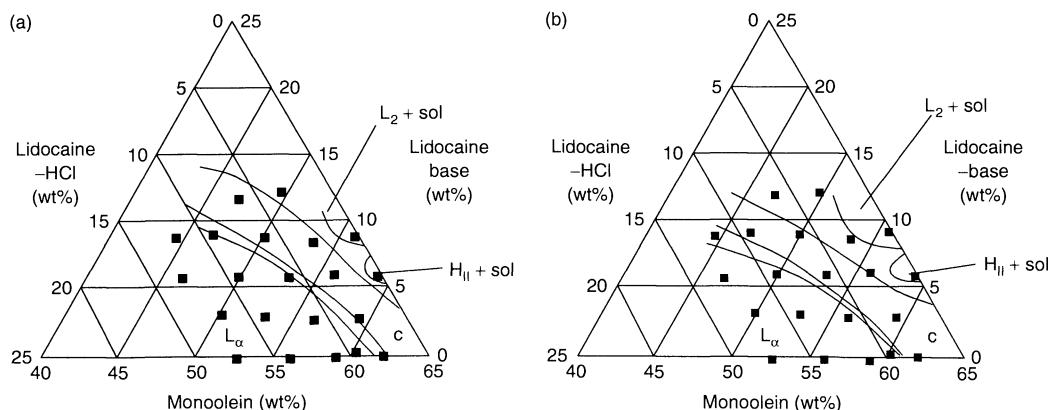


Figure 1.4. Phase diagrams of the sub-system lidocaine base/lidocaine-HCl/monoolein at 35 wt% water at 20°C (a) and 37°C (b) (data from ref. (21))

incorporation. On the other hand, the drug BIBP3226 is a charged molecule which is insoluble in the oil phase but slightly soluble in water, and with an affinity for the lecithin layer. Therefore, this molecule partitioned itself between the lecithin layer and the water phase, which caused incorporation of water due to the charge of this substance, and at higher concentrations a transition from a bicontinuous to an o/w structure.

In addition, the self-assembly of amphiphilic (co)polymers is influenced by the presence of drugs and other cosolutes. For example, the temperature-induced gelation of PEO-PPO-PEO block copolymer systems (PPO being poly(propylene oxide)), discussed below, has been found to depend on the presence of cosolutes, such as electrolytes (where a lyotropic behaviour is observed) (25, 26), oils (25–27) and surface-active species (27, 28). In particular, the gelation has also been found to depend on the presence of drugs. Depending on the properties of the drug, different effects on the gelation of such systems have been observed. For example, Scherlund *et al.* investigated the effects of the local anesthetic agents lidocaine and prilocaine on gels formed by Poloxamer F127 and F68, and found that at pH 8, where lidocaine and prilocaine are largely uncharged, the gelation temperature is reduced due to their presence (28). Since these gels form as a consequence of temperature-induced micellization, this is analogous to the finding that oily substances may reduce the critical micellization concentration (CMC) of surfactant systems (19, 25).

As clearly shown by these and numerous other findings in the literature (see, e.g. ref. (29)), the effects of the drug itself on the structures and stabilities of pharmaceutical of these must be considered when designing the formulation, which also means that each of these will have to be optimized for each drug to be formulated. In the following, the interplay between active substances and drug carriers, as well as the practical uses of the latter, will be discussed for a range of formulation types.

4 DRUG DELIVERY THROUGH DISPERSED COLLOIDAL SYSTEMS

4.1 Emulsions

Despite their finite stability, dispersed colloidal systems, such as emulsions, dispersions, aerosols and liposomes, have several advantages as drug delivery systems. For example, emulsions offer opportunities for solubilizing relatively large amounts of hydrophobic active

ingredients, with advantages relating to, e.g. the effective drug solubility, the drug release rate and chemical stability, taste masking, etc. Furthermore, the amount of surfactant required is generally quite low, and relatively non-toxic surfactants, such as phospholipids and other polar lipids, as well as block copolymers, can be used as stabilizers.

Sparingly soluble hydrophobic drugs frequently display a poor bioavailability, not the least following oral administration. Naturally, there are several reasons for this, including degradation of the drug in the gastrointestinal tract, physical absorption barriers due to the charge and size of the drug (particularly relevant for protein and oligopeptide drugs (30–32)), etc. Perhaps even more important than the low uptake of orally administered hydrophobic drugs, however, is the frequently observed strong intra- and inter-subject variability in the uptake, which naturally causes problems relating to the possibilities to administer the required dose in a safe and reproducible manner (33–37). However, it has been found that the uptake of orally administered drugs may be improved by the use of o/w emulsions as drug carrier systems. Additional benefits with this approach, naturally, are that the effective solubility of the drug increases, that hydrolytic degradation may be reduced, that it offers a way to obtain taste masking, etc. For example, o/w emulsions were used by Tarr and Yalkowsky in order to improve the pharmacokinetics of cyclosporine, an oligopeptide drug used as an immunosuppressive agent for prolonging allograft survival in organ transplantation and in the treatment of patients with certain auto-immune diseases (35). Interestingly, the intestinal absorption could be increased by reducing the droplet size, thus suggesting that the droplets, analogously to, e.g. biodegradable polymer particles used in oral vaccination (see discussion below), are taken up in a size-dependent manner. (Not surprisingly, o/w microemulsions, with their very small oil “droplets”, have been found to be even more efficient than emulsions for the oral administration of cyclosporine (see below).)

Naturally, there have also been a very large number of investigations relating to the formulation of specific drugs in order to achieve these and other advantages following from the use of emulsion systems. These, however, are too numerous to discuss in this present overview treatise. Just to mention one example, Scherlund *et al.* prepared a gelling emulsion system for administration of the local anaesthetic agents lidocaine/prilocaine to the peridontal pocket. By stabilizing the lidocaine/prilocaine droplets by either nonionic,

anionic, or cationic surfactants in the simultaneous presence of a gelling polymer system (Lutrol F68 and Lutrol F127), an *in situ* gelling local anesthetic formulation with a high release rate could be obtained (27). Furthermore, intravenous, intraarterial, subcutaneous, intramuscular and interperitoneal administrations of emulsions have been performed for, e.g. barbituric acids, cyclandelate, diazepam and local anaesthetics. Other substances formulated in such emulsions include valinomycin, bleomycin, narcotic antagonists and corticosteroids. Emulsions are also used as adjuvants in vaccination. For oral administration, examples of drugs administered through emulsions include sulfonamides, indoxole, griseofulvin, theophylline and vitamin A. Examples of topical emulsion systems, finally, include, e.g. those containing corticosteroids (38, and refs therein).

Moreover, emulsions are also used essentially without solubilized drugs in a couple of interesting medical applications. For example, parenteral administration of o/w emulsions has been used for the nutrition of patients who cannot retain fluid or who are in acute need of such treatment (38–41). In these, soybean, cottonseed, or safflower oil are typically emulsified with a phospholipid (mixture) in an aqueous solution containing also, e.g. carbohydrates. A number of these systems, e.g. Intralipid[®], Lipofundin[®], Travemulsion[®] and Liposyn[®], exist on the market. Furthermore, emulsions have been used parenterally as blood substitute formulations (42, 43). The latter are perfluorochemical (PFC) emulsions with a typical droplet size of about 100–200 nm, which increase the oxygen-carrying capacity through dissolution of oxygen rather than oxygen binding. Such systems are therefore fundamentally different from haemoglobin. Although the composition is certainly crucial both for the function and the safety of such systems, formulations have been found which effectively and safely can act as carrier systems (e.g. Fluosol-DA[™]).

4.2 Liposomes

4.2.1 Parenteral administration

For several decades, liposomes have been considered promising for drug delivery. There are many reasons for this, including the possibility to encapsulate both water-soluble, oil-soluble, and at least some surface-active substances, thereby, e.g. controlling the drug release rate, the drug degradation, and the drug bioavailability (44–50). Liposomes, similarly to other colloidal drug carriers, may also have advantageous effects, e.g. for directed administration to tissues related to

the reticuloendothelial system (RES), e.g. liver, spleen and marrow, as adjuvants in vaccines formulations, etc. (see below). However, liposome-based formulations have also been found to have numerous weaknesses and difficulties, e.g. related to complicated or at least expensive preparations, difficulties with sterilization, poor storage stabilities, limitations concerning poor solubilization capacities for more hydrophobic drugs, difficulties in controlling the drug release rate, and limitations in how much the drug release can be sustained, etc. In parenteral administration, another problem with this type of formulation has been the rapid clearance from the bloodstream, thus resulting in poor drug bioavailability and local toxicity in RES-related tissues. However, during the last decade or so, the development of so-called Stealth[®] liposomes, i.e. liposomes which have been surface-modified by PEO derivatives, as well as other developments, have resolved at least some of these issues, and there has been an increased activity in this area. In fact, several liposome-based products have recently been commercialized (e.g. AmBisome[™] (amphotericin B), DaunoXome[™] (daunorubicin citrate) and Doxil[™] (doxorubicin)), while many more are currently being tested and documented.

On intravenous administration of liposomes and other colloidal drug carriers, these are accumulated in the RES, which leads to a short bloodstream circulation time and an uneven tissue distribution, with a preferential accumulation in RES-related tissues, such as the liver, spleen, and marrow (51–56). This, in turn, may cause poor drug bioavailability and accumulation-related toxicity effects. The RES uptake, as well as the drug circulation time and tissue distribution, depends on, e.g. the surface properties of the drug carrier. This is related to the adsorption of serum proteins at the drug carrier surface, which induces biological responses related to complement activation, immune response, coagulation, etc. In fact, an inverse correlation has been found between the total amount of serum proteins adsorbed, on the one hand, and the bloodstream circulation time, on the other (Figure 1.5) (54, 55). In particular, through the use of PEO derivatives and surface modifications to induce steric stabilization, the adsorption of serum proteins at the drug carrier surface can be largely eliminated, which has been found to lead to an increased bloodstream circulation time and a more even tissue distribution (8, 44, 49–73).

An area where sterically stabilized liposomes are of particular interest is cancer therapy. Thus, by the

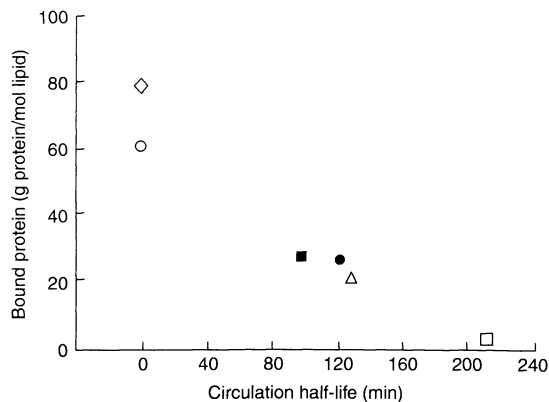


Figure 1.5. Correlation between the total amount of protein adsorbed and circulation time before plasma clearance of large unilamellar vesicles (LUVs) containing trace amounts of [^3H]cholesteryl-hexadecyl ether administered intravenously in CD1 mice at a dose of about $20\ \mu\text{mol}$ of total lipid per 100 g of mouse weight. Results are shown for liposomes containing SM:PC:ganglioside GM1 (72:18:10) (open square), PC:CH (55:45) (filled circle), PC:CH:plant PI (35:45:20) (filled square), SM:PC (4:1) (open triangle), PC:CH:dioleoylphosphatidic acid (DOPA) (35:45:20) (open diamond), and PC:CH:DPG (35:45:20) (open circle) (SM, sphingomyelin; PC, phosphatidyl choline; CH, cholesterol; PI, phosphatidylinositol; DPG, diphosphatidyl glycerol) (data from ref. (55))

use of such liposomes, enhanced antitumour capacity and reduced toxicity of the encapsulated drug can be achieved for a variety of tumours, even those that do not respond to the free drug or the same drug encapsulated in conventional liposomes. Just to mention one example, Papahadjopoulos *et al.* investigated the use of PEO-modified liposomes consisting of distearoyl phosphatidylethanolamine-PEO1900, hydrogenated soy phosphatidylcholine and cholesterol, for the administration of doxorubicin to tumour-bearing mice (57). It was found that the liposomes have a longer bloodstream circulation time than liposomes composed of, e.g. egg phosphatidylcholine. Furthermore, the prolongation of the circulation time in blood was correlated to a decrease of accumulation in RES-related tissues such as liver and spleen, and a correspondingly increased accumulation in implanted tumours (Figure 1.6). These and other aspects of parenteral administration, e.g. in cancer therapy, have been extensively reviewed previously (8, 44, 47, 49, 50).

4.2.2 Targeting of liposomes

An interesting use of liposomes related to their parenteral administration concerns targeting of the drug

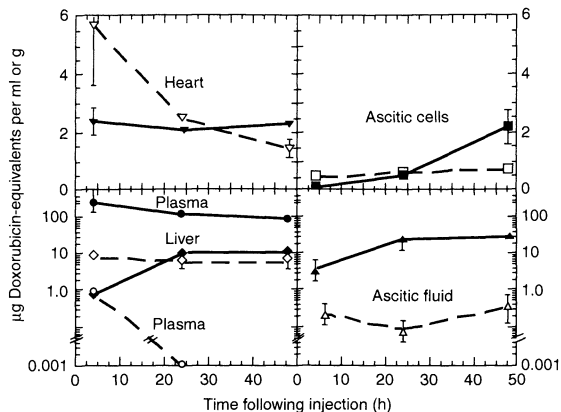


Figure 1.6. Doxorubicin in tumour-bearing mice, either as the free drug (open symbols/dashed lines) or in liposomes consisting of distearoylphosphatidylethanolamine-PEO/hydrogenated soy phosphatidylcholine/cholesterol (0.2:2:1 mol/mol) (filled symbols/continuous lines) (data from ref. (57))

to a desired tissue or cell type. In particular, sterically stabilized liposomes and other types of PEO-modified colloidal drug carriers are of potential interest in this context, due to the long circulation times and relatively even tissue distributions of such systems after intravenous administration. If a biospecific molecule, e.g. a suitable antibody (fragment), a peptide sequence, oligosaccharide, etc., is covalently attached to such a carrier, the long circulation time reached ideally would improve the possibilities for targeting to a localized antigen. As an example of this, Khaw *et al.* investigated cytoskeleton-specific immunoliposomes with the goal of either “sealing” hypoxic cells or using them in the intracellular delivery of DNA (74, 75). Thus, by the use of antimyosin-immunoliposomes, a highly improved survival rate could be demonstrated for hypoxic cells compared to those of the controls. Furthermore, by electron microscopy, these investigators could infer that the liposomes act by “plugging” the microscopic cell lesions present in hypoxic cells. Furthermore, Holmberg *et al.* investigated the binding of liposomes to mouse pulmonary artery endothelial cells (76). As can be seen in Figure 1.7, the amount of lipid bound to these cells was significant with two different relevant antibodies, and also displayed a strongly increasing binding with the liposome concentration, whereas the binding of both the bare liposomes and liposomes modified with an irrelevant antibody was negligible. Positive results from the use of conjugated liposomes were also found, e.g. by Muruyama *et al.* (77), Ahmad *et al.* (78), Gregoriadis and Neerunjun (79), Torchilin and co-workers (80–82).

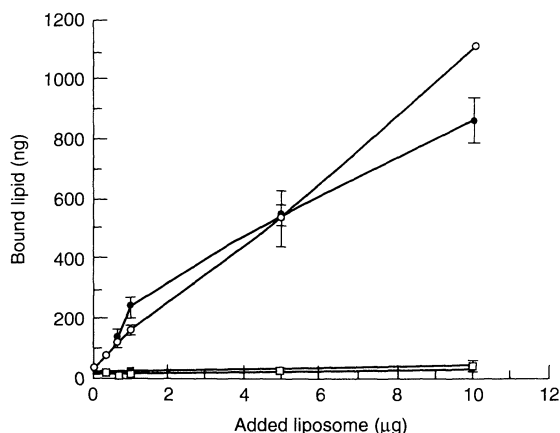


Figure 1.7. Binding to mouse pulmonary artery endothelial cells of two liposome preparations functionalized with relevant antibodies (34A and 201B) (filled and open circles, respectively), functionalized with an irrelevant antibody (open squares) or uncoated liposomes (filled squares) (data from ref. (76))

Naturally, liposomes as such are not unique in this context. Instead, the same approach can be used for other PEO-modified colloidal drug carriers, e.g. copolymer micelles. For example, Kabanov *et al.* have demonstrated specific targeting of fluorescein isothiocyanate solubilized in PEO-PPO-PEO block copolymer micelles conjugated with antibodies to the antigen of brain glial cells (α_2 -glycoprotein) (83, 84). Furthermore, incorporation of haloperidol into such micelles was found to result in a drastically improved therapeutic effect in mice, as inferred from horizontal mobility and grooming frequency studies.

One should also note that although beneficial therapeutic effects have been observed for both liposomes and micelles, the presence of the recognition moiety in the conjugated carrier may also have detrimental effects, e.g. causing the long circulation time in the absence of such entities to decrease drastically. As an example of this, Savva *et al.* conjugated a genetically modified recombinant tumour necrosis factor (TNF)- α to the terminal carboxyl groups of liposome-grafted PEO chains (85). However, although the liposomes in the absence of such conjugation displayed a long circulation in the bloodstream, incorporation of as little as 0.13% of the PEO chains resulted in a rapid elimination from the bloodstream. Clearly, the use of immunoliposomes for targeting may indeed be rather complex. The use of liposomes in parenteral drug delivery has been extensively reviewed previously (44, 47, 49, 50).

4.2.3 Topical administration

Another area where liposomes have been found useful is in topical and dermal drug delivery. Thus, the major problem concerning topical drug delivery is that the drug may not reach the site of action at a sufficient concentration to be efficient, e.g. due to the barrier properties of the *stratum corneum*. To overcome this problem, topical formulations may contain so-called penetration enhancers, such as dimethyl sulfoxide, propylene glycol and Azone[®]. However, although these yield an improved transport of the drug, they typically also result in an increased systemic drug level, which is not always desired, and may cause irritative or even toxic effects (86–89). As discussed below, one way to achieve an increased drug penetration without the use of penetration enhancers is to use microemulsions. Another approach for this, however, is to use liposomes or other types of lipid suspensions, e.g. so-called transfersomes (86). Although there are a large number of drugs which could be of interest in relation to liposomal transdermal drug delivery, perhaps of particular interest are local anaesthetics, retinoids and corticosteroids. For example, Gesztes and Mezei compared a formulation prepared by encapsulating tetracaine into a multilamellar liposome dispersion to a control cream formulation (Pontocaine[™]) and found the liposome formulation to be significantly more efficient (90). Positive results were found by Schäfer-Korting *et al.* for tretinoin formulations for the treatment of *acne vulgaris* (91).

However, although liposomes have indeed been successfully used commercially (e.g. Pevaryl[™] Lipogel, Ifenec[™] Lipogel, Micotef[™] Lipogel, Heparin Pur[™] and Hepaplus Eugel[™]), other types of lipid dispersions are also interesting in this context. In particular, Cevc has convincingly argued for the advantages of so-called transfersomes, i.e. self-assembled lipid structures, which due to their highly deformable lipid bilayers have shown superior membrane penetration when compared to traditional liposomes for a number of systems (86).

4.2.4 Liposomes in gene therapy

Yet another area where liposomes are of interest is gene therapy (48, 92–97). Thus, on mixing lipids with DNA, compact complexes may be obtained, particularly for cationic lipids. More specifically, most DNA condensation methods yield similar particles, i.e. torus-shaped with a 40–60 nm outer and 15–25 nm inner diameter, or rods of about 30 nm in diameter and a length of 200–300 nm, although this naturally depends on a number of parameters, such as the lipid/DNA ratio (48). By

the use of liposomes, an increased efficiency of DNA delivery has been observed. It has been found that the transfection efficiency depends on the net charge of the complex. However, this dependence is not straightforward, and different cell lines require different complex charges for optimal expression (93). Although considerable work has been performed with both positively and negatively charged liposome complexes, as well as with titrating ones, cationic liposome complexes have received particular attention in gene therapy. However, there are several potential problems with the *in vivo* gene delivery through cationic charge-mediated uptake. For example, on intravenous administration the complex carrier encounters net negatively charged serum proteins, lipoproteins and blood cells, with the risk of flocculation and emboli formation. Carriers administered through the airway, on the other hand, face problems related to the lung surfactants, etc. In both cases, there is a risk of the carriers not being able to maintain their positive charges until they reach their target, which will deteriorate their performance. Furthermore, intravenously administered carriers are cleared from circulation rapidly by the RES. Despite these obstacles, however, DNA administered through cationic liposome complexes has been found to be more efficient than naked DNA delivery (48).

Cationic lipid-based systems have also been found to be comparatively efficient for gene delivery to a range of tissues *in vivo*. These include, e.g. pulmonary epithelial cells, endothelial cells after direct application to the endothelial surfaces or after intravenous administration, solid tumours after interstitial administration, metastases after intravenous delivery, etc. (93, and refs therein). Furthermore, therapeutic cDNAs have been delivered by cationic liposomes in human gene therapy trials and no toxicity has been observed at the low doses administered. Naturally, the positive findings when using complexes between DNA and cationic liposomes and lipids are analogous to those of the enhanced gene delivery efficiencies obtained for cationic (co)polymers or polymer complexes, as has been extensively reviewed recently (98). Comprehensive, recent reviews of the use of liposomes in gene therapy are also available (48, 92–94).

4.3 Dispersed lipid particles

4.3.1 Dispersed liquid crystalline phases

Although emulsions and liposomes are probably the most frequently studied and used dispersed lipid systems for pharmaceutical applications, there are also

others of interest, based on, e.g. dispersed crystalline or liquid crystalline phases. For example, formulations based on dispersed cubic liquid crystalline phases, frequently referred to as Cubosomes[®], are of interest for parenteral administration, since these can solubilize both water-soluble and oil-soluble substances (99–103). Such carrier systems are prepared through high pressure homogenization of cubic liquid crystalline phases which are also stable in equilibrium with excess water. The dispersed cubic-phase particles are stabilized against flocculation and coalescence, which can be achieved, e.g. by a PEO-containing copolymer. Due to the small size that can be reached (≈ 100 – 300 nm) and the PEO-based coatings, it is hardly surprising that these particles are capable of bloodstream circulation for a considerable time. Therefore, such systems offer potential advantages relating to increased drug bioavailability and reduced toxic side-effects in RES-related tissues, at the same time as both water-soluble and oil-soluble substances may be solubilized in the particles, and released in a controlled manner. For example, Engström investigated the use of Cubosomes for parenteral administration of somatostatin in rabbits, and found a much longer circulation time than that displayed by the free drug (99). Furthermore, Schröder *et al.* compared Cubosomes to a number of other immunological adjuvants, and found the former to work both as a parenteral and a mucosal adjuvant in mice, using diphtheria toxoid as a model antigen (101).

4.3.2 Dispersed solid lipid particles

Another class of dispersed colloidal particles of interest in pharmaceutical applications are those prepared either by crystallization and/or precipitation in o/w emulsion systems, or by dispersion through high-pressure homogenization at elevated temperature, followed by cooling and solidification of the lipids droplets (104–115). In particular, such systems are attractive since they allow a high load of hydrophobic drugs, since hydrolytic degradation is limited, since the drug release rate can be controlled by the particle size and composition, etc. At least some solid lipid nanoparticles (SLNs) combine the advantages of polymeric nanoparticles (in that they provide a solid matrix for controlled release) and o/w emulsions (in that they consist of physiological compounds and can straightforwardly be produced industrially on a large scale), but simultaneously avoid the disadvantages of these systems, such as the use of solvents for the preparation of polymer particles and the burst release frequently observed for emulsion systems.

In particular, emulsification of molten lipid systems at elevated temperatures, followed by cooling, is an efficient way to prepare small solid particles of high concentration of hydrophobic substances. On cooling, the glycerides are expected to recrystallize and thereby form the solid carrier. However, as shown, e.g. by Siekmann and Westesen, the crystallization in the SLNs may be more complex than that of the bulk glyceride systems (109). For example, a reduced degree of crystallinity was found for SLNs prepared from tripalmitate or "hard fat", although this depended on the nature and the concentration of the emulsifier used for the melt homogenization. Furthermore, incorporation of ubidecarenone resulted in a reduced crystallinity and in a precluded transition of residual α -polymorphic material into the stable β -polymorph. Clearly, the physical structure and formation of SLNs may be rather complex.

In addition, emulsification in the presence of a solvent, followed by solvent evaporation and solidification, has been used as a means of preparing solid lipid particles. For example, Sjöström *et al.* previously devised a way to prepare small solid particles containing hydrophobic drugs, based on dissolving these substances in a suitable solvent, followed by emulsification, and thereafter evaporation of the solvent (111–115). By using this approach, solid particles as small as 50 nm and less could be reached by a suitable emulsifier mixture. However, although the solvent used for the emulsification can be rather efficiently evaporated, residual solvent may still hinder these from being used, e.g. in parenteral drug delivery applications.

Similarly to polymeric particles, the solid matrix of SLNs protects incorporated drugs from degradation, and offers a very large flexibility regarding the drug release rate. For example, using model drugs it has been shown that the release could be varied from minutes to many weeks (see, e.g. ref. 108). In addition, other aspects of SLNs have been investigated, such as their enzymatic degradation, the effect of light and temperature on their physical stability, and aspects of large-scale production (106–108).

4.4 Dispersed polymer particles

A further class of colloidal dispersions of interest in pharmaceutical applications are polymer lattices. In particular, systems of interest include those formed by biodegradable polymers, notably polylactides and polyglycolides and their copolymers, the degradation products of which are essentially non-toxic and readily resorbable. As discussed more extensively below,

dispersed particles prepared from such polymers are interesting, e.g. for oral delivery of drugs not stable in the stomach, for oral vaccination, and for formulations where bioadhesion is desirable.

Both oral and parenteral uptake of colloidal carrier systems have been found to depend on the nature of the carrier as such. In the latter case, the RES uptake of colloidal drug carriers depends on a number of factors, notably the surface properties of the carrier (see above). This is related to the adsorption of certain serum proteins (opsonins) at the carrier surface, which initiates various biological responses. For example, it is known that macrophages, major components in the RES system, have Fc receptors at their surfaces, which means that carriers with adsorbed IgG are more likely to be captured by these cells (52). By reducing the adsorption of the opsonins at the carrier surface, e.g. by surface treatment using PEO derivatives, a very low serum protein adsorption can be reached, thereby prolonging the bloodstream circulation time and obtaining a more uniform tissue distribution (see above).

However, while the factors governing the RES uptake of intravenously administered colloidal drug carriers are by now rather well known, the oral uptake of such systems is considerably less well known and understood. The oral uptake of such carriers has been found to depend on a number of factors, including size, hydrophobicity and chemical functionality (116–123). For example, Florence *et al.* investigated the effects of size on the oral uptake of carboxylated latex particles, and found the uptake to be due to Peyer's patches and other elements of the gut-associated lymphoid tissue (GALT) (117). Furthermore, the uptake of the untreated particles was found to increase with decreasing particle size, a finding which has also been reported by Ebel (122) and Tabata *et al.* (118). Moreover, Florence *et al.* found that surface modification with hydrophilic PEO–PPO–PEO block copolymers reduces the uptake of polystyrene particles by intestinal GALT (117). A decreased uptake of colloidal particles with an increasing particle hydrophilicity have also been suggested by findings by, e.g. Jepson *et al.* (123).

An interesting approach to achieve an increased uptake after oral administration of colloidal drug carriers is to use site-specific adherence through surface modification of the colloidal systems with various entities, e.g. lectins, to a selected site in the gastrointestinal tract (124). By using this approach, Lehr *et al.* were able to achieve an enhanced adherence of polystyrene particles to enterocytes *in vitro* (125). Similarly, Rubas *et al.* were able to enhance the uptake of liposomes into Peyer's patches *in vitro* through incorporation

of the reovirus M cell attachment protein into the liposomes (126). Furthermore, Pappo *et al.* modified polystyrene microparticles with a monoclonal antibody with specificity to rabbit M cells, and found that this promoted the uptake of these particles into the M cells (127).

In addition, bioadhesion has also been inferred to be of importance for the resulting bioavailability in nasal administration (128). Here also, bioadhesion mediated through specific interactions has been shown to give advantageous effects. For example, Lowell *et al.* investigated the intranasal immunization of mice with human immunodeficiency virus (HIV) rgp 160, and found enhanced responses for bioadhesive emulsions (129). Similarly, Florence *et al.* investigated the oral uptake of polystyrene latex particles, and found that modification of the polymer particle surfaces with specific ligands, e.g. tomato lectin molecules, resulted in a significant uptake enhancement (117). Findings along the same lines have also been previously described by Naisbett and Woodley (130, 131).

An interesting issue in relation to oral drug delivery, not the least with particular drug carriers, but also in other types of administration, is that of bioadhesion, by which one usually means the adhesion/adsorption at mucosal surfaces. Since mucins are negatively charged and contain hydrophobic domains, it is possible to use a number of approaches, other than those based on specific interactions, for achieving efficient bioadhesion, including positively charged carriers, small hydrophobic carriers or those at least containing some hydrophobic part, or carriers not stable but rather aggregating and depositing at the conditions prevalent at the administration site. By the use of bioadhesive formulations, the residence time, e.g. in the gastro-intestinal tract, can be prolonged, which tends to improve the drug uptake.

For example, Luessen *et al.* investigated mucoadhesive polymers in relation to the oral drug delivery of busserelin (132). It was found that the use of, e.g. the positively charged polyelectrolyte chitosan, resulted in a significantly improved bioavailability after intradouneal administration, which most likely is an effect of the enhanced electrostatically driven bioadhesion of the formulation. Furthermore, Soane *et al.* investigated the clearance characteristics of nasal drug delivery systems consisting of, e.g. chitosan solutions and microspheres (133). By the use of a technetium labelling approach, it was found that both of these formulations resulted in a prolonged residence time. Particularly for the latter, the

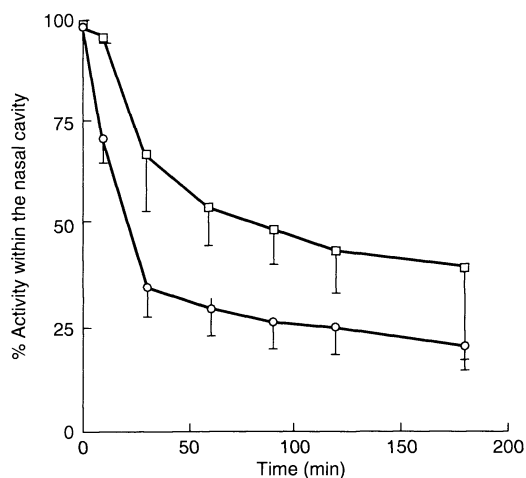


Figure 1.8. The clearance of ^{99m}Tc -sodium pertechnetate and ^{99m}Tc -diethylenetriaminepentaacetic acid, respectively, from the nasal cavity following administration of a chitosan particulate formulation (squares) and the control without such carrier (circles) (data from ref. (133))

clearance half-life was strongly pronounced when compared to the control (Figure 1.8). Analogous results were found by Felt *et al.*, who observed a threefold increase of the corneal residence time in the presence of chitosan in comparison to the control (134). Furthermore, an ocular irritation test demonstrated good tolerance of chitosan after topical administration on to the corneal surface. As yet another example of findings along these lines, Gåserød *et al.* found chitosan-coated alginate beads to adhere more extensively to pig stomach tissues than the corresponding uncoated alginate beads (135).

Note, however, that other mechanisms for obtaining bioadhesion than those based on electrostatic or specific interactions may also be used. For example, those based on poor solvency of a carrier polymer have been used successfully. As an example of this approach, Rydén and Edman investigated the effects of polymers displaying reversed temperature-dependent gelation, i.e. gelation on heating, on the nasal absorption of insulin in rats (136). Two of the systems investigated, i.e. ethyl(hydroxyethyl)cellulose (EHEC) and poly(*N*-isopropyl acrylamide), display a lower consolute temperature of 30–32 and 32–34°C, respectively. At elevated temperatures, these systems undergo a transition from relatively low-viscous solutions to relatively rigid gels (137–139). It was found that both systems were able to enhance the reduction of the blood glucose level compared to the reference, which is most likely due to gelation-induced bioadhesion of these formulations.

4.5 Aerosols

Aerosols are dispersions of either liquid droplets or solid particles in a gas – in the context of pharmaceutical applications, notably air. Such systems are of interest, e.g. for the delivery of therapeutic proteins and peptides, e.g. since the bloodstream can be reached from the alveolar epithelium without penetration enhancers, and since respiratory diseases can be treated by direct action at the site of interest (140, 141). Aerosol droplets/particles deposit in the airways by either gravitational sedimentation, inertial impaction, or diffusion. Since particles greater than about 5 μm in diameter deposit primarily in the upper airways, while an efficient drug uptake requires that the droplets/particles reach the lower airways, and since submicron particles are generally exhaled, most aerosol particles are of the size range 0.5–5.0 μm . It has been shown that the pulmonary absorption of macromolecules decreases with increasing molecular weight of the macromolecule (142). Nevertheless, for a range of smaller macromolecules, e.g. hormones, a significant absorption has been found. For example, compared to intravenous administration, the oral bioavailability of leuprolide, a potent luteinizing hormone-releasing hormone with a molecular weight of 1.2 kDa, is less than 0.05%, while the transdermal and nasal bioavailabilities are less than 2%. On the other hand, the bioavailability after inhalation was much higher (143). Furthermore, although the pulmonary absorption of macromolecules decreases with increasing molecular weight, pulmonary administration is not limited to small molecules. Instead, a number of larger polypeptides and proteins, e.g. growth hormone (22 kDa), α -interferon (18 kDa), and α_1 -antitrypsin (51 kDa) have been found to be absorbed in the lung (141, and refs therein).

5 DRUG DELIVERY THROUGH THERMODYNAMICALLY STABLE SYSTEMS

The use of thermodynamically stable systems in drug delivery applications has obvious advantages relating to stability, in some cases to ease of preparation, and frequently to optical clarity, etc. It is important to note, however, that although a formulation may be stable when stored, it may breakup at or after administration as a result of, e.g. a change in temperature, pH and excess electrolyte concentration, as well as the extensive dilution with water which usually occurs after administration. Furthermore, even for thermodynamically stable

systems, there may be stability problems relating to the chemical degradation of the drug carrier system. These issues will be discussed further below.

5.1 Micellar solutions

Micellar solutions are useful for increasing the solubility of sparingly soluble drugs. Thus, while the solubility of hydrophobic molecules may be quite low in the absence of surfactants or copolymers, or in the presence of such species below the critical micellization concentration (CMC), it is generally found to strongly increase above the CMC (19, 144–146). Naturally, this is due to incorporation of the molecules in the hydrophobic interior of the micelles. Due to the incorporation of the hydrophobic substance in the micelle hydrophobic interior, there may also be other positive effects relating to decreased hydrolysis rate, controlled release rate of the drug, taste masking, etc.

The capacity of a micellar solution to incorporate hydrophobic drugs depends on a number of factors, including the nature of the surfactant, the size and shape of the micelles formed, and the hydrophobicity and size of the drug, as well as the drug solubility, just to mention a few important aspects. For example, although PEO–PPO–PEO block copolymer micelles are able to solubilize a range of hydrophobic substances, the solubilization capacity has been found to depend on the solute hydrophobicity, e.g. being much larger for aromatic than for aliphatic compounds (144). Although hydrophobic drugs may be solubilized in the hydrophobic core of surfactant or block copolymer micelles, this solubilization will depend on, e.g. the drug solubility. By increasing the charge of the drug molecules, e.g. by changing the pH, their incorporation into micelles may be affected. For example, the solubilization of indomethacin, a non-steroidal anti-inflammatory agent, in PEO–poly(β -benzyl L-aspartate) (PBLA) block copolymer micelles was applied by La *et al.* in order to reduce irritation of the gastrointestinal mucosa and central nervous system toxicity (147). While the release of indomethacin from the PEO–PBLA micelles at low pH, i.e. when the drug is uncharged, is quite slow, the release rate increases strongly on increasing the pH to above the pK_a of the drug ($pK_a \approx 4.5$). Naturally, this is due to a decreased preference for the hydrophobic core of the micelles by the charged indomethacin molecules. Similarly, Scherlund *et al.* investigated the release of lidocaine and prilocaine from block copolymer micelles consisting of Lutrol F68 and Lutrol F127, and found the release rate to increase with decreasing pH, i.e. with an

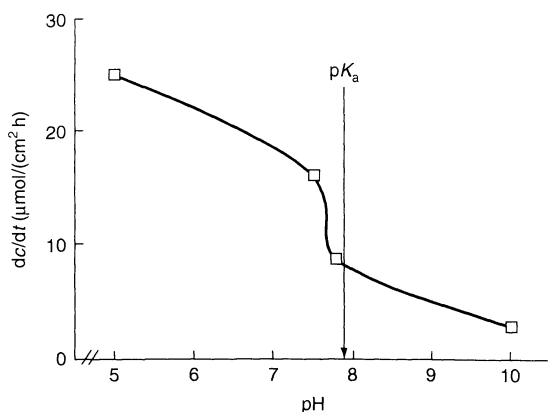


Figure 1.9. Initial release rate of a 50/50 mixture of lidocaine and prilocaine from a formulation containing 15.5 wt% Lutrol F127, 5.5 wt% Lutrol F68 and 5 wt% of the active ingredients, versus pH. The arrow indicates the pK_a of lidocaine and prilocaine (data from ref. (28))

increasing degree of ionization of the active substances (Figure 1.9) (28).

Micellar solutions may also be used to increase the chemical stability of a drug. Hence, since the micellar core is generally essentially free of water, there is typically a reduction of the hydrolysis rate on solubilization. As an example of this, Lin *et al.* found that the hydrolysis of indomethacin was lowered when it was solubilized into PEO–PPO–PEO block copolymer micelles (148). In particular, the hydrolysis rate was reduced at higher copolymer concentrations and molecular weights (constant EO/PO ratio), which follows the solubilization capacity of these block copolymers (Figure 1.10).

Another approach to achieve “solubilization” is to couple the active ingredient to a self-associating amphiphilic substance through a labile bond, i.e. essentially a prodrug approach (149–152). As an example of this, PEO–polyaspartate conjugates with adriamycin (ADR), a potent anti-cancer drug, have been found to form small micelles (15–60 nm), in which the ADR is solubilized/anchored to the micelle interior. These conjugate micelles have been found to display a very long residence time for the individual polymer molecules in the micelles (\approx days), which means that the micelles do not disintegrate as a result of the extensive dilution following intravenous administration. Furthermore, the micelles were found to display a very long circulation time in the bloodstream after parenteral administration. In addition, any side-effects found for ADR when administered in aqueous solution at concentrations higher than about 10 mg/kg were observed to

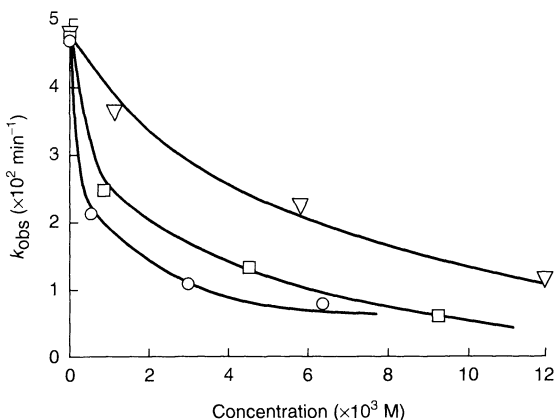


Figure 1.10. Degradation rate constant (k_{obs}) of indomethacin as a function of polymer concentration for Pluronic F68 (triangles), F88 (squares) and F108 (circles) in alkaline aqueous solution at 37°C (data from ref. (148))

occur at 1–2 orders of magnitude higher ADR concentrations when the ADR was present in the micelles. Thus, the use of these conjugate micelles increases the maximum ADR concentration usable in therapy without occurrence of toxic side-effects. Due to this and to the longer circulation time in the bloodstream, the cytotoxicity of the block copolymer conjugate micelles is much better than that of ADR in aqueous solution. Naturally, this is analogous to the positive effects of PEO-modified liposomes in cancer therapy discussed above. The use of PEO-containing block copolymer micelles in drug delivery has been extensively discussed previously (149–153).

Block copolymer micelles with solubilized drugs have also been successfully used for targeting, i.e. the selective administration of drugs to certain tissues or cells. Just to mention one example, Kabanov *et al.* have demonstrated targeting of fluorescein isothiocyanate solubilized in PEO–PPO–PEO block copolymers to the brain when the copolymer was conjugated with antibodies to the antigen of brain glial cells (α_2 -glycoprotein) (84). Furthermore, incorporation of haloperidol into such micelles was found to result in a drastically increased therapeutic effect.

5.2 Cyclodextrin solutions

Although micellar solutions are successfully and extensively used in order to solubilize sparingly soluble hydrophobic drugs, e.g. to increase their solubility, to reduce hydrolytic degradation, to obtain a controlled

drug release, for taste masking, etc., there are also other possibilities for this. Notable in this respect are cyclodextrin inclusion complexes, which have been investigated in pharmaceutical research and development for a long time, and which are now also used in a number of commercial formulations, e.g. Prostvasin™, Brexin™, Cycladol™ and Optalmon™. Although a considerable amount of work has been devoted to the application of natural cyclodextrins, they have some undesirable properties as drug carriers, and therefore cyclodextrin derivatives have received considerable attention. Furthermore, although hundreds of cyclodextrin derivatives have been prepared and a large number of these investigated in the context of pharmaceutical formulations, only a few seem useful as commercial excipients (e.g. hydroxypropyl, methyl and sulfobutylether derivatives) (154–156).

Naturally, it is the cavity of the cyclodextrins which determines their capacity to form inclusion complexes, and which makes these substances interesting for pharmaceutical and other applications. In addition, for naturally occurring cyclodextrins the cavity readily participates in inclusion complex formation, and thereby facilitates solubilization of sparingly soluble hydrophobic drugs. Through hydrophobization of the cavity, e.g. with alkyl groups, this natural tendency is enhanced. Due to the hydrophobic nature of the cavity, the capacity of cyclodextrins to form inclusion complexes depends also on the drug physico-chemical properties. Typically, cyclodextrins bind neutral drugs better than their ionic forms. For example, Otero-Espinar *et al.* found that the binding constant of naxopren in β -cyclodextrin decreased dramatically on increasing the pH, as a result on the pH-dependent ionization of this drug (157). Analogous effects were observed by van der Houwen *et al.* for mitocycin C/ γ -cyclodextrin complexes (158). Naturally, the cavity hydrophobicity also has consequences for the drug release rate. More precisely, with an increasing cavity hydrophobicity, the release rate of hydrophobic drugs is reduced (154–156, and refs therein).

Due to this inclusion complex formation, cyclodextrins have a wide applicability within pharmaceuticals, as a consequence of the positive effects on solubility and dissolution rate, hydrolytic degradation rate, drug absorption, suppression of volatility, powdering of liquid drugs, taste masking, and reduction of adverse biological responses, such as local irritancy and haemolysis (although, e.g. some highly alkylated and surface-active cyclodextrins may have such detrimental effects on their own (154)). In particular, the enhanced solubility of a large number of hydrophobic drugs through the addition of both natural and derivatized cyclodextrins has been

reported. Overall, it seems that while natural cyclodextrins are particularly useful as hydrophilic carriers for increasing the solubility, and at least in some cases the dissolution rate of sparingly soluble drugs, hydrophobic cyclodextrin derivatives are preferable for modifying and controlling the release of drugs. Cyclodextrins have also been found to stabilize various esters, amides and glycosides from hydrolytic degradation, although cyclodextrins may both enhance and reduce drug degradation (154–156).

Cyclodextrins have been found to be beneficial for the bioavailability of poorly soluble drugs and for reducing the occurrence of side-effects. For example, Uekama *et al.* investigated the administration of digoxin to dogs and found that incorporation of this drug into γ -cyclodextrin resulted in increased plasma levels after administration (159), as well as reduced haemolytic effects *in vitro* (160). Furthermore, Kaji *et al.* were able to demonstrate the selective transfer of carmofof, a hydrophobic prodrug of 5-fluorouracil, into the lymphatics from the lumen and the large intestine in rats through the use of a carmofof/cyclodextrin/polymer system (161). Moreover, due to the inclusion in cyclodextrins, the toxicity of such drugs may be reduced. For example, cyclodextrins have been shown to be able to reduce membrane disruption due to amphiphilic drugs, and to protect erythrocytes from morphological changes and following haemolysis induced by certain drugs, e.g. chlorpromazine and flufenamic acid. The chemistry, pharmaceutical applications and safety considerations of cyclodextrins have been extensively discussed previously (154–156).

5.3 Microemulsions

Microemulsions are systems consisting of water, oil and amphiphile(s), which constitute a single optically isotropic and thermodynamically stable liquid solution (162, 163). They are fundamentally different from homogenized emulsion systems, which are generally thermodynamically unstable, and which will therefore break up and form two macroscopic phases after a sufficiently long time. There are many aspects of microemulsions which make them interesting from a drug delivery point of view, including excellent storage stability, ease of preparation, optical clarity, low viscosity, etc. So far, microemulsions have found applications in primarily topical and oral administrations, whereas the use of microemulsions in, e.g. parenteral drug delivery, is much less explored due to both stability and toxicity concerns.

5.3.1 Oral administration

One area where microemulsions are of interest to drug delivery is in oral administration of sparingly soluble hydrophobic drugs. Thus, it is commonly found that on oral administration of such substances a low and strongly varying uptake occurs. The latter also depends significantly on a number of factors, e.g. on the state of feeding/fasting. As discussed above, the broadly occurring low and strongly varying bioavailability of orally administered hydrophobic drugs may be improved through the use of *o/w* emulsions. The mechanism of this is not entirely understood, but it is interesting to note that it has been found that the uptake for formulations based on *o/w* emulsions is improved on decreasing the droplet size (see above). (See also the discussions of the gastrointestinal uptake of particulate drug carriers and oral vaccination.) Considering this, it is perhaps not entirely surprising that *o/w* microemulsions have been found to be efficient in oral administration of hydrophobic drugs. For example, when given orally, the absorption of cyclosporine, an immunosuppressive agent which is used in the treatment of patients with certain autoimmune diseases, and which prolongs allograft survival in organ transplantation, is only about 30% of the dose or less. Moreover, there is a considerable intra- and inter-subject pharmacokinetic variability, which is affected by physiological and pharmaceutical factors such as bile and food. Most likely, this is related to the high molecular weight and hydrophobicity of cyclosporine. However, as has been found by a number of investigators, significantly better results regarding both uptake and pharmacokinetic variability are obtained when cyclosporine is administered in an *o/w* microemulsion (Figure 1.11) (33–37).

Apart from improving the uptake and decreasing the variability, the use of microemulsions for oral delivery of hydrophobic drugs can be applied in order to protect drugs which are unstable at the conditions present in the stomach. For example, Novelli *et al.* formulated WR2721, a substance employed in cancer therapy which needs to be protected from acid hydrolysis in the stomach in order to retain its biological activity (164). By formulating this substance in a *w/o* microemulsion consisting of cetyltrimethyl ammonium bromide (CTAB), iso-octane and butanol, these authors were able to slow down the hydrolysis considerably when compared to the aqueous solution.

5.3.2 Topical administration

Due to the rather high surfactant concentrations typically present in microemulsion systems, there are some

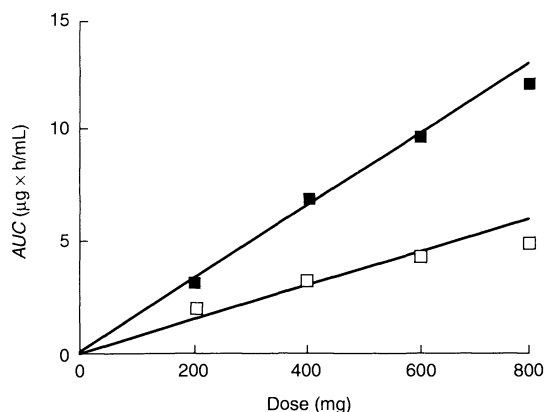


Figure 1.11. Relationship between cyclosporine bioavailability, given as the integral of the blood concentration versus time curve (*AUC*) and dose after oral administration of an *o/w* microemulsion (filled symbols) and a crude *o/w* emulsion (open symbols) (data from ref. (36))

limitations to their general application in drug delivery. However, this high surfactant concentration can also contribute to the functional advantages of such systems, which is most probably the case for topical administration of both hydrophobic and hydrophilic substances using microemulsions. There are numerous examples of studies in which an improved bioavailability of topically administered drugs has been achieved through the use of microemulsions, e.g. that of Ziegenmeyer and Führer, who found the transdermal penetration of tetracycline hydrochloride from a *w/o* microemulsion, prepared from dodecane, decanol, water and an ethoxylated alkyl ether surfactant, to be better than that observed with conventional formulations (165), and that by Willimann *et al.*, who found that the transport rate for transdermally administered scopolamine and broxaterol was much higher for lecithin-based microemulsion gels than for an aqueous solution at the same concentration (Figure 1.12) (166). Further examples include the work of Bhatnagar and Vyas, who found an improved bioavailability of transdermally administered propranolol when using a lecithin based *w/o* microemulsion (167), and that of Gasco *et al.*, who found that a viscosified *o/w* microemulsion, formed by water, propylene glycol, decanol, dodecanol, Tween 20, 1-butanol and Carbopol 934, gave a significantly better penetration of azelaic acid, e.g. when used for treating a number of skin disorders, than the corresponding water, propylene glycol and Carbopol “gel”, through full-thickness abdominal skin (168).

The origin of the advantageous effects of microemulsions for topical drug delivery is not entirely understood.

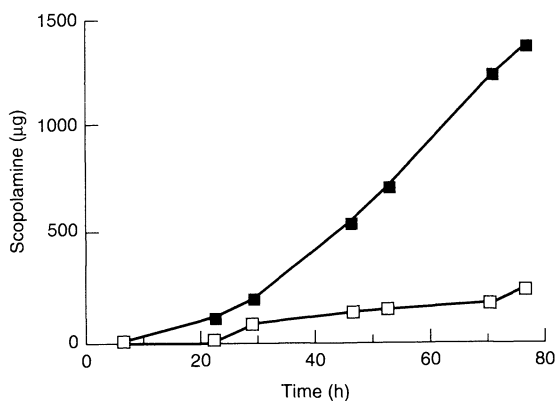


Figure 1.12. Transport of scopolamine through human skin from a lecithin–isopropyl palmitate–water microemulsion (filled symbols) and from an aqueous buffer solution (open symbols) (data from ref. (166))

However, it is known that the outermost layer of the skin, the *stratum corneum*, consists of keratin-rich dead cells embedded in a lipid matrix. The most important function of the *stratum corneum* is to limit transdermal transport in order to prevent dehydration and to protect the body from chemical and biological attack. The lipids, which only constitutes about 10% of the *stratum corneum*, seem to be particularly important for its function. Studies in which the natural lipids of the *stratum corneum* have been replaced by model lipids indicate that the former consists of layered structures, and it has therefore been inferred that it is the structure of the lipid self-assemblies which governs the barrier properties (169, 170). In this context, it is also interesting to note that Azone[®], a commonly used penetration enhancer in topical drug delivery (89, 171), favours reversed-type structures, such as the reversed hexagonal and reversed bicontinuous cubic structure, at least in certain lipid systems (172). Thus, disruption of layered structures and generation of water and oil channels seem to correlate with an increased penetration of the *stratum corneum*. The solubilization of membranes by surfactants, as well as strategies for passive enhancement in topical and transdermal drug delivery, have previously been discussed in some detail (89, 173).

Since microemulsions are capable of solubilizing both hydrophobic and hydrophilic substances, it is not entirely unexpected that microemulsions can disrupt the *stratum corneum* and increase the penetration and transdermal drug absorption. Their use in topical formulations are therefore interesting. A drawback with this approach, however, is that there is a risk of skin irritation. It is possible that the latter effect depends on the

structure formed at the skin after evaporation of water and other volatile components (e.g. whether a lamellar liquid crystalline phase, a reversed structure phase, etc., is formed) (see below).

5.3.3 Parenteral administration

There are several potential difficulties relating to the use of microemulsions in parenteral administration. In particular, the high surfactant concentration generally present in such systems severely limits the types of surfactant that can be used in the formation of such systems. Furthermore, many microemulsions are not stable on dilution with water, and hence intravenous use of such systems demands knowledge on what happens to the microemulsion on dilution with blood. However, microemulsions have indeed been investigated and also found promising for this administration route. For example, von Corswant *et al.* studied a microemulsion system composed of a medium-chain triglyceride, soybean phosphatidylcholine and poly(ethylene glycol)(660)-12-hydroxystearate (12-HSA-EO15), the structure of which was found to be bicontinuous even at high oil concentrations (174). On dilution of the microemulsion with water, there is a transition into an emulsion phase, i.e. there is a spontaneous *in situ* emulsification, resulting in emulsion droplets of a size acceptable for intravenous applications (Table 1.2), and in fact smaller than that of typical commercial nutrition formulations (see above). Furthermore, it was found that it was possible to administer up to 0.5 ml/kg of the microemulsion (oil weight fraction, 50%) without significant detrimental effects on the acid–base balance, blood gases, plasma electrolytes, mean arterial blood pressure, heart rate, and time lag between depolarization of atrium and chamber. Therefore, it seems that also for intravenous

Table 1.2. Mean droplet diameter and polydispersity index of o/w emulsions resulting from dilution by water of a microemulsion consisting of a medium-chain triglyceride, soybean phosphatidylcholine, and poly(ethylene glycol)(660)-12-hydroxystearate, poly(ethylene glycol) 400 and ethanol (from ref. (174) Reprinted by permission of Wiley-Liss, Inc., a subsidiary of John Wiley & Sons, Inc)

Oil weight fraction	Diameter (nm)	Polydispersity index
0.06	187.9	0.54
0.21	65.8	0.32
0.38	67.8	0.23
0.60	105.3	0.08
0.72	132.5	0.19

administration, microemulsion-based formulations may indeed be of interest.

5.4 Liquid crystalline phases

There are a number of liquid crystalline phases formed by amphiphilic molecules, notably surfactants, polar lipids and block copolymers, including discrete and bicontinuous cubic phases, hexagonal phases (and their reversed counterparts), lamellar phases, intermediate phases, etc. A number of these phases are interesting from a drug delivery point of view. This is due to the frequently large solubilization capacity of both hydrophilic and hydrophobic substances, possibilities to control the drug release rate, favourable rheological properties, suitable water transport rates, excellent stability, etc.

Perhaps of particular interest to drug delivery are cubic liquid crystalline phases, especially those which are bicontinuous. Such systems are stiff, transparent, and can act as a “solubilizing” and controlled release reservoir of both low- and high-molecular-weight hydrophilic, hydrophobic or surface-active ingredients (175–185). For many substances and bicontinuous cubic phases, the solubilization capacity for all of these types of drugs can be considerable, which also contributes to making cubic phases interesting for drug delivery. (Naturally, the release at a given mesh size of the cubic phase depends to a large extent on both the size and hydrophobicity of the solubilized drug.) The solubilization capacity of bicontinuous cubic phases also relates to another interesting possibility with the use of these phases as drug carriers, since large biomolecules, e.g. enzymes, can be incorporated into the cubic phase. This, in turn, may allow an increased use of rather potent protein drugs, which, if not effectively immobilized, could result in detrimental side-effects (see below).

Unless the cubic phase is dispersed as described above, its stiffness can render its administration rather difficult. However, through the knowledge of the phase diagram of the system (in the presence of the active component), one can utilize the natural tendency for the system to undergo phase changes depending on the conditions. This, in turn, may allow *in situ* formation of the liquid crystalline phase. As an example of this, Norling *et al.* previously investigated such *in situ* formation in a dental gel application (175). The system used for this consisted of monoolein, sesame oil and metronidazole. By administering such a system as a suspension, which transforms into either a cubic or a reversed hexagonal phase at higher water content, it is

possible to use the excess water present in the oral cavity in order to achieve the transition from the relatively low viscous, and hence easily administered, L2 formulation, into the stiffer cubic and reversed hexagonal phases *in situ* (cf. Figure 1.13). In particular, the reversed hexagonal phase was found to have the most favourable sustained release properties. It was further showed by Engström *et al.* that lamellar and cubic phases formed by the monoolein–water system display moderate to excellent bioadhesive properties (176).

Furthermore, temperature can be used in order to obtain an *in situ* formation of liquid crystalline phases which otherwise would be difficult to administer, e.g. due to their high viscosity. For example, Engström *et al.* studied the *in situ* formation of a bicontinuous cubic phase constituted by monoolein and water (177). Thus, in a certain concentration range this system displays a transition from the lamellar phase to the cubic phase with increasing temperature, and by tuning the system a transition temperature between room and body temperature may be obtained (see Figure 1.13). By using this approach, the favourable drug delivery properties of the cubic phase can be combined with the relative ease of administration of the more low-viscous lamellar phase. The formation and properties of such *in situ*-forming carrier systems were also demonstrated with a number of lipid systems and a variety of drugs.

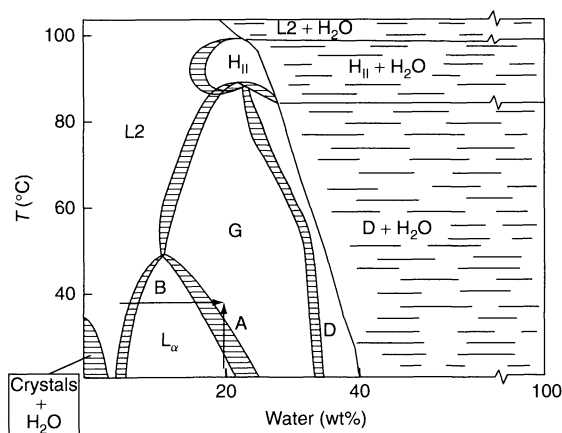


Figure 1.13. Phase diagram of the monoolein/water system. The cubic phases are denoted G (the gyroid type) and D (the diamond type). The arrows indicate two different means to reach an *in situ* formation of a bicontinuous cubic phase, i.e. through increasing the temperature of a lamellar phase at a fixed composition (A), and through dilution with water of a reversed micellar phase at a fixed temperature (B) (data from ref. (266))

Liquid crystalline phases also seem to play an important role in topical and transdermal drug delivery. As discussed above, the protective properties of the *stratum corneum* seems to depend on the properties of its lipid fraction. More specifically, these have been found to form lamellar structures (169, 170), which could be expected to reduce the transdermal penetration of drugs, as well as water evaporation. On the other hand, the presence of Azone[®] may induce reversed-type phases (172). Thus, the generation of oil and water channels seems to correlate with the commonly observed enhanced transdermal penetration of drugs caused by this penetration enhancer (186).

On application of a liquid crystalline or other type of surfactant-based formulation (e.g. microemulsions) to the skin its composition, and hence its structure, will change as a result of differential evaporation of the formulation components (169, 170). A little while after application, therefore, the amounts of the more volatile components (e.g. water) are reduced. This is expected to have implications for both drug penetration and skin irritation. For example, if the formulation after evaporation consists of a (reversed) microemulsion structure, solubilization of lipid biomembranes could be expected to be substantial (see above), thus leading to good skin penetration of the drug but also risking the occurrence of skin irritation. If, on the other hand, the remaining system is a lamellar liquid crystalline phase, skin irritation is less likely, and water evaporation from the application site may be reduced, although the drug uptake may be less efficient. In any case, a controlled dermal application of such formulations requires knowledge of the phase behaviour of the system in general, and of the effects of evaporation on the structures formed in particular.

Liquid crystalline phases are also of interest from the point of view of controlled or sustained release, or even the *absence* (e.g. in the case of certain potent enzymes) of such release of bioactive molecules. For example, due to the presence of both water and oil channels in bicontinuous cubic structures, such systems are capable of solubilizing both hydrophilic, hydrophobic and amphiphilic drugs, the release of which can be sustained over extended periods of time. Particularly interesting in this respect is the incorporation of large oligopeptide or macromolecular drugs (e.g. enzymes). For example, Ericsson *et al.* investigated the incorporation of lysozyme in a cubic phase formed by monoolein and water, and found that a considerable amount could be solubilized in the liquid crystalline phase (182). Furthermore, the incorporation of α -lactalbumin, bovine serum albumin and pepsin was found to resemble that

of lysozyme. Analogously, Portmann *et al.* incorporated α -chymotrypsin in a cubic phase composed of 1-palmitoyl-*sn*-glycero-3-phosphocholine and water, and inferred through UV/VIS and circular dichroism studies that the conformation of the enzyme is quite similar to that in water (183). Moreover, Razumas *et al.* investigated the incorporation of cytochrome *c* (184) and of glucose oxidase, lactate oxidase, urease and creatinine deiminase in a cubic liquid crystalline phase formed by monoolein and water (185). It was found that the latter enzymes could indeed be incorporated, although the relative activities of the enzymes were found to decrease over a time-span of a few days to a couple of weeks.

5.5 Gels

The use of gels in pharmaceuticals depends to some extent of the structure of the particular gel being considered. The term “gel” is frequently used in pharmaceutical research and development to describe “thick” or “non-flowing” systems. This means that different systems may have drastically different compositions, even consisting of entirely different kinds of sub-units, therefore having widely different structures. (In fact, some gels of interest to pharmaceutical applications are two-phase systems, and therefore not even thermodynamically stable.) More often than not, however, the gels used in pharmaceutical applications contain water-soluble polymers. While some are suitable for molecular solubilization of sparingly soluble drugs due to the presence of hydrophobic domains, others are not capable of this due to the absence of such domains. However, although the solubilization capacity may be an important aspect in a particular drug delivery system, it is generally other aspects, e.g. the rheological properties or their consequences (e.g. relating to the drug release rate, bioadhesion, etc.), which make these systems particularly interesting from a drug delivery point of view, and therefore these systems are discussed together here.

One type of “gel” which has been extensively investigated in relation to pharmaceutical applications is that formed by certain PEO–PPO–PEO block copolymers (153). These systems are particularly interesting since even a concentrated polymer solution is quite low-viscous in nature at low temperature, whereas a very abrupt “gelation” (liquid crystal formation (25, 187, 188)) occurs on increasing the temperature. The precise value of the transition temperature depends on the polymer molecular weight, composition and concentration, the concentration and nature of the drug, etc., but by

combining these aspects, the gelation temperature can be straightforwardly controlled.

Such systems have the capacity to solubilize particularly hydrophilic or moderately hydrophobic drugs. Apart from this, however, they are also interesting from the point of view of drug delivery, e.g. since they can be easily administered at low temperatures through their low viscosities, whereas they gel rapidly at the administration site. One area where this is of obvious importance is in topical, dermal and buccal administration. As an example of this, Scherlund *et al.* investigated the gels formed by two PEO–PPO–PEO block copolymers (Lutrol F68 and Lutrol F127) and the local anaesthetic agents, lidocaine and prilocaine. By a suitable choice of composition, the low viscosity of a refrigerator-chilled or room-temperature formulation can be combined with gelation at the administration site, bioadhesion in the oral cavity, and a suitable release rate of the active ingredients, with the latter being an important aspect of these types of formulation (Figure 1.14) (28).

One reason for the use of gel-based drug delivery formulations is that they allow sustained and controlled release. As expected for PEO–PPO–PEO-based gels, the drug release rate depends on the drug hydrophobicity. More precisely, the drug release rate has been found to decrease with increasing drug hydrophobicity for these types of formulations (see Figure 1.9). For example, Wang and Johnston investigated the sustained release of interleukin-2 (IL-2) after intramuscular injection in rats (189). This substance has been found promising in the treatment of several cancers in both experimental animal models and in humans, in which the toxicity of IL-2 is a major problem. However, the

antitumour effect of IL-2 has been found to correlate with the time that this substance remains in the serum, rather than with the peak serum concentration, and therefore a sustained-release formulation could be expected to improve the therapeutic efficiency and reduce toxic side-effects. Therefore, the reduced peak serum IL-2 concentration and the longer circulation of IL-2 observed after intramuscular administration for a gel formulation (Pluronic F127), when compared to the aqueous IL-2 solution, is promising for IL-2 intramuscular therapy.

Apart from effectively increasing the solubility of hydrophobic drugs and achieving a controlled release of the drug after administration, block copolymer gels may be used to improve the chemical stability of the active substance (cf. micellar and cyclodextrin solubilization (see Figure 1.10)). For example, Tomida *et al.* investigated PEO–PPO–PEO block copolymer gels containing indomethacin regarding their suitability as topical drug delivery systems, and found that the hydrolysis rate of indomethacin was reduced in the gels when compared to the aqueous solution (190). This protective property makes these gels interesting, e.g. for oral administration of substances sensitive to acid-catalysed hydrolysis.

Another application where PEO–PPO–PEO block copolymer gels have shown promise is as wound dressings in the treatment of thermal burns. Such dressings should be easy to apply, and should adhere to the uninjured skin surrounding the wound, but also come off easily when removed. Furthermore, the adherence should be uniform since small areas of non-adherence may lead to fluid-filled pockets where bacteria could proliferate. Moreover, dressings should absorb fluid and

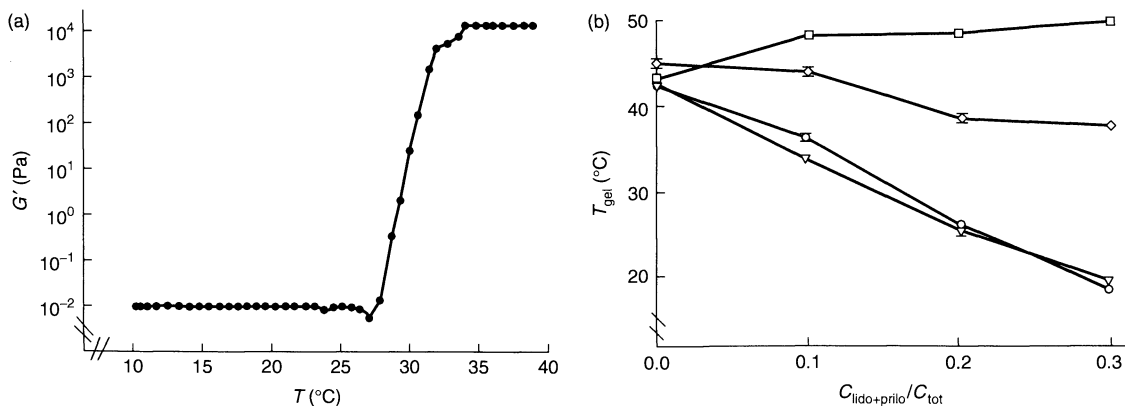


Figure 1.14. (a) Elastic modulus (G') of formulations containing 14.5 wt% Lutrol F127, 5 wt% Lutrol F68 and 5 wt% of a 50/50 mixture of lidocaine and prilocaine. (b) The effect of the concentration of the active ingredients on the gelation temperature of a formulation containing 15.5 wt% Lutrol F127 and 4 wt% Lutrol F68 at pH 5 (squares), pH 7 (diamonds), pH 8 (circles), and pH 10 (triangles). The pK_a of lidocaine (lido) and prilocaine (prilo) are 7.86 and 7.89, respectively (267) (data from ref. (28))

maintain a high humidity at the wound, and should also provide a bacterial barrier, either on their own or by the inclusion of antibacterial agents, the release of which should preferably be sustained. Although it is difficult to meet all of these requirements, PEO-PPO-PEO block copolymer gels have been found useful for such wound dressings. For example, Nalbandian *et al.* found that Pluronic F127 is an efficient formulation for bacteriocidal silver nitrate and silver lactate following full-thickness thermal burns in rats (191). No inhibition of skin growth and repair was noted and the dressings were equally efficient against *Pseudomonas aeruginosa* and *Proteus mirabilis*. The dressings also showed promise regarding electrolyte imbalances, heat loss and bacterial invasion.

While the “gels” formed by the PEO-PPO-PEO block copolymers are generally liquid crystalline phases (187, 188), those formed by polysaccharides occur as a consequence of network formation, frequently involving coil-helix transitions, and in at least some cases, helix aggregation (192–195). For example, pectin and galactomannan are of interest, e.g. for specific targeting of the drug to the large intestine, due to their enzymatic degradation in the colon (see below) (196, and refs therein). Furthermore, *in situ*-forming polysaccharide gels are interesting for sustained drug release in the stomach (197, and refs therein). A relatively frequently investigated type of polysaccharide gels are those formed by alginates or gellan gum in the presence of calcium ions. Irrespective of the nature of these types of gels, however, they lack substantial hydrophobic domains. As such, they can only solubilize either fully soluble (hydrophilic) drugs, or dispersed drug (-containing) colloids. Nevertheless, a considerable drug loading can be reached by utilizing poor solvency conditions for the drug. For example, Kedzierewicz *et al.* were able to achieve very high drug loading capacities of propranolol in gellan gum microgel particles by increasing the pH prior to particle formation to above the pK_a of propranolol (198).

Yet another class of gels of some interest in drug delivery is that formed by polymer-surfactant mixed aggregates. Thus, on mixing polymers and surfactants, there is frequently surfactant binding to the polymer backbone, as well as polymer-induced surfactant self-assembly (199, 200). Although the polymer-surfactant aggregates so formed may have different structures, frequently they are described with the so-called bead-necklace structure, in which surfactant micelles are “bound” along the polymer chains. Considering this, it is not surprising that the surfactant micelles may act as transient cross-links, and that an effective “gelation”

can result under at least certain specific conditions (137–139, 199–203).

Polymer systems which have been found to be particularly interesting in this context are cellulose ethers and hydrophobe-modified cellulose ethers. In the presence of ionic surfactants, some cellulose ethers, e.g. ethyl(hydroxyethyl)cellulose (EHEC), display a reversible temperature-induced gelation on heating (137–139, 202, 203). Thus, while such polymer systems are relatively low-viscous in nature at low temperatures, they form loose gels at elevated temperatures. As an example of this, Figure 1.15 shows the temperature-induced gelation of a local anaesthetic formulation, intended for the periodontal pocket, consisting of lidocaine/prilocaine, EHEC and myristoylcholine bromide, the latter being a readily biodegradable and antibacterial cationic surfactant.

In a couple of investigations, Lindell and Engström studied the *in situ* gelation of EHEC/surfactant systems in the presence of timolol maleate and timolol chloride, where the former is a potent β -blocker (202, 203). It was found that timolol maleate could be incorporated in the thermogelling EHEC system at a concentration relevant to commercial eye drops, thus indicating a potential use of these systems in ocular drug delivery. Furthermore, by comparison of formulations containing timolol maleate and timolol chloride, as well as those with different surfactants, it was inferred that for a gel to form at a low concentration of ionic surfactant, (i) the ionic drug should typically be a co-ion to the surfactant, (ii) the counterion of the drug and the surfactant should be inorganic and have a low polarizability, and (iii) the surfactant should have a low CMC, but a Krafft temperature not higher than ambient.

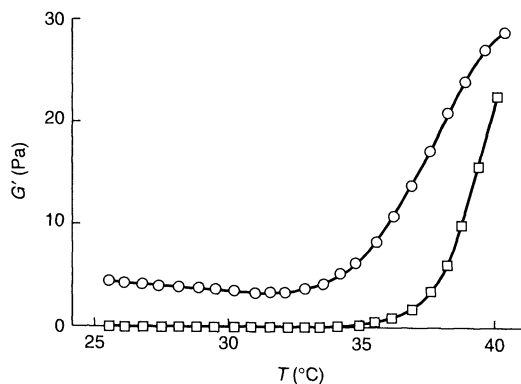


Figure 1.15. Elastic modulus (G') of formulations containing EHEC (1 wt%) and myristoylcholine bromide (3 mM) in the presence (circles) and absence (squares) of 0.5 wt% prilocaine/lidocaine (50/50), at pH 9.8 (data from ref.(139))

6 RESPONSIVE SYSTEMS

Of particular appeal for more advanced drug delivery is the use of responsive systems, which on a given change in one parameter change their properties dramatically, e.g. regarding adsorption/desorption, colloidal stabilization/destabilization, self-assembly, gel formation, swelling/deswelling, etc. Such systems may be responsive to a number of parameters, including temperature, pH, electrolyte concentration, presence of divalent ions, etc. Depending both on the type of response and the parameter inducing the response, such systems find different applications in pharmacy. In the following, a few of the different types of such systems will be briefly discussed.

6.1 Temperature-responsive systems

Of great interest to drug delivery in general are temperature-responsive systems, especially if the system displays a reversed temperature dependence, i.e. a deteriorating solvency with increasing temperature. This decreased solvency, in turn, favours adsorption, self-assembly, gelation, deswelling, etc. Of particular interest for drug delivery in this respect so far have been PEO-PPO-PEO copolymers (see above). These substances have been the subject of numerous investigations, not only due to their interesting temperature-dependent physico-chemical properties, but also due to these polymers being among the first to become commercially available in a range of molecular weights and compositions, and due to the toxicities of at least some of them being comparably low (204). Specifically, a considerable amount of work involving the use of such polymers in drug delivery systems based on their temperature-dependent properties has been performed over the last decade or so. As discussed above, one such temperature response which has been particularly extensively used and investigated in drug delivery is the reversed temperature-dependent gelation displayed by some of these systems, e.g. for *in situ* gelation in periodontal drug delivery, treatment of thermal burns and other wounds, ocular therapy, etc.

Temperature-responsive systems have also been used in conjunction with bioadhesion. For example, ethyl(hydroxyethyl)cellulose, with a lower consolute temperature of 30–32°C and displaying gelation on heating (cf. discussion above), was previously found by Rydén and Edman to cause a rapid decrease in the blood glucose level when co-administered with insulin (136). A similar, although quantitatively smaller effect, was

found for poly-*N*-isopropyl acrylamide (lower consolute temperature, 32–34°C (205)). The positive effects were attributed to the temperature-induced gelation and contraction after administration. Thus, the temperature-dependent gelation may be beneficial simply through the mechanical properties being suitable. However, the temperature increase causes the solvency to deteriorate, which makes alternatives to a molecular solution relatively more favourable. Naturally, this is the origin of the gelation in itself, but the poor solvency conditions at elevated temperatures also enhances the surface activity of these polymers (206–209), which should also contribute to the observed bioadhesive properties. Similarly, Sakuma *et al.* investigated the oral administration of salmon calcitonin (sCT), and found that polystyrene nanoparticles with poly(*N*-isopropyl acrylamide) surface grafts increase the absorption enhancement of sCT (210, 211). Furthermore, the effect was larger for poly(*N*-isopropyl acrylamide) than for a series of ionic nanoparticles. These effects were ascribed to bioadhesion of the particles to the gastric mucosa.

The transition temperatures for thermoresponsive systems depend on a number of factors. Of these, the molecular weight and composition of the polymer systems are perhaps the most obvious ones. For example, the lower consolute temperature, the critical micellization temperature, the gelation temperature, etc., may be drastically changed by the copolymer composition. This is the case, e.g. for the frequently employed PEO-PPO-PEO copolymers (25, 153) and cellulose ethers (212), just to mention a few examples. The transition temperatures have also been found to depend on the presence of cosolutes, such as electrolytes (26, 208), alcohols (208), surfactants (27, 139, 213), hydrotropes (214) and drugs (27, 28, 139, 215). For example, Scherlund *et al.* investigated the gelation of local anaesthetic formulations containing PEO-PPO-PEO block copolymers (Lutrol F127 and Lutrol F64) in the presence of lidocaine and prilocaine, and found that the temperature-induced gelation depended on both the concentration of the active ingredients and on the pH, with the latter as a consequence of the degree of ionization of the active ingredients (see Figure 1.14) (28).

Moreover, Lowe *et al.* examined the thermally responsive hydrogels of *N*-isopropylacrylamide-containing hydrophobic comonomers in both the absence and presence of ephedrine and ibuprofen (216). It was found that the positively charged and hydrophilic drug ephedrine caused deswelling of negatively charged copolymer gels due to attractive electrostatic interactions between the drug and the polyelectrolyte, whereas no such deswelling due to ephedrine was observed for the uncharged gels.

Furthermore, addition of hydrophobic ibuprofen resulted in a collapse of all of the gels. The latter is analogous to the findings by Scherlund *et al.* on the temperature-induced gelation of PEO–PPO–PEO block copolymers on addition of lidocaine and prilocaine in their base forms (see Figure 1.14), as well as to the findings by Carlsson *et al.* on pH-dependent reductions of the cloud points of poly(*N*-isopropyl acrylamide) solutions on addition of either lidocaine or prilocaine (215).

Although most temperature-responsive systems used in pharmaceutical applications are formed by polymers, lipid systems may also be used in this respect. For example, such systems may display temperature-dependent phase transitions. Such transitions of interest could be, e.g. micellar to liquid crystalline phase transitions, transitions between different liquid crystalline phases, emulsion phase inversions, or temperature-induced structural changes in microemulsion systems (17–19, 153). Just to mention one example, Engström *et al.* used the temperature-induced transition displayed by the monoolein–water system from the lamellar phase to the cubic phase as a means of combining the advantageous properties of the cubic phase regarding, e.g. the drug release rate, with the relatively larger ease of administration of the lamellar phase (see Figure 1.13) (177). In fact, these authors compared their system to the temperature-responding systems formed by PEO–PPO–PEO block copolymers and ethyl(hydroxyethyl)cellulose/surfactant systems, and found a comparable performance.

6.2 Electrostatic and pH-responsive systems

Systems responding to changes in pH or electrolyte concentration offer interesting opportunities for drug delivery. In particular, swelling/deswelling transitions of polymer systems, e.g. particles or gels, are quite interesting since they allow the exposure of the drug to the surrounding aqueous solution to be controlled, e.g. in relation to oral administration, with advantageous effects relating to drug stability, release, etc. In particular, polyacids are interesting in this context, since they are protonized at the low pH in the stomach, thus resulting in a compact and somewhat dehydrated structure under these conditions. This, in turn, may lead to a low release rate and some protection against hydrolysis. On the other hand, the deprotonation at a higher pH, e.g. corresponding to that in the small intestine, causes the polymer system to swell as a result of intramolecular electrostatic interactions. This, in turn, facilitates the

release of the drug in a region where it is absorbed more effectively, and where it is more stable against hydrolytic degradation. Microgel particles displaying such pH-dependent swelling have been investigated, e.g. by Carelli *et al.* (217), Bilia *et al.* (218), Morris *et al.* (219), Saunders *et al.* (220), and Kiser *et al.* (221).

For example, Carelli *et al.* investigated the incorporation and release of prednisolon (PDN) from pH-sensitive hydrogel particles prepared from poly(methacrylic acid-*co*-methacrylate) and cross-linked PEO 8000 (217). It was found that the PDN release depends on pH and the hydrogel composition, the latter as a consequence of the different pH sensitivity displayed by particles of different compositions (Figure 1.16). Thus, the higher degree of swelling, then the faster is the release of the drug. Furthermore, Bilia *et al.* investigated the release from pH-sensitive hydrogels prepared by poly(acrylic acid) and PEO (218). (Similar gels have been discussed, e.g. by Buonagidi *et al.* (222).) The drugs investigated were salicylamide, nicotinamide, clonidin hydrochloride and prednisolone. It was found that the release rates of all of these substances were determined by the pH-dependent swelling of the matrix, with a more rapid drug release in simulated intestinal fluid than in simulated gastric fluid. It was therefore concluded that these hydrogels are of potential interest in gastrointestinal drug delivery. Naturally, cross-linked protein systems may also be used as pH-responding gel systems. For example, Park *et al.* studied the swelling of denatured albumin gels, and found the swelling ratio to depend on pH (223). More precisely, minimum swelling was observed at the isoelectric point of the protein.

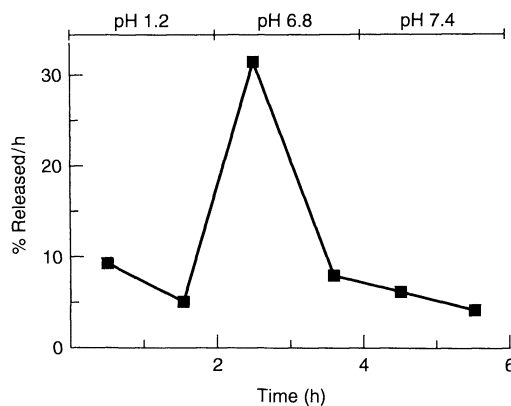


Figure 1.16. Fractional release rate of prednisolone from a hydrogel formed by cross-linked PEO and poly(methacrylic acid-*co*-methylmethacrylate) versus time. The effects of pH changes on the release rate are also shown (data from ref. (217))

Another interesting type of electrostatically responding system is that which depends on the electrolyte concentration. For example, Conaghey *et al.* studied the release of nicotine from ion-exchange resins containing carboxyl groups (224). At pH 7.4, where nicotine is present in its positively charged form, and therefore extensively bound electrostatically to the negatively charged ion-exchange resin, the release of nicotine was found to increase with increasing ionic strength (Figure 1.17). This is expected, since increasing the ionic strength reduces the electrostatic attraction between nicotine and the resin, thus facilitating the release of the former. Somewhat analogous effects have also been found by, e.g. Schacht *et al.* (225), Raghunathan *et al.* (226) and Irwin *et al.* (227).

Furthermore, pH-sensitive multicomponent systems have been investigated in this context. For example, Fernandez-Hervas *et al.* prepared chitosan-alginate beads, and investigated the release of diclofenac salt from these beads, e.g. as a function of pH (228). The background to this study is that diclofenac, a widely used non-steroidal anti-inflammatory drug for the treatment of, e.g. *rheumatoid arthritis*, may cause bleeding, ulceration and perforation upon chronic oral administration. Therefore, enteric coated or sustained release formulations of this substance are interesting. Under conditions mimicking those in the stomach, the release of the drug was limited, even after several hours. On increasing the pH to 7.4, on the other hand, the release rate increased drastically as a consequence of the increased negative charge of alginate and the decreased positive charge of chitosan. This, in turn, reduces interparticle electrostatic attractive interaction

and consequent contraction, thereby facilitating an increased release rate.

Another type of responding system of interest in drug delivery is polysaccharide gels. In particular, microgel particles can be formed in a responsive manner through addition of Ca^{2+} . Examples of such systems include alginate and gellan gum. In particular, such systems are interesting for the preparation of pH-sensitive gel particles highly loaded with the active substance. Just to mention one example, Kedzierewicz *et al.* investigated the loading of gellan gum particles with propranolol (198). By increasing the pH, and thereby reducing the solubility of this drug, prior to gel formation, the drug loading of these particles could be significantly increased. The formation of polysaccharide gel (particles) has also been investigated by others, e.g. Hwang *et al.* (229), Huguet and Dellacherie (230) and Lim and Wan (231).

It is interesting to note that Ca^{2+} alginate beads coated with chitosan have also been found to be of interest due to their bioadhesive properties (cf. the discussion on bioadhesion above). For example, Gåserød *et al.* investigated the adherence of such particles at pig stomach and oesophageal mucosa, and also the adhesion of alginate beads at pig stomach tissue, and found a much higher degree of adhesion of the chitosan-coated alginate beads (135). Naturally, this is in line with numerous previous findings on the bioadhesion of chitosan-containing formulations (cf. the discussion above).

7 BIODEGRADABLE SYSTEMS

Biodegradable systems are interesting for pharmaceutical applications for a number of reasons. In particular, the degradation can be used in order to control the release rate of the drug, but it may also be valuable for protecting the drug from degradation, to reduce the risk for accumulation-related diseases, to control the biological responses to the active substances, etc. By the use of biodegradable chemical links, it is possible to make particles, gels, surface coatings, self-assembled structures, etc., which degrade with half-lives which are orders of magnitude in difference.

The degradation is affected by a number of factors, most notably the nature of the unstable link, composition, pH and temperature. A particular emphasis in this area over the last decade or so has been placed on polyester (co)polymers, and particularly those consisting of polylactides and/or polyglycolides. Through control of the copolymer composition, the degradation

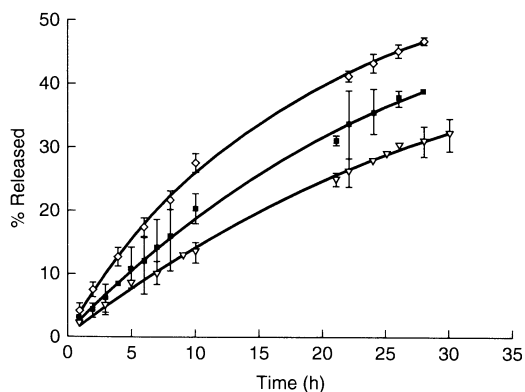


Figure 1.17. Release rate of nicotine from a negatively charged resin (Amberlite IRC50) at pH 7.4 at ionic strengths of 0.11 M (triangles), 0.22 M (squares) and 0.44 M (diamonds) (data from ref. (224))

rate may be controlled to quite some extent (232, 233). Analogous to low-molecular-weight esters, the degradation of polyesters is accelerated at low and high pH (234–236). This makes them interesting regarding oral administration, since a biodegradable drug carrier may be used in order to protect the active substance in the stomach, which is particularly important if the latter is sensitive to hydrolysis, after which it is released after passage through the stomach. Since the degradation rate is quite low at neutral pH or in the dried formulation, on the other hand, one could expect the storage stabilities for such systems to be good.

7.1 Solid systems

Biodegradable particles and other solid systems are probably the types which have been most extensively investigated in this context. In particular, emphasis in these studies have been placed on biodegradation as a means of controlling the drug release rate. It has been found in some cases that there is a close correlation between the degradation and the drug release rate. For example, Domb and Langer investigated the degradation of discs composed of poly(carbophenoxyvaleric acid), as well as the release of *p*-nitroaniline for these, and were able to demonstrate that the release occurs as a consequence of the degradation (Figure 1.18(a)) (237). Since the degradation rate may be controlled over orders of magnitude through the choice of copolymer composition, the drug release rate may be widely controlled with some accuracy. Furthermore, a drug release sustained over extremely long times may be achieved by using this approach.

It is important to note, however, that the drug release from biodegradable polymer systems may be significantly more complex than this. In particular, both the polymer degradation and the drug physico-chemical properties are frequently of importance for the drug release. For example, Sung *et al.* studied the effects on the drug release rate of both the drug physico-chemical properties, notably the hydrophobicity, and the copolymer composition for a series of nalbuphine prodrugs and polylactide–polyglycolide copolymers of different compositions (238). As can be seen in Figure 1.18(b), the drug release rate decreases with an increasing drug hydrophobicity, thus indicating that the drug partitioning is important to the release rate. On the other hand, these investigators also found in the same study that the release rate increases with increasing polyglycolide content in the copolymer, thus indicating that the faster the degradation/erosion, then the faster the release.

In fact, the relation between degradation, drug partitioning and drug release may be even more complex than this, since the drug may also affect the degradation rate. For example, basic drugs may behave as base catalysts, which may enhance the degradation rate and hence also the release rate. On the other hand, basic drugs may also neutralize the polymer terminal carboxyl residues of polyesters, thereby reducing the autocatalysis due to the acidic end-groups, and therefore also the degradation rate and the release rate (238–241).

An area where biodegradable particulate drug carriers have been found promising is in the development of oral vaccines (242–258). Because most infectious species enter the body through mucosal surfaces, immunization involving these surfaces can be expected to be an

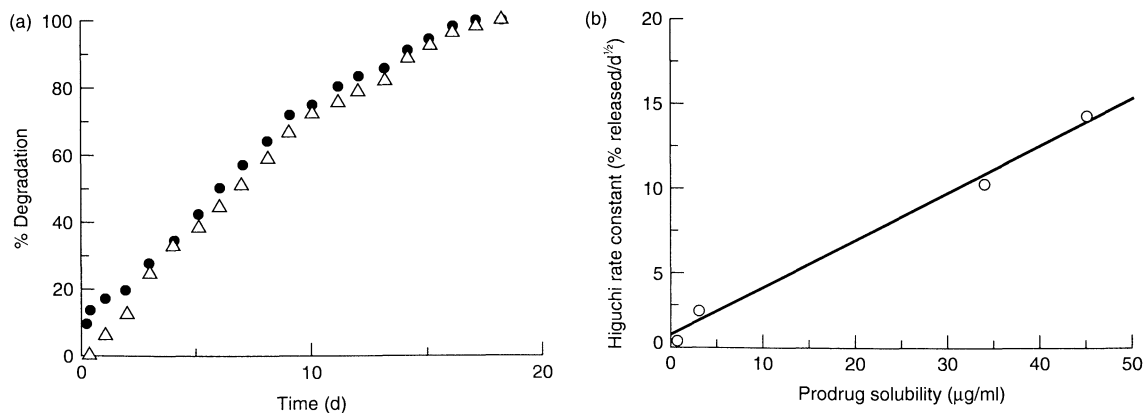


Figure 1.18. (a) *In vitro* release of *p*-nitroaniline (circles) from a poly(carbophenoxyvaleric acid) matrix, as well as the fractional degradation of the matrix (triangles) (data from ref. 237). (b) Relationship between the release rate and the aqueous solubility of various nalbuphine prodrugs (data from ref. (238))

efficient approach for vaccination. The gastrointestinal tract has been mainly investigated in this context, although in addition, other mucosal surfaces, e.g. the pulmonary, genitourinary and nasopharyngeal surfaces are all coated with mucus-containing immunoglobulins, notably IgA, and could therefore be of interest in this respect.

From a delivery point of view, particle encapsulation is an interesting route to facilitate a successful vaccination through the oral route. One reason for this is the harsh conditions prevalent in the stomach, which cause rapid degradation of the material used for immunization, e.g. peptides, proteins, cells, viruses, etc. By encapsulation, on the other hand, degradation of the species provoking the immune-response may be reduced or eliminated. Furthermore, in analogy to parenteral immunization, particles may also be beneficial for immunization by acting as adjuvants (259). Thirdly, since orally administered particles are typically taken up by Peyer's patches, which constitute one of the main immune systems in the gastrointestinal tract, a beneficial localization effect may also occur. In fact, considering the key role played by Peyer's patches, the successful use of particles in oral vaccines seems to depend extensively on the uptake of the latter in these patches. This uptake, in turn, has been found to depend on a number of factors, notably particle size, hydrophobicity and charge, as well as the feeding state of the patient.

Although a number of different particle systems may be used for oral vaccination, biodegradable polylactides and polyglycolides, or their copolymers, are particularly interesting in this context, e.g. since they are taken up very efficiently by Peyer's patches, as they are readily biodegradable, and since the resulting degradation products are essentially non-toxic and readily resorbable. A number of groups have investigated the use of these types of particles in oral vaccination, and stimulation of both mucosal (sIgA antibodies) and systemic (IgG antibodies) have been observed (see, e.g. ref.121). For example, Elridge *et al.* studied the immune response resulting from *Staphylococcal enterotoxin B* encapsulated in poly(DL-lactide-co-glycolide) particles, and found that particles in the size range 1–10 μm were efficient as carriers for this antigen (256). In contrast, the soluble antigen was relatively ineffective (Figure 1.19). Furthermore, Elridge and co-workers demonstrated that particles of different sizes can be co-administered in order to provoke a biphasic immune response (246). Similarly, Nellore *et al.* investigated the performance of microparticles with *hepatitis B* surface antigen vaccine and found enhanced antibody responses (255), while Stevens *et al.* investigated biodegradable

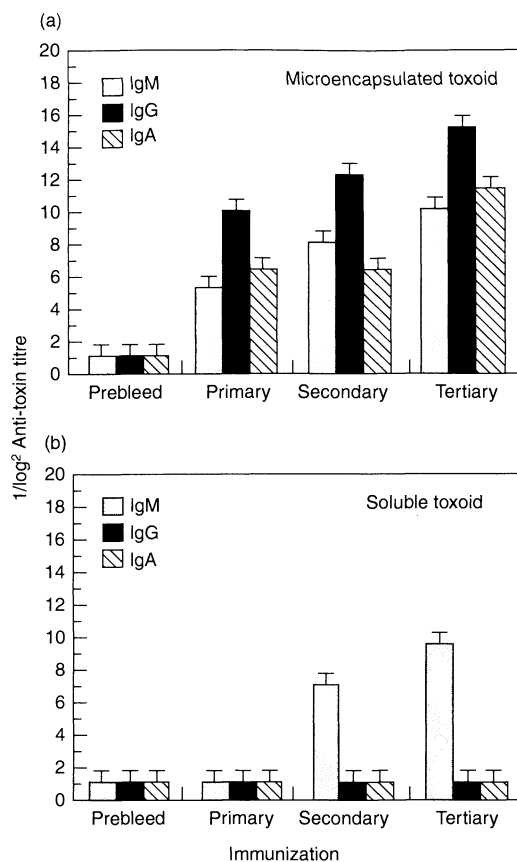


Figure 1.19. Plasma anti-toxin antibody levels of the IgM, IgG and IgA isotypes induced following oral immunizations with 100 μg doses of *staphylococcal enterotoxin B* vaccine either encapsulated (a) or free (b) (data from ref. (256))

microparticles in vaccination for fertility control, and found promising results (260). Biodegradable particles have also been found useful for provoking immune responses to viruses, including parainfluenza virus (244) and influenza virus (248).

Another area where biodegradable polymer systems are of interest is in drug delivery to the lymphatic system (121). This, in turn, is interesting since transport via the intestinal lymphatics circumvents first-pass metabolism through the liver and may enhance the drug bioavailability. Furthermore, uptake in the GALT constitutes an access route to the lymphatic system, and the successful use of this may provide an absorption pathway for encapsulated drug molecules (e.g. peptides and proteins) which are otherwise subject to luminal degradation. As discussed above, the uptake in Peyer's patches depends on the particle size, generally decreasing with increasing

particle size. Furthermore, it has been found that the surface characteristics of particulate drug carriers affect the uptake of the latter in the lymphatic system. For example, more hydrophilic particles are less effectively retained in the regional lymph nodes than hydrophobic particles.

7.2 Polymer gels

Biodegradable polymer gels are interesting, e.g. for oral, buccal, topical, ocular, nasal and vaginal drug delivery. Such systems are frequently preferred due to suitable rheological properties, bioadhesion, optical clarity, etc. Biodegradation of such systems, in turn, offers advantages related to ease of removal or lack of need of removal, sustained release, etc. Considering the advantageous properties of PEO and PEO-containing copolymers in many drug delivery applications, as well as the advantages of biodegradable systems in general, the possibility of producing biodegradable gels from functional PEOs, as discussed previously, e.g. by Zhao and Harris (261) and by Singh *et al.* (262), is certainly interesting.

An area where biodegradable gels are of particular interest is in colon drug delivery (196). The main reason for this is that the fermentation of polysaccharide carriers caused by microbial enzymes in the large intestine may be used, together with the inherent tendency for such systems to display sustained release of solubilized drugs, to obtain efficient controlled release formulations, e.g. for the treatment of Crohn's disease, ulcerative colitis, spastic colon, constipation and colon cancer. Moreover, colon administration is also interesting for systemic absorption of, e.g. peptides and proteins, which are extensively degraded in the gastrointestinal tract. Naturally, a number of systems are of interest in this context, e.g. coatings of by amylose, cyclodextrins, galactomannan or pectin, as well as matrices formed by, e.g. chondroitin sulfate, dextran, pectin or galactomannan. Just to provide one illustrative example, Figure 1.20 shows the results obtained by Rubinstein and Sintov on the release of indomethacin from a calcium pectate gel in the absence and presence of pectinolytic enzyme (known to be present in the colonic region) (263). As can be seen from this figure, essentially no release is observed in the absence of digestive enzymes, whereas a significant release was observed in the presence of such enzymes. Therefore, the release to the colon may be controlled by the stability of the matrix to enzymatic degradation, and, more importantly, a specific targeting to the large intestine can be obtained by this approach.

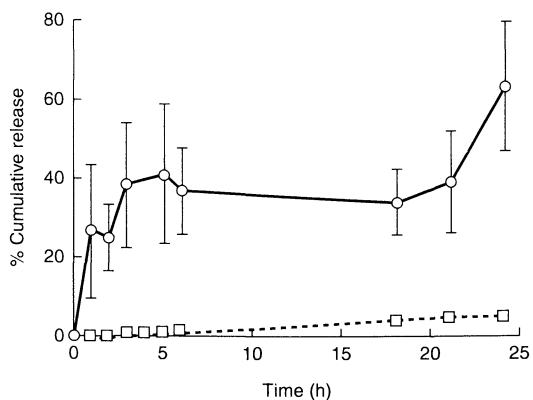


Figure 1.20. Cumulative release of indomethacin from a calcium pectate gel in citrate buffer in the presence (circles) and absence (squares) of pectinolytic enzyme (data from ref. (263))

7.3 Surface coatings

Biodegradable surface coatings of drug carriers could be expected to be of interest in a number of pharmaceutical applications, but particularly so in relation to parenteral drug delivery of colloidal drug carriers. As discussed above in relation to liposomes, sterically stabilized, and particularly PEO-modified colloidal drug carriers, are quite interesting due to prolonged bloodstream circulation times, a comparably even tissue distribution, reduced toxicity effects, etc. Even with PEO-modified particles or surface coatings, however, the bloodstream circulation time is generally of the order of a couple of days at most, and hence a PEO-based surface coating needs to be stable over that particular time only. After this, the fairly good chemical stability of PEO has no advantage, and indeed it may even be detrimental to the degradation and excretion of this substance.

As discussed above, the origin of the advantageous effects of PEO-containing coatings of colloidal drug carriers in intravenous drug delivery is the low serum protein adsorption caused by the PEO chains. On biodegradation, on the other hand, the PEO chains are released and the serum proteins can adsorb once more. For example, Muller *et al.* have previously investigated the adsorption of a number of PEO-poly lactide copolymers at hydrophobic methylated silica surfaces, as well as the adsorption of fibrinogen, a well-known opsonin (8) at such surface coatings, e.g. before and after degradation of the poly lactide anchoring block (264). It was found that when the poly lactide moiety is intact, the polymer is strongly anchored at the hydrophobic surface, and prevents the protein from adsorbing. On degradation of the poly lactide block, however, the polymer does not adsorb

as extensively and strongly at the surface, and hence it is no longer capable of reducing the protein adsorption.

Analogous to this, Kirpotin *et al.* investigated the properties of liposomes with detachable polymer coatings through incorporation of a disulfide-linked PEO–phospholipid conjugate (distearoyl phosphatidylethanolamine–dithiopropionyl (DTP)–PEO₂₀₀₀) in dioleoyl phosphatidylethanolamine (DOPE) liposomes (265). It was found that the liposomes in the absence of such a conjugated lipid, but in the presence of not readily degradable DOPE/mPEO–distearoyl phosphatidylethanolamine, displayed a long circulation time in the bloodstream, stability to flocculation, and a slow release of an entrapped fluorescence marker. On the other hand, the stability of the liposomes decreased drastically on degradation of the carbamate links. Moreover, modifying pH-sensitive DOPE/cholesterol hemisuccinate liposomes with mPEO–DTP–distearoyl phosphatidyl ethanolamine (DSPE) resulted in a decrease in the pH-sensitivity. After cleavage, on the other hand, the pH-sensitivity was restored. Such degradable surface coatings therefore seem feasible.

8 ACKNOWLEDGEMENTS

This work was financed by the Institute for Research and Competence Holding AB, Sweden.

9 REFERENCES

- Richardson, N. E. and Meakin, B. J., The sorption of benzocaine from aqueous solution by nylon 6 powder, *J. Pharm. Pharmacol.*, **26**, 166–174 (1974).
- Seeman, P. M. and Baily, H. S., The surface activity of tranquilizers, *Biochem. Pharmacol.*, **12**, 1181–1191 (1963).
- (a) Abe, I., Kamaya, H. and Ueda, I., Activated carbon as a biological model: comparison between activated carbon adsorption and oil–water partition for drug activity correlation, *J. Pharm. Sci.*, **77**, 166–168 (1988). (b) Matsuki, H., Hashimoto, S., Kaneshina, S. and Yamanaka, M., Surface adsorption and volume behavior of local anesthetics, *Langmuir*, **10**, 1882–1887 (1994). (c) Matsuki, H., Hashimoto, S., Kaneshina, S. and Yamanaka, M., Incorporation of micelle-forming local anesthetics into surface-adsorbed films and micelles of decylammonium chloride, *Langmuir*, **13**, 2687–2693 (1997). (d) Okahata, Y. and Ebato, H., Adsorption behaviour of local anaesthetics in synthetic lipid membranes coated on a quartz-crystal microbalance and correlations with their anaesthetic potencies, *J. Chem. Soc. Perkin Trans.* **2**, 475–480 (1991).

- Malmsten, M. and Veide, A., Effects of amino acid composition on protein adsorption, *J. Colloid Interface Sci.*, **178**, 160–167 (1996).
- Malmsten, M., Burns, N. and Veide, A., Electrostatic and hydrophobic effects of oligopeptide insertions on protein adsorption, *J. Colloid Interface Sci.*, **204**, 104–111 (1998).
- Arnebrant, T. and Ericsson, B., Adsorption of arginine vasopressin and desamino-8-D-arginine vasopressin on to silica and methylated silica surfaces, and at the air/water interface, *J. Colloid Interface Sci.*, **150**, 428–435 (1992).
- Norde, W., Adsorption of proteins from solution at the solid–liquid interface, *Adv. Colloid Interface Sci.*, **25**, 267–340 (1986).
- Malmsten, M. (Ed.), *Biopolymers at Interfaces*, Surface Science Series, vol. 75, Marcel Dekker, New York, 1998.
- Arnebrant, T. and Nylander, T., Adsorption of insulin on metal surfaces in relation to association behaviour, *J. Colloid Interface Sci.*, **122**, 557–566 (1988).
- Nilsson, P., Nylander, T. and Havelund, S., Adsorption of insulin on solid surfaces in relation to the surface properties of the monomeric and oligomeric forms, *J. Colloid Interface Sci.*, **144**, 145–152 (1991).
- Delgado, C., Francis, G. E. and Fisher, D., The uses and properties of PEG-linked proteins, *Crit. Rev. Ther. Drug Carrier Syst.*, **9**, 249–304 (1992).
- Zalipsky, S., Chemistry of polyethylene glycol conjugates with biologically active molecules, *Adv. Drug Delivery Rev.*, **16**, 157–182 (1995).
- Harris, J. M. (Ed.), *Poly(ethylene glycol) Chemistry – Biotechnical and Biomedical Applications*, Plenum Press, New York, 1992.
- Harris, J. M. and Zalipsky, S. (Eds), *Poly(ethylene glycol) Chemistry and Biological Applications*, ACS Symposium Series 680, American Chemical Society, Washington, DC, 1997.
- Jeon, S. I., Lee, J. H., Andrade, J. D. and de Gennes, P. G., Protein–surface interactions in the presence of polyethylene oxide. I. Simplified theory, *J. Colloid Interface Sci.*, **142**, 149–158 (1991).
- Jeon, S. I. and Andrade, J. D., Protein–surface interactions in the presence of polyethylene oxide. II. Effect of protein size, *J. Colloid Interface Sci.*, **142**, 159–166 (1991).
- Israelachvili, J. N., *Intermolecular and Surface Forces*, Academic Press, London, 1992.
- Schick, M. J., *Nonionic Surfactants – Physical Chemistry*, Surface Science Series, Vol. 23, Marcel Dekker, New York, 1987.
- Lindman, B. and Wennerström, H., *Micelles – Amphiphile Aggregation in Aqueous Solution*, Topics in Current Chemistry, Vol. 87, Springer, Berlin, 1980.
- Evans, D. F., and Wennerström, H., *The Colloidal Domain – Where Physics, Chemistry, Biology and Technology Meet*, VCH, New York, 1994.
- Engström, S. and Engström, L., Phase behaviour of the lidocaine–monoolein–water system, *Int. J. Pharm.*, **79**, 113–122 (1992).

22. Lawrence, M. J., Surfactant systems: microemulsions and vesicles as vehicles for drug delivery, *Eur. J. Drug Metab. Pharmacokinet.*, **3**, 257–269 (1994).
23. Carlfors, J., Blute, I. and Schmidt, V., Lidocaine in microemulsion – a dermal delivery system, *J. Dispersion Sci. Technol.*, **12**, 467–482 (1991).
24. von Corswant, C. and Thorén, P. E. G., Solubilization of sparingly soluble active compounds in lecithin-based microemulsions: influence on phase behavior and microstructure, *Langmuir*, **15**, 3710–3717 (1999).
25. Alexandridis, P. and Hatton, T. A., Poly(ethylene oxide)–poly(propylene oxide)–poly(ethylene oxide) block copolymer surfactants in aqueous solutions and at interfaces: thermodynamics, structure, dynamics, and modeling, *Colloids Surf. A*, **96**, 1–46 (1995).
26. Malmsten, M. and Lindman, B., Self-assembly in aqueous block copolymer solutions, *Macromolecules*, **25**, 5440–5445 (1992).
27. Scherlund, M., Malmsten, M. and Brodin, A., Stabilization of a thermosetting emulsion system using ionic and nonionic surfactants, *Int. J. Pharm.*, **173**, 103–116 (1998).
28. Scherlund, M., Malmsten, M., Holmqvist, P. and Brodin, A., Thermosetting microemulsions as drug delivery systems for periodontal anaesthesia, *Int. J. Pharm.*, **194**, 103–116 (2000).
29. Seddon, J. M., Structure of the inverted hexagonal (H_{II}) phase, and non-lamellar phase transitions of lipids, *Biochim. Biophys. Acta*, **1031**, 1–69 (1990).
30. Lee, V. H. L., Peptide and protein drug delivery: opportunities and challenges, *Pharm. Int.*, **8**, 208–212 (1986).
31. Lee, V. H. L., Enzymatic barriers to peptide and protein absorption, *Crit. Rev. Ther. Drug Carrier Syst.*, **5**, 69–97 (1988).
32. Sarciaux, J. M., Acar, L. and Sado, P. A., Using microemulsion formulations for oral drug delivery of therapeutic peptides, *Int. J. Pharm.*, **120**, 127–136 (1995).
33. Kovarik, J. M., Mueller, E. A., van Bree, J. B., Tetzloff, W. and Kutz, K., Reduced inter- and intraindividual variability in cyclosporine pharmacokinetics from a microemulsion formulation, *J. Pharm. Sci.*, **83**, 444–446 (1994).
34. Kovarik, J. M., Mueller, E. A., van Bree, J. B., Flückiger, S. S., Lange, H., Schmidt, B., Boesken, W. H., Lison, A. E. and Kutz, K., Cyclosporine pharmacokinetics and variability from a microemulsion formulation – a multicenter investigation in kidney transplant patients, *Transplantation*, **58**, 658–663 (1994).
35. Tarr, B. D. and Yalkowsky, S. H., Enhanced intestinal absorption of cyclosporine in rats through the reduction of emulsion droplet size, *Pharm. Res.*, **6**, 40–43 (1989).
36. Mueller, E. A., Kovarik, J. M., van Bree, J. B., Tetzloff, W., Grevel, J. and Kutz, K., Improved dose linearity in cyclosporine pharmacokinetics from a microemulsion formulation, *Pharm. Res.*, **11**, 301–304 (1994).
37. Drewe, J., Meier, R., Vonderscher, J., Kiss, D., Posanski, U., Kissel, T. and Gyr, K., Enhancement of the oral absorption of cyclosporin in man, *Br. J. Clin. Pharmacol.*, **34**, 60–64 (1992).
38. Davis, S. S., Hadgraft, J. and Palin, K. J., Medical and pharmaceutical applications of emulsions, in *Encyclopedia of Emulsion Technology – Applications*, vol. 2, Becher, P. (Ed.), Marcel Dekker, New York, 1983, pp. 159–238.
39. Boyett, J. B. and Davis, C. W., Injectable emulsions and suspensions, in *Pharmaceutical Dosage Forms: Disperse Systems*, Vol. 2, Lieberman, H. A., Rieger, M. M. and Banker, G. S. (Eds), Marcel Dekker, New York, 1989, pp. 379–416.
40. Johnston, I. D. A. (Ed.), *Current Perspectives in the Use of Lipid Emulsions*, Marcel Dekker, New York, 1983.
41. Becher, P. (Ed.), *Encyclopedia of Emulsion Technology – Applications*, vol. 2, Marcel Dekker, New York, 1983.
42. Zuck, T. F. and Riess, J. G., Current status of injectable oxygen carriers, *Crit. Rev. Clin. Lab. Sci.*, **31**, 295–324 (1994).
43. Schneider, P., Artificial blood substitutes, *Transfus. Sci.*, **13**, 357–370 (1992).
44. Gregoriadis, G. (Ed.), *Liposome Technology*, vol. 3, CRC Press, Boca Raton, FL, 1984.
45. Uchegbu, I. F. and Vyas, S. P., Non-ionic surfactant based vesicles (niosomes) in drug delivery, *Int. J. Pharm.*, **172**, 33–70 (1998).
46. Gulati, M., Grover, M., Singh, S. and Singh, M., Lipophilic drug derivatives in liposomes, *Int. J. Pharm.*, **165**, 129–168 (1998).
47. Senior, J. H., Fate and behavior of liposomes *in vivo*: a review of controlling factors, *Crit. Rev. Ther. Drug Carrier Syst.*, **3**, 123–193 (1987).
48. Lasic, D. D. and Tempelton, N. S., Liposomes in gene therapy, *Adv. Drug Delivery Rev.*, **20**, 221–266 (1996).
49. Lasic, D. and Martin, F. (Eds), *Stealth Liposomes*, CRC Press, Boca Raton, FL, 1995.
50. Gregoriadis, G., Engineering liposomes for drug delivery: progress and problems, *TIBTECH*, **13**, 527–537 (1995).
51. Patel, H. M., Serum opsonins and liposomes: their interaction and opsonophagocytosis, *Crit. Rev. Ther. Drug Carrier Syst.*, **9**, 39–90 (1992).
52. Tabata, Y. and Ikada, Y., Phagocytosis of polymer microspheres by macrophages, *Adv. Polym. Sci.*, **94**, 107–141 (1990).
53. Eldem, T. and Speiser, P., Endocytosis and intracellular drug delivery, *Acta Pharm. Technol.*, **35**, 109–115 (1989).
54. Semple, S. C. and Chonn, A., Liposome–blood protein interaction in relation to liposome clearance, *J. Liposome Res.*, **6**, 33–60 (1996).
55. Chonn, A., Semple, S. C. and Cullis, P. R., *J. Biol. Chem.*, **267**, 18759–18765 (1992).
56. Szebeni, J., The interaction of liposomes with the complement system, *Crit. Rev. Ther. Drug Carrier Syst.*, **15**, 57–88 (1998).
57. Papahadjopoulos, D., Allen, T. M., Gabizon, A., Mayhew, E., Matthey, K., Huang, S. K., Lee, K.-D., Woodle, M. C., Lasic, D. D., Redemann, C. and Martin, F. J.,

- Sterically stabilized liposomes: improvements in pharmacokinetics and antitumor therapeutic efficacy, *Proc. Natl. Acad. Sci. USA*, **88**, 11460–11464 (1991).
58. Gabizon, A. and Papahadjopoulos, D., Liposome formulations with prolonged circulation time in blood and enhanced uptake by tumors, *Proc. Natl. Acad. Sci. USA*, **85**, 6949–6953 (1988).
 59. Allen, T. M., The use of glycolipids and hydrophilic polymers in avoiding rapid uptake of liposomes by the mononuclear phagocyte system, *Adv. Drug Delivery Rev.*, **13**, 285–309 (1994).
 60. Allen, T. M., Hansen, C., Martin, F., Redemann, C. and Yau-Young, A., Liposomes containing synthetic lipid derivatives of poly(ethylene glycol) show prolonged circulation half-lives *in vivo*, *Biochim. Biophys. Acta*, **1066**, 29–36 (1991).
 61. Klibanov, A. L., Maruyama, K., Torchilin, V. P. and Huang, L., Amphiphatic polyethyleneglycols effectively prolong the circulation time of liposomes, *FEBS Lett.*, **268**, 235–237 (1990).
 62. Mori, A., Klibanov, A. L., Torchilin, V. P. and Huang, L., Influence of the steric barrier activity of amphiphatic poly(ethylene glycol) and ganglioside GM1 on the circulation time of liposomes and on the target binding of immunoliposomes *in vivo*, *FEBS Lett.*, **284**, 263–266 (1991).
 63. Blume, G. and Cevc, G., Liposomes for the sustained drug release *in vivo*, *Biochim. Biophys. Acta*, **1029**, 91–97 (1990).
 64. Gabizon, A., Price, D. C., Huberty, J., Bresalier, R. S. and Papahadjopoulos, D., Effect of liposome composition and other factors on the targeting of liposomes to experimental tumors: biodistribution and imaging studies, *Cancer Res.*, **50**, 6371–6378 (1990).
 65. Uster, P. S., Working, P. K. and Vaage, J., Pegylated liposomal doxorubicin (DOXIL[®], CAELYX[®]) distribution in tumour models observed with confocal laser scanning microscopy, *Int. J. Pharm.*, **162**, 77–86 (1998).
 66. Vaage, J., Mayhew, E., Lasic, D. and Martin, F., Therapy of primary and metastatic mouse mammary carcinomas with doxorubicin encapsulated in long circulating liposomes, *Int. J. Cancer*, **51**, 942–948 (1992).
 67. Mayhew, E. G., Lasic, D., Babbar, S. and Martin, F. J., Pharmacokinetics and antitumor activity of epirubicin encapsulated in long-circulating liposomes incorporating a polyethylene glycol-derivatized phospholipid, *Int. J. Cancer*, **51**, 302–309 (1992).
 68. Huang, S. K., Stauffer, P. R., Hong, K., Guo, J. W. H., Phillips, T. L., Huang, A. and Papahadjopoulos, D., Liposomes and hyperthermia in mice: increased tumor uptake and therapeutic efficacy of doxorubicin in sterically stabilized liposomes, *Cancer Res.*, **54**, 2186–2191 (1994).
 69. Yuan, F., Leunig, M., Huang, S. K., Berk, D. A., Papahadjopoulos, D. and Jain, R. K., Microvascular permeability and interstitial penetration of sterically stabilized (stealth) liposomes in a human tumor xenograft, *Cancer Res.*, **54**, 3352–3356 (1994).
 70. Williams, S. S., Alosco, T. R., Mayhew, E., Lasic, D. D., Martin, F. J. and Bankert, R. B., Arrest of human lung tumor xenograft growth in severe combined immunodeficient mice using doxorubicin encapsulated in sterically stabilized liposomes, *Cancer Res.*, **53**, 3964–3967 (1993).
 71. Allen T. M., Mehra, T., Hansen, C. and Chin, Y. C., Stealth liposomes: an improved sustained released system for 1- β -D-arabinofuranosylcytosine, *Cancer Res.*, **52**, 2431–2439 (1992).
 72. Huang, S. K., Mayhew, E., Gilani, S., Lasic, D. D., Martin, F. J. and Papahadjopoulos, D., Pharmacokinetics and therapeutics of sterically stabilized liposomes in mice bearing C-26 colon carcinoma, *Cancer Res.*, **52**, 6774–6781 (1992).
 73. Vaage, J., Donovan, D., Mayhew, E., Uster, P. and Woddle, M., Therapy of mouse mammary carcinomas with vincristine and doxorubicin encapsulated in sterically stabilized liposomes, *Int. J. Cancer*, **54**, 959–964 (1993).
 74. Khaw, B. A., Narula, J., Vural, I. and Torchilin, V. P., Cytoskeleton-specific immunoliposomes: sealing of hypoxic cells and intracellular delivery of DNA, *Int. J. Pharm.*, **162**, 71–76 (1998).
 75. Khaw, B.-A., Torchilin, V. P., Vural, I. and Narula, J., Plug and seal: prevention of hypoxic cardiocyte death by sealing membrane lesions with antimyosin-liposomes, *Nature Med.*, **1**, 1195–1198 (1995).
 76. Holmberg, E., Maruyama, K., Kennel, S., Klibanov, A., Torchilin, V., Ryan, U. and Huang, L., Target-specific binding of immunoliposomes *in vivo*, *J. Liposome Res.*, **1**, 393–406 (1990).
 77. Maruyama, K., Kennel, S. J. and Huang, L., Lipid composition is important for highly efficient target binding and retention of immunoliposomes, *Proc. Natl. Acad. Sci. USA*, **87**, 5744–5748 (1990).
 78. Ahmad, I., Longenecker, M., Samuel, J. and Allen, T. M., Antibody-targeted delivery of doxorubicin entrapped in sterically stabilized liposomes can eradicate lung cancer in mice, *Cancer Res.*, **53**, 1484–1488 (1993).
 79. Gregoriadis, G. and Neerunjun, E. D., Homing of liposomes to target cells, *Biochem. Biophys. Res. Commun.*, **65**, 537–544 (1975).
 80. Torchilin, V. P., Targeting of drugs and drug carriers within the cardiovascular system, *Adv. Drug Delivery Rev.*, **17**, 75–101 (1995).
 81. Toonen, P. A. H. M. and Crommelin, D. J. A., Immunoglobulins as targeting agents for liposome encapsulated drugs, *Pharmaceut. Weekbl. Sci. Edn*, **5**, 269–280 (1983).
 82. Müller, R. H., *Colloidal Carriers for Controlled Drug Delivery and Targeting*, CRC Press, Boca Raton, FL, 1991.
 83. Kabanov, A. V., Chekhonin, V. P., Alakhov, V. Y., Batrakova, E. V., Lebedev, A. S., Melik-Nubarov, N. S., Arzhakov, S. A., Levashov, A. V., Morozov, G. V., Severin, E. S. and Kabanov, V. A., The neuroleptic activity of haloperidol increases after its solubilization in surfactant micelles, *FEBS Lett.*, **258**, 343–345 (1989).
 84. Kabanov, A. V., Batrakova, E. V., Melik-Nubarov, N. S., Fedoseev, N. A., Dorodnich, T. Y., Alakhov, V. Y.,

- Chekhonin, V. P., Nazarova, I. R., and Kabanov, V. A., A new class of drug carriers: micelles of poly(oxyethylene)-poly(oxypropylene) block copolymers as microcontainers for drug targeting from blood to brain, *J. Controlled Release*, **22**, 141–158 (1992).
85. Savva, M., Duda, E. and Huang, L., A genetically modified recombinant tumour necrosis factor- α conjugated to the distal terminals of liposomal surface grafted polyethyleneglycol chains, *Int. J. Pharm.*, **184**, 45–51 (1999).
86. Cevc, G., Transfersomes, liposomes and other lipid suspensions on the skin: permeation enhancement, vesicle penetration, and transdermal drug delivery, *Crit. Rev. Ther. Drug Carrier Syst.*, **13**, 257–388 (1996).
87. Schaller, M. and Korting, H. C., Interaction of liposomes with human skin: the role of the stratum corneum, *Adv. Drug Delivery Rev.*, **18**, 303–309 (1996).
88. Schmid, M.-H. and Korting, H. C., Therapeutic progress with topical liposome drugs for skin disease, *Adv. Drug Delivery Rev.*, **18**, 335–342 (1996).
89. Hadgraft, J., Passive enhancement strategies in topical and transdermal drug delivery, *Int. J. Pharm.*, **184**, 1–6 (1999).
90. Gesztes, A. and Mezei, M., Topical anaesthesia of the skin by liposome-encapsulated tetracaine, *Anesth. Analg.*, **67**, 1079–1081 (1988).
91. Schäfer-Korting, M., Korting, H. C. and Ponce-Pöschl, E., Liposomal tretinoin for uncomplicated *acne vulgaris*, *Clin. Invest.*, **72**, 1086–1091 (1994).
92. Lee, R. J. and Huang, L., Lipidic vector systems for gene transfer, *Crit. Rev. Ther. Drug Carrier Syst.*, **14**, 173–206 (1997).
93. Rolland, A. P., From genes to gene medicines: recent advances in nonviral gene delivery, *Crit. Rev. Ther. Drug Carrier Syst.*, **15**, 143–198 (1998).
94. Kato, Y. and Sugiyama, Y., Targeted delivery of peptides, proteins, and genes by receptor-mediated endocytosis, *Crit. Rev. Ther. Drug Carrier Syst.*, **14**, 287–331 (1997).
95. Gershon, H., Ghirlando, R., Guttman, S. B. and Minsky, A., Mode of formation and structural features of DNA-cationic liposome complexes used for transfection, *Biochemistry*, **32**, 7143–7151 (1993).
96. Felgner, J. H., Kumar, R., Sridhar, C. N., Wheeler, C. J., Tsai, Y. J., Border, R., Ramsey, P., Martin, M. and Felgner, P. L., Enhanced gene delivery and mechanism studies with a novel series of cationic lipid formulations, *J. Biol. Chem.*, **269**, 2550–2561 (1994).
97. Sternberg, B., Sorgi, F. L. and Huang, L., New structures in complex formation between DNA and cationic liposomes visualized by freeze-fracture electron microscopy, *FEBS Lett.*, **356**, 361–366 (1994).
98. Garnett, M. C., Gene-delivery systems using cationic polymers, *Crit. Rev. Ther. Drug Carrier Syst.*, **16**, 147–207 (1999).
99. Engström, S., Drug delivery from cubic and other lipid-water phases, *Lipid Technol.*, **2**, 42–45 (1990).
100. Larsson, K., Cubosomes and hexosomes for drug delivery, *Int. Symp. Control. Rel. Bioact. Mater.*, **24**, 198–199 (1997).
101. Schröder, U., Björk, E. and Artursson, P., Cubic and L2 lipid suspensions as parental and mucosal immunological adjuvants, *Int. Symp. Control. Rel. Bioact. Mater.*, **24**, 573–574 (1997).
102. Gustafsson, J., Ljusberg-Wahren, H., Almgren, M. and Larsson, K., Submicron particles of reversed lipid phases in water stabilized by a nonionic amphiphilic polymer, *Langmuir*, **13**, 6964–6971 (1997).
103. Neto, C., Aloisi, G. and Baglioni, P., Imaging soft matter with the atomic force microscope: cubosomes and hexosomes, *J. Phys. Chem. B*, **103**, 3896–3899 (1999).
104. Bargoni, A., Cavalli, R., Caputo, O., Fundaro, A., Gasco, M. R. and Zara, G. P., Solid lipid nanoparticles in lymph and plasma after duodenal administration to rats, *Pharm. Res.*, **15**, 745–750 (1998).
105. Boltri, L., Canal, T., Esposito, P. and Carli, F., Relevant factors affecting the formation and growth of lipid nanosphere suspension, *Eur. J. Pharm. Biopharm.*, **41**, 70–75 (1995).
106. Olbrich, C. and Müller, R. H., Enzymatic degradation of SLN-effect of surfactant and surfactant mixtures, *Int. J. Pharm.*, **180**, 31–39 (1999).
107. Freitas, C. and Müller, R. H., Effect of light and temperature on zeta potential and physical stability in solid lipid nanoparticle (SLNTM) dispersions, *Int. J. Pharm.*, **168**, 221–229 (1998).
108. Müller, R. H., Mehnert, W., Lucks, J.-S., Schwarz, C., zur Mühlen, A., Weyhers, H., Freitas, C. and Rühl, D., Solid lipid nanoparticles (SLN) – an alternative colloidal carrier systems for controlled drug delivery, *Eur. J. Pharm. Biopharm.*, **41**, 62–69 (1995).
109. Siekmann, B. and Westesen, K., Thermoanalysis of the recrystallization process of melt-homogenized glyceride nanoparticles, *Colloids Surf. B*, **3**, 159–175 (1994).
110. Siekmann, B. and Westesen, K., Submicron-sized parenteral carrier systems based on solid lipids, *Pharm. Pharmacol. Lett.*, **1**, 123–126 (1992).
111. Sjöström, B., Kaplun, A., Talmon, Y. and Cabane, B., Structures of nanoparticles prepared from oil-in-water emulsions, *Pharm. Res.*, **12**, 39–48 (1995).
112. Sjöström, B., Kronberg, B. and Carlfors, J., A method for the preparation of submicron particles of sparingly water-soluble drugs by precipitation in oil-in-water emulsions. I. Influence of emulsification and surfactant concentration, *J. Pharm. Sci.*, **82**, 579–583 (1993).
113. Sjöström, B., Bergenstahl, B. and Kronberg, B., A method for the preparation of submicron particles of sparingly water-soluble drugs by precipitation in oil-in-water emulsions. II. Influence of the emulsifier, the solvent and the drug substance, *J. Pharm. Sci.*, **82**, 584–585 (1993).
114. Sjöström, B., Westesen, K. and Bergenstahl, B., Preparation of submicron drug particles in lecithin-stabilized o/w emulsions. II. Characterization of cholesterol acetate particles, *Int. J. Pharm.*, **94**, 89–101 (1993).

115. Sjöström, B. and Bergenståhl, B., Preparation of submicron drug particles in lecithin-stabilized o/w emulsions. I. Model studies of the precipitation of cholesteryl acetate., *Int. J. Pharm.*, **84**, 107–116 (1992).
116. Lavelle, E. C., Sharif, S., Thomas, N. W., Holland, J. and Davis, S. S., The importance of gastrointestinal uptake of particles in the design of oral delivery systems, *Adv. Drug Delivery Rev.*, **18**, 5–22 (1995).
117. Florence, A. T., Hillery, A. M., Hussain, N. and Jani, P. U., Factors affecting the oral uptake and translocation of polystyrene nanoparticles: histological and analytical evidence, *J. Drug Targeting*, **3**, 65–70 (1995).
118. Tabata, Y., Inoue, Y. and Ikada, Y., Size effect on systemic and mucosal immune responses induced by oral administration of biodegradable microsphere, *Vaccine*, **14**, 1677–1685 (1996).
119. Desai, M. P., Labhassetwar, V., Amidon, G. L. and Levy, R. J., Gastrointestinal uptake of biodegradable microparticles: effect of particle size, *Pharm. Res.*, **13**, 1838–1845 (1996).
120. Amselem, S., Domb, A. J. and Alving, C. R., Liposomes as a vaccine carrier system: effects of size, charge, and phospholipid composition, *Vaccine Res.*, **1**, 383–395 (1992).
121. Porter, C. J. H., Drug delivery to the lymphatic system, *Crit. Rev. Ther. Drug Carrier Syst.*, **14**, 333–393 (1997).
122. Ebel, J. P., A method for quantifying particle absorption from the small intestine of the mouse, *Pharm. Res.*, **7**, 848–851 (1990).
123. Jepson, M. A., Simmons, N. L., O'Hagan, D. T. and Hirst, B. H., Comparison of poly(DL-lactide-co-glycolide) and polystyrene microsphere targeting to intestinal M cells, *J. Drug Targeting*, **1**, 245–249 (1993).
124. Russell-Jones, G. J., The potential use of receptor-mediated endocytosis for oral drug delivery, *Adv. Drug Delivery Rev.*, **20**, 83–97 (1996).
125. Lehr, C.-M., Bouwstra, J. A., Kok, W., Noach, A. B. J., de Boer, A. G. and Junginger, H. E., Bioadhesion by means of specific binding of tomato lectin, *Pharm. Res.*, **9**, 547–553 (1992).
126. Rubas, W., Banerjee, A. C., Gallati, H., Speiser, P. P. and Joklik, W. K., Incorporation of the retrovirus M cell attachment protein into small unilamellar vesicles: incorporation efficiency and binding capability to L929 cells *in vitro*, *J. Microencapsulation*, **7**, 385–395 (1990).
127. Pappo, J., Ermak, T. H. and Steger, H. J., Monoclonal antibody-directed targeting of fluorescent polystyrene microspheres to Peyer's patch M cells, *Immunology*, **73**, 277–280 (1991).
128. Dondeti, P., Zia, H. and Needham, T. E., Bioadhesive and formulation parameters affecting nasal absorption, *Int. J. Pharm.*, **127**, 115–133 (1996).
129. Lowell, G. H., Kaminski, R. W., VanCott, T. C., Slike, B., Kersey, K., Zawoznik, E., Loomis-Price, L., Smith, G., Redfield, R. R., Anselem, S. and Birx, D. L., Proteosomes, emulsomes, and cholera toxin B improve nasal immunogenicity of human immunodeficiency virus gp160 in mice: induction of serum, intestinal, vaginal and lung IgA and IgG, *J. Infect. Dis.*, **175**, 292–301 (1997).
130. Naisbett, B. and Woodley, J., The potential use of tomato lectin for oral drug delivery: 1. Lectin binding to rat small intestine *in vitro*, *Int. J. Pharm.*, **107**, 223–230 (1994).
131. Naisbett, B. and Woodley, J., The potential use of tomato lectin for oral drug delivery: 2. Mechanism of uptake *in vitro*, *Int. J. Pharm.*, **110**, 127–136 (1994).
132. Luessen, H. L., de Leeuw, B. J., Langemeyer, M. W. E., de Boer, A. B. G., Verhoef, J. C. and Junginger, H. E., Mucoadhesive polymers in peroral peptide drug delivery. VI. Carbomer and chitosan improve the intestinal absorption of the peptide drug busserelin *in vivo*, *Pharm. Res.*, **13**, 1668–1672 (1996).
133. Soane, R. J., Frier, M., Perkins, A. C., Jones, N. S., Davis, S. S. and Illum, L., Evaluation of the clearance characteristics of bioadhesive systems in humans, *Int. J. Pharm.*, **178**, 55–65 (1999).
134. Felt, O., Furrer, P., Mayer, J. M., Plazonnet, B., Buri, P. and Gurny, R., Topical use of chitosan in ophthalmology: tolerance assessment and evaluation of precorneal retention, *Int. J. Pharm.*, **180**, 185–193 (1999).
135. Gåserød, O., Jolliffe, I. G., Hampson, F. C., Dettmar, P. W. and Skjåk-Bræk, G., The enhancement of the bioadhesive properties of calcium alginate gel beads by coating with chitosan, *Int. J. Pharm.*, **175**, 237–246 (1998).
136. Rydén, L. and Edman, P., Effect of polymers and microspheres on the nasal absorption of insulin in rats, *Int. J. Pharm.*, **83**, 1–10 (1992).
137. Carlsson, A., Karlström, G. and Lindman, B., Thermal gelation of nonionic cellulose ethers and ionic surfactants in water, *Colloids Surf.*, **47**, 147–165 (1990).
138. Nyström, B., Thuresson, K. and Lindman, B., Rheological and dynamic light scattering studies on aqueous solutions of a hydrophobically modified cellulose ether and its unmodified analogue, *Langmuir*, **11**, 1994–2002 (1995).
139. Scherlund, M., Malmsten, M. and Brodin, A., Nonionic cellulose ethers as potential drug delivery systems for periodontal anaesthesia, *J. Colloid Interface Sci.*, **229**, 365–374 (2000).
140. Johnson, K. A., Preparation of peptide and protein powders for inhalation, *Adv. Drug Delivery Rev.*, **26**, 3–15 (1997).
141. Yu, J. and Chien, Y. W., Pulmonary drug delivery: physiologic and mechanistic aspects, *Crit. Rev. Ther. Drug Carrier Syst.*, **14**, 395–453 (1997).
142. Morita, T., Yamamoto, A., Hashida, M. and Sezaki, H., Effect of various promoters on pulmonary absorption of drugs with different molecular weights, *Biol. Pharm. Bull.*, **16**, 259–262 (1993).
143. Okumura, K., Iwakawa, S., Yoshida, T., Seki, T. and Komada, F., Intratracheal delivery of insulin. Absorption from solution and aerosol by rat lung, *Int. J. Pharm.*, **88**, 63–73 (1992).
144. Nagarajan, R., Barry, M. and Ruckenstein, E., Unusual selectivity in solubilization by block copolymer micelles, *Langmuir*, **2**, 210–215 (1986).

145. Hurter, P. N. and Hatton, T. A., Solubilization of polycyclic aromatic hydrocarbons by poly(ethylene oxide-propylene oxide) block copolymers micelles: effects of polymer structure, *Langmuir*, **8**, 1291–1299 (1992).
146. Gabelle, F., Koros, W. J. and Schechter, R. S., Solubilization of aromatic solutes in block copolymers, *Macromolecules*, **28**, 4883–4892 (1995).
147. La, S. B., Okano, T. and Kataoka, K., Preparation and characterization of micelle-forming polymeric drug indomethacin-incorporated poly(ethylene oxide)-poly(β -benzyl L-aspartate) block copolymer micelles, *J. Pharm. Sci.*, **85**, 85–90 (1996).
148. Lin, S.-Y. and Kawashima, Y., Kinetic studies on the stability of indomethacin in alkaline aqueous solution containing poly(oxyethylene)poly(oxypropylene) surface-active block copolymers, *Pharm. Acta Helv.*, **60**, 345–350 (1985).
149. Kwon, G. S., Diblock copolymer nanoparticles for drug delivery, *Crit. Rev. Ther. Drug Carrier Syst.*, **15**, 481–512 (1998).
150. Kwon, G. S. and Kataoka, K., Block copolymer micelles as long-circulating drug vehicles, *Adv. Drug Delivery Rev.*, **16**, 295–309 (1995).
151. Yokoyama, M., Block copolymers as drug carriers, *Crit. Rev. Ther. Drug Carrier Syst.*, **9**, 213–248 (1992).
152. Kataoka, K., Design of nanoscopic vehicles for drug targeting based on micellization of amphiphilic block copolymers, *Pure Appl. Chem.*, **11**, 1759–1769 (1994).
153. Alexandridis, P. and Lindman, B. (Eds), *Block Copolymers – Fundamentals and Applications*, Elsevier, Amsterdam, 2000.
154. Thompson, D. O., Cyclodextrins-enabling excipients: their present and future use in pharmaceuticals, *Crit. Rev. Ther. Drug Carrier Syst.*, **14**, 1–104 (1997).
155. Albers, E. and Müller, B. W., Cyclodextrin derivatives in pharmaceuticals, *Crit. Rev. Ther. Drug Carrier Syst.*, **12**, 311–337 (1995).
156. Uekama, K. and Otagiri, M., Cyclodextrins in drug carrier systems, *Crit. Rev. Ther. Drug Carrier Syst.*, **3**, 1–40 (1987).
157. Otero-Espinar, F. J., Anguiano-Igea, S., Garcia-Gonzalez, N., Vila-Jato, J. L. and Blanco-Mendez, J., Interaction of naproxen with β -cyclodextrin in solution and in the solid state, *Int. J. Pharm.*, **79**, 149–157 (1992).
158. Van der Houwen, O. A. G. J., Bekers, O., Bult, A., Beijnen, J. H. and Underberg, W. J. M., Computation of mitomycin C/ β -cyclodextrin complex stability constant, *Int. J. Pharm.*, **89**, R5–R7 (1993).
159. Uekama, K., Fujinaga, T., Hirayama, F., Otagiri, M., Yamasaki, M., Seo, H., Hashimoto, T. and Tsuruoka, M., Improvement of the oral bioavailability of digitalis glycosides by cyclodextrin complexation, *J. Pharm. Sci.*, **72**, 1338–1341 (1983).
160. Uekama, K., Irie, T., Sunada, M., Otagiri, M. and Tsubaki, K., Protective effects of cyclodextrins on drug-induced hemolysis *in vitro*, *J. Pharm. Dyn.*, **4**, 142–144 (1981).
161. Kaji, Y., Uekama, K., Yoshikawa, H., Takada, K. and Muranishi, S., Selective transfer of 1-hexylcarbamoyle-5-fluorouracil into lymphatics by combination of β -cyclodextrin polymer complexation and absorption promoter in the rat, *Int. J. Pharm.*, **24**, 79–89 (1985).
162. Kumar, P. and Mittal, K. L., *Handbook of Microemulsion Science and Technology*, Marcel Dekker, New York, 1999.
163. Attwood, D., Microemulsions, in *Colloidal Drug Delivery Systems*, Kreuter, J. (Ed.), Marcel Dekker, New York, 1994, pp. 31–72.
164. Novelli, A., Rico, I. and Lates, A., Novel microemulsion formulation reduces acid hydrolysis of radioprotector WR 2721, *New J. Chem.*, **16**, 395–398 (1992).
165. Ziegenmeyer, J. and Führer, C., Microemulsionen als topische arzneiform, *Acta Pharm. Tech.*, **26**, 273–275 (1980).
166. Willmann, H., Walde, P., Luisi, P. L., Gazzaniga, A. and Stroppolo, F., Lecithin organogel as matrix for transdermal transport of drugs, *J. Pharm. Sci.*, **81**, 871–874 (1992).
167. Bhatnagar, S. and Vyas, S. P., Organogel-based system for transdermal delivery of propranolol, *J. Microencapsulation*, **11**, 431–438 (1994).
168. Gasco, M. R., Gallarate, M. and Pattarino, F., *In vitro* permeation of azelaic acid from viscosized microemulsions, *Int. J. Pharm.*, **69**, 193–196 (1991).
169. Friberg, S. E., Kayail, I., Beckerman, W., Rhein, L. D. and Simion, A., Water permeation of reaggregated stratum corneum with model lipids, *J. Invest. Dermatol.*, **94**, 377–380 (1990).
170. Friberg, S. E., Micelles, microemulsions, liquid crystals, and the structure of stratum corneum lipids, *J. Soc. Cosmet. Chem.*, **41**, 155–171 (1990).
171. Degim, I. T., Uslu, A., Hadgraft, J., Atay, T., Akay, C. and Cevheroglu, S., The effects of Azone and capsaicin on the permeation of naproxen through human skin, *Int. J. Pharm.*, **179**, 21–25 (1999).
172. Engblom, J., Engström, S. and Fontell, K., The effect of the skin penetration enhancer Azone[®] on fatty acid–sodium soap–water mixtures, *J. Controlled Release*, **33**, 299–305 (1995).
173. Jones, M. N., Surfactants in membrane solubilisation, *Int. J. Pharm.*, **177**, 137–159 (1999).
174. von Corswant, C., Thorén, P. and Engström, S., Triglyceride-based microemulsions for intravenous administration of sparingly soluble substances, *J. Pharm. Sci.*, **87**, 200–208 (1998).
175. Norling, T., Lading, P., Engström, S., Larsson, K., Krog, N. and Nissen, S. S., Formulation of a drug delivery system based on a mixture of monoglycerides and triglycerides for use in the treatment of periodontal disease, *J. Clin. Periodontol.*, **19**, 687–692 (1992).
176. Engström, S., Ljusberg-Wahren, H. and Gustafsson, A., Bioadhesive properties of the monoolein–water system, *Pharm. Technol. Eur.*, Publication Number 0063, (February 1995).

177. Engström, S., Lindahl, L., Wallin, R. and Engblom, J., A study of polar lipid drug carrier systems undergoing a thermoreversible lamellar-to-cubic phase transition, *Int. J. Pharm.*, **86**, 137–145 (1992).
178. Landau, E. M. and Luigi Luisi, P., Lipidic cubic phases as transparent, rigid matrices for the direct spectroscopic study of immobilized membrane proteins, *J. Am. Chem. Soc.*, **115**, 2102–2106 (1993).
179. Landh, T., From entangled membranes to eclectic morphologies: cubic membranes as subcellular space organizers, *FEBS Lett.*, **369**, 13–17 (1995).
180. Larsson, K., Cubic lipid–water phases: structures and biomembrane aspects, *J. Phys. Chem.*, **93**, 7304–7314 (1989).
181. Landh, T., Phase behavior in the system pine oil monoglycerides–poloxamer 407–water at 20°C, *J. Phys. Chem.*, **98**, 8453–8467 (1994).
182. Ericsson, B., Larsson, K. and Fontell, K., A cubic protein–monoolein–water phase, *Biochim. Biophys. Acta*, **729**, 23–27 (1983).
183. Portmann, M., Landau, E. M. and Luisi, P. L., Spectroscopic and rheological studies of enzymes in rigid lipidic matrices: the case of β -chymotrypsin in a lysolecithin/water cubic phase, *J. Phys. Chem.*, **95**, 8437–8440 (1991).
184. Razumas, V., Larsson, K., Mieziš, Y. and Nylander, T., A cubic monoolein–cytochrome c–water phase: X-ray diffraction, FT-IR, differential scanning calorimetric, and electrochemical studies, *J. Phys. Chem.*, **100**, 11766–11774 (1996).
185. Razumas, V., Kanapienienė, J., Nylander, T., Engström, S. and Larsson, K., Electrochemical biosensors for glucose, lactate, urea, and creatinine based on enzymes entrapped in a cubic liquid crystalline phase, *Anal. Chem. Acta*, **289**, 155–162 (1994).
186. Hadgraft, J., Williams, D. G. and Allan, G., Azone. Mechanisms of action and clinical effect, *Drugs Pharm. Sci.*, **59**, 175–197 (1993).
187. Alexandridis, P., Olsson, U. and Lindman, B., Self-assembly of amphiphilic block copolymers: the (EO)₁₃-(PO)₃₀(EO)₁₃–water–*p*-xylene system, *Macromolecules*, **28**, 7700–7710 (1995).
188. Alexandridis, P., Olsson, U. and Lindman, B., Phase behaviour of amphiphilic block copolymers in water–oil mixtures: the Pluronic 25R4–water–*p*-xylene system, *J. Phys. Chem.*, **100**, 280–288 (1996).
189. Wang, P.-L. and Johnston, T. P., Sustained-release interleukin-2 following intramuscular injection in rats, *Int. J. Pharm.*, **113**, 73–81 (1995).
190. Tomida, H., Kuwada, N. and Kiryu, S., Hydrolysis of indomethacin in Pluronic F-127 gels, *Acta Pharm. Suec.*, **25**, 87–96 (1988).
191. Nalbandian, R. M., Henry, R. L. and Wilks, H. S., Artificial skin. II. Pluronic F-127 silver nitrate or silver lactate gel in treatment of thermal burns, *J. Biomed. Mater. Res.*, **6**, 583–590 (1972).
192. Piculell, L., Gelling polysaccharides, *Curr. Opinion Colloid Interface Sci.*, **3**, 643–650 (1998).
193. Morris, V. J. and Wilde, P. J., Interactions of food biopolymers, *Curr. Opinion Colloid Interface Sci.*, **2**, 567–572 (1997).
194. Clark, A. H. and Ross-Murphy, S. B., Structural and mechanical properties of biopolymer gels, *Adv. Polym. Sci.*, **83**, 57–192 (1987).
195. Piculell, L. and Nilsson, S., Effects of salt on association and conformational equilibria of macromolecules in solution, *Prog. Colloid Polym. Sci.*, **82**, 198–210 (1990).
196. Hovgaard, L. and Brøndsted, H., Current applications of polysaccharides in colon targeting, *Crit. Rev. Ther. Drug Carrier Syst.*, **13**, 185–223 (1996).
197. Hwang, S.-J., Park, H. and Park, K., Gastric retentive drug-delivery systems, *Crit. Rev. Ther. Drug Carrier Syst.*, **15**, 243–284 (1998).
198. Kedziewicz, F., Lombry, C., Rios, R., Hoffman, M. and Maincent, P., Effect of the formulation on the *in-vitro* release of propranolol from gellan beads, *Int. J. Pharm.*, **178**, 129–136 (1999).
199. Kwak, J. C. T., *Polymer–Surfactant Systems*, Surface Science Series Vol. 77, Marcel Dekker, New York, 1998.
200. Goddard, E. D. and Ananthapadmanabhan, K. P. (Eds), *Interactions of Surfactants with Polymers and Proteins*, CRC Press, Boca Raton, FL, 1993.
201. Iliopoulos, I., Wang, T. K. and Audebert, R., Viscometric evidence of interaction between hydrophobically modified poly(sodium acrylate) and sodium dodecyl sulfate, *Langmuir*, **7**, 617–619 (1991).
202. Lindell, K. and Engström, S., *In vitro* release of timolol maleate from an *in situ* gelling polymer system, *Int. J. Pharm.*, **95**, 219–228 (1993).
203. Lindell, K. and Engström, S., Investigation of surfactant alkyl chain length and counterion effects on the thermogelling EHEC system, *Int. J. Pharm.*, **124**, 107–118 (1995).
204. Schmolka, I. R., Poloxamers in the pharmaceutical industry, in *Polymers for Controlled Drug Delivery*, Tarcha, P. J., (Ed.), CRC Press, Boca Raton, FL, 1991, pp. 189–214.
205. Schild, H. G., Poly(*N*-isopropylacrylamide): experiment, theory and application, *Prog. Polym. Sci.*, **17**, 163–249 (1992).
206. Fleer, G. J., Cohen Stuart, M. A., Scheutjens, J. M. H. M., Cosgrove, T. and Vincent, B., *Polymers at Interfaces*, Chapman & Hall, London, 1993.
207. Napper, D. H., *Polymeric Stabilization of Colloidal Dispersions*, Academic Press, London, 1983.
208. Malmsten, M. and Lindman, B., Ellipsometry studies of cellulose ethers, *Langmuir*, **6**, 357–364 (1990).
209. Tiberg, F., Malmsten, M., Linse, P. and Lindman, B., Kinetic and equilibrium aspects of block copolymer adsorption, *Langmuir*, **7**, 2723–2730 (1991).
210. Sakuma, S., Suzuki, N., Kikuchi, H., Hiwatari, K. I., Arikawa, K., Kishida, A. and Akashi, M., Absorption enhancement of orally administered salmon calcitonin by polystyrene nanoparticles having poly(*N*-isopropylacrylamide) branches on their surfaces, *Int. J. Pharm.*, **158**, 69–78 (1997).

211. Sakuma, S., Sudo, R., Suzuki, N., Kikuchi, H., Akashi, M. and Hayashi, M., Mucoadhesion of polystyrene nanoparticles having surface hydrophilic polymeric chains in the gastrointestinal tract, *Int. J. Pharm.*, **177**, 161–172 (1999).
212. Karlström, G., Carlsson, A. and Lindman, B., Phase diagrams of nonionic polymer–water systems. Experimental and theoretical studies of the effects of surfactants and other cosolutes, *J. Phys. Chem.*, **94**, 5005–5015 (1990).
213. Kokufuta, E., Suzuki, H. and Sakamoto, D., On the local binding of ionic surfactants to poly(*N*-isopropylacrylamide) gels, *Langmuir*, **13**, 2627–2632 (1997).
214. Dhara, D. and Chatterji, P. R., Effect of hydrotropes on the volume phase transition in poly(*N*-isopropylacrylamide) hydrogel, *Langmuir*, **15**, 930–935 (1999).
215. Carlsson, F., Elofsson, U., Arnebrant, T. and Malmsten, M., Interactions between local anaesthetic agents and poly (*N*-isopropylacrylamide) through phase behaviour, surface tension, and adsorption measurement, *J. Colloid Interface Sci.*, **233**, 320–328 (2001).
216. Lowe, T. L., Virtanen, J. and Tenhu, H., Interactions of drugs and spin probes with hydrophobically modified polyelectrolyte hydrogels based on *N*-isopropylacrylamide, *Polymer*, **40**, 2595–2603 (1999).
217. Carelli, V., Coltelli, S., Di Colo, G., Nannipieri, E. and Serafini, M. F., Silicone microspheres for pH-controlled gastrointestinal drug delivery, *Int. J. Pharm.*, **179**, 73–83 (1999).
218. Bilia, A., Carelli, V., Di Colo, G. and Nannipieri, E., *In vitro* evaluation of a pH-sensitive hydrogel for control of GI drug delivery from silicone-based matrices, *Int. J. Pharm.*, **130**, 83–92 (1996).
219. Morris, G. E., Vincent, B. and Snowden, M. J., Adsorption of lead ions on to *N*-isopropylacrylamide and acrylic acid copolymer microgels, *J. Colloid Interface Sci.*, **190**, 198–205 (1997).
220. Saunders, B. R., Crowther, H. M. and Vincent, B., Poly[(methylmethacrylate)-*co*-(methacrylic acid)] microgel particles: swelling control using pH, consolvency, and osmotic deswelling, *Macromolecules*, **30**, 482–487 (1997).
221. Kiser, P. F., Wilson, G. and Needham, D., A synthetic mimic of the secretory granule for drug delivery, *Nature*, **394**, 459–462 (1998).
222. Buonaguidi, M., Carelli, V., Di Colo, G., Nannipieri, E. and Serafini, M. F., Evaluation of a pH-sensitive semi-interpenetrating polymer network for control of GI drug delivery, *Int. J. Pharm.*, **147**, 1–10 (1997).
223. Park, H.-Y., Song, I.-H., Kim, J.-H. and Kim, W.-S., Preparation of thermally denatured albumin gel and its pH-sensitive swelling, *Int. J. Pharm.*, **175**, 231–236 (1998).
224. Conaghey, O. M., Corish, J. and Corrigan, O. I., The release of nicotine from a hydrogel containing ion exchange resins, *Int. J. Pharm.*, **170**, 215–224 (1998).
225. Schacht, E., Goethals, E., Gyselinck, P. and Thienpont, D., Polymer drug combinations VI. Sustained release of levamisole from ion exchange resins, *J. Pharm. Belg.*, **37**, 183–188 (1982).
226. Raghunathan, Y., Amsel, L., Hinsvark, O. and Bryant, W., Sustained-release drug delivery system I: coated ion-exchange resin system for phenylpropanolamine and other drugs, *J. Pharm. Sci.*, **70**, 379–384 (1981).
227. Irwin, W. J., MacHale, R. and Watts, P. J., Drug-delivery by ion-exchange. Part VII: Release of acidic drugs from anionic exchange resinates complexes, *Drug Dev. Ind. Pharm.*, **16**, 883–898 (1990).
228. Fernández-Hervás, M. J., Holgado, M. A., Fini, A. and Fell, J. T., *In vitro* evaluation of alginate beads of a diclofenac salt, *Int. J. Pharm.*, **163**, 23–34 (1998).
229. Hwang, S.-J., Rhee, G. J., Lee, K. M., Oh, K.-H. and Kim, C.-K., Release characteristics of ibuprofen from excipient-loaded alginate gel beads, *Int. J. Pharm.*, **116**, 125–128 (1995).
230. Hugué, M. L. and Dellacherie, E., Calcium alginate beads coated with chitosan: effect of the structure of encapsulated materials on their release, *Process Biochem.*, **31**, 745–751 (1996).
231. Lim, L. Y. and Wan, L. S. C., Propranolol hydrochloride binding in calcium alginate beads, *Drug Dev. Ind. Pharm.*, **23**, 973–980 (1997).
232. Leong, K. W., Synthetic biodegradable polymer drug delivery systems, in *Polymers for Controlled Drug Delivery*, Tarcha, P. J. (Ed.) CRC Press, Boca Raton, FL, 1991, pp. 127–148.
233. Bruck, S. D. (Ed.), *Controlled Drug Delivery*, CRC Press, Boca Raton, FL, 1983.
234. Belbella, A., Vauthier, C., Fessi, H., Devissaguet, J.-P. and Puisieux, F., *In vitro* degradation of nanospheres from poly(D,L-lactides) of different molecular weights and polydispersities, *Int. J. Pharm.*, **129**, 95–102 (1996).
235. Wallis, K. H. and Müller, R. H., Comparative measurements of nanoparticle degradation velocity using an accelerated hydrolysis test, *Pharm. Ind.*, **55**, 168–170 (1993).
236. Bamford, C. H. and Tipper, C. F. H., Ester formation and hydrolysis and related reactions, in *Chemical Kinetics*, Vol. 10, Bamford, C. H. and Tipper, C. F. H. (Eds), Elsevier, Amsterdam, 1972, pp. 146–161.
237. Domb, A. and Langer, R., Polyanhydrides: stability and novel composition, *Makromol. Chem., Macromol. Symp.*, **19**, 189–200 (1988).
238. Sung, K. C., Han, R.-Y., Hu, O. Y. P. and Hsu, L.-R., Controlled release of nalbuphine prodrugs from biodegradable polymeric matrices: influence of prodrug hydrophilicity and polymer composition, *Int. J. Pharm.*, **172**, 17–25 (1998).
239. Miyajima, M., Koshika, A., Okada, J., Kusai, A. and Ikeda, M., The effects of drug physico-chemical properties on release from copoly (lactic/glycolic acid) matrix, *Int. J. Pharm.*, **169**, 255–263 (1998).
240. Cha, Y. and Pitt, C. G., The acceleration of degradation-controlled drug delivery from polyester microspheres, *J. Controlled Release*, **8**, 259–265 (1989).
241. Li, S., Girod-Holland, S. and Vert, M., Hydrolytic degradation of poly(DL-lactic acid) in the presence of caffeine base, *J. Controlled Release*, **40**, 41–53 (1996).

242. O'Hagan, D. T., Microparticles as oral vaccines, in *Novel Delivery Systems. Oral Vaccines*, O'Hagan, D. T. (Ed.), CRC Press, Boca Raton, FL, 1994, pp. 175–205.
243. Bhagat, H. R., Dalal, P. S. and Nellore, R., Oral vaccination by microspheres, *Drugs Pharm. Sci.*, **77**, 381–399 (1996).
244. Ray, R., Novak, M., Duncan, J. D., Matsuoka, Y. and Compans, R. W., Microencapsulated human parainfluenza viruses induce a protective immune response, *J. Infect. Dis.*, **167**, 752–755 (1993).
245. Stevens, V. C., Future perspectives for vaccine development, *Scand. J. Immunol.*, **36**, 137–143 (1992).
246. Eldridge, J. H., Staas, J. K., Meulbroek, J. A., McGhee, J. R., Tice, T. R. and Gilley, R. M., Biodegradable microspheres as a vaccine delivery system, *Mol. Immunol.*, **28**, 287–294 (1991).
247. McGhee, J. R., Mestecky, J., Dertzbaugh, M. T., Eldridge, J. H., Hirasawa, M. and Kiyono, H., The mucosal immune system: from fundamental concepts to vaccine development, *Vaccine*, **10**, 75–88 (1992).
248. Moldoveanu, Z., Novak, M., Huang, W.-Q., Gilley, R. M., Staas, J. K., Schafer, D., Compans, R. W. and Mestecky, J., Oral immunization with influenza virus in biodegradable microspheres, *J. Infect. Dis.*, **167**, 84–90 (1993).
249. Eldridge, J. H., Gilley, R. M., Staas, J. K., Moldoveanu, Z., Meulbroek, J. A. and Tice, T. R., Biodegradable microspheres: vaccine delivery system for oral immunization, *Curr. Topics Microbiol. Immunol.*, **146**, 59–66 (1989).
250. Eldridge, J. H., Staas, J. K., Meulbroek, J. A., Tice, T. R. and Gilley, R. M., Biodegradable and biocompatible poly(DL-lactide-co-glycolide) microspheres as an adjuvant for staphylococcal enterotoxin B toxoid which enhances the level of toxin-neutralizing antibodies, *Infect. Immun.*, **59**, 2978–2986 (1991).
251. Marx, P. A., Compans, R. W., Gettie, A., Staas, J. K., Gilley, R. M., Mulligan, M. J., Yamshchikov, G. V., Chen, D. and Eldridge, J. H., Protection against vaginal SIV transmission with microencapsulated vaccine, *Science*, **260**, 1323–1327 (1993).
252. Burke, C. J., Hsu, T.-A. and Volkin, D. B., Formulation, stability, and delivery of live attenuated vaccines for human use, *Crit. Rev. Ther. Drug Carrier Syst.*, **16**, 1–83 (1999).
253. Strannegård, Ö. and Yurchison, A., Formation of agglutinating and reaginic antibodies in rabbits following oral administration of soluble and particulate antigens, *Int. Arch. Allergy*, **35**, 579–590 (1969).
254. Cox, D. S. and Taubman, M. A., Oral induction of the secretory antibody response by soluble and particulate antigens, *Int. Arch. Allergy Appl. Immunol.*, **75**, 126–131 (1984).
255. Nellore, R. V., Pande, P. G., Young, D. and Bhagat, H. R., Evaluation of biodegradable microspheres as vaccine adjuvant for hepatitis B surface antigen, *J. Parenteral Sci. Technol.*, **46**, 176–180 (1992).
256. Eldridge, J. H., Hammond, C. J., Meulbroek, J. A., Staas, J. K., Gilley, R. M. and Tice, T. R., Controlled vaccine release in the gut-associated lymphoid tissues. I. Orally administered biodegradable microspheres target the Peyer's patches, *J. Controlled Release*, **11**, 205–214 (1990).
257. Mauduit, J., Bukh, N. and Vert, M., Gentamycin/poly-(lactic acid) blends aimed at sustained release local antibiotic therapy administered per-operatively. I. The case of gentamycin base and gentamycin sulfate in poly (DL-lactic acid) oligomers, *J. Controlled Release*, **23**, 209–220 (1993).
258. Mestecky, J., Moldoveanu, Z., Novak, M., Huang, W.-Q., Gilley, R. M., Staas, J. K., Schafer, D. and Compans, R. W., Biodegradable microspheres for the delivery of oral vaccines, *J. Controlled Release*, **28**, 131–141 (1994).
259. Paul, W. E. (Ed.), *Fundamental Immunology*, Raven Press, New York, 1993.
260. Stevens, V. C., Powell, J. E., Rickey, M., Lee, A. C. and Lewis, D. H., Studies various delivery systems for a human chorionic gonadotropin vaccine, in *Gamete Interaction: Prospects for Immunocontraception*, Wiley, New York, 1990, pp. 549–563.
261. Zhao, X. and Harris, J. M., *Novel Degradable Poly-(ethylene glycol) Esters for Drug Delivery*, Harris, J. M. and Zalipsky, S. (Eds), ACS Symposium Series 680, American Chemical Society, Washington, DC, 1997.
262. Singh, M., Rathi, R., Singh, A., Heller, J., Talwar, G. P. and Kopecek, J., Controlled release of LHRH-DT from bioerodible hydrogel microspheres, *Int. J. Pharm.*, **76**, R5–R8 (1991).
263. Rubinstein, A. and Sintov, A., Biodegradable polymeric matrices with potential specificity to the large intestine, in *Oral Colon-Specific Drug Delivery* Friend, D. R. (Ed.), CRC Press, Boca Raton, FL, 1992, pp. 233–257.
264. Muller, D., Malmsten, M., Tenodekaew, S. and Booth, C., Adsorption of diblock copolymers of poly(ethylene oxide) and polylactide at hydrophobized silica from aqueous solution, *J. Colloid Interface Sci.*, **228**, 326–334 (2000).
265. Kirpotin, D., Hong, K., Mullah, N., Papahadjopoulos, D. and Zalipsky, S., Liposomes with detachable polymer coatings: destabilization and fusion of dioleoylphosphatidylethanolamine vesicles triggered by cleavage of surface-grafted poly(ethylene glycol), *FEBS Lett.*, **388**, 115–188 (1996).
266. Hyde, S. T., Andersson, S., Ericsson, B. and Larsson, K., A cubic structure consisting of a lipid bilayer forming an infinite periodic minimum surface of the gyroid type in the glycerolmonooleat–water system, *Z. Kristallogr.*, **168**, 213–219 (1984).
267. Nyqvist-Mayer, A. A., Brodin, A. F. and Frank, S. G., Drug release studies on an oil–water emulsion based on a eutectic mixture of lidocaine and prilocaine as the dispersed phase, *J. Pharm. Sci.*, **75**, 365–373 (1986).

CHAPTER 2

Surface Chemistry in Food and Feed

Björn Bergenståhl

Lund University, Lund, Sweden

1	Introduction	39	3.6	Liquid bridges	44
2	Colloids in Liquids	39	4	Surface-Active Components	44
	2.1 Chemically homogeneous dispersions	40	4.1	Lipids	44
	2.2 Chemically heterogeneous dispersions	40	4.2	Proteins	46
	2.2.1 Emulsions	40	4.3	Polysaccharides	46
	2.2.2 Suspensions	41	5	Particles and Surfaces in Air	48
	2.2.3 Foams	41	5.1	Wettability	49
3	Interparticle Interactions in Liquids	42	5.2	Cohesive and repulsive surface interactions	50
	3.1 van der Waals interactions	42	5.3	The chemical composition of the surface	50
	3.2 Electrostatic repulsion	42	5.4	Characterisation of powder surfaces	51
	3.3 Hydration interactions	42	6	Concluding Remarks	51
	3.4 Solvent structure	43	7	References	51
	3.5 Polymer-induced interactions	43			

1 INTRODUCTION

Almost all food and feed materials are heterogeneous, with structural entities in size ranges from 1 nm to 1 μm , or larger. Colloid and surface chemistry aspects strongly affect all properties of these materials, while such aspects are also involved when we want to understand and describe the properties of various food and feed materials and systems. Hence, we cannot follow a headline such as the one above with a complete description of the area, but rather we will give a few examples and ideas concerning important aspects of colloid and surface chemistry in relation to food and feed industrial problems.

2 COLLOIDS IN LIQUIDS

Most of our food and feed materials are dispersed in a liquid medium forming the continuous phase of the

system, either in their final state or during the production process. They are all thermodynamically unstable, with the kinetics of the instability processes describing their life times.

All dispersed systems have common characteristic properties which are determined by three key parameters: the particle size, the volume fraction of the dispersed phase and the interparticle interactions.

Food suspensions may be *aqueous* dispersions, for instance tomato ketchup, mustard, etc., or *oil-continuous* dispersions, such as melted chocolate. The interparticle interactions are strongly influenced by the properties of the continuous phase, which will make oil-continuous systems very different from water-continuous systems. In addition, the solution, structural and chemical properties of the dispersed phase strongly influence the properties of these systems.

In order to understand the mechanisms involved, it might be useful to divide the various dispersions

Table 2.1. Instability mechanisms in homogeneous and heterogeneous dispersions

Mechanism	Homogeneous	Heterogeneous
Sedimentation	Less important due to the small density difference and the high volume fraction	Usually very important unless the particle size is very small
Flocculation	Unimportant due to the large particle size	Important if the particle size is below 1 μm
Coalescence	Most systems contain solid particles	Important in liquid/liquid and liquid/gas systems
Ostwald ripening	Very important for small particles (<1–10 μm).	Important in foams
Nucleation	Important during the formation of the dispersed system	Might be important during foam formation
Material bridges	Important	Only important for water bridges in oil-continuous dispersions (sucrose in oil)

into two groups, depending on the degree of chemical heterogeneity between the phases. The first of these, *chemically heterogeneous systems*, are those where the dispersed phase consists of components with different solubility properties and a different chemical character to that of the continuous phase. The second type comprises *chemically homogeneous systems*, where the dispersed phase is obtained by crystallization or precipitation of a major part of the continuous phase.

2.1 Chemically homogeneous dispersions

Chemically homogeneous dispersions are defined here as dispersions where the dispersed phase and the continuous phase have chemical compositions with important similarities. Examples of such systems are honey, where we have saccharide crystals dispersed in a concentrated syrup, or semi-solid fat, which consists of solid triglyceride crystals dispersed in a solution of liquid triglycerides.

Major characteristics of homogeneous dispersions are the dynamic characters of their phase boundaries. There is a continuous flux of material from the dissolved state into the solid state, and vice versa. The interfaces are dynamic and changing, with the process of ostwald ripening rapidly eliminating the smaller particles. Surface-active components may influence both the crystal growth and the nucleation.

Important examples of homogeneous dispersions are ice crystals in concentrated protein and salt solutions (frozen animal tissue materials and other frozen low-carbohydrate foods), or ice crystals dispersed in a concentrated syrup (frozen desserts, ice cream, etc.).

2.2 Chemically heterogeneous dispersions

The most characteristic food model colloid in this class is that of triglycerides dispersed in water. Triglycerides

display an extremely low solubility in water, suppressing the ripening processes, and thus make instability mechanisms far more important. Suspensions of insoluble materials, such as fibre particles (for instance, clouding materials in soft drinks), or protein and carbohydrate particles in oil (for instance, chocolate systems which normally consist of about 70% of sucrose dispersed in cacao liquid) are also examples of heterogeneous dispersions. Such colloidal systems might be described as being either emulsions, suspensions or foams. The various instability mechanisms occurring in homogeneous and heterogeneous dispersions are compared in Table 2.1.

2.2.1 Emulsions

Emulsions are created by applying mechanical agitation to an oil phase, thus dispersing it into droplets. In order to stabilize the droplets, they need to be protected by an adsorbed layer of emulsifiers or protecting colloids. The emulsifying material creates repulsive and attracting interaction patterns, which determines the properties of the final food system.

Such destabilising factors are different between oil-in-water and water-in-oil systems, as shown in Table 2.2.

Water-in-oil emulsions, are commonly exemplified by systems such as butter, spreads and margarine. These consist of water droplets formed in an oil phase of a liquid oil or a semi-solid partially crystalline oil phase. These systems are typically stabilized by oil-soluble emulsifiers and by the presence of solid particles. The water solubility in a triglyceride, in contrast to the triglyceride solubility in water, is about 0.5%, thus making the ripening processes fast unless the droplets are stabilized by the inclusion of a totally oil-insoluble material such as salt.

A second factor that differs between oil-in-water and water-in-oil systems is the role of fat crystals. In oil-in-water systems, such crystals induce coalescence. However, the finalization of the droplet fusion is also slowed

Table 2.2. Characteristics of water-in-oil and oil-in-water food emulsions

	Oil-in-water	Water-in-oil
Stabilizing components	Proteins, hydrophilic surface-active lipids	Hydrophobic surface-active lipids, fat crystals
Destabilizing mechanisms	Flocculation, coalescence, fat crystals (partial coalescence)	Ostwald ripening, coalescence
Particle size	Typically 0.5–5.0 μm	Typically 5.0–50 μm
Examples	Mayonnaise, cream	Butter, spreads

Table 2.3. Properties of food and feed suspensions

Colloidal parameter	Rheological properties	Consolidation properties
Particle size	Smaller particles—more connections and higher strength	Smaller particles—faster consolidation
Interparticle interaction	Attractive interaction—higher strength	Attractive interactions—slower consolidation.
Volume fraction	High volume fraction—high strength	High volume fraction—slow consolidation
Density difference between continuous and dispersed phases.	No effect	Larger density difference—faster consolidation
Container height	No effect	High container—large consolidation stress and faster process

down in the presence of a high-fraction solid fat. Hence, partial coalescence is a typical state for an emulsified semi-solid fat (1, 2). In water-in-oil emulsions, the role of the fat crystals is in the opposite direction, i.e. it contributes to the stability of the system.

2.2.2 Suspensions

Suspensions of insoluble material are commonly found in many food and feed systems. Some of their properties are summarized in Table 2.3. The particles are almost always obtained from the grinding operation of a biological tissue or of a pure solid food material (typically sucrose or protein). These processes generate particles with a typical size range of 5–500 μm . The sedimentation of particles of these sizes is rapid under dilute conditions, which thus makes such dilute suspensions unstable. More concentrated systems produce stable suspensions by the formation of a concentrated network, which then only slowly change due to a consolidation process.

The strength of this particle network is of large technical importance. For example, it gives rise to various rheological characteristics such as the yield values of more or less plastic dispersions, and determines the sensitivity to consolidation. A developed consolidation process in a suspension gives a layer of clear liquid on top of the suspension.

Feed suspensions are usually prepared by dispersing a powdered, agglomerated or pelleted material in

water just before feeding to animals. These suspensions display a rapid sedimentation, which is mainly determined by the size of the particles and their effective densities. A rapid sedimentation during the distribution of the feed slurry could commonly lead to problems with the feed composition.

2.2.3 Foams

Foams consist of gases dispersed in a liquid. The nature of such foams varies depending on the situation. Some foams are transient with a short lifetime, for instance a Champagne foam, while other foams are more or less permanent, e.g. the foam formed in bread.

A typical feature of foams is that diffusion between the phases (Ostwald ripening or disproportionation) is of critical importance rapidly eliminating all particles in the colloidal range (3). The density difference between the two phases is always large, and consequently a densely packed layer of comparatively large bubbles is always rapidly formed (typically 90–99% of the dispersed phase) if the viscosity is low (4). The stability of these foams is largely determined by the film rupture characteristics (of the film separating the bubbles) and by film drainage. The surface-active components present in the liquid form two-dimensional layers along the air-water interfaces, displaying surface rheological properties which contribute to the stability of the film via a range of different mechanisms, as illustrated in Table 2.4.

However, a range of very important food foams are stabilized by a three-dimensional gel through the foam

Table 2.4. Destabilizing mechanisms and stabilizing factors in foams with viscous or low-viscous lamellae

	Low-viscous lamellae	Viscous lamellae
Important mechanisms determining the stability	The formation of a two-dimensional viscous layer along the surface. Repulsive interactions between adsorbed layers	The formation of a three-dimensional viscous layer through the foam lamellae. Formation of interfacial gels
Important components contributing to the foam performance	Adsorbed surface-active components, e.g. proteins, peptides and lipids. Absences of defoaming components such as free oil	Proteins sensitive to surface denaturation. Monoglycerides forming gel phases by partial crystallization (α -gels). Fat particles able to form aggregated networks at the air-water interface
Stability character	Transient	More or less permanent
Dispersed phase/overrun	90–99% dispersed phase; $\geq 800\%$ overrun	50–85% dispersed phase; 100–800% overrun
Examples	Beer, champagne	Bread, meringue, shortenings

lamellae. Such foams generally have very thick lamellae and a less dispersed phase (typically 50–85% – which corresponds to overruns of 100–500%). The structure of the foam is viscous to solid, and the foam may be permanent.

The stabilizing mechanisms displayed under these two conditions are different, and thus when dealing with food foams one has to recognize the role of the solidifying structure of the foam lamella in many important technical systems.

3 INTERPARTICLE INTERACTIONS IN LIQUIDS

Colloidal interparticle interactions are important in all systems dispersed in liquids, and consequently play an importance role in many types of food dispersions (5). The relative importance of the different interactions depends on the properties of the surfaces involved and of the continuous phase.

3.1 van der Waals interactions

Dipolar and induced dipolar interactions cause this general and fundamental attractive interaction. The character of this interaction is comparatively weak and comparatively long-range in order. The interaction is, in principal, proportional to the refractive index difference between the phases. The difference between oil and water is large and only fairly high concentrations of dissolved material reduce the van der Waals interactions significantly.

3.2 Electrostatic repulsion

Electrostatic repulsion is generally considered to be the main source of stability in typical colloidal systems.

This repulsive interaction is caused by charge at the interfaces, with the range of the interactions being determined by the counterion concentration. Three reasons reduce the significance of electrostatic interactions in food systems, as follows:

1. The surface charges are usually low. Only a few charged emulsifiers are permitted and used. Food polyelectrolytes are always of a heterogeneous nature. For instance, the polyacid, pectic acid, contains partly esterified acid groups, thus reducing the actual charge. Proteins contain nonionic, cationic and anionic amino acids, hence creating a surface with complex charge properties.
2. The salinity is usually high. Most food systems have a salt level around the physiological concentration (0.9% NaCl, approximately equal to 150 mmol/l). Animal foods have an original salinity at this level, while for recombined vegetable-based foods about this same amount of salt is added.
3. The pH is usually low. Typical pH values for fermented food and fruits are around 4, while the pH for most vegetables and meat is between 5 and 6. Only a few foods have almost neutral pH values, i.e. between 6 and 7, e.g. shellfish, milk, egg, etc.

Consequently, DLVO-type interactions (a combination of van der Waals and electrostatic interactions) are rarely sufficient to explain the functionality of typical food systems.

3.3 Hydration interactions

Hydration interactions are empirically identified short-range repulsive interactions, which operate between hydrophilic surfaces (6). The strength of the interaction is larger than the electrostatic or van der Waals interactions, although the range is very short, i.e. typically

Table 2.5. Structural interactions

Molecule	Shape	Number of oscillations	Interaction Distance Å	Reference
Water	Approximately spherical, $d \approx 2-3 \text{ \AA}$	10	25	8
Octamethylcyclotetrasiloxane	spherical, $d \approx 9 \text{ \AA}$	10	90	9
Triolein	$25 \times 10 \times 10 \text{ \AA}$	3	60	10

2 nm. The final nature of this interaction is still under debate (7), although it has been empirically identified between a wide range of surfaces (mica, phospholipids, monoglycerides and protein surfaces).

3.4 Solvent structure

Interactions between surfaces are usually assumed to depend on the average properties of the specific liquid between the surfaces. However, at very short distances, the size of the molecule becomes comparable to the distance separating the actual particles. At such short distances, the interaction becomes oscillating due to the packing constraints of the solvent molecules (Table 2.5). The propagation of this ordering depends on the sphericity, polydispersity and size of the interacting surfaces. For water this happens only at very short distances (typically 5 Å), while for larger molecules it becomes more important at much larger distances. Structural interactions can be expected to have a particular importance for solutions with large molecules, such as triglyceride systems and systems with non-adsorbing polymers.

3.5 Polymer-induced interactions

Polymers in solutions are characterized by the low level of mixing entropy, which makes the interaction terms much more important with respect to the solution properties. This is also the main reason why polymer solutions tend to separate when two or more polymers are mixed together. The phase separation could be associative if there is an attractive interaction between both polymers or segregative when there is a repulsive interaction between the polymers. Food and feed systems which include various types of polymers can be very complex. Thus, there are strong tendencies to various types of phase separation. It has also been observed that such behaviour is of significance during processing at high temperatures, for instance during peleting. However, due to the complexity and the presence of other

colloids it has been difficult to characterize this property in food systems. During the last few years, however, it has been described in several systems (Table 2.6).

Polymers present in solution also influence the interactions between particles. Such interactions depend on the solution properties of the polymers and on the polymer-to-surface concentration ratio (Table 2.7).

It is clear from this table that there is a range of different properties that could be obtained in the presence of polymers. A low fraction of a strongly adsorbing polymer might cause bridges between the particles, thus destabilizing the system. This is typically used industrially in flocculent systems, for instance in clarifying cider or beer. The best efficiency is obtained when the adsorbing polymer generates fairly long-range interactions, e. g. electrostatic interactions.

Table 2.6. Examples of phase-separating polymer food systems

Polymer 1	Polymer 2	Observation	Reference
Starch	Galactomannan	Phase separation	11
Casein	Galactomannan	One phase; phase separation occurs above a salinity of 0.1–0.2 M	12
Na-caseinate	Na-alginate	Phase separation	13
Gelatine	Maltodextrin	Phase separation	14

Table 2.7. Interparticle interactions caused by the presence of polymers

Type of interaction	Polymer surface interaction	Other conditions
Bridging	Adsorbing	Low surface coverage
Steric repulsion	Adsorbing	High surface coverage, good solvent conditions
Depletion attraction	Non-adsorbing	Intermediate polymer concentration

Table 2.8. Amphiphilic properties of polar lipids

Character	Solubility	Self-assembling aggregates	HLB ^a	Use
Hydrophilic	Water-soluble	Micelles	Above 12	Detergents, wetting
Balanced	Dispersible in water and oil	Bilayer structures	8–6	Water-continuous emulsions, foam
Lipophilic	Oil-soluble	Reversed aggregates	Below 6	Oil-continuous systems

^aHydrophilic–lipophilic balance.

An adsorbed layer of a well-solvated polymer (good solvent conditions) creates a steric barrier protecting the particles from flocculating. This type of interaction is very common in food and feed systems as a result of protein adsorption. Under some conditions, steric repulsion could also be caused by the adsorption of surface-active polysaccharides, such as gum arabic.

Non-adsorbing polymers generate attractive interactions and depletion attractions, thus causing the system to phase-separate into one polymer-depleted and one particle-depleted solution. Typical polymers that could cause this behaviour are large non-adsorbing polysaccharides, such as xanthan or starch. This effect is usually observed as an increased creaming or a coarsening of the system.

3.6 Liquid bridges

Precipitating material between dispersed particles causes material bridges. The necessary conditions include that the precipitating material should wet the particles (contact angle less than 90°) and that there is a surface tension between the precipitating phase and the surrounding liquid. Typical systems where this may occur are triglyceride-continuous dispersions, where dissolved water may precipitate and form bridges between hydrophilic particles, such as sucrose particles in a chocolate dispersion. This will lead to a stiffening of the dispersion and result in a change in the sensoric properties of the product. However, a hydrophobic additive, such as lecithin, will adsorb to the sucrose particles, thus reducing their hydrophilicity, and hence reduce the formation of water bridges, and consequently the viscosity (10).

4 SURFACE-ACTIVE COMPONENTS

The generation of surface interactions is closely connected to the presence of surface-active material which

is naturally present in food and feed systems, as well as surface-active technical additives. Various national authorities (for instance, the USA Food and Drug Administration) regulate the use of additives in food systems. For feed systems, there are similar restrictions regulating their use. The chemical origin could belong to three classes of compounds, i.e. lipids, proteins and polysaccharides.

4.1 Lipids

The functional properties of polar lipids are determined by their solution properties. The amphiphilic character of such properties can be described as follows (Table 2.8):

1. By the solubilities, ranging from oil-soluble to water-soluble. This was first expressed by the Bancroft rule, which states that water-soluble emulsifiers favour emulsions with an aqueous continuity, while oil-soluble emulsifiers favour emulsions with an oil continuity.
2. By the *hydrophilic–lipophilic balance* (HLB) system, according to Griffin (15). The HLB ratio is expressed as a number based on the emulsifying properties of the emulsifier. The HLB can also be estimated from the chemical structure according to the molecular group contributions, as repeated by Davies (16). HLB numbers are closely related to the functional properties of the emulsifiers.
3. The *phase-inversion temperature*, according to Shinoda and Saito (17). The effective HLB value is strongly temperature-dependent (the emulsifier becomes less hydrophilic with increasing temperature) when ethoxylated surfactants are used. In an emulsion system, this can be followed by the phase-inversion temperature, which corresponds to the temperature at which the effective HLB is about 6. In food and feed applications, this is fairly rarely used as purely ethoxylated surfactants are seldom used in such systems.

4. By the formation of self-assembling structures in the presence of surplus water. The type of structures formed range from micellar structures (hydrophilic emulsifiers) to reversed structures (reversed micelles, L2 phases or reversed hexagonal phases) for the more lipophilic emulsifiers. Balanced emulsifiers (HLB around 7) form lamellar liquid crystals. A dispersed lamellar phase appears as liposomal dispersions. Krog has reviewed the liquid crystalline phases formed by common food emulsifiers (18). Friberg and Wilton, plus other workers, have suggested that the presence of lamellar liquid crystalline phases is a strong indication of a good emulsifier (in simple systems) (19). There is also a strong relation between the presence of swelling self-assembling structures and the ability to generate repulsive interactions (5) on one hand and between non-micellar phases and dense adsorbed layers on the other. The critical packing parameter (CPP) is a generalization of the self-assembling properties of surfactants, describing the properties as a geometrical balance between the area needed for the polar group relative to the area needed for the hydrophobic group (20).

The melting properties are of crucial importance to the technical functionality of emulsifiers, in addition to their amphiphilic properties. Most food and feed emulsifiers are based on natural fat sources, thus giving different melting properties. The consequences of the melting properties can be expressed as the Krafft temperature (i.e. the temperature at which the solubility is above the critical micelle concentration) or as the transition temperature (chain melting temperature, i.e. the melting temperature of the fatty acids in a semicrystalline bilayer). The transition temperature in an emulsifier water system forming a lamellar liquid crystalline phase

represents the transformation between a swelling lamellar phase (above the transition temperature) and an α -gel phase (below the transition temperature). The fully crystalline form of the emulsifier is the β -form. The melting temperature of the β -phase is higher than the transition temperature. In order to form a liquid crystalline phase or a hydrated gel phase (α -phase) from a solid (β -crystalline) emulsifier, the latter needs to be mixed above the melting temperature of the β -phase. Technical functionality (such as foaming and emulsifying action) is only obtained when the emulsifier is present in the liquid crystalline form or in the α -gel form. The high-melting monoglycerides used in the baking industry are usually distributed as a stable α -gel in order to overcome the high melting point of the pure emulsifier. The stability of the α -gel is achieved by mixing complex mixtures of different fatty acids, sodium soap and different modified monoglycerides into the gels.

The activation temperatures of the emulsifiers are strongly dependent on the fat base (Table 2.9). High-melting fat bases (fully hardened C_{18} -dominated fats) create high-melting emulsifiers with Krafft or transition temperatures in the range 40–60°C. Precipitating emulsifiers may contribute to fat crystallization, while solid emulsifiers may have a textural functionality, but for most applications such high-melting points are unsuitable. Intermediate-melting fat bases (C_{14} – C_{18} fats with some unsaturation) give emulsifiers with Krafft or transition temperatures between 30 and 50°C. These emulsifiers could be used to create stable α -gels and do usually display well performing properties in baking applications. Low-melting fats (highly unsaturated fats) give Krafft points below 0°C. Typical of such systems are soybean phospholipids which have the native fatty acid composition. These are present in the liquid crystalline state under all conditions.

Table 2.9. Technical fat bases and emulsifier properties

Fat	Typical fatty acids (% composition)	MP ^a (°C)	Iodine value ^b
Lard	18:1 (35), 16:0 (25), 18:0 (20)	30–35	50
Tallow	18:1 (50), 16:0 (25), 18:0 (15)	30–35	50
Hardened fish oil	16:0 (30), 18:0 (30), 20:0 (20), 22:0 (12)	50–55	0
Coconut butter	12:0 (44), 14:0 (18), 16:0 (8)	25	10
Sunflower	18:2 (65), 18:1 (25), 16:0 (6)	–15	125
Soybean	18:2 (50), 18:1 (30), 16:0 (10), 18:3 (6)	–15	130
Rapeseed oil	18:1 (50), 18:2 (20), 18:3 (10)	–15	100
Hardened rapeseed oil	18:0 (82), 16:0 (4), 20:0 (3), 22:0 (2)	50–55	0

^aMelting point of the corresponding triglyceride.

^bA measure of the degree of unsaturation; 86 is equal to a monounsaturated fat (triolein).

Ricinic (castor) oil is a special oil which is of significant use in the emulsifier industry. This consists of 85% of esters of *cis*-12-hydroxy-9-octadecenic acid. The free hydroxy group is used as a starting point for the formation of chemical derivatives such as esters or ethers, for instance, in polyethoxylated or polyglycerol surfactants.

There is a range of different polar groups available for food and feed applications, thus giving a range of different properties. Some examples are given in Table 2.10, while more details are available in the text by Hasenhuettl and Hartel (21).

4.2 Proteins

The consequences of the presence of proteins are nearly always important when we want to understand the colloidal functionalities of food and feed systems as such species are almost always present and are always surface-active in nature. There are a few key parameters, or rather descriptors, that are helpful when we need to understand protein functionalities in technical systems.

Solubility. The surface-active functionality is closely related to the solubility. A well-soluble protein forming a true solution adsorbs to surfaces and thus creates steric repulsions. The precipitation of a protein from a solution may lead to linkages between dispersed particles, hence resulting in gelation of the system. Totally insoluble proteins, perhaps resulting from harsh processing conditions, act as insoluble particles, maybe with swelling and waterholding properties.

Denaturation temperature. Denaturation is an irreversible reduction of the protein solubility at a certain critical temperature.

Isoelectric point. The isoelectric point is the pH when a protein displays a zero net charge. The solubility of proteins is reduced in solutions at a pH close to the isoelectric point and enhanced at pH values above and below the isoelectric point. The pH of the solution relative to the isoelectric point also highly influences its aggregation properties, denaturation temperature and solubility.

Molecular parameters. The molecular parameters include a range of various parameters on a molecular

level, which may be more or less difficult to measure and sometimes even to quantify. They include the molecular weight, for most proteins very well defined, but technically most important for proteins like gelatine where it may vary and be less defined, and the molecular structure, which might be globular (whey proteins), random coil (sodium caseinate) or helical (gelatine). The molecular flexibility is a more descriptive but less well defined parameter, describing the willingness or the resistance of the molecule towards conformational changes. A further parameter, the protein surface hydrophobicity, is a chemical descriptor based on the binding of a probe to the molecular surface.

Functionality tests. A wide range of functionality tests are available for use in connection with certain protein products and their applications. These include emulsification index according to Kinsella (a measure of the amount of oil that can be emulsified the using the tested protein preparation), the Bloom strength (a gel strength test used to characterize gelatine) and Heini numbers (a measure of egg white quality). A common feature of most of these tests are that they are very sensitive towards the protein solubility, which may influence the results obtained when applied to technical samples.

The characteristic properties of a range of important technical proteins are summarized in Table 2.11.

4.3 Polysaccharides

Most polysaccharides are not very surface active. For instance, starch and dextrane display very weak surface activities in various tests (for instance, in the classical “Gold number” tests). Xanthane has been shown to create depletion flocculation in several types of experiment, as shown by an unpredicted fast creaming. However, other polysaccharides, for instance, gum arabic and modified cellulose, do display surface activity. The latter is defined here as the ability to adsorb to surfaces. The ability to reduce the interfacial tension is associated with the ability to adsorb, as the surface tension represents the strength of the molecule–surface interactions. However, for large molecules, where the mixing entropy is only a minor contribution to the free energy, adsorption can also be achieved also when the adsorption energy is small. The surface activity of gum arabic is explained by the proteinaceous components associated with the molecule (22). When these parts are eliminated, the surface activity is lost. With modified cellulose, the surface activity is more related to

Table 2.10. Surface-active lipids (soaps, lecithins, monoglyceni- des, monoglyceni- de derivatives, etc.) used in food and feed applications (emulsifiers)

Lipid	Examples and USFDA and EEC E numbers	Properties	Uses
Soaps	Sodium and potassium soaps of common fatty acids (-) (-)	Strongly hydrophilic (HLB above 20) at pH values above the pK_a of the fatty acid (about 6). Forms micelles with water. Strong soapy taste	Limited use due to the poor taste and high pH. Is included as a hydrophilizing additive in commercial monoglyceride gels used in the baking industry
Lecithin	Natural mixture of phosphatidylcholine (pc), phosphatidylethanolamine and other phospholipids (184.1400) (E 322)	The standard lecithin (mainly of soybean origin) is a hydrophobic mixture dominated by the properties of phosphatidylethanolamine (effective HLB about 4). Forms a reversed hexagonal phase with water	Used over a wide range of the industry. Typically used in margarines and spreads as a hydrophobic emulsifier and in chocolates as a viscosity regulator. Used as a wetting additive for powders, and in the feed industry to improve fat digestion
PC-enhanced lecithin	PC concentration increased through a selective extraction of non-PC components of the lecithin (184.1400) (E 322)	More hydrophilic than the native mixture. When the PC concentration is high enough (about 60–80%), lamellar liquid crystalline phases might be formed	Used in applications where more hydrophilic properties are required. The product has less taste and a purer character than the original material, which might be beneficial in some applications. However, the increased cost level limits its use
Hydrolysed lecithin	Lysophospholipids (184.1400) (E 322)	More hydrophilic than the standard lecithin. Water dispersible, and may form lamellar liquid crystals (depending on the quality)	Used in water-continuous applications such as mayonnaise and dressings
Distilled mono-glycerides (MGs)	About 90% MG, with fatty acid composition depending on fat base; typically lard, tallow, vegetables (182.4505) (E 471)	Slightly on the more lipophilic side (HLB about 5). Forms lamellar liquid crystalline phases with water	Used over a wide range of the industry, e.g. in the margarine industry as a lipophilic emulsifier, in the baking industry as an additive retarding the staling of bread, and in whipped toppings
Monoglycerides/diglycerides (DGs)	Typically 40% MG and 60% DG (182.4505) (E 471)	More lipophilic than distilled monoglyceride (HLB less than 5). Forms an L_2 phase with water	Used as an emulsion destabilizer in the ice-cream industry
Modified monoglycerides	Lactylated monoglycerides (172.852) (E 472) Acetylated monoglycerides (172.828) (E 472) Ethoxylated monoglycerides (172.834) (-) Diacetyltartaric acid esters of monoglycerides (182.4101) (E 472)		Baked products, whipped toppings Baked goods Frozen desserts, cakes Baked goods, dairy-type emulsion replacers

(continued overleaf)

Table 2.10. (continued)

Lipid	Examples and US FDA and EEC E numbers	Properties	Uses
	Citric acid esters of monoglycerides (172.832) (E 472)		Emulsion products
Polyglycerol esters	(172.854) (E 475)	A hydrophobic emulsifier (HLB typically less than 4)	Limited use due to restrictive legislation. Some use in the chocolate industry in combination with lecithin as a viscosity regulator Cake mixes
Propyleneglycol esters	(17.854) (E 477)		
Sorbitane esters	Sorbitane stearate (solid) and sorbitane oleate (liquid) (172.842) (E 491)	A lipophilic emulsifier (HLB about 4). Forms an L ₂ phase with water	Emulsions
Polysorbates	Polysorbate 80 (oleate-liquid) (172.480) (E 433)	A hydrophilic emulsifier (HLB typically about 12-16). Forms micellar solutions	Frozen desserts, dressings, etc.
Sucrose esters	(172.859) (E 173)	An intermediate emulsifier (HLB estimated as about 8)	Limited use due to restrictive legislation and high cost level
Calcium and sodium stearyl lactylates	(172.844) (172.846) (E 482) (E 481)		Bread, coffee whiteners
Ethoxylated ricinic oil	(-) (-)	Emulsifiers with somewhat intermediate hydrophilicity (HLB about 6-8). Dispersible in water	Only permitted in the feed industry. Used as an emulsifier in self-emulsifying feed mixtures

the hydrophobicity of parts of the molecule itself. Modified cellulose also gives a reduction in the interfacial tension.

A second interfacially active component may also induce the surface activity of weakly surface-active proteins due to strong intermolecular interactions. Electrostatic interactions from anionic bile salts enhance the adsorption of cationic chitosan on emulsion droplets emulsified by using a mixture of phospholipids, cholesterol and such bile salts. Carrageenan interacts strongly with milk proteins, which is of importance in relation to the association to emulsions and to its application in stabilizing neutral dairy products.

5 PARTICLES AND SURFACES IN AIR

A number of food systems, as well as most feed systems consist of particles in air. Several important application properties depend strongly on the surface properties of the particles and interparticle interactions, and consequently on the chemical composition of the surface.

The *cohesive* properties are important for keeping the designed particles intact when exposed to mechanical abrasion. This is essential for foods such as breakfast cereals in flakes or for feeds in pellet form. For agglomerated systems, this is dependent on adhesive interparticle interactions.

Wetting properties are of importance when particles need to be dispersed and dissolved in water, or if the particles are expected to float or sink in a controlled way (e.g. fish feed). Oil wetting and capillary suction is of importance if pellets are to be filled with a liquid fat (high-fat feed systems).

Handling properties are of importance when powdered systems are packed, transported and handled by the final customer. These include flowability (closely related to the cohesive properties), dust formation and storage stability (lump formation due to cohesion or related to fat migration in high-fat powders).

Chemical stability may also be surface-related. The lipid exposure at the surface influences the oxidation sensitivity of cholesterol in a dairy-type powder. An encapsulating procedure using gelatine during the drying process enhances the chemical stability of

Table 2.11. Characteristic properties of a range of important technical proteins

Preparation	Main components	Characteristic properties	Use
<i>Dairy proteins</i>			
Spray-dried skimmed-milk powder	Micellar casein, whey proteins, lactose	Soluble; reacts chemically (develops aromas) when heated	Milk-replacing systems, such as baby food, ice cream, etc.
Drum-dried milk powder	Micellar casein, whey proteins, lactose, fat	Low solubility due to denaturation during processing	Chocolate, meat products
Sodium caseinate	Free casein components	Highly soluble and very surface active	Emulsions and foam products
Whey protein	Lactoglobulin, lactoalbumin and lactose, depending on the processing; denaturates at 80°C	Soluble under acid conditions, but coagulates with heating	Emulsifying or foaming additive
<i>Egg proteins</i>			
Egg white powder	Ovoalbumine, lysozyme; denaturates at 75°C	Soluble; denaturates at air/water interfaces; very heat sensitive	Foam stabilizer
Egg yolk	Phosvitin, egg yolk lecithin	Dispersible and heat sensitive; Both the protein and the lipids contribute to the functionality	Emulsifier (e.g. mayonnaise and dressings), baking products
<i>Animal protein</i>			
Gelatine	Partially hydrolysed collagen	Cool gelling properties	Texture-provided in spread emulsions and other food systems; foaming additive in candy foams
Meat powder	Myosine	Technical meat powder is a highly denaturated protein product with no solubility	Feed products, although the BSA problematic has caused limitations and restrictions
Albumin	Mainly BSA	Good solubility; denaturates with heating, at 65°C.	Meat products
Haemoglobin		Dark colour; poor solubility	Feed products
Fish protein	Mainly myosin	Technical fish powder is a highly denaturated protein product with no solubility	Feed products; of particular importance in fish feed
<i>Vegetable protein</i>			
Soybean protein	Denaturates at 92°C	Solubility varies depending on processing	As milk or meat replacer in emulsion or gel products; feed products
Potato protein		Technical potato protein is a highly denaturated protein product with absent solubility	Feed products
Gluten		Technical gluten has poor solubility but swells with water	Feed products and as an extender in certain gel products

astaxanthin (a colouring additive used in the salmon fish industry).

5.1 Wettability

The process of dissolving or dispersing a dry material in water can be divided into several steps: the wetting step, when water is surrounding and penetrating the particles, the sinking, the dispersing, when the particles

are being separated and evenly dispersed, and finally, the dissolving process, when the primary particles dissolve.

The wetting process of a porous material (for instance, a powder bed) can be described by the Washburn equation (23). This equation relates the capillary force and the flow resistance, approximating the powder as parallel capillaries with a certain radius r , as follows:

$$\frac{dh}{dt} \propto \frac{\gamma \cos(\theta)r}{h\eta} \quad (2.1)$$

where h is the penetrating height, t the time, θ the contact angle, γ the interfacial tension, r the capillary radius, and η the viscosity.

The above equation shows that the penetration is fast if, e.g. the radius is large, the viscosity is low, the interfacial tension is high and the contact angle is low (well-wetted surfaces). The initial part of the wetting is expected to be very fast (dh/dt goes to infinity when h goes to zero).

In the Washburn treatment, all parameters are assumed to be constants. However in many situations this is not true. The viscosity will increase if dry material is dissolved in the rising liquid. If the penetration is slow (a small capillary radius which corresponds to a small particle in a powder bed) and if the area is large, the viscosity increase will reduce the penetration significantly. It can easily be observed that powdered sucrose is more difficult to disperse in water than standard sucrose. Several hydrocolloids are extremely difficult to dissolve due to the viscous liquid gluing the lumps together. Agglomeration, enhancing the wetting by a larger radius and reducing the dissolution rate, improves the situation. Ethanol in the first dispersing water stage could also improve the situation due to its lower solubility to most hydrocolloids.

A second parameter that varies is the contact angle. The latter increases with increasing wetting rate according to various experiments carried out with moving surfaces penetrating through an air–water interface. This effect is particularly important when lipid-covered surfaces are wetted, causing the wetting in such systems to be a linear process with time, rather than the retarding process as predicted by the Washburn equation.

5.2 Cohesive and repulsive surface interactions

A range of interparticle interactions operates between particles dispersed in air, as with particles dispersed in water. The balance between these has its main impact on the handling properties of the particles and is consequently of significant technical interest.

van der Waals interactions are very short-range in order and as powder systems commonly consist of fairly large particles (typically 20–2000 μm), their magnitudes are most commonly insignificant.

Gravity and friction are more important when the density difference is large and the particle sizes are large. For compact large particles (like seeds), such factors

dominate, while for smaller particles (like flour or coffee powder) other interactions are of more importance.

Electrostatic interactions in air are very different compared to the electrostatic interactions in aqueous systems, as there is no ion solubility and no double layer is formed. The source of the surface charges is also different. In air, there are no possibilities for acid–base interactions or for ion disassociation. Charging in air is caused by static electricity and is stable for non-conducting particles. This makes the interaction coulombic in nature, with a range comparable to the radius of the particle. The electrostatic interactions easily dominate when the particle size is large, the density is low, and there is a low water content (low conductivity). Typical examples could be during the drying of milk powder or the transport of coffee powder.

Water bridges are formed between hydrophilic particles as a result of water condensing in the gaps between the powder particles. The driving force behind condensation depends on the sizes of such gaps. The smaller the gap, then the stronger is the driving force. Hence, water bridges are formed under almost all normal humidity conditions, although they will be smaller under dry conditions than under wet conditions. The strength of an individual water bridge is directly proportional to the radii of the surfaces in contact. The cohesive strength due to water bridges dominates in finely dispersed systems, with the number of contacts increasing as a function of the third power of the reduced particle size. A very wide particle size distribution reduces the strength due to a high frequency of large–small–large particle interaction events. This feature is commonly used when small particulates, such as silica particles, are used as anti-cohesive additives in powder systems. Water bridges in a system with soluble material, e.g. sucrose, could dissolve fractions of the material and then precipitate it to form solid bridges that may result in severe caking.

5.3 The chemical composition of the surface

The chemical composition of the surface influences the interaction (hydrophilic or hydrophobic), and the wettability (soluble, hydrophilic or hydrophobic), as well as the chemical stability. The chemical composition of the powder is a result of its technical processing, or, if non-processed, its biological structure.

If a powder, or a dry matrix, is generated from a wet system, the surface composition depends strongly

on the speed of drying. *Slow drying* (oven drying, drum drying and roller drying, among other techniques) allows the phase with the lowest interfacial tension (against air) to cover the surface. As an example, fat has been shown to cover the surface obtained by roller drying of whole milk. Similarly, the internal surfaces of fish protein pellets are covered with fat. With *fast drying* (e.g. spray drying), the air/particle surface is formed very rapidly from the liquid/water interface without allowing the system to equilibrate. Consequently, the composition of the air/particle interface is very similar to the composition of the air/water interface before drying. Surface-active material present in the system before drying (for instance, protein in a skimmed-milk system) dominates the powder after drying, while insoluble components usually stay well encapsulated. However, fat may leak out of the surface due to air/water contact before drying or because of sensitivity towards the mechanical treatment after the immediate drying. *Freeze-drying* is a special drying form carried out under solid/solid conditions. Ideally, this method should give a composition similar to the composition in solution, but if the ice contains non-frozen water the latter may cause enrichments at the ice/water interfaces that could appear in the final freeze-dried powder.

5.4 Characterisation of powder surfaces

A range of methods are used to characterize powder surfaces. Important techniques include methods for describing the cohesive character, compressibility, particle sizes, porosity, density and wettability. However, in this section we will focus on chemical characterization as a novel contribution to the understanding of powder properties.

The classical chemical surface analysis method is free-fat extraction. This technique gives a measure of the fraction of the fat component which is accessible to the solvent used during a rapid extraction. The data obtained are only a crude measure, which is very sensitive to the amount of exposed surface.

A new technique has been developed using Electron Spectroscopy for Chemical Analysis (ESCA) (24). This method is based on the surface sensitivity of ESCA, where the analytical depth is about 2 nm, which allows the outer surface to be analysed separately from the bulk of the material. ESCA gives the elemental composition (except hydrogen) which thus allows the user to divide the surface into components of the same number as the number of elements presents (normally three, i.e. protein, carbohydrate and fat).

6 CONCLUDING REMARKS

Food and feed dispersions vary enormously in character. We face problems with an extreme complexity in terms of chemical heterogeneity and structural diversity. Clearly, this limits our expectations about the ability to predict and design the properties of various formulations. However, at the moment we are increasing our understanding in the fundamental field of surface chemistry, as well as in food chemistry and structure. By selecting the appropriate knowledge based on the chemical and structural constraints of the systems, and by applying the colloidal theories with care, a lot more understanding should be obtained.

7 REFERENCES

1. Boode, K. and Walstra P., Partial coalescence in oil-water emulsions 1. Nature of the aggregation, *Colloid Surf. A*, **81**, 121-137 (1993).
2. Boode, K., Walstra P. and De Groot-Mosterd, A.E.A., Partial coalescence in oil-water emulsions 2. Influence of the properties of the fat, *Colloid Surf. A*, **81**, 139-151 (1993).
3. Gandolfo, F. G. and Rosano, H. L., Interbubble gas diffusion and the stability of foams, *J. Colloid Interface Sci.*, **194**, 31-36 (1997).
4. Weaire, D., Hutzler, S., Verbist, G. and Peters, E., A review on foam drainage, in *Advances in Chemical Physics*, Vol. 102, Prigogine, I. and Stuart, A. R. (Ed.), Wiley, New York, 1997, pp. 315-374.
5. Bergenstahl, B. and Claesson P., Surface forces in food emulsions in *Food Emulsions*, Friberg, S. and Larsson, K. (Eds.), Marcel Dekker, New York, 1997, pp. 57-110.
6. Parsegian, V. A., Fuller N. and Rand P., Measured work of deformation and repulsion of lecithin bilayers, *Proc. Natl. Acad. Sci. USA*, **76**, 2750-2754 (1979).
7. Israelachvili, J. N. and Wennerström, H., Entropic forces between amphiphilic surfaces in liquids, *J. Phys. Chem.*, **96**, 520-531 (1992).
8. Israelachvili, J. N. and Pashley, R. M., Molecular layering of water at surfaces and origin of repulsive hydration forces, *Nature (London)*, **306**, 249-250 (1983).
9. Christensson, H. K. and Blom, C. E., Solvation forces and phase-separation of water in a thin-film of nonpolar liquid between mica surfaces, *J. Chem. Phys.*, **86**, 419-424 (1987).
10. Dedinaitė, A., Claesson, P. M., Campbell, B. and Mays, H., Interactions between modified mica surfaces in triglyceride media, *Langmuir*, **14**, 5546-5554 (1998).
11. Closs, C. B., Conde-Petit, B., Roberts, I. D., Tolstoguzov, V. B. and Escher, F., Phase separation and rheology of aqueous starch galactomannan systems, *Carbohydrate polym.*, **39**, 67-77 (1999).

12. Antonov, Y. A., Lefebvre, J. and Doublier, J. L., On the one phase state of aqueous protein uncharged polymer systems: Casein-guar gum systems, *J. Appl. Polym. Sci.*, **71**, 471–482 (1999).
13. Pacek, A. W., Ding, P., Nienow, A. W. and Wedd, M., Phase separation and drop size distribution in homogenous Na-alginate/Na-caseinate mixtures, *Carbohydrate Polym.*, **42**, 401–409 (2000).
14. Loren, N., Langton, M., and Hermansson, A. M., Confocal scanning microscopy and image analyses of kinetically trapped phase separated gelatine maltodextrin gels, *Food Hydrocolloids*, **13**, 185–198 (1999).
15. Griffin, W. C., Classification of surfactant active agents by HLB, *J. Soc. Cosmetic Chem.*, **1**, 311–326 (1949).
16. Davies, J. T., A quantitative kinetic theory of emulsion type I. Physical chemistry of the emulsifying agent, in *Proceedings of the 2nd Congress on Surface Activity*, Vol. 1, Butterworths, London, 1957, pp. 426–438.
17. Shinoda, K. and Saito, H., The stability of O/W emulsions as a function of temperature and HLB of the emulsifier/the emulsification by HLB, *J. Colloid Interface Sci.*, **30**, 258–263 (1968).
18. Krog, N., Food emulsifiers, in *Food Emulsions*, Friberg, S. and Larsson, K. (Eds.), Marcel Dekker, New York, 1997, pp. 141–188.
19. Friberg, S. and Wilton, I., Liquid crystals – the formula for emulsions, *Am. Parfum. Cosmet.*, **85**, 27–30 (1970).
20. Israelachvili, J., Mitchell, D. J. and Ninham, B., Theory of self-assembly of hydrocarbon amphiphiles into micelles and bilayers, *J. Chem. Soc. Faraday Trans. 1*, **72**, 1525–1568 (1976).
21. Hasenhuettl, G. L. and Hartel, R. W. (Eds.), *Food Emulsifiers and their Applications*, Chapman Hall, New York, 1997.
22. Islam, A. M., Phillips, G. O., Sljivo, A., Snowden, M. J. and Williams, P. A., A review of recent developments on the regulatory, structural and functional aspect of gum arabic, *Food Hydrocolloids*, **11**, 493–505 (1997).
23. Washburn, E. W., The dynamics of capillary flows, *Phys. Rev.*, **1**, 273–283 (1921).
24. Fäldt, P. and Bergenståhl, B., The surface composition of spray-dried protein-lactose powders, *Colloid Surf. A*, **90**, 183–90 (1994).

CHAPTER 3

Surface Chemistry in Detergency

Wolfgang von Rybinski

Henkel, Düsseldorf, Germany

1	Introduction	53	5	Liquid/Liquid Interface	65
2	Surface Tension and Wetting	54	6	Phase Behaviour of Surfactant Systems	67
3	Adsorption at the Solid/Liquid Interface	58	7	Foaming	71
4	Complexation and Ion Exchange	61	8	References	72

1 INTRODUCTION

Washing and cleansing are processes in which many interfacial effects are involved. Therefore, a fundamental description of detergency is very complex. The interfacial processes range from the wetting of fabrics or hard surfaces and the dissolution of stains from fabrics, to the removal of ions from the washing liquor or the interaction of softeners with the fabric in the rinse cycle (1). Table 3.1 shows the different types of interfacial processes involved in the washing process. Besides this, the components involved in the washing process can be very different, including the variety of fabrics to be cleaned, liquid or solid stains with different structures and the ingredients of the detergent (2). Grouping of the different processes leads to the following main steps in washing or cleaning:

- formulation of the detergents and cleansers
- wetting of the substrate to be cleaned or washed
- dissolution of the detergent formulation
- complexation or removal by ion exchange of the ions of the washing liquor
- interaction of the detergent or cleanser with the stains
- removal of the stains from the fabric
- stabilization of the soil in the washing liquor
- modification of the substrate (e.g. by softener in the rinse cycle).

Table 3.1. Interfacial processes involved in detergency

<i>Air–water interface</i>
surface tension
film elasticity
film viscosity
foam generation
<i>Liquid–liquid interface</i>
interfacial tension
interfacial viscosity
emulsification
electric charge
active ingredient penetration
<i>Solid–liquid interface</i>
adsorption
dispersion
electric charge
<i>Solid–solid interface</i>
adhesion
flocculation
heterocoagulation
sedimentation
<i>Interfaces in multicomponent systems</i>
wetting
rolling-up processes

All of these processes occur either consecutively or simultaneously and are influenced by the different interfacial parameters.

Table 3.2 gives an overview of the different substrates and soil materials (3). The soils can either

Table 3.2. Substrates and soils in the washing process

<i>Water-soluble materials</i>	<i>Pigments</i>
inorganic salts	metal oxides
sugar	carbonates
urea	silicates
perspiration	humus
	carbon black (soot)
<i>Fats</i>	<i>Proteins (from)</i>
animal fat	blood
vegetable fat	egg
sebum	milk
mineral oil	skin residues
wax	
<i>Bleachable dyes (from)</i>	<i>Carbohydrates</i>
fruit	starch
vegetables	
wine	
coffee	
tea	

be solid pigments or a liquid phase like oils and fats. Usually, they occur as mixtures. The removal of soils can be either by mechanical force or by chemical degradation, e.g. by enzymes or bleaching agents.

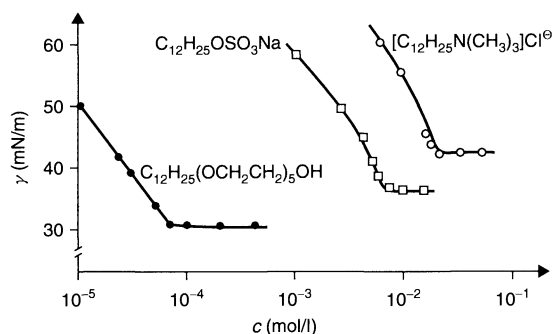
The composition of the detergent may also be very complex, containing different types of substances. Table 3.3 shows the typical major components of detergents and cleansers (4). In addition to this complex formulation, the components themselves are mixtures, as they are usually of technical grade. This makes the description and interpretation of the interfacial processes even more complex.

In the following sections, the major characteristics of the individual interfacial processes of the washing procedure relating to Table 3.1 are summarized,

concentrating on the more general features applicable to different detergent types. We will concentrate on the major components of detergents. Minor but equally important ingredients such as enzymes, soil-repellents, perfume oils, etc. have also been studied to a certain extent regarding their interfacial effects. As these effects are quite similar to those of the mentioned major components, they are not described in detail in the following.

2 SURFACE TENSION AND WETTING

The characteristic effect of surfactants is their ability to adsorb on to surfaces and to modify the surface properties. At the gas/liquid interface, this leads to a reduction in surface tension. Figure 3.1 shows the dependence of surface tension on the concentration for different surfactant types (5). It is obvious from this figure that the nonionic surfactants have a lower surface

**Figure 3.1.** Surface tensions of several surfactants with the same chain length as a function of concentration (5)**Table 3.3.** Major components of powder detergents

Ingredients	Composition (%)			
	United States, Canada, Australia	South America, Middle East, Africa	Europe	Japan
<i>Surfactants</i>	8–20	17–32	8–20	19–25
Foam boosters	0–2	–	0–3	–
Foam depressants	–	–	0.3–5.0	1–4
<i>Builders</i>				
– Sodium triphosphate	25–35	20–30	20–35	0–15
– Mixed or non-phosphate	15–30	25–30	20–45	0–20
– Sodium carbonate	0–50	0–60	–	5–20
Antiredeposition agents	0.1–0.9	0.2–1.0	0.4–1.5	1–2
Anticorrosion agents	5–10	5–12	5–9	5–15
Optical brighteners	0.10–0.75	0.08–0.50	0.10–0.75	0.1–0.8
Bleach	–	–	15–30	0–5
Enzymes	–	–	0–0.75	0–0.5
Water	6–20	6–13	4–20	5–10
Fillers	20–45	10–35	5–45	30–45

tension for the same alkyl chain length and concentration than the corresponding ionic surfactants. The reason for this is the repulsive interaction of ionic surfactants in the adsorption layer, which leads to a lower surface coverage than for the nonionic surfactants. In detergent formulations, this repulsive interaction can be reduced by the presence of electrolytes which compress the electrical double layer and therefore increase the adsorption density of the anionic surfactants. The second effect which can be seen from Figure 3.1 is the discontinuities of the surface tension–concentration curves, with constant values for the surface tension above these point. The breakpoint of the curves can be correlated to the critical micelle concentration (cmc), above which the formation of micellar aggregates can be observed in the bulk phase. These micelles are characteristic of the ability of surfactants to solubilize hydrophobic substances in aqueous solution. Therefore, the concentration of surfactant in the washing liquor has at least to be just above the cmc .

The presence of electrolytes increases the adsorption of anionic surfactants at the gas/liquid interface, as already mentioned. This leads to a reduction of the surface tension at an equal solution concentration (5) and to a strong decrease of the cmc (Figure 3.2). This effect can be of the magnitude of several decades in order. Similar to this are the effects of mixtures of surfactants with the same hydrophilic group and different alkyl chain lengths or mixtures of anionic and nonionic surfactants (6). Such mixtures follow the mixing rule (equation (3.1)) in the ideal case, as follows:

$$\frac{1}{cmc_{\text{mix}}} = \frac{\alpha}{cmc_1} + \frac{1-\alpha}{cmc_2} \quad (3.1)$$

where cmc_{mix} , cmc_1 and cmc_2 are the critical micelle concentrations of the mixture, surfactant 1 and

surfactant 2, respectively, and α is the mole fraction of the surfactant in the bulk solution.

According to a theory, which is itself based on the regular solution theory, the deviation from ideal behaviour can be described by the introduction of the activity coefficients, f_1 and f_2 , as follows:

$$\frac{1}{cmc_{\text{mix}}} = \frac{\alpha}{f_1 cmc_1} + \frac{1-\alpha}{f_2 cmc_2} \quad (3.2)$$

$$f_1 = \exp \beta(1-x_1)^2 \quad (3.3)$$

$$f_2 = \exp(\beta x_1^2) \quad (3.4)$$

$$\Delta H_m = \beta RT x_1(1-x_1) \quad (3.5)$$

where f_1 and f_2 are the activity coefficients of components 1 and 2, respectively, β is the interaction parameter, x_1 is the mole fraction of component 1 in the micelle, and ΔH_m is the micellization enthalpy.

The interaction parameter β characterizes the deviation from ideal behaviour. If β has negative values, there is an attractive interaction between the surfactants, and the cmc of the mixture is lower than that expected for ideal behaviour. For $\beta > 0$, there is a repulsive interaction and the cmc is higher than for ideal behaviour. For highly negative values of β and cmc values for the surfactants which are quite similar, the cmc of the mixture is even lower than those of the single surfactants. The strongest interactions are observed for mixtures of anionic and cationic surfactants, due to the electrostatic forces between the head groups. An example of the influence of the interaction of the surfactant molecules on the cmc is shown in Figure 3.3. The interaction between the surfactants has not only an influence on the cmc , but also on various other properties which are relevant to washing and cleaning. Thus, a synergistic effect has

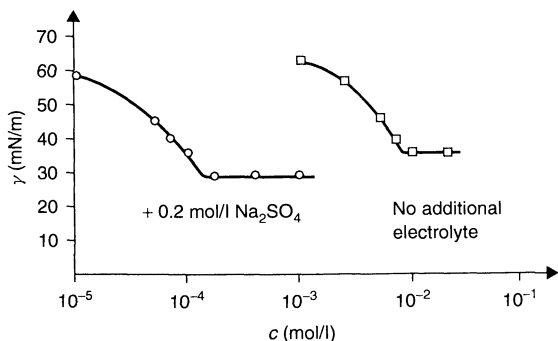


Figure 3.2. Influence of counterions on the surface activity of a typical anionic surfactant as a function of the surfactant concentration (5)

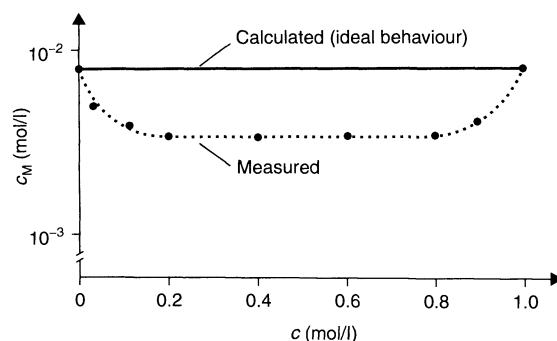


Figure 3.3. Critical micelle concentrations of mixtures of sodium *n*-dodecyl sulfonate and *n*-octylnona glycol ether (5)

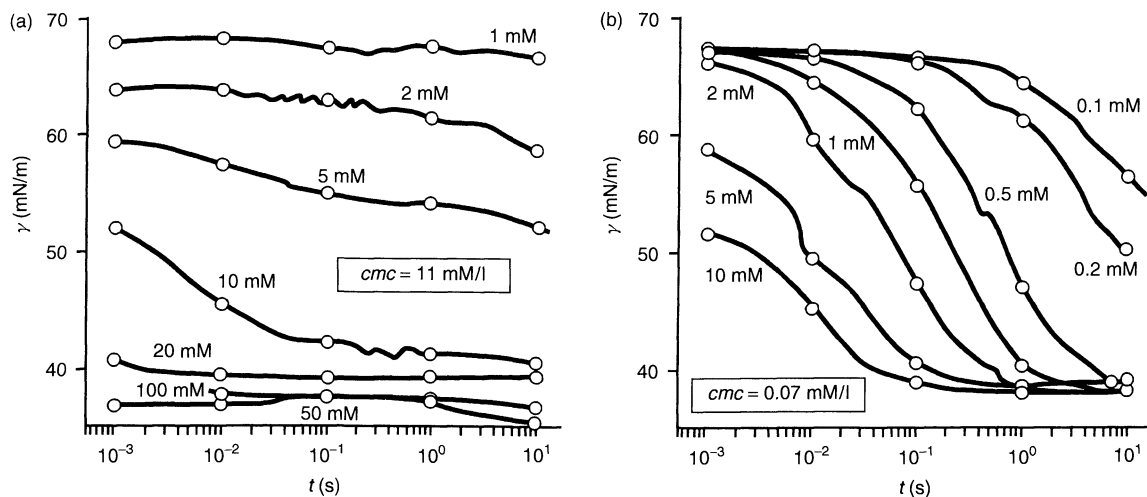


Figure 3.4. Dynamic surface tensions of (a) $C_{12}SO_3Na$ ($c_{ms} = 11$ mmol/l) and (b) $C_{12}E_6$ ($c_{mc} = 0.07$ mmol/l) as a function of concentration at $40^\circ C$ (7)

been observed for foaming, emulsification and dispersing properties, and even washing and cleaning efficiency for negative β parameters (6).

An aspect which has been underestimated for a long time regarding the mechanisms of washing and cleaning is the kinetics of surface effects. Particularly at lower concentrations, there might be a strong influence of time on the surface and interfacial tensions. Figure 3.4 shows the dependence of time on the dynamic surface tensions of both a pure anionic and a pure nonionic surfactant at different concentrations (7). For both surfactants, the time dependence of the surface tension is greatly reduced when the concentration increases. This effect is especially pronounced when the critical micelle concentration is reached. The reason for this dependance is the diffusion of surfactant molecules and micellar aggregates to the surface, which thus influences the surface tension at newly generated surfaces. This dynamic effect of the surface tension can probably be attributed to the observation that an optimum of the washing efficiency usually occurs well above the critical micelle concentration. This effect is an important factor for cleaning and institutional washing where short process times are common.

Connected with the surface tension parameter is the wetting process of the surface, e.g. fabrics or hard surfaces. This wetting can be described by the Young equation (see Figure 3.5):

$$\gamma_s = \gamma_{sl} + \gamma_l \cos \theta \quad (3.6)$$

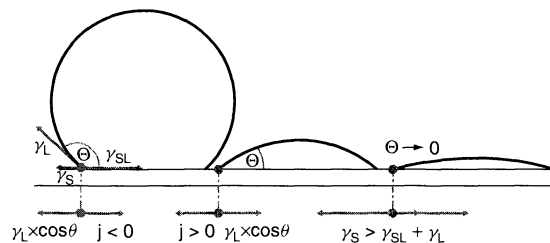


Figure 3.5. Schematic of the wetting of solid surfaces

where γ_s and γ_{sl} are the solid/gas and solid/liquid interfacial tensions, respectively, γ_l is the liquid/gas surface tension, and θ is the contact angle.

The so-called wetting tension j can be defined by the following equation:

$$j = \gamma_s - \gamma_{sl} = \gamma_l \cos \theta \quad (3.7)$$

A complete wetting of a solid is only possible for spontaneous spreading of a drop of the liquid at the surface, i.e. for $\theta = 0$ or $\cos \theta = 1$. For a specific solid surface of low surface energy, a linear correlation is observed between $\cos \theta$ and the surface tension. This is demonstrated for polytetrafluoroethylene in Figure 3.6. The limiting value, i.e. $\cos \theta = 1$, is a constant for a solid and is called the critical surface tension of a solid, γ_c . Therefore, only liquids with $\gamma_l \leq \gamma_c$ are able to spontaneously spread on surfaces and to wet them completely.

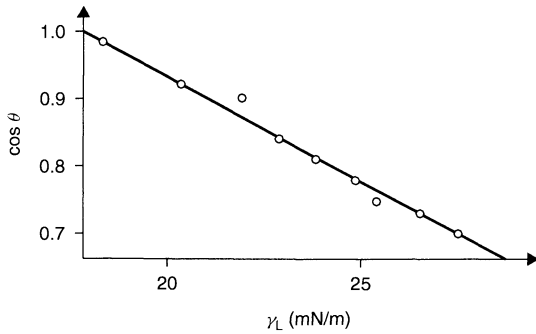


Figure 3.6. Influence of the surface tensions of various fluids on the wetting of polytetrafluoroethylene according to Fox and Zismann (cf. ref. 4)

Table 3.4. Critical surface tension values of a number of polymer solids (8)

Polymer	γ_c at 20°C (mN/m)
Polytetrafluoroethylene	18
Polytrifluoroethylene	22
Poly(vinyl fluoride)	28
Polyethylene	31
Polystyrene	33
poly(vinyl alcohol)	37
poly(vinyl chloride)	39
poly/(ethylene terephthalate)	43
poly(hexamethylene adipamide)	46

Table 3.4 gives an overview of the critical surface tension values of different polymer surfaces (8). From these data, it is obvious that polytetrafluoroethylene surfaces can only be wetted by specific surfactants with a very low surface tension, e.g. fluoro surfactants. Figure 3.7 shows the wetting tensions of two all-purpose cleaners for different surfaces (9). As these tensions are in very good agreement with the surface tensions of the cleaners, a spreading of the cleaner solution on the surfaces and therefore a good wetting can be assumed. It is only on polytetrafluoroethylene surfaces that an incomplete wetting is observed.

In cleaning and washing, the situation becomes more complicated due to the presence of oily or fatty soils on the surface. In this case, there is a competition between the wetting by the surfactant solution and that of the oily soil (Figure 3.8). When two droplets – one of the surfactant solution and one of the oily soil – are set on a solid surface, the two wetting tensions j_A and j_B will act on the basal plane (3). When the two droplets approach each other, so that a common interface is formed, the difference between the wetting tensions will act at the contact line. This parameter is called the oil

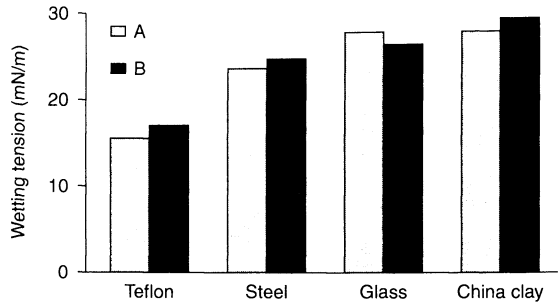


Figure 3.7. Wetting tensions of two all-purpose cleaners (A and B) on different surfaces (9)

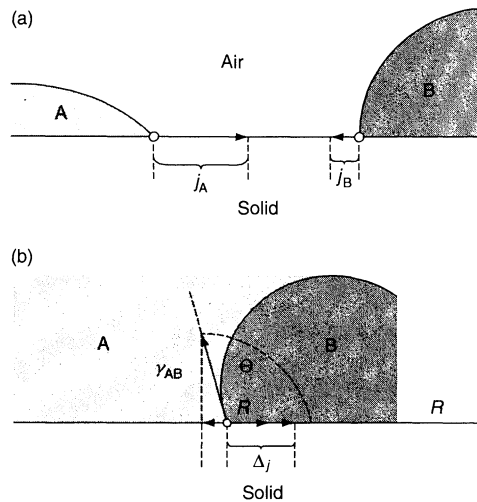


Figure 3.8. Two liquids, A (detergent) and B (oily soil), on a solid surface, shown for (a) separated and (b) in-contact situations: j_A and j_B = wetting tensions; γ_{AB} = interfacial tension; R = interfacial wetting tension (3)

displacement tension, as follows:

$$\Delta j = j_A + j_B \tag{3.8}$$

By the adsorption of the surfactant from the phase A, j_A is increased and thus Δj becomes larger. In addition to this, a fraction of the interfacial tension γ_{AB} acts in the basal plane with a value of $\gamma_{AB} \cos \theta$, with θ being the contact angle in B, i.e. the oily phase. The resulting force R is called the contact tension and is defined as follows:

$$R = \Delta j + \gamma_{AB} \cos \Theta \tag{3.9}$$

When R becomes equal to zero, equilibrium is reached. For the washing and cleaning processes, the complete

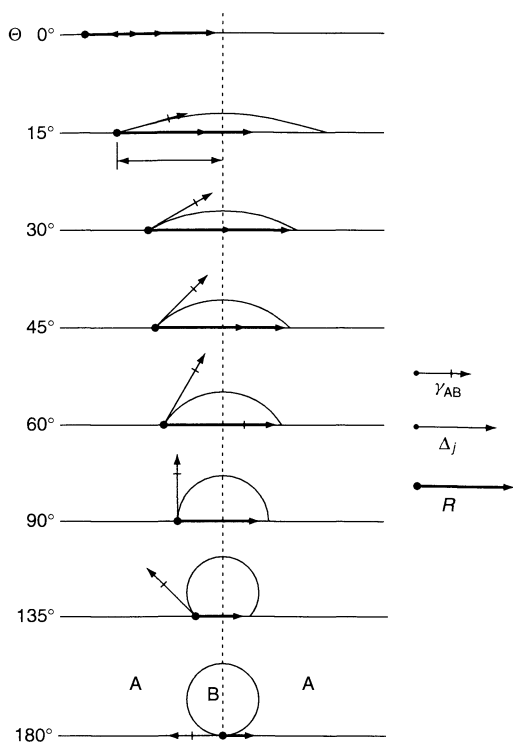


Figure 3.9. Schematic of the displacement phases of an oily drop B by a cleanser A (10)

removal of the oil B by the surfactant solution A is the important step. This process is shown schematically in Figure 3.9 (10). The interfacial tension γ_{AB} for $90^\circ > \theta > 0^\circ$ supports the contraction of the oil drop in the first step. For a contact angle $\theta > 90^\circ$, this will change and the interfacial tension acts in an opposite way. Dependent on Δ_j and γ_{AB} , a complete removal of the oil can occur. In practice, the rolling-up is never complete, so that support of the removal of the oil drop from a solid surface by mechanical forces is necessary for the washing and cleaning step.

3 ADSORPTION AT THE SOLID/LIQUID INTERFACE

The physical separation of soil from fabrics is based on the adsorption of surfactants and ions on the fabric and soil surfaces. For a pigment soil, the separation is caused by an increased electrostatic charge due to the adsorption (Figure 3.10) (11). In the aqueous washing liquor, the fabric surface and the pigment soil are charged negatively due to the adsorption of OH^- ions

and anionic surfactants. This leads to an electrostatic repulsion. In addition to this effect, a disjoining pressure occurs in the adsorbed layer which supports the lift-off process of the soil from the surface. For a spherical particle with a radius r the, separation force (f_d) is described by the following (11):

$$f_d = 2\pi r(\pi_s + \pi_p) \quad (3.10)$$

where π_s and π_p are the disjoining pressures in the adsorption layers of the substrate and particle, respectively.

The non-specific adsorption of surfactants is based on the interaction of the hydrophilic head-group and the hydrophobic alkyl chain with the pigment and substrates surfaces, as well as the solvent. For the adsorption of surfactants, different models have been developed which take into account different types of interactions. A simple model which excludes lateral interactions of the adsorbed molecules is the Langmuir equation:

$$\frac{1}{Q_\infty} = \frac{1}{bQ_m} \frac{1}{c} + \frac{1}{Q_m} \quad (3.11)$$

where Q_∞ and Q_m are the amounts absorbed at equilibrium and in a fully covered mono layer, respectively, c is the equilibrium concentration in solution, and b is a constant.

This model is restricted to only a very few systems. A more widely applicable model is presented in Figure 3.11 which shows a visualization of the dependence of the structure of the adsorbed molecules on surface coverage (12). Three different ranges can be distinguished. In the low concentration range, single molecules are adsorbed on the surface with no interactions between the molecules. The molecules are preferably arranged on the surface in a flat structure or at a certain tilt angle. For ionic surfactants, the adsorption sites on the surface are determined by the locations of surface charge. When the surfactant concentration increases, a strong rise in the adsorbed amounts is observed due to the lateral interactions of the hydrophobic parts of the surfactant molecules. The latter have a perpendicular arrangement on the surface. There are different models for the structure of the adsorbed layer in this concentration range, either assuming a flat monolayer or a hemimicellar structure, depending on the structure of the surfactants and the charge distribution on the solid surface. The hydrophilic groups of the surfactants can be directed either to the surface of the solid or to the solution depending on the polarity of the solid surface. In the third part of the adsorption isotherm, a plateau value is observed. During a further increase of the surfactant concentration,

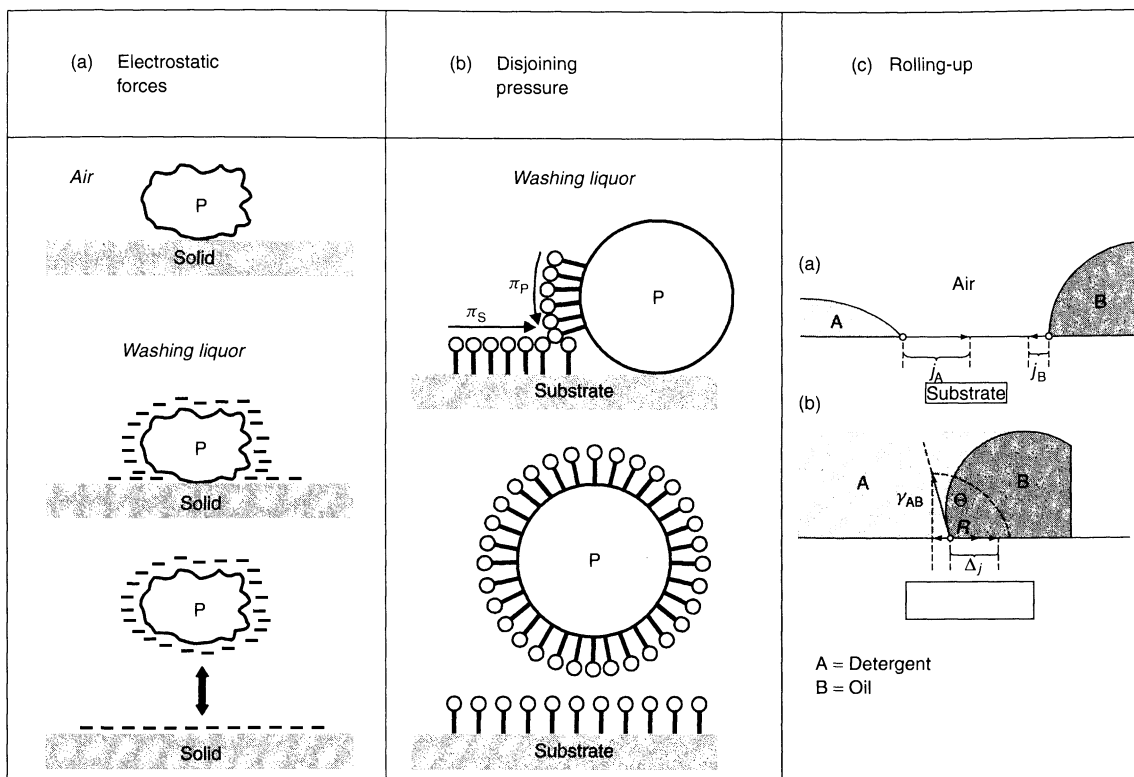


Figure 3.10. Separation mechanisms of detergency (11)

a rise in the adsorbed amounts occurs. In this range of the adsorption isotherm, a fully covered monolayer or double layer is adsorbed on to the surface, hence making the surface either hydrophilic or hydrophobic.

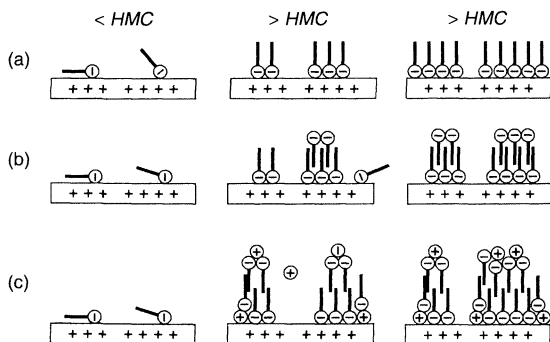


Figure 3.11. Adsorption models for surfactants: (a) model of Fuerstenau; (b) model of Scamehorn and co-workers; (c) model of Harwell and co-workers (12) (*hmc*, hemimicelle concentration)

Depending on the type of the surface, in some cases micellar structures of the adsorbed surfactants have been postulated instead of flat double layers. Typical examples of adsorption isotherms of sodium dodecyl sulfate on to different surfaces are shown in Figure 3.12 (11). The adsorption isotherms for the carbon black and the graphitized carbon black (Graphon) are completely different. For graphitized carbon black, a step-like adsorption isotherm is observed which indicates the flat arrangement of the surfactant molecules on the surface at low concentrations with a perpendicular structure at higher concentrations (see Figure 3.11). The adsorption process is exothermic with an adsorption enthalpy of about -128 to -36 kJ mol^{-1} . The adsorption of sodium dodecyl sulfate on titanium dioxide is an example of the specific adsorption via the hydrophilic group on to the polar pigment surface. A second adsorption layer is formed via hydrophobic interaction with the first adsorption layer, which thus makes the pigment surface hydrophilic again in the range of the plateau of the adsorption isotherm. Figure 3.12 also demonstrates the effect of the addition of electrolytes which are

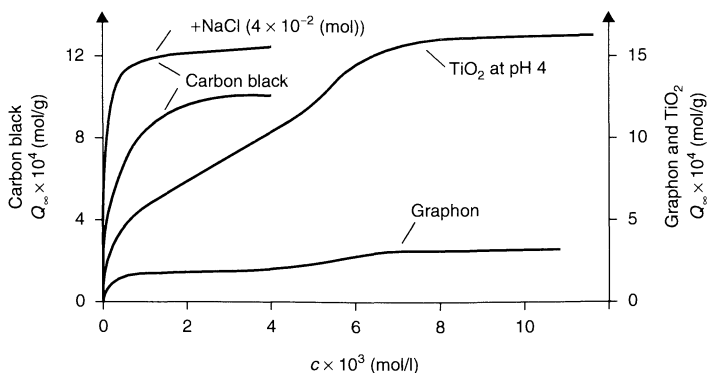


Figure 3.12. Equilibrium adsorption isotherms of sodium *n*-dodecyl sulfate on carbon black, TiO_2 , and Graphon at room temperature (11)

present in the washing process. In the presence of ions, the amounts adsorbed of the anionic surfactant are increased. This is due to a decreased electrostatic repulsion of the negatively charged hydrophilic groups of the anionic surfactant in the presence of electrolytes. Therefore, the adsorption density in equilibrium can be enhanced significantly. A similar effect can be observed in a comparison of an anionic and nonionic surfactant with the same alkyl chain length adsorbed on to a hydrophobic solid (Figure 3.13) (11). The nonionic surfactant gives higher adsorbed amounts than the anionic surfactants at the same concentrations. This is especially valid at low concentrations, whereas at very high concentrations both surfactants reach the same plateau value. For a hydrophilic solid surface, this effect can be almost opposite due to a higher affinity of anionic surfactant to the surface via specific interactions.

The electrolyte effect for the adsorption of anionic surfactants which leads to an enhancement of soil removal is valid only for low water hardness, i.e. low

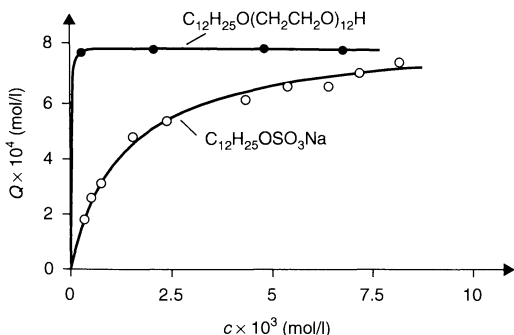


Figure 3.13. Surfactant adsorption on to carbon black: $T = 298 \text{ K}$; surface area = $1150 \text{ m}^2 \text{ g}^{-1}$ (BET) (11)

concentrations of calcium ions. High concentrations of calcium ions can lead to a precipitation of calcium surfactant salts and therefore to a reduction in concentration of the active molecules. In addition to this, the electrical double layer is compressed such an extent that the electrostatic repulsion between pigment soil and surface is reduced. Therefore, for many anionic surfactants the washing performance decreases with lower temperatures in the presence of calcium ions. This effect can be compensated by the addition of complexing agents or ion exchangers (see Section 4 below).

The characteristic change of the surface charge of the solid, which depends on the nature of the hydrophilic groups of the surfactant, is a consequence of the non-specific adsorption of the surfactants on pigments and fabrics or hard surfaces. This can be shown in aqueous solutions of different surfactants with the same alkyl chain length by the change of electrophoretic mobility of pigments, which is a measure of the surface charge (Figure 3.14) (11). The carbon black shown as an example has a negative surface charge in water at an

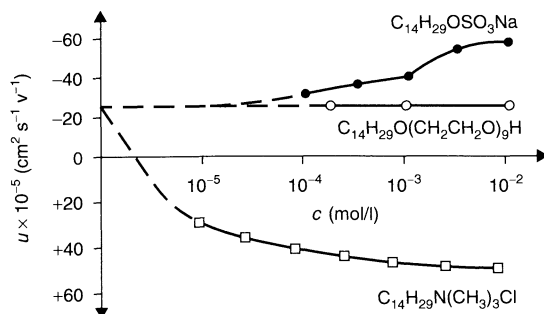


Figure 3.14. Electrophoretic mobility u of carbon black in solutions of different surfactants at 308 K (11)

alkaline pH value, as for most pigments present in the washing process the isoelectric point is below pH 10. The nonionic surfactant shows no influence on the electrophoretic mobility, whereas the anionic surfactant increases the negative surface charge of the pigment due to the adsorption. By the adsorption of the cationic surfactant the surface charge can be changed from a negative to a positive value during the adsorption process. This picture explains quite well the mode of action of different surfactant types for pigment removal in the washing process. As nonionic surfactants do not influence the electrostatic repulsion of pigment and fabric, their washing efficiency is mainly caused by the disjoining pressure of the adsorption layer. Anionic surfactants also increase the electrostatic repulsion, but usually have lower amounts adsorbed than the nonionic surfactants. Cationic surfactants show similar effects in the washing process as anionic surfactants, but in spite of this they are not suited for most washing processes due to their adverse effects in the rinse cycles. In these cycles, the positively charged surfaces (due to the adsorption of cationic surfactants) are recharged to negative values due to the dilution of the washing liquor and the consecutive desorption of cationic surfactants. As the different fabrics and pigment soils have different isoelectric points, positively and negatively charged surfaces are present in the washing liquor which leads to heterocoagulation processes and a redeposition of the already removed soil on to the fabric. Therefore, cationic surfactants are not used in the washing process, but only as softeners in the rinse cycle when no soil is present any more and a strong adsorption of cationic softener on the negatively charged fabric is desired.

4 COMPLEXATION AND ION EXCHANGE

Water-soluble complexing agents or water-insoluble ion exchangers are part of detergent formulations in order to remove calcium ions, in particular from the washing liquor (1). These calcium ions have an disadvantageous effect in the washing process due to formation of insoluble calcium salts, especially calcium carbonate which precipitates on the fabrics or on the surfaces of washing machines. In addition, the solubility of anionic surfactants is decreased by calcium ions. Besides these primary effects of complexing agents and ion exchangers, they enhance the washing efficiency by their interaction with interfaces and modify the physical properties of powder detergents. Therefore, they are

Table 3.5. Typical builders for detergents

Pentasodium triphosphate
Sodium aluminium silicate (zeolites A and X)
Sodium nitrilotriacetate
Sodium polycarboxylate
Sodium citrate

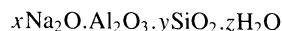
often called *builders*. Some typically used complexing agents and ion exchangers are given in Table 3.5.

Water-soluble complexing agents show a specific adsorption on to fabrics and pigment soil. If one considers the adsorption of multivalent ions on to aluminium oxide, the adsorption of sodium sulfate, for example, follows the form of the Langmuir-type isotherm. In particular, efficient builders have an isotherm of the high-affinity type, i.e. there are high amounts adsorbed at very high concentrations. This indicates a high adsorption energy, which is characteristic of chemisorption.

A well-studied system is sodium tripolyphosphate (STP). Figure 3.15 visualizes the interaction of STP with γ -Al₂O₃ for different pH values, shown at, above and below the isoelectric point (5). Below the isoelectric point, OH as well as OH₂ groups are substituted by the polyanions. At pH values above the isoelectric point, the surface of aluminium oxide has a negative charge. The electrostatic interaction between the surface and the polyanions interferes with the adsorption. Ions such as sulfate are not adsorbed any longer due to their (only possible) physical adsorption. Complexing agents such as STP or 1-hydroxyethane-1,2-diphosphonic acid (HEDP) are still adsorbed. The adsorption of complexing agents decreases in the sequence: HEDP > STP > citrate.

The adsorption of the complexing agents has a significant impact on the dispersion properties. This can be shown for the sedimentation of graphitized carbon black and kaolinite in solutions of STP (Figure 3.16) (11).

Zeolites have been used since the 1980s to replace phosphate in many detergents for preventing eutrophication of stagnant and slowly flowing surface waters. The main type of zeolite used in detergents is zeolite A. This substance is a water-insoluble, finely dispersed ion exchanger which differs regarding its properties from water-soluble complexing agents. The general formula of sodium aluminium silicates with a zeolite structure is:



The main properties of zeolites in the washing process, besides ion exchange of the calcium and magnesium ions from the water hardness, are as follows:

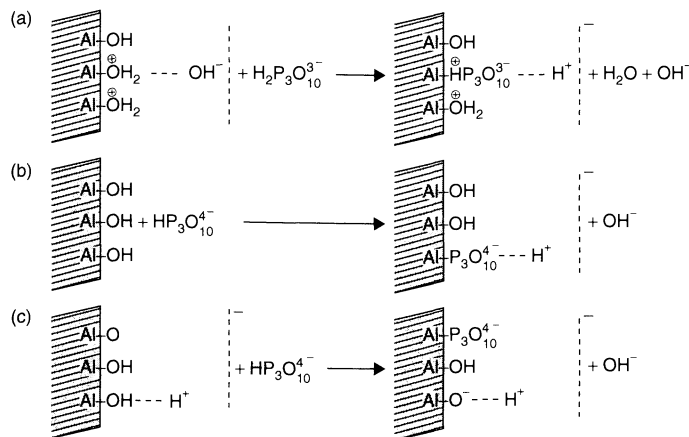


Figure 3.15. Chemisorption of the triphosphate anion on aluminium oxide: (a) pH < isoelectric point; (b) pH = isoelectric point; (c) pH > isoelectric point (5)

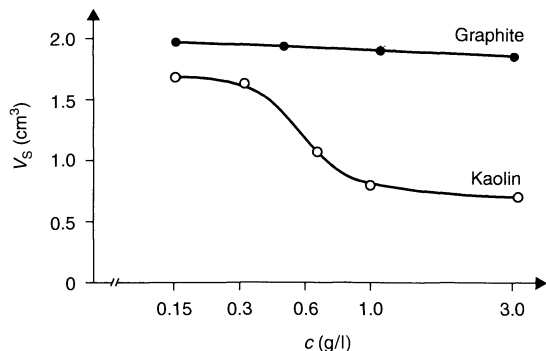


Figure 3.16. Settling volumes of graphitized carbon black and kaolinite in sodium triphosphate solutions: 16°dH water hardness; 0.30 g/(10 ml) graphitized carbon black; 0.50 g/(10 ml) kaolinite (11)

- adsorption of water-soluble substances, e.g. dyes on the zeolite particles
- heterocoagulation of pigments and solid fats with the zeolite
- action as crystallization nuclei for sparingly soluble salts.

All of these effects support the mode of action of zeolites in the washing process. The most characteristic feature of zeolites is the ion exchange of the sodium ions in the crystal structure by calcium and magnesium ions. Figure 3.17 shows the ion-exchange kinetics of zeolites A and X for calcium and magnesium ions (13). Calcium ions diffuse with a high rate into both types of zeolite, with a slight preference for the wider-pore

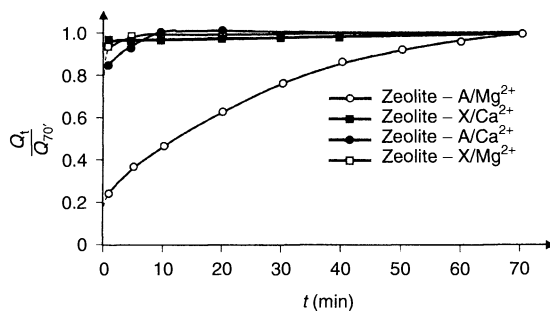


Figure 3.17. Kinetics of ion exchange of calcium and magnesium ions for zeolite A and zeolite X: $T = 25^\circ\text{C}$; ion concentration = 5.36×10^{-3} mol/l; zeolite concentration = 1 g/l (13)

zeolite X. These differences are only evident for short times which are not of practical importance for the washing process. The ion-exchange kinetics are more strongly dependent on the pore size of the ion exchanger for magnesium ions. Despite the smaller ion radius at 25°C , the magnesium ion has a more stable and bigger hydration shell than the calcium ion and therefore penetrates more slowly into the pore system of the zeolite.

A comparison between the decrease of water hardness by ion exchange and washing performance is given in Figure 3.18 (14). A decrease of the water hardness from 16 down to 3–4°dH only slightly influences the detergency performance. Only a further decrease of the calcium ion concentration leads to a significant increase of soil removal from the fabric. Due to the fact that zeolite A is an ion exchanger, the calcium ion exchange

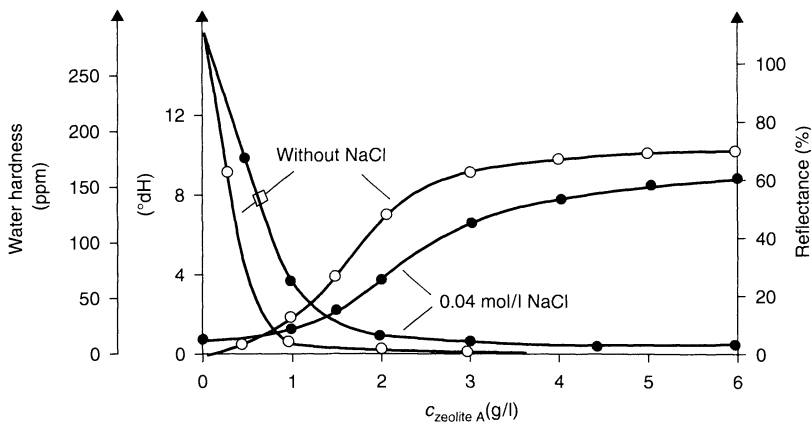


Figure 3.18. Influence of NaCl on the water-softening effect and the washing performance of zeolite A: water-softening effect at measured 90°C after 15 min; washing performance measured at 90°C and 285 ppm water hardness on particulate-sebum-soiled cotton (14)

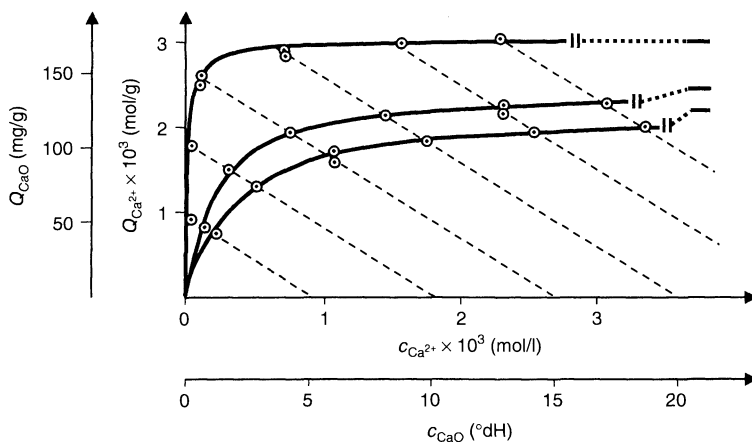


Figure 3.19. Comparison of calculated and measured isotherms of calcium ion exchange by zeolite A: $T = 22^\circ\text{C}$; 1 h exchange time (15)

is decreased by a high concentration of sodium ions, despite the high selectivity of the ion-exchange process. According to this, the detergency behaviour in the presence of sodium ions slightly decreases. The ion exchange of the zeolite can be described by the following equation:

$$Q_{\text{Ca}^{2+}} = \frac{Q_m c_{\text{Ca}^{2+}}}{c_{\text{Ca}^{2+}} + 2 \frac{b_2}{b_1} c'_{\text{Na}^+} + 2 Q_{\text{Ca}^{2+}}} \quad (3.12)$$

where $Q_{\text{Ca}^{2+}}$ is the exchanged amount of calcium ions, Q_m is the maximum exchanged amount of calcium ions, $c_{\text{Ca}^{2+}}$ is the equilibrium concentration of calcium

ions, c'_{Na^+} is the initial concentration of sodium ions, and b_1 and b_2 are constants.

Figure 3.19 shows a comparison of experimental data of the ion exchange with the calculated curves (15). Both sets of data are in good agreement. With increasing sodium concentration, not only do the maximum exchanged amounts of calcium ions decrease, but also a higher calcium ion concentration is necessary to reach the equilibrium values.

Zeolites show significant adsorption properties regarding the washing process and conditions in the waste water. Figure 3.20 demonstrates the adsorption of a cationic dye (Methylene Blue) and an anionic dye (benzopurpurine) on to zeolite A (16). The cationic

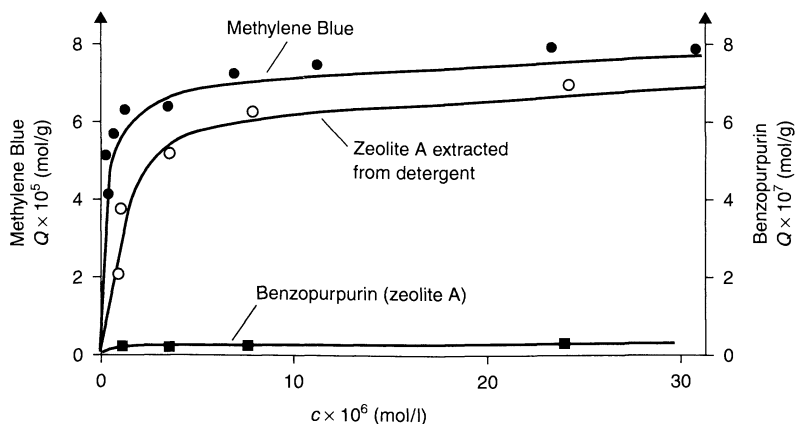


Figure 3.20. Adsorption of dyes on zeolite A, at $T = 23^\circ\text{C}$ (16)

dye is strongly adsorbed on the negatively charged surface of zeolite A, whereas the anionic dye is only adsorbed on zeolite A which is extracted from a detergent formulation produced on a technical scale. This is due to a hydrophobization of the zeolite surface in the production process, which increases the interaction of the dye and the zeolite surface.

Due to the negatively charged zeolite surface at alkaline pH values, cationic surfactants are strongly adsorbed on to zeolite A (Figure 3.21). For mixtures of cationic and nonionic surfactants, a strong increase of the adsorbed amounts is observed in a certain concentration range (17). Because of hydrophobic interactions between the adsorbed cationic surfactants and nonionic surfactant molecules, additional nonionic surfactant molecules are probably adsorbed in a second layer from mixtures. These effects have an impact on the behaviour of zeolites in waste water.

In modern detergents, zeolites are used in combination with water-soluble complexing agents or polycarboxylates. The dissolution of calcium by zeolite A is enhanced by complexing agents which specifically adsorb on calcium-containing particles and subsequently desorb after sequestering calcium ions. Even small amounts of water-soluble complexing agents increase the dissolution rate of calcium carbonate by zeolites to the extent that the dissolution rate approaches that of the water-soluble complexing agent alone. This increase is particularly pronounced over the range of small complexing agent concentrations and with short reaction times. As the water-soluble complexing agents act as carriers for the transfer of calcium from the precipitate to the water-insoluble ion exchanger, this process is known as a “carrier-effect” in the literature.

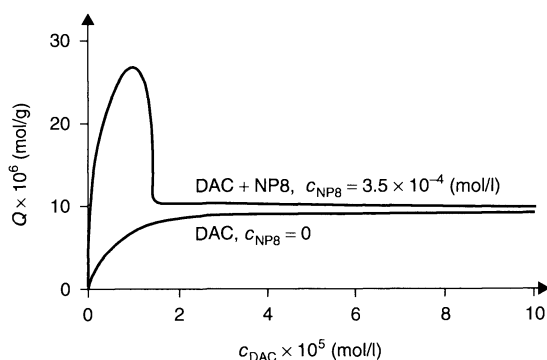


Figure 3.21. Mixed adsorption of cationic and nonionic surfactants on to zeolite A: $T = 25^\circ\text{C}$, DAC, ditallowalkyl dimethylammonium chloride; NP8, nonylphenol octaglycol ether (17)

A different effect occurs with the use of polycarboxylates in combination with zeolites. Small amounts of polycarboxylates or phosphonates can retard the precipitation of sparingly soluble calcium salts such as CaCO_3 (the “threshold effect”). As they behave as anionic polyelectrolytes, they bind cations (counterion condensation), and multivalent cations are strongly preferred. Whereas the pure calcium salt of the polymer is almost insoluble in water, mixed Ca/Na salts are soluble, i.e. only overstoichiometric amounts of calcium ions can cause precipitation. Polycarboxylates are also able to disperse many solids in aqueous solutions. Both dispersion and the threshold effect result from the adsorption of the polymer on to the surfaces of soil and CaCO_3 particles, respectively.

The stabilization of sparingly soluble salts such as CaCO_3 in a colloidal state is one of the possible

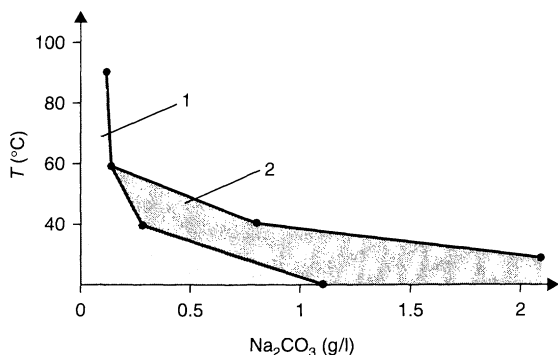


Figure 3.22. Precipitation inhibition of calcium carbonate by polycarboxylates as a function of temperature and soda concentration (3.04×10^{-3} mol/l calcium ions): (1) 105 mg/l polycarboxylate; (2) 210 mg/l polycarboxylate (18)

effects of polycarboxylates in detergents. The advantage is that, in contrast to ion exchange or complexation, the concentration of the cobuilder can be much lower than the calcium concentration in the washing liquor. Thus, small amounts of threshold-active compounds could be used as cobuilders, even in soda-based laundry detergents.

The effect, however, is strongly dependent on the experimental (or washing) conditions, i.e. temperature, and soda and cobuilder concentrations. Figure 3.22 (18) illustrates the range of effectiveness of polycarboxylates in a carbonate-containing system for typical central European conditions of water hardness (3.04×10^{-3} mol/l Ca^{2+}). The results are based on turbidity measurements. The appearance of a CaCO_3 particle larger than approximately $0.2 \mu\text{m}$ within 30 min was taken as an indicator of the threshold effect. The soda concentrations in the test include the hydrogen carbonate content of the tap water as well as the soda content of the detergent. The results show that for typical German phosphate-free, heavy-duty detergents, polycarboxylate is no longer threshold-active at temperatures above 40°C . This is valid even more for higher carbonate concentrations, i.e. purely soda-based detergents.

For zeolite A and soda-containing products, the participation of zeolite A in the elimination of calcium ions during the washing process has to be taken into account. For typical test concentrations, the amount of coarsely dispersed CaCO_3 is reduced in the presence of zeolite A over the whole range of washing temperatures. The effect of polycarboxylate on the total amount of precipitation is strongly dependent on the presence of zeolite A. In the absence of zeolite, precipitation is inhibited only below 40°C .

With increasing temperature, the precipitated amounts strongly increase. In this case, on addition of CaCO_3 , polycarboxylate is precipitated as calcium salt, as can be seen from the respective measurements of the residual concentrations of water-soluble polycarboxylate. In contrast, the amount of precipitates in the presence of zeolite A and polycarboxylate is negligibly low, and the residual concentration of water-soluble polycarboxylate is as high as in the zeolite A/polycarboxylate systems without soda.

These results can be explained by the binding of calcium ions by zeolite A and by polycarboxylate in its water-soluble form. This is possible because the calcium ion concentration of the water is lowered by zeolite A. Thus, Ca^{2+} is no longer in excess of polycarboxylate and thus formation of the insoluble calcium salt of polycarboxylate is no longer possible.

5 LIQUID/LIQUID INTERFACE

The phenomena observed at the liquid/liquid interface are of outstanding importance for the removal of oily soil from the surface. As already shown in Section 2 above, the interfacial tension is one of the decisive parameters in the rolling-up process. This parameter can be very different depending on the surfactant structure and the type of oily soil (9). Figure 3.23 shows this for two different oils and two anionic surfactants. The interfacial tension here has been recorded as a function of time. For both surfactants, the interfacial tension is the same, with lower values for the non-polar decane. To demonstrate the influence of the polarity of the oil on the efficiency of the surfactant, a more polar oil is chosen (see Figure 3.24). In this case, the interfacial tension is significantly lower when the fatty alcohol sulfate is used instead of the linear alkylbenzene sulfonate. The increase of the interfacial tension with time is probably caused by solubility of the surfactant in the oil phase. Figure 3.25 shows the interfacial tension of different detergent formulations against mineral oil. For overall low values of the interfacial tension there are significant differences between the detergents, which thus indicate a different performance against this non-polar oil.

As the interfacial tension needs to be minimized in detergency, there is therefore the need for a further decrease of the interfacial tension in formulations. A suitable way is again to create mixed adsorption layers of suitable surfactants (3, 6). For example, the interfacial tension of the system water/olive oil as a function of composition for a surfactant mixture containing the

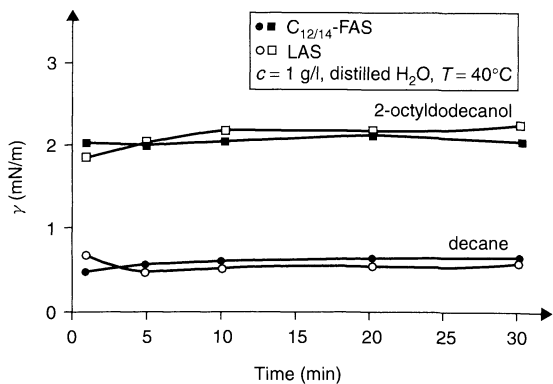


Figure 3.23. Interfacial tensions between a solution of $C_{12/14}$ -fatty alcohol sulfate (FAS) and linear alkylbenzene sulfonate (LAS) and two different oils as a function of time (9)

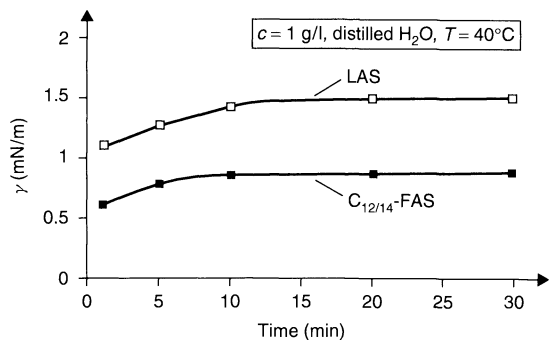


Figure 3.24. Dynamic interfacial tensions of $C_{12/14}$ -fatty alcohol sulfate (FAS) and linear alkylbenzene sulfonate (LAS) for isopropyl myristate (9)

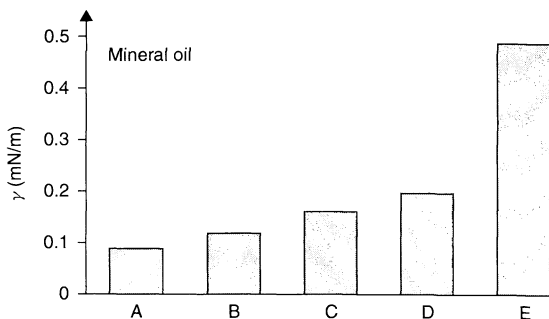


Figure 3.25. Interfacial tensions of different detergents for mineral oil (9)

anionic surfactant sodium *n*-dodecyl sulfate and the non-ionic surfactant nonylphenol octaethyleneglycol ether shows a pronounced minimum at a certain concentration ratio for a constant total surfactant concentration. Even

small additions of one surfactant to another can lead to a significant reduction of the interfacial tension. For this specific example, a minimum value of the interfacial tension is reached with a ratio of anionic surfactant to nonionic surfactant of about 4 to 1. Kinetic effects play an important part in this process. The behaviour of the mixtures can be completely different depending on the time involved, either showing a minimum of the interfacial tension for a certain concentration ratio of the surfactants or not (6). This has to be taken into account in the search for an effective surfactant system. Thus, the interfacial tension can be used to optimize detergent formulations.

The interfacial tension can be influenced by the penetration of the surfactant solution into the oily phase and the formation of new phases. A typical example is given in Figure 3.26 (19). This optical micrograph, taken under polarized light conditions, for oleic acid in contact with an aqueous solution of sodium dodecyl

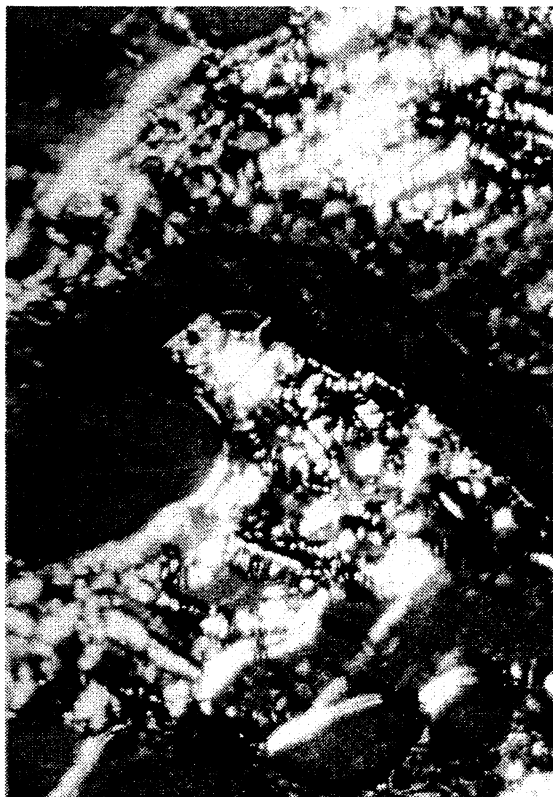


Figure 3.26. Polarized light micrograph, showing the spontaneous formation of liquid crystalline mixed phase zones (light areas) from sodium dodecyl sulfate solution (2.5%) and oleic acid (19)

sulfate illustrates the formation of liquid crystalline mixed phases. Such phases influence both the rolling-up and the emulsification of oil by surfactant solutions. For this model system, an increased removal of oil from the fabric surfaces was proven by this formation of mixed phases. These effects are described in more detail in the following section.

6 PHASE BEHAVIOUR OF SURFACTANT SYSTEMS

The phase behaviour of surfactant systems is decisive for the formulation of liquid and solid products and the mode of action of the surfactants in soil removal during the washing and cleaning processes. Due to the different phases of surfactant systems at higher concentrations, e.g. the flow properties can vary greatly depending on the concentration and type of surfactants. This is of crucial importance for the production and handling of liquid products. In addition to this, the phase behaviour influences the dissolution properties of solid detergents when water is added, forming or preventing high-viscous phases. One can distinguish between the phase behaviour of surfactant–water systems and multicomponent systems including an additional oil phase which occurs when soil is released from the surfaces.

As an example of the different phases of surfactants, Figure 3.27 shows the phase diagram of a pure nonionic surfactant of the alkyl polyglycol ether type (20). In particular, the phase behaviour of nonionic surfactants with a low degree of ethoxylation is very complex. As the lower consolute boundary is shifted to lower temperatures with a decreasing EO (ethylene oxide) number of the molecule, an overlapping of this boundary

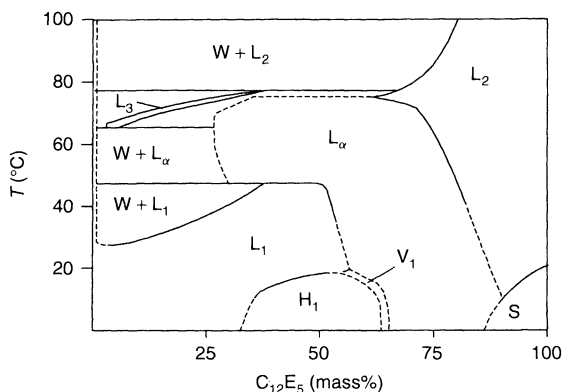


Figure 3.27. Phase diagram of the binary system water–penta-oxethylene *n*-dodecanol ($C_{12}E_5$) (20)

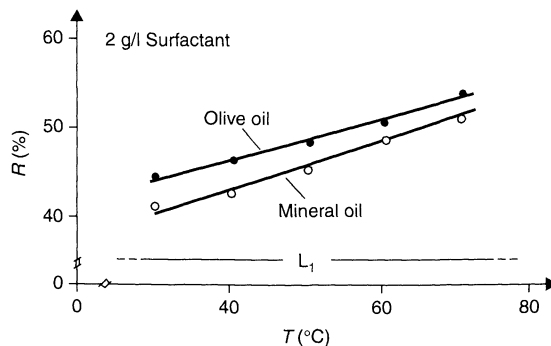


Figure 3.28. The effect of the phase behaviour of $C_{12}E_9$ on detergency (21)

with the mesophase region may result, as depicted in Figure 3.27. At low surfactant concentrations in such systems, several two-phase areas are observed in addition to the single-phase isotropic L_1 range, namely two co-existing liquid phases ($W + L_1$), a dispersion of liquid crystals ($W + L_\alpha$) and a two-phase region of water and a surfactant liquid phase ($W + L_2$).

The phase behaviour can have a significant impact on the detergency (21). If there is no phase change for the surfactant–water system, a linear dependence of the detergency on temperature is observed (Figure 3.28). The surfactant exists in an isotropic micellar solution at all temperatures. The cloud point of the surfactant used here is 85°C at the given concentration (2 g/l), i.e. above the highest washing temperature.

Tests with other pure ethoxylated surfactants have revealed that a discontinuity is observed with respect to oil removal versus temperature in cases of the existence of dispersions of liquid crystals in the water–surfactant binary system. Figure 3.29 shows that the detergency

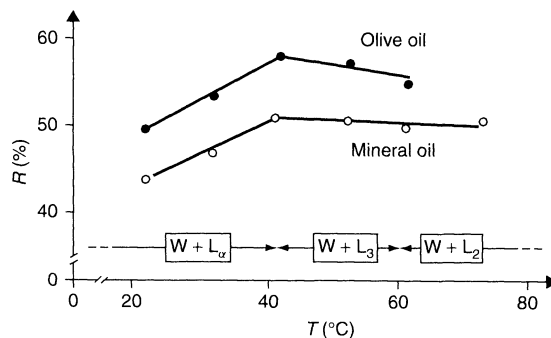


Figure 3.29. The effect of the phase behaviour of the poly-oxethylene alcohol $C_{12}E_3$ on detergency, using 2 g/l surfactant (21)

values for mineral oil and olive oil, i.e. two oils with significantly different polarities, are at different levels. This also demonstrates that in both cases a similar reflectance versus temperature curve exists. In the region of the liquid crystal dispersion, i.e. between 20 and 40°C, the oil removal increases significantly. Above the phase transition $W + L_\alpha \rightarrow W + L_3$, between 40 and 70°C, no further increase in oil removal takes place. For olive oil, a small decrease in detergent performance is observed. The interfacial tensions between aqueous solutions of $C_{12}E_3$ and mineral oil lie at about 5 mN m^{-1} at 30 and 50°C. These relatively high values indicate that in this system the interfacial activity is not the decisive factor in oil removal from fabrics. The macroscopic properties of the liquid crystal dispersion seem to be responsible for the strong temperature dependence. It can be assumed that fragments of liquid crystals are adsorbed on to fabric and oily soil in the $W + L_\alpha$ region during washing. The local surfactant concentration is therefore substantially higher in comparison to the molecular surfactant layer that forms when surfactant monomers adsorb. As the viscosity of liquid crystals in the single-phase range is strongly temperature-dependent, it can be assumed that the viscosity of a fragment of a liquid crystal deposited on a fabric also significantly decreases with increasing temperature. Thus, the penetration of surfactant into the oil phase and removal of oily soil are both promoted.

Technical-grade surfactants are of specific interest for applications. As in the case of pure nonionic surfactants, definite ranges exist in which there is only a slight dependence of oil removal on the temperature (Figure 3.30). For $C_{12/18}E_5$, this is in the range of the two co-existing liquid phases ($W + L_1$), while for $C_{12/18}E_4$ it is in the range of the surfactant liquid phase ($W + L_2$). An unusually strong increase of oil removal with increasing temperature occurs in the region of the

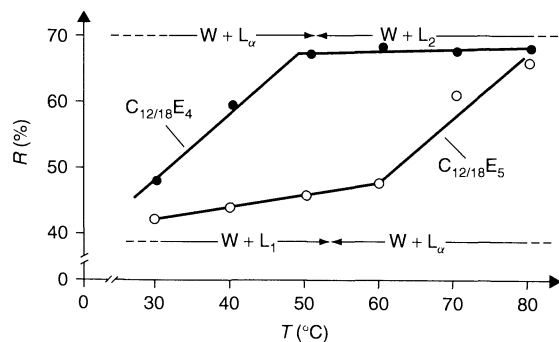


Figure 3.30. The effects of the phase behaviours of the polyoxyethylene alcohols $C_{12/18}E_4$ and $C_{12/18}E_5$ on detergency (21)

liquid crystal dispersion ($W + L_\alpha$). At 30 and 50°C, the interfacial tensions between aqueous surfactant solutions and mineral oil and the contact angles on glass and polyester were determined for $C_{12/18}E_4$. Whereas the values of interfacial tensions are practically identical (approximately $10^{-1} \text{ mN m}^{-1}$), the contact angles on both substrates are slightly less advantageous at higher temperatures. Hence, the increased oil removal between 30 and 50°C cannot be attributed to an increase in the adsorbed amounts of surfactants. Rather, in both cases, the decisive part is probably played by the macroscopic properties of the liquid crystal dispersion and their temperature dependence.

During the oil removal from fabrics or hard surfaces, ternary systems occur where three phases co-exist in equilibrium. These systems are also referred to as three-phase microemulsions. These effects have been studied in detail for alkyl polyglycol ethers (22). Depending on the temperature, different phases exist, having a three-phase region between the temperature T_1 and T_u (Figure 3.31). When these three phases are formed,

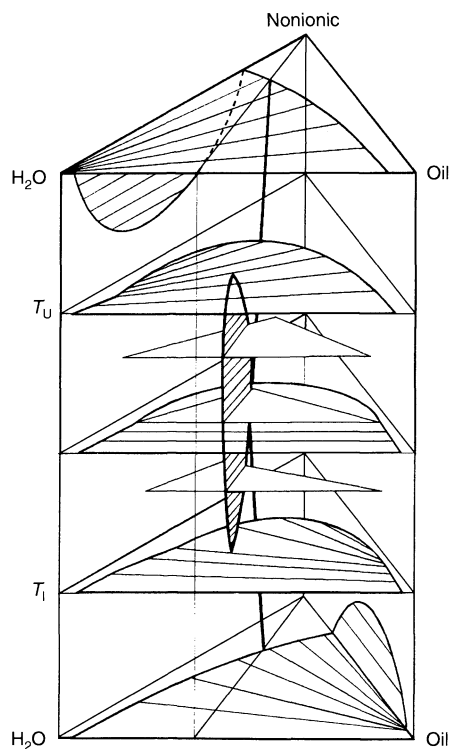


Figure 3.31. Schematic phase diagram of a ternary system consisting of water, oil and an ethoxylated nonionic surfactant (22)

extremely low interfacial tensions between two phases are observed. Because the interfacial tension is generally the restraining force, with respect to the removal of liquid soil in the washing and cleaning process, it should be as low as possible for optimal soil removal. Other parameters such as the wetting energy and the contact angle on polyester, as well as the emulsifying ability of, e.g. olive oil, also show optima at values of the same mixing ratio at which the minimum interfacial tension is observed.

Figure 3.32(b) represents the three-phase temperature intervals for $C_{12}E_4$ and $C_{12}E_5$ versus. the number n of carbon atoms of several n -alkanes, while Figure 3.32(a) shows the detergency of these surfactants for hexadecane. Both parts of this figure indicate that the maximum oil removal is in the three-phase interval of the oil used (n -hexadecane) (23). This means that not only the solubilization capacity of the concentrated surfactant phase, but probably also the minimum interfacial

tension existing in the range of the three-phase body, are responsible for the maximum oil removal. Further details about the influence of the polarity of the oil, the type of surfactant and the addition of salt are summarized in the review by Miller and Raney (24).

Studies of diffusional phenomena have direct relevance to detergency processes. Experiments have been reported which investigate the effects of changes in temperature on the dynamic phenomena, which occur when aqueous solutions of pure nonionic surfactants contact hydrocarbons such as tetradecane and hexadecane. These oils can be considered to be models of non-polar soils such as lubricating oils. The dynamic – contacting phenomena, at least immediately after contact, are representative of those which occur when a detergent solution contacts an oily soil on a synthetic fabric surface. With $C_{12}E_5$ as the nonionic surfactant at a 1 wt% level in water, quite different phenomena were observed below, above, and well above the cloud point when tetradecane or hexadecane were carefully layered on top of the aqueous solution. Below the cloud point temperature of 31°C , very slow solubilization of oil into the one-phase micellar solution occurred. At 35°C , which is just above the cloud point, a much different behaviour was observed. The surfactant-rich L_1 phase separated to the top of the aqueous phase prior to the addition of hexadecane. Upon addition of the oil, the L_1 phase rapidly solubilizes the hydrocarbon to form an oil-in-water microemulsion containing an appreciable amount of the non-polar oil. After depletion of the larger surfactant-containing drops, a front developed as smaller drops were incorporated into the microemulsion phase.

Unlike the experiments carried out below the cloud point temperature, appreciable solubilization of oil was observed in the time-frame of the study, as indicated by upward movement of the oil–microemulsion interface. Similar phenomena were observed with both tetradecane and hexadecane as the oil phases. When the temperature of the system was raised to just below the phase-inversion temperatures of the hydrocarbons with $C_{12}E_5$ (45°C for tetradecane and 50°C for hexadecane), two intermediate phases formed when the initial dispersion of L_1 drops in the water contacted the oil. One of these was the lamellar liquid crystalline phase L_α (probably containing some dispersed water). Above this was a middle-phase microemulsion. In contrast to the studies carried out below the cloud point temperature, there was appreciable solubilization of hydrocarbon into the two intermediate phases. A similar progression of phases was found at 35°C when using n -decane as the hydrocarbon. At this temperature, which is near the phase-inversion temperature of the water– $C_{12}E_5$ –decane system, the

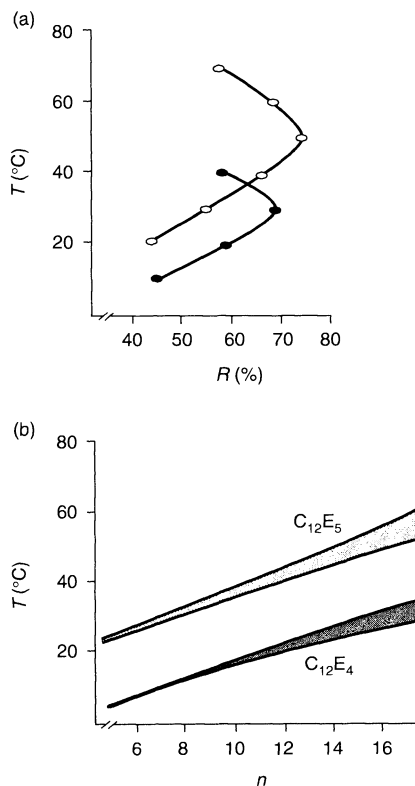


Figure 3.32. Detergency effects of $C_{12}E_4$ and $C_{12}E_5$ against hexadecane as a function of temperature (a) and the corresponding three-phase ranges for these surfactants as a function of the number n of carbon atoms of various n -alkanes (b) (23)

existence of a two-phase dispersion of L_{α} and water below the middle-phase microemulsion was clearly evident. These results can be utilized to optimize surfactant systems in detergents, and in particular to improve the removal of oily soils. The formation of microemulsions is also described in the context of the pretreatment of oil-stained textiles with a mixture of water, surfactants and cosurfactants.

Besides the effects on detergency the liquid crystalline phases of surfactant systems at higher concentrations are of crucial importance for the processing of concentrated surfactant systems and the formulation, as well as the application, of liquid products. This will be demonstrated with the help of the phase diagram of anionic surfactants for the example of fatty alcohol sulfates. Figure 3.33 shows the complete phase diagram

of sodium dodecyl sulfate (25). At higher concentrations of the surfactant, a multitude of different liquid crystalline phases occur. These liquid crystalline phases significantly influence the rheological properties of the surfactant systems (26). This is demonstrated by a comparison of the simplified phase diagram of hexadecyl sulfate and the viscosity at a constant shear rate and the yield point (Figure 3.34). With increasing surfactant concentration and a transition from the micellar solution to the hexagonal phase, a strong increase in viscosity is observed. At even higher concentrations, a lamellar liquid crystalline phase occurs which leads to a decrease in the viscosity. This high-viscous region of many surfactants in the medium-concentration range has a strong impact on the formulation and production of concentrated surfactant systems. The same is valid for

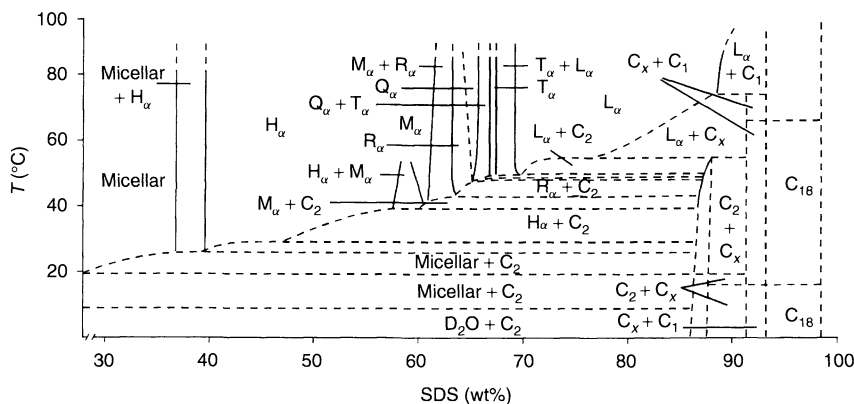


Figure 3.33. Phase diagram of sodium dodecyl sulfate (SDS) (25)

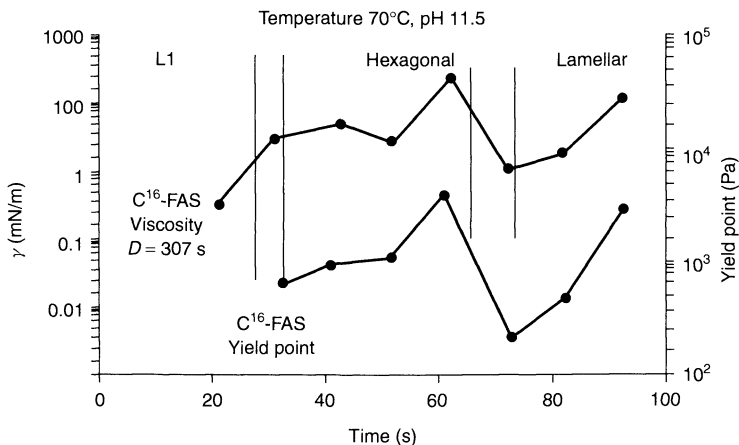


Figure 3.34. Comparison of the liquid crystalline phases with viscosities and yield points for C_{16} -fatty alcohol sulfate (FAS) as a function of concentration (26)

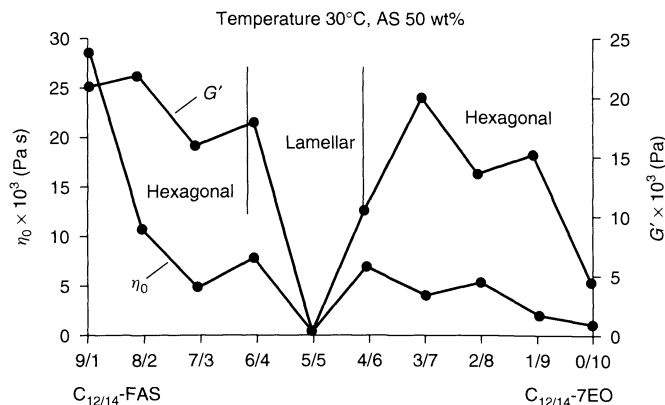


Figure 3.35. Zero shear viscosity η_0 and elastic shear modulus G' for mixtures of $C_{12/14}$ -fatty alcohol sulfate (FAS) and $C_{12/14}$ -fatty alcohol ethoxylate (7EO) as a function of the concentration ratio at a constant concentration (26)

the dissolution of concentrated solid detergents where intermediate high-viscous phases have to be avoided. The addition of nonionic surfactants to the anionic surfactants may have a strong influence of the rheological behaviour (Figure 3.35). A decrease is observed both in viscosity and yield point, which leads to improved flow properties.

7 FOAMING

Foaming and the control of foam is an important factor in the application of detergents and cleansers. This concerns high-foaming systems for, e.g. manual dish-washing detergents, as well as low-foaming systems for use in textile or dish-washing machines. The foam properties of the products are mainly governed by the surfactant system and the use of anti-foams. Besides this, the chemical composition of the product or the washing liquor, e.g. electrolyte content and soil, strongly influences the foam properties. Physical parameters, such as temperature and pH, or the mechanical input in the system, have also to be taken into account.

The basis for the foam properties is given by interfacial parameters. An overview of these parameters and the correlation with the foam properties is shown in Figure 3.36 (7). All of these parameters influence the foam properties in a complex way and have been studied in detail. Although correlations have been shown between a single parameter and foam properties, there is still the lack of a general correlation between interfacial properties and the foam behaviour of complex systems in detergency. As foam is not the specific subject of this particular chapter, the influences of the single parameters will not be discussed in detail here, and

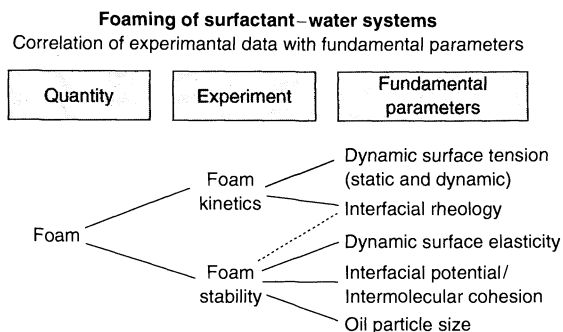


Figure 3.36. Foam properties and interfacial parameters (7)

only a specific example regarding detergency will be given. The simplest approach to correlate an interfacial parameter to the foam properties is to compare the surface activity measured by the surface tension of a surfactant system and the foam stability. This has been carried out for a series of pure surfactants. Within a specific class of surfactants, the surface tension directly correlates to the foam stability of the surfactant–water system. A more general form of this concept is not possible due to the influence of other parameters (as summarized in Figure 3.36).

As foam generation and also foam stability are dynamic processes generating and reducing the surface area, in a surfactant–water system the diffusion of the surfactant to the surface and the change in surface coverage, at least locally during bubble generation and drainage of the film, is a more useful way of describing the foam properties. If one distinguishes between foam formation and foam stability, a good correlation can be found between the relative dynamic surface pressure

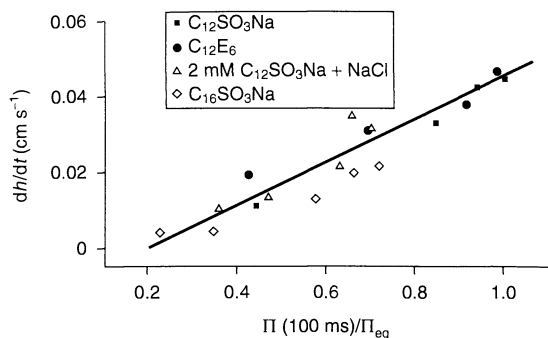


Figure 3.37. Correlation of relative dynamic surface pressures with foam kinetics data (dh/dt) as a function of the type of surfactant, alkyl chain length and salt concentration (7)

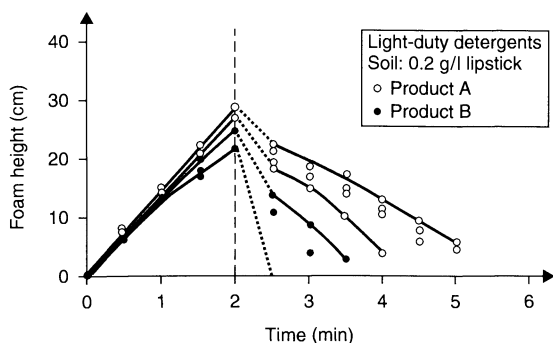


Figure 3.38. Foam stabilities of fine-textile detergents (at recommended dosage levels): $T = 40^\circ\text{C}$, 160 mg/l CaO (7)

derived from the time-dependent surface tension and the rate of foam formation (Figure 3.37). The specific time for the relative dynamic surface pressure was chosen empirically. The correlation of the two parameters is valid for different surfactant types and addition of electrolyte. This effect can be explained by the micellar kinetics of the surfactant solution and the diffusion of the molecules and micelles to the surface. The importance of these effects for finding the optimum surfactant system in detergency is shown in Figure 3.38. For high-foaming detergents, the foam stability of the products is shown in the presence of oily soils which usually suppress the foam formation. It can be demonstrated that foam stability strongly depends on the formulation, i.e. the surfactant system, and can be adjusted to a high level in this case when considering 'care aspects' of the detergents towards sensitive textiles.

8 REFERENCES

1. Cutler, W. G. and Kissa, E. *Detergency – Theory and Applications*, Marcel Dekker, New York, 1987.
2. Lange, K. R., *Detergents and Cleaners*, Hanser, Munich, 1994.
3. Jakobi, G. and Löhr, A., *Detergents and Textile Washing*, VCH, Weinheim, 1986.
4. Showell, M. S., *Powdered Detergents*, Marcel Dekker, New York, 1997.
5. Berth, P. and Schwuger, M. J., *Tenside Surfactants Det.* **16**, 3–12 (1979).
6. Jost, F., Leiter, H. and Schwuger, M. J., *Colloids Polym. Sci.*, **266**, 554–561 (1988).
7. Engels, Th., von Rybinski, W. and Schmiedel, P., *Prog. Colloid Polym. Sci.*, **111**, 117–126 (1998).
8. Shafrin, E. G. and Zisman, W. A., *J. Phys. Chem.*, **64**, 519–524 (1960).
9. Nickel, D., Speckmann, H. D. and von Rybinski, W., *Tenside Surfactants Det.*, **32**, 470–474 (1995).
10. Kling, W., *Kolloid-Z. Z. Polym.*, **115**, 37–44 (1949).
11. Schwuger, M. J., *Ber. Bunsenges. Phys. Chem.*, **83**, 1123–1137 (1979).
12. Dobias, B., Qiu, X. and von Rybinski, W., *Solid-Liquid Dispersions*, Marcel Dekker, New York, 1999.
13. Schwuger, M. J. and Smolka, H. G., *Colloid Polym. Sci.*, **254**, 1062–1069 (1976).
14. Schwuger, M. J. and Smolka, H. G., *Tenside Surfactants Det.*, **16**, 233–239 (1979).
15. Schwuger, M. J. and Smolka, H. G., *Colloid Polym. Sci.*, **256**, 1014–1020 (1978).
16. Schwuger, M. J., *J. Am. Oil Chem. Soc.*, **59**, 265–271 (1982).
17. Schwuger, M. J., von Rybinski, W. and Krings, P., *Prog. Colloid Polym. Sci.*, **69**, 167–173 (1984).
18. Schwuger, M. J. and Liphard, M., *Colloid Polym. Sci.*, **267**, 336–344 (1989).
19. Kurzendörfer, C. P. and Lange, H., *Fette, Seifen, Anstrichmittel*, **71**, 561–567 (1969).
20. Mitchell, D. J., Tiddy, G. J. T., Warring, L., Bostock, T. and McDonald, M. P., *J. Chem. Soc. Faraday Trans. 1*, **79**, 975–1000 (1983).
21. Schambil, F. and Schwuger, M. J., *Colloid Polym. Sci.*, **265**, 1009–1017 (1987).
22. Kahlweit, M., *Tenside Surfactants Det.*, **30**, 83–89 (1993).
23. (a) Benson, H. L., Cox, K. R. and Zweig, J. E., *Happi*, **21**, (1985); (b) Kahlweit, M. and Strey, R., in *Proceedings of the 5th International Conference on Surface and Colloid Science*, Potsdam, New York, 1985.
24. Miller, C. A. and Raney, K. H., *Colloids Surf.*, **A 74**, 169–215 (1993).
25. Fontell, K., *Mol. Cryst., Liq. Cryst.*, **63**, 59–82 (1981).
26. Hofmann, R., Nickel, D. and von Rybinski, W., *Tenside Surfactants Det.*, **31**, 63–66 (1994).

CHAPTER 4

Surface Chemistry in Agriculture

Tharwat F. Tadros

Wokingham, Berkshire, UK

1	Introduction	73	4	Surface Chemistry in Suspension Concentrates	78
2	Surface Chemistry in Emulsifiable Concentrates	74	5	Surface Chemistry in the Application of Agrochemical Formulations	80
3	Surface Chemistry of Emulsion Concentrates	76	6	References	83

1 INTRODUCTION

The formulations of agrochemicals cover a wide range of systems which range from simple aqueous solutions (for water-soluble actives) and self-emulsifiable oils to disperse systems of suspensions, emulsions and microemulsions. More complex formulations such as multiple emulsions and suspoemulsions (mixtures of suspensions and emulsions) are also applied in some cases. Microencapsulation of active ingredients for controlled and sustained release represents a more sophisticated approach to the formulation of agrochemicals. Solid formulations of wettable powders, grains, granules and tablets are also used in many applications.

In all of the above formulations, the role of surface chemistry is crucial, both in the formulation of the product and its subsequent application. Even for simple formulations of water-soluble actives, surface-active agents (sometimes referred to as “wettters”) are needed to enable the spray solution to adhere to the target surface and spread over a large area. The surface-active agents also play a more subtle role in optimization of biological efficacy. With self-emulsifiable oils (referred to as emulsifiable concentrates (ECs)), surfactants are added in high concentrations to ensure the spontaneity of emulsification on dilution. The adsorption and conformation of the surfactant molecules at the oil/water (O/W) interface is crucial for spontaneous emulsification of the oil

in the spray tank. With disperse systems such as suspensions (referred to as suspension concentrates (SCs) and emulsions (referred to as (EWs)), the role of surfactants and polymers in preparation of the disperse system, its long term stability and application is crucial. This requires a fundamental surface chemical approach to understand the adsorption and conformation of the surfactant and/or polymer at the interface. Microemulsions, which are thermodynamically stable systems of O/W or W/O, also require an understanding of the surface chemistry involved for production of an ultra-low interfacial tension (which is the driving force for their formation and stability).

One may list a large number of surface chemical phenomena that are crucial in the preparation of more complex systems such as multiple emulsions and microcapsules. In the first case, the formulation is a complex system of an “emulsion in an emulsion”, with the most common being a water-in-oil-in-water (W/O/W) multiple emulsion, which requires the preparation of a stable W/O emulsion that is further emulsified into an aqueous solution of another surfactant to produce the final system. Microencapsulation is a process whereby the active ingredient is surrounded by a polymer shell that allows the controlled and slow release of the active. The most common procedure for encapsulation is interfacial polymerization, whereby two monomers are allowed to react at the interface (by condensation) to produce the

required polymer shell. The role of surface chemistry in this process is obvious.

With solid formulations, such as wettable powders (micronized active ingredients plus filler and surfactant), water-dispersible grains (prepared by extrusion of a paste, spray drying or agglomeration), granules (porous substrates with the active absorbed) and tablets, surfactants are added to aid the wetting and disintegration of the solid matrix. Again, a surface chemical approach is required to ensure adequate adsorption of the surfactant molecules, reduction of the dynamic surface tension to enhance wetting and disintegration of the powder and maintenance of stability of the particles in the aqueous solution.

It is clear from the above introduction that understanding the various interfacial phenomenon involved in agrochemical formulations is crucial for the formulation chemist. Fundamental knowledge is required at a molecular level to enable the formulation chemist to select the optimum surfactants or polymers. These investigations are also essential for assessment and prediction of the long-term stability of the formulation as well as its application. For detailed information on the role of surfactants in agrochemicals the interested reader should refer to a recent book by this present author (1).

In this chapter, which is by no means comprehensive, we will give some examples of agrochemical formulations to illustrate the importance of surface chemistry in their preparation and subsequent preparation. As far as possible, we will describe the main fundamental principles that are involved.

2 SURFACE CHEMISTRY IN EMULSIFIABLE CONCENTRATES

Many agrochemicals are formulated as emulsifiable concentrates (ECs) which when added to water produce O/W emulsions either spontaneously or after gentle agitation. Such formulations are produced by the addition of surfactants to the agrochemical if the latter is an oil with a reasonably low viscosity, or to an oil solution of the chemical if the latter is a solid or a liquid with high viscosity.

Spontaneous emulsification requires a number of criteria that may be met by control of the properties of the interfacial region. Usually, a mixture of two or more emulsifiers are used, such as calcium dodecylbenzene sulphonate and an ethoxylated non-ionic surfactant (2). With such blends, a 5% emulsifier concentration in the formulation may be sufficient for spontaneous emulsification and adequate stability within

the time of application. As stated by Becher (3), the hydrophilic–lipophilic balance (HLB) method that is normally used for selection of surfactants in emulsions is inadequate for the formulation of ECs. This is not surprising, since with ECs one requires in the first place spontaneity of dispersion on dilution, which as mentioned above is governed by the properties of the interfacial region.

The importance of the properties of the interfacial region for spontaneous emulsification was first demonstrated by Gad (4), who observed that when a solution of lauric acid in oil was carefully placed on an aqueous alkaline solution, an emulsion spontaneously formed at the interface. The reason for this spontaneous emulsification is the formation of a mixed film of lauric acid and sodium laurate (produced by partial neutralization of the acid by alkali) which produces an ultra-low interfacial tension.

Several mechanisms may be proposed to explain the process of spontaneous emulsification, all of which are related to the properties of the interfacial film. The first mechanism is due to interfacial turbulence that may occur as a result of mass transfer or by non-uniform adsorption of the surfactant molecules at the O/W interface. The interface shows unsteady motions – streams of one phase are ejected and penetrate into the second phase. This is illustrated in Figure 4.1(a) which shows the localized reduction in interfacial tension caused by non-uniform adsorption of surfactants or mass transfer of surfactants across the interface (5–7). When the two phases are not in chemical equilibrium, convection currents may be formed which transfers the liquid rich in surfactants towards the areas deficient in surfactants. These convection currents may give rise to

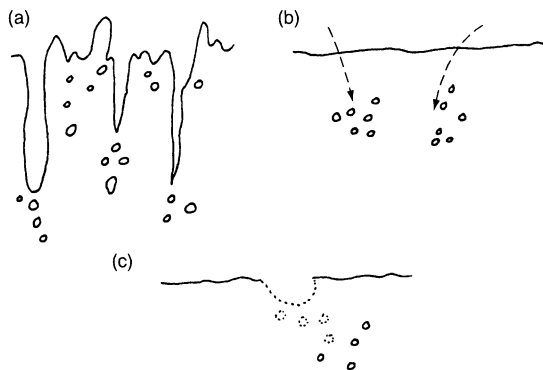


Figure 4.1. Schematic representation of spontaneous emulsification; (a) interfacial turbulence; (b) diffusion and stranding; (c) ultra-low interfacial tension

local fluctuations in the interfacial tension, hence causing oscillation of the interface. Such fluctuations may grow in amplitude, leading to violent interfacial perturbations and an eventual disintegration of the interface, when liquid drops of one phase are “thrown” into the other phase.

The second mechanism of spontaneous emulsification is based on diffusion and stranding, as represented in Figure 4.1(b). This is best illustrated by carefully placing an ethanol–toluene mixture (containing, say, 10% alcohol) on to water. The aqueous layer eventually becomes turbid as a result of the presence of toluene droplets (8). The alcohol molecules diffuse into the aqueous phase, carrying some toluene in a saturated three-component sub-phase (9). At some distance from the interface, the alcohol becomes sufficiently diluted in water to cause the toluene to precipitate as droplets in the aqueous phase. This process occurs when the third component (the alcohol) increases the mutual solubility of the two previously immiscible phases (oil and water).

The third mechanism of spontaneous emulsification may be due to the production of an ultra-low (or transiently negative) interfacial tension (see Figure 4.1(c)). The same mechanism accounts for the formation of microemulsions, which usually require the presence of two surfactant molecules (10), with one being essentially water soluble and the other essentially oil soluble. The mechanism of reduction of interfacial tension when using two surfactants can be understood from a consideration of the effect of addition of a cosurfactant on the interfacial tension γ –log concentration (c) curves (10), as illustrated in Figure 4.2. Addition of surfactant to the aqueous or oil phase causes a gradual lowering of γ , reaching a limiting value at the critical micelle concentration (cmc). Any further increase in c above the cmc causes little or no further decrease in γ . The limiting

γ value reached with most single surfactants is seldom lower than 0.1 mN m^{-1} . This value is not sufficient for microemulsion formation or spontaneous emulsification. If a surfactant mixture is used with one component predominantly water soluble, such as sodium dodecyl sulphate (SDS), and one predominantly oil soluble, such as a medium-chain alcohol (usually referred to as the cosurfactant), the limiting γ can reach very low values ($<10^{-2} \text{ mN m}^{-1}$), or can even become transiently negative (11). In the latter case, the interface expands spontaneously adsorbing all surfactant molecules until a small positive γ is reached. This behaviour is shown in Figure 4.2. As can be clearly seen, addition of the cosurfactant causes a shift of the γ –log c curve of a surfactant to lower values and the cmc is reduced.

The reason for the reduction in γ to very low values when using two surfactants can be understood from a consideration of the Gibbs adsorption equation, which may be extended for multicomponent systems (11), as follows:

$$d\gamma = - \sum \Gamma_i d\mu_i = - \sum \Gamma_i RT d \ln c_i \quad (4.1)$$

where Γ_i is the surface excess (amount of surfactant adsorbed in moles per unit area), μ_i is the chemical potential of the i th species, R is the gas constant, T is the absolute temperature and c_i is the surfactant concentration.

Integration of equation (4.1) for surfactant (s) and cosurfactant (co) gives the following:

$$\gamma = \gamma_0 - \int_0^{c_s} \Gamma_s RT d \ln c_s - \int_0^{c_{co}} \Gamma_{co} RT d \ln c_{co} \quad (4.2)$$

which clearly shows that γ_0 is lowered by two terms, from both surfactant and cosurfactant (which have surface excesses of Γ_s and Γ_{co} , respectively). It should be mentioned, however, that the both types of molecules should become simultaneously adsorbed and should not interact with each other, or otherwise they will lower their respective activities. This explains why the two types of molecules should vary in nature, i.e. with one being predominantly water-soluble and the other predominantly oil-soluble.

Several other mechanisms have been proposed to explain the dynamics of spontaneous emulsification. Direct observation by using phase contrast and polarizing microscopy showed that in some cases vesicles (closed bilayers) are produced in the oil phase near the interface with the water. These vesicles tend to “explode”, thereby pulverizing oil droplets into the aqueous phase. The above structures can be produced, for example, by using a mixture of nonionic surfactant (alcohol ethoxylate) and a long-chain alcohol such

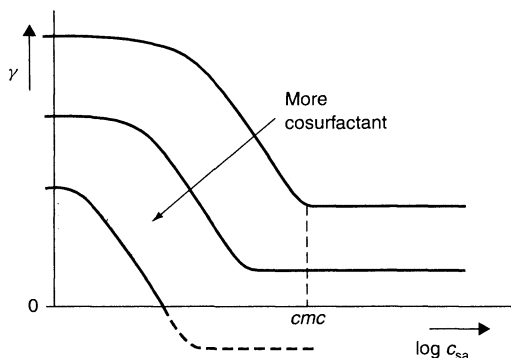


Figure 4.2. Interfacial tension (γ) versus log concentration (c) curves for surfactant plus cosurfactant

as dodecanol and an oil such as hexadecane. The oil/surfactant mixture is transparent, but on addition of a small amount of water it becomes turbid and vesicles can be observed under the microscope. The interfacial tension of the oil–surfactant mixture–water system is very low.

3 SURFACE CHEMISTRY OF EMULSION CONCENTRATES

Many agrochemicals are formulated as O/W emulsions, referred to as emulsion concentrates (EWs). These systems offer many advantages over the self-emulsifiable oils (ECs). Being aqueous-based, they produce less safety hazard to human operators, and may be less phytotoxic to plants.

In order to produce an emulsion from two immiscible liquids, one requires a third component, i.e. an emulsifier. The role of the latter can be clearly understood from a consideration of the process of emulsification, as illustrated in Figure 4.3.

The free energy of formation of the emulsion from the bulk oil (state I) is given by the following:

$$\Delta G^{\text{form}} = \Delta A\gamma_{12} - T\Delta S^{\text{conf}} \quad (4.3)$$

The first term on the right-hand side of equation (4.3) is the energy required to expand the interface (ΔA is the increase in interfacial area when the bulk oil is subdivided into a large number of droplets and γ_{12} is the interfacial tension). The second term on the right-hand side of the equation is the entropy of dispersion of the emulsion into a large number of droplets.

Since γ_{12} is positive, then the energy required to expand the interface to form a large number of droplets is positive and this term can be reduced by reducing γ_{12} , e.g. by surfactant adsorption. The entropy term, however, is positive and this favours the formation of the emulsion. With macroemulsions, $|\Delta A\gamma_{12}| > -T\Delta S^{\text{conf}}$, and hence ΔG^{form} is positive. This means that the process of emulsification is non-spontaneous and the

emulsion breaks down on storage by the processes of flocculation and coalescence. In order to maintain stability for the emulsion, one needs to introduce an energy barrier (repulsive energy) to prevent state II from converting to state I. The higher the energy barrier, then the longer the stability of the emulsion.

The above discussion shows the importance of the interfacial region in stabilizing the emulsion. For prevention of flocculation, electrostatic and/or steric repulsion is required to overcome the everlasting van der Waals attraction. The basic theory for stabilization of dispersions by using electrostatic repulsions was formulated by Deryaguin and Landau (12) and Verwey and Overbeek (13), and is thus usually referred to as the DLVO theory. The stability arises from the presence of electrical double layers around the particles (which could be the result of the presence of ionic surfactants). When two droplets with a radius R approach each other to a separation distance h that is less than twice the double layer thickness ($1/\kappa$, which depends on electrolyte concentration and valency), repulsion occurs as a result of the interaction of the double layers (which have the same charge sign). In the simple case of two large droplets and a low surface (or zeta) potential ψ_0 , the repulsion interaction free energy is given by the following expression:

$$G_E = 2\pi R\epsilon_r\epsilon_0\psi_0^2 \ln[1 + \exp(-\kappa h)] \quad (4.4)$$

where ϵ_r is the permittivity of the medium and ϵ_0 that of free space.

The van der Waals attraction between two droplets with a radius R and a Hamaker constant A (the effective Hamaker constant) is given by the following expression (14):

$$G_A = -\frac{AR}{12h} \quad (4.5)$$

Combination of the electrostatic repulsion (which decays exponentially with distance h) with the van der Waals attraction energy (which decreases as an inverse-power law) results in the total energy–distance curve, as shown schematically in Figure 4.4. The energy–distance curve is characterized by two minima at short and long distances and an energy maximum at intermediate distance. The height of the energy maximum determines the stability of the dispersion. Generally speaking, an energy maximum in excess of $25 kT$ (where k is the Boltzmann constant and T is the absolute temperature) is sufficient to maintain the long-term stability of the emulsion against flocculation. The height of the maximum is determined by the magnitude of the surface or zeta potential and the electrolyte concentration and valency. Generally speaking a zeta potential in excess of

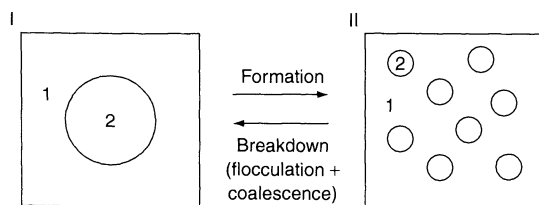


Figure 4.3. Schematic representation of emulsion formation and breakdown

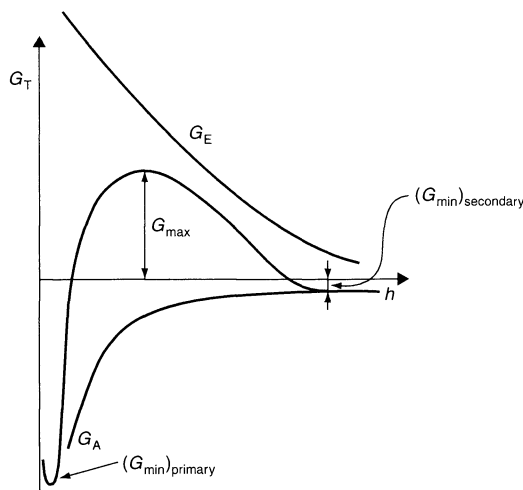


Figure 4.4. Schematic representation of the total energy–distance curve according to the DLVO theory

40–50 mV and an electrolyte concentration lower than 10^{-2} mol dm $^{-3}$ (for a 1:1 electrolyte) is sufficient for maintenance of stability.

The second stabilization mechanism for emulsions is referred to as steric repulsion. This arises from the presence of adsorbed nonionic surfactant and/or polymers. Generally speaking these surfactants or polymers are of the A–B, A–B–A block- and BA $_n$ graft-type systems, where the B chain (the “anchor” group) is strongly adsorbed at the O/W interface (or is soluble in the oil) and the A chain (the stabilizing chain) is soluble in the medium and highly solvated by its molecules. When two droplets, with adsorbed surfactant or polymer molecules having a thickness δ for the A chains, approach each other to a distance of separation h that is smaller than 2δ , repulsion occurs when these layers begin to overlap (and/or undergo some compression). Two main effects can be described. The first is referred to as the mixing free energy of interaction, G_{mix} , which arises from the unfavourable mixing of the A chains when these are in good solvent conditions. G_{mix} is given by the following expression (15):

$$\frac{G_{\text{mix}}}{kT} = \frac{4\pi}{3V_1} \phi_2^2 N_{\text{av}} \left(\frac{1}{2} - \chi \right) \times \left(3R + 2\delta + \frac{h}{2} \right) \left(\delta - \frac{h}{2} \right)^2 \quad (4.6)$$

where V_1 is the molar volume of the solvent, ϕ_2 is the volume fraction of surfactant or polymer in the adsorbed layer, N_{av} is the Avogadro constant and χ is the Flory–Huggins interaction parameter.

It is clear from equation (4.6) that G_{mix} is positive (i.e. repulsive) when $\chi < 0.5$, i.e. the A chains are in good solvent conditions. When $\chi > 0.5$, G_{mix} becomes negative and the interaction becomes attractive. There is one point at which $\chi = 0.5$ and this is referred to as the θ -point for the chain that determines the onset of flocculation.

The second repulsive effect resulting from the presence of the adsorbed layers is the loss in configurational entropy of the chains when significant overlap occurs. This effect, which is always repulsive, is referred to as an entropic, volume-restriction or elastic interaction, G_{el} .

Combination of G_{mix} and G_{el} with G_A results in an other form energy–distance curve, as illustrated in Figure 4.5. It can be seen from this that G_{mix} starts to increase rapidly as soon as h becomes smaller than 2δ . On the other hand, G_{el} begins to increase with decrease of h when the latter becomes significantly smaller than 2δ . When G_{mix} , G_{el} are combined with G_A , the total energy G_T –distance curve shows only one minimum, whose location depends on both the Hamaker constant and the droplet radius R . It is clear that when δ is made sufficiently large and R sufficiently small, the depth of the minimum becomes very small and one may approach thermodynamic stability. This is the basis of formation of nanoemulsions.

The properties of the interfacial region are also important in preventing other breakdown processes in

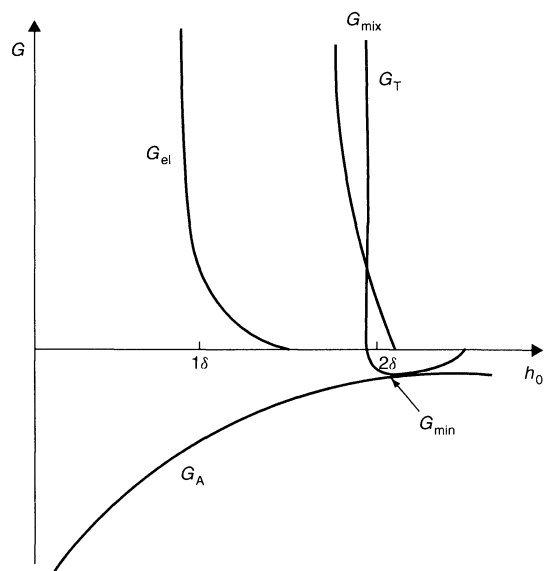


Figure 4.5. Schematic representation of the variation of G_{mix} , G_{el} , G_A and G_T with h

emulsions, such as Ostwald ripening and coalescence. Ostwald ripening occurs as a result of the difference in solubility between the small and large emulsion droplets. The higher solubility of the smaller droplets is due to the higher radius of curvature, as predicted by the Laplace equation ($S \propto 2\gamma/R$). For two droplets with radii R_1 and R_2 (where $R_1 < R_2$):

$$\frac{RT}{M} \ln \frac{S_1}{S_2} = \frac{2\gamma}{\rho} \left(\frac{1}{R_1} - \frac{1}{R_2} \right) \quad (4.7)$$

where S_1 and S_2 are the solubilities of the small and large droplets, respectively, M is the molecular weight and ρ is the density.

For a polydisperse emulsion with some solubility for the oil phase, the smaller droplets disappear by oil diffusion and become deposited on the larger ones. This process may be significantly reduced by proper choice of the interfacial layer. The lower the interfacial tension, then the lower the rate of Ostwald ripening. More important is the Gibbs elasticity ε , which arises from interfacial tension gradients:

$$\varepsilon = \frac{d\gamma}{d \ln A} \quad (4.8)$$

The higher the Gibbs elasticity, then the lower the rate of Ostwald ripening. The Gibbs elasticity can be enhanced by using polymeric surfactants that strongly adsorb at the O/W interface. An oil-soluble polymeric surfactant could be advantageous in reducing Ostwald ripening.

Coalescence of emulsions can also be controlled by proper choice of the interfacial film. When two emulsion droplets come into close contact in a floc or during Brownian collision, thinning and disruption of the liquid film between the droplets may occur, resulting in its eventual rupture and hence the joining together of the droplets. This process can be prevented by the presence of a proper interfacial film which opposes the rupture process. A useful picture describing the prevention of thinning and rupture was introduced by Deryaguin and Obucher (16), who described the film properties in terms of a disjoining pressure $\pi(h)$ that balances the excess normal pressure $P(h) - P_0$ in the film. Here, $P(h)$ is the normal pressure of a film of thickness h , whereas, P_0 is the normal pressure of a sufficiently thick film such that the interaction energy is zero; $\pi(h)$ is the net force per unit area acting across the film, i.e. normal to the interfaces. Thus, $\pi(h)$ is simply equal to $-dV_T/dh$, where V_T is the net force acting across the film, and consists of three main contributions, namely van der Waals, electrostatic and steric, as follows:

$$\pi(h) = \pi_A + \pi_E + \pi_S \quad (4.9)$$

In order to produce a stable film, $\pi_E + \pi_S > \pi_A$. Thus, to reduce coalescence one needs to enhance the repulsion between the surfactant layers, e.g. by using a charged film and/or using surfactants with long hydrophilic chains that produce strong steric repulsions.

For reduction of coalescence, one needs to dampen the fluctuations of the interface that occur during close approach of the droplets. This can be achieved by enhancement of the Gibbs elasticity. For this reason, mixed surfactant films are ideal for reducing coalescence. Such mixed films may also produce lamellar liquid crystalline phases at the interface which prevent coalescence as a result of their multilayer structure (17).

Another method of reducing coalescence is the use of macromolecular surfactants such as gums, proteins and synthetic polymers, e.g. A-B, A-B-A block and BA_n graft copolymers. Examples of such molecules are poly(vinyl alcohol) and polyethylene oxide-polypropylene oxide block copolymers.

4 SURFACE CHEMISTRY IN SUSPENSION CONCENTRATES

The formulation of agrochemicals as aqueous suspensions (suspension concentrates) has attracted considerable attention in recent years. This is due to the advantages produced by these systems, e.g. control of particle size distribution, ease of application (flowable systems that can be easily dispersed in the spray tank) and the possibility of incorporation of high surfactant concentrations which in many cases are essential for biological control.

Suspension concentrates are prepared in two steps. The active ingredient powder is first dispersed in an aqueous solution of the required dispersing agent (surfactant and/or polymer) and this is then followed by a wet milling process (bead milling) to reduce the particle size to the desirable range. In both processes, it is important to control the surface chemical characteristics of the suspension. For example, when dispersing the powder into the liquid, it is essential to have adequate wetting of the powder. Both external and internal surfaces (in pores) need to be completely wetted by the liquid. This process requires the presence of a wetting agent (surfactant) that lowers the surface tension of the liquid and also produces a zero contact angle at the solid/liquid (S/L) interface. Wetting of a solid is usually described in terms of the equilibrium contact angle θ and the appropriate interfacial tensions, by using the classical Young's equation, as follows:

$$\gamma_{SV} - \gamma_{SL} = \gamma_{LV} \cos \theta \quad (4.10)$$

where γ represents the interfacial tension and the symbols S, L and V refer to the solid, liquid and vapour, respectively.

It is clear from equation (4.10) that if $\theta < 90^\circ$, a reduction of γ_{LV} improves wetting. Hence, the use of surfactants that reduce both γ_{LV} and γ_{SL} to aid wetting is clear. However, the process of wetting of particulate solids is more complex and involves three distinct types of wetting (18), i.e. adhesive wetting, immersionsal wetting and spreading wetting. This is schematically represented in Figure 4.6 for a simple cube of solid. Assuming that the surface area of the cube is unity, then the work of dispersion is given by the following expression:

$$W_d = W_a + W_i + W_s = -6\gamma_{SL} - 6\gamma_{SV} \\ = -6\gamma_{LV} \cos \theta \quad (4.11)$$

Thus, wetting of a solid by a liquid depends on γ_{LV} and θ , both of which are reduced by the addition of surfactants. Thus, wetting of a powder by an aqueous surfactant solution is usually spontaneous since θ is close to zero. This only applies for the external surface. However, wetting of the internal surface requires penetration of the liquid into channels between and inside the agglomerates and this requires a high capillary pressure P , as follows:

$$P = -\frac{2\gamma_{LV} \cos \theta}{r} \quad (4.12)$$

Equation (4.12) shows that to increase penetration one has to make θ as small as possible (by adsorption of surfactant on the solid surface). However, when $\theta = 0$, $P \propto \gamma_{LV}$ and a high surface tension is required. These two opposing effects show that the proper choice of a surfactant for dispersing the powder into the liquid is not simple and a compromise has to be made to minimize θ while still keeping a moderate surface tension.

The dispersion of aggregates and agglomerates and subsequent reduction of particle size by wet milling (a process referred to as comminution) also requires

fundamental understanding of the surface chemical processes involved. Surfactants and polymers which become adsorbed on the particle surface aid these processes. For the breakdown of single crystals into smaller units, mechanical energy is required and this is supplied in the bead mill. As a result, permanent deformation of the crystals and crack initiation result. This will eventually lead to the fracture of crystals into smaller units. Of particular importance is the effect of various surface-active agents and polymers on the grinding efficiency. Rhebinder and co-workers (19, 20) explained that as a result of surfactant adsorption at the solid/liquid interface, the surface energy at the boundary is reduced and this facilitates the process of deformation or destruction. In addition, the adsorption of surfactants at the solid/solution interface in cracks facilitates their propagation. This process is usually referred to as the *Rhebinder effect*.

After preparation of the aqueous suspension, it is essential to ensure its long-term physical stability. A shelf life of two years is required under various climatic conditions and thus this requires a careful understanding of the interaction forces that occur between the particles in the suspension. Three main stabilities should be considered, namely stability against irreversible aggregation, stability against crystal growth (Ostwald ripening) and stability against sedimentation and separation on storage. In order to prevent irreversible flocculation, one should ensure the presence of sufficient repulsion (energy barriers) between the particles. This process has been discussed in detail in Section 3 above, where both electrostatic and steric stabilities were considered. In order to reduce Ostwald ripening (crystal growth), one has to consider the structure of the interfacial region. In some cases, strong adsorption of macromolecular surfactants of the A-B-A block or BA_n graft copolymer types may reduce crystal growth. Additives that become incorporated in the crystal and "block" the active sites on which growth occurs may also be used. In general, one should avoid the presence of high micellar concentrations which may solubilize the active ingredient and thus enhance crystal growth.

Reduction of sedimentation and separation of the suspension concentrate on storage requires the addition of a "suspending agent". The latter may consist of a high-molecular-weight polymer such as xanthan gum (a high-molecular-weight polysaccharide) which produces a "gel" network in the continuous phase which has a yield value and a very high viscosity at low shear rates. Finely divided particulate solids, such as sodium montmorillonite (swellable clay) or fumed silica, may also be used to reduce sedimentation and separation of

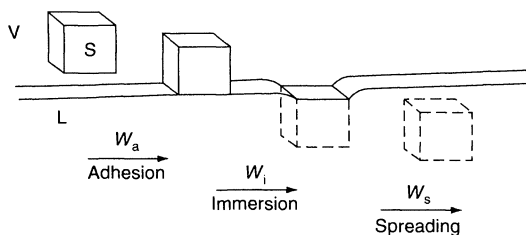


Figure 4.6. The three stages involved in the complete wetting of a solid cube by a liquid

the suspension. In most cases, a combination of the particulate solid with the high-molecular-weight polymer produces a “structure” in the continuous phase that overcomes the stresses exerted by the particles. These suspending agents (sometimes referred to as *antisettling agents*) produce the right rheological characteristics for prevention of sedimentation and separation of the suspension on storage. They are also shear-thinning systems and hence can be easily poured from the container and on dilution they spontaneously disperse in the aqueous phase. For further details on this subject, the reader may refer to a review by this present author (21).

5 SURFACE CHEMISTRY IN THE APPLICATION OF AGROCHEMICAL FORMULATIONS

Optimization of the transfer of agrochemicals to the target requires careful analysis of the various steps involved in the application (22). Most agrochemicals are applied as liquid sprays, particularly for foliar application. Hydraulic nozzles are commonly used for this spraying process to produce droplets in the range 100–400 μm . For application parameters such as the droplets size spectrum, and their impaction and adhesion, wetting and spreading are of prime importance. In addition to these “surface chemical factors”, i.e. the interaction with various interfaces, other parameters that affect biological efficiency are deposit formation, penetration and interaction with the site of action. Enhancement of penetration is sometimes crucial to avoid removal of the agrochemical by environmental conditions such as rain and/or wind. All of these factors are affected by the surfactants and polymers added to the formulation and hence the surface chemistry of the various processes involved is crucial in designing formulations with optimum biological efficacy.

In a spraying process, a liquid is forced through an orifice (the spray nozzle) to form droplets by the application of hydrostatic pressure. The effect of surfactants and/or polymers on the droplet size spectrum of a spray can be described in terms of their effects on the surface tension. Since surfactants lower the surface tension of the liquid, one would expect that their presence in the spray solution would result in the formation of smaller droplets. However, when considering the role of surfactants in droplet formation, one should consider the dynamics of surfactant adsorption at the air/liquid interface. In a spraying process, a fresh liquid surface is continuously being formed. The surface tension of this

liquid depends on the relative ratio between the time taken to form the interface and the rate of adsorption of the surfactant from the bulk solution to the air/liquid interface. The rate of adsorption of a surfactant molecule depends on its diffusion coefficient D and its concentration, according to the following:

$$\frac{d\Gamma}{dt} = \frac{D}{\delta} \frac{N_a}{100} c(1 - \theta) \quad (4.13)$$

where Γ is the surface excess (number of moles of surfactant adsorbed per unit area), t is the time, δ is the diffusion layer thickness, N_A is the Avogadro constant and θ is the fraction of the surface already covered by adsorbed molecules.

Equation (4.13) shows that the rate of adsorption increases with an increase in both D and c . The diffusion coefficient of a surfactant molecule may be calculated from the Stokes–Einstein equation, as follows:

$$D = \frac{kT}{6\pi\eta R} \quad (4.14)$$

where k is the Boltzmann constant, T is the absolute temperature, η is the viscosity of the medium and R is the radius of the surfactant molecule. Equation (4.14) predicts that smaller molecules diffuse faster and hence they reduce the dynamic surface tension more efficiently. However, the situation is more complex, since micelles play a major role in determining the kinetics of adsorption. The shorter the lifetime of the micelle and the smaller its size, then the more efficient is the surfactant in reducing the dynamic surface tension. For full detail, the reader should refer to a recent text by Dukhin, *et al.* (23).

If the rate of formation of the interface is much faster the rate of adsorption of the surfactant, the surface tension of the spray solution will not be far from that of pure water. Alternatively, if the rate of surfactant adsorption is faster than the rate of formation of the fresh interface, the surfactant will lower the dynamic surface tension and hence smaller droplets are produced. With liquid jets, an important factor may be considered that enhances surfactant adsorption (24). Addition of surfactants reduces the surface velocity (which is in general lower than the mean velocity of flow of the jet) below that obtained with pure water. This results from surface tension gradients which enhances adsorption (the molecules will move to the areas with high surface tension).

Surface chemistry also plays a major role in droplet impaction and its subsequent adhesion. The latter process is determined by the difference between the surface

energy of the drop in flight, E_0 , and its value at the target surface, E_s . This difference should exceed the kinetic energy of the drop ($0.5mv^2$, where m is the mass of the drop and v its velocity) for adhesion to take place. The parameter E_0 simply depends on the dynamic surface tension ($E_0 = 4\pi R^2\gamma$), whereas E_s depends on the contact angle θ of the drop on the substrate (25), as follows:

$$\frac{E_0 - E_s}{E_0} = 1 - 0.39[2(1 - \cos\theta) - \sin^2\theta \cos\theta] \times \left[1 - \cos\theta + \frac{1}{3}(\cos^3\theta - 1) \right] \quad (4.15)$$

The term $(E_0 - E_s)/E_0$ is the minimum energy barrier between attached and free drops which is necessary for the kinetic energy to overcome, expressed as a fraction of the free energy of the free drop. A plot of $(E_0 - E_s)/E_0$ versus θ is shown in Figure 4.7, which illustrates that this ratio decreases rapidly from its value of unity when $\theta = 0^\circ$ to a near-zero value when $\theta > 160^\circ$. The master curve shown in Figure 4.7 can be used to calculate the critical contact angle required for the adhesion of water droplets with various sizes and velocities. For droplets with a size of $100\ \mu\text{m}$, and a velocity of $0.25\ \text{ms}^{-1}$, the critical contact angle for adhesion is 160° and in this case no surfactant is

required for adhesion. However, with larger droplets ($200\text{--}400\ \mu\text{m}$) and higher velocities, the critical contact angle required for adhesion becomes smaller than 90° . For example, for a drop of $200\ \mu\text{m}$ and a velocity of $1.5\ \text{ms}^{-1}$ (twice the terminal velocity), a contact angle of 54° is required for adhesion. This shows the importance of surfactants in the spray solution.

Many agrochemical applications involve high-volume sprays, whereby with continuous spraying the volume of the drops continues to grow in size by impaction of more spray drops on them and by coalescing with neighbouring drops on the surface. During this process, the amount of spray retained steadily increases provided that the liquid drops that are impacted are also retained. However, on further spraying the drops continue to grow until they reach a critical size above which they begin to slide down the surface and "drop off" (the so-called *run-off condition*). At the point of run-off, the volume of spray retained is at a maximum. The retention at this point is governed by the movement of liquid drops on the solid surface. Bikerman (26) stated that the percentage of drops sticking to a plant after having touched it should depend on the tilt of the leaf, the size of the droplets and the contact angle at the plant leaf/droplet/air interface.

Furmidge (27) analysed the process of retention of drops on a tilted substrate by considering the advancing and receding contact angles, θ_A and θ_R , respectively. This is illustrated in Figure 4.8, which shows the profile and plan view of a drop during sliding.

By using a simple analysis whereby the gravity force (given by $mg\sin\alpha$, where m is the drop mass, g is the acceleration due to gravity and α is the angle of tilt) is balanced by the difference in the work of dewetting and wetting (determined by the receding and advancing contact angles, respectively) Furmidge derived the following expression for the

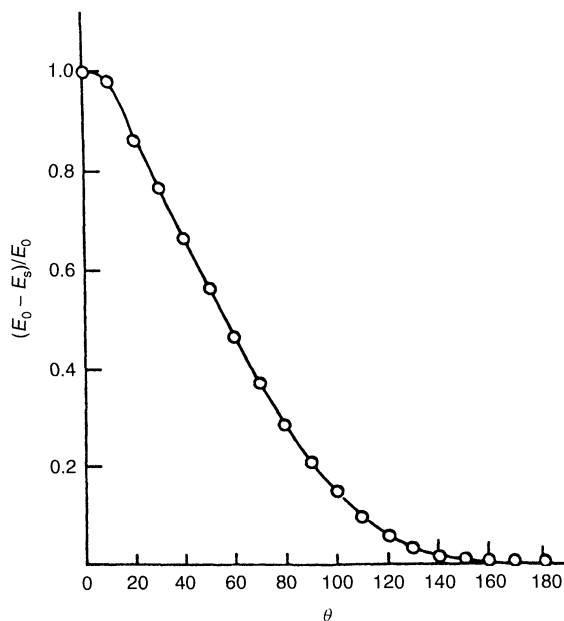


Figure 4.7. Variation of $(E_0 - E_s)/E_0$ with θ for a drop on a solid surface

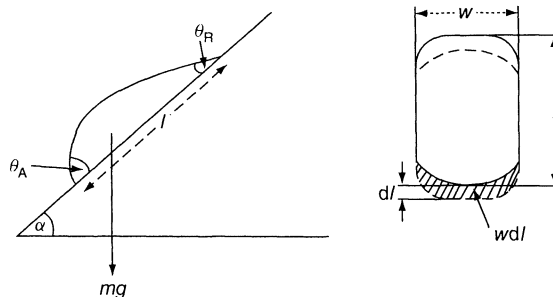


Figure 4.8. Profile and plan view of a drop during sliding

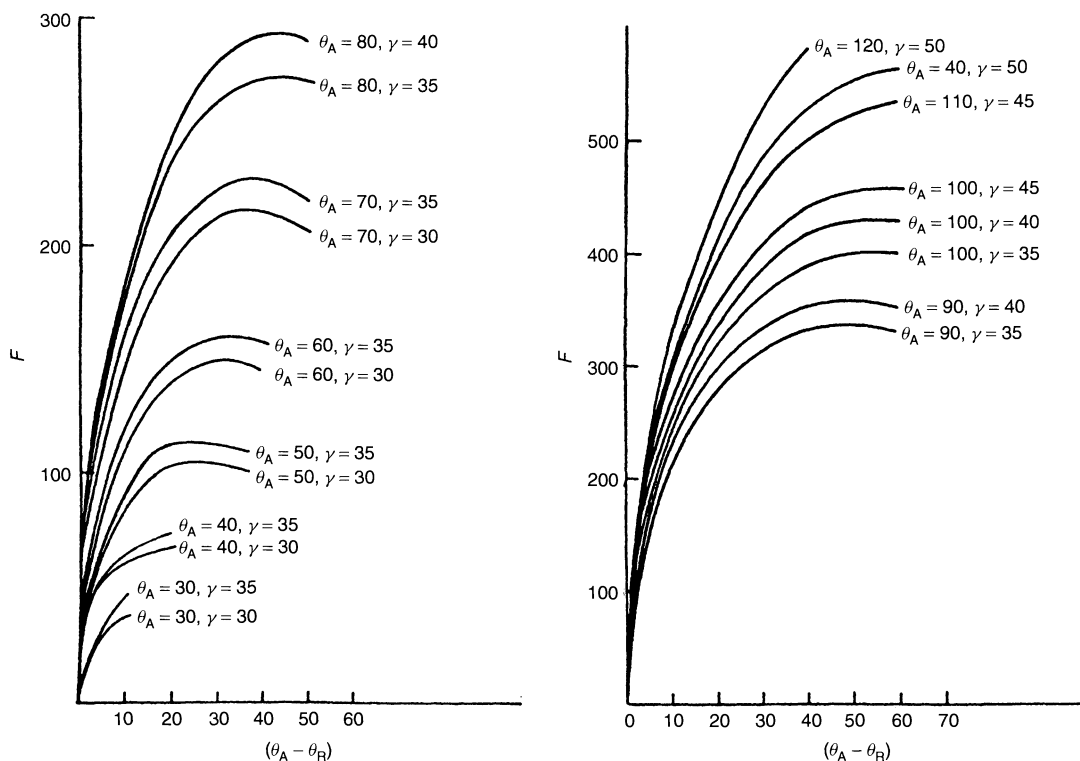


Figure 4.9. Variation of the retention value with the contact angle hysteresis

retention factor F :

$$F = \theta_M \left[\frac{\gamma_{LA} (\cos \theta_R - \cos \theta_A)}{\rho} \right]^{1/2} \quad (4.16)$$

where θ_M is the mean value of the contact angles and ρ is the density of the spray solution. Equation (4.16) shows that F depends on the value of γ_{LA} , the difference between θ_R and θ_A (referred to as the contact-angle hysteresis), and θ_M . This is illustrated in Figure 4.9. It can be seen from Figure 4.9 that at any given value of $(\theta_A - \theta_R)$ and γ_{LA} , F increases rapidly with an increase in the contact-angle hysteresis, reaching a maximum and then decreases.

Another surface chemical factor that can affect the efficacy of the foliar spray application of agrochemicals is the extent to which the liquid wets, spreads and covers the foliage surface. A very convenient parameter describing spreading is the spread factor SF , which is simply the ratio of the diameter of the area wetted, D , and the diameter of the drop applied, d , as follows:

$$SF = \frac{D}{d} \quad (4.17)$$

The spread factor depends on the contact angle, and provided that θ is not too small ($>5^\circ$), is given by the following expression:

$$SF = \left[\frac{4 \sin^3 \theta}{(1 - \cos \theta)^2 (2 + \cos \theta)} \right]^{1/3} \quad (4.18)$$

A plot of SF versus θ is shown in Figure 4.10 which clearly illustrates the rapid increase in SF when θ becomes lower than 35° .

A useful index for measuring the spreading of a liquid on a solid surface is the Harkin spreading coefficient S , (28), which is the change in tension when solid/liquid and liquid/air interfaces are replaced by a solid/air interface:

$$S = \gamma_{SA} - (\gamma_{SL} + \gamma_{LA}) \quad (4.19)$$

By using Young's equation (equation (4.10)), S is then given by the following:

$$S = \gamma_{LA} (\cos \theta - 1) \quad (4.20)$$

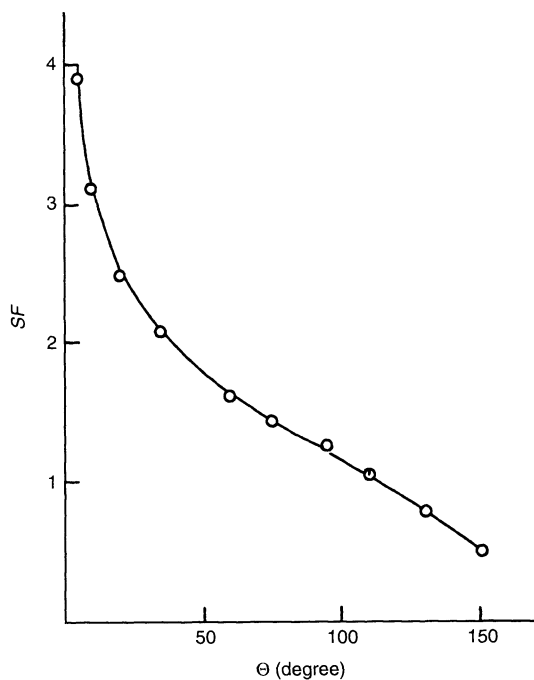


Figure 4.10. Variation of the spread factor with the contact angle

If $\theta > 0$, S is negative and this implies only partial wetting. In the limit $\theta = 0$, $S = 0$, and this represents the onset of complete wetting. A positive S value implies rapid spreading of the liquid on the solid surface. This shows the importance of the presence of surfactant and the structure of the interfacial region which determines the values of the surface tension and contact angle.

Several other factors where surface chemistry plays a major role in biological efficacy may be listed. For example, the evaporation of drops and the formation of deposits that may contain various liquid crystalline phases may play a major role in retention of the active ingredient on the leaf surface. This is particularly important for systemic fungicides. These deposits also reduce the loss of the active ingredient by falling rain. Another important factor is the presence of micelles, which solubilize the active ingredient and may enhance penetration of the chemical through the leaf surface and the cuticle. All of these factors rely on specific interactions between the active ingredient, the surfactant, the leaf surface and the active sites involved. However, a detailed analysis of these effects is beyond the scope of this present chapter.

6 REFERENCES

1. Tadros, Th. F., *Surfactants in Agrochemicals*, Marcel Dekker, New York, 1995.
2. Fischer, E., *Farm. Chem.*, **126**(3), 18 (1963).
3. Becher, D. Z., in *Encyclopedia of Emulsion Technology*, Vol. 2, Becher, P. (Ed.), Marcel Dekker, New York, 1958, Ch. 4.
4. Gad, J., *Arch. Anat. Physiol.*, 181 (1878).
5. Lewes, J. B. and Pratt, H. R. C., *Nature (London)*, **171**, 1155 (1953).
6. Garner, F. H., Nutt, C. W. and Mohtadi, M. F., *Nature (London)*, **175**, 603 (1955).
7. Davies, J. T. and Rideal, E. K., *Interfacial Phenomena*, 2nd Edn, Academic Press, New York, 1963.
8. Kaminski, A. and McBain, J. W., *Proc. R. Soc. London, A*, **198**, 447 (1949).
9. Ogino, K. and Ota, M., *Bull. Chem. Soc. Jpn*, **49**, 1187 (1976).
10. Overbeek, J. Th. G., *Faraday Discuss. Chem. Soc.*, **65**, 7 (1978).
11. Overbeek, J. Th. G., de Bruyn, P. L. and Verhoecks, F., in *Surfactants*, Tadros, Th. F. (Ed.), Academic Press, London 1984, p. 111.
12. Deryaguin, B. V. and Landau, L., *Acta Phys. Chem. USSR*, **14**, 633 (1939).
13. Verwey, E. J. W. and Overbeek, J. Th. G., *Theory of Stability of Lyophobic Colloids*, Elsevier, Amsterdam, 1948.
14. Hamaker, H. C., *Physica*, **4**, 1058 (1937).
15. Napper, D. H., *Polymeric Stabilisation of Dispersions*, Academic Press, London, 1983.
16. Deryaguin, B. V. and Obucher, E. J. *Colloid Chem.*, **1**, 385 (1930).
17. Friberg, S., Jansson, P. O. and Cederberg, E., *J. Colloid Interface Sci.*, **55**, 614 (1967).
18. Parfitt, G. D., *Dispersion of Powders in Liquids*, Applied Science Publishers, London, (1973).
19. Rhebinder, P. A., *Colloid J. USSR*, **20**, 493 (1958).
20. Schukin, E. D. and Rhebinder, P. A., *Colloid J. USSR*, **20**, 601 (1958).
21. Tadros, Th. F., in *Solid/Liquid Dispersions*, Tadros, Th. F. (Ed.), Academic Press, London, 1987.
22. Tadros, Th. F., *Aspects Appl. Biol.*, **14**, 1 (1987).
23. Dukhin, S.S., Kretzschmar, G. and Miller, R., *Dynamics of Adsorption at Liquid Interfaces*, Elsevier, Amsterdam 1995.
24. Davies, J. T. and Makepeace, R. W., *AICHE J.*, **24**, 524 (1978).
25. Hartley, G. S. and Brunskill, R. G., *Surface Phenomena in Chemistry and Biology*, Pergamon Press, New York, 1958, pp. 214–223.
26. Bikerman, J. J., *J. Colloid Interface Sci.*, **5**, 349 (1950).
27. Furnidge, C. G. L., *J. Colloid Interface Sci.*, **17**, 309 (1962).
28. Harkins, W. D., *J. Phys. Chem.*, **5**, 135 (1937).

CHAPTER 5

Surface and Colloid Chemistry in Photographic Technology

John Texter

Strider Research Corporation, Rochester, New York, USA

1	Introduction	85	3	Particles and Colloids in Photographic Technology	94
1.1	Support base	85	3.1	Silver halide	94
1.2	Antistat layers	86	3.2	Surface charge	96
1.3	Overcoats	87	3.3	Chemical sensitization	97
1.4	Emulsion layers	87	3.4	Sensitizing dye adsorption	98
1.5	Coating methods	88	3.5	Spectral sensitization	98
1.6	Black and white photography	88	4	Coupler Dispersions	99
1.7	Colour negative photography	89	4.1	Emulsification	99
1.8	Other types of photographic elements	89	4.2	Mixed micellization	100
2	Surfaces and Particles in Photographic Technology	90	4.3	Nanocrystalline coupler dispersions	100
2.1	Length scales	90	5	Adsorber Dyes and Filter Dyes	101
2.2	Particulate materials	91	5.1	Light management	101
2.3	Development	92	5.2	Dye dispersions	101
2.4	Coupling stoichiometry and reactivity	93	5.3	Dispersion electrokinetics	102
			6	Matte Beads	103
			7	References	104

1 INTRODUCTION

In order to better discuss the role of surface chemistry in photography, it is useful to consider some of the basic features of photographic elements (paper, film, etc.) morphology, exposure and processing. As a start, consider a multilayer photographic element such as that pictured in Figure 5.1. The layer structure illustrated is typical of a simple colour print material, such as colour paper or colour movie print films. Such materials comprise many different types of layers (1), and each layer is prepared as a thin film *coating*.

1.1 Support base

The thickest layer is the support. This provides a base upon which to coat the other layers, discussed below, and also provides dimensional stability during manufacture, storage, exposure, processing and display. In the case of a typical reflection print material, the support would be some type of high-grade photographic paper. Such paper supports often consist of several different layers, including reflection layers containing inorganic pigments (barium sulfate, titania, etc.) in gelatin or polyethylene binders. The preparation of

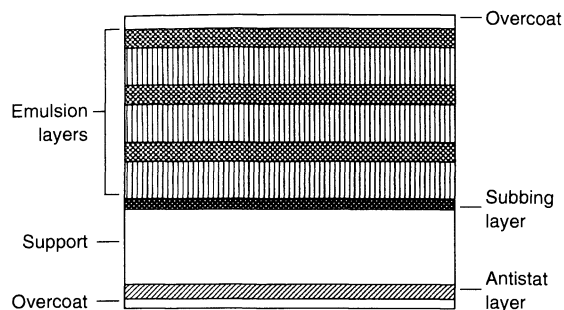


Figure 5.1. Generic multilayer photographic film element shown in cross-section, illustrating the key morphological components: overcoats, emulsion layers, subbing layer, support and antistat layer. The layer thicknesses are not drawn proportionately to scale. A typical emulsion layer may be 3–6 μm thick, a typical overcoat or interlayer may be 1–2 μm thick, and the support is typically of the order of 100 μm in thickness

paper coatings is discussed elsewhere in this volume by Tiberg *et al.* (see Chapter 7). Transparent supports are important for colour negative, movie and slide films. The main materials used for such supports are cellulose triacetate (CTA), poly(ethylene terephthalate) (PET) and poly(ethylene naphthalate) (PEN). The thickness of these supports ranges from 60 to 200 μm . CTA supports are typically of the order of 130 μm , PET supports are about 100 μm thick, and PEN supports are about 80–90 μm in thickness. PEN was recently introduced to allow thinner, more tightly wound roles of film for cartridge storage. Its mechanical properties give it superior performance in comparison to PET.

A subbing layer is usually coated in order to provide good wetting and good adhesion between the support and the layer coated upon it. Good adhesion is required in order to make sure that the multilayer element will maintain its mechanical integrity throughout all of the physical and chemical processes it is put through. The composition of subbing layers varies with the composition of the layers to be joined. Prior to applying a subbing layer, the support may be physically or chemically treated to improve wetting and adhesion. For example, corona discharge may be applied in order to increase the surface energy of the support, thereby improving wettability. Solvents for the support material may be applied to provide limited swelling. Such swelling will promote polymeric entanglement of the polymers applied in the subbing layer, thereby improving the adhesive interaction.

Gelatin is often used in subbing layer compositions, since it is the most prevalent binder used in the emulsion and overcoat layers. Gelatin in the subbing

layer promotes adhesion of an overcoated layer containing gelatin. This adhesion is promoted further by chemical cross-linking of the gelatin, between various amine and carboxyl sites in the latter. Cross-linking of interpenetrating gelatin strands from the subbing and overcoated layers results in covalently based adhesion. Good binding to polyester supports is promoted by subbing layer polymers that contain chlorine, such as poly(vinyl chloride)- and poly(vinylidene chloride)-containing copolymers (1). Using copolymers that interact strongly with the support provides good adhesion on one side of the subbing layer–support interface. Having subbing layer copolymers which also contain blocks or components that strongly adhere to the emulsion layer is also important. Monomer components containing carboxylic acid functionalities or maleic anhydride groups provide chemical sites with which amine groups, from overcoated gelatin layers, can chemically cross-link. Various mixtures of gelatin, poly(alkyl acrylate)s, vinyl acrylate copolymers and polyurethanes can be used as the components of such subbing layers, wherein the glass transition temperature and stress accommodation properties can be varied.

1.2 Antistat layers

An antistat layer is a conductive layer prepared in order to dissipate electrostatic charge that builds up during manufacture (e.g. slitting operations), exposure (e.g. amateur roll film and, movie film) and viewing (e.g. motion picture film) processes. Unwanted discharge can cause fog and other defects in unexposed elements and can also cause sparks during projection. Since it is useful to dissipate electrostatic charge both before and after development processing, it is important to have layers formulated with materials that will withstand the harsh chemical treatments attendant to development processing of photographic papers and films. Antistat layers have been formulated with a wide variety of organic and inorganic conductive materials (2). Conductive materials that dissolve in aqueous processing solutions must be protected with a water-resistant overlayer in certain circumstances. Ionically conductive polymers, typically containing monomers having quaternary nitrogen groups and halide counterions, have been used in antistat layers for a long time. They suffer, however, in that their conductivities vary appreciably with relative humidity. Antistat layers comprising carbon black are very effective in providing electronic conductivity and insensitivity to humidity. The requisite removal of the carbon black from transparent print supports

(slide film and movie print film) demands fairly expensive processing steps. Colloidal tin oxide and vanadium pentoxide have been successfully used to provide electronic conductivity in antistat layers. Nanoparticles (80 Å diameter) of antimony-doped tin oxide can provide humidity-insensitive conductivity. Vanadium pentoxide is typically nanoscopic in two dimensions, and provides excellent electronic conductivity, although it requires protection from aqueous processing solutions. More recently, electronically conducting polymers and latexes have been introduced. These materials are very competitive with the nanoparticulate semiconductors in their efficacy.

1.3 Overcoats

The overcoat layers are thin layers, typically less than 1 µm in thickness, that can provide both chemical (e.g. water barrier properties to protect a water-sensitive antistat layer material) and mechanical (e.g. abrasion and wear resistance) protection to the undercoated layers. They also often provide lubrication and may contain wax dispersions or other lubricants. To guard against blocking or ferrotyping, where adhesion between touching surfaces causes one or more layers to strip off when elements are stacked or rolled, relatively large beads, known as *matte beads*, are often coated in these overcoat layers. Such beads are typically formulated from polystyrene or polymethacrylate and are up to several µm in diameter. They are typically coated at a relatively low number concentration and do not materially affect the gloss or light scattering from the materials. They serve to prevent strong interactions between adjacent planar surfaces by providing point contacts that prevent large surface area contacts. Matte beads are typically prepared by using suspension polymerization methods, sometimes following limited coalescence (see Section 6 below).

1.4 Emulsion layers

Finally we address the emulsion layers that contain light-sensitive silver halide. Some of these other layers, as discussed above, contain particulates such as matte beads in overcoats, nanoparticulate semiconductors in antistat layers, copolymeric latexes in subbing layers, etc. Such layers are intrinsically composite multiphase layers, and this is also the case for the light-sensitive emulsion layers. In addition to microcrystals or nanocrystals of silver halide, present to capture light and to form developable

latent image, much of the image dye-forming chemistry (for colour-negative films and papers and for colour positive films, papers and transparencies) is incorporated as nanoparticles. This is especially the case for dispersions of couplers that react with oxidized developer to form cyan, magenta or yellow image dyes. Other important chemicals are also often incorporated in particulate form. Dyes and organic pigments are used to manage light transmission and reflection through such elements (to control speed and to prevent halation). Such materials are often prepared as nanoparticulate dispersions and incorporated in thin interlayers between thicker light-sensitive layers containing silver halide.

The silver-halide-containing layers may be of different types, depending on whether the silver halide therein is “slow”, “fast” or “something in between”. The layers that generate the bulk of the colour density are typically termed “slow” layers, and these layers are thickest because they contain a larger stoichiometric amount of dye-forming chemistry, namely silver halide and coupler dispersion. “Fast” layers are typically much thinner and contain much less dye-forming coupler. These combinations of slow and fast layers may be coated in several different formats or layer orders. The most common situation is to have the slow red-sensitive layer coated closest to the support. If the element is a print material (e.g. colour paper and motion picture print film), there probably will be no distinguishable fast layers. A fast red-sensitive layer will then typically be coated on top of the slow layer. There may or may not be an interlayer between these two layers – typically, there is not. An interlayer often will be coated above the fast red-sensitive layer. This interlayer may contain oxidized developer scavenger to reduce chemical “cross-talk” between different colour records during development and/or a magenta filter dye to prevent green light from reaching the red-sensitive record. Slow and fast green-sensitive layers are then coated in sequence, often with another interlayer coated above these. Such an interlayer may also contain oxidized developer scavenger and a yellow filter dye dispersion. This yellow dispersion absorbs blue light, and keeps blue light from exposing the underlying green- and red-sensitive layers, all of which are intrinsically blue-sensitive. An alternative coating order used in some products is to coat the slow layers in sequence, i.e. red-sensitive, green-sensitive and blue-sensitive, and then coat the fast layers in the same sequence above the slow layers. Some products contain slow, medium and fast layers, and there are many permutations possible. However, those articulated here illustrate the main function of some of the auxiliary particulate materials, such as filter dye dispersions and

oxidized developer scavengers. The composite nature and prevalent use of nanoparticulate materials in photographic elements will be discussed further below.

1.5 Coating methods

These thin layers may be coated and prepared by using a variety of different coating technologies. While the coating industry as a whole uses dip coating and doctor blades for high volumes of coating manufacturing, the uniformity and low-defect-level requirements and the multiple number of coated layers present in a particular element necessitate more sophisticated coating processes than those generally available in other industries. For the coating of multilayer elements out of aqueous melts, extrusion, slide hopper and curtain coating processes are predominant in the photographic industry. Extrusion coating, also known as (“Ex”) “X-hopper” coating, involves pumping a melt composition out of an “extrusion” slot in near-contact with a moving substrate (web). This mode of coating usually is carried out one layer at a time. After coating, the applied film is typically chill set and then dried. At a given coating speed, there typically will be an upper and lower limit to the wet coating thickness that can be applied. If too much melt is extruded at a given web speed, the resulting thin film will not be uniform. If too little melt is extruded, break-lines will develop. For a given (linear) coating speed, melts having greater viscosity can typically be coated in thicker layers. Slide hopper coating has revolutionized the manufacture of multilayer films and papers. Up to 15 layers have been successfully coated simultaneously by using slide hopper coating, although three to five layers is a more usually encountered situation. A given melt is pumped out of an extrusion slot on to a hopper chute that is gravity fed onto a moving web. Each succeeding (overcoating) layer is pumped out and gravity fed on to the lower layer. Curtain coating involves a similar cascading of multilayers, but instead of crossing a narrow gap onto a moving web, the array of contiguous layers falls as a curtain onto a moving web. This approach offers faster coating speeds. Whether coating one or multiple layers, the surface energy of the substrate and each succeeding layer must be tuned to insure wetting of each interface by the overcoating layer melt.

1.6 Black and white photography

The image-wise exposure, processing and viewing of a negative-working black and white element are illustrated

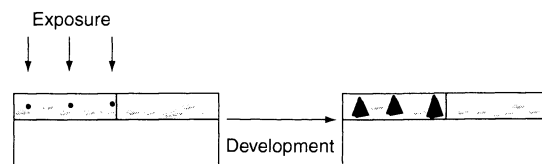


Figure 5.2. Schematic of simple black and white photographic element illustrating “negative” development. A region of film that is exposed produces silver halide microcrystals containing a latent image speck. During development, this speck catalyses the complete reduction of the silver halide crystal to silver metal. Silver halide crystals without latent image are not reduced to silver during the limited development process time

in Figure 5.2. Microcrystals or nanocrystals of silver halide (generally AgCl or AgBr with some iodide doping) provide light sensitivity in photographic elements. The nature and formation of silver halide microcrystals are discussed in greater detail below. These crystals are the primary particulate component of the emulsion layer in black and white elements and are known as photographic emulsions. This usage of “emulsions” is, as a term of art, restricted to photographic technology, and does not refer to the more usually understood meaning of a dispersion of one immiscible liquid in another. Such crystals can be chemically and/or spectrally sensitized (as discussed below) to respond to very narrow or to very broad segments of the visible (or near-infrared) spectrum. Light exposure of the emulsion layer results in the formation of a latent image. The structure of latent image specks has not been unequivocally identified, but much indirect evidence suggests such specks are charged silver clusters, comprising neutral silver atoms and charged silver cations (3). This latent image is typically located at or on the surface of a silver halide particle and is chemically amplified by chemical processing or development which produces an image density in developed silver metal in response to the degree of light (photo) exposure (Figure 5.3). The latent image catalyses development of the rest of the crystal to elemental silver, at a rate faster than the rate at which crystals without latent image will be reduced to silver metal. This catalytic discrimination provides the basis for modern silver halide photographic development, and the effective degree of amplification obtainable (e.g. 10^8) has not been matched by other competing technologies. When the amount of image developed is directly proportional to the amount of exposure, the photographic element is called “negative” working. When this proportionality is an inverse one, the element is called “positive” working, and a density versus $\log E$ plot would appear as the dotted line

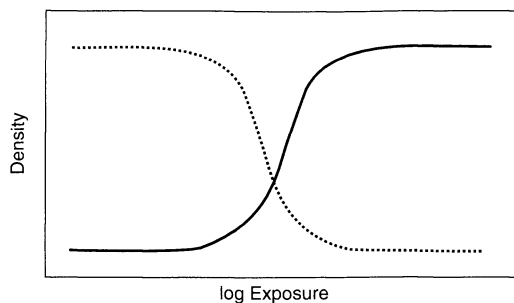


Figure 5.3. Relationship between exposure (E) and developed silver density (D). The continuous curve illustrates the basic sensitometry obtained in negative-working systems. Increasing exposure results in increasing developed (optical) density (elemental silver or image dye in the case of colour systems). The dotted curve illustrates positive-working sensitometry, where increasing exposure results in decreasing developed density

shown in Figure 5.3. Either type of response can be obtained, depending on the details of the chemistry incorporated in the emulsion layer. A more thorough discussion of such options is beyond the scope of this present chapter, although further information is readily accessible (4). The negative development of black and white elements is typically carried out with aqueous alkaline hydroquinone solutions. The partially ionized hydroquinone chemically reduces silver halide to silver metal. Other popular black and white reducing agents include aminophenols, catechols, pyrogallols and ascorbic acid.

1.7 Colour negative photography

Amateur colour negative photographic elements have one or more emulsion layers for each of three regions of the visible spectrum, i.e. red, green and blue (5, 6). Water-insoluble organic couplers are incorporated as submicron diameter dispersions in each of these layers. Typically, red-sensitive layers contain cyan dye-forming couplers (e.g. phenols and naphthols), green-sensitive layers contain magenta dye-forming couplers (e.g. pyrazolones and pyrazolotriazoles), and blue-sensitive layers contain yellow dye-forming couplers (e.g. benzoylacetanilides and pivaloylacetanilides). Such layers typically contain three phases, i.e. silver halide, coupler and a continuous gelatin (as binder) phase. Spectral sensitivity is imparted by spectral sensitizing dyes that are adsorbed on to the silver halide particle surfaces (discussed at greater length below). This method of subtractive colour generation produces (negative) dye densities

in proportion to the amount of “minus” exposure. For example, the amount of yellow image dye produced is in proportion to the amount of blue light converted to latent image, the amount of magenta image dye produced is in proportion to the amount of green light converted to latent image, and similarly, the amount of cyan dye produced is in proportion to the amount of red light converted to latent image. A schematic of a typical colour negative film element is similar to that depicted in Figure 5.1, except that there are typically additional interlayers above, between and below the various light-sensitive emulsion layers. For example, in colour negative print materials, such as papers and colour transparencies, a UV filter dye layer is often included right below the overcoat layer. Such a UV layer typically comprises a UV filter dye dispersed in particulate form and protects the resulting image dyes from UV-induced photodegradation.

A schematic basis for colour development chemistry is illustrated in Figure 5.4 (6). Silver halide is reduced by colour developer to metallic silver. Paraphenylenediamines (PPDs) are preferred colour developers, but aminophenols may also be used. The PPD undergoes a two-electron oxidation process and produces two silver atoms and one quinonediimine, (QDI) molecule. This two-equivalency is illustrated in the top part of Figure 5.4. Surrounding the silver halide microcrystals in a given layer are much smaller coupler dispersion particles. The coupler in these particles is partially ionized under dilute alkaline development conditions ($\text{pH} \sim 10\text{--}11$) and reacts with QDI to form indoaniline image dyes. The formation of some of these image dyes is illustrated in Figure 5.4. The coupler dispersion particles are typically of the order of 100–500 nm in diameter, and surface chemistry is key to their formation, as well as affecting their coupling kinetics.

1.8 Other types of photographic elements

There are many other important types of photographic elements (7) which space limitations do not allow us to discuss at length here. For example, colour separation photography allows one to capture the colour information in a scene by exposing three different black and white films, one to each of the principle scene colors, i.e. red, green and blue. Each of these exposures can then be put through a black and white development, chemically fogged, and then “colour developed” using aqueous diffusible couplers to produce the appropriate subtractive colour. The resulting three colour images

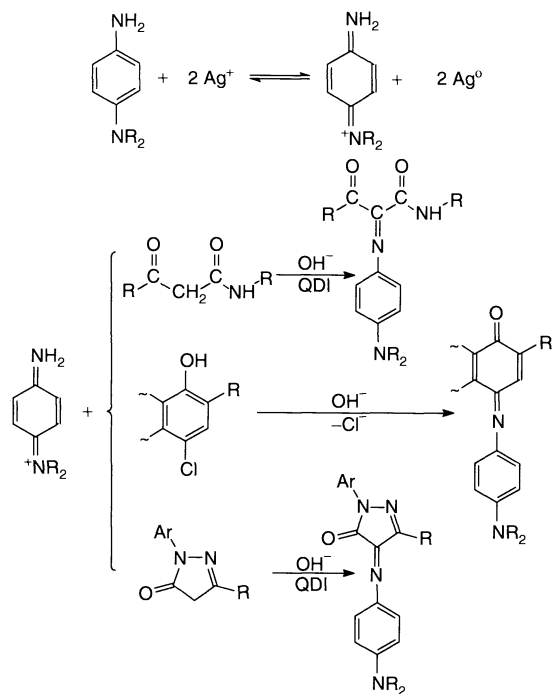


Figure 5.4. Brief summary of colour development and coupling chemistry. The reaction depicted at the top corresponds to the two-equivalent development of silver halide, AgX, by a paraphenylenediamine (PPD) developer species. The latter reduces two silver ions to elemental silver and is transformed by a two-electron oxidation to quinonediimine, (QDI). The R substituent may be the same or different in the developers and in the couplers. In addition, the PPD may have other ring substituents. The reactions depicted at the bottom illustrate indoaniline image-dye formation from QDI and various classes of couplers. The middle coupling examples represent coupling with phenols or naphthols to produce cyan image dyes. In this example, there is a Cl coupling-off group at the *para* position. The coupler is activated by hydroxide, thus ionizing the hydroxyl group, and then reacts with one QDI to form a cyan image dye. The yellow (upper) and magenta (lower) dye-forming reactions are examples of four-equivalent couplings. The corresponding couplers do not have coupling-off groups. After activation by hydroxide and ionization, reaction with QDI produces a leuco-dye intermediate. The latter undergoes a two-electron oxidation by another QDI to produce the final dye molecule

must then be placed in mechanical registry to produce a final colour print of the original scene. Such processes are still pursued for certain commercial applications, such as in proofing for colour advertising. The old Kodachrome[®] process was based on some related chemistry, but relied on carefully timed and diffusion-controlled processing to produce such separations in an integral multilayer pack.

Colour instant photography has much in common with colour negative photography. There are 50–100% more layers in a colour instant element. Some of the additional layers required include base releasing layers, timing layers to release pH-adjusting chemicals to shut down development chemistry, dye-permeable opacifying layers, mordant layers (to bind diffusible dyes) and incorporated developer layers. Some colour instant systems have been built by using colour developers such as PPD. More common is the use of dye-developers or so-called redox dye releasers. Dye-developers diffuse to developable silver halide, and upon reduction of the latter they release a diffusible image dye. This dye will then diffuse through an opacifying layer to a mordant.

Heat-developable silver halide elements make it possible to avoid wet-development processing, and the elimination of wet-processing chemistry has some environmental motivation. The only commercially available heat-developable products are microfilms. There is a large patent literature on heat-developable materials. The key limitation to the commercialization of colour heat-developable systems is the problem of getting rid of undeveloped silver halide. In normal wet-developable systems, fixing agents such as thiosulfate (hypo) are used to dissolve undeveloped AgX. Silver halide microcrystals typically provide a lot of scattering, so it is generally necessary to fix out such AgX and to bleach (in the case of colour systems) the silver image.

2 SURFACES AND PARTICLES IN PHOTOGRAPHIC TECHNOLOGY

2.1 Length scales

The importance of surface chemistry in photographic technology spans 10 decades in the length scale, i.e. from nanometres to metres. The largest length scales are encountered in the manufacturing of photographic film and paper support materials and in the coating of such supports with the incorporated chemistries that make up image-forming photographic elements. Most reflection print materials are coated on high-grade photographic papers, and such papers are typically manufactured in high-speed paper mills. Such mills typically operate with webs of the order of three metres in width and at coating speeds of up to 30 metres per second. A detailed consideration of the surface chemistry of paper manufacturing is beyond the scope of this present section, and the reader is referred to the companion chapter by Tiberg

et al. (Chapter 7) for more information, although certain critical preparative treatments are described below. Alternative reflection base materials may perhaps be described as synthetic papers, in that the inherent reflection properties are achieved solely from coated pigment layers or from processes producing voids in polymeric layers, so as to produce scattering (reflecting) layers from synthetic polymeric compositions. Transparent film support materials are typically manufactured in coating mills approaching two metres in web width. A detailed discussion of the manufacture of such coating supports is beyond our present scope, but physical and chemical surface treatments are very important, as was discussed earlier in the application of subbing layers. Chemical and surface treatments of coating supports are critical for the successful coating of chemistry-containing layers, for the storage of such coated elements (e.g. to prevent coiled and stacked layers from adhering strongly to one another during storage and for the dissipation of static electrical energy), and to maintain dimensional stability and structural integrity during processing and long-term storage. While the width (> metres) and length (10^3 metres) scales are certainly macroscopic, the thickness of these supports typically is microscopic and in the range of 80–200 μm .

2.2 Particulate materials

The bulk of chemicals incorporated into photographic elements is in particulate form. This can be illustrated by reviewing Table 5.1, where classes of various particulate materials are listed. Silver halide crystals cover

a wide range of sizes. Those used in light capture as three-dimensional grains are typically in the range of 300 nm to 3 μm in the largest dimension. Tabular high-aspect-ratio grains may have their largest dimensions closer to 5 μm . The so-called Lippmann emulsions are just a few hundred angstroms in diameter, and are used for astronomical plates where high resolution is required. Silver halides, therefore, span two orders of magnitude in their largest dimension. Colloidal silver can be prepared as monodisperse dispersions varying in colour from blue to yellow, depending on the particle size (e.g. 7–12 nm). Yellow silver dispersions are used in filter layers to absorb blue light. The small particle size makes them insignificant as scattering centres. Semiconducting oxides such as tin oxide are useful as antistats. The preferred sizes are less than 10 nm, so that the particles do not contribute to light scattering. Opacifying pigments, such as titania and barium sulfate, are typically dispersed as highly scattering particles, ranging in sizes from 0.5 to 5 μm in their largest dimension. Such inorganic pigments are often coated on photographic papers to increase opacity and diffuse reflectivity. Most of the binders used in photographic elements are organic, but nanoparticulate silica (20–30 nm) has been used as a binder in certain layers, usually with a small amount of gelatin to provide cross-linking sites.

Many water-insoluble organic materials are also incorporated as particulates. Foremost in colour photography are photographic couplers. They are typically prepared as amorphous dispersions by an emulsification process (discussed below), with or without various plasticizers (coupler solvents). They also can be prepared as nanocrystalline dispersions by comminution processing, and as metastable mixed micelles by precipitation from homogeneous solution. Coupler particles are also prepared as latexes, where coupler monomers are copolymerized with other monomers, typically using emulsion polymerization, to produce submicron water-borne dispersions. Such polymeric couplers can be attached permanently to the polymeric backbone, or attachments can be made through a coupling-off group. In the latter case, once the oxidized developer has reacted with the coupling moiety, the resulting image dye is separated from the polymeric backbone and is free to diffuse if soluble or mobile in the continuous phase. Such formulations are useful in diffusion-transfer imaging elements. Particle sizes range from 10 to 30 nm for the mixed micelle formulations to fractions of a micron for dispersions prepared by comminution or by emulsification.

Absorber, filter and antihalation dyes can be prepared by several different processes. All three types can be prepared as dispersions by the emulsification

Table 5.1. Particulate materials in photographic elements

<i>Inorganic</i>
Silver halide
Silver
Antistats (oxides)
Opacifying materials (TiO ₂ , BaSO ₄)
Binders (SiO ₂)
<i>Organic</i>
Couplers
Absorber dyes, filter dyes, antihalation dyes
Sensitizing dyes
Oxidized developer scavengers
Developers
Dye-Developers
Antistats (latexes)
Mordants (latexes)
Opacifying materials (hollow polymer spheres)
Binders (gelatin, latexes, microgels)

process discussed below for couplers. They also can be imbibed into swollen latexes (latex loading – also discussed below), made part of a latex through copolymerization, and dispersed as small solid particles by using comminution processing. While sensitizing dyes have historically been added to finishing processes as solutions, they more recently have been dispersed as submicron-sized solid particle dispersions prepared by comminution. Their small aqueous solubility is generally sufficient to afford diffusion transfer to silver halide surfaces. Oxidized developer scavengers and incorporated developers and developer precursors can be dispersed by emulsification and by comminution. Dye-developers are important molecules in colour instant processing, and are also dispersed by emulsification and by comminution.

Traditional polymeric antistats relying on ionic conductivity and comprising quaternary halide groups or acidic groups can be prepared as latexes. Electrically conducting polymers are also typically prepared as aqueous latexes. In dye-diffusion-transfer processes, especially for anionically charged dyes, mordent polymers are also prepared as latexes.

Organic light scattering pigments produced as hollow spheres in the submicron and larger size ranges have been used as alternatives to inorganic pigments such as titania. Various polymers have been evaluated as binders, but gelatin is still the most widely used material for this application. Various latexes, as small as 40 nm and less, have been used as binders, usually in conjunction with gelatin. Microgels of water-swellaible polymers are now beginning to be used as binder components. Matte beads in the range of 1 to 10 μm are used to guard against layer-to-layer adhesion and are typically made from polystyrene, poly(methyl methacrylate) and related polymers. Such beads may be chemically cross-linked, for example, by incorporating divinyl benzene in the monomer mix.

This range of scales may be qualitatively considered in terms of the transmission electron micrograph (TEM) shown in Figure 5.5, where a thin cross-section of an amateur colour-negative film is depicted. Thirteen distinct layers are evident, as is the particulate nature of almost every layer. Starting from the right-hand side of the figure, one can identify the following layers: an overcoat layer, a UV-filter dye layer, fast blue, slow blue, two distinct interlayers, fast green, slow green, an interlayer, fast red, slow red, antihalation layer and PET support, plus a subbing interlayer (which is not visible). With the exception of some lengthy artifacts spanning two or more layers and arising from the formation of folds in the very thin (100 nm) cross-section used in this TEM, the black particles are silver halide or

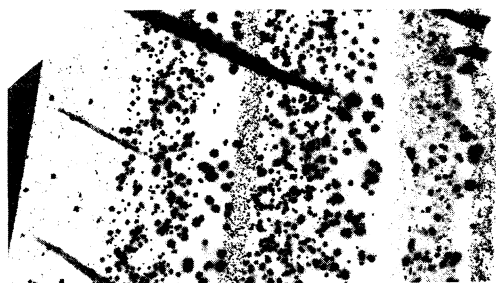


Figure 5.5. Transmission electron micrograph of a thin (~ 100 nm thick) cross-section of commercial VR100 amateur colour-negative film. The top overcoat layer is at the far right. The next is a UV layer with a Lippmann emulsion, followed by the fast and slow blue-sensitive layers, two interlayers, fast and slow green-sensitive layers, an interlayer, fast and slow red-sensitive layers, an antihalation layer, and a portion of the PET support. The overall width of the figure corresponds to a total thickness of 53 μm

colloidal silver. In the UV layer (second from right) one sees evidence of two kinds of particles. The small black particles are Lippmann emulsion particles that serve to filter and adsorb surface-active compounds that accumulate in seasoned developer baths. The apparent voids appearing as ellipsoidal shapes are holes left by UV-filter dye dispersion particles. The size of the silver halide crystals in the fast emulsion layers is larger than the slow-layer silver halide. This is particularly the case in the blue record. The rightmost interlayer between the blue and green records contains colloidal silver of very fine particle size. This yellow colloidal silver is used to absorb blue light that passes through the blue record. The voids evident in this layer are due to particles of oxidized developer scavenger which are incorporated to retard “cross-talk” between the blue and green records. The interlayer between the green and red records contains a Lippmann emulsion. This very small-sized emulsion serves to adsorb development inhibitors released as coupling-off groups by certain of the couplers, and to keep such inhibitors from crossing over to other records.. Insufficient contrast exists to clearly image the coupler dispersion particles, but many of these are visible as apparent voids in the green and red records. Almost all of them are less than 1 μm in diameter, and most are smaller than 0.5 μm .

2.3 Development

Silver halide development, whether in black and white or in colour elements, occurs by an autocatalytic redox process. For example, in the case of

development with hydroquinone, aminophenols and paraphenylenediamines, a two-equivalent reduction of silver halide occurs (as illustrated in the top part of Figure 5.4 for paraphenylenediamine development). The characterization of this equivalency carries over to the dye-formation chemistry, where the equivalency of image-dye formation is expressed in terms of the amount of silver halide that must be reduced. The couplers illustrated in Figure 5.4 exemplify so-called two-equivalent and four-equivalent couplers. Because they have coupling-off groups, only one QDI is required to form an image dye from a two-equivalent coupler. One QDI molecule attacks and reacts with the coupler to produce the dye. An example of such a two-equivalent coupling is given by the cyan dye-forming class of couplers in the middle of the bottom part of Figure 5.4. When the coupler does not have a coupling-off group, a leuco-dye is formed instead. This leuco-dye must undergo a two-electron oxidation in order to convert to the final dye molecule, and this oxidation is typically effected by another QDI molecule. Such couplers are therefore known as four-equivalent couplers. The acetanilide and pyrazolone coupling species shown in Figure 5.4 are examples of four-equivalent couplers. More recently, efforts in research have been directed towards developing one-equivalent and less-than-one-equivalent couplers. A simple method of producing one-equivalent couplers is to incorporate a dye molecule as the coupling-off group. Thus, after coupling, there exist two image-dye molecules. Such efforts are particularly useful in dye-diffusion transfer elements.

2.4 Coupling stoichiometry and reactivity

Although the stoichiometry between silver development and image-dye formation is well defined, achieving near-stoichiometric yields can be difficult or impossible because of system inefficiencies in the utilization of QDI. One can view QDI as the messenger that transforms the information in the developed silver image to information in the image dye. QDI that does not react to form an image dye in the record of choice is, in a yield sense, wasted. QDI can diffuse out of the emulsion layer in which it was to form dye. This species reacts with hydroxide and sulfite, present in most developer solutions, to form other by-products. Hydroxide is present in developer solutions to activate the couplers (typical pH in the range 9–12) and sulfite is present in many developer solutions as a preservative against aerial oxidation of PPD. If we define Y as the molar dye yield, i.e. the number of moles of image dye produced per mole

of silver halide reduced or developed, one can invoke a steady-state approximation in oxidized developer (generation and consumption) and derive this yield in terms of the dye-forming rates, R_c , and competition rates, R_x , and the respective equivalencies, e_c and e_x . This relationship is given in terms of the Weaver–Bertucci equation (7), as follows:

$$Y = \frac{1}{e_c + e_x \left(\frac{R_x}{R_c} \right)} \quad (5.1)$$

This equation shows that the yield obtained depends on the *ratio* of the coupling rates to the system competition (loss) rates, and the general relationships are illustrated in Figure 5.6. We see from this figure, for either two-equivalent or four-equivalent couplings, that stoichiometric yields, respectively, of 0.5 or 0.25 are only obtained when the ratio of coupling-to-loss rates are of the order of 10 or higher. When this ratio is of order unity, the heterogeneous reactivity of the coupler dispersion comes into play. Various factors can affect the coupler dispersion reactivity. First, it has been very well established that ionized couplers are much more reactive in the coupling reaction than are unionized couplers. The coupling reaction is, by and large, a surface reaction and occurs at the continuous phase–coupler particle interface. At a given pH, a certain fraction of the coupler will be ionized, and activated, in analogy to the ionization of fatty acids in monolayers. The observed coupling rates will vary widely, depending on the intrinsic bimolecular reactivity of a particular coupler type, just as has been

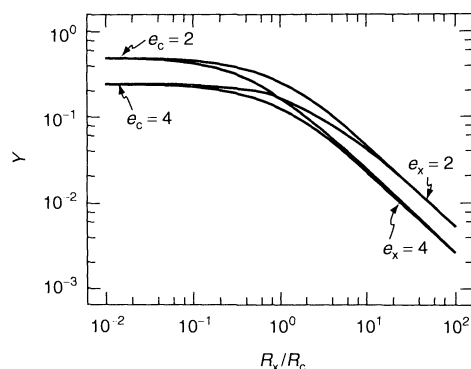


Figure 5.6. Graphical representation of the Weaver–Bertucci equation, illustrating how the molar dye yield, Y , varies as a function of the ratio of the system competition rate, R_x , to the coupling (dye-forming) rate R_c . Four different curves corresponding to different combinations of two-equivalent and four-equivalent coupling (e_c) and competition (e_x) are illustrated

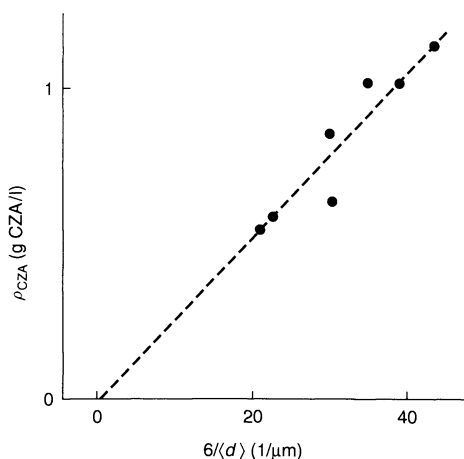
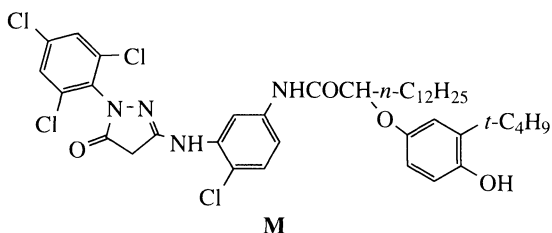


Figure 5.7. Coupling reactivity as a function of surface-to-volume ratio (proportional to the specific surface area) for the coupler **M** prepared as an NS dispersion. This coupling reactivity is expressed as ρ_{CZA} in units of g CZA per litre. Both the coupler **M** and CZA (citrazinic acid) are four-equivalent. The specific surface-to-volume ratio for monodisperse spheres is $6/d$. The average diameters $\langle d \rangle$ for the various dispersions were measured by disc centrifugation with turbidity detection. (Data by courtesy of Dr Andrew Sierakowski)

modelled in homogeneous physical organic chemistry. However, another important contribution to coupling reactivity is the specific surface area of the coupler dispersion particles. Thus, for certain classes of couplers, the specific surface area increases with decreasing particle diameter, while the coupling reactivity increases as the particle size decreases. Some example data are illustrated in Figure 5.7, where decreasing size yields increased reactivities for “NS” dispersions (i.e. those formulated without (coupler) solvents – see Section 4.1 below) of the coupler **M**:



Whether or not increased coupling reactivity results in increased dye yields, according to the Weaver–Bertucci equation, it also depends on how much system competition or QDI loss is prevalent during the development process. The reactivity illustrated

in Figure 5.7 of the coupler **M** dispersions, ρ_{CZA} , is defined (8) in terms of the amount of added competitor, in this case CZA (citrazinic acid), that is required in the developer in order to decrease the molar dye yield by a factor of 50% over that obtained in the absence of added competitor. Both the coupler **M** and CZA are four-equivalent with respect to their utilization of QDI, so in this case $e_x = e_c = 4$. The linearity illustrated in Figure 5.7 shows that interfacial (specific surface) area (particle size) is a kinetically limiting parameter in the heterogeneous coupling of **M**.

3 PARTICLES AND COLLOIDS IN PHOTOGRAPHIC TECHNOLOGY

The discussion above of Figure 5.5 illustrated that there are many different types of organic and inorganic particles in photographic elements. The formation and stabilization of these particles, before, during and after element manufacture represent important practical applications of surface and colloid chemical concepts. Some of these concepts are illustrated here in our discussion of some of the most important particle classes.

3.1 Silver halide

Silver halide microcrystals are solid-state sensors that, after exposure to visible light, generate a latent image that can subsequently be developed and amplified to produce a silver image. The process of latent image generation is discussed briefly below. The formation of silver halide microcrystals in different shapes (habits) and sizes is the most highly developed area of inorganic particle precipitation, and is very well understood from many viewpoints, although particular aspects still remain as empirical art. This applies for AgCl, AgBr and AgI, as well as for mixed halide crystals (e.g. $\text{AgBr}_{0.96}\text{Cl}_{0.04}$ and $\text{AgBr}_{0.97}\text{I}_{0.03}$) and pseudohalides (e.g. AgCN and AgSCN).

These various silver halides are usually precipitated in batch or continuous reactors by mixing aqueous solutions of alkali halide salts and silver nitrate. One, two or more reagents may be pumped into the reactor under programmed or feedback control. Key control variables are reagent mixing and delivery, temperature, and especially silver ion activity. The latter can be electrochemically monitored by using silver or silver salt electrodes, and the relative potentials measured by such electrodes provide a means to impose feedback control

on reagent addition in many different types of reactors. Supersaturation is induced in such solutions when the respective solubility product is exceeded, where the solubility product

$$K_{\text{sp,AgX}} = a_{\text{Ag}^+} a_{\text{X}^-}$$

in which a_{Ag^+} and a_{X^-} are the activities of silver ion and halide ion, respectively (cf. Table 5.2 below). These activities can usually be adequately approximated by concentrations, and when required, augmented with activity coefficients. Nucleation is an important, but as yet incompletely characterized process for silver halides. Homogeneous nucleation from reagent ions and complexes is an important colloidal concept that balances the free energy of silver halide condensation and phase formation with the unfavourable surface free energy of growing nuclei that must be overcome to sustain growth. A very useful review of the balance of nucleation and growth processes has been provided by Leubner (9). Seeded nucleation, a concerted form of heterogeneous nucleation, is an important practical approach in many processes. Typically, nanoparticulate silver halide crystallites, e.g. AgBr, AgI or Ag(Br,I), are added to the reactor and used as growth centres to grow particular types of silver halides. Such approaches are particularly useful for growing core-shell types of particles, wherein the core and shell regions have substantially different halide compositions. Such core-shell approaches are also useful for constructing crystallites that will promote internal latent image sites, wherein defects and internal fog centres can easily be created on the surface of grains of a given size, and then covered with a silver halide shell. Such core-shell particles are used in certain reversal or direct positive applications.

A key to the control of crystal habit is in controlling the electrochemical potential by maintaining a constant halide (alternatively, silver ion) concentration during growth. This is usually achieved by using feedback potential control in batch reactors or by maintaining a given reagent flow rate in continuous reactors.

For the case of AgBr, one can vary the habit from cubic to octahedral to tabular by simply adjusting the excess bromide concentration. This concentration controls how the silver ion in solution is complexed or coordinated. At very low excess bromide levels, the silver ion is tetrahedrally aquated as $\text{Ag}(\text{H}_2\text{O})_4^+$ (10). As the bromide concentration increases, $\text{AgBr}(\text{H}_2\text{O})_3$, $\text{AgBr}_2(\text{H}_2\text{O})_2^-$, $\text{AgBr}_2(\text{H}_2\text{O})^{-2}$ and AgBr_4^{-3} complexes compete for silver ion complexation. The interactions of these complexes with the various AgBr crystalline facets dictates the growth rates of such facets, while

the competition in growth rates of the different facets determines the resulting habit. Facets that grow more quickly tend to disappear, and those facets we see are those that grew more slowly. At bromide concentrations less than 10^{-3} M, primarily cubic AgBr is obtained (or less than 0.1 M chloride in the case of AgCl). The $\text{AgBr}(\text{H}_2\text{O})_3$ and $\text{Ag}(\text{H}_2\text{O})_4^+$ complexes predominate under these conditions. As bromide is increased and the $\text{AgBr}_2(\text{H}_2\text{O})^{-2}$ complex becomes competitive in concentration with $\text{AgBr}(\text{H}_2\text{O})_3$, the octahedral habit predominates. At bromide concentrations greater than 10^{-2} M, tabular crystals of AgBr predominate. Under these high halide conditions, the largest exposed surfaces are (111) surfaces and are essentially covered with hexagonally close packed halide. More rapid growth occurs parallel to these planes, along one or more (111) twin planes.

The solubility of silver halides varies markedly because of the common ion effect and because of the formation of various mononuclear complexes, such as those articulated above for AgBr. The solubility of AgBr as a function of pAg ($-\log[\text{Ag}^+]$) is illustrated in Figure 5.8. Along the right side of the parabolic solubility curves, excess bromide provides ever increasing solubilization from the silver bromide complexes articulated above. On the left-hand side of these parabolas where there is excess free silver ion, multinuclear (positively charged) silver complexes provide a mechanism for increasing solubilization. These solubility variations with pAg have also repeatedly been observed

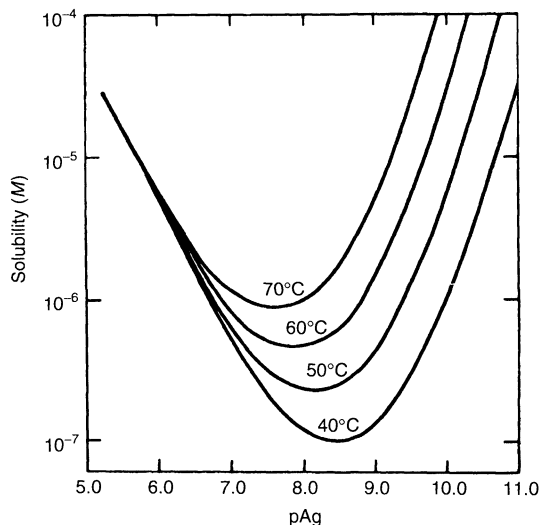
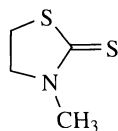


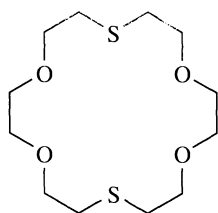
Figure 5.8. AgBr solubility (M) in water as a function of pAg at various temperatures. (Date by courtesy of Dr Jacob Cohen)

for silver halide growth rates, because Ostwald ripening is a very important mechanism of growth. Ostwald ripening is a growth mechanism wherein larger crystallites grow at the expense of smaller crystallites. The greater solubility of the smaller crystallites results in the mass of these smaller particles being redeposited on larger particles having a larger mean radius of curvature. Transport of material is generally ionic or molecular, and anything that increases the continuous-phase solubility of the condensing materials will increase the growth rate.

In addition to the surface chemical effects of intrinsic components such as these complexes, growth restraint can be effected by many kinds of specifically and non-specifically adsorbing species. Organic ligands that tend to form stable and soluble complexes with silver ion, will generally act to promote Ostwald ripening rates. Sulfur-containing ligands generally complex silver ion to some extent, and this tendency makes such species surface active with respect to silver halides. The thiolate thione (**1**) and thioether (**2**) species provide, respectively, relative growth rates about 30-fold and 100-fold greater at 10^{-3} M bromide (pBr 3), relative to a bromide-only control, so that cubooctahedral crystallites twofold and tenfold larger, respectively, were obtained relative to the control. The thioether compound binds silver ion about four orders of magnitude more strongly than does the thiolate thione species. These size and growth rates are simple functions of the solution-phase silver ion solubility.



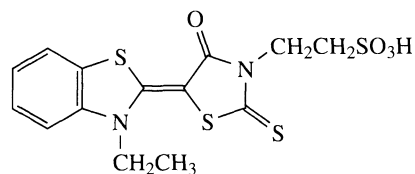
(1)



(2)

Alternatively, organic ligands and compounds that tend to form sparingly soluble silver salts will generally act as growth restrainers. It was mentioned above that the range of 10^{-3} to 10^{-2} M excess bromide (pBr 2) is a transition region from the cubic to the octahedral habit for AgBr. Within this region, other additives can be used to modify the crystal habit. The use of gelatin as a peptizing agent, at $\text{pH} > 5$ where most of the carboxy groups are ionized, tends to maintain the cubic or cubooctahedral habits. Cationic copolymers having

trimethylammonium pendant chains, on the other hand, tend to promote octahedral AgBr formation. A myriad of organic compounds have been found to promote one sort of habit or another. The surface-active species **3** has been found to restrain growth on (111) AgCl surfaces, and promote octahedral grain growth.



(3)

The crystal size of silver halides ranges from less than 10 nm to more than several microns. High speed X-ray films typically contain large crystallites, since sensitivity to X-ray radiation is intrinsically a volume effect. The crystallites used for blue light detection in colour negative films are also large, often of the order of 1 μm in diameter or larger (cf. the fast blue silver halide in Figure 5.5). Particle sizes fall to 100–300 nm for print materials, where there is more control of exposure and high speed is not an issue. Particle sizes less than 100 nm are used for microfilm products, which typically are very slow but require high spatial resolution. Finally, astronomical plates requiring the greatest spatial resolution utilize the smallest crystallites in the 8–50 nm size range. Control of crystal size distribution is often achieved by Ostwald ripening to eliminate small crystallites.

3.2 Surface charge

Many of these growth effects can be related to surface chemistry. Honig and Hengst(11) made the important discovery that all of the silver halides are negatively charged at their equivalence points. These data are summarized in Table 5.2. One would expect the equivalence point to be an isoelectric point. However, all of the silver halides exhibit a preference for halide adsorption at their equivalence points. The corresponding isoelectric points (IEPs) are also given in Table 5.2. Specific adsorption studies show experimentally that nearly twice as much bromide can adsorb on octahedral (111) AgBr surfaces than on cubic (100) surfaces. This is as expected for the corresponding lattice layers, wherein bromide is hexagonally close packed in (111) layers and cubically arranged in (100) planes.

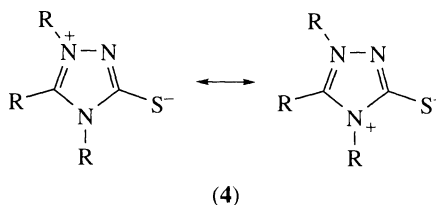
Table 5.2. Solubility products, equivalence points (EPs) and isoelectric points (IEPs) for silver halides

AgX	pK_{sp}	EP (pAg)	IEP (pAg)
AgCl	9.8	4.9	4.6
AgBr	12.3	6.1	5.3
AgI	16.1	8.1	5.6

The surface charge of silver halides, as well as the electrokinetic charge, may be varied by various surface-active species. For example, the effects of adsorbed gelatin on the electrokinetics of AgBr are illustrated in Figure 5.9. For both gelatin types, the same IEP is obtained on AgBr and on glass beads. Glass (silica) typically has an IEP that is very low, usually at a pH less than 3. Moreover, for the pig gelatin, an identical IEP was measured by a streaming current detector on polyethylene. These measured electrophoretic mobility data show that the electrokinetic charge reflects the charge state of the adsorbed gelatin, not of the underlying solid surfaces. The zero mobility points occur at the isoelectric points of the corresponding gelatins, at about pH 4.8 for bone gelatin and at about pH 8.5 for pig gelatin.

Various charged and neutral species have been shown to modify the surface charge or the electrokinetic charge of silver halides. The adsorption of positively charged quaternary species at pBr 3 has been shown to reverse the sign of the electrophoretic mobility of cubic AgBr. The adsorption of triazolium thiolates (4), molecules

with large dipoles that carry no net charge, has been shown to lead to electrokinetic charge reversal by an adsorption mechanism that displaces adsorbed halide ions, and so such reversals are due to surface charge reversals (12). Such triazolium thiolates also strongly bind silver ion and are very effective growth promoters (ripening agents).



3.3 Chemical sensitization

Most latent image sites for negative-working silver halide systems are believed to be surface sites. Surfaces offer the highest frequency of defects and other sites that may stabilize a latent image cluster. This preponderance is increased by chemical sensitization, by forming latent image precursors or an increased number of surface or near-surface sites that will stabilize the latent image. Typical chemical sensitization chemistries involve treatment with sulfur, gold and reducing agents, such as hydrogen and hydrazine. Many other metals and diverse complexes and species have been investigated

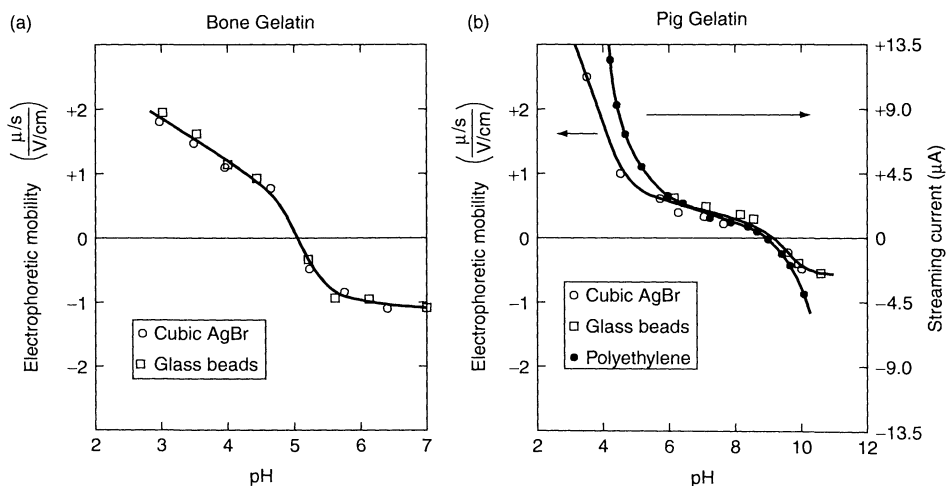
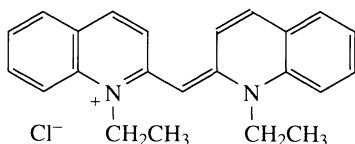


Figure 5.9. Electrophoretic mobility effects of (a) bone and (b) pig gelatins adsorbed on cubic AgBr, glass beads and polyethylene at 24°C. Reproduced by permission from J.I. Cohen, W.L. Gardner and A.H. Herz, *Advances in Chemistry Series*, **145**, 198–217 (1975); © 1975 by The American Chemical Society

as well. The most prevalent form of chemical sensitization is the use of sulfur and gold. Sulfiding, often by chemical decomposition of thiosulfate, is believed to form latent image precursors involving Ag_2S and $\text{Ag}_n\text{S}_{mn}^{+n-m}$ clusters or aggregates. Gold is often introduced as an auric complex (e.g. KAuCl_4) or as an aurous complex (AuSCN , Au_2S or as an Au-triazolium thiolate salt). It is believed that Au^+ occupies Ag^+ vacancies and forms mixed AuAg_n latent image specks that are superior catalysts to homogenous silver specks. Reduction sensitization can be achieved with a variety of reducing agents, such as with hydrogen gas, hydrazine derivatives and reducing gelatins, to name just a few. It is believed that such treatments produce latent image precursors involving silver atoms that require only one or a couple of additional silver atoms to produce a stable latent image speck. Chemical sensitization processes, for negative-working emulsions, are usually carried out as a separate operation after crystal formation. Temperature, pH and pAg are the parameters that are typically varied, and often cycled, to promote surface sensitization chemistry.

3.4 Sensitizing dye adsorption

Silver halides are spectrally sensitized to visible light by adsorbed sensitizing dyes. Aspects of this electronic coupling are discussed below. A requisite for this process is to get the sensitizing dyes in a condensed state on the surfaces of the silver halide microcrystals. This process is often facilitated by surface aggregation processes. These processes are exemplified by distinguishing monomeric dye adsorption states from dye aggregate adsorption states. The adsorption of pseudoocyanine **5** on to AgBr surfaces is illustrated in Figure 5.10. The monomeric absorption envelope is that which is characteristic of the isolated dye molecule in an adsorbed state. As the solution-phase dye concentration increases, co-operativity in dye-dye interactions come into play, and a condensed-surface dye aggregate, in this case the J-aggregate, forms. This class of aggregates is characterized by intense long-wavelength absorption maxima at longer wavelengths than the adsorbed monomer



(5)

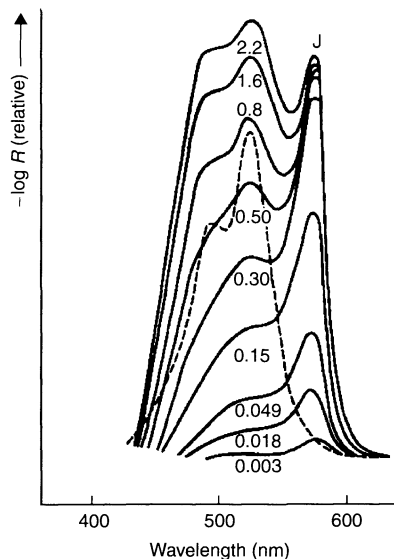


Figure 5.10. Pseudocyanine aggregation on AgBr illustrating the adsorbed J-aggregate spectrum generated from adsorbed monomeric dye. The solution spectrum of the dye is illustrated as the dashed curve. Each spectrum for adsorbed dye is annotated with the number of millimoles of dye added per mole of AgBr. Relative reflectance (R) measurements were made on turbid suspensions relative to a control suspension containing no added dye. Increasing absorbance corresponds to a decreasing R and an increasing $-\log R$. Adapted from A.H. Herz, *Adv. Colloid Interface Sci.*, **8**, 237–298 (1977)

absorption band. The so-called H-aggregate produces an absorption maximum at shorter wavelengths than the adsorbed monomer.

Adsorption isotherms can conveniently be measured for sensitizing dyes on silver halides. The formation of a J-aggregate indicates a close-packed condensed state that corresponds to a certain limiting area per dye molecule. Such areas are conveniently measured by performing adsorption measurements on monodisperse emulsions of a given silver halide type. Limiting areas can then be used to estimate surface areas of polydisperse emulsions of the same halide type.

3.5 Spectral sensitization

Silver halides have intrinsic spectral sensitivities that correlate with their absorption cross-sections. However, these intrinsic sensitivities are essentially limited to the UV region for AgCl, and the blue and UV regions for AgBr and AgI. In order to make silver halides really useful over the visible spectrum, and to make them

useful for capturing the red, green or blue components of coloured scenes, spectral sensitizing dyes are adsorbed and electronically coupled to silver halide valence and conduction bands (13). Various mechanisms of spectral sensitization have been described, although no single mechanism covers the behaviour of all sensitizing dyes. The details depend on the electronic properties, including the photoelectrochemical properties, of these dyes. Such details affect how a particular dye, or dye aggregate, couples into the electronic structure of the silver halide microcrystal. In simple terms, photoexcitation raises an electron to the lowest unoccupied molecular orbital (LUMO) of the sensitizing dye. This electron can then tunnel into the conduction band of the silver halide and be trapped at a latent image site. Alternatively, this electron can be competitively returned to the sensitizing dye molecule (electron-hole recombination).

4 COUPLER DISPERSIONS

4.1 Emulsification

Dispersion formation by emulsification is an effective way to disperse couplers, and any of the other water-insoluble organics that are useful in photographic elements (cf. Table 5.1 and the discussion above of organic materials) (14). A very widely applicable technique for preparing amorphous organic nanoparticulates is to dissolve the water-insoluble organic coupler in a water-immiscible solvent having a relatively high vapor pressure (e.g. ethyl acetate) in order to form an "oil phase" containing the substrate. Such water-immiscible solvents are often known as "auxiliary" solvents. In addition to such auxiliary solvents that are subsequently (generally) removed to condense the coupler as an amorphous particle, other low-vapour-pressure water-immiscible solvents (coupler solvents, plasticizers, etc.) are often included in the formulation at weight fractions of 0.2–2 relative to the coupler. Di-*n*-butyl phthalate, diethyldodecanamide and tri(2-ethylhexyl) phosphate are typical examples of coupler solvents. Dispersions formulated without coupler solvents are often known as "NS" dispersions.

This dissolution step is often aided by heating. The amount of heating (temperature of dissolution) is determined by the thermal stability of the organic substrate, the viscosity required during emulsification, and the amount of auxiliary solvent utilized. It is sometimes possible to omit the auxiliary solvent, or nearly so, when the melting point of the organic substrate is not too high. It is generally desired to

obtain dissolution of the organic substrate by using the least amount of auxiliary solvent necessary, so as to minimize the amount of auxiliary solvent (volatile organic components (VOCs)) that must subsequently be removed.

This organic solution is then emulsified with an aqueous solution containing stabilizers such as surfactant and polymeric dispersants (e.g. gelatin, poly(vinyl alcohol), poly(*N*-vinylpyrrolidone), etc.). Generally, increasing surfactant levels lead to decreasing particle sizes, as the specific surface area stabilized increases in direct proportion to the surfactant added. Charged surfactants provide charge stabilization. Nonionic surfactants and polymeric stabilizers provide steric stabilization. All of the surfactants when adsorbed to the aqueous–oil interface lower the interfacial tension and facilitate smaller droplet production with a given amount of input shear energy. Many high-shear methods for achieving emulsification are available. Such shear methods in decreasing order of effectiveness are high-pressure homogenization, colloid milling with rotor-stator devices, ultrasonic mixing, and very high speed stirring.

The final steps centre on removal of the auxiliary solvent. Two methods are used in practice, i.e. evaporation and washing. On the laboratory scale, evaporation is easily carried out by using a rotovap apparatus. The emulsion is circulated over a large surface area under reduced pressure and the water-immiscible solvent gradually diffuses out of the emulsion into the vapor phase, where it is vented or condensed for recycling. Larger-scale industrially practical flow systems generally condense the auxiliary solvent for recycling. These techniques are only practical for certain classes of solvents, as the auxiliary solvents must exhibit a sufficiently high vapour pressure. Ethyl acetate and cyclohexanone are two examples of auxiliary solvents well suited for evaporative removal. There are, however, several limitations of evaporative solvent removal. One limitation is that evaporation may be too slow at the desired processing temperature, while another is that the amorphous physical state of the organic substrate may be too unstable at the processing temperature and untoward physical ripening, particle growth or crystallization may occur.

Although the auxiliary solvents are water-immiscible, they usually have finite water solubility. It is sometimes preferred to use countercurrent washing techniques to remove unwanted auxiliary solvent. If the emulsion is not gelled, then constant-volume dialysis or ultrafiltration can effectively be used to wash out the auxiliary solvent. If the emulsion gels, as is easily obtained when using gelatin or some other gelling polymeric stabilizer,

one can chill (causing gelation) and then “chunk” the emulsion to produce a high surface area. This gelled emulsion is then repeatedly washed with a stream of wash water (containing appropriate electrolyte to control swelling) to remove the auxiliary solvent.

As the auxiliary solvent is removed and the temperature of the emulsion cools, the solubility of the organic substrate decreases. After the auxiliary solvent is removed, one usually obtains an amorphous (solid) state for the organic substrate. In some cases, particularly when the substrate has few degrees of internal freedom, intraemulsion particle crystallization may occur. However, for most organics having molecular weights > 300 or so, condensation into an amorphous solid state is the rule rather than the exception. Low-vapour-pressure organic solvents or plasticizers can be included in such dispersion formulations for various chemical and physical reasons. Such solvents, plasticizers and additives typically do not very effectively solubilize the substrate. Sufficient water-insoluble solvent, dramatically less water-miscible than auxiliary solvents, can be included to prevent condensation of the organic substrate and to keep the substrate in a solution state.

4.2 Mixed micellization

Micelles are thermodynamically stable nanoparticles that can be used to template metastable nanoparticles of coupler. Preist (15) developed a mixed micellization process for dispersing couplers as extremely small particles. Since the coupling sites in couplers are tied to weak acid sites, and couplers also often have other weak acid functionalities, such as $-\text{COOH}$, $-\text{OH}$ and $-\text{SO}_2\text{NH}-\text{R}$ groups that can be ionized at sufficiently high pH, they can usually be dissolved at sufficiently high pH levels. When dissolved, they are surface-active and exhibit surfactant properties just as fatty acids and related amphiphiles do. When dissolved and mixed with a micellar solution of a conventional charged surfactant, they form mixed micelles that are thermodynamically stable. When this mixed micellar solution is acidified, for example with an organic acid (e.g. acetic acid), the coupler molecules are neutralized. These mixed micelles are thereby transformed from thermodynamically stable nanoparticles (5–20 nm in diameter) to metastable particles. With appropriate stabilization against phase separation, such metastable coupler dispersions can remain stable for many, many months while still maintaining their ultra-small particle size.

Various methods can be used to provide kinetic stabilization of such reprotinated couplers. Charge stabilization is a key approach. The most effective way to utilize charge stabilization is to use anionic surfactants having sulfo groups that remain charged at $\text{pH} < 1$. After acidification and reprotonation of the weakly acidic organic compounds, the ionic surfactants remain charged and provide charge stabilization. The ionic strength of the suspension must be kept suitably low so that excess electrolyte does not shield the electrostatic repulsion afforded by the surfactant head-groups. Nonionic surfactants and polymeric stabilizers (nonionic and polyelectrolytes) can provide steric stabilization of the reprotinated coupler dispersion particles. The combined use of polymeric stabilizers in conjunction with charged surfactants generally provides improved overall stabilization.

In addition to the kinetic stabilization against phase separation afforded by charge and steric stabilization, one must also be cognizant of untoward chemical consequences of alkaline dissolution of complex organics such as couplers. Couplers often have a variety of linking groups that are susceptible to hydrolysis reactions, and such reactions are often catalysed by nucleophiles such as hydroxide groups. Water-miscible organic solvents are therefore sometimes used to provide some chemical stabilization, so that dissolution of coupler can be effected at a lower pH, and thereby avoid or diminish hydrolysis of the coupler that may occur at higher pH levels.

A flow chart of this general process is illustrated in Figure 5.11. Surfactant and alkaline coupler solutions are combined to form a solution wherein surfactant and coupler form mixed micelles. This solution is then acidified and the coupler is reprotonated to create metastable coupler (nano)particles. Excess salt is then removed by washing (ultrafiltration or dialysis). Steric stabilization may be imparted by adding polymeric stabilizers or nonionic surfactants at the initial or final process stages.

4.3 Nanocrystalline coupler dispersions

An alternative approach to incorporating couplers into photographic layers is to disperse them as nanocrystalline particles by using conventional comminution (media milling, ball milling, etc.) processing. Submicron particle sizes can easily be obtained. Depending on the weak acid functionality of the coupler molecule, photographic coupling activity competitive with that obtained by the above described emulsification approach

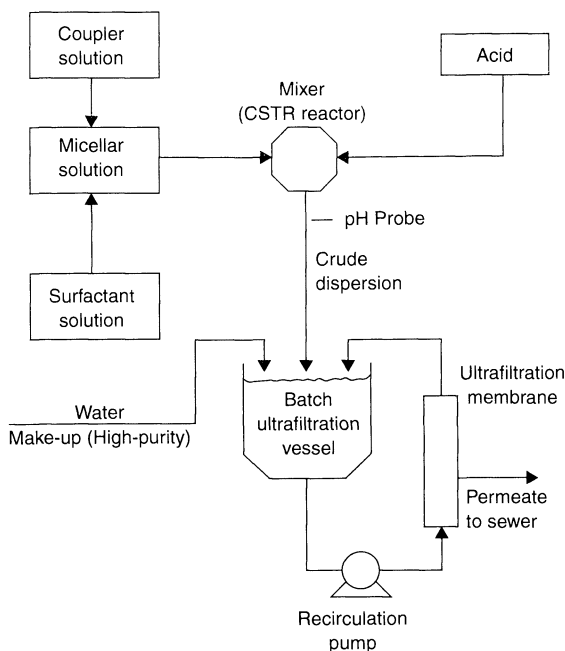


Figure 5.11. Flow chart of the mixed micellization process for preparing stable nanodispersions of couplers. A continuous stirred tank reactor (CSTR) is used to acidify and reprotonate ionized coupler in the mixed micelles. Excess salt is removed by ultrafiltration. Reproduced by permission from K. Chari and J.T. Beck, US Patent 5256527 (1993)

may be obtained (16). This approach, however, generally requires that the nanocrystalline particles be coated with a water-immiscible organic solvent to promote coupling activity, in much the same way that such solvents are found to be effective in emulsification formulations.

5 ADSORBER DYES AND FILTER DYES

5.1 Light management

Dyes and pigments are used to manage the flow of light prior to, within, between and under the light-sensitive emulsion layers. For example, absorber dyes are used to create antihalation layers at the bottom of sensitized elements, so that light that gets through all of the layers of an element is absorbed, and can thereby not reflect back up through the element and cause exposure laterally away from the incident light ray. Another use of such absorber dyes is to decrease the speed of a particular sensitized layer. by adding a

dye to a layer that competes for light with the sensitizing dye on the silver halide, the effective speed of that layer will be decreased. Another important use of absorber dyes is in interlayers. For example, yellow absorber dyes are placed in interlayers beneath blue-sensitive silver halide layers so that light that gets through such a blue-sensitive layer does not cause exposure of any underlying green- or red-sensitive layers. This is a practical concern, since most silver halide is intrinsically blue-sensitive. Similarly, magenta absorber dyes are often put in interlayers beneath green-sensitive layers so that green light not absorbed by the green-sensitized silver halide does not expose the underlying silver halide layers. For example, underlying red-sensitive silver halide often is also somewhat green-sensitive, due to the breadth of the sensitizing dye absorption envelopes. Finally, UV absorber dyes are often coated in overcoats to protect the image dyes formed from UV-induced photodegradation.

There are a variety of ways to introduce absorber dyes into particular layers. The simplest approach is to add the dye to the layer as a solution. A major limitation of such an approach is that dye solutions are prone to diffuse into other layers where the efficacy of the dye may be nil. Preferred approaches utilize incorporation methods wherein the absorber dye cannot diffuse out of the layer into which it is incorporated.

5.2 Dye dispersions

A very effective approach to dispersing water-insoluble absorber dyes is to use the emulsification–dispersion process described above for coupler molecules. NS dispersions of such dyes are straightforward. A limitation that must be considered is whether or not the dye will transform after formation from an amorphous physical state into a crystalline state. Absorption properties often change upon crystallization.

Another approach is to imbibe water-insoluble absorber dyes into latexes by controlled swelling. A latex is put into a solvent mixture which causes swelling and which also solubilizes the dye of interest. As the latex swells, the solubilized dye is imbibed into the particle. The solvent composition is then shifted to cause the latex particle to condense, with entrapped absorber dye. Provided that the latex polymer and dye are sufficiently miscible, the dye may be incorporated into any layer by adding a suspension of the loaded latex into the layer melt composition.

Comminution techniques also effectively produce solid particle dispersions of absorber dyes. Aqueous

suspensions of dye particles ranging from 30 to 300 nm in size may easily be prepared by a variety of small media milling processing techniques. Recent advances in such technology have demonstrated the possibility of producing extremely small particles in certain cases, wherein most of the (mass is in) particles are less than 40 nm in size.

Solvent shifting is a process by which the solubility of a component is altered by changing the composition of the solvent. High solubility in one solvent can be mitigated by the addition of another solvent in which the soluble component is much less or only sparingly soluble. Similarly, high solubility can often be obtained by ionizing an organic species, such as a weak carboxylic acid, in dilute alkali solution. Subsequent neutralization by pH shifting, or by dropping the pH through the pK_a of the acid, generally yields a significant drop in solubility, and is often accompanied by precipitation of the weak acid component.

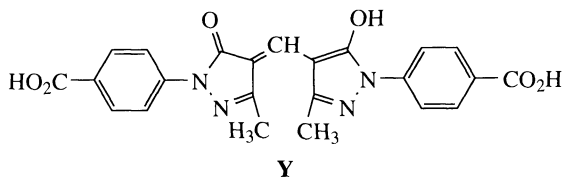
Precipitation into submicron-sized particles is another direct approach. Precipitation by pH shifting can be an effective approach for dyes that have weak acid functionality. A number of different families of such dyes have been dispersed by acidification of weakly alkaline dye solutions, in the presence of stabilizers such as surfactants and polymers. Alternatively, solvent shifting has been demonstrated to be an effective method of preparing absorber dye dispersions. Recent work by Brick *et al.* (14) has shown how such dyes can be very effectively precipitated from a variety of water-miscible organic solvents. Finally, another approach for incorporation of absorber dyes is to precipitate or condense them on the surface of a high-surface-area carrier species, such as colloidal silica. Such preparations can be prepared by pH- and solvent-shifting processes, in the presence of the carrier particles.

5.3 Dispersion electrokinetics

Surface chemistry is very important for most of the organic particulates incorporated in photographic elements. We saw earlier that coupler dispersion reactivity can be a sensitive function of the dispersion's specific surface area. Surfactant adsorption plays a major role in determining such areas (and particle sizes). Surfactant adsorption is also important for physical reasons, such as colloidal stabilization. Charged surfactants provide a means for charging the particle surfaces, and this adsorbed charge is useful in generating double-layer repulsion between approaching particles. The characterization of adsorption onto polydisperse particulates,

particularly organic particulates, is not so well developed as it is for silver halides. However, essentially all of the same colloidal and surface chemical techniques may be applied.

Here, we examine the adsorption of an anionic surfactant, sodium oleoylmethyltaurine (OMT), onto a yellow pigment dispersion of **Y**, used in various filter layers and antihalation layers in different kinds of photographic products. An aqueous dispersion of **Y** was prepared by grinding in water in a small-scale ball mill using ceramic media (17). No surfactant was added to the mixture during grinding, so that the resulting particles could be used as substrates for studying surfactant adsorption. Very small particles were obtained; such particles were lathe-like in shape. Detailed image analysis showed that the particles had a volume-average equivalent-spherical diameter of about 100 nm and a specific surface area of about $50 \text{ m}^2 \text{ g}^{-1}$.



The adsorption of OMT onto this dispersion was studied in two ways. First, an electroacoustic technique was used to study the electrophoretic mobility of the pigment particles as a function of added surfactant. In this technique, the electroacoustic sonic amplitude (*ESA*), is measured in a flow cell. The *ESA* magnitude represents the ultrasonic pressure amplitude generated in response to a unit applied rf field, and is proportional to the electrophoretic mobility (18). The experimental results obtained are illustrated in Figure 5.12(a). At the pH (5.05) of the experiments, the particle surfaces are initially negatively charged due to ionization of surface carboxy groups. This is why the electrophoretic mobility is negative before any anionic surfactant is adsorbed. As OMT is added to the dispersion, the surfactant adsorbs and drives the electrophoretic mobility more negative. The breakpoint illustrated by the arrow in Figure 5.12(a) corresponds to where the adsorption effect appears to saturate. This point corresponds to $5.3 \times 10^{-5} \text{ mol g}^{-1}$ (OMT/**Y**).

In separate experiments (17), the adsorption of OMT onto this dispersion of **Y** was measured. The data are plotted in Figure 5.12(b) to facilitate a linear regression analysis in terms of Langmuir adsorption parameters.

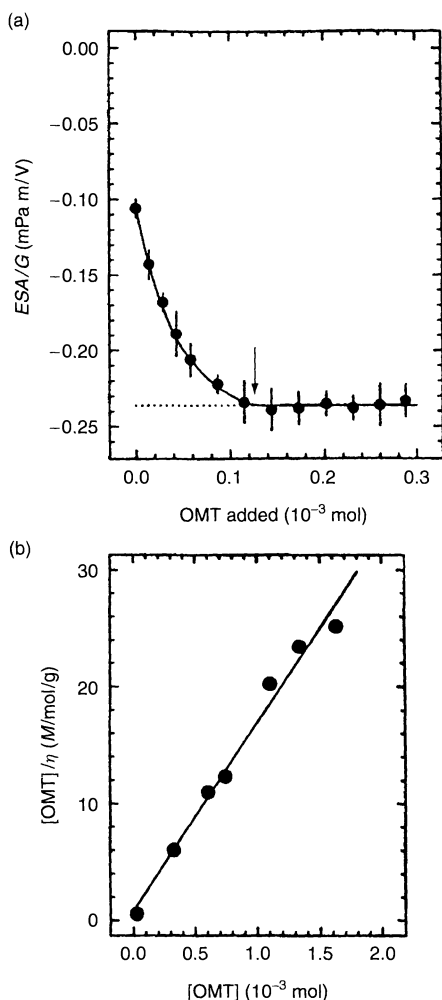


Figure 5.12. (a) Variation of ESA (G is an instrumental constant) with added OMT for a dispersion of pigment Y at a volume fraction of 0.0135, pH 5.05 and 25°C . The breakpoint denoted with the arrow corresponds to $5.3 \times 10^{-5} \text{ mol g}^{-1}$ (OMT/Y). (b) OMT adsorption isotherm on Y at volume fractions ranging from 0.017 to 0.025 and at pH 5.05 and 25°C . The adsorption, η (mol OMT/g Y) was measured by phase separation. The Langmuir adsorption isotherm saturation parameter, η_s , was $6.23 \times 10^{-5} \text{ mol g}^{-1}$, and the binding constant was $10^{4.2} \text{ l mol}^{-1}$. Reproduced by permission from ref. (17); © 1992 by The American Chemical Society

The key result is that the saturation adsorption determined from these data, i.e. $6.2 \times 10^{-5} \text{ mol g}^{-1}$, is very close to the breakpoint value illustrated by the arrow in Figure 5.12(a). It appears that the ESA experiment provides a rapid route to determining saturation surfactant adsorption.

6 MATTE BEADS

Adhesive forces and attractive interactions are greatest for parallel planar surfaces and decrease in proportion to the contact area. Matte beads in the 1 to $5 \mu\text{m}$ diameter range, when coated at a low-number density in overcoat layers, mechanically retard adhesion interactions between stacked layers (as in a box of sheet film or paper) and rolled layers (as in large rolls during manufacturing or in consumer roll film), since only point contacts can be made with a surface coming in contact with an overcoat layer containing matte beads.

The synthesis of large polymeric particles can be challenging, especially if uniform particle size is desired. Emulsion polymerization is unsuitable, because the basic mechanism maintains a very high number of polymerization sites and very small particle sizes are produced. Alternatively, emulsification of monomer followed by suspension polymerization can be used to produce large beads, but the emulsification process generally produces a wide particle size range, and so a plethora of particles too small to be useful will generally be obtained. A particularly useful method for making large beads is to use limited coalescence to produce a uniformly sized emulsion of monomer, and then carry out suspension polymerization (19, 20).

For a given final particle size, d , the volume, V , of beads to be synthesized is selected. From the simple relationship for the surface (area)-to-volume ratio, S/V , for monodisperse spheres:

$$S/V = \frac{6}{d} \quad (5.2)$$

the surface area to be stabilized can easily be calculated from the total volume and the individual particle size specified. This total surface area is then used to compute the amount of stabilizer to be added to the monomer–water mixture prior to emulsification. One can use any suitable surfactant, many of which are known to close pack at oil–water interfaces with a given limiting molecular area. Alternatively, one might use nanoparticles of inorganics, such as silica, or various other stabilizing materials. Such materials also have a typical limiting area per particle that is known or can easily be determined experimentally. The stabilizer is then added to the emulsion mixture, and the mixture is then emulsified or homogenized to a droplet diameter *smaller* than the final, desired droplet size. The “crude” emulsion is then incubated with stirring, typically overnight, to promote collisions between the droplets. As the droplets collide, they will tend to coalesce and grow in size. However, when the emulsion droplets have grown essentially to the target size, each

droplet will be essentially saturated with surface stabilizer, and further coalescence will be strongly kinetically retarded. At this point, suspension polymerization is initiated, by standard means, and the monomer in each particle is polymerized, thus producing polymeric beads of the desired size.

7 REFERENCES

1. Fleischer, C., Bauer, C. L., Massa, D. J. and Taylor, J. F., Film as a composite material, *MRS Bull.*, **21**, 14–19 (1996).
2. Texter, J. and Lelental, M., Network formation in nanoparticulate tin oxide – gelatin thin films, *Langmuir*, **15**, 654–661 (1999).
3. Sturmer, D. M. and Marchetti, A. P., Silver halide imaging, in *Imaging Processes and Materials*, 8th Edn, Sturge, J., Walworth, V. and Shepp, A. (Eds), Van Nostrand Reinhold, New York, 1989, pp. 71–109.
4. Bacon, R. E., Latent image effects leading to reversal or desensitization, in *The Theory of the Photographic Process*, 4th Edn, James T. H. (Ed.), Macmillan, New York, 1977, pp. 182–193.
5. Krause, P., Color photography, in *Imaging Processes and Materials*, 8th Edn, Sturge, J., Walworth, V. and Shepp, A. (Eds), Van Nostrand Reinhold, New York, 1989, pp. 110–134.
6. Kapecki, J. and Rodgers, J., Color Photography, in *Kirk-Othmer Encyclopedia of Chemical Technology*, 4th Edn, Vol. 6, Wiley, New York, 1993, pp. 965–1002.
7. Sturge, J., Walworth, V. and Shepp, A. (Eds), *Imaging Processes and Materials*, 8th Edn, Van Nostrand Reinhold, New York, 1989.
8. Texter, J., *In situ* measurement of coupling reactivity by dye density yield competition, *J. Photogr. Sci.*, **36**, 14–17 (1988).
9. Leubner, I., Particle nucleation and growth models, *Curr. Opinion Colloid Interface Sci.*, **5**, 151–159 (2000).
10. Texter, J., Hastreiter, J. J. and Hall, J. L., Spectroscopic confirmation of the tetrahedral geometry of $\text{Ag}(\text{H}_2\text{O})_4^+$, *J. Phys. Chem.*, **87**, 4690–4693 (1983).
11. Honig, E. P. and Hengst, J. H., Points of zero charge of inorganic precipitates, *J. Colloid Interface Sci.*, **29**, 510–520 (1969).
12. Texter, J., Hydroquinone development acceleration by triazolium thiolates, *J. Photogr. Sci.*, **40**, 83–88 (1992).
13. West, W. and Gilman, P. B., Spectral sensitivity and the mechanism of spectral sensitization, in *The Theory of the Photographic Process*, 4th Edn, James T. H. (Ed.), Macmillan, New York, 1977, pp. 251–290.
14. Texter, J., Organic particle precipitation, in *Reactions and Synthesis in Surfactant Systems*, Texter, J. (Ed.), Marcel Dekker, New York, 2001, pp. 577–607.
15. Priest, W. J., *Res. Disc.* (No. 16468), 75–80 (December, 1977).
16. Texter, J., Multiphase coupling with nanocrystalline coupler dispersions, *J. Imaging Sci. Technol.*, **39**, 340–354 (1995).
17. Texter, J., Electroacoustic characterization of electrokinetics in concentrated pigment dispersions: 3-methyl-1-(4-carboxyphenyl)-2-pyrazolin-5-one monomethineoxonol, *Langmuir*, **8**, 291–298 (1992).
18. Hunter, R. J., The electroacoustic characterization of colloidal suspensions, in *Handbook on Ultrasonic and Dielectric Characterization Techniques for Suspended Particulates*, Hackley, V. A. and Texter, J. (Eds), American Ceramic Society, Westerville, OH, 1998, pp. 25–46.
19. Bennett, J. R. and Smith, D. E., Limited coalescence process, *US Patent 5 354 799* (1994).
20. Whitesides, T. H. and Ross, D. S., Experimental and theoretical analysis of the limited coalescence process: Stepwise limited coalescence, *J. Colloid Interface Sci.*, **169**, 48–59 (1995).

CHAPTER 6

Surface Chemistry in Paints

Krister Holmberg

Chalmers University of Technology, Göteborg, Sweden

1	Introduction	105	4	Pigment Dispersant	113
2	Competitive Adsorption of Surfactants	105	4.1	Paint pigments	113
3	The Binder–Emulsion Preparation and Film Formation	107	4.2	Pigment dispersants	114
3.1	Latices	107	4.2.1	Dispersants for water-borne paints	116
3.2	Post-emulsified binders	111	4.2.2	Dispersants for solvent-borne paints	119
3.2.1	The role of the surfactant	111	5	Wetting of the Substrate	119
3.2.2	Emulsification of short oil alkyds	113	6	Use of Speciality Surfactants	121
			7	Bibliography	122

1 INTRODUCTION

Water-borne paints formulations are among the most complex of systems from a surface and colloid chemistry point of view. Surfactants are needed in order to reduce the free energy of the various interfaces of the system, thus providing kinetic stability to the formulation. Surfactants are used as binder emulsifiers and as pigment dispersants, they are added to improve wetting on low-energy substrates, to control foaming during application and processing, and to prevent film defects caused by surface tension gradients. In addition, surface-active polymers, often referred to as associative thickeners, are widely used to optimize the rheological properties of the formulation, and anionic polyelectrolytes such as polyphosphates are commonly used as dispersing agents for pigments and fillers. Taken together, a water-borne paint formulation is extremely complex, with a plethora of low- and high-molecular-weight compounds competing for available surfaces, such as binder droplets, pigment particles, and, although much smaller in surface area, the substrate to be painted. The situation is schematically illustrated in Figure 6.1.

2 COMPETITIVE ADSORPTION OF SURFACTANTS

Competitive adsorption of surface-active agents is a common problem in paints. In fact, in a paint formulation, with its many different surface-active species and its variety of interfaces, it is virtually impossible to maintain full control of the surface interactions. Uncontrolled desorption/adsorption of surfactants frequently gives rise to unexpected rheological effects and lack of dispersion stability. For instance, the nonionic surfactant needed as a steric stabilizer of latex particles may preferentially adsorb on a hydrophobic pigment surface where it replaces the original dispersant. The net result will be that the latex particle will no longer be fully covered with nonionic surfactant, thus leading to reduced stability, particularly in formulations of high-electrolyte concentration.

Most latex-based paint formulations contain both anionic and nonionic surfactants (see discussion in Section 3 below). Figure 6.2 shows the results obtained from a model experiment in which such a surfactant pair is added to a polystyrene latex and adsorption of the

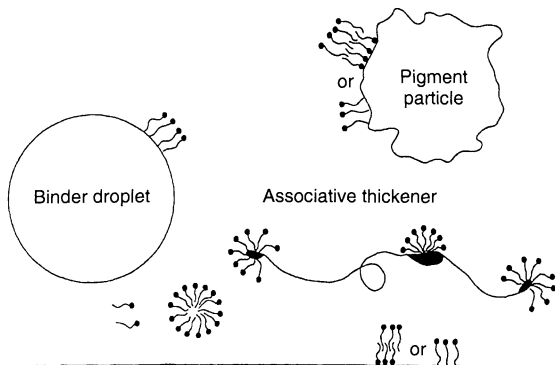


Figure 6.1. A paint formulation containing emulsion droplets, pigment particles, associative thickener and surfactant

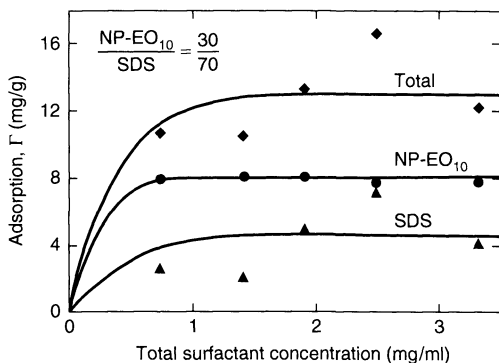


Figure 6.2. Simultaneous adsorption of a nonionic surfactant, a nonylphenol ethoxylate (NP-EO₁₀) and an anionic surfactant, sodium dodecyl sulfate (SDS), on polystyrene latex. (From B. Jönsson *et al.*, *Surfactants and Polymers in Aqueous Solution*, John Wiley, Chichester, 1998, p. 291, Reproduced with permission)

individual components monitored. The surfactants used are nonylphenol (NP) ethoxylate (10 EO) and sodium dodecyl sulfate (SDS), and the molar ratio of the NP ethoxylate to SDS is 30:70. Such a ratio of nonionic to anionic surfactant is common as a latex surfactant system. Additional nonionic surfactant is often introduced into the formulation as mill base dispersant or as wetting agent. Additional anionic surfactant, a sulfate or a sulfonate, may be introduced as a pigment or filler dispersant. This figure shows that the nonionic surfactant is in abundance at the surface in spite of being in lower concentration in the bulk phase. Thus, the nonionic amphiphile adsorbs preferentially on the hydrophobic latex surface.

Figure 6.3 gives another illustration of the preferred adsorption of nonionics over anionics on a hydrophobic

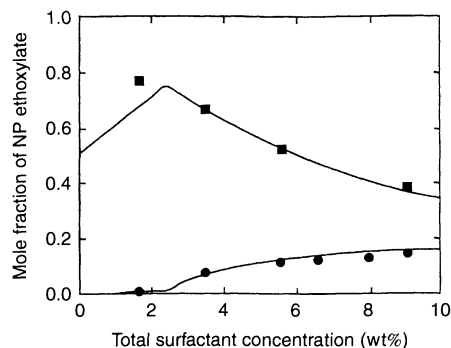


Figure 6.3. Mole fraction of NP ethoxylate at the particle surface (■) and in the aqueous phase (●) as a function of total surfactant concentration in the aqueous phase using a mixture of nonylphenol ethoxylate (NP-EO₁₀) and sodium dodecyl sulfate in a molar ratio of 16:84. (From M. Huldén and B. Kronberg, *J. Coatings Technol.*, **66**, 67 1994, Reproduced with permission of Federation of Societies for Coatings Technology)

latex surface. The same surfactant pair, NP ethoxylate (10 EO) and SDS, is used, this time in a 16:84 molar ratio and the latex is poly(butyl methacrylate). The composition at the latex surface is monitored and the result is given as mole fraction of the NP ethoxylate as a function of total surfactant concentration in the bulk phase. As can be seen from this figure, at low total surfactant concentration almost all nonionic surfactant is present on the latex particle surface. As the surfactant concentration is increased, the ratio of nonionic to anionic surfactant at the surface approaches that in the bulk. The surfactant composition at the surface clearly varies with the total amount in the formulation and the preferential adsorption is greatest at the onset of micellization. It has also been shown that the presence of polar solvents, which are commonly used to facilitate coalescence, affect the ratio of nonionic to anionic surfactant at the surface. The experimentally determined surface composition from such surfactant mixtures agrees well with values predicted by treating the system as a pseudo three-phase system, consisting of a surface phase, a micellar phase and a monomer phase, with only monomers adsorbing at the surface. The micelle–monomer equilibrium in the aqueous phase is given by the regular solution theory for mixed micelles.

The surfactant composition at a hydrophobic surface can be estimated from the values of the critical micelle concentration (CMC) of the individual surfactants. This is a result of the fact that the solution properties of surfactants dominate the adsorption. The molar fraction of nonionic surfactant at the surface, X_n^s , is related

to the fraction in solution, α , through the following expression:

$$X_n^s = \frac{\alpha CMC_a}{\alpha CMC_a + (1 - \alpha) CMC_n}$$

where CMC_a and CMC_n are the critical micelle concentrations for the anionic and nonionic surfactants, respectively. We note that the surface is not a parameter in the equation; the expression is valid for all hydrophobic surfaces. This equation is akin to the expression for composition in a mixed micelle composed of an anionic and a nonionic surfactant.

The problem related to competitive adsorption has been accentuated with the incorporation of associative thickeners in the paint formulation. These polymers, being highly surface-active, have a strong driving force for hydrophobic surfaces such as latex particles. The adsorption behaviour of hydrophobically modified polyurethanes, so-called HEUR thickeners, has been investigated in some detail. If the latex surface is not fully covered by surfactant, these surface-active polymers adsorb at the particle surface, often resulting in gels. Addition of extra nonionic surfactant usually gives fluid, uniform dispersions, suggesting that the nonionic surfactant displaces the polymer from the latex surface.

In a systematic study on the adsorption of mixtures of associative thickeners of the polyurethane type and nonylphenol ethoxylates on a hydrophobic latex, it was demonstrated that polymers with hydrophobic side chains along the backbone could displace the nonionic surfactant provided that the concentration of polymer hydrophobe units was high enough. For associative thickeners with only terminal hydrophobic chains, it was found that the size of these chains is a decisive factor in competitive adsorption. In addition, the distance between the hydrophobic end-groups is of importance; the shorter the distance, i.e. the higher the concentration of hydrophobic chains, then the more effective the polymer is in displacing the nonionic surfactant.

Competitive adsorption at solid surfaces is complex and it is therefore difficult to predict the outcome when new mixtures of amphiphiles or a new particle surface is introduced. The adsorption behaviour may, for instance, be very different at a pigment surface as compared to a latex surface. An anionic surfactant may adsorb more strongly than an associative thickener on the former but not on the latter. This type of competitive adsorption is difficult to predict *a priori*, the more so as most pigments are being surface modified by the pigment producer who usually does not reveal the exact surface composition.

3 THE BINDER – EMULSION PREPARATION AND FILM FORMATION

3.1 Latices

The majority of water-borne paints are latex paints, i.e. aqueous dispersions of water-insoluble polymers made by emulsion polymerization using free-radical initiators. In the majority of cases, the polymers are based on combinations of monomers, often with a high content of water-insoluble entities such as methyl methacrylate, butyl acrylate and styrene, and a much smaller fraction of water-soluble monomers such as acrylic and methacrylic acid. The water-soluble monomers give oligomeric acid segments at the latex particle surface which improves the colloidal stability of the formulation and adhesion and curing characteristics of the film. Most latices for paints have an average particle diameter in the range 100–500 nm.

The emulsifier used in latex preparation is often a combination of nonionic and anionic surfactants. The nonionic surfactant has traditionally been an alkylphenol ethoxylate, but environmental concern has caused a change-over to other ethoxylated surfactants, such as fatty alcohol ethoxylates or fatty acid monoethanolamide ethoxylates. The ethoxylate is the surfactant mainly responsible for dispersion stabilization. The steric stabilization provided by surfactants with relatively long polyoxyethylene chains (>10 EO) is needed in order to retain stability at high-solids content in the presence of electrolytes. Steric stabilization also gives proper shear stability to the latex. The presence of an anionic surfactant, usually an alkyl sulfate or an alkylaryl sulfonate, during the latex synthesis is needed to compensate for the reverse temperature dependence of ethoxylated surfactants. For nonionics, an increase in temperature leads to a decrease in water solubility and an increase in oil solubility. During the course of the emulsion polymerization, there is an increase in temperature which would lead to formation of a water-in-oil emulsion if nonionic surfactants were the sole emulsifier. Upon depletion of the monomer phase, i.e. at high conversion, there would be a phase inversion into an oil-in-water emulsion. Such a phase inversion leads to a very broad particle size distribution, since particle nucleation as well as reaction kinetics will be out of control. A way to circumvent the problem is to use a semi-continuous polymerization process with the monomer being slowly fed into the reactor during the polymerization.

Figure 6.4 shows a typical surfactant monolayer at the surface of latex droplets. It is important to realize that

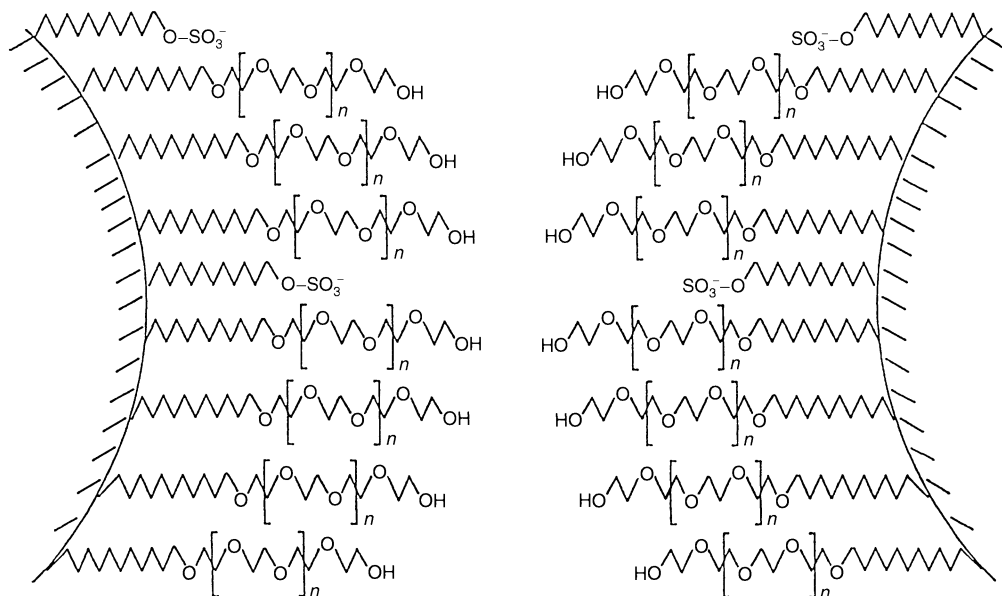


Figure 6.4. A mixed monolayer of nonionic and anionic surfactants usually stabilizes latex droplets

the surfactants are not permanently adsorbed at the surface but subject to a continuous adsorption–desorption process. As was discussed above, the driving force for adsorption at a hydrophobic latex surface is stronger for nonionic surfactants than for anionics, unless the electrolyte concentration is very high. This leads to a higher ratio of nonionic to anionic surfactant at the surface than in the bulk solution.

Anionic surfactants provide electrostatic stabilization and such latices exhibit good storage stability in formulations containing low or moderate salt concentrations. However, latices made with only anionic emulsifier are not stable at high electrolyte concentrations. Evaporation of water during the drying process leads to a continuous raise in ionic strength of the formulation. Often, the stability limit is exceeded at a relatively early stage, leading to particle coagulation and consequent loss in film gloss. Steric and electrostatic stabilization of dispersions is further discussed in Section 4.2 below.

In recent years, there has been a considerable interest in the use of polymerizable surfactants for latices. Such surfactants contain a polymerizable group which may be an acrylate, a methacrylate, an allyl ether or a maleate double bond. Both anionic and nonionic reactive surfactants are commercially available. The polymerizable surfactant is usually added from the beginning, in essence serving as a comonomer in the emulsion polymerization. The reactive surfactant may

also be added at the end of the polymerization process, in which case conventional surfactants are needed to prepare the latex.

By using surfactants that become covalently bonded to the latex particle, many of the problems encountered with conventional surfactants can be avoided or at least minimized. Positive effects are often obtained both on the dispersion itself and on the dried film.

The surfactant-related problems in latices, as well as in many other dispersions, arise from the fact that surfactants physically adsorbed on the particle surface may desorb into the bulk aqueous phase and that the equilibrium between surface and bulk surfactant concentration is governed by factors such as particle concentration, temperature, ionic strength and pH, all of which may be changed during storage, paint application and film formation. Since a certain surface concentration of surfactant is needed to give proper latex stabilization, a change in the adsorption–desorption equilibrium may severely affect the rheology and stability of the dispersed system.

Formulations containing a latex in combination with another dispersion, such as a pigment slurry, constitute a particular problem from a stability point of view. As discussed above in Section 2, the physically adsorbed latex surfactant may have a higher affinity for the pigment than for the latex, a situation which often leads to latex instability. The surfactants used as pigment

dispersants are usually different from those used as emulsifiers in the emulsion polymerization process. Hence, the different surfactants will compete for both surfaces, i.e. the latex and the pigment, and the surface composition and coverage obtained in the equilibrium situation may be very different from that of the two components before mixing. This type of competitive adsorption may drastically affect the rheology and stability of a formulation.

The presence of surfactant in the dried latex film may also impair the film properties. During drying, the surfactant is adsorbed on the latex particles. As the particles coalesce during the annealing process, the surfactant migrates out of the bulk phase and concentrates at the interface. It has been shown that surfactant molecules preferably go to the film–air interface, where they align with their hydrophobic tails pointing towards the air. Calculations from ESCA (Electron Spectroscopy for Chemical Analysis) spectra show that a lacquer film containing 1% surfactant may have an average surface surfactant concentration of around 50%. Such a high concentration of a non-chemically incorporated, water-soluble component at the film surface will adversely affect the adhesion properties and create problems in terms of repaintability. It may also impair the water resistance of the film.

Furthermore, AFM (Atomic Force Microscopy) studies have shown that during the film-forming process many conventional surfactants phase separate from the binder. When the surfactant has phase separated, the water flux may carry it to the film surface. Alternatively, it may accumulate in the interstices between

the particles from where it will migrate to the film–air or film–substrate interfaces through a long-term exudation process. Eventually, the surfactant will be present in aggregates of considerable size, seen by AFM as “hills”. After treatment with water, the surfactant aggregates are washed away and the hills are replaced by distinct “valleys”. The rough surface will give rise to poor gloss.

It has been shown that many of the surfactant-related problems in latex paints can be minimized by the use of a polymerizable surfactant as emulsifier in the emulsion polymerization process. Several types of reactive surfactants are used for this purpose, some of which are shown in Figure 6.5. Block copolymers of ethylene oxide and propylene or butylene oxide with a polymerizable group at the far end of the hydrophobic segment (compounds I and II) have become popular, partly due to ease of preparation. Of particular interest from the performance point of view are surfactants which preferably undergo copolymerization rather than homopolymerization. A good example of such surfactants are the maleate half-esters of fatty alcohols, such as compound III in Figure 6.5. However, even surfactants based on highly reactive groups such as maleate do not become quantitatively copolymerized during the emulsion polymerization.

As mentioned above, AFM is an excellent method to evaluate the influence of the latex surfactant on the film topography. A smooth film with as little as possible of hills and craters is needed in order to obtain high gloss. Figures 6.6 and 6.7 illustrate the difference in topography, as seen during the film formation process,

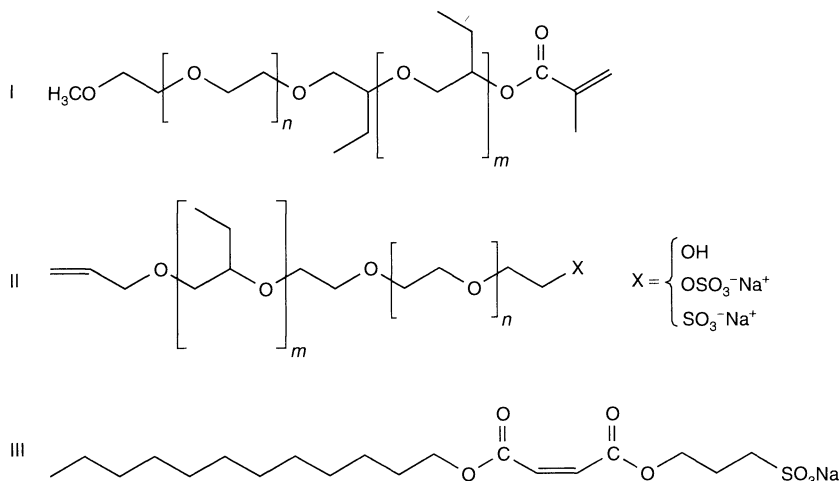


Figure 6.5. Examples of polymerizable surfactants for latices

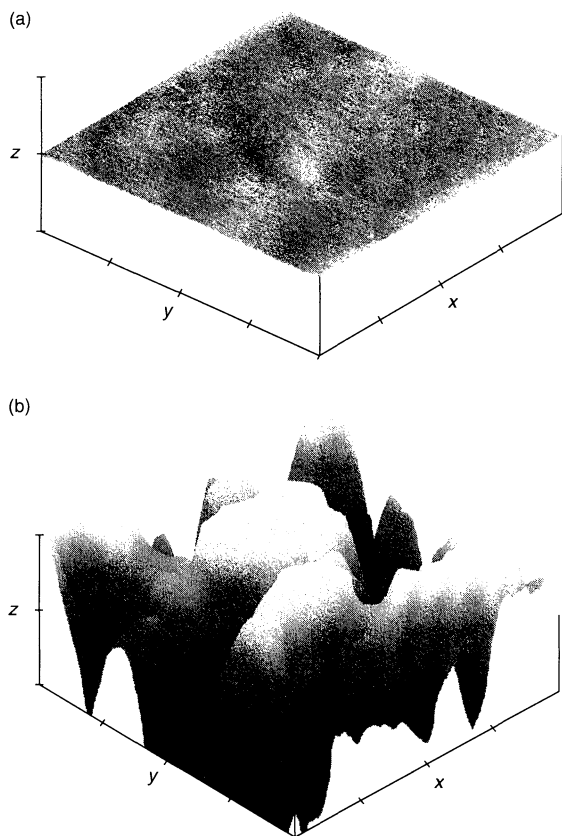


Figure 6.6. AFM images of films cast from a butyl acrylate–styrene–acrylic acid latex stabilized by sodium dodecyl sulfate: (a) before rinsing with water; (b) after rinsing with water: x - and y -axes, $0.500\ \mu\text{m}/\text{division}$; z -axis, $25.000\ \text{nm}/\text{division}$. (From A.-C. Hellgren *et al.*, *Prog. Org. Coatings*, **903**, 1 (1999) Reprinted with permission from Elsevier Science)

that can be obtained with a conventional anionic surfactant, sodium dodecyl sulfate (SDS), and with a polymerizable anionic surfactant, i.e. compound III in Figure 6.5. The same scale is used in all of the figures, but one should note that in each picture the z -dimension is plotted at 20 times larger magnification than the x - and y -dimensions.

Figure 6.6(a) shows a film formed from the SDS-stabilized latex. The film has a smooth, wavy surface, as would be expected after annealing for 48 h far above the glass transition temperature of the film. After rinsing with water, large pits were created, as shown in Figure 6.6(b). This change in the film morphology is an effect of migrating surfactant. During the drying stage, SDS moves with the evaporating water towards the

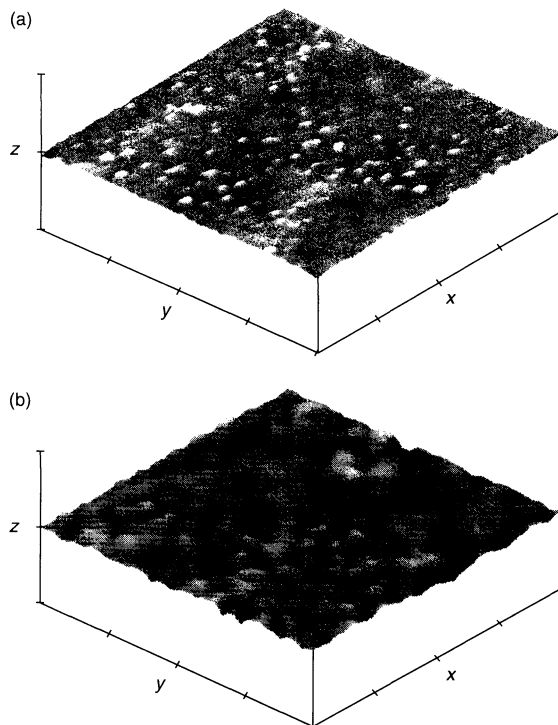


Figure 6.7. AFM images of films cast from a butyl acrylate–styrene–acrylic acid latex stabilized by the maleate surfactant, compound III in Figure 6.5: (a) before rinsing with water; (b) after rinsing with water: x - and y -axes, $0.500\ \mu\text{m}/\text{division}$; z -axis, $25.000\ \text{nm}/\text{division}$. (From A.-C. Hellgren *et al.*, *Prog. Org. Coatings*, **903**, 1 (1999) Reprinted with permission from Elsevier Science)

film surface where it crystallizes to form a continuous separate phase, thus covering the total surface area. Upon rinsing with water, the highly water-soluble SDS is washed away. The roughness of the remaining film surface is caused by the migrating surfactant phase preventing orderly packing of the latex particles.

Figures 6.7(a) and (b) show the topographies of films cast from maleate-stabilized latex, before and after rinsing, respectively. The film before rinsing showed “hills”, indicative of surfactant aggregates at the surface. After the film was rinsed with water, holes appeared in a regular pattern. This is indicative of removal of surfactant from the surface. The situation is much improved compared to the appearance of the films from the SDS-based latex but, evidently, even with the reactive maleate surfactant, a substantial portion is not anchored to the latex particle. Chemical analysis showed that about 1/3 of the surfactant was not chemically incorporated into the film.

3.2 Post-emulsified binders

Another common approach to water-based coating formulations is post-emulsification of a polymer in water. Several condensation polymers, e.g. alkyds, i.e. fatty-acid-modified polyesters, polyurethanes and epoxy resins, have been made into dispersions by the use of a suitable emulsifier and application of high shear. For instance, long oil alkyd resins of the type used in white-spirit-based formulations have been successfully emulsified by using nonionic surfactants such as fatty alcohol ethoxylates, alkylphenol ethoxylates or fatty acid monoethanolamide ethoxylates. Neutralization of alkyd carboxylic groups helps in producing small emulsion droplets and with the proper choice of surfactant, droplet diameters of less than 1 μm can be obtained. Such dispersions are sufficiently stable for most applications.

3.2.1 The role of the surfactant

Figure 6.8 illustrates the important fact that whereas a nonionic surfactant needs to be added in an amount sufficient to give close packing of the emulsifier on the surface in order to give sufficiently small droplets, an anionic surfactant already gives small droplets at concentrations that give a very low packing density. This is consistent with the different mechanisms by which nonionic and anionic surfactants exert stabilization, as discussed above. Figure 6.9 shows that there is a good correlation between droplet size and mechanical stability, i.e. the smaller the droplet, then the higher the shear rate needed for coalescence. As for latex dispersions, alkyd emulsions stabilized with only anionic surfactants are highly sensitive to electrolytes.

The main drawback of water-borne alkyd paints is slow drying. This is partly due to the comparatively low evaporation rate of water, although there is also strong evidence that catalysis of autoxidation does not work properly in water-borne systems. The distribution of the drier, in particular cobalt alkanolate, between the alkyd and water phases is believed to influence the early stages of drying of alkyd emulsions. Figure 6.10 illustrates that the distribution of cobalt between the phases is strongly affected by the pH of the formulation. This is a practically important observation since it is known that there is often a drop in pH on storage of paints.

Surfactants capable of participating in autoxidative drying are of interest for the post-emulsification of alkyd resins. Ethoxylated monoethanolamides of unsaturated fatty acids are one such type of surfactant that can be chemically incorporated into the network during drying

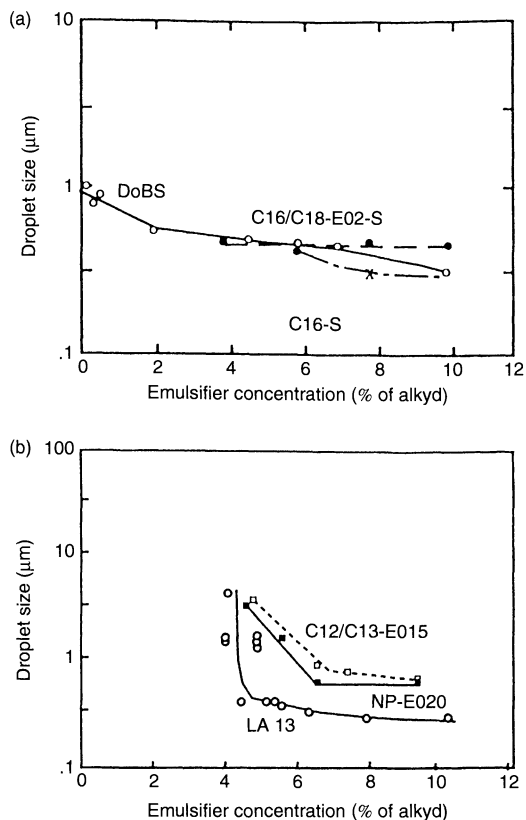


Figure 6.8. Effect on initial droplet size of concentrations of (a) the anionic surfactants sodium dodecylbenzene sulfonate (DoBS), sulfated hexadecyl alcohol (C16-S) and sulfated hexadecyl/octadecyl alcohol ethoxylate (2 EO) (C16/C18-EO2-S) and (b) the nonionic surfactants dodecyl/tridecyl alcohol ethoxylate (15 EO) (C12/C13-EO15), nonylphenol ethoxylate (20 EO) (NP-EO20) and linseed oil fatty acid monoethanolamide ethoxylate (13 EO) (LA 13). (From G. Östberg *et al.*, *Colloids Surf. A*, **94**, 161 (1995))

of an alkyd-based coating film. The general structure of this surfactant type is as follows:



where R-CO is an unsaturated acyl group, derived from an unsaturated triglyceride such as soy bean oil, linseed oil, sunflower oil or tall oil. (There must be more than one double bond in the acyl chain; oleoyl is not reactive enough.)

Figure 6.11 illustrates the difference in surface composition with respect to the surfactant for a polymerizable amide ethoxylate and a conventional nonionic surfactant of similar hydrophilic-lipophilic balance (HLB). Surfactant concentrations at the film-air interface were

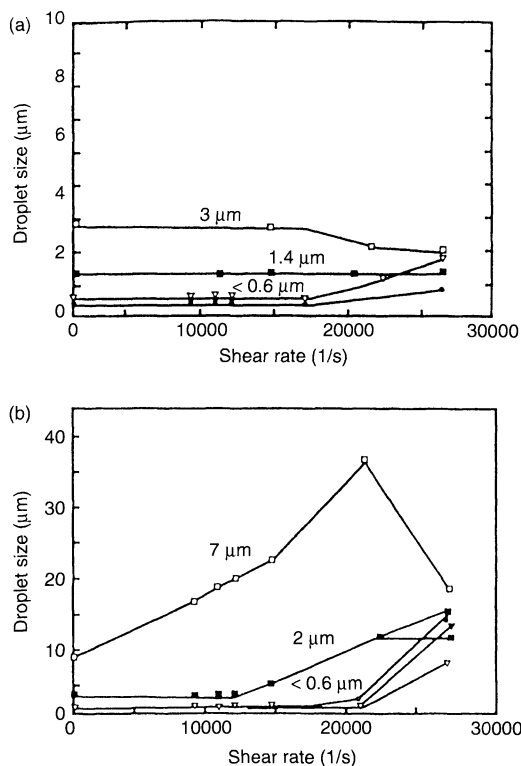


Figure 6.9. Mechanical stability of emulsions stabilized by (a) the anionic surfactant sodium dodecylbenzene sulfonate, and (b) the nonionic surfactant linseed oil fatty acid monoethanolamide ethoxylate (13 EO). The initial droplet sizes are given on the figures. Increase in droplet size on shearing is a sign of coalescence. The decrease in droplet size for the 7 μm droplets of part (b) reflects shear-induced disintegration of the large aggregates formed. (From G. Östberg *et al.*, *Prog. Org. Coatings*, **24**, 281 (1994) Reprinted with permission from Elsevier Science)

measured by ESCA. As can be seen from this figure, both the conventional surfactant, a nonylphenol ethoxylate, and the amide ethoxylate accumulate at the surface and the concentration increases with time. Whereas the concentration versus time curve is almost linear for the nonylphenol ethoxylate, it levels off for the amide ethoxylate. For the latter species, the distribution of surfactant in the film seems to be established within three days of drying.

The difference in behaviour between the nonylphenol ethoxylate and the amide ethoxylate is probably due to the fact that the latter surfactant becomes immobilized through coupling to binder molecules during the drying process. Once covalently incorporated into the network, the migration process will cease. Another contributing

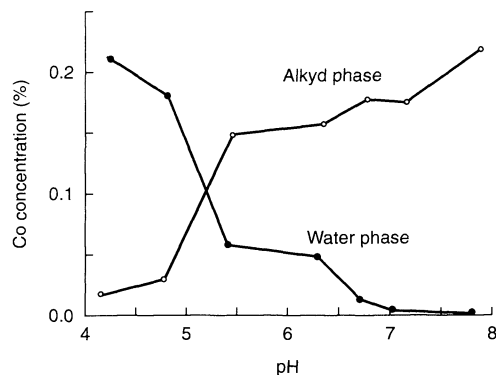


Figure 6.10. Concentration of cobalt in the alkyd and water phases as a function of pH. Cobalt 2-ethylhexanoate was used in an amount of 0.2% of alkyd. The oil-in-water alkyd emulsions were made without emulsifier. (From G. Östberg *et al.*, *Prog. Org. Coatings*, **24**, 281 (1994) Reprinted with permission of Elsevier Science)

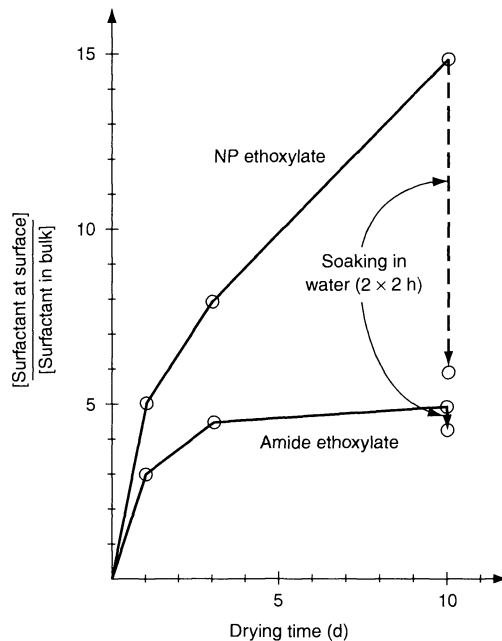


Figure 6.11. Relative surface concentration of surfactant as a function of drying time, as determined by ESCA. The NP ethoxylate is nonylphenol ethoxylate (12 EO) and the amide ethoxylate is linseed oil fatty acid monoethanolamide ethoxylate (14 EO). (From K. Holmberg, *Prog. Colloid Polym. Sci.*, **101**, 69 (1996))

factor for the low degree of migration of the amide ethoxylate could be that this surfactant is likely to be very compatible with the binder, a long oil alkyd resin. Surfactant-polymer compatibility is often decisive for

the distribution of surfactants in films. Surfactants are carried towards the surface by the flux of water during film drying and this process is particularly effective when there is poor compatibility between surfactant and polymer.

The effect on the surface composition of soaking the dried film in water is also shown in Figure 6.11. Whereas more than half of the nonylphenol ethoxylate disappears from the outermost surface layer (the analysis depth is approximately 5 nm), the effect on the amide ethoxylate is small, in spite of the fact that both surfactants have about equal water solubility. This is a further indication of the amide ethoxylate being immobilized during the drying process, although one must keep in mind that the evidence shown in Figure 6.11 is only indirect. The sensitivity of ESCA is not sufficient for monitoring the disappearance of carbon-carbon double bonds, which would have been the most direct way of studying surfactant polymerization. However, studies on cobalt-initiated autoxidation of ethyl esters of unsaturated fatty acids have shown that oleate ester does not polymerize over a period as long as 110 days, whereas linoleate ester polymerises almost completely over three days. These findings support the view that amide ethoxylates based on fatty acids with a high degree of unsaturation become covalently incorporated in the dried film.

3.2.2 *Emulsification of short oil alkyds*

Alkyd emulsions are also of interest in the industrial coatings market. The alkyds used for such applications, so-called short oil alkyds, have a much higher viscosity and are most conveniently emulsified in a phase-inversion process. The emulsifier, which can either be a nonionic surfactant, an anionic surfactant or a combination of these, is dissolved in the alkyd at high temperature and water is added under low shear so that a water-in-oil emulsion is formed. For alkyds of very high viscosity, the process must be performed in pressurized vessels to prevent boiling of the water. By adding more water and/or lowering the temperature, the emulsion is made to invert and form an oil-in-water emulsion.

The location of the emulsifier prior to phase inversion has been found to be of prime importance. Emulsions of smallest droplet size (less than 1 μm) is obtained when all the emulsifier is added to the alkyd before the addition of pure water. The mobility (or migration) of the surfactant during phase inversion is also decisive for the size of the oil-in-water droplets. The mobility is controlled by both the hydrophilicity (water solubility) of the surfactant and its molecular size, with a very high-molecular-weight surfactant diffusing relatively slowly

across the interface. However, bulky emulsifiers with very long polyoxyethylene chains may be able to give proper emulsion stability in spite of large droplets being formed due to their ability to induce a long-range steric repulsive force. Mixtures of anionic and nonionic surfactants, with the latter typically having long (>30) polyoxyethylene chains, seem to work well in most instances.

Post-emulsification is simplified if the polymer itself is surface-active. This can be achieved by using polymers of high acid values or by using polymers with noncharged, hydrophilic segments such as polyoxyethylene chains. Such polymers can often be emulsified with considerably less surfactant, but the trade-off is water and chemical resistance of the paint film. If the polymer is sufficiently polar, no emulsifier at all is needed. However, such binders need to be cross-linked during curing in order to give acceptable film properties.

4 PIGMENT DISPERSION

4.1 Paint pigments

Pigments are used in paints to give desired colour, hiding and other optical properties to the coating. In addition, pigments often impart mechanical strength and protective properties to the paint. Anti-corrosion pigments are a well known example of pigments whose prime role is to confer a specific technical property rather than colour or hiding to the paint film.

Pigments can be organic or inorganic, and can be natural or synthetic. Some of the organic pigments are actually hybrids with an inorganic core, e.g. aluminium hydroxide, coated with an organic substance. Many inorganic pigments are dug out of the earth's crust, then washed and graded by size. The majority of the organic pigments used today are synthetic. Generally, pigments produced via a precipitation step have a more uniform particle size than pigments obtained by crushing of natural oxides or salts.

In order to effectively obliterate the underlying substrate (which may be a paint film of different colour), the pigments used must prevent light from passing through the film to the substrate and back to the eye of the observer. Pigments achieve this by absorbing and by scattering the incoming light. The hiding power of a pigment is a function of the refractive index of the pigment and the pigment particle size. (In addition, pigment shape influences the hiding power because the shape of the particles affects their packing in the film.) The hiding power of the pigment is high if the refractive index of

the pigment is much higher than that of the binder used in the paint formulation. Most pigments have a refractive index above 2.0, while most binder resins have a refractive index of 1.4–1.6. The very common white pigment, titania (titanium dioxide), has an unusually high refractive index, i.e. 2.55 for the anatase crystallographic form and 2.76 for the rutile form.

The perfect particle size for maximum scattering of light is equal to the wavelength of the light within the particle, which roughly corresponds to half the wavelength of light in air, i.e. 0.2–0.4 μm . Some pigments are far below this value, e.g. iron blue with a typical particle size range of 0.01–0.2 μm ; some are in this range, e.g. rutile titanium dioxide which is usually 0.2–0.3 μm in size, while some are far above, e.g. micaceous iron oxide with particle sizes in the range 5–100 μm . The right particle size in combination with the high refractive index is the main reason for the excellent hiding power of titania.

Inorganic pigments with low refractive indices (below 1.65) and with concomitant poor hiding power are usually referred to as extenders or fillers. They are employed in paint formulations to control the rheological properties (thickening agents, anti-sag agents, etc.), to reduce gloss (flattening agents), to improve mechanical properties (reinforcing agents) or to improve the barrier properties of the film. Silica, barium and calcium sulfates, calcium carbonates, and silicates such as china clay, talk, mica and bentonite, are the most common types of extenders. The average particle size of extenders is often large.

Pigments need to be finely dispersed in the paint in order to retain good hiding power. Pigment dispersion has therefore been a key process in paint making throughout the long history of paints and still remains an important issue today. The pigment is usually supplied as a powder with the primary particles clustered into agglomerates. The agglomerates must be broken and the primary particles obtained must be dispersed throughout the coating formulation. In this way, a colloidal dispersion of the pigment is produced, with either water or an organic solvent (or more often a solvent mixture) as the continuous phase. The dispersion stage is performed in some kind of grinding process with an input of high shear. Various types of mills have been developed for the purpose, such as high-speed dispersers, ball mills (with the cylinder partly filled with steel or porcelain balls) and bead mills (with glass beads or coarse sand as the grinding medium).

In order to economize the grinding process, only a part of the total paint formulation is charged into the mill. Together with all of the pigment and pigment

dispersants, a fraction of the binder is added together with enough solvent to reduce the viscosity to an acceptable level. After milling, a rather stiff paste is obtained to which the remaining amounts of binder and solvent are added, together with the various types of additives used in the specific formulation.

The pigment dispersion process can be viewed as being composed of three stages, although the stages overlap in any actual grinding process:

- i *Wetting*, i.e. displacement of air by a liquid.
- ii *Grinding*, i.e. mechanical breakup and separation (deagglomeration) of the particle clusters to isolated primary particles.
- iii *Dispersion*, i.e. movement of the wetted particles into the body of the coating to affect a long-term particle separation.

In the dispersion process each particle must become surrounded with sufficient liquid so that particle–particle interaction is minimized. All particle dispersions are thermodynamically unstable, however, and prolonged storage will inevitably lead to clustering of the particles in the wet-coating formulation. Such a clustering is usually referred to as flocculation. Figure 6.12 illustrates the difference between agglomerated and flocculated pigments.

4.2 Pigment dispersants

The additives used in the grinding process are called pigment dispersants. Their primary function is to surround the suspended pigment particles with a barrier envelope that by either ionic repulsion or steric hindrance, or both, prevents random contact with other pigments. In water-borne paints, electrostatic repulsion is usually the most important stabilizing mechanism and the well known DLVO theory that accounts for the balance of

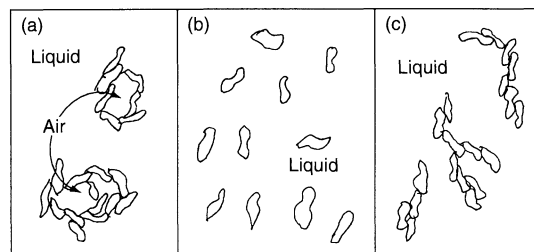


Figure 6.12. Schematic representations of (a) agglomerated, (b) dispersed, and (c) flocculated pigments

attractive van der Waals forces and repulsive electrostatic forces in suspensions can be used as a tool to understand the stability characteristics of the system. In media of low dielectric constant, such as white spirit or xylene, steric repulsion is the dominating force. Steric repulsion is achieved by polymers with an anchoring group attached to the particle surface and a segment with high compatibility with the continuous phase extending away from the particle. Steric repulsion can be explained as a loss of entropy when the polymer chains attached to two different pigment particles are forced to penetrate into each other. In order to maximize this loss in entropy, i.e. to achieve maximum stabilization, the density of polymer chains on the particle surface must be high. Sometimes, a stabilizing system is used that provides both electrostatic and steric stabilization; this is referred to as electrosteric stabilization. Figure 6.13

illustrates electrostatic, steric and electrosteric stabilization. (Electrosteric stabilization is very common for latices, with Figure 6.4 showing latex particles stabilized by this mechanism.)

Most inorganic pigments are oxides. These exhibit a surface charge in aqueous systems that is characteristic of the oxide and the pH of the water. Each pigment has an isoelectric point which corresponds to the pH at which the positive and negative charges on the oxide surface are balanced. By moving away from this pH, a net charge, positive or negative, starts to develop that leads to pigment particle repulsion. Since the introduction of an ionic dispersant on to the oxide surface alters the balance of charges on this surface, it also acts to alter the isoelectric point of the pigment particle, as shown in Figure 6.14. For any given pH, adding an ionic dispersant may improve or reduce

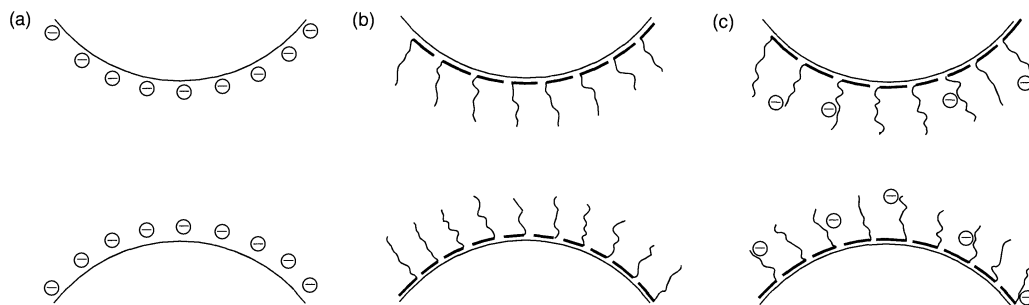


Figure 6.13. Electrostatic (a), steric (b) and electrosteric (c) stabilization of a dispersion

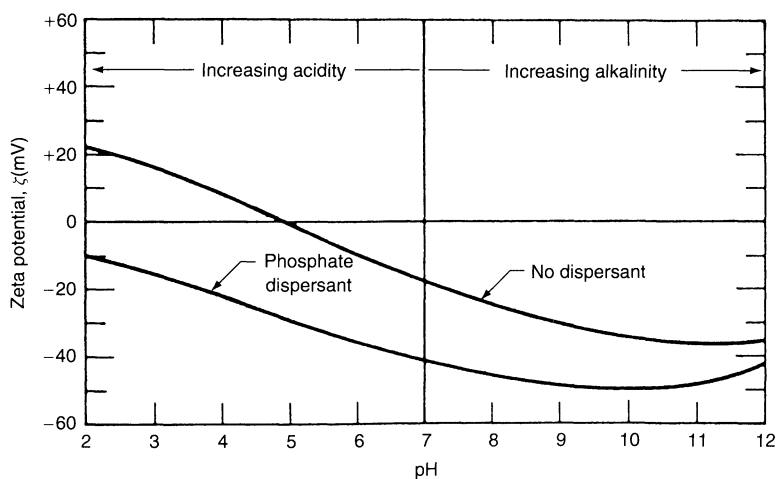


Figure 6.14. Plot of zeta potential (ζ) of aqueous dispersions of kaolin pigment particles as a function of pH with and without a phosphate dispersant present. (From T. C. Patton, *Paint Flow and Pigment Dispersion*, 2nd Edn, John Wiley, New York, 1979, p. 292, Reproduced with permission)

dispersion stability depending on whether the charge will increase or decrease.

In principle, electrostatic stabilization can be achieved by either anionic or cationic pigment dispersants. In order to be compatible with the other components of a paint formulation, in particular the latex which is almost always negatively charged, anionic dispersants are usually employed. A good dispersant for inorganic pigments for water-borne paints should (i) give a low isoelectric point of the coated particle, i.e. should be the salt of a relatively strong acid, and (ii) have a strong affinity for the pigment surface.

4.2.1 Dispersants for water-borne paints

The most common type of dispersants for inorganic pigments for use in water-borne paints are polyelectrolytes. These may be inorganic, e.g. various types of polymeric phosphates, or organic, such as polyacrylates or styrene-maleate copolymers. Organic polyelectrolyte dispersants are polymers of relatively low molecular weight. For instance, polyacrylate dispersants usually give the best performance when composed of between 12 and 18 monomer units. The optimum in length probably reflects the balance between proper anchoring at the particle surface, which is favoured by a high molecular weight, and the rate of adsorption at the surface, which is faster for species of lower molecular weight. In evaluating the dispersion efficiency of added dispersants, one must also take into account the wetting-dispersing properties of the binder used in the formulation. Alkyd resins, in particular, have good wetting properties, and often contribute considerably to the dispersing power of the total coating formulation.

Polyphosphates are versatile inorganic polyelectrolytes that at relatively low concentrations disperse a variety of inorganic pigments. Table 6.1 shows some common polyphosphates used as pigment dispersants. Polyphosphates are suitable as pigment dispersants on two accounts. First, the polyphosphoric acids are relatively strong acids, i.e. the first pK_a s are low, and

thus the polyphosphate-coated particles become strongly negatively charged at all relevant pH values. Secondly, the phosphates bind remarkably strongly to many inorganic surfaces. The anchoring can occur by either of two mechanisms, i.e. acid-base interactions or chemisorption. Acid-base interactions usually occur with oxide or hydroxide pigments, and the polyphosphate molecule with its regular pattern of P-O⁻, P=O and P-OH units can act both as the base, being an electron donor, or acid, being an electron acceptor, in the interaction with the pigment surface. Chemisorption may occur at the surface of pigments such as CaCO₃, BaSO₄ and ZnO, since phosphates form insoluble precipitates with calcium, barium and zinc ions (as well as with many other metal ions). Regardless of the mechanism of anchoring, the binding of polyphosphates to an inorganic pigment can often be regarded as irreversible. For this reason, polyphosphates are very efficient dispersants for many inorganic pigments in water-based formulations.

However, a number of problems are associated with the use of polyphosphates. They contribute to eutrophication, thus leading to an acceleration of the metabolism and reproduction of some fungi on paint films and at runoff areas. Polyphosphates may also give rise to blooming, although this occurs much less with potassium than with sodium salts, and less with polymeric phosphates than with monomeric species. The bloom is a frosty, crystalline deposit that may appear on the surface of aged paint films. The blooming problem is the reason why the more expensive potassium polyphosphates are preferred to the corresponding sodium salts. Furthermore, polyphosphates may degrade by hydrolysis, particularly when the paints are kept at an alkaline pH (and most latex paints are formulated at a pH of 8-9), or when certain transition metals, which form strong complexes with phosphates, are present. The degradation may lead to unexpected rheological changes in the formulation.

Other types of polyelectrolytes that are now being used as pigment dispersants include polysilicates, polyaluminates and polyborates. These polyelectrolytes function in the same way as the polyphosphates. Blooming is not usually a problem with these other inorganic dispersants as it is with the polyphosphates. The anchoring to the pigment surface is often not as good with other polyelectrolytes when compared to the polyphosphates. However, the pigment-polyelectrolyte interaction can be very specific, leading to a chemisorption type of binding. In practice, it is not uncommon to use mixtures of inorganic dispersants, for instance, various ratios of soluble alumina and silica. The isoelectric point of the

Table 6.1. Examples of alkali phosphate dispersing agents

Common name	Ratio of basic oxide to acidic oxide ^a	Number of P atoms	Representative formula
Orthophosphate	3.00	1	K ₃ PO ₄
Pyrophosphate	2.00	2	K ₄ P ₂ O ₇
Tripolyphosphate	1.67	3	K ₅ P ₃ O ₁₀
Metaphosphate	1.00	<i>n</i>	Na _{<i>n</i>} (PO ₃) _{<i>n</i>}

^aBasic oxide: Na₂O, K₂O; acidic oxide: P₂O₅.

pigment particles can then be adjusted by varying the $\text{Al}_2\text{O}_3:\text{SiO}_2$ ratio.

In addition organic dispersants are used with inorganic pigments for water-borne coatings. For instance, polyamines impart excellent dispersion properties to many inorganic pigments. In order to achieve optimum properties, the spacer length between the amino groups must be such that it matches the distance between the adsorption sites on the pigment surface. As an example, 1,3-propylene diamine, with three carbons between the amino nitrogen atoms, is a better dispersant for clay particles than either ethylene diamine (with a two-carbon spacer) or 1,4-butylene diamine (with a four-carbon spacer).

Various types of amino alcohols are excellent dispersants for some inorganic pigments used in water-based formulations. The amino group anchors the molecule to the pigment surface and the hydrophilic hydroxyl group extends out into the aqueous phase. Amino diols are often preferred to simple amino alcohols.

Organic pigments for water-borne paints are often more hydrophobic in character than inorganic pigments. Table 6.2 gives a list of the *HLB* values for common paint pigments, both organic and inorganic. (*HLB* stands for hydrophilic–lipophilic balance, on a numerical scale from 0 (extremely hydrophobic) to 20 (extremely hydrophilic).) Inorganic polyelectrolytes often do not bind strongly to the surface of these hydrophobic particles. Instead, surfactants of various types are commonly used. Anionic surfactants may be employed to provide electrostatic stabilization, nonionics to give steric

stabilization, or a mixture of the two used to impart electrosteric stabilization, as discussed above and illustrated in Figure 6.13. Alkylbenzene sulphonates are the most commonly used anionic surfactants for this purpose, while alkylphenol ethoxylates with relatively long polyoxyethylene chains, typically 20–30 oxyethylene units, have been the nonionic surfactants of choice. For environmental reasons, the slowly biodegradable alkylphenol ethoxylates are gradually being replaced by fatty alcohol ethoxylates of similar *HLB* values. The switch away from alkylphenol ethoxylates is not, however, without problems. Anchoring of the fatty alcohol chain to the pigment surface is often not as good as for alkylphenols. It is probable that alkylphenol derivatives can form electron donor–acceptor (EDA) complexes with pigment surfaces that contain electron-deficient groups, as is illustrated in Figure 6.15. Such EDA complexes may also form with alkylbenzene sulfonates. No

Table 6.2. *HLB* values of various organic and inorganic pigments. (From R. H. Pascal and F. L. Reig, *Off. Dig.*, **36**, 839 (1964))

Pigment	<i>HLB</i>
<i>Organic pigments</i>	
Phthalocyanide blue (green shade)	14–16
Azo yellow	13–15
Quinacridone red	12–14
Phthalocyanide green (yellow shade)	12–14
Nickel azo yellow	11–13
Quinacridone violet	11–13
Phthalocyanide blue (red shade)	11–13
Phthalocyanide green (blue shade)	10–12
Toluidine yellow	9–11
Toluidine red (medium)	8–10
BON red (dark)	6–8
<i>Inorganic pigments</i>	
Iron oxide (yellow)	20
Chrome yellow	18–20
Titanium dioxide	17–20
Molybdate orange	16–18
Iron oxide (red)	13–15

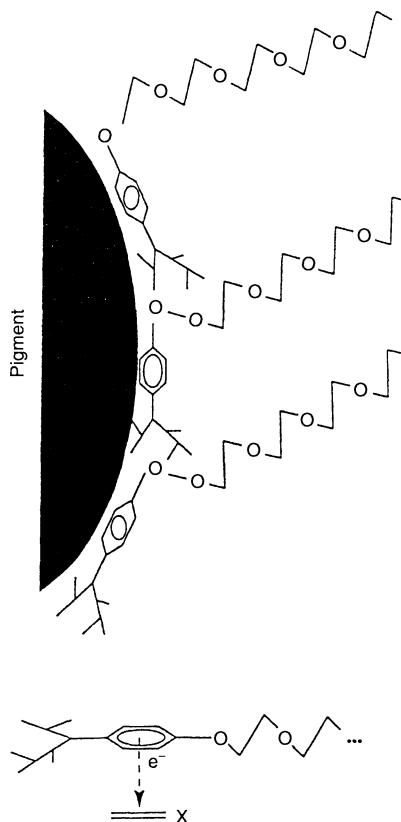


Figure 6.15. Schematic representation of an electron donor–acceptor complex formed between an alkylphenol ethoxylate and unsaturated moieties on a pigmented surface. (From K. Holmberg, *Surf. Coatings Int.*, **76**, 481 (1993))

such contribution is, of course, possible in the case of alcohol ethoxylates which are always based on saturated alkyl chains. Monoethanolamide ethoxylates of polyunsaturated fatty acids, which were discussed above in Section 3 are an interesting class of surfactants in this context. This type of nonionic surfactant seems to work well as a pigment dispersant and it is likely that these compounds, which contain π -electrons in the acyl chain, can form EDA complexes with some organic pigment surfaces, although these complexes may not be as strong as for alkylphenol ethoxylates. Figure 6.16 shows the structures of an alkylbenzene sulfonate, an alkylphenol ethoxylate, an alcohol ethoxylate and a monoethanolamide ethoxylate of a di-unsaturated fatty acid, i.e. linoleic acid. The latter is the main fatty acid found in common drying oils such as soy bean oil and sunflower oil. Figure 6.16 also shows the structure of lecithin, a zwitterionic surfactant which has a long tradition as a efficient of organic pigments in paints.

Dispersion of pigments in aqueous formulations is in reality a more complex issue than has been described above. First, many pigments, and in particular the inorganic pigments, have been surface treated by the pigment producer and relevant details about the composition of the applied coating is often kept as proprietary information. The common white pigment, rutile titanium dioxide, for instance, can be obtained with an anionic or a cationic surface charge and its *HLB* value can vary from very hydrophilic to extremely hydrophobic. The paint formulator may not possess the detailed knowledge of the pigment surface characteristics needed to perform the dispersion experiments in a scientific manner. For this reason, the process of pigment dispersion in the paint industry is still more of an art rather a science.

Another complicating factor is that optimized electrostatic stabilization of pigment particles in water-based formulations may lead to sub-optimization when

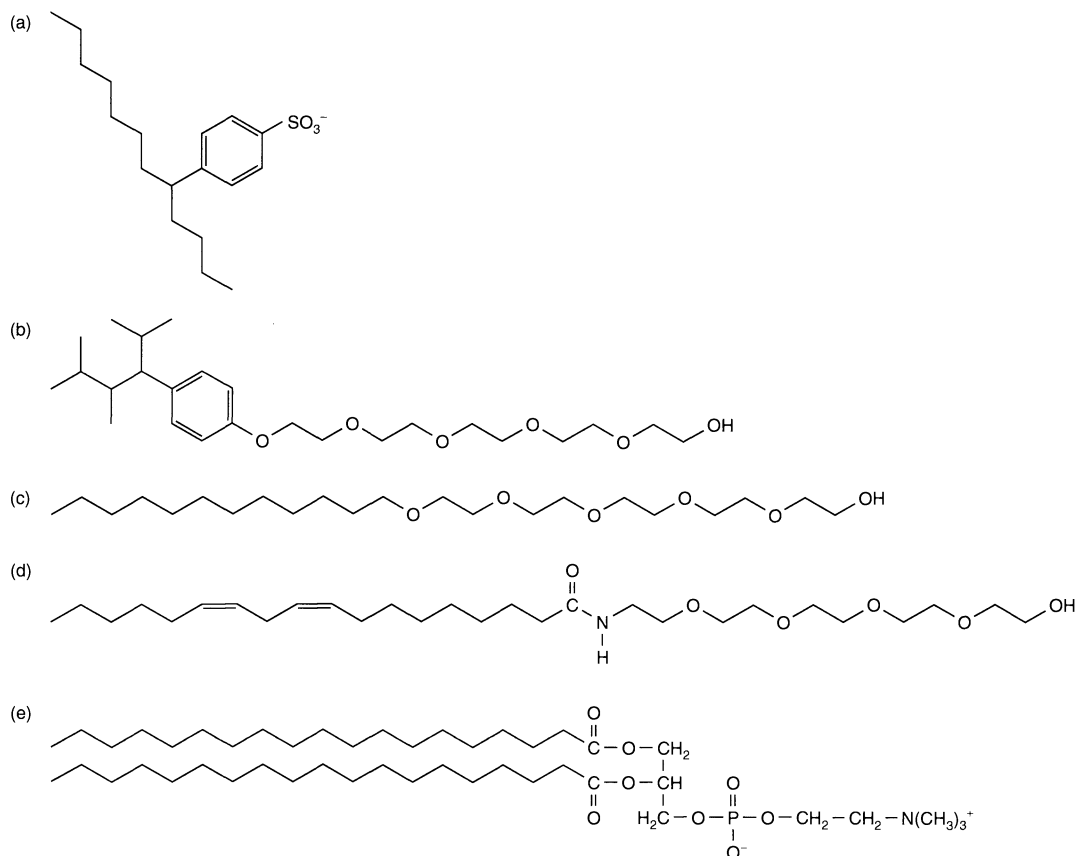


Figure 6.16. Structures of (a) dodecylbenzene sulfonate, (b) nonylphenol ethoxylate, (c) dodecyl alcohol ethoxylate, (d) the monoethanolamide ethoxylate of linoleic acid, and (e) lecithin (phosphatidylcholine)

it comes to binder–pigment compatibility. If, at the formulation pH, the pigment particles carry a very strong negative charge, the interaction with the binder, which is usually slightly negatively charged, will be strongly repulsive in character. Such incompatibility may lead to phase separation in the film forming step with adverse effects on the optical properties of the dried film. For this reason, a compromise may be needed between the efficiency in pigment dispersion and the compatibility between the pigment and the binder. As a general rule, the best pigment–binder compatibility is achieved if the two surfaces do not carry the same charge and if the degree of hydrophobicity of the binder and the coated pigment, for instance, expressed in terms of the *HLB*, is approximately the same.

4.2.2 Dispersants for solvent-borne paints

Pigment dispersions in organic solvent formulations are based on steric stabilization, since electrostatic interactions in media of low dielectric constant are weak. In order to give proper stabilization, the lyophilic part of the dispersant molecule, i.e. the part that stretches out into the continuous liquid phase, must be relatively large; thus, pigment dispersants for solvent-borne paints are polymeric in nature. It can be shown from calculations using Hamaker constants of the particles across the liquid medium that the thickness of the stabilizing layer needs to be in the range of 5–20 nm for most pigments of particle size 0.1–1.0 μm . An extension of 5–20 nm is not very large for a polymer; the molecular weight of polymeric dispersants, therefore, need not be high. In practice, polymeric dispersants are seldom above 40 000 in molecular weight.

Pigment dispersants have for a long time been the most important application for polymeric surfactants and both graft and block copolymers are used for this purpose. Graft copolymers, often referred to as “comb polymers”, have now become more important than block copolymers. It is important that the segments that extend away from the pigment surface are very compatible with the binder–solvent mixture, or, expressed in other words, that the binder–solvent mixture is a very good solvent for those segments. Only then do the dispersants keep the particles well separated, which is a necessary condition in order to achieve a low viscosity with a minimal amount of solvent in the formulation. Different lyophilic segments, with different solubility characteristics, are needed for different types of binder–solvent mixtures. One approach to this problem has been to use the solubility parameter concept of

Hildebrand. Maximum dispersion efficiency is obtained when the solubility parameters of the binder–solvent mixture match the solubility parameters of the polymer segments that stretch out in to the solution.

The polymeric dispersants need to contain groups that provide strong anchoring of the molecule to the pigment surface. As was discussed above for dispersants for pigments in water-borne paints, the choice of an anchoring group depends on the type of pigment used in the formulation. The anchoring mechanism is usually based on acid–base interaction, with the pigment surface constituting either the acid or the base moiety. For instance, acidic pigments are properly dispersed by graft copolymers with a poly(alkylene imine) backbone that forms a multiple of acid–base interactions with the pigment surface. Pigments with a basic character, on the other hand, may be dispersed by copolymers containing pendant carboxylic acid groups. Poly(12-hydroxystearic acid) is a well known example of such a polymeric dispersant. Hydrogen bonding should be regarded as one example, and indeed a very important example, of acid–base interactions, and the anchoring of dispersant to pigments in solvent–based paints can often be viewed as hydrogen-bonding interactions. For instance, phthalimine groups, which are typical hydrogen-bond acceptors, can be used as anchoring groups of polymeric dispersants to hydroxyl-containing pigments. Such an interaction is illustrated in Figure 6.17.

5 WETTING OF THE SUBSTRATE

Proper wetting of the surface by the coating is an absolute requirement in order to achieve good film properties. Wetting is normally measured by determining the contact angle obtained when a drop of the liquid formulation is put on a planar solid surface. Whether or not a given liquid spreads on a given substrate depends on both the liquid and the solid. In a scientific approach to wetting, it is important to be able to determine the wetting characteristics of the substrate. Determination of surface tension or surface free energy for a solid surface is not as straightforward as it is for a liquid. The most common approach is that devised by Zisman who introduced a useful scheme for classifying low-energy surfaces with respect to their wettability. For many series of liquids on solids – including plastics, metals and metal oxide – it was shown that the contact angle decreases with decreasing surface tension of the liquid. For a homologous series of non-polar liquids, the increase in $\cos\theta$ with decreasing liquid surface tension is linear for a given solid, as illustrated in Figure 6.18.

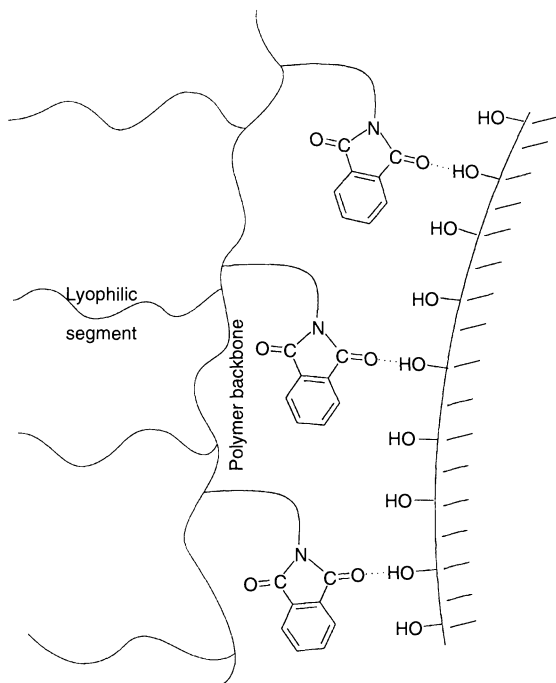


Figure 6.17. Stabilization of a pigment with hydroxyl groups at the surface by a graft copolymer containing phthalimide anchoring groups

The critical liquid surface tension, γ_C , is defined as the point where the plotted line intersects the $\cos \theta$ line, i.e. the line representing complete wetting. In theory, all liquids with a liquid-gas surface tension (γ_{LG}) equal to or lower than the γ_C will spread on that surface. In practice, however, γ_C is not a constant for any given solid, but varies somewhat with the liquid type.

These regularities in the wetting properties of low-energy surfaces, such as polymers, and adsorbed oriented monolayers of organic materials on high-energy surfaces are significant. Even for non-homologous liquids, a plot of γ_{LG} against $\cos \theta$ shows points lying in a narrow rectilinear band. However, the line may exhibit curvature if hydrogen bonding can take place between the liquid molecules and the molecules in the solid surface.

The use of a “Zisman plot” to determine the critical surface tension is relatively straightforward and has become a widely used method to characterize a low-energy solid with respect to the surface free energy. Table 6.3 gives the critical surface tension values for a number of common polymers, while Table 6.4 shows such values for various surface functional groups. The

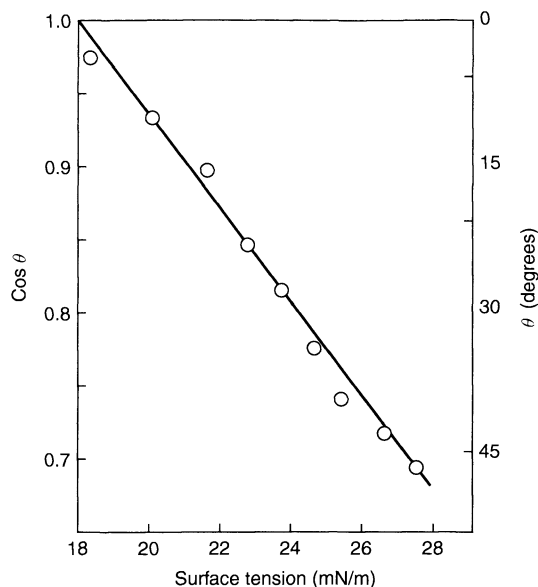


Figure 6.18. A Zisman plot for *n*-alkanes on polytetrafluoroethylene

latter values have been calculated from a large collection of experimentally determined γ_C values for polymers.

As can be seen from Table 6.4, the value of γ_C for a solid is indicative of the molecules that make up its surface. The surfaces having the lowest value of γ_C , and hence the lowest surface energy, consist of closely packed CF_3 groups. Replacing one fluorine atom by hydrogen considerably raises the value of γ_C . This low

Table 6.3. Critical surface tension, γ_C , for various polymers at 20°C

Polymer	γ_C (mN/m)
Poly(1,1-dihydroperfluorooctyl methacrylate)	10.6
Polyhexafluoropropylene	16.2
Polytetrafluoroethylene	18.5
Polytrifluoroethylene	22
Poly(vinylidene fluoride)	25
Poly(vinyl fluoride)	28
Polyethylene	31
Polytrifluorochloroethylene	31
Polystyrene	33
Poly(vinyl alcohol)	37
Poly(methyl methacrylate)	39
Poly(vinyl chloride)	39
Poly(vinylidene chloride)	40
Poly(ethylene terephthalate)	43
Cellulose	45
Poly(hexamethylene adipamide)	46

Table 6.4. Critical surface tension, γ_c , in relation to the surface constitution at 20°C

Surface group	γ_c (mN/m)
<i>Fluorocarbon surfaces</i>	
-CF ₃	6
-CF ₂ H	15
-CF ₃ and -CF ₂ -	17
-CF ₂ -CF ₂ -	18
-CF ₂ -CFH	22
-CF ₂ -CH ₂ -	25
-CFH-CH ₂ -	28
<i>Hydrocarbon surfaces</i>	
-CH ₃ (crystal)	20-22
-CH ₃ (monolayer)	22-24
-CH ₂ -CH ₂ -	31
-CH-(phenyl ring edge)	35
<i>Chlorocarbon surfaces</i>	
-CClH-CH ₂ -	39
-CCl ₂ -CH ₂ -	40
=CCl ₂	43

Table 6.5. Surface tension, γ , for selected solvents at 20°C.

Solvent type	γ (mN/m)
Alcohols	21-35
Esters	21-29
Ketones	23-27
Glycol ethers	27-35
Glycol ether esters	28-32
Aliphatic hydrocarbons	18-28
Aromatic hydrocarbons	28-30
Water	73

value of the critical surface tension indicates that the adhesion between liquids and surfaces containing trifluoromethyl groups is very low. (Sometimes, however, the introduction of a terminal CF₃ group does not decrease the wettability very much since the introduction of the dipole associated with the CF₃-CH₂ group gives an effect in the other direction.) Another observation that can be made from Table 6.4 is that CH₃ groups have very low values when compared with CH₂ groups. This implies that surfaces rich in methyl groups should have low surface tensions, which indeed is true. The most common type of silicone oil, i.e. polydimethylsiloxane, is probably the best example of such a methyl-rich surface.

The concept of the critical surface tension of a solid is useful for many practical applications, e.g. surface coatings. In order for a coating to spread on a substrate, the surface tension of the liquid coating must be lower than the critical surface tension of the substrate. (In addition, since a liquid is easier to break up and atomize when the surface tension is low, a lower surface tension means a better sprayability of the coating.) The well known coatings defect, "cratering", is also surface-tension related. Contaminants on the surface, such as fingerprints and oil spots, usually have lower critical surface tension values than those of the surrounding areas, thus putting extra demand on the coating with regard to low surface tension.

The surface tension of the coating is largely determined by the polymer and the solvent. The polymers usually have relatively high surface tensions, with values between 35 and 45 mN/m being typical. The organic

solvents have surface tension values between 20 and 30 mN/m, as can be seen from Table 6.5.

In general, when comparing solvents within the same solvent class it has been found that faster evaporating solvents usually have lower surface tension values than their slower evaporating counterparts. Furthermore, increased branching of the solvent molecule leads to a lowering of the surface tension. Isopropyl alcohol, which fulfils the two above-mentioned requirements, has an extremely low surface tension, i.e. 21.4 mN/m. Evidently, the higher the solvent content of the coating, the lower the surface tension. Conventional coatings normally lie in the range of 25-32 mN/m. This is low enough to give proper wetting on most surfaces, i.e. to move below the values of the critical surface tension of the substrates (see Table 6.3).

As the resin becomes the major component of the coating, problems related to surface tension are frequently encountered. So-called high-solids coatings are, therefore, extremely sensitive to dirt and fingerprints (the surface tension of which is around 24 mN/m). Paint defects, such as "cratering" and "picture framing" occur more frequently with high-solids coatings than with conventional systems.

Water is a liquid of high surface tension and is obviously not suitable for wetting of surfaces. Use of water-borne paints would have been very limited had it not been possible to use surfactants in the formulation. A good surfactant reduces the surface tension of water down to 28-30 mN/m, i.e. to the same range as that of the organic solvents used in paints and lacquers.

6 USE OF SPECIALITY SURFACTANTS

The majority of surfactants used in coatings formulations are standard anionic and nonionic amphiphiles, such as fatty alcohol sulfates, alkylaryl sulfonates and alcohol ethoxylates. Cationic and amphoteric surfactants

are rarely used. A few types of speciality surfactants have found specific niches. Fluorosurfactants and silicone surfactants reduce the surface tension to extremely low values. They are used in paint formulations to eliminate surface-tension gradients that can form due to faster evaporation of the solvent from the coating edges than from the centre. Acetylenic glycols, characterized by having two short, bulky hydrocarbon chains surrounding the polar group, are another type of niche surfactant. These non-micelle-forming surfactants form expanded films on water surfaces which can withstand high surface pressures. Such surfactants are widely used as antifoaming agents in coatings.

7 BIBLIOGRAPHY

1. Calbo, L. J., *Handbook of Coatings Additives*, Marcel Dekker, New York, 1992.
2. Holmberg, K., Role of surfactants in water-borne coatings, *Prog. Colloid Polym. Sci.*, **109**, 254–259 (1998).
3. Karsa, D. R., *Additives for Water-based Coatings*, Royal Society of Chemistry, Cambridge, UK, 1990.
4. Östberg, G., Huldén, M., Bergenståhl, B. and Holmberg, K., Alkyd emulsions, *Prog. Org. Coatings*, **24**, 281–297 (1994).
5. Patton, T. P., *Paint Flow and Pigment Dispersion*, 2nd Edn, Wiley, New York, 1979.
6. Paul, S., *Surface Coatings, Science and Technology*, 2nd Edn, Wiley, New York, 1996.

CHAPTER 7

Surface Chemistry of Paper

Fredrik Tiberg, John Daicic and Johan Fröberg

Institute for Surface Chemistry, Stockholm, Sweden

1	Introduction	124	6.2.1	Pigments	147
2	Fibre Properties	125	6.2.2	Dispersants	147
3	Paper Formation	128	6.2.3	Thickeners and rheology modifiers	148
3.1	The paper machine and the formation of the sheet	128	6.2.4	Starches as co-binders	149
3.2	Flocculation and retention	129	6.2.5	Binders	149
3.3	Control of interparticle interactions	130	6.3	Rheology	149
3.3.1	Colloidal stability and surface forces	130	6.3.1	Steady shear	149
3.3.2	Polymer adsorption	132	6.3.2	Viscoelasticity	151
3.3.3	Polymer effects on colloidal interactions and retention	136	6.4	Dewatering	152
4	Internal Sizing of Paper	138	6.5	Surface sizing and barrier coatings	152
4.1	Effects and side effects of sizing	138	6.5.1	Surface sizing	153
4.2	Internal sizing sub-processes	140	6.5.2	Barrier coatings	153
4.2.1	Retention of sizing agents	141	7	Wettability and Absorbency of Paper	154
4.2.2	Redistribution of sizing agent on paper surfaces	142	7.1	Basic concepts	154
4.2.3	Reactions and side-reactions of sizing agents	143	7.1.1	Wetting of rough and chemically heterogeneous surfaces	155
4.2.4	Analysis of size content in paper	144	7.1.2	Wetting dynamics	156
5	Dry and Wet Strength of Paper	145	7.1.3	Adhesion	157
5.1	Dry strength	145	7.2	Wetting properties and surface energy characteristics of paper	158
5.2	Wet strength	145	7.3	Capillary rise and flow dynamics	159
6	Surface Treatment of Paper	146	7.4	Absorption of liquids in paper	160
6.1	Why coat paper?	146	8	Characterization of Paper Properties	162
6.2	Coating components	147	8.1	Surface chemical properties	162
			8.1.1	X-ray photoelectron spectroscopy	162
			8.1.2	Secondary ion mass spectrometry	163

8.1.3	Infrared and Raman spectroscopy	163	8.3.1	Gas adsorption	167
8.2	Surface topography	163	8.3.2	Mercury porosimetry	168
8.2.1	Experimental methods	164	8.3.3	Microscopy	170
8.3	Porosity	167	9	Acknowledgements	171
			10	References	171

1 INTRODUCTION

Paper is a complex composite produced from various natural cellulose fibres to which mineral pigments and fillers are often added to form the material bulk. The physico-chemical properties of the paper depend greatly on the source of these materials, as well as the methods used for their refinement. Substantial quantities of performance chemicals are usually added to the bulk material in the papermaking process to improve, for instance, retention of fine particles (to increase bulkiness), to optimize the dewatering rate, to modify the dry and wet strength properties, and to increase resistance against liquid absorption. Most of these additives play their specific roles at the surfaces of the bulk material. Moreover, the papermaking process involves the dewatering and consolidation of a complex suspension of materials, in particular the fibres and fillers, which lie within the colloidal size domain (≈ 1 nm to $1 \mu\text{m}$) where surface forces are the dominating influence on the state of the suspension. It is thus clear that surface and colloid chemistry is crucial for the papermaking process. This is even so from an economic perspective, since for most paper grades profit margins are narrow and based on incremental performance and pricing differences. For example, specialized performance chemicals are usually added at levels below 5% by weight of the papermaking furnish, but this represents a substantial cost in comparison to the bulk material. Considerable savings can be achieved by cost-effective use of chemicals. Furthermore, control of the surface chemistry is vital if product quality is to be maintained.

The versatile usage of paper as a packaging material, an absorbent, and perhaps most importantly as an information carrier, very often requires the implementation of various surface treatments to optimize the product with respect to end-use requirements. This indicates again the important role of surface chemistry in the making and application of paper, particularly if one bears in mind the interaction of the (modified) paper surface with fluids of various kinds, ranging from simple liquids

such as water, to complex inks and even physiological fluids.

Paper is generally produced in a number of different steps, namely:

- Pulping, milling and other fibre treatments
- Dispersing of fibres (and filler) and mixing with chemical additives
- Formation
- Pressing and drying
- Surface treatment
- Calendering

This present chapter is concerned with the surface and colloid chemistry of the papermaking process, including preparation of the fibre suspension, production of the base sheet and modification of its surface. The focus lies on surface chemical sub-processes of papermaking discussed with a view to end-use applications. A brief introduction to the surface chemical properties of cellulose fibres is also provided. For more comprehensive descriptions of different aspects of papermaking, the reader is referred to refs (1–3).

Surface chemistry is important in pulping as well as milling operations, for instance, in refining steps where wood fibres are being washed and delignified. However, a lengthy discussion of this subject is beyond the scope of this present chapter. In the paper formation area, surface chemistry plays important roles in the retention of fines, in the dewatering process, and during drying and consolidation. The additive systems used for retention are frequently based on cationic polymers with possible additions of a second polymer or nanoparticles. Their function relies on their adsorption and interfacial behaviour and the effect that this has on the colloidal interactions between components in the papermaking furnish. The desired function of retention chemicals is to retain colloidal particles at fibre surfaces without causing inter-fibre aggregation and thus bad formation. The surface and colloid chemistry of retention is non-trivial due both to the complexities of the systems used and the “out-of-equilibrium” conditions prevailing in the paper machine. Dry strength is built up in the

consolidation and drying steps under the influence of capillary forces between thinning inter-fibre water necks. For improving the dry strength of the ready paper, hydrophilic polymer additives are commonly added, which act by increasing the fibre surface energy, the hydrogen bonding ability, and the effective contact areas between fibres, which together result in more efficient fibre bonding. Other important additives for paper modification added in the wet-end of the paper machine, include hydrophobic sizing agents. These are often added in the form of emulsions or dispersions, requiring expertise in this important field of colloidal technology. The role of sizing agents is to spread and anchor at fibre and filler surfaces, thus rendering these hydrophobic. Thereby, a capillary plug is established against penetration of polar liquids, which is desired in many paper grades, such as packaging and printing papers. In contrast, wetting promoters, in the form of surface-active agents and block copolymers, are also frequent additives in, for instance, tissue grades in order to improve water absorption properties. There exists, indeed, a whole range of performance chemicals, other than those mentioned above, which based on surface chemical principles are used in the papermaking process to facilitate production and optimize product performance. In this present chapter, we will focus on the more common types, whose major role is to modify the basic surface chemical properties, such as charge, surface polarity and surface morphologies, and thus also the nature of colloidal interactions, wetting and adhesion.

The surface finishing of paper is often as important as the actual papermaking process. This includes several processes including surface sizing, coating and calendaring. Surface sizing is often carried out in order to improve the resistance to liquids and increase the surface strength of paper. This is achieved by adding film-forming starch, sometimes together with sizing agents in a size press. Mineral and organic particles can also be included to improve surface smoothness and other properties of the substrate surface. However, this is more commonly done in coating operations, where thicker surface layers of mineral pigments are spread, for instance, by a doctor blade over the base paper surface to improve printability and optical properties. The pigment content is often above 50 wt%. It is not a trivial task to formulate coating colours for storage, coating, consolidation and dewatering, especially when considering that modern high-speed coating processes can run at rates of more than 2000 m/min.

One highly important characteristic of paper is its interactions with a number of liquids and solutions,

including water, surfactant solutions, physiological fluids, fountain solutions, various water- and oil-borne ink systems, polymer melts, etc. Processes of interest include wetting, absorbency and adhesion. To understand these and other phenomena, the evaluation of paper characteristics with respect to their "topochemical" properties is of importance. A number of techniques are used for this purpose. A selection of these will be discussed in the present chapter.

2 FIBRE PROPERTIES

Of the bulk materials used in papermaking, cellulose fibre is the most abundant, indeed in itself defining paper as a material. The wood fibre is a composite, built up in different layers, as shown schematically in Figure 7.1.

The main constituents in these layers are cellulose, lignin and hemicellulose. Fatty acids and fatty acid esters, rosins and sterols are also found in the fibre and are usually referred to as extractives. The surface chemical nature of the papermaking fibre depends on the fibre origin, as well as on the refining processes employed. Soft wood pulp from evergreens is often preferred in pulp products because of its longer fibres. These generally have a higher percentage of lignin and a lower percentage of hemicellulose than hard woods. In addition to wood fibres, various plant fibres are also used in papermaking. The pulp fibres are classified according to the treatment method as either mechanical or chemical, or as combinations thereof. In mechanical pulping, the fibres are separated by employing mechanical energy, whereas the fibres in chemical processing are removed from the wood matrix by chemically removing the lignin bonding material. Mechanical pulping results in high yields and fibres with chemical properties similar to those in native wood. However, the fibre damage and amounts of debris due to the mechanical treatment are large. Chemical pulping results in large reductions of the fibre lignin and hemicellulose content, which facilitates easy separation of fibres. The low lignin content of chemical fibres results in large bond strengths due to high surface energies and the formation of strong hydrogen bonds. Both mechanical and chemical pulps are normally bleached in order to increase brightness and remove lignin. Bleaching of mechanical pulps is generally done in a lignin-conserving manner called *brightening* in which chromophores are chemically modified and little bond cleavage and lignin removal occurs. Conversely, the goal of chemical pulp bleaching is often to maximally remove residual lignin. Nearly all bleaching agents used for chemical pulp bleaching are oxidizing

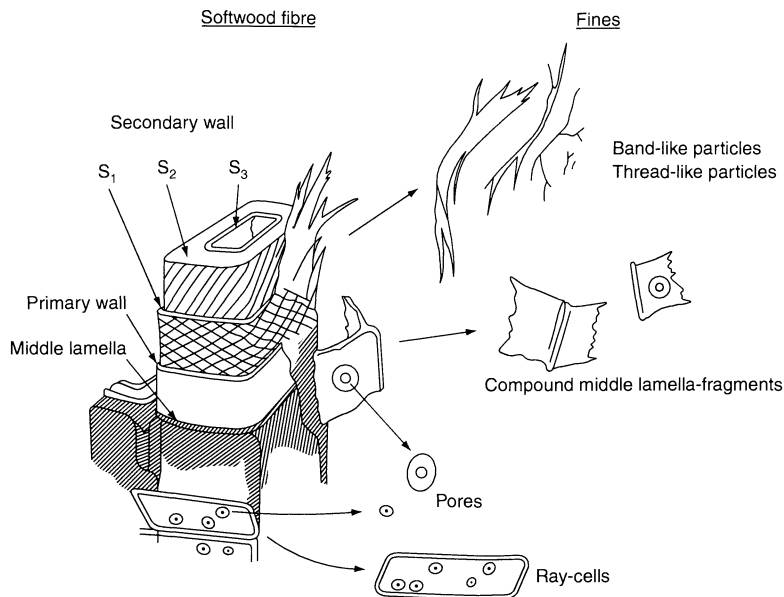


Figure 7.1. Structure of softwood fibre showing the architecture of the fibre wall with a lignin-rich middle lamella, the primary wall enforced by a network of cellulose fibrils, and the secondary wall built up of three layers with different fibrillar orientations. (Reproduced from Mr. Rundlöf, Licentiate thesis, Royal Institute of Technology, Stockholm 1996, with permission from the author)

agents, which act to lower the lignin molecular weight and increase its solubilization. Before being formed into a sheet, most pulps are subjected to mechanical action in order to improve the strength and other properties of the finished sheet. In this refining step, cellulose fibres are swollen, cut and fibrillated to make the fibre more flexible and compliant, and to increase the fibre–fibre bonding ability developed during drying. The mechanical and chemical processing discussed above affects a number of important fibre properties including:

- Chemical composition of the fibre surface
- Surface charge of the fibres in aqueous environments
- Surface morphology and fibre porosity
- Wetting properties

Together, these properties will influence retention, dewatering and paper strength developments, as well as liquid–paper interactions important in converting, printing and end use applications (see Sections 3–7 below). Some illustrative examples of the interrelationship between fibre treatment processes and fibre properties are given below.

The fibre lignin content is a central issue since high lignin contents tend to impact negatively on strength development in paper and paper wettability, as well as on the long-term stability of paper. Figure 7.2 shows

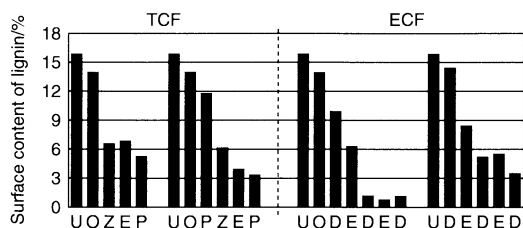


Figure 7.2. Effects of different bleaching sequences on the fibre surface content of lignin: TCF, total chlorine free; ECF, elemental chlorine free. The bleaching steps are oxygen delignification (O), ozone (Z), peroxide (P), chlorine dioxide (D) and alkali extraction (E). (From ref. (4) with permission)

how the surface lignin content of paper decreases after being subjected to various bleaching treatments (4). Decreasing the amount of lignin has been shown to decrease the fibre charge density, thus causing an increase in the tensile strength of the final product. The surface charge of fibres is important to papermaking, since it affects, among other things, polyelectrolyte adsorption and retention, and the swelling behaviour of the fibre. The surface charge arises from ion adsorption and dissociation of certain molecular groups and is determined by the fibre composition and properties of the solution, such as pH and ionic strength. The fibre charge can be estimated by using conventional

conductometric and potentiometric titration techniques or by electrokinetic methods, such as electrophoresis, electro-osmosis and streaming potential measurements (5). However, the surface charge of fibres is difficult to quantify correctly, due to their complex surface morphology and low charge density. A common method is to measure polyelectrolyte adsorption isotherms for high-molecular-weight polymers and estimate the charge density by assuming no penetration of the polyelectrolyte into the fibre interior, as well as stoichiometric charge compensation (see Section 3 below).

The surface morphology and porosity of fibres is a complex issue and varies with the ambient media due to swelling and other effects. Atomic Force Microscopy (AFM) and Scanning Electron Microscopy (SEM) are very useful for the characterization of the surface topography of fibres. The image quality of AFM is less than that of some SEM techniques, but instead AFM offers several advantages: simple sample preparation, measurements in most ambient media and greater sensitivity to thickness variations. Variations in the fibril structure are readily visualized by AFM as well as measurements of the individual micro-fibril properties. In addition, surface-to-surface interaction force measurements can be performed. In the phase-imaging mode, in-plane variations of the viscoelastic properties of the surface can also be studied, and provide information about the local distribution of different surface groups on the fibre. AFM provides many more features, such as force modulation measurements, where the local resistance of the surface is probed, and lateral force microscopy (probing friction). Considering the potential of AFM for fibre characterization, very little work has been published in the area. A particularly useful reference describing the use of AFM for fibre characterization was published a few years ago by Hanley and Gray (6).

SEM is a commonly used technique in the paper industry for high-resolution visualization of fibre and sheet properties (see also Section 8 below). Recent technological developments have substantially improved its range of applicability by making it possible to perform measurements at relatively high vapour pressures. The environmental SEM (ESEM) has great potential in the field of fibre and paper research. Among other things, it can be used to study fibre swelling and local wetting phenomena, as illustrated in Figure 7.3 (7).

The porosity of fibers can be measured using techniques such as gas-adsorption and cryoporometry, which are sensitive to pore sizes in the sub-micron size range. These techniques are discussed further in Section 8 below. Wetting properties and the surface energy of

fibres are important for dewatering, adhesion and dry strength, absorbency, etc. The most direct means of measuring fibre wettability is the single fibre capillary-graphic technique (8), where the contact angle of a liquid is determined from the wetting tension.

The force F exerted on the fibre dipped into a liquid (see Figure 7.4), is the capillary minus the buoyancy force, as follows:

$$F = P\gamma \cos \theta - \rho Agh + F_{\text{abs}}(t) \quad (7.1)$$

where P is the fibre perimeter, γ the liquid surface tension, θ the contact angle, ρ the liquid density, A the fibre cross-sectional area, and h the depth of immersion; $F_{\text{abs}}(t)$ corrects for the time-dependent absorption in the fibre. This can be usually be neglected for single fibres due to the fast equilibration. The force intercepts from measurements during advancement and retraction of the fibre in liquid, respectively, are then given by the



Figure 7.3. High-magnification image of wet-base stock showing the presence of 1–20 μm partially wetting water drops at the fibre surfaces. (From ref. (7) with permission)

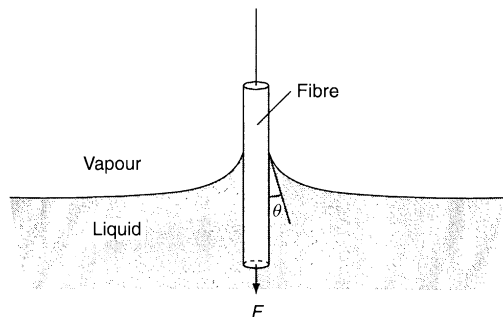


Figure 7.4. Single fibre wetting measurement geometry

following equations:

$$F_a = P\gamma \cos \theta_a \quad (7.2)$$

and

$$F_r = P\gamma \cos \theta_r \quad (7.3)$$

where θ_a and θ_r are the advancing and receding contact angles, respectively. The buoyancy contribution in equation (7.1) is usually negligible for single fibres, so θ_a and θ_r can be determined at any point during immersion or retraction of the fibre, as long as the perimeter is known. This is often not the case. The parameter θ_a is then often calculated from the F_a and F_r values along the fibre with the assumption that θ_r is zero, which often seems to be the case for cellulose fibres. Figure 7.5 shows the advancing contact angles measured along bleached and unbleached single fibres, where the bleaching process clearly has increased the fibre wettability. From contact angle measurements in different liquids, the surface energy of the fibres can be estimated (see Section 7 below). This possibility was explored and discussed in a comprehensive study by Berg (9), in which the effect of pH variations on the fibre wetting properties was also investigated. This author found that acidic and basic groups co-exist on bleached kraft pulp, and that their $pK_{1/2}$ values were of the order of 3–5 and 11, respectively, while chemithermo-mechanical pulp (CTMP) fibres only had basic groups, with a $pK_{1/2}$ value around 12.

The wetting properties of fibres can also be estimated from contact angle measurements on sheets and liquid penetration measurements. As is shown later in Table 7.1, the microscopic fibre measurements seem to correlate well with measurement on hand-sheets and paper. This is discussed in more detail later in Section 7.

Table 7.1. Surface energy components measured for single fibres (sf), hand sheets (hs) and films (f) of hard-, soft- and mixed-wood bleached kraft (HWBK, SWBK and HSWBK, respectively) pulp and cellulose films

Substrate	γ_s	γ_s^{LW}	γ_s^-	γ_s^+	Reference
HWBK (sf)	48.3	43.2	16.3	0.40	54
SWBK (sf)	46.2	41.8	24.5	0.20	54
HSWBK (hs) ^a	42.6	41.6	15.0	0.02	–
Cellulose (f)	54.5	44.0	17.2	10.50	53
Cellulose acetate (f)	52.6	44.9	18.5	0.80	53
Cellulose nitrate (f)	45.1	44.7	13.9	0.002	53
Cellulose (f)	56.7	39.1	39.7	2.00	55
Cellulose acetate (f)	43.1	38.2	28.2	0.21	55

^aData obtained from Figure 7.36.

3 PAPER FORMATION

3.1 The paper machine and the formation of the sheet

Paper manufacturing involves turning a complex suspension of fibres, fines, fillers and chemical additives into a thin paper sheet of width 1 to 10 metres. The paper machine typically runs at high speeds, ranging from 500 to 2000 metres per minute. The overriding challenge for the paper manufacturer is to produce a sheet of uniform lateral consistency with respect to strict criteria of dimensionality, strength, appearance and surface physico-chemical properties. Thus, control of the dewatering and flocculation of the paper fibre suspension is an essential step in ensuring an acceptable outcome. In this section, we emphasize the colloidal and surface chemical aspects of the paper formation process.

The formation process already needs to be controlled at the level of the fibre suspension in the head-box of the paper machine. Following Deng and Dodson (10), one way to describe the concentration of the fibre suspension is to introduce the crowding number, n_{crowd} , which is the number of fibres in a spherical volume with diameter of the order of the mean fibre length, $\bar{\lambda}$, in the suspension. The crowding number is related to the mass concentration, c , via the coarseness of the fibres δ , i.e. the mass per unit length – a measure of the flexibility. In the formation step, the crowding number may increase by up to two orders of magnitude during a time period of the order of 100 ms during which the paper may have passed the major part of the wire section.

Initially, some 10^{10} fibres are suspended in each section in the head-box unit. These typically have an average fibre length of 1 mm. In the entrance to the paper machine, the height of the fibre suspension is

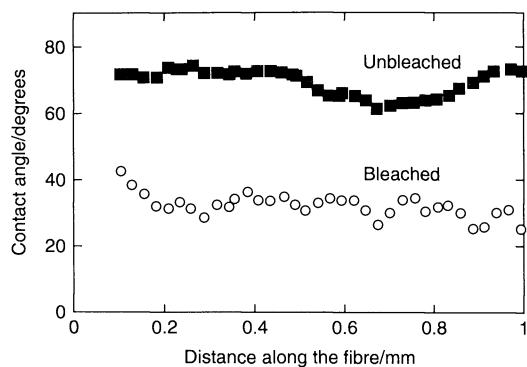


Figure 7.5. Advancing contact angles versus immersion distance along a bleached and an unbleached thermomechanical pulp fibre using equations 7.2 and 7.3 and assuming that the receding contact angle is zero

about 10 mm thick, which means that 10 fibres can span the distance if put in an end-to-end geometry. After dewatering in the wire section and pressing, the thickness of the sheet is about 0.1 mm for newsprint (holding some 10 fibre layers), up to, in extreme cases, a thickness of 1 mm for board. It is thus clear that one faces a very delicate problem of structuring when forming the paper sheet. Despite this, the local mass per unit area does not typically vary more than 10% (in the mm size regime).

The fibres usually have a log-normal distribution in length, with a mean value of the order of a few mm, depending on the type of pulp. The width of the fibres shows a normal distribution around a mean value of typically tens of microns. Apart from the dimensions of the fibres, the flexibility plays an important role in the formation characteristics. Increasing the wet fibre flexibility will affect both the fibre packing and bonding, and the more flexible the fibres are in a system, then the lower the tendency to flocculate. Despite the high aspect ratio of the fibres, typically 20–50, each fibre in the sheet only penetrates one or two fibre thicknesses and the structure of the paper sheet should therefore be characterized as layered rather than felted.

Despite being a well-established industrial process, the understanding of flow characteristics in the paper machine is still meagre. In principle, there is an overall general forward fluid motion with superimposed small-scale variations of turbulent flow. These fluctuations are very short-lived and in periods of decaying turbulence or regions of steady flow there is the possibility for flocs to form. In order for the water to be removed, there also needs to be a flow from the centre of the fibre matt towards the surface of the sheet. When considering flocculation and retention in the paper machine, it is important to keep in mind that fairly strong shear forces prevail and these will have a tendency to break up weakly flocculated aggregates.

Due to the forward motion of the fluid it is possible to detect a preferential orientation of the fibres in the plane of the sheet along the machine direction (MD). The anisotropy is on average 2:1 (MD/cross direction (CD)) but increases in regions of lower density due to fibre–fibre interactions. This anisotropy can also easily be detected by trying to tear paper apart in different directions.

Starting at the wet end of the paper machine, the fibre suspension is introduced through the head-box on to the vira where the formation takes place and initial stages of dewatering occur. The forming sheet then enters the wet pressing section before it reaches the final drying section. Today, many paper machines are integrated with

equipment for coating and other post-treatment of the paper, which follows directly at the end of the dryer.

The aim of the formation process is to produce a sheet with controlled structure, porosity, surface topography, strength and optical properties. Several of these are altered at later stages of the production by, e.g. calendaring. The fibres in the sheet are mainly held together by hydrogen-bonds, interfacial tension forces and chemical and mechanical interlocking. The fraction of hydrogen bonding hydroxyl groups on the fibre surfaces is claimed to be of the order of 1%, but this figure is difficult to verify experimentally. Hydrogen bonds extend some fraction of a nanometre and hence operate only at very short fibre–fibre distances. Hence, small-scale fibre roughness will impact strongly on the hydrogen-bonding capacity. The fibres are brought in contact during the later stages of dewatering through capillary forces, which result from the negative curvature in the thinning inter-fibre water neck. This pulls the fibre surfaces in contact and can also lead to local fibre-surface deformation. Most of the fibre shrinkage occurs at a late stage of the drying process when a specific solids content is reached. The fibre collapse point (FCP) is defined as the point when the water left in the fibre wall is equal to the bound water. This usually occurs at around 85–88% solids content.

3.2 Flocculation and retention

As emphasized above, one of the major challenges in paper manufacturing is to obtain a good formation of the paper sheet. The process of forming the sheet is complicated by the large number of components present in the furnace. Apart from the basic constituent, i.e. cellulose fibres, the process solution also contains finer pulp originating materials, collectively called fines. Mineral or latex particles (fillers) of different types are added to give the paper either bulk or volume, and the desired light scattering properties, or to change the physical properties of the end product. A comparison of the sizes of these different types of constituents and the mesh size in the wire used as the base for the sheet formation is shown in Figure 7.6 (11). This figure nicely illustrates the retention problem at hand. The system is made even more complex by the variety of additional chemicals, which are needed to control the end-use properties, either by giving specific properties to the sheet or by facilitating the production process itself. These chemicals tend to alter the interactions present in the furnace considerably and the balance between different types of aggregates is thus

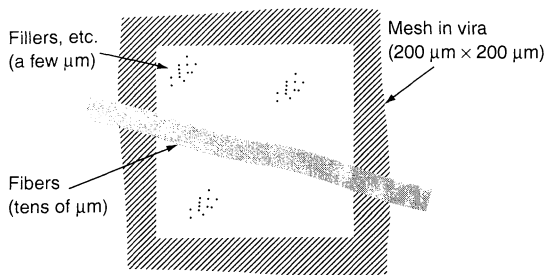


Figure 7.6. Characteristic dimensions of the central components in the formation and retention step in papermaking. (Redrawn from ref. (11))

changed. The sheet formation itself is achieved through a combination of two mechanisms: filtration, resulting from the structure formation of the fibres on the wire, and enhanced colloidal interactions brought about by the added chemicals. The first prerequisite is that the fibres need to be well dispersed. If not, the sheet will form unevenly, and instead of producing a relatively homogenous sheet with the fibres arranged in a network, the structure will be built up by a large number of flocs. Fibres are typically 1–3 mm long and some tens of microns wide. They have a tendency to entangle and form aggregates when present at concentrations typically prevailing during papermaking. However, the charge repulsion between cellulose fibres in aqueous solution makes it fairly simple to break up such aggregates. This can be achieved by shearing the system. High turbulence is consequently maintained in the head-box in order to prevent floc formation. If such conditions are not fulfilled, the paper will be unevenly formed.

Unfortunately, the fibre network structures formed during filtration on the wire are not small-scale enough to retain the finer materials, which are also needed in order for the paper to have the desired properties and prevent buildup in the white water of fillers and fines. In the design of chemical retention systems, it is important to strive for efficient bonding of smaller-sized materials, while keeping the fibres from forming large flocs and non-uniform lateral properties.

In order to understand the retention and flocculation problems at hand, we need to discuss the forces prevailing between the components as well as how these can be manipulated. The colloidal interactions prevalent in such systems can be described by using the classical DLVO theory, which is presented below. Subsequently, a short description of polymer adsorption and the effect that this has on the interactions between surfaces is given. This is followed by a short presentation of flocculation and retention mechanisms in papermaking systems.

3.3 Control of interparticle interactions

3.3.1 Colloidal stability and surface forces

The problem of *colloidal stability*, that is the balance of forces which stabilizes systems that contain particles too large to be buffeted by Brownian forces (approx. larger than 1 nm), but too small to be subject to significant sedimentation (smaller than 1 μm) is of central importance to the understanding of suspension properties. This, in turn, is useful in many applications, and in papermaking the issue arises not only in retention, but also, e.g. in the stability of the suspensions used to coat paper. Fines and coating pigments are good examples of colloidal particles. Their suspension stability is effectively dominated by surface forces (and thus surface chemistry), which can be modified by the addition of other components to the system, e.g. salts, polymers, binding agents, etc. However, we first need to (briefly) review the fundamentals of colloidal stability for simple systems, which contain charged surfaces in aqueous solution. Most surfaces are charged in an aqueous environment. The charge mechanism can be one of many, including desorption of lattice ions, acid–base equilibria of surface groups, dissociation of ionizable surface groups and preferential adsorption of charged species. For pulp fibres, the charge is principally due to the presence of negatively charged carboxylic acid groups.

DLVO theory

The DLVO theory of interactions between charged surfaces was developed independently by Deryaguin and Landau in Russia and Verwey and Overbeek in the Netherlands in the early 1940s. The theory was originally formulated in terms of a system where, in a first approximation, the charge is assumed to be *spread out* over the surface. By necessity (electroneutrality of macroscopic systems is such a necessity), the system contains a quantity of dissolved ions which when summed is equal to the total surface charge, but is opposite in sign. In order to simplify matters, these ions are assumed to be point charges (i.e. of zero size), and in terms of their thermodynamics are assumed to satisfy a Boltzmann distribution. Additionally, the theory allows for other simple ion species to be present, usually referred to as “added salt”. In practice, this is used to “screen” or reduce the electrostatic interaction. The counterion density profile is such that there is a high concentration near the surface, with a monotonic decay away until the bulk concentration is reached. A

single charged surface and its dissolved counterions are collectively known as the *electrostatic diffuse double-layer*. Since the range of the electrostatic interaction is for many practical cases relatively short compared to the size of the charged particles, an approximation can reasonably be made whereby (model) spherical particles are replaced by (model) parallel infinite planes. Evidently, many simplifications and assumptions were made in the DLVO formulation, and since this early work many researchers have laboured with the task of removing these and further refining and improving the theory. Still, as a qualitative description of colloidal stability, the DLVO theory remains a useful tool.

The DLVO theory assumes that there are two forces at play in simple colloidal systems which balance each other in such a way as to *kinetically stabilize* the suspension. It is important to emphasize that the true *equilibrium* state of nearly all colloidal systems is the fully aggregated one, i.e. given enough time, colloidal systems will ultimately collapse. The DLVO theory captures both features, and this is the key to its appeal. The balance of repulsive electrostatic and attractive dispersion forces produces a kinetic barrier to full aggregation; often, “stable” colloidal systems are in effect in a state of “suspended animation” before ultimate collapse.

That a repulsive force should exist between like-charged surfaces comes as no surprise; however, given the consideration that the system *overall* is electroneutral suggests that some additional thinking is required. What should be borne in mind is that the diffuse layer is compressed by the surfaces, and hence from a thermodynamic point of view the repulsive force arises from a favourable increase in ion entropy as the surfaces separate. The role of added electrolyte in reducing the electrostatic repulsive force is actually one of reducing entropy gains on separation, by collapsing the diffuse part of the double layer.

The attractive component of the DLVO force balance arises from *van der Waals* or *dispersion* interactions. In summary, all molecular species (apart from the proton) have, via the interaction of the electron cloud with the background electromagnetic field, the ability to induce dipoles in nearby molecules, and to be so affected themselves. This *dipole–dipole interaction* leads to an attractive force between molecules, and indeed between macroscopic bodies (although it is important to point out that dispersion forces are not, in general, pair-wise additive).

In order to give the DLVO theory a semi-quantitative description, the electrostatic and dispersive components are (individually) approximated analytically. Even given

the constraints described above, the Poisson–Boltzmann (PB) differential equation, which describes the electrostatic potential as a function of the surface separation D , is nonlinear and thus nontrivial to solve, with the solution for like-charged parallel plates providing a rather opaque set of equations in special functions known as elliptic integrals. A further simplification can be made, whereby the potential (or charge) at the surface is assumed to be low, and this simplifies the PB equation to the linear Debye–Hückel equation, with the very simple solution for an isolated double-layer given as follows:

$$V_{el} = V_0 e^{-\kappa x} \quad (7.4)$$

where V_0 is the electrostatic surface potential, x is the distance from the surface, and $\lambda_D (\equiv 1/\kappa)$ is the Debye length, given by:

$$1/\kappa = \sqrt{\frac{\epsilon_r \epsilon_0 k_B T}{\sum_i n_i z_i e^2}} \quad (7.5)$$

where n_i and z_i are the bulk concentrations and valencies of the salt ions, respectively. An inspection of the above two expressions shows clearly that the Debye length is a measure of the range over which the diffuse part of the double-layer extends. Addition of salt collapses the layer and the screening effect becomes more pronounced for salts with high valence ions. The Debye length at 25°C is $1/\kappa = \text{const.}/\sqrt{c_s}$, where the constant is 0.304 for a 1:1 salt such as NaCl, 0.176 for a 2:1 or 1:2 salt such as CaCl_2 , and 0.152 for a 2:2 salt such as MgSO_4 .

The quantification of the van der Waals dispersion interaction between colloidal bodies is a complex problem in quantum electrodynamics. A naive picture can be obtained from considerations of what occurs in the interaction between two simple atoms. At any instance of time, the distribution of electrons around an atom will give rise to an instantaneous dipole. This transient dipole will in turn induce dipoles in neighbouring molecules, via the background electromagnetic field. The interactions arising from these fluctuating dipoles decay with separation as a power law (power of -6 or -7 depending on the separation) and are proportional to the polarizabilities of the interacting species. For macroscopic bodies, one may make the approximation of pair-wise summation of all such interactions arising from atoms in the two bodies. However, this is but an approximation as three-body and higher interaction terms contribute to the full interaction. Hamaker was the first to provide the pair-wise additive solution for two parallel infinite planes of the same molecular composition, interacting across a gap. The interaction energy between two bodies

at a separation D can be described as follows:

$$V_{vdw} = -\frac{A}{12\pi D^2} \quad (7.6)$$

where A is a material constant, known as the Hamaker constant.

A more sophisticated approach, based on the interaction of continuous media mediated by the quantum electromagnetic field, was later developed by Lifshitz, but this theory is outside the scope of this present chapter.

In order to describe the colloidal interactions within the DLVO approach, one now simply has to add the two derived relationships to obtain the total interaction energy:

$$V_{tot} = V_{el} + V_{vdw} \quad (7.7)$$

Figure 7.7 illustrates qualitatively the interaction of two colloidal bodies under the assumptions detailed above. The interaction energy can, in principle, be divided into different regions. The longer-range force is the electrostatic interaction, the range of which decreases with increasing electrolyte concentration, while the magnitude increases with increasing surface charge or surface potential. At intermediate separations, a shallow minimum may be present in the case of a strong van der Waals force and/or weak electrostatic repulsion. This minimum is where the particles reside when “kinetically trapped” in a flocculated state. Closer to contact, a maximum in the interaction energy may occur, again primarily depending on the magnitude of the electrostatic repulsion. This is the barrier which hinders closer

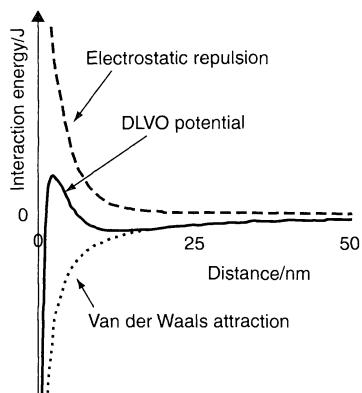


Figure 7.7. DLVO-type interaction (continuous line) obtained as the sum of the electrostatic repulsion (dashed line) and van der Waals attraction (dotted line). The interaction curve is calculated for a sphere with a $1 \mu\text{m}$ radius, a surface potential of 20 mV , a Hamaker constant of $20 \times 10^{-20} \text{ J}$, immersed in a 10 mM 1:1 salt solution

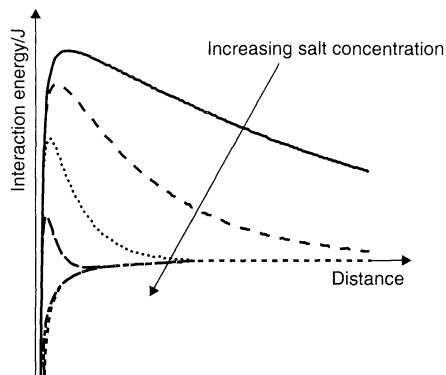


Figure 7.8. Influence of the salt concentration on the DLVO potential between two charged surfaces. The system is, aside from the varying salt concentration, the same as in Figure 7.7

contact between the particles. However, once this maximum is passed the particles then reach the deep primary minimum regime. The parameters which can be altered when attempting to control the system behaviour are the surface charge/potential and ionic strength, which determines the magnitude and range of the repulsion, respectively, and the Hamaker constant which determines the magnitude of the van der Waals or dispersion force. The latter is more difficult to alter but may be changed by adding a polymer to the system that adsorbs to the particles in high enough amounts in order for its polarizability to alter the interaction of the material with the electromagnetic field. (However it should be noted that this is usually not the primary reason for adding polymers to the system; a full discussion will be given below.) Finally, we will summarize the discussion about DLVO interactions by showing the effect of changing salt concentration (Figure 7.8) and surface potential (Figure 7.9) on the DLVO potential. Figure 7.8 shows how the range and the magnitude of the potential decreases with increasing salt concentration from low- to high-salt limits. The repulsive barrier vanishes completely in the high-salt limit. Decreasing the surface potential results in a decreasing magnitude of the repulsive electrostatic interaction. However, that the range of the interaction is unchanged is easily understood from equation 7.4 and seen in Figure 7.9.

3.3.2 Polymer adsorption

Nearly all retention aid systems used in paper manufacturing contain a high-molecular-weight polymer as a key component. The adsorption of polymers at the surfaces of fibres, fines and fillers in the papermaking

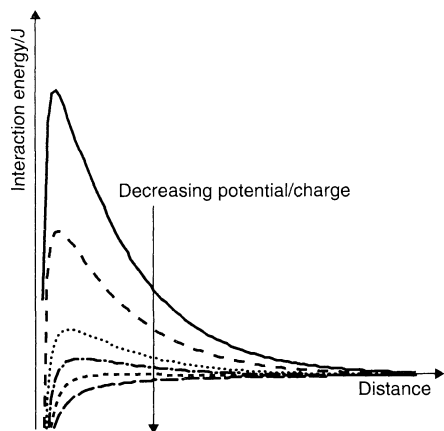


Figure 7.9. Influence of the surface potential on the DLVO potential between two charged surfaces. The system is, apart from the varying surface potential/charge, the same as in Figure 7.7

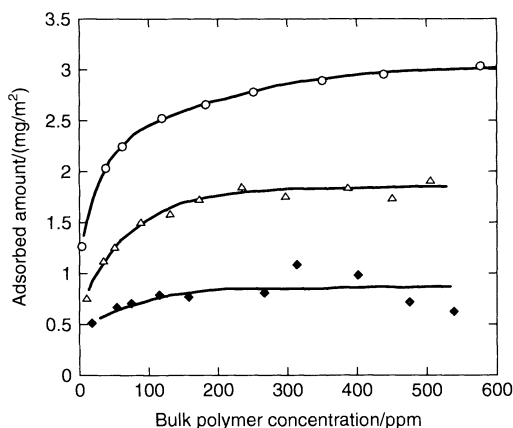


Figure 7.10. Adsorption isotherms for different narrow-molecular-weight poly(vinyl alcohol) at the polystyrene-water interface. The molecular weights used are 8000 (filled diamonds), 28 000 (open triangles) and 67 000 (open circles). (Redrawn from ref. (13))

furnish is used in different ways to facilitate retention. The purpose of polymer adsorption is to modify the interactions between the colloidal components so that the fines and fillers are effectively retended at fibre surfaces. Introducing polymers into a colloidal system can result in a colloidal stability increase or decrease depending on the structure and density of the polymers at the surfaces of the colloidal material. There are several fundamental reasons for a polymer to adsorb at a surface. The first reason is specific attractive interactions

between the polymeric groups and the surface, such as the attraction of opposite charges of a cationic polymer (polyelectrolyte) and a negatively charged surface. The other, which is more specific to polymers, is the entropy gained when surface-bound molecules are released into solution when replaced by surface-anchoring polymer groups. The entropy gained by the many solvated molecules is much larger than the rather small loss in degree of conformational freedom of the polymer. Due to the fact that polymer adsorption is entropically favoured, only a small specific adsorption energy is needed for polymers to anchor at a surface and substitute small surface-bound molecules. By considering the entropic driving force for polymer adsorption, it is easy to understand that the necessary energy for substituting, for instance, a solvent molecule with a polymer group at the surface will decrease with an increasing size of the polymer molecule. High-molecular-weight polymers are more inclined to adsorb than their low-molecular-weight analogues. Indeed, high-molecular-weight polymers adsorb strongly even at very low concentrations, thus leading to high-affinity isotherms having constant adsorption at higher concentrations where the surface has become saturated, as shown in Figure 7.10 (13). Generally, the adsorbed amount increases with the molecular weight of the polymer, becoming independent of molecular weight for very large polymers (12). As can be understood from the earlier discussion, the saturation adsorption tends to increase with the molecular weight. The high-affinity character of polymer isotherms means that the polymers in a practical sense are irreversibly adsorbed, since the concentration difference between any rinsing solution and the sub-surface outside the adsorbed layer is very small. This will lead to very slow mass-transfer from the interfacial region to the bulk. Even fairly low-molecular-weight polymers can appear irreversibly adsorbed. This is often due to the polydispersity, i.e. the polymer contains a high-molecular-weight fraction that adsorbs preferentially due to the larger entropic driving force.

Before going into the details of polymers at interfaces, a few points about solution behaviour are worth mentioning. Long flexible-chain polymers tend to adopt a random coil conformation in dilute solutions. An important measure of this structure is the radius of gyration, which depends on the molecular weight and the solvency in the ambient medium. Solvency describes the relative strength of the polymer segment/segment and segment/solvent interactions. A high affinity of the polymer for the solvent, i.e. a good solvent, leads to an osmotically swollen coil with a radius of gyration tending to its maximum. The coil collapses and adopts a

more close-packed unit when the polymer affinity for the solvent decreases. Finally, the polymer will precipitate. The intermediate situation when the affinities are equal is referred to as the θ -temperature. Decreasing the polymer solvency will also promote adsorption of polymers at surfaces. Close to conditions of bulk precipitation, this tendency will be high and may result in the formation of multiple layers of polymers at the surface. For polymers that carry a net charge, commonly referred to as polyelectrolytes, the intra-chain electrostatic repulsion between charged groups along the polymer backbone results in a more extended conformation than that of a random coil. A common measure of the chain rigidity is the persistence length L_p , which increases with increasing charge density of the macromolecule and decreasing ionic strength. A high rigidity leads to deviation from the random-coil conformation. A highly charged polyelectrolyte will, at very low ionic strengths, behave more like a stiff rod. As salt is added to a polyelectrolyte solution, the intra-chain repulsion becomes screened and the polyelectrolyte will behave more and more as a flexible non-ionic polymer. The effects described above can also be seen for adsorbed polymers, as is emphasized below.

We shall now mention some basic facts about the manner in which polymers organize at interfaces. Adsorbed polymer segments are classified into trains, loops and tails, depending on whether the segment is anchored at the interface, forms a loop out from the surface, or extends into the solution with only one end attached at the surface, as illustrated in Figure 7.11. The relative contribution of trains, loops, and tails will depend on the interaction strength between the polymer monomers and the surface, the solvency of the polymer chain, and also the polymer charge density in the case of polyelectrolytes (12). If the polymer is a copolymer built up of different monomers, then the structure will also depend on the distribution of different segments along the chain. The following trends apply in most

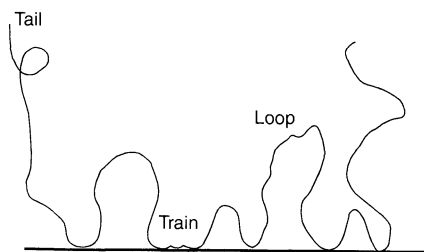


Figure 7.11. Schematic illustration of the structure of an adsorbed polymer chain. Segments are distributed into trains, loops and tails

cases, providing all other factors affecting adsorption are constant:

- Increasing the molecular weight usually results in an increase of adsorption, thicker layers, and a larger relative fraction of loops at the expense of tails.
- Improving the solvency conditions results in a decrease of the overall adsorption, but frequently to an increase of the size of loops and tails and their extension into solution.
- Increasing the strength of the monomer surface interaction leads, at least initially, to an increase of adsorption and an increase of the loop and tail extensions into solution.

Since polymers used in papermaking are often oppositely charged to the surface, we need also to consider some basic electrostatic effects:

- Increasing the fraction of charged groups results, for purely electrosorbing polymers, initially in a strong increase of adsorption followed by a slower decrease at higher charge densities. In the latter regime, the layer thickness tends to decrease strongly with increasing polymer charge density. The maximum is for low-ionic-strength solutions observed at polymer charge densities of only a few percent.
- Increasing the salt concentration shifts the position of the maximum to higher charge densities and the adsorption to lower values. However, the layer thickness given by loop and tail sizes increases with the salt concentration. In the limit of high ionic strengths, electrostatic interactions are strongly screened, thus resulting in desorption. This effect becomes even larger if the competing ions are multivalent or interact specifically with the surface.

The adsorption maximum observed on increasing the polymer charge density can be explained as follows. Initially, the increased electrostatic attraction results in more polymers being bound to the surface. However, this effect competes with the fact that an increased charge density results in more train segments, and thus fewer and shorter loops and tails. Low-charged polyelectrolytes tend as a general rule to adsorb in more extended conformations with loops and tails than highly charged polyelectrolytes, which adopt flatter conformations, due both to the larger stiffness of the polymer chain and the increased chain density of conceivable anchoring sites. It should in this context be noted that purely electrosorbing polymers tend to fully charge-compensate the surface in the low-salt limit (12).

In many cases, adsorption is driven both by electrostatic and non-electrostatic interactions. In conjunction

with adsorption close to the saturation limit, this often results in an overcompensation of the surface charge. The outcome of varying different properties, such as the ionic strength, becomes less transparent when both electrostatic and non-electrostatic interactions are important. Increasing the salt concentration may, for instance, also lead to an increased adsorption in the high-salt limit for such a system. The reasons for the increase may in such a case be twofold. Increasing the salt concentration decreases the electrostatic intra-chain repulsion and can thereby result in denser packing of the polyelectrolyte chain in the interfacial region. It may also reduce the solubility of the polymer and thereby cause an increased adsorption. The two effects are strongly interrelated.

In the case of like-charged polymers and surfaces, polymers are depleted from the surface (negative adsorption) unless non-electrostatic interactions aid adsorption (typically hydrophobic attraction in aqueous media). In such a case, adsorption increases with increasing salt concentration, due to the screening of repulsive electrostatic interactions between the polymer and the surface.

The retention systems used in papermaking are often multi-component systems. Nanoparticles, for instance silica sols, are frequently added to a high molecular weight cationic flocculants in order to improve retention and flocculation properties. Nanoparticles compete with the colloidal fibre, filler and fines surfaces for the polyelectrolyte. In terms of adsorption properties, nanoparticles seem to have similar, but more pronounced, effects than salts. Relatively small additions result in a large swelling of the adsorbed cationic polyelectrolyte layers. The nanoparticle can be viewed as a multi-ion competing with the surface for polyelectrolyte charges. When present in the adsorbed layer, they may mutually repel each other and thereby further aid in swelling of the adsorbed polyelectrolyte layer. Many multi-component systems are used in papermaking, but an attempt to rationalize their respective complex interfacial behaviour is beyond the scope of this present chapter.

Before discussing the effects that adsorbed polymers have on interactions between surfaces and colloidal bodies, a brief discussion about the kinetic aspects of polymer adsorption phenomena is given. This is an important aspect to consider since papermaking is a dynamic process. At least at low coverage, polymer adsorption tends to be mass-transfer limited, implying that the adsorption rate can be written as follows:

$$\frac{d\Gamma}{dt} = \frac{D_p}{\delta} [C_b - C_s(\Gamma)] \quad (7.8)$$

where D_p is the diffusion coefficient for the polymer, δ is the diffusion distance (or stagnant layer thickness), C_b the bulk polymer concentration, and $C_s(\Gamma)$

the sub-surface concentration for a given surface excess. This is equal to the inverse isotherm value $C(\Gamma)$ and hence directly accessible from experimental adsorption isotherm data. Due to the high-affinity nature of most polymer isotherms, the surface concentration $C_s(\Gamma)$ can be set to zero for the major part of the adsorption process ("perfect sink" condition). Surprisingly good fits to experimental adsorption data for polymers and block copolymers have been obtained by using the simple local equilibrium approach of equation (7.8). The simple mass-transfer-limited model (based on the assumption of local equilibrium) has indeed been shown to predict rather nicely the adsorption kinetics up to 75% of the plateau surface coverage and for Reynolds numbers ranging from 1 to 200 (the experimentally accessible regime), as discussed in ref. (12). By using this simple model, we can also, as was mentioned above, explain the slow desorption kinetics observed for polymer and polyelectrolyte systems. The parameter $C_s(\Gamma)$ also decays very rapidly during desorption under local equilibrium conditions, and extremely slow mass-transfer is predicted. The prediction is, indeed, in agreement with experimentally observed desorption rates, which, however, are often interpreted in terms of adsorption irreversibility. Therefore, the concept of irreversibility is not necessary for explaining the very slow desorption rates observed experimentally for adsorbed polymer systems. A further indication of the reversibility of polymer adsorption processes is the fact that most polymers are easily displaced by associates of higher molecular weight (12). The driving force for the displacement is the concomitant entropy increase of the system. In the case of charged polymer adsorption, it is more likely that adsorption is partially irreversible. The strong electrostatic bonds with the surface may inhibit relaxation and trap the polymer in a metastable state. This issue is, however, still unresolved.

There are naturally many situations when polymer adsorption is not mass-transfer limited, and mixed kinetics, taking into account adsorption barriers and slow surface relaxation phenomena, more appropriately describe the adsorption kinetics. However, in many practical cases it is quite sufficient to consider the implications of the simple mass-transfer-limited kinetics discussed above, keeping in mind that the technical retention systems used are inherently polydisperse. The papermaking furnish is furthermore exposed to high shear, which must be carefully considered in the kinetic analysis. The collision frequency of the colloidal components in the system is also high. This is important and means that polymers may be transferred between colliding surfaces as

well as becoming structurally distorted in the adsorbed state.

The fact that most solid components in a papermaking furnish are rough and porous is an issue that we so far have not discussed. Conceptually, it is logical that the adsorption at fibre surfaces resembles the corresponding process occurring at a smooth surface having the same surface properties. A distribution of trains, loops, and tails, will thus form on the surface, depending on the various properties discussed earlier. However, with time, polymer may start to penetrate the small pores present in fibre surfaces, and relax in crevices. This is schematically illustrated in Figure 7.12. Such relaxation phenomena will naturally affect the impact that the polymers have on colloidal interactions in terms of flocculation and retention tendencies. It is important to note that low-molecular-weight polymers may diffuse into fibre pores, and thus become inactivated in a practical sense. This diffusion often reverses the molecular-weight dependence of adsorption on micro-porous surfaces, since the surface area available for small polymers is larger than that for high-molecular-weight polymers. Hence, it is of no surprise that adsorption isotherms on pulps reveal an apparent decrease of adsorption with increasing molecular weight.

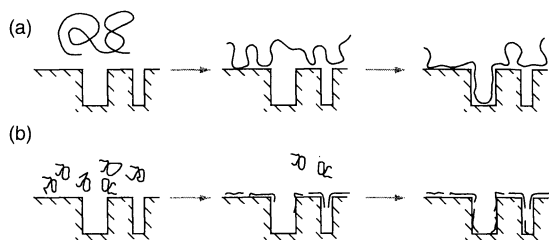


Figure 7.12. Sequence of processes following the anchoring of polymers on porous materials, schematically depicted for (a) high- and (b) low-molecular-weight polymers

3.3.3 Polymer effects on colloidal interactions and retention

Retention involves binding fines, filler, sizing agents, etc. to the fibre surface. This often involves both flocculation of fine materials into larger aggregates and binding of the fine materials and aggregates at fibre surfaces. A good retention system should facilitate these processes without causing the fibres to aggregate. The high shear forces in parts of the paper machine can result in floc breakup and detachment from the fibre surfaces. Hence, reflocculation properties are also important. The reflocculation tendency may vary strongly between different retention systems, and optimization of this aspect is important when choosing a retention system. Before discussing these aspects in more detail, a brief review of polymer-induced forces will be given.

Addition of polymer to a colloidal system may facilitate both attractive and repulsive interactions, depending on the properties of the interfacial polymer layers.

Attractive interactions resulting in flocculation and binding to fibre surfaces may, for like-charged colloidal system, be generated by the action of adsorbing polymers through three basic mechanisms (14):

- Polymer bridging
- Charge neutralization
- Electrostatic patch aggregation

Polymer bridging results from the fact that polymer chains can anchor at different surfaces concurrently when particles are brought together, as depicted in Figure 7.13. Bridging flocculation is most effective when the polymer surface coverage is not too high. The reason why high-molecular-weight polyelectrolytes are effective can readily be understood from the postulated mode of action. For the bridging attraction to take effect, it is necessary that the spatial extension of polymer loops and tails exceeds a distance of the order

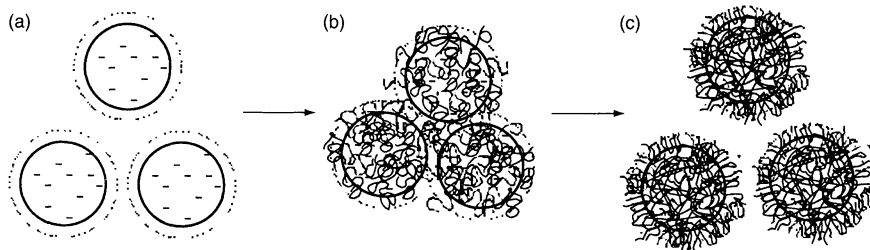


Figure 7.13. Sequence showing schematically (a) charge-stabilized particles, (b) particles flocculated by the polymer bridging mechanism, and (c) particles restabilized by steric repulsive (chain overlap) interactions at higher levels of polymer surface coverage

of the sum of the electrostatic double-layers. Lower-molecular-weight polymers can generally be used when flocculation is effected at high salt concentrations, where the double-layer is compressed and adsorbed polyelectrolyte layers expand. The mechanism of adding salt to enhance bridging flocculation is called *sensitization*. Note that in the limit of high ionic strength, desorption and contraction of the adsorbed layer may occur. A prerequisite for effective bridging flocculation is that an individual polymer anchors with at least one segment at each surface. For cationic polymers and anionic colloidal material, as is common in papermaking, charge interactions promote anchoring. It is found in some cases, however, that negatively charged particles can be flocculated by anionic polymers. There is evidence for the fact that this is facilitated by multivalent counterions, such as Ca^{2+} , which act as "bridges-within-bridges" to promote polymer binding at the surface. A low-molecular-weight cationic polymer can be added to a high-molecular-weight anionic polymer system to generate the same effect. Attraction between hydrophobic polymer segments and surface groups driven by the hydrophobic effect can also facilitate anchoring and bridging, irrespective of the charge nature of the system. With good mixing and control of the polymer concentration, a highly effective aggregation (flocculation) of colloidal dispersions can indeed be obtained based on the bridging flocculation mechanism. Charge neutralization is conceptually trivial and simply involves compensating the surface charges with the charges of an adsorbing polymer. Practically, however, it is not so easy to achieve since surfaces readily become over-compensated. Steric repulsive contributions between adsorbed chains may also oppose the desired aggregation effect. However, charge neutralization flocculation may in other situations be improved by polymer bridging. A further consequence

of the charge neutralization mechanism is that, acting alone, it results in floc structures that are sensitive to shear.

A related mechanism to charge neutralization is the patch flocculation mechanism. This presupposes that the cationic polyelectrolyte adsorbs to form patches on the negatively charged surface, as is illustrated in Figure 7.14. Electrostatic interactions between such mosaics of charges may then drive aggregation during forced or Brownian collision. This is actually a type of bridging attraction, although it differs to some extent by the requirement of a strong heterogeneity in the surface distribution of adsorbed polyelectrolyte. During papermaking, the mentioned attractive interactions may all be in effect to different degrees, since each of them are usually most effective when the surfaces are unsaturated with adsorbed polymer. The bridging efficiency should be at a maximum when the fractional surface coverage is half the value at surface saturation. The fact that high-molecular-weight polymers are used in nearly all retention system points to the fact that bridging flocculation is often critical for good retention. This can partly be related to the fact that the bridging flocs are long-range in nature, relatively strong and thus resistant to shear.

Floc breakup, however, still occurs during papermaking, despite the presence of bridging polymers. The process of reflocculation is therefore significant. The breakup of particle aggregates frequently results in breakage of the polymer chains and hence in a decreased molecular weight distribution. In combination with possible reformation effects, this will negatively influence the tendency for reflocculation. There is some evidence that polymeric retention systems containing microparticles exhibit better reflocculation properties than one-component polymer systems (15). The reason

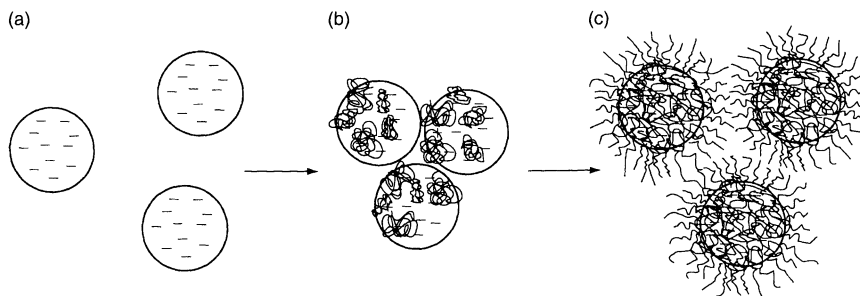


Figure 7.14. Sequence showing schematically (a) charge-stabilized particles, (b) particles flocculated by the patch flocculation mechanism, and (c) particles restabilized by steric repulsive (chain overlap) interactions at higher levels of polymer surface coverage

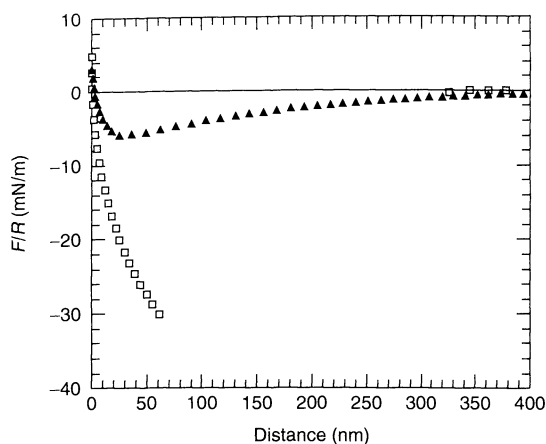


Figure 7.15. Interaction forces measured on separation for two glass spheres in 1 mM KCl in the presence of 3 ppm highly charged AM–MAPTAC cationic polymer (squares) and 3 ppm highly charged AM–MAPTAC together with silica nanoparticles (triangles); AM–MAPTAC, copolymer of acrylamide and (3-meth acrylamido propyl)tri methylammonium chloride. (From ref. (16) with permission)

for this is unclear, but may be related to the type of network formed in the bridging situations. A recent study indicates that the attractive bridging interaction between surfaces in the presence of nanoparticles is more elastic, exhibits a more shallow adhesion minimum, and is more long-ranged, as shown in Figure 7.15 (16). The role of nanoparticles in retention systems is, however, still far from being fully understood. Besides giving good reflocculation properties, these systems tend also to have favourable dewatering properties.

Finally, the effect that polymeric retention aids have on fibre flocculation must be emphasized. There is always a cost in terms of poorer formation when adding a polymeric flocculant. The effect is largest at high dilution below the threshold concentration for fibre network formation (15).

In effect, we have mainly covered attractive interactions introduced when adding polymer to a system. This is because our interest here was mainly focused on retention aids which function by enhancing the attractive interactions in the papermaking system. Polymeric systems tuned to increase the repulsive force between surfaces by way of steric interactions (caused by chain overlap and loss of conformational entropy on compression), electrosteric interactions (between charged polymer brushes), and/or electrostatic repulsions (due to charge over-compensation), are equally important in practical applications. However, repulsive polymeric forces should not by any means be viewed as purely

detrimental, as they are beneficial in applications such as stabilizing papermaking emulsions during storage, pumping, protecting against homoflocculation, and for control of pitch and stickies. Interested readers can consult one of the many textbooks devoted to colloidal interactions for more detailed information on this topic, such as refs (12, 14, 17, 18).

4 INTERNAL SIZING OF PAPER

Internal sizing aims at the establishment of a capillary barrier for the penetration and spreading of liquids, often water and aqueous solutions, through the capillary pore system of the paper sheet. The process of sizing (hydrophobizing) paper surfaces can involve a range of chemicals and surface chemical sub-processes including emulsification, retention, molecular spreading and anchoring. Sizing is furthermore performed with the goal of altering the surface-related properties of paper such as wetting and absorption, which are discussed in more detail in Section 7 below. Common side effects of the sizing process usually include adhesion and friction problems, which have their origin in the surface chemistry of the sized product.

4.1 Effects and side effects of sizing

Generally speaking, the term *sizing* refers to the process of making paper fibres and fillers hydrophobic with the aim of controlling liquid–paper interactions. An example is the control of spreading and the introduction of absorption barriers for polar liquids and solutions, such as water-borne inks, fountain solutions, water and milk. Many grades of printing paper require sizing treatments in order to control ink spreading and absorbency. It is also frequently necessary to size paper in order to retard or prevent the penetration of liquids in cartons, packaging paper and board, paper cups, etc. The role played by sizing agents in such applications is to increase the hydrophobicity of the paper to levels where capillary penetration is avoided. Therefore, a discussion of the capillary mechanism is germane to the issue of sizing, and this is where we begin our exposition.

The capillary pressure in an ideal cylindrical pore is given by the following:

$$P_c = \frac{2\gamma \cos \theta}{r} \quad (7.9)$$

where γ is the surface tension of the liquid, θ the contact angle, and r the pore radius. Negative capillary pressures

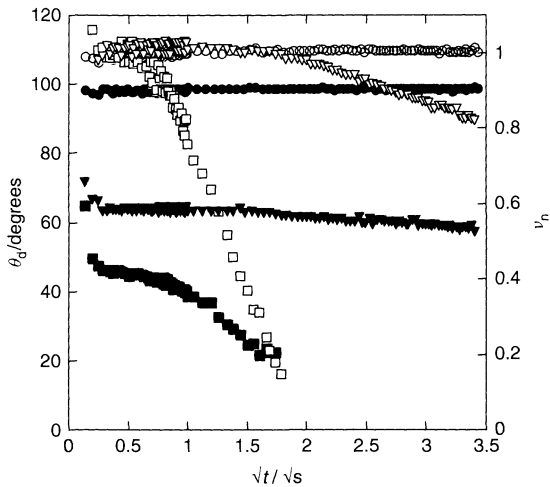


Figure 7.16. Time-dependence of the dynamic contact angle (filled symbols) and drop volume normalized to its original value before contact with the paper (open symbols). The amount of sizing agent in the different papers increased by a factor of three, following the order: squares, triangles and circles

arise for contact angles larger than 90° , which in absorbency terms means an effective resistance against liquid penetration. The advancing water contact angle of a well-sized paper grade should therefore be higher than 90° . As is indicated in Figure 7.16, this is sufficient for hindering the spontaneous uptake of water by the paper sheet. Negative capillary pressure for a hydrophobic capillary can none the less rather easily be overcome by an externally applied pressure gradient. For a paper with a water contact angle of 110° , and an average pore size of $10\ \mu\text{m}$, the resisting pressure for water will only be about $\sim 0.1\ \text{atm}$. It is also worth noting that the capillary plug created by the sizing process has no effect on vapour penetration, as the driving force for this process is the mixing entropy. Since internal sizing results in hydrophobizing the fibre and filler surfaces in the paper, the tendency for capillary condensation of vapours in pores and cracks may still be decreased. Attractive interactions between sized fibre surfaces in water may also contribute to an increased wet strength. We can from this reasoning conclude that internal sizing of paper provides:

- A decreased spreading tendency of polar liquids (through an increased contact angle)
- A weak capillary resistance against absorption of polar liquids $\sim 0.1\ \text{atm}$

- A decreased tendency for capillary condensation of polar liquids
- An increased wet strength through hydrophobic attractive interactions

It is worth noting that the above discussion on capillary penetration is based on an idealized pore system. In reality, this is of course not the case. Sizing agents are, furthermore, not distributed evenly, as is evident from the large contact angle hysteresis seen for sized papers, where the receding angle is often the same as for a non-sized product. Despite these precautions, the 90° contact angle threshold for water resistance seems valid for sized paper grades, at least for short contact times, as shown in the example given in Figure 7.17. The resistance to liquid imbibition obtained through internal sizing is not always sufficient, since condensation phenomena can occur in sized paper exposed to liquid vapours because of incomplete size coverage. This can shift the wetting balance from initially being controlled by the advancing contact angle to a situation where the receding angle dominates the wetting behaviour. Furthermore, liquids may penetrate into the cellulose fibres and thus cause fibre swelling as well as a change of apparent surface hydrophobicity. For obtaining long-term stability against water penetration in paper, it is often necessary to cover paper surfaces by polymer laminate or completely impregnate the paper with a hydrophobic liquid or wax.

Unfortunately, the very important resistance against capillary penetration achieved through internal sizing

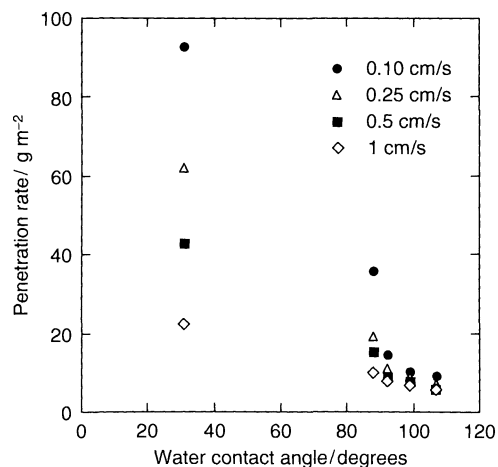


Figure 7.17. Penetration rate, measured using the Bristow wheel as function of the advancing water contact angle for different AKD sized paper grades

does not come alone. Internal sizing frequently results in unwanted side effects including:

- Reduced adhesion between, for instance, paper and polyethylene surface films or between paper and toner, due to a decreased surface energy of the paper surface.
- Reduced paper-to-paper friction values, where sizing agents in combination with the surface energy reduction effect can also lubricate the paper surfaces.
- Contamination of the white water system and formation of deposits.
- Deterioration of the mechanical properties of paper (folding ability, etc.).

The adhesion problems arising due to sizing are generally related to the fact that the surface energy of the paper becomes so low that the wetting of the surface by, for instance, a polymer is no longer sufficiently effective (see also Section 7 below). Reduced friction may have both its *pros* and *cons*. A typical example of the latter concerns sack papers, where sizing may cause a low frictional resistance and hence difficulties with stapling. The reason for the friction reduction often resulting from sizing is partly due to the lowering of the surface energy of the paper. Spread and unspread sizing agents may also have a strongly lubricating effect on the paper surface. Poor retention of size particles on fibre and filler surfaces may result in a buildup in the wet end and thus contaminate the white water and result in the buildup of deposits.

The most commonly used sizing agents today are rosins, commonly used in acidic papermaking systems, and synthetic sizing agents such as alkyl ketene dimer (AKD) and alkenyl succinic anhydride (ASA), as shown in Figure 7.18. The latter two components are suitable for papermaking processes under neutral and alkaline conditions.

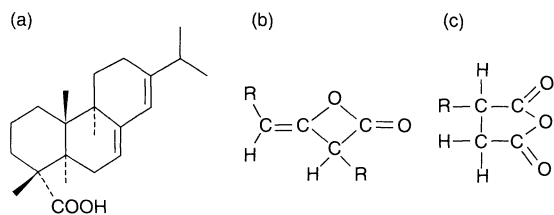


Figure 7.18. Chemical structures of: (a) abietic acid, which is one of the more common constituents of rosin; (b) alkyl ketene dimer (AKD), with $R = C_{14}-C_{18}$ (saturated or unsaturated); (c) alkenyl succinic anhydride (ASA) with $R = C_{14}-C_{18}$ (unsaturated)

4.2 Internal sizing sub-processes

The aim of internal sizing is to cover the paper surfaces with a strongly anchored monomolecular hydrophobic layer. Since most sizing agents are added in the form of emulsions/dispersions, this involves a number of steps before the individual sizing molecules can anchor at fibre and filler surfaces. The following principal steps can be identified as critical for the buildup of hydrophobicity during internal sizing:

- Retention of sizing agent at fibre and filler surfaces
- Spreading and redistribution of sizing agent over fibre and filler surfaces
- Anchoring of sizing agents with surface groups on fibres and fillers

Depending on the sizing system used, the importance of these different processes varies. Rosin soap sizes used together with alum as a retention aid in acidic papermaking processes have high melting points and do not extensively redistribute following the retention step. For these sizing agents, it is very important that the retention process results in a uniform distribution of rosin particles at the fibre surfaces and that the particle size is small in order to achieve a high sizing efficiency. So-called free rosin dispersions (with high fractions of free rosin acid) do, however, redistribute after the deposition step of the dispersed rosin particles/droplets. For these systems, the spreading and surface anchoring of individual size molecules during curing will also affect the outcome of the rosin sizing process. The same is true for synthetic sizing agents like AKD and ASA, which are often referred to as cellulose-reactive sizes. Note that the extent to which these molecules actually bond covalently to cellulose under papermaking conditions is rather unclear. Nevertheless, they do redistribute on fibres and filler surfaces and through this process the hydrophobicity of the fibre surfaces is increased. The mode in which redistribution occurs is also a matter of some debate, as will be discussed later in this section. All of the above-mentioned processes are indeed occurring after the size deposition/retention step. However, their respective importance in terms of the resulting sizing efficiency will vary depending on drying and storage conditions, molecular structure and the melting point of the sizing agent.

We will now give some illustrative examples of the importance of different surface chemistry related mechanisms for sizing, concentrating chiefly on AKD sizing, but also with a mention of some aspects of ASA and rosin sizing. In addition to sizing mechanisms, some useful techniques for measuring the surface chemical

properties of sized paper are also presented, together with a discussion of the implications for product performance. More extensive reviews on the subject of internal sizing can be found in refs (19, 20).

4.2.1 Retention of sizing agents

Cationic polyelectrolytes are generally used as retention aids for synthetic sizing agents such as AKD and ASA. In addition to their role as retention aids, these polyelectrolytes may also serve as a part or all of the emulsifying/stabilization system. The driving force for size retention at neutral and basic pH values is the electrostatic attraction, resulting in adsorption of positively charged (due to adsorption of, e.g. cationic starch or synthetic cationic polyelectrolytes) AKD particles at the negatively charged fibre surface. The charge character of the polyelectrolyte determines the electrophoretic mobility of the particles, as is demonstrated in Figure 7.19 (21). In this case, the cationic groups were tertiary amino groups for which deprotonation occurs at higher pH, which is clearly indicated by the decrease in their mobility. For particles stabilized by a polyelectrolyte quaternary amino group with constant charge, no change in mobility is expected over the same pH interval. It is worth noting, however, that other polymers and surfactants may be added to increase the stability of the size particles against homoflocculation. These and ionizable groups on the size molecule (see

below) may also influence the pH dependence of the electrophoretic mobility of the size particles. The pulp type is another important factor for the retention efficiency. It is well known that thermomechanical pulp (TMP) and waste ground-wood is difficult to size. This may be related to less effective retention, but can alternatively be due to slow surface spreading of size molecules or weak anchoring. Besides attractive electrostatic interactions, retention of size particles may also be promoted by charge neutralization and bridging phenomena, in particular in situations where the polyelectrolyte coverage on size particles and fibres is limited.

The traditional retention systems used for rosin sizes under acidic papermaking conditions differ to some extent from the systems used for synthetic sizing agents. Aluminium sulfate is generally used for retaining rosin soaps (and dispersed rosin emulsion droplets) at the fibre surfaces. Ferrous or ferric ions can also be efficient, but these are not used commercially. The role of the metal salts is effectively to impart a positive charge to the dispersed rosin particles, which then are retained on to the negatively charged fibre surfaces by attractive electrostatic interactions. Figure 7.20 shows the mobility of rosin particle–aluminium ion complexes at different pH values (22). Increasing the pH decreases the retention due to dissociation and deprotonation of the hydrated aluminium complex. Hydrated aluminium ion complexes are sufficiently polyvalent up to pH values of about 6 to efficiently recharge the surfaces of dispersed rosin ($pK_a \text{Al}(\text{H}_2\text{O})_6^{3+} = 4.9$). Retention is therefore usually relatively effective up to pH 6. Above this value, a noticeable decrease in retention is usually

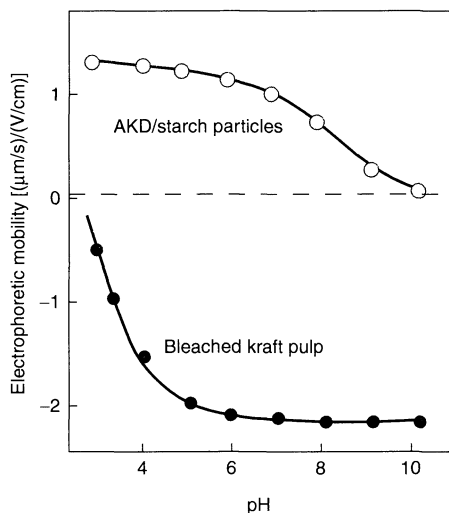


Figure 7.19. Electrophoretic mobility as a function of pH for AKD particles stabilized by cationic starch and for bleached kraft pulp. (Redrawn from ref. (21))

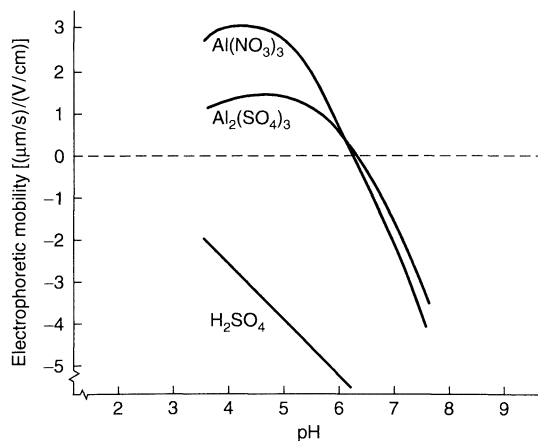


Figure 7.20. Electrophoretic mobility of rosin precipitate as a function of pH in the presence of $\text{Al}(\text{NO}_3)_3$, $\text{Al}_2(\text{SO}_4)_3$ and H_2SO_4 . (Redrawn from ref. (22))

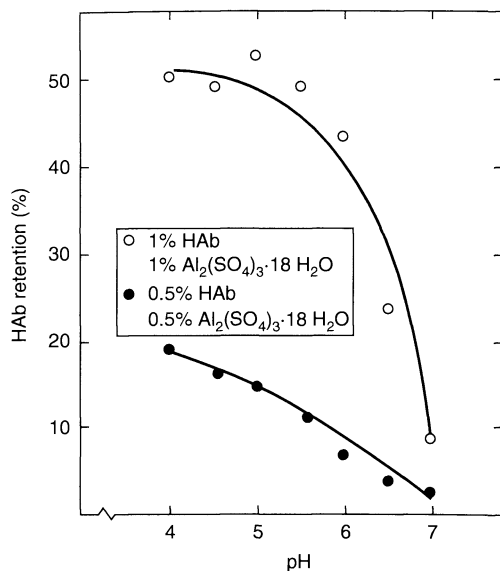


Figure 7.21. Retention of rosin precipitate (HAb) on bleached kraft pulp as a function of pH in deionized water with different additions of aluminium sulfate. (Redrawn from ref. (23))

observed, as shown in Figure 7.21 (23). Note that it is not sufficient that the retention in itself is efficient. A further requirement is that the rosin particles are well dispersed against homoflocculation and are thereby retained evenly on the fibre surfaces. Both the stability and the driving force for retention by heterocoagulation decreases with increasing salt concentration due to the screening of electrostatic interactions. Increasing ionic strength results in more effective screening of the double-layer forces. High concentrations of divalent anions are for the same reason more detrimental to the retention efficiency than monovalent anions. It is further observed that the stability of dilute rosin solutions results in less aggregation and hence in a more even surface coverage than retention from a more concentrated solution of rosin–aluminium hydroxide complexes.

It has been difficult to use rosin as a sizing agent at neutral and basic pH values, due partly to the relatively low pK_a value of the aluminium ion complex used for promoting retention. The substitution of aluminum sulfate by poly(aluminium chloride) (PAC) and organic polyelectrolytes has however extended the pH range in which rosin sizing is applicable. These are only a few of many different strategies for increasing the pH interval for rosin sizing which can be found in the literature (see, e.g. (19, 20)).

4.2.2 Redistribution of sizing agent on paper surfaces

Internal sizing agents are almost always added in the form of emulsions or dispersions. After retention at a surface, these will naturally only cover a limited area, given by the number density of particles/droplets at the surfaces and their respective areas. Potentially, however, the size content in these particles/droplets may spread at the surface and form a thin hydrophobic film, which then will cover a much greater surface area and thereby render the paper significantly more hydrophobic. The common view has been that after retention, AKD spreads in a wetting fashion to ultimately form a thin monomolecular film. A simple calculation shows that this would lead to a large increase of exposed hydrophobic area. One adsorbed AKD droplet/particle with a radius of, say, $0.1 \mu\text{m}$, covers an area of approximately $0.03 \mu\text{m}^2$. If the content of the same AKD droplet could spread into a monomolecular film with a thickness of about 10 \AA , the resulting hydrophobic area would be about $2.4 \mu\text{m}^2$, i.e. roughly 100 times larger. It is easy to understand that spreading would greatly benefit the sizing efficiency. However, the mechanism of spreading of sizing agents is not yet well understood. Potentially, there exist at least three likely routes for redistribution of sizing agent on the fibre surfaces:

- Wetting flow when the drop spreads to an equilibrium contact angle between 180 and 0° by surface tension forces.
- Surface diffusion of a monolayer from the foot of the macroscopic drop. The sizing agent in the macroscopic drop does not spread on the monolayer due to surface-ordering effects (an effect referred to as autophobicity).
- Gas-phase transfer of vaporized sizing agent followed by readsorption on paper surfaces.

The first mechanism, resulting in a monolayer coverage (i.e. complete wetting), has long been assumed to be the relevant one. However, recent studies have shown that AKD also does not form a zero contact angle when contacted with a relatively high-energy surface, such as silica or pure cellulose. Wetting does indeed occur, but results in non-zero contact angles. The reason for this behaviour is that a monomolecular film of surface-ordered sizing molecules spreads ahead of the macroscopic drop. The bulk liquid cannot spread on this film, due to surface ordering and preferential orientation of the hydrophobic groups towards air. The effect is commonly referred to as autophobicity. However, further spreading of sizing agents occurs by

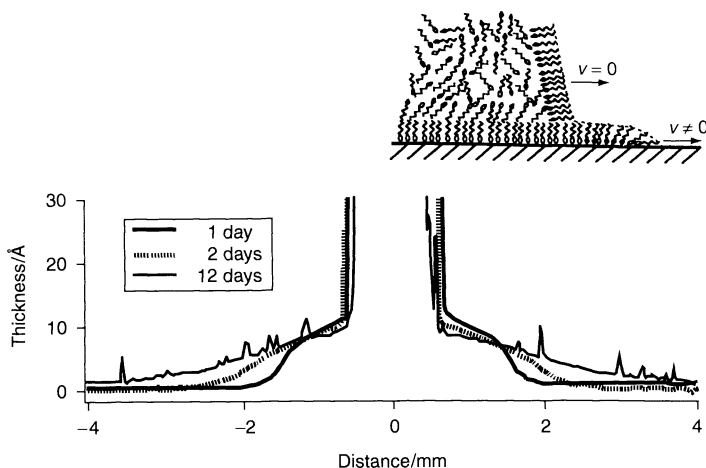


Figure 7.22. Laterally resolved ellipsometry profile showing an AKD precursor that spreads out from the foot of a macroscopic AKD drop (melting point $<10^{\circ}\text{C}$), which has been put in contact with a silica surface. The inset shows schematically the spreading of an autophobic precursor from the foot of the AKD droplet. (From ref. (24) with permission)

surface diffusion and spreading of the monolayer, as is clearly seen in Figure 7.22 (24). The apparent diffusion coefficient in the AKD monolayer is $\sim 10^{-11} \text{ m}^2/\text{s}$. This value was found to increase in proportion to the ambient temperature, whereas it decreased with the increasing melting point of the sizing agent. The relatively slow rate of monolayer spreading explains why, in practice, the sizing efficiency builds up with time during the storage of paper, as shown in Figure 7.23 (24). Attention has also been focused on the redistribution of sizing agent through a different mechanism, involving desorption, vapour diffusion, and readsorption (25). At temperatures above 80° , higher than usual storage temperatures in the paper rolls, this mechanism seems to play a role. However, if the tendency for readsorption is low, this can also cause de-sizing, which is seen for single paper sheets exposed to ambient air after long storage times in Figure 7.23 (24). Despite the importance of size redistribution through surface spreading, few fundamental studies have dealt with this issue and very little is indeed known for systems other than AKD.

In the case of ASA, it is clear that sizing develops much faster than with AKD. However, the reason for this has not yet been established. In the case of rosin, spreading is claimed for the dispersion type with high fractions of free rosin acids, as opposed to what occurs with the sodium soap particulate form. Little mechanistic information about the redistribution process is available for rosin sizes. Most likely, similar mechanisms are involved as in the case of AKD. Their respective importance will depend on the temperature,

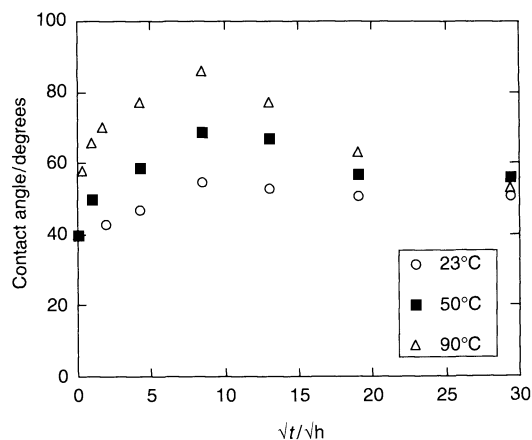


Figure 7.23. Influence of storage time and storage temperature on the hydrophobicity of bleached kraft pulp sized with 0.04 wt% AKD. The hydrophobicity is given in terms of advancing water contact angle recorded when the drop base expansion was first observed to stabilize. (From ref. (24) with permission)

melting points, vapour pressure, surface tension and other process conditions.

4.2.3 Reactions and side-reactions of sizing agents

The commonly claimed reaction mechanism for AKD is a direct covalent linkage with cellulose via β -keto

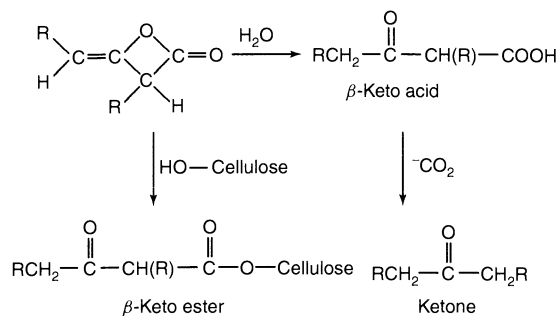


Figure 7.24. Proposed reactions of AKD with cellulose and hydrolysis in aqueous media

ester formation, as shown in Figure 7.24. The molecule can also be hydrolysed by water leading to a β -keto acid that will spontaneously transform to a ketone. The reactivity with cellulose under papermaking conditions is quite low and it is not clear to which extent AKD actually reacts with cellulose and other surface groups on papermaking fibres. There are many claims about reaction promoters and so forth, but their roles are unclear and promotion may well be related to improved retention. Despite the fact that AKD sizing research has a long history, the issue is still not resolved and remains under debate by researchers active in the paper chemistry field. In the case of AKD, the hydrolysis with water to form keto acids and subsequently ketones is also shown to have important implications for the sizing result. In particular, ketones are claimed to make paper slippery and difficult to handle in some operations. If AKD actually forms covalent linkages with cellulose, the competing ketone formation will also decrease the reaction efficiency with cellulose. Even if this is not the case and AKD is only physisorbed at the surface, the ketone formation may result in less efficient binding between the size molecules and the fibre surface. The fact that the ketone has a higher melting point than AKD is also noteworthy. This may, for instance, reduce the spreading tendency of the ketone on the paper surface, in comparison to AKD.

Alkenyl succinic anhydride (ASA) may also, like AKD, either react with cellulose hydroxyl groups or with water, as shown in Figure 7.25. Note that the side reaction of ASA leads to the formation of a dicarboxylic acid, which due to its amphiphilic nature can lower the surface tension of polar liquids, such as water, and thereby also decrease the sizing efficiency. The reactivity of ASA is claimed to be much higher than that of AKD and “full sizing” develops immediately in the paper machine, and suggests that covalent bonds

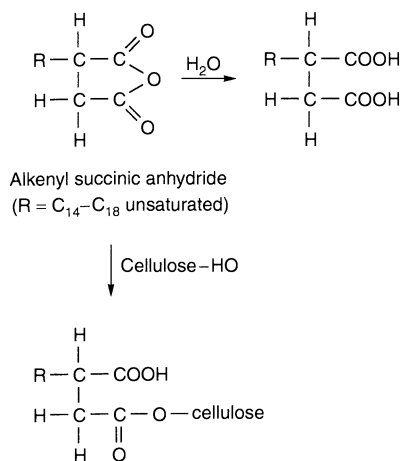


Figure 7.25. Proposed reactions of ASA with cellulose and hydrolysis in aqueous media

between sizing agents and fibre surfaces are more frequent in ASA-sized paper than for AKD-sized paper. The high reactivity of ASA necessitates on-site emulsification, using cationic starch as the stabilizing system. The surfactant nature and higher solubility of the dicarboxylic acid side product may affect the properties of the ASA emulsion. This may change emulsion stability criteria and also influence the surface charge of the emulsion droplets. This can further increase the accessibility of water and thereby also the rate of hydrolysis. The dicarboxylic acid by-product may also increase the paper wettability due to its surfactant nature.

4.2.4 Analysis of size content in paper

The sizing efficiency is commonly determined indirectly through various wetting and absorption measurements made on sized paper products. However, it is often preferable to quantify the amount of sizing agents retained in the paper. Furthermore, it is desirable to identify whether or not these are bound at papermaking surfaces and if they are non-reacted, reacted with fibre surfaces, or hydrolysed. This is usually done indirectly by extracting the paper in different steps and then analysing the liquid phase by gas chromatography or other analytical techniques. This is still the most common approach, but there are many questions unanswered regarding the specificity and efficiency of the extraction steps used in the different analyses employed. X-ray photoelectron spectroscopy (XPS) (discussed below in Section 8.1.1) is a straightforward technique with the

capacity to give quantitative information on the content of a surface-spread sizing agent in a sheet. However, it cannot be used to determine if the sizing agent is in its natural, surface-reacted or hydrolysed state. For this purpose, time-of-flight secondary ion mass spectrometry (ToF-SIMS) seems to be a good candidate, as described below in Section 8.1.2. This technique can also provide information about the in-plane distribution of sizing agents, but does not provide quantitative information such as that obtained by XPS.

5 DRY AND WET STRENGTH OF PAPER

5.1 Dry strength

The dry strength of paper relates strongly to the distribution of fibres and bonds (controlled by the formation process) and the mechanical properties of the fibres. Surface chemistry plays the main role in the development and strength of fibre–fibre bonds. Fibres are often chemically and/or mechanically refined to increase bond areas and strength. This is not always desired since it may slow down drainage and decrease the paper porosity, which may result in loss of bulk, and detrimentally affect stiffness, tearing resistance and opacity.

A different strategy is to add dry-strength additives, which basically are hydrophilic polymers. To be efficient, these must be adsorbed or retended at fibre (and filler) surfaces. The effective driving forces for adsorption/retention in aqueous solutions are, as discussed previously, hydrophobic and electrostatic interactions. Ionic exchange and the concomitant increase in the counterion entropy play an important role in the latter case. Considering the above, it is easily understood that dry-strength agents frequently are charged (like cationic starch, gums, polyacrylamide and its copolymers) or have some hydrophobic substitutions. The optimum character of the agent depends on the chemical nature of the fibre surfaces under process conditions, which may vary strongly from system to system. In the case of anionic dry-strength agents, alum or some similarly adsorption-mediating cationic polymer may be added. Hydrogen bonds and van der Waals interactions are believed to be responsible for the adsorption of dry-strength agents. In an aqueous environment, however, this interaction can only help by reducing the cost of displacing surface-bound water; van der Waals interactions are, for the system discussed, simply too small to be of importance.

The question now arises as to how the surface adsorbed dry-strength agent fulfils its task of enhancing the inter-fibre bond strength. This can be attributed to two basic mechanisms, or a combination thereof:

- An adsorbed layer of dry-strength agents can act to smoothen the fibre and filler surfaces, e.g. fill existing inter-fibre cavities or those arising in the drying phase, thereby increasing the real area of inter-fibre contact.
- By increasing the surface energy of the fibre surfaces, the hydrogen-bonding ability, and also allowing increased intermingling of surface-bonded polymer chains, hydrophilic dry-strength agents will also strengthen inter-fibre bonds.

During drying, the capillary force acts to effectively attract the surfaces between hydrophilic fibres and thereby reshape and increase the real area of contact. This phase may naturally also be modified by the presence of interfacial layers of hydrophilic dry-strength agents. Secondary effects related to the viscoelastic properties of the inter-fibre joints can also have a large impact on paper strength properties. More details on the subject of dry-strength of paper and strength additives can be found in ref. (26).

5.2 Wet strength

Dry strength can be augmented by hydrophilic polymers, which enhance the effective bonding area, surface energy and/or hydrogen-bonding ability. Since water is a very strong structure breaker of hydrogen bonds, a completely different strategy must be employed in order to enhance paper wet strength.

In principle this may be carried out by the following (see refs (2, 27) for details):

- Increasing the fibre surface hydrophobicity, thus relying on the attraction between hydrophobic surfaces in water.
- Cross-linking of fibres by use of polymerizable wet-strength resins such as urea–formaldehyde, melamine–formaldehyde and polymeric amine–epichlorohydrin resin systems.
- Hydrophobization and cross-linking of fibre surfaces by use of cationic latexes.

Increasing the surface hydrophobicity is generally not a successful strategy since this will inflict on the dry-strength properties. Cross-linking using polymerizable resins is the method currently used for increasing the wet-strength properties of, e.g. tissue and towelling,

linerboard and carton. Two mechanisms are proposed for explaining the wet-strength development. The protection theory proposes that the additive forms a restraining three-dimensional network, which also protects hydrogen bonds from water exposure. The restraining three-dimensional network model seems plausible, but the protection of hydrogen binding inter-fibre areas seems unlikely since water penetrates rather quickly through the fibres. The reinforcement theory suggests the formation of covalent fibre–fibre bonds. The real reason behind wet-strength development is likely to be a combination of the two. Whatever the right answer is, it is clear that it involves formation of new covalent bonds.

Recently, it has been suggested and shown that cationic latexes can increase the dry strength. Such systems can, due to the size of the latex particles, probably form new fibre–fibre bridges while still allowing the fibre–fibre bonds necessary for dry strength to develop. If applied after the sheet is formed in, for instance, a surface-sizing step, latexes may introduce new bonds between the fibres, and in conjunction with spreading partially protect bonding areas necessary for dry strength.

Besides being important for the strength of paper, wet-strength agents can also increase the absorbency of paper. The reason for this is that fibre-swelling phenomena in the absence of wet-strength agents can hinder penetration and lead to a collapse of the three-dimensional structure of the sheet.

6 SURFACE TREATMENT OF PAPER

6.1 Why coat paper?

For some paper grades, such as most newsprint stock, it is possible to print directly on the fibre surface and attain acceptable performance outcomes for the given product requirements. In many cases, however, demands are placed on the final product (such as glossy magazine grades) which require a coating layer to be deposited on the base paper surface to achieve acceptable optical and printability outcomes. (Even in cases where this is not done, significant additions and treatments, such as filler inclusion in the base paper, or supercalendering, are required.) This section deals mainly with paper coating as it is “traditionally” defined: the application of a thin layer (of the order of 10 μm), consisting mainly of mineral (sometimes plastic) pigments and binders, to one or both sides of the paper surface. Again, we focus on the surface chemical aspects of this process and its consequences for product performance.

Viewed generally, the coating of paper is, as Lepoutre (28) noted, carried out for “aesthetic reasons”. As these reasons include improving smoothness, optical properties (brightness, opacity, etc.) and printability, this is a clear case where aesthetic and commercial considerations are in harmony. Indeed, it is consumer demand based on heightened expectations of performance in these areas that largely drives improvements in technology and further research into the surface treatment of paper. An added factor in more recent times has been the market desire for multi-purpose grades, which can, e.g. be used both in ink-jet printers and photocopiers. This places a high demand on the surface treatment in terms of a number of key factors where surface chemistry plays a role: surface energy, surface and sub-surface structure, and rheology and consolidation of the coating during application. In many respects, an optimal solution is still under development. That these factors also are significant to one extent or another (depending on the grade and usage) for more conventional single-purpose coated papers is further reason still to develop a good understanding of the underlying physico-chemical mechanisms which play a significant role in controlling coating performance.

It is important to bear in mind the conditions in the coater unit and in particular the coater “nip”. A good review has been provided by Brander and Thorn (29). For our purposes here, it is sufficient to note that modern paper coating processes have exceedingly high technical demands: modern units run at over 1500 m/min and must produce a uniform 10 μm layer from a suspension which arrives at the blade or roll at up to 70% solids content. Blade coating, the most common implementation of the process, imposes shear rates of the order of 10⁶ s⁻¹. Because of the very short residence times at the blade/roll, the coating process is therefore a *low-deformation*, but *high-deformation-rate* process.

The coating “colour” itself is a multi-component colloidal suspension designed to achieve the target properties of the final coating layer and also run well in the coater under the extreme conditions discussed above. Achieving these aims requires some finesse in colloidal engineering. The 50–70% solids component of the colour consists of pigments, binders, dispersants, thickeners or rheology modifiers, and other additives such as fluorescence brighteners and antifoaming agents. Surface chemistry plays a significant role in the coating process, namely through stabilization of the suspension, and meeting the broad range of rheological demands during pumping to, and application at, the coating unit. In addition, the manner in which the applied layer dewateres, immobilizes and adheres to the base

sheet, and thus ultimately the performance of the dry coating layer, are areas where surface chemistry plays a significant role.

6.2 Coating components

6.2.1 Pigments

A variety of pigments are employed in coatings, with the most common being clay (chiefly kaolin) and calcium carbonate (usually ground mineral calcite, but with an increasing use of precipitated varieties). It is therefore worthwhile noting some basic properties of these two materials.

Kaolin

Clays are aluminosilicates, built up of two-dimensional arrays of silica and alumina in layers, with hydrogen bonds providing a strong inter-layer adhesion. Kaolinite is one of the more common varieties (bentonite and other clay types are also used in paper coatings). The layered sub-structure imbues an extremely high aspect ratio on the kaolinite particles: they are plate-like in nature. At the edges, the silica and alumina layers are disrupted and an oxide-like surface is produced, being typically sensitive to pH variations. Above pH 7, the surface is overall negatively charged, and below this pH it is positively charged. The basal planes, on the other hand, retain their overall negative charge across a broad range of pH values, with the likely cause being the presence of silanol groups.

Calcium carbonate

Calcium pigments are either derived from the processing of mineral limestone (ground calcium carbonate (GCC)) or from precipitation (precipitated calcium carbonate (PCC)). GCC, usually calcite, tends to have a more isotropic, but also more irregular, shape than clay, whereas PCC can indeed be produced in needle-like shapes ("rosettes"). The surface properties of CaCO_3 in solution are quite complex, due mainly to the fact that both Ca^{2+} and CO_3^{2-} are released in water, and this in turn leads to a dependence of the surface charge on the particle concentration. For GCC, a charge reversal (negative to positive) occurs at particle concentrations greater than about 2.5 wt%.

6.2.2 Dispersants

The classical DLVO picture of colloidal forces, whereby typically repulsive electrostatic forces are balanced by typically attractive dispersion forces, are insufficient in themselves to properly disperse coating pigments under typical conditions of pH and salt concentration. The repulsive electrostatic barrier will be insufficient to inhibit diffusion-initiated coagulation, resulting in strongly bound agglomerates, and the suspension being rendered of no use. Indeed, pigment dispersal needs to be finely tuned just to avoid less drastic situations where isolated agglomerates cause runnability problems at the coating unit, or lead to defects or tears in the final product. Dispersion is achieved through the addition of suitable polyelectrolytes, commonly polyacrylates or polyphosphates, into the colour.

Järnström (30) demonstrates how optimization of the dosage of sodium polyacrylate (NaPA), can be achieved by investigating the viscosity of GCC suspensions dispersed with NaPA. The minimum in the viscosity as a function of dispersant dose gives an indication of where flocculated structures have best been prevented and the particles stabilized. It was seen that for suspensions of approximately 55 wt% of pigment, an NaPA dose of approximately 0.5 parts per hundred (pph) optimized the viscosity, as shown in Figure 7.26 (30). Given that at these pigment concentrations the surface charge of GCC is expected to be positive, electrostatic adsorption of NaPA occurs. A point of interest is that this same author observed that NaPA adsorption to GCC is maximized at a dosage of about 0.12 pph, followed by plateaux for higher dosages. Thus, optimal stabilization cannot be explained by an adsorption mechanism alone. This author's interpretation is related to the fact that NaPA

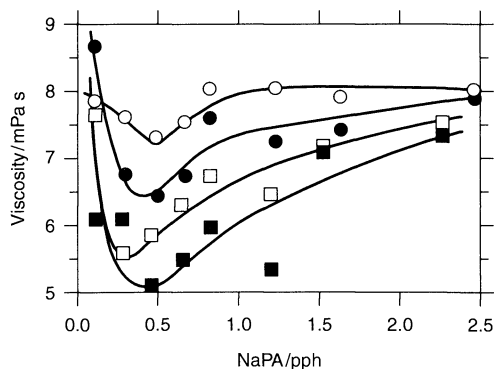


Figure 7.26. Viscosity versus polymer concentration curves, which can be used in the optimization of the dispersant dose. (From ref. (30) with permission)

induces a dissolution of Ca^{2+} ions from the pigments, which then complex with the NaPA. However, as the NaPA dose is increased, the number of bound Ca^{2+} ions per NaPA monomer effectively decreases, thus leading to a greater overall net negative charge, and improved dispersion. Hence the optimal dose is related not only to NaPA adsorption, but also to a reduction of bound Ca^{2+} per monomer of dispersant.

6.2.3 Thickeners and rheology modifiers

CMC compared to synthetic associative thickeners

Clearly, control of rheological properties of coating colours is desirable, and this is achieved through polymeric additives. The aim is not only to favourably adjust the viscosity and other rheological parameters of the suspension *per se*, but also to improve the water retention properties of the colour. If the suspension dewaters too quickly before or on application, this can lead to severe runnability problems, such as the formation of streaks, dry “stalagmites” and uneven binder distribution.

The most common of these polymeric additives (thickeners, “co-binders”) is carboxymethylcellulose (CMC), a cellulose derivative (29). Different grades may be produced from chemical substitution of hydroxyl groups. The main thickening mechanism is through entanglement formation in the aqueous phase. While there may be some effect of adsorption on to pigments, Järnström *et al.* (31) showed that this can be strongly hindered by the presence of NaPA dispersant for clay-based colours, through a competitive adsorption. Similarly, Fadat *et al.* (32) showed that CMC does not adsorb at all to the other major particulate component in most colours, i.e. the latex binder.

A relatively recent development has been the use of associative thickeners, which had their origin in the paint industry. A review of the varieties available has been provided by Hawe (33). Generally speaking, they often involve a repeat sequence of hydrophilic and hydrophobic groups, sometimes with pendant surfactant side groups. Examples of these are emulsion copolymers, swellable emulsions and “true” associative thickeners, such as alkali-activated associative thickeners. These polymers do more than just increase the viscosity of the background solution – they form networks, usually with the latex binder particles and with each other, through selective adsorption of hydrophobic groups, or even micellization of the surfactant side chains. Clearly, the system so formed is rheologically more complex than that created by conventional thickeners. Fadat (34) elegantly showed this by comparing

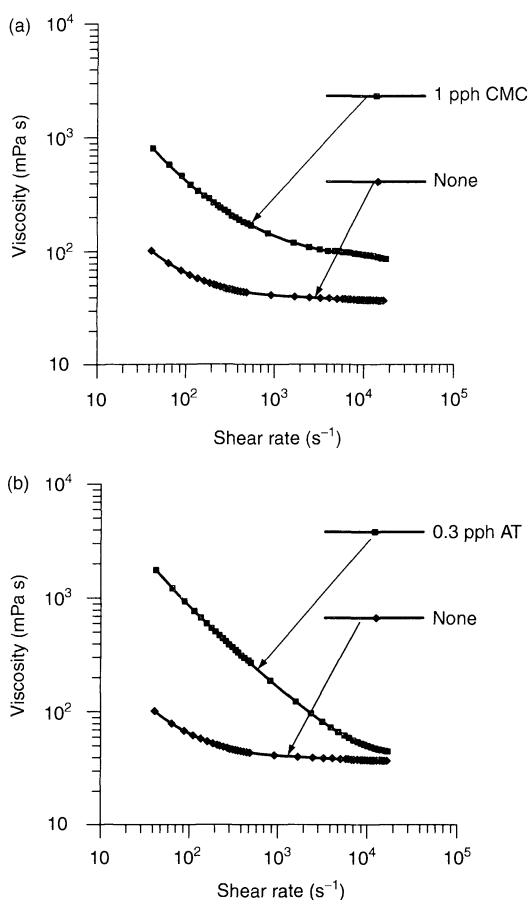


Figure 7.27. A comparison of the effects on the shear-thinning behaviour of a coating colour containing clay, calcium carbonate and styrene–butadiene binder of (a) CMC and (b) associative thickener (AT). (redrawn from ref. (34))

the viscosities of two colours, identical in all respects other than one having CMC as a co-binder and the other an associative thickener, over a broad shear-rate range of 10–10⁶ s⁻¹, and then compared both of these with the same colour without co-binder. The viscosity increased in both cases compared to the co-binder-free system (indicating desirable improved water retention); however, at higher shear rates the networks formed by the associative thickener were broken down, and a more pronounced shear-thinning effect was observed. On the other hand, the more simple “background viscosity” nature of the CMC co-binder manifested itself: it simply shifted the entire thickener-free curve to higher viscosity. This is demonstrated in Figure 7.27 (34). Clearly, associative thickeners may provide a useful means for tuning coating rheology in desirable ways. Co-binders

of all types have a real effect on coating viscoelasticity and thereby runnability. Adolfsson *et al.* (35) showed that increasing the amount of CMC in a clay coating had an effect on the relaxation time as measured by stress experiments, which in turn had a strong correlation to the width of a streak deliberately introduced into the wet coating layer.

6.2.4 Starches as co-binders

Starches are very common natural products heavily used by the paper and other industries (29). In paper coatings, they are used as both binders and co-binders (thickeners). They naturally occur in two fractions, namely linear amylose and branched amylopectin, with usually the latter being the more abundant. Modification may be performed in numerous ways (29) in order to provide desirable physico-chemical properties, tailored to usage. For example, it is possible to cationically modify starch by using cationization reagents at high pH, in order to produce starches suitable as pigment binders. Nonionic, oxidized, anionic, amphoteric, hydrophobically modified, and other starch variants may also be produced.

These possibilities, and the two basic starch fractions, allow for interesting behaviour when starch is used as a co-binder. Husband (36) has shown that adsorbing anionic (phosphate ester) starches on to clay does not reveal fractionation, i.e. amylose and amylopectin are adsorbed with no preference, although the introduction of NaPA reduces starch adsorption due to competitive effects, similar to the behaviour of CMC. However, for non-ionic starch (hydroxyethylated), there was significant fractionation of adsorption, with amylose being preferred. No sensitivity was shown with respect to NaPA. Furthermore, the system where both fractions equally absorbed seemed to flocculate at high starch doses. This author suggested that this may be due to size exclusion effects and therefore a depletion mechanism. It is interesting to note the consequence for system viscoelasticity, with the flocculating system clearly demonstrating a more elastic nature.

6.2.5 Binders

As mentioned previously, starches may be used as binders. More common are latex particles, spheres of 0.1–0.3 μm produced by emulsion polymerization. They are thermoplastic in nature and may be derived from a variety of monomers, i.e. styrene–butadiene, styrene–acrylate and vinyl acetate–acrylate. They are

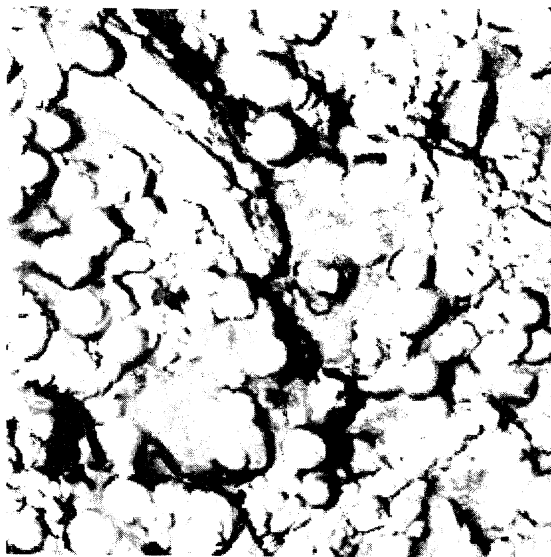


Figure 7.28. An AFM image of a clay-based coating layer. Latex binders and clay particles are clearly visible. (Micrograph supplied by courtesy of R. Seppänen)

stabilized in water either with grafted surfactant or ionic surface groups.

An important feature during drying is that the latex has film-forming capabilities. The latex particles deform and are drawn together through capillary forces, as the solids content and temperature increases in the drier unit. Furthermore, the particles adhere to the pigment and thereby bind them to the substrate and to one another, so forming a consolidated layer. Atomic force microscopy (AFM) images provide useful information as to the state of latex binder in the final coated layer, as shown in the image presented in Figure 7.28.

6.3 Rheology

6.3.1 Steady shear

As stated above, coating rheology is of utmost importance for runnability. It will, to a large extent, determine pressure changes and forces at the blade/roll, and the relaxation of the colour after its brief residence in the coating head. Moreover, we can use rheological measurements as a tool to investigate interactions in coating suspensions and thus engineer desired outcomes. From a rheological point of view, coating colours are highly non-trivial in nature, displaying a complicated rheological response to external stresses, as is

typical of highly concentrated particulate suspensions. An excellent reference for those new to the rheology of complex fluids is the text by Larson (37).

The nature of shear stresses in the coating process, including the delivery to the coating head, application at the nip, and the drying stage, are extremely complex. Laboratory methods must be judiciously chosen in order to either mimic these conditions as best as possible so as to evaluate performance in a controlled manner, or alternatively provide other information regarding coating microstructure which can then be “fine-tuned”. In the latter category are low shear-rate measurements in laboratory rheometers based on cell geometries such as the cone–plate, plate–plate or concentric cylinders, employing controlled shear or controlled stress mechanisms, and also capillary viscometers. The latter in turn are also used to make high-shear-rate devices, where the suspension is driven into the capillary under pressure. Alternatively, some pressure-driven devices use slit geometries in order to simulate the blade coater.

Coating colours, as one would expect from their composition, are in general non-Newtonian fluids, so that the steady-shear viscosity $\eta(\dot{\gamma})$ is shear rate-dependent, for a given shear stress σ :

$$\eta(\dot{\gamma}) = \sigma \dot{\gamma} \quad (7.10)$$

This is not simply because of the presence of rheology modifiers or other polymers; a simple NaPA-stabilized GCC suspension will also show a plastic-like behaviour. Typically, this involves the suspension behaving like a solid at low shear rates and stresses, and only “yielding” to liquid-like behaviour above a certain yield stress σ_y . This behaviour can be modelled in various ways, with two common ones being the Bingham:

$$\sigma = \sigma_y + \eta_{pl} \dot{\gamma} \quad (7.11)$$

and the Casson:

$$\sigma^{1/2} = \sigma_y^{1/2} + \eta_{pl}^{1/2} \dot{\gamma}^{1/2} \quad (7.12)$$

models, where η_{pl} is the plastic viscosity.

For such materials, the steady-shear viscosity decreases with increasing shear rate, $\dot{\gamma}$. This is known as “shear-thinning” and is in itself a vitally important feature for the coating process: without shear thinning, coating colours would be difficult to handle at low shear (i.e. pouring or pumping) and would have severe runnability problems at the high shear rates present at the coater. Shear thinning can be understood in terms of the formation of layers of particles (layered in the flow direction) in the sheared suspension; in other words, shearing induces a suspension structure which reduces resistance to further shearing. An elegant example of this was in fact shown with clay particles sheared in a cuvette cell and examined by neutron scattering, whereby the suspension microstructure can be inferred (38), as shown in Figure 7.29. Indeed, increasing shear rate indicated the breakdown of clay particle “domains” and the formation of conveniently oriented layers as $\dot{\gamma}$ was increased. While this is conceptually appealing for plate-like clays, it also occurs for other particles (such as GCC). An important quantity in the consideration of phenomena such as shear thinning is the *Peclet number*, $Pe = a^2 \dot{\gamma} / D_0$, where a is the mean particle radius and D_0 the diffusion constant. Essentially, the shear rate must be such that the particles do not have time to diffuse back to their equilibrium mean positions, so that shear thinning is expected when $Pe \geq 1$. The opposite effect, shear thickening, is speculated to be, conversely, the result of the induction of an increasingly unfavourable suspension structure with increasing shear rate. This may occur, for example, when the layers induced through shear thinning are broken up at higher shear rates. Clearly, shear thickening can cause severe runnability problems in the coating process if it occurs at unfavourable shear rates. The characteristic behaviour of non-Newtonian fluids is illustrated in Figure 7.30. Indeed, similar particles, but with different size distributions, can behave very differently in the same shear-rate interval (the appearance of the radius a in the expression for Pe

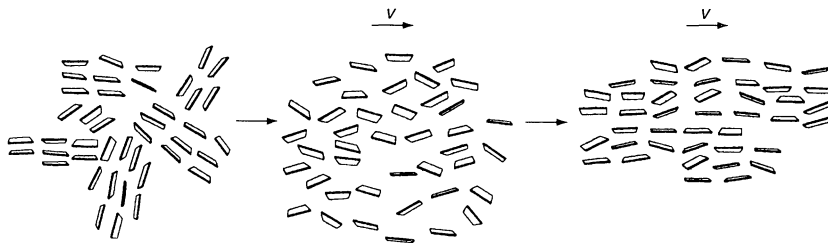


Figure 7.29. Schematic representation of shear thinning of clay particles. (Taken from ref. (38))

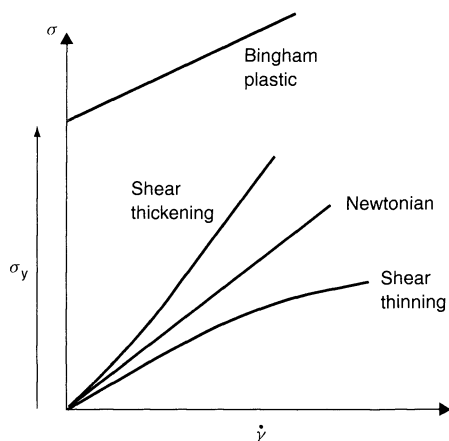


Figure 7.30. Generic rheological behaviour of non-Newtonian fluids – shear stress versus shear rate

could indicate why). However, this might be used to advantage: Alince and Lepoutre (39) showed how two GCC populations, one shear thickening and the other shear thinning, might be combined to give, remarkably, a nearly Newtonian suspension of relatively low viscosity. (It should be remarked, however, that this may not be a general phenomenon, and also difficult to implement in practice.)

An important property from both a bulk rheological and microstructural point of view is the relative plastic viscosity:

$$\eta_r = \eta_{pl}/\eta_0 \quad (7.13)$$

where η_0 is the viscosity of the liquid phase, which depends on the volume fraction of solids ϕ . A number of semi-empirical models exist, one being the *Krieger–Dougherty (KG) equation*, which accounts for viscosity increases with ϕ through a mean-field approximation, while accounting for the divergence in η_r at the maximum packing fraction η_m empirically, as follows:

$$\eta_r = \left(1 - \frac{\phi}{\phi_m}\right)^{-[\eta]\phi_m} \quad (7.14)$$

where $[\eta]$ is the *intrinsic viscosity* (or shape factor) of the particles. An example of such a plot is given in Figure 7.31. Not only do plots of η_r against ϕ give important information about viscosity increases with solids content, but they can also be used to investigate structure formation in particulate suspensions. If flocculation has been induced in the system, such as through the introduction of salt or through a polymeric mechanism, then the impact upon the viscosity of these flocs may be inferred by the replacement $\phi \rightarrow \phi_f$ in the KG

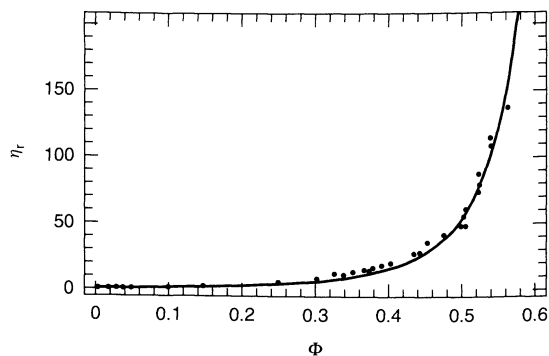


Figure 7.31. Volume-fraction dependence of relative viscosity for a suspension of calcium carbonate dispersed with NaPA

equation, where ϕ_f is the volume fraction of flocs. This leads to the definition of a *flocculation index*, as follows:

$$C_f = \phi_f/\phi \quad (7.15)$$

which characterizes the extent of flocculation in the system.

6.3.2 Viscoelasticity

An alternative to a steady-shear measurement is oscillatory shear, described in the linear regime by the following:

$$\sigma(t) = \gamma_0 [G'(\omega) \sin(\omega t) + G''(\omega) \cos(\omega t)] \quad (7.16)$$

where the sample is sheared at an oscillatory frequency ω and strain amplitude γ_0 , and the *storage modulus* G' and *loss modulus* G'' respectively indicate the degree of elastic response to, and viscous dissipation of, the time-dependent shear stress $\sigma(t)$. This type of measurement is useful because it can indicate the nature of relaxation processes acting with the suspension, through the *Deborah number*, given by the following:

$$De = \tau \omega \quad (7.17)$$

where τ is a characteristic relaxation time. As ω is increased, the elastic nature of suspensions often decreases and the viscous nature increases. The suspensions start to behave more like fluids. Note that increasing ω is akin to reducing an “impulse time”. If G' and G'' cross over at a given ω , then that may indicate a value of τ , the shortest time-scale on which restoring forces act in the system.

Coating colours do indeed show viscoelastic behaviour; however, estimating τ for such materials is

not straightforward, as relaxation processes appear to occur on many time-scales, and the G' and G'' moduli rarely cross over. Triantafillopoulos (40) has reviewed viscoelasticity in paper coatings. He suggested that a more straightforward method may be to determine the time it takes for the shear modulus to drop to a predetermined value. Such measurements by several authors indicate that $0.1 \leq \tau \leq 1$ ms, and since in practice the impulse time at the nip is of the order of 10^{-5} s, we can assume that for coating colours, $De \gg 1$. The consequence of this is that coatings may behave more like elastic solids than fluids at the blade. Furthermore, large values of G' indicate that there may be insufficient time for the colour to relax at the nip, so that coating thickness is affected by elasticity; in addition, partial recovery before drying may preserve non-uniformities and defects.

A useful manner in which to quantify the relative contributions of elastic and viscous effects is through the *loss angle* δ , as follows:

$$\tan \delta = G'/G'' \quad (7.18)$$

with larger values of δ indicating a relatively more viscous, as opposed to elastic, material. One neat conclusion that can be drawn from such an analysis (40) is that GCC coatings are generally more viscous in character than their relatively elastic clay counterparts; this again may well be an indication of the role of particle morphology in determining the rheological properties. The elastic nature of clay suspensions could be related to the domain formation alluded to previously, or indeed the often-postulated "house-of-cards" structure which may form at low pH values. In practice, this viscoelastic information may well indicate why clay and carbonate-based coatings can have quite different responses to the impulse at the coating nip under the same mechanical conditions.

6.4 Dewatering

As mentioned previously, the dewatering process is vital to the structure of the final coated layer. Understanding the mechanisms at play in the dewatering step is a challenging task. Indeed, a debate has developed (41, 42) as to the exact mechanisms at work, especially during blade coating. The question has arisen as to whether dewatering proceeds as a thickening mechanism, whereby a vertical concentration gradient is formed in the coating layer, or as to whether a distinct immobilized layer is established with a fixed concentration (FCC, the first critical concentration) forming a filter cake through

which the supernatant bulk coating dewaters through a filtration mechanism. If the latter is true, then the fluid flux q should obey Darcy's law, given by the following:

$$q = -\frac{k(\phi)}{\eta} \nabla P \quad (7.19)$$

where η is the liquid viscosity and ∇P is the pressure gradient, and where the solids volume fraction, ϕ -dependent permeability $k(\phi)$ is given by the Kozeny-Carman relationship:

$$k(\phi) = \frac{(1 - \phi)^3}{CS^2\phi^2} \quad (7.20)$$

with C a constant and S the average surface area of the particles forming the consolidated bed.

Interestingly, the resolution may be somewhat of a compromise. Recently, Lohmander *et al.* (41) investigated the pressure filtration of a model monodisperse polystyrene sphere system. By using conventional filtration methods, as well as magnetic resonance imaging, these authors observed a filter cake with a near-linear density gradient reducing to the bulk concentration at a fixed height, and were able to modify the existing models for filtration through porous beds to account for this compressible layer.

In practice, dewatering is a complex process. Sandås and Salminen (43) have evaluated different co-binders and their effects on dewatering and suspension viscosity and attempted to correlate to runnability. These authors noted that starch, with good water retention, has excellent runnability, even with relatively high viscosity. On the other hand, poly (vinyl alcohol) (PVOH) performed poorly because of high viscosity, whereas some synthetic thickeners also did so because of poor water retention.

6.5 Surface sizing and barrier coatings

The majority of the discussion in this section on surface treatment has dealt with traditional pigment-based coatings, which are chiefly designed to improve the optical, smoothness and printability properties of paper. Another major function of surface treatment is to heighten the liquid and gas resistance of the base sheet. A classic example of this is liquid packaging board, where the requirements for the resistance of the substrate to liquids are extremely high. A *barrier dispersion coating*, meaning a non-porous polymeric film, is applied to the base sheet in such cases. In related applications, *surface sizing* is used as an alternative or

complement to *internal sizing*, which has been discussed extensively above in Section 4. Surface sizing most often refers to a system consisting of a transport medium and strengthening agent (often starches) along with hydrophobizing agents (alkyl ketene dimers, rosins, etc.). Furthermore, pigments may in some cases be added at a low solids content (compared to a full-weight traditional coating) in order to improve the optical or surface properties. Alternatively, surface sizing can be used as a surface “pre-treatment” before another coating step, for example in order to improve the coating “hold-out” (resistance to penetration of the coating layer into the base sheet). With film-forming starches and synthetic hydrophobizing agents which produce highly resistive layers, the distinction between surface sizing and barrier coating begins to blur significantly, and the question is more of how to achieve, in practice, the best result for given demands in a specific situation. Here, we present a brief overview of the surface sizing and barrier coating processes. An extensive account is available in the text edited by Brander and Thorn (29).

6.5.1 Surface sizing

The traditional method of application of the sizing to the sheet is through the “size press”, whereby two rolls are pressed together to form a nip, and the paper sheet fed through a pond of sizing liquid. An important issue in this regard with respect to runnability is “misting”, whereby droplets form after the sizing is applied and the paper moves away from the nip. These drops then deposit on the surface, hence causing an uneven appearance and poor printability. A related effect is “orange-peel”, where small pockets are formed on the surface. These complex problems are due to film-splitting and filament formation in the part of the sizing layer that is not immobilized on the sheet directly after application. A good account is given in the paper by Roper *et al.* (44). It has been speculated that the underlying cause for this is essentially due to a cavitation process. The normal pressure profile across the nip is such that a local minimum is achieved inside the wet layer, and if this is below the vapour pressure for the fluid, splitting can then occur. Moreover, the problem can be adversely affected by the presence of surface-active material, such as surfactants from latex pigments, which will lower the energy of surface formation by a lowering of the surface tension of the liquid–air interface, and thus increase the tendency for cavitation. Once the interface is formed, the adsorption kinetics of surface-active material will play a role in as to

whether the cavity can be healed, or whether it persists and grows. A further factor is that the sizing fluid is viscoelastic in nature and has a complex *elongational rheology*, that is its response to longitudinal stresses (pure stretching). At the nip exit, the sizing layer experiences both shear and elongational stresses. A further factor at hand is the relaxation of the layer and its ability to heal pocket cavities and to level drops after the nip, which again are reliant upon the viscoelastic character of the sizing liquid, in a broadly similar fashion to that of traditional coatings. The overall problem of misting and orange-peel is at least in some significant part surface chemical in nature; however, a complete understanding (and control) of it is yet to be achieved.

6.5.2 Barrier coatings

The film press has been tested in the application of polymeric (predominantly polyethylene) barrier coatings, and issues such as misting and film splitting indeed arise to an extent where more reliable methods, such as blade or roll coating, are still used. The critical step in achieving a barrier coating layer which effectively seals the surface and has good uniformity is the film formation step. This is traditionally viewed as a step-wise process whereby a particle consolidation process is followed by coalescence of the polymer particles and finally interdiffusion of polymer chains from particles in contact. A schematic diagram of this process is shown in Figure 7.32. The underlying physico-chemical mechanisms, however, are complex, thus providing a challenge in attempts to control the process. The coalescence step can be very crudely described by a DLVO-type picture of interparticle forces. While this is hardly sufficient in realistic situations, it is true to say that schematically a DLVO-type pair particle potential applies and a repulsive barrier must be overcome in order for the particles to come into close enough contact for interdigitation of individual polymer chains to occur. Once in contact, particle deformability is critical for allowing the intermingling of polymer chains. Ideally, the process therefore is one of delivering the coating as a dispersion of (semi)hard spheres and then controlling the evaporation and consolidation, chiefly through the drying temperature, so that the film may form sufficiently before the coating has levelled and set. Other factors that need to be considered are the temperature-dependence of the viscoelastic properties of the dispersion, since this will affect the ability of the particles to deform once they have coalesced. On the other hand, evaporation will lead to cavitation of the liquid between the particles and thus

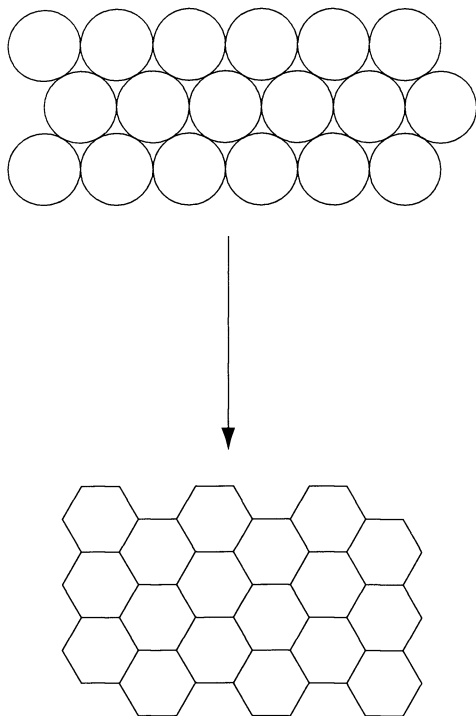


Figure 7.32. Schematic representation of the film-formation process

an enhanced driving force for coalescence due to an attractive capillary force.

7 WETTABILITY AND ABSORBENCY OF PAPER

Paper wettability studies are very often undertaken when optimizing paper properties with regards to the requirements set by converting and end use. Polymer lamination, gluing and printing are typical converting operations which set high demands on the wetting and surface energy characteristics of paper. Environmental concerns and regulations pushing the industry from traditional solvent-based formulations to more environmentally friendly aqueous-based systems stress the importance of wetting control.

7.1 Basic concepts

Spontaneous spreading of a liquid on a solid occurs only if the free energy of the system decreases during this

process. The wetting tendency of a liquid in contact with a solid is reflected by the initial spreading coefficient, as follows:

$$\begin{aligned} S &\equiv -\Delta G_s/A \\ &= \gamma_{so} - \gamma - \gamma_{sl} \end{aligned} \quad (7.21)$$

where ΔG_s is the free energy change due to spreading; γ_{so} , γ_{sl} and $\gamma (= \gamma_{lv})$ denote the interfacial free energies per unit areas (surface tensions) of the solid–air, solid–liquid and liquid–vapour interfaces, respectively. A liquid drop will completely wet the solid surface when $S \geq 0$, while only partial wetting will be the result if $S < 0$. A large positive S value favours the spreading of a liquid. Equation (7.21) shows importantly that the equilibrium wetting behaviour is controlled by the surface chemistry of the different materials in question.

The equilibrium state of a partially wetting droplet put in contact with a flat solid surface can be derived by using the principle of free-energy minimization. The optimum state is a hemispherical cap (see Figure 7.33), with a contact angle given by Young's equation:

$$\cos \theta = \frac{\gamma_{sv} - \gamma_{sl}}{\gamma} \quad (7.22)$$

where γ_{sv} is the liquid–vapour interfacial tension, taking into account the surface pressure exerted by equilibrium-adsorbed vapour film at the solid surface. The “sv” surface tension can be written as follows:

$$\gamma_{sv} = \gamma_{so} - \pi_{sv} \quad (7.23)$$

where π_{sv} is the “sv” surface pressure. The surface pressure can at any arbitrary interface be calculated by using the Gibbs integral method, yielding the following:

$$\pi_{sv} = RT \int_0^{P_{\text{sat}}} \Gamma(P) d \ln P \quad (7.24)$$

where $\Gamma(P)$ is the amount of adsorbed vapour. The central parameter in wetting science is the contact angle,

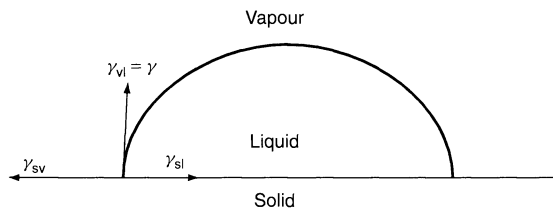


Figure 7.33. Side-view of a partially wetting drop on a solid surface showing the macroscopic contact angle and the three interfacial tension vectors acting on the three-phase contact line (tcl)

which can easily be observed directly by using various optical techniques or indirectly by measuring capillary forces, as described below. Since the surface tension, γ , also can be determined quite readily, it is possible to deduce the wetting tension $\gamma_{sv} - \gamma_{sl}$ for systems exhibiting partial wetting.

In many practical applications, the wetting liquid in question is a solution, e.g. an aqueous solution containing surface-active components. Then, the possibility of adsorption at all interfaces surrounding the three-phase contact-line (tcl) must be considered. According to the Gibbs isotherm for adsorption at the ij interface:

$$d\gamma_{ij} = -\Gamma_{ij} d\mu \quad (7.25)$$

Under the assumption that the solution is ideal, one can therefore write:

$$\pi_{ij} = RT \int_0^c \Gamma_{ij}(c) d \ln c \quad (7.26)$$

where the spreading pressure $\pi_{ij} (= \gamma_{ij}^0 - \gamma_{ij})$ is the difference between the surface tension of the pure solvent and the surface tension of the solution at concentration c . In the case of partial wetting, preferential solute adsorption at the “sl” interface will increase the wetting tendency of the solution, as is often the case when adding surfactants to a solution in contact with a hydrophobic surface, while preferential adsorption at the “sv” interface will cause dewetting, as often is observed when small amounts of cationic surfactants are added to solution in contact with a negatively charged surface. This effect is commonly referred to as autohydrophobicity. If the adsorption isotherms are known, the contact angle of the solution can be calculated by combining equations (7.22) and (7.26).

7.1.1 Wetting of rough and chemically heterogeneous surfaces

As has been pointed out several times, the surface of paper is far from being a smooth ideal surface. This has great consequences on the wetting behaviour that is observed. For “random” rough surfaces, the influence of surface roughness can be described by using Wenzel’s equation:

$$\cos \theta_r = \frac{A_{act}}{A_{proj}} \cos \theta \quad (7.27)$$

which simply states that the contact angle can be calculated if the ratio between the actual-to-projected surface areas are known. The important conclusion drawn from equation (7.27) is that roughness promotes

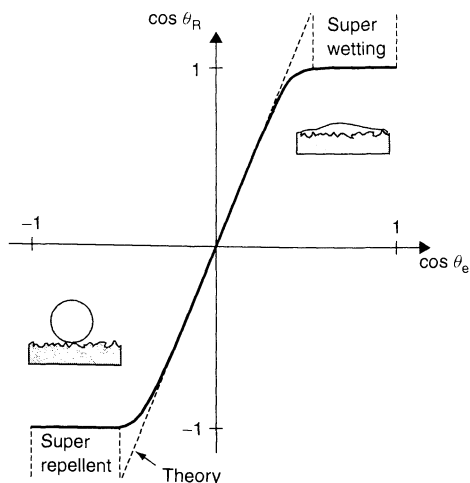


Figure 7.34. Illustration of the effect that surface roughness has on the wetting of a solid by a liquid drop. The plot shows schematically the evolution of the cosine of the contact angle on a rough surface (θ_R) versus the same quantity on a smooth surface with the same surface composition (θ_e). The theoretical line refers to equation (7.27)

wetting in the partial wetting regime ($0 < \theta < 90^\circ$), while the wetting tendency decreases in the non-wetting regime ($0 < \theta < 90^\circ$). Figure 7.34 show schematically how the roughness effect may manifest itself in practice. If the roughness defects are sharp and large enough, the contact angle may be pinned also for wetting liquids and Wenzel’s equation is no longer valid. This situation may give rise to a large hysteresis in the measurement of advancing and receding contact angles. Due to pinning of the contact line, the advancing contact angle, θ_a , is always larger than the receding contact angle, θ_r .

Chemical heterogeneity is also highly important when discussing the wetting of paper. For surfaces composed of different surface groups that are ideally mixed, the contact angle can be estimated simply from the relative fractions of the two components “1” and “2”, as follows:

$$\cos \theta_{1+2} = f_1 \cos \theta_1 + f_2 \cos \theta_2 \quad (7.28)$$

However, this situation is seldom realized in papermaking systems for which the chemical heterogeneity is often observed on the micron-size scale. This can give rise to contact line pinning on defects due to line tension effects, which also causes contact-angle hysteresis. This is illustrated below in Figure 7.35, which shows a large difference between the advancing and receding contact angles measured on paper. In the advancing mode, the measured contact angle increases rapidly with

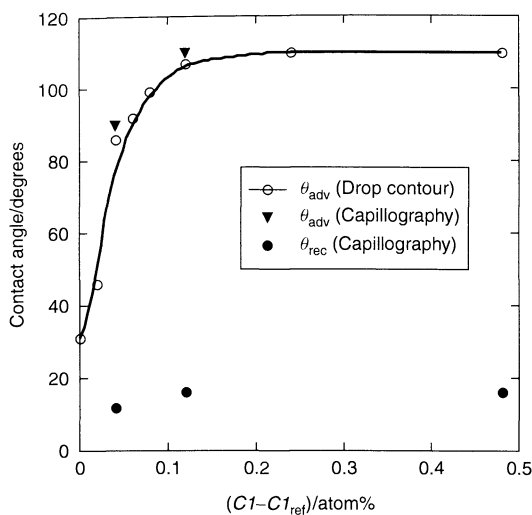


Figure 7.35. Quasi-static advancing and receding contact angles versus the fibre surface coverage of AKD sizing agents (given as the relative CI -to total carbon ratio minus that measured for the non-sized reference, as described below). The CI value represents aliphatic carbons (see Section 8)

increased surface coverage of hydrophobic domains, whereas small contact angles are measured in the receding mode. This is in agreement with previous findings for heterogeneous materials (45). In the study of paper wettability, it is always important to consider if receding or advancing wetting modes apply to the practical problem at hand.

7.1.2 Wetting dynamics

Wetting dynamics is highly important in converting operations, coating, and printing on paper, since equilibrium conditions are seldom realized in these fast processes. The spreading of a liquid on a solid can be driven by hydraulic pressure, inertia, gravity and wetting tension. The energy of the moving liquid can be dissipated through viscous drag in the bulk liquid or by molecular friction at the wetting front. Together, this generates a seemingly overwhelming challenge in formulating an understanding of wetting dynamics, in particular when considering the various possible wetting geometries and the large range of wetting speeds encountered in practice. Comprehensive reviews of this difficult topic have been published by de Gennes (46), Blake (47) and Kistler (48). Here, we will only touch upon some rather trivial issues related mostly to the spontaneous spreading of liquids and solutions on solid surfaces.

When discussing wetting dynamics, the dynamic contact angle θ_d is the central parameter. In the so-called capillary regime, spreading is promoted by the in-plane and out-of-balance interfacial tension force, which often is expressed as follows:

$$F_s = \gamma \cos(\theta_d - \theta) \quad (7.29)$$

from which one can conclude that the spreading force is largest far from equilibrium for completely wetting systems. A net dissipation associated with the motion of a spreading liquid compensates the unbalanced capillary force. The main theories available for describing wetting dynamics differ in the way in which one accounts for this dissipation. In the hydrodynamic approach, dissipation occurs by viscous drag in the bulk liquid, whereas according to the molecular kinetic theory, the dissipation takes place at the moving three-phase contact line. In the hydrodynamic theories, the dependence of spreading rate on the contact angle is, in the case of the complete wetting regime, accounted for by the $\theta_d^3 \sim Ca$ power law. This is referred to as the Hoffman–Voinov–Tanner law. For partial wetting, the approximate spreading law $\theta_d^3 - \theta^3 \sim Ca$ is suggested; $Ca = \eta U / \gamma$ is the *capillary number*, where η is the liquid viscosity, U the spreading rate, and γ the surface tension. Hence, the rate of spreading in the complete wetting regime is given by the following:

$$U \sim \frac{\gamma}{\eta} \theta_d^3 \quad (7.30)$$

showing (as in the case of capillary flow discussed below) that the rate is proportional to the surface tension and inversely proportional to the viscosity. In the capillary spreading regime, the radius of a spreading drop is predicted to exhibit an approximate $r \sim t^{1/10}$ dependence. It should be noticed that deviations from the spreading laws referred to above are common, in particular for high Ca numbers. The dynamic contact angle θ_d is often observed to rise rapidly for $Ca > 0.2$. In high-speed coating processes, this often results in the entrainment of air and ultimately to a situation in which the substrate is not coated at all.

For spontaneous wetting processes involving complex solutions under conditions of fast hydrostatic equilibration, the wetting dynamics are often controlled by the kinetics of interfacial adsorption and its effect on the dynamic wetting tension. Due to the fact that several interfaces are involved and that mass transfer can occur over the three-phase contact line, it is frequently difficult to predict wetting rates for such systems. However, in the case of drop spreading on hydrophobic surfaces, the time-limiting step is often the adsorption at the expanding liquid–vapour interface. Inserted into the surface

tension balance in equation (7.22), the dynamic contact angle then becomes:

$$\cos \theta_d(t) = \frac{\gamma_{sv} - \gamma_{sl}}{\gamma(t)} \quad (7.31)$$

This simple law can be used to predict the spontaneous spreading of ink drops on hydrophobic paper from surface tension relaxation data.

7.1.3 Adhesion

The thermodynamic work of adhesion between two materials A and B is given by the following:

$$W_a = (\gamma_A + \gamma_B) - \gamma_{AB} \quad (7.32)$$

For a solid and a liquid, this can be expressed as follows:

$$W_a = (\gamma_{sv} + \pi_{sv} + \gamma) - \gamma_{sl} \quad (7.33)$$

where $(\gamma_{sv} + \pi_{sv})$ is the surface energy of the solid in air. If the spreading pressure term is omitted, then the work of adhesion refers to the separation of the liquid from a solid, which still is covered with an adsorbed vapour layer. Substituting $(\gamma_{sv} - \gamma_{sl})$ with $\gamma \cos \theta$ by using the Young equation gives the following:

$$W_a = \gamma(1 + \cos \theta) + \pi_{sv} \quad (7.34)$$

This equation describes quite accurately the situation of an adhesive drop on a solid surface. The surface energies do not alter profoundly as the liquid solidifies, although stresses may build up due to shrinkage. Hence, the equation is also valid for the situation of a solid adhesive on a substrate. It follows that the adhesion maximum is obtained when $\cos \theta = 0$, that is when the liquid spreads completely. This implies the existence of larger forces between the liquid molecules and the solid, compared to that between the liquid molecules themselves, which further implies a high π_{sv} value. The adhesive force will tend to zero for contact angles above 90° , in which case π_{sv} is small.

The work of cohesion of a liquid W_c is defined as that which is required to create two new interfaces with a total interfacial tension of 2γ . Under conditions of complete wetting, $W_a = 2\gamma + \pi_{sv}$, which shows that the work of adhesion for completely wetting liquids is always larger than the work of cohesion. Adhesion problems generally require the consideration of aspects other than wetting alone. An important issue is to determine the surface energies of solids. The surface tensions of liquid–vapour and liquid–air interfaces can easily be determined from the pressure difference across

an interface having principal curvature radii of r_1 and r_2 , as follows:

$$\Delta P = \gamma \left(\frac{1}{r_1} + \frac{1}{r_2} \right) \quad (7.35)$$

which reduces for a spherical drop to the well-known relationship, $\Delta P = 2\gamma/r$. No such simple and direct method of measuring the surface energy exists for solid surfaces, due to their rigidity. However, it is the surface energy of the solid that to a large degree determines wetting, adhesion, cohesion and friction properties.

In a study that has proven highly useful in the design of products with prescribed wettability, Zisman found that a liquid drop will wet a surface completely when its surface tension, γ , is smaller than a critical value, γ_c , which is characteristic of the solid (49). This critical surface tension of wetting is often measured by using a homologous series of liquids with different surface tension values. By using the following function:

$$\cos \theta = 1 - const.(\gamma - \gamma_c) \quad (7.36)$$

and plotting $\cos \theta$ versus γ , γ_c is obtained at the intercept, $\cos \theta = 1$. The importance of Zisman's method is that the desired wetting properties for a specified liquid can be obtained by modifying surfaces using coatings or other chemicals with suitable values of γ_c . Liquids will furthermore completely wet a surface only when $\gamma \geq \gamma_c$. Hence, when laminating paper with, e.g. polyethylene, with a surface tension of about 30 mN/m, the paper substrate should preferably have a higher γ_c in order to achieve good wetting and adhesion. The adhesion will decrease strongly with decreasing γ_c below this value. The measured γ_c values may vary rather strongly between different commercial grades of, for instance, paper board (50). Increasing the surface energies of surfaces for improved wetting and adhesion in converting operations is often achieved by using corona discharge.

Fowkes and Mostafa (51) demonstrated another fruitful approach to the problem of estimating surface energies of solids by separating the surface free energy into different components, of which dispersive and polar acid-base interactions dominate, thus giving the following:

$$\gamma = \gamma^d + \gamma^{ab} \quad (7.37)$$

This work was followed by others, notably that of van Oss *et al.* (52), and was developed into a theory of surface free energies and adhesion (see ref. (53)). The complete combining rule can for a "polar" system be expressed in terms of the adhesion energy and the contact angle, as follows:

$$W_a = \gamma(1 + \cos\theta) = 2 \left[(\gamma_1^{LW} \gamma_s^{LW})^{1/2} + (\gamma_1^- \gamma_s^+)^{1/2} + (\gamma_1^+ \gamma_s^-)^{1/2} \right] \quad (7.38)$$

By using several liquids with known surface tension components and determining their contact angles in contact with a given solid, the surface energy of the solid may be calculated using the above equation. It is worth noting that this theory has been questioned from several standpoints, including the use of the combining geometric mean rule. Furthermore, the surface tension values of the reference liquids used to determine the surface energy components of the solids have been debated. The theory is nevertheless extensively used in practice in an effort to understand the interrelationships between wetting, adhesion and molecular surface properties.

7.2 Wetting properties and surface energy characteristics of paper

It should be stressed from the beginning that paper substrates are not compliant to the assumptions of Young's equation. Paper surfaces are naturally rough, porous, chemically heterogenous, and also dynamic to some degree. Contact angles measured for such substrates reflect to different degrees these properties, usually in a non-trivial way. Techniques for measuring contact angles are discussed elsewhere in this compendium (see Chapter 37). The heterogenous features of paper and fibre surfaces are clearly indicated by the large difference between advancing and receding contact angles, as illustrated in the example shown in Figure 7.35. Wetting studies on paper and fibre nevertheless provide very important and useful information for understanding adhesion, absorption and printing. This is, for instance, seen in Figures 7.16 and 7.17, which show clearly the interrelation between the advancing contact angle and the absorptivity of paper. Furthermore, as seen in Figures 7.35 and 7.23, such studies can also provide semi-quantitative information about the chemical compositions of the paper surfaces. This information is highly useful when trying to rationalize important end-use properties such as absorbency, adhesion and friction.

The surface energy of paper can be calculated from quasi-static advancing contact angles. The best approach for doing this seems to be to treat spreading and penetration as separate processes. The quasi-static advancing contact angle is identified as the contact angle measured when drop base expansion is first stabilized, which for low-viscous fluids occurs in fractions of a second. In

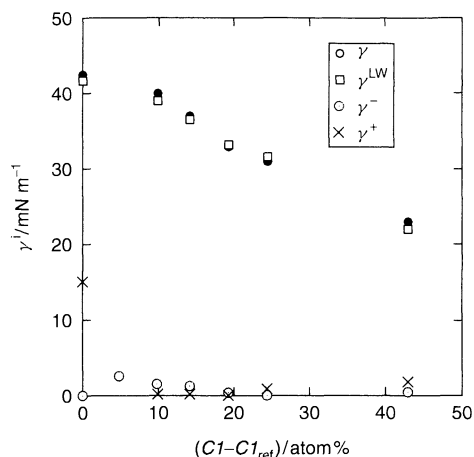


Figure 7.36. Evolution of surface energy components for kraft pulp hand-sheets versus the fibre surface coverage of AKD sizing agents (given as the relative $C1$ -to total carbon ratio minus that measured for the non-sized reference sheet, as in Figure 7.35). The surface energies were calculated by using equation (7.37) from the quasi-static advancing contact angles for water, formamide, ethylene glycol and diiodomethane

the case of adsorbing papers, the effect on the contact angle of the drop volume decrease during spreading is accounted for by extrapolation to $t = 0$. Figure 7.36 shows the evolution of the surface energy components for AKD sized hand-sheets. As can be clearly seen, there is more or less an inverse linear relationship between these quantities. The values obtained for the non-sized sheet agrees well with those previously reported for different cellulosic material, as shown in Table 7.1. The agreement in the Lifshitz–van der Waals and basic components is very good indeed. Variations seen in the total surface energy value are mainly caused by variations in the small acid component, whose magnitude often is of the same order as the measurement accuracy. Very low surface energies are obtained for high surface coverage of AKD. In this case, the paper surface must be seen as a heterogenous composite of cellulose fibre, AKD and entrapped air voids. However, the physical meaning of the measured surface energy is under such circumstances somewhat questionable. The results have none the less some value in the prediction of, for instance, polymer adhesion on paper.

The influence of paper roughness on wetting dynamics is illustrated in Figure 7.37, which shows the spreading of ethylene glycol on different coated paper grades having the same surface chemistry but different mean roughness values. Surface roughness was altered by calendering. The glossy art paper was hard-calendered,

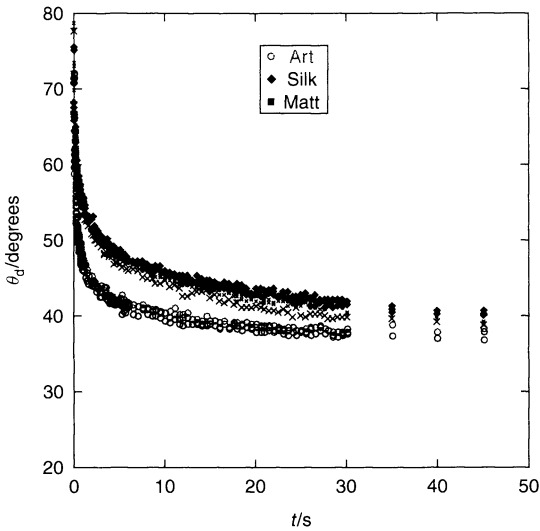


Figure 7.37. Spreading of ethylene glycol on three coated paper grades (art, silk and matt) with the same surface chemical composition. Each curve represents three different measurements at three different positions on the papers, and is perfectly reproducible. The rms roughness values of the samples depends on the scale length and the waveband analysed, but for all scales measured by atomic force microscopy and white-light profilometry increase in the order: art < silk < matt (see also Figures 7.44 and 7.45 below)

and the silk paper soft-calendered, while the matt paper was not calendered at all. Spreading of ethylene glycol is initially fastest on the glossy paper, due to the fact that roughness defects retard the spreading less on this smoother surface. However, the spreading on the rougher surfaces relaxes within 50 s to approximately the same value as that observed for the glossy art paper. This long-time relaxation is facilitated by sub-surface penetration in the surface pores of the coating. Hence, as predicted from the equations of capillary dynamics discussed below, this relaxation should be faster for the non-calendered matt sample when compared to the soft-calendered silk grade. Spreading of different completely wetting poly(dimethyl siloxane)s (PDMSs) did not reveal any differences between the two samples. Roughness defects thus do not seem to pin the contact angle of a completely wetting fluid, which intuitively seems to be correct. Overall, spreading on paper must be considered as a mix between surface spreading and sub-surface penetration. The physical laws for the latter process are discussed below. The dominance of different phenomena will depend on the wettability of the solid by the liquid, and the liquid viscosity, which retards sub-surface penetration more than surface spreading.

Future work will hopefully help to clarify the relationship between paper surface morphology and spreading dynamics.

7.3 Capillary rise and flow dynamics

The driving force for liquid penetration into a capillary is given by the following:

$$\Delta P = \frac{2\gamma \cos \theta}{r} \quad (7.39)$$

In a dynamic situation, this force is opposed by viscous drag and gravity. For a viscous non-compressible liquid in a long cylindrical capillary, the capillary flow dynamics are described by the following differential equation:

$$\rho[zz'' + (z')^2] = \frac{2}{r}\gamma \cos \theta - \frac{8}{r^2}\eta zz' - \rho gz \quad (7.40)$$

where ρ is the density, η the viscosity, γ the surface tension, θ the wetting angle of the liquid, z the height of capillary rise, r the capillary radius and g the acceleration due to gravity. Equation (7.40) can only be solved analytically in different asymptotic regimes, as was shown by Lucas (56) and Washburn (57). For viscous fluids in the short-time regime under quasi-static conditions (i.e. the acceleration term is zero), the capillary flow can be described by the Washburn equation as follows (57):

$$z(t) = \sqrt{\frac{r\gamma \cos \theta}{2\eta}} t \quad (t \rightarrow 0) \quad (7.41)$$

which predicts the well-established fact that liquid penetration in the short-time regime often is proportional to the square root of time. Furthermore, the rate of penetration increases with increasing size of the capillary, decreasing viscosity and increasing capillary force. In the long-time limit, the penetration slows down and exhibits an exponential relaxation towards the equilibrium height, z_∞ :

$$z(t) = z_\infty \left[1 - \exp\left(-\frac{\rho g r^2}{8\eta z_\infty} t\right) \right] \quad (t \rightarrow \infty) \quad (7.42)$$

where z_∞ is defined by the balance of capillary and hydrostatic pressures:

$$z_\infty = \frac{2\gamma \cos \theta}{\rho g r} \quad (7.43)$$

So far we have only discussed the dynamics of capillary rise in a cylindrical capillary. However, when interpreting flow in paper, it is also worthwhile to consider other

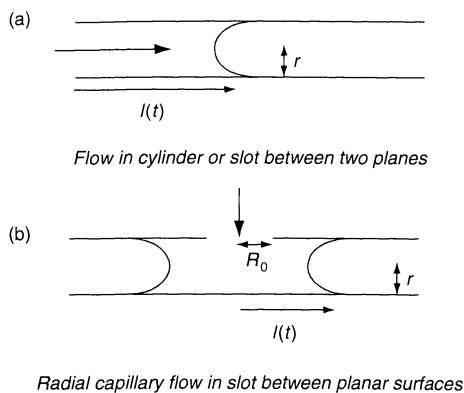


Figure 7.38. Schematic illustrations of (a) the capillary flow in a cylinder or a slot between two planes and (b) the radial capillary flow in a slot between planar surfaces

geometries, such as a slot between planar surfaces. Figure 7.38 shows some simple geometries for which the general dynamics equation can be solved in the short-time regime. The penetration distance versus time dependences for the geometries shown in Figure 7.38 can be written as follows:

$$l(t) = \sqrt{\frac{r\gamma \cos \theta}{2\eta}} t, \quad \text{cylindrical capillary} \quad (7.44)$$

$$l(t) = \sqrt{\frac{2r\gamma \cos \theta}{3\eta}} t, \quad \text{one-directional flow between two planes} \quad (7.45)$$

$$l(t)^2 \left(\ln \frac{l(t)}{R_0} - \frac{1}{2} \right) + \frac{1}{2} R_0^2 = \frac{2r\gamma \cos \theta}{3\eta} t, \quad (7.46) \\ \text{radial capillary}$$

where the penetration distance rate is highest for the one-directional planar flow and lowest for the radial capillary flow, due to the continuous expansion of the liquid–vapour interface. In the first two cases, the penetration distance scales as $t^{1/2}$.

Only cases of spontaneous penetration into pores of simple geometry have been considered above. In real papers and coatings, the situation becomes much more complex, and accurate modelling of flows requires a detailed knowledge about pore distributions, swelling effects and the connectivity of pores. Such properties are not trivial to determine.

The penetration kinetics of complex solutions such as printing inks and fountain solutions are often controlled by time-dependent interfacial adsorption phenomena, as is discussed in detail in ref. (58). Surfactant adsorption

will naturally aid penetration in hydrophobic capillaries, whereas the opposite effect is often observed for hydrophilic capillaries due to the decrease of the capillary pressure with decreasing surface tension.

7.4 Absorption of liquids and solutions in paper

Liquids can be transported into paper by capillary penetration, surface spreading or vapour sorption mechanisms. In many practical situations, these tend to be coupled processes. Capillary penetration in paper can be strongly influenced by adsorption and surface wetting processes ahead of the liquid front, which can cause fibre swelling and molecular rearrangement of various surface groups. Liquids can be imbibed from drops or liquid films deposited on the paper surface, or penetrate through the edge of the paper sheet, thus causing edge wicking. Absorption from the vapour phase through adsorption and pore condensation mechanisms is also frequently encountered.

We start by discussing the surface penetration phenomenon. This can, for instance, be investigated by using what in paper science is known as the *Bristow wheel*, where absorption in a paper strip mounted on a rotating wheel is studied. The absorption time in such a set-up is controlled by simply varying the peripheral speed or the applicator box width. Figure 7.39 (59) shows some early absorption results obtained by using the Bristow wheel absorption technique. All curves show some measurable absorption volume, visible also for

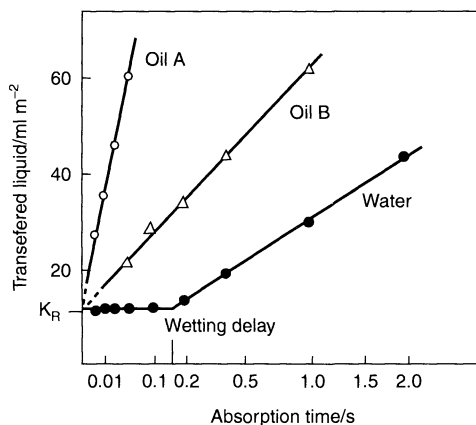


Figure 7.39. Liquid absorption in paper as a function of adsorption time; note the logarithmic time-scale. (Redrawn from ref. (59))

very short contact times (<1 ms). This volume is generally claimed to be the void volume associated with the surface roughness of the paper. The oils studied exhibit a $V \sim t^{1/2}$ relationship from the outset (59), agreeing with the simple Washburn kinetics. For water in contact with the sized paper, however, there is quite an interesting short-time behaviour with an induction period before further absorption occurs. In the drop spreading experiment shown above in Figure 7.16, a similar induction period can be identified. The reason for this so-called “wetting delay” has been the subject of different hypotheses. It seems, however, reasonable that the delay relates to the rate of establishment of a precursor wetting film on the fibre surfaces, which thus enables further capillary penetration into the sized paper. The establishment of a precursor wetting film on sized grades is no surprise considering the heterogeneous chemical nature of the paper surfaces, with both hydrophilic and hydrophobic patches, as described above. This pre-wetting phase, either due to surface spreading or vapour sorption, must be emphasized for all partially hydrophobic paper grades. Once absorption is initiated, however, Washburn-type kinetics seems also to prevail for these qualities. This is also indicated for the sized paper qualities represented above in Figures 7.16 and 7.18. It should be mentioned however, that in an extensive study of liquid penetration in paper by Salminen, both linear and square-root relationships were obtained, although the cause of the discrepancy between the different data was not fully explained. It may be concluded that a wetting induction time is commonly observed for water absorbing in paper, whereas this effect is not seen for non-polar liquids. The time-dependence of penetration can often be described by using a Washburn-type equation suited for the particular experimental geometry at hand. The effects of typical liquid and substrate characteristics, such as viscosity, surface tension and pore size distribution, can thus at least qualitatively be accounted for by using equations (7.44), (7.45) or (7.46).

A frequently encountered problem in paper applications is the edge penetration or wicking of liquids. Packaging grades are often polymer-laminated but have unprotected edges where liquids and vapours may penetrate, hence resulting in edge wicking. As can be seen in Figure 7.40, internal sizing can be used to efficiently prevent the capillary transport of water into the paper edge. However, as can also be seen in this Figure, the protective effect of the sizing treatment vanishes when surfactant is added or when the temperature of the liquid is increased. The surfactant effect has been discussed above, and the increased penetration rate is due to adsorption at the solid–liquid interface, thus resulting in

a decrease of the liquid–vapour interfacial tension and hence an increase in the wetting tension ($= \gamma_{sv} - \gamma_{sl}$). Note that the adsorption depletes the solution front of the surfactant and that this effect becomes larger with a smaller average pore size of the network. Hence, high concentrations of surfactants are required for penetration into hydrophobic porous structures having small pores. This issue is discussed in detail in ref. (58). An important point to make with regards to the dynamics of the capillary penetration of surfactant solutions is that this is mainly determined by the rate of interfacial relaxation in the system under study, which may vary strongly between seemingly similar surfactants. Hence, the Washburn equation developed for describing simple liquid penetration is no longer relevant in this case.

The fast penetration of water into the highly sized paper which is observed at higher temperatures seems at first counterintuitive, since the water surface tension is only weakly dependent on the temperature. However, the important penetration mechanism is, in this case, most likely vapour transport and capillary condensation, where the latter occurs in accord with the Kelvin equation, as follows:

$$P = P^0 \exp\left(\frac{2v_l\gamma \cos\theta}{R_m RT}\right) \quad (7.47)$$

where P is the partial pressure of the vapour condensing into a circular pore of mean radius R_m , P^0 the vapour

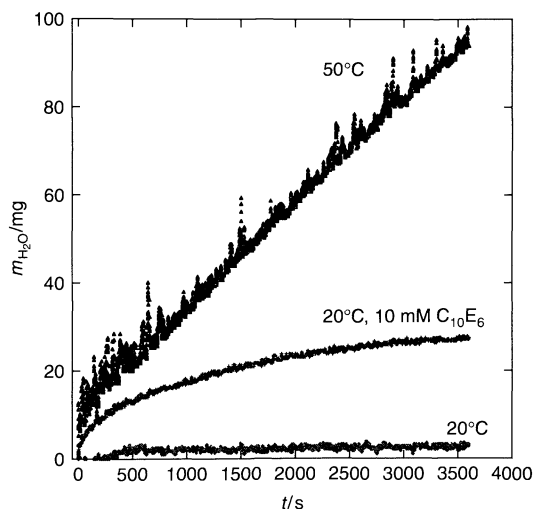


Figure 7.40. Edge penetration of water and an aqueous solution of hexaethylene glycol tetradecyl ether ($C_{10}E_6$) into a highly sized paper, with an advancing contact angle of $\sim 110^\circ$ as a function of the contact time

pressure, and v_l the molar volume of the vapour condensate. Capillary condensation occurs only when the contact angle is smaller than 90° , hence requiring hydrophilic patches in the paper, which as mentioned previously are also present in highly sized paper grades. The rate of imbibition into sized paper is strongly temperature-dependent and scales with the vapour pressure. Hence, sizing treatments are much less effective at elevated water temperatures.

Liquid transport in paper is, as can be understood from the above examples, a complex issue. Imbibition can occur by various mechanisms and is affected by many factors, such as the structure of the fibre network which controls the size of the capillaries and continuity, fibre surface chemistry and morphology, sizing and other chemical treatments of the fibre surfaces. Each practical case must be carefully thought over in order to make fruitful predictions of the absorbency behaviour and a correct analysis of the experimental data.

Paper is, as described above, often surface treated with a mineral coating in order to optimize ink-vehicle absorption. In this case, the resulting paper structure is heterogeneous. The absorbing liquid is often present in limited quantities, thus rendering important the nature of the pore size distribution. This is because the capillary pressure is higher in the small pores, thus leading to preferential penetration in small pore regions. Ink-bottle pores, which are large voids connected to small capillaries, tend to become more important in the more closed coating structures than in the more open fibrous paper structure. However, even if the capillaries in a (coated) paper sheet are not cylindrical and they are interconnected in a non-trivial way, a theoretical framework based on ideal penetration geometries provides an important basis for understanding liquid penetration phenomena.

8 CHARACTERIZATION OF PAPER PROPERTIES

8.1 Surface chemical properties

We have emphasized throughout this chapter that the surface chemical composition of paper is important since it affects among other things the wetting properties, adhesion, friction and surface strength of paper, which are important for converting and end-use applications. There exists a whole range of surface-chemistry-sensitive techniques, many of which are spectroscopic, that are being applied for the purpose of determining the surface chemistry of paper. These include Infrared

Spectroscopy (IR), Raman Spectroscopy, X-ray Photoelectron Spectroscopy (XPS) or Electron Spectroscopy for Chemical Analysis (ESCA), and Secondary Ion Mass Spectrometry (SIMS). More recently, Atomic Force Microscopy (AFM) has also found important use in the characterization of the local surface distribution of paper. Below, we will briefly discuss the use of some different surface-sensitive techniques in paper applications and relate the results obtained to paper characteristics and end-use properties. For a more detailed description of these and other available techniques for characterizing the chemistry of paper surfaces, readers are referred to ref. (60).

8.1.1 X-ray photoelectron spectroscopy

X-ray photoelectron spectroscopy (XPS) is widely used for surface characterization and analysis of polymers, biomedical materials and paper. The technique was developed by Kai Siegbahn in the 1960s, who realized that technical development had come to a point where the photoelectric effect discovered by Einstein could be used for surface chemical analysis. The photoelectric effect is the phenomenon that occurs when a material is exposed to photons with sufficiently high energy and electrons contained in the material with a lower binding energy are emitted. Therefore, we can write:

$$E_k = \frac{mv^2}{2} = h\nu - E_b$$

where E_k is the kinetic energy of the photoelectron, m , v and E_b are the kinetic energy, mass and binding energy of the electron, respectively, and $h\nu$ is the energy of the incident photon (X-ray) beam. Due to the fact that the kinetic energy of the photoelectrons is small, these can only travel small distances in the solid material. This makes XPS a truly surface-sensitive technique with an analysis depth of ~ 10 nm. However, the small kinetic energy also imposes the restriction of high-vacuum measurements, as gas molecules would otherwise scatter photoelectrons.

The information that can be obtained from an XPS measurement includes elemental compositions, the chemical state, the depth and in-plane distributions of elemental compositions, and the layer thickness values. Problems associated with the technique include the high-vacuum treatment of the sample, which may lead to evaporation of volatile components. Figures 7.41 and 7.42 give two examples of ESCA spectra obtained for paper materials.

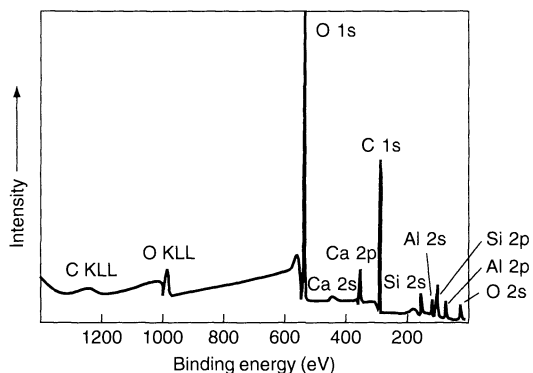


Figure 7.41. Typical XPS (ESCA) spectrum obtained on a coated paper grade, where peaks due to emission of core electrons can be clearly seen. The positions of these peaks are used to identify the elements present and to provide information about their oxidation states and chemical surroundings. The intensities of the peaks are furthermore used for quantification

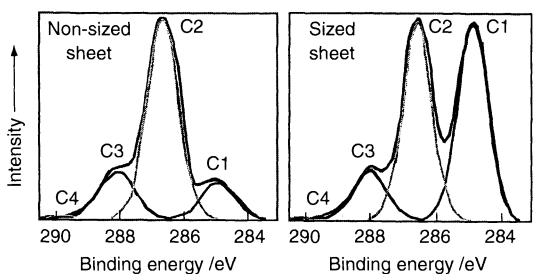


Figure 7.42. High-resolution XPS (ESCA) spectra obtained for non-sized and sized bleached kraft pulp hand-sheets. Such spectra are used to quantify the amounts of, for instance, sizing agents, extractives, ketones, etc., present on cellulose surfaces

8.1.2 Secondary ion mass spectrometry

Secondary ion mass spectrometry SIMS is the most surface-sensitive spectroscopic technique available today, with an analysis depth of some nanometres. The mass of secondary ions emitted from a substrate surface during the bombardment of a surface with primary ions is analysed by using this technique. Using time-of-flight (ToF) mass analysers, the complete mass spectrum can be recorded for every pulse of the primary ion source. This provides extremely high surface sensitivity. The output data from SIMS techniques include the total area spectrum used to identify surface groups and molecules and the total ion image from which conclusions about the in-plane distributions of the surface groups can be obtained. The typical practical resolution of a commercial ToF-SIMS instrument is 1–2 μm enabling,

for instance, the detection of retarded size particles at fibre or filler surfaces of paper (61).

8.1.3 Infrared and Raman spectroscopy

Infrared IR and Raman spectroscopy are today commonly used for the chemical analysis of paper. IR spectroscopy relies on the vibrational excitation of molecules due to photon absorption, whereas Raman spectroscopy exploits the photon frequency shift corresponding to a particular vibrational transition. Compared to XPS, both techniques are much less surface-sensitive, with analysis depths in the micron range. Both IR and Raman techniques are powerful tools in the identification of paper components, molecules and molecular segments. They can also be used for quantification purposes, although this requires the use of calibration curves with known compositions. Raman spectroscopy is in general less sensitive than IR, but is better suited for studies of heterogenous samples where IR suffer from Rayleigh scattering of infrared photons. Raman spectroscopy can also be used for time-resolved measurements by using a spectrometer equipped with a pulsed laser. Readers interested in further information on this topic are referred to refs (62) and (63), which provide detailed information about different IR and Raman spectroscopic techniques.

8.2 Surface topography

The surface topography of paper is an important characteristic influencing, as mentioned earlier, the wetting, adhesion and friction properties, as well as the light scattering of paper, and thereby its visual appearance in terms of gloss. Consequently, it is one of the key control parameters in the evaluation and design of paper products. The surface topography of paper can be controlled by various treatments including coating and surface sizing treatments and calendering in hard and soft nips. The process used depends on the value of the end product, as well as on the specific end-use requirements for strength, appearance and printability. The surface topography is consequently a key measure in the development of, e.g. new coating colours and coating procedures and during press trials for new paper machine settings.

Surface topography is technically the variation of the height z -direction along the lateral x - and y -coordinate space of the paper surface. A map of $z(x, y)$ gives a three-dimensional image of the surface. This information can be used in itself to evaluate the

topography. However, it is common and more practical to use various statistical measures. The subject of exactly which such parameters, as well as that of different models for light interaction with paper, is vast and it suffices here to say that many parameters are based on the calculation of some deviation of the surface structure from a best-fitted surface of well-known geometry, such as a plane or sphere, to the measured topography. It is important to be aware of the differences between the different measures and to consult suitable monographs on the subject before deciding on which parameter to use as the measure of topography. Depending on what the purpose of the measurement is, the different measures may be more or less suitable as they might emphasize or diminish certain effects.

Another powerful tool when analysing surface topography is filtering, which can be used to divide the topography according to the length scale of the surface features. By employing, for instance, wavelength filtering, much like the filtering of sound or any other frequency/wavelength-dependent property, it is possible to distinguish between roughness on different scales. The interesting scale for paper is often set by the size of the building stones at the paper surface, i.e. the fibres, pigments or pigment aggregates. The division is, however, somewhat arbitrary and the cut-off values between different ranges will be strongly dependent on the type of surface and the practical question of interest. In the case of the visual appearance, the interesting scale is set by the wavelengths of white light. In such cases, topography studies can gain much in terms of practical relevance by being combined with test panel studies in order to distinguish, for instance, within which wavelength band structural variations are most disturbing to the end-user.

With decreasing wavelength, or increasing spatial frequency, the different ranges are usually referred to as form (or shape), waviness, roughness and noise. As the very long wavelength variations rarely are of great importance, at least not in relation to surface chemistry, such variations can be removed by fitting an appropriate surface (e.g. a plane or sphere) to the form of the sample. Applying a low- and a high-pass filter will then divide the topography into the remaining three waviness, form and noise regimes. The noise is usually as much a measure of the sensitivity of the instrument as it is an intrinsic characteristic of the substrate and can therefore often be omitted. What remains then are the waviness and roughness features, which can be used in the pursuit of structure–property relationships, e.g. correlating with experimental spreading, gloss variation and printability measurements.

When studying topography images, especially two-dimensional (2D) measurements over large distances, it is important to bear in mind the frequently very large aspect ratio between the scales on the z -direction, on the one hand, and xy -plane, on the other.

8.2.1 Experimental methods

There are a number of experimental techniques available for measuring the surface topography of paper and other materials. Several methods are commonly employed by paper manufacturers for fast assessment of the average surface roughness. Such techniques include the use of air-leak-type instruments as well as indirect measurements of light scattering.

Direct imaging of surface topographical features can be obtained by using either contact methods, where a sharp tip is used to track the height variations in the plane of the surface, or techniques relying on the interaction of a light probe with the surface. Since the paper surface is often quite soft, it is important when using contact techniques to ensure that the measured response is not convoluted with characteristics of the measuring device. The measurement speed, resolution (in both lateral and normal directions) and measurement range are among the characteristics which determine the most suitable technique for a particular user and problem area. Figure 7.43 shows the resolution of a few chosen contact and non-contact methods. Note already at this stage that one should in presentations of topography-related results always present the range used in the experiment, since statistical roughness measures are

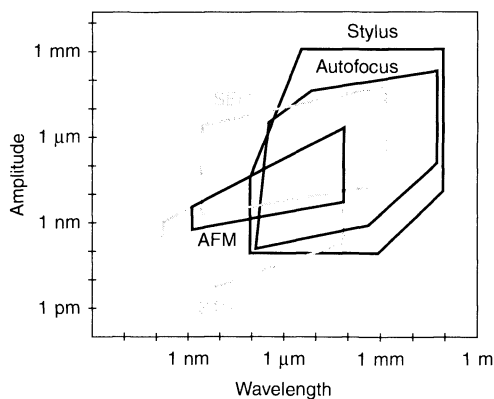


Figure 7.43. The resolution of different experimental techniques used for surface topography studies. (Redrawn from Stout, K. J. and Blunt, L., *Surface Coating Technol.*, **71**, 69–81 (1995). Reprinted with permission from Elsevier Science)

usually dependent on the measurement area. We divide the discussion of the techniques into indirect, contact and non-contact or optical methods, according to their modes of interaction with the surface. The different methods have both different technical limitations and different resolutions in normal as well as in the lateral directions. Atomic force microscopy (AFM) provides the highest lateral resolution images on paper but has a limited xy -range, whereas the stylus, autofocus and interferometry techniques have a much lower lateral resolution but larger working window.

Indirect methods

Common methods used by the paper industry for obtaining indirect surface roughness measures are those based on measurements of the amount of air that leaks out under the rim of a pressurized cup placed upside down on the paper surface. Two commercial instruments based on this principle are the Bendtsen and the Parker–Print–Surf (PPS) test. Such techniques provide an average value which is rather related to the surface roughness but do not provide a map of the surface and information about local properties. A serious problem with these methods is that they are not suitable for highly porous materials in which a significant fraction of air can be transported through the paper. However, they are simple and rapid to apply and are therefore frequently used in industry. Their primary usefulness is to follow the product reproducibility. The results obtained with the PPS method has, however, been scaled to physical roughness values and the technique is frequently used in the evaluation of paper for different printing techniques. As mentioned above in Section 7.4, the Bristow wheel wetting technique can also be used for evaluating surface roughness, or rather surface volume. Other indirect measures include light scattering methods but these require the use of an optical model for calculating roughness properties, and the input data are seldom known for constructing such models.

Contact methods

In contact methods, a sharp object is contacted with the sample and the variation in height position of this stylus is recorded as it scans the x - and/or y -directions of the surface. Contact methods are available both for 2D and three-dimensional (3D) measurements. From a 3D $z(x, y)$ map it is possible to calculate all relevant topography measures. However, since the method relies on the contact between the surface and a sharp object

which is scanned along the surface while in contact, considerable damage may be done to soft materials such as paper. The size of the stylus will also limit the xy resolution. Only features larger than the radius of the stylus tip can be measured. The maximum amplitude is of course also limited by the size and shape of the tip that is used for imaging the paper surface.

The principle of atomic force microscopy, (AFM) is very similar to the stylus contact method. A sharp nano-sized tip is used here to image small areas of a surface. Although a stylus is used, the probe and the surface do not necessarily need to be in physical contact when using the AFM technique. The reason for this is that the technique is highly sensitive, thus allowing measurement of more long-range physical interactions, such as electrostatic fields, on the colloidal scale. There exist various methods by which a constant force can be maintained between the tip and the sample without coming into physical contact with the imaging tip. This makes AFM ideal for imaging both hard and soft samples. The disadvantage of the technique is its small maximum measurement area, which is typically $50 \times 50 \mu\text{m}$ for paper. When determining roughness parameters from AFM data, it is recommended to use input from many repeated measurements in order to get reasonable statistics. The resolution is, on the other hand, very good and lateral structures of the order of a few nanometers can be detected without difficulty. The resolution in the vertical direction is even better, i.e. fractions of nanometers. Figure 7.44 shows examples of topography images of a glossy and a matt paper imaged by using AFM. When determining roughness parameters from AFM data, it is recommended to use input from many repeated measurements in order to get reasonable statistics from the small scan size used with this technique. The AFM technique can be applied in both air and liquid ambient media, which is unique and very useful when studying, e.g. swelling of fibres in water. Furthermore, as was discussed previously, AFM can be used for much more than simply determining the topography. This includes mapping the viscoelastic response of surfaces and thus gaining information about the chemical heterogeneity of a surface, and measuring normal and lateral force interactions between surfaces.

Non-contact methods

One of two basic principles is employed in most commercial optical non-contact methods. The first is the laser-focusing technique, which works according to the same basic principle as a CD-player, and can best be described as an optical equivalent of the stylus

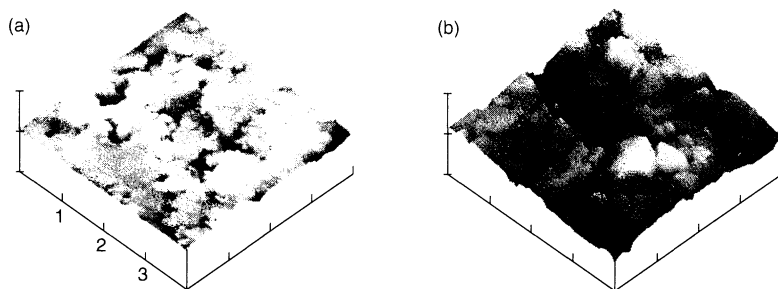


Figure 7.44. AFM images of (a) a glossy and (b) a matt paper with a scan size of $4 \times 4 \mu\text{m}$: x - and y -axes, $1.000 \mu\text{m}/\text{division}$; z -axis, $1000 \text{ nm}/\text{division}$. Roughness data for the same papers measured by the white-light interferometric technique are provided in Figure 7.45. The same paper grades are also used in the spreading experiments shown in Figure 7.36

method. The local height $z(x, y)$ is, by this method, determined from the measured position of a surface-reflected laser light probe at some distance away from the substrate as this surface is being moved in the xy -plane. A 3D map of the surface can then be constructed from this set of data. This method also has the advantage of being a non-contact method and having quite a large lateral measurement range, as can be seen from Figure 7.43. However, the technique is quite slow when compared to the non-contact interferometric technique, which is the second principle on which many commercial non-contact profilometers are based.

The basis of the interferometric technique is that when white light is used to illuminate both the sample and an internal reference surface, the reflected light from these two sources will produce a standing-wave pattern due to interference of the electromagnetic waves. The fringe pattern of reinforced and extinguished light is analysed after being transferred to a computer via a charge-coupled device (CCD)-camera. By scanning the focus of the interferometer microscope in the z -direction, fringe patterns corresponding to different heights on the surface are obtained and can be analysed in order to determine the variation in height at different positions on the surface. The lateral resolution obtained with this technique is of the order of $1 \mu\text{m}$, while the surface height information can be resolved down to about 1 nm . The area investigated is dependent on the objective used, as with all microscopes, but it can easily be increased by using a “stitching” methodology in which several images are assembled into a larger combined image. The technique has similar limitations as the stylus and laser-focusing techniques, but is much faster and it also allows easy filtering of the roughness in different wavelength bands, as is nicely illustrated in Figure 7.45. From experience gained at the

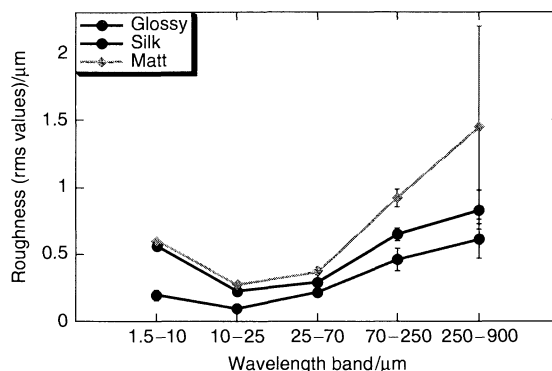


Figure 7.45. Roughness data of glossy, silk and matt paper grades as a function of the wavelength band. The coating colour recipes of the silk and matt grades are identical; however, the silk grade has been calendered in a soft nip. It can be clearly seen that the effect of calendering is largest for the larger roughness features and is not visible at low wavelengths, thus indicating that pigments and primary aggregate structures are unaffected by soft-calendering. The roughness for the glossy paper grade calendered in a hard nip is much smaller at all wavelengths when compared with the other grades. The papers featured in the plots are the same as those used in the spreading experiments shown in Figure 7.36

authors' laboratory, this technique, together with AFM, provides a very powerful combination in the study of the surface roughness of paper and similar materials which have roughness features that span several orders of magnitude. Common to all techniques used to study surface topography are problems related to very rapidly varying surface features. As mentioned above, contact techniques may run into problems because the stylus tip is relatively large and can be convoluted with the surface features. Such problems also provide difficulties for the optical non-contact techniques and should not be neglected.

8.3 Porosity

As we have emphasized previously in this chapter, some critical target properties for a paper coating include high smoothness, printability and print quality, outstanding optical qualities such as opacity, reflectance and finish (gloss/matt), and good performance with regards to surface strength and other mechanical properties. All of these qualities, to various degrees, are influenced by not only the physical and chemical surface characteristics of the coating layer, but also the nature of the sub-surface pore space. In particular, print quality can, to a large extent, be determined by ink drying times, which in turn are strongly influenced by the pore size distribution and connectivity in the sub-surface zone of the coating layer. Optical properties are significantly determined by the morphology of the void space and its influence on the scattering of impinging light. The printability of uncoated paper grades, however, are much less dependent on the sub-surface pores (chiefly inter-fibre pores in this case) than for coated papers, simply because the pore sizes in the base sheet are on average too large to induce large capillary forces, being of the order of tens of microns.

Bearing the above in mind, it is not surprising that obtaining reliable and reproducible characterizations of the pore space in a coating is an important aspect of paper research and analysis. The relevant range of pore sizes for a paper coating spans four decades, approximately between 1 nm and 10 μm , and this presents a considerable technical challenge. In this section, we will describe various methods now in use for the characterization of the pore structure of paper coatings. As the methodologies are broadly applicable to many kinds of porous systems (e.g. mesoporous silicates, zeolites, rocks, and even foods and biological materials) the discussion of these techniques will be rather general.

The IUPAC system classifies pores according to size as follows: micropores, <2 nm; mesopores, 2–50 nm; macropores, >50 nm. Paper coatings very often contain pores in all three categories; however, the distribution is commonly peaked somewhere in the range of 100 to 500 nm. The (somewhat arbitrary) delineation between micropores and mesopores is based on the role of capillary condensation in adsorption, which dominates in the mesopore regime but is itself dominated by direct adsorbent–adsorbate interactions in the micropore regime. Macroporous materials are such that the pores cannot induce capillary condensation at reasonable pressures; the base paper sheet is characteristically such a material.

The characterization of pore structure often exploits, in a highly controlled way, the phenomena which

relate to its interaction with liquids and gases, such as imbibition, capillary condensation and melting/freezing temperature suppression. Non-intrusive methods, such as scattering, imaging and tomography, are also used.

8.3.1 Gas adsorption

The sorption of gases to porous and rough materials has been used as a characterization method throughout the past century (64, 65). For paper coatings, it is a very useful technique for the investigation of smaller pores, which are important, e.g. in the initial stages of fluid imbibition. The pioneering work of Freundlich and Langmuir allowed a systematic description of the phenomenon of physisorption to evolve, centred around the concept of surface “condensation”. Langmuir’s chief contribution was the idea of *monolayer coverage*, whereby a single layer of adsorbant molecules is formed. The plateau of the *adsorption isotherm* (defined as the relationship between the amount of gas adsorbed by a unit mass of solid at a given relative pressure, p/p_0) represents completion of the monolayer, and if the average area per molecule can be independently determined, then the surface area can, in principle, be deduced. In practice, multilayer adsorption takes place, which can complicate this picture. Differences can be seen in the different classes of adsorption isotherm (under the IUPAC classification), with the more significant being the following:

- Type I.* The isotherm rises sharply at low p/p_0 , reaching a plateau, indicative of monolayer adsorption.
- Type II.* The isotherm rises sharply at low p/p_0 , becomes linear, and then increases rapidly, indicating multilayer adsorption.
- Type IV.* Isotherms commonly showing adsorption–desorption hysteresis, and always a steep drop in the absorbed amount on reduction of p , due to capillary evaporation effects.

The full range of adsorption isotherms under the IUPAC system is shown in Figure 7.46. Brunauer, Emmett and Teller were able to extend Langmuir’s theory of monolayer adsorption to obtain an isotherm (the BET equation) which models Type II behaviour, for meso- and macroporous systems. Briefly, in the theory, molecules in one layer act as adsorption sites for molecules in the next layer, so that the adsorbed layer is not of uniform thickness, but rather is made up of a random stack of molecules. The theory has limitations, such as the assumption of liquid-like behaviour in all adsorbed layers but the first; however, it has become a

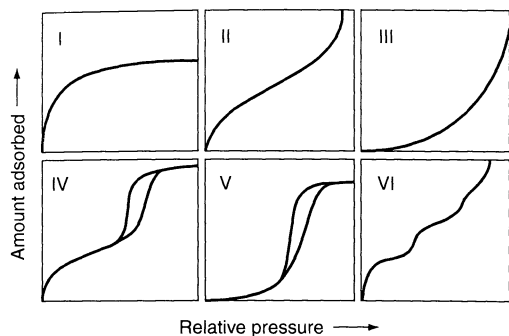


Figure 7.46. Gas adsorption isotherms according to the IUPAC system. (Taken from ref. (64). Reprinted with permission from Elsevier Science)

standard means by which to determine the surface area of rough and porous solids, and is commonly used in the paper industry to investigate smaller pores in paper coatings, and also the *intra-fibre* pores in the base sheet.

Performing a BET surface area measurement involves determination of the adsorption isotherm, and then the fitting of the theory to the linear (multilayer adsorption) part of the isotherm by using an established procedure (65). The measurement principle itself can be manometric (gas pressure measurement), gravimetric (measurement of mass change of the sample), or measurement of gas flow. An inert gas (e.g. He, N₂ or Ar) is commonly used at a fixed temperature (usually 77 K). This is often done discontinuously. For example, in the gravimetric method, the pressure is ramped by introduction of the gas, equilibrium obtained at the required p , and the mass change recorded. The specific BET surface area $a(\text{BET})$ is then given through the relationship between the *monolayer capacity* n_m (the amount required to cover the surface with a monolayer), which appears in the theoretical BET isotherm and is determined by fitting to the measurement, and the average area per molecule σ :

$$a(\text{BET}) = n_m N_A \sigma \quad (7.49)$$

where N_A is the Avogadro number.

Gas adsorption can also be used in systems with mesopores to measure pore size distributions. In this range of pore sizes, the surface energy of the pore walls causes a condensation of the gas (usually N₂ in practice) at pressures where it would remain in the gas state if not confined; an interface forms with surface tension γ and the reduced vapour pressure on the convex side of the meniscus, as expected from the Laplace equation, explains the condensation at equilibrium. Equating the

chemical potentials of the gas and liquid phases, and application of Laplace's equation:

$$\Delta p = -\frac{2\gamma \cos \theta}{r_p} \quad (7.50)$$

where Δp is the pressure difference across the interface, θ is the contact angle of the liquid–vapour–wall, and r_p is the radius of the pore wall, leads to the Kelvin equation, as follows:

$$\ln \frac{p}{p_0} = -\frac{2\gamma v^l}{r_K RT} \quad (7.51)$$

where r_K is the mean radius of curvature of the condensate, v^l is the molar volume of liquid, and the contact angle is now assumed to be 0.

As stated above, a Type IV isotherm is indicative of capillary condensation and provides a means of determining the pore size distribution of mesoporous materials through gas adsorption. The hysteresis often seen in these isotherms is due to the establishment of metastable states, more commonly a feature of adsorption rather than desorption. Moreover, on desorption from a full pore, the *inner* layers of the condensed phase tend to be removed first, so that the contact angle θ remains 0. In the Barrett, Joyner and Halenda (BJH) method, a stepwise procedure is used to determine the pore size distribution by following the desorption branch of the isotherm, whereby the differential volume of removed gas at each pressure step is related to the differential volume of pores emptied in that step, through the Kelvin equation. Consideration has to be given to the fact that not only is the condensate being removed from pores above a certain size, determined by the Kelvin equation for a given pressure, but also layers of adsorbed gas are being stripped away from pores emptied of liquid, at the same time (as is done in a BET experiment). Measurement of the amount of nitrogen desorbed at each reduction in pressure gives the pore size distribution. Some subtleties must be dealt with in connection with the assumption of pore shape and the range of validity of the Kelvin equation (65). The theoretical and practical complications for the interpretation of adsorption to both micro- and macroporous systems effectively restrict the method to the mesoporous regime.

8.3.2 Mercury porosimetry

As stated above, for many systems of interest, including paper coatings, the majority of pores lie somewhere near to or in the macroporous regime, where gas adsorption

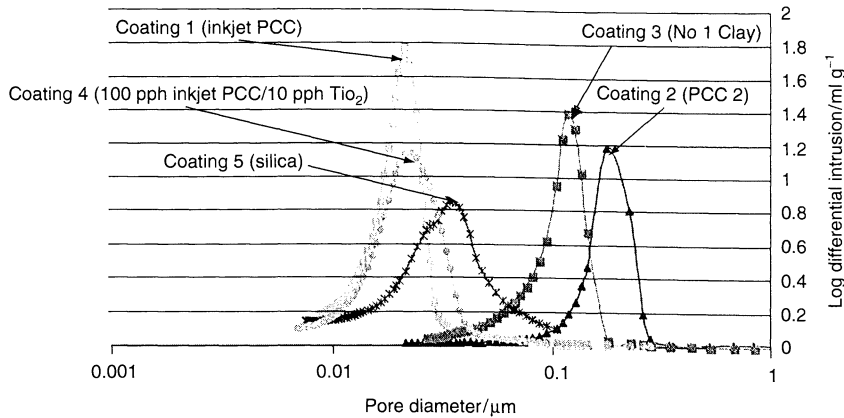


Figure 7.47. Comparison of pore size distributions obtained by using Hg porosimetry. (Taken from ref. (66))

becomes less effective. The technique commonly used to investigate these larger pores is mercury porosimetry.

For a non-wetting fluid ($90^\circ < \theta < 180^\circ$) like mercury, the Laplace equation predicts that the liquid will recede from the pore. Hence, Hg must be forced hydraulically into the pore space. The principle of mercury porosimetry uses this fact to provide a simple means to determine pore size distributions: The amount of non-wetting liquid that intrudes into pores as a function of applied pressure is monitored. Equation (7.50) provides a relationship between the pressure and the size of the smallest pore intruded. Some artefacts have to be considered, such as ink-bottle effects, where pores with small opening “necks” fill only when the minimum pressure is sufficient to force the liquid past the opening. Moreover, at the lower end of the mesopore regime, very large pressures are required (207 MPa at 7.2 nm) to access the pores, thus causing deformation of the sample which must be taken into account. However, the method has proven accurate (and popular) in the measurement of pore size distributions of larger mesoporous, and macroporous, systems. By using Fick’s law to describe fluid diffusion through cylindrical paths, it is even possible to deduce the *tortuosity* of the pore network, which is a measure of the deviation of diffusion paths away from aligned straight cylinders.

Modern mercury porosimeters can reach pressures up to ≈ 400 MPa, and perform intrusion and extrusion measurements automatically. This is carried out in either a stepwise or scanning mode. Recently, there has been a move towards the scanning mode method, as the stepping mode approach has several drawbacks, including the possibility of missing important information during the filling of smaller mesopores. Other issues of

importance are accurate determination of the contact angle of mercury on solid surfaces, the use of mercury of high purity, and the control of deformation effects by running scans on a non-porous sample of similar compressibility and comparing the results to those obtained from analysis on the real sample. The technique has been used on a wide variety of porous materials, from porous rocks to paper. An example for a comparative measurement on several ink-jet coating grades is given in Figure 7.47 (66).

Thermoporosimetry (cryoporometry)

Thermoporosimetry (67–69) is another technique where, similarly to gas adsorption, a capillary-induced phase transition is exploited as a pore characterization method. However, in this case, it is the liquid-to-solid, rather than vapour-to-liquid, transition that forms the basis of the method. As described by Gibbs and Thompson (Kelvin) over a century ago, the melting (and freezing) temperature of a crystalline solid in a pore is lowered relative to the bulk melting temperature, due to the limitation on crystal size and the large surface-to-volume ratio in a confined region. The Gibbs–Thompson equation describing the melting temperature suppression in a porous material can be derived by applying the Laplace equation at the solid–liquid interface and equilibrating the chemical potentials of the two phases, thus leading to the suppression in the melting temperature of magnitude ΔT_m :

$$\Delta T_m = T_m - T_m(r_p) = \frac{2\gamma T_m}{r_p \Delta H_f \rho} \equiv \frac{k}{r_p} \quad (7.52)$$

where T_m is the melting temperature in the bulk, $T_m(r_p)$ is the melting temperature in a pore of radius r_p , ΔH_f is

the bulk enthalpy of fusion of the solid–liquid transition, and ρ is the density of the solid. The physical constants for a given material can therefore be grouped as k . In practice, performing experiments during melting rather than freezing is preferable, as supercooling and contact angle effects are avoided.

The thermoporosimetry measurement exploits the Gibbs–Thompson phenomenon as follows: A sample is saturated with a wetting liquid (usually purified water or cyclohexane, depending on the material), and the sample quenched to well below the bulk melting temperature, such that liquid in pores of all feasible sizes is frozen. (A temperature of -60°C is sufficient to ensure this for water.) Equation (7.52) in fact predicts that ice in successively larger pores will be melted as the temperature is increased. Thus, to obtain the pore size distribution, all that is needed is a probe that can either distinguish between the relative amounts of liquid and solid in the pores, or monitor the progressive transition between the two phases. Nuclear magnetic resonance (NMR) spectroscopy can be used in the former case, where the two widely different spin–spin relaxation times of the liquid (long) and the solid (short) are used to determine the liquid and solid fractions of the substance imbibed in a porous sample. Alternatively, differential scanning calorimetry (DSC) can be used to monitor the progressive phase transition as the temperature is continuously raised.

The technique has proven successful in measuring the pore size distribution in the mesopore regime, for a variety of model (67–69) and practical (67) systems. An example of a measurement on a glossy coated paper is given in Figure 7.48 (67). For pores with $r_p > 50$ nm, instrument resolution, temperature control and

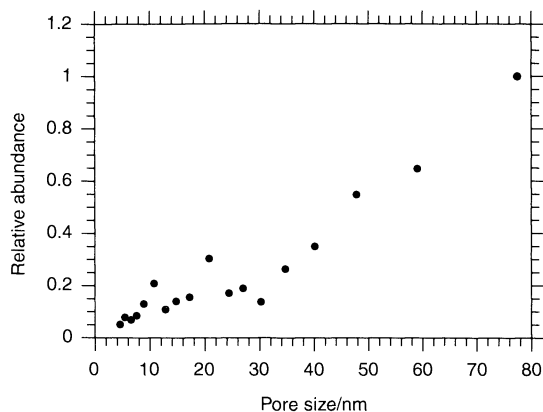


Figure 7.48. Pore size distribution of pores up to 80 nm in diameter of a glossy coated paper. (Taken from ref. (67))

defect formation in the pore ice restrict the usefulness of the technique. Its advantage for mesopores over mercury porosimetry is in significantly reduced material deformation, whereas the detection method, especially in the NMR implementation, is more direct and less model-based than the procedure for gas desorption. However, issues regarding the pore damage caused by the density changes during the freezing and melting of the probe fluid must be borne in mind.

8.3.3 Microscopy

The methods described above are generically intrusive: they require the invasion of the pore space by either a gas or liquid. Non-intrusive methods for studying pore structure are also commonly used, with microscopy being the main such method. With the lengths of interest often residing at the nanometre to micron scale, it is not surprising that scanning electron microscopy (SEM) has been widely used to image the internal pore structure of paper and paper coatings. A concise review is given in ref. (70).

The sample preparation procedure for SEM imaging of paper involves the embedding of small cuttings (e.g. cm width) of sheets into epoxy resin and either microtoming, or as has recently been introduced (70), polishing and chemical removal of a thin (μm) resin layer. These are then mounted in the SEM unit. Both secondary and back-scattered electron images can be used to investigate the cross-sections. In secondary electron mode, SEM relies on differences in surface topography to provide images, and hence the new trend towards exposure of the section surface by removal of the resin. Computer-based image analysis can then be applied to identify the distribution of different components (fibres, fillers, pigments and binders) and to quantitatively evaluate the distribution of pores. An example of the SEM imaging of paper cross-sections is shown in Figure 7.49. Advantages of this approach chiefly centre on the ability to identify the transverse distribution of individual components and to obtain a direct image of the sub-surface environment, including the pore structure. The disadvantages lie mainly in the fact that one is attempting to construct a three-dimensional overview of the sample from a series of two-dimensional images. This is a classic issue in microscopy, tomography and imaging. It is hoped that new methods, such as confocal microscopy and X-ray tomography, will provide more direct means of imaging the sub-surface zone of paper and coating layers.

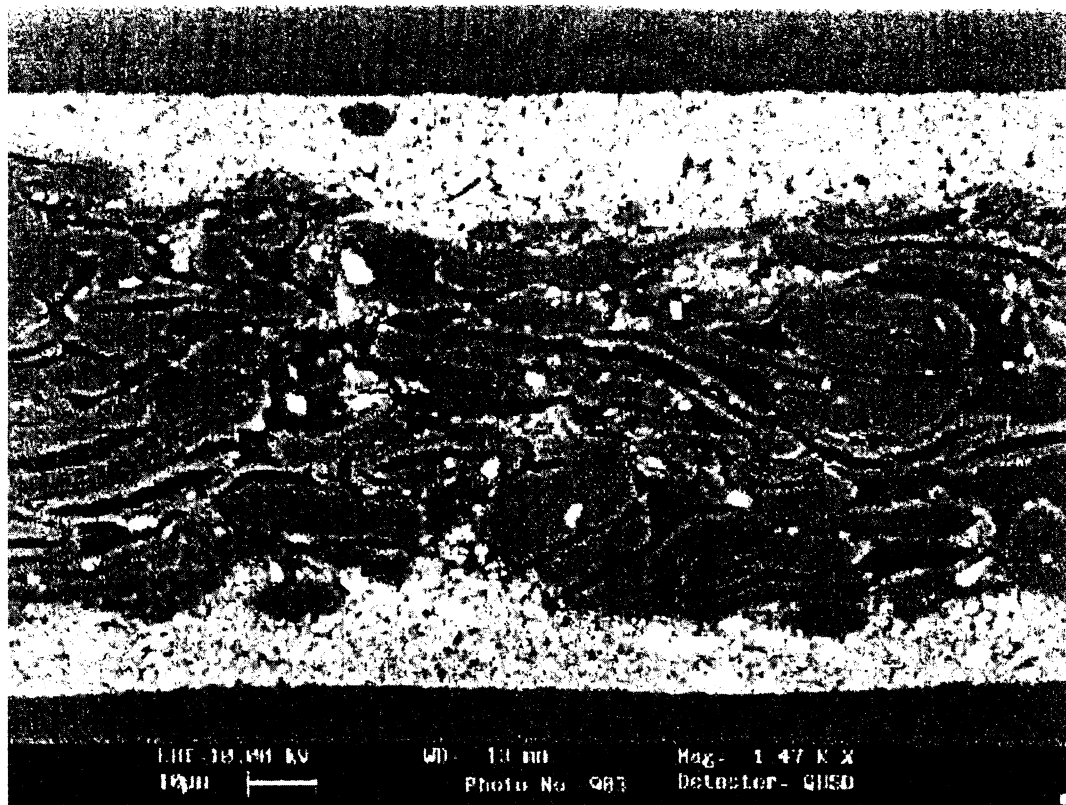


Figure 7.49. SEM image of a coated paper. (Micrograph supplied by courtesy of G. Ström)

9 ACKNOWLEDGEMENTS

IRECO and KK-stiftelsen are acknowledged for financing this work. Karin Hallstensson is thanked for help with the artwork, and Boris Zhmud is thanked for valuable comments on the manuscript.

10 REFERENCES

1. Lyne, B., Paper, in *Kirk-Othmer Encyclopedia of Chemical Technology*, Vol. 18, 4th Edn, Howe-Grant, M. (Ed.), John Wiley & Sons, New York, 1996, pp. 1–34.
2. Dulany, M., Batten, G. L., Peck, M. C. and Farley, C. E., Papermaking additives, in *Kirk-Othmer Encyclopedia of Chemical Technology* Vol. 18, 4th edn, Howe-Grant, M. (Ed.), John Wiley & Sons, New York, 1996, pp. 35–60.
3. Roberts, J. C. (Ed.), *Paper Chemistry*, Blackie Academic Press, London, 1996.
4. Laine, J., Stenius, P., Carlsson, G. and Ström, G., The effect of ECF and TCF bleaching on the surface chemical composition of kraft pulp as determined by ESCA, *Nordic Pulp Paper Res. J.*, **11**, 201–210 (1996).
5. Lindström, T., Electrokinetics of the paper making industry, in *Paper Chemistry*, 2nd Edn, Roberts, J. C. (Ed.), Blackie Academic Press, London, 1996, pp. 25–43.
6. Hanley, S. J. and Gray, D. G., Atomic force microscopy, in *Surface Analysis of Paper*, Conners, T. E. and Banerjee, S. (Eds), CRC Press, Boca Raton, FL, 1995, pp. 301–324.
7. de Silveira, G., Forsberg P. and Conners, T. E., Scanning electron microscopy: A tool for the analysis of wood pulp fibers and paper, in *Surface Analysis of Paper*, Conners, T. E. and Banerjee, S. CRC Press, Boca Raton, FL, 1995, pp. 41–71.
8. Okagawa, A. and Mason, S. G., Capillography: A new surface probe, in *Fibre-Water Interactions in Paper-Making*, Vol. 2, Committee, F. R. (Ed.), The British Paper and Board Industry Federation, London, 1978, pp. 581–586.
9. Berg, J. C., The importance of acid-base interactions in wetting, adhesion and related phenomena, *Nordic Pulp Paper Res. J.*, 75–85 (19931).
10. Deng, M. and Dodson, C. T. J., *Paper: An Engineered Stochastic Structure*, Tappi Press, Atlanta, GA, 1994.

11. Norman, B., *Pappersteknik*, Kungliga Teknisk Högskolan, Stockholm, 1992.
12. Fleer, G. J., Cohen Stuart, M. A., Scheutjens, J. M. H. M., Cosgrove, T. and Vincent, B., *Polymers at Interfaces*, Chapman & Hall, London, 1993.
13. Garvey, M. J., Tadros, T. F. and Vincent B., A comparison of the volume occupied by macromolecules in the adsorbed state and in bulk solution. Adsorption of narrow molecular weight fractions of poly(vinyl alcohol) at the polystyrene/water interface, *J. Colloid Interface Sci.*, **49**, 57–68 (1974).
14. Napper, D. H., *Polymeric Stabilization of Colloidal Dispersions*, Colloid Science series, Otteville, R. H. and Rowell, R. L. (series Eds), Academic Press, London, 1983.
15. Swerin, A. and Ödberg, L., Some aspects of retention aids, in *The Fundamentals of Papermaking Materials*, Vol. 1, Baker, C. F. (Ed.), Pira International, Leatherhead, UK, 1997, pp. 265–350.
16. Sennerfors, T., Froberg, J. C. and Tiberg F., Adsorption of polyelectrolyte–nanoparticle systems on silica: Influence on interaction forces, *J. Colloid Interface Sci.*, **228**, 127–134 (2000).
17. Israelachvili, J. N., *Intermolecular and Surface Forces*, Academic Press, London, 1991.
18. Evans, D. F., and Wennerström, H. K., *The Colloidal Domain where Physics, Chemistry, Biology, and Technology Meet.*, VCH, New York, 1994.
19. Roberts, J. C., Neutral and alkaline sizing, in *Paper Chemistry*, Robert, J. C. (Ed.), Blackie Academic Press, London, 1996, pp. 140–160.
20. Roberts, J. C., A review of advances in internal sizing, in *The Fundamentals of Papermaking Materials*, Vol. 3, Baker, C. F. (Ed.), Pira International, Leatherhead, UK, 1997, pp. 1541–1545.
21. Lindstrom, T. and Soderberg, G., On the mechanism of sizing with alkyl ketene dimers. Part 3, The role of pH, electrolytes, retention aids, extractives, Ca-lignosulfonates and mode of addition on alkylketene dimer retention, *Nord. Pulp Paper Res. J.*, **1**(2), pp. 31–38 (1986).
22. Lindström, T. and Söremark, C., Electrokinetic aspects of internal rosin sizing, *Svensk Papperstidning*, **80**(1), 22–28 (1977).
23. Lindström, T. and Söderberg, G., Studies on internal rosin sizing. Part 3. Effects of pH, electrolyte concentration and concentration of calcium-lignosulfate on size retention, *Svensk Papperstidning*, **87**(3) R2–R7 (1984).
24. Seppänen, R., Tiberg, F. and Valignat, M. P., Mechanism of internal sizing by alkyl ketene dimers (AKD). The role of the spreading monolayer precursor, *Nordic Pulp Paper Res. J.*, **15**, 452–458 (2000).
25. Yu, L. P. and Garnier, G., Mechanism of internal sizing with alkyl ketene dimers: the role of vapour deposition, in *The Fundamentals of Papermaking Materials*, Vol. 2, Baker, C. F., (Ed.), Pira International, Leatherhead, UK, 1997, pp. 1021–1046.
26. Marton, J., Dry-strength additives, in *Paper Chemistry*, 2nd Edn, Roberts, J. C., (Ed.), Blackie Academic Press, London, 1996, pp. 83–97.
27. Dunlop-Jones, N., Wet-strength chemistry, in *Paper Chemistry*, 2nd Edn, Roberts, J. C. (Ed.), Blackie Academic Press, London, 1996, pp. 98–119.
28. Lepoutre, P., The structure of paper coatings: An update, *Prog. Org. Coat.*, **17**, 89–106 (1989).
29. Brander, J. and Thorn, I. (Eds), *Surface Application of Paper Chemicals*, Blackie Academic press, London, 1997.
30. Järnström, L., The polyacrylate demand in suspensions containing ground calcium carbonate, *Nordic Pulp Paper Res. J.*, **8**, 27–33 (1993).
31. Järnström, L., Ström, G. and Stenius, P., The adsorption of dispersing and thickening polymers and their effect on the rheology of coating colors, *Tappi J.*, **70**, 101–107 (1987).
32. Fadat, G., Engström, G. and Rigdahl, M., The effect of dissolved polymers on the rheological properties of coating colours, *Rheol. Acta*, **27**, 289–297 (1988).
33. Hawe, M., The development and properties of associative thickeners, *Nordic Pulp Paper Res. J.*, **8**, 188–190 (1993).
34. Fadat, G., The influence of associative rheology modifiers on paper coating, *Nordic Pulp Paper Res. J.*, **8**, 191–194 (1993).
35. Adolfsson, M., Engström, G. and Rigdahl, M., The effect of the relaxation time of coating colours on the elimination of blade streaks, in *Proceeding of the 1989 Coating Conference*, Chicago, IL, 14–17 May 1989, Tappi Press, Atlanta, GA, 1989, pp. 55–58.
36. Husband, J., Interactions in coating colours containing clay, latex and starch, in *Proceedings of the Coating Conference*, Nashville, TN, 19–22 May 1996, Tappi Press Atlanta, GA, pp. 99–114.
37. Larson, R. G., *The Structure and Rheology of Complex Fluids*, Oxford University Press, New York, 1998.
38. Ramsey, J. D. F., and Lindner, P., Small-angle neutron scattering investigations of the structure of thixotropic dispersions of smectic clay colloids, *J. Chem. Soc., Faraday Trans.*, **89**, 4207–4214 (1993).
39. Alince, B. and Lepoutre, P., Flow behaviour of pigment blends, *Tappi J.*, **66**, 57–60 (1983).
40. Triantafillopoulos, N., *Paper Coating Viscoelasticity*, Tappi Press, Atlanta, 1996.
41. Lohmander, S., Martinez, M., Lason, L., Rigdahl, M. and Li, T.-Q., Dewatering of coating dispersions – model experiments and analysis, in *Proceedings of the 1999 Advanced Coating Fundamentals Symposium*, Toronto, Canada, 29 April–1 May 1999, Tappi Press, Atlanta, GA, 1999, pp. 43–58.
42. Letzelter, P., Dewatering of coating colours: A filtration or thickening mechanism?, in *Proceedings of the 1997 Advanced Coating Fundamentals Symposium*, Philadelphia, PA, 9–10 May 1997, Tappi Press, Atlanta, GA, 1997, pp. 103–131.
43. Sandås, S. E. and Salminen, P. J., The influence of the interaction between pigment and various cobinders on the rheology, dewatering and coating performance, in *Proceedings of the 1991 Coating Conference*, Montreal, Canada, 19–22 May 1991, Tappi Press, Atlanta, GA, 1991, pp. 51–59.

44. Roper, J. A., Bousfield, D. W., Urscheler, R. and Salminen, P., Observations and proposed mechanisms of misting on high-speed metered size press coaters, in *Proceedings of the 1997 Coating Conference*, Philadelphia, PA, 11–14 May 1997, Tappi Press, Atlanta, GA, 1997, pp. 1–14.
45. Adamson, A. W. and Gast, A. P., *Physical Chemistry of Surfaces*, John Wiley & Sons, New York, 1997.
46. de Gennes, P. G., Wetting: statics and dynamics, *Rev. Mod. Phys.*, **57**, 827–863 (1995).
47. Blake, T. D., Dynamic contact angles and wetting kinetics, in *Wettability*, Berg, J. C. (Ed.), Surfactants Science Series, Marcel Dekker, New York, 1993, pp. 251–309.
48. Kistler, S. F., Hydrodynamics of wetting, in *Wettability*, Berg, J. C. (Ed.), Surfactants Science Series, Marcel Dekker, New York, 1993, pp. 311–429.
49. Zisman, W. A., Relation of equilibrium contact angle to liquid and solid constitution, in *Contact Angle, Wettability, and Adhesion*, Fowkes, F. W. (Ed.), Advances in Chemistry Series, Vol. 43, American Chemical Society, Washington, DC, 1964, pp. 1–51.
50. Etzler, F. M., and Conners, J. J., The surface chemistry of paper: Its relationship to printability and other paper technologies, in *Surface Analysis of Paper* Conners, T. E. and Banerjee, S. (Eds), CRC Press, Boca Raton, FL, 1995, pp. 90–108.
51. Fowkes, F. M. and Mostafa, M. A., Acid–base interactions in polymer adsorption, *Ind. Eng. Chem. Prod. Res. Dev.*, **71**, 3–7 (1978).
52. van Oss, C. J., Chaudhury, M. K. and Good, R. J., Interfacial Lifshitz–Vanderwaals and polar interactions in macroscopic systems, *Chem. Rev.*, **88**, 927–941 (1988).
53. van Oss, C. J., *Interfacial Forces in Aqueous Media*, Marcel Dekker, New York, 1994.
54. Berg, J. C. and Pearson, S. W., The acid–base characterization of cellulosic fibers using inverse gas-chromatography, *Abstr. Papers Am. Chem. Soc.*, **203**, 256-COLL (1992).
55. Toussaint, A. F. and Luner, P., The wetting properties of grafted cellulose films, *J. Adhesion Sci. Technol.*, **7**, 635–648 (1993).
56. Lucas, R., *Kolloid Z* **23**, 15–22 (1918).
57. Washburn, E. W., Penetration of liquids into capillaries, *Phys. Rev. Ser. 2*, **17**, 273–283 (1921).
58. Tiberg, F., Zhmud, B., Hallstenson, K. and von Bahr, M., Capillary flow of surfactant solutions, *Phys. Chem. Chem. Phys.*, **2**, 5189–5196, (2000).
59. Bristow, J. A., Water vapor transmission rates through paper and board, *Svensk Papperstidning*, **70**, 623–629 (1965).
60. Conners, T. E. and Banerjee, S., (Eds), *Surface Analysis of Paper*, CRC Press, Boca Raton, FL, 1995, p. 346.
61. Dettler-Hoskin, L. D. and Busch, K. L., SIMS: Secondary ion mass spectroscopy, in *Surface Analysis of Paper*, Conners, T. E. and Banerjee, S. (Eds), CRC Press, Boca Raton, FL, 1995, pp. 206–234.
62. Friese, M. A. and Banerjee, S., FT-IR spectroscopy, in *Surface Analysis of Paper*, Conners, T. E. and Banerjee, S. (Eds), CRC Press, Boca Raton, FL, 1995, pp. 119–141.
63. Agarwal, U. P. and Atalla, R. H., Raman spectroscopy, in *Surface Analysis of Paper*, Conners, T. E. and Banerjee, S. (Eds), CRC Press, Boca Raton, FL, 1995, pp. 152–181.
64. Neimark, A. V. (Ed.), *Characterization of Porous Materials: From Angströms to Millimeters*, *Adv. Colloid Interface Sci.* (special issue), 76–77 (1998).
65. Rouquerol, F., Rouquerol, J. and Sing, K., *Adsorption by Powders and Porous Materials*, Academic Press, San Diego, 1999.
66. McFadden, M. G. and Donigian, D. W., Effects of coating structure and optics on inkjet printability, in *Proceedings of the 1999 Coating Conference*, Toronto, Canada, 2–5 May 1999, Tappi Press, Atlanta, A, 1999, pp. 169–178.
67. Furó, I. and Daicic, J., NMR cryoporometry: A novel method for the investigation of the pore structure of paper and paper coatings, *Nordic Pulp Paper Res. J.*, **14**, 221–225 (1999).
68. Ishikiriyama, K., Tudoki, M. and Motomura, K., Pore size distribution (PSD) measurements of silica gels by means of differential scanning calorimetry, *J. Colloid and Interface Sci.*, **171**, 92–102 (1995).
69. Strange, J. H., Rahman, M. and Smith, E. G., Characterization of porous solids by NMR, *Phys. Rev. Lett.*, **71**, 3589–3591 (1993).
70. Williams, G. J. and Drummond, J. G., Preparation of large sections for the microscopical study of paper structure, *J. Pulp Paper Sci.*, **26**, 188–193 (2000).

CHAPTER 8

Surface Chemistry in the Polymerization of Emulsion

Klaus Tauer

Max Planck Institute of Colloids and Interfaces, Golm, Germany

1	Introduction	175	6	Polymerization of (or in) Monomer Emulsions	191
2	A Little Relevant Thermodynamics	176	6.1	General features of suspension polymerization	192
3	Emulsification	179	6.2	General features of emulsion polymerization	193
3.1	General considerations	179	6.3	General features of miniemulsion polymerization	195
3.2	Preparation of emulsions by comminution–structure of the emulsion	180	7	Fixation of an Emulsion by Radical Polymerization in Aqueous Media–Fact or Fancy?	196
3.3	Preparation of emulsions by comminution–some practical considerations	181	8	References	198
3.4	Preparation of emulsions by condensation	184			
4	Stability of Emulsions	186			
5	Comminution or Condensation Techniques–What Makes the Difference?	190			

1 INTRODUCTION

Matter is, in our world, regardless of whether inorganic or organic, very often organized in such a way that a high surface- or interface-to-volume ratio represents a characteristic feature. All four fundamental elements of early Greek philosophy – earth, water, air and fire – contain millions of hectares of interfaces essential for maintaining life on our planet. It is evident that under these circumstances surface or interface chemistry¹ plays an essential role. Interface chemistry is necessary to preserve the interface, to support the exchange of matter and energy, and to allow chemical

reactions. Examples of such colloidal systems include fog, mist, smoke, mineral alloys, natural latex, milk, cells in living organisms and blood, but also nanometre-thick cellulose fibre bundles or the capillary system in plants and the muscular tissue and the vein system in living organisms. In the energy balance of colloidal systems, the interface or surface energy cannot be neglected. From a thermodynamic point of view the interface area adds to the extensive quantities of volume and amount of substance. Many of the colloidal systems are in the form of dispersions. The latter consists of at least two phases of one or more components. However, in most cases colloidal dispersions appear to the human eye as homogeneous. The characteristic dimension of the dispersed phase of a colloidal system is, independent of the shape, which can be either spherical,

¹ The terms interface and surface chemistry will be used interchangeably in the following text.

coil-like, fibre-like, cylindrical, ellipsoid, or any other, in the nanometre range and hence less than a thousandth of a millimetre. Sophisticated techniques, as for instance, light, X-ray and neutron scattering, electron microscopy, atomic force microscopy, confocal microscopy, fluorescence techniques, and analytical or preparative ultracentrifugation are needed to study dispersions.

Starting from the three states of matter – gas, liquid and solid – dispersed systems can consist of all possible combinations of interfaces, except the gas–gas interface. This present chapter is focused on the surface chemistry of liquid–liquid and solid–liquid dispersions. In detail, some thermodynamics is refreshed as is necessary for an understanding of emulsions, followed by a review of preparation methods and some remarks regarding emulsion stability, always with special emphasis regarding subsequent radical polymerization. Then, emulsion and suspension polymerizations are considered as technically important processes for the production of polymer dispersions. A polymer dispersion is considered as a colloidal system consisting of almost spherical polymer particles dispersed in water. The hydrophobic polymer is the dispersed phase (also called the inner phase), with water being the continuous phase (also called the outer phase or dispersion medium). In this sense, an emulsion consists of a polymerizable hydrophobic monomer or monomer mixture dispersed in water. Surface chemistry is important to keep the hydrophobic phase dispersed, and refers in particular to the chemical composition of the monomer and of the polymer interface which is influenced by the presence of surface-active compounds and also by the initiator system employed for the polymerization. In the following, the terms oil, organic phase or monomer will be used interchangeably and the term organic phase as a generic term may comprise both monomer and polymer. The use of the expressions *emulsion*, *suspension* and *dispersion* are, for historic reasons not unambiguous, and therefore an exact as possible a definition is necessary. A dispersion¹ is considered as a generic term for various systems which differ regarding the state of matter forming the dispersed and the continuous phases, respectively. Table 8.1 contains some definitions and examples of dispersed systems where the continuous phase is exclusively a liquid. These definitions are widely accepted in colloid science (1–3).

Water is by far the most important liquid forming the continuous phase in dispersions in both the natural and the technical world. Examples include all kinds of living organisms and synthetic latexes. It is necessary to point

Table 8.1. Dispersions with a liquid continuous phase^a

Dispersed phase	Technical term	Example
Gas	Foam	Meringue, Whipped Cream
Liquid	Emulsion ^b	Milk, Mayonnaise
Solid	Sol, Suspension ^c	Latex, Paint, Blood

^aBoth the continuous and the disperse phase can be composed of different components. Of particular importance is the liquid state of matter, i.e. the existence of a certain short-range order but no long-range order. In this sense, both the continuous and the disperse phase can be a polymer solution. This is of some importance in the following.

^bEmulgere (Latin): to milk out.

^cSuspendere (Latin): to keep in, to keep (in) floating.

out that a sol or a suspension made from inorganic solids is called a *slurry* (4). On the other hand, in the polymer colloids community the term dispersion is frequently used, e.g. it is quite common to call a polymer latex a polymer dispersion. Polymer dispersions can be prepared by different procedures, where the generic term for the direct synthesis is heterophase polymerization (5). This means that at least the polymer is insoluble in the dispersion medium and precipitates in the course of the reaction, thus forming the dispersed particle phase. In the sense of the definitions given in Table 8.1, the technical terms *emulsion* polymerization and *suspension* polymerization (both resulting in polymer-in-water suspensions) are somewhat irritating as the former refers to the state before polymerization and the latter to the final state after polymerization. Nowadays, it is quite common to subdivide the term emulsion into *macroemulsion*, *miniemulsion* and *microemulsion* with regard to the decreasing average droplet size. These droplet sizes for macroemulsions, miniemulsions and microemulsions are in the range of several micrometres, hundreds of nanometres, and some tens of nanometres, respectively. Each of these types of emulsions has been subjected to polymerization. In addition to emulsion and suspension polymerization, the so-called miniemulsion polymerization is considered in this review, as a great deal of work has been carried out on such systems over the past 25 years. Microemulsions are outside the scope of this present chapter. Features of the other polymerization techniques are discussed here especially with regard to the fate of the emulsion droplets.

2 A LITTLE RELEVANT THERMODYNAMICS

Some introductory remarks are necessary concerning the thermodynamics of the formation of interfaces and the relation to heterophase polymerization techniques. If two components are completely compatible they do

¹ Dispergere (Latin): to remove, to redistribute.

not form an interface, as is the case for dilute gases or two mutually soluble liquids. In this case, the free energy of mixing is negative. It is exactly the opposite if two incompatible components form an interface upon mixing. If a stable interface is formed, the free energy of formation must be positive. This behaviour finds its expression in a special form of the Gibbs–Helmholtz equation (equation (8.1)), where U^S is the total surface energy for a given interface (S), σ is the interfacial tension, and T is the absolute temperature¹:

$$U^S = \sigma - T \left(\frac{\partial \sigma}{\partial T} \right)_S \quad (8.1)$$

From the thermodynamic point of view only microemulsions are stable, i.e. their formation follows other laws different to these for the formation of macro- and miniemulsions (for some exceptions, see below). In the thermodynamic sense, stability means that the structure of the emulsion does not change with time and that it is independent of the preparation technique. However, emulsions can be prepared in such a way that their structure remains unchanged over longer periods of times, even up to years. In such cases, the emulsion is said to be kinetically stable. In the following text, the technical term “emulsion” is used in order to describe macroemulsions as well as miniemulsions. The preparation of emulsions requires energy to disperse the organic phase (monomer or polymer solution in an organic solvent) in water. In order to obtain some ideas about the thermodynamics, the change in the Gibbs free energy of the system (ΔG), provided by the particular dispersing procedure at constant composition and pressure, can be expressed by the following:

$$\Delta G = \Delta H - T \Delta S \quad (8.2)$$

The entropy (ΔS) is a measure of the extent of disorder in the system and hence measures the extent of size reduction of the organic phase (or increase in droplet number). The increasing disorder during the formation of an emulsion means a positive ΔS contributing to the stability. The term ΔH is the enthalpy of the system and can be considered as the binding energy of the organic bulk material or the energy input needed to achieve a certain average droplet size. If a volume change during the emulsification is neglected, the enthalpy corresponds to the internal energy which is the sum of the work required to expand the interfacial area (ΔW) and an amount of heat which results from wasting a

part of the energy input². The latter effect may lead to a temperature increase during emulsification. The term ΔW is given by equation (8.3) where ΔA is the increase in interfacial area and σ is the interfacial tension between the organic phase and water. Note that, the increase in the energy of the emulsion compared to the non-emulsified components is equal to ΔW . This amount of energy can be considered as a measure of the thermodynamic instability of an emulsion.

$$\Delta W = \sigma \Delta A \quad (8.3)$$

In the above equation, ΔW is the free energy of the interface and corresponds to the reversible work brought permanently into the system during the emulsification process³. This makes an emulsion very prone to coalescence processes which lead to a decrease in ΔA and subsequently in ΔW . The conclusion is straightforward that ultimate stability against coalescence processes is only achieved if σ approaches zero.

Equation (8.3) describes the influence of the interfacial tension on the emulsification process. For a given energy input, ΔA is lower the higher the value of σ , and vice versa. Thus, σ is a crucial parameter for any process that leads to a dispersion. If we define the interface as the area where the molecules of different phases meet a relationship must then exist between σ and the surface tensions (γ) of the neat phases⁴. The interfacial tension is in any case lower than the surface tension of the component with the higher value. The precise relationship between σ and the surface tensions of the organic phase and water depends on the chemical composition (more polar or more non-polar) and the orientation of the molecules at the interface (more flat or more stretched) (1, 6). A simple relationship (equation (8.4) below) allows an estimation of σ only from the interfacial tensions of the components (γ_o for the organic phase and γ_w for water) where Φ is a correction term which takes into account the different molar volumes⁵. Applying this equation to predict σ between polar organic liquids and water gives at least the same tendency as that obtained from experimental values (1).

$$\sigma = \gamma_o + \gamma_w - 2\Phi(\gamma_o\gamma_w)^{1/2} \quad (8.4)$$

² The amount of energy wasted as heat can be as high as 99% of the total input.

³ The total energy of the interface per surface area under isothermal conditions is given by equation (8.1).

⁴ Surface tension means the interfacial tension of the particular component to air, which is for a liquid saturated with its vapour and for a solid neat air.

⁵ $\Phi = 4(v_o v_w)^{1/2} / (v_o^{1/2} + v_w^{1/2})^{1/2}$, where v_o and v_w are the molar volumes of the organic and water phases, respectively.

¹ Note, for almost all systems $(\partial\sigma/\partial T)$ is negative.

However, for a detailed description it is also necessary to take into account dispersion and polar forces. Thus, it is usual to express the interfacial tension in the form of the following equation (7):

$$\sigma = \gamma_w + \gamma_o - 2(\gamma_w^d \gamma_o^d)^{1/2} - 2(\gamma_w^p \gamma_o^p)^{1/2} \quad (8.5)$$

The superscripts, "d" and "p" in the above equation refer to the contributions of dispersion and polar forces to the interfacial tension, respectively. Using the values for water, i.e. $\gamma_w = 72.8 \text{ mN m}^{-1}$, $\gamma_w^d = 22.1 \text{ mN m}^{-1}$ and $\gamma_w^p = 50.7 \text{ mN m}^{-1}$, and with some rearrangements, we obtain the following equation where X_o^p is the polarity of the organic phase (7):

$$\sigma = 72.8 + \gamma_o - \left[9.4 - 4.7X_o^p + 14.2(X_o^p)^{1/2} \right] \gamma_o^{1/2} \quad (8.6)$$

Table 8.2 summarizes the γ_o and σ values for water for different organic compounds and relates these values to the water solubility. The values given in Table 8.2 reveal that σ is a measure of the compatibility of an organic compound with water, which means that it inversely relates to the water solubility of pure hydrocarbons. This relationship is broken if the molecule contains a hydrophilic group which can strongly interact with water (compare 1-octanol vs. benzene). This means that, on the other hand, a strong interaction with water leads to a stronger decrease in σ despite the water solubility. Consequently, the values of the interfacial tensions between pure water and pure organic liquids vary over a quite broad range, from some

Table 8.2. Values of γ_o , σ and water solubility (C_w) for different organic compounds at 25°C

Organic compound	γ_o (mN m ⁻¹)	σ (mN m ⁻¹)	C_w (M) ^c
Hexadecane ^a	27.3	53.3	2.4×10^{-11}
Ethylbenzene ^a	29.2	38.4	1.6×10^{-3}
Benzene ^a	28.9	33.9	2.3×10^{-2}
1-Octanol ^a	27.5	8.5	4.2×10^{-3}
Ethyl acetate ^a	23.9	6.8	1.0
1-Butanol ^a	24.6	1.8	1.08
Methylacrylate ^b	24.2	13–14	0.64
Vinyl acetate ^b	22.9	18–19	0.30
Ethyl acrylate ^b	24.7	21–22	0.15
n-Propyl acrylate ^b	24.8	26–27	5.0×10^{-2}
n-Butyl acrylate ^b	–	30–31	1.7×10^{-2}
Styrene ^b	30.9	40–43	3.0×10^{-3}

^a γ_o and σ values from ref. (1).

^b γ_o values from ref. (8) and σ values from ref. (7).

^c C_w values from ref. (9).

50 mN m⁻¹ to about 1 mN m⁻¹ depending on the particular functional groups. In contrast to σ , the γ -values do not show any spectacular changes as they are in a quite close range between about 23 mN m⁻¹ and 30 mN m⁻¹.

This chapter treats the subject of interfacial effects while a monomer is converted into its polymer. Hence, the question arises concerning the interfacial properties of polymers. For some polymers typically prepared by heterophase polymerizations, values of the surface tension (γ_p) and interfacial tension to water are listed in Table 8.3. Compared to the data shown in Table 8.2, the values for the polymers are higher and especially the σ data can be understood in the same way as those of the low-molecular-weight compounds.

Equations (8.4)–(8.6) clarify that there is, for a given organic phase, a possibility to influence the interfacial tension by changing the dispersion medium, and hence changing γ_w . This is possible by adding organic water-soluble compounds as, for instance, alcohols. Methanol, ethanol, *n*-propanol and *n*-butanol are very efficient additives for reducing the surface tensions of aqueous solutions down into the range below 40 or 30 mN m⁻¹. The higher the carbon number and the concentration of the alcohol, then the greater is the decrease in γ_w (10). This effect is utilized in so-called dispersion polymerizations for the preparation of large and fairly monodisperse particles (11, 12).

Another possibility for altering σ is a complete change of the dispersion medium. Besides water other classes of suitable liquids are alkanes or perfluorocarbon fluids. By using such materials a drastic decrease in γ can be achieved (cf. Table 8.4) when compared to water ($\gamma_w = 72.8 \text{ mN m}^{-1}$). Indeed, it is the state of the art (also in larger-scale technical processes) to use certain petroleum fractions as continuous phases for the polymerization of hydrophilic monomers (so-called inverse heterophase polymerizations) to prepare, for instance flocculants for waste-water treatment or as aids for paper production (14). The large-scale application of perfluorocarbon fluids, however, is restricted

Table 8.3. Values of the surface tension and interfacial tension to water for various polymers^a

Polymer	γ_p (mN m ⁻¹)	σ (mN m ⁻¹)
Poly(butyl methacrylate)	31.2	36.7
Poly(vinyl acetate)	36.5	23.5
Polystyrene	40.7	32.7
Poly(methyl methacrylate)	41.1	26.0
Poly(vinyl chloride)	41.9	37.8

^a data from ref. (7) at 20°C.

¹ $X_o^p = \gamma_o^p / \gamma_o$; $X_o^d = \gamma_o^d / \gamma_o$; $X_o^p + X_o^d = 1$; $(1 - X_o^p)^{1/2} \approx 1 - X_o^p/2$.

Table 8.4. Surface tension values of alkanes and perfluorocarbon fluids (25°C)

N	γ (mN m ⁻¹) of C _n H _{n+2} ^a	γ (mN m ⁻¹) of C _n F _{n+2} ^b
6	17.9	12
7	19.8	13
8	21.1	14

^adata from ref. (8).^bdata from ref. (13).

due to the higher price and the special solubility characteristics. Nevertheless, the benefits of using perfluorocarbon fluids as continuous phases is evident, as due to the low γ values these fluids are capable of dispersing organic monomers without additives (13).

Regarding the topic of this chapter, possibly the most important way to influence the interfacial tension of a dispersion is the addition of surfactants¹. The special importance of surfactants in heterophase polymerizations is treated below. If an interface is completely covered by surfactants, σ is governed by the hydrophilic head groups of the surfactant. This situation can be treated approximately in analogy to a micelle. The free energy contribution of the head group (ΔG_{hg}) can be expressed by the following equation, according to ref. (15):

$$\Delta G_{\text{hg}} = \Delta G_{\text{el}} + A_{\text{hg}}\sigma_{\text{mic}} \quad (8.7)$$

The first term on the right-hand side of equation (8.7) is the contribution of the head group repulsion, while the second is the interfacial energy contribution where A_{hg} is the total surface area of the head groups and σ_{mic} is the interfacial tension. Within the framework of the GOUY-CHAPMANN theory, the dressed micelle model allows the estimation of σ_{mic} values, which are for sodium dodecyl sulfate (SDS), sodium octyl sulfate, and teradecyltrimethylammonium bromide, 15–16, 11 and 11–14 mN m⁻¹, respectively (15). Note that these values are up to a factor of 3 lower than those of the pure monomers (cf. Table 8.2). A further decrease of σ is possible in the case of emulsions of organic liquids where the interface is saturated with stabilizer. For example, a value of about 4 mN m⁻¹ was determined for a toluene emulsion stabilized with potassium laurate (16).

¹ The terms surfactant, stabilizer and emulsifier will be used interchangeably in the remainder of this chapter.

3 EMULSIFICATION

3.1 General considerations

An emulsion has been defined above as a thermodynamically unstable heterogeneous system of two immiscible liquids where one is dispersed in the other. There are two principal possibilities for preparing emulsions: the destruction of a larger volume into smaller sub-units (comminution method) or the construction of emulsion droplets from smaller units (condensation method). Both methods are of technical importance for the preparation of emulsions for polymerization processes and will be discussed in more detail below. To impart a certain degree of kinetic stability to emulsions, different additives are employed which have to fulfil special demands in the particular applications. The most important class of such additives, which are also called emulsifying agents, are surface-active and hence influence the interfacial properties. In particular, they have to counteract the rapid coalescence of the droplets caused by the van der Waals attraction forces. In the polymerization sense, these additives can be roughly subdivided into surfactants for emulsion polymerization, polymers for suspension and dispersion polymerization, finely dispersed insoluble particles (also for suspension polymerization), and combinations thereof (cf. below).

In any case, the formation of an emulsion is a dynamic process and hence, instead of the static interfacial tensions, the corresponding dynamic values are much more meaningful². The dynamic surface tension is always higher than the static value. The difference can be as high as 40 mN m⁻¹ and depends, in addition to the age of the interface, mainly on the kind of the surfactants and on the solution viscosity (17, 18).

The general actions of emulsifying agents in emulsions, independently of the emulsification method, are: (i) lowering of the interfacial tension, hence supporting the emulsification, (ii) formation of a barrier around the droplets, thus delaying the coalescence by changing the electrostatic, steric, viscous and elastic properties of the interface, and (iii) generation and maintaining of a gradient of the interfacial tension (gradient of the interfacial density of surfactant molecules) across the droplet surface during undulations caused by thermal or

² Dynamic surface tension refers to the fact that the surface tension needs a certain time to reach a static value (time-independent or equilibrium value) due to diffusion of the surfactants to the interface and possibly rearrangements to find the thermodynamically favoured conformation. Note, however, that for pure liquids the dynamic and static surface tensions have the same values.

mechanical stresses. The latter effect also contributes to the stability of emulsions and is strongly connected with the Gibbs–Marangoni effect (19). The interfacial tension gradient leads to a stress at the droplet interface, which causes a flow inside the droplets opposing the water and surfactant drainage between two approaching droplets. Note that film rupture between two droplets is a prerequisite for droplet coalescence. This stabilization mechanism is especially effective at surfactant concentrations below or at about the critical micelle concentration, for surfactants with slow dynamics, and if the difference between the dynamic and static surface tension is high.

An important conclusion of these considerations is that a practically useful emulsion is by no means a neat two-component system but contains a variety of additives to impart a certain kinetic stability (cf. Section 4 below).

3.2 Preparation of emulsions by comminution – structure of the emulsion

Emulsification by comminution (20–22) is very common, the most widely used procedure for emulsion preparation. It can be carried out with very simple equipment, as for instance, a spoon in a bowl during the preparation of salad dressing in the kitchen for mixing water and oil.

Under the action of intense mechanical energy, any combination of immiscible and mutually non-reactive liquids can be broken up into an emulsion. The most interesting question to be asked after completion of the emulsification is that concerning the structure of the emulsion, i.e. which liquid forms the dispersed phase and which will be the continuous one? The result of the emulsification process is influenced by the volume ratio of the liquids, the kind of emulsifying agent, and its concentration in close relation with the temperature. The most important property of the emulsifying agent is its solubility (in both phases), or in the case of solid stabilizers, the wetting behaviour of both liquids.

Bancroft summarized the results of emulsification experiments carried out from the late 19th until the early 20th century by a “rule of thumb” which stated that in order to have a kinetically stable emulsion the emulsifying agent must be soluble in the continuous phase (23). In principle, this rule finds its expression in the empirical system of the HLB values (hydrophilic–lipophilic balance) which was developed in the middle of the 20th century to allow the

selection of the most effective emulsifier for a desired type of emulsion (24). Such HLB values were determined from tedious emulsification experiments. Consequently, several attempts have been made to develop predictive methods based on the HLB concept for the classification of surfactants. A summary of group numbers for hydrophilic and hydrophobic groups, together with some good guidance as to when the use of the HLB concept is helpful, but also hints as to when problems may occur, can be found in refs. (2, 25, 26). For heterophase polymerizations, both Bancroft’s rule and the HLB concept are quite useful in selecting surfactants for “normal” polymerizations where water is the continuous phase or for inverse systems where a non-polar organic liquid is the medium. Typical emulsifiers for “normal” emulsion polymerizations are, for instance, sodium dodecyl sulfate, sodium alkyl sulfate (average carbon chain length of 15), sodium palmitate or poly(ethylene glycol)(15) cetyl ether with HLB values of about 40, 10.9, 19.8 and 15.4, respectively. In contrast, sorbitan monostearate and sorbitan monolaurate, which are typical surfactants for inverse polymerizations, have HLB numbers of 4.7 and 8.6, respectively (26). These examples illustrate that emulsifiers with HLB values lower than 10 are good for inverse polymerizations, while those with values larger than 10 are suitable for polymerizations in water (as the continuous phase). As mentioned above, temperature has a strong influence on the result of the emulsification process, especially if a surfactant with a poly(ethylene glycol) chain is used. In this case, consideration must be given to the fact that poly(ethylene glycol)s are soluble in both organic phases and water, where the solubility at highest temperatures is highest in organic solvents (also in monomers such as styrene and acrylates). Hence, poly(ethylene glycol)-based surfactants may stabilize either an oil in water or the inverse emulsion, depending on the temperature employed. This behaviour is the consequence of a lower critical solution temperature (or a cloud point) at approximately 100°C in aqueous solutions (27). The change in the properties with temperature is considered via the concept of the phase inversion temperature (PIT) (2). This is very useful in predicting the properties of nonionic surfactants based on poly(ethylene glycol), where the latter is the most important hydrophilic group in nonionic emulsifiers, and also for polymerizations. It is interestingly to note that at the PIT, both the interfacial tension and the droplet size are at their minima. The consequences of these properties of the poly(ethylene glycol) chain for heterophase polymerizations will be briefly discussed below.

3.3 Preparation of emulsions by comminution – some practical considerations

The input of mechanical energy into a two component liquid system causes a stepwise increase in the interfacial area until a steady state is reached. This process, as schematically illustrated in Figure 8.1, is assumed to be independent of the particular comminution procedure. There are four main groups of comminution techniques, namely rotor/stator systems (including all type of stirrers), high-pressure homogenizers, ultrasound devices and membrane techniques. Besides membrane techniques all of the other techniques are based on the input of mechanical energy, in the course of which eddies are formed, thus transferring the mechanical energy to the droplets. As almost all technical heterophase polymerizations utilize stirrers, the principles of emulsification with stirrers are considered here in more detail. Furthermore, stirring is the technically most important procedure for enhancing heat, as well as mass transfer processes and to counteract sedimentation, creaming and coalescence. The stirrer generates macro-eddies or macro-turbulences with a characteristic length of the order of the stirrer diameter. These macro-eddies decompose into micro-eddies with a characteristic length λ which is also called the Kolmogorov length (28). These micro-eddies are eventually responsible for the energy transfer and hence the breakage of the macroscopic phase. The Kolmogorov length relates to the kinematic viscosity of the solution (ν) and the dissipation rate (ε), which is the power input by the stirrer

(P) per mass (m) (cf. equation (8.8)) (29):

$$\lambda = \left(\frac{\nu^3}{\varepsilon} \right)^{1/4} \quad (8.8)$$

The emulsification proceeds in such a way that as soon as the shear exerted by the turbulent micro-eddies on the droplet interface exceeds the cohesive forces of the liquids in the drops, they split up to smaller units (cf. (a)–(b) in Figure 8.1). The cleavage occurs as long as a balance between the external stress and the internal stress is achieved. At this steady state, the droplet size distribution (DSD) becomes time-independent (Figure 8.1(d)). The droplet size distribution curve is frequently self-preserving during the emulsification process. This means that the median diameter characterizes the time evolution and that a master size distribution curve can be constructed by normalizing the size with respect to the median value (30). Note, however, that the external stress is governed by ε and the internal stress by the product of the interfacial tension and droplet diameter (D_d). In other words, the interfacial tension forces a spherical shape on the droplets and counteracts the droplet deformation and subsequent breakage by the shear stress. The attack of the shear stress upon the droplet leads to a deformation of the interface (cf. Figure 8.1). This leads to an increase in the Laplace pressure difference (ΔP) according to equation (8.9) as the curvature is locally decreased:

$$\Delta P = \frac{\sigma}{(r_a + r_b)} \quad (8.9)$$

where (r_a and r_b are the principal radii of curvature) and ΔP is related to capillary forces which also try to preserve a given drop. A third class of forces counteracting droplet breakage is the viscoelastic force of the dispersed phase. The solution viscosity is a direct measure of the viscoelastic force, and its influence on the emulsification process can be verified comparatively simply. The results obtained by the emulsification of an aqueous bovine serum albumin solution in dichloromethane containing poly(methyl methacrylate) (PMMA) as stabilizer with different agitation machines are summarized in Table 8.5 (31). The viscosity in both phases was varied by changing the PMMA and the bovine serum albumin concentration, respectively. The data shown in Table 8.5 clearly confirm the influence of the viscoelastic forces on the emulsification. The dependence of D_d on η_d is as expected: the higher the η_d , then the less effective is the emulsification and the higher the equilibrium droplet size. However, it is interesting to note that the equilibrium droplet size decreases much more

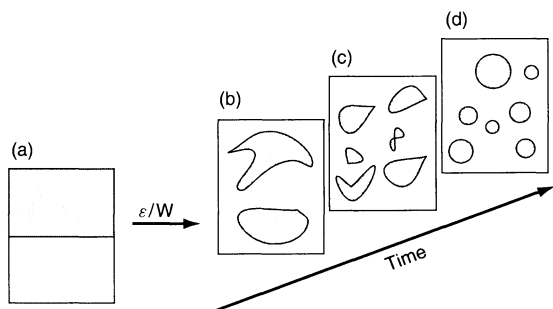


Figure 8.1. Schematic representation of the advancing emulsification process of two immiscible liquids during the input of mechanical energy (ε or W), where the white areas within the frames represent the continuous phase and the shaded areas the dispersed phase; (not to scale). The formation of locally different curvatures is clear to see. The equilibrium state (d) is characterized by the lowest average curvature and a spherical drop shape with a certain drop size distribution

Table 8.5. Relationship between the average droplet size and the viscosity of the dispersed phase (η_d) and the continuous phase (η_c) in different agitation machines (31)

Agitation machine	Relationship
Rotor/stator homogenizer	$D_d \propto \eta_d^{0.11} \eta_c^{-0.43}$
Baffled mixed tank	$D_d \propto \eta_d^{0.22} \eta_c^{-0.42}$
Static mixture	$D_d \propto \eta_d^{0.004} \eta_c^{-0.56}$

strongly with an increasing viscosity of the continuous phase. This clearly shows that the shear stress acting on the droplets during the emulsification increases with increasing viscosity. Furthermore, the data show that the kind of emulsification apparatus employed has a more or less pronounced influence. This is quite evident, as the energy input and its microscopic action is different for the different devices.

In a systematic study, the emulsification of paraffin oil ($\eta_d = 32 \text{ mPa s}$) in water with an oil volume fraction of 0.1, in the presence of 50 mM sodium dodecyl sulfate (SDS) as emulsifier at 20°C was investigated in various agitation machines (32). The interfacial tension in this particular system was determined to be 7 mN m^{-1} . The conditions were adjusted in such a way that the diminution energy (W_V) in each machine was equal to $5 \times 10^6 \text{ J m}^{-3}$. The diminution energy is defined as the power input per volume. The data presented in Table 8.6 reveal, on the one hand, how different the necessary condition are for the different devices to achieve the same W_V , and on the other hand, the influence of the geometry of the device on the droplet size distribution.

These data allow us to estimate ΔW according to equation (8.3), as well as the efficiency of the emulsification process. For the STR system, the increase in ΔA is about 180 m^2 (assuming an average $D_d = 65 \text{ }\mu\text{m}$) which corresponds to a reversible work value

of 63 J m^{-3} . This estimation makes clear that most of the diminution energy is not required according to equation (8.3) but is needed for other purposes or wasted is as heat. A considerable part of this energy is used to break up the viscous resistance during the stirring. Note that the energy efficiency of an emulsification process by agitation is extraordinarily low. In general, D_d decreases with increasing ε , but increases with increasing volume fraction of the dispersed phase.

The same authors (32) also reported on the influences of the sodium dodecyl sulphate (SDS) concentration on the DSD. The latter distribution is basically bimodal in form and the main fraction is shifted towards smaller diameters with increasing SDS concentrations from 5 mM up to 100 mM. It is interesting to note that the range of the DSD remains almost unchanged, between 30 μm and 500 nm, over the entire investigated concentration range.

A special kind of energy input during the emulsification process is the application of ultrasound. As acoustic energy is not absorbed by molecules, its action is also purely mechanical. To achieve a good result for the comminution, high-power ultrasound must be used. Ultrasound refers here to the application of high-frequency vibrations. In a first step, larger drops ($D_d \gg 100 \text{ }\mu\text{m}$) are produced in such a way that instabilities of the interfacial waves will be enhanced, thus leading finally to the crushing. These drops are subsequently fragmented into smaller ones by acoustic cavitation. The use of ultrasound in emulsification processes is much more efficient than the application of rotor/stator systems. This was shown in a systematic comparison between an Ultra Turrax ($n = 10000 \text{ rpm}$, 170 W) and an ultrasound horn (20 kHz, 130 W) in emulsification experiments with kerosene in water (25 vol% kerosene; total volume of 80 ml) with a polyethoxylated (20EO) sorbitan monostearate surfactant (interfacial tension of kerosene to

Table 8.6. Influence of different rotor/stator systems on the steady-state droplet size distribution (32): n , stirrer speed in rotations per minute; t_d , dispersion time; v , volume flow rate

Machine	Conditions for $W_V = 5 \times 10^6 \text{ J m}^{-3}$	Maximum D_d in DSD
STR ^a	$n = 500 \text{ rpm}$, $t_d = 60 \text{ min}$	60–70 μm
Screw loop ^b	$n = 4000 \text{ rpm}$, $v = 350 \text{ l h}^{-1}$	10–11 μm and 2 μm
Ultra Turrax ^c	$n = 10000 \text{ rpm}$, $t_d = 2 \text{ min}$	10–11 μm and 2 μm

^aSTR, stirred tank reactor consisting of a cylindrical vessel (diameter 30 cm, volume 21.2 l) with a flat bottom and four symmetrical baffles and a six-blade disc impeller with a diameter of 10 cm.

^bScrew loop reactor, with the volume of the dispersing zone about 64 ml and a reactor volume of 1.67 l.

^cUltra turrax T50 (from IKA) with the dispersing tool (type S50-G45F) used in a cylindrical vessel with a volume of 8 l.

water, 9.5 mN m^{-1}) (33). The results clearly show that ultrasonification leads to a smaller D_d , a less polydisperse DSD, more stable emulsions, and less surfactant consumption for a desired D_d . With ultrasound emulsification, it was possible to obtain droplets with diameters down to 200 to 300 nm. In contrast, the smallest droplet size obtained with the Ultra Turrax was about $1.5 \mu\text{m}$. The values of D_d increase with an increase in the oil volume fraction for both techniques. However, this increase is considerably stronger for the Ultra Turrax system. Furthermore, these same authors also showed that for the ultrasound horn only 53 W were wasted as heat, whereas for the Ultra Turrax system a heat flux of 120 W was determined.

A common feature of all of the comminution processes considered so far is a stepwise fragmentation, up until a balance of forces and hence a steady-state DSD is reached. The final average D_d is very different for different comminution techniques. Furthermore, the droplet breakage is influenced by the viscosity of both phases. As the emulsion viscosity is different from that of the starting liquids, the following question then arises: "what would happen if an emulsion which was prepared by a certain comminution technique is exposed to a different shear stress?"¹. This subject was recently treated very successfully by Mason and Bibette (34). These authors subjected emulsions which were prepared in a stirred tank by normal agitation to a shear stress formed in a Couette flow. These pre-emulsions consisted of polydimethylsiloxane oil (volume fraction ϕ) in water stabilized with a nonionic surfactant (nonylphenol with seven ethylene oxide units; mass fraction with respect to water, C). At shear rates larger than 10 s^{-1} in the Couette flow the polydisperse pre-emulsions start to convert into monodisperse ones. This was exemplified, in a C versus ϕ diagram where the monodisperse region is located at a shear rate of 10^3 s^{-1} between C and ϕ values of $0.6 < 0.9$ and $0 < \text{ca. } 0.9$, respectively. The dependence of the final droplet size on the emulsifier concentration is as expected; i.e. D_d decreases with increasing C . However, in contrast to other mechanical comminution techniques like ultrasound, Ultra Turrax (33), and the screw loop reactor (32), during the fragmentation of prefabricated emulsions in a Couette flow, D_d decreases with the increasing volume fraction of the organic phase. This is a remarkable result as it indicates fundamental differences in the comminution mechanisms. This possibility for producing highly monodisperse emulsions is of

some practical importance regarding emulsion stability and also the use of individual droplets as micro- or nano-reactors for polymerization processes (see below).

The above emulsification methods (perhaps except the Couette flow technique) have as a common feature that the final DSD is primarily determined by the interaction of turbulent eddies with interfaces. Note, however, that turbulence is hard to control and to maintain consistently throughout the whole reactor volume. From a practical point of view, it is almost impossible to predict the DSD after a scale-up based on laboratory-scale experiments. Emulsification techniques based on other principles are necessary to overcome these drawbacks. An alternative technique is the so-called membrane emulsification method where the liquid forming the disperse phase is pressed through a porous membrane². The other side of the membrane where the droplets are formed is in contact with the continuous phase. This concept is simple and it is assumed to be superior to the above techniques (35). The basic relationship of membrane emulsification (equation (8.10)) correlates the trans-membrane pressure required to start the dropwise flow through the pores (P_C) with the average pore diameter of the membrane (D_M) with Θ being the contact angle of the mixture with the wall of the pore:

$$P_C = \frac{4\sigma \cos \Theta}{D_M} \quad (8.10)$$

For the successful preparation of emulsions, the wetting conditions on the membrane surface are crucial. It is necessary that the membrane surface is only wetted by the liquid that forms the continuous phase. The droplet size correlates with the membrane pore size by a simple relation, $D_d = f D_M$, where f is a value typically between 2 and 8 (35). Droplets can be produced with diameters in the μm -, as well as in the sub-micrometre range. This technique has been successfully applied to produce monodisperse emulsions and multiple emulsions, as well as to carry out polymerizations leading to polymer particle in the μm size range with narrow size distributions (36, 37). Further advantages (38) are as follows: the droplet size is controllable and generally a quite narrow DSD can be achieved, the method is reproducible and the scale-up is easy just by increasing the number of membrane modules, the characteristic features are independent of scale-up, batch as well as continuous operations modes are possible, the continuous phase is exposed to a lower stress,

¹ Note that the shear stress is the product of shear rate and viscosity and hence it combines the emulsion properties with the properties of the comminution technique.

² This technique was first reported at the 1988 Autumn Conference of the Japanese Chemical Engineering Society, utilizing a microporous glass membrane made of $\text{CaO-Al}_2\text{O}_3\text{-B}_2\text{O}_3\text{-SiO}_2$.

and the required diminution energy to obtain a D_d of 1 μm is orders of magnitude lower when compared to a rotor stator/system or a high-pressure homogenizer. The latter is important for preventing chemical degradation or polymerization already occurring during the emulsification.

In concluding this part, the emulsification process is influenced by various parameters, such as the volume phase ratio, the viscosity of both phases, the mutual solubility of both phases, the kind and concentration of additives, the power input, the stirrer as well as the vessel geometry, the diminution energy and the thermodynamic changes during the emulsification process (reactions, temperature etc.).

3.4 Preparation of emulsions by condensation

In contrast to comminution techniques, the preparation of emulsions by condensation techniques does not require mechanical energy, except sometimes gentle stirring to avoid creaming or settling due to density differences between the two phases. These condensation processes are mainly determined by thermodynamic principles. There are basically two different types of condensation methods, i.e. droplet nucleation and swelling of dispersed phases, although also a combination of the two has some meaning, especially for heterophase polymerizations.

The nucleation of droplets requires the creation of a supersaturation¹ of "liquid-l" (the liquid that will form the disperse phase) "in liquid-w" (the liquid that will form the continuous phase). Normally, the supersaturation is created starting from a solution of liquid-l in liquid-w by changing the solubility conditions for liquid-l. This can be done either by changing the temperature, pressure or solvency power. Droplet nucleation occurs at a critical supersaturation as soon as the droplet nucleus has a size (D_d^c) that allows it to surmount the free energy barrier (ΔG_{max})². The drop formation is an energy-consuming process regarding the formation of the interface, although some energy is gained (ΔG_v) as the new, dispersed phase is thermodynamically more stable than the supersaturated solution. The energy gain (ΔG_v) depends on the drop volume, and hence the change in the free energy of homogeneous droplet formation (ΔG_{nuc}) can be expressed by the following

equation:

$$\Delta G_{\text{nuc}} = \pi \sigma D_d^2 - \frac{\pi}{6} D_d^3 \Delta G_v \quad (8.11)$$

Both the size of the critical nucleus (see equation (8.12)) and the energy barrier (see equation (8.13)) strongly depend on the supersaturation and the interfacial tension, where v_m is the size of a molecule of liquid-l and $k_B T$ is the thermal energy.

$$D_d^c \propto \frac{\sigma v_m}{k_B T \ln S} \quad (8.12)$$

$$\Delta G_{\text{max}} = \frac{\sigma^3 v_m^2}{(k_B T \ln S)^2} \quad (8.13)$$

In the above, ΔG_{max} is essentially the barrier to the formation of the dispersed phase. If once a nucleus with the critical size is formed, the addition of the next molecule makes it free-growing and consequently, a liquid drop will appear. The presence of emulsifying agents preserves the stability of the droplets. However, surface-active materials can also influence σ and thus, may have a direct influence on the nucleation.

Emulsification by swelling presupposes that already a phase exists which can be swollen. Another prerequisite is that the swelling agent has to diffuse through the continuous phase and hence it must have a certain solubility in it. The phase capable of swelling can either consist of micelles, microemulsion droplets or dispersed particles. Each of these phases can be swollen with a liquid that is a solvent for it. In this sense, microemulsions can be considered as swollen micelles. They are thermodynamically stable since the huge number of microemulsion droplets causes a high entropy gain during their formation which exceeds the energy cost of the large interface. Additionally, σ contributes to the stability as it is of the order of 10^{-5} N m^{-1} . For instance, a mixture of 10.5% SDS, 15% 1-pentanol, 59.5% water and 15% *n*-dodecane forms a microemulsion with an average diameter of 10 nm (39). If such a microemulsion is diluted into a 50-fold amount of water, it decomposes into a miniemulsion with an average droplet diameter of 60 nm. Although the droplet size increases during the dilution, it is not a swelling process. Coalescence processes seem to play a role as well, since the droplet number decreases. The miniemulsion is no longer thermodynamically stable since σ has increased to about 10^{-3} N m^{-1} . Immediately after their formation, the miniemulsion droplets starts to grow in size.

It has been known for almost 50 years that fatty alcohols (for instance, lauryl alcohol) acts as an emulsifying adjuvant for ammonium fatty acid soaps during emulsion polymerizations (40). In the presence of

¹ Supersaturation is the ratio of concentration and solubility.

² This is not the case if nucleation occurs along the spinodal or is completely heterogeneous, as in both cases, ΔG_{max} is zero.

soap and alcohol, in a 2:1 stoichiometry, polymerizable miniemulsion droplets are formed. This process obviously also involves the diffusion of the monomer through the aqueous phase into the structures formed by the mixed surfactant system. The synergistic action of the alcohol surfactant mixture results in less energy demand for the emulsification process (gentle stirring is enough) and an enhanced droplet stability. This effect is called *spontaneous emulsification* and its mechanism is still a matter of controversial discussion (41). These same authors also report that the presence of small amounts of a highly water-insoluble compound in the monomer phase prevents the formation of a miniemulsion¹. This is a remarkable experimental observation as it underlines the importance of diffusion processes through the aqueous phase for the spontaneous emulsification. In this context, it is interesting to note that surfactant-alcohol mixtures possess a variety of exceptional properties, as for instance, the highest packing density, the lowest interfacial tension, the highest surface viscosity, a minimum in the droplet/bubble size, and formation of the most stable microemulsions (2, 42, 43).

A pure swelling process of a very fine emulsion which has been prepared by intense homogenization of a low-molecular-weight compound (Y)² with an extremely low water solubility is described in ref. (41). Subsequent addition of an oil to this pre-emulsion leads to the formation of a stable emulsion. The swelling capacity of the droplets of "compound-2" is up to 10⁴ times higher than that of the polymer particles. Compound-2 can be, for instance, hexadecane or another highly water-insoluble substance which can be active during a radical polymerization (for example, a monomer or an initiator). However, the so prepared emulsion droplets are not very monodisperse, although their size and size distribution can be controlled to some extent by the homogenization process during the preparation of the Y-emulsion (41).

A modified technique to produce emulsion droplets is the so-called activated swelling method starting from polymer particles (41). Note, as per the definition given above, a polymer solution is also considered to form an emulsion. This procedure implies that the first seed particles, which may be composed of any polymer, are swollen with the highly water-insoluble compound-2 in a volume ratio between 1:1 and 5:1. These seed particles can be very monodisperse if prepared by the

right heterophase polymerization technique. In a second step, the oil is added and again, compound-2 increases the swelling capacity drastically when compared to the neat seed particles. This procedure leads finally to very monodisperse droplets where the compound-2 acts as the swelling promoter.

Another suitable way for preparing emulsions by condensation methods is the combination of droplet nucleation and swelling. Again, the phase to be swollen consists of latex particles. The oil droplets swelling these particles are nucleated from a supersaturated solution by changing stepwise the solvency for the oil. This technique is called the *dynamic swelling method* (44). The following example clarifies the principle of action where the oil phase is styrene and the seed particles consist of polystyrene. In a mixture of 6 g ethanol and 4 g water as solvent, 0.4 g styrene, 0.004 g benzoyl peroxide and variable amounts of poly(vinyl alcohol) (PVAI) stabilizer (between 3.75 and 37.5 wt% based on styrene) are dissolved. The supersaturation is created by adding 40 g water using a micro-feeder with a rate between 0.53 and 800 ml h⁻¹. Due to the stepwise addition of water, the solvency power for styrene gets increasingly worse until the conditions for droplet nucleation are met. In the absence of seed particles, the nucleated droplets will form a styrene emulsion. However, this emulsion has a rather polydisperse DSD. The average droplet size is the higher for both a lower PVAI concentration and water feeding rate. This situation changes completely if seed particles are present which soak up the oil as soon as it is nucleated from the aqueous phase. This is exemplified by the case where, at a water feeding rate of 2.88 ml h⁻¹ and in the presence of 3.75 wt% PVAI, together with 0.004 g polystyrene seed particles with a particle diameter (D_p) of 1.8 μm , which were prepared by dispersion polymerization in an ethanol-water mixture, a monodisperse styrene emulsion is formed with a D_d of 8.5 μm . Again, as in the above-mentioned example of the activated swelling method, the presence of monodisperse polymeric seed particles leads to the formation of an emulsion with a monodisperse DSD. Note that in the latter case no swelling promoter is necessary. The driving force for the enhanced swelling is the high Laplace pressure inside the small styrene droplets after nucleation compared to the seed particles, and the swelling proceeds via Ostwald ripening (see below). Additionally, the freshly nucleated droplets are rather unstable due to the high dynamic interfacial tension of PVAI, which as a polymer only slowly adsorbs and equilibrates.

¹ Note that the same effect can be used to stabilize emulsion droplets against dissolution (see below).

² The "Y-component" is the original name given by the authors; however, the notation "compound-2" is used henceforth in the following discussion.

4 STABILITY OF EMULSIONS

As stated above, emulsions are thermodynamically unstable but they can be made kinetically stable by the use of additives. These additives are either surface-active compounds soluble in the continuous phase, or polymers, which can be soluble in both phases. Emulsion can degrade via different mechanisms as illustrated in Figure 8.2. Basically, four different mechanisms are involved i.e. phase separation, Ostwald ripening, aggregation (as a generic term for flocculation or coagulation and coalescence) and phase inversion. Generally, it has to be heeded that changes in the thermodynamic conditions (composition and temperature) compared to the preparation conditions may have a devastating influence on emulsion stability.

Phase separation (route 1 in Figure 8.2) means that an emulsion may separate into two phases: one phase enriched with the droplets and the other enriched with the continuous phase. These kinds of separation are called *creaming* or *sedimentation* if the upper phase and the lower phase is formed by the drops, respectively. Note that the sediment or the cream are themselves both dispersions, but with a much higher volume fraction of the dispersed phase. The phase separation is macroscopic and does not lead to a coalescence of the dispersed drops. The stationary velocity for laminar conditions during phase separation

(V_{ps}) depends, according to equation (8.14) on the difference of the densities of the dispersed (ρ_d)¹ and the continuous phases (ρ_c), on D_d , on η_c , and on the gravitational acceleration field g :

$$V_{ps} = (\rho_d - \rho_c) \frac{D_d^2 g}{18\eta_c} \quad (8.14)$$

As a rule of thumb, if D_d is above 1 μm , sedimentation and creaming may occur for $\rho_d > \rho_c$ and $\rho_d < \rho_c$, respectively. If the droplet size is smaller than 1 μm and if water is the continuous phase and a common monomer being the oil, then Brownian motion is able to keep the droplets almost evenly distributed throughout the emulsion.

Ostwald ripening (route 2 in Figure 8.2) as a degradation mechanism is a direct consequence of the polydispersity of the DSD whereby even a thermal fluctuation in D_d or in the curvature may cause it. It is easy to show that the chemical potential of a dispersed phase, compared to that of the same bulk material, is increased by $4\sigma v_m/D_d$ (45). Consequently, for the concentration of the disperse phase just at the interface ($C(D)$ where σ holds), we obtain equation (8.15)² with C_0 being the solubility of the disperse phase in the continuous medium:

$$k_B T \ln C(D) = \frac{4\sigma v_m}{D_d} + k_B T \ln C_0 \quad (8.15)$$

For colloid chemistry, an important conclusion to be drawn from equation (8.15) is that the smaller the species are, then the higher is the $C(D)$. As D_d goes to infinity, $C(D)$ will then equal C_0 . This means that, smaller species have a tendency to dissolve, whereas larger species grow by the uptake of matter which is released from the smaller ones. Two important points should be noted, however, i.e. (i) Ostwald ripening needs to occur at a certain water solubility of the liquid-1, and (ii) direct contact between the droplets is not necessary as molecular diffusion through the continuous phase leads to an increase in D_d . Based on these considerations, it was supposed that it might be

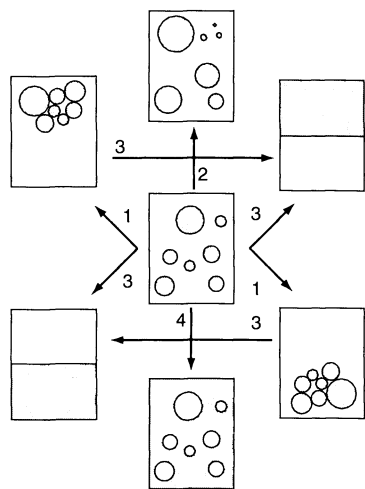


Figure 8.2. Schematic representation of the different degradation mechanisms of emulsions, where the white areas within the frames represent the continuous phase and the shaded areas the dispersed phase (not to scale): 1, phase separation; 2, Ostwald ripening; 3, aggregation (coalescence as the final state is shown); 4, phase inversion

¹ The density of the disperse phase means exactly the density of the droplets during the motion. A moving droplet is composed of liquid-1 and stabilizers, and in some cases also a certain amount of continuous phase which is entrapped in a layer surrounding the droplets.

² The free energy of a dispersion (G_{disp}) can be expressed as $G_{disp} = G_{bulk} + \sigma A$, where G_{bulk} is the free energy of the same amount of liquid-1 as bulk phase. By differentiating this equation after n (the number of molecules forming a droplet, i.e. $n = \pi D_d^3 / (6v_m)$), the chemical potential, $\mu_{disp} = \mu_{bulk} + (4\sigma v_m / D_d)$, follows. The chemical potential of liquid-1 dissolved in the continuous phase is expressed as $\mu_c = \mu_{c0} + k_B T \ln C$, where μ_{c0} is a reference value. At equilibrium, $\mu_{disp} = \mu_c$, and with $\mu_{bulk} - \mu_{c0} = k_B T \ln C_0$, equation (8.15) then follows. Note that both $C(D)$ and C_0 are volume fractions.

possible to stabilize emulsions against Ostwald ripening by the addition of small amounts of a third component which preferentially should dissolve in liquid-1 and not in the continuous phase. This was carried out by Higuchi and Misra (46) and experimentally verified by the stabilization of a carbon tetrachloride emulsion in water with hexadecane. Ostwald ripening in the presence of compound-2 was theoretically investigated by Kabalnov *et al.* (47). Two cases are of special interest regarding polymerizations. First, the solubility of the second component in the continuous phase is zero ($C_{02} = 0$) which means that the total number of particles remains constant. However, the distribution of liquid-1 from small to large particles changes the composition of the particles. This increases the volume fraction of compound-2 (ϕ_2) in the smaller particles and decreases it in the larger ones. Indeed, investigations carried out on Ostwald ripening with sedimentation field-flow fractionation in fluorocarbon emulsions confirmed the theoretical prediction that compound-2 is enriched in smaller drops (48). This recondensation comes to an end when the capillary and the concentration forces (Raoult's law) are in equilibrium. The equilibrium requires that the chemical potential of liquid-1 (subscript 1) is the same in all particles. Equation (8.16) illustrates the situation at equilibrium (subscript e) regarding the second component (subscript 2) for two particles (superscripts ' and ") with different diameters:

$$\phi'_{2,e} - \left(\frac{4\sigma v_{m,1}}{k_B T} \right) \left(\frac{1}{D'_{d,e}} \right) = \phi''_{2,e} - \left(\frac{4\sigma v_{m,1}}{k_B T} \right) \left(\frac{1}{D''_{d,e}} \right) \quad (8.16)$$

Compensation for the Ostwald ripening requires ϕ_2 -values depending on the droplet size, in the sense that smaller drops require a higher ϕ_2 , and vice versa. However, this is practically impossible to control during the initial emulsification process.

From the chemical potential at equilibrium follows a condition for $\phi_{2,i}$ that the system can reach equilibrium and Ostwald ripening will stop (see equation (8.17)). Here the subscript "i" stands for initial conditions, and $\bar{D}_{d,i}$ stands for the initial average droplet size¹.

$$\phi_{2,i} > \frac{4\sigma v_{m,1}}{3k_B T \bar{D}_{d,i}} \quad (8.17)$$

¹ The equilibrium condition for liquid-1 is $\Delta\mu_1 = \frac{4\sigma v_{m,1}}{D_{d,e}} + k_B T \ln \left[1 - \phi_{2,i} \left(\frac{D_{d,i}}{D_{d,e}} \right)^3 \right] = \text{constant}$. This can be approximated by $\Delta\mu_1 \approx \frac{4\sigma v_{m,1}}{D_{d,e}} - k_B T \phi_{2,i} \left(\frac{D_{d,i}}{D_{d,e}} \right)^3$. Differentiation after D_d leads to relationship given in equation (8.17).

If this condition is not met the particles cannot reach equilibrium and Ostwald ripening will further increase the differences in the chemical potentials for particles with different sizes. This also means that the addition of a completely water-insoluble hydrophobe during the emulsification does not *per se* prevent Ostwald ripening. Ostwald ripening takes place in any case, except for the case of an exactly monodisperse droplet size distribution, and will either lead to an equilibrium after a certain maturation time or not. Note that an additional effect arises if compound-2 is surface-active. During the equilibration of liquid-1, σ decreases in the small drops and increases in the large ones. This decreases the driving force for the redistribution of liquid-1 and hence would additionally stabilize the emulsion against Ostwald ripening.

Secondly, if compound-2 has a low but non-zero solubility in the continuous phase (with $C_{0,1} \gg C_{0,2}$)² an equilibrium condition according to the case where $C_{0,2} = 0$ can be applied. There exists a critical drop size ($D_{d,c}$) in the DSD for which the flux of compound-2 out of the drops is zero³. Note that for $D_d > D_{d,c}$ and for $D_d < D_{d,c}$, the flux is positive and negative, respectively.

The volume growth rate of the droplets (W) is given by equation (8.18) below which is valid under the assumption that all three of the molecular volumes ($v_{m,i}$), the interfacial tensions (σ_i) and the diffusion coefficients (D_i) in the continuous phases of liquid-1 and compound-2 are comparable:

$$W = \left(\frac{\phi_1}{w_1} + \frac{\phi_2}{w_2} \right)^{-1} \quad (8.18)$$

where w_1 and w_2 are the rates in the case of the pure components (i) and are given by the Lifschitz/Slezov theory (49) (cf. equation (8.19)):

$$w_i = \frac{d\bar{D}_d}{dt} = \frac{8}{9} \frac{D_i C_{0,i} v_{m,i} \sigma_i}{\phi_i k_B T} \quad (8.19)$$

The behaviour of a two-component emulsion is determined by the solubility of compound-2. Equation (8.18) is highly unsymmetrical as small ϕ_2 -values have a large effect on W but even substantial amounts of liquid-1 are unable to retard the Ostwald ripening of compound-2 to any great extent. In other words, if $\phi_2 \ll w_2/w_1$, then liquid-1 governs the mass transfer, while if $\phi_2 \gg$

² Note that the solubilities $C_{0,i}$ are given as dimensionless volume fractions.

³ The critical drop size is given by the relationship $D_{d,c} = \frac{4v_{m,2}\sigma}{k_B T \ln[C_2/C_{02}\phi_2(D_{d,c})]}$, where C_2 is the concentration of compound-2 in the continuous phase.

w_2/w_1 , Ostwald ripening is governed by the mass transfer of the second component.

Important for all attempts to polymerize emulsions is that with C_0 between 10^{-5} and 10^{-8} , the characteristic time of Ostwald ripening for compound i ($\tau_{OR} = (\bar{D}_d)^3/w_i$) is the order of 10^2 to 10^5 s. These relationships allow an estimate of how fast the polymerization should be in order to be able to compete with Ostwald ripening (cf. below).

Aggregation (route 3 in Figure 8.2 and Figure 8.3(a)) processes (flocculation, coagulation, coalescence) can take place when the average distance between the emulsion droplets is so close that attractive forces become dominating. It is useful to discriminate between flocculation on the one hand, and coagulation and coalescence, on the other hand, in the way that this is

illustrated in Figure 8.3a. In this sense, flocculation is an aggregation in a shallow secondary energy minimum (about $-1.5 k_B T$) and is hence reversible by the supply of a proper amount of energy. In contrast, both coalescence (in the case of emulsions) and coagulation (for sols or suspensions) result in a durable breakdown of the colloidal systems. In principal, this state is depicted in Figure 8.3(a) as the primary minimum. Coalescence is not a single stage process but comprises at least four elementary steps: (a) contact at a distance that allows attractive interaction, (b) the drainage of the continuous phase film between the drops, (c) the rupture of the film, and (d) finally, the collapse of the droplets. This qualitative picture also provides ideas as to how effective protection against droplet coalescence can be achieved. Useful precautions in this respect are the use of effective surfactants at high concentrations and low ionic strengths to enlarge the screening between the particles, a high η_c to retard film drainage, and a high η_d to slow down the confluence.

Nowadays, the stability of emulsions can be controlled very effectively by the addition of proper stabilizers in sufficient concentrations so that generally in practice the aggregation of emulsions is not a serious problem anymore. Stabilizers can act either in an electrostatic or steric way, or in a combination of both, to prevent aggregation processes. The interaction of colloidal particles (micelles, emulsion droplets, or that of polymeric particles after polymerization) is determined by the effective interaction energy resulting from a superposition of the van der Waals attraction, electrostatic repulsion, steric repulsion, electrosteric repulsion, and the Born repulsion of the electron clouds. A schematic representation of an interaction energy–distance curve is depicted in Figure 8.3(a). It seems to be didactically useful to include the Born repulsion as this is the general prerequisite for the ability to form colloidal systems. As the stabilization of colloids against aggregation is of enormous practical importance, almost innumerable treatises on this subject have been published. From this author's experience, the refs (1, 2, 50–52) can be recommended for more detailed information. Specifically regarding emulsions, the appropriate chapters in ref. (53) give a good insight.

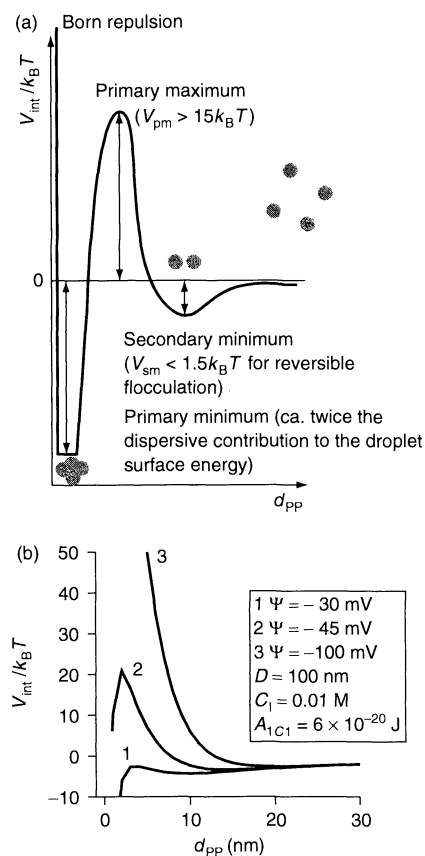


Figure 8.3. Electrostatic stabilization of colloidal particles: (a) schematic representation of the electrostatic interaction energy–distance curve for two approaching particles (not to scale); (b) calculated electrostatic interaction curves according to equations (8.20a–8.20c)

In order to get an idea as to how the interaction energy ($V_{int}(d_{PP})$) between two approaching droplets changes as a function of the distance (d_{PP}) of their surfaces, equations (8.20a)–(8.20c) from ref. (51) are quite useful. These equations describe, according to the DLVO theory, the interaction of electrostatically

stabilized particles, as follows¹:

$$V_{\text{int}}(d_{\text{PP}}) = \pi \frac{D_{\text{d}}}{2} \left[- \left(\frac{A_{\text{IC1}}}{12\pi} \right) \left(\frac{1}{d_{\text{PP}}} \right) + \frac{64k_{\text{B}} T C_{\text{I}} \Gamma_0^2}{\kappa^2} \exp(-\kappa d_{\text{PP}}) \right] \quad (8.20a)$$

$$\kappa^{-1} = \left[\frac{\varepsilon \varepsilon_0 k_{\text{B}} T}{\sum_i (z_i e)^2 C_{\text{I}i}} \right]^{0.5} \quad (8.20b)$$

$$\Gamma_0 = \tanh \left(\frac{ze\Psi}{4k_{\text{B}} T} \right) \quad (8.20c)$$

In the above equations, A_{IC1} is the complex Hamaker constant of droplets of liquid-1 interacting through the continuous phase, C_{I} is the ionic strength, κ^{-1} is the Debye screening length (cf. equation (8.20b)), ε and ε_0 are respectively the permittivities in the continuous phase and in vacuum, z is the stoichiometric valency of the electrolyte, and Ψ is the surface potential of the droplets. Figure 8.3(b) shows interaction energy distance curves calculated by using equations (8.20a)–(8.20c). The formation of the primary maximum protecting the drops from coalescence with increasing surface potential can be clearly seen. Increasing Ψ can be realized practically, for instance, with a higher concentration of ionic surfactants or a lower ionic strength. The latter causes a higher degree of ionization due to a reduced counterion condensation. The Debye screening length, which is a measure at which distance two charges of the same sign “start to notice each other”, decreases with increasing ionic strength. For example, at concentrations of a 1:1 electrolyte of 10^{-3} , 10^{-2} , 10^{-1} and 1 M, κ^{-1} is (at 25°C) 9.2, 2.9, 0.92 and 0.29 nm, respectively. It is an “experimental experience” that at C_{I} between 10^{-1} and 10^{-2} M, where κ^{-1} is between 1 and 2 nm, purely electrostatically stabilized droplets/particles can come so close together that they will aggregate.

Nonionic surfactants stabilize colloidal systems not by electrostatics but basically by osmotic forces. If two sterically stabilized particles approach each other, the soluble parts of the adsorbed chains causes a higher concentration in the interstitials when compared to the average continuous phase. This will cause a flux of continuous phase into the interstitials, which subsequently leads again to drop separation. As nonionic stabilizers are mainly polymeric in nature (for instance, poly(ethylene glycol) chains), elastic forces may contribute to the stability as well. The elastic force per

chain (P_{el} , cf. equation (8.21)) depends directly on the adsorbed layer thickness (ΔR , also called the *corona thickness*) and inversely on the second power of the square of the average end-to-end distance ($R_0 = P_{\text{n}}^{1/2} a$), where P_{n} is the average degree of polymerization and a is a characteristic monomer length:

$$P_{\text{el}} \propto \frac{k_{\text{B}} T \Delta R}{R_0^2} \quad (8.21)$$

The above equation elucidates that the longer the chain length, then the lower is the elastic force. In other words, a compression of the corona is the easier possible the longer the stabilizing chain. If the stabilizer is a long polyelectrolyte chain, the osmotic force (P_{osm}) is determined mainly by counterion condensation and can be expressed in the form of the following equation (54):

$$P_{\text{osm}} \propto \frac{k_{\text{B}} T P_{\text{n}}}{\Delta R^4 C_{\text{I}}} \quad (8.22)$$

Both forces act into opposite directions: the osmotic force tries to stretch the chain into the continuous phase, whereas the elastic force pulls the chain back to the interface. Setting $P_{\text{el}} = P_{\text{osm}}$ shows that $\Delta R \propto C_{\text{I}}^{-1/5}$. This is a much lower electrolyte dependence than in the case of low-molecular-weight ionic stabilizers where an exponential dependence of V_{int} is predicted (cf. equations (8.20)). Note, this scaling behavior of ΔR with C_{I} is the same as for polyelectrolyte chains in solution [2]. Regarding colloid stability, this means that polyelectrolyte-decorated droplets/particles possess an extraordinary electrolyte stability when compared to low-molecular-weight ionic stabilizers. Indeed, the *Pincus brush* behaviour ($\Delta R \propto C_{\text{I}}^{-1/5}$) was experimentally observed for polystyrene particles stabilized with poly(styrene sulfonate) chains (55). These particles were stable up to a sodium chloride concentration of 5 M. This is almost two orders of magnitude higher than for low-molecular-weight electrostatic stabilizers (cf. above) and reaches the region for nonionic surfactants, which are almost always a part of technical stabilizer systems for increasing the electrolyte stability.

Phase inversion (route 4 in Figure 8.2) is a process, where for a given stabilizer, the continuous phase becomes the dispersed one and vice versa. This is mainly observed in the case of polymeric surfactants with a stabilizing moiety possessing a *critical solution temperature*. Prominent examples of these are surfactants with poly(ethylene glycol) units. Increasing the temperature leads to a decrease in the HLB of the surfactant and it may subsequently, in accordance with Bancroft’s rule, promote the stabilization of a water-in-oil instead of an oil-in-water emulsion. Furthermore, whether or not

¹ During the 1940s, Derjaguin and Landau in the Soviet Union, as well as Verwey and Overbeek in the Netherlands, developed independently a theory of interparticle interaction based on attractions due to van der Waals forces and electrostatic repulsion.

phase inversion occurs depends on the polarity of the oil phase, the kind of electrolyte and its concentration, other additives, as for instance, organic, water-soluble solvents increasing the oil solubility in water, and the oil volume fraction.

To conclude, the stability of emulsions depends on droplet size, the presence of electrostatic, and/or steric, and/or electrosteric repulsion forces, the viscosity of both phases and the temperature. In addition, the kind and concentration of all stabilizers electrolytes and additives play a major role as well.

5 COMMINATION OR CONDENSATION TECHNIQUES – WHAT MAKES THE DIFFERENCE?

There are considerable differences in the properties of emulsions prepared by the swelling of polymeric seed particles and emulsions prepared by comminution techniques. Possibly the most important difference is regarding the stability. “Normal” swelling (*not* the methods of enhanced swelling, cf. above) is an important step during emulsion polymerization as this is the process by which the monomer is delivered to the reaction loci, which are the monomer swollen latex particles. Furthermore, the frequently applied seed polymerization technique¹ requires swelling as well. Swelling itself is, from the colloid chemical point of view, an extraordinarily interesting effect as an organic solvent (say, toluene) which dissolves bulk samples of a polymer (say, polystyrene) is unable, even if it is present in excess, to dissolve the polymer if this is present in the form of colloidal particles dispersed in water. This was first treated theoretically and experimentally by Morton *et al.* (56). The next benchmark was set by Ugelstad and co-workers while theoretically underpinning the enhanced swelling method discussed above (57). Note that latexes have, after enhanced swelling, a polymer concentration of about 1% inside the droplets. Interestingly, for such emulsions no problems regarding their stability have been reported (44, 57). It is obvious that their stability is higher than that of emulsions prepared by comminution techniques. There are arguments that swollen latex particles can be considered as being thermodynamically stable as the free energy of swelling goes through a minimum at the equilibrium size of the swollen particles (58). Both the normal and the enhanced swelling

are exclusively thermodynamically controlled. A general swelling relationship is possibly given with equation (8.23) where subscript 3 refers to the polymer, $\chi_{i,j}$ are the corresponding interaction parameters, and P_{sw} is the swelling pressure (56, 57, 59):

$$\begin{aligned} \ln \phi_1 + \left(1 - \frac{1}{P_{n,2}}\right) \phi_2 + \left(1 - \frac{1}{P_{n,3}}\right) \phi_3 + \phi_2^2 \chi_{1,2} \\ + \phi_3^2 \chi_{1,3} + \phi_2 \phi_3 \left(\chi_{1,2} + \chi_{1,3} - \frac{\chi_{2,3}}{P_{n,2}}\right) \\ - \frac{4v_{m,1}\sigma}{D_d k_B T} - \frac{P_{sw} v_{m,1}}{k_B T} \end{aligned} \quad (8.23)$$

The left-hand site of equation (8.23) describes the entropy and the enthalpy of mixing, where both are promoting swelling. The dissolution is prevented as the interfacial energy and the swelling pressure counteract the swelling process. For practical applications, equation (8.23) describes, at least qualitatively, the swelling of polymer particles in accordance with experimental findings. The swelling is the higher for the lower $P_{n,2}$, the larger the seed particles, the lower σ , the higher the temperature, the better the solubility of the polymer in the oil, and the lower the swelling pressure (56–59). Additionally, the influence of surfactants has to be considered. It is an experimental fact that as soon as free surfactant is present the swelling capacity is apparently enhanced (56, 59). This is caused by solubilization in the continuous phase and if present also in micelles or by adsolubilization in adsorbed stabilizer layers at the particle water interface. Swelling is of special interest in context with both the preparation of emulsions and heterophase polymerizations as it bridges both fields (cf. below).

Possibly the most important difference between swelling and comminution techniques in preparing emulsions is as outlined in Figure 8.4. All comminution techniques are governed by the input of energy which is much larger than necessary according to equation (8.3). In contrast, swelling is a process driven purely by thermodynamic forces. The idea illustrated in Figure 8.4 describes swelling as a process driven by entropy and energy changes as a concentrated solution will be diluted. This a thermodynamically favoured process unlike comminution where a solution with a given concentration is crushed, which is an energetically costly process. There are today two general possibilities known to achieve highly swollen particles with a polymer volume fraction of about 1%: (i) the use of a swelling promoter (compound-2) or (ii) the dynamic swelling method. Compound-2 acts according to equation (8.23). Due to its low molecular weight, the swelling promoter

¹ Seeded procedures are industrially the most important emulsion polymerization techniques since all uncertainties in connection with particle nucleation can be avoided see also ref. (81).

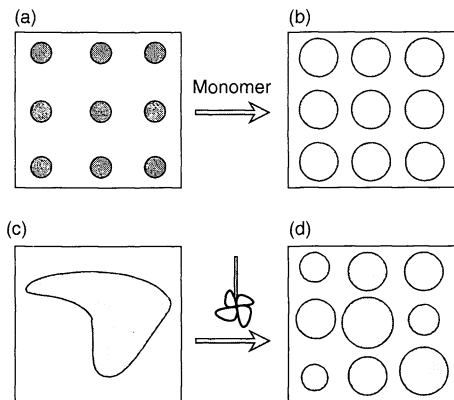


Figure 8.4. Schematic representation of the difference between emulsion preparation by swelling of seed particles (from (a) to (b)) and by comminution (from (c) to (d)) (not to scale). The different degrees of shading indicate different concentrations in the disperse phase

increases the entropy gain of mixing as the $1/P_{n,2}$ -term cannot be neglected. Again, the swelling promoter can be either a low-molecular-weight, highly water-insoluble compound or an oligomer which was generated during the preparation of the seed particles utilizing a chain-transfer agent. Principally, the dynamic swelling method uses Ostwald ripening. The monomer droplets are generated with a size which is much smaller than the seed particles. The small monomer droplets have a high Laplace pressure that drives the monomer into the aqueous phase and subsequently into the seed particles which absorb it eagerly. However, in both cases the use of a monodisperse seed ensures almost complete stability against degradation by Ostwald ripening. Furthermore, Ostwald ripening is impeded, as the swollen particles are in thermodynamic equilibrium and the seed particles consist of absolutely water-insoluble compounds, namely the polymer molecules.

In concluding these considerations, it is obvious that for subsequent polymerization reactions the preparation of emulsions by swelling (a condensation technique) has considerable advantages when compared to comminution techniques.

6 POLYMERIZATION OF (OR IN) MONOMER EMULSIONS

Any polymerization reaction causes a change in the existing thermodynamic conditions compared to those during the emulsification process. The question immediately originates whether or not it is possible to convert

the characteristic features of monomer droplets into that of polymer particles. Characteristic features of monomer emulsion droplets are, for instance, average size, size distribution and composition. Suspension, miniemulsion and emulsion polymerization are suited to a very different degree to preserve the droplet properties during polymerization.

In order to look in some more detail at the conditions during the transfer of a monomer emulsion into a polymer dispersion it seems apt to consider some characteristic time and length scales.

The characteristic time of the exchange of monomer from droplets during Ostwald ripening (τ_{ex}) is given by the following relationship, where ϕ_w is the dimensionless solubility of the monomer in water ($\phi_w = C_w v_{mon}$) and D_{mon} is the monomer diffusion coefficient¹:

$$\tau_{ex} \propto \frac{D_d^2}{\phi_w D_{mon}} \quad (8.24)$$

The polymerization competes with the bleeding of an emulsion droplet. For radical polymerizations, the initiation rate (r_i), given by equation (8.25) below, is a measure of how fast a certain number of free radicals capable of starting a polymerization are formed. The equilibrium radical concentration (P^*), obtained under the assumption that the rates of radical formation and termination are equal, is given by the following equation (8.26). In these equations f is the radical efficiency factor ($f \approx 0.5$), k_d is the initiator decomposition rate constant, C_1 is the initiator concentration, and k_t is an average termination rate constant. The time τ_{ini} is defined below by equation (8.27) and is a measure how long it takes to generate, for each droplet, at least one radical. Note that equations (8.25)–(8.27) are only useful for estimations concerning the condition in the aqueous phase but not for detailed mechanistic consideration.

$$r_i = 2fk_d C_1 \quad (8.25)$$

$$P^* = \left(\frac{r_i}{k_t} \right)^{1/2} \quad (8.26)$$

$$\tau_{ini} = \left(\frac{N_d}{r_i N_A} \right) \quad (8.27)$$

The time needed to polymerize the monomer in one droplet (τ_{pol}) is given by the relationship shown in equation (8.28), where \bar{n} is the average radical number in the droplet, k_p is the propagation rate constant, and $C_M = 1/v_{mon}$ is the monomer concentration in the

¹ Note that ϕ_w corresponds to C_0 from above.

droplet, v_{mon} is the molar volume of the monomer, and N_A is the Avogadro constant:

$$\tau_{\text{pol}} \propto \frac{D_d^3 N_A}{k_p C_M \bar{n} v_{\text{mon}}} \quad (8.28)$$

The time between two successive monomer additions at a growing chain (τ_{madd}) is given by equation (8.29), where C_{mon} is the monomer concentration either in the aqueous phase (C_W) or in the droplets (C_M):

$$\tau_{\text{madd}} = \frac{1}{k_p C_{\text{mon}}} \quad (8.29)$$

The interesting length scales are, on the one hand, the average distance between two drops (d_{pp}) given by equation (8.30) where N_d is the drop number, and on the other hand, the average path (root-mean-square displacement) that a radical can diffuse between two consecutive monomer additions (λ_{madd}) given by equation (8.31):

$$d_{\text{pp}} = \left(\frac{1}{N_d} \right)^{1/3} \quad (8.30)$$

$$\lambda_{\text{madd}} = (2D_{\text{mon}}\tau_{\text{madd}})^{0.5} \quad (8.31)$$

Another size scale, which, however, is important for each polymerization technique, is the shrinkage of the reaction volume due to the density increase during polymerization¹. The size of a monomer droplet decreases due to polymerization of the monomer according to equation (8.32), where ρ_{mon} and ρ_{pol} are the densities of the monomer and polymer, respectively:

$$D_p = \left(\frac{\hat{r}_{\text{mon}}}{\rho_{\text{pol}}} D_d \right)^{1/3} \quad (8.32)$$

6.1 General features of suspension polymerization

Suspension polymerization (60–63) is of special meaning for the production of technically important polymers, as for instance, expanded polystyrene and poly(vinyl chloride). Suspension polymerization refers to the carrying out of a polymerization in micron-sized droplets with oil-soluble initiators. Emulsification and polymerization take place in the same vessel and at the same time. A polymeric stabilizer or protective colloid is

used. Typical examples include poly(vinyl alcohol) or cellulose derivatives. Rather unusual, but of some technical importance, are Pickering stabilizers which consist of small-sized, insoluble inorganic particles as for example, $\text{Ca}_3(\text{PO}_4)_2$ or BaSO_4 . Sometimes, additionally low-molecular-weight, water-soluble surfactants are used either to support the initial state of the emulsification or to improve wettability. Compared to other heterophase polymerizations, the stabilizer concentration with respect to the monomer mass is low. This is typically of the order of less than 0.5%, and is usually between 0.06 and 0.1%. The polymerization is started by an oil-soluble initiator or an initiator mixture. In principle, suspension polymerization is an example of successfully converting a monomer emulsion into a polymer dispersion, if precautions are taken to avoid extensive polymerization in the aqueous phase or fouling of the reactor walls by applying radical scavengers that prevent polymerization at unwanted loci. Due to the inhomogeneity of the stirrer shear field throughout the reactor volume, the droplets formed in the vicinity of the stirrer become unstable during their way through the reactor and degenerate. This process continues as long as the viscosity inside the droplets (i.e. the conversion) becomes high enough that both coalescence and breakage of the droplets is no longer possible. The conversion range where this occurs is called the *point of particle identity*. Afterwards, the droplets are practically stable and keep their identity throughout the remaining polymerization time². The processes of droplet breakage and coalescence can be influenced by the stabilizer properties. These stabilizers form a layer at the droplet–water interface, thus leading to a steric stabilization which reduces the rate of droplet coalescence. However, the droplet breakage is also altered as the dilational modulus of the interface is increased and the droplet deformation is hindered. An increase in the viscosity of the dispersed phase acts in a similar way, although the latter takes place during the polymerization in any case. An increase in the continuous phase viscosity acts in two ways, both of which favour smaller drops. On the one hand, this decreases the droplet collision frequency, thus reducing the coalescence rate, while on the other hand, it enhances the shear stress acting on the drop interface during the emulsification. However, if the hindrance of the droplet coalescence is too strong, the interface to be stabilized becomes too large and hence flocs or aggregates can be formed. The later two species may lead upon further polymerization to “raspberry-like” particles.

¹ The higher density of a polymer in comparison to its monomer is the consequence of the smaller average distance between the molecules in the polymer. This effect surpasses the alterations in the bond length that the reverse dependence would have expected as the double bond is shorter than the single bond.

² Note that the transition from an emulsion droplet to a polymer particle proceeds from this point to the process very smoothly. The droplets solidify step-by-step with increasing conversion.

The molecular weight of the stabilizer also has a strong influence, since it determines its mobility. As a rule of thumb, it may serve that for a given polymeric stabilizer, the stabilization of the drops is rather more supported than comminution if the molecular weight is higher than a critical value. In contrast, if the molecular weight is lower, then comminution is more favoured than stabilization. Obviously, in the former case the droplet identity is more preserved than in the latter situation where droplet coalescence occurs.

In addition, the dependence of the final particle diameter on the stirrer speed is not unambiguous as, in principal D_p decreases with n over a wide range. However, if n is higher than a critical value, then instabilities may occur due to slow stabilizer adsorption or low surfactant concentration leading to an increased D_p . A typical reaction during a suspension polymerization at the interface is a grafting reaction on to the stabilizer molecules. This reaction is important as it leads to a better anchoring of the stabilizer, already at low conversions, and hence to an early formation of a protecting membrane. This membrane protects against coalescence, but also against radical exit into the aqueous phase, thus reducing the probability of both aqueous phase polymerization and reactor fouling. Additionally, if poly(vinyl alcohol) is used, cross-linking via the hydroxyl groups with borate is frequently used to increase membrane stability.

The Pickering stabilizers (cf. ref. (63)) have special importance for styrene suspension polymerization. In this case, the initial suspension is a three-phase colloidal system, rather than a two-phase systems (as is usual). The third phase (a sol or suspension) is formed by the stabilizers which are located in an interfacial layer between styrene and water where both liquids compete to wet the inorganic particles. Mixed wetting is necessary to achieve stabilization which means that the interface of the inorganic particles must be amphiphatically modulated to be effective. This is very often achieved by the use of low-molecular-weight surfactants. Figure 8.5 illustrates schematically the action of inorganic particles as stabilizers. A contact angle Θ , larger or smaller than 90° , determines which kind of emulsion is formed (63). If Θ between the inorganic particle and water is smaller than 90° an oil-in-water emulsion is formed, while if Θ is above 90° the inverse oil-in-water emulsion is preferably formed. Frequently, an optimum stabilization is observed for both cases if Θ is close to 90° . Inorganic particles as stabilizers in suspension polymerization have at least two advantages when compared to polymers, i.e. they are cheaper and can be removed completely after the polymerization very easily.

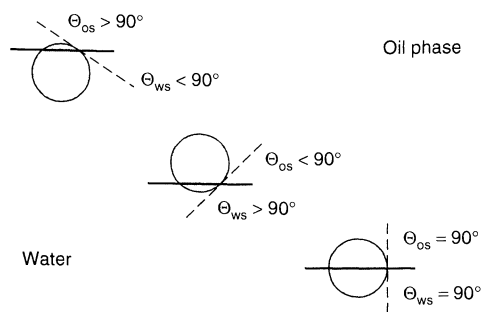


Figure 8.5. Principle of the action of Pickering stabilizers (not to scale). The horizontal line indicates the oil–water interface, with the oil phase being assumed to be located above the latter: Θ_{os} , contact angle between a Pickering stabilizer particle and the oil phase; Θ_{ws} , contact angle between a Pickering stabilizer particle and the water phase

Besides the stabilizer, the solubility of the polymer in the monomer strongly influences the morphology of the polymer beads. If the polymer is soluble in the monomer, as for instance, polystyrene in styrene or poly(methyl methacrylate) in methyl methacrylate, beads with homogeneous spatial densities and smooth surfaces are formed. The transition from an emulsion droplet to a polymer bead proceeds smoothly, with the drops solidifying slowly during the polymerization. In contrast, vinyl chloride monomer only swells its polymer and hence poly(vinyl chloride) precipitates at low conversions. Inside the drops, small polymer granules are formed which are unstable towards coagulation. The internal structure of poly(vinyl chloride) suspension beads is characterized by a coagulation structure with a certain morphological assembly. In some cases, phase separation is induced in the drops for the preparation of porous beads by the presence of alkanes which do not solvate the polymer. The hydrocarbons form a separate phase inside the drops and can be removed at the end of the polymerization process.

As suspension polymerization is based on an *in situ* emulsification by turbulence, problems may arise during scale-up. The emulsification process is the real problem during the scale-up of laboratory-scale suspension polymerizations to an industrial level where today a typical reactor size is 200 m^3 .

6.2 General features of emulsion polymerization

There are innumerable scientific papers and patents available on emulsion polymerization which also cover

several aspects of surface chemistry (64–67). As the average size of the species is smaller than in suspension polymerization the enlarged interface requires higher emulsifier concentrations. Typically these are between 1 and 5% with respect to the monomer weight. Additionally, end groups originating from the water-soluble initiators contribute to the surface chemistry, as well as water-soluble comonomers. In technical polymerizations, a mixture of different emulsifier is used so that all kinds of stabilization mechanisms are acting i.e. electrostatic due to ionic groups, steric due to nonionic stabilizers, and electrosteric due to copolymers formed with the small amounts of ionic comonomers present in almost any recipe. Only such a combination ensures an optimum stability against electrolytes and temperature changes during storage and application.

In contrast to suspension polymerization, the use of water-soluble initiators is typical for emulsions polymerization, although oil-soluble initiators can also be used. Emulsion polymerization differs from the other heterophase polymerization techniques in one important point: it does not require the existence of a free monomer phase, or in other words, a neat monomer emulsion is not a prerequisite. The monomer can be fed into the reactor continuously from an external reservoir during continuous or semi-batch procedures. This is carried out in the case of almost all technically and commercially important polymerizations. A monomer feed allows an easy control of the rate of polymerization and hence the avoidance of peaks in the heat development during the reaction. Based on the fact that feeding techniques are possible and advantageous two important conclusions are straightforward. First, seed particles can be used and hence all problems in connection with particle nucleation can be avoided. Secondly, swelling is very important, as the polymer particles are the loci where the main part of the polymerization takes place. The latter requires conditions ensuring a fast transport of the feed throughout the entire reaction volume. The swollen polymer particles may be considered, as agreed above, as emulsion droplets and hence the name emulsion polymerization is, at least to seeded polymerizations, completely applicable.

Besides seed and feed procedures, batch polymerizations with a free monomer phase are also very popular. In these so-called *ab initio* polymerizations, water, emulsifier and monomer are charged into the reactor and allowed thermally to equilibrate under gentle stirring. Then, the polymerization is started by adding initiator. The stirrer speed is, compared to suspension polymerization, only of minor importance as both the final particle sizes and particle properties are not governed by the

droplet size. Nevertheless, in industrial practice, the stirrer speed must be carefully controlled. It must be, on the one hand, high enough to ensure an appropriate mixing of the reactor content, but on the other hand, carefully controlled enough to avoid shear instabilities. However, there are experimental results available which indicate an influence, on styrene emulsion polymerization, of the stirrer speed on the particle size, the molecular weight and the polymerization rate (68). These results indicate that below a critical stirrer speed, where a bulky styrene phase exists, the monomer diffusion is too low to maintain the equilibrium concentration in both the water and the particles. The slow monomer diffusion was also confirmed by investigations of surfactant-free polymerizations with on-line surface tension measurements (69). Just after initiation, the surface tension increased due to the styrene consumption and then levelled off at a value close to water. This indicates that the diffusion from the bulky styrene phase is much slower than the polymerization process.

Regarding the mechanism of an *ab initio* emulsion polymerization, the following statements, which have been experimentally verified, should be generally accepted as having a common basis, despite all contrary opinions in (important) details:

1. Monomer swollen polymer particles are the main reaction loci.
2. Transfer of matter through the particle–water interface in both directions is essential for the process (radicals and monomers).
3. The average particle size and number, as well as the particle size distribution, in the final latex are governed by the kinds and concentrations of stabilizers, initiators and other additives.
4. Particles are nucleated at the beginning of the polymerization, but a multiple formation of particles is also possible in the further course of the polymerization.
5. Monomer droplets with an average size of some microns are not the loci of particle formation, and serve only as reservoirs for monomers.

In particular, statement (1) above underlines the importance of surface or interface chemistry for the whole process. The particle–water interface may be, on the one hand either charged or uncharged, and on the other hand, either smooth or rough (fibrous). How the particular look of the interface influences the overall polymerization kinetics was recently shown by means of calorimetric data (67). For instance, the greater ΔR (stabilizer corona), then the more is the maximum in the polymerization time curves shifted towards longer times. The

corona was built up of polyelectrolytes with different P_n values and charge distributions along the chain (cf. above part swelling discussion).

Irespective of the particular polymerization procedure, it should be pointed out that the adsorption behaviour of surfactants depends on the nature of the substrate. This was shown for polymer dispersions in ref. (7). The area covered by a surfactant molecule (A_m) depends strongly on the polarity of the polymer, e.g. the higher the polarity, then the higher the A_m . For instance, the corresponding values for sodium lauryl sulfate adsorption on to polystyrene and poly(vinyl acetate) latexes differ by more than a factor of two. This has consequences regarding the stability, as the higher the A_m , then the lower the amount of surfactant adsorbed and the more diminished the stability against flocculation. The author points out that experimentally determined values of A_m can be used to estimate the composition of copolymer latex particles at the interface where frequently an enrichment of the more polar polymer is observed. This is a general behaviour for copolymerizations, as well as for two- or multistage polymerizations, in accordance with thermodynamic considerations (70). The more polar polymer tries to reach the interface to water. However, as the whole process is governed by a competition between thermodynamics and kinetics, the thermodynamically favoured morphology can be suppressed if the mobility of the chains is drastically reduced (for instance by fast polymerization, high conversion, low feed rate, etc.). However, by swelling of the composite particles the equilibrium structure will be formed. From the surface chemistry point of view, it is interesting to note that if, for instance, the amount of hydrophilic groups in a polystyrene particle is high (either brought into the particles by initiator end-groups or comonomers), a kind of phase separation takes place in the swollen particles. This phase separation leads to the formation of porous particles, either due to microphase separation or ionic repulsion (71). Generally, ionic repulsion between charged surface groups leads to the formation of a "hairy" or hydrodynamic layer, and may also contribute to an enhanced swelling (58).

However, the nature of surface groups is not completely predictable, as side reactions can lead to alterations. Water is not an inert media, and is indeed the main source of side-reactions with radicals. For both persulfate and azo initiators, a variety of end-groups, other than the expected ones, have been detected. These are mainly hydroxyl and carboxyl groups and it seems that their formation cannot be avoided as long as water is used as the continuous phase (72, 73).

Furthermore, surface groups may have an influence on the film formation of latex particles. They may slightly counteract particle coalescence, but will in any case influence the film properties at least in two ways. Covalently bound ionic groups will evenly distribute in the film but adsorbed ionic or hydrophilic compounds will migrate to the interface. There they will assemble in hydrophilic domains, thus leading to an enhanced water uptake. It is worth nothing briefly that so-called reactive surfactants, which are covalently bound or grafted on the polymer particles in the course of the polymerization, may overcome the drawbacks of free surfactants during film formation (74, 75). Furthermore, latexes prepared with surfimers exhibit an improved freeze-thaw stability.

6.3 General features of miniemulsion polymerization

Suspension and emulsion polymerizations have been technically and commercially very successful. Both techniques are controlled by different mechanisms and lead to products for fundamentally different applications. Simply expressed, suspension polymerization can be considered as a bulk polymerization inside μm -sized droplets, where the properties of the monomer drops, governed by the emulsification process as well as by the chemical composition, determine the properties of the polymer beads. Emulsion polymerization operates on the nm-size range, where the process is controlled by many exchange processes among the swollen particles via the continuous phase where the droplet properties have essentially no influence on the process. From this, the question arises whether or not it is possible to control the latex properties in a range typical for emulsion polymerization latexes, simply by controlling the properties of the initial monomer droplets (size and composition). This requires the preparation of monomer emulsions with droplet sizes of about 100 nm (so-called miniemulsions) (40, 41, 76–79) and their subsequent polymerization to achieve an almost "1:1 copy". In this sense, the term "miniemulsion polymerization" may be considered as being just as suitable as the term "minisuspension polymerization". The motivation for this polymerization technique can be understood as an attempt to combine the advantages of suspension and emulsion polymerizations. This seems to be very promising and consequently an enormous number of papers have been published during the last decade mainly devoted to polymerization experiments. On the other hand, there is clearly a lack of theoretical studies concerning such systems.

There is no problem in preparing emulsion droplets with sizes of about 100 nm. These small droplets are prepared by high-power comminution techniques, mainly the application of a high-energy ultrasound source and/or a microfluidizer in the presence of a stabilizer system at concentrations below the critical micelle concentration. This is done in order to avoid particle nucleation via a micellar mechanism during the subsequent polymerization. The stabilizer system consists of a "normal" emulsifier and a second component, where the latter is either a fatty alcohol or hexadecane. The former acts mainly as an emulsifying aid and the latter as "compound-2". Additionally, a few per cent of a polymer can be added. All of these represent attempts to increase the droplet stability. The latter case formally resembles seed particles, although not prepared in a "thermodynamic way". At a more or less defined time after the emulsification (which can be carried out in one or two steps), the polymerization is started. During the polymerization, only gentle stirring is applied so as to avoid creaming or sedimentation. There is at this present time no conclusive experimental results known that verify a complete 1:1 copy of a miniemulsion by polymerization. This is independent of both the initiator and the stabilizer system employed. There are several arguments, on the basis of the above considerations, that a 1:1 copy of a so-called miniemulsion by polymerization is rather unlikely, as follows:

1. The emulsion at the start of the polymerization is not well characterized, in particular regarding the DSD and stability.
2. The energy input during the emulsification is very high, in particular when using ultrasonification, which can lead either to a temperature increase high enough to start thermal polymerization (e.g. styrene and acrylates) or to radicals formed, e.g. during the ultrasonification of water (80), which are able to start the polymerization¹. Both effects may cause irreproducible starting conditions.
3. During the time span between emulsion preparation and polymerization, the temperature is not constant, which may cause changes in the emulsion properties.
4. The emulsions, even in the presence of hexadecane and polymer, are not stable *per se*; if they are stable, this is a fortunate case where the conditions according to equations (8.16) and (8.17) are fulfilled.

¹ In some cases (30% as a rough estimate), we have observed, from electron microscopy evidence, a polymerization of styrene miniemulsions during or after ultrasonification. These miniemulsions showed an extraordinary stability during storage when compared to non-polymerised systems.

However, these conditions can be met after a certain maturation time (this is really a complicated situation which needs experimental as well as theoretical investigations).

5. The DSD in the presence of polymer in the miniemulsion droplets before polymerization was found to be very broad (78) which promotes droplet instability.
6. The distribution of the particle composition is, in the case of composite particles, rather broad, which indicates that exchange processes take place during the polymerization (81).
7. In all cases, N_p was found to be smaller than N_d , indicating also exchange processes or instabilities (77, 78).

Taking all facts into account, the situation is characterized in such a way that the important question is to what extent it is possible to *copy* a miniemulsion by polymerization and not to realize a *true* 1:1 copy.

However, there is no doubt that the monomer miniemulsion itself has a strong effect on the polymerization. Due to the large droplet interface, all exchange processes are enhanced according to equation (8.33) where $C_{M,I}$ is the monomer concentration at the droplet-water interface. (Note that this is a similar expression to the relationship given by equation (8.24) for the characteristic exchange time of a droplet.)

$$\frac{dC_M}{dt} \propto \frac{D_{\text{mon}}(C_{M,I} - C_w)}{D_d^2} \quad (8.33)$$

The monomer stream from the droplets into the aqueous phase causes a much higher polymerization rate in water and subsequently also a higher capture rate of species from the aqueous phase by the droplets. This is particularly important when compared with the much larger droplet sizes observed during suspension or emulsion polymerization.

7 FIXATION OF AN EMULSION BY RADICAL POLYMERIZATION IN AQUEOUS MEDIA – FACT OR FANCY?

To fix an emulsion by polymerization requires precautions in two aspects: (i) to enhance emulsion stability, and (ii) to choose a rapid polymerization process advancing from the interface into the droplet core. Thus, the fixation of droplets by polymerization is in principle possible. The crucial parameters are droplet size and size distribution, viscosity of both phases, and the polymerization procedure. It is perfectly possible to fix a droplet size distribution in the μm -sizerange, typical for

a suspension polymerization, by interfacial polycondensation reactions. For instance, if an oil-soluble monomer (e.g. terephthaloyl dichloride, 0.05 vol% of the amount of oil) is dissolved in the oil phase, the DSD can be fixed by adding piperazine. The interfacial polycondensation is fast enough to “freeze” the DSD (30).

For the radical heterophase polymerizations considered here, the situation is pretty much different in each case. In suspension polymerizations, emulsification and polymerization occur at the same time. After the point of particle identity, the droplets are stable and the polymerization then proceeds smoothly until completion. The properties of the final particles are mainly determined by the droplet properties, in particular by their size distribution and composition.

During emulsion, as well as miniemulsion polymerization, the situation is considerably different, with the exception of seeded emulsion polymerizations. Normal seed particles or highly swollen particles can be polymerized without difficulties under maintenance of the particle concentration. Agglomeration as well as secondary nucleation, can be avoided. This is the “state of the art” in many industrial processes (82) and also for scientific (research) investigations (64). The method of enhanced swelling with swelling promoters (low-molecular-weight, highly water-insoluble compounds)

has been successfully applied to produce large monodisperse particles for a variety of applications (83, 84). In addition, the dynamic swelling method has been proven to be a suitable way to produce monodisperse particles in the μm -sizerange (44). In both cases, the utilization of radical scavengers in the continuous water phase prevents secondary nucleation. During normal seed processes, this is usually not necessary as the capture efficiency of species from the aqueous phase by the existing particles is high enough. These are all examples showing that a performed emulsion can be successfully copied by polymerization. Note that all of these emulsions have been prepared via the thermodynamic route.

The situation in the case of emulsions prepared by comminution techniques can be partly illustrated with the help of the characteristic quantities defined above. These data are summarized in Table 8.7 for two emulsions, namely one with an average drop size of 50 μm (e.g. prepared by a common rotor/stator device) and one with an average droplet size of 100 nm (e.g. prepared by ultrasonification).

Some important conclusions which can be drawn from Table 8.7 include the following:

1. Small drops of neat styrene degenerate very fast ($\tau_{\text{ex}} \approx 10^{-3}$ s).

Table 8.7. Characteristic data for two neat styrene emulsions with different drop sizes subjected to polymerization initiated with potassium peroxodisulfate ($C_1 = 2$ mM) at 60°C ; $\phi_0 = 0.2$; total emulsion volume, 1 dm³; N_{mon} is the number of monomer molecules soluble in the continuous phase, and n_{mon} is the number of monomer molecules per droplet; indices E and w refer to emulsion and water, respectively; $N(\text{size})$ and $N(\text{size})^2$ represent the product of number and size of the corresponding species according to collision and diffusion theory, respectively (85). In addition, the following values have been used: $C_W = 5 \times 10^{-2}$ M; $v_{\text{mon}} = 0.12$ M⁻¹; $\rho_{\text{mon}} = 0.87$ g cm⁻³; $\rho_{\text{pol}} = 1.054$ g cm⁻³; $k_p = 3 \times 10^2$ M⁻¹ s⁻¹; $k_t = 10^8$ M⁻¹ s⁻¹; $k_d = 8.5 \times 10^{-5}$ s⁻¹ (73) or 5.5×10^{-6} s⁻¹ (64), where the higher k_d -value was determined experimentally during aqueous styrene polymerization with potassium persulfate (73)

Parameters	H ₂ O	Droplets		Remarks
Size	$a \approx 0.7$ nm	$D_d = 50$ μm	$D_d = 100$ nm	–
N_d	–	3×10^{10} dm _E ⁻³	3.8×10^{17} dm _E ⁻³	–
N_{mon}	1.8×10^{21} dm _w ⁻³	–	–	–
$N(\text{size})$	1.3×10^{13} dm ⁻²	1.5×10^7 dm ⁻²	3.8×10^{11} dm ⁻²	Diffusion (85)
$N(\text{size})^2$	9×10^4 dm ⁻¹	7.5×10^4 dm ⁻¹	4×10^5 dm ⁻¹	Collision (85)
n_{mon}	–	4×10^{13}	3×10^5	Per drop
d_{pp}	8.2 nm	32 μm	140 nm	–
τ_{madd}	0.3 s	4×10^{-4} s	4×10^{-4} s	–
λ_{madd}	25 μm	900 nm	900 nm	–
τ_{ex}	–	200 s	10^{-3} s	–
τ_{pol}	–	10^{11} s	10^3 s	$\bar{n} = 1$
r_i	1.1×10^{-8} M s ⁻¹	–	–	k_d from (64)
	1.7×10^{-7} M s ⁻¹	–	–	k_d from (73)
	–	4.5×10^{-6} s	60 s	k_d from (64)
τ_{mi}	–	3×10^{-7} s	4 s	k_d from (73)
P^\bullet	6×10^{15}	–	–	k_d from (64)
	2.5×10^{16}	–	–	k_d from (73)

2. A much more hydrophobic monomer is needed (ϕ_w should be decreased at least by a factor of 10^6) to increase τ_{ex} into a range where it can compete with τ_{pol} .
3. Even with oil-soluble initiators, the finer the emulsions, then the more important are aqueous phase reactions, as low-molecular-weight radicals can diffuse hundred of nanometres between two monomer additions and hence their exit from small droplets is very likely.
4. Regarding the radical production (r_i , τ_{ini} , P^*), the situation is quite promising as enough radicals can be generated for all droplets within a short period of time (τ_{ini} is less than 1 min).
5. According to the diffusion theory, there is a higher probability that a radical in the aqueous phase will meet a dissolved styrene molecule rather than a drop, whereas according to the collision theory, both events should occur almost with the same probability.
6. In the case of the larger drops, precautions are really necessary to avoid water-phase polymerization with subsequent nucleation, $d_{pp} \gg \lambda_{madd}$ (cf. $N(size)$ and $N(size)^2$ values).

Finally, under well-defined conditions, it is possible to polymerize performed emulsion droplets. This is especially true for emulsions prepared by condensation methods where the conditions can be controlled in such a way that both secondary nucleation can be avoided and droplet or particle stability can be maintained during the entire polymerization. In the case of emulsions prepared by comminution techniques, suspension polymerization is a good example of a system where the (conditions) properties of emulsions can be converted into the corresponding properties of sols/suspensions. For smaller drop sizes, the solubility of the monomer in water is crucial, but unfortunately, very hydrophobic monomers are technically unimportant, at least nowadays. The addition of hydrophobic molecules needs tailored emulsification procedures regarding \bar{D}_d and DSD, and a certain maturation time to result in stable emulsions. Miniemulsion polymerization is a promising way, although the question as to what extent a 1:1 copy of an emulsion is possible is still waiting for an answer.

8 REFERENCES

1. Birdi, K. S., Surface and colloid chemistry, in *Handbook of Surface and Colloid Chemistry*, Birdi, K. S. (Ed.), CRC Press, Boca Raton, FL, 1997, pp. 1–5.
2. Jönsson, B., Lindman, B., Holmberg, K., and Kronberg, B., *Surfactants and Polymers in Aqueous Solution*, Wiley, Chichester, 1998.
3. Tadros, Th. F., Suspensions, in *Surfactants*, Tadros, Th. F. (Ed.), Academic Press, London, 1984, pp. 197–220.
4. Conley, R. F., *Practical Surfactant: A Guide to Understanding and Formulating Slurries*, VCH, New York, 1996.
5. Hunkeler, D., Candau, F., Pichot, C., Hamielec, A. E., Xie, T. Y., Barton, J., Vaskova, V., Guillot, J., Dimonie, V. L., and Reichert, K. -H., Heterophase polymerizations: A physical and kinetic comparison and categorization, *Adv. Polym. Sci.*, **122**, 115–133 (1994).
6. Eliseeva, V. I., *Polymeric Dispersions* (in Russian), Chimija, Moscow, 1980.
7. Vijayendran, B. R., Polymer polarity and surfactant adsorption, *J. Appl. Polym. Sci.*, **23**, 733–742 (1979).
8. Daubert, T. E., Danner, R. P., Sibul, H. M., and Stebins, C. C., *Physical and Thermodynamic Properties of Pure Chemicals: Data Compilation*, Taylor and Francis, Washington, DC, 1998.
9. Lide, D. R. (Ed.), *CRC Handbook of Chemistry and Physics: A Ready Reference Book of Chemical and Physical Data*, 80th Edn, CRC Press, Boca Raton, FL, 1999.
10. Gliniski, J., Chavepeyer, G., Platten, J. -K., and Smet, P., Surface properties of diluted aqueous solutions of normal short-chain alcohols, *J. Chem. Phys.*, **109**, 5050–5053 (1998).
11. Barton, J. and Capek, I., *Radical Polymerization in Dispersed Systems*, Ellis Horwood, New York, 1994, pp. 216–248.
12. Sudol, E. D., Dispersion polymerization, in *Polymeric Dispersions: Principles and Applications*, Asua, J. M. (Ed.), Kluwer, Dordrecht, The Netherlands, 1997, pp. 141–154.
13. Zhu, D. -W., Perfluorocarbon fluids: Universal suspension polymerization media, *Macromolecules*, **29**, 2813–2817 (1996).
14. Candau, F., Inverse emulsion and microemulsion polymerization, in *Emulsion Polymerization and Emulsion Polymers*, Lovell, P. A., and El-Aasser, M. S. (Eds), Wiley, Chichester, 1997, pp. 724–741.
15. Stokes, R. J. and Evans, D. F., *Fundamentals of Interfacial Engineering*, Wiley-VCH, New York, 1997.
16. Roe, C. P. and Brass, P. D., Interfacial tension from the swelling of latex particles, *J. Colloid Sci.*, **9**, 602–603 (1954).
17. Fainerman, V. B., Makievski, A. V., and Miller, R., The measurement of dynamic surface tensions of highly viscous liquids by the maximum bubble pressure method, *Colloid Surf. A*, **75**, 229–235 (1993).
18. Kihm, K. D. and Deignan, P., Dynamic surface tension of coal water slurry fuels, *Fuel*, **74**, 295–300 (1995).
19. Wasan, D. T. and Christiano, S. P., Foams and antifoams: A thin film approach, in *Handbook of Surface and Colloid Chemistry*, Birdi, K. S. (Ed.), CRC Press, Boca Raton, FL, 1997, pp. 179–215.
20. Vincent, B., Emulsions and foams, in *Surfactants*, Tadros, Th. F. (Ed.), Academic Press, London, 1984, pp. 175–196.

21. Davis, H. T., Factors determining emulsion type: hydrophile-lipophile balance and beyond, *Colloid Surf. A*, **91**, 9–24 (1994).
22. Mason, T. G. and Bibette, J., Shear rupturing of droplets in complex fluids, *Langmuir*, **13**, 4600–4613 (1997).
23. Bancroft, W. D., The theory of emulsification. I, *J. Phys. Chem.*, **16**, 177–233 (1912).
24. Griffin, W. C., Classification of surface-active agents by HLB, *J. Soc. Cosmetic Chem.*, **1**, 311–326 (1949).
25. Lin, I. J., Friend, J. P., and Zimmels, Y., The effect of structural modifications on the hydrophile-lipophile balance of ionic surfactants, *J. Colloid Interface Sci.*, **45**, 378–385 (1973).
26. Myers, D., *Surfactant Science and Technology*, 2nd Edn, VCH, New York, 1992.
27. Harris, J. M., Introduction to biotechnical and biomedical applications of poly(ethylene glycol), in *Poly(ethylene glycol) Chemistry*, Harris, J. M. (Ed.), Topics in Applied Chemistry, Plenum, New York, 1992, pp. 1–14.
28. Grassmann, P., *Physikalische Grundlagen der Verfahrenstechnik*, 2nd Edn, Sauerländer AG, Aarau, Germany, 1970.
29. Kolmogorov, A. N., On the comminution of droplets in turbulent flow (in Russian), *Dokl. Akad. Nauk SSSR*, **66**, 825–828 (1949).
30. Polat, H., Polat, M., and Chander, S., Kinetics of oil dispersion in the absence and presence of block copolymers, *AIChE J.*, **45**, 1866–1874 (1999).
31. Maa, Y.-F. and Hsu, C., Liquid-liquid emulsification by rotor/stator homogenization, *J. Controlled Release*, **38**, 219–228 (1996).
32. Ludwig, A., Flechtner, U., Prüss, J., and Warnecke, H.-J., Formation of emulsions in a screw loop reactor, *Chem. Eng. Technol.*, **20**, 149–161 (1997).
33. Abismail, B., Canselier, J. P., Wilhelm, A. M., Delmas, H., and Gourdon, C., Emulsification by ultrasound. Drop size distribution and stability, *Ultrasonics Sonochem.*, **6**, 75–83 (1999).
34. Mason, T. G. and Bibette, J., Shear rupturing of droplets in complex fluids, *Langmuir*, **13**, 4600–4613 (1997).
35. Peng, S. J. and Williams, R. A., Controlled production of emulsions using a crossflow membrane, Part 1: Droplet formation from a single pore, *Trans IChemE*, **76**, 894–901 (1998).
36. Omi, S., Preparation of monodisperse microspheres using the Shirasu porous glass emulsification technique, *Colloid Surf. A*, **109**, 97–107 (1996).
37. Omi, S., Ma, G. H., and Nagai, M., Membrane emulsification – a versatile tool for the synthesis of polymeric microspheres, *Macromol. Symp.*, **151**, 319–330 (2000).
38. Williams, R. A., Peng, S. J., Wheeler, D. A., Morley, N. C., Taylor, D., Whalley, M., and Houldsworth, D. W., Controlled production of emulsions using a crossflow membrane, Part 2: Industrial scale manufacture, *Trans IChemE* **76**, 902–910 (1998).
39. Taylor, P. and Ottewill, R. H., Ostwald ripening in o/w miniemulsions formed by the dilution of o/w microemulsions, *Colloid Polym. Sci.*, **97**, 199–203 (1994).
40. Dewald, R. C., Hart, L. H., and Carroll, Jr, W. F., PVC miniemulsion polymerization I. Origin of droplet families, *J. Polym. Sci., Polym. Chem. Edn.*, **22**, 2923–2930 (1984).
41. Ugelstad, J., Mork, P. C., and Berge, A., Vinyl chloride polymerization, in *Emulsion Polymerization and Emulsion Polymers*, Lovell, P. A., and El-Aasser, M. S. (Eds), Wiley, Chichester, 1997, pp. 589–618.
42. Patist, A., Axelberd, T., and Shah, D. O., Effect of long chain alcohols on micellar relaxation times and foaming properties of sodium dodecyl sulfate solutions, *J. Colloid Interface Sci.*, **208**, 259–265 (1998).
43. Oh, S. G., Jobalia, M., and Shah, D. O., The effect of micellar lifetime on the droplet size in emulsions, *J. Colloid Interface Sci.*, **155**, 511–514 (1993).
44. Okubo, M., Shiozaki, M., Tsujihira, M., and Tsukuda, Y., Preparation of micron-size monodisperse polymer particles by seeded polymerization utilizing the dynamic swelling method, *Colloid Polym. Sci.*, **269**, 222–226 (1991).
45. Webster, A. J. and Cates, M. E., Stabilization of emulsions by trapped species, *Langmuir*, **14**, 2068–2079 (1998).
46. Higuchi, W. I. and Misra, J., Physical degradation of emulsions via the molecular diffusion route and the possible prevention thereof, *J. Pharm. Sci.*, **51**, 459–466 (1962).
47. Kabalnov, A. S., Pertzov, A. V., and Shchukin, E. D., Ostwald ripening in two-component disperse phase systems: application to emulsion stability, *Colloid Surf.*, **24**, 19–32 (1987).
48. Weers, J. G. and Arlauskas, R. A., Sedimentation field-flow fractionation studies of Ostwald ripening in fluorocarbon emulsions containing two disperse phase components, *Langmuir*, **11**, 474–477 (1995).
49. Lifschitz, I. M. and Slezov, V. V., Kinetics of diffusive decomposition of supersaturated solid solutions, *J. Exp. Theor. Phys.*, **35**, 479–492 (1958) (in Russian); English translation in *Sov. Phys. JETP*, **35**, 331–339 (1959).
50. Hunter, R. J., *Foundations of Colloid Science*, Vol.1, Clarendon Press, Oxford, UK, 1995.
51. Evans, D. F. and Wennerström, H., *The Colloidal Domain*, VCH, New York, 1994.
52. Napper, D. H., *Polymeric Stabilization of Colloidal Dispersions*, Academic Press, London, 1983.
53. Smith, A. L., *Theory and Practice of Emulsion Technology*, Academic Press, London, 1976.
54. Pincus, P., Colloid stabilization with grafted polyelectrolytes, *Macromolecules*, **24**, 2912–2919 (1991).
55. Tauer, K., Müller, H., Rosengarten, L., and Riedelsberger, K., The use of polymers in heterophase polymerization, *Colloid Surf. A*, **153**, 75–88 (1999).
56. Morton, M., Kaizerman, S., and Altier, M. W., Swelling of latex particles, *J. Colloid Sci.*, **9**, 300–312 (1954).
57. Ugelstad, J., Mork, P. C., Herder Kaggerud, K., Ellingsen, T., and Berge, A., Swelling of oligomer-polymer particles. New methods of preparations of emulsions and polymer dispersions, *Adv. Colloid Interface Sci.*, **13**, 101–140 (1980).
58. Antonietti, M., Kaspar, H., and Tauer, K., Swelling equilibrium of small polymer colloids: influence of surface

- structure and a size-dependent depletion correction, *Langmuir*, **12**, 6211–6217 (1996).
59. Tauer, K., Kaspar, H., Antonietti, M., Equilibrium swelling of colloidal polymeric particle with water-insoluble organic solvents, *Colloid Polym. Sci.*, **278**, 814–820 (2000).
 60. Bieringer, H., Platau, K., and Reese, D., Industrial aspects of suspension polymerization, *Angew. Makromol. Chem.*, **123/124**, 307–334 (1984) (in German).
 61. Dowding, P. J. and Vicent, B., Suspension polymerization to form polymer beads, *Colloid Surf. A.*, **161**, 259–269 (2000).
 62. Vivaldo Lima, E., Wood, P. E., Hamielec, A. E., and Penlidis, A., An updated review on suspension polymerization, *Ind. Eng. Chem. Res.*, **36**, 939–965 (1997).
 63. Lagaly, G., Schulz, O., and Zimehl, R., *Dispersions and Emulsions: An Introduction to the Colloid Science of Finely Dispersed Matter*, Steinkopff, Darmstadt, German 1997 (in German).
 64. Gilbert, R. G., *Emulsion Polymerization. A Mechanistic Approach*, Academic Press, London, 1995.
 65. Fitch, R. M., *Polymer Colloids. A Comprehensive Introduction*, Academic Press, London, 1997.
 66. Lovell, P. A. and El-Aasser, M. S. (Eds.), *Emulsion Polymerization and Emulsion Polymers*, Wiley, New York, 1997.
 67. Tauer, K., Emulsion polymerization, in *Reactions and Synthesis in Surfactant Systems*, Texter, J. (Ed.), Marcel Dekker, New York, 2000, pp. 429–453.
 68. Tauer, K., Schellenberg, C., and Zimmermann, A., Nucleation in heterophase polymerizations, *Macromol. Symp.*, **150**, 1–12, 2000.
 69. Tauer, K., Dessy, C., Corkery, S., and Bures, K. -D., On-line surface tension measurements inside stirred reactors, *Colloid Polym. Sci.*, **277**, 805–811, 1999.
 70. V. L., Dimonie, Daniels, E. S., Shaffer, O. L., and El-Aasser, M. S., Control of particle morphology, in *Emulsion Polymerization and Emulsion Polymers*, Lovell, P. A., and El-Aasser, M. S. (Eds.), Wiley, New York, 1997, pp. 293–326.
 71. Tauer, K., Riedelsberger, K., Deckwer, R., Zimmermann, A., Dautzenberg, H., and Thieme, J., A new way to control particle morphology in heterophase polymerizations, *Macromol. Symp.*, **155**, 95–104 (2000).
 72. Tauer, K. and Deckwer, R., Polymer end groups in persulfate-initiated styrene emulsion polymerization, *Acta Polym.*, **49**, 411–416 (1998).
 73. Tauer, K., Deckwer, R., Kühn, I., and Schellenberg, C., A comprehensive experimental study of surfactant-free emulsion polymerization of styrene, *Colloid Polym. Sci.*, **277**, 607–626 (1999).
 74. Guyot, A. and Tauer, K., Reactive surfactants in emulsion polymerization, *Adv. Polym. Sci.*, **111**, 43–65 (1994).
 75. Guyot, A., Tauer, K., Asua, J. M., van Es, S., Gauthier, C., Hellgren, A. C., Sherrington, D. C., Montoya-Goni, A., Sjöberg, M., Sindt, O., Vidal, F., Unzue, M., Schoonbrood, H., Schipper, E., and Lacroix-Desmazes, P., Reactive surfactants in heterophase polymerization, *Acta Polym.*, **50**, 57–66 (1999).
 76. Ugelstad, J., El-Aasser, M. S., and Vanderhoff, J., Emulsion polymerization: initiation of polymerization in monomer droplets, *J. Polym. Sci., Polym. Lett. Edn*, **11**, 503–513 (1973).
 77. Sudol, E.D. and El-Aasser, M. -S., Miniemulsion polymerization, in *Emulsion Polymerization and Emulsion Polymers*, Lovell, P. A., and El-Aasser, M. -S. (Eds.), Wiley, New York, 1997, pp. 699–722.
 78. Blythe, P. J., Morrison, B. R., Matthauer, K. A., Sudol, E. D., and El-Aasser, M. S., Polymerization of miniemulsions containing pre-dissolved polystyrene using hexadecane as costabilizer, *Langmuir*, **16**, 898–904 (2000).
 79. Miller, C. M., Sudol, E. D., Silebi, C. A., and El-Aasser, M. S., Polymerization of miniemulsions prepared from polystyrene in styrene solutions. I. Benchmarks and limits, *Macromolecules*, **28**, 2754–2764 (1995).
 80. Makino, K., Mossoba, M. M., and Riesz, P., Chemical effects of ultrasound on aqueous solutions. Formation of hydroxyl radicals and hydrogen atoms, *J. Phys. Chem.*, **87**, 1369–1377 (1983).
 81. Erdem, B., Sudol, E. D., Dimonie, V. L. and El-Aasser, M. S., Encapsulation of inorganic particles via miniemulsion polymerization, *Macromol. Symp.*, **155**, 181–198 (2000).
 82. Distler, D., *Aqueous Polymer Dispersions*, VCH-Wiley, Weinheim, 1999 (in German).
 83. Ugelstad, J., Mfutakamba, H. R., Mork, P. C., Ellingsen, T., Berge, A., Schmid, R., Holm, L., Jorgendahl, A., Hansen, F. K., and Nustad, K., Preparation and application of monodisperse polymer particles, *J. Polym. Sci., Polym. Symp. Edn*, **72**, 225–240 (1985).
 84. Ugelstad, J., Stenstad, P., Kilaas, L., Prestvik, W. S., Rian, A., Nustad, K., Herje, R., and Berge, A., Biochemical and biomedical application of monodisperse polymer particles, *Macromol. Symp.*, **101**, 491–500 (1996).
 85. Fitch, R. M. and Shih, L. -B., Emulsion polymerization: kinetics of radical capture by the particles, *Prog. Colloid Polym. Sci.*, **56**, 1–11 (1975).

CHAPTER 9

Colloidal Processing of Ceramics

Lennart Bergström

Institute for Surface Chemistry, Stockholm, Sweden

1	Introduction	201	5.2	Stable and flocculated suspensions	209
2	Powder Processing of Ceramics	202	5.3	The effect of solid loading	210
	2.1 Colloidal processing	203	5.4	Compression rheology	211
3	Interparticle Forces and Colloidal Stability	203	6	Consolidation	212
	3.1 van der Waals forces	203	6.1	Drained casting techniques	212
	3.2 Electrostatic double-layer forces	204	6.2	Electrophoretic deposition	213
	3.3 Polymer-induced forces	205	6.3	Extrusion and injection molding	214
4	Deagglomeration and Dispersion	206	6.4	Dry pressing	214
5	Rheological Properties of Ceramic Suspensions	208	6.5	Direct casting techniques	215
	5.1 Basic concepts	208	6.6	Solid freeform fabrication	216
			7	Drying and Binder Burnout	216
			8	Acknowledgements	217
			9	References	217

1 INTRODUCTION

Mankind has used ceramics for thousands of years. The oldest findings of ceramic objects date back more than 20 000 years with a larger scale production of bowls and storage vessels starting from 6000 BC in China. All ancient ceramics were based on clay but the properties varied greatly depending on the composition and firing temperature. The traditional ceramics still form the basis for dinner-ware, household items and works of art, but it is the advent of advanced, non-clay ceramics that has sparked the current large interest in ceramic materials. During the last 50 years, we have seen a tremendous development of advanced ceramics for functional, biomedical and structural applications (1). Structural ceramics possess unique material properties such as high strength from room temperature to very high temperatures (up to 1500°C), good wear, and erosion and corrosion resistance in most environments. Functional

ceramics are characterized by specific electrical, dielectric, magnetic and optical properties. Advanced ceramics are currently being used in a large number of applications such as cutting tools, heat engine parts, body implants, sensors, capacitors and actuators, with new applications continuously evolving.

Ceramics are brittle materials at moderate temperatures, which means that a ceramic material is prone to catastrophic failure when the fracture stress is exceeded. The strength of a ceramic material can be described by the Griffith equation (1), as follows:

$$\sigma = YK_{IC}/\sqrt{C} \quad (9.1)$$

where σ is the fracture stress, K_{IC} the fracture toughness, C the defect size, and Y a factor that depends on the position and shape of the defect. This relationship suggests that there are two ways of increasing the strength of a ceramic material, namely by increasing the fracture toughness or by decreasing the flaw size. A flaw or defect can be thought of as an inhomogeneity in the

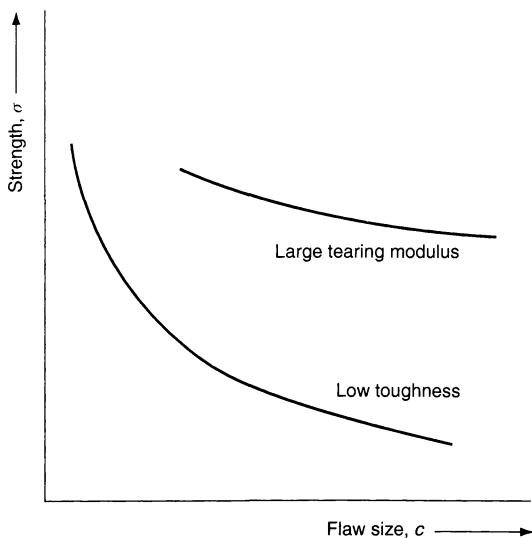


Figure 9.1. Effects of damage on the strength of low- and high-toughness ceramics

material. These flaws can be cracks, inclusions, agglomerates or pores. If the fracture toughness is increased, the strength of the material becomes more insensitive to flaw size (Figure 9.1). This can be accomplished by the incorporation of a second phase such as whiskers, platelets or particulates (1). In order to obtain the optimal increase in fracture toughness and to avoid the formation of new defects, the reinforcing phase has to be well dispersed in the matrix.

Although high strength can be achieved by defect minimization, the flaw size distribution can vary from specimen to specimen, thus leading to a very broad strength distribution, i.e. low reliability. For design purposes, the scatter in fracture strength should be kept at a minimum. Hence, the defect minimization has to be so effective that defects above a certain size never occur. The performance at high temperatures is also controlled by the microstructure of the ceramic material. The composition and the amorphous or crystalline nature of the grain boundary phases often determine the creep or slow crack growth tendency, which are the most important mechanisms for failure at high temperatures. The uniformity of the microstructure is also important for the electrical properties of functional ceramics. For example, a maximum dielectric constant of BaTiO_3 is achieved when the final grain size distribution is uniform and small. This is very important for multi-layer capacitors where a high dielectric constant relates to a small size and high efficiency of the capacitor.

In summary, a ceramic material should have a microstructure characterized by a small defect size, other phases which are well dispersed and a homogeneous grain boundary phase composition to perform optimally at both room temperature and elevated temperatures. How can such a microstructure be obtained? In order to answer this question, we have to consider how a ceramic material is produced.

2 POWDER PROCESSING OF CERAMICS

Most advanced ceramics are formed as powder compacts and densified by sintering. Other forming techniques commonly employed for metals and polymers, e.g. deformation methods and melt casting, are unsuitable. Powder processing involves five basic steps (2): (i) powder production, (ii) preparation of powders for consolidation, (iii) consolidation to an engineering shape, (iv) removal of solvent and organic additives (drying and burnout), and (v) densification. Each step has the potential for introducing a detrimental heterogeneity, which will either persist during further processing or develop into a new heterogeneity during densification and microstructure development. Hence, the microstructural inhomogeneities that occur in the early processing steps, e.g. powder mixing and powder consolidation, are very difficult, if not impossible, to remove during the later processing steps, e.g. burnout and sintering. This means that handling of fine (usually submicron-sized) ceramic powders in large quantities requires a high degree of process control to reach the desired microstructural characteristics.

Many of the detrimental heterogeneities stem from the powder itself, e.g. large, hard agglomerates and contamination by foreign phases. Other heterogeneities are introduced in the powder preparation step, e.g. an inhomogeneous phase distribution due to insufficient mixing of the ingoing components. The consolidation method used can also introduce heterogeneities. Hence, in order to produce reliable ceramic materials, methods must be developed which can eliminate heterogeneities from the powders and avoid the introduction of other types of heterogeneities in the subsequent processing steps.

The sensitivity of ceramic materials to heterogeneities, and the difficulty in removing them in subsequent processing, means that the microstructure and homogeneity of the consolidated powder (before sintering) is strongly related to the properties of the final material (2, 3). In general, the powder body (which

is called the *green body* in the ceramics community) should have the following characteristics: (i) a high, uniform packing fraction of particles, (ii) small and narrow size pores, and (iii) a high degree of homogeneity (sintering additives and reinforcing phases being well mixed). Furthermore, common heterogeneities such as agglomerates, organic inclusions and gas bubbles, have to be avoided. There is also a desire to decrease the size of the ingoing powders (typically $<1 \mu\text{m}$) in order to enhance sinterability at lower temperatures and to reduce the scale of mixing homogeneity of different components.

2.1 Colloidal processing

The present methods of manufacturing ceramic green bodies of a complicated shape on an industrial level include dry-pressing with subsequent machining, slip casting, tape casting, pressure casting and injection moulding (4, 5). All of these forming methods start with a suspension where the ceramic particles (powders, whiskers, platelets, etc.) are mixed with a liquid or a polymer melt, a proper dispersant, and possibly further additives (such as binders, plasticizers, and anti-foaming agents). With the growing awareness of the detrimental effect of different types of heterogeneities on the material properties, a concept called *colloidal processing* has been successfully applied to improve product reliability. The colloidal processing concept involves the manipulation and control of the interparticle forces in powder suspensions (2, 6), in order to remove heterogeneities and to optimize the suspension properties. For example, repulsive interparticle forces can be used to create colloidally stable suspensions where weak agglomerates are broken down and good mixing of different powders is facilitated. Large, hard agglomerates can also be removed by sedimentation or filtration at low volume fractions. Colloidally stable suspensions usually facilitate the good mixing of different powders. Flocculation of such a composite suspension can be used as a way of avoiding mass segregation during storage and handling.

Interparticle forces play a pivotal role in determining the suspension rheology (4, 7). For example, a highly concentrated suspension can be transformed from an easily pourable liquid to a stiff paste by changing the interparticle forces from repulsive to attractive. Such a transformation is also related to a change in the microstructure of the suspension. In general, a colloidally stable suspension has a homogeneous microstructure, where the single particles are separated

from each other. A flocculated concentrated suspension, on the other hand, consists of clusters of particles touching each other and, hence, creates an inhomogeneous suspension microstructure. This difference in suspension microstructure and suspension rheology can have a large impact on the behaviour during consolidation. For example, an inhomogeneous microstructure can be expected to influence the filtration rate in pressure filtration and slip casting. Liquid flow is facilitated by the existence of larger channels between the clusters.

This review intends to cover the field of colloidal processing of ceramics. To support the understanding of the underlying colloidal concepts, we will briefly introduce a background on the major particle interactions. This is followed by a section on deagglomeration and dispersion. An orientation on how the rheological properties of concentrated suspensions can be manipulated is also given. The various colloidal consolidation routes are presented and we also discuss the drying and burnout behaviour.

3 INTERPARTICLE FORCES AND COLLOIDAL STABILITY

It is critical to understand how one may manipulate suspension properties to generate the desired rheological behaviour for the chosen forming technique. The ability to control and manipulate the sign of particle interactions represents a first step towards optimised colloidal processing. Attempts to estimate the properties of ceramic slurries by calculations are generally hampered by the complex nature of these systems. Accurate calculations require many parameters to be defined, but this information is usually difficult to obtain. Hence, although calculations can lead a long way, direct measurements of the interparticle forces and rheological properties are indispensable for an improved understanding of these complex systems. The dominating interparticle forces in most ceramic systems are the van der Waals, double-layer (electrostatic) and steric (polymer-induced) forces. We will give a brief account of the theories underlying each of these interactions, with examples of direct measurements in ceramic systems.

3.1 van der Waals forces

All ceramic powders experience van der Waals forces. This force is electrodynamic in origin as it arises from

the interactions between oscillating or rotating dipoles within the interacting media. This ubiquitous interaction may be of varying importance depending on the system, and the Hamaker constant (A) represents a conventional and convenient way of assessing its magnitude (7, 8). For example, the van der Waals interaction free energy, $V_{\text{vdW}}(D)$, between two spheres of radius R at a surface separation D , can be approximated by the following:

$$V_{\text{vdW}}(D) = -AR/12D \quad (9.2)$$

providing that $D \ll R$. As can be seen from equation (9.2), there is a direct proportionality between the magnitude of the van der Waals interaction and the Hamaker constant. The latter is a materials constant that depends on the dielectric properties of the two materials and the intervening media. The distance dependence of the van der Waals energy depends essentially on the geometry of the two interacting bodies, being proportional to D^{-2} for parallel plates, and scales to D^{-1} for two spherical particles.

In the original treatment, also called the *microscopic approach*, the Hamaker constant was calculated from the polarizabilities and number densities of the atoms in the two interacting bodies. Lifshitz presented an alternative, more rigorous approach where each body is treated as a continuum with certain dielectric properties. This approach automatically incorporates many-body effects, which are neglected in the microscopic approach. The Hamaker constants for a number of ceramic materials have been calculated from the Lifshitz theory using optical data of both the material and the media (Table 9.1) (9). Clearly, all ceramic materials are characterized by large unretarded Hamaker constants in air. When the materials interact across a liquid, their Hamaker constants are reduced, but still remain rather high, except for silica.

If we want to create a colloidal stable system, some type of interparticle repulsion needs to be introduced to overcome the van der Waals attraction. In a stable system, the maximum attractive interparticle energy should be less than $1-2 kT$ to allow thermal motion to readily break all particle-particle bonds. Since the magnitude and range of the attractive van der Waals interaction scales with the effective Hamaker constant, a relatively long-range repulsion is needed to stabilize suspensions of ceramic powders such as alumina and silicon carbide; silica, however, is stabilized by a very short-range repulsion.

Below, we will describe the two most common methods of stabilizing a colloidal suspension, i.e. either by creating an electrostatic double-layer at the solid-liquid

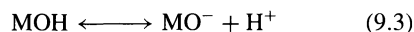
Table 9.1. Calculated values of Hamaker constants between identical ceramic materials. (Adapted from ref. (9))

Material	Non-retarded Hamaker constants (10^{-20} J)	
	Vacuum (Air)	Water
α -Al ₂ O ₃	15.2	3.67
BaTiO ₃ (average)	18.0	8.0
BeO (average)	14.5	3.35
CaCO ₃ (average)	10.1	1.44
CaF ₂	6.96	0.49
CdS	11.4	3.40
MgO	12.1	2.21
Mica	9.86	1.34
PbS	8.17	4.98
6H-SiC	24.8	10.9
β -Si ₃ N ₄	18.0	5.47
Si ₃ N ₄ (amorphous)	16.7	4.85
SiO ₂ (quartz)	8.86	1.02
SiO ₂ (silica)	6.50	0.46
SrTiO ₃	14.8	4.77
TiO ₂ (average)	15.3	5.35
Y ₂ O ₃	13.3	3.03
ZnO	9.21	1.89
ZnS (cubic)	15.2	4.80
ZnS (hexagonal)	17.2	5.74
3Y-ZrO ₂	20.3	7.23

interface, or by adsorbing polymers or surfactants on the particle surfaces.

3.2 Electrostatic double-layer forces

Immersing a ceramic powder in a polar liquid, such as water, usually results in the buildup of a charge at the solid-liquid interface. The interfacial charge is a result of adsorption or desorption of ionic species in solution, e.g. by proton transfer reactions with the surface hydroxyl groups, or by adsorption of specifically adsorbed ions. The site-dissociation reactions for an amphoteric oxide (MO) can be written as follows:



Both the pH and the reaction constant for the respective dissociation reaction control the net charge. The point of zero charge (pzc) is the pH where the surface concentration of (MO^-) and (MOH_2^+) are equal. The surface charge is negative at a $\text{pH} > \text{pH}_{\text{pzc}}$ and positive at $\text{pH} < \text{pH}_{\text{pzc}}$. Ions of opposite charge (counterions) are attracted to the charged interface and form a diffuse ion "cloud" adjacent to the particle surface. The thickness of this electrical double-layer is a very important parameter, which determines the range of the double-layer repulsion. The concentration and valency of the

ions in solution control this; a high concentration of ions (high ionic strength) results in a thin double-layer. The thickness is commonly identified with the Debye length, which is the inverse of the Debye parameter, κ :

$$\frac{1}{\kappa} = \left(\frac{\epsilon \epsilon_0 k T}{e^2 \sum_i n_i z_i^2} \right)^{1/2} \quad (9.5)$$

where e is the electronic charge, n_i is the concentration of ions with charge z_i , ϵ is the dielectric constant of the liquid and ϵ_0 is the permittivity of vacuum.

The interaction between two charged particles in a polar media is related to the osmotic pressure created by the increase in ion concentration between the particles where the electrical double-layers overlap. The repulsion can be calculated by solving the Poisson–Boltzmann equation, which describes the potential, or ion concentration, between two overlapping double-layers. The full theory is quite complicated, although a simplified expression for the double-layer interaction energy, $V_{DL}(D)$, between two spheres, can be written as follows:

$$V_{DL}(D) = 2\pi R \epsilon \epsilon_0 \psi_0^2 \exp(-\kappa D) \quad (9.6)$$

where ψ_0 is the surface potential.

Combining the attractive van der Waals interaction and the repulsive double-layer repulsion is the foundation of the well-known DLVO theory (7, 8), which provides an overall net interaction energy, as illustrated in Figure 9.2. The interaction energy displays an

energy barrier with a magnitude related to the Hamaker constant, surface potential and ionic strength. At a low surface potential or at a high ionic strength, the repulsive barrier will vanish, thus allowing particles to flocculate. This suggests two routes for flocculating an electrostatically stabilized suspension, namely either by reducing the charge on the particle surfaces through a change in pH towards the pH_{pzc} or by increasing the ionic strength to reduce the range of the double layer repulsion.

3.3 Polymer-induced forces

In many ceramic systems it is not possible to create a stable suspension simply by controlling pH. Large additions of acid or base can result in dissolution of the particles, or provide a too high ionic strength. Hence, addition of suitable polymeric dispersants is commonly used to create colloidal stable suspensions. These polymeric additives can induce an interparticle repulsion that prevents coagulation. Upon the close approach of two particles covered with adsorbed polymer layers, the interpenetration of the polymer layers give rise to a repulsive force, the so-called *steric stabilization* (10). There are some simple requirements for steric stabilization of colloidal suspensions, as follows:

- (i) The adsorbed polymer layer should be thick enough to prevent the particles from coming into close contact where the van der Waals forces will give rise to a net attraction.
- (ii) The adsorbed polymer layer should completely cover the particles and be as dense as possible. If the coverage is incomplete or the layer density is too low, the particles may come into close contact. Bridging flocculation might also occur if the coverage is incomplete.
- (iii) The polymer should be firmly “anchored” to the surface of the particle. If the adsorption is too weak, the polymer may desorb or be “pushed” away during a particle collision.
- (iv) The stabilizing moieties should be in a *good-solvent* condition. If the solvent condition is bad, interaction between two polymer layers will result in an attractive, and not a repulsive force. The solvent quality is commonly characterized by the Flory–Huggins parameter, χ , where poor solvent quality has $\chi > 0.5$.

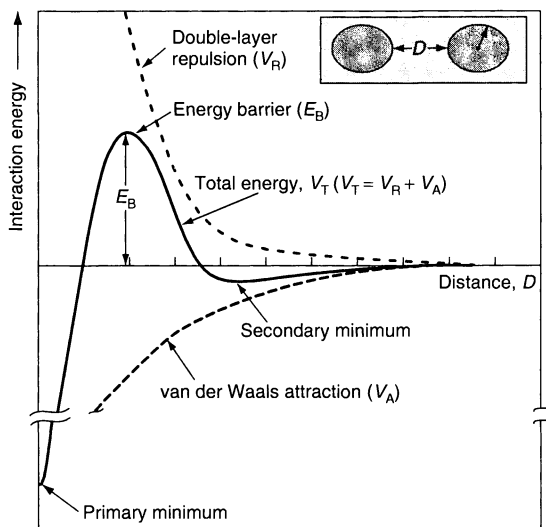


Figure 9.2. Schematic energy versus distance curves for double layer repulsion and van der Waals attraction. (Adapted from ref. (15) with permission of The American Ceramic Society)

The thickness of the adsorbed layers, the affinity of the polymer to the surface, the adsorbed amount and the solvency of the polymer in the media are all strongly

interrelated. This provides several ways in which to manipulate the stability of sterically stabilized systems.

Any theory trying to describe the magnitude and range of the interaction between polymer layers needs to account for both the solution properties of the polymer and the conformations of the polymer at the solid–liquid interface (7, 10). The repulsive steric forces for polymers in a good solvent can be characterized by using De Gennes scaling theory (11). In scaling theory, the adsorbed polymer conformation is assumed to be either a low surface coverage *mushroom*, in which the volume of the individual polymer is unconstrained by neighbours, or a high surface coverage *brush*, where the proximity of neighbouring polymer chains constrains the chain volume and causes extension of the polymer into the solvent. The normalized force for two spheres as a function of separation distance can be expressed by using a scaling expression valid for polymer brushes:

$$\frac{F(D)}{R} = \frac{8\pi kT}{35} \frac{L}{s^3} \left[7 \left(\frac{2L}{D+2\delta} \right) + 5 \left(\frac{D+2\delta}{2L} \right)^{7/4} - 12 \right] \quad (9.7)$$

where s is the distance between the chain anchoring points, L denotes the interaction range from each surface and δ is the thickness of the highly compressed polymer layer.

The term electrosteric stabilization is often used to describe how polyelectrolytes act as dispersants. Electrosteric stabilization is a combination of a pure electrostatic repulsion and a polymeric repulsion where the relative importance of the respective contributions is closely related to the segment density profile at the interface. If the polyelectrolyte adsorbs in a flat conformation, the polymeric repulsion is short-range in nature, and the stabilization mechanism is mainly

electrostatic. This is usually the case when the polyelectrolyte is highly charged, has an extended conformation, and the particle surface is oppositely charged. With thicker adsorbed layers, having chains protruding into the solution, the polymeric contribution will become more important. In addition to the steric contribution, there is always an electrostatic contribution since the adsorption of a highly charged polyelectrolyte on a weakly charged, amphoteric oxide surface usually results in an increase of the net surface charge density.

4 DEAGGLOMERATION AND DISPERSION

The deagglomeration and dispersion of ceramic powder processing is crucial for obtaining a high reliability and high strength in the final material. Any inhomogeneity in the suspension, e.g. segregation, density gradients or presence of agglomerates, is a potential flaw in the sintered material. Hence, the agglomerates, which exist in most starting powders, either have to be broken down or removed. The definition of an agglomerate depends on the chosen length scale and what is defined as the primary unit. The crystallites, i.e. the single crystal units in a powder, are typically quite small, <100 nm, which means that the “primary” particles, typically of a size between 0.5 and 1 μm , are, in fact, small agglomerates. These “primary” particles (more correctly called primary agglomerates) constitute the building blocks of secondary agglomerates of a typical size between 50 and 200 μm (Figure 9.3). With the current interest in using finer and finer particles and going into the so-called nanosized (<100 nm) range, it becomes necessary to break down not only the secondary agglomerates but also disintegrate the primary agglomerates.

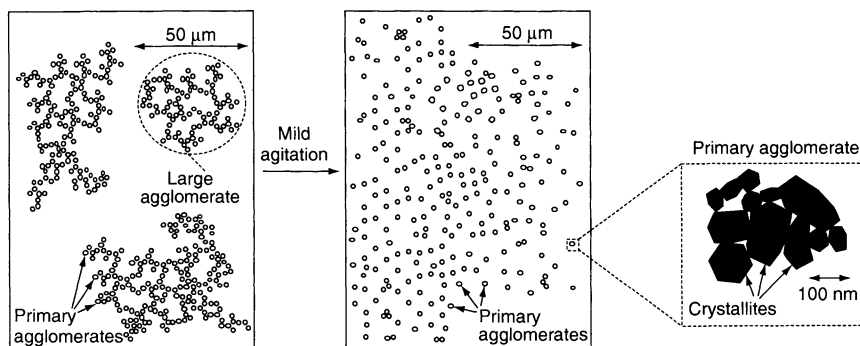


Figure 9.3. Schematic showing the hierarchical structure of ceramic powders. (From E. Laarz, B. V. Zhmud and L. Bergström, *J. Am. Ceram. Soc.*, **83**, 2394–2700 (2000), reprinted with permission from The American Ceramic Society)

Deagglomeration proceeds through the breakup of interparticle bonds in the aggregates. For this to happen, the applied force has to be larger than the adhesion force between the particle and the aggregate. For a dilute suspension subjected to mild agitation, hydrodynamic drag will be the dominating force on the aggregate. The drag force exerted on a single particle of radius R in a flow field is of the order of:

$$F_d \approx 6\pi v\eta R \quad (9.8)$$

where v is the fluid velocity and η is the viscosity. Therefore, the drag force should be directly proportional to the particle size and the fluid velocity. For a concentrated suspension subjected to high-energy milling, the situation is much more complex; inertial forces transmitted through collisions with other clusters or the milling media become important and make the deagglomeration process a mixture of cluster erosion and attrition.

Although the mechanism for hydrodynamic detachment is poorly understood, it is clear that the hydrodynamic drag force required to detach a particle is proportional to the interparticle adhesion force:

$$F_d = \gamma F_{ad} \quad (9.9)$$

where γ is a numerical constant. This parameter is close to unity when the drag force is perpendicular to the surface but much smaller than 1 when the hydrodynamic force is parallel to the surface.

The particles in an aggregate are held together by attractive van der Waals (vdw) forces. This interaction is described by equation (9.2), which show that the magnitude of the vdW attraction is determined by the Hamaker constant and the separation distance of the particles in the aggregate. The adhesive interparticle force can be reduced by creating a surface charge on the particles and thus induce an electrostatic repulsion. Another possibility is to prevent the particles from coming into close contact by coating them with a layer of a suitable substance, e.g. surfactants or small organic molecules that adsorb strongly to the particle surface.

In addition to the surface forces, it is also possible that the particles are held together by rigid interparticle bridges, so-called necks. These solid bridges can result from reprecipitation of soluble material during drying or from partial sintering of crystallites during pyrolysis or calcination in the powder manufacturing stage (2). For sparingly soluble non-oxide ceramics, such as silicon nitride, the necks may also develop through oxidation during storage or by a dissolution/precipitation processes at the particle contact points. The size of the necks may be quite large (10–100 nm) for systems where a

large amount of material is reprecipitated but should be of the same order as the thickness of the oxidized surface layer (1–10 nm) for sparingly soluble non-oxide powders.

The neck radius, h , holding two particles of different size, R_1 and R_2 , together may be expressed as follows:

$$h = 2(r\bar{R})^{1/2} \quad (9.10)$$

where \bar{R} is the geometrical mean of the particle radii and r is the curvature radius of the neck. The decay of the neck radius with time, $h(t)$, is related to the dissolution rate, k_m , according to the following:

$$h(t) \approx h - \frac{k_m t}{\rho} \quad (9.11)$$

assuming that reprecipitation can be neglected. This is a reasonable assumption at early stages of dissolution where the bulk concentration of soluble species is much less than the saturation concentration. The strength of a neck, F_n , is proportional to the cross-sectional area of the neck, which gives the following approximate expression for the time-dependence of the adhesion force:

$$F_n \approx E\varepsilon\pi \left(h - \frac{k_m t}{\rho} \right)^2 \quad (9.12)$$

where ρ is the neck density, E is the elastic modulus of the material, typically of the order of 1 to 10 GPa, and ε is the elongation at fracture, typically of the order of 0.01 for brittle materials. Equating the adhesion force with the drag force (equation 9.8), one can define the critical length, h^2/a , as follows:

$$\frac{h^2}{a} = \frac{6v\eta}{E\varepsilon} \quad (9.13)$$

which shows that even a small neck (<10 nm) can induce a very strong interparticle bond. Hence, the neck has to be essentially completely dissolved to allow deagglomeration under mild agitation. In highly concentrated suspensions, it is expected that cluster attrition becomes more important in the deagglomeration process, although the breakup of interparticle necks by dissolution may still be of significance.

These simple force-balance estimates show that the interparticle bonds either have to be dissolved or broken by excessive mechanical forces to give a deagglomerated suspension. Although intense milling is often the solution, optimization of the dissolution rate may solve a deagglomeration problem at a shorter time with a smaller energy consumption. For most oxide materials, rapid dissolution can be obtained by shifting the pH away from the stable region and increasing the

temperature. For example, the silica-like oxide layer on silicon carbide and silicon nitride can easily be dissolved at high pH (>11) and elevated temperatures.

5 RHEOLOGICAL PROPERTIES OF CERAMIC SUSPENSIONS

Rheological methods are widely used to determine the properties of concentrated ceramic suspensions. Rheology can be used as an analysis method, e.g. when determining the optimal amount of dispersant from measurements of viscosity versus the amount of dispersant added. In addition, rheological measurements are often used for quality control in order to minimize the batch-to-batch variation before a ceramic suspension is processed further, e.g. spray dried or tape cast. The rheological behaviour can also be used as a direct process parameter, which should be appropriately adjusted to obtain the optimal green-body properties after forming.

Fundamentally, the rheological properties of concentrated colloidal suspensions are determined by the interplay of thermodynamic and fluid mechanical interactions. This means that there exists an intimate relationship between the particle interactions, including Brownian motion, the suspension structure (i.e. the spatial particle distribution in the liquid), and the rheological response. With particles in the colloidal size range (at least one dimension <1 μm), the range and magnitude of the interparticle forces will have a profound influence on the suspension structure and hence, the rheological behaviour (4, 7). Both the fluid mechanical interactions and the interparticle forces are

strongly dependent on the average separation distance between the suspended particles. Hence, the rheological behaviour of concentrated suspensions is a function of the solids concentration, the particle size and shape, and the range and magnitude of the interparticle forces. Below, some of the salient features of concentrated suspensions, which relate to the colloidal processing of ceramics, are described, after a brief introduction of some basic concepts.

5.1 Basic concepts

The different types of viscous response in steady shear can be illustrated by plots of shear stress versus shear rate or viscosity versus shear rate (Figure 9.4). In the simplest case (a), so-called Newtonian behaviour, the flow curve is a straight line passing through the origin, with the slope of the curve being equal to the viscosity, η . In practice, most concentrated suspensions show a more complicated flow behaviour where the viscosity is shear-dependent. A shear thickening (also called a dilatant) system is characterized by an increasing apparent viscosity with shear rate (curve (b)). If the viscosity decreases with shear rate, the system is described as being shear-thinning (curve (c)). If the decrease in viscosity is very large at small shear rates, the system is sometimes called pseudoplastic. Commonly, concentrated suspensions show a plastic behaviour with no response until a limiting yield stress, σ_y , has been exceeded. If the flow curve is linear above σ_y , the system is said to be a Bingham plastic (curve d), described by the Bingham model (12), as follows:

$$\sigma = \sigma_y + \eta_{pl}\dot{\gamma} \quad (9.14)$$

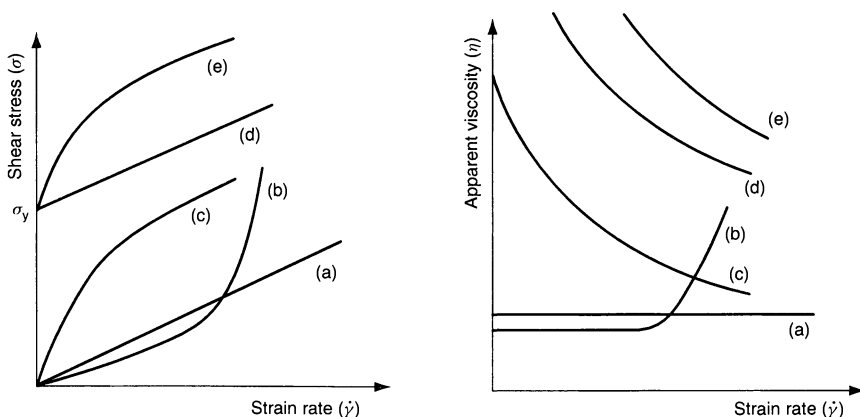


Figure 9.4. Classification of rheological behaviour under steady-shear conditions, plotted as shear stress and viscosity versus strain rate; (a) Newtonian; (b) shear thickening; (c) shear thinning; (d) Bingham plastic; (e) nonlinear plastic. (From ref. (4) with permission from Marcel Dekker Inc.)

where η_p , the plastic viscosity, is defined as the slope of the flow curve at $\sigma > \sigma_y$. The yield stress, σ_y , in the Bingham model is sometimes called the Bingham yield stress, σ_B . The curve above the yield stress can also be nonlinear (curve (e)).

The rheological properties of concentrated suspensions are often time-dependent. If the apparent viscosity continuously decreases with time under shear, with a subsequent recovery of the viscosity when the flow is stopped, the system is said to be *thixotropic*. The opposite behaviour is called *antithixotropy*, or sometimes *rheopexy*. Thixotropy should not be confused with shear-thinning which is a time-independent characteristic of a system. Systems which show an irreversible decrease in viscosity with shear should be termed shear-destructive and not thixotropic.

The viscoelastic behaviour of concentrated suspensions can be studied using several different methods (4, 7). The most widely used method consists of subjecting the material to a continuously oscillating strain over a range of frequencies and then measuring the peak value of the stress, σ_0 , and the phase difference between the stress and strain, δ . A sinusoidal deformation is usually employed.

In the linear viscoelastic region, the mathematical analysis of the data is substantially simplified since the ratio of stress to strain:

$$G^* = \sigma_0/\gamma_0 \quad (9.15)$$

where G^* is called the complex or the dynamic modulus, is independent of the magnitude of the stress or strain. The dynamic modulus can also be expressed in complex form in terms of a storage modulus, G' , and a loss modulus, G'' , as follows:

$$G^* = G' + iG'' \quad (9.16)$$

where i (the complex number) is equal to $\sqrt{-1}$. The storage modulus, G' , represents the in-phase stress-to-strain ratio and gives a measure of the elastic properties. The loss modulus, G'' , represents the out-of-phase stress-strain ratio and gives a measure of the viscous properties. All of these rheological parameters, G^* , G' , G'' , etc., vary with frequency. Phenomenological models such as the Maxwell, Kelvin or Berger models can be used to describe the frequency dependence of the rheological parameters (7). These models are mechanical analogues consisting of combinations of springs representing an elastic, Hookean response and dash-pots representing a viscous response.

5.2 Stable and flocculated suspensions

Concentrated colloidally stable suspensions display a shear-thinning behaviour under steady shear because of a perturbation of the suspension structure by the shear. At low shear rates, the suspension structure is close to equilibrium because thermal motion dominates over the viscous forces. At higher shear rates, the viscous forces affect the suspension structure, and shear-thinning occurs. At very high shear rates, the viscous forces dominate and the plateau value of the viscosity measures the resistance to flow of a suspension with a completely hydrodynamically controlled structure. Both the degree of shear-thinning and the viscosity at high shear rates increases with increasing volume fraction of the solids.

Models describing this type of shear-thinning behaviour have been developed by Krieger and Cross (see ref. (4)). Figure 9.5 illustrates how well the high-shear form of the Cross equation can describe the steady shear properties of stable silicon nitride suspensions. The full form of these models could not be utilized due to the inability of reaching the low-shear region. Near the high-shear-rate limit, where $b\dot{\gamma}^p \gg 1$, the Cross equation takes the following form:

$$\eta = \eta_\infty + \frac{\eta_0 - \eta_\infty}{b\dot{\gamma}^p} \quad (9.17)$$

which is essentially a three-parameter equation, with b and p being fitting parameters and $\dot{\gamma}$ being the shear rate; η_0 and η_∞ represent the low-shear and high-shear limiting viscosities, respectively.

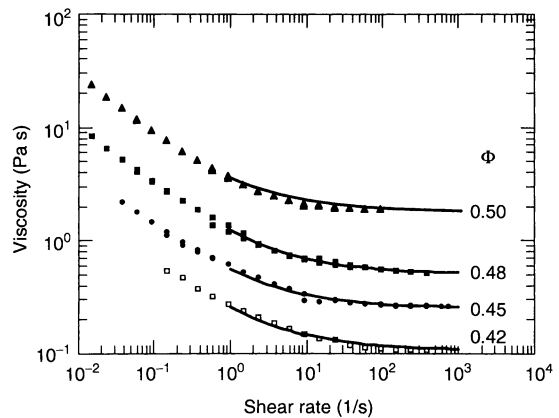


Figure 9.5. Degree of shear thinning of silicon nitride suspensions at different solids content. (From L. Bergström, *Colloids Surf. A*, **133**, 151–155 (1998) with permission from Elsevier Science)

The viscoelastic response of a colloiddally stable concentrated suspension is strong when the average distance between the suspended particles is of the same order as the range of the repulsive interparticle potential. Hence, the viscoelastic properties originate from this latter potential. The magnitude of the viscoelastic response becomes stronger with an increase of the overlap of the repulsive forces, e.g. by increasing the solids loading or decreasing the particle size, which results in a decrease of the average distance between the particles. An alternative way of influencing the viscoelastic properties of electrostatically stabilized suspensions is to change the ionic strength. A low ionic strength results in a long-range electrostatic repulsion, thus leading to a strong viscoelastic response at low volume fractions.

Shear-thickening is a phenomenon which needs to be controlled and often minimized in several ceramic processing steps, such as the filling of a mould or during general suspension handling e.g. pumping and pouring. Colloiddally stable, concentrated suspensions may show either continuous or discontinuous shear-thickening. The severity of the shear-thickening increases with increasing particle concentration, while the critical shear rate for the onset of shear thickening decreases with increasing particle concentration (13). The shear-thickening phenomenon is associated with a order–disorder transition. Because of this, shear-thickening is strongly dependent on the particle size distribution. Shear-thickening is most pronounced for monodisperse systems and becomes less severe when using a polydisperse system.

Flocculation occurs when the net force between the particles is attractive. At low volume fractions, aggregation results in clusters, or flocs, which have a fractal structure (7). For most systems, the properties of the aggregating suspension changes drastically at a certain critical particle concentration, ϕ_g , which corresponds to the formation of a space-filling particle network. In dilute suspensions, at $\phi < \phi_g$, suspensions have no yield stress and the discrete clusters will settle more or less independently. Above ϕ_g , the suspension can sustain a stress before yielding; the elasticity may be significant, and the rate of settling is very slow.

The viscoelastic properties, in particular how the elastic modulus scales with the volume fraction, have been modelled based on the assumption that the particle network consists of close-packed fractal flocs. Although differing in details, these models all predict a power-law behaviour, which can be written as follows:

$$G = G_0 \phi^p \quad (9.18)$$

where G_0 is the pre-exponential factor. The exponent, p , is related to the structure through the fractal dimension of the flocs.

If a stress above the yield stress is applied, the gelled structure is broken into smaller units (flocs), which can then move past each other. If floc attrition is affected by the strength of the hydrodynamic and attractive forces, pseudoplastic behaviour is observed and the viscosity decreases with shear rate. The strong shear forces at high shear cause flow units to be smaller and flow is facilitated. The destruction of flocs releases constrained solvent, which results in a decrease in the effective volume-fraction of the flocs. This phenomenon may create thixotropic behaviour in the system if the breakup and formation of flocs is reversible.

These qualitative differences in suspension properties based on the attractive or repulsive nature of the interparticle forces have been utilized in the optimization of colloidal processing concepts and have led to the development of the direct casting techniques which will be described in more detail below.

5.3 The effect of solid loading

The viscosity of a suspension is strongly dependent on the solids loading, with the viscosity approaching infinity at a maximum volume fraction, ϕ_m . The latter relates to the particle concentration at which the average separation distance between the particles tends to zero and the particles pack together, thus making flow impossible. The maximum volume fraction is strongly dependent on the particle size distribution and the particle shape. A broad particle size distribution displays a higher value of ϕ_m because the small particles can fit into the voids between the large particles.

When the particles in suspension are non-spherical, the rotation of the particles due to Brownian motion results in an excluded volume, which is higher than the volume-fraction of the particles. As the degree of anisotropy increases, the effects become more dramatic. Figure 9.6 shows the volume-fraction dependence of the viscosity of silicon nitride, alumina and silicon carbide whisker (SiC_w) suspensions. The experimental points were fitted to a modified Krieger–Dougherty equation:

$$\eta_r = \left(1 - \frac{\phi}{\phi_m}\right)^{-n} \quad (9.19)$$

where ϕ_m and n are used as fitting parameters. The best fit of the experimental data to equation 9.19 shows that the maximum volume fraction is drastically lower for the SiC_w suspension ($\phi_m = 0.28$) when compared to the

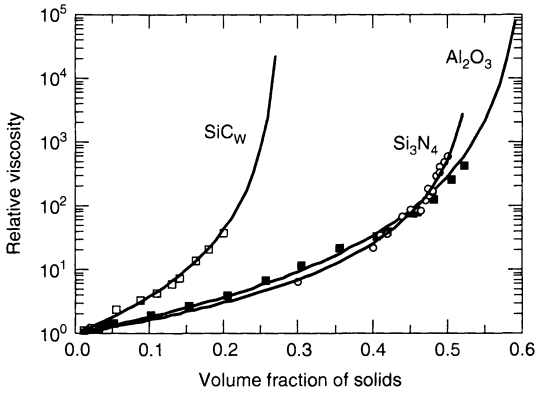


Figure 9.6. Relative high-shear viscosity as a function of volume fraction of solids for different materials. (From L. Bergström, *Colloids Surf., A*, **133**, 151–155 (1998) with permission from Elsevier Science)

Al_2O_3 suspension ($\phi_m = 0.61$) or the Si_3N_4 suspension ($\phi_m = 0.54$). The low values of the maximum volume fractions, illustrates the poor packing behaviour of rods. This demonstrates that the effect of aspect ratio in pure suspensions can be quite dramatic and thus a serious concern in ceramic processing.

When the solids concentration approaches dense packing, the range and magnitude of the interparticle forces become very important in controlling the rheological response. Irrespective of the origin of the repulsion, the repulsive barrier will occupy a certain volume, thus preventing the particles from coming into close contact. This effect can be calculated by adding the volume of the repulsive range, e.g. the thickness of an attached polymer layer, to the volume fraction of the solid phase, ϕ , to yield an effective volume fraction, ϕ_{eff} . In the case of monodisperse, spherical particles, ϕ_{eff} can be defined as follows:

$$\phi_{\text{eff}} = \phi \left(1 + \frac{\delta}{R} \right)^3 \quad (9.20)$$

where δ is the thickness of the repulsive barrier and R is the radius of the spherical particle. The effective volume fraction in an electrostatic system relates to the particle size and the salt concentration through the Debye length, $\Lambda = 1/\kappa$. Figure 9.7 illustrates the effect of using two different thicknesses of the repulsive barrier ($\delta = 5$ and 20 nm) on the maximum packing density of the solid particles. A thickness of 5–20 nm corresponds to polymer layer thicknesses commonly encountered in practical systems when using commercially available dispersants. It is assumed that the spherical, monodisperse (coated) particles will pack to a maximum volume fraction of $\phi_{\text{eff,m}} = 0.64$ (random close packing).

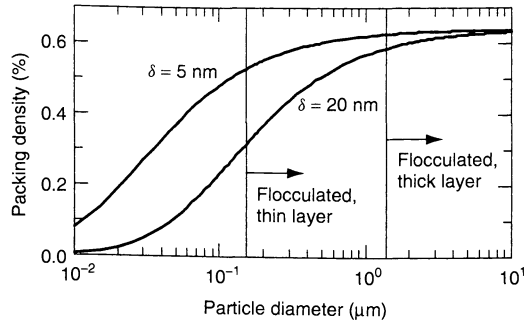


Figure 9.7. The effect of particle size and the repulsive range on the particle packing density. (From ref. (15) with permission of The American Ceramic Society)

Figure 9.7 shows that the packing density decreases strongly when the particle size is lowered, in particular in the nanosized particle range ($R = 10\text{--}100$ nm). With the use of a relatively thick coating, $\delta = 20$ nm, the packing density is $\phi < 0.50$ when the particle size is < 0.5 μm . Decreasing the layer thickness to $\delta = 5$ nm, the calculated packing density is only reduced to $\phi \sim 0.60$ at a particle size of $2R = 0.5$ μm .

However, when the range of the interparticle repulsion is decreased sufficiently, the van der Waals attraction will dominate and the particles will aggregate and form flocs. Using typical values for the Hamaker constant of alumina in dodecane, we estimate that particles with $2R > 0.17$ μm will flocculate when the repulsive barrier is $\delta = 5$ nm; particles with $2R > 1.3$ μm will flocculate when the barrier is 20 nm thick. Hence, if a colloiddally stable suspension is desired, it is not possible to use the thin coating ($\delta = 5$ nm) when working with micron-sized particles. On the other hand, using the thick coating ($\delta = 20$ nm) for nanosized particles will result in very low packing densities, i.e. $\phi < 0.30$. Thus, the optimal situation would be if the dispersant, and thus the range of the repulsion, could be tailored to just be sufficiently thick to prevent aggregation, hence minimizing the occupied volume.

5.4 Compression rheology

In many of the ceramic forming operations, such as slip casting, pressure filtration and centrifugal casting, the suspensions are subjected to compressive stresses. Although shear rheology provides important information, it is also of great interest to investigate the compressive response of concentrated suspensions. Colloiddally stable suspensions display a compressive response once the particles starts to interact. The

transmitted compressive stress relates to the osmotic pressure, which can be directly related to the magnitude of the repulsive interparticle forces. When the particles are forced close together, i.e. the volume fraction increases, the interparticle repulsion becomes stronger and thus also the osmotic pressure of the suspension. If the repulsion is very soft, e.g. for electrostatically stabilized systems at low ionic strength, we will observe a compressive stress that increase gradually over a relatively wide volume fraction range. If the repulsion is short range, e.g. for sterically stabilized systems having a dense surfactant layer adsorbed on the particle surfaces, we will observe a compressive stress that sets in at a well defined volume fraction and then increases rapidly over a very narrow volume fraction range.

One feature of most colloiddally stable suspensions is that the compressive properties are more or less reversible, provided that no major changes in suspension structure occur. However, in the case of flocculated suspensions, the compressive properties are irreversible. In concentrated flocculated suspensions, a continuous particle network forms which can support some stress up to a critical value. Once this critical stress, also called the *compressive yield stress*, P_y , is exceeded, the network consolidates to a higher volume fraction with a higher critical stress.

6 CONSOLIDATION

Dense, homogeneous green bodies can be prepared from dry powder, suspensions or pastes. The green body should be characterized by a high, uniform packing fraction of particles, small and narrow size pores, and a high degree of homogeneity, irrespective of the forming method being used. The green body should also possess a sufficient strength to allow handling without shape distortion. The different forming methods utilize solid–liquid separation, particle flow and compaction, solidification of the continuous medium or gelation to produce ceramic components with different geometries and microstructures. The features of the various methods are outlined below.

6.1 Drained casting techniques

All of the drained casting techniques, e.g. slip casting, pressure casting and centrifugal casting, involve a solid–liquid separation process to form a dense green body (Figure 9.8). A mould is filled with a suspension and the liquid is separated from the solid particles.

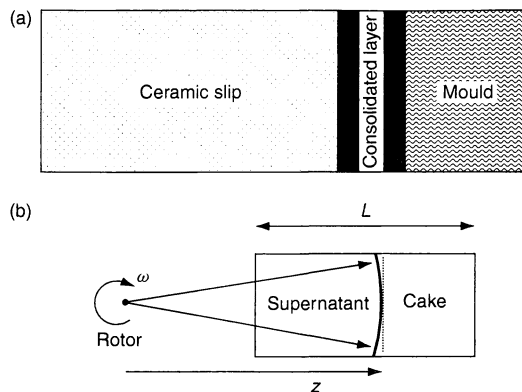


Figure 9.8. Schematic representations of (a) slip casting and (b) centrifugal casting

Slip casting is a low-pressure filtration method where capillary suction provides the driving force (of the order of 0.1–0.2 MPa) for liquid removal and formation of a cast layer at the mould surface. The casting rate is controlled by the resistance to flow by the cast layer and the mould. Usually, the mould resistance is negligible and the increase in the cast layer thickness, Z , with time, t , can be written as follows:

$$Z \propto \sqrt{\frac{\Delta P t}{\alpha}} \quad (9.21)$$

where ΔP is the capillary suction pressure of the mould and α is the specific cake resistance. Equation (9.21) illustrates the parabolic decrease of the casting rate with time; this makes slip casting a relatively slow process, which is mainly suitable for small or thin-walled objects. Pressure casting, which is an established forming technique in the fabrication of traditional clay-based ceramic materials such as pottery and sanitary porcelain, is a modification of slip casting that was developed to accelerate the consolidation stage and to obtain a higher green density. In pressure casting methods, an external pressure ($\Delta P \approx 1\text{--}10$ MPa), which is substantially higher than the capillary suction pressure of the mould, is applied to the ceramic suspension.

Centrifugal consolidation is based on consolidating a dense particle layer by subjecting the ceramic suspension to a centrifugal force field. Centrifugation and sedimentation are essentially identical, with the only differences being the magnitude of the force field and the time-scale of the process. Although sedimentation in normal gravity is not a viable ceramic forming operation, studies of transient settling can give important information regarding the behaviour during centrifugal casting. Hence, appropriate models describing

transient settling can also be applied to centrifugal casting.

The settling velocity, U_0 , of particles in a dilute suspension is described by the well-known Stokes law, as follows:

$$U_0 = \frac{2\Delta\rho R^2 g}{9\eta_{\text{sol}}} \quad (9.22)$$

where g is the normal gravity, $\Delta\rho$ is the density difference between the particles and the medium, and η_{sol} is the viscosity of the medium. The centrifugal settling rate is obtained by exchanging g for $\omega^2 z$ in equation (9.22), where ω is the angular velocity and z is the distance from the rotor centre. Because no liquid is forced through the cast layer in centrifugal casting, this method results in a casting rate that does not change with time. Hence, the body force exerted on the particles creates a buildup of a cast layer with a thickness increasing linearly with time. This feature makes centrifugal casting an attractive candidate for the casting of large objects from fine powders.

The structure of the suspension and the compression rheological properties determine much of the consolidation behaviour. Colloidally stable, dilute suspensions of monodisperse spherical particles are well described by the relationships described above. The effect of the shape of the particles and the particle concentration can be accounted for by multiplying the expression given in equation (9.22) by suitable factors. For flocculated suspensions, the situation is much more complex. The attractive interparticle forces can produce a cohesive network of particles, which will resist consolidation depending on its strength. Because flocculation generally affects the suspension microstructure, the permeability will change.

Colloidally stable suspensions result in higher packing densities, relative to strongly flocculated suspensions (4). In addition, well dispersed suspensions produce incompressible powder bodies, whereas flocculated suspensions result in compressible powder bodies. Compressible powder bodies and low packing densities are in general undesirable since they can produce shape distortions and cracks in the sintered material. However, inducing attractive forces between the particles can be beneficial since the mass segregation of different phases can be avoided (2) and a flocculated powder is more resistant to shape distortions after removing the shaped body from the mould. Recent work has also shown that packing densities as high as those produced from stable suspensions can be attained by the use of certain additives, hence producing weakly flocculated suspensions (2, 4).

6.2 Electrophoretic deposition

Electrophoretic Deposition (EPD) is a forming process where charged particles are consolidated on a substrate in a DC electric field (14). This field causes the particles to move, and deposit on, the oppositely charged electrode (Figure 9.9). EPD is a combination of two processes, i.e. electrophoresis and deposition. Electrophoresis controls the motion of the charged particles in the electric field while the deposition mechanisms control the buildup of the dense particle layer on the electrode. EPD should not be confused with electrodeposition, where ions are deposited and discharged at the electrode.

EPD requires colloidally stable suspensions where the particles carry a substantial charge. The most common dispersion medium used in EPD is ethanol, because aqueous-based suspensions have the disadvantage of electrolysis. Although electrostatic stabilization is considered most effective in aqueous medium, a substantial surface charge density – with the associated counterion layer in solution – can also be created in ethanolic media. In aqueous media, high surface charge densities can be obtained by working far away from the point of zero charge (pH_{pzc}) of the powder. A similar approach can also be used in non-aqueous media, providing that an operational pH scale (pH^*) and thus an

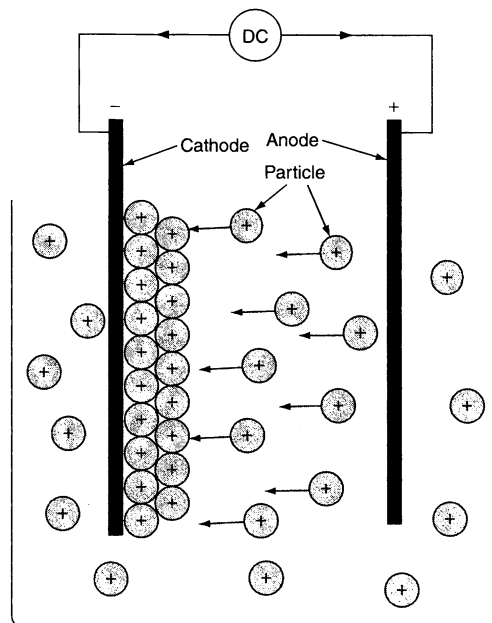


Figure 9.9. Schematic representation of the electrophoretic deposition process. (From ref (14) with permission of The American Ceramic Society)

isoelectric point, pH_{iep}^* , for the specific solvent can be defined (14). The operational pH can be controlled by adding strong acids and bases to the suspension, e.g. HCl and LiOH.

The rate of formation of the consolidated layer during EPD is directly proportional to the amount of charge that has passed through the cell. When EPD is operated under constant-current conditions, the deposited weight increases linearly with time. However, in order to maintain constant-current conditions, the voltage has to be continuously increased as the deposit induces an increased electrical resistance to the system. Under constant-voltage conditions, the potential between the electrodes is maintained constant, which thus results in a decreased deposition rate as the deposit builds up.

6.3 Extrusion and injection molding

Extrusion and injection moulding are commonly used for the manufacturing of polymers, and have also found applications in the shaping of ceramic green bodies (3). These un-drained, plastic forming technique are based on forming a green body from a paste consisting of 50–70 vol% ceramic powder dispersed in a polymeric binder. In extrusion, the plastic paste is forced through a die of a selected geometry. When the paste leaves the die, it solidifies into the desired shape. Extrusion is used to make long axi-symmetric materials of a relatively simple shape, such as pipes and honeycomb structures. In injection moulding (Figure 9.10), the paste is forced into an impermeable mould where the binder is solidified, usually by a the use of temperature gradient. Injection moulding has proven to be an excellent forming technique for smaller objects of complex shape with high precision at relatively high production rates.

The rheological properties of the paste control to a large extent the final properties of the extruded or injection moulded part. Different additives, such as dispersants and lubricants, are added to the powder–polymer mixture to promote deagglomeration and reduce the

die-wall friction. The adsorption of the additives on the particles, and the distribution, and possible phase separation of the additives and the polymer during processing, are important phenomena which have to be controlled for optimal performance.

The major problem confronting extrusion and injection moulding is the removal of the binder. Binder burnout must proceed at a slow rate (taking up to several days) so as to avoid problems with slumping and crack formation. The polymer removal time increases drastically when the size of the green body increases, thus making it difficult, if not impossible, to produce parts with thick cross-sections.

6.4 Dry pressing

Dry pressing and cold isostatic pressing are probably the most important forming techniques for the industrial production of ceramic materials. Green bodies are formed by pressing free-flowing granules in a die. Pressing is an established forming technique which has existed for decades, having been used for numerous applications, ranging from dinner-ware to the production of insulators and spark plugs. The high productivity makes pressing the method of choice for most industrial ceramic operations, despite the problems associated with density gradients, inhomogeneous microstructures, and the need to machine most complex shaped objects.

The free-flowing granules are formed from a suspension by using a granulation technique, e.g. spray drying or freeze granulation. Spray drying involves spraying a suspension through an atomizer (often a small nozzle) into a hot-air drying chamber. Freeze granulation is a relatively new technique based on the instant freezing of sprayed suspension drops, followed by solvent removal through freeze-drying. Prior to granulation, the powder has to be dispersed in a suspension containing all of the necessary pressing additives, e.g. binders and lubricants. The suspension should preferably be of high solids concentration and possess a relatively low viscosity to facilitate spray drying.

The quality of the pressed body depends strongly on the properties of the granules. If the granules are not completely broken down during pressing, the remnant structure may induce large defects during sintering. Hence, the granules should not be too hard. However, too soft granules may cause problems with handling and mould filling, since granule fracture and deformation will have a negative effect on the flowability.

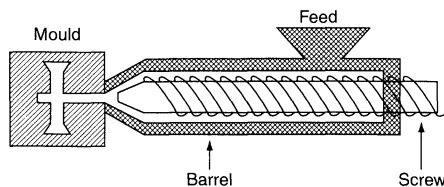


Figure 9.10. Schematic representation of an injection moulding machine. (From ref. (4) with permission from Marcel Dekker Inc.)

6.5 Direct casting techniques

During the last decade, an increasing number of novel “near-net-shape” forming techniques have been presented to the ceramic community (15). One class of these new methods, the direct casting methods, utilizes some of the inherent properties of dense suspensions to transform a fluid suspension into a stiff gel. The general concept is to retain the homogeneous state of the dense slurry during the green-body formation step. By minimizing the disturbance to the slurry during gelation, introduction of larger heterogeneities can be avoided and density gradients minimized. The physical or chemical processes responsible for the formation of a solid green body differ greatly but all methods require a well dispersed suspension with (very) high solid loading of reasonably low viscosity to facilitate the mould filling process. Hence, maximizing the solid loading by tailoring the range and magnitude of the interparticle repulsion and optimizing the particle size distribution become very important issues.

The underlying mechanisms for most of the direct casting methods are related to the formation of either physical or chemical bonds between either the particles and/or some species in the dispersion. At high solid loading, particle gels can develop a sufficient strength to support their own weight and thus be handled without shape distortion. The division between physical and chemical gels is somewhat arbitrary, differing mainly in the strength of the green body, with chemical gels being substantially stronger than physical gels. Physical particle gels rely on the formation of a physical bond between the particles in dense suspensions. This is mainly achieved by manipulating the interparticle forces to become attractive. In electrostatically stabilized slurries this can be achieved by increasing the salt content to compress the electric double-layer (Figure 9.11). Such changes can, of course, be induced by adding acid, base or salt. However, there is a large risk that the simultaneous mixing and gelation may result in large inhomogeneities in the dense suspension. A better idea is to use a reaction that produces the desired pH or salt change *in situ*. Examples of such reactions are thermally activated decomposition of urea and formamide, which change the pH from acidic towards a neutral pH by slowly forming ammonia. Autocatalytic reaction temperatures can be lowered by introducing catalysts. This is carried out in Direct Coagulation Casting (DCC) where enzymes trigger chemical reactions that release salt and/or shift the pH at room temperature (15). The interparticle forces in sterically stabilized systems can be manipulated by changing the solution properties of the

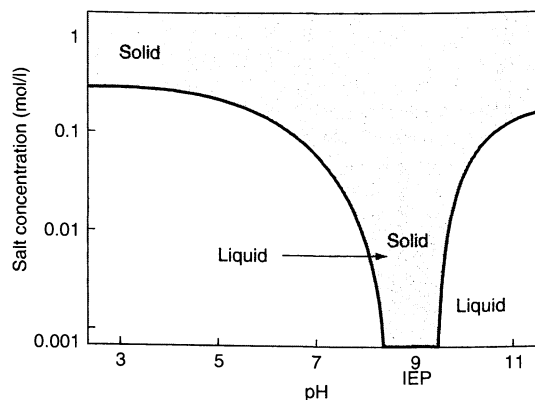


Figure 9.11. Stability diagram for an electrostatically stabilized alumina suspension as a function of pH and salt concentration. (Adapted from Graule *et al.*, *Ind. Ceram.*, **16**, 31–34 (1996))

polymer. Changing temperature or pH, or adding salt, may have a drastic influence on, e.g. the layer thickness and the adsorbed amount. When the solvency reaches a critical level, the sterically stabilized dispersion flocculates – the so-called incipient flocculation.

The formation of strong gels is commonly accompanied by the formation of permanent chemical bonds between either the particles or some species in the dispersion. Typical examples are the formation of a percolating polymer network by polymerizing a monomer in the slurry and gelation of dissolved polymers. In comparison to the physical gels, chemical gels usually require a higher amount of organic processing aids and thus a separate burnout step.

Gel casting uses a dispersion of particles and monomer in a dispersing media which is poured into a mould. The monomer is then polymerized *in situ* and permanently gels around the ceramic powder to retain the desired shape. Vinyl monomers and cross-linking agents are commonly used in the process and, because they undergo a free-radical chain polymerization reaction, the setting is very rapid. Organic or aqueous dispersing media can be used, although the chemistry has to fit the physical and chemical data of the solvent, i.e. processing temperature, solubility, etc. This process has been adapted to a variety of ceramic materials and the green parts have a high green strength that allows for machining beyond the limits of the mould design. Cross-linking of proteins has also been applied in gel casting. Proteins that contain the amino acids, cysteine or cystin, cross-link on heating and thus form a chemical gel.

Direct casting processes using responsive non-adsorbed polymers are commonly referred to as

Aqueous Injection Moulding (AIM). One of the early applications used methylcellulose derivatives, which are very soluble at room temperature due to polymer hydration. With increasing temperature, the polymer becomes more and more dehydrated until the chain–chain interaction is stronger than the chain–water interaction. Above 50°C, it forms a percolated network that stiffens the dispersing media and gels. The process is reversible on cooling. Another example is agarose (a purified polysaccharide), which has to be handled close to the boiling point and gels below 37°C. Irreversible processes that form percolated networks have also been proposed. One of them is the gelation of slurries containing a swellable polymer, such as starch. Here, the slow dissolution and swelling of 100 µm size polymer particles consumes the dispersing medium and thus gel the polymer–particle mixture.

6.6 Solid freeform fabrication

Until recently, prototypes had to be constructed by skilled model makers from two-dimensional (2-D) engineering drawings. This time-consuming and expensive process is now being replaced with novel layer manufacturing and computer aided design (CAD) technologies. Ceramic prototypes and small series production may now be produced by solid freeform fabrication (SFF) techniques (15). These methods allow the mould-less manufacturing of ceramics. The general process includes the virtual slicing of the three-dimensional (3D) CAD-data of a ceramic component into thin sheets. These slices are then developed through computer-controlled devices that fabricate the component. Prototypes of advanced ceramics can be formed through stacking of greensheets (made by tape-casting), by immobilization of free-flowing powder, or by solidification of suspended particles.

Stereolithography (SL), one of the first freeform fabrication technologies for polymeric materials, involves the polymerization of liquid monomers through exposure to UV-laser radiation. A computer-controlled laser beam scans across the surface of a container filled with liquid photopolymer, solidifying the liquid at each point of impact. Ceramic green bodies can be created by using SL methods where a ceramic slip consisting of 40–55 vol% ceramic powder is dispersed within an ultraviolet-curable solution. Three-Dimensional Printing (3DP™) creates parts by a layered printing process. A free-flowing powder (large particles or granules), or a thin slurry layer, is spread and after drying, the particles are selectively joined by ink-jet printing binder material.

Direct Ink-Jet Printing (DIP) is a forming process in which droplets of ceramic ink are printed on to previous layers. These inks, which consist of ceramic particles, organic solvents and additives, need to be designed to match printer requirements for optimum output.

7 DRYING AND BINDER BURNOUT

When the green body has been formed, it has to be dried and all of the organic processing additives have to be removed prior to sintering. If solvent or organic binder remains in the powder body at the sintering stage, large volumes of gas can be released in an uncontrolled manner, which can result in cracking. Both drying and binder burnout can be controlled by temperature; the heat for evaporation of the solvent and the heat of reaction for binder decomposition control the extent and rate of these processes. Hence, the heat transfer in the porous powder body is of great importance and can be rate-limiting in both drying and binder decomposition. The large volumes of gas that are released must diffuse through the porous powder and this mass transfer step can also limit the drying or binder burnout rate. From heat and mass transfer considerations, it is clear that drying and binder burnout have much in common (3). Drying and binder burnout are also associated with induced stresses, caused by thermal gradients or gas or liquid pressure gradients in the powder body. These stresses, which are additive, have to be controlled to avoid cracking and warping.

Drying of a saturated porous powder body proceeds in several steps, schematically shown in Figure 9.12. The saturated powder body dries at a constant rate, controlled by the geometry of the body, the partial vapour pressure and the temperature. At this stage, the surface of the powder body is always wet, since liquid flows from the interior to the surface. The volume fraction of particles increases continuously with the evaporation of solvent until the particles touch each other and no more shrinkage can occur. At this critical point, the liquid–vapour interface starts to recede into the pores and the drying rate decreases significantly as the transport of fluid to the surface of the powder body becomes rate-limiting. When the liquid in the large pores has evaporated, the drying rate decreases even more as diffusion of vapour from the fluid trapped inside the powder body becomes rate-limiting.

The desired end in ceramic parts' production is attaining fast drying rates; however, quick drying causes cracks. Cracking is inhibited by strengthening the solid network, increasing pore size and reducing capillary

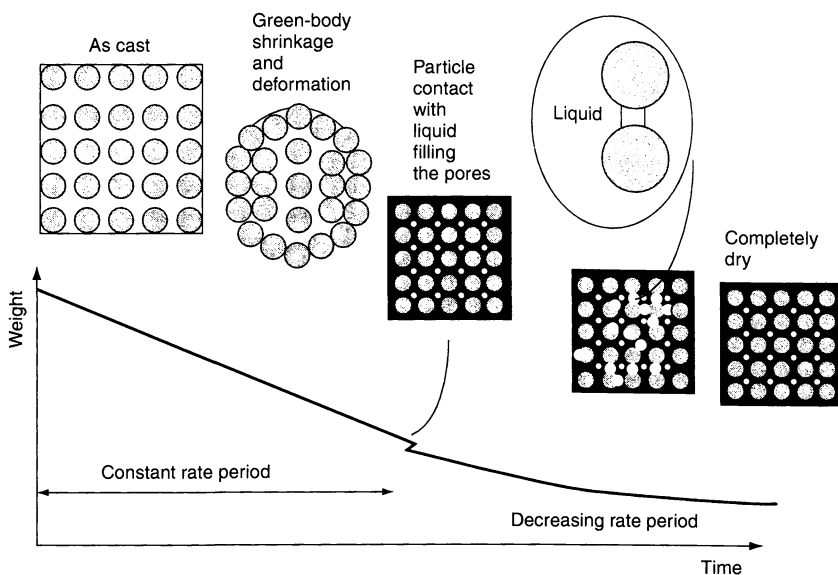


Figure 9.12. Schematic representation of the drying of a saturated powder body showing the weight loss with time. (From ref. (3) with permission from Academic Press)

pressure. The transport of the evaporating dispersing media can also cause migration of binder and small particles to the surface, which can lead to additional problems on burnout and sintering.

Organic binders are mainly used to provide strength to the green body. In the various casting methods, e.g. slip casting, only a small amount is needed, while substantially higher additions are common in dry pressing. In extrusion and injection moulding, the binder is the continuous phase, comprising typically about 30–45 vol% of the green body. The dominating method to remove the organic binders is pyrolysis, although solvent extraction can be used for special applications.

Pyrolysis proceed mainly by three different mechanisms, i.e. thermal degradation, oxidative degradation and evaporation (4). The oxidative degradation is limited by the oxygen diffusion in the green body. Deep within the green body, the oxygen partial pressure is frequently low because it cannot diffuse fast enough to keep up with the reactions taking place. Oxidative degradation often needs an induction period before it sets in. This induction period can be reduced by increasing the temperature. Many metals act as catalysts and reduces the induction period essentially to zero.

Thermal degradation involves chain scission, which occurs throughout the body, providing that the thermal gradients are minor. The chain scission products are volatile with a partial pressure corresponding to the

molecular weight. During pyrolysis, chains can also cross-link to another chain; this is, in general, an undesirable complication since the molecular weight increases and thus the partial pressure of the reaction product decreases, thus resulting in slow burnout. Polymers that undergo depolymerization in a well-controlled manner are desirable as binders, because they burn-out cleanly and leave little carbon residue (3).

8 ACKNOWLEDGEMENTS

The author gratefully acknowledges the Brinell Centre-Inorganic Interfacial Engineering, and the Institute for Research and Competence Holding (IRECO) for financial support. Wolfgang Sigmund, Brian Sundlof, Eric Laarz, and Anders Meurk are thanked for stimulating discussions.

9 REFERENCES

1. Richerson, D. W., *Modern Ceramic Engineering – Properties, Processing and Use in Design*, 2nd Edn, Marcel Dekker, New York, 1992.
2. Lange, F. F., Powder processing science and technology for increased reliability, *J. Am. Ceram. Soc.*, **72**, 3–15 (1989).

3. Ring, T. A., *Fundamentals of Ceramic Powder Processing and Synthesis*, Academic Press, San Diego, CA, 1996.
4. Pugh, R. J. and Bergström, L. (Eds), *Surface and Colloidal Chemistry in Advanced Ceramics Processing*, Marcel Dekker, New York, 1994.
5. Reed, J. S., *Introduction to the Principles of Ceramics Processing*, Wiley, New York, 1988.
6. Aksay, I. A., Microstructure control through colloidal consolidation, in *Advances in Ceramics*, Vol. 9, Mangels J. A. and Messing, G. L. (Eds), American Ceramics Society, Columbus, OH, 1984, pp. 94–104.
7. Russel, W. B., Saville, D. A. and Schowalter, W. R., *Colloidal Dispersions*, Cambridge University Press, Cambridge, UK, 1989.
8. Israelachvili, J. N., *Intermolecular and Surface Forces*, 2nd Edn, Academic Press, London, 1992.
9. Bergström, L., Hamaker constants of inorganic materials, *Adv. Colloid Interface Sci.*, **70**, 125–169 (1997).
10. Napper, D. H., *Polymeric Stabilization of Colloidal Dispersions*, Academic Press, London, 1983.
11. de Gennes, P. G., Polymers at an interface; a simplified view, *Adv. Colloid Interface Sci.*, **27**, 189–209 (1987).
12. Bingham, E. C., *Fluidity and Plasticity*, McGraw-Hill, New York, 1922.
13. Barnes, H. A., Shear-thickening (“dilatancy”) in suspensions of nonaggregating solid particles dispersed in Newtonian liquids, *J. Rheol.*, **33**, 329–366 (1989).
14. Sarkar, P. and Nicholson, P. S., Electrophoretic deposition (EPD): mechanisms, kinetics, and applications to ceramics, *J. Am. Ceram. Soc.*, **79**, 1987–2002 (1996).
15. Sigmund, W. M., Bell, N. S. and Bergström, L., Novel powder processing methods for advanced ceramics, *J. Am. Ceram. Soc.*, **83**, 1557–1574 (2000).

CHAPTER 10

Surface Chemistry in Dispersion, Flocculation and Flotation

Brij M. Moudgil, Pankaj K. Singh and Joshua J. Adler

University of Florida, Gainesville, Florida, USA

1	Introduction	219	7.1	Adsorption of surfactants at the solid–liquid interface	233
2	Surface Chemistry	220	7.1.1	Mechanisms of adsorption	233
2.1	Surface charge development	220	7.1.2	Contributions to the adsorption energy	233
2.2	Measurement of surface charge	221	7.2	Surfactant structures at the solid–liquid interface	236
3	The Electrical Double-Layer	222	8	Particle Processing	238
3.1	Helmholtz model	222	8.1	Dispersion of particles	238
3.2	Gouy–Chapman model	222	8.1.1	Characterization of the state of dispersion	239
3.3	Stern–Graham model	223	8.1.2	Control of dispersion through surface chemistry	240
4	Zeta Potential (Electrokinetic Potential)	224	8.2	Selective flocculation of particles	243
4.1	Measurement of zeta potential	224	8.2.1	Design of selective reagents based on surface chemistry	243
4.2	Manipulation of zeta potential	225	8.2.2	Modifying surface chemistry and structure to enhance selectivity	244
5	Electrostatic Forces	226	8.3	Flotation of minerals	246
5.1	Calculation of electrostatic forces	227	8.3.1	Collector selection based on surface charge	246
5.1.1	Boundary conditions	227	8.3.2	Collector selection based on surface reactions	247
5.1.2	The linearized Poisson–Boltzmann approach	228	9	References	249
5.1.3	Analytical formulae	228			
6	Manipulating Surface Behaviour by Polymer Adsorption	229			
6.1	Solution behaviour of polymers	229			
6.2	Adsorption of polymer at the particle surface	230			
6.3	Role of surface chemistry and structure in polymer adsorption	231			
7	Manipulating Surface Behaviour by Surfactant Adsorption	232			

1 INTRODUCTION

Particulate processing plays a crucial role in industries such as mineral processing, chemicals, pharmaceutical,

food processing, microelectronics and cosmetics, to name just a few. Many of the industrial applications involve particles, which are in the micron or the sub-micron size range. In such ranges, the surface

properties or the surface chemistry controls the processing behaviour of the particles. It is imperative to understand and manipulate the surface chemistry in order to control the processing conditions to achieve consistent and desired products. In this chapter, the surface chemistry relevant to dispersion/flocculation and flotation processes is discussed.

The surface chemistry, and more specifically, the charge development on the surface of particles in aqueous systems is briefly reviewed. The manipulation of surface chemistry by the adsorption of organic reagents, such as surfactants and polymers, is also considered. Finally, to illustrate the importance of surface chemistry in particulate processing, the practical applications of ore flotation, dispersion of particles and selective flocculation are discussed.

2 SURFACE CHEMISTRY

Solid surfaces are heterogeneous in nature, and may have sites with different energies. The presence of surface defects, and the different arrangement of the atoms in and around the surface defects, lead to surface sites with wide ranging energies. Depending on the method of preparation of the surface, the relative concentrations of atoms in the surface defects can be varied, thus resulting in different surface structure and energetics. Changes in the local environment can result in dynamic restructuring of the surface. This rearrangement of surface atoms can occur on the chemisorption time-scale ($\sim 10^{-13}$ s), on the time-scale of catalytic reactions (seconds), and at longer times (hours). This makes the study of surfaces extremely complex. In certain cases, both polar and non-polar sites can co-exist on the same solid surface, thus leading to more complex surface structures. For example, on the surface of silicon oxide (SiO_2), the Si–O–Si sites are hydrophobic, whereas the Si–OH (silanol) sites are polar in nature. In order to understand the surface phenomena, detailed information about the surface atomic structure and the chemical composition of a thin surface layer is required. For the study of solid surfaces in gases, a number of experimental techniques have been used that employ heat, electric fields, electrons, photons, ions or molecules in order to excite the surface. The response of the surface to these excitations results in the emission of electrons, photons, ions or molecules whose energy, mass, or direction can be measured. These techniques have significantly enhanced the understanding of surfaces, but are limited in use because they all rely on the use of high vacuum, i.e. 10^{-6} to 10^{-9} torr. Some of

the techniques that have been used include low-energy electron diffraction (LEED), field-ion microscopy, electron impact Auger spectroscopy, ion neutralization spectroscopy, X-ray photoelectron spectroscopy, ultraviolet photoelectron spectroscopy, electron energy loss spectroscopy (EELS), appearance potential spectroscopy and scanning tunnelling microscopy. The study of surfaces in aqueous environments becomes difficult, due to various changes occurring at the interface, and the lack of instrumentation to detect such changes. The development of surface charges and the measurement techniques are summarized in the following sections.

2.1 Surface charge development

When the solid surfaces are immersed in aqueous media, they exhibit a net surface charge. A great majority of colloidal particles are charged by the following mechanisms.

1. *Ion adsorption* Charge can develop at surfaces by unequal adsorption of oppositely charged ions. Ion adsorption may be positive or negative. Surfaces in contact with aqueous media are more often negatively charged due to the fact that cations are more hydrated when compared to anions. Hydrocarbon oil droplets and air bubbles exhibit net negative charges because of negative adsorption of ions. Cations move away from the air–water and oil–water interface more than anions. Surface charge may also be established by the adsorption of charged surfactant molecules. Preferential adsorption of one type of ion on the surface can occur due to either London–van der Waals interactions or hydrogen or hydrophobic bonding.
2. *Ion dissolution* Unequal dissolution of ions in the case of ionic substances can lead to a net charge on the substrate. A classical example of this mechanism is the silver iodide surface. When silver iodide is immersed in an aqueous environment, dissolution occurs as $\text{AgI} \leftrightarrow \text{Ag}^+ + \text{I}^-$. Since the solubility product for this equilibrium is relatively small ($K_{\text{sp}} = a_{\text{Ag}^+} a_{\text{I}^-} \sim 10^{-16}$), the concentrations of Ag^+ and I^- in solution are small. The surface of the crystal consists of an array of Ag^+ and I^- ions in cubic close packing, and no net charge develops when the number of each ion is the same. However, an equal number of each ion on the surface does not occur at the concentration where there are equal numbers of Ag^+ and I^- ions in the solution. Instead, due to their higher affinity for the surface, the iodide ions tend to

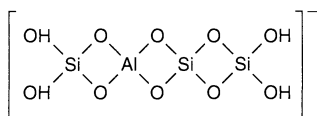


Figure 10.1. Schematic representation of charge development in SiO_2 tetrahedra by the substitution of a Si atom by an Al atom

be preferentially adsorbed at the surface. A detailed mathematical treatment of the AgI surface is given in ref. (1).

3. *Lattice imperfections and isomorphous substitutions* In the case of most clay mineral systems, lattice defects result in very large charge densities. The defect in such cases is in the form of an isomorphous replacement of one ionic species by another of lower charge. For example, the replacement of a Si atom by an Al atom in the SiO_2 tetrahedra will yield a net negatively charged surface (Figure 10.1).
4. *Ionization/Dissociation* The ionization of groups such as carboxyl ($-\text{COOH}$), sulfate ($-\text{O.SO}_2.\text{OH}$), sulfonate ($-\text{SO}_2.\text{OH}$), sulfite ($-\text{O.SO.OH}$), amine ($-\text{NH}_2$) and quaternary amine ($-\text{N}^+\text{R}_3$), may take place at the surface, thus resulting in the development of surface charges. The dissociation of these surface groups is pH dependent. This mechanism represents the charge development in proteins and in, polymer latex systems, which have carboxyl, sulfate and sulfonate groups on their surfaces. In addition, this mechanism is applicable to the behaviour of oxide surfaces. For a detailed description of such dissociation models, the reader is referred to ref. (1).

2.2 Measurement of surface charge

The surface charge is measured by titrating the surface with the potential-determining ions (e.g. H^+ and OH^- ions for oxides, and Ag^+ and I^- ions for silver iodide) for the surface. In such an experiment, a certain known mass, m (typically < 1 g) of the particle is added to a known volume, v ($200 \text{ cm}^3 < v < 1000 \text{ cm}^3$) of an “indifferent” electrolyte solution (e.g. $0.01M \text{ NaNO}_3$), and the suspension is equilibrated for 30–60 min at fixed temperatures (22 or 25°C), followed by purging with nitrogen to expel any dissolved carbon dioxide. Care should be taken to purge out the dissolved carbon dioxide completely, because this dissolved gas can lower the solution pH, thus resulting in incorrect measurements. A schematic of a typical set-up for measuring the surface charge is shown in Figure 10.2.

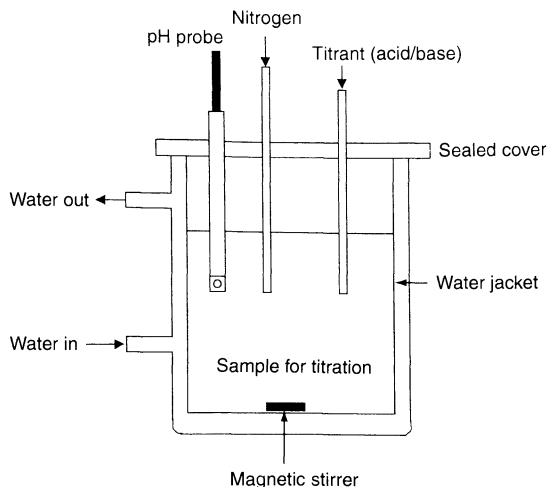


Figure 10.2. Schematic of an experimental set-up used for surface charge measurement

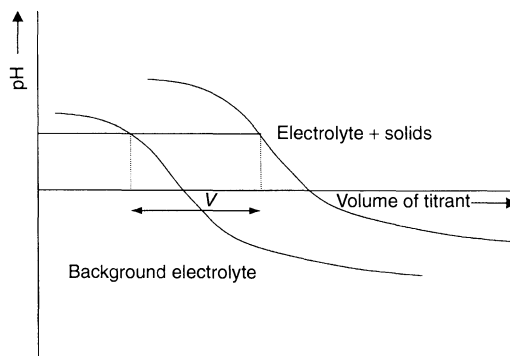


Figure 10.3. Schematic representation of the typical results obtained from a surface titration experiment for the calculation of surface charge

After equilibration, the initial pH is noted. If the initial pH is low, a base titration (e.g. $0.01M \text{ NaOH}$) is used to move to a higher final pH (pH_{final}). If the initial pH is high, an acid titration is used to move to a low pH_{final} . The delay time between titrant addition for complete reaction is usually between 5 and 30 min. A blank titration is also carried out on the electrolyte solution and the results obtained from the two titrations are then superimposed. A typical result is shown in Figure 10.3. From such a figure, by subtracting the two curves (i.e. subtract the blank electrolyte curve from the curve for electrolyte + solids), the relative amounts of OH^- or H^+ adsorbed on the solid surface at any particular pH can be determined from the following

equation:

$$-(\Gamma_+ + \Gamma_-) = \frac{eN_a[C]V}{m(SSA)} \quad (10.1)$$

where e is the charge on an electron, N_a is the Avogadro constant, $[C]$ is the electrolyte concentration, V is the additional amount of acid or base required for the same pH change in the presence of solid particles, and SSA is the specific surface area.

The calculation is repeated for all pH values greater than initial pH, pH_0 , and the titrations are repeated with acid to cover the full pH range (if necessary). The relative amount of OH^- adsorbed is also equal to the relative surface charge (σ_0). The latter is then plotted as a function of the pH for a particular electrolyte concentration. The experiment is then repeated for other electrolyte concentrations (e.g. 0.1 M and 0.3 M $NaNO_3$). The results can then be plotted on the same graph, as shown in Figure 10.4. The common intersection point (CIP) (Figure 10.4(a)) is also the point of zero charge (PZC) (Figure 10.4(b)), since it is only at the PZC that the relative surface charge (σ_0) is independent of the background electrolyte concentration. The CIP is then translated to $\sigma_0 = 0$ to generate a plot of the absolute values of σ_0 at any given pH.

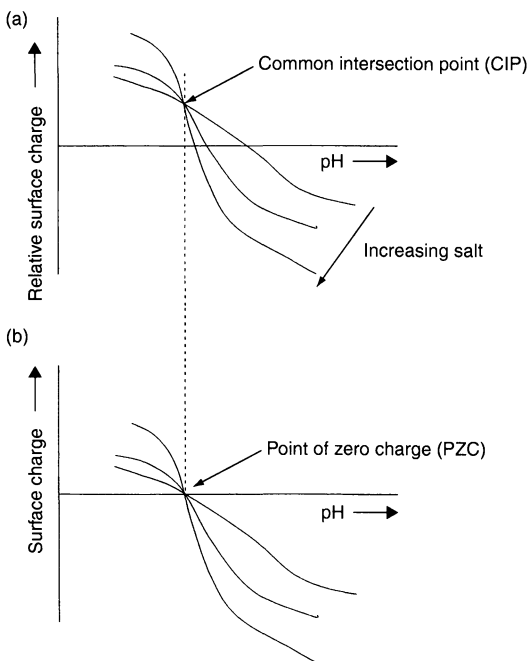


Figure 10.4. Schematic showing the conversion of relative surface charge (a) into absolute surface charge (b). The common intersection point (CIP) defines the point of zero charge (PZC)

Some of the experimental considerations required in order to obtain accurate results are as follows:

- The background electrolyte used should be “indifferent”.
- The surfaces of the particles should be insoluble.
- Sufficient delay time should be allowed between titrant additions.
- The pH probe used for the experiments should be very accurate (± 0.01 pH units or better).

3 THE ELECTRICAL DOUBLE-LAYER

Surface charge on a particle results in an unequal distribution of ions in the polar medium in the vicinity of the surface. Ions of opposite charge (counterions) are attracted to the surface, and ions of like charges (co-ions) are repelled away from the surface. This unequal distribution gives rise to a potential across the interface. The exact distribution of the counterions in the solution surrounding the charged surface is very important, since it determines the potential decay into the bulk from the charged surface. Electrostatic attraction, thermal motion and forces other than electrostatic (specific adsorption) influence the counterions in the vicinity of the surface.

Several models have been proposed for the distribution of ions in the vicinity of the surfaces, and are summarized below.

3.1 Helmholtz model

In 1879, von Helmholtz proposed that all of the counterions are lined up parallel to the charged surface at a distance of about one molecular diameter (Figure 10.5). The electrical potential decreases rapidly to zero within a very short distance from the charged surface in this model. Such a model treated the electrical double-layer as a parallel-plate condenser, and the calculations of potential decay were based on simple capacitor equations. However, thermal motion leads to the ions being diffused in the vicinity of the surface, and this was not taken into account in the Helmholtz model.

3.2 Gouy–Chapman model

This model, proposed by Gouy (1910 and 1917) and Chapman (1913), consists of a diffuse distribution of the counterions, with the concentration of such ions falling off rapidly with distance near to the surface, because

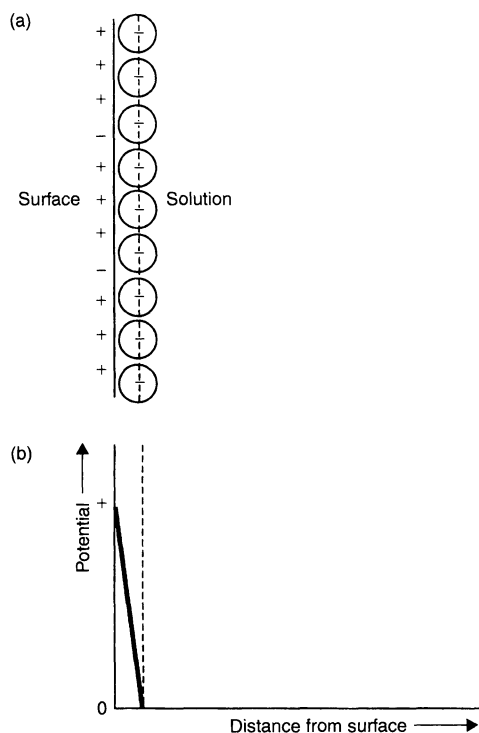


Figure 10.5. Schematic representation of the Helmholtz model of the electrical double-layer: (a) distribution of counterions in the vicinity of the charged surface; (b) variation of electrical potential with distance from the surface

of the screening effect, and then falling off gradually (Figure 10.6). Such a model is accurate for planar charged surfaces with low surface charge densities, and distances far away from the surface, but is inaccurate for surfaces with high surface charge densities, especially at small distances from the charged surfaces, since it treats the ions as point charges and neglects their ionic diameters.

3.3 Stern–Graham model

This model, shown in Figure 10.7, divides the double-layer into two parts, i.e. (i) a fixed layer of strongly adsorbed counterions, adsorbed at specific sites on the surface, and (ii) a diffuse layer of ions similar to that of the Gouy–Chapman model. The fixed layer of ions is known as the Stern layer, and the potential decays rapidly and linearly in this layer. The potential decay is much more gradual in the diffuse layer. In the case of specifically adsorbing ions (multivalent ions, surfactants, etc.) the sign of the Stern potential may be reversed.

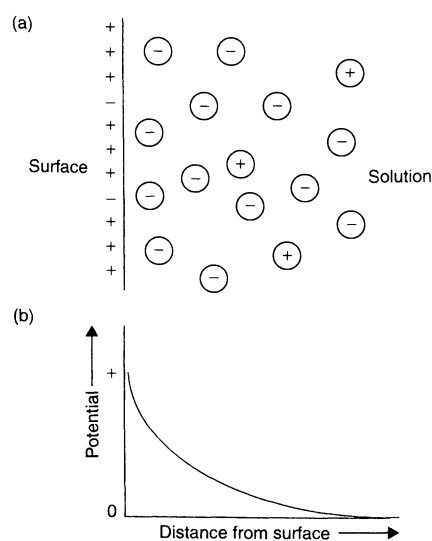


Figure 10.6. Schematic representation of the Gouy–Chapman model of the electrical double-layer: (a) distribution of counterions in the vicinity of the charged surface; (b) variation of electrical potential with distance from the surface

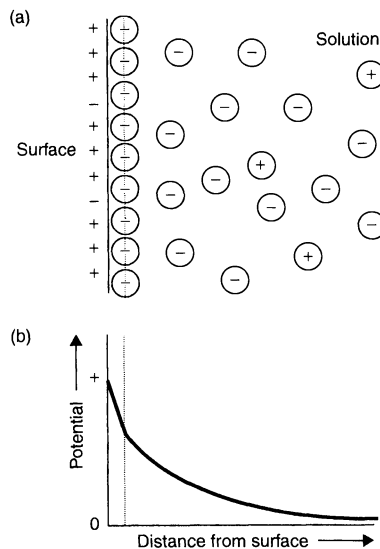


Figure 10.7. Schematic representation of the Stern–Graham model of the electrical double-layer: (a) distribution of counterions in the vicinity of the charged surface; (b) variation of electrical potential with distance from the surface

Mathematical treatment of the electrical double-layer is given in refs (1) and (2) and the interested reader is referred to these books for detailed mathematical descriptions of the various models.

4 ZETA POTENTIAL (ELECTROKINETIC POTENTIAL)

Zeta potential is the potential of the surface at the plane of shear between the particle and the surrounding medium as the particle and medium move with respect to each other. In the presence of an applied electric field, the charged surface (and the attached material) tends to move in the appropriate direction, while the counterions in the mobile part of the double-layer would have a net migration in the opposite direction. On the other hand, an electric field would be created if the charged surface and the diffuse part of the double-layer were made to move relative to each other. The plane of shear is beyond the Stern plane, and the zeta potential facilitates easy quantification of the surface charge. The pH at which the calculated zeta potential value is zero is known as the isoelectric point (IEP).

4.1 Measurement of zeta potential

The zeta potential of a particle is calculated from electrokinetic phenomena such as electrophoresis, streaming potential, electro-osmosis and sedimentation potential. Each of these phenomena and the determination of zeta potential by using each technique will be discussed briefly in this section.

1. *Electrophoresis* This is the movement of a charged surface along with the adsorbed ions, in relation to a stationary liquid under the influence of an applied electric field. The electrophoresis cell consists of a horizontal glass tube with inlet and outlet taps and an electrode at each end. Platinum black electrodes are employed for salt concentrations in the range from 10^{-3} to 10^{-2} mol dm $^{-3}$, or otherwise appropriate reversible electrodes such as Ag/AgCl or Cu/CuSO $_4$ must be used so as to avoid gas evolution. A flat microelectrophoresis cell is shown in Figure 10.8. The mobility of the particle is viewed under the microscope at a “stationary plane” in the cell, where the electro-osmotic flow of the liquid caused by the charged surface of the cell is compensated by the return flow of the liquid. For a cylindrical cell, the stationary plane is located at 0.2 and 0.8 of the total depth, with the exact location depending on the width/depth ratio.

The electrophoretic mobility is calculated from the time that a particle takes to travel a fixed distance. The zeta potential, ξ (potential at the shear plane), is calculated by using the Smoluchowski equation

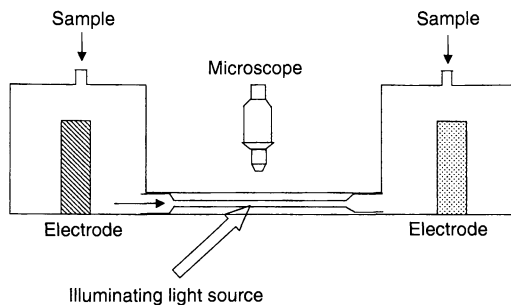


Figure 10.8. Schematic of a vertically mounted flat microelectrophoresis cell

for spherical particles, which can be treated as point charges, as follows:

$$U_E = \frac{\xi \varepsilon}{\eta} \quad (10.2)$$

where U_E is the mobility under an applied potential E , ε is the permittivity of the electrolyte medium, and η is the viscosity of the medium.

Electrophoretic-mobility-measurement-based instruments are more suited for the determination of zeta potentials of fine particles.

2. *Streaming potential* The liquid in the capillary of a porous plug carries a net charge given by the mobile part of the electrical double-layer. When the liquid flows through the capillary or the plug, it gives rise to a streaming current and consequently a potential difference. An apparatus suitable for studying streaming potentials is illustrated in Figure 10.9.

The streaming potential can be measured by using a micrometer instead of an electrometer. To minimize

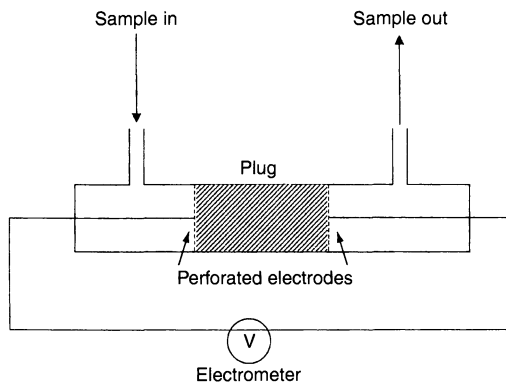


Figure 10.9. Schematic of an apparatus for measuring streaming potential

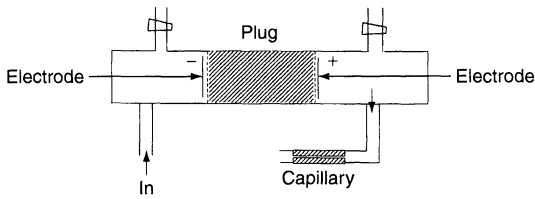


Figure 10.10. Schematic of the capillary method used for the measurement of electro-osmosis

electrode polarization, an alternating streaming current can be generated by forcing the liquid through the plug by a reciprocating pump.

If E is the potential difference developed across a capillary of radius a and length l , for an applied pressure difference p , we can write the following:

$$E = \frac{\varepsilon p \zeta}{\eta K_0} \quad (10.3)$$

where ε is the permittivity of the medium, ζ is the zeta potential, η is the viscosity of the liquid, and K_0 is the conductivity of the electrolyte solution.

- Electro osmosis** This technique involves the movement of a liquid relative to a stationary charged surface (e.g. a capillary or porous plug) by the application of an electric field. Experimentally, zeta potentials may be measured by this method by means of an apparatus such as that shown in Figure 10.10. The potential is supplied by electrodes, as shown in the schematic, and the transport of liquid across the tube is observed through the motion of an air bubble in the capillary providing the return flow. For water at 25°C, a field of about 1500 V/cm is needed to produce a velocity of 1 cm/s if the surface potential (ψ_0) is 100 mV.
- Sedimentation potential** This is the creation of an electric field when charged particles move relative to a stationary fluid. This technique is the least commonly used for the determination of zeta potential, because of several limitations associated with the measurement and calculation of the zeta potential.

A selection of some of the commercially available instruments for measuring zeta potential, and the relevant techniques employed by these, is presented in Table 10.1.

4.2 Manipulation of zeta potential

The zeta potential has wide ranging applications in particulate processing. However, control of the zeta

Table 10.1. Commercially available instruments for measuring zeta potential, and the corresponding techniques employed

Instrument	Technique
Zeta Meter 3.0+	Electrophoresis
Rank Brothers Mark II	Electrophoresis
Zpi, Inc.- Zeta Reader	Electrophoresis
Laval Lab Zetaphoremeter III	Electrophoresis
Micromeritics Zeta Potential Analyser 1202	Electrophoresis
Laval Lab Zetacad	Streaming potential
Brookhaven-BI-EKA (Electro Kinetic Analyser)	Streaming potential
Dispersion Technology (DT200, DT300, DT 1200)	Acoustophoresis
AcoustoSizer II	Acoustophoresis
Brookhaven Zeta Plus/Zeta Pals	Laser Doppler/Photon correlation (PCS)
Coulter Delsa 440 SX	Laser Doppler/Photon correlation (PCS)

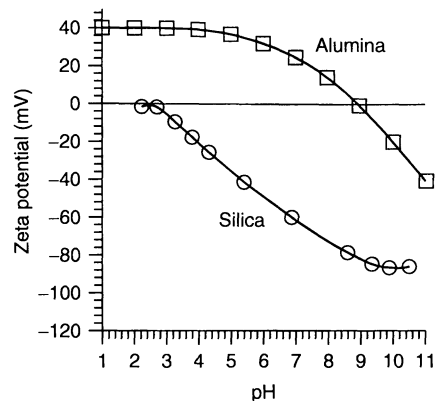


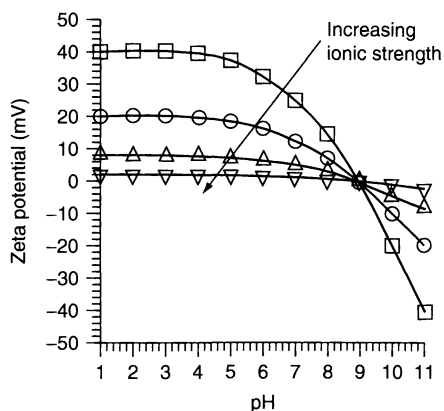
Figure 10.11. Variation of the zeta potential as a function of pH for silica and alumina

potential within a specific range is necessary in order to control such processing. In this present section, the use of solution pH and ionic condition for manipulating the zeta potential will be illustrated.

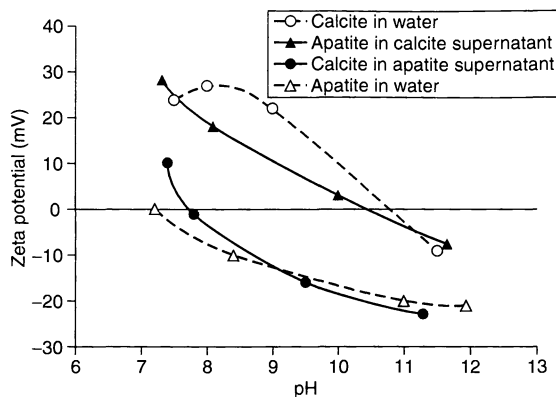
- pH** The variation of the zeta potential with pH is shown in Figure 10.11. It can be seen that at low pH values the zeta potential is positive and as the pH is increased, the zeta potential decreases, goes through zero at a pH known as the isoelectric point (IEP), and finally becomes negative as the pH is further increased. The IEPs of some common oxides and minerals are presented in Table 10.2.

Table 10.2. Isoelectric points (IEPs) of some common oxides and minerals

Material	Chemical formula	IEP
Quartz	SiO ₂	2.0
Sol-gel silica	SiO ₂	2.5
Alumina	Al ₂ O ₃	8–9
Titania	TiO ₂	5–6
Zirconia	ZrO ₂	4–6
Hematite	Fe ₂ O ₃	8–9
Magnesia	MgO	12.0
Molybdenum oxide	MoO ₃	0.5–1
Vanadium oxide	V ₂ O ₅	0.5–1
Zinc oxide	ZnO	9.0
Chromium oxide	Cr ₂ O ₃	6–7
Tin oxide	SnO ₂	4–5
Calcium carbonate	CaCO ₃	9–10
Mullite	3Al ₂ O ₃ · 2SiO ₂	6–8
Kaolin (edge)	Al ₂ O ₃ · SiO ₂ · 2H ₂ O	6–7
Apatite	10CaO · 6PO ₂ · 2 H ₂ O	4–6
Potassium feldspar	K ₂ O · Al ₂ O ₃ · 6SiO ₂	3–5

**Figure 10.12.** Illustration of the effect of increasing ionic strength on the zeta potential for alumina

2. **Ionic strength** In the presence of indifferent ions, the zeta potential is reduced and goes towards zero as the ionic strength is increased (Figure 10.12). However, in the presence of specifically adsorbing ions, depending on the nature of such ions, the IEP shifts and the sign of the zeta potential may be reversed (Figure 10.13 (3)). In this figure, for calcite in apatite supernatant, the specifically adsorbing ion is PO₄³⁻, and we see that the IEP shifts to lower pH and the sign of the zeta potential is reversed. In case of apatite in calcite supernatant, Ca²⁺ acts as the specifically adsorbing ion and shifts the IEP to a higher pH value.

**Figure 10.13.** Effects of specifically adsorbing ions on the zeta potentials of calcite and apatite (after ref. (3))

5 ELECTROSTATIC FORCES

The presence of surface charges leads to the development of a potential gradient in the vicinity of the surface. The Poisson–Boltzmann (PB) distribution, which assumes ions as point charges and *non-interacting*, defines the potential distribution as a function of the distance from the surface as follows:

$$\frac{d^2\psi}{dx^2} = \frac{2Zen}{\epsilon_r\epsilon_0} \sinh\left(\frac{Ze\psi}{kT}\right) \quad (10.4)$$

where Z is the electrolyte valency, e the elementary charge (C), n the electrolyte concentration (#/m³), ϵ_r the dielectric constant of the medium, ϵ_0 the permittivity of a vacuum (F/m), k the Boltzmann constant (J/K), and T the temperature (K).

When solved, the PB equation gives the potential (ψ), the electric field (differential of the potential) and the counterion density at any distance (x) away from the surface.

The Debye–Huckel parameter (κ) describes the decay length of the electrical double-layer, while the inverse of the parameter, κ^{-1} , which is known as the Debye length, indicates the distance away from the surface where the distribution of ions in the solution is affected by the presence of a charged surface:

$$\kappa = \left(\frac{2nZ^2e^2}{\epsilon_r\epsilon_0kT}\right)^{1/2} \quad (10.5)$$

where all of the symbols are as defined above for equation (10.4). Figure 10.14 shows the variation of the

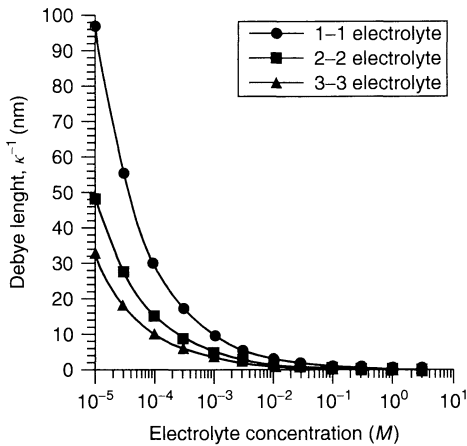


Figure 10.14. Variation of the Debye length with electrolyte concentration for different $z-z$ electrolytes

Debye length as a function of the electrolyte concentration for electrolytes with different valences. The extent of the double-layer decreases with increasing electrolyte concentration due to the shielding of surface charge, with ions of higher valences being more effective in screening such charge.

The overlap of similar electrical double-layers leads to a repulsive interaction, which will be summarized in the following sub-section. A schematic showing the overlap of electrical double-layers is presented in Figure 10.15, where part (b) illustrates the potential distribution after overlapping of such layers. In this figure, the dashed lines show the potentials expected from single double-layers, while the continuous line represents the potential due to the overlap. The expected potential due to the latter is higher, thus leading to a higher counterion concentration, which results in a higher osmotic pressure, which tends to push the particles further apart.

5.1 Calculation of electrostatic forces

5.1.1 Boundary conditions

1. *Constant potential surfaces* Under the assumption of a constant potential, the potential distribution near the surface remains constant. In order to maintain electro-neutrality, as the electrical double-layers overlap, the concentration of the counterion

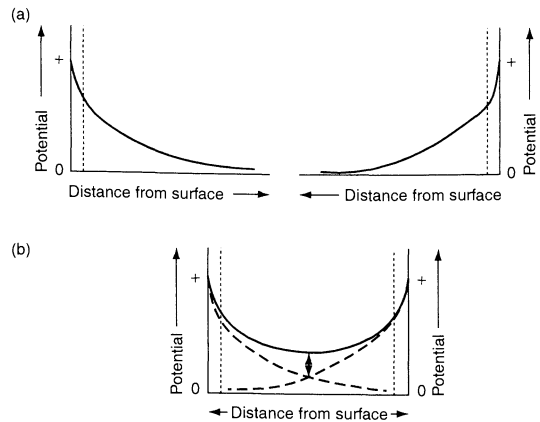
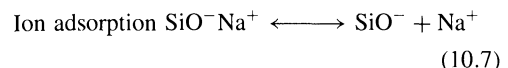
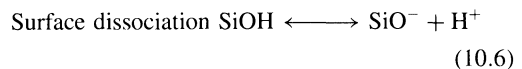


Figure 10.15. Schematic representations of the potential distribution between two approaching surfaces, shown (a) before, and (b) after overlap of the electrical double-layer; overlap leads to a higher potential between the planes, thus resulting in repulsion

increases. This increase leads to more counterion adsorption on the approaching surfaces, thus resulting in a decrease of the Stern charge. As a result, such a model predicts the minimum repulsion. Surfaces that develop charge by ion adsorption (AgI, NaCl, KCl, air bubbles, etc.) are best represented by this boundary condition.

2. *Constant charge surfaces* In these systems, as the surfaces approach each other, the charge on the surfaces remains constant, thus resulting in a maximum predicted repulsion between them. This model is the closest fit for surfaces that develop charges through site dissociation (Al_2O_3 , TiO_2 , latex, microbes, etc.).
3. *Charge regulated surfaces* In reality, most surfaces display an intermediate behaviour between constant charge and constant potential. For example, silica (SiO_2) can develop surface charge by both site dissociation and ion adsorption:



Information about the number of sites per unit area for each site is needed to calculate the surface charge. Because of the complexity of the charge-regulation model, many experiments under different conditions (pH, ionic strength, etc.) are needed in order to

extract the dissociation constants for the (surface) reactions responsible for surface charge development. The charge-regulated-surface assumption predicts the magnitude of the repulsion to be between that of constant charge and constant potential.

5.1.2 The linearized Poisson–Boltzmann approach

In order to calculate the repulsive interaction due to the overlap of the electrical double-layers (EDLs), the PB equation (equation (10.4)) needs to be solved numerically, which is difficult and computationally intensive. An easier approach is to produce analytical formulae by using a series of approximations. The PB equation can be written in terms of series expansion terms; for low-surface-charge and low-ionic-concentration conditions, even the first term of the expansion results in a more or less accurate estimate of the repulsive interaction.

5.1.3 Analytical formulae

Based on the above simplifications, analytical formulae can be produced for the calculation of the electrostatic energy of interaction between two flat surfaces. Appropriate formulae for two different models, i.e. constant potential and constant charge, are given as follows:

Constant potential (4)

$$W_{\psi}(H)_{\text{fl/fl}} = 2Z^2 n_i kT \left(\frac{e\psi_s}{kT} \right)^2 \frac{1}{\kappa} \left(1 - \tanh \frac{\kappa H}{2} \right) \quad (10.8)$$

Constant charge (4)

$$W_{\sigma}(H)_{\text{fl/fl}} = 2Z^2 n_i kT \left(\frac{e\psi_s}{kT} \right)^2 \frac{1}{\kappa} \left(\coth \frac{\kappa H}{2} - 1 \right) \quad (10.9)$$

where $W_{\text{fl/fl}}$ is the energy between two flat plates (J/m^2), H the separation distance (m), Z the valency, n_i the ion concentration ($\#/m^3$), k the Boltzmann constant (J/K), T the temperature (K), e the electron charge (C), ψ_s the Stern potential (V), and κ the Debye–Huckel parameter (m^{-1}).

For large separation distances, $W_{\psi} \cong W_{\sigma}$, and is given by the following equation (4):

$$W_{\psi}(H)_{\text{pl/pl}} = W_{\sigma}(H)_{\text{pl/pl}} = \frac{64nkT}{\kappa} \times \tanh^2 \left(\frac{Ze\psi_s}{4kT} \right) e^{-\kappa H} \quad (10.10)$$

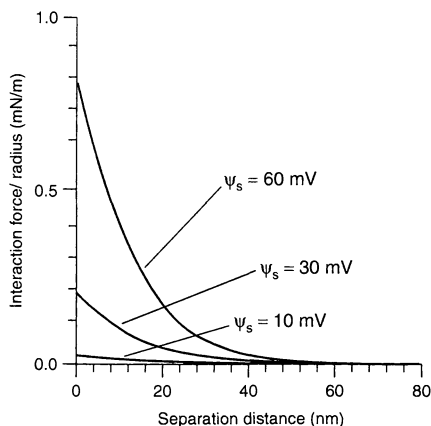


Figure 10.16. Variation of the electrostatic interaction energy with separation distance for different surface potentials, calculated by using the constant-potential assumption (ionic strength, $0.001M$; κ^{-1} , 905 nm)

Figure 10.16 illustrates the variation of the electrostatic interaction energy (mN/m) as a function of separation distance for three different surface potentials by using the constant-potential assumption. As mentioned earlier, the constant-charge assumption will yield higher repulsion energies in all cases. It can be seen that as the separation distance increases, the interaction energy decreases. In addition, the interaction energy decreases with decreasing surface potential. Figure 10.17 depicts this by showing that as the ionic strength of the solution is increased, the Debye length decreases, and hence the range of the interaction energy also decreases due to shielding of the surface charges.

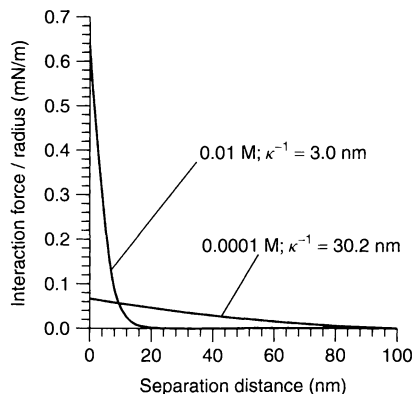


Figure 10.17. Variation of the electrostatic interaction energy with separation distance for different ionic strengths, calculated by using the constant-potential assumptions (ψ_s , 30 mV)

So far, only basic concepts have been outlined about the surface charge behaviour and its implications concerning interactions between charged surfaces. Most applications demand a control of interaction forces and/or surface behaviour, e.g. dispersion/agglomeration or the wettability of particulate systems. This is achieved by the use of polymer/surfactant or particulate coatings on core particles. The manipulation of surface behaviour and/or interactions by polymeric coatings is discussed next.

6 MANIPULATING SURFACE BEHAVIOUR BY POLYMER ADSORPTION

The word polymer is derived from the Greek, with “poly” meaning *many* and “mer” meaning *part*. According to the IUPAC definition, “A polymer is a substance composed of molecules characterized by the multiple repetition of one or more species of atoms or groups of atoms (constitutional repeating units), linked to each other in amounts sufficient to provide a set of properties that do not vary markedly with the addition of one or a few of the constitutional repeating units”. Polymers are made from repeating units of chemical species known as monomers, with typical molecular weights between 50 and 100 Da. Some of the polymers used in particulate processing are illustrated in Figure 10.18.

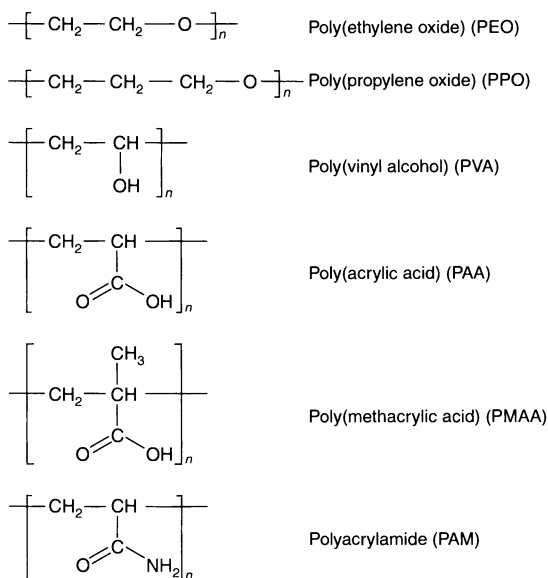


Figure 10.18. Some common polymers used in particulate processing

Polymers at particle surfaces play an important role in a range of technologies such as stabilization, flocculation, enhanced oil recovery and lubrication. In order to control and optimize these technologies, it is very important to understand the adsorption of polymers at the particle surfaces.

6.1 Solution behaviour of polymers

In order to understand the role played by polymers at interfaces in particle processing, it is important to understand the solution behaviour of such materials. The two major theories concerning this are briefly described below.

1. *Flory–Huggins theory* This theory calculates the free energy of mixing of pure amorphous polymers with pure solvent. The entropy and the enthalpy of mixing can be calculated separately, and the following relationship applies:

$$\Delta G^M = \Delta H^M - T\Delta S^M \quad (10.11)$$

where ΔG^M is the total free energy change, ΔH^M is the enthalpy change, and ΔS^M is the change in entropy, all with respect to mixing.

The entropy of mixing was originally calculated by Flory using a lattice approach, but it can also be derived by using a free volume approach. The entropy of mixing, ΔS^M , can be denoted by the following equation (1):

$$\Delta S^M = -k(n_1 \ln v_1 + n_2 \ln v_2) \quad (10.12)$$

where k is the Boltzmann constant, n_1 the number of solvent molecules, n_2 the number of polymer molecules, v_1 the volume fraction of the solvent in the polymer solution, and v_2 the volume fraction of the polymer.

The enthalpy of mixing is calculated by considering mixing to be a quasi-chemical reaction (1) between the dissimilar solvent contacts and segment contacts, which can be expressed as follows:

$$1 - 1 + 2 - 2 = 2(1 - 2) \quad (10.13)$$

Equation (10.13) depicts the formation of two solvent–polymer contacts (1–2) from a solvent–solvent contact (1–1), and a polymer segment–segment (2–2) contact. An interaction parameter, χ_1 , is defined where $\chi_1 kT$ is the difference in energy of a solvent molecule immersed in pure polymer, relative to that in pure solvent. For n_1 solvent molecules,

the energy change is $n_1\chi_1kT$. The probability of a solvent molecule being in contact with a polymer segment in a polymer solution is ν_2 , and hence the enthalpy of mixing, ΔH^M , can be denoted by the following equation [1]:

$$\Delta H^M = n_1\nu_2\chi_1kT \quad (10.14)$$

Therefore, by combining equations (10.11), (10.12) and (10.14), the free energy of mixing is given by:

$$\Delta G^M = kT(n_1 \ln \nu_1 + n_2 \ln \nu_2 + n_1\nu_2\chi_1) \quad (10.15)$$

It can be seen that the dominating reason for dissolution of a polymer is the increase in entropy of the solvent (e.g. water) molecules.

2. *Free volume theory* In the Flory–Huggins theory, χ_1 was considered primarily as an enthalpy term, although it was later shown experimentally that for many non-aqueous polymer–solvent systems, positive values of χ_1 , which oppose the mixing of solvent and polymer, are determined by entropic considerations. The enthalpy terms are relatively small, and the sign can vary depending on the conditions (1). In addition, it was found that χ_1 depends on the polymer concentration, and varies between 0.1 and 0.5, with χ_1 becoming more positive as the polymer concentration increases. The Flory–Huggins theory predicts that the mixing would be favoured as the temperature increases, since the mixing is entropy driven. However, phase separation has been observed for most polymer solutions near the critical point of the solvent. (The latter is defined as the temperature at which the transition takes place from a *good* solvent to a *poor* solvent)

Most of the shortcomings of the Flory–Huggins theory have been overcome by the use of the free volume theory (1). The entropic contribution to χ_1 was attributed to the difference in free volume between the solvent and the polymer. The increase in the value of χ_1 with concentration was explained on the basis of the ordering of the solvent molecules on increasing the segment concentration. The phase separation near the critical temperature of the solvent was attributed to the decrease in entropy on mixing the solvent and polymer under such conditions.

An important length-scale associated with polymer solutions is the root-mean-square radius of the polymer coil in the solution. For an unperturbed coil, this is known as the unperturbed radius of gyration, R_g , and is given by the following (1):

$$R_g = \frac{l\sqrt{n}}{\sqrt{6}} = \frac{l\sqrt{M/M_0}}{\sqrt{6}} \quad (10.16)$$

where n is the number of segments, l the effective segment length, M the molecular weight and M_0 the segment molecular weight. Equation (10.16) is valid so long as the solvent is “ideal” for the polymer, i.e. there are no interactions, either attractive or repulsive, between the segments in the solvent. In real (non-ideal) solvents, the effective size of a coil can be larger or smaller than the unperturbed radius R_g , and is sometimes referred to as the Flory radius, R_F , where $R_F = \alpha R_g$, and α is the intramolecular expansion factor, which depends on the nature of the solvent.

6.2 Adsorption of polymer at the particle surface

The free energy of the overall process must be favourable in order for a polymer to adsorb at a particle surface. The different factors contributing to the free energy change, when polymer adsorption takes place, are as follows (5):

- the adsorption energy, due to contacts of the polymer segments with the surface
- the conformational entropy of the chains
- the entropy of mixing of chains and solvent
- the polymer–solvent nearest-neighbour interactions

Adsorption takes place only if the energy of a segment–surface interaction is lower than that of a solvent–surface interaction (the first factor given above). A quantitative measure for this energy is the dimensionless parameter χ_s , which is defined such that the net effect of the exchange of a solvent molecule on the surface and a segment in the bulk solution is $-\chi_s kT$. For polymer adsorption to take place, χ_s has to be positive and the adsorption energy is proportional to the number of adsorbed segments. Polymers bond with surfaces through a variety of mechanisms, including electrostatic interactions, hydrogen bonding, hydrophobic interactions and specific chemical bonding, and the free energy for adsorption can be given by the following formula:

$$\Delta G_{\text{ads}}^0 = \Delta G_{\text{elec}}^0 + \Delta G_{\text{chem}}^0 + \Delta G_{\text{hydrophobic}}^0 + \Delta G_{\text{h-bonding}}^0 + \dots \quad (10.17)$$

Depending on the surface chemistry, and the nature and energetics of the sites on the surface of the particle, different factors contribute to the adsorption energy. In order to control polymer adsorption on surfaces, the interplay between the different adsorption mechanisms should also be considered.

The second and third factors listed above represent the entropy loss occurring upon adsorption, and hence can be considered as the opposing forces for polymer adsorption. The second accounts for the reduction of the internal degrees of freedom within the chains when they adsorb, while the third is related to the configurational entropy loss, which occurs when the homogeneous polymer solution is separated into a polymer-rich surface “phase” and a solution that becomes enriched with respect to the solvent.

The final factor results from the mutual interaction between segments and solvent molecules. In a poor solvent, the segment–solvent interaction is unfavourable. This forces the polymer out of the solution, thus promoting adsorption. In a good solvent, the segment–solvent interaction is favourable, while the aggregation of segments is unfavourable and as a result the adsorbed amount is less.

At equilibrium, in order to minimize the energy the adsorbed layer consists of polymer chains with several stretches of segments in the surface layer (*trains*), with the parts connecting the trains sticking out into the solution (*loops*). Moreover, at the chain ends, freely dangling *tails* may protrude into the solution. (Figure 10.19). The relative amount of the polymer segments, in trains, loops and tails, depends on the energetics of the polymer adsorption process discussed earlier.

6.3 Role of surface chemistry and structure in polymer adsorption

For a particular polymer functionality, the adsorption depends on the nature and energetics of the adsorption sites that are present on the surface. The adsorption of polymers via electrostatics, chemical bonding and hydrophobic attraction is relatively well understood,

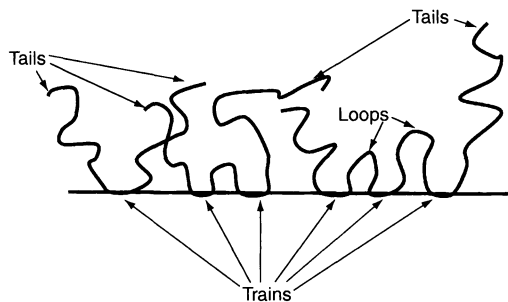


Figure 10.19. Structure of an adsorbed polymer layer at the solid–liquid interface

and most of the unexpected adsorption behaviour is attributed to hydrogen bonding, which is ubiquitous in nature. In this section, the dependence of hydrogen bonding on the surface chemistry will be presented, to illustrate how, by clever manipulation of the surface chemistry, hydrogen bonding can be controlled and predicted.

For a hydrogen-bonding polymer such as poly(ethylene oxide) (PEO), whose ether oxygen linkage acts as a Lewis base, it was illustrated that not only does the number of hydrogen-bonding sites differ from one surface to another, but the energy of such sites also varies (6). Based on adsorption studies of PEO on silica and other oxides (6), it was demonstrated that the amount of adsorbed polymer depends on the nature of the Brønsted acid sites on the particles. (Brønsted acids are defined as proton donors.) Hence, the more electron-withdrawing is the underlying substrate, then the greater is the Brønsted acidity, and thus the lower the isoelectric point of the material. It can be seen from Figure 10.20 that SiO_2 , MoO_3 and V_2O_5 strongly adsorb PEO, whereas oxides with a point of zero charge (pzc) greater than that of silica, such as TiO_2 , Fe_2O_3 , Al_2O_3 and MgO , did not exhibit significant adsorption of PEO. However, within a single system (silica) it has been found that PEO will adsorb to

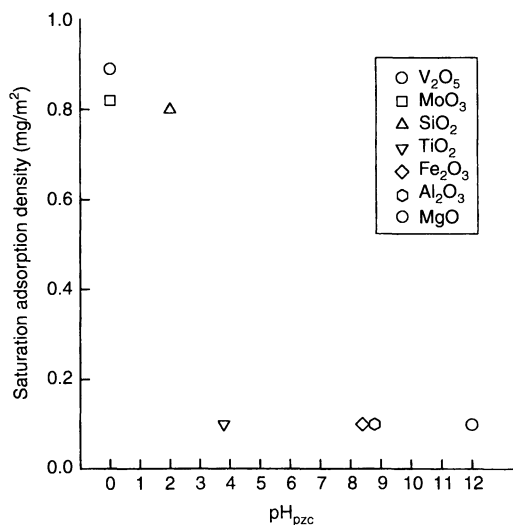


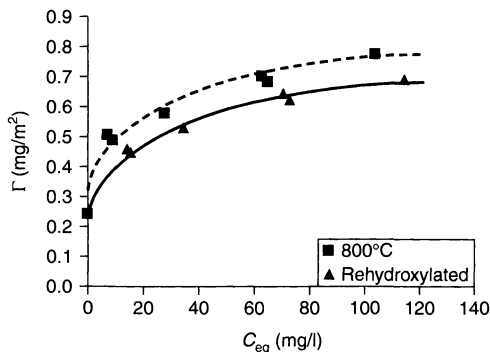
Figure 10.20. The effect of surface-Brønsted acidity on the adsorption of a hydrogen-bonding polymer, poly(ethylene oxide) (PEO) (after ref. (6)). (“Reprinted from *International Journal of Mineral Processing*, **58**, S. Mathur, P. Singh and B. M. Moudgil, Advances in selective flocculation technology for solid–solid separations, Page 212, Copyright (2000), with permission from Elsevier Science”)

Table 10.3. Correlation of polymer functionality with the surface absorption sites: PEO, poly(ethylene oxide); PVA, poly(vinyl alcohol); PAA, poly(acrylic acid); PAM, polyacrylamide(non-ionic); PAH, polyalamine

Polymer	Repeat unit	Functionality	Adsorbs (to)	Adsorption site
PEO	$\left[\text{CH}_2 - \text{CH}_2 - \text{O} \right]_n$	Ether	SiO ₂	Brønsted
PVA	$\left[\begin{array}{c} \text{CH}_2 - \text{CH} \\ \\ \text{OH} \end{array} \right]_n$	Hydroxyl	SiO ₂	Brønsted
PAA	$\left[\begin{array}{c} \text{CH}_2 - \text{CH} \\ \\ \text{O} = \text{C} - \text{OH} \end{array} \right]_n$	Carboxylic acid	Fe ₂ O ₃ , Al ₂ O ₃ , TiO ₂	Lewis
PAM	$\left[\begin{array}{c} \text{CH}_2 - \text{CH} \\ \\ \text{O} = \text{C} - \text{N} - \text{H} \\ \\ \text{H} \end{array} \right]_n$	Amide	Fe ₂ O ₃ , Al ₂ O ₃ , TiO ₂	Lewis
PAH	$\left[\begin{array}{c} \text{CH}_2 - \text{CH} \\ \\ \text{CH}_2 \\ \\ \text{NH}_2 \end{array} \right]_n$	Amine	SiO ₂	Brønsted

sol-gel-derived silica but not to glass or quartz at high pH values (6). This suggests that not only is the type of Brønsted acid site important, but that its strength, as determined by the surface molecular architecture, also influences the adsorption process. It was also proven that by surface modification, using techniques such as calcination and re-hydroxylation (7), the nature and energetics of the surface sites could be modified. Upon calcination of silica surface to 800°C, the number of

isolated surface hydroxyl groups and three-membered silicate rings increased, thus resulting in a higher surface acidity. These changes led to higher adsorption of the PEO polymer (Figure 10.21) (7). Based on the polymer functionality, it may be possible to predict the surface molecular architecture or the surface sites that are required for the polymer to adsorb. Table 10.3 correlates the polymer functionalities with the nature of the surface sites on which they adsorb (Lewis acid, Brønsted acid, etc.).

**Figure 10.21.** Adsorption of PEO on sol-gel silica after different treatments (calcined at 800°C; rehydroxylated) (after ref. (7))

7 MANIPULATING SURFACE BEHAVIOUR BY SURFACTANT ADSORPTION

A surfactant (surface-active agent) is a substance which, when present at low concentrations in a system, adsorbs on to the surface or interface of the system, and alters, to a marked degree, the surface or interfacial free energies of the surface. Surface-active agents have a molecular structure consisting of two distinct groups, namely the head and the tail. The tail is a structural unit that has very little attraction for the solvent, and is known as a lyophobic group. The head has a strong attraction for the solvent, and is called the lyophilic group. This kind of structure, consisting of lyophobic and lyophilic

groups, is known as the amphipathic structure. When a surface-active agent is dissolved in a solvent, the presence of the lyophobic group may cause solvent molecules to form an ordered structure, thus reducing the entropy of these species, and hence increasing the free energy of the system. As a result, the surfactant molecule is driven out of the bulk towards the interface. Thus, less work is required to create a unit area of surface, so resulting in the lowering of the interfacial energy or tension. The surfactant, however, cannot be completely removed from the system, since it has a lyophilic group, and complete expulsion of the surfactant would involve dehydration of such groups, which is energetically unfavourable. The chemical structures of suitable lyophobic and lyophilic groups vary with the nature of the solvent, and the conditions of use. In a highly polar solvent, such as water, the lyophobic group may be a hydrocarbon, fluorocarbon or siloxane chain of a suitable length, while the lyophilic group may be an ionic or highly polar group. Depending on the nature of the hydrophilic group, surfactants are classified as (i) anionic (net negative charge), (ii) cationic (net positive charge), (iii) zwitterionic (both positive and negative charges may be present), and (iv) nonionic (no apparent ionic charge). Some examples of commonly used surfactants are given in Table 10.4.

7.1 Adsorption of surfactants at the solid–liquid interface

7.1.1 Mechanisms of adsorption

Some of the most common mechanisms for surfactant adsorption are as follows:

- (i) Ion Exchange. This mechanism involves the replacement of counterions adsorbed on the surface by similarly charged surfactant ions.
- (ii) Ion Pairing. This mechanism involves the adsorption of surfactant ions from solution on to oppositely charged sites unoccupied by counterions.
- (iii) Acid–Base Interaction. The adsorption can take place via hydrogen-bond formation between the surfactant and the surface.
- (iv) Hydrophobic Bonding. This occurs when the adsorption of a surfactant molecule from the liquid phase takes place on to or adjacent to an other surfactant molecule already adsorbed on the surface.

7.1.2 Contributions to the adsorption energy

The contributions to the total free energy of adsorption can be divided into several different components, as follows [8]:

$$\Delta G_{\text{ads}}^0 = \Delta G_{\text{elec}}^0 + \Delta G_{\text{h-h}}^0 + \Delta G_{\text{chem}}^0 + \Delta G_{\text{c-c}}^0 + \Delta G_{\text{c-s}}^0 + \Delta G_{\text{solv/desolv}}^0 \dots \quad (10.18)$$

where ΔG_{elec}^0 represents the electrostatic contribution, $\Delta G_{\text{h-h}}^0$ the contribution from hydrogen-bond attraction, ΔG_{chem}^0 the possible chemical interactions between the substrate and surfactant, such as covalent bond formation and acid–base interactions, and $\Delta G_{\text{c-c}}^0$ the contribution from the lateral interaction between the adsorbed hydrocarbon chains. In addition, $\Delta G_{\text{c-s}}^0$ represents the interaction between hydrocarbon chains and non-polar solids (hydrophobic bonding), and $\Delta G_{\text{solv/desolv}}^0$ the change in energy due to the changes in solvation of the surface and the surfactant species upon adsorption. It should be noted that the division of the total free energy into these various contributions is to illustrate here such different contributions; these terms are *not* independent, and interplay between the different contributions is also very important.

Depending on the particle–surfactant system, one or more of the above contributions can be responsible for adsorption. The dominating one would depend on the nature and concentration of the surfactant, the surface chemistry of the particle, and solution properties such as pH and ionic strength. Electrostatic and lateral interaction forces are usually the major factors determining the adsorption of surfactants on oxides and other non-metallic minerals. Chemical interactions become more dominant for surfactant adsorption on salt-type minerals, such as carbonates and sulfides.

1. *Electrical interactions* As discussed earlier, most solids in aqueous solution exhibit a net surface charge depending on the pH and ionic strength of the solution. The surface charge results in an electrochemical potential in the vicinity of the surface. Oppositely charged surfactant molecules are attracted to the surface, and adsorb via electrostatic interactions. To maintain electroneutrality, the adsorption of ionic surfactants occurs through either exchange with co-ions in the double layer, or with an equivalent co-adsorption of counterions.

The electrical interaction becomes very important in the case of ionic surfactants. This interaction can be broken down into two contributions (8), i.e. Coulombic and dipole, as follows:

$$\Delta G_{\text{elec}}^0 = \Delta G_{\text{Coul}}^0 + \Delta G_{\text{dip}}^0 \quad (10.19)$$

Table 10.4. Some examples of commonly used surfactants

Long-chain amines derived from animal and vegetable acids, tall oil and synthetic amines $R-NH_2$	Polyoxyalkylenated alcohols, alkyl phenols and alcohol ethoxylates, including derivatives from nonyl phenol, coconut oil, tallow, and synthetic alcohols $R-(O-R')_n-OH$
Diamines and polyamines, including ether amines and imidazolines $R'-NH-R''-NH_2$	Polyoxyethylenated glycols $R-(O-CH_2-CH_2)_n-OH$
Quaternary ammonium salts, including tertiary amines and imidazolines $\begin{array}{c} H \\ \\ R'-N^+-R'' \\ \\ R''' \end{array} x^-$	Polyoxypropylenated glycols $R-\left(O-CH_2-\underset{\begin{array}{c} \\ CH_3 \end{array}}{CH}\right)_n-OH$
Quaternized and unquaternized polyoxyalkylenated long-chain amines $R'-(O-R''')_n-\begin{array}{c} H \\ \\ N^+-R'' \\ \\ R''' \end{array} x^-$	Esters of carboxylic acid and alkylene oxides $R'-\overset{\overset{O}{ }}{C}-O-R''$
Amine oxides derived from tertiary amines oxidized with hydrogen peroxide $\begin{array}{c} R'' \\ \\ R'-N=O \\ \\ R''' \end{array}$	Alkanolamine condensates with carboxylic acids $R'-\overset{\overset{O}{ }}{C}-NH-R''-OH$
	Polyoxyalkylenated mercaptans $R'-S-(OR')_n-OH$

Acrylic acid derivatives with amine functionality $R'-NH-R''-\overset{\overset{O}{ }}{C}-O^-M^+$
Substituted alkylamides $R'-\overset{\overset{O}{ }}{C}-N-R''-N\begin{array}{l} \nearrow R'''-\overset{\overset{O}{ }}{C}-O^-M^+ \\ \searrow R'''-\overset{\overset{O}{ }}{C}-O^-M^+ \end{array}$
<i>n</i> -alkyl betaines $\begin{array}{c} R'' \\ \\ R'-N^+-R''' \\ \\ R'' \end{array} \begin{array}{c} O \\ \\ C-O^-M^+ \end{array} x^-$
<i>n</i> -alkyl sulfobetaine $\begin{array}{c} R'' \\ \\ R'-N^+-R''' \\ \\ R'' \end{array} \begin{array}{c} O \\ \\ S-O^-M^+ \\ \\ O \end{array}$
Thio alkyl amines and amides $R'-S-R''-NH_2$

where:

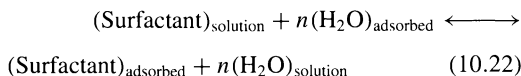
$$\Delta G_{\text{dip}}^0 = \sum \Delta n_j \mu_j E_s \quad (10.20)$$

and:

$$\Delta G_{\text{coul}}^0 = z F \psi_s \quad (10.21)$$

In the dipole expression (equation (10.20)), Δn_j is the change in the number of adsorbed molecules (dipoles), j , μ_j the dipole moment of j , and E_s the field strength at the Stern plane. For the adsorption of ionic surfactants, only the dipole moment of water needs to be considered.

The dipole term arises due to the replacement of water dipoles by surfactants upon adsorption, according to the following scheme (8):



In the Coulombic expression (equation (10.21)), z is the valency of the ionic surfactant, ψ_s represents the potential at the Stern plane in the electrical double layer, and F is the Faraday constant. Zeta potential can be used in place of ψ_s without introducing any significant errors in the calculations. At the isoelectric point (IEP), the contribution from the Coulombic term is expected to be negligible. In the absence of other contributions, Coulombic adsorption should proceed to the point where the adsorption reduces the zeta potential of the particle to zero. Any adsorption beyond this can be attributed to other types of interactions. Figure 10.22 (8) shows the adsorption of dodecyl sulfate on alumina. The adsorption of the negatively charged surfactant on the initially positively charged alumina surface decreases the zeta potential, eventually reducing the latter to zero. However, it is interesting to note that the adsorption continues to increase, although at a slower rate, even when the zeta potential is negative and the surface has the same sign as the oncoming surfactant molecules. This clearly indicates that even in systems where electrostatics is the dominant mechanism for adsorption, the latter may proceed through other mechanisms, such as chain-chain interactions between the adsorbed surfactant molecules.

Experimental evidence suggests that the electrostatic term in equation (10.18) can be overridden by the other terms. In fact, flotation of most sulfide minerals is accomplished with anionic surfactants under conditions where the mineral is negatively charged, i.e. the surfactant and the surface have the same charge and electrostatic interaction is unfavourable

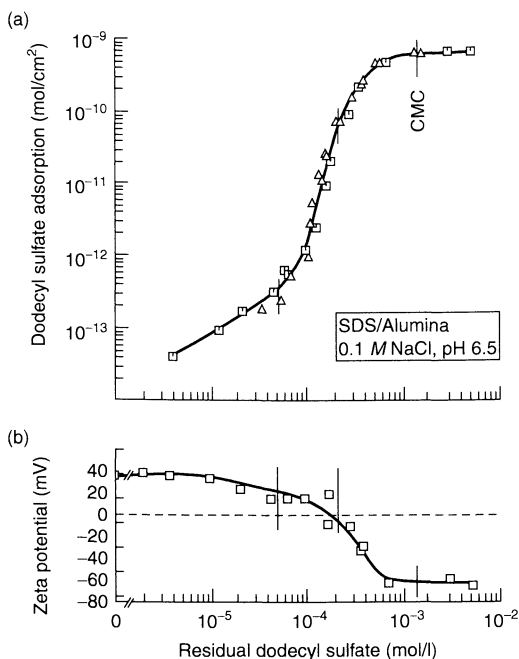


Figure 10.22. Adsorption (a) and zeta potential (b) behaviours of the dodecyl sulfate-alumina system (after ref. (8))

for adsorption. In the case of adsorption of fatty acids or alkyl sulfonates on oxides or salt-type minerals, ΔG_{chem}^0 plays a dominant role in the adsorption processes, and adsorption can take place irrespective of the zeta potential of the surfaces.

By assuming that the Stern potential can be approximated by the zeta potential, ΔG_{coul}^0 can be calculated by using equation (10.21). Table 10.5 (8) presents the corresponding values of ΔG_{coul}^0 for different values of the zeta potential. As shown in this table, the energy involved is very small, and even at very high zeta potentials, such as 60 mV, ΔG_{coul}^0 is only 1.38 (kcal/mol). This value is much

Table 10.5. Calculated values of ΔG_{coul}^0 , from equation (10.21), for different values of the potential (after ref. (8))

Zeta potential (mV)	ΔG_{coul}^0 (kcal/mol)
10	0.23
20	0.46
30	0.69
40	0.92
50	1.15
60	1.38

smaller than the ΔG_{c-c}^0 (7 kcal/mol for a hydrocarbon chain with 12 carbon atoms), the hydrogen-bonding (4–8 kcal/mol), and the chemical interaction contributions. Equation (10.21) may underestimate the value of ΔG_{coul}^0 , because of the fact that the double-layer theory assumes the surface to be uniformly charged. A better model would involve the presence of localized charges, which will increase the contribution of ΔG_{coul}^0 .

2. *Lateral chain–chain interactions* At a certain surfactant concentration, there is a sharp increase in the slope of the adsorption isotherm. This sharp increase clearly indicates an enhanced affinity of the surfactant for the surface. The increase in adsorption is also accompanied by a sharp increase in the zeta potential, and in some cases, a reversal in the zeta potential is observed. Such observations have been attributed to lateral interactions between the adsorbed surfactant tails, which lead to the formation of self-assembled two-dimensional structures known as “hemimicelles”. The formation of such structures resulting from hydrophobic interactions between the surfactant tails, was first proposed in 1955 by Gaudin and Fuerstenau, and later verified by Somasundaran and co-workers (refer to refs (9–11) for further details of these studies). Such aggregation occurs due to the fact that surfactant molecules decrease the entropy of the water molecules in the bulk solution, and are forced out of the latter in a process similar to the formation of the micelles in the bulk. In order to form hemimicelles, a certain critical amount of the adsorbed surfactant is required, and this concentration is known as the *critical hemimicelle concentration*. The hemimicelle concentration depends on the strength of the interaction between the surfactant and the surface, the surfactant structure (number of CH₂ or aromatic groups, arrangement of atoms in the hydrocarbon chain, etc.), and solution conditions (pH, ionic strength and temperature).

The energy for lateral chain interaction, ΔG_{c-c}^0 , has been proposed to be proportional to the number of CH₂ groups in the surfactant (n), according to the following equation (8):

$$\Delta G_{c-c}^0 = n\phi \quad (10.23)$$

where ϕ is the cohesive energy per mole of CH₂ groups. This factor has been calculated to be about 0.6 kcal/mol per CH₂ group, and hence for surfactants with chain lengths of 12 to 18 carbon atoms, the ΔG_{c-c}^0 would be 7–10 kcal/mol (8). This energy contribution is significantly higher than the electrostatic contribution, and would explain the increased

adsorption in some systems, even when the surfactant is similarly charged to the substrate.

3. *Chemical interactions* The chemical contribution may result from interactions such as covalent or complex bond formation between the surfactants and the surface sites. Surfactants such as fatty acids, alkyl sulfates, alkyl sulfonates, amines and alkylhydroxamates have been proposed to adsorb by means of chemical interactions on a variety of particles. In addition, surfactants containing hydroxyl, phenolic, carboxylic and amine groups can hydrogen-bond with the surface sites. Infrared spectroscopy has been used to understand the chemisorption of surfactants at the surface, by examining the shift in the characteristic peaks of the surfactants upon adsorption.

Surfactants can react with the dissolved ionic species in the bulk to form insoluble complexes. It has been proposed that adsorption of the surfactant can take place through similar reactions with ions on the surface, or by surface precipitation, under conditions where no bulk precipitation takes place, but where the interfacial concentration is high enough to exceed the solubility product in the interfacial region (8).

7.2 Surfactant structures at the solid–liquid interface

The aggregation of surfactants into spherical, cylindrical and lamellar micelles in the bulk solution, and the factors controlling the aggregation, are relatively well understood, when compared to the self-assembly of surfactants at the solid–liquid interface (9). At interfaces, apart from the entropic conditions that favour aggregation in the bulk, additional factors such as surfactant–surface and solvent–surface interactions play an important role in the self-assembly. Adsorption isotherms, combined with techniques such as contact angle and zeta potential, have been used traditionally to probe the self-assembled surfactant structures at the solid–liquid interface. Recently, surfactant structures adsorbed at the solid–liquid interface have been directly imaged by using atomic force microscopy (AFM) (for further information on these studies, the interested reader is referred to refs (10), and (11)). Various factors, such as the nature and morphology of the substrate, solution conditions, surfactant type and time, have been investigated by a number of authors (10, 11), in order to understand the self-assembly process. However, owing to the instability of the self-assembled surfactant structures at lower concentrations under

the experimental conditions encountered during AFM experiments, most of the measurements using such a technique have been performed at relatively high surfactant concentrations (twice the bulk critical micelle concentration (CMC)). However, as mentioned earlier, surfactant self-assembly at the interface in the form of "hemimicelles" is known to initiate at concentrations much below the bulk CMC.

Some theoretical models based on the thermodynamics of surfactant self-assembly have also been recently used to predict the critical surface aggregation concentration (the bulk concentration at which surfactants start to self-assemble at the solid-liquid interface), and the self-assembled surfactant structure at the solid-liquid interface (11). These models, although providing useful insight into the surfactant self-assembly process, require an estimate of the interaction energies, which are difficult to determine experimentally. Variations in the estimated interaction energies can lead to different self-assembled surfactant structures, depending on the values used for the calculations.

Several different experimental techniques, such as fluorescence decay, electron spin resonance (ESR) spectroscopy, Raman spectroscopy, nuclear magnetic resonance (NMR) spectroscopy, neutron reflectometry, calorimetry, Fourier-transform infrared (FT-IR) adsorption spectroscopy, small-angle neutron scattering (SANS), ellipsometry and surface force measurements, have been used to study self-assembled surfactant structures at the solid-liquid interface (11). These measurements, although providing insight into the hemimicellization process, critical aggregation numbers

and adsorption kinetics, have not been able to illustrate the morphology and structural transitions taking place within the self-assembled surfactant films at the solid-liquid interface.

Presented below is an example of structure development at the solid-liquid interface for the silica/dodecyltrimethylammonium bromide ($C_{12}TAB$) system, at pH 4.0 and 0.1 M NaCl as the background electrolyte, obtained by Singh *et al.* (11). A combination of different techniques such as adsorption, zeta potential, contact angle and FT-IR attenuated total reflection (ATR) measurements, have been used in this study to clearly illustrate the structural transitions, and the structure of self-assembled surfactant films at different adsorbed amounts of the surfactants at the interface.

The adsorption, zeta potential and contact angle measurements of silica surfaces, in 0.1 M NaCl at pH 4.0 as a function of the solution $C_{12}TAB$ concentration, obtained in this study are presented in Figure 10.23. Based on the observations, various possible self-assembled surfactant structures as a function of the surfactant concentration were suggested. Based on the interface properties, the entire self-assembly process was divided into six stages, marked as "A-F" on the figure. At low concentrations (below 0.007 mM, Region A on Figure 23), individual surfactant adsorption takes place. The next structural transition in this system was the formation of hemimicelles, which is evidenced by a significant effect on both the zeta potential and hydrophobicity of the surface. At approximately 0.1 mM in region B, the sign of the zeta potential reverses, although the contact angle continues to increase, indicating that the reversal in

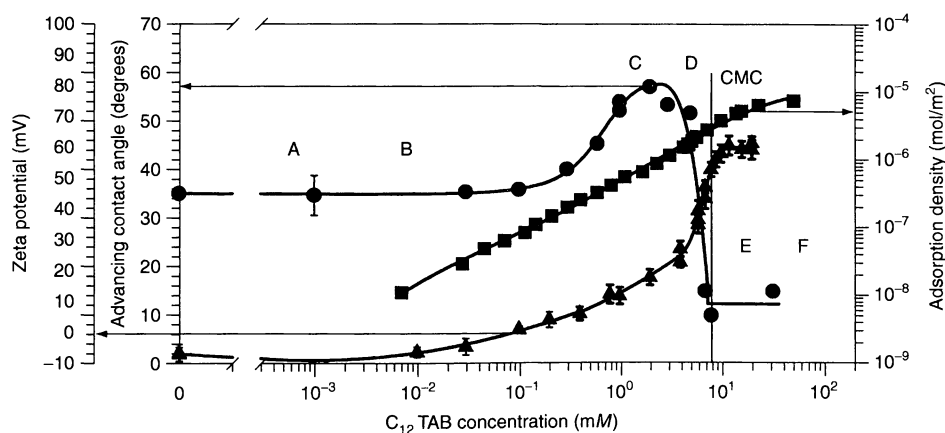


Figure 10.23. Adsorption isotherm (squares), zeta potential (triangles), and contact angle (circles) data of silica surfaces, obtained in 0.1 M NaCl at pH 4.0 as a function of the solution $C_{12}TAB$ concentration (after ref. (10)). ("Reproduced with permission from *Langmuir*, 2000, 16, 7255–7262, Copyright (2000) American Chemical Society")

zeta potential is not due to formation of bilayers, as has been suggested in earlier literature. This reversal in zeta potential, while the hydrophobicity continues to increase, was attributed to either hydrophobic association between the surfactant tails, thus resulting in the formation of hemimicelles, or due to some kind of specific adsorption. In regions B and C, the contact angle continues to increase, hence indicating an increasing concentration of hemimicelles at the interface. Beyond a certain concentration (approximately 2.3 mM), the hydrophobicity decreases (region D), and is accompanied by an increase in the rate of increase of the zeta potential. This indicates the formation of structures which have an increasing number of their polar heads oriented towards the solution. The sharp increase in zeta potential, and the corresponding decrease in contact angle, was attributed to the transition of the surfactant structure from hemimicelles to either bilayers, spherical aggregates (imaged at surfaces by using AFM), or structures having “semi-spheres” on top of perfect monolayers. At higher surfactant concentrations beyond the bulk CMC (Regions E and F), based on AFM imaging, spherical aggregates or composite semi-spheres on top of perfect monolayers (it is not possible to distinguish between these structures, based just on AFM imaging) are known to exist. Thus, based on the adsorption, zeta potential and contact angle results, several plausible surfactant structures were proposed at the interface at different concentrations of the surfactant. To illustrate the exact structural transitions taking place at the interface, the FTIR/ATR spectroscopic technique (with a polarized IR beam), which can probe the adsorbed structures directly, was employed.

The FTIR/ATR technique is based on the fact that individual surfactant molecules, hemimicelles, monolayers, bilayers and spherical/cylindrical aggregates at the interface will have different average orientations of the alkyl chain with respect to the surface normal. Different average orientations would result in different absorptions of the plane-polarized IR beam, and can thus be used to identify the surfactant structures at the interface (11).

Based on the FT-IR study, the proposed surfactant structures in the different regions were verified. In region D, it was found that spherical aggregates are formed directly from hemimicelles, without the formation of bilayers. In fact, no evidence of bilayer formation was seen in this system, even at very high surfactant concentrations.

By using the contact angle, FTIR, zeta potential and adsorption data, the above structural transitions are summarized by the schematic shown in Figure 10.24,

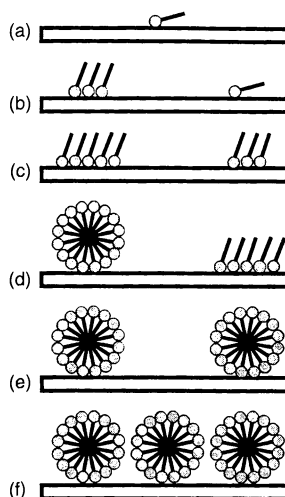


Figure 10.24. Schematic representation of the proposed self-assembled surfactant films at concentrations corresponding to regions A–F in Figure 10.23: (A) individual surfactant adsorption; (B) low concentration of hemimicelles on the surface; (C) higher concentration of hemimicelles on the surface; (D) hemimicelles and spherical surfactant aggregates formed due to increased surfactant adsorption and transition of some hemimicelles to spherical aggregates; (E) randomly oriented spherical aggregates at the onset of steric repulsive forces; (F) surface fully covered with randomly oriented spherical aggregates (after ref. (11)). (“Reproduced with permission from *Langmuir*, 2001, **17**, 468–473, Copyright (2001) American Chemical Society”)

which illustrates the structures present at the interface for the concentration regions A–F in Figures 10.23.

8 PARTICLE PROCESSING

8.1 Dispersion of particles

Different types of dispersions are encountered in industrial applications, the most common ones include solid/liquid (suspension), liquid/liquid (emulsions), gas/liquid (foams), liquid/solid (gels), and liquid/gas (aerosols). These dispersions are encountered in almost every industry in some form or the other during the preparation or as end product. Examples of industrial applications of dispersions include paints, dyestuffs, printing ink, paper coatings, cosmetics, ceramics, microelectronics, agrochemical and pharmaceutical formulations, and various household products. In the following sections, the characterization and properties of solid/liquid suspensions will be described. However, the same concepts would be valid for other kinds of dispersions also.

8.1.1 Characterization of the state of dispersion

There are numerous techniques available for characterization of the state of dispersion. Some of the most common methods are as described in the following.

1. *In Situ Particle size measurement* If the particle's primary particle size is known, then measurements of the size distribution in the suspension state can indicate if the powder is dispersed or flocculated. Table 10.6 presents some *in situ* particle sizing techniques, along with the size ranges that they are capable of measuring and the concentrations of samples which can be used. Caution should be exercised, however, when using such techniques, since no one method is appropriate for all slurries. Most of the ensemble techniques, such as light scattering, photon correlation spectroscopy, referenced light scattering, acoustic spectroscopy, flow field fractionation and sedimentation, are not sensitive to the tails of the particle size distribution plots. There is definitely a need for developing size distribution techniques that are sensitive to large particles, are able to measure slurries without dilution, and may be modified for in-line particle size analysis.
2. *Consolidation behaviour* The state of the dispersion can be assessed by monitoring powder consolidation rates, such as sedimentation, filtration or casting rates. Poorly dispersed suspensions will tend to undergo more rapid consolidation when compared to well-dispersed samples because of the large particle (i.e. floc/agglomerate) size. This effect is illustrated in Figure 10.25 for titania suspensions prepared at various pH levels, showing the sediment height as a function of the suspension pH. A lower sediment height indicates that the initial settling rate and coagulation is fast and the suspension is unstable. At about pH 7.0, which is the IEP for the system, the system is most unstable, since there are no repulsive

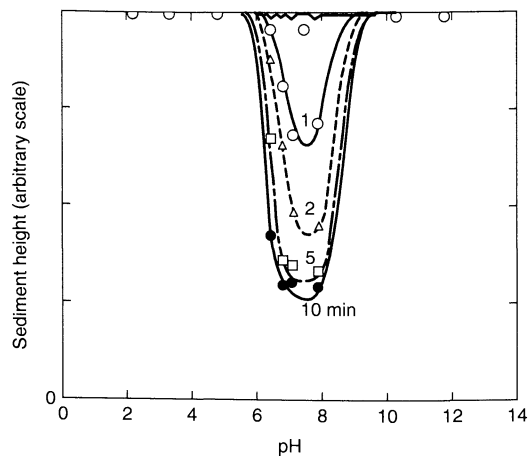


Figure 10.25. Sediment height of TiO₂ particles as a function of pH and time (in 10⁻²M KNO₃ solution)

electrostatic forces to keep the particles apart, and the particles coagulate due to attractive van der Waals forces. Another way to observe sedimentation would be to measure the turbidity of the suspension. A higher turbidity indicates a higher scattering of the incident light, which in turn indicates a stable slurry.

Settling, however, may not be feasible or practical for nanosized particles unless strong agglomeration is present. Settling is also influenced by other factors such as viscosity and structure formation. The turbidity measurements are most reliable when used on non-settling and translucent slurries.

3. *Consolidated structure* The consolidated structure (i.e. powder compact) that forms after the liquid is removed from the suspension depends on the state of the dispersion. Well-dispersed suspensions tend to form consolidated structures with a higher particle packing density (lower total porosity) when compared to samples prepared from suspensions with flocs/agglomerates (Figure 10.26) (12). In addition, the samples prepared from well-dispersed suspensions tend to have a smaller average pore size and a narrower pore size distribution.
4. *Rheology* This is the science dealing with the flow and deformation of materials. The rheological behaviour of particle/liquid systems is important in most processing operations, including powder and batch preparation, materials transport, coating and deposition, and shape forming. Rheological properties are highly dependent upon the physical structure of the particle/liquid system. The structure is governed by factors such as the particle size and shape

Table 10.6. Different techniques used for particle size measurements in suspension, and the corresponding size ranges and concentrations

Technique	Size range	Solids range (vol%)
Electrical sensing zone	400 nm–1.2 mm	Dilute
Light scattering	40 nm–2 mm	Dilute
Photon correlation spectroscopy	2 nm–5 μm	Dilute
Referenced light scattering	30 nm–5 μm	Dilute–5.0
Acoustic spectroscopy	100 nm–10 μm	2.0–50.0
Flow field fractionation	15 nm–2 μm	2.0–20.0
Sedimentation	100 nm–100 μm	Dilute

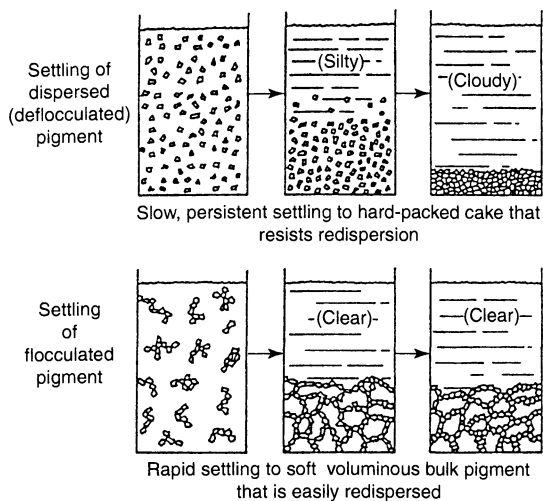


Figure 10.26. Consolidated structures for dispersed and flocculated suspensions (after ref. (12))

distribution, solid/liquid volume ratio and interparticle forces. Rheological measurements can often be used to deduce information about the state of the particulate dispersion in the suspension.

The viscosity, η , is defined as the ratio of the shear stress (τ) to the shear rate (D), as follows:

$$\eta = \frac{\tau}{D} \quad (10.24)$$

At low solids loading, flocs/agglomerates may remain as individual flow units, which do not interact extensively. Flow behaviour may be Newtonian, although the viscosity will be higher than that observed in the corresponding dispersed suspension. This is due to the immobilized liquid in the intra-floc (intra-agglomerate) voids, which results in an increase in the “effective” solids loading of the suspension (Figure 10.27). As the solids loading increases, agglomerated suspensions tend to show shear-thinning behaviour (i.e. the viscosity decreases as the shear rate is increased). Extensive structure (floc/aggregates) exist at low shear rates. The viscosities tend to be significantly higher than the corresponding dispersed suspensions due to immobilized liquid. As the shear rate is increased, the structure is broken down, entrapped liquid is released, and the viscosities are observed to decrease. Whether or not the flow units are broken down to primary particle size levels depends on the shear rate and the strength of the agglomerates.

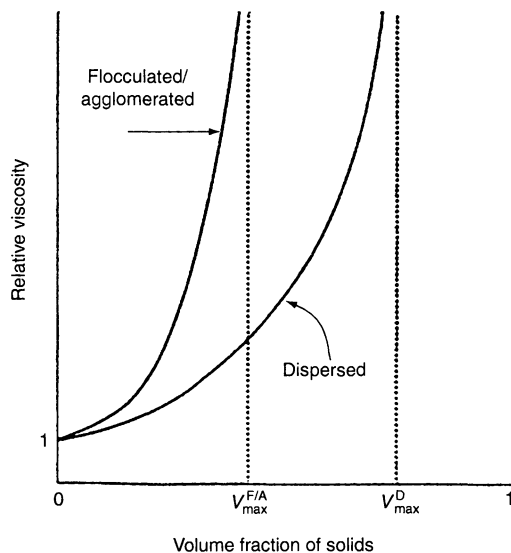


Figure 10.27. Variation of the relative viscosity as a function of the volume fraction for flocculated/agglomerated and dispersed suspensions

8.1.2 Control of dispersion through surface chemistry

1. *pH and ionic strength* As illustrated earlier, both pH and ionic strength control the surface charge and hence the suspension stability. The effect of pH is shown in Figure 10.25 for a titania suspension, which exhibits minimum stability at the isoelectric point of titania, where the net surface charge is zero, and there is no electrostatic repulsive force to prevent the particles from agglomerating due to attractive van der Waals forces. Figure 10.28 (13) shows the effect of electrolyte concentration on the stability of a silica suspension under different pH conditions. At low electrolyte concentration, the suspensions are stable at all pH values (indicated by high turbidity), whereas, at higher salt concentrations, suspensions are unstable under pH conditions where the surface potential is lower.
2. *Surfactant adsorption at the surface* As discussed in an earlier section, the adsorption of ionic surfactants can lead to charge development on the surface, and hence lead to stabilization of particulate dispersions. It has been shown recently by Adler *et al.* (10), that self-assembled surfactant layers at the particle surface can impart stability to nanoparticulate suspensions in extreme environments. It was proposed that the resistance to elastic deformation of the surface surfactant structures was the primary stabilization mechanism.

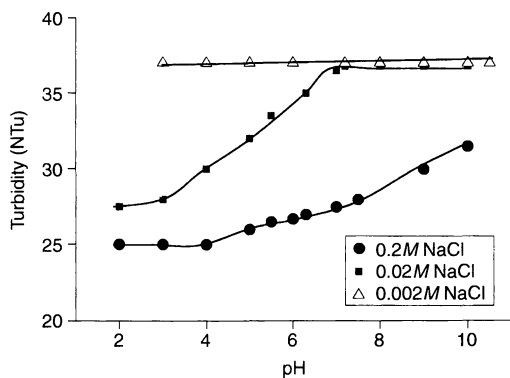


Figure 10.28. Illustration of the effect of electrolyte concentration on the coagulation of suspensions (after ref. (13))

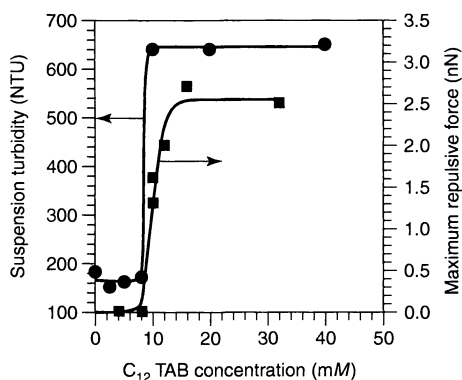


Figure 10.29. Turbidity of a 0.02 vol% suspension of sol-gel-derived 250 nm silica particles after 60 min in a solution of 0.1 M NaCl at pH 4 as a function of the C_{12} TAB concentration, and the measured interaction forces between an AFM tip and the chemical vapour deposited (CVD) silica substrate under identical solution conditions. A significant repulsive force arises upon a change in concentration from 8 to 10 mM, which directly corresponds to the formation of a stable suspension (after ref. (10)). ("Reproduced with permission from *Langmuir*, 2000, **16**, 7255–7262, Copyright (2000) American Chemical Society")

Figure 10.29 (10) depicts the suspension turbidity, a measure of the stability of a suspension of 0.25 μm sol-gel-derived silica particles and the surface forces measured with an atomic force microscope, as a function of the surfactant (C_{12} TAB) concentration at pH 4.0 and 0.1M NaCl. Under these conditions, the silica suspension without the dispersant is unstable, as determined by turbidity measurements. It is seen that there exists a critical concentration of the surfactant, above which repulsive forces between

surfactant-coated surfaces are observed, and particle stability occurs. This transition from an unstable to a stable suspension, from no repulsive forces to steric repulsive forces, occurs just beyond the bulk critical micelle concentration (CMC) of the surfactant. These authors reported the stability of silica suspensions under 5M NaCl concentration conditions, where the zeta potential is approximately zero. Stability under relatively high electrolyte concentrations further indicates that electrostatic repulsion may not be the only stabilization mechanism in the presence of self-assembled surfactant structures at the surface of the particle. It is important to note that the repulsive forces measured between the microscope tip and the silica surface in the presence of the self-assembled layer is at least an order of magnitude higher than the repulsive force expected from pure electrostatic interactions.

3. *Polymer adsorption at the surface—steric barrier* As two polymer-coated particles approach each other, the outer segments of the adsorbed polymer layers begin to overlap, thus leading to steric repulsive forces. This overlap usually takes place when the separation between the particles is less than a few R_g (radius of gyration) units (introduced earlier, see equation (10.16)). The repulsive steric force is, in fact, a repulsive osmotic force due to the unfavourable entropy resulting from the compression of the chains between the surfaces. This repulsive force is critical in particulate processing, because it can be used to stabilize dispersions which are otherwise unstable. In order for the steric repulsion to be effective, the range of the latter should be greater than distances at which van der Waals forces become dominant.

The steric repulsive force depends on the quantity or coverage of the polymer on each surface, and on the quality of the solvent. Three domains of close approach for sterically stabilized particles can be defined (1), based on the separation distance between the particles, d , and the thickness of the steric layers, l (Figure 10.30).

- (i) $d > 2l$. This region is referred to as the non-interpenetrational domain, since the adsorbed polymer layers cannot interact, and no steric repulsive forces are observed.
- (ii) $l \leq d \leq 2l$. When the distance between the surfaces is less than twice the steric layer thickness, interpenetration occurs between the adsorbed polymer molecules on both the surfaces – this domain is referred to as the interpenetrational domain. Due to such interpenetration, the solvent molecules are

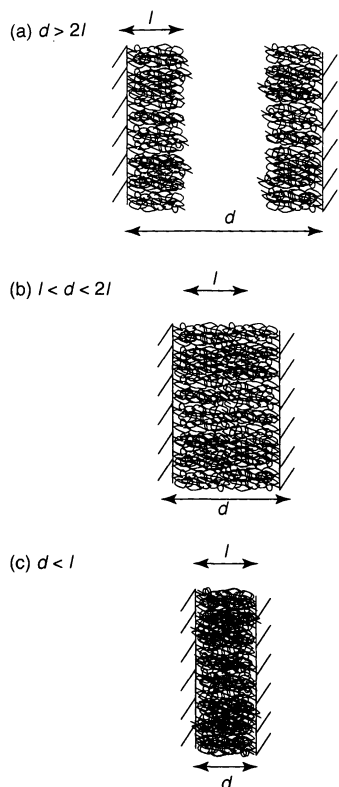


Figure 10.30. The three domains of sterically stabilized flat plates: (a) non-interpenetration; (b) interpenetration; (c) interpenetration and compression of the adsorbed layer

driven out of the overlap region, thus resulting in de-mixing. In good solvents, this de-mixing of segments and solvent leads to repulsion, due to the increase in the free energy of the system.

- (iii) $d < l$. When the separation distance is less than the adsorbed layer thickness, apart from interpenetration, compression of the adsorbed polymer molecules also takes place. In addition to the de-mixing of solvent and segments, the reduction in elasticity of the polymer segments also contributes to the free energy of the system. This elasticity arises from the reduction in the configurational entropy of the adsorbed surfactant molecules, and irrespective of the quality of the solvent, leads to steric repulsion.

For a detailed mathematical description of these three domains, the interested reader is referred to ref. (1).

A direct measure of the interaction energy can be obtained by using atomic force microscopy (AFM).

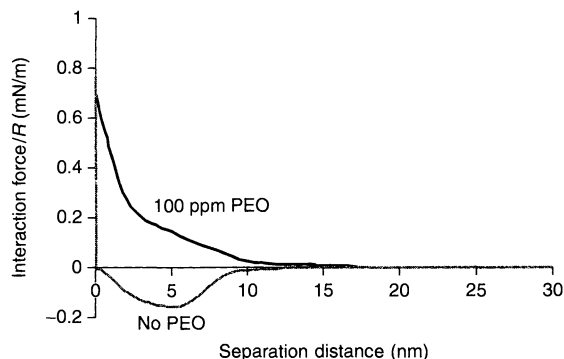


Figure 10.31. Interaction force between a silica sphere and a flat silica substrate (pH 3.0, 0.01 M NaCl), both in the absence and presence of 100 ppm of PEO (M_w 7500) dispersant

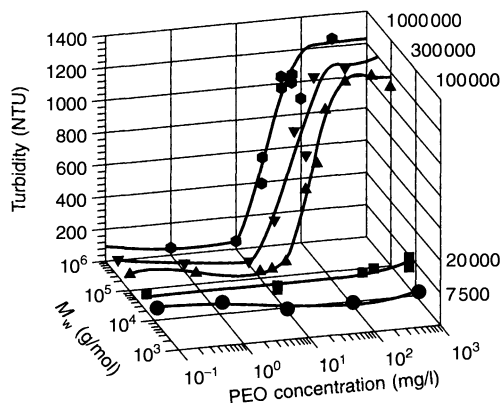


Figure 10.32. Stability of silica particles (pH 3.0, 0.01 M NaCl) as a function of the PEO dosage, showing the variation with different molecular weights of the polymer

Figure 10.31 depicts the force between a silica sphere and a flat silica surface measured by using such a technique, both with and without poly(ethylene oxide) (PEO) (M_w 7500). Under the conditions of the experiment (pH 3.0, 0.01 M NaCl), in the absence of the polymer, the electrostatic repulsive forces are not strong enough, and the van der Waals forces become dominant and lead to an attractive interaction between the surfaces. In the presence of the polymer, steric repulsive forces are observed between the surfaces, and no net attractive force is measured. Figure 10.32 illustrates the stability of silica particles under similar conditions, but using PEO with different molecular weights. In the absence of polymer, the turbidity of the silica suspension is low, hence indicating an unstable suspension, and this correlates with the attractive interactions observed

Table 10.7. Some commonly used dispersants, their formulae and the mechanisms of dispersion involved in application

Dispersant	Formula	Dispersion mechanism
Sodium silicate	Na_2SiO_3	Electrostatic
Sodium Hexametaphosphate	$(\text{NaPO}_3)_n$	Electrostatic
Dodecyl trimethyl ammonium bromide	$(\text{CH}_2)_{12}\text{N}(\text{CH}_3)_3\text{Br}$	Electrostatic, steric
Poly(acrylic acid)	$(\text{CH}_2-\text{CH}-\text{COOH})_n$	Electrostatic, steric
Poly(ethylene oxide)	$(\text{CH}_2-\text{CH}_2-\text{O})_n$	Steric
Polyacrylamide	$(\text{CH}_2-\text{CH}-\text{CONH}_2)_n$	Electrostatic, steric
Poly(vinyl alcohol)	$(\text{CH}_2-\text{CHOH})_n$	Steric
Poly(methacrylic acid)	$(\text{CH}_2-\text{C}(\text{CH}_3)(\text{COOH}))_n$	Electrostatic, steric
Poly(vinyl amine)	$(\text{CH}_2-\text{CHNH}_2)_n$	Electrostatic, steric

in Figure 10.31. Above a certain dosage of the added polymer, a stable suspension is observed, and this again correlates to the steric forces observed in the presence of the polymer.

A list of commonly used dispersants, including both inorganic and polymeric materials, is provided in Table 10.7.

8.2 Selective flocculation of particles

The process of selective flocculation is used for solid–solid separations (i.e. to separate a desired component from a mixture of particles). The process involves the selective adsorption of a polymeric flocculant on the desired component, resulting in the formation of agglomerates known as flocs, and the separation of such aggregates from particles of other component(s) in the dispersed phase. The competition between different surfaces for the flocculant has to be controlled in order to achieve adsorption on the targeted component(s). The flocs are separated from the suspension either by sedimentation/elutriation or floc-flotation. In order to improve the concentrate grade, if possible, the flocs may be subjected to further washing.

The selective flocculation process involves four steps (6): (i) dispersion of the fine particles by addition of inorganic or organic dispersants, (ii) selective adsorption of the polymer on the flocculating component and formation of the flocs, (iii) floc growth, which is generally achieved by conditioning at low shear, and (iv) floc separation, either through sedimentation/elutriation/sieving or flotation, followed by cleaning

of the flocs by repeated redispersion and flocculation, if necessary.

The principles of selective flocculation as well as the underlying surface chemistry has been reviewed earlier by various authors, including the groups of Kitchener, Attia and Moudgil and their co-workers. (The interested reader is referred to ref. (6) for details of these publications.)

The process of selective flocculation is being used industrially by companies such as the Engelhard Corporation (process for removal of titania from clays), Thiele Kaolin Georgia (separation of titania from clays) and the Cleveland Cliffs Company (beneficiation of non-magnetic taconites, and separation of silica). Although the primary application of selective flocculation has been in the mineral processing industry, many potential uses also exist in biological and other colloidal fields. These include purification of ceramic powders, separation of hazardous solids from chemical wastes, and removal of deleterious components from paper pulp.

It is important to note that the choice of selective reagents/flocculants based on single-mineral tests does not guarantee a successful separation scheme. In general, the selectivity observed in single-component tests is lost in mixed-component or natural systems because of one or more of the following reasons: heterocoagulation, charge patch neutralization, dissolved ion interference, slime coating, physical entrapment, entrainment, heteroflocculation, and cross-contamination during the size reduction process (6). In order to develop selective separation schemes, the role of these factors and their dependence on the surface chemistry of the components becomes very important. In the following section, the choice of selective flocculants based on surface chemistry will be discussed.

8.2.1 Design of selective reagents based on surface chemistry

The surface property which has the greatest difference between flocculating and nonaggregating particles should be the basis for selection of a flocculant. The latter materials are high-molecular-weight polymers and can adsorb through hydrogen bonding, hydrophobic interactions, electrostatic interactions, chemical bonding and van der Waals forces.

Flocculant selection based on surface charge

The differences in surface charge, either natural or induced by controlling the pH and solution conditions,

can be used to achieve selective adsorption of the flocculant. For example, a hydrolyzed polyacrylamide, which is negatively charged, can be employed to separate apatite from clay under appropriate dosage and pH conditions. In this system, clay is negatively charged in the pH range 4–10, while apatite has an IEP at pH 6.5, and hence by selecting the pH of the solution such that the minerals are oppositely charged, selectivity can be achieved based on surface charge.

However, the possibilities of achieving an adequate selectivity based on electrostatic interactions alone are limited since the particulates involved may have similar isoelectric points (e.g. the apatite–dolomite system) or there may be specific interactions between the polymer and mineral surface.

Selectivity based on specificity of hydrogen bonding

The specificity of hydrogen bonding of surface hydroxyls with PEO was discussed in Section 6.3 above (see Figure 10.20 (6)). Those oxides which did not adsorb PEO displayed no flocculation with this polymer, while SiO_2 , MoO_3 , and V_2O_5 flocculated with PEO. In general, highly acidic oxides of the type MO_3 , M_2O_5 , and MO_2 are expected to adsorb and flocculate with poly(ethylene oxide).

Flocculant selection based on specific interactions

Flocculants can be designed on the basis of certain specific interactions, such as chemical reactions of the flocculant with surface sites or ions present on the surface. For example, poly(acrylic acid) (PAA) can react with calcium sites on surfaces. However, such an approach fails when the cations participating in the complexation reactions on the surfaces are the same or chemically similar.

Selectivity based on molecular recognition

An alternative approach to the selective creation of adsorption sites on the surface, appropriate to the polymer adsorption mechanism(s), would be to design the flocculant molecule such that its configuration is compatible with the molecular architecture of the surface.

Based on the molecular/ionic recognition mechanisms, the need to take into account the surface structure, rather than simple interactions with single sites on the

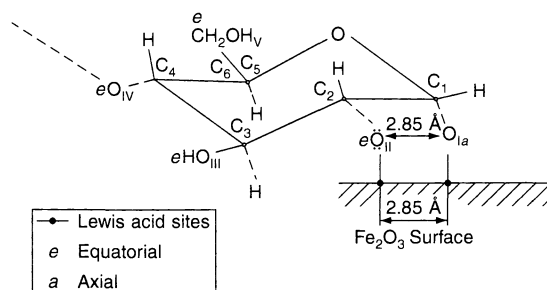


Figure 10.33. Schematic illustrating the mechanism of starch adsorption through binuclear complexation with Fe sites on the surface of haematite (after ref. (6)). (“Reprinted from *International Journal of Mineral Processing*, **58**, S. Mathur, P. Singh and B. M. Moudgil, Advances in selective flocculation technology for solid–solid separations, Page 218, Copyright (2000), with permission from Elsevier Science”)

surface, in designing novel reagents for selective separation, has been suggested (6). Polymeric reagents having two or more functional groups, with an appropriate spacing between them, to achieve structural/stereochemical compatibility with the surface are likely to exhibit enhanced structure specificity, and hence act as more selective dispersants and flocculants. Thus, the choice of selective reagents on the basis of molecular recognition (structural compatibility) mechanisms could help in enhancing selectivity in natural ore systems, particularly with respect to overcoming the adverse effects of soluble-ion activation, heteroflocculation and slime coating. For instance, the unusual selectivity of starch-based reagents for haematite and alumina has been attributed to the structural compatibility between the interacting oxygens in the starch end-groups and the Fe–Fe distance on the surface of haematite (or Al–Al in the case of alumina). Figure 10.33 (6) schematically illustrates this concept of structural compatibility.

8.2.2 Modifying surface chemistry and structure to enhance selectivity

A knowledge of the polymer adsorption mechanism(s) can be used to create sites for adsorption in systems where such sites do not exist. In such cases, the binding sites for the polymer functionality may be selectively created by altering the surface chemistry and surface molecular architecture. Some of the methods by which appropriate surface bonding sites can be created are discussed below. These include modifying the surface by changing the pH, heat treatment of the substrate and selective coating on to the particles.

Effect of pH

In the case of hydrogen-bonding polymers, such as PEO, the nature of the surface hydroxyl groups can be manipulated by pH to control the adsorption and desorption behaviour of the polymer, and hence the flocculation of the material.

Effect of heat treatment

Figure 10.34 (6) illustrates the effect of heat treatment of sol-gel-derived silica powders on the adsorption of PEO. The adsorption and flocculation of PEO on silica increases with temperature up until 700°C and then decreases (see Figure 10.34). This behaviour of

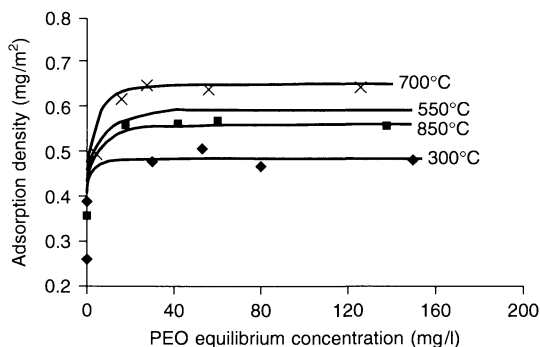


Figure 10.34. Adsorption isotherms for differently treated silica particles (at pH 5.6). The adsorption density of PEO increases with temperature up until 700°C and then decreases (after ref. (6)). (“Reprinted from *International Journal of Mineral Processing*, 58, S. Mathur, P. Singh and B. M. Moudgil, Advances in selective flocculation technology for solid-solid separations, Page 216, Copyright (2000), with permission from Elsevier Science”)

Table 10.8. Some commonly used flocculants, their functional groups and the adsorption (bonding) mechanisms involved in application

Flocculant	Type	Functional group	Adsorption mechanism
Starch	Natural	-OH	Hydrogen bonding
Gums	Natural	-OH	Hydrogen bonding
Cellulose	Natural	-OH	Hydrogen bonding
Alginates	Natural	-OH, $-\text{SO}_3^-$, $-\text{NH}_2^+$	Hydrogen bonding, electrostatic, chemical bonding
Carboxylic salts of poly(acrylic acid)	Anionic	$-\text{COO}^-$	Hydrogen bonding, electrostatic, chemical bonding, hydrophobic bonding
Poly(styrene sulfonate)	Anionic	$-\text{SO}_3^-$	Electrostatic, hydrogen Bonding, chemical bonding
Poly(vinyl phosphonate)	Anionic	$-\text{PO}_3^{2-}$	Electrostatic, hydrogen bonding
Polyethylenimine	Cationic	$-\text{NH}_2^+$	Electrostatic, coordination bonding
Poly(ethyldimethyl sulfonium chloride)	Cationic	$-\text{S}(\text{CH}_3)_2^+$	Electrostatic
Poly(vinyl alcohol)	Nonionic	-OH	Hydrogen bonding
Poly(ethylene oxide)	Nonionic	-O-	Hydrogen bonding, hydrophobic bonding
Polyacrylamide	Nonionic	$-\text{CONH}_2$	Hydrogen bonding, coordination bonding

silica upon heat treatment was correlated with the concentration of isolated silanol groups on the surface; adsorption and flocculation were found to be highest at the maximum isolated silanol concentration.

Recently, it has been shown by using NMR spectroscopic measurements (8) that heat treatment can be used to alter the acidity of the silica surface, and hence to control the adsorption of polymers (such as PEO) that bind by hydrogen bonding.

Effect of surface coating

It was observed (6) that the source of the mineral strongly influences its interaction with a given reagent. Dolomite samples obtained from Florida exhibited flocculation with PEO whereas those from Perry Mines, Georgia and New Jersey did not flocculate at all. A detailed characterization of these dolomite samples revealed that the flocculating dolomite is surface-coated with a minor amount of palygorskite clay. The latter material, due to the presence of strong Brønsted acid sites on the surface, adsorbs and flocculates with PEO. This phenomenon can thus be used to introduce selectivity in to a system, where the pure components are inert to the given polymer, by coating of the desired components.

In natural systems, the presence of even trace levels of surface-active impurities can alter significantly the surface characteristics and hence the flocculation behaviour of the constituent minerals. In order to achieve a better control of selectivity, surface characterization techniques for analysing impurities and surface contaminants are therefore essential.

A list of some commonly used flocculants is provided in Table 10.8.

8.3 Flotation of minerals

In the processing of fine particles, it is often necessary to separate certain components of the mixture from the others. For carrying out such a solid–solid separation, differences in the physical or chemical attributes between the components can often be utilized. One such property is the surface hydrophobicity, with froth flotation being the most common industrial process based on this approach. The term surface hydrophobicity refers either to the tendency of the particle not to closely associate with water or to repel it from the surface. Particles that are hydrophobic have a tendency to associate with oily or hydrocarbon-based materials. The process of froth flotation is based on the simple idea of using air bubbles to provide an escape mechanism for the hydrophobic particles from the water-based mixture of particles. Because of the free-energy driving forces associated with hydrophobic surfaces in water, the hydrophobic particles prefer to attach themselves to the air bubbles rather than remain in the water. Once the particles are attached to the bubble, they are carried up by the latter to the surface of a constantly agitated water–solids mixture (referred to as “pulp”). At the surface, a stabilized froth is formed which can then be removed (skimmed) from the surface. The component left behind in the pulp (referred to as “gangue”) is then either discarded or reprocessed.

However, in mineral systems, the difference in hydrophobicity between the components, may not be significant with most of the naturally occurring minerals having some kind of hydrophilic characteristic associated with their surfaces. In order to achieve selectivity in separation, the surface of the components therefore has to be modified to render it hydrophobic, while at the same time ensuring that the component which is not to be floated remains hydrophilic in character. In almost all flotation processes, selective development of hydrophobicity is achieved by adsorption of surfactants to render the surfaces hydrophobic. In the flotation literature, these surfactants are known as “collectors”. A list of some of such commonly used collectors is given in Table 10.9.

The success of any flotation scheme depends on several factors, such as (i) the production of appropriate particle sizes of the liberated components in the mixture of the solids to be separated, (ii) the creation of selective hydrophobicity, and (iii) the formation of a stable froth containing the desired component on the surface of the agitated mixture of the particles (pulp).

Each of these steps is very important, but the selective modification of the surfaces by surfactant

Table 10.9. Collectors used for froth flotation and their chemical structures

Collector	Formula ^a
Primary amine Salt	$\text{RNH}_3^+\text{Cl}^-$
Secondary amine Salt	$\text{RR}'\text{NH}_2^+\text{Cl}^-$
Tertiary amine Salt	$\text{R}(\text{R}')_2\text{NH}^+\text{Cl}^-$
Quaternary ammonium salt	$\text{R}(\text{R}')_3\text{N}^+\text{Cl}^-$
Sulfonium salts	$\text{RS}(\text{R}')_2^+\text{Cl}^-$
Carboxylate	RCOO^-Na^+
Sulfonate	$\text{RSO}_3^-\text{Na}^+$
Alkyl sulfate	$\text{R-O-SO}_3^-\text{Na}^+$
Hydroxamate	$\text{R-CO-NHO}^-\text{Na}^+$
<i>O</i> -Alkyl dithiocarbonates	$\text{R-O-CS}_2^-\text{Na}^+$
Dialkyl dithiocarbamate	$\text{R}_2\text{N-CS}_2^-\text{Na}^+$
Dialkyl dithiophosphates	$(\text{R-O})_2\text{-PS}_2^-\text{Na}^+$

^aR represents a hydrocarbon chain, usually ≥ 10 carbon atoms; R' is a short alkyl chain, usually a methyl group.

adsorption is the key to a successful flotation process. The procedure for selecting the optimum collector is very complex, because not only is the surface chemistry important, but also the economics of the process in terms of collector dosage. In the remainder of this section, the selection of collectors on the basis of surface chemistry will be discussed in detail.

8.3.1 Collector selection based on surface charge

In these flotation schemes, the electrostatic interaction between the collector and the mineral plays an important role. In all cases, the flotation of the mineral using the collectors is carried out under pH conditions when the mineral and the collector are oppositely charged. For example, oxide-based minerals, such as corundum (aluminium oxide), haematite (iron oxide) and goethite (iron oxide), can be floated by using cationic collectors such as primary, secondary, tertiary and quaternary amines, plus other collectors such as alkyl pyridinium salts above their isoelectric points (IEPs) (14), or they can be floated by using anionic collectors such as sodium alkyl sulfates, or sodium alkyl sulfonates below their IEPs (15). Figure 10.35 shows the zeta potential under different salt conditions, plus the flotation recovery data for goethite when using three different surfactants (8). It can be seen from this figure that the recovery is at a maximum when the collector and the mineral surfaces are oppositely charged, whereas the recovery drops to zero when the surface charges are similar in nature.

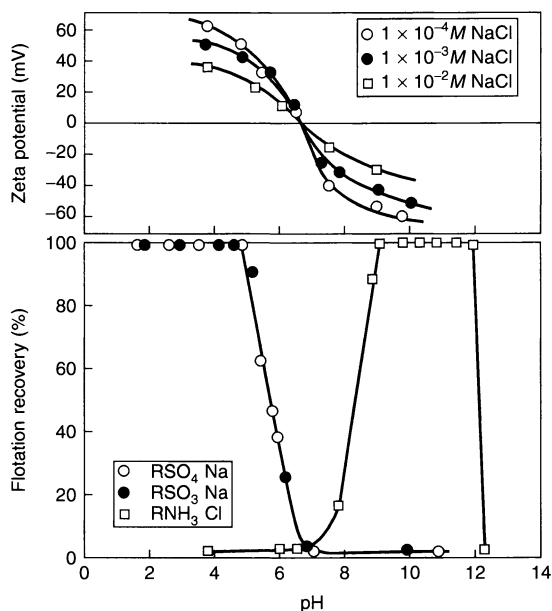


Figure 10.35. Flotation of geothite with $10^{-3}M$ solutions of dodecylammonium chloride (open squares), sodium dodecyl sulfate (open circles) and sodium dodecyl sulfonate (filled circles), illustrating the dependence of flotation recovery on surface charge (after ref. (8))

8.3.2 Collector selection based on surface reactions

Surface reactions, such as ion exchange, where surfactant anions can replace crystal lattice ions, or actual surface reactions where the surfactant forms complexes with the ions present on the surface, can lead to surfactant adsorption, and have been used in several systems to achieve flotation selectivity.

For example, as shown in Figure 10.36 (15), no adsorption of myristate (an anionic surfactant) occurs below the isoelectric point (pH 7.0) of chromite (even though the surfaces are oppositely charged), while essentially complete flotation is achieved at about pH 9.0 (when the surfactant and surface are similarly charged). The lack of flotation below the IEP was attributed to the limited solubility of myristic acid under these conditions. A similar behaviour has been observed for the flotation of haematite with myristate. Chemisorption of another anionic collector, octyl hydroxamate, has also been observed on haematite at pH 9.0 (15).

In the case of oxides, experimental evidence indicates that the following phenomena must occur in order for the adsorption to take place by surface reactions: (i) slight mineral dissolution, followed by hydrolysis

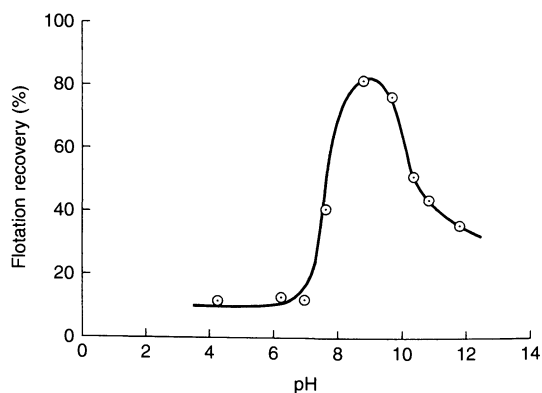


Figure 10.36. Flotation of chromite with $10^{-4}M$ myristate, as a function of pH. Note that very little flotation occurs below the IEP of chromite (pH 7.0) with a negatively charged collector, while flotation increases when similar charges exist on both surfactant and surface—an indication of chemisorption (after ref. (15))

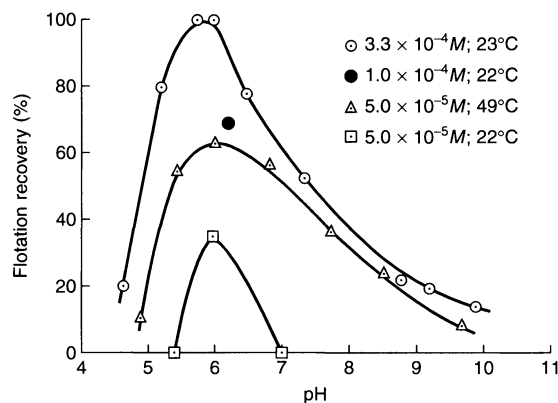


Figure 10.37. Flotation of chrysocolla as a function of pH with different concentrations of octyl hydroxamate (after ref. (15))

of the contained metal ions to hydroxy complexes, (ii) adsorption of hydroxy complexes by hydrogen bonding, and (iii) collector adsorption on these metal ion sites. For example, the flotation of chrysocolla (copper oxide) with octyl hydroxamate (Figure 10.37) takes place in the pH range in which CuOH^+ is present in significant concentration (Figure 38) (15). Optimum flotation occurs at approximately pH 6.3, which is also the pH at which the zeta potential becomes positive in the presence of Cu^{++} . The infrared analysis data for this system is presented in Figure 10.39, which shows the spectra of chrysocolla, cupric octyl hydroxamate and chrysocolla after being treated with

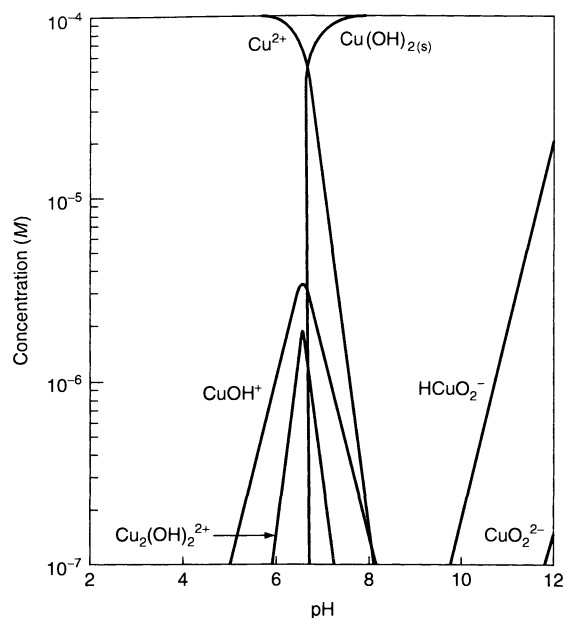


Figure 10.38. Species diagram for $10^{-4}M\text{Cu}^{2+}$ as a function of pH (after ref. (15))

0.001M octyl hydroxamate. Cupric octyl hydroxamate has major bands at 925, 1095, 1380, 1450, and 1535 cm^{-1} , while bands at 1380, 1450 and 1535 cm^{-1} are observed on chrysocolla after it has been treated with the collector, hence indicating the formation of cupric octyl hydroxamate at the surface during the adsorption process. This surface reaction is evident from the fact that chrysocolla changes colour from its natural blue-green to a vivid green colour upon adsorption of the collector.

The chemisorption of fatty acids, such as oleic, or their soaps, on salt-type minerals, such as calcite, or apatite, is another example of the use of chemical interactions to achieve selectivity. In salt-type minerals, this becomes significant, since the minerals to be separated have similar physico-chemical properties. The separation process is further complicated due to the presence of several ions in the solution, owing to the fact that the minerals are "semi-soluble". Chemisorption in these systems is thought to occur by an ion-exchange process in which the oleate anions replace an equivalent amount of the crystal lattice ions, such as F^- , CO_3^{2-} and SO_4^{2-} , to build a surface layer of the alkaline earth oleate (16).

Oleate has been observed to adsorb on calcite and apatite, electrostatically below their points of zero charge, and chemically above these points.

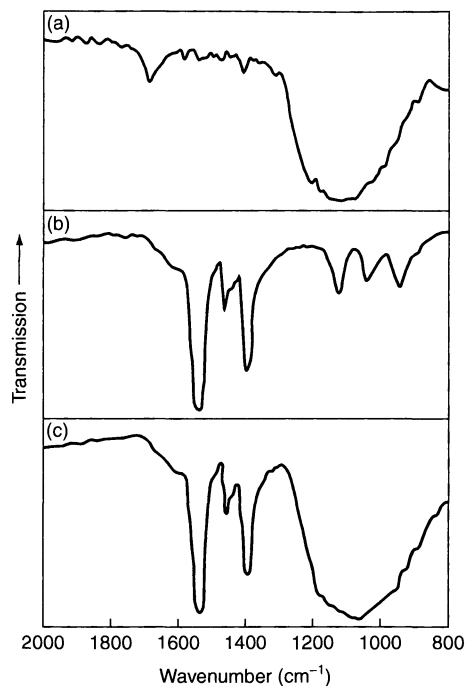


Figure 10.39. Infrared spectra of (a) chrysocolla, (b) cupric octyl hydroxamate, and (c) adsorbed hydroxamate on chrysocolla (at pH 6.0) (after ref. (15))

Figure 10.40 (16) illustrates the adsorption of different amounts oleate on to calcite at a natural pH of 9.6, plus the corresponding zeta potential data as a function of pH. Adsorption at pH 9.6, when the surfactant and surface are similarly charged, takes place due to the interaction of the surfactant with the calcium species on the surface. The sharp increase in the adsorption above $3 \times 10^{-5}\text{ mol/l}$ was attributed to possible precipitation of calcium oleate, since, with calcium present at a concentration of $\sim 1.5 \times 10^{-4}\text{ mol/l}$, the solubility limit is exceeded for calcium oleate above $\sim 5 \times 10^{-5}\text{ mol/l}$ of oleate. Corresponding measurements at constant ionic strength reveal little change in the zeta potential below concentrations of $\sim 10^{-6}\text{ mol/l}$ of oleate. Adsorption on calcite at these concentration levels and at pH values below the IEP (pH 8.2) can therefore be considered due to electrostatic attraction between the negative oleate ions and the positive surface sites.

Above its IEP, the zeta potential of calcite is seen to change continuously with oleate concentration. Simple electrostatic adsorption under constant ionic strength will not lead to the observed changes in the zeta potential, thus implying that there is some specific kind of interaction taking place. It was found that the calcium

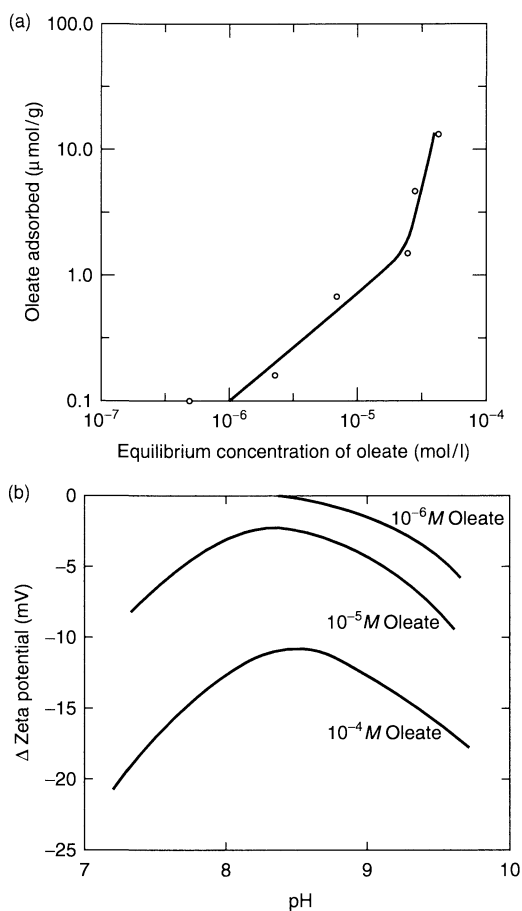


Figure 10.40. Adsorption (a) and zeta potential (b) behaviour for the calcite–oleate system (after ref. (16))

concentration in solution at pH 12.1 is significantly increased by the presence of oleate. This suggests chemical bonding of calcium and/or its complexes with the oleate in the solution, and even precipitation of calcium oleate. Similar chemical interactions with the surface calcium species, leading to the adsorption of oleate on to calcite have also been demonstrated by using infrared spectroscopy (16).

The multilayer adsorption of fatty acids on minerals has been shown to occur by the direct adsorption of precipitated metallic salts of the collectors. In fact, it has been shown, on the basis of solubility product data for a number of cationic soaps of fatty acid collectors, that the precipitation of such salts is indeed required for the incipient flotation.

9 REFERENCES

- Hunter, R. J., *Foundations of Colloid Science*, Vol. I, Oxford Science Publications, Oxford, UK, 1986.
- Adamson, A. W., *Physical Chemistry of Surfaces*, 4th Edn., Wiley-Interscience, New York, 1982.
- Amankonah, J. O. and Somasundaran, P., Effects of dissolved mineral species on the electrokinetic behavior of calcite and apatite, *Colloids Surf.*, **15**, 335–353 (1985).
- Derjaguin, B. V., *Surface Forces* (English translation from the Russian by Kisin, V. I.; Translation Ed. Kitchner, J. A.), Consultants Bureau (Plenum Publishing), New York, 1987.
- Fleer, G., Cohen Stuart, M., Cosgrove, T. and Vincent, B., *Polymers at Interfaces*, Chapman & Hall, London, 1993.
- Mathur, M., Singh, P. K. and Moudgil, B. M., Advances in selective flocculation technology for solid–solid separations, *Int. J. Min. Process.*, **58**, 201–222 (2000).
- Bjelopavlic, M., Singh, P. K., El-Shall, H. and Moudgil, B. M., Role of surface molecular architecture and energetics of hydrogen bonding sites in selective adsorption of polymers and surfactants, *J. Colloid Interface Sci.*, **226**, 159–165 (2000).
- Moudgil, B. M., Soto, H. and Somasundaran, P., Adsorption of surfactants on minerals, in *Reagents in Mineral Technology*, Somasundaran, P. and Moudgil, B. M. (Eds), Surfactant Science Series, Vol. 27, Marcel Dekker, New York, 1988, pp. 79–104.
- Rosen, M. J., *Surfactants and Interfacial Phenomena*, Wiley, New York, 1989.
- Adler, J. J., Singh, P. K., Patist, A., Rabinovich, Y. I., Shah, D. O. and Moudgil, B. M., Correlation of particulate dispersion stability with the strength of self-assembled surfactant films, *Langmuir*, **16**, 7255–7262 (2000).
- Singh, P. K., Adler, J. J., Rabinovich, Y. I. and Moudgil, B. M., Investigation of self-assembled surfactant structures at the solid–liquid interface using FT-IR/ATR, *Langmuir*, **17**, 468–473 (2001).
- Reed, J. S., *Principles of Ceramic Processing*, Wiley, New York, 1988.
- Yotsumoto, H. and Yoon, R. H., Application of extended DLVO theory, II. Stability of silica suspensions, *J. Colloid Interface Sci.*, **157**, 434–441 (1993).
- Smith, R. W. and Akhtar, S., Cationic flotation of oxides and silicates, in *Flotation*, Vol. 1 (A. M. Gaudin Memorial Volume), Fuerstenau, M. C. (Ed.), AIME, New York, 1976, pp. 87–116.
- Fuerstenau, M. C. and Palmer, B. R., Anionic flotation of oxides and silicates, in *Flotation*, Vol. 1 (A. M. Gaudin Memorial Volume), Fuerstenau, M. C. (Ed.), AIME, New York, 1976, pp. 148–196.
- Hanna, H. S. and Somasundaran, P., Flotation of salt type minerals, in *Flotation*, Vol. 1 (A. M. Gaudin Memorial Volume) Fuerstenau, M. C. (Ed.), AIME, New York, 1976, pp. 197–272.

CHAPTER 11

Surface Chemistry in the Petroleum Industry

James R. Kanicky, Juan-Carlos Lopez-Montilla, Samir Pandey and Dinesh O. Shah

Center for Surface Science and Engineering, Departments of Chemical Engineering and Anesthesiology, University of Florida, Gainesville, Florida, USA

1	Introduction	251	3.1	Drilling mud	259
2	Fundamentals	252	3.2	Enhanced oil recovery	259
2.1	Adsorbed films	252	3.2.1	Surfactant-polymer flooding	259
2.2	Self-assembly of surfactant molecules	252	3.2.2	Foams in enhanced oil recovery	262
2.3	Contact angle and wetting	254	3.2.3	Acid fracturing for oil well stimulation	263
2.4	Foams	254	3.3	Antifoaming and defoaming	263
2.5	Emulsions	256	3.4	Corrosion inhibition	263
2.5.1	Hydrophilic-lipophilic balance (HLB)	257	3.5	Oil spill clean-up	264
2.5.2	Winsor's R ratio	258	3.6	Fluidization of bitumen	265
2.5.3	Phase-inversion temperature	258	3.7	Asphaltic emulsions	265
2.5.4	Surfactant affinity difference	258	3.8	Oil/water separation and crude oil dehydration	265
2.5.5	Microemulsions	258	4	Summary	266
3	Applications	259	5	References	266

1 INTRODUCTION

It is well recognized that the energy consumption per capita and the standard of living of a society are interrelated. Among various sources of energy, fossil fuels or crude oils play an important role in providing the energy supply of the world. Crude oil is the most readily exploitable source of energy available to humankind, and is also a source of raw materials for feed stocks in many of the chemical industries on which our present civilization relies. The field of surface chemistry is intricately connected to most

(if not all) processes of petroleum technology – from the drilling of crude oil to petroleum refining and petrochemical processing – as well as to allied and dependent applications and industries. All of these processes involve interfacial phenomena and surface chemical interactions.

In the context of petroleum technology, surface chemistry deals with the surface properties of crude oil/air, crude oil/brine (or water) and crude oil/solid surfaces. Thus, surface tension, interfacial tension (IFT), contact angle, wetting and surface charge (zeta potential) are the parameters that one measures for surface

chemical studies. The next section deals with the fundamental aspects of surface chemistry and how they relate to the petroleum industry. Following this discussion, we will describe several major areas in the petroleum industry – enhanced oil recovery, corrosion inhibition, oil spill clean-up, fluidization of bitumen, asphaltic emulsions, oil/water separation and crude oil dehydration – where knowledge of surface chemistry plays a vital role.

2 FUNDAMENTALS

A surfactant molecule has two functional groups, namely a hydrophilic (water-soluble) or polar group and a hydrophobic (oil-soluble) or non-polar group. The hydrophobic group is usually a long hydrocarbon chain (C₈–C₁₈), which may or may not be branched, while the hydrophilic group is formed by moieties such as carboxylates, sulfates, sulfonates (anionic), alcohols, polyoxyethylenated chains (nonionic) and quaternary ammonium salts (cationic) (1). Crude oil contains organic acids and salts, alcohols and other natural surface-active agents. When crude oil is brought in contact with brine or water, these natural surfactants accumulate at the interface and form an adsorbed film which lowers the interfacial tension of the crude oil/water interface.

Depending on the type of crude oil, the adsorbed film at the interface can be either fluid or very viscoelastic and able to form a skin. Depending on the properties of the crude oil (e.g. API gravity (2), sulfur, salt and metals content, viscosity, pour point, etc.), the structure of the film can vary significantly. Therefore, the molecular packing, surface viscosity, surface elasticity and surface charge of the adsorbed film are very important parameters that determine various phenomena such as coalescence of emulsion droplets, as well as oil drop migration in porous media.

2.1 Adsorbed films

Adsorption is an entropically driven process by which molecules diffuse preferentially from a bulk phase to an interface. Due to the affinity that a surfactant molecule encounters towards both polar and non-polar phases, thermodynamic stability (i.e. a minimum in free energy or maximum in entropy of the system) occurs when these surfactants are adsorbed at a polar/non-polar (e.g. oil/water or air/water) interface. The difference between solute concentration in the bulk and that at the interface is the *surface excess* concentration. The latter

is related to surface and interfacial tension by the *Gibbs Adsorption Equation* (3–5), which in its practical form, is as follows:

$$\Gamma = -\frac{1}{RT} \frac{d\gamma}{d \ln C} \quad (11.1)$$

where Γ is the surface excess per unit area (moles/cm²) of surfactant measured, R the universal gas constant, T the temperature (in kelvin), γ the surface tension (often replaced by σ for interfacial tension), and C the bulk concentration of surface-active species. Once the surface excess Γ is known, the area per molecule of adsorbed surfactant can be calculated by using the following equation:

$$\text{Area per molecule}(\text{\AA}^2) = \frac{10^{16}}{N_A \Gamma} \quad (11.2)$$

with units of area/molecule in $\text{\AA}^2/\text{molecule}$, and where N_A is the Avogadro constant (6.023×10^{23} molecules per mole).

The Gibbs adsorption equation allows for calculation of area per molecule from very simple measurements of surface (or interfacial) tension versus surfactant concentration in the solution. This calculation, in turn, enables one to study the relative area/molecule of a surfactant. Tighter molecular packing in the adsorbed film lowers the interfacial tension.

In addition, for very surface-active molecules, a slight increase in bulk phase concentration produces a dramatic reduction in the interfacial tension.

With the use of specific surfactants, and with appropriate physico-chemical conditions, the interfacial tension of a crude oil/water interface can drop as low as 10^{-4} mN/m (6). As will be discussed below, such ultra-low interfacial tensions are very important in technologies such as enhanced oil recovery processes for recovering crude oil from depleted oil wells.

The presence of surfactant molecules at an interface leads to a dramatic change in many surface properties, including surface and interfacial tensions (as discussed above), contact angle, wettability, surface charge and surface rheology (i.e. surface viscosity). Surfactants can also act as a barrier when they adsorb at an interface, thus influencing mass and heat transfer between the adjacent phases as well as dispersion stability (1).

2.2 Self-assembly of surfactant molecules

The adsorption of surface-active molecules from a bulk phase to a surface or interface is governed by an equilibrium rate constant, and the adsorption occurs at any

concentration. If the concentration of a soluble surfactant in water is increased gradually, the surface concentration also increases and reaches a maximum level at a specific bulk concentration. Beyond this concentration, individual surfactant monomers begin to aggregate with their hydrophilic heads pointing outwards towards the solution and the hydrophobic tails pointing inwards away from the water in order to minimize the free energy (i.e. maximize the entropy) of the system. The concentration at which this aggregation occurs is called the critical micelle concentration (CMC), and the aggregates are called micelles. In general, micelles are spherical aggregates of surfactant molecules about 4–10 nm in diameter that are in equilibrium with single surfactant monomers in the bulk aqueous solution (Figure 11.1). The critical micelle concentration depends upon the structure of surfactant molecules, as well as physico-chemical conditions such as temperature, pH and the ionic composition of the solution.

As total surfactant concentration is further increased, other cylindrical, hexagonal-packed and lamellar

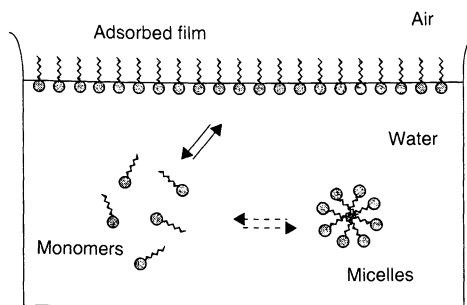


Figure 11.1. Schematic representation of the three environments (monomer, micelle and adsorbed film) in which surfactant molecules reside in water above the CMC

structures may form, depending on the surfactant structure and physico-chemical conditions (Figure 11.2). If the bulk phase is non-aqueous, reverse micelles may form with polar heads pointing inwards into a water core and hydrophobic tails pointing outwards into the oil.

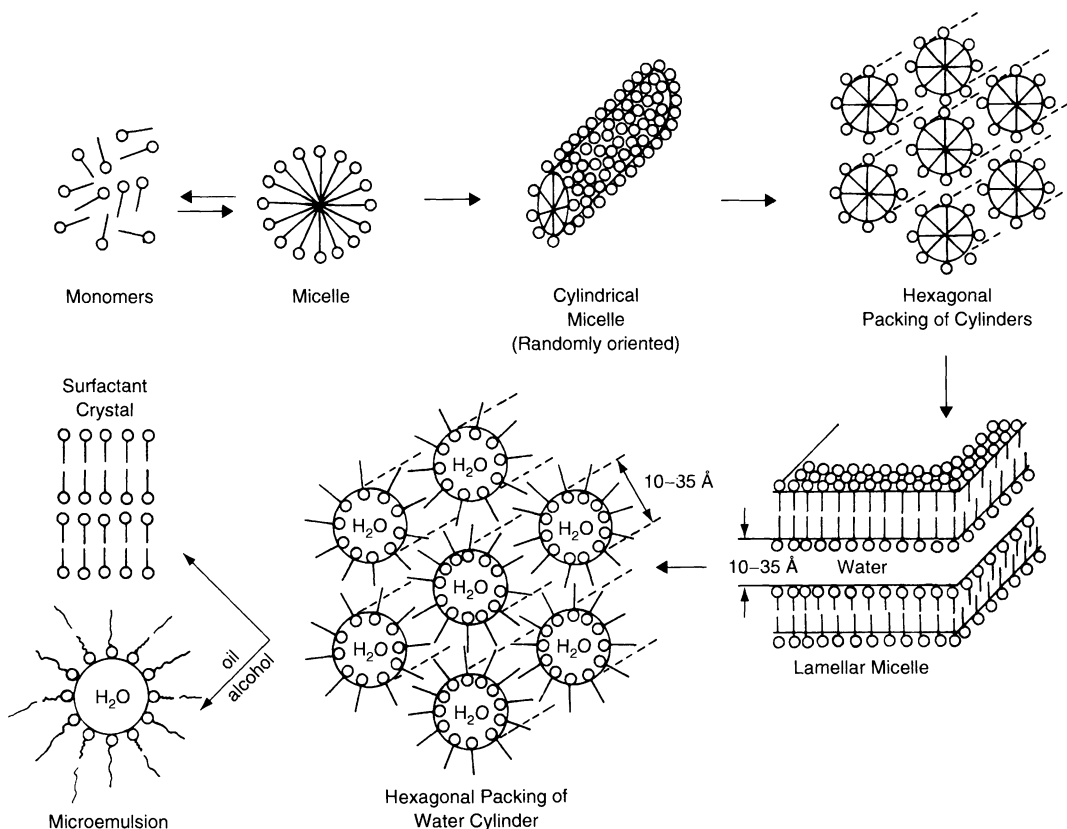


Figure 11.2. Possible structures formed in a surfactant solution

When an oil phase is present in contact with the aqueous phase, the water/oil partition coefficient of the surfactant, degree of surface activity and molecular structure determine whether an oil-in-water (o/w) emulsion, water-in-oil (w/o) emulsion, or liquid crystalline structure is formed (1).

Surfactant aggregates are dynamic systems. Thermal energy and coulombic forces keep surfactant monomers and aggregates in motion, and influence the rates of formation and break-up of these structures. Micellar systems, for example, exhibit two characteristic "relaxation" times, known as τ_1 and τ_2 , corresponding to the rate at which single monomers enter and exit a micellar aggregate, and to the rate of formation and break-up of an entire micelle, respectively. The kinetics of micellization has been shown to strongly affect such interfacial phenomena as wetting time, foamability, emulsion droplet size, oil solubilization rate and detergency (7).

2.3 Contact angle and wetting

The wetting of a surface by a liquid and the ultimate extent of spreading of that liquid are very important aspects of practical surface chemistry. Porous media in a petroleum reservoir can be water-wet or oil-wet, depending on the chemical composition of the solids and the crude oil. The extent to which crude oil wets the porous media is directly related to the work required to bring this oil to the surface, as will be seen later. Wetting of a solid surface by a liquid is determined by the contact angle (measured through the liquid) that this liquid makes with the surface (Figure 11.3). Usually, complete wetting means that the contact angle between a liquid and a solid is zero, or so close to zero that the liquid spreads on the solid spontaneously. Non-wetting occurs when the angle is greater than 90° , so that the liquid beads up like water on a waxy surface (8).

Young's equation, as follows:

$$\cos \theta = \frac{\gamma_{SV} - \gamma_{SL}}{\gamma_{LV}} \quad (11.3)$$

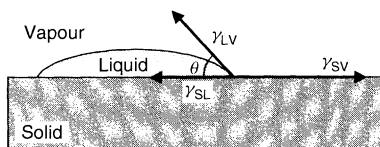


Figure 11.3. Force balance among the three surface tensions (Young's equation) acting at each point in the contact line; θ is the contact angle of the liquid with the solid surface

describes the relationship between contact angle (θ) and the solid–vapour (γ_{SV}), solid–liquid (γ_{SL}) and liquid–vapour (γ_{LV}) interfacial tensions. This equation is usually helpful and sufficient for describing wetting equilibria in most circumstances. However, sometimes it is useful to determine thermodynamically whether wetting will occur. For a spontaneous process (such as spreading) to occur, the free energy of the process must be negative (8). In terms of surface tensions, we define the *spreading coefficient*, $S_{L/S}$, where:

$$S_{L/S} = \gamma_{SV} - \gamma_{LV} - \gamma_{SL} \quad (11.4)$$

Spontaneous spreading occurs when $S_{L/S} > 0$. Thus, to encourage wetting, γ_{LV} and γ_{SL} should be made as small as possible. This is achieved by adding a surfactant to the liquid phase to decrease the solid/liquid and liquid/vapour interfacial tensions.

Contact angle and wetting are closely related to the interaction of crude oil with the rock surface and solid particles in the reservoir porous media. The silica in sand, for example, is preferentially water-wet so that oil will not wet its surface. Silica is negatively charged, and the negative charges found in the adsorbed film around crude oil droplets leads to repulsion and a beading effect between the water-wet solid and oil. On the other hand, limestone, having a net positive charge, will preferentially bind to the negatively charged surfactants from crude oil such as organic acids. Hence, the surfactant tail will be facing outward and the oil can spread on the limestone. Both excessive beading (non-wetting) and complete wetting of porous media by a crude oil make it very difficult to coalesce oil droplets and move oil ganglia through porous media to the surface.

Figure 11.4 shows how the wettability of a water-wet solid surface in contact with an oil droplet can change when surfactant molecules adsorb on to it. As is shown, if the solid surface has some negative sites where cationic surfactants can be adsorbed, the hydrophobic tails of these molecules will point towards the oil, thus making the solid surface more wettable by the oil droplet.

2.4 Foams

For a liquid to produce a foam, it must be able to (i) expand its surface area so as to form a thin film around gas bubbles, (ii) possess the correct rheological and surface properties to retard thinning of the lamellae leading to bubble coalescence or collapse, and

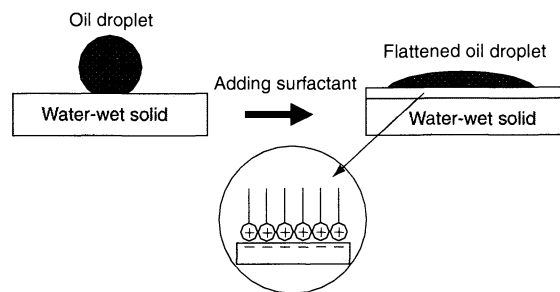


Figure 11.4. The wettability of a water-wet solid surface in contact with an oil droplet increases when surfactant molecules adsorb on to the surface

(iii) retard the diffusion of trapped gas from small to large bubbles or to the surrounding atmosphere. Foaming does not occur in pure liquids because such a system cannot meet the above three criteria. When surface-active molecules or polymers are present in the liquid, however, rheological effects and adsorption of molecules aid in stabilizing the interface, thus impeding the diffusion of gas through the lamellae, and resulting in a more mechanically stable system (Figure 11.5) (9).

As previously discussed, the Gibbs adsorption equation demonstrates how an increase in the amount of surface-active material will result in a decrease in the surface tension of a liquid. Because the Gibbs adsorption equation was derived on a thermodynamic basis, the surface tension is an equilibrium value that does not take into account the time necessary for molecules to diffuse and adsorb to an interface. The instantaneous, or dynamic surface tension of a newly created interface is always higher than the equilibrium surface tension value(s). In the laboratory, the dynamic surface tension of an adsorbed film can be obtained by

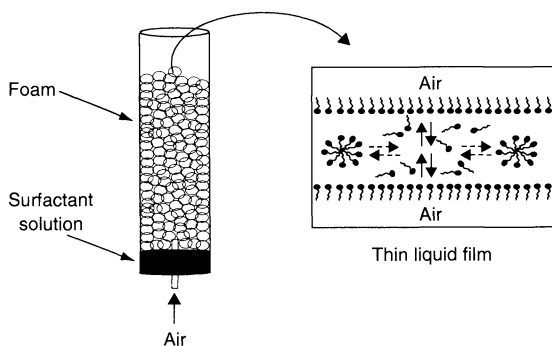


Figure 11.5. Schematic representation of the adsorption of surfactant on the newly created air/water interface during foam generation

measuring the maximum pressure realized within a soap bubble as a function of the bubble lifetime (Figure 11.6). If the interface (i.e. bubble) formation time is long, surfactants have time to flow from the bulk solution to the interface. Given enough time, the dynamic surface tension approaches an equilibrium value. However, if the interface is created very quickly (by a very small bubble lifetime), surfactants do not have the opportunity to diffuse from the bulk to the interface and hence higher values of the dynamic surface tension are observed.

The effect on surface tension by surfactant adsorption from the bulk solution (Gibbs effect) and by diffusion along an interface (Marangoni effect) is often referred to as the combined Gibbs–Marangoni effect (Figure 11.7).

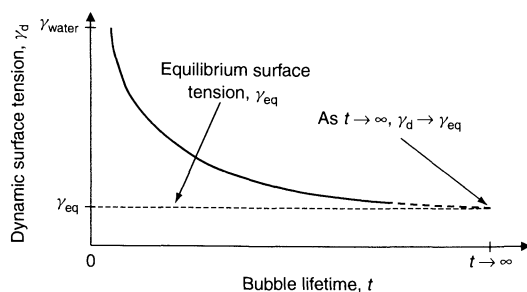


Figure 11.6. Dynamic surface tension of a newly created interface as a function of bubble lifetime

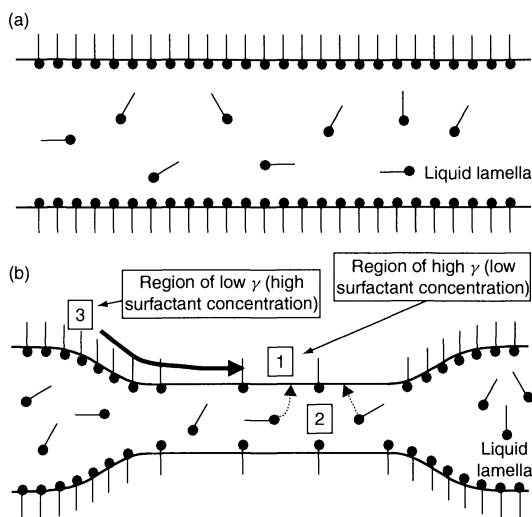


Figure 11.7. Schematic representation of the Gibbs–Marangoni effects. (a) Unstretched film. (b) Stretched film. Film stretching causes localized areas of high surface tension, γ [1]. Surfactant molecules flow from the bulk phase [2] to the surface (Gibbs effect) and along the interface [3] (Marangoni effect) to “heal” the stretched film [1]

As a foam lamella is stretched (e.g. by gravity, agitation, thermal fluctuation or drainage), it becomes thinner and a new surface is generated having a lower transient surfactant concentration at the surface, and consequently a higher surface tension, than its neighbouring surface. The surface tension gradient that is generated results in the flow of surfactant (and associated boundary layer water) from areas of low γ to those of high γ , thereby opposing film thinning. Likewise, the diffusion of surfactant molecules with associated water also occurs from the bulk in the direction of the newly created surface. These mechanisms can be thought of as producing a “healing” effect at the site of thinning. While the Gibbs and Marangoni effects are complementary, each of them are generally important in different surfactant concentration regimes. However, both mechanisms rely on the presence of a surface tension gradient and are ineffective at very low and very high surfactant concentrations. At very low surfactant concentrations, not enough surfactant monomers exist in the bulk or interface to diffuse to the thinning film. At very high concentrations, so many monomers are present in the system that an adequate concentration gradient is not established between the thinning film and the bulk and neighbouring surfaces.

Other factors can also affect the stability of foam; among these are temperature, surfactant structure, surface viscosity, rate of drainage and bulk viscosity.

2.5 Emulsions

Working with emulsion systems is nothing new to people in the petroleum industry. Historically and economically, the most important problems in the oil industry have been in the area of breaking up o/w emulsions formed within reservoirs. However, the breaking and formation of emulsions plays a very important role in other technological applications in the oil industries. Because of their wide-ranging practical importance, it is necessary to discuss the fundamental aspects and methods of characterization of emulsions.

An emulsion (sometimes referred to as a macroemulsion in order to distinguish it from a microemulsion) is defined as a thermodynamically *unstable* mixture of two immiscible liquids, one existing as a dispersed phase and the other as a continuous phase. Note that emulsions are formed from surfactant, oil, and water at concentrations found in the two-phase and three-phase regions of the surfactant/oil/water phase diagram (Figure 11.8). However, emulsions are not thermodynamically stable and thus are not labelled on the phase diagram. The

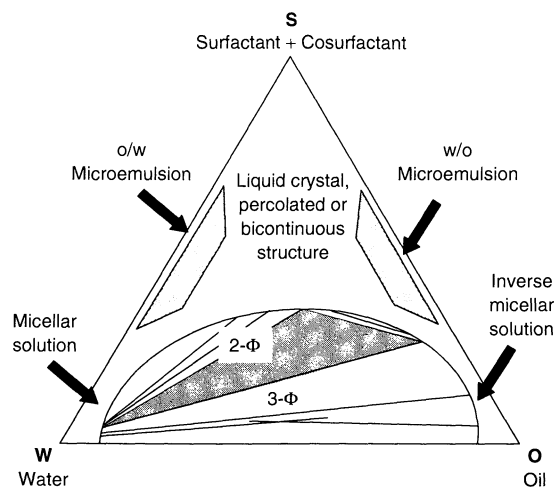


Figure 11.8. Typical phase diagram for the Oil (O)/Water(W)/Surfactant + Cosurfactant (S) system. Emulsions are formed from surfactant, oil and water at concentrations found in the two-phase (2- Φ) and three-phase (3- Φ) regions of the diagram

common types of emulsions relevant to the petroleum industry are oil-in-water (o/w) and water-in-oil (w/o) emulsions, although water-in-oil-in-water (w/o/w) and oil-in-water-in-oil (o/w/o) multiple emulsions are sometimes encountered. The thermodynamic instability of an emulsion system dictates that the suspension will separate over time into water and oil. This phase separation is dependent, among other factors, upon the rate of emulsion droplet coalescence. The level of emulsion stability required in a process is dependent upon application of the emulsion system. For example, microemulsions formed with brine and crude oil within a reservoir aid in mobilizing the oil trapped in the porous medium and in pumping the oil to the surface. However, it is preferred that once the emulsion has been brought to the surface, it quickly and easily (i.e. inexpensively) breaks up into its individual oil and water phases. On the other hand, sometimes it is required that emulsions be stable for a long time, such as in the case of Orimulsion[®], a low-viscosity (150–350 CP) o/w emulsion made from heavy crude oil (10).

Common emulsion properties such as droplet size distribution, emulsion type, stability, and rheological properties depend on many factors, including the following:

- chemical composition (molecular structure and concentration) of oil
- chemical composition (types and concentrations of salts present) of water

- chemical composition (nonionic, anionic, cationic, zwitterionic and polymeric) and concentration of surfactants
- structure and concentration of cosurfactants (e.g. short-chain alcohols)
- number and types of finely divided particles present
- temperature and pressure of the system
- order of mixing of emulsion constituents
- energy input.

It is clearly evident that emulsions are very complicated systems. Progress has been made on theoretical studies attempting to clarify the complexities of these systems. However, the majority of predictions of the type and stability of emulsions derives more from empirical observation than from theory. Emulsion formulation is still considered to be an art rather than a scientific method in many circles of industry (11).

2.5.1 Hydrophilic–lipophilic balance (HLB)

A very useful numerical rating scheme, known as the *hydrophilic–lipophilic balance* (HLB) number, was introduced by Griffin (12). In this empirical method, surfactants are assigned a number based on their solubility behaviour in water (Table 11.1). This method correlates well with Bancroft's rule, which states that the external (continuous) phase of an emulsion will be that in which the emulsifying agent (surfactant) is the most soluble (13). Each surfactant is then rated according to this scale. Surfactant mixtures are assigned an HLB number on a weight-prorated basis. Molecular functional groups (e.g. $-\text{OH}$, $-\text{COONa}$, $-\text{CH}_2-$, etc.) have also been assigned HLB numbers (14). The empirical HLB number is calculated by adding 7 to the algebraic sum of the functional group numbers given in Table 11.2. For example, the calculated HLB number for sodium laurate

Table 11.1. The hydrophilic–lipophilic balance (HLB) scale

Surfactant solubility/ Behaviour in water	HLB number	Application
No dispersibility in water	{ 0 2	–
Poor dispersibility	{ 4 6	W/O emulsifier
Milky dispersion, unstable	{ 8	
Milky dispersion, stable	{ 10	Wetting agent
Translucent-to-clear solution	{ 12	
Clear solution	{ 14	Detergent
	{ 16	
	{ 18	
		Solubilizer

Table 11.2. Group HLB numbers^a

Hydrophilic group	HLB	Lipophilic group	HLB
$-\text{SO}_4\text{Na}$	38.7	$-\text{CH}-$	-0.475
$-\text{COOK}$	21.1	$-\text{CH}_2-$	
$-\text{COONa}$	19.1	$-\text{CH}_3-$	
Sulfonate	~ 11.0	$-\text{CH}=\text{}$	
$-\text{N}$ (tertiary amine)	9.4	$-(\text{CH}_2-\text{CH}_2-\text{CH}_2-\text{O}-)$	-0.15
Ester (sorbitan ring)	6.8		
Ester (free)	2.4		
$-\text{COOH}$	2.1		
$-\text{OH}$ (free)	1.9		
$-\text{O}-$	1.3		
$-\text{OH}$ (sorbitan ring)	0.5		

^aTo calculate the HLB number for a given surfactant, add 7 to the algebraic sum of the group numbers.

(C₁₁H₂₃COONa) would be:

$$7 + 11(-0.475) + 19.1 = 20.9$$

The HLB empirical approach is still very popular because of its extreme simplicity, but it does not take into account the effects of the kind and concentration of electrolyte, temperature and other factors.

2.5.2 Winsor's *R* ratio

The introduction by Winsor (15) of the theoretical concept that an emulsion formulation could be represented by a single parameter relating the "ratio of the interaction energies" between adsorbed surfactant molecules and the oil and water in the system was the next step in understanding emulsion formulation. It was shown that the state and properties of a system at equilibrium were directly related to a particular combination of the interactions between surfactant, water and oil. This combination of interactions was expressed as the ratio *R*. A ratio *R* < 1 means that the interactions between surfactant and oil are stronger than those between surfactant and water. In this case, the surfactant/oil/water systems have a tendency to form w/o emulsions. When *R* = 1, the surfactant–oil and surfactant–water interactions are balanced. Such a system forms a thermodynamically stable bicontinuous microemulsion. Finally, *R* > 1 means that the interactions between the surfactant and water molecules are stronger than the interactions between the surfactant and oil molecules, which thus leads to o/w emulsions.

A major drawback to this method, however, is that Winsor's so-called *R* ratio could not be numerically calculated as in the HLB method, which made it difficult to use for practical emulsion formulations.

2.5.3 Phase-inversion temperature

The *phase-inversion temperature* (PIT) is the temperature at which the continuous and dispersed phases of an emulsion system are inverted (e.g. an o/w emulsion becomes a w/o emulsion, and vice versa). This phenomenon, introduced by Shinoda (16), occurs for emulsion systems containing nonionic surfactants, and can be a valuable tool for predicting the emulsion behaviour of such systems. The phase inversion occurs when the temperature is raised to a point where the interaction between water and the nonionic surfactant molecules decreases and the surfactant partitioning in water decreases. Hence, surfactant molecules

begin to partition in the oil phase beyond this temperature. The PIT phenomenon does not occur with ionic surfactants, where a normal temperature–solubility relationship exists (i.e. solubility increases with increased temperature), so its use is limited. However, emulsion formulations are quite often stabilized by a mixture of both ionic and nonionic surfactants, where the PIT may still be important.

2.5.4 Surfactant affinity difference

Enhanced oil recovery research in the 1970s led to the development of empirical correlations that numerically describe the conditions for attaining ultra-low interfacial tension and maximum oil mobilization. The correlation, the *surfactant affinity difference* (SAD), is a measure of the difference between the standard chemical potentials or the Gibbs free energy of surfactant in the oil and water phase, as follows:

$$\text{SAD} = \mu_w^* - \mu_o^* = \Delta G_{\text{oil} \rightarrow \text{water}} = -RT \ln K_p \quad (11.5)$$

where *K_p* is the partition coefficient of the surfactant between water and oil at the corresponding temperature, a value that can be measured. At a SAD = 0, the surfactant affinity for the water phase exactly equals its affinity for the oil phase, thus resulting in the optimum formulation (i.e. an ultra-low interfacial tension). The sign of the SAD indicates the dominant affinity of the surfactant, whereas the value denotes the magnitude of deviation from an optimum formulation. A SAD < 0 means that surfactant–oil interactions dominate, while a SAD > 0 indicates that surfactant–water interactions prevail.

2.5.5 Microemulsions

Under certain conditions, the oil or water droplets in emulsions can be made small enough (< 100 nm) that the emulsions appear transparent. Such dispersions are called microemulsions. Three types of microemulsions can be formed, namely oil-in-water, water-in-oil, and middle-phase microemulsions. The latter microemulsions occur when the Winsor's ratio *R* = 1, and when the SAD = 0. All microemulsions are thermodynamically stable, which implies that they form spontaneously at certain concentrations of oil, water and surfactant, and the formation is limited only by the diffusion of the molecules. It has been reported (17) that the change in free energy of dispersions shows a minimum at an equilibrium droplet size in the range of 100–1000 Å for

microemulsion systems. Microemulsions require a relatively large amount of surfactant in order to stabilize the large interfacial area created by the nano-droplets. They also often require the addition of cosurfactants such as short-chain alcohols to attain an appropriate interfacial fluidity or surface viscosity of the oil/water interface.

3 APPLICATIONS

3.1 Drilling mud

The drilling mud used in prospecting for petroleum is a complex system made from a variety of materials used to perform several functions in the drilling process: water, with its high heat capacity, removes the heat generated by friction between the rocky material and the drilling tip, oil lubricates the drilling tip, clay provides the appropriate rheology, and salts of heavy metals increase the density of the mud, so that the particles of rock (debris) can rise with the mud up to the ground level, where they are separated. Dispersant and emulsifying surfactants are used to stabilize this complex mixture. It is important to mention that drilling mud is formulated for each region, because of the variation in geology and physico chemical conditions from one place to another (18).

3.2 Enhanced oil recovery

One of the most attractive energy sources today is the petroleum remaining in a depleted oil well, where it is trapped in the reservoir's porous media by capillary and viscous forces. To recover this trapped oil, several technologies based on enhanced oil recovery (EOR) processes have been developed. Examples of these technologies (also referred to as "tertiary oil recovery") are surfactant-polymer flooding, foaming and acid fracturing (6, 19-22). However, the presence of many interfaces and the complexity of the physico-chemical and geological characteristics of the reservoirs make enhanced oil recovery an immense scientific and technological challenge. A detailed knowledge of the petroleum reservoir, transport through porous media, and various interfacial phenomena are required. Furthermore, enhanced oil recovery technologies are usually very expensive because enormous quantities of costly chemicals are injected into an oil well and are completely lost during the process.

In spite of the above-mentioned difficulties, enhanced oil recovery technologies are appealing since indeed the

depleted oil wells still contain approximately 65% of the original oil in place.

3.2.1 Surfactant-polymer flooding

This present section will deal in a general way with all of those technologies referred to as "surfactant-polymer flooding" or "chemical flooding". Basically, the purpose of surfactant-polymer flooding is to produce oil from an exhausted petroleum well by injecting into the reservoir a slug of surface-active agents capable of mobilizing the residual oil (Figure 11.9) (6, 19-22). Figure 11.10 shows schematically the surfactant-polymer flooding process. The first step is to inject a solution (preflush) to condition the reservoir by eliminating undesirable salts that would otherwise bind to the valuable surfactants and render them ineffective (20, 23-26). Next, a surfactant solution is injected to decrease the interfacial tension of the oil ganglia (6, 19-22, 27), and to mobilize the ganglia through narrow necks of the pores (6, 21), thus forming an oil bank (as shown in Figure 11.11). The formation of an oil bank is indispensable, since it will allow the efficient mobilization of the trapped crude oil. The surfactant slug is driven by a slug of thickened aqueous polymer solution that is in turn driven by a water slug (6, 20, 21). The viscous polymer slug prevents fingers of water from penetrating the oil bank, which would otherwise make the process less effective (22).

In order to optimize the surfactant-polymer flooding process, the oil bank formed must be propagated through the porous media while the oil ganglia continue to coalesce with the leading edge of the oil bank. The volumetric coverage of the process is optimized by adjusting the mobility of each slug (Figure 11.11) (6, 22). This is accomplished by maintaining the ultra-low interfacial tension at the oil bank/surfactant slug interface (6, 28).

There also exists a need to avoid surfactant aggregate structures such as lamellar liquid crystals which exhibit high viscosity (29-32). System parameters should be such that mixing between the fluids in the surfactant, oil and polymer slugs does not occur. A dispersion of surfactant and oil would form an undesired emulsion, while a dispersion of surfactant and polymer, if incompatible, could lead to phase separation, which would decrease the effectiveness of the process. Other points to take into account are (i) the mass transfer of surfactant to the oil bank can change the interfacial tension, and (ii) surfactant-polymer incompatibility leads to a phase separation, which would reduce the efficiency of the process (30, 31).

Displacement of oil in petroleum reservoirs
by water or chemical flooding (five-spot pattern)

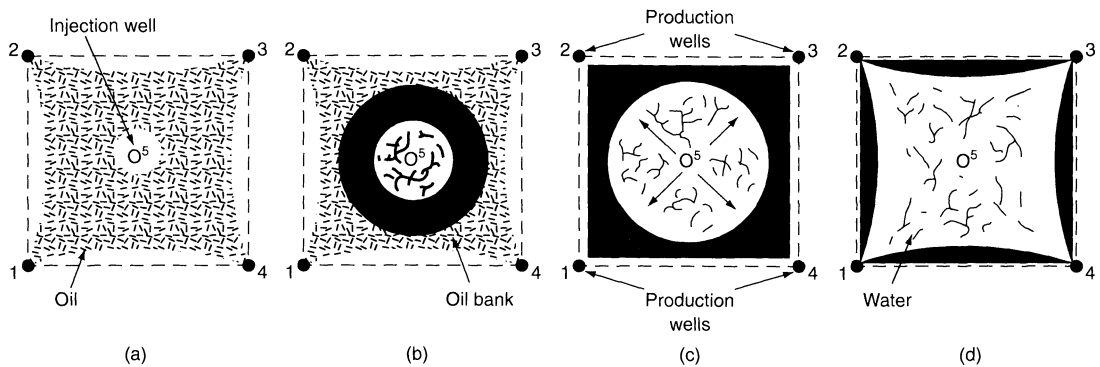
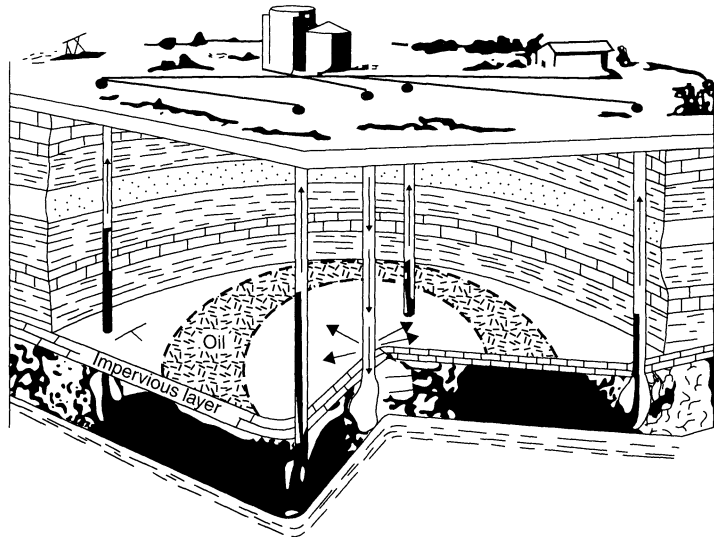


Figure 11.9. Schematic representation of an oil reservoir and the displacement of oil by water or chemical flooding

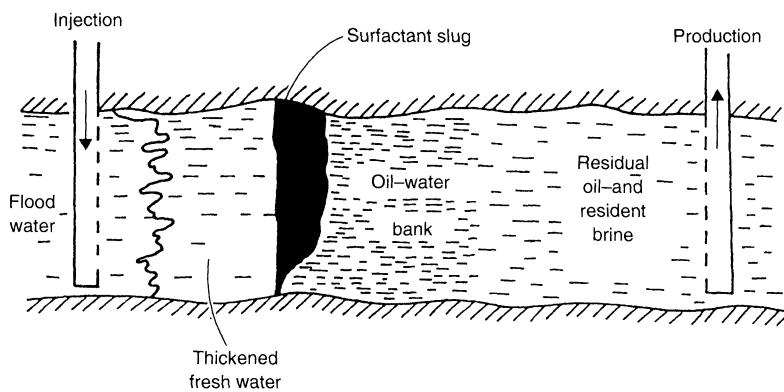


Figure 11.10. Schematic representation of the surfactant-polymer flooding process

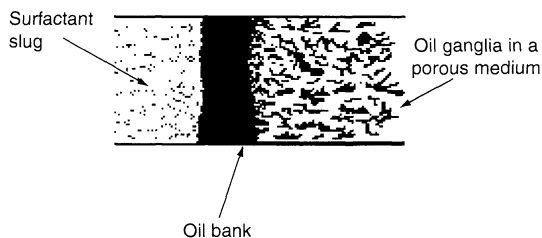


Figure 11.11. Schematic representation of the role of ultra-low interfacial tension on the formation of the oil bank

After secondary oil recovery (water flooding), the oil ganglia are trapped inside the pores by viscous and capillary forces, the magnitude of which can be accounted for by the capillary number, N_c , which is defined as follows:

$$N_c = \left(\frac{\mu_w v_w}{\gamma_{ow}} \right) \quad (11.6)$$

where μ_w is the viscosity of water, v_w is the water velocity and γ_{ow} is the oil/water interfacial tension (6, 19–22). At this stage in the oil recovery process, the capillary number is about 10^{-6} , which means that the forces trapping the oil ganglia are enormous. As indicated by equation (11.6), to overcome these forces it is necessary to increase the capillary number by three orders of magnitude to 10^{-3} by increasing the viscosity or velocity of the fluid, or by decreasing the interfacial tension from 30 to 10^{-3} – 10^{-4} mN/m. Any attempt to increase the fluid velocity involves the use of high pressures which can collapse the rock structure, thus

creating preferred paths of high porosity, and possibly leading to channelling (22). Increasing the viscosity is also impractical (try blowing honey through a straw!). Therefore, in order to increase the capillary number, one must decrease the interfacial tension (IFT) of the entrapped oil.

Interfacial tensions can reach ultra-low values at low as well as high surfactant concentrations (Figure 11.12) (6, 21). At low surfactant concentrations, the system appears to be a two-phase one, namely oil and brine in equilibrium with each other. A small change in the surfactant concentration around this region could strongly affect the interfacial tension. Such a change in surfactant concentration might occur due to adsorption of surfactant molecules on to surfaces of the reservoir porous media. On the other hand, in high-surfactant-concentration systems (approximately 4–8 wt% surfactant), a microemulsion middle phase exists in equilibrium with the excess oil and brine phases. These high-concentration systems are close to the optimal formulation (i.e. the concentration at which the most oil can be mobilized), and are therefore preferred to low-concentration systems (Figure 11.13).

Surface charge density is another parameter that can strongly and favourably affect the displacement efficiency of oil ganglia by changing the interfacial tension, surface viscosity and electrical repulsion of the ganglia entrapped in the porous media (Figure 11.14) (6, 21, 22, 33).

Figure 11.15 indicates that there exists an optimal salinity where the high surfactant concentration formulations exhibit a minimum interfacial tension

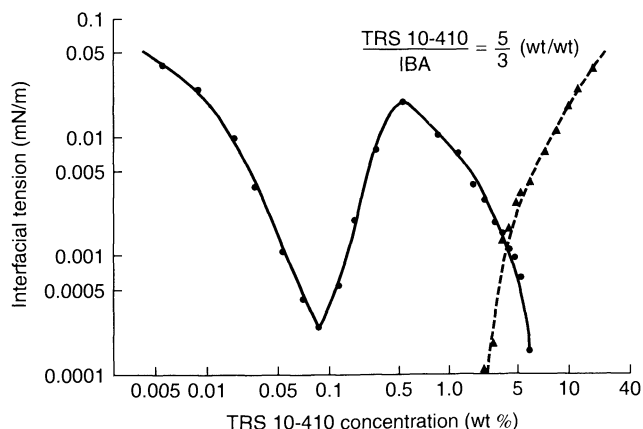


Figure 11.12. Effect of surfactant concentration on the interfacial tension (IFT) of TRS 10-410 (a petroleum sulfonate surfactant) + isobutyl alcohol (IBA) in 1.5% NaCl with dodecane. An ultralow IFT can occur at low or high surfactant concentrations: ●, interfacial tension of o/w micro emulsion; ▲, interfacial tension of w/o micro emulsion. A three-phase system (oil-continuous, water-continuous and middle-phase regions) exists where the (●) and (▲) data overlap

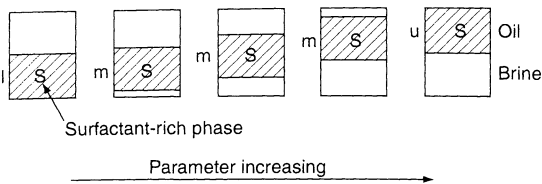


Figure 11.13. Factors that can affect the partitioning of surfactant from the water to the oil phase. The transition from the lower to the middle to the upper phase (I–m–u) can occur by (a) increasing the salinity, (b) decreasing the oil chain length, (c) decreasing the temperature, (d) increasing the total surfactant concentration, (e) increasing the brine/oil ratio, (f) increasing the surfactant solution/oil ratio, or (g) increasing the molecular weight of the surfactant

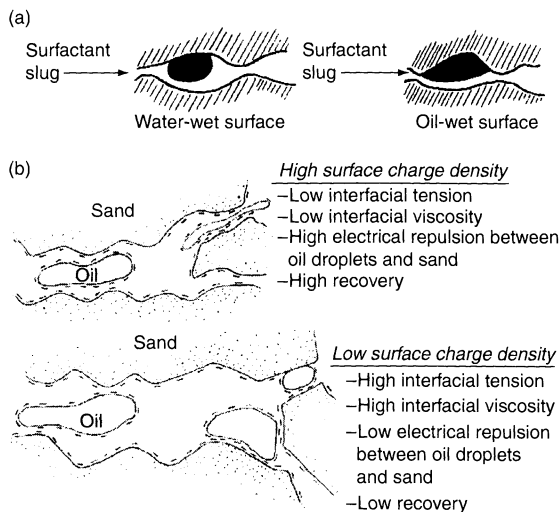


Figure 11.14. (a) Shape of an oil drop on a water-wet or an oil-wet surface. (b) The role of surface charge in the oil displacement process

between oil and water, a middle-phase microemulsion formation with equal oil and water solubilized in the middle phase, a minimum loss of surfactant in the porous media, and a minimum phase separation time of the three phases, as well as a minimum pressure buildup while pumping these multiphase systems through the porous media, and a maximum oil displacement efficiency. This figure also suggests that these are all interrelated interfacial phenomena.

3.2.2 Foams in enhanced oil recovery

In the petroleum industry, foam finds applications mainly in the area of enhanced oil recovery. The basic

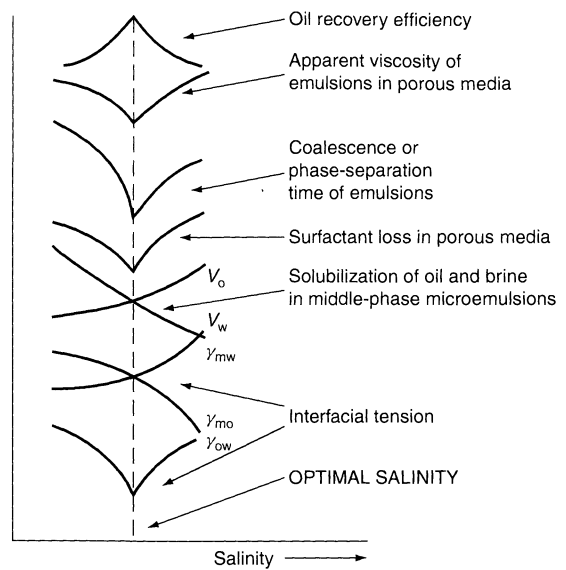


Figure 11.15. The various phenomena occurring at optimal salinity in relation to enhanced oil recovery

concept involves the use of the unique rheological properties of foam in porous media to block highly permeable areas (from where the oil has already been swept) and to allow oil to be recovered from the low-permeability zones.

Carbon dioxide is often used in the foaming process as a displacing fluid. The carbon dioxide fluid is miscible in all proportions with the lighter hydrocarbons. This behaviour is very different from that of displacement by water, where a significant amount of oil remains trapped because of the immiscibility of the two phases. Another advantage of using carbon dioxide is that it has limited solubility in water, so nearly all of the CO_2 injected can be used to solubilize the oil, and little is wasted by dissolving into the water.

Surfactants are used to overcome some of the disadvantages that the CO_2 flooding system offers. The crucial disadvantage of CO_2 flooding is the low viscosity of liquid CO_2 when compared to the heavy fractions in the oil. A low viscosity implies a higher mobility and this means a possibility of CO_2 leakage via finger formation or channelling. Surfactants are used to decrease this higher mobility by enhancing foam stability.

Steam is also used as a foaming fluid. The problem in this case is similar to that of the CO_2 system, i.e. a high mobility of the steam. Once again, surfactants with or without non-condensable gas are used to increase the foam stability. Since the operating temperatures involved are high, the surfactant system must be

designed to remain effective over a wide range of temperatures. The adsorption of surfactants on to reservoir rock surfaces is minimal at high temperatures, unless ionic species are present. If the foam is made out of "pure" steam (saturated steam in equilibrium with water as the lamella), according to Kelvin's equation, the smaller bubbles, which have a higher pressure, will collapse and be absorbed by larger bubbles, thus resulting in decreased foam stability. Small amounts of non-condensable gas are added to increase the foam stability by decreasing the rate of steam condensation and foam collapse.

The text by Schramm (34) covers most aspects of the use of foams in the petroleum industry, ranging from fundamentals to enhanced oil recovery. It also provides field data from several oil fields along with the "in-laboratory" experimental methods that are used to correlate field data to proposed theories.

3.2.3 Acid fracturing for oil well stimulation

Acid fracturing is an oil well stimulation process in which acid (HCl or HF, depending on the rock structure) is injected into an oil well at sufficiently high pressure to fracture the porous media or to widen existing natural fractures. Various principles of surface chemistry are employed in this process in order to avoid excessive and costly fluid loss, and to decrease the rate of acid spent.

For controlling fluid loss, surfactants are used as thickeners which gel the acid by forming micelles. These gelled acids are shear-stable because micellar chains can quickly reform following shearing. The advantages of surfactants as thickeners is that they can be designed to provide high viscosity to "live" (i.e. active) acid solutions, while at the same time providing low viscosity to the spent acid. This is possible because of the disruption of the micellar structure due to the increased concentration of reaction products formed during spending of acid. The decreased spent acid viscosity aids in recovery of the treating fluids (35).

The employment of foamed acid and acid-external emulsions (oil as the dispersed phase and gelled acid as the continuous phase) are other methods used to control the loss of acid solutions. The disadvantage of using oils is that a large concentration of oil is required to increase the viscosity of the emulsion formulation, which reduces the acid concentration and, therefore, the amount of acid available for fracture etching. Foaming the acid also reduces the amount of acid available for etching since less acid is present per unit volume injected.

To control the reaction rate of the acid, retarders such as alkyl sulfonates, alkyl phosphonates and alkyl amines are used to form hydrophobic films on carbonate surfaces. These protective films act as a barrier to slow acid attack. Another method involves the use of foaming agents to stabilize the carbon dioxide foam that is created when CO₂ is released as a product of the acid-etching reaction. This CO₂ foam acts as a barrier to slow acid attack. Yet another method for controlling the acid activity in an oil well is the use of emulsions containing kerosene or diesel as the continuous oil phase and hydrochloric acid as the dispersed aqueous phase. Acid-in-oil emulsions are most commonly used because oil separates the acid from the carbonate surface (and from machine parts, thus reducing the level of corrosion). Moreover, acid reaction rates can be further decreased by surfactant retarders that increase the wettability of the carbonate surface for oil.

3.3 Antifoaming and defoaming

Foam shows peculiar properties that are useful in enhanced oil recovery. However, foam turns out to be a major problem in all downstream processing of the recovered crude oil. The causes of foaming are usually related to naturally occurring impurities and corrosion products found in process streams. Antifoaming and defoaming agents are added in all major unit operations to avoid foaming. Antifoaming agents are added to prevent the formation of new foam, while defoamers are added to destroy the existing foam (34). Hydrophobic silicas, silicone oils, glycol-based polymers, amides, mineral oils and fatty acids are common antifoaming agents (34).

3.4 Corrosion inhibition

The petroleum industry does not remain unaffected by corrosion (as was alluded to in the discussion on acid-in-oil emulsions above). Indeed, corrosion is a common phenomenon endured by almost every industry. The metallic parts used everywhere from oil wells to refineries and petrochemical plants are susceptible to corrosion. In 1999, in the USA alone, corrosion was held responsible for approximately \$300 billion of lost revenue, of which more than one third could have been saved by using available methods of corrosion control (36).

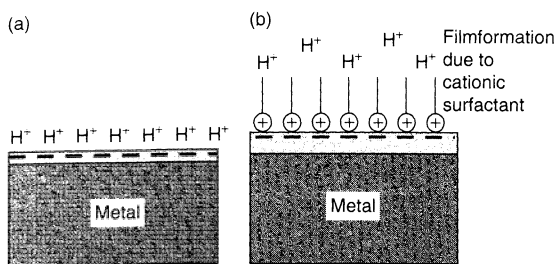


Figure 11.16. Schematic representations of (a) a Bare metal surface, and (b) a surface where the Presence of a surfactant film acts as a barrier to corrosion

The most commonly observed corrosion in the oil industry begins with the adsorption of protons on metallic surfaces, followed by an irreversible electrochemical reaction between the protons and the metallic atoms. Metallic cations may either dissolve in the aqueous phase or react with anions such as sulfur, thus exposing more metallic surface for subsequent attacks.

Surface chemistry provides an important corrosion control method (Figure 11.16). Ohmic inhibitors, also known as filming inhibitors, are cationic surfactants that have a tendency to preferentially adsorb to all available negative sites on the metallic surface, forming a compact and hydrophobic film. This low-permeability film will (i) decrease the wettability of the surface to water and brine, (ii) decrease the mobility of various ions, (iii) lessen the spread of conductive bridges between the anode and cathode, and (iv) reduce the possible chemical interactions of oxidizing agents (e.g. protons, acids, etc.) with negative sites on the metallic surface.

Robinson (18) describes in detail the possible solutions to corrosion-related problems which are encountered in the various steps of petrochemical operations.

3.5 Oil spill clean-up

The introduction of petroleum into the marine environment is a direct consequence of the production and transportation of crude oil and refined products. Oil spills have justifiably earned ill fame for polluting the environment by being responsible for some of the worst environmental disasters in (recent) human history. Oil spills jeopardize the dissolved oxygen-dependent aquatic life because the oil film acts as a barrier for oxygen transport across the air–water interface. Seabirds are unable to fly or even float on water once oil wets their feathers, thus leading to their untimely death. In addition to aesthetic and ecological concerns, coastal regions

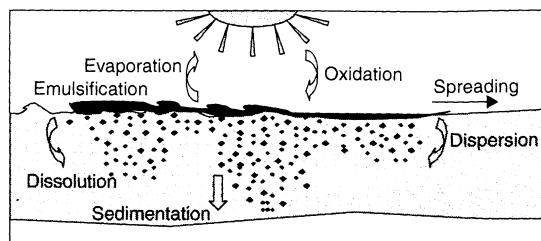


Figure 11.17. Schematic showing some of the phenomena governing the fate of an oil spill after a spillage at sea

can suffer economically from damage done by oil spills to recreational areas, harbours and vessels, commercial shellfish grounds and intake sources for desalination and power plants. Figure 11.17 shows some of the phenomena that decide the fate of spilled oil on the sea surface.

For removal of spilled oil, a surfactant solution (a dispersant) is added along the circumference of the oil (sprayed from boats and aircraft), which creates a surface tension gradient that forces the oil to contract to the centre of the oil lens, so making the job of removal of the oil easier. The effectiveness of this process depends on sea conditions and application techniques, as well as the chemical nature of both the oil and dispersant. The time elapsed after an oil spill remains one of the critical factors in this process, because with weathering, the viscosity of oil increases rapidly, hence resulting in slower migration of surfactant to the oil/water interface and a decreased dispersion effectiveness.

Once the oil is collected, it is then pumped to on-ship coalescers that use surfactants and oil-wet or water-wet filters to break the crude oil–brine emulsion.

Even after removal of the bulk of the spilled oil, a thin layer of oil still exists – this remains a barrier for oxygen absorption. Moreover, the native microbial populations cannot degrade it. It then becomes imperative to break this film into tiny droplets so as to quicken the oil degradation and to increase oxygen transport from the atmosphere to the water. This is achieved by adding a surfactant solution to the oil lens.

The surfactants traditionally used as dispersants are not without their share of problems. Lately, there has been some debate on the toxicological impact of these dispersants on marine organisms and the coastal environment, and so the search for new, less toxic formulations remains ongoing.

The interested reader is referred to ref. (37) for further studies on the chemistry and physics of dispersants and dispersed oil, methods for toxicological testing and the techniques employed, logistics, monitoring and

application strategies for using various dispersants in the United States.

3.6 Fluidization of bitumen

Bitumen is a naturally occurring hydrocarbon that exists in a semi-solid or solid phase in natural deposits. The most important reservoirs of bitumen are found in Canada and Venezuela. Among the problems encountered when recovering bitumen, its high viscosity is one of the greatest. Natural bitumen has a viscosity greater than 10 000 mPa, measured on a gas-free basis at its original temperature in the deposit and atmospheric pressure (38, 39).

Current technology has made possible the recovery and use of this huge source of energy (38–41). Moreover, since the extraction process of this raw material requires much less energy than the refining process required for other fossil fuels, (the bitumen extraction industry is flourishing.) Gas-oil, which is an intermediate product created during the refining of crude oil, is pumped into the oil well to reduce the viscosity of the bitumen and allow it to be pumped from underground to a flow station (at ground level.)

A commercial product known as Orimulsion® is an example of the application of surface chemistry to the technology of conferring special properties to heavy crude oil¹. This is an oil-in-water emulsion made from bitumen stabilized by a nonionic surfactant, which decreases the viscosity of the bitumen from 10^5 to less than 10^2 mPa, and reduces the NO_x emissions while still maintaining a high combustion performance (42).

It is worth mentioning here that to optimize the low viscosity of an emulsion, two emulsions of different drop size distributions are mixed, with the smaller one being about 25% and the larger one about 75% of the total concentration (43).

3.7 Asphaltic emulsions

Another very important application of surface science in the petroleum industry that has recently been receiving much attention is the creation of oil-in-water asphaltic emulsions (asphalt dispersed in a brine continuous phase) which are used to pave roads (44). The idea is to decrease the viscosity of asphalt, while at the same time avoiding the use of gasoline. The latter is presently

being used to fluidize asphalt, but has high economic and environmental costs.

For this technological application, the main types of surfactants used have been cationics, since most rock surfaces are negatively charged. By using this method, when the asphaltic emulsion contacts the ground, surfactant molecules migrate from the surface of the asphalt droplets to the rock surfaces, which results in the breaking of the asphaltic emulsion and a permanent spread of asphalt on to the rock surfaces. Cationic surfactants are preferred, despite their high cost, because they promote faster breakup of the asphalt emulsion, which is often necessary to prevent the possibility of rain washing away the asphalt before it has solidified. However, work is currently being carried out to incorporate non-ionic surfactants into the emulsion in order to reduce costs and to improve the mechanical properties of the asphalt.

3.8 Oil/water separation and crude oil dehydration

Oil-water emulsion systems are often desirable in cases such as the transportation of crude oil and increased fuel efficiency of light oil fractions. By the same token, these systems are undesirable for distillation and catalytic cracking of crude oil. More than 50% of all of the petroleum recovered is in the form of water-in-oil emulsions. These emulsions are formed because crude oil contains natural surfactants and the oil and water are emulsified as they pass through mechanical devices such as pumps or valves. Water must be removed before any refinery operation can be performed on this oil material. It is not economically viable to distill crude oil in emulsion form because of the incremental energy costs that would be encountered when producing fractions in the established standard viscosity range. Moreover, water may poison or reduce the activities of the catalysts used in catalytic cracking processes further down the processing line.

In earlier days, the method used to destabilize a crude oil/water emulsion was gravity-heating sedimentation. Nowadays, however, chemical de-emulsification and improved electromagnetic and gravitational techniques are the main methods used to break down an emulsion.

Such methods take advantage of inexpensive de-emulsifying chemicals to enable the collision and fusion of droplets that ultimately lead to oil/water phase separation. This is achieved by adjusting the surface charge density, counterion concentration and temperature. Polymers are also added to promote flocculation. A detailed

¹ Note: Orimulsion® is a trademark of INTEVEP, SA, a branch company of Petróleos de Venezuela, SA (PDVSA).

discussion of the electrostatic phenomena used in this process can be found in ref. (45).

The coagulants (typically multivalent counterions) commonly used are the salts of aluminium and iron and salts or the bases of calcium and magnesium. The transition from stabilized to destabilized emulsions on changing the temperature is very sharp at the critical flocculation temperature (CFT) when nonionic surfactants are used. Generally, aqueous dispersions destabilize upon increasing temperature, while non-aqueous dispersions destabilize with decreasing temperature.

To dissolve the stabilizing agent, the use of cosolvents such as carbon disulfide, carbon tetrachloride, acetone and ether is in current practice. For specific examples of oil/water separations and for further details about the use of dissolved air floatation, deep bed filtration, and the selection and sizing of various equipment, the interested reader is referred to ref. (46).

4 SUMMARY

Surfactants have very special qualities that make them invaluable to the petroleum industry. The relevance of various interfacial phenomena, such as adsorbed surfactant films, self-assembly, contact angle, wetting, foams and emulsions, in nearly every process in the industry has been discussed. In addition, this chapter summarized the importance of the adsorption and aggregation behaviour of surfactants with regard to drilling, enhanced oil recovery, antifoaming, corrosion inhibition, oil spill clean-up, oil/water separation and fluidization of highly viscous materials.

5 REFERENCES

- Shah, D. O., The world of surface science, in *Chemical Engineering Education*, Anderson, T. J. (Ed.), American Society for Engineering Education, Winter 1977, pp. 14–48.
- Gary, J. H. and Handwerk, G. E., *Petroleum Refining: Technology and Economics*, 3rd Edn, Marcel Dekker, New York, 1994.
- Gibbs, J. W., *The Collected Works of J. W. Gibbs*, Vol. I, Longmans & Green, New York, 1931.
- Guggenheim, E. A. and Adam, N. K., The thermodynamics of adsorption at the surface of solutions *Proc. R. Soc. London, A*, **139**, 218–236 (1933).
- Adamson, A. W. and Gast, A. P., *Physical Chemistry of Surfaces*, 6th Edn, Wiley, New York, 1997.
- Shah, D. O., Fundamental aspects of surfactant–polymer flooding process, Keynote paper presented at the *European Symposium on Enhanced Oil Recovery*, Bournemouth, UK, September 21–23, 1981, Elsevier, Lausanne, Switzerland, 1981.
- Patist, A., Jha, B. K., Oh, S. -G. and Shah, D. O., Importance of micellar relaxation time on detergent properties. *J. Surfactants Deterg.*, **2**, 317–324 (1999).
- Davies, J. T. and Rideal, E. K., *Interfacial Phenomena*, 2nd Edn, Academic Press, New York, 1963.
- Myers, D., *Surfaces, Interfaces, and Colloids: Principles and Applications*, 2nd Edn, Wiley-VCH, New York, 1999.
- Battelle, *Testing and Characterization of Orimulsion®-400*, Volume 1 – Technical Report, Battelle Memorial Institute, Duxbury, MA, 1998.
- Salager, J. L., Phase inversion and emulsion inversion on the basics of catastrophe theory, in *Encyclopedia of Emulsion Technology*, Vol. 3, Becher, P. (Ed.), Marcel Dekker, New York, 1983, pp. 79–134.
- Griffin, W. C., Classification of surface active agents by “HLB”, *J. Soc. Cosmet. Chem.*, **1**, 311–326 (1949); Griffin, W. C., Calculation of HLB values of non-ionic surfactants *J. Soc. Cosmet. Chem.*, **5**, 249–256 (1954).
- Bancroft, W. D., The theory of emulsification V, *J. Phys. Chem.*, **17**, 501–519 (1913); Bancroft, W. D., The theory of emulsification VI, *J. Phys. Chem.*, **19**, 275–309 (1915).
- Becher, P., HLB – A survey, in *Surfactants in Solution*, Vol. 3, Mittal, K. L., (Ed.), Plenum, New York, 1984 pp. 1925–1946; Becher, P., Hydrophile–lipophile balance–History and recent developments (Langmuir Lecture, 1983), *J. Disper. Sci. Technol.*, **5**, 81–96 (1984).
- Winsor, P. A., *Solvent Properties of Amphiphilic Compounds*, Butterworth, London, 1954.
- Shinoda, K. and Arai, H., The correlation between phase inversion temperature in emulsion and cloud point in solution of nonionic emulsifier, *J. Phys. Chem.*, **68**, 3485–3490 (1964).
- Ruckenstein, E. and Chi, J. C., Stability of microemulsions, *J. Chem. Soc., Faraday Trans. 2*, **71**, 1690–1707 (1975).
- Robinson, J. S., *Corrosion Inhibitors – Recent Developments*, Noyes Data Corporation, Park Ridge, NJ, 1979.
- Rivas H., Gutierrez, X., Ziritt, J. L., Anton, R. E. and Salager, J. L., Microemulsion and optimal formulation occurrence in pH-dependent systems as found in alkaline-enhanced oil recovery, in *Industrial Applications of Microemulsions*, Solans, C. and Kunieda, H. (Eds), Surfactant Science Series, Vol. 66, Marcel Dekker, New York, 1997, pp. 305–329.
- Baviere, M. and Canselier, J. P., Microemulsion in the chemical EOR process, in *Industrial Applications of Microemulsions*, Solans, C. and Kunieda, H. (Eds), Surfactant Science Series, Vol. 66, Marcel Dekker, New York, 1997, pp. 331–353.
- Pillai, V., Kanicky, J. R. and Shah, D. O., Applications of microemulsions in enhanced oil recovery, in *Handbook of Microemulsion Science and Technology*, Kumar P. and Mittal, K. L. (Eds), Marcel Dekker, New York, 1999, pp. 743–753.

22. Willson, Jr., L. A., Physicochemical environment of petroleum reservoirs in relation to oil recovery systems, in *Improved Oil Recovery by Surfactant and Polymer Flooding*, Shah, D. O. and Schechter, R. S. (Eds), Academic Press, New York, 1977, pp. 1–26.
23. Somasundaran, P. and Hanna, H. S., Physico-chemical aspects of adsorption at solid/liquid interfaces. I. Basic principles, in *Improved Oil Recovery by Surfactant and Polymer Flooding*, Shah, D. O. and Schechter, R. S. (Eds), Academic Press, New York, 1977, pp. 205–251.
24. Hanna, H. S. and Somasundaran, P., Physico-chemical aspects of adsorption at solid/liquid interfaces. II. Mahogany sulfonate/berrea sandstone, kaolinite, in *Improved Oil Recovery by Surfactant and Polymer Flooding*, Shah, D. O. and Schechter, R. S. (Eds), Academic Press, New York, 1977, pp. 253–274.
25. Malmberg, E. W. and Smith, L., The adsorption losses of surfactants in tertiary recovery systems, in *Improved Oil Recovery by Surfactant and Polymer Flooding*, Shah, D. O. and Schechter, R. S. (Eds), Academic Press, New York, 1977, pp. 275–291.
26. Willhite, G. P. and Dominguez, J. G., Mechanisms of polymer retention in porous media, in *Improved Oil Recovery by Surfactant and Polymer Flooding*, Shah, D. O. and Schechter, R. S., Academic Press, New York, 1977, pp. 511–554.
27. Morgan, J. C., Schechter, R. S. and Wade, W. H., Recent advances in the study of low interfacial tensions, in *Improved Oil Recovery by Surfactant and Polymer Flooding*, Shah, D. O. and Schechter, R. S., Academic Press, New York, 1977, pp. 101–118.
28. Stegemeier, G. L., Mechanisms of entrapment and mobilization of oil in porous media, in *Improved Oil Recovery by Surfactant and Polymer Flooding* Shah, D. O. and Schechter, R. S., Academic Press, New York, 1977, pp. 55–91.
29. Mashiko, A. B. E., Microemulsions in enhanced oil recovery: Middle-phase microemulsion formation with some typical anionic surfactants, in *Industrial Applications of Microemulsions*, Solans, C. and Kunieda, H. (Eds), Surfactant Science Series, Vol. 66, Marcel Dekker, New York, 1997, pp. 279–303.
30. Lissant, K. J., Emulsification and demulsification in oil recovery, in *Improved Oil Recovery by Surfactant and Polymer Flooding*, Shah, D. O. and Schechter, R. S. (Eds), Academic Press, New York, 1977, pp. 93–100.
31. Shah, D. O., Bansal, V. K., Chan, K. S. and Hsieh, W. C., The structure, formation, and phase inversion of microemulsions, in *Improved Oil Recovery by Surfactant and Polymer Flooding*, Shah, D. O. and Schechter, R. S. (Eds), Academic Press, New York, 1977, pp. 293–337.
32. Metzner, A. B., Flows of polymeric solution and emulsions through porous media: Current status, in *Improved Oil Recovery by Surfactant and Polymer Flooding*, Shah, D. O. and Schechter, R. S. (Eds), Academic Press, New York, 1977, pp. 439–451.
33. Wasan, D. T. and Mohan, V., Interfacial rheological properties of fluid interfaces containing surfactants, in *Improved Oil Recovery by Surfactant and Polymer Flooding*, Shah, D. O. and Schechter, R. S. (Eds), Academic Press, New York, 1977, pp. 161–203.
34. Schramm, L. L. (Ed.), *Foams: Fundamentals and Applications in the Petroleum Industry*, Advances in Chemistry Services, Vol. 242, American Chemical Society, Washington, DC, 1994.
35. Economides, M. J. and Nolte, K. G., *Reservoir Stimulation*, Prentice Hall, Englewood Cliffs, NJ, 1989.
36. Davis, J. R. (Ed.), *Corrosion: Understanding the Basics*, ASM International, Materials Park, OH, 2000.
37. Committee on Effectiveness of Oil Spill Dispersants, *Report of the Marine Board Commission on Engineering and Technical Solutions*, National Research Council, National Academy Press, Washington, DC, 1989.
38. Miller, C. A., Linak, W. P., King, C. and Wendt, J. O. L., Fine particle emissions from heavy fuel oil combustion in a firetube package boiler, *Combust. Sci. Technol.* **134**, 477–502 (1998).
39. Miller, C. A. and Srivastava, R. K., The combustion of Orimulsion and its generation of air pollutants, *Prog. Energy Combust. Sci.*, **26** 131–160 (2000).
40. Rivas, H. and Colmenares, T., ORIMULSION®: New generations and future perspectives, *Vis. Tecnol.* (Special Issue), 49–60, (1999).
41. Anon, Dalhousie Orimulsion conversion and scrubber facility wins 1995 Powerplant of the Year Award, *Power*, **139**, 27–32 (1995).
42. Zaki, M. I., Nael, N., Ahmed, N. S. and Nassar, A. M., Sodium lignin sulfonate to stabilize heavy crude oil-in-water emulsions for pipeline transportation, *Petrol. Sci. Technol.*, **18**, 1175–1193 (2000).
43. Nuñez, G. A., Sanchez, G., Gutierrez, X., Silva, F., Dalas, C. and Rivas, H., Rheological behavior of concentrated bitumen in water emulsions, *Langmuir*, **16**, 6497–6502 (2000).
44. Puzinauskas, V. P. and Jester, R. N., Design of emulsified asphalt paving mixtures, National Cooperative Highway Research Program Report 259, Transportation Research Board, Washington, DC, 1983.
45. Hunter, R. J. and White, L. R., *Foundations of Colloid Science*, Oxford University Press, New York, 1987.
46. Wasan, D. T., Ginn, M. E. and Shah, D. O., *Surfactants in Chemical/Process Engineering*, Marcel Dekker, New York, 1998.

PART 2
SURFACTANTS

CHAPTER 12

Anionic Surfactants

Antje Schmalstieg and Guenther W. Wasow

Berlin, Germany

1	Introduction	271	12.1	Phosphated and polyphosphated alcohols	285
2	Soap	272	12.2	Polyoxyalkylene phosphate esters	287
3	Alkyl Sulfates	273	12.3	Applications of phosphorus- containing surfactants	288
4	Alkyl Ether Sulfates	275	13	Sulfosuccinates	289
5	Alkyl Ether Carboxylates	275	14	Anionic Surfactants with Special Properties	291
6	α -Olefinesulfonates	276	14.1	Cleavable surfactants	291
7	α -Sulfo Fatty Acid Methyl Esters	277	14.2	Short-chain sulfonates	291
8	Esters and Amides of Fatty Acids	278	14.3	Anion-active sequestrents	291
9	Petrol Sulfonates	278	14.4	Fluorosurfactants	291
10	Alkylbenzene Sulfonates	278	14.5	Silicosurfactants	291
11	Alkane Sulfonates	282	14.6	Ligninsulfonates	292
	11.1 Sulfochlorination	282	15	Acknowledgements	292
	11.2 Sulfoxidation	284	16	Bibliography	292
	11.3 Properties and applications of alkane sulfonates	284			
12	Esters of Phosphoric Acid	285			

1 INTRODUCTION

The surface-active agent first made by man was soap, with this being an anionic surface-active agent. Indeed, soap was already known to the Sumerians (Babylonians) as early as 2500 years BC. Vegetable oils were cooked with potassium carbonate from burnt wood. The next step was the use of potassium hydroxide made from potash and calcium oxide. In this way, soap has been produced for millennia, mainly by the reaction of potassium hydroxide and tallow. During the 17th century, Marseille, in particular, was well known for its production of soap.

If the hydrophobic part of a surfactant molecule acts as an anion in aqueous solution, the compound is called

an anionic surfactant. Thus, many structures are known which are covered by this definition.

In technical-scale production, it is mainly the carboxylates, sulfates, sulfonates and phosphates which act as the hydrophilic parts of surface-active molecules. In addition to soap, the carboxylic group also plays this role in polyether carboxylates, sarcosinates and asparaginates.

In monoesters of sulfuric acid, the sulfate ion is the hydrophilic part of the molecule which results in its solubility in water. Sodium salts of fatty alcohol monoesters of sulfuric acid are the best known examples of this kind of surfactant. The sulfate group is also present in alkyl polyglycol ether sulfates and in some reaction products of starting materials containing a double bond or an OH-group in the molecule, e.g. sulfated castor oil.

If the central sulfur atom of the hydrophilic group is directly bonded to a carbon atom, the resulting compound is called a sulfonate. Because aromatic ring systems will easily react with sulfuric acid or sulfur trioxide, alkylbenzene sulfonates were one of the earliest types of surface-active compounds to be produced. The sulfonate group is the hydrophilic part in many surfactants in the trade. Besides alkylbenzene sulfonates, alkane sulfonates, olefine sulfonates, α -sulfo fatty acid methyl esters, taurates and isothionates should also be mentioned.

In a similar way, the phosphorus atom gives rise to the surface-active esters of phosphoric acid (alkyl phosphates) and the alkyl phosphonates, in which the phosphorus atom is directly bonded to a carbon atom.

Although many other surfactants can be prepared which will exhibit anionic properties, the bulk of anionics in the market today are covered by the types mentioned above.

The different demands of a surface-active system can be met either by blending these main types with each other or with other types of surfactants. This is, in most cases, the best way to optimize costs, performance and environmental impact.

2 SOAP

Although soap had already been known for millennia, the industrial production of soap was particularly favoured by the rising textile industry and the importation of tropical fats. Soap became an item for common consumption when the Leblanc process for the production of sodium carbonate was set into operation in 1820.

Soaps have now almost completely been replaced by synthetic surfactants in many fields of their former application, although they are still in use today in bodycare products and cosmetics. In Western Europe alone, production still exceeds 700 000 t per year. In less developed countries, soap is still the most important surfactant in detergents and cleaners, as was always the case.

Soaps are mainly produced from coconut oil, palm kernel oil and tallow. High proportions of unsaturated fatty acids are unwanted because they will easily become rancid. However, if their double bonds are hydrogenated, they may also be used as basic materials in soap production. The preferred mixture for the production of soap bars contains 80 wt% of tallow and 20 wt% of coconut oil. The use of synthetic fatty acids has virtually no importance any more.

Soap can be produced by the neutralization of fatty acids from the fat-splitting process with caustic soda, soda ash or potash. In the saponification process of natural fats and oils, glycerol is obtained as an important by-product. At first, a viscous gel is produced, and from this, by the addition of common salt, "curd soap" is separated. The lower phase consists of a viscous solution of salt and glycerol. The upper phase is cooled and transferred into moulds in which it will solidify to give the curd soap. This soap contains ca. 60% of active matter, calculated as fatty acid. Soap powder or flakes can be obtained by vacuum drying on roll dryers or in spray-drying towers to a fatty acid content of ca. 80%. Glycerol, obtained by saponification of fats and oils, is a component of the lower phase and is isolated by a special process. The production of highly pure glycerol gives a considerable contribution to the profitability of a soap-production plant.

In addition to sodium soaps, corresponding saponification and neutralization reactions of fatty acids can also be carried out to produce the softer potassium and ammonium soaps. Soaps prepared from coconut oil or oleic acid by the use of nitrilotriethanol are semi-solid or liquid in form. Salts of polyvalent ions such as calcium, zinc and aluminium, the so-called "metal soaps", also form part of the market.

In larger plants, the production of soap is nowadays carried out by a continuous process. Soaps based on pure fatty acids can be prepared in crystalline form, although they will absorb water from the humidity in air up to an equilibrium level. The solubility of soaps depends on the length of the carbon chain and increases sharply with a rise in temperature. Sodium laurate is already soluble in water at 30°C to a considerable amount, while sodium stearate will not show a comparable solubility until a temperature above 70°C is reached. All solutions of soap in water are colloidal, and thus will easily form gels.

The precipitation of soaps by polyvalent ions in aqueous solutions is considered to be troublesome in many applications. However, because metal soaps are soluble in organic solvents, mineral oils and fats, they are valuable additives in the production of plastics where they are used as mould-separation agents, emulsifiers and stabilizers. The fatty acid salts of lead and cobalt are used as siccatives in varnish and paints.

Because soaps are salts of weak acids and strong bases, they undergo hydrolysis. Thus, their aqueous solutions behave as alkaline systems. If the negative influence from the water hardness is cancelled out by using soft water or by the addition of sequestrants, then soaps will show excellent detergency. They combine good wetting ability and foaming power with a

high detergency and work as good dispersants for soil pigments. Simultaneously, they support the release of soil by swelling the fibres and pigments due to their alkaline reaction.

Soaps are still major components of modern detergents. On the one hand, the formation of lather will be controlled by the addition of soap with long carbon chains. On the other hand, soaps based on coconut oil acids are components of liquid soaps, where they form lime soap by reaction with the components in hard water. In this way, they bind the polyvalent ions resulting from the water hardness. The formed insoluble lime soap is dispersed by an excess of soap or by other surfactants in the product so that it cannot deposit on the fibres. The major application of soap lies mainly in the field of human cleansing agents. Toilet soaps with different properties are easily obtained by the addition of lime soap dispersants, perfume oils, re-fattening agents, herbal extracts and other active substances.

3 ALKYL SULFATES

With the expansion of the textile industry, other surfactants besides soap began to achieve importance. For example, industry a surface-active product, produced by sulfonation of castor oil, possesses outstanding properties. Under the name of "turkey red oil", it is still in use today. It was found that the sulfuric acid semi-ester of the OH-group of ricinoleic acid was the surface-active moiety in this material. At first, the carboxylic group of the ricinoleic acid was transformed into an ester to avoid forming insoluble salts from the water hardness. Later, Bertsch logically arrived at the use of fatty alcohols instead of ricinoleic acid as suitable hydrophobic starting materials.

Only a few natural sources of fatty alcohols were known at this time. Production on a technical scale could be first realized by the reduction of methyl or butyl esters of fatty acids with metallic sodium after the Bouveault-Blanc process. Nearly simultaneously, the high-pressure hydrogenation of fatty acids to the resulting alcohols was developed by Schrauth. Hence, fatty alcohols were soon available on the market in a price range that made it possible to produce fatty alcohol sulfates for use in detergents.

Fatty alcohol sulphates are surfactants that show many interesting properties. They are relatively insensitive towards water hardness, display no biodegradable problems, and can be produced from renewable raw materials.

The surface-active characteristics of these materials are mainly dominated by their alkyl chains. The homologous series of the sodium salts of *n*-alkyl sulfuric acid mono esters with an even number of carbon atoms in the alkyl chain are the most thoroughly investigated substances of this kind. While alkyl chains with two to eight carbon atoms show the basic character of a salt, the surface-active properties dominate for those compounds with greater than 10 carbon atoms in the chain. The solubility of sodium tetradecyl sulfate and its higher homologues in water is poor at a temperature of 25°C, while sodium dodecyl sulfate combines sufficient solubility with good surface activity. Therefore, it is often used as a standard substance.

Sodium alkyl sulfates are esters. Thus sodium dodecyl sulfate is sensitive towards hydrolysis, especially in acid solutions. In this case, the starting fatty alcohol and sodium hydrogen sulfate is formed. Hydrolysis, once started, will run autocatalytically because the sodium hydrogen sulfate formed in this reaction is an acid in itself. Alkyl sulfates are stable in storage when in their highly pure states.

However, the surface-active behaviour will already be drastically changed by the presence of traces of fatty alcohols or other substances with a strong hydrophobicity.

Fatty alcohols are preferentially adsorbed at phase boundaries due to their high surface activities. Such behaviour, however, can often lead to the distortion of test data. With increasing concentration, the fatty alcohol (being a hydrophobic substance) will be encased in micelles of Sodium dodecyl sulfate, where the latter begin forming at the so-called critical micelle concentration (CMC). This is due to desorption from the surface boundary.

This course of adsorption and desorption can be used as a sensitive test for small amounts of hydrophobic impurities in a solution of surfactants. If the surface tension of the solution is plotted against the logarithm of the concentration of the surfactant, the so-called sigma/ln *c* curve will be obtained. The surface tension steadily decreases with increasing concentration of surfactant, until reaching a minimum shortly before the CMC.

At this stage, the hydrophobic impurities will be enclosed inside the micelles. The surface tension of the solution will rise slightly until reaching constant value due to the fact that now the whole surface is covered with molecules of the surfactant. A minimum in the plot will only occur if there are impurities in the solution which show a stronger surface activity than the surfactant itself, e.g. traces of unreacted fatty alcohol.

On the other hand, the behaviour discussed above offers the possibility to eliminate hydrophobic impurities from aqueous solutions of surface-active agents.

If foam is produced by blowing an inert gas through the solution of alkyl sulfate (or any other surfactant), the bulk of hydrophobic impurities will be enriched in the thin films of the foam bubbles. The remaining solution will then become more and more purified. Another method uses the primary adsorption of substances with the strongest surface activity at interfaces. Hence, the hydrophobic impurities will adsorb at the water/air interface and can then be sucked away from the surface. Automatic devices can decrease the surface area of the solution to concentrate the surfactant-containing layer, suck away these layers, expand the surface again for repeated adsorption, and repeat the cycle, etc. After some hundred cycles, the solution will become "interfacially pure".

To use sodium alkyl sulfate as a standard material, one has to ensure that the substance does not contain any impurities. One of the ways to create such a pure substance is to use the reaction of *n*-dodecanol with an adduct of chlorosulfuric acid and diethyl ether. The fatty alcohol is added to the ether solution while being cooled with ice. A stoichiometric surplus of 5–10% of chlorosulfuric acid is used to avoid forming the dialkyl sulfuric acid ester. The major part of the hydrogen chloride gas formed will evaporate.

After completion of the reaction, the ether solution is added to a surplus of an aqueous solution of sodium hydroxide while the solution is strongly stirred. It is essential to avoid any acid sites in the solution, or otherwise hydrolysis takes place, thus reforming undesired dodecanol. Carbon dioxide is then blown (in the form of small bubbles) into the alkaline aqueous solution to neutralize any surplus sodium hydroxide. The solution now contains sodium dodecyl sulfate, sodium chloride and sodium hydrogen carbonate, as well as diethyl ether in the upper phase. The organic phase is then separated and the aqueous solution washed three times with ether.

Next, the aqueous phase is evaporated to dryness (the temperature should not exceed 35°C), and the residue obtained is extracted by ethanol at 60°C. Only the required sodium dodecyl sulfate is soluble in ethanol, while the sodium chloride and sodium hydrogen carbonate are barely soluble in this solvent. The clear ethanolic solution is then cooled, where upon sodium dodecyl sulfate separates as white crystals. In order to obtain a highly pure substance, it is advisable to keep the first and second fractions separate from the mother liquor.

The dried crystals are stable without any limitations when kept in a closed container. On the other hand, hydrolysis will start and continue autocatalytically if the crystals are allowed to come into contact with water (from moisture in the air) or acid gases allowed to enter. At temperatures above 110°C, an intramolecular redox reaction will take place, even in an inert atmosphere, leading finally via dodecanal to dodecene and sodium hydrogen sulfite.

The properties of alkyl sulfates differ depending upon the structures of the alkyl chains and the counterions present. While alkali and ammonium salts are similar in behaviour, the solubilities of the alkaline-earth salts are reduced in water. On the other hand, the solubilities in organic solvents of alkyl sulfates with polyvalent ions is increased. Due to this fact, fatty pollutants can be better detached from fabrics by a detergent solution of moderate water hardness than by a solution showing extremely low water hardness. In particular, the wetting of textile fibres will be measurably accelerated by using calcium or magnesium as counterions.

The use of amines or tetraalkylammonium groups as counterions results in alkyl sulfates with good solubilities in water and in many organic solvents. That is of particular interest for many technical applications. The above-mentioned statements about the influences of different counterions on the behaviour of anionic alkyl sulfates applies largely to all anionic surfactants. The range of this influence differs according to the type of surfactant and hydrophobic unit present in the molecule.

The alkyl chain of a particular alkyl sulfate depends, of course, on the alcohol used in its synthesis. For technically relevant alkyl sulfates, such alcohols are available from the catalytic reduction of natural fatty acids and synthesized fatty acids or alcohols from the Oxo Process. Alcohols produced via the Ziegler process ("alfols") contain mainly 10 to 22 carbon atoms in their main chains and are in accordance with fatty alcohols obtained from natural sources.

In the Oxo Process, carbon monoxide and hydrogen are added to olefines in such a way that aldehydes are created having one carbon atom more than the starting olefine. These are simultaneously converted into the corresponding alcohols. The main products of the Oxo Process are butanols, methylheptanol, 2-ethylhexanol, and alcohols containing 8 to 13 carbon atoms in the alkyl chain.

Alcohols from the Oxo Process used for the synthesis of alkyl sulfates contain links of even and uneven numbers in the alkyl chain depending on the starting olefine employed. Although they are largely unbranched, they always contain a certain ratio of methyl and ethyl

side-chains in α -positions to the OH-group. However, this has only a slight influence on the surface-active properties of the corresponding alkyl sulfates.

4 ALKYL ETHER SULFATES

It is only a small step from the alkyl sulfates to the so-called alkyl ether sulfates. These surface-active agents are made from alcohols which are ethoxylated. The formed fatty alcohol polyglycol ethers possess a final OH-group which then reacts with sulfuric acid. Fatty alcohol polyglycol sulfates are characterized by an insensitivity to water hardness and low irritation of the skin. Their aqueous solutions can be easily thickened by the addition of sodium chloride. These properties thus attract attention for the use of fatty alcohol polyglycol sulfates in cosmetic products.

The sodium salts of coconut oil fatty alcohols (12–14 C-atoms), with a degree of ethoxylation of 2–3, are mainly used. These surfactants still contain – due to the statistical contribution of the ethylene oxide adducts – considerable amounts of the starting alcohol, which is converted by sulfation and neutralization reactions into the corresponding alkyl sulfate (as described below).

Besides the ether sulfates derived from coconut oil fatty alcohols, it is possible to produce other compounds with a higher degree of ethoxylation by using, other alcohols as starting materials. In this way, the hydrophilic/lipophilic balance (HLB) value can be widely varied. Thus, additives can be produced for oil-in-water (O/W) or water-in-oil (W/O) emulsions, for use in saline water, for detergents, and for dispersants of lime soap.

Ether sulfates are prepared in substantial quantities in short-time reactors by using gaseous sulfur trioxide. The quality of the ether sulfates depends on a short reaction time and a reaction temperature not exceeding 60°C. It is also necessary to keep the ratio of SO₃ to the ethylene oxide adduct exactly in the range of 1.1–1.3.

Amidosulfuric acid or chlorosulfuric acid can also be used for the sulfation of alkyl polyglycol ethers. The formed sulfuric acid semi-ester can be neutralized by either caustic soda solution, ammonia or nitrilotriethanol. The acid reaction mixture has to be neutralized immediately so as to avoid disintegration reactions which take place in the acid environment. Such reactions would otherwise lead not only to “dark” by-products but also to the formation of dioxane. The ether sulfates produced nowadays cover all demands for safety from toxic by-products.

Ether sulfates are sensitive to hydrolysis in acid solution and because an acid salt is formed by hydrolysis, the reaction would then become autocatalytic. Therefore, commercially available ether sulfates are usually buffered. Such products contain concentrations of ether sulfates of < 30%, or 65–70%. In the region between these concentrations, ether sulfates form very rigid gels.

The viscosity of aqueous solutions of ether sulfates can be increased by adding an electrolyte, usually common salt. This effect depends on salt concentration and the structure of the particular ether sulfate. As a general rule, it can be said that this thickening effect will happen at lower concentrations of salt, the more branched parts there are in the alkyl chain. This means, in practice, that thickening of solutions of alkyl ether sulfates based on oxoalcohols with a proportion of branched alkyl chains will occur at lower concentration of salt than is the case for alkyl ether sulfates based on pure linear alcohols. The increase of viscosity by the addition of salt also takes place in mixtures of ether sulfates with other types of surfactants.

Because ether sulfates are good foam-forming substances and also possess good solubilities in hard water they are used in many liquid formulations. In particular, they are used in cosmetic products like body cleansing lotions, shampoos and shower gels. They are also part of many liquid household cleaners and dishwashing agents.

5 ALKYL ETHER CARBOXYLATES

The hydrophilic component of these molecules is a carboxylic group, as is the case in the soap molecule. In general, an aceto- or propiocarboxylic group is attached to the polyoxyethylene chain by an ether bond. The free alkylcarboxylic acids can be prepared from salts such as fatty acid soaps. In contrast to alkyl ether sulfates, alkyl ether carboxylates contain no ester bonds and therefore they are not susceptible to hydrolysis.

A straight forward method involves a preparation after the Williamson synthesis, which does have some industrial application. In this, the OH end-group of the alkyl polyoxyethylene as starting material is converted by monochloroacetic acid and metallic sodium to form the ester carboxylate and sodium chloride.

Alkyl polyglycolether carboxylates are produced industrially by a modified method where sodium hydroxide solution is used instead of metallic sodium. A molar excess of 20–30% of NaOH/chloroacetic acid with respect to the alkyl polyglycolether is necessary to obtain a high yield of the ether carboxylate. Alkylphenol polyoxyethylene carboxylates or alkyl

polyoxypropylene carboxylates can be obtained by the same procedure.

The necessary creation of sodium chloride is a disadvantage in industrial production. It is possible to form the carboxylic acids by stirring solutions of ether carboxylates with hydrochloric acid or sulfuric acid at ca. 80°C. After stirring, an upper layer is formed containing the ether carboxylic acid, while the lower layer consists of a (high-concentration) saline solution and some by-products such as glycolic or diglycolic acid.

Another procedure for the production of ether carboxylates is the catalytic oxidation of the nonionic surfactants by oxygen or air. While in the Williamson synthesis with chloroacetic acid, two carbon atoms are added to the nonionic, the oxidation route converts a CH₂OH group into a carboxylic group. This process is carried out in the presence of platinum or palladium as catalysts at a temperature of 40–100°C.

Ether carboxylic acids are able to undergo the same reactions as fatty acids, e.g. esterification, and the formation of amides and acid chlorides. This leads to a great variety of different structures for tailoring the desired properties.

Alkyl polyether carboxylates are mainly produced by synthetic methods involving monochloroacetic acid. They are in general, shipped as ester carboxylic acids, which are clear liquids. If necessary, they can be neutralized before use. Alkyl polyether carboxylates offer outstanding stability against water hardness. They are mild to the skin and show excellent dispersing and emulsifying properties. They are readily used in cosmetic formulations and household cleaners. In recent years, polyether carboxylates have been reported as useful additives in enhanced oil recovery, due to their outstanding emulsifying properties under saline conditions and at high temperatures.

6 α -OLEFINESULFONATES

The reaction of sulfur trioxide with α -olefines in molecular ratios gives rise to two main products, i.e. isomeric alkenesulfonates and sultones. The 1,2-sulfone is produced first, followed by transformation into the 1,3- and 1,4-sultones. Hydrolysis then leads to hydroxyalkanesulfonates. The overall synthesis is a four-stage process of sulfonation, transformation, neutralization and hydrolysis. The complex mixture of isomeric alkenesulfonates and hydroxyalkanesulfonates is known under the collective term of " α -olefinesulphonates", an anionic surfactant that is itself a blend of different

surfactants. In addition, the final product also contains multiply-sulfonated olefines and other by-products. Particularly in the USA and Japan, the manufacturing of olefinesulfonates has been thoroughly studied after α -olefines became available on a large scale from ethylene oligomerization. Olefinesulfonates are produced by the electrophilic addition of sulfur trioxide to alkenes containing a double bond in the α -position. This reaction is very exothermic. A discoloration or even the formation of coal-like materials can easily take place. Therefore, the heat of reaction must be removed immediately. In particular, in the manufacture of olefinesulfonates, reactors for achieving sulfonation in a short time have been developed. The latter are nowadays also used for preparing alkylbenzene sulfonates and alkyl sulfates under mild conditions.

In such reactors, the starting material comes into contact with diluted SO₃ gas for only a short time. The reaction heat is removed by indirect cooling. Reaction takes place in a tubular reactor which is cooled from the outside by water. In these (falling-film) reactors the α -olefines are sulfonated with SO₃ gas diluted with air or nitrogen. A molar ratio of 1.0 to 1.2 of SO₃ is used at a temperature of 25–30°C.

The mixture has to be allowed to age for rearrangement of the unstable 1,2-sultone to alkenesulfonic acids and 1,3- and 1,4-sultones. That is carried out to minimize the content of the 1,2-sulfone, or otherwise this would be transformed by hydrolysis to the insoluble 2-hydroxyalkanesulfonate. The highly reactive 1,2-sulfone, the rearranged sultones or the formed alkenesulfonic acid may further react with SO₃ to give disulfonic acids and sultone sulfonic acids.

In the following stage, the reaction mixture is neutralized by caustic soda solution. In this neutralization step, only the free sulfonic acid component will be dissolved. The water-insoluble mixture of sultones must undergo an alkaline or acid hydrolysis. This takes place in a reactor at a hydrolysis temperature of 150–160°C for ca. 30 min. This leads to a nearly complete hydrolysis of the sultones to sodium 3-hydroxyalkanesulfonates and sodium 4-hydroxyalkanesulfonates.

The composition of the final product depends on the olefine feedstock, the sulfonation process and the manufacturing conditions. A typical product composition contains 2 parts of sodium alkenesulfonate to 1 part of hydroxyalkanesulfonate, apart from 0–10% of sodium disulfonate and less than 2% of unsulfonated matter and sodium sulfate. Unhydrolysed sultones and unreacted matter are only present in concentrations of ≤ 50 ppm. In addition, no severe toxic effects are known for α -olefinesulfonates.

In the USA, this surfactant is a well established product used in many household and industrial formulations. In particular, in light-duty liquid detergents the water solubility and soil removal ability of α -olefinesulfonates are excellent. In addition, α -olefinesulfonates are compatible with many other surfactants on the market, including alkyl sulfates, alkylbenzene sulfonates and alcohol ethoxylates. Therefore, α -olefinesulfonates can be used to obtain synergistic effects in binary or ternary mixtures.

The reaction product is a mixture of 50–60 individual structural forms of alkenesulfonates and 40–50 forms of hydroxyalkanesulfonates. The final product is bleached by hydrogen peroxide and is available as a slurry of 30–40% active matter. Although the α -olefinesulfonates offer a lot of properties which are valuable in many applications, these materials have not achieved great importance in Europe. Their sodium salts are non-hygroscopic and will easily crystallize. Thus, they can be favourably used for the production of free-flowing powder detergents which will not become sticky under conditions of high humidity. However, the final product partly contains unsaturated compounds. Therefore, they are somewhat susceptible to autoxidation. Olefinesulfonates derived from olefines with 12–14 carbon atoms are very soluble in water, while already with 16–18 carbon atoms the solubility will, remarkably decrease. The feedstock of α -olefinesulfonates for technical applications is mainly a blend of C_{14-16} olefines. The critical micelle concentration of this α -olefinesulfonate mixture is 0.6 g/l, while its aqueous solution shows a depression of the surface tension to 32 mN/m. Such α -olefinesulfonates are good detergents and form stable foams, although their wetting ability is only moderate. The detergency rises with increasing alkyl chain length of the starting olefine. This also means that the best detergency properties are to be expected at higher temperatures, where these compounds will have a sufficient solubility.

The properties of α -olefinesulfonates used in the trade alter according to their proportions of hydroxyalkane- and alkenesulfonates. Hydroxyalkanesulfonates with the hydroxy group in the 2-position are poorly soluble in water, while the hydroxy group in the 3- or 4-positions results in a very good solubility.

Such properties thus enable their use in detergents, cleaners, dishwashing formulations, and also in body-cleansing products. They are particularly useful in dry cleaner, formulations, e.g. for carpet cleaners. The world-wide consumption of α -olefinesulfonates in the last decade was of the order of 85 000 t, that is 1.5% of the total consumption of surfactants.

7 α -SULFO FATTY ACID METHYLESTERS

Fatty acids in the form of their methylesters are basic starting materials for the production of surface-active α -sulfo fatty acid methylesters. While the reaction of fats and oils with concentrated sulfuric acid or oleum was limited to compounds with double bonds or OH-groups in the molecule, saturated fatty acids also became available as feedstock after the introduction of sulfonation with diluted sulfur trioxide gas. The sulfonate group enters in the α -position to the carboxylic group in this process.

The sodium salts of α -sulfo fatty acid methylesters are soluble in water and resistant to hydrolysis in the pH range of 3–10. They are also only slightly sensitive to water hardness and offer good detergency in combination with other surfactants. Their foaming ability decreases strongly from the lauric methylester to the stearic methyl ester.

The preparation of α -sulfo fatty acid methylesters is a two-stage process taking place at two different rates. At first, an addition compound of 1 mol of methylester with 2 mol of SO_3 is formed. Then, in the following reaction, 1 mol, of SO_3 is split off, to form the final ester. This sulfur trioxide will slowly react further with another methyl ester. Using the fatty acid methylester and SO_3 in a molar ratio results in an undesirably long reaction time. Therefore a surplus of sulfur trioxide is used. The reaction mixture then consists of the main product, the α -sulfo fatty acid methylester and also its anhydride with SO_3 . By neutralization with a solution of caustic soda, on the one hand the desired sodium salt of the required ester is formed, while on the other hand the anhydride is transformed to the corresponding disodium salt and sodium methylsulfonate. In order to achieve a complete transformation of the fatty acid methylester, a certain amount of the undesired disodium salt has to be expected.

In practice, the sulfonation process is carried out in two stages. In the first stage, the methylester is converted at temperatures below 50°C by SO_3 which is obtained – diluted with air and nitrogen – by the burning of sulfur, followed by catalytic oxidation. In the second stage, the reaction mixture is allowed to go to completion at 70–90°C over a period of ca. about 1 h. Sulfur trioxide is used in an excess of 10–20 mol%.

The reaction products are dark-coloured and are bleached by the addition of water and hydrogen peroxide, followed by neutralization with sodium hydroxide. The final ester product contains 10–20% of the barely soluble disodium salt, and is marketed as a paste of

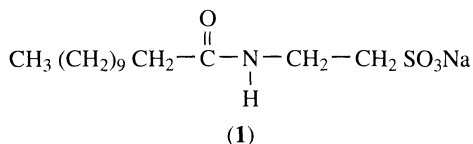
40% active matter. In the range of 40–70 wt%, slurries of these esters show a high viscosity, which leads to considerable problems in handling.

These esters have found only a small use in fabric detergents due to their expensive production process. However, they have been suggested for use in cosmetics because they show only a slight irritation of the skin. They are also used as lime soap dispersants.

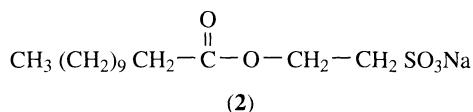
8 ESTERS AND AMIDES OF FATTY ACIDS

Fatty acids can also act as the hydrophobic component of a surface-active substance by reaction of the carboxylic group with OH- or NH-containing molecules. One example of this is the class of so-called protein fatty acid condensates, which are soft to the skin and are therefore used in cosmetic products. The fatty acid esters or acid chlorides are converted to amides or esters of amino acids or sulfonic acids containing an OH-group. In this way taurates are formed by the reactions of 2-aminoethane sulfonic acid with fatty acids such as lauric, myristic or stearic acid.

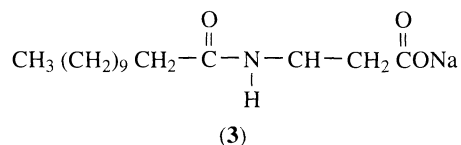
In sodium lauroyl taurate, the sodium ion is attached to the sulfo group while the carboxyl group of the fatty acid is converted to an amide (1).



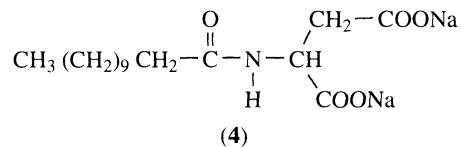
In a similar way, the fatty acid can be attached to 2-hydroxyethanesulfonic acid, thus forming an ester instead of an amide. The sodium salt is the so-called sodium isethionate (2).



Reaction of *N*-methylaminoacetic acid with fatty acids such as lauric, myristic or stearic acids leads to the sarcosinates. The *N*-methylglycine can be easily obtained from the reaction of formaldehyde, sodium cyanide and methylamine. In this compound, the hydrophilic group is a carboxylic group as in soap. The hydrophobic part results from the fatty acid attached to the sarcosine by an amide bond (3).



Asparaginate are the reaction products of 2-amino succinic acid (aspartic acid) with fatty acids or their acid chlorides. For instance, the sodium salt of lauroyl asparaginate (4), formed by this reaction, is shown below.



9 PETROL SULFONATES

When petroleum or kerosene (as the raw materials for gas oil or lubricants) are purified by using oleum or sulfuric acid, a reaction with the aromatic compounds takes place. While these substances were originally seen as waste products, later their chemical structures and surface-active properties were identified, thus leading to special applications for such products. Nowadays, petroleum fractions with a high content of aromatic hydrocarbons are treated with sulfur trioxide to form alkylaryl sulfonates. These products are then transformed into the sodium, ammonium or alkaline-earth salts. They are soluble in oils and therefore are of some importance as additives in lubricants, oil fuels and corrosion-inhibiting oils. Further more, they are also used as auxiliaries in production of fabrics and as dispersants in enhanced oil recovery processes.

10 ALKYL BENZENE SULFONATES

The anionic surface-active compounds with the largest volume of production are the alkylbenzene sulfonates. Here, the possibility of an easy insertion of a sulfonic acid group into the benzene molecule is used to obtain inexpensive surfactants. Suitable starting materials are alkylbenzenes with an alkyl chain length of ca. 12 carbon atoms, obtained by the application of olefines or monochloroalkanes to the benzene ring.

Tetrameric propene is used as the basic starting material for the synthesis of the so-called tetrapropylenebenzene sulfonate (TPS), which offers favourable application properties at a relatively low cost of production. Thus, it soon found use as a detergent prior to the introduction of the above-mentioned alkyl sulfates and alkanesulfonates. However, TPS contains a highly branched alkyl chain, and as a result its biodegradability was so poor that effluents with a high concentration of detergent began to occur in slowly flowing rivers and lakes, so giving rise to thick layers of foam. Therefore, already by the 1960s the use of TPS was restricted in many industrial countries.

The chemical industry reacted quickly to this challenge by producing alkylbenzene sulfonates with straight alkyl chains which are easily biologically degradable. These compounds are nowadays the basis of most detergent formulations.

In contrast to TPS with its branched alkyl chain, *n*-dodecylbenzene sulfonate exhibits an extremely fast rate of biodegradability. The change-over from a branched to a straight-chain structure is easily achieved, and thus by the use of Ziegler synthesis and molecular-sieve extraction techniques, industrial processes for the production of linear olefines and *n*-alkanes soon became readily available. These are the basic starting materials for the synthesis of linear alkylbenzene derivatives.

The sulfonation of an alkylbenzene is carried out by using sulfur trioxide (diluted to 4–8% by air or nitrogen). The reaction is very rapid and is accompanied by generation of heat. Therefore, in modern continuous-operation facilities a film reactor is used which allows reaction to take place in thin and well-cooled falling films. The sulfur trioxide is often produced by rapid burning of elementary sulfur, followed by catalytic oxidation of the sulfur dioxide thus produced by oxygen from an excess of air. In the manufacture of detergents, alkylbenzene sulfonates are produced often from the respective alkylbenzene and sulfur trioxide in synthesis facilities directly adjacent to the production line of the detergent.

The alkylbenzene sulfonic acid produced is neutralized with sodium hydroxide solution, forming a viscous slurry containing 50–60% of active matter. It can be shipped in the acid form or neutralized with other alkalis like potassium hydroxide or amines. Neutralization is in most cases carried out continuously by feeding the alkaline solution into a stream of circulated neutralized product to avoid forming Gel-like structures.

Alkylbenzene sulfonic acids are strong acids, which are easily soluble in water for up to 12–14 carbon atoms in the side-chain. Alkylbenzene sulfonates with

longer alkyl chains and containing alkaline-earth ions are soluble in mineral oil. The colour of the acids is yellow to brown, depending on the temperature regime, which would be lightened by neutralization. Often, the product is bleached by using hydrogen peroxide or chlorine.

Commercial dodecylbenzene sulfonate is a mixture of decyl- to tridecylbenzene sulfonates, made from alkylbenzenes produced from an aluminium chloride catalysed synthesis. Thus, it contains a significant proportion of the 2-alkyl isomers. Its solubility in water is better than the solubility of the corresponding sulfonate derived from alkylbenzenes catalysed by hydrofluoric acid. The viscosity of concentrated slurries is lower in the case of aluminium chloride catalysed alkylbenzenes.

The surface activity of alkylbenzene sulfonates depends on the length of the alkyl chain and the solubility in water. An optimum occurs at 11 to 15 carbon atoms in the side-chain. Technical-grade alkylbenzene sulfonates show a critical micelle (forming) concentration of ca. 0.5 g/l at a surface tension of the solution of 35 mN/m.

Alkylbenzene sulfonates, as a mixture of homologous and isomeric decyl- to tridecylbenzene sulfonates, with an average of 12 carbon atoms, is an universally applicable surfactant. Due to the fact that it is even stable in acid solution – in contrast to alkyl sulfates or alkyl ether sulfates – it can be used over a widespread field of applications.

Alkylbenzene sulfonates are the main surfactants used in household cleaners, detergents and sanitary formulations, as well as in industrial and institutional cleaners. They are used in the production of fabrics. They are also used as emulsifiers, in many technical processes as wetting agents and dispersants. e.g. in polymerisation processes and in the formulation of plant protection products.

These sulfonates can be used to optimize the efficacy of cationic inhibitors for protecting metals against corrosive acids. Such inhibitors form adsorption layers on the surface of a metal which will act as a penetration barrier for the acid medium, as well as for the reaction products. However, there is no continuous layer formed by the cationic surfactant because the surfaces show sites of different charges. An inhibitor consisting of a mixture of cationic and anionic surfactants leads to a compact adsorption layer and to a high effectiveness of the inhibitor system. Although the adduct of anionics and cationics is poorly soluble in aqueous acid solutions, an inhibitor concentration of ca. 5 ppm is already sufficient for the protection of the metal.

Linear alkylbenzene sulfonates are the surfactants that have been most comprehensively tested for their environmental behaviour. Due to their extensive application, the ways of degradation and mineralization of the substance itself, its by-products and metabolites have been comprehensively studied. Under aerobic conditions, these sulfonates are easily biologically degraded. Although biological degradation will not take place under anaerobic conditions, traces of sulfonates that appear in sewage sludges by forming insoluble salts, e.g. with calcium ions, will be easily mineralized, undergoing aerobic degradation once more when the rotted sludge is brought into contact with soil.

Alkylbenzene sulfonates are on the market in the form of slurries with a proportion of active matter of 50–60%, or as powders or granules with 80–90% active content.

The linear sulfonates are inexpensive surfactants with optimal properties for many applications. By mixing with other kinds of surface-active agents synergistic effects can occur that allow adjustment of the properties of the mixtures to special demands.

A well known example is the mixture of an alkylbenzene sulfonate with soap. Both of these types of surfactants alone result in a strong formation of foam when used in water free from hardness and at higher temperatures. The stability of the foam is lowered drastically by the forming of mixed films in the lamellae of the foam if soap is added to the sulfonate.

A regime for the formed foam can be achieved by selecting the right fatty acids in the soap component. In detergents for the washing of laundry, a good foaming ability in the temperature range of 20–40°C

is desired. However, with rising temperatures in the washing drum too much foam will be created. By mixing an alkylbenzene sulfonate with soap containing alkyl chains from 18 to 22 carbon atoms the soap will show a notable solubility only at temperatures above 50°C. In this way, any influence on the forming of foam will only arise at higher temperatures. Figure 12.1(a) shows the foam height as a function of the alkyl chain length, proportion of components in the mixture, and temperature.

A punched disc rotating in a glass cylinder creates the foam (see Figure 12.1(b)). Depending on the temperature, an equilibrium occurs when as many foam bubbles are newly produced in the same time interval as the number that disappear. The foam increases sharply with rising temperature when soap is absent. If soap is added in a sufficient amount, a depression of the foam is achieved, although the observed height of lather depends on the solubility of the soap used. Soaps with alkyl chains of 12 to 16 carbon atoms are soluble at low temperatures. Thus, the foam is already depressed over the temperature range from 20 to 40°C, where a thicker foam layer is desired in handwashing. In comparison, soaps with alkyl chains containing of 18 to 22 carbon atoms will only depress the foam significantly at higher temperatures.

For a decisive removal of fatty dirt from hydrophobic fibres, it is necessary for that a fat-soluble surfactant to penetrate into the fat layer, thus supporting its removal. That can be achieved by using ethoxylated alcohols at a low level of ethoxylation.

Mixtures of adducts of ethylene oxide with alkylbenzene sulfonates therefore show a division of the

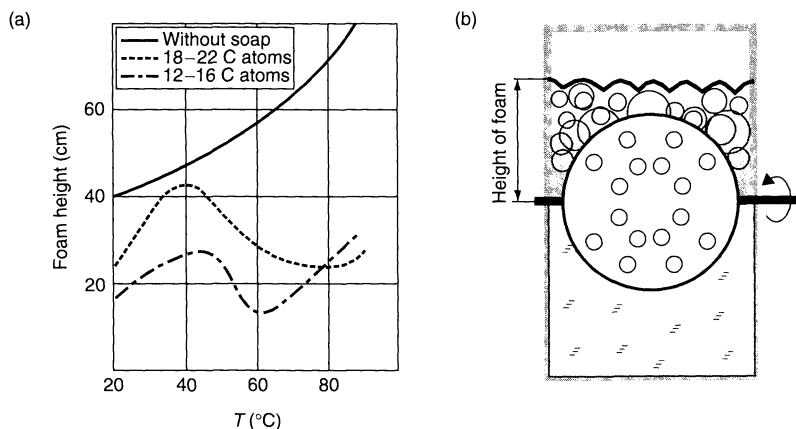


Figure 12.1. The formation of foam: (a) variation of foam height as a function of temperature on the addition of 4% soap to an alkylbenzene sulfonate-based detergent system; (b) apparatus used to create the foam

work that leads to a better cleaning performance. The nonionic surfactants take over the job of removing the fatty film on the fabric and decreasing the interfacial tension between the hydrophobic solid surface and the aqueous solution. The alkylbenzene sulfonates, on the other hand, take the role of dispersing pigments and raising the stability of the dispersion of soil in the washing liquor. Similar synergistic effects can be observed with other kinds of surfactants.

Nearly all surfactants used in the trade are already mixtures of homologues and isomers by themselves. Thus, any additional beneficial effects will occur only between classes of different surfactants. Such synergisms make it possible to obtain the required effects at lower total concentrations of the surfactant mixture than those of the single components. This is important for the proportion of cost to performance, as well as for the reduced effects on the environment.

Many publications report the interactions between various surfactants. In most cases, well-defined physical methods are used. This leads to well-defined conditions for the tests to yield reproducible results. To avoid distortion of the results by the presence of by-products, pure surfactants are used, which are dissolved in distilled water or in solutions of salts such as sodium chloride or potassium chloride in known concentrations. Under these conditions, the properties of the solutions can be very accurately studied for their dependence on concentration, proportion of mixture, temperature and time.

Often, synergistic effects are observed. This means that the measured value will not change corresponding to the molecular fraction of the mixture, but will show a maximum or minimum, often within narrow limits. Depending on the test procedure being used, different extreme values can be observed, e.g. the maxima of stability of foam films, and of elasticity or viscosity of surface films, and of the depression of surface tension, or the minima of the critical micelle (forming) concentration. Because the interfacial activity of the single components may be very different, such extreme values will often already arise at a small proportion of the component with the stronger interfacial activity in the mixture.

However, in the daily practice of the application of surfactants there is in most cases an interaction of the surfactant mixtures with the extended surfaces of solids. This leads to a decrease in the amount of the most surface-active components in the solution by adsorption at the solid surface. Any synergisms observed in laboratory tests will therefore not occur any more, and a shift of the synergistic effects to higher concentrations will be observed. This changes drastically the proportion of the synergistic-effective mixture. Especially in systems

with several components, the desired effect of a mixture can be lost by adsorption of one or more components on extended solid surfaces.

This is the case, for instance, when microemulsions are used for enhanced oil recovery. By adsorption of minor components at the rock matrix, the proportion of the mixture can be so drastically altered that the forming of a microemulsion with the oil is no longer possible. The ratio of the surfactants present is then far away from the necessary range under the given thermal conditions.

However, changing of the composition and properties of surfactant mixtures while in use can also be required, e.g. in breaking oil-in-water emulsions of the effluents in car washing installations. By dilution with rinsing water and reaction of the calcium ions from the water hardness, insoluble salts of, e.g. alkylbenzene sulfonates will be formed. Thus, the remaining concentration of surfactants is not further able to stabilize the emulsion. Simultaneously the water-insoluble calcium alkylbenzene sulfonate will attract small oil droplets. In this way, the emulsion is broken up and a separate phase of oil is formed that can be separated.

In mixtures, a mutual solubilization of the surfactants takes place. Thus, the solubility and as a result the efficiency of difficultly soluble surfactants can be shifted to a lower temperature range.

Figure 12.2 shows a triangular diagram for a mixture of an alkylbenzene sulfonate, alkyl sulfate and $C_{16/18}$ -soap, relating to the detergency behaviour cotton at 25°C. The performance is presented in the form of contour lines as a percentage of the measured brightness to the theoretically possible level. This diagram shows

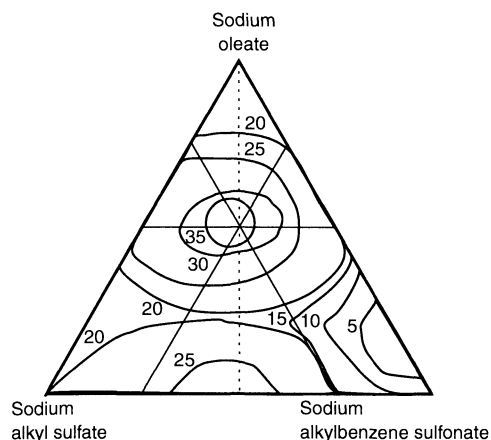


Figure 12.2. Triangular diagram illustrating the detergency performance of a mixture of surfactants on soiled cotton at 25°C, as a function of the proportions of the three components

that it is only in a small area of ca. 25% alkylbenzene sulfonate, 25% alkyl sulfate, and 50% soap will a maximum of detergency performance be obtained. It is especially remarkable that ca. 50% of soap is needed to achieve this maximal effect.

Beginning with 100% of sulfonate, the measured detergency drops from 10 to 5% by the addition of 2–10% of soap. This could give rise to the statement that the addition of soap lowers the detergency of the alkylbenzene sulfonate under the conditions of the study. However, on further addition of soap, the detergency increases to 25% and this is a higher value than both components will show when used as single surfactants. Although the washing liquor was of medium hardness, a sufficient amount of sodium triphosphate was added to avoid precipitation of lime soap.

In this study of detergency at a low temperature, the effect of the alkylbenzene sulfonate as a single surfactant was very small. The alkyl sulfate shows a slightly higher performance. The mixture of these two surfactants shows an increase to 30%. The ternary mixture, with soap in all proportions of alkylbenzene sulfonate and alkyl sulfate, leads at first in a drop in detergency performance. A significant rise of detergency occurred first above a content of 40% soap in the mixture.

In actual practice, the synergistic effects of detergency often only occur if the proportion of the components is high enough to be effective in the presence of extended surfaces from fibres and soil particles. Therefore, it is very difficult to correlate results obtained on pure systems with those obtained for actual applications.

11 ALKANE SULFONATES

By the radical addition of sodium bisulfite to α -olefines, alkane sulfonates are obtained which carry a sulfo group at the end of the chain. These compounds possess relatively poor solubility in water. In contrast, the sulfo group in technical alkane sulfonates is statistically distributed along the alkyl chain. This leads to a good solubility.

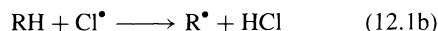
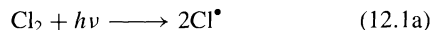
Alkane sulfonates are mainly produced by two methods, i.e. the process of sulfochlorination and the process of sulfoxidation. In both processes, a radical chain reaction takes place and therefore the alkane starting material must be free from branched compounds, olefines and aromatics because such compounds will act as chain-stoppers in the chain reactions. Highly pure straight alkanes of paraffin fractions from 13 to 18 carbon atoms are used, with an optimum in the range of 14–17 carbons in the chain.

In both cases, a mixture of alkanes with sulfur dioxide and chlorine or oxygen, respectively, is irradiated by actinic light, giving radicals which lead to sulfochlorides or sulfonic acids. Because this reaction can take place repeatedly at one alkane molecule, the process is interrupted after 1 to 30% of the starting material has reacted, the formed alkane sulfonate extracted after the addition of caustic soda solution, and the remaining alkane recycled back into the process.

11.1 Sulfochlorination

The main products of the sulfochlorination process are the alkane sulfochlorides, which in turn are saponified to the desired alkane sulfonates. This process was first discovered in the 1930s, and industrially realized shortly afterwards. Sulfochlorination is a radical chain reaction, initiated by irradiation with short-wavelength light.

Because the dissociation enthalpy of chlorine is 250 kJ/mol, the reaction can be initiated by using visible light in the wavelength range 370–478 nm, forming chlorine radicals as follows:



The yield of alkane sulfochloride depends on the molar ratio of SO_2 to Cl_2 , the purity of the feedstock and the reaction temperature. Optimal conditions in the technical process are 35–40°C and a molar ratio of SO_2 to Cl_2 of 3:1. Nevertheless, there are side-reaction such as the chlorination of the alkane, chlorination of the formed alkane sulfochlorides, and the formation of sulfuric acid from traces of water. In addition, a second sulfochlorination reaction may take place. Thus, the main components of the sulfochlorination process are the desired alkane monosulfochloride, di- and trisulfochlorides and chlorinated products of these species, as well as monochloroalkanes and dichloroalkanes.

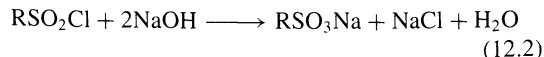
The sulfochlorination process is carried out in acid-proof coated vessels. These reactors (with a volume of 10–12 m³) are equipped with gas-inlet nozzles and glass pipes containing fluorescent lamps. The reaction mixture is pumped to heat exchangers in a circuit, because at higher temperatures chlorination instead of sulfochlorination will dominate. The advantage of using fluorescent tubes radiating visible light is a long lifetime of four to six years for these lamps. Eight vessels of this

kind are connected in a reactor cascade arrangement. In this way, the formation of poly sulfochlorinated alkanes is limited. Circulating and cooling systems of appropriate design also avoid the formation of di- and polysulfochlorides.

An initial reaction time of 4 to 5 h is necessary for a conversion of ca. 25% of the starting material. The exhaust gas contains mainly hydrogen chloride and sulfur dioxide. While hydrogen chloride is absorbed adiabatically by water, the excess of sulfur dioxide can be liquefied for recycling back into the process or be converted into sulfite solution. Residues of hydrogen chloride and sulfur dioxide are stripped off from the sulfochloride mixture by using warm air. A schematic of a typical sulfochlorination plant is shown in Figure 12.3.

The reaction mixture is saponificated by 10% caustic sodium solution at ca. 90°C. After this stage, the mixture is conveyed into a settler where an upper phase of non-reacted alkane will separate, which is then fed back into the process after refining. The lower phase contains sodium chloride in addition to the formed sodium alkane

sulfonates, according to the following equation:



In addition, the reaction mixture also contains 4–8% of unreacted solubilized alkane. The pH value may be adjusted in the range of 3–5 to improve the conditions for separation. After cooling the NaCl brine, which contains trace quantities of the alkane monosulfonate, 1.5–2.0% di- and polysulfonates will separate out. Almost all of the alkanes and sulfonates are completely present in the upper phase. The alkanes are mainly stripped off by steam distillation at ca. 200°C, while at this temperature molten alkane sulfonate is simultaneously formed. This is then transformed into flakes on cooling rolls or other cooling equipment.

Sodium alkane sulfonates are hygroscopic and therefore they have to be shipped in sealed waterproof packages. They are also available in the trade as ca. 35% solutions or 60–70% pastes. These consists of ca. 90% monosulfonate, ca. 10% di- and polysulfonates, and very small amounts of NaCl and neutral oil.

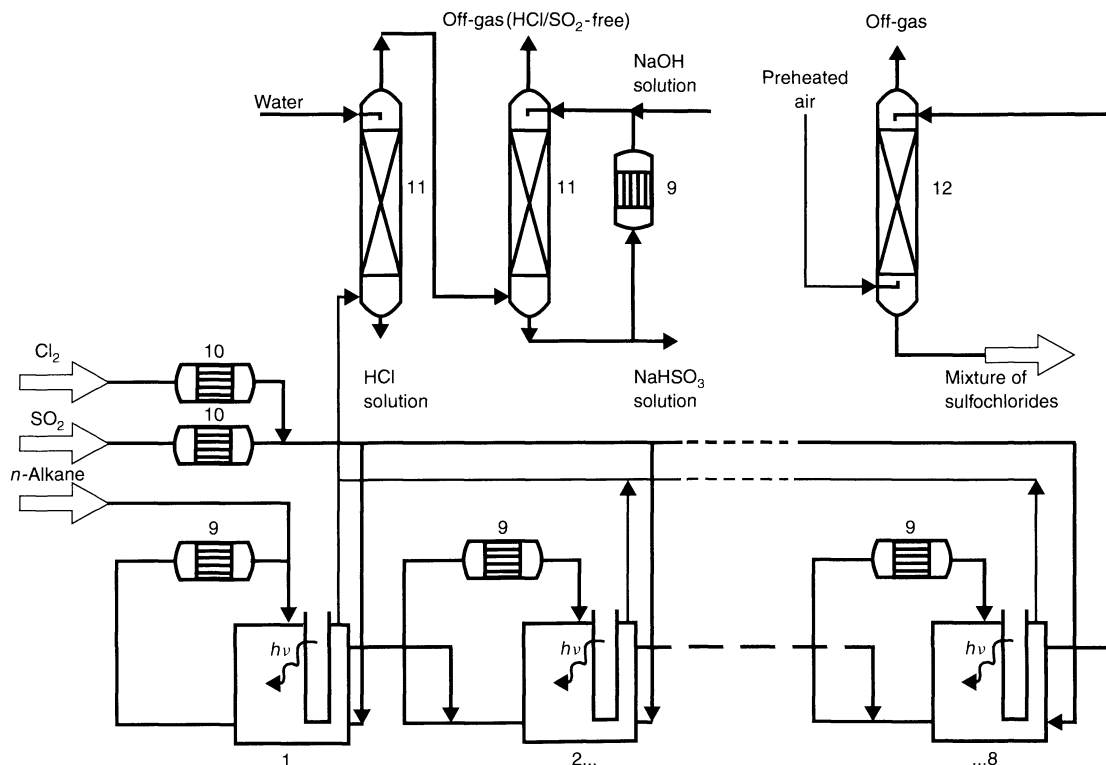
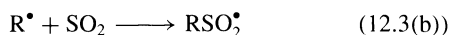
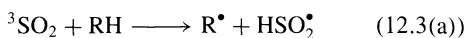


Figure 12.3. Schematic of a typical continuous sulfochlorination plant: (1, 2–8) sulfochlorination reactors; (9) recirculation coolers; (10) vaporizers; (11) absorption columns; (12) blow-off column

Sulfochlorination was the first successful procedure for preparing alkane sulfonates. Nowadays, however, these materials are mainly produced by the sulfoxidation process.

11.2 Sulfoxidation

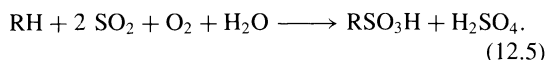
This reaction, of *n*-alkanes with sulfur dioxide and oxygen, was introduced in the 1940s. Sulfoxidation is also started by a radical chain reaction. By using ultraviolet light of wavelengths longer than 320 nm, excited triplet sulfur dioxide is formed, and the reaction combines according to the following:



The very unstable peroxy sulfonic acid is a source of many complex reactions, the presence of which will be minimized by using an excess of sulfur dioxide and water:



Because the paraffin/water mixture has to be in close contact with the gases sulfur dioxide and oxygen (in a molar ratio of 2:1), these three phases must be thoroughly mixed. The simplified overall equation of the total reaction is as follows:



Compared to sulfochlorination, multiple substitution is dominant in the sulfoxidation process. Therefore, the conversion is restricted to 1 mol% of each passage in a continuously working facility. The weakly exothermic reaction is run in the temperature range from 30 to 38°C.

The reaction mixture is circulated by the continuous addition of alkane and water. It is pumped to a separator where an aqueous phase and an upper phase of practically pure alkane are formed. In the aqueous phase, there is sulfuric acid and unreacted alkane in addition to the alkane sulfonic acid. After separation of the sulfuric acid, the alkane sulfonic acid, containing some alkane, is neutralized. The alkane is then separated by steam distillation and recycled. The final product is obtained as molten sodium alkane sulfonate and is available as either flakes or pastes.

11.3 Properties and applications of alkane sulphonates

Monoalkane sulfonates are the preferred materials because their properties are very similar to those of the alkylbenzene sulfonates. Products containing a higher proportion of di- or polysulfonated compounds show a limited detergency but are useful wetting agents.

The ratio of mono- to di- and polysulfonates in commercial products lies in the range of 5.5:1 to 8.6:1 for products derived from the sulfochlorination process and 9:1 to 10:1 in the case of sulfoxidation. Alkanes, measured as neutral oils have a content in all products of < 0.6 wt%. The origin of the manufacturing process can be traced by determining the presence of chloroalkanes. Typical for the sulfochlorination route are chloro organics up to 0.15% of measured chlorine. Their absence indicates the sulfoxidation process. However, the content of adsorbable organic halogen (AOX)-containing substances in the products derived from sulfochlorination will be completely mineralized by biological sewage treatment.

The biological degradation of alkane sulfonates occurs somewhat more easily than the degradation of alkylbenzene sulfonates. Alkane sulfonates are toxicologically harmless and ecologically safe. From recent investigations, it was found that even under anaerobic conditions adapted strains of bacteria are able to desulfonate alkane sulfonates.

Some “no-effect concentration” (NOEC) values where alkanesulfonates show no effect on biological samples are shown in Table 12.1. Owing to their good solubility in water, the stability of concentrated aqueous solutions at low temperatures and their chemical stability over the whole pH range and against oxidation agents, alkane sulfonates can be widely applied. These properties make alkane sulfonates valuable for preparing liquid cleaners, laundry detergents and dishwashing formulations. They are also a helpful auxiliary in emulsion polymerization processes.

However, alkane sulfonates cannot be produced as inexpensively as alkylbenzene sulfonates. Therefore, they are mainly used as special surfactants in blends

Table 12.1. NOEC values for various species at which alkane sulfonates show no biological activity

Species	NOEC value (mg/l)
Fish	1.2
Daphnia	0.6
Algae	6.1

with other surfactants in order to adjust the properties of the mixture to special requirements. They show synergistic effects in mixtures with nonionics, ether sulfates and alkyl polyglucosides. Blends of alkane sulfonates of high purity with surfactants gentle to the skin – such as amphoteric, fatty alkanolamides and protein fatty acid condensates – are also suitable for cosmetic formulations.

Because of their rapid wetting ability, alkane sulfonates are used in many production stages in the textile industry. They are also useful in the pulp and paper industries as well as in many industrial and institutional cleaning processes.

Alkane sulfonates are components of bleaching and disinfecting solutions due to their stability towards strong alkaline solutions and oxidizing agents such as hydrogen peroxide and sodium hypochlorite.

The high wetting ability and thermostability are utilized by the addition of alkane sulfonates to water in fire-fighting applications. Such water systems will wet burning wood and plastics and penetrate into charcoal, thus cooling it below its flash-point. Furthermore, foam can be created to cover the burning material and separate it from the oxygen in the air.

Alkane sulfonates are applied in a widespread manner in emulsion polymerization. They are used as processing aids, in particular in the emulsion polymerization of vinyl chloride, vinyl acetate, styrene and acrylonitrile. Because they possess no double bonds, alkane sulfonates do not act as radical chain stoppers. Well-known lattices derived from emulsion polymerization are poly(vinyl chloride), ethylene-vinylacetate copolymers, polyacrylates, and butadiene and chloroprene rubbers. Alkane sulfonates also offer good stabilizing effects in lattices against coagulation by fillers.

The annual production of alkane sulfonates – which are mainly produced in Europe – lies in the region of 60 000 t, about 20% of which are exported to countries outside of Europe.

12 ESTERS OF PHOSPHORIC ACID

Although in most cases the bulk of anionic surfactants on the market are of the sulfonate, sulfate, or carbonate type, derivatives of phosphoric acid also show surface activity, with very interesting properties. The proportion of phosphorus-containing surfactants reaches about 1% of total surfactant production. It can be fundamentally stated that surfactants covering nearly all applications can be derived from phosphoric acid. It is often only the somewhat higher price which blocks the same

widespread use of phosphorus-containing surfactants when compared to the total output of surfactants in general.

Orthophosphoric acid, containing three acid OH groups in the molecule, offers many opportunities for the realization of surface-active molecule structures. However, phosphoric acid possesses additionally the ability to form polyacids in wide manner. Pyrophosphoric acid and triphosphoric acid are substances that have been known for a long time. This fact presents further possibilities for some interesting syntheses.

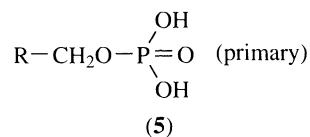
Phosphorus-containing surfactants exhibit a good solubility in saline solutions, they are insensitive to water hardness, they are able to disperse lime soap, and they act as corrosion inhibitors in acid media. They are also valuable components for obtaining synergistic effects due to the variety of possible molecule structures. However, until now this opportunity has only been seldom used, as can be deduced from the literature. In some fields of application, phosphorus-containing surfactants obviously offer many benefits when compared to other types of surfactants. In such cases, they have been applied to great advantage.

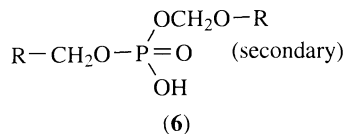
There are many parallels between the phosphates and sulfates of aliphatic alcohols. Both types of surfactants contain ester bonds which undergo hydrolysis in strong acid solutions. As a result, the production of esters is a key stage in the preparation of these phosphorus-containing surfactants.

By dry heating of the salts above a temperature of 140°C, decomposition will occur, forming the corresponding alkenes and an inorganic acid salt. In the same way that sulfonic and sulfinic acids are formed by C–S bonds, C–P bonds lead to phosphonic and phosphinic acids.

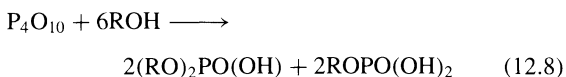
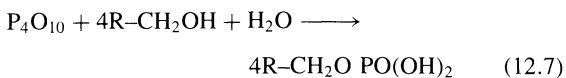
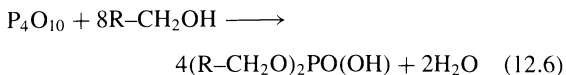
12.1 Phosphated and polyphosphated alcohols

In most cases, aliphatic alcohols with a chain length in the range of 10 to 20 carbon atoms are converted with phosphorus pentoxide to yield a mixture of alkyl dihydrogen esters (primary) (5) and dialkyl hydrogen esters (secondary) (6).





The reaction follows the following simplified equations:



Although the yield of the dialkyl hydrogen esters can be influenced by the ratio of alcohol to P_4O_{10} , in practice, mixtures of primary and secondary esters are obtained always, e.g. changing the molecular ratio of alcohol to P_4O_{10} from 2:1 to 4:1 results in an increase of the secondary ester in the mixture from 35 to 65%.

Long-chain alcohols, as well as traces of water in the alcohol or from P_4O_{10} , lead to a higher proportion of monoalkyl esters. Alkyl phosphates are described as being low-skin-irritant anionic surfactants, and are used in paste- and liquid-type skin cleansers. However, there are also some specific routes for the syntheses of defined primary or secondary esters.

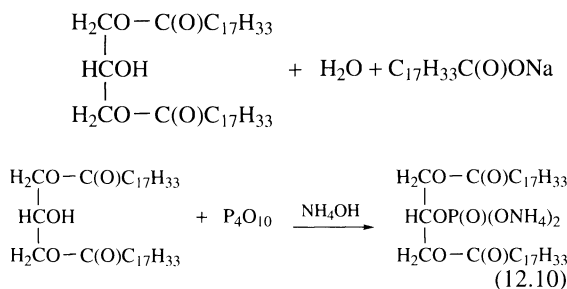
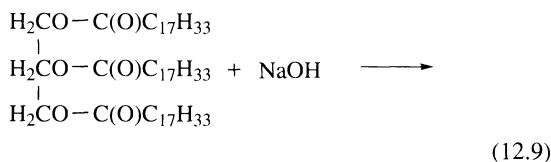
Monoester salts of phosphoric acid, for instance, are prepared by the reaction of alcohol (or ethoxylated alcohol), alkali fluoride and pyrophosphoryl chloride $(\text{Cl}_2\text{PO})_2\text{O}$ in a molar ratio of 0.9–1.5:0.05–1:1.0 at -50 to $+10^\circ\text{C}$, followed by hydrolysis of the Cl^- containing intermediates with a base. In this way, for example, 32.3 g $(\text{Cl}_2\text{PO})_2\text{O}$ was treated at -50°C with 23.9 g lauryl alcohol in the presence of 0.7 g KF and the mixture was slowly warmed to room temperature and then hydrolysed with H_2O and 40% NaOH to give 83% sodium monolauryl phosphate. These monoester salts show better washing and foaming efficiencies when compared to the corresponding commercial products.

One can also use OH-containing nonionic surfactants, with an OH end-group, for the reaction with P_4O_{10} . The optimal ratio of surfactant/ P_4O_{10} is 2.5–3:1. While the yield of mono- and diesters is significantly influenced by the water content of the starting materials, it does not depend on the reaction temperature. However, the quality of the surfactants is improved by using

tetraalkylammonium hydroxide as the base and a reaction temperature below 60°C .

Surfactants can also be obtained by the reaction of glycerol derivatives such as $\text{RCO}_2[\text{CH}_2\text{CH}(\text{OH})\text{CH}_2\text{O}]_n\text{H}$ ($\text{R} = \text{C}_{6-16}$ alkyl, $n = 1-5$) with P_4O_{10} at $60-80^\circ\text{C}$, followed by subsequent neutralization of the resulting phosphate ester acids with aqueous alkali or alkanolamine solution at $50-70^\circ\text{C}$. The preparation of surfactants by the reaction of P_4O_{10} with fats, oils and diglycerides is also described in early patents.

A specific example describes the reaction of P_4O_{10} with diglycerides from vegetable oil in the presence of isopropyl ether. The reaction product was neutralized with ammonia or other alkaline reagents, as follows:



Defined phosphoric acid diesters can be prepared by treating a liquid slurry of a phosphate monoester with epoxides in the presence of alkali compounds, e.g. a mixture of monolauryl phosphate sodium salt and triethylamine in water was treated with glycidol at 80°C for 8 h to give 98% of the lauryl(2,3-dihydroxypropyl)phosphate sodium salt.

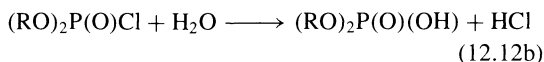
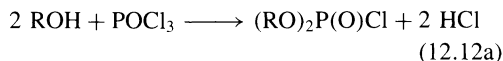
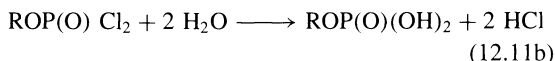
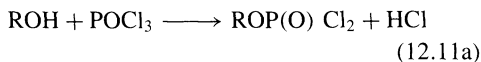
However, definite primary or secondary alkyl phosphates are seldom produced in practice. There are two reasons for this. First, the production costs are generally too high, and secondly the mixture of both esters in combination with the unreacted starting material often offers the most interesting properties for practical applications.

Although temperature has no influence on the ratio of reaction products, it does influence the rate of reaction and the formation of coloured by-products. The addition of acetic acid anhydride or acetyl chloride was found to accelerate the reaction. In some instances, the use of other solvents has been described.

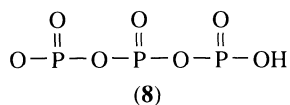
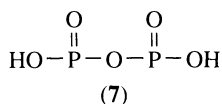
The reaction of 2-ethylhexanol and POCl_3 (or P_4O_{10}) has been studied in an effort to maximize the formation

of di-2-ethylhexyl hydrogen phosphate. It was found that POCl_3 was the preferred reagent for obtaining a pure product.

The reaction between an alcohol and phosphorus oxychloride also gives mono- or diesters, according to the following:



The ability of certain phosphoric acids to form condensed molecules is an additional effect. Such acids include pyrophosphoric acid, $\text{H}_4\text{P}_2\text{O}_7$ (7) and triphosphoric acid $\text{H}_5\text{P}_3\text{O}_{10}$ (8).



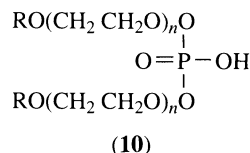
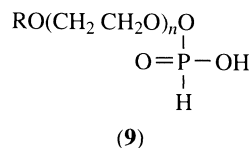
In living cells, adenosin triphosphate plays an important role in the transfer of energy. As an example, the reaction of condensed phosphoric acid with castor oil gave a polyphosphoric acid ester, which after neutralization with ammonia shows a high wetting power. For the production of detergent builders and inhibitors against soil-redeposition, starch was reacted with NaH_2PO_4 and partially neutralized hexametaphosphoric acid. In a similar way, vinyl monomers were heated with phosphorus compounds, e.g. PCl_3 , PBr_3 , triethyl phosphine, tripropyl phosphine, triallyl phosphine, or methyl or ethyl dimethoxy phosphine ester, to give polymers useful as antistatic agents, surfactants and plasticizers.

12.2 Polyoxyalkylene phosphate esters

Compounds with a suitable length of a hydrophilic group may be reacted with ethylene oxide, thus resulting in

alkyl polyglycol ethers which in turn can be treated with phosphorus pentoxide or phosphoric acid to give surface-active polyoxyalkylene phosphate esters. The properties of phosphoric acid esters based on alkylene oxide adducts can be controlled by the kind and length of the hydrophilic alkylene oxide chain, as well as by changing the length and structure of the hydrophobic alkyl chain. Furthermore, they can be easily adapted to special demands by using either ethylene oxide or propylene oxide.

The general formulae of the polyoxyethylene mono- and diesters of phosphoric acid are shown in structures 9 and 10, respectively, where R is either an alkyl or an alkylphenyl group, and n is between 2 and 18.



Anionic polyoxyethylene phosphate surfactants are produced by two general reactions. Either the terminal hydroxy group of a polyoxyethylated hydrophobic compound is reacted with a phosphorylating agent, or a phosphate ester is oxalkylated. Often, aliphatic and aromatic alcohols are first treated with an alkylene oxide, and afterwards with a suitable phosphorylating agents, such as P_4O_{10} , POCl_3 , phosphoric acid or polyphosphoric acid.

Phosphoric acid esters of polyoxyalkylenes with a high degree of alkoxylation are only mildly anionic and still show many properties of the base products. However, they have a better performance in application systems containing a high percentage of alkaline builders, e.g. institutional and industrial cleaners.

Phosphoric acid esters based on linear primary alcohols ($\text{C}_{11}-\text{C}_{15}$) solidify in general below 24°C whereas phosphate esters derived from nonylphenol are liquid at temperatures as low as 2°C (see Table 12.2). Hydrolysis with 1–3% water at $60-110^\circ\text{C}$ decomposes polyphosphates without hydrolysing the phosphate ester product, thus giving esters having good colour, clarity and resistance to discolouration and acid drift in storage.

Table 12.2. Pour points of phosphate esters

Esters (of)	Content ^a (%)	Pour point (°C)
Nonylphenol,	54.5 EO	2
Nonylphenol,	64 EO	2
Tridecyl alcohol (oxo),	56.9 EO	2
Linear primary alcohol, C ₁₁ -C ₁₅	54.5 EO	24
Linear primary alcohol, C ₁₁ -C ₁₅	64 EO	27
Linear primary alcohol, C ₁₁ -C ₁₅	68 EO	24
Linear primary alcohol, C ₁₄	57 EO	24
Linear primary alcohol, C ₁₄	57 PO	21

^aEO, ethylene oxide; PO, propylene oxide.

Mixtures of novel nonionic derivatives of phosphate esters of polyoxyethylenated partial glycerides of higher fatty acids are manufactured by reacting ethoxylated fatty mono- and diglycerides with polyphosphoric acid containing 82–84% P₄O₁₀, followed by treatment of the reaction products with ethylene oxide or propylene oxide.

Phosphate derivatives of ethylene oxide adducts exhibit good colour stability upon contact with sodium hydroxide, whereas nonionic ethylene oxide adducts discolour badly under these conditions. The free surface-active acids show little tendency to hydrolyse. They have a pH value of about 2 in aqueous solution. However, in the presence of strong acids, polyoxyethylated phosphate esters undergo hydrolysis to the base nonionic and phosphoric acid.

12.3 Applications of phosphorus-containing surfactants

Phosphorus-containing surfactants provide a combination of desired characteristics, e.g. wettability, detergency, sequestering ability and anticorrosive behaviour. Therefore a classification into separate fields of application is difficult.

Wetting is often one of the first steps for the effect of a surfactant. A special case is the penetration of fluids into porous material such as a bundle of fibres in the dyeing process or the stone matrix in enhanced oil recovery. One of the steps of lubrication is wetting of the surfaces by lubricant liquids. Because often further conditions have to be considered, the use of phosphorus-containing surfactants can be favourable.

Alkylphosphates and phosphonates are valuable components of cleaners, especially when anticorrosive behaviour is also asked for. Their solubility in saline solutions extends their field of application above the limits for other common surfactants.

Alkyl phosphonates are outstanding sequestering agents and builders. The latter influence precipitation of solid soil and promote the soil suspending ability of washing liquors.

They are further able to reduce the catalytic effects of heavy metal ions. Thus, they support the stabilization of peroxides in detergents. In a similar way, alkyl phosphonates also help to reduce the possibilities of catalytic processes taking place which cause soaps and fragrances to become rancid.

Far below stoichiometric amounts of sequestrants, precipitation of insoluble salts from water hardness can be avoided by the so-called *threshold effect*, in which formation of crystal nucleation sites is hindered by sequestrants. This process has been used for a long time to prepare feeding water for boilers e.g. steam vessels in rail way engines. Sodium pyrophosphate was originally used for this task. However, in particular alkyl phosphonic acids and their derivatives have a superior effect when compared to sodium pyrophosphate.

Heavy metal ions not only behave as catalysts in the destruction of peroxide compounds, but also catalyse other chemical processes often caused by oxygen and air. Sequestering these metal ions by phosphorus-containing compounds will decrease these undesired effects. Salts of alkylene diphosphonic acid and aminotri(methylphosphonic) acid are effective in stabilizing peroxide and chlorine bleaching solutions.

Phosphate esters based on alkanols, polyethoxylated alkanols and alkylphenols are favourably applied in emulsion polymerization processes. Especially in low-temperature polymerization, high requirements are demanded of emulsifiers for solubility and surface activity at ca. 5°C.

The dispersing ability of phosphorus-containing anionics is made use of in many applications. The sequestering abilities of polyphosphoric acid derivatives and derivatives of phosphonic acids are additional valuable properties for their use as dispersants. Their main task is to secure a stable distribution of particles in suspension. This is a strong demand in the production of photographic emulsions, as well as in the production of recording tapes and disk.

Poly(ethylene glycol) alkylaryl ether phosphates and poly(ethylene glycol) alkyl ether phosphates have been used as inhibitors for the deposition of salts in the petroleum field. These reagents have high surface activity and are adsorbed on the nuclei of crystallization centres, thus preventing further crystallization and thus inhibiting the deposition of salts.

In recent years, bi- and polyfunctional phosphorus-containing surfactants have attracted interest, mainly for

their combination of surface activity and sequestering ability. However, anticorrosive properties and biologically active behaviour are also effects that need to be considered. Alkyl phosphonic acids and their derivatives represent the largest group amongst these. Surfactants which contain carboxylic acid ester or amide chains with terminal phosphonic acid groups are prepared from poly(hydroxystearic) acid or polycaprolactone. Such reaction products are useful as dispersants, emulsifiers, and in some cases, as bactericides, disinfectants and antiseptics.

The diethylethanolamine salt of oleyl phosphate is effectively used as a dispersant for antimony oxide in a mixture of xylene-type solvent and water. Such a combination is useful as an additive for preventing the activity deterioration of the fluid catalytic cracking material for heavy petroleum fractions.

Phosphoric acid esters of alcohols are recommended as surfactants which are mild to the skin. Therefore, they are used in cosmetics such as shampoos and lotions. In analogy to alkyl sulfates and alkylether sulfates mildness to the skin and especially to mucous membranes will be increased by using ethoxylated alkanols as the starting materials.

Some phosphorus-containing surfactants possess bacteriostatic properties. In combination with their physiological acceptance, they are therefore used in cosmetics and pharmaceuticals, e.g. in oral anticaries compositions, the combination of alkyl phosphates and nonionic surfactants stabilizes mutanase without decreasing foaming behaviour.

13 SULFOSUCCINATES

Mono- or dialkyl esters of succinic acid are formed by the addition of fatty alcohols or ethoxylated fatty alcohols to maleic anhydride in the presence of acid catalysts. These are the hydrophobic starting material for sulfosuccinates. The next step is the addition of sodium hydrogensulfite in aqueous methanol, which forms the surface-active sulfosuccinates via a radical reaction.

In the case of sulfosuccinates, fatty alcohols with short alkyl chains that would otherwise give no useable surface activity, owing to their chain length, in other surfactants such as alkyl sulfates, can be used as starting materials. Very pronounced is the large rise in surface activity between diesters with six carbon atoms and diesters with eight carbon atoms in the alkyl chain, but we have to remind ourselves that this means a difference of four carbon atoms in the whole molecule.

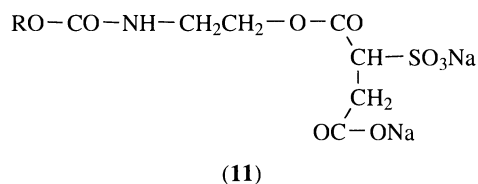
Alkyl sulfates as monoesters of the dibasic sulfuric acid have only one hydrophobic group in the molecule, while in the case of the tribasic sulfosuccinic acid, both monoesters and diesters can be formed. This gives a broader variation and influence of the surface-active properties. In general, it can be said that sulfosuccinates containing less than eight to ten carbon atoms in each ester group exhibit a sufficient solubility in water.

Sulfosuccinates are in general on the market as neutral aqueous solutions. However, especially the sodium salts of the diesters will easily crystallize by evaporating. In this form, they are used as components of cleaners in powder form, e.g. in carpet dry cleaning formulations. The dialkyl sulfosuccinates with alkyl groups such as butyl, hexyl or ethylhexyl show outstanding wetting properties and good dispersing ability. They are used as quick-acting wetting agents in the textile industry. The best results are obtained with esters containing from 14 to 18 carbon atoms in the hydrophobic unit.

The monoesters of sulfosuccinic acid possess good washing ability and high foam stability, and are gentle to the skin. Therefore they are in widespread use in bodycare products such as shower gels and baby shampoos. However, their ester bonds are sensitive to hydrolysis in alkaline solutions. Thus, they cannot be used in common detergents.

In particular, the monoesters of ethoxylated fatty alcohols with three to twelve ethylene oxide groups in the molecule are gaining importance in bodycare products. They are indifferent to water hardness and non-irritating to the skin.

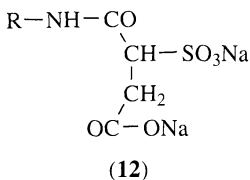
The same properties are shown by the sulfosuccinates of fatty acid alkanolamines (11). These materials can be combined with other anionics, resulting in cleaners which show good solubility and excellent foam ability.



The sulfosuccinates also need to be mentioned here. These materials can be produced by the reaction of fatty amines with maleic anhydride, followed by the addition of sodium bisulfite (12).

They are used in flotation processes of non-sulfidic ores to adjust the wetting properties.

The great variety and number of ester components of all kinds results in adaptation to many demands in



application. Therefore, they may be found in detergents and cleaners, in body cleansers and bodycare products, in disperse colourants, and in auxiliaries for the pulp and paper industries. They are also used as emulsifiers in polymerization processes, as foam boosters in flotation, and as wetting agent in electrodeposition processes.

The production of sulfosuccinate on an industrial scale began in the early 1960s. This followed a sharp decline in the price of maleic anhydride, a raw material which was of great importance in the production of plastics. In the previous years, only a few diesters of short-chain fatty alcohols had been used as wetting agents, largely in the textile industry. In the class of ethanolamides of sulfosuccinate, the monoethanolamide of undecylenic acid shows microbiological properties and is used in hair shampoos as an anti-dandruff agent. A large variety of sulfosuccinates are now available.

For the synthesis of sulfosuccinate monoesters, the fatty alcohol is loaded into a reactor vessel and heated to 60–70°C. The temperature is kept at this level and maleic anhydride is continuously added up to a slight excess above the theoretically required amount. The heat of reaction causes the anhydride to melt. The reaction is continued by stirring the mixture for ca. 1 h at 70–90°C. Afterwards, an aqueous solution (~20%) of sodium sulfite or sodium bisulfite is added. The reaction is completed by continuous stirring at 70–90°C for at least for 1 h. The pH value of the reaction mixture is then adjusted to neutral.

In the final stage, ca. 80% of the mixture is transformed to the monoester of the sulfosuccinate, resulting in a 40% aqueous solution which in most cases is used in formulations. An excess of sulfite can be eliminated by the addition of hydrogen peroxide. Solutions of sulfosuccinates in their most common product form contains 40% active material.

The production of diesters is similar to the synthesis of the monoesters. In this case, however, after addition of the maleic anhydride, the temperature is raised to 100–120°C and under a slight vacuum the formed water of reaction is evaporated so as to shift the reaction towards the diesters. The use of an esterification catalyst is also necessary. The addition of inert solvents for the removal of water (by forming azeotropic mixtures)

is very helpful for lowering the required temperature. Unlike the monoesters, the diesters of succinic acid are obtained in high yield.

Sulfosuccinates obtained from OH-group containing substances other than fatty alcohols are produced in the same manner as described before.

For the synthesis of sulfosuccinates, maleic anhydride is reacted with the particular amine needed to give the required maleic acid monoamide, which can then be transformed to the sulfosuccinate by sulfonation with sodium bisulfate in aqueous solution. The preparation of diamides is similar to that used for preparing diesters.

As already mentioned, the finished monoester product is always in the form of a blend because neither of the reaction steps are completed. Often the starting material by itself contains many components. That is especially the case when using ethoxylated fatty alcohols, which offers a low sensitivity against the alkaline-earth ions in hard water. This starting material even contains unreacted fatty alcohol due to the statistical distribution of the ethoxylates. However, it is possible to reduce the amounts of unwanted by-products such as 1,4-dioxine or nitrosamines in the alkanolamine-based sulfosuccinates below the detection limits by using modern production methods.

In the diester class, the di-2-ethylhexyl sulfosuccinate and the diisodecyl sulfosuccinate have gained importance. These materials combine a high wetting power, a good foaming ability and a strong decrease of the surface tension in aqueous solution. Furthermore di-2-ethylhexyl sulfosuccinate is soluble in a number of organic solvents, such as alcohols and acetone, and even carbon tetrachloride and other non-polar solvents. Another important sulfosuccinate of the diester type is diisooctyl sodium sulfosuccinate. Due to its low toxicity, this sulfosuccinate is even used in pharmaceuticals and in plastics for the packaging of food, e.g. beverages. Because of its presence in these polymeric coatings and in emulsifiers, the diisooctyl ester has to be considered as a food additive. Therefore, the pharmacological and toxic side-effects of this sulfosuccinate have been thoroughly studied. An incorporation of ca. 37 mg per day is estimated as being non-toxic. In medical use, even a consumption of up to 200 mg per day is tolerated. Because of its extended use in recent years, the safety of sulfosuccinates is considered as proven.

Sulfosuccinates are very useful in emulsion polymerization processes. In this technique the interfacial tension between the monomer and the water phase must be lowered in order to secure the best contact of the components for an optimal reaction rate. Furthermore, the surfactant has to function not only as a wetting agent

but also as a solubiliser and dispersant to ensure the full effects of the various auxiliaries which are added to alter the properties of the polymer latex. Sulfosuccinates are soluble not only in water but also in many of the monomers. This is helpful in producing concentrated and finely dispersed lattices important for stable dispersions of the polymers. Sulfosuccinates are also used for the preparation of latex paints in which a thorough dispersion of pigments is necessary to achieve stable dispersions. For this purpose, the dioctyl and dihexyl sulfosuccinates are used in a concentration range of 0.2 to 1.0%.

14 ANIONIC SURFACTANTS WITH SPECIAL PROPERTIES

There are various other materials with special structures which show anionic surface-active properties.

14.1 Cleavable surfactants

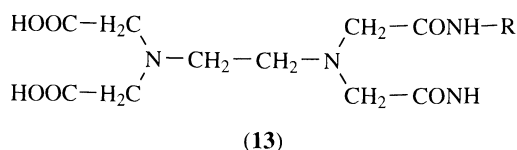
The so-called cleavable surfactants possess a planned "site of break" in their molecules. Surface-active agents which reduce the surface tension of water to values lower than 45 mN/m are highly toxic substances. They have a harmful influence on the gills of fish and nutrients for fish such as tiny crustaceans. Therefore, the primary degradation is of great importance besides the total mineralisation. Chemodegradable surfactants are compounds with an acetal group in their structures. Hence, their surface-active properties will rapidly decrease after use when they arrive into sewage systems. Surfactants of this kind include sodium *cis*- or *trans*-(2-*n*-alkyl-1,3-dioxan-5-yl) sulfates or carboxylates.

14.2 Short-chain sulfonates

Another class of surfactants are those compounds with short alkyl chains where the hydrophobic part of the molecule dissociates in water as an anion. They will not show any pronounced surface-active properties but in combination with other anionic surfactants they will influence the solubilities and viscosities of concentrated solutions. A well-known compound of this kind is cumene sulfonate (sodium propylbenzene sulfonate) which is often used to decrease the viscosity of *n*-alkylbenzene sulfonate pastes.

14.3 Anion-active sequestrants

There is another special type of surfactant where a fatty amine is attached to a carboxylic group to create surface activity. Reaction of 1 mol ethylenediaminetetraacetic acid (EDTA) with 1 mol of alkyl amine results in the monoalkyl amide of the EDTA (13). This compound still possesses the sequestering properties for multivalent ions of the original EDTA. However, in addition it behaves as a surface-active agent. Hence, in aqueous solution it will be driven by thermodynamic forces towards the interfaces. In this way, its concentration will be increased at solid surfaces where its sequestering properties are desired.



14.4 Fluorosurfactants

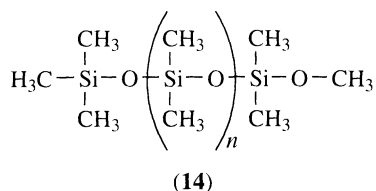
In fluorosurfactants, the hydrophobic group is a per-fluoroalkyl unit in which all of the hydrogen atoms are replaced by fluorine. Anionic fluorosurfactants can be prepared from all classes of anionics. Their critical micelle (forming) concentration is remarkably low and therefore they depress the surface tension of water to a very low value, even at small concentration levels. Furthermore, they are stable against thermal and chemical influences. Hence, fluorosurfactants can be used in aggressive media and at high temperatures.

For economic reasons, they are only used if there is a strong demand for outstanding properties. Typical fields of application are as wetting agents in the production of photographic material, as soil- and oil-resistant finishings in the textile industry, and in fire-extinguishing agents. The surface tension of water will be lowered by fluorosurfactants to a value that makes it possible to extinguish burning oil that otherwise would "swim" on the water.

14.5 Silicosurfactants

Silicosurfactants also possess outstanding properties. Such materials display strong hydrophobic behaviour, as is already known from the silicane oils used as effective foam inhibitors.

Depending on their structure, silicone surfactants are surface-active not only in water but also in organic solvents. They are structurally derived from polydimethylsiloxanes (14) in which the methyl groups are partly substituted by anionic groups.



Silicone surfactants show outstanding surface activity, e.g. the surface tensions of their aqueous solutions can be lowered to the level of 21–22 mN/m. They are in most cases oligomeric or polymeric substances. Silicone sulfonates show thermal stability and will not crystallize at low temperatures due to their highly branched structures. They show a great variety of molecular weights and structures (linear, branched, comb-like, etc). The variability of the synthetic routes also leads to a large number of products with different properties.

Although most of the silicone surfactants on the market are of the nonionic or amphoteric type, there are also some anionic materials. For instance, by the reaction of an epoxysiloxane intermediate with sodium sulfite, a silicone sulfonate can be obtained. Silicone surfactants, including the anionic forms continue to find new fields of application.

The use of silicone surfactants as foam regulators in the production of polyurethane foams played a key role in bringing polyurethane foams on to the market. They have also shown their technical usefulness in many other applications. A high number of modifying groups can be realized to cover the demands for industrial use. They are used as wetting agents for surfaces of many different kinds, as surface-active lubricants and as defoamers, as well as foam regulators.

14.6 Ligninsulphonates

Aqueous solutions of ligninsulphonates do not form micelles, although the surface tensions are lowered to levels of 40 mN/m. In paper making, wood chips are cooked in a sulfite digester with calcium bisulfite

and excess sulfur dioxide. The waste liquor contains lignin compounds which show surface-active properties. Ligninsulphonates are prepared from this sulfite lye. The molecular weight of ligninsulphonates is between 10 000 and 50 000, depending on the grade of digestion and on the chips used – either from hard or soft wood.

Calcium or sodium salts of ligninsulphonates are available as brown translucent solutions containing ca. 25% active material or as yellow powder, (by spray drying). They are easily soluble in water, forming neutral solutions which are effective dispersants.

Ligninsulphonates are used as admixtures to increase the flowability of concrete, as levelling agents in the dyeing of fabrics, as protective agents for wool fibres against the action of alkalies, and for the preparation of drilling fluids. They also show sequestering properties for heavy metal ions.

15 ACKNOWLEDGEMENTS

The authors express their gratitude to Professors Hermann G. Hauthal and Bogdan Burczyk, and to Drs Helmut W. Stache, Kurt Kosswig, Gunter Czichocki and Rainer Holzbauer for providing valuable and informative material for this review.

16 BIBLIOGRAPHY

1. Chhabra, V., Free, M. L., Kang, P. K., Truesdail, S. E. and Shah, D. O., Microemulsions as an emerging technology, *Tenside Surf. Det.*, **34**, 156–68 (1997).
2. Kosswig, K. and Stache, H., *Die Tenside*, Carl Hanser Verlag, Muenchen, 1993.
3. Morrow, N. R. (Ed.), *Interfacial Phenomena in Petroleum Recovery*, Surfactant Sciences Series, Vol. 36, Marcel Dekker, New York, 1991.
4. Schoeberl, P., Ecological assessment of surfactants, *Tenside Surf. Det.* **33**, 28–36 (1996).
5. Schwuger, M. J., (Ed.), *Detergents in the Environment*, Surfactant Sciences Series, Vol. 65, Marcel Dekker, New York, 1997.
6. Solans, C. and Kunieda, H., (Eds.), *Industrial Applications of Microemulsions*, Surfactant Sciences Series, Vol. 66, Marcel Dekker, New York, 1997.
7. Stache, H. W., (Ed.), *Anionic Surfactants*, Surfactant Sciences Series, Vol. 56, Marcel Dekker, New York, 1996.
8. Wasow, G. W. and Schmalstieg, A., The use of surface active substances as corrosion inhibitors, *Tenside Surfactants Det.*, **30**, 128–132 (1993).

CHAPTER 13

Nonionic Surfactants

Michael F. Cox

Sasol North America, Inc., Austin, Texas, USA

1	Introduction	294	4.3.2	Manufacture	303
2	Nonionic Hydrophobes	294	4.3.3	Advantages/disadvantages . . .	303
	2.1 Primary alcohols	294	4.3.4	Impact of molecular composition on properties . . .	304
	2.2 Alkylphenols	296	4.4	Alkylpolyglycosides	304
	2.3 Alkylene oxides	296		4.4.1 Applications	304
	2.4 Amines	297		4.4.2 Manufacture	304
	2.5 Esters	297		4.4.3 Advantages/disadvantages . . .	304
	2.6 Fatty acids	297		4.4.4 Impact of molecular composition on properties . . .	304
	2.7 Odd versus even chain length	297	4.5	Alkyl <i>N</i> -methylglucamides	305
	2.8 Branching	297		4.5.1 Applications	305
	2.9 Average molecular weight/carbon chain distribution	297		4.5.2 Manufacture	305
3	Nonionic Hydrophiles	298		4.5.3 Advantages/disadvantages . . .	305
	3.1 Ethylene oxide	298		4.5.4 Impact of molecular composition on properties . . .	305
	3.1.1 Ethoxymer distribution	299	4.6	Amine oxides	305
	3.2 Propylene oxide	300		4.6.1 Applications	306
	3.3 Carbohydrates	300		4.6.2 Manufacture	306
4	Common Nonionic Surfactants	301		4.6.3 Advantages/disadvantages . . .	306
	4.1 Alcohol ethoxylates	301		4.6.4 Impact of molecular composition on properties . . .	306
	4.1.1 Applications	301	4.7	Alkanolamides	306
	4.1.2 Manufacture	301		4.7.1 Applications	306
	4.1.3 Advantages/disadvantages . . .	301		4.7.2 Manufacture	306
	4.1.4 Impact of molecular composition on properties . . .	302		4.7.3 Advantages/disadvantages . . .	306
	4.2 Alkylphenol ethoxylates	302		4.7.4 Impact of molecular composition on properties . . .	306
	4.2.1 Applications	302	4.8	Amine ethoxylates	307
	4.2.2 Manufacture	302		4.8.1 Applications	306
	4.2.3 Advantages/disadvantages . . .	302		4.8.2 Manufacture	306
	4.2.4 Impact of molecular composition on properties . . .	303		4.8.3 Advantages/disadvantages . . .	307
	4.3 Ethylene oxide/propylene oxide block copolymers	303		4.8.4 Impact of molecular composition on properties . . .	307
	4.3.1 Applications	303			

4.9	Methyl ester ethoxylates	307	4.9.4	Impact of molecular composition on properties . . .	308
4.9.1	Applications	307	4.10	Other surfactants	308
4.9.2	Manufacture	307	5	References	308
4.9.3	Advantages/disadvantages . . .	308			

1 INTRODUCTION

Surfactants have historically been classified according to the charge they carry when dissociated in water at neutral pH. This results in four categories, as follows:

- *Nonionic* surfactants – do not ionize in solution
- *Anionic* surfactants – carry a negative charge when dissociated in water
- *Cationic* surfactants – carry a positive charge when dissociated in water
- *Amphoteric* surfactants – can carry both a positive and a negative charge when dissociated in water

Anionics are the largest class of surfactants in terms of volume, and include the work-horse surfactants, linear alkylbenzene sulfonate (LAS), alcohol sulfate (AS) and alcohol ether (or ethoxy) sulfate (AES). Cationic surfactants generally include various quaternary salts, used predominantly as fabric conditioners (“fabric softeners”), anti-static agents and anti-microbial agents. Amphoteric surfactants represent the smallest class of surfactants, and generally are used when solubility, mildness and compatibility issues are important.

More than approximately 2 million metric tons of various nonionic surfactants are used annually in the world today, and are prepared by more than 150 different manufacturers. There are three reasons for the popularity of nonionic surfactants: nonionic feedstocks are readily available and generally inexpensive, nonionics are relatively easy to make, and nonionic surfactants can vary significantly in structure so that the chances of finding an acceptable nonionic surfactant for any given application are quite good.

This present chapter deals with nonionic surfactants, which include a broad array of different types of molecules. However, as we shall see, the vast majority of nonionic surfactants, at least in terms of volume, arise from a very limited number of oleochemical and/or petrochemical feedstocks. This chapter first discusses the feedstocks used to produce the hydrophobic portion of the nonionic molecule, and why they are used. The second portion of the chapter deals with the hydrophilic portion of the molecule in the same way. The final

segment of the chapter describes the major nonionic surfactants that are used in the world today.

2 NONIONIC HYDROPHOBES

There are two general sources of hydrophobic feedstocks, namely oleochemical and petrochemical. Oleochemical feedstocks are those derived from oleochemical sources such as palm kernel oil, coconut oil, tallow, and so forth. Petrochemical feedstocks are derived from petroleum. In the 1980s and 1990s, there was significant debate about the pros and cons of oleochemical vs. petrochemical feedstocks. This debate has subsided as technical information has more clearly defined such pros and cons. Oleochemical feedstocks are indeed “renewable”, but they have not been shown to be superior to petrochemical feedstocks in terms of their impact on the environment (energy consumed in processing, wastes produced during processing, etc.). In addition, the availability of oleochemical feedstocks can vary, as does the pricing. Petrochemical feedstocks are not renewable, although the amount of petroleum used to produce surfactants is miniscule in comparison to the amount used for energy. Thankfully, there now appears to be a general consensus in the industry that both types of feedstocks have their various pros and cons, and that both are needed for future growth. Approximately half of the alcohol used today to make various alcohol-based nonionic surfactants originates from oleochemical feedstocks, while the remainder is of petrochemical origin.

2.1 Primary alcohols

The most common hydrophobe used to produce nonionic surfactants is alcohol. Alcohol can be produced by using both petrochemical and oleochemical feedstocks.

There are two petrochemical processes for converting ethylene into various synthetic alcohols. The Ziegler process employs aluminium metal and ethylene to grow alkyl chains which are then oxidized and hydrolyzed to produce a broad distribution of primary alcohols (see Figure 13.1). This chemistry is practiced by the Sasol North America, Inc. in the USA, and by Sasol Germany GmbH, and their

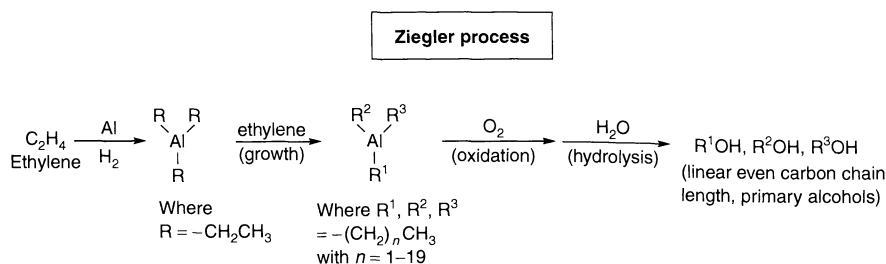


Figure 13.1. The Ziegler process for the preparation of alcohols from ethylene

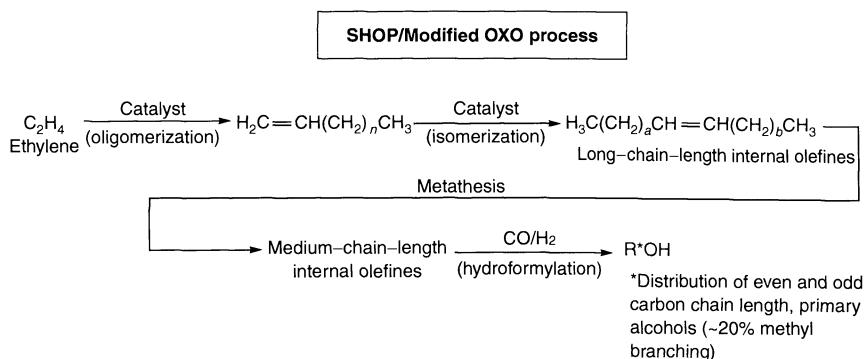


Figure 13.2. The Shell Oil Company's SHOP/modified-OXO process for the preparation of alcohols from ethylene

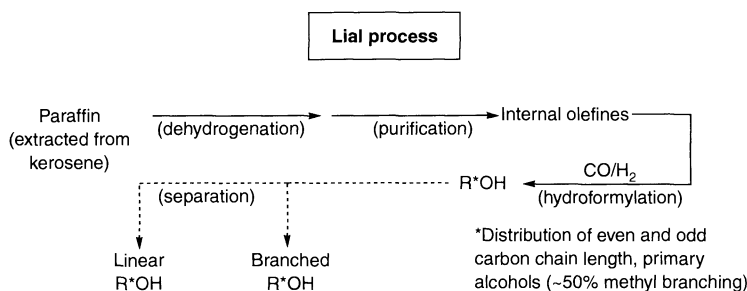


Figure 13.3. CONDEA's Lial process for the preparation of alcohols from paraffins

process has been licensed to others. Albemarle also uses a modified version of the Ziegler process; their process converts aluminium trialkyl to alpha olefins in order to market and/or consume the shorter chain (C_4 – C_{10}) homologues. The C_{12} – C_{18} alpha olefins are then converted to alcohols through transalkylation to produce the C_{12} – C_{18} aluminium trialkyl, which is then oxidized and hydrolyzed to produce alcohol.

Shell's SHOP (Shell Higher Olefin Process) also converts ethylene to alcohol, but makes use of a different route that produces both even and odd carbon chain length alcohols that contain a moderate level

(approximately 20%) of mostly methyl-branching (see Figure 13.2). This process first produces even carbon chain alpha olefins which are then converted to a mixture of internal olefins of even and odd carbon chain length. A modified-OXO process then converts the internal olefins to alcohols.

An additional petrochemical route is practiced by Sasol Italy SpA (see Figure 13.3). This process starts with the dehydrogenation of paraffins to produce olefins, which are then reacted with carbon monoxide (via hydroformylation) to produce "Oxo" alcohols containing 40–50% mostly methyl-branching.

Petrochemical alcohols are also produced via the oligomerization of propylene and butylene, followed by hydroformylation of the olefine to the alcohol.

A variety of oleochemical feedstocks (fats and oils) can be employed to make alcohols. Coconut and palm kernel oils, however, are most often used because they produce alcohols predominantly in the lauryl (C₁₂ and C₁₄) range, which is considered most desirable from a performance point of view, and because they produce highly saturated alcohols which helps to minimize the degree of hydrogenation required during alcohol manufacture.

The oldest route for converting oils and fats to alcohol involves the “splitting” of triglycerides (see

Figure 13.4). This route first produces fatty acids which are then hydrogenated to produce alcohols. Another common route for converting triglycerides to alcohols involves the transesterification of triglycerides to methyl esters, which are then hydrogenated to alcohols (Figure 13.4). This process is practiced by Procter & Gamble, Henkel and Kao.

Both oleochemical routes have process advantages and disadvantages, and both produce high-quality primary alcohols of even numbered carbon chain lengths.

Because of the difficulty in producing surfactant derivatives from secondary and tertiary alcohols, they are not typically used as feedstocks.

2.2 Alkylphenols

Alkylphenols are produced by reacting phenol with propylene or isobutylene oligomers. As shown in Figure 13.5, the reaction of a propylene trimer with phenol produces various isomers of nonylphenol, the most common feedstock for alkylphenol-based nonionic surfactants. Dimerization of isobutylene yields an octene which leads to octyl(diisobutylene)phenol. Similarly, propylene tetramer, on reaction with phenol, yields dodecyl(tetrapropylene)phenol.

2.3 Alkylene oxides

Blocks of alkylene oxide (other than ethylene oxide) are also commonly used as hydrophobes (see Figure 13.6). The most common type is produced with propylene oxide, although butylene oxide is also used.

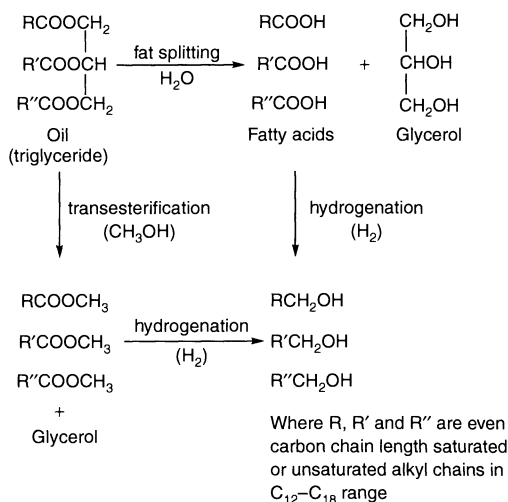


Figure 13.4. Major oleochemical routes for producing alcohols

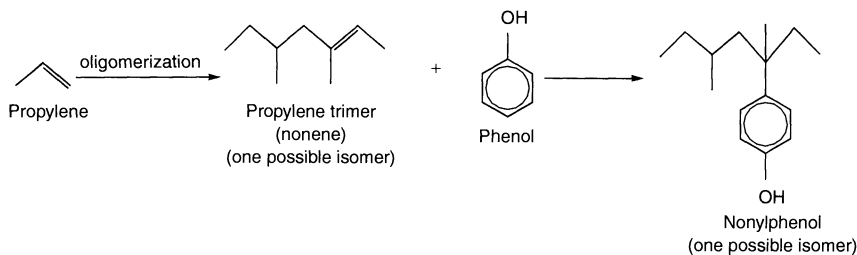


Figure 13.5. Preparation of alkylphenol; in this example, propylene is used to produce nonylphenol

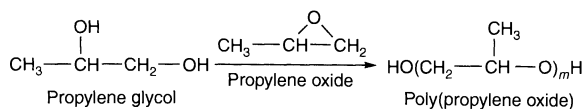


Figure 13.6. Preparation of poly(propylene oxide)

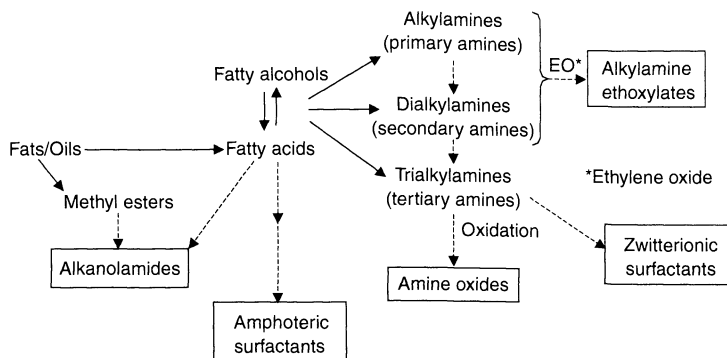


Figure 13.7. Preparation of various nitrogen-based feedstocks (and nitrogen-based nonionic surfactants)

2.4 Amines

A variety of amines can serve as nonionic feedstocks (see Figure 13.7). Amines are generally made from petrochemical-based or oleochemical-based alcohols, or from fatty acids.

2.5 Esters

Alkoxylation catalysts have been developed that allow the ready conversion of methyl esters, as well as their precursor triglycerides, into nonionic surfactants. Methyl esters are produced from triglycerides (see Figure 13.4), or by esterifying fatty acids with methanol.

2.6 Fatty acids

Fatty acids are also used to produce nonionic surfactants.

2.7 Odd versus even chain length

At one point, the debate over oleochemical vs. petrochemical feedstocks also encompassed the question of odd-versus-even-numbered carbon chain lengths. The carbon chain length clearly has an impact on hydrophobicity and therefore surface activity, but beyond this, whether a molecule has an even or odd number of carbons is insignificant. The claim that even carbon chain lengths promote faster biodegradation because microorganisms can better metabolize even-carbon-chain molecules has not proven to be true.

Oleochemical-based feedstocks produce even-numbered carbon chain length alcohols, as does the ziegler petrochemical route. All other petrochemical routes produce both even and odd carbon chain length alcohols.

2.8 Branching

A higher degree of branching is sometimes preferred by the formulator because this produces better solubility, can enhance wetting, foaming and emulsifying power, and can positively impact on the physical properties. Although very high branching can depress the rate of biodegradation, minor branching (simple methyl-branching) has little impact on environmental acceptability.

Oleochemical feedstocks and Ziegler alcohols are linear. Shell's SHOP process produces alcohols with approximately 20% predominantly methyl-branching, while other OXO-type alcohols contain approximately 40–50% predominantly methyl-branching. Alkylphenols and alcohols based on oligomerized alkylenes are generally highly branched.

2.9 Average molecular weight/carbon chain distribution

Average molecular weight and carbon chain distribution are adjusted by the manufacturer through distillation and blending to meet the needs of the formulator. These parameters are perhaps the most important factors when selecting a hydrophobe because they strongly influence surface activity and solubility.

3 NONIONIC HYDROPHILES

3.1 Ethylene oxide

The most common hydrophile for nonionic surfactants is a polymeric chain made from ethylene oxide (EO). EO is a commodity chemical made from ethylene and oxygen (see Figure 13.8). Although EO production consumes a significant portion of the ethylene produced worldwide (roughly 13% in the USA), the ethylene market is more strongly driven by polyethylene production which consumes significantly more (almost 30% of USA-produced ethylene). Consequently, EO pricing varies depending on ethylene pricing, which varies depending on the volatility of the polyethylene market.

Addition of ethylene oxide to hydrophobic feedstocks requires an alkoxylation catalyst. Most alkoxylation catalysts use sodium or potassium hydroxide. These (and similar catalysts) work by first removing a labile hydrogen from the hydrophobe to produce a reactive anion (see figure 13.9). This reactive anion then reacts with ethylene oxide, one unit at a time, to “grow” the ethylene oxide chain. However, different hydrophobic molecules react with EO at different rates, thus yielding a distribution of isomers (also called “ethoxymers” and “homologues”). Figure 13.10 shows the distribution

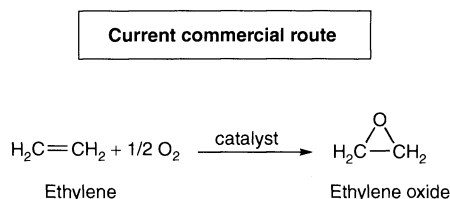


Figure 13.8. Preparation of ethylene oxide (EO)

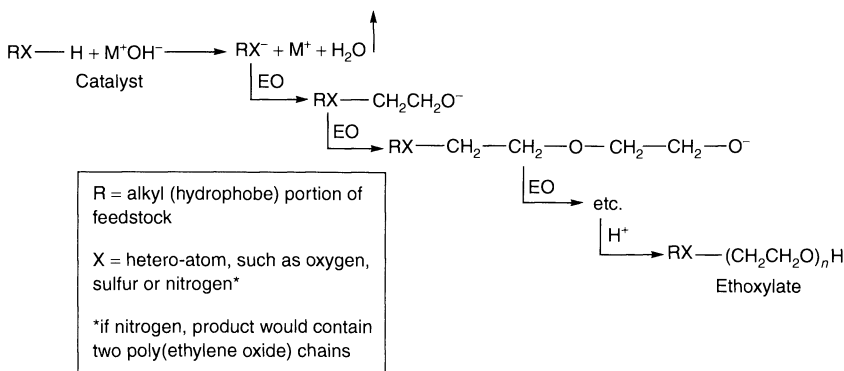


Figure 13.9. Ethoxylation with conventional catalysts

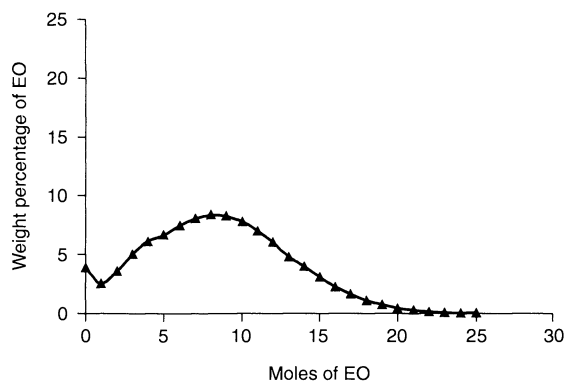


Figure 13.10. Distribution of ethoxymers for the sodium-hydroxide-catalysed ethoxylation of dodecanol (to 60% EO by weight)

of ethylene oxide for dodecanol “ethoxylated” to 60 wt% (where the hydrophobe makes up 40% of the molecule and the hydrophile (EO) makes up 60%).

Ethoxylates are typically described by the average amount of EO added to the hydrophobe, either as the average weight percent added, or as the average number of moles (units) of EO added. The advantage of using percent is that it gives the user some idea of the solubility characteristics of the ethoxylate. In general, if the wt% EO is greater than 50, the surfactant is water-soluble, while weight percentages below 50% are oil-soluble (with 50% being borderline). The advantage of describing the surfactants in terms of moles of EO is that it more accurately describes the composition of the molecule. It is important, however, to keep in mind that the relationship between wt% and moles is not linear (see Figure 13.11).

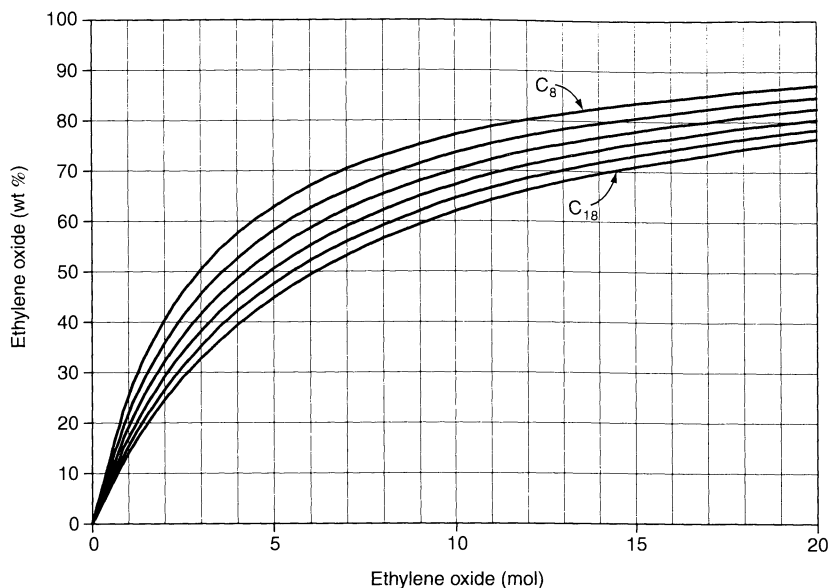


Figure 13.11. Relationship between wt% EO and moles of EO for C₈–C₁₈ linear alcohol ethoxylates

As described above, conventional ethoxylation catalysts (NaOH, KOH, etc.) require a “labile” or “active” hydrogen to promote ethoxylation. To become active and labile, these hydrogens require an adjacent heteroatom, such as oxygen, sulfur or nitrogen. For many years, this requirement served as a practical limit to which hydrophobic feedstocks could and could not be ethoxylated. Alcohols, amines, and to some extent, fatty acids, could be ethoxylated, while triglycerides, methyl esters, etc. could not.

The first crack in this paradigm, however, occurred in 1989. Although not commercially attractive from a conversion and reactivity point of view, Hoechst (1) and Henkel (2) demonstrated that alkoxylation catalysts based on alkali/alkaline-earth metals and calcined hydrotalcites (aluminium–magnesium hydroxycarbonates), respectively, promoted the ethoxylation of esters. In 1990, Vista Chemical Company (now Sasol North America, Inc.) demonstrated that their proprietary catalyst (activated calcium and aluminium alkoxides), and similar catalysts, efficiently and effectively ethoxylated a variety of esters (3). That same year, Lion showed that magnesium oxide-based catalysts also worked well (4). Henkel followed with the discovery that hydrotalcites become effective catalysts for esters when combined with co-catalysts such as ethylene glycol, fatty acids and standard alkali catalysts (5, 6). These discoveries effectively launched the development

of ester ethoxylates, and initiated the commercial introduction of methyl ester ethoxylates by Lion in the late 1990s. Esters, such as oleochemical oils and methyl esters, are now recognized as alkoxylation feedstocks, and ester alkoxyates are an active area of research and development.

Although there hasn’t been a great deal of research on the mechanisms involved in the ethoxylation of esters, one mechanism that has been proposed involves transesterification (7). As shown in Figure 13.12, it is the catalyst (in this case, a mixture of calcium and aluminium alkoxides) that first becomes “ethoxylated” (forms the metal alkoxyethoxylate). After the catalyst picks up a mole of EO, it then transesterifies with the ester to form methyl ester ethoxylate, alkyl ester ethoxylate, and metal-coordinated methoxide. These steps occur continuously until the available EO is exhausted and a distribution of methyl ester ethoxylate homologues (ethoxymers) is obtained.

3.1.1 Ethoximer distribution

With the exception of some small volume 1- and 2-mol products, all ethoxylates consist of a distribution of ethoxymers. These distributions are not statistically determined because there exist finite differences in the relative reactivities of various homologues to

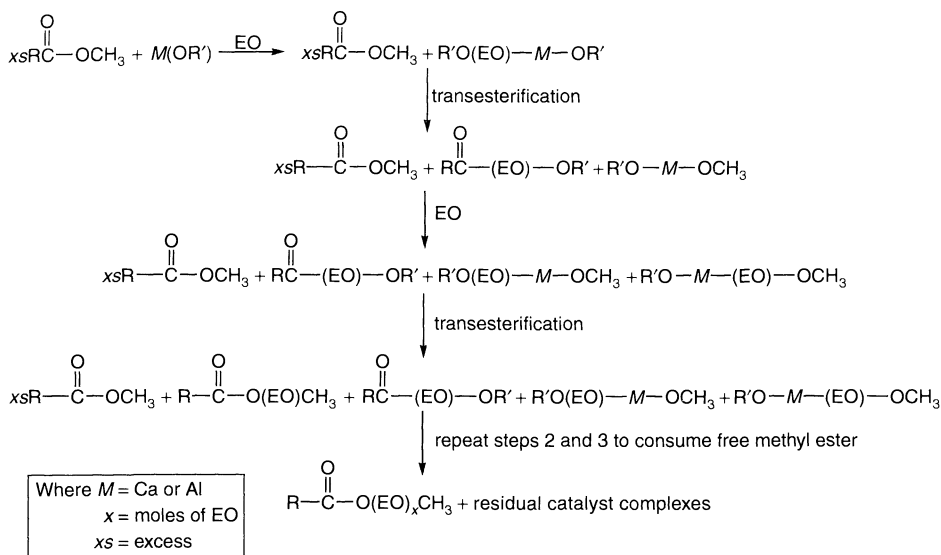


Figure 13.12. Ethoxylation of a methyl ester by using a complex catalyst

EO, and because these relative reactivities are influenced by the ethoxylation catalyst employed. With linear alcohols, conventional ethoxylation catalysts, such as sodium hydroxide and potassium hydroxide, produce similar, somewhat broad distributions, as illustrated earlier in Figure 13.10 for dodecanol ethoxylated to 60% EO. Most formulators accept the fact that ethoxylates contain a certain level of unethoxylated feedstock (e.g. free alcohol in alcohol ethoxylates) because it does not significantly impact upon the performance or physical properties. However, some feedstocks are relatively volatile and/or have an odour associated with them. Significant levels of unethoxylated feedstock therefore can cause processing problems (e.g. in the preparation of a spray-dried powder) or odour concerns. In order to address these concerns, alkoxylation manufacturers have developed catalysts that “peak” the ethoxymer distribution. The resulting ethoxylates are called “peaked” or “narrow-range” ethoxylates. An example of a 60 wt% ethoxylate of dodecanol, made with a “peaked distribution” catalyst, is shown in Figure 13.13. Note that in comparison to the sodium hydroxide-catalysed ethoxylate, free dodecanol (unethoxylated alcohol) drops from about 4 to less than 1%, and that the concentrations of homologues below and above the central molecule (7 mol ethoxymer) are reduced. “Peaked” ethoxylates offer certain performance benefits which are described later in this chapter.

3.2 Propylene oxide

In surfactant manufacture, propylene oxide (PO) is employed both as a hydrophobe (see Section 2.3 above), and as a modifier for poly(ethylene oxide). Propylene oxide is similar to EO except that it contains an additional methyl group, which adds steric bulk, and is significantly more hydrophobic in nature. If PO is inserted in the middle of a poly(ethylene oxide) chain, different properties (e.g. greater liquidity) are obtained. Since this approach requires three separate alkoxylation, it is only used when modification of specific properties is required. More common is the use of PO to “cap” the end of the poly(ethylene oxide) chain. This significantly reduces foaming, which can be critical in certain applications (e.g. machine dishwashing).

3.3 Carbohydrates

The use of simple sugars as hydrophiles is attractive in terms of both their ready availability and renewability, and in terms of their inherent consumer acceptance. Simple sugars are more readily available than vegetable oils, and come from a variety of sources, including cane, beet, corn, and so on. Unfortunately, the chemistry involved in linking sugars to hydrophobes is more difficult with respect to purity and yield, thus making the cost of sugar-based surfactants relatively high.

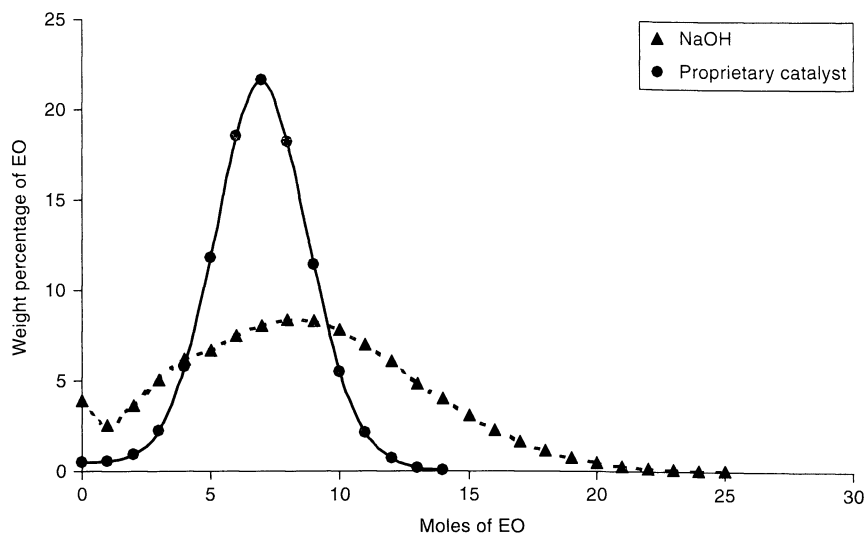
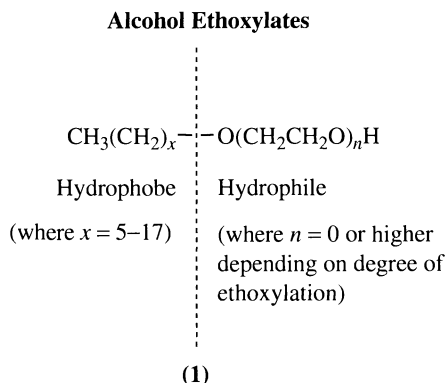


Figure 13.13. Distribution of ethoxymers for the preparation of 60% EO ethoxylates by using sodium hydroxide (NaOH) and a proprietary “peaked distribution” catalyst

4 COMMON NONIONIC SURFACTANTS

4.1 Alcohol ethoxylates

The (general) structure of alcohol ethoxylates (AEs) (1) is as follows:



4.1.1 Applications

Almost 2 billion pounds of various alcohol ethoxylates are consumed annually in the world today, which is more than any other class of nonionic surfactant. They are widely used in laundry detergents (second only to linear

alkylbenzene sulfonates) and liquid dishwashing liquids (used mostly as a cosurfactant with anionic surfactants), and are commonly used as the primary surfactant in various hard-surface, industrial and institutional cleaners.

4.1.2 Manufacture

The ethoxylation of primary alcohols is straightforward, but requires care because of the hazardous nature of EO. Conventional catalysts (sodium hydroxide, potassium hydroxide, etc.) are readily available, and ethoxylation products do not require purification or clean-up. Ethoxylation is typically run in high-pressure autoclaves with overhead stirring, although recirculation-type reactors have been introduced which provide enhanced mixing and process control.

4.1.3 Advantages/disadvantages

Alcohol ethoxylates are relatively inexpensive and readily available, and are considered to be one of the key “work-horse” surfactants. The primary advantage of alcohol ethoxylates, however, lies in the flexibility of their structure. The hydrophobe can vary in terms of carbon chain length (from C_6 to C_{20+}), carbon chain distribution (single homologues or various blends), feed-stock source (petrochemically based or oleochemically based), and the degree of minor (methyl) branching.

The hydrophile can vary in terms of EO chain length and distribution (conventional vs. “peaked”). This give this nonionic class significant flexibility in meeting a wide range of physical property and performance criteria.

4.1.4 Impact of molecular composition on properties

Increasing average carbon chain length decreases the critical micelle concentration (CMC), while both average carbon chain length and EO content determine the surface activity. Increasing carbon chain length also generally decreases the aqueous solubility and foaming, but generally increases the solution viscosity. Increasing carbon chain length and EO content also raises the melting point.

Most detergent applications use a carbon chain distribution averaging in the C_{12} – C_{16} range, and an average of about 60–65% (7–9 mol) of EO. Some hard-surface cleaners use shorter carbon chain lengths (C_6 – C_{10}) with 50–60% (3–5 mol) EO because a shorter carbon chain length has been shown to improve the hard-surface cleaning performance, presumably because the surfactant is better able to penetrate solid, greasy soils.

As discussed earlier in this chapter, “peaked” or “narrow-range” ethoxylates are available which have peaked or narrow ethoximer distributions. Peaking the distribution effectively concentrates certain ethoxymers. If these ethoxymers are key to performance, then the latter (soil removal, wetting, etc.) will be enhanced. However, the opposite is also true, which is why utilizing peaked ethoxylates requires optimization of EO content in order to obtain the benefit of peaking.

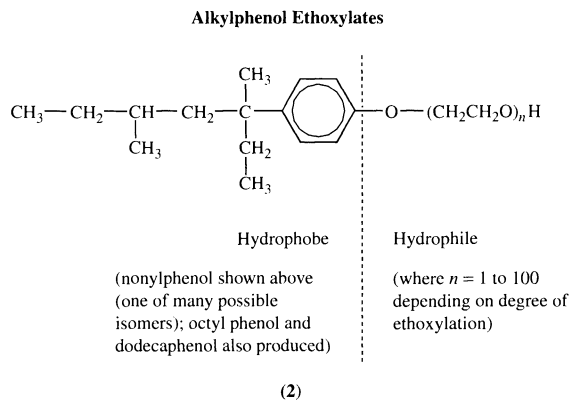
Peaking also improves the water solubility by reducing the concentrations of the lower, more insoluble homologues.

As discussed earlier, peaking can also significantly reduce the free (unethoxylated) alcohol content, as well as the “lower-mole” ethoxymers. This can have a significant impact on odour, especially if the parent alcohol is volatile and/or pungent. A lower concentration of unethoxylated alcohol also results in the reduction of pluming during the processing of spray-dried powders. If the ethoxylate is to be converted to an ether sulfate via a sulfation reaction, then the lower free alcohol content translates to a lower alcohol sulfate content in the alcohol ether sulfate. This can result in an improvement in the ability of the anionic to be thickened through the addition of salt, and potentially improve product

mildness through a reduction in the concentration of alcohol sulfate.

4.2 Alkylphenol ethoxylates

The general structure of alkylphenol ethoxylates (APEs) (2) is as follows:



4.2.1 Applications

Alkylphenol ethoxylates have been used for more than 50 years in a variety of applications. Questions regarding APE environmental acceptability have led to their diminished use, particularly in major USA and European liquid laundry and dishwashing products. They are still used in smaller-volume detergent products, particularly in the USA, and in a wide variety of institutional and industrial products.

4.2.2 Manufacture

The ethoxylation of alkylphenols is similar to that of linear alcohols.

4.2.3 Advantages/disadvantages

A key advantage of alkylphenol ethoxylates is that they contain essentially no free (unethoxylated) alkylphenol. The level of alkylphenol left after ethoxylation is dependent on two factors, i.e. the relative reactivity of the alcohol to EO in comparison to the reactivity of the various ethoxymers, and the level of EO added to the feedstock. With linear alcohols, the alcohol itself is

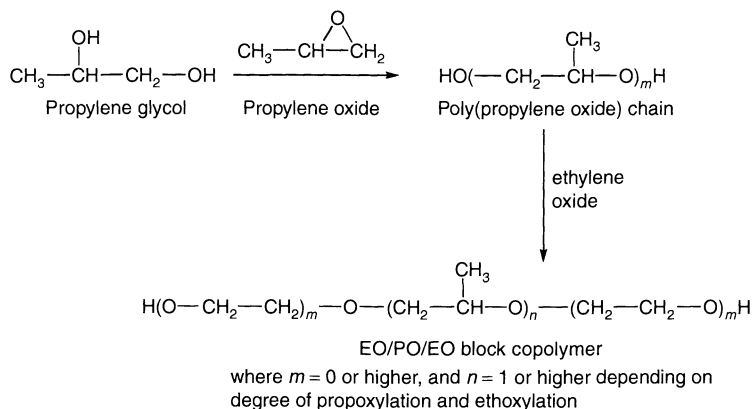


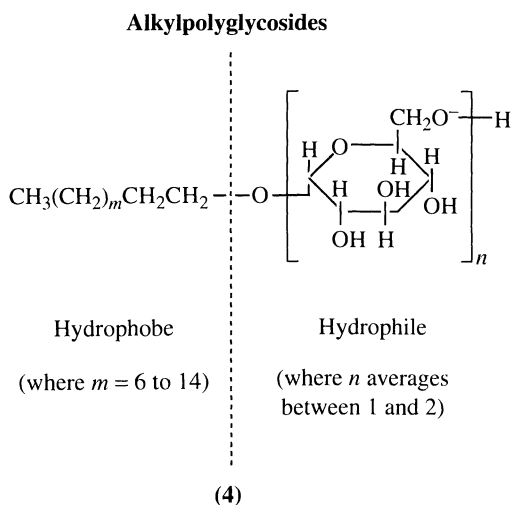
Figure 13.14. Preparation of EO/PO/EO block copolymers

4.3.4 Impact of molecular composition on properties

In general, increasing EO content increases the water solubility, improves the ability to thicken and form gels, and reduces wetting. PO/EO/PO block copolymers foam less, are more effective defoamers, and have less of a tendency to form gels in aqueous solutions than EO/PO/EO block copolymers.

4.4 Alkylpolyglycosides

The general structure of alkylpolyglycosides (4) is as follows:



4.4.1 Applications

Alkylpolyglycosides (APGs®) are formulated into dish-washing liquids (along with anionic surfactants) and in various specialty applications. They were the first major surfactant to utilize an oleochemical feedstock for the hydrophilic portion of the surfactant molecule.

4.4.2 Manufacture

APGs® are prepared by reacting alcohol (petrochemical or oleochemical) with glucose (dextrose) using processes based on Fischer glycosylation.

4.4.3 Advantages/disadvantages

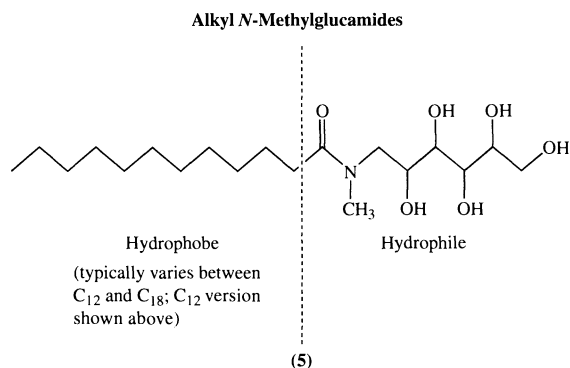
Alkylpolyglycoside (APG®) surfactants are premium-priced, high-foaming nonionics that are mild and ionic-strength tolerant.

4.4.4 Impact of molecular composition on properties

Increasing alcohol chain length increases the surface activity, but decreases water solubility, foaming and tolerance to ionic strength. Limitations of existing processes restrict the degree of glycosidation that can occur such that the average number of moles of glucose added is generally between 1.4 and 1.7. This gives a relatively narrow range to adjust the hydrophilic behaviour.

4.5 Alkyl *N*-methylglucamides

These surfactants were developed and are being largely consumed by a single detergent manufacturer (Procter & Gamble). They are included here because a significant quantity is produced, and because they represent the first major surfactant utilizing oleochemical feedstocks for both the hydrophobic and hydrophilic portions of the surfactant. The general structure of these surfactants (5) is as follows:

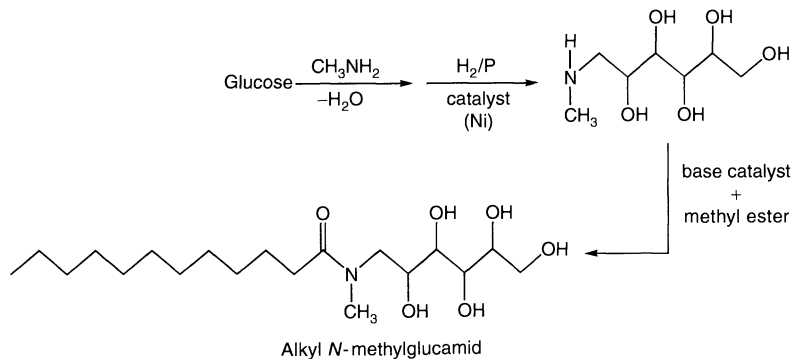


4.5.1 Applications

Alkyl *N*-methylglucamides find application predominantly in laundry and hand dishwashing liquids.

4.5.2 Manufacture

These surfactants are produced by preparing *N*-methylglucamine, followed by reaction of the latter with an alkyl (or fatty) methyl ester, using a base catalyst, to form the required glucamide (see Figure 13.15).



4.5.3 Advantages/disadvantages

The advantages of alkyl *N*-methylglucamides as surfactants are similar to those of APGs[®]. They are based on renewable resources, and are high-foaming, mild surfactants that emulsify well.

4.5.4 Impact of molecular composition on properties

These surfactants can be made from C₁₂–C₁₄ (cocoa) or C₁₆–C₁₈ methyl esters. The cocoa version foams better and is more soluble than the C₁₆–C₁₈ version.

4.6 Amine oxides

Amine oxides (6) are considered to be nonionic surfactants because they are neutral when dissociated in water at neutral pH. In an acid environment, however, amine oxides are cationic. The general structure of these surfactants is as follows:

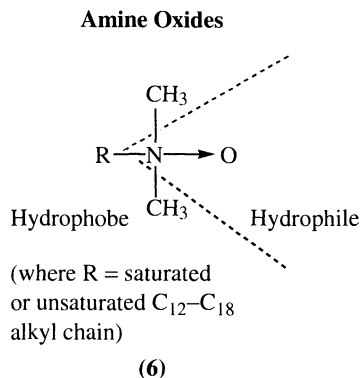


Figure 13.15. Preparation of an alkyl *N*-methylglucamide from glucose and a methyl ester

4.6.1 Applications

The principal application of amine oxides is boosting the foam formation of alcohol-ether-sulfate-based hand dishwashing formulations. They are also used in applications that require solubility in a high-ionic-strength environment, or when strong oxidants are present.

4.6.2 Manufacture

Amine oxides are prepared by the oxidation of tertiary amines (e.g. cocoa dimethylamine).

4.6.3 Advantages/disadvantages

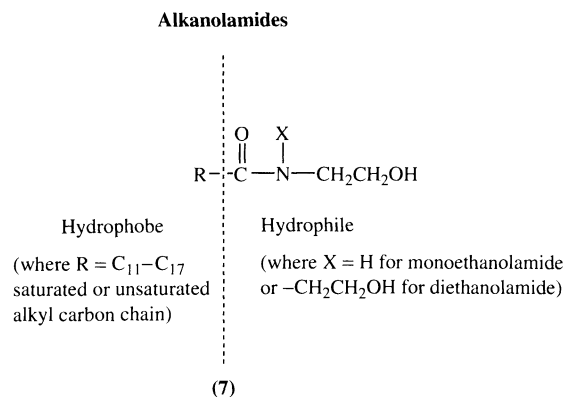
Amine oxides excel at stabilizing alcohol sulfate/alcohol ether sulfate foam, and are relatively unaffected by ionic strength and oxidants, but are relatively expensive.

4.6.4 Impact of molecular composition on properties

There is not a large degree of freedom with respect to structure. Most amine oxides are based on C₁₂–C₁₈ alkyldimethylamines. A small volume of amine oxides derived from acylamidopropyldimethylamines is also available commercially.

4.7 Alkanolamides

The general structure of these surfactants (7) is as follows:



4.7.1 Applications

Alkanolamides are similar to amine oxides in that their principal application is as foam stabilizers (boosters) in hand dishwashing formulations. Alkanolamides, however, are generally preferred in linear alkylbenzene sulfonate/alcohol-ether-sulfate-based formulations, while amine oxides seem to be the preferred foam stabilizer for alcohol sulfate/alcohol-ether-sulfate-based formulations.

Alkanolamides are also used in shampoos as thickening agents, and as anti-static and anti-corrosion agents in detergents.

4.7.2 Manufacture

These surfactants are produced by reacting fatty acids or fatty methyl esters with ethanolamine or diethanolamine. With fatty acids, conventional amides (sometimes called “Kritchevsky” alkanolamides) are obtained that consist of approximately 50% amide, 25% unreacted diethanolamine and 25% of various by-products (the amine ester the amide ester, and the amine soap). With methyl esters, higher-active (90% amide) alkanolamides are produced; these are known as “super amides”.

Alkanolamides can also be produced by ethoxylating fatty amides.

4.7.3 Advantages/disadvantages

Alkanolamides are excellent at stabilizing foam and thickening formulations, and are moderately priced.

4.7.4 Impact of molecular composition on properties

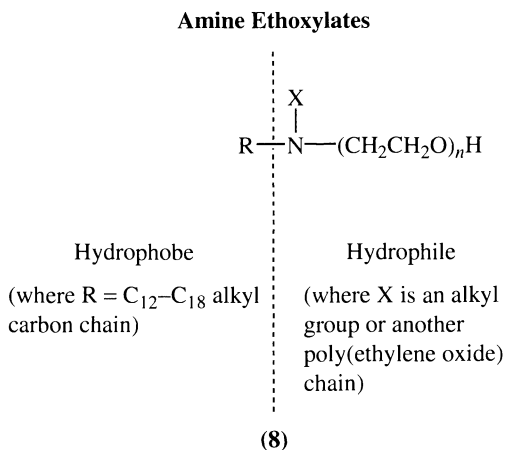
Most alkanolamides are made with lauric-range (C₁₂–C₁₄) fatty acids or methyl esters. Increasing the carbon chain length decreases the water solubility, which is why higher-molecular-weight versions are used in oil-soluble applications (e.g. metalworking fluids).

Diethanolamides are generally more soluble than monoalkanolamides, while super amides are less water soluble than regular (Kritchevsky) amides. Super amides are generally preferred in household products because they have a lower odour (due to their lower free amine content). Monoethanolamides are more effective than diethanolamides in building viscosity, while super amides are better at building viscosity than regular amides.

Note – alkanolamides can also be ethoxylated to improve water solubility.

4.8 Amine ethoxylates

The general structure of these surfactants (8) is as follows:



4.8.1 Applications

Amine ethoxylates are found in a wide variety of applications as corrosion inhibitors (oilfield applications), emulsifiers (asphalts), and as wetting agents processing aids, antistatic agents and lubricants (textiles).

4.8.2 Manufacture

Primary and secondary amine ethoxylates are prepared similarly to alcohol and alkylphenol ethoxylates. Like APEs, amines are highly reactive towards EO, thus resulting in a low level of unethoxylated amine.

In the ethoxylation of amines, EO first replaces the available hydrogens on the nitrogen. This reaction does not require an ethoxylation catalyst, and is one mechanism for preparing alkanolamines. Further ethoxylation (development of the poly(ethylene oxide) chains) requires an ethoxylation catalyst.

4.8.3 Advantages/disadvantages

Low-mol amine ethoxylates represent a balance between cationic and nonionic character. Varying the degree of ethoxylation changes the balance and produces

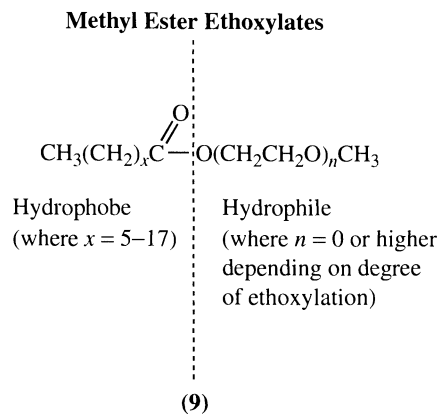
surfactants with the desired interaction with either anionic species and/or negatively charged surfaces.

4.8.4 Impact of molecular composition on properties

Increasing EO content decreases the cationic behaviour (increases the nonionic character), improves water solubility and decreases surface activity. The hydrophobe can be varied to achieve the desired surface activity and balance between cationic and nonionic character. Unsaturated hydrophobes produce better wetting agents.

4.9 Methyl ester ethoxylates

Although very little methyl ester ethoxylates are produced at the present time they are included here because of their potential to have a significant impact on the nonionic surfactants market in the future. The general structure of these surfactants (9) is as follows:



4.9.1 Applications

Methyl ester ethoxylates (MEEs) are a new introduction to the stable of feedstocks which can be ethoxylated, and have only recently become commercially available (currently being produced and utilized in a detergent formulation in Japan by the Lion Corporation). Based on recent literature, however, a significant amount of effort is being focused on the development of MEEs for detergent applications.

4.9.2 Manufacture

The ethoxylation of methyl esters is similar to that of linear alcohols (explained earlier in this chapter),

but requires specialized (proprietary) catalysts that have been developed by most major ethoxylators.

4.9.3 Advantages/disadvantages

A key advantage for ethoxylators is that MEEs introduce a new option for ethoxylatable feedstocks. For the formulator, MEEs offer the advantage of having a significantly lower tendency to gel which can be important when formulating liquid products.

The primary disadvantage of MEEs (or any ester ethoxylates) are that they will hydrolyse at pH levels above about 9. This makes these materials unacceptable for high pH (caustic) cleaners.

MEEs also foam less than alcohol ethoxylates. This can be both an advantage and a disadvantage, depending on what is desired in the application.

4.9.4 Impact of molecular composition on properties

The general relationship described above between hydrophobe structure and EO chain length of alcohol ethoxylates also applies to MEEs. However, since the catalysts used to prepare MEEs are often the same catalysts used to produce “peaked” ethoxylates, the ethoxymer distributions for MEEs are in fact already “peaked”. The degree of peaking, however, varies significantly depending on the catalyst used.

4.10 Other surfactants

There are a number of other, smaller-volume, nonionic ethoxylates that will not be discussed in this chapter.

These include secondary alcohol ethoxylates, tridecyl alcohol ethoxylates, fatty acid ethoxylates, PO-capped ethoxylates and various alcohol propoxylates.

5 REFERENCES

1. Scholz, H. J., Suehler, H., Quack, J. M., Schuler, W. and Trautmann, M., Process for the preparation of carboxylic esters of alkylene glycol ethers and their utilization, *European Patent Application 89105357.1*, to Hoechst AG (1989); *Chem. Abstr.*, **112**, 181911.
2. Behler, A., Raths, H. C., Friedrich, K. and Herrmann, K., Use of calcined hydrotalcites as catalysts for ethoxylation or propoxylation of fatty acid esters, *German Patent DE 3914131.4*, to Henkel KGaA (1990); *Chem. Abstr.*, **114**, 206576.
3. Weerasooriya, U., Aeschbacher, C. L., Leach, B. E., Lin, J. and Robertson, D. T., Process for alkoxylation of esters and products produced therefrom; using a calcium-based catalyst to react a lower alkyl oxide and a methyl ester of a fatty acid to obtain a product having a narrow weight distribution, *US Patent 5220046*, to Vista Chemical Company (1993); *Chem. Abstr.*, **120**, 57218.
4. Hirofumi, N., Itsuo, H., Yuji, F. and Yuichi N., Method and manufacturing of fatty acid esters of polyoxyethylene alkyl ethers, *US Patent 5374750*, to Lion Corporation (1994).
5. Pi, R. S. and Bigorra, J. L., Process for preparation of alkoxyated fatty acid alkyl esters, *German Patent DE 19611508 C1*, to Henkel KGaA (1997); *Chem. Abstr.*, **127**, 137366.
6. Behler, A. and Folge, A., Method of preparation of alkoxyated fatty acid alkyl esters, *German Patent DE 19611999 C1*, to Henkel KGaA (1997); *Chem. Abstr.*, **127**, 108708.
7. Cox, M. F. and Weerasooriya, U., Methyl ester ethoxylates, *J. Am. Oil Chem. Soc.*, **74**, 847–859 (1997).

CHAPTER 14

Cationic Surfactants

Dale S. Steichen

Akzo Nobel Surface Chemistry, Stenungsund, Sweden

1	General Introduction	310	6.1	Amine oxides	326
2	The Synthesis and Manufacture of Cationic Surfactants	311	6.2	Ethoxylated amines	327
3	Cationic Surfactants in Fabric Softening	314	6.3	Glucamides	327
	3.1 Introduction	314	6.4	Amidopropylamines	327
	3.2 Softener-active molecules	315	6.5	Quaternary ammonium compounds	327
	3.2.1 Dialkyldimethyl quaternaries	315	6.6	Nitrogen-containing polymers	327
	3.2.2 Diethylene triamine compounds	315	7	Cationic Surfactants in Personal Care	327
	3.2.3 Ester quaternaries	316		7.1 Introduction	327
	3.3 Softener product trends	317		7.2 Functionality of cationic surfactants on hair and skin	327
4	Cationic Surfactants in Biocides	318		7.2.1 Hair	328
	4.1 Introduction	318		7.2.2 Skin	328
	4.2 Fatty amines and derivatives	318		7.3 Cationic surfactant chemistry and applications	328
	4.3 Disinfection	318		7.3.1 Alkylamines	328
	4.4 Biostatic activity	319		7.3.2 Ethoxylated amines	328
	4.5 Biocidal activity	320		7.3.3 Quaternaries	329
	4.5.1 Wood preservation	320	8	Cationic Surfactants in Paper Processing	331
	4.5.2 Temporary protection	320	9	Cationic Surfactants in Conveyor Lubricants	332
	4.5.3 Permanent protection	321		9.1 Cationic surfactants as chain lubricants	333
	4.6 Wood preservatives	321		9.2 Cationic surfactants as chain lubricant additives	333
5	Cationic Surfactants in Hard Surface Cleaning	321	10	Cationic Surfactants in Road Construction	334
	5.1 Introduction	321		10.1 Adhesion promoters	334
	5.2 Hydrotropes	321		10.1.1 Heat stability of adhesion promoters	335
	5.3 Thickening	323			
	5.4 Foaming	325			
	5.5 Wetting	325			
6	Cationic Surfactants in Laundry Detergents	326			

11	Cationic Surfactants in Viscose/Rayon Production	337	12.4.4	Miscellaneous oilfield applications	340
11.1	Mercerization, xanthogenation, dissolving and ripening	337	13	Cationic Surfactants in Agricultural Formulations	341
11.2	Spinning, regeneration, washing and spin finishing	337	13.1	Adjuvants	341
12	Cationic Surfactants in Oilfield	337	14	Cationic Surfactants in Organoclays	343
12.1	Rheology	338	15	Cationic Surfactants in Mining	344
12.2	Corrosion inhibition	340	15.1	Flotation of oxide minerals	345
12.3	Other applications	340	15.1.1	Silicates from calcite	345
12.4	Recent trends and developments	340	15.1.2	Silicates from iron ore	345
12.4.1	Environmental	340	15.1.3	Feldspar from quartz	346
12.4.2	Surfactant-based fracturing fluids	340	15.2	Potash	346
12.4.3	Hydrate inhibitors	340	15.2.1	Flotation of sylvite	346
			15.2.2	Flotation of halite	347
			16	Acknowledgements	347
			17	References	347

1 GENERAL INTRODUCTION

Cationic surfactants represent one of the smaller classes of surfactants, with a consumption estimated to be 700 000 tons per year. Typically, reviews and market studies include in this class of materials all amine-based surfactants, whether they be charged or uncharged. In this present chapter we will use the same definition, but exclude amphoteric materials, which will be covered in the next chapter in this volume.

The demand for this class of surfactants is usually found to be 10% of the total demand of surfactants, although this figure varies depending upon the development in different regions of the globe. More developed regions typically show a higher use for these type of surfactants, driven partly by the use of fabric softeners.

While cationics are a smaller class of surfactants, they nevertheless represent an irreplaceable category of surface-active agents. This particular class of surfactants has several unique features, which cannot be duplicated by other surfactant materials. Such features include the ability to make a cationically charged surfactant, the basicity of the nitrogen lone pair in uncharged amine surfactants, the ability to change the hydrophilic–lipophilic balance (HLB) of the amine surfactant by protonating/deprotonating the nitrogen via changing the pH, and the cationically charged surfactant's proclivity for formation of ordered structures in aqueous solution.

The cationic charge leads to the use of these types of surfactants in fabric softening and other surface treatments where the cationic charge assists in deposition on to surfaces, which due to the construction of our

universe and matter, are typically negatively charged. The adsorption on to surfaces also accounts partly for the bactericidal properties of some cationic surfactants. The basicity of the nitrogen atom in amine surfactants can be used to impart a local basic environment at the surface that can be employed to improve detergency and other dispersive processes. The ability to change the HLB of an amine surfactant at will is useful in the breaking of emulsions created with amine surfactants. This type of behaviour is similar to the cleavable nonionic surfactants that have recently been commercialized. Cationic surfactants more easily form ordered structures in aqueous solution than other classes of surfactants. While in the past this has been a limitation to the use of cationics, it is now being employed where thickening in high-salt solutions is required, or where suspensions of particulate materials are needed.

The approach in this chapter is to review the use of cationic surfactants by application. I have taken this approach rather than a structural approach listing various applications for each type of surfactant. I hope the advantage for the reader will be a more in-depth knowledge of the individual applications and the contribution that the use of cationic surfactants can have. For those applications which are not covered, an understanding of the physical characteristics and behaviours of cationic surfactants from the applications described, should provide the basis for the sound use of these surfactants.

A section on the syntheses of the different classes of amine surfactants is given first. This provides a baseline of knowledge about the structures of the various

amine surfactants, which determine their performance in different applications. It should also be mentioned that the use of cationic surfactants, and surfactants in general, in various applications is often well patented. Prior to commercial exploitation of any of the technologies discussed in this chapter, a review of the patent literature is therefore strongly recommended.

I have called upon my colleagues in Akzo Nobel Surface Chemistry, who individually possess extensive application knowledge in each subject, to prepare the individual sections of this chapter. Their names are provided in the particular sections.

2 THE SYNTHESIS AND MANUFACTURE OF CATIONIC SURFACTANTS (*Maurice Dery*)

The majority of commercially produced amines originate from three materials, i.e. (i) natural fats and oils, (ii) *alpha*-olefins, and (iii) fatty alcohols. Most large commercial manufacturers of quaternary ammonium compounds are fully back-integrated to at least one of these three sources of amines. Such amines are then used to produce a wide array of commercially available cationic surfactants. Some individual quaternary ammonium compounds can be produced by more than one synthetic route.

Presently, most amine-containing surfactants are produced from fatty nitriles which are in turn made from a natural fat or oil derived fatty acid and ammonia (Figure 14.1). The nitriles are then reduced to the amines. There are a variety of reducing agents which accomplish this. Catalytic hydrogenation over a nickel-containing catalyst is the one which is most often used

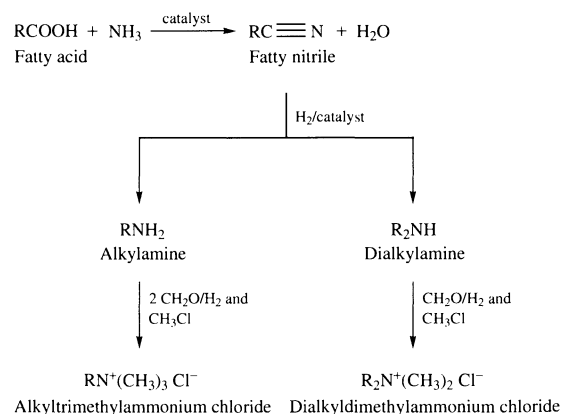


Figure 14.1. Preparation of cationics from fatty nitriles

on a commercial scale. Bimetallic catalysts have been investigated for use in this synthesis. Secondary and tertiary amines are often by-products whose formation can be hindered by the addition of acetic anhydride or excess ammonia. In some cases, it is desired to produce secondary amines and the reaction conditions can be controlled so that this is the favoured product. The amines can then be quaternized or derivatized as discussed below.

Nearly all fatty nitrile plants require considerable technological expertise and capital investment to operate. Presently, the largest volume product types are the di(hydrogenated tallow) alkyldimethylammonium (DHTMAC) quaternaries which are sold as the chloride or methyl sulfate salts.

The major products produced directly from fats, oils or fatty acids without a nitrile intermediate are the quaternized amidoamines and imidazolines, and their ethoxylated derivatives (Figure 14.2). Reaction of fatty acids or tallow with various polyamines produces the intermediate dialkylamidoamines. It is not necessary to stop the reaction at the dialkylamidoamine stage. By

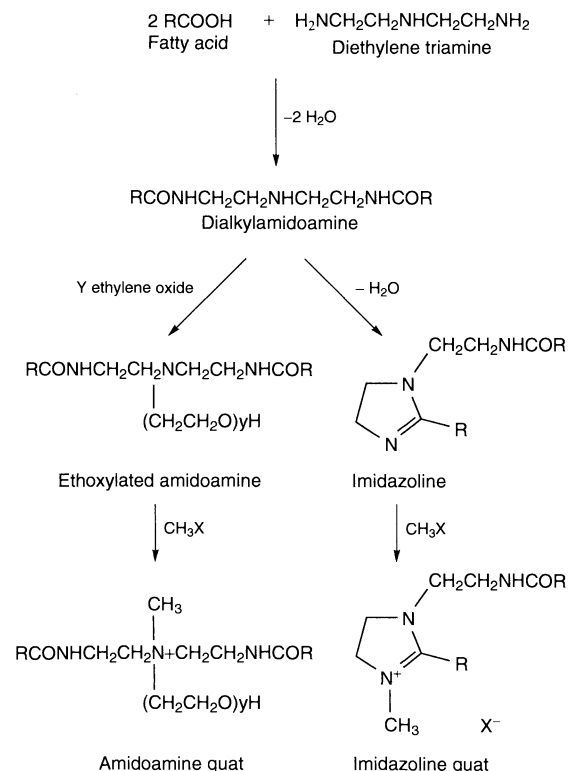


Figure 14.2. Cationic surfactants from amidoamines and imidazolines

controlling the reaction conditions, the dehydration can be continued until the imidazoline is produced. Quaternaries are produced from both amidoamines and imidazolines by reaction with methyl chloride or dimethyl sulfate. The amidoamines can also be reacted with ethylene oxide to produce ethoxylated amidoamines, which are then quaternized.

These compounds and their derivatives can be manufactured by using relatively simple equipment compared to that required for the fatty nitrile derivatives. The cyclization of amidoamines to imidazolines requires higher reaction temperatures and reduced pressures, which accounts for the higher prices of the imidazolines.

Alkylbenzyltrimethylammonium (ABDM) quaternaries are usually prepared from *alpha*-olefin or fatty alcohol precursors. Manufacturers that start from the fatty alcohol usually prefer to prepare the intermediate alkyl dimethylamine directly with dimethylamine and catalyst, rather than from the fatty alkyl chloride, although this route is commercially utilized (Figure 14.3). Small volumes of dialkyldimethyl and alkyltrimethyl quaternaries in the C₈–C₁₀ range are also manufactured from these precursors.

Some tertiary amines are used as surfactants, but the major use is as intermediates for preparing other classes of surfactants such as quaternary ammonium compounds and amine oxides. Primary and secondary amines are

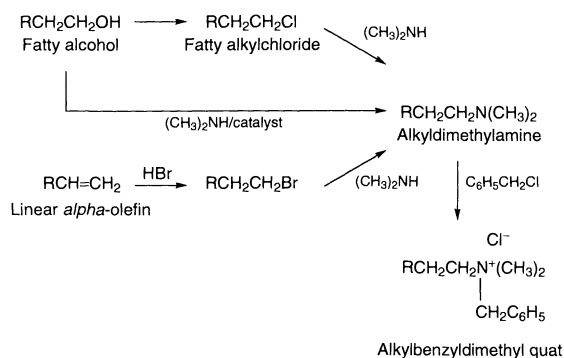


Figure 14.3. Cationics from *alpha*-olefins of fatty alcohols

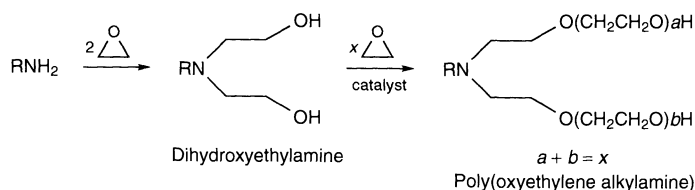


Figure 14.5. Synthesis of poly(oxyethylene alkylamine)s

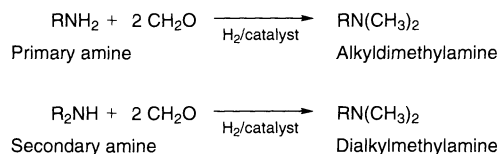


Figure 14.4. Reductive methylation of amines

usually converted to tertiary amines with formaldehyde and hydrogen in the presence of a catalyst (Figure 14.4). This is known as reductive alkylation and is an attractive commercial process. The desired amines are produced in high yields and without significant by-product formation. The resultant alkyldimethyl- and dialkylmethyl amines can then be quaternized by reaction with an appropriate alkylating reagent or oxidized to the amine oxide as described below.

Ethoxylated amines are prepared by the reaction of epoxides with primary amines. This reaction is well known, and an example is shown in Figure 14.5. In a typical manufacturing process, two moles of ethylene oxide are reacted with primary amine to produce a dihydroxyethylamine. Addition of more than two moles of ethylene oxide usually requires the presence of a catalyst. Typical catalysts are sodium or potassium hydroxide.

Non-catalytic reactions to produce poly(oxyethylene amine) adducts were reported to proceed at lower reaction temperatures via a quaternary ammonium intermediate. These catalysts do not result in a product with a symmetrical distribution of oxyethylene units. This has led to the development of catalysts intended to produce narrower ranges of oxyethylene units on the surfactant molecule. The narrow range ethoxylate catalysts are composed of cations with valency higher than 1. These include, (but are not limited to) calcium, barium, strontium and magnesium. The surfactant properties and manufacturing costs of poly(oxyalkylene amine)s produced using narrow-range catalysts are expected to be different compared to those made by using more traditional catalysts. Examples have recently appeared claiming to have produce lower coloured ethoxylated amines.

There are a wide variety of methods available for the preparation of quaternary ammonium compounds. A significantly lower number of methods exist which can be used on a commercial scale. A summary of the most common commercially used methods is discussed below.

Quaternary ammonium compounds are usually prepared from the reaction of a tertiary amine with an alkylating agent (Figure 14.6). The most widely used alkylating agents are summarized in Table 14.1. Some of these alkylating reagents pose significant health concerns and require special handling techniques. The alkylation reactions are usually run at moderate temperatures, i.e. 60–100°C. When using methyl chloride, the reactions are performed under moderate pressures, i.e. 60–115 psi.

The reaction of a tertiary amine with alkylating agent can be classified as S_N2 (substitution nucleophilic bimolecular). The rate of the reaction is influenced by several parameters, i.e. basicity of the amine, steric effects, reactivity of the alkylating agent and solvent polarity. The reaction is often carried out in a polar solvent such as isopropanol, which may increase the rate of reaction and make handling of the product easier.

Dialkyldimethyl and alkytrimethyl quaternaries can be prepared directly from secondary and primary amines respectively (Figure 14.7). This process is known as exhaustive alkylation and is usually not the method of choice on a commercial scale. This technique requires the continuous addition of basic material over the course of the reaction to prevent the formation of amine salts. Furthermore, products such as inorganic salt and water, are produced which must be removed from the product; the salt, in particular, represents a significant disposal problem.

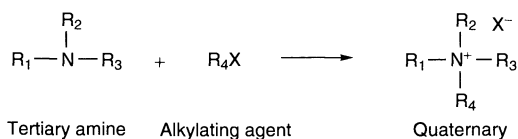


Figure 14.6. Cationics from alkylation of tertiary amines

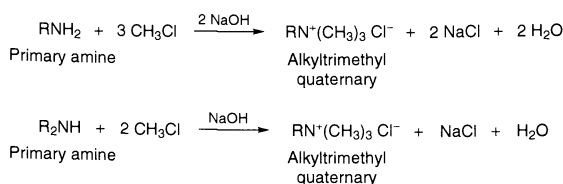


Figure 14.7. Cationics from exhaustive alkylation of primary and secondary amines

Ester quaternaries have begun to gain a market share in Western Europe and in the USA, with this growth expected to continue. These molecules are believed to be rapidly biodegraded and can be formulated into products such as fabric softeners that have good shelf-stability. The industry has developed many examples of this type of molecule.

Quaternized esteramines are usually derived from fat or fatty acid which is reacted with an alkanolamine to give an intermediate esteramine. The esteramines are then quaternized. A typical reaction scheme for the preparation of a diester quat is given in Figure 14.8. Two moles of fatty acid methyl ester are reacted with one mole of triethanolamine in the presence of sodium methoxide catalyst. The resultant esteramine is then quaternized with dimethyl sulfate. Free fatty acids and glycerides have been used in place of the fatty acid methyl ester.

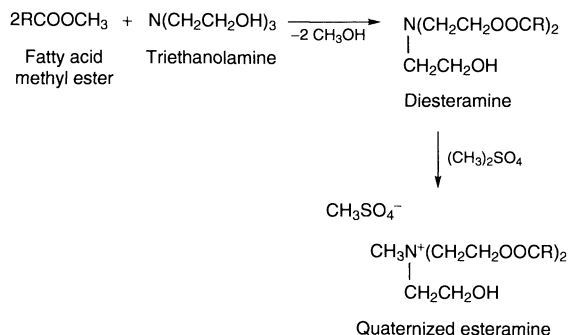


Figure 14.8. Preparation of a quaternized esteramine

Table 14.1. Typical alkylating agents used for the preparation of quaternaries

Alkylating agent	Chemical formula	Typical amine	Final quaternary
Methyl chloride	CH ₃ Cl	R ₃ N	R ₃ N ⁺ CH ₃ Cl ⁻
Dimethyl sulfate	(CH ₃) ₂ SO ₄	R ₃ N	R ₃ N ⁺ CH ₃ CH ₃ SO ₄ ⁻
Diethyl sulfate	(CH ₃ CH ₂) ₂ SO ₄	R ₃ N	R ₃ N ⁺ CH ₃ CH ₂ CH ₂ SO ₄ ⁻
Benzyl chloride	C ₆ H ₅ CH ₂ Cl	R ₂ N	R ₃ N ⁺ CH ₂ C ₆ H ₅ Cl ⁻

Tertiary amines can be readily oxidized to amine oxides by using peracids and Caro's acid (H_2SO_5). On a commercial scale, the preferred reagent is hydrogen peroxide. The reaction is performed in water or an alcohol-water mixture. The reaction is quite facile and can be completed by using relatively moderate temperatures, i.e. $70\text{--}80^\circ\text{C}$. In order to ensure complete conversion of the amine, a slight excess of hydrogen peroxide is often used which must be decomposed when the desired reaction is complete. The simplest method to accomplish this is to raise the reaction temperature slightly and monitor the disappearance of the hydrogen peroxide. Chelating agents are usually added to the reaction mixture to prevent contact of trace metals with the hydrogen peroxide solution. The mechanism was reported to proceed via an alkyl peroxide which decomposes to an amine oxide. The reaction is catalysed by carbon dioxide. The kinetics of the reaction are first order with respect to the amine concentration and three-halves order with respect to the hydrogen peroxide concentration (Figure 14.9).

Another important class of cationic surfactants are the polyamine-based or polyquaternaries. Generally, the synthesis of the polyamine-based surfactants is similar to that for the monomeric counterparts, and will not be discussed any further here.

Cationic surfactants, containing two hydrophilic groups and two hydrophobic groups in the same molecule, are referred to as "Gemini" surfactants. Although these materials were first prepared in 1971, they have not yet found any significant commercial application. Many cationic "Gemini" surfactants have been prepared with the intention of studying their chemical and physical properties. The synthetic methodology used to prepare these compounds is similar to that used for preparing more traditional cationic surfactants, with the exception being that the starting materials contain multiple functionality. An example of a "Gemini" surfactant preparation is given in Figure 14.10. The developments in this area are being monitored by the industry

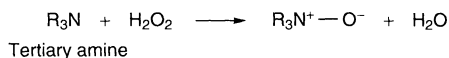


Figure 14.9. Preparation of amine oxides

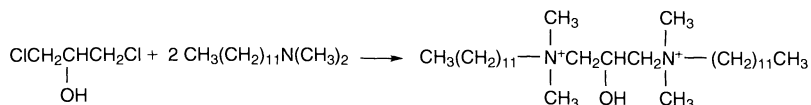


Figure 14.10. Preparation of a cationic "Gemini" surfactant

with hopes that a significant commercial application is imminent.

3 CATIONIC SURFACTANTS IN FABRIC SOFTENING (*Joe Zachwieja*)

3.1 INTRODUCTION

The use of amine surfactants is varied and found throughout a diverse number of industries. One industry, detergents, employs the largest use of amine surfactants as fabric softener actives. Out of the approximately 700 000 metric tons of amine surfactants consumed globally on an annual basis, roughly 50%, or 300 000 metric tons, find their way into household, industrial, and textile fabric softener applications. Of the three end-uses as fabric conditioners, the household fabric softener segment commands the lion's share of cationic surfactants at approximately 270 000 metric tons.

The need for a fabric softener owes its origins to the replacement of soaps with synthetic detergents shortly after World War II. Soaps derived from fats that had been reacted with caustic had been used for hundreds of years. These soaps were efficient at removing dirt from fabrics, although they also reacted with water hardness (Ca and Mg ions) to form an insoluble residue that deposited on to the fabrics. This residue resulted in the undesirable benefit of greying fabrics; however, the residue also provided a beneficial effect, i.e. it improved the feel or "hand" when the fabric was rubbed across the skin. With the introduction of the synthetic detergents, which were formulated with builders or sequestering agents to eliminate the water hardness residues, this perceived "softness" benefit was lost.

In the late 1940s, the Armour Industrial Chemical Company (now Akzo Nobel Surface Chemistry) discovered that the softness lost during laundering with synthetic detergents could be replaced by the use of a nitrile-based chemical, i.e. dihydrogenated tallow dimethylammonium chloride (DHTDMAC). However, the commercial use of DHTDMAC in a household fabric softener was not realized until the mid-to-late 1950s. A. E. Staley and Procter & Gamble first introduced the household

fabric softeners, “Sta-Puf” and “Downy”, respectively, in the United States. The softener brands, “Comfort”, “Soupline”, “Lenor” and “Humming” were launched about 10 years later in Europe and Japan. The level of active softener in all of these systems ranged from 3 to 8 wt% of DHTDMAC.

Household fabric softeners have been formulated to be utilized by the consumer in either a rinse-added, dryer-added, or wash-added (softergent = detergent plus softener) application. It must be noted that there have been many cationic compounds developed since the introduction of DHTDMAC to meet the needs of formulators.

3.2 Softener-active molecules

The fabric softener actives exploited today evolved primarily as a result of (i) formulation and performance demands, (ii) major trends in marketing, such as concentrated products to allow for greater throughput in manufacturing, reduction of packaging and associated costs and globalization of formulations, and (iii) legislative environmental pressures. The nature of the softener actives that are commercially viable in today’s marketplace fall into three chemical types of cationic surfactant, i.e. (i) dialkyldimethyl quaternary ammonium salts, (ii) diethylenetriamine (DETA) compounds, and (iii) ester quaternaries. All of these are quaternary ammonium compounds, meaning that they contain a positively charged nitrogen atom having four hydrocarbon groups attached to it by covalent bonds. For each positively charged nitrogen centre there is an associated anion, typically chloride or methyl sulfate. The structures that represent these three major types of quaternaries in fabric softening applications are shown in Figure 14.11. A recent review on quaternary ammonium compounds covering their properties, synthesis and manufacture, and applications has been given by Dery (1).

3.2.1 Dialkyldimethyl quaternaries

The first commercial fabric softener active, DHTDMAC, shown as Structure 1 in Figure 14.11, accounts for approximately one third or 90 000 metric tons of the quaternaries sold for use in fabric softening. DHTDMAC is known to form a liquid crystalline phase when dispersed in water. The liquid crystalline phases of DHTDMAC and water are comprised of lipid-like bilayers and alternating water layers. This structure is best described as a “multiwalled vesicle” which resembles the multiple

layers of an onion. Due to the large amount of water enclosed within the bilayer structure, the disperse phase volume is much greater, thus resulting in a higher viscosity of the dispersion. This viscosity can be reduced by the addition of an electrolyte, such as sodium or calcium chloride, which affects the spacing of the bilayers and causes a lowering of the disperse phase volume via osmotic shrinking of the lipid-like phase.

Data available from the commercial textile-treating industry suggested that two fatty chains of 16–18 carbons each, which are commonly found in tallow, lard and some seed oils, such as palm, soybean or canola, resulted in the best softening performance. The alkyl groups can be saturated, unsaturated, or a mixture of both. The effect of alkyl chain saturation on the softener active performance is readily seen in Table 14.2.

In general, softeners based on hydrogenated tallow triglycerides or stearic acid which have a low Iodine Value (IV) exhibit higher melting and storage temperatures (and usually require more solvent for ease of handling), but provide premium softening and lubricating qualities. The major detriment of these highly saturated compounds is their inability to be formulated into dispersions containing greater than about 15 wt% active. When the level of alkyl chain unsaturation is increased in these compounds, the dispersion forms a lower-viscosity isotropic phase in which the packing of the alkyl chains is disordered. This results in a reduced softening effect; however, it does facilitate easier formulation of concentrated products through the addition of electrolytes.

The methyl sulfate version (DHTDMAMS), which is the primary softener active found on tumble-dryer sheets also provides some softening, but more importantly, static charge control. The methyl sulfate counterion is used due to the corrosivity of chloride ions against the drums of tumble dryers.

3.2.2 Diethylene triamine compounds

The softener actives based on diethylene triamine (DETA) that are of commercial significance today are diamidoamine ethoxylate quaternary ammonium methyl sulfate (DAAEQAMS) and imidazolium quaternary ammonium methyl sulfate (IQAMS) (see Structures 2 and 3, respectively, in Figure 14.11). These compounds account for only about 10%, or 26 000 metric tons, of the quaternaries sold for use in fabric softeners. Such compounds were developed as an alternative to DHTDMAC and were found to provide better static control and similar softening performance on a cost/performance basis.

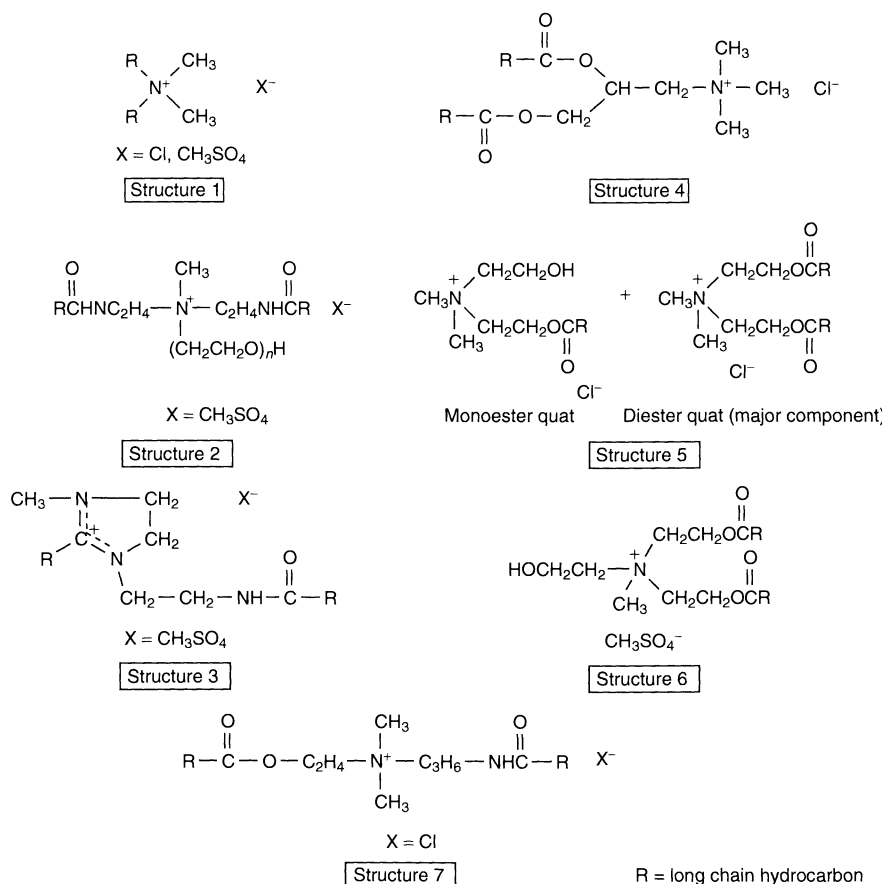


Figure 14.11. Chemical structures of major softener actives

Table 14.2. Effect of alkyl chain saturation on the characteristics of fabric softener actives

Characteristic	Unsaturation (IV) ^a	
	Low, IV = 1–10	High, IV = 45–60
Handling temperature	> 65°C	40–55°C
Softening Hand	Premium Slick	Good–excellent Dry
Stable concentration (aqueous)	~ 15% (maximum)	~ 25% (maximum)

^aIV, iodine value.

The major advantage of this class of quaternaries is that they can be derived from whole triglycerides, which are cheap and available from a variety of naturally occurring sources. DAAEQAMS and IQAMS based on unsaturated fatty chains can be readily formulated to 25 wt%

and 20 wt%, respectively. For saturated fatty chains, these compounds suffer the same problem of formulation as seen with DHTMAC. The trade-off for this class of compounds is ease of formulation in exchange for premium softening. The IQAMS materials are also used as tumble dryer sheet actives and in industrial (textile) applications.

3.2.3 Ester quaternaries

The third class of quaternary ammonium compounds, i.e. ester quaternaries (Structures 4–7 in Figure 14.11) has the greatest commercial significance in the fabric softener market today. These compounds represent almost 60%, or 155 000 metric tons, of the quaternaries sold for use as fabric softeners. A recent and very comprehensive review of ester quaternaries was presented by Kruger *et al.* in 1998 (2).

Ester quaternaries have been known since the 1930s, but found limited commercial use in earlier years. However, their commercial relevance took a “quantum leap” forward in 1991, when European detergent manufacturers reformulated their rinse-added softeners because of pressure from environmental authorities in some European Union member states. A major benefit or feature of the ester quat structure is its decomposition into non-surface-active fragments upon hydrolysis. However, this benefit, i.e. hydrolytic instability, also posed a challenge to the formulator. Ester quaternaries are stable in aqueous solutions only over a narrow pH range, unlike the traditional alkyl quaternaries. Softener dispersions based on ester quaternaries are typically adjusted to $\text{pH} < 4$ to maintain hydrolytic stability.

The ester quaternaries used in fabric softening are based on alkanolamines reacted with fatty acids or esters. Ester quaternaries derived from 3-(dimethylamino)-1,2-propane diol (DMAPD) and methyldiethanolamine (MDEA) result in structures (4 and 5, respectively, in Figure 14.11) which resemble the dialkyl quaternaries and exhibit similar softening performance. However, triethanolamine (TEA)-based ester quaternaries (Structure 6 in Figure 14.11) contain a mixture of mono- and triester quaternaries, in addition to the diester quat, and lack the same level of performance as the true diester quaternaries. There have been recent developments in improving the diester quat content in these TEA-based compounds. One development includes a process to make a higher diester quat compound which exhibits improved softening performance, water absorbancy and formulation stability, and is non-yellowing to fabrics. It is apparent from these developments that manipulation of molecular parameters such as the degree of esterification, ratio of mono-, di- and triesters, unsaturation, and isomerization of the alkyl chain, can result in ester quaternaries having improved, if not unique, benefits. Another interesting development utilizing these techniques describes a novel, biodegradable polyolester quat based on dimethylethanolamine (DMEA) capable of producing low-viscosity, stable aqueous dispersions/solutions up to 60 wt% actives. The above-mentioned ester quat structures are primarily available in North America and Europe. There is an amide-ester quat (Structure 7 in Figure 14.11) commercially available in Asia which is a hybrid between a diamidoamine and an ester quat.

3.3 Softener product trends

The primary use of fabric softeners world-wide is in the rinse-aid area. This product form is typically

added to the rinse water during the deep-rinse cycle. Rinse-added softeners aim to deliver about 0.25% of active softener per load of fabric (e.g. for a 3 kg load = 7 g of active softener). Regular-strength formulations (3–8 wt% actives) were the work-horse products from their introduction in the 1950s until the development of concentrates and dilutable concentrates in the 1980s. These products contained three to five times the active softener when compared to the regular-strength product and primarily were designed to be diluted with tap water by the consumer to make a 5–8 wt% dispersion. Such products met the following consumer demands, i.e. (i) for less bulky and more concentrated products, and (ii) to reduce plastic container waste and promote recycling. Formulators continued to use the DHTDMAC- and DETA-based actives for these concentrated products, but needed to employ viscosity modifiers such as ethoxylated fatty amines, fatty alcohols and poly(ethylene glycol) esters to reduce the viscosity of the dispersion. However, these new systems, in particular those above 15–20 wt% actives, suffered from the weakness of gelation upon their addition to cool rinse water, which caused fabric staining. This problem was solved in the early 1990s with the development of the ultra fabric softener formulations which are in use today. New softener actives were developed which could be formulated to 20–30 wt% without the fear of fabric staining upon addition to the cool rinse water.

In addition to new softener actives development, the formulator has been focused on delivering other benefits via the fabric softener formulation. Recent developments include concentrated, biodegradable softener formulations which are clear or translucent and deliver improved softening and water absorbency, and most importantly, reduced wrinkling of fabrics, with a combination of higher-IV materials and also the inclusion of solvents to maintain solution clarity.

Another important fabric softener product form is the dryer-added product. This product form has been a staple commodity in the North American market-place since its introduction in the late 1960s to alleviate the buildup of static electricity or “static cling” on fabrics produced during the tumble drying process. Such a dryer-added product consists of a non-woven substrate or sheet on to which is coated a mixture of cationic surfactant and a release or distribution agent. The dryer sheet is tossed in the tumble dryer along with the damp fabrics and aims to deliver about 1–2 g of fabric softener actives per fabric load. Since dryer sheets have a considerably lower loading of softener actives when compared to the rinse-added products, it is not surprising that they provide only a limited softening performance. This feature, coupled

with the fact that outside of North America a relatively smaller percentage of households have tumble dryers, also explains why rinse-added softeners command the lion's share of the world-wide market.

The methyl sulfate dialkyldimethyl quaternaries and ester quaternaries are the cationic surfactants of choice for tumble dryer sheets. The compounds typically used to optimize the softener actives release from the dryer sheet include poly(ethylene glycol) esters and fatty amine soaps. Recent data indicate that through the proper selection of release agent (such as a 4 mol alkoxyolate), the melt characteristics of the dryer sheet actives can be optimized to deliver the softener actives more consistently over the entire tumble drying cycle.

The final commercially significant product form incorporates a cationic fabric softener active with laundry detergent and is better known as a "softergent". The softergent product form is a trade-off on cleaning and softening performance with convenience or ease of use. Due to the antagonism between cationic softener actives and anionic detergents, a considerable amount of work has been directed at finding the right cationic and anionics. One result was to incorporate hydrophilic substituents into the cationic molecule to overcome the formulation issues. Other strategies included the simple addition of cationics or quaternaries into the detergents at very high concentrations, delayed release of cationics via encapsulation, use of substitutes for the cationic surfactant, such as montmorillonite clays, and replacement of the anionic detergent with a nonionic surfactant. Like the dryer-added product form which has found a niche in one geographical area (North America), the softergent product form has found considerable success in Europe. Because fabrics are typically line dried in Europe, the softergents can provide a perceptible level of softness that cannot be met for those regions employing tumble dryers. However, as tumble dryers continue to penetrate the European market-place, the benchmark for softening performance will be raised to a level that cannot be met by the current softergents.

4 CATIONIC SURFACTANTS IN BIOCIDES (*Johan Tiedink*)

4.1 Introduction

Microbes are ever present in our world. Wherever there is moisture and nutrients – basically everywhere on earth – microbes thrive, potentially leaving disease and destruction in their wake. Microbes take many forms, such as viruses, bacteria, fungi or algae. They cause

rot and slime – which affect products and health. An important means of defense against these tiny terrors are biocides. The use of biocides ensures effective performance of products and processes, reduces the cost of maintenance, provides health protection and safeguards the natural environment.

4.2 Fatty amines and derivatives

A number of fatty amines and their derivatives, especially quaternary ammonium compounds, are widely used in formulations for the control of bacteria, fungi, viruses and algae, in disinfectant/sanitizers and wood-preservation applications. Table 14.3 presents the fatty amines and derivatives which are frequently used in biocidal formulations.

The positive ionic charge, based on the nitrogen atom of a quaternary ammonium group, provides the antimicrobial properties. Quaternary ammonium compounds have a number of advantages, i.e. they are readily biodegradable, non-toxic, non-corrosive (at in-use concentration) and have no odour.

4.3 Disinfection

Disinfectants, in their various specific formulations, are used to destroy bacteria, viruses, spores, fungi and other dangerous microbes. Disinfectants prevent disease and food poisoning. They also prevent the spread of microbes in hospitals, surgeries, public places, breweries and in the food processing industry. Disinfecting of

Table 14.3. Biocidal cationic surfactants

Amines

Cocoamine
 Cocopropylenediamine
 Bis(3-aminopropyl); laurylamine
 Monoalkyl quaternary ammonium compounds
 Tetradecyltrimethylammonium bromide
 Hexadecyltrimethylammonium chloride
 Cocotrimethylammonium chloride
 Coco(fractionated)trimethylammonium chloride

Dialkyl ammonium quaternaries

Diocyltrimethylammonium chloride
 Didecyltrimethylammonium chloride
 Didecyltrimethylammonium bromide
 Dialkyltrimethylammonium chloride
 Dicocodimethylammonium chloride
 Benzyl quaternary ammonium compounds
 Cocobenzyltrimethylammonium chloride
 Coco(fractionated)benzyltrimethylammonium chloride

animal housing and equipment protects the animals and produce from lethal microbes such as *Salmonella sp.* and *Listeria sp.*

Disinfectants are often applied by spraying or brushing. In order to achieve the best results, the surfaces to be disinfected have to be cleaned first. Dust, litter and other deposits contain substantial levels of microbes. After disinfecting, the surfaces are usually rinsed with water, although the purity of the water employed for rinsing can impact on how ultimately successful was the initial disinfecting of the surface.

The antimicrobial properties of cationic surfactants are evident in their ability to eliminate or inhibit the

growth or viability of microorganisms. The concentration used in the formulations determines whether the microorganisms are eliminated or are inhibited from growth.

4.4 Biostatic activity

Biostatic activity is defined as the concentration at which the growth of the microorganism is inhibited. Depending on the actual microorganism involved, formulations are called either bacteriostatic, fungistatic or algaestatic. In Tables 14.4 and 14.5, the fatty amine

Table 14.4. MIC values as measures of bacteriostatic activity

Product ^a	Gram-negative bacteria		Gram-positive bacteria		
	<i>Escherichia coli</i>	<i>Proteus mirabilis</i>	<i>Pseudomonas aeruginosa</i>	<i>Staphylococcus aureus</i>	<i>Streptococcus faecalis</i>
Cocoamine acetate (Armac [®] C)	50–100	400	3200	25	12
Cocopropylenediamine (Duomeen [®] C)	25–50	800	100–200	12–25	6–12
Didecyldimethylammonium chloride (Arquad [®] 2.10-50)	6	50–100	100–200	3	3–6
Dialkyldimethylammonium chloride (Arquad [®] NF-50)	25–50	400	200	6–12	25
Dicocodimethylamminium chloride (Arquad [®] 2C-75)	400	800	400	3	12–25
Cocobenzylidimethylammonium chloride (Arquad [®] B-50)	100	200	200	6	12–25
Coco(fractionated)benzylidimethylammonium chloride (Arquad [®] MCB-50)	50–100	100–200	200	3–6	6

^aThe values given have been determined specifically for Akzo Nobel Surface Chemistry products with the trade names given in brackets.

Table 14.5. MIC values as measures of fungistatic activity

Product ^a	Yeasts		Fungi	
	<i>Candida albicans</i>	<i>Saccharomyces cerevisiae</i>	<i>Aspergillus niger</i>	<i>Penicillium funicolosum</i>
Cocoamine acetate (Armac [®] C)	25	6–12	100–100	100
Cocopropylenediamine (Duomeen [®] C)	12–25	6	200	50–100
Didecyldimethylammonium chloride (Arquad [®] 2.10-50)	3	3	6–12	3
Dialkyldimethylammonium chloride (Arquad [®] NF-50)	25	25	100–200	25
Dicocodimethylamminium chloride (Arquad [®] 2C-75)	400	800	12	6–12
Cocobenzylidimethylammonium chloride (Arquad [®] B-50)	50	12	100–200	12
Coco(fractionated)benzylidimethylammonium chloride (Arquad [®] MCB-50)	25	6	25–50	3–6

^aThe values given have been determined specifically for Akzo Nobel Surface Chemistry products with the trade names given in brackets.

derivatives exemplified above are compared in their biostatic activities against gram-negative bacteria, gram-positive bacteria, yeasts and fungi. The Minimum Inhibitory Concentration (MIC) is the concentration at which the growth of the microorganism is inhibited. Such MIC values are given in parts per million (ppm) of active material.

4.5 Biocidal activity

The biocidal activity of a formulation is determined by the concentration of the active ingredient and by the effective contact time. Depending on the microorganism to be killed, formulations are classified as being either bactericidal, fungicidal or algicidal, fungicidal or algacidal. In disinfectant applications, the successful elimination of microorganisms is usually confirmed in a suspension test. Tables 14.6 and 14.7 present test results obtained on didecyltrimethylammonium chloride and coco(fractionated)benzyltrimethylammonium chloride. The tests employed are performed according to the new European standards for the evaluation of disinfectants. (*Note for formula tables* – in most applications, these products will be part of a specific formulation, and consequently an effect on the antimicrobial properties can be expected.)

Table 14.6. Biocidal activity of coco(fractionated)benzyltrimethylammonium chloride and didecyltrimethylammonium chloride determined according to pr EN1276^a for clean conditions (0.03% BSA)

Microorganism	Lowest test concentration to pass the test (ppm active substance)	
	Coco(fractionated)-benzyltrimethylammonium chloride ^b	Didecyltrimethylammonium chloride ^c
<i>Enterococcus faecium</i>	30	10
<i>Staphylococcus aureus</i>	40	10
<i>Escherichia coli</i>	100	25
<i>Pseudomonas aeruginosa</i>	700	250
<i>Salmonella typhimurium</i>	150	40
<i>Proteus mirabilis</i>	300	200
<i>Campylobacter jejuni</i>	45	4
<i>Legionella pneumophila</i>	80	30
<i>Listeria monocytogenes</i>	25	5

^apr EN1276–quantitative suspension test for the evaluation of bactericidal activity of chemical disinfectants and antiseptics used in food, industrial, domestic and institutional areas.

^bArquad[®] MCB-50 (Akzo Nobel Surface Chemistry) used as test substance.

^cArquad[®] 2.10-50 (Akzo Nobel Surface Chemistry) used as test substance.

Table 14.7. Fungicidal activity of coco(fractionated)benzyltrimethylammonium chloride and didecyltrimethylammonium chloride determined according to pr EN1650^a for clean conditions (0.03% BSA)

Microorganism	Lowest test concentration to pass the test (ppm active substance)	
	Coco(fractionated)-benzyltrimethylammonium chloride ^b	Didecyltrimethylammonium chloride ^c
<i>Candida albicans</i>	225	40
<i>Saccharomyces cerevisiae</i>	150	20
<i>Aspergillus niger</i>	1500	150

^apr EN1650–quantitative suspension test for the evaluation of fungicidal activity of chemical disinfectants and antiseptics used in food, industrial, domestic and institutional areas.

^bArquad[®] MCB-50 (Akzo Nobel Surface Chemistry) used as test substance.

^cArquad[®] 2.10-50 (Akzo Nobel Surface Chemistry) used as test substance.

4.5.1 Wood preservation

In general, hard-wood is more durable than soft-wood but, due to its slow growth rate, is not commercially available in large quantities and is also extremely costly. On the other hand, timber cut from soft-wood is often attacked by fungi, thus causing discoloration deep within the wood structure. The most common of these fungi is the blue stain fungi (see Section 4.5.2 below). Soft-wood is also prone to attack from wood-rotting fungi (see Section 4.5.3 below). The chemical treatment of wood, to counter the effect of fungi, involves additional costs; however, these costs are fully justified if the correct preservatives are used. Wood that is properly protected with the right preservative has a service lifetime that is many years longer than that of unprotected wood. This, in turn, reduces commercial soft-wood consumption, which is itself an important environmental issue. The use of hard-wood, often sourced from indigenous rain forests, can similarly be reduced drastically.

4.5.2 Temporary protection

Wood is used as a source of nutrition and energy by many microorganisms, including fungi and bacteria. Fungi, such as the blue stain fungi, can be especially damaging since their mycelia, or filaments, are able to develop inside the wood cells. The damage caused by these fungi shows as dark patches of discoloration both on and beneath the surface of the timber. In certain

conditions, these patches can spread to cover wide areas until the entire length of the timber is affected. The damaged, discolored wood can become spongy and more water-absorbent than healthy wood. Fungal growth may be treated in different ways, and the use of a proven, effective fungicide is often the best of these.

4.5.3 *Permanent protection*

For soft-woods, the most damaging form of attack is from the wood-rotting fungi, the so-called *Basidiomycetes*. While some wood species are more durable than others, none are completely resistant and will eventually succumb in time. This group of fungi can be split into two types, known as “Brown rot” and “White rot”. “Brown rot” destroys the cellulose skeleton of the wood so that the timbers become brown and crumble easily. “White rot” damages both the cellulose and the lignin in the wood cells, causing only minor changes in colour, although the wood will become soft and fluffy. The presence of water, oxygen, suitable temperatures and nutrients – in this case the wood itself – are necessary for the germination and development of fungi spores to take place. Wood preservation systems rely on the permanent elimination of the fungi.

4.6 **Wood preservatives**

The use of quaternary ammonium compounds as biocides in wood preservation formulations is increasing rapidly. Their low toxicity and biodegradable properties, combined with their favourable adsorption characteristics, have led to an increase in the popularity of these products as an alternative to other wood preservative formulations such as pentachlorophenate (PCP) and chromated copper arsenate (CCA). Due to growing environmental pressure, the use of these latter products is declining and the development of alternative wood preservatives is gaining momentum.

Used by themselves, or in combination with other modern biocides – such as systematic fungicides, bactericides or insecticides – the long-alkyl-chain quaternary ammonium compounds offer a useful tool in the development of new environmentally acceptable wood preservative formulations. The most commonly used quaternary ammonium compounds are coco(fractionated) benzyltrimethylammonium chloride and didecyltrimethylammonium chloride.

5 **CATIONIC SURFACTANTS IN HARD SURFACE CLEANING** (*Eva Cassel and Magnus Franck*)

5.1 **Introduction**

Hard surface cleaning applications cover a very wide scope and encompass both Industrial and Institutional (I&I) and Household (HSHLD) concerns. This sub-set of cleaning applications is very complex due to geographical differences in formulation design, plus the wealth of technical and environmental requirements on the cleaners themselves. However, a common denominator is the importance of formulation knowledge.

5.2 **Hydrotropes**

Hydrotropes belong to a very diverse group of compounds that are of great importance in the formulation of cleaning products. These range from simple molecules such as ethanol and glycols, to sodium toluene/cumene sulfonates, phosphate esters, alkyl polyglucosides, amphoteric surfactants and quaternized fatty amine ethoxylates. While there are different definitions of (and theories about) the mechanisms of the hydrotropes, their primary role is to solubilize surfactants and salts in aqueous cleaning systems. The appropriate selection of the hydrotrope will achieve not only a stable cleaner but may also offer additional benefits which could include enhanced cleaning efficiency. Sometimes a hydrotrope that offers multiple benefits is called a “cosurfactant”. There is no such thing as a “panacea” or “universal” hydrotrope. Before the formulation work starts, the cleaning conditions have to be clearly defined, for example, the substrate to be cleaned, the type of soil, the cleaning temperature and methodology, the desired foam characteristics and the environmental requirements. On the basis of this information, the surfactant(s), complexing agents, pH adjusters and the hydrotrope can be chosen. In the I&I area, non-ionic surfactants are often preferred due to their very good surface-active properties, hard water tolerance and compatibility with other surfactant types.

The complexing agents and pH adjusters are in many cases necessary auxiliaries to achieve good cleaning efficiency but they also change a vital parameter of nonionic cleaning formulations, namely the cloud point. The latter is the upper temperature limit where the nonionic is no longer soluble in an aqueous system. Above this temperature, phase separation occurs. For optimal detergency performance, the cloud point should

be close to the desired cleaning temperature. Use of a hydrotrope makes it possible to balance the formulation and adjust the cloud point according to this desired temperature.

From the virtual “smorgasbord” of hydrotropes that are available, products from the cationic (quaternized fatty amine ethoxylates) and amphoteric families can be combined with nonionic surfactants to produce water-based formulations for the cleaning or degreasing of hard surfaces.

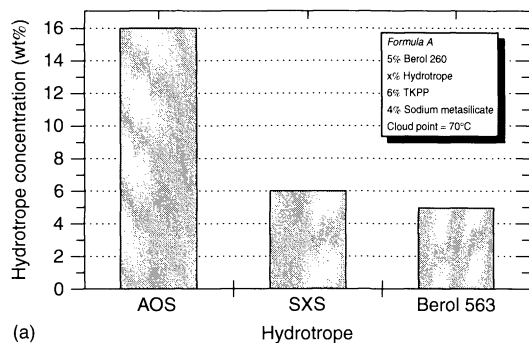
It is important to take the efficiency of the hydrotrope into consideration. The performance and quantity of the hydrotrope is linked to the nonionic in the system and the type and quantity of the builders used. Figure 14.12 illustrates the requisite amounts of hydrotrope needed to reach a cloud point of 70°C in (a) an alkaline (Formula A) and (b) a neutral formulation (Formula B), using a modelling system consisting of a “peaked” or “narrow-range” ethoxylated fatty alcohol (C₉₋₁₁ + 4EO) with good emulsifying and soil penetrating properties (Berol[®] 260), and different builders, including tetrapotassium pyrophosphate (TKPP), sodium metasilicate and trisodium citrate. The hydrotropes

are a quaternized fatty amine ethoxylate (Berol[®] 563), α -olefin sulfonate (AOS) and sodium xylene sulfonate (SXS). The hydrotrope concentrations are adjusted based on the active material present.

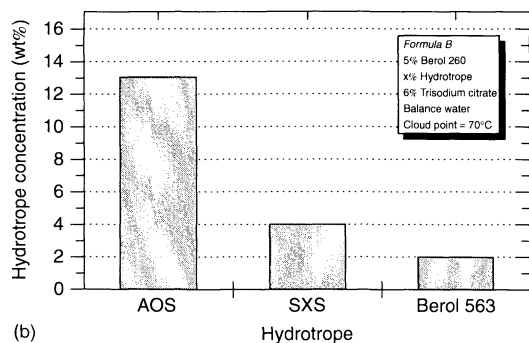
In this modelling system, the quaternary is the most effective hydrotrope for this particular nonionic. In Figure 14.13, the results of a detergency test using the above-mentioned formulations are presented. There are many types of soils (depending on the application), but in this case the sample is a “real world” soil from a diesel engine containing soot and grease. The test method is a laboratory evaluation where the soil is smeared on coated metal panels, the formulation is applied to the panels and the detergency of the different products is measured by using a reflectometer.

For the sake of clarity, the reference solution containing the nonionic surfactant and the builders (no hydrotrope) was dispersed mechanically before application to the panels. Regardless of the builder used, the quaternized fatty amine ethoxylate (Berol[®] 563) enhances the soil removal.

Interestingly, quaternaries have the ability to remove both greasy and particulate soil. The hydrotropic

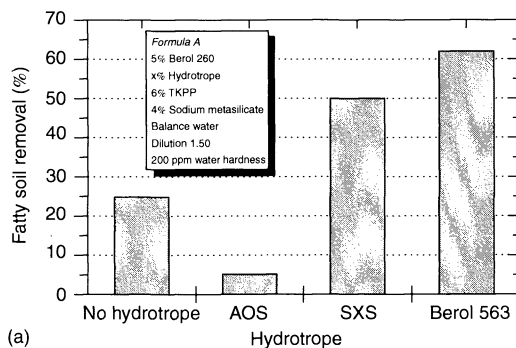


(a)

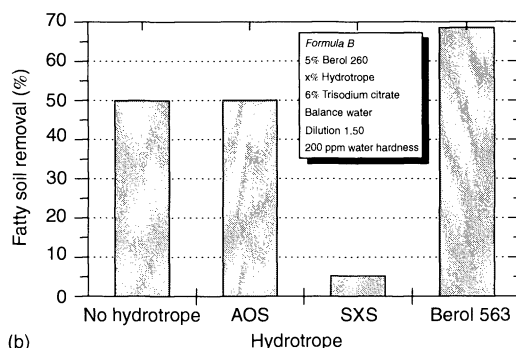


(b)

Figure 14.12. Required amounts of hydrotropes needed to obtain a cloud point of 70°C, shown for alkaline (a) and neutral (b) formulations



(a)



(b)

Figure 14.13. Detergency testing results obtained for the same formulations used in Figure 14.12

properties of specific quaternized fatty amine ethoxylates are a function of their alkyl chain length and the ethylene oxide content. When selecting the proper quaternary for the specific cleaning condition, it is critical to achieve the right balance between the alkyl chain and the ethylene oxide for greatest efficiency. This highlights the fact that a well-balanced formulation of non-ionics and quaternaries makes a potent, water-based, degreasing system for hard surfaces and provides for a powerful alternative to solvent-based degreasing. However, this type of combination does not perform well in all instances. If a low-foam, high-caustic stability or a highly concentrated product is the goal, a different composition would be required. One option is to use certain amphoteric surfactants. In Figure 14.14, the initial foam heights for three different hydrotrope systems (using Formula A, as above) are evaluated according to a method in which cylinders containing the formulations were put in a support and simultaneously turned upside down for a given time. The amount of hydrotrope is adjusted to produce a clear solution above 45°C (Berol® 522 is a phosphate ester).

In this case, use of an amphoteric substantially lowered the foam quantity (height). In Figure 14.15, sodium cumene sulfonate (SCS) is included as a reference and the amount of hydrotrope is again adjusted to produce a clear solution above 45°C. The amphoteric offers a secondary benefit as it solubilizes a highly concentrated Na₃NTA (trisodium salt of nitrilotriacetic acid) solution, while other hydrotropes have solubilization maxima for the salt below this figure. The curves presented in Figure 14.15 show how much hydrotrope is needed at a certain Na₃NTA concentration. The far right of each curve indicates the solubilization maximum. With Berol

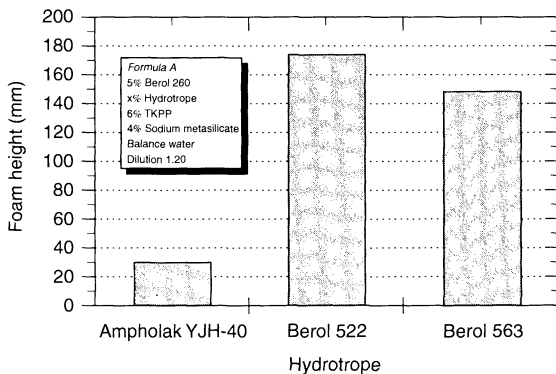


Figure 14.14. Foam-height evaluation results obtained for three different hydrotrope systems, employing the same alkaline formulation used in Figure 14.12

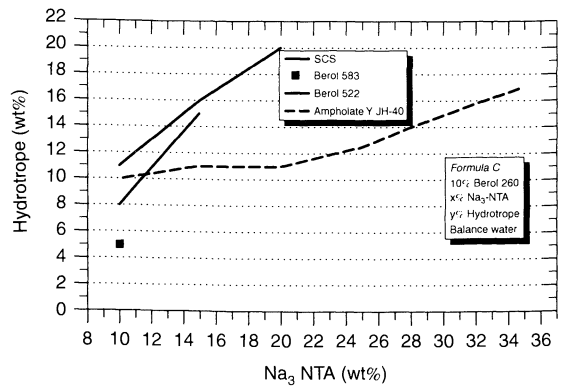


Figure 14.15. Selecting the proper hydrotrope for a highly concentrated liquid cleaner

Table 14.8. Starting point for hard surface cleaning formulations

Cleaning conditions check-list	Main ingredients of cleaner
<ul style="list-style-type: none"> • Type of surface • Soil composition • Foam/low foam/no foam • Temperature • Corrosion risk • Legislative environmental concerns • Viscosity required 	<ul style="list-style-type: none"> • Surfactant(s) • Hydrotropes • Builders/salts

563 and 10% Na₃NTA in this formulation, the use of Ampholate Y JH-40 allows for a maximum above 30%. In summary, it is of the utmost importance to know the exact details the cleaning conditions for any particular application (see Table 14.8).

5.3 Thickening

Formulations are most frequently thickened in order to increase the contact time on inclined or vertical surfaces such as toilet bowls and tile walls. The longer adherence achieved in this way results in an improved removal of soil, limestone and microorganisms, as well as in an enhanced perfume release for better air freshening. Different types of thickeners can be used, for example, natural thickeners (cellulose ethers, xanthan and guar gums, starch, etc.), synthetic thickeners (polyacrylates, polyurethanes and poly(ethylene glycol)s) and cationics thickeners (quaternary ammonium salts, amine oxides and ethoxylate amines). The stabilities of various thickeners over different pH ranges are shown given in

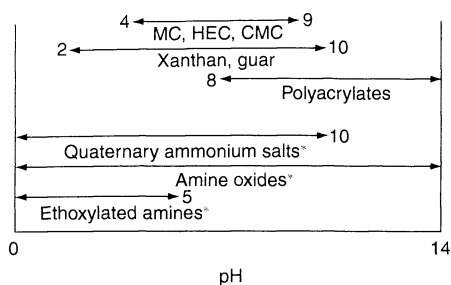


Figure 14.16. Stability of various types of thickener over different pH ranges: MC, methyl cellulose; HEC, hydroxy ethyl cellulose; CMC, carboxy methyl cellulose; *, includes blends with anionics

Figure 14.16. As can be seen from this figure, an amine oxide mixed with an anionic as a thickener gives excellent stability over the broad pH range of 0 to 14.

The unique ability of cationic surfactants to act as thickeners is a result of the formation of long, rod-like micelles which become entangled to give three-dimensional networks. The packing of these micelles into a network has been observed as the source of the increased viscosity. The solubility of the cationic plays a key role in the thickening action. If the cationic is highly soluble, it forms spherical micelles, which do not increase the viscosity of the system. Therefore, a desolubilizer (such as an anionic surfactant or electrolyte) must be added to initiate the formation of the rod-like micelles and the increase in viscosity. The latter will increase until a maximum level is reached, after which it will decrease. Conversely, with poorly soluble or insoluble cationic surfactants, a solubilizer must be added to dissolve the surfactant and create the rod-like micelles, to achieve the increased viscosity. However, adding too much of the solubilizer will result in a non-viscous system, as shown in Figure 14.17.

Amine oxides are powerful thickeners for anionic surfactants, especially in acid formulations. The addition of a very low amount of salt results in a high viscosity. It is not only surfactant solutions that can be thickened by amine oxides, for example, in hypochlorite bleach formulations amine oxides offer a good thickening effect as well as chlorine stability. The alkyl chain length of the amine oxide has a significant impact. In particular, myristamine oxide, $C_{14}N(CH_3)_2O$ (Aromox[®] 14 D-W), gives both a high viscosity and chlorine stability. A “middle-cut” coco amine oxide, $C_{12-14}N(CH_3)_2O$ (Aromox[®] MCD-W), gives limited or no thickening effect, but can act as a fragrance (solubilizing) agent. However, the use of “full-cut” coco amine oxides (containing a certain proportion of C_{16-18} alkyl chains),

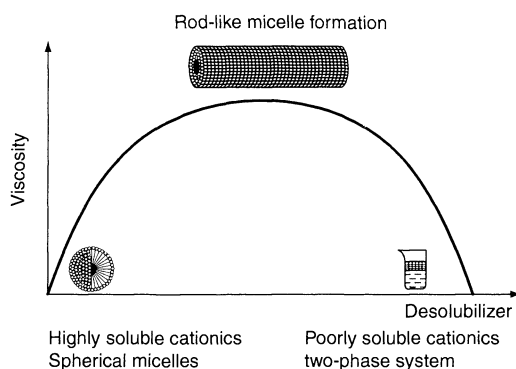


Figure 14.17. Schematic of the formation of rod-like micelles

in combination with certain anionic surfactants, leads to an effective thickening system.

In some cases, an alternative to sodium hypochlorite bleach cleaners may be desired for a variety of reasons, including product odour. Acid bleach cleaners based on hydrogen peroxide are a good alternative. A formulation based on a quaternary ammonium compound, a nonionic and a desolubilizer in citric acid, will give excellent sanitation, including cleaning, descaling, mild bleaching and bactericidal activity. The formulation shown in Table 14.9 has excellent stability regarding viscosity and active oxygen content.

In acid solutions, amine oxides have a very efficient thickening performance when used with both organic and mineral acids. These thickened acid formulations are widely used in industries where the removal of soil, limestone, metal oxides and microorganisms are desired, including applications such as metal and vehicle cleaning, industrial kitchen and bathroom cleaning. Depending on the type of acid, thickening is efficiently done with a combination of a poorly soluble cationic

Table 14.9. Formulation for a bleach cleaner based on hydrogen peroxide^a

Component	Content (wt%)
Citric acid monohydrate	3.0
Arquad [®] 16-29 (hexadecyltrimethylammonium chloride)	3.5
Berol [®] 175 (C_{12-14} alcohol, 7.5 EO)	0.1
Fragrance IFF 4329	0.1
Hydrogen peroxide (a.m.) ^b	5.0
Sodium xylene sulfonate (40%)	1.5
Demineralized water	(added to balance)

^aViscosity: 250 mPa s (20°C, Brookfield LVT (spindel), 60 rpm).

^ba.m., active matter.

thickener and a cationic solubilizer, or the appropriate anionic counterion and a cationic solubilizer. The thickening effect of a citric acid formulation containing a cationic solubilizer and an anionic counterion is shown in Figure 14.18.

When thickening an organic acid, e.g. citric acid, a broad range of cationic surfactants can be used, such as amine oxides, ethoxylated amines or quaternary ammonium compounds, in combination with a desolubilizer (e.g. an aromatic sulfonate) (see Figure 14.19).

When a desolubilizer is added to the acid formulation, an increase of the viscosity is observed, where the rod-like micelles increase in length. When the maximum viscosity is reached, a phenomenon occurs which is often observed with cationic surfactants, namely viscoelasticity. The latter occurs when the system of very long rod-like micelles with numerous entanglements becomes a stable, three-dimensional network, which at

low shear stress behaves like gum. If this network is broken down by applying a suitable shear rate, the solution then starts to flow. This viscoelastic region, which is very small, can be easily avoided by adding small amounts of either nonionic surfactants or fragrance components. In neutral-pH products, the only effective cationics are the quaternary ammonium compounds in combination with aromatic sulfonates.

5.4 Foaming

Foam, which is a dispersion of a gas in a liquid, has a wide field of applications within I&I and HSHLD cleaning. One of the main functions of amine oxides is the generation of foam. The greatest amount of foam is obtained when using amine oxides having chain lengths of C_{12} – C_{14} . Cocoamine oxide, $C_{12-14}N(CH_3)_2O$ (Aromox[®] MCD-W), in combination with an alkyl sulfate, yields a voluminous, creamy foam that is highly stable in the presence of fat. The combination of an amine oxide and an alkyl sulfate shows excellent foaming height characteristics, even in high-water-hardness systems.

5.5 Wetting

Water is a good solvent and is commonly used because it is safe, inexpensive, effective and has no odour. However, its polar character makes it difficult to wet a hydrophobic surface, thus requiring the use of a wetting agent. Good wetting allows the active solution to penetrate more quickly to the surface and the cleaning to be more efficient. Amine oxides with chain lengths of around C_{12} yield the fastest wetting times, where the latter are measured as the sinking times of a standard piece

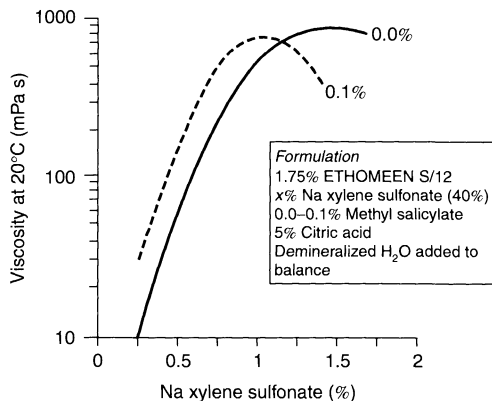


Figure 14.18. Thickening effect (represented by increase in viscosity) of citric acid formulations

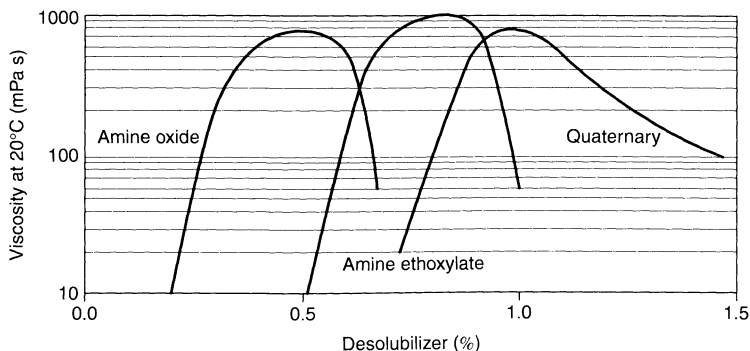


Figure 14.19. Thickening effect (represented by increase in viscosity) as a function of added desolubilizer (xylene sulfonate) for different cationic surfactants in citric acid formulations (5% citric acid monohydrate; 2% cationic surfactant (C_{16} – C_{18} type))

of cotton in an aqueous surfactant solution. Accordingly, amine oxides are effective wetting agents in different types of formulations of alkaline degreasers, for example, oven cleaners or low-temperature detergents. Most recently, a combination of alkyl amine derivatives and short-chain glycosides has been shown to have a synergistic effect, thus resulting in even better wetting properties. Amine oxides with chain lengths of C_{12-14} and C_{12-18} and a cocotrimethylammonium chloride, together with both branched and linear octyl and hexyl glycosides, have been used. In laboratory tests, different ratios of alkylamine derivatives and alkyl glucosides were mixed and then evaluated by using dynamic contact angle measurements (against Parafilm[®] as a reference). These tests showed that a ratio of one part alkylamine to nine parts alkyl glucosides gave the optimum wetting performance.

6 CATIONIC SURFACTANTS IN LAUNDRY DETERGENTS (Jeff Chang)

The major surfactants used in laundry detergents have traditionally been linear alkylbenzene sulfonates, alcohol

ethoxylate sulfates, alkyl sulfates and alcohol ethoxylates. This is due to their favorable cost-to-performance position. The choice of surfactants to be used depends not only on performance criteria but also on compatibility issues. The surfactants employed must be compatible with the myriad of other components in the formulation such as builders, enzymes, bleaching agents, fluorescent whitening agents and dye-transfer inhibitors. The use of amine surfactants in laundry detergents remains that of a specialty surfactant additive. Common usage rates of amine surfactants within laundry detergent formulations are in the range of 0.1–5 wt%. The performance characteristics enhanced by amine surfactants are typically soil removal, soil anti-redeposition, and in-wash softening.

6.1 Amine oxides

Amine oxides are well known for their ability to remove oily/greasy soils from hard surfaces. This ability is retained in the laundry operation. Amine oxides have the general Structures A and B shown in Figure 14.20

Polymers with amine oxide units have also found utility in laundry detergents to increase detergency, i.e.

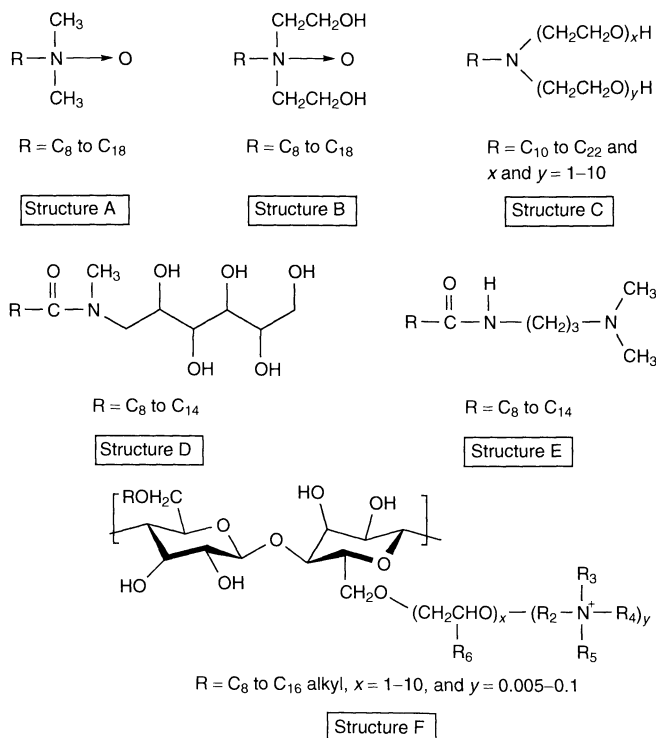


Figure 14.20. Structures of cationic surfactants used in detergents

soil removal. Amine *N*-oxide polymers have also been shown to act as dye-transfer inhibitors.

6.2 Ethoxylated amines

In some cases, the removal of oily soils and sebaceous dust from fabrics has been shown to be enhanced by ethoxylated amines, (see Figure 14.20 Structure C). Studies have also demonstrated that ethoxylated amines are very effective in removing grass stains on cotton fabrics. An ethoxylated amine with a tallow alkyl chain and two moles of ethylene oxide has been shown to be especially effective against oily soils deposited on cotton/polyester blends and grass stains on cotton fabrics.

6.3 Glucamides

This class of compounds is covered by a large number of application and formulation patents. Such surfactants are claimed to have superior cleaning efficiency with respect to oily/greasy and enzyme-sensitive soils. Glucamides are polyhydroxy fatty acid amides, having the typical Structure D shown in Figure 14.20.

6.4 Amidopropylamines

Amidopropylamines, whose generic structure is given as Structure E in Figure 14.20, have been shown to soften fabrics when used in a formulation containing its corresponding betaine, where the nitrogen group has been functionalized by reaction with chloroacetic acid. To date, betaines on their own have not made significant inroads into the laundry detergents market. Amidopropylamines, along with the glucamides discussed above, have been used to increase detergency.

6.5 Quaternary ammonium compounds

Quaternary ammonium compounds have been utilized for a number of purposes in laundry detergents. The performance characteristics where benefits are seen include fabric softening and soil removal. Laundry detergents that also provide fabric softening can utilize relatively simple quaternary ammonium compounds of structures such as alkyldimethylammonium quaternaries with an alkyl chain length of 12 to 18 carbon atoms.

Ethoxylated quaternary ammonium compounds have been also shown to aid in the removal of particulate/clay

soils from fabrics. The mechanism by which this occurs involves the positively charged cationic group absorbing on to the negatively charged layers of the clay particles which are attached to the fabric. The hydrophilic ethoxylate units of the surfactant swell the clay particles so that they lose their cohesive character and are thus swept away in the wash liquor. Some complexes of anionic and cationic surfactants have been found to remove oily soils from fabrics better than either the anionic or cationic parent surfactants from which they were formed.

6.6 Nitrogen-containing polymers

Nitrogen-containing polymers are a recent addition to the use of amine surfactants in detergent formulations. The first of these is a cellulose-based polymer where quaternary ammonium groups have been added to the polymer backbone. This structure allows the molecules to attach themselves to the fabric through the quaternary ammonium group while the cellulosic backbone covers the fabric, thus effectively forming a protective sheath around the latter. The generic structure of this cellulose-based material is given as Structure F in Figure 14.20.

Polyalkyleneimines in the molecular weight range from 1000 to 25 000 g/mol have also been used as soil dispersants in laundry detergents. In these compounds, ethoxy and propoxy groups are attached to the nitrogen-carbon backbone of the alkyleneimine. Such alkoxy groups are able to attach themselves to soil materials and keep them in solution.

7 CATIONIC SURFACTANTS IN PERSONAL CARE (*Diana Tang*)

7.1 Introduction

Cationic surfactants, characterized by their amphiphilic properties, contain an alkyl hydrophobe and a hydrophilic positively charged head-group. Among cationic surfactants, quaternary ammonium salts are notable for their ability to reduce surface and interfacial tensions by ready adsorption to a surface or interface, such as hair and skin. This ability to adsorb on to substrates makes the use of cationic surfactants extremely important in the personal care industry.

7.2 Functionality of cationic surfactants on hair and skin

For conditioning and improving the substrate (hair and skin), the cationic surfactants or conditioning agents

must first deposit on to such substrates. Because of the proteinaceous surface structure of both hair and skin, quaternary ammonium compounds are attracted to the negatively charged cuticle surface of hair and the stratum corneum of skin. The interactions of quaternaries with hair or skin surfaces contribute to surface improvements such as smoothness, softness, enhanced manageability, etc. This improvement of surface quality on hair or skin is called "conditioning".

7.2.1 Hair

Human hair is a biological composite consisting of the cortex, a spindle-shaped assemblage of cells which serves as supporting material for the hair fibre, plus surrounding cuticle layers overlapping each other to provide the hair outer surface. The cuticle surface consists of amino acid functional side groups, which are potential binding sites for cosmetic components. The mechanism of interaction of cationic surfactants with the outer surfaces of hair fibres has recently been studied by surface analysis techniques, e.g. x-ray photoelectron spectroscopy, (XPS) by which the amount of adsorption and uptake can be quantitatively determined.

The deposition and uptake of cationic surfactants on the cuticle surface ultimately neutralizes the negatively charged surface and thereby reduces the repulsive forces between the cuticle scales to provide the following conditioning benefits: enhanced appearance, lubricity, manageability, wet/dry combability, reduced static charge "flyaway" and detangling.

7.2.2 Skin

Skin is a living organism and has a more complex structure than hair. This means that irritation and skin compatibility are major concerns when the creams and lotions are formulated. One of the most important aspects for skin conditioning is to prevent the evaporation of water from the skin surface to the atmosphere. Consequently, emollients and humectants are commonly used in skin care formulations to condition the skin surface.

Cationic surfactants play an important role and offer specialized benefits for certain skin care and sun care formulations. The emollients, humectants and cationic emulsifiers used in skin care products provide the following skin conditioning benefits: smoothness, moisturizing effects, increased elasticity, less irritation and improved appearance.

7.3 Cationic surfactant chemistry and applications

Nearly all hair care products incorporate one or more cationic conditioning agents, where the latter can be either cationic surfactants or cationic polymers. The cationic surfactants can be further divided into four major classes, i.e. alkylamines, ethoxylated amines, alkyl imidazolines, and quaternaries. The quaternaries are the most widely used in the personal care industry because of their strong affinity to the hair fibre surface.

7.3.1 Alkylamines

The structures of the different types of alkylamines are shown in Figure 14.21. These amines, which are used extensively in the cosmetic industry (typically as their salts with phosphoric, citric or acetic acid), exhibit surface activity, water solubility and compatibility with a variety of other surfactants. They can also serve as neutralizing agents for resins and acrylate thickeners.

Although alkylamines are extensively used as conditioning agents, amidoamines have recently gained a considerable amount of attention due to certain performance advantages. The presence of the amido group, positioned between the cationic nitrogen and the hydrophobe (Figure 14.22), influences the amine functionality and helps impart strong cationic properties.

7.3.2 Ethoxylated amines

Compared to ordinary amines, ethoxylated amines (Figure 14.23) become progressively more water-soluble and nonionic in character as the degree of ethoxylation

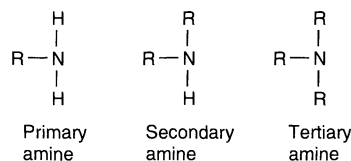


Figure 14.21. Structures of the different types of alkylamines

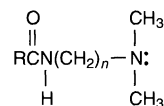


Figure 14.22. General structure of amidoamines

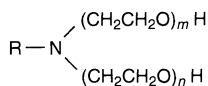


Figure 14.23. General structure of ethoxylated amines

increases. Most ethoxylated amines are water-soluble and compatible with a wide range of other surfactants, in particular anionics. Ethoxylated amines are generally used as emulsifying, conditioning and anti-static agents in shampoos and conditioners. In addition, they are employed as plasticizing agents in hairspray formulations to detackify and to provide flexibility, as well as to neutralize hair fixative resins.

7.3.3 Quaternaries

Quaternary ammonium compounds play a vital role in the formulation of hair and skin care products, and for use in the personal care industry can be divided into three categories, i.e. (i) alkyl quaternary ammonium compounds (including mono-, di- and trialkyl quaternaries), (ii) ethoxylated quaternaries, and (iii) ester quaternaries. The synthetic route for preparing such compounds is shown in Figure 14.24.

The conditioning performance of these compounds is largely determined by their molecular structures. As shown in Figure 14.25, the performance, in general, improves as the number of alkyl groups and the length of the alkyl chains increase.

Alkyl quaternary ammonium compounds

Mono-, di- and trialkyl quaternaries are an extremely important group of surfactants for use as hair conditioning ingredients (Figure 14.26). The conditioning performance and benefits depend upon the number of alkyl groups and the alkyl chain length, as well as the degree of unsaturation.

Monoalkyl quaternaries, such as cetrimonium chloride, are cost-effective light conditioning additives, the dialkyl quaternaries, such as dicyldimethylammonium

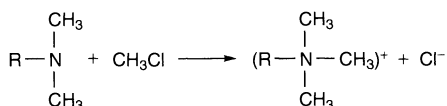


Figure 14.24. Synthetic route used to prepare quaternary ammonium compounds

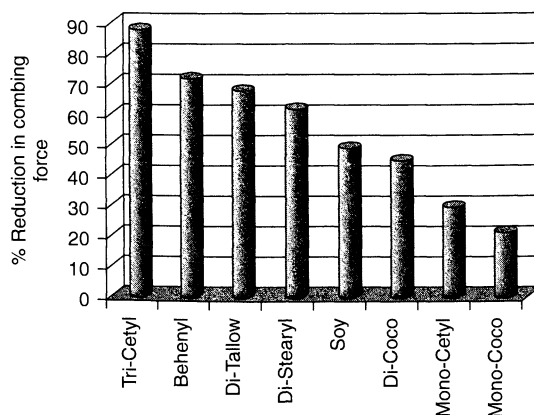


Figure 14.25. Conditioning performances of various quaternaries. The abbreviations used represent the following INCI (International Nomenclature Cosmetic Ingredient) names, with the respective trade names given in brackets: Tri-Cetyl, tricetylmonium chloride (Arquad[®] 316); Behenyl, behentrimonium methosulfate (Arquad[®] B-72-PG); Di-Tallow, quaternium-18 (Arquad[®] 2HT-75-PG); Di-Stearyl, steartrimonium chloride (Arquad[®] 18-50); Soy, soytrimonium chloride (Arquad[®] SV-60-PG); Di-Coco, cocotrimonium chloride (Arquad[®] C-50); Mono-Cetyl, cetrimonium chloride (Arquad[®] 16-29); Mono-Coco, cocotrimonium chloride (Arquad[®] C-33W)

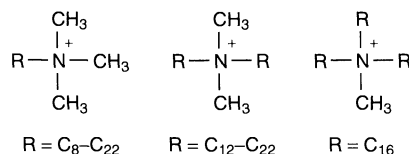


Figure 14.26. Structures of some typical alkyl quaternary salts

chloride, are moderate to strong conditioning actives with excellent rinsing properties, while trialkyl quaternaries, such as tricetylmonium chloride, are strong conditioning actives with superior compatibility and anti-static properties. Furthermore, trialkyl quaternaries offer excellent compatibility with anionic surfactants for "2-in-1" conditioning shampoo formulations due to the shielding of the cationic centre by the three large hydrophobes.

The branched quaternary compound with the Cosmetics, Toiletries Fragrances Act (CFTA) name designation, stearyl octyldimonium methosulfate (Figure 14.27), is a molecule offering strong conditioning performance. Unlike conventional long-chain dialkyl quaternary compounds, stearyl octyldimonium methosulfate is water-soluble, and thus can be used in clear conditioning formulations.

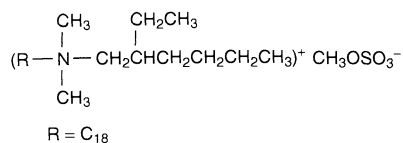


Figure 14.27. Structure of the branched quaternary compound, stearyl octyldimonium methosulfate (Arquad[®] HTL8-MS)

Ethoxylated quaternary ammonium compounds

Ethoxylated quaternary salts are used primarily as light-conditioning additives in both anionic and nonionic surfactant systems. However, these quaternaries have less substantivity due to their greater water solubility. Increasing either the alkyl chain length or the number of alkyl groups results in increased conditioning performance (see Figure 14.28).

Ester quaternary ammonium compounds

Ester quaternaries, prepared by quaternization of the condensates of alkanolamines with fatty acids (see

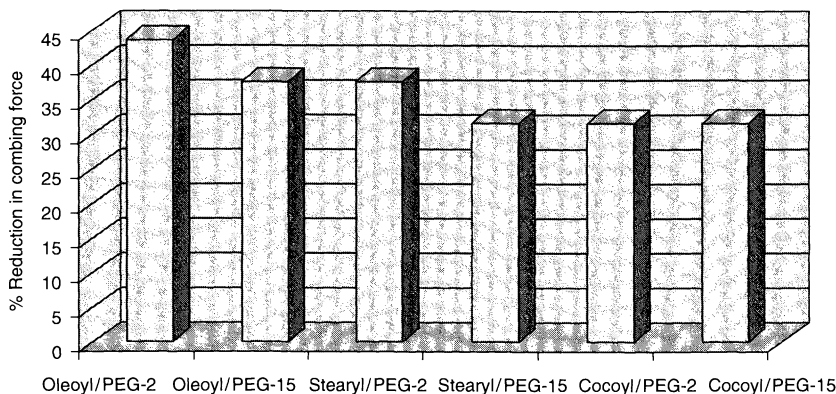


Figure 14.28. Combability measurements for a range of ethoxylated quaternary compounds

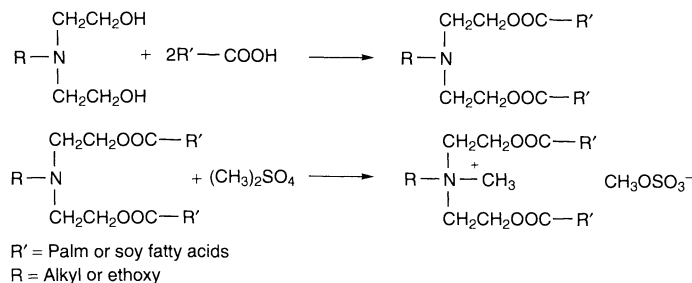


Figure 14.29. Synthetic route used to prepare ester quaternaries

Figure 14.29), are a new family of quaternary ammonium salts designed for addressing a broad variety of hair and skin conditioning needs.

The conditioning benefits of ester quaternaries can be demonstrated by using a Dia-Stron Tensile Tester to measure the combing force. The unique ability of these quaternaries to improve the combability of both wet and dry hair is illustrated in Figure 14.30.

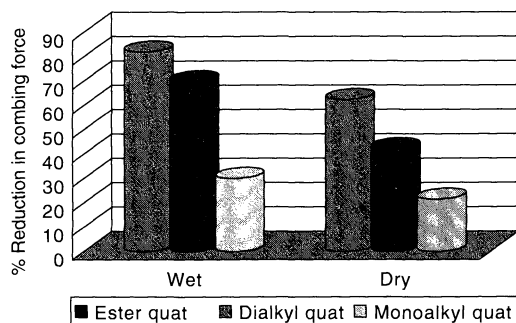


Figure 14.30. Comparative combability measurements (both wet and dry hair) for monoalkyl, dialkyl and ester quaternaries

8 CATIONIC SURFACTANTS IN PAPER PROCESSING (*Karin Bergstrom*)

Tissue paper and fluff pulp, which are used in diapers, towelling, napkins and facial and toilet tissue products, find extensive application in modern society. During recent years, a growing demand for fluff/tissue products has been seen, which is closely related to the economic development within this area. In industrialized countries, there is a clear drive towards high-quality products. To produce tissue or fluff of high quality and acceptable cost, it is important to optimize properties such as bulk adsorption, softness and wetting, but at the same time reduce energy consumption during the paper manufacturing process.

It is well known that conventional quaternary ammonium compounds, such as dialkyldimethylammonium salts (e.g. ditallow dimethylammonium chloride and ditallow dimethylammonium methyl sulfate), or quaternized imidazolines are effective chemical debonding agents in paper. Such compounds interact with the natural fibre-to-fibre bonding that occurs during the paper-making process, where hydrogen bonds are formed between the hydroxyl groups of the fibre. The hydrophilic cationic portion of the surfactant is believed to be attracted to the negatively charged cellulose fibres and thus reduces the inter-fibre bonding. The hydrophobic portions of the molecule are exposed on the surface, forming a thin lubricant film, thus making the fibres more hydrophobic. This reduction of the inter-fibre bonding, together with the lubricating effect, imparts a soft feel to the paper. In the mechanical fluff pulp process, the lubricating property protects the fibres against damage and reduces the defibration energy needed. However, since such properties are obtained largely due to the effect of fatty chain of the cationic debonder, the absorbency and rewetting properties of the cellulose can be negatively influenced (3).

It has been shown that bis(ethoxy 2-hydroxypropylene) quaternary ammonium compounds, which are cationic surfactants with both nonionic and cationic hydrophilic groups, give excellent softening properties, while at the same time preserving good wetting behaviour in fluff and tissue paper. This debonding agent has been synthesized by reacting a long-chain alcohol with ethylene oxide in the presence of an alkaline catalyst. The resulting fatty alcohol ethoxylate is reacted with epichlorohydrin, thus producing the corresponding chloroglycerol ether, which is then reacted with a secondary amine such as dimethylamine. The cationic part will adsorb, thus reducing inter-fibre bonding and give softness, while the hydrophilic nonionic part will

provide good wettability. If the number of oxyethylene units is increased, e.g. from two to ten, the wettability of the cellulose increases, while the number of inter-fibre bonds between cellulose chains is somewhat increased. As the number of carbon atoms in the fatty alcohol increases, the wettability decreases and the effect in reducing the inter-fibre bonds between the cellulose chains is increased. Thus, by appropriate adjustment of the chain length of the alcohol and the number of oxyethylene units, it is possible to "fine-tune" a desired combination of hydrophilicity and softness. A good balance is usually obtained with a stearyl alcohol and an ethoxylation average of four. An additional benefit from the hydroxy groups is the decrease in melting point of the product, thereby improving the handling properties.

Additional incorporation of 2-hydroxy oxypropylene groups by propoxylation of the fatty alcohol ethoxylate described above has been shown to give additional benefits. While improving softness and preserving good hydrophilic properties, this also reduces the electrostatic charge in the cellulose materials, thus also giving the molecule anti-static properties. Reducing electrostatic buildup during the pulp and paper processes is important for maintaining a fast and safe production line. It is quite remarkable that the oxypropylene units, which could be expected to impart some hydrophobic character to the system, in this case do not affect the desirable hydrophilic properties of the material. The anti-static properties are most likely to be due to an increased binding of water molecules to the secondary hydroxyl group.

Another way of obtaining good softening properties, combined with good wetting and anti-static properties, is by mixing cationic and nonionic surfactants. The behaviour of a mixture is often very different from that of a pure surfactant as synergistic effects are often observed. When ionic surfactants are mixed with nonionic surfactants, the change in electrostatic interactions between the head-groups becomes significant and the mixture deviates from ideality. The critical micelle concentration (CMC) for a cationic/nonionic mixture will be lower than that of the corresponding single surfactant system. This will increase the driving force for adsorption on to the cellulose fibres and will also considerably increase the effectiveness of the softening agent. The adsorbed layer will also be denser since the nonionic surfactant will decrease the repulsion between the cationic head-groups. This effect is even more pronounced for cationic/anionic surfactant mixtures, which have been used for fabric softening. A combination of an alkylbenzyltrimethylammonium chloride and a linear fatty alcohol ethoxylate (or fatty acid ethoxylate) gives good softening properties combined

with anti-static properties. This profound positive effect of the cationic–nonionic surfactant adsorption on the surface conductivity may be understood from Harwell's theory assuming that a dense film adsorption will take place, which acts as a conducting element.

Environmental issues are driving developments in the chemical industry towards more efficient chemical additives, which meet the new legislative standards. In order to achieve these demands, new softening agents have been developed. It has been shown that quaternized esteramine compounds (normally referred to as ester quaternaries), such as diester ditallow dimethylammonium chloride, work well as softening agents and can be substituted for conventional softeners in tissue paper and fluff pulp. Due to the hydrolytic instability of the ester bond, these molecules are classified as being "readily biodegradable" and have aquatic toxicity profiles which can meet government standards. Cleavage of the ester bond yields fatty acid soaps, in addition to highly water-soluble quaternary ammonium diols. The cationic charge close to the ester bond makes these ester quaternaries unusually stable to acids, which being labile to alkalis. The hydrolysis rate is at a minimum between pH 3 and 4 and accelerates strongly above pH values of 5–6. Thus, formulations containing ester quaternaries must be maintained at low pH levels.

9 CATIONIC SURFACTANTS IN CONVEYOR LUBRICANTS (*Andress Doyle*)

The USA food and beverage industry consumes 700 million gallons of lubricants every year, including greases, process oils and chain lubricants. Conveyor or chain lubricants are a very specialized type of boundary lubricant which are used in this industry. The main use of these lubricants is to facilitate the movement of chain/belt and containers on the conveyor systems running from filling to packing stations (at very high speeds) in food and beverage processing plants.

The formulation of chain/conveyor lubricants is very complex due to various requirements placed on these products. The primary function of a conveyor lubricant is to reduce friction between the chain/conveyor and its support. The reduction of friction between the chain/conveyor and the container is a secondary requirement of such products. Added to this, the chain lubricant needs to be formulated to provide both detergency, and in many cases, biocidal functions, in order to maintain the processing plants chains in a sanitary condition.

These formulations should also be non-corrosive, stable and compatible with a broad spectrum of materials.

One of the first fluids tried as a lubricant on these chains was water and the formulations used in the industry today are still 99% water-based. A conveyor lubricant formulation concentrate contains 5–20% active lubricant which is diluted 1:100 on site. This dilute product is combined with water at low levels and sprayed through nozzles on to the conveyor belt or chain. The active lubricant component is consequently usually less than 1 mg/l when in final use at the food or beverage processing plant. A packaging plant can use up to ~40 gallons of lubricant per hour and this places extreme demands on the products cost/performance and environmental profile.

There are two main classes of chain lubricants used in the industry today, namely the traditional soap-based lubricants and soap-less lubricants. The soap-based lubricants are most commonly used due to their low cost. A typical soap-based formulation is shown in the table below. The pH of this formulation is usually between 8 and 10, and the fatty acids typically used are oleic or tall oil, with hydrotropes that can include isopropyl alcohol (IPA) or glycols, and surfactants which can be taken from the nonionic, anionic or amphoteric classes. These formulations have several drawbacks, but the primary problem is their inability to tolerate hard water conditions. The insoluble salts formed with calcium or magnesium ions can result in blocking of the spray nozzles and consequently shutting down of the packaging line. Therefore, the presence of chelating agents, such as ethylenediaminetetraacetic acid (EDTA), are critical to their long-term performance. However, incompatibility with aluminum cans has limited the use of EDTA in such formulations.

Component	Content (wt%)
Fatty acid	10–20
Tetrasodium EDTA (40%)	5–12
Hydrotrope	5–10
Surfactants	5–10
KOH (45%)	5–10
Remainder	(to 100)

The second class is the soap-less lubricants, with these being based on a growing list of surfactant types. The most common ones used today are the phosphate esters and cationic-based chain lubes; recently, polyalkylphoglucosides have been added to this list. Phosphate-ester-based chain lubricants have had limited use due to legislative restrictions in certain regions.

However, the cationic-based chain lubricants are now being used more extensively in today's market.

9.1 Cationic surfactants as chain lubricants

Several classes of cationic surfactant have found utility in chain lubricants as the active component; these include amines, diamines, polyamines, etheramines and the acetate salts of the various amine types shown in Figure 14.31.

The use of amine chemistry in this application was first developed as an additive to traditional soap-type formulations, where it was found that the lubricity of the fatty acid soap was enhanced. This resulted in the use of fatty amines alone as lubricants without any fatty acids being present. However, simple fatty amines had limited use in this particular field due to their interactions with carbonates, phosphates and sulfates in certain water supplies, thus leading to the formation of insoluble salts. However, it was found the latter could be avoided by using diamines and polyamines (and their salts) in the same formulations. A typical polyamine chain lubricant formulation is shown in Figure 14.32. Examples of the chemistries included under polyamines as chain lubricants include diamines, etherdiamines, triamines and tetramines, with chain lengths of C_{12-18} . The acid that is most commonly used to neutralize the polyamine is acetic acid, although other acid types can also be used. The hydrotropes used in this type of formulation can include glycols and alcohols. The

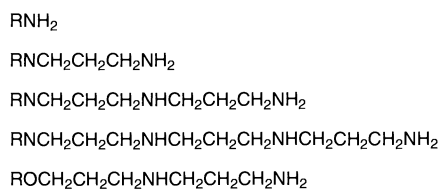


Figure 14.31. Structures of some typical cationic surfactants which are used as chain lubricants

Polyamine	5–20%
Acid	1–7%
Surfactant	10–20%
Hydrotrope	5–10%
Remainder	Water

Figure 14.32. Typical formulation of a soap-less, polyamine-based chain lubricant concentrate

most common type of surfactant used with polyamine formulations is nonionic.

The most successful features that have resulted from the application of amine chemistry in chain lubricants have been their lubrication efficiency, water stability, biocidal action and improved compatibility with poly(ethylene terephthalate) (PET) containers when compared to traditional soap-based formulations. The key features of these molecules that are considered critical to lubricity are the alkyl chain length, ionizable sites and unsaturation in the alkyl chain. The alkyl chain length should be between C_{12} and C_{18} . However, C_{18} is usually considered to be optimal for lubricity, while C_{12} tends to provide better biocidal action. The amount of ionization sites, which in the case of polyamines is the amount of nitrogen, is considered to be key in the binding of the lubricant to the chains or containers. Therefore, the more nitrogen groups (which are positively charged), then the better is the lubricant attachment to the surface. The amount of double bonds or unsaturation is also considered to improve binding to the surface. However, this may also reduce the chain length effect and give similar values to those for a shorter alkyl chain. Unsaturation in longer-alkyl products may provide an added benefit by keeping the lubricant liquid and stable in the formulation.

Traditionally, the oleyl diamines used in this particular application should have an Iodine Value (IV) of above 70 g I_2 per 100 g. Lower IVs can result in chain lubricant formulation stability issues, which could lead to sediment in the final application, hence resulting in blocked spray nozzles. Many of the recent developments in cationic-surfactant-based chain lubricants have been a consequence of improving formulation stability and PET compatibility via the development of polyamine formulations and etherdiamine formulations.

9.2 Cationic surfactants as chain lubricant additives

Cationic surfactants can also be used as functional additives in traditional chain lubricant formulations, including biocides, stress-craze inhibitors and coupling agents. As mentioned above, the first use of alkylamines in chain lubricants was as an additive in a traditional, soap-based formulation to improve the stability of the system. Ethoxylated amines have also been employed as coupling agents in an alkaline diamine track lubricant, while tertiary amines have found utility as saponifying agents in traditional, soap-based chain formulations.

The use of cationic surfactants in chain lubricant formulations for biocidal action can be split

into two groups, i.e. traditional quaternary ammonium compounds as biocides in soap-less and soap-based chain lubricants. However, the use of quaternary ammonium compounds as biocides in any type of formulation is banned from brewery sites due to concerns about their impact on the yeast population. The use of amines, diamines and polyamines as biocidal additives has increased in these types of formulations as they do not show the same anti-microbial activity towards yeast (*Saccharomyces*)-type organisms, but will reduce the growth of organisms such as *Pseudomonas* and *Staphylococcus*. The optimal chain length for biocidal action is C₁₂, while C₁₈ gives the best lubricity; thus, many formulators will mix or compromise on chain lengths in order to obtain a balance between the lubricity and anti-microbial action.

The last additive area which has been gaining in importance is that of the stress-craze inhibitor, because the use of PET bottles continues to grow within the beverage industry. The main problem with the use of such bottles upon exposure to traditional, soap-based chain lubricant formulations is the formation of stress cracks or crazing, which weakens the integrity of the container. The stress-crazing problem is not as severe with soap-less based formulations, although the problem can still occur on long-term exposure. The addition of amines, secondary amines, tertiary amines, diamines and quaternary ammonium compounds have found utility in traditional, soap-based formulations for preventing or reducing stress crazing in PET bottles.

As can be seen above, the formulation of chain lubricants is extremely complex, as evidenced by the demands placed on these formulations to include functions that can have opposing effects, thus impacting their efficiency. The complex nature of this area has resulted in a very rich patent field, which makes the formulation of these products even more complex.

10 CATIONIC SURFACTANTS IN ROAD CONSTRUCTION (Alan James)

Bitumen (asphalt) is used as a binder in road construction and in protective coatings and adhesives used in the construction industry (4, 5). In the most common processes, the bitumen is heated to 100–200°C until fluid enough to mix with aggregate. The “hot-mixed” materials must themselves be stored, transported and used hot to maintain their workability. The final strength of a roadway is developed as the mixture cools. Alternatively, the bitumen is diluted with petroleum solvents such as kerosene until fluid, with the final strength of the

material only developing when the solvent evaporates. Bitumen emulsions provide an alternative approach in which the bitumen is liquefied by dispersing in water. Such emulsions can be used with cold and wet aggregates, with the final strength of the road material developing as the emulsion “sets” – reverts to a continuous bitumen phase – plus water is removed. Cationic surfactants are used as adhesion promoters for hot bitumen, as emulsifiers and adhesion promoters in bitumen emulsions, and as peptizing agents which improve the emulsifiability of bitumen and slow down its age-hardening. Together, these applications account for ca. 10% of all cationic surfactants consumption.

10.1 Adhesion promoters

Bitumen is a non-polar oily material, whereas the aggregates used in road construction have polar surfaces. The result is that bitumen may have difficulty in spreading over (coating) the aggregates, especially when the aggregate is wet or dusty, and the bitumen coating may be displaced by water during the service life of the roadway (known in the asphalt industry as “stripping”). Moisture damage is an important cause of the failure of asphalt roadways.

The adhesion of bitumen to aggregate depends on the chemistry of both the bitumen and the aggregate surface. Aggregates may be of an acidic type whose surfaces have a tendency to become negatively charged, or basic with a tendency to become positively charged. Acidic aggregates include those with high silica contents such as granites and quartzites, while basic aggregates include limestones. Bitumen, although mostly hydrocarbon in nature, contains chemical groups such as carboxylic acids, phenols, pyridines, sulfoxides, anhydrides, etc. which are mainly associated with the high-molecular-weight polar cyclic components known as asphaltenes.

The amount and nature of these polar groups depend on the source and processing of the asphalt and can influence the adhesive properties of the asphalt on to different aggregate types. Most bitumens are low in cationic amino compounds and so there are particular problems with the adhesion to acidic aggregates. Addition of 0.2–2% cationic surfactants (called adhesion promoters or anti-stripping agents) to bitumen markedly improves its adhesion to aggregate. The result is that the bitumen may coat wet aggregate and/or the coating is not displaced by water. Traditional adhesion promoters were based on tallow diamines but these have now been largely replaced by liquid products based on tall oil fatty acid condensates of polyethylenepolyamines. It has

been shown that the cationic surfactants are adsorbed on to the aggregate surface and are preferentially adsorbed when compared to the polar components of the asphalt.

10.1.1 Heat stability of adhesion promoters

Bitumens are stored at 120–200°C and at these temperatures amine groups in the adhesion promoters can react with acid groups in the bitumen to form less active amido compounds, or can degrade by oxidation. The rate of degradation depends on the acid value of the bitumen and the chemistry of the adhesion promoter. Where possible, the adhesion promoters should be added to the bitumen just before use. So-called heat-stable products based on less reactive tertiary amines or polyamines have been developed for situations where the treated bitumen must be stored for longer than a few hours. Field studies have shown that treatment of bitumens with adhesion promoters improves the performance of roadways.

Bitumen emulsions

Bitumen emulsions are normally of the oil-in-water (O/W) type, although there is evidence that bitumen can form multiple water–oil–water (W/O/W) emulsions. Emulsions containing from 40 to 80% bitumen are brown liquids with consistencies ranging from that of milk to double cream. The droplets range from 0.1–20 µm in diameter (see Figure 14.33) and can have a positive (cationic emulsions) or negative (anionic emulsions) charge.

Emulsions are usually prepared by mixing hot bitumen (110–180°C) and a warm solution of emulsifier

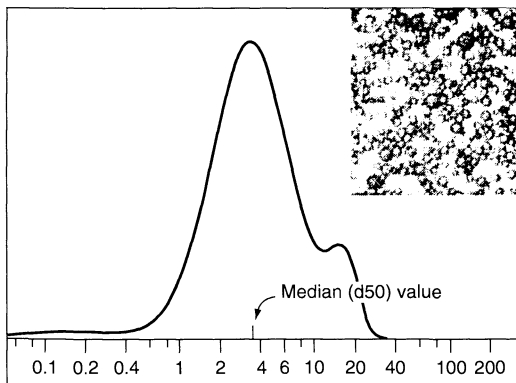


Figure 14.33. Particle size distribution of bitumen emulsion droplets

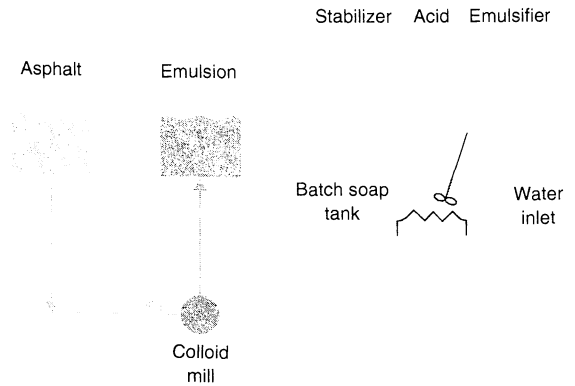


Figure 14.34. Schematic of a batch emulsion plant

(soap) (20–80°C) in a colloid mill (see Figure 14.34). The emulsification temperature (i.e. after mixing the soap and bitumen phases) can range from 80 to 140°C, although the higher temperatures are only possible in pressurized systems.

The soap contains cationic surfactant as well as hydrochloric, or less usually, acetic or phosphoric acids. The acids are needed to convert amine-type emulsifiers to their protonated cationic forms but also to inhibit the ionization of acid groups in the bitumen. Cationic soaps typically contain 0.5–2.0% cationic surfactant, acid to pH 1 to 5, and optional additives such as water-soluble thickeners, electrolytes, latex, stabilizers and adhesion promoters which modify the physical properties or reactivity of the emulsion, or the properties of the bitumen film when cured. Some typical emulsion recipes are shown in Table 14.10.

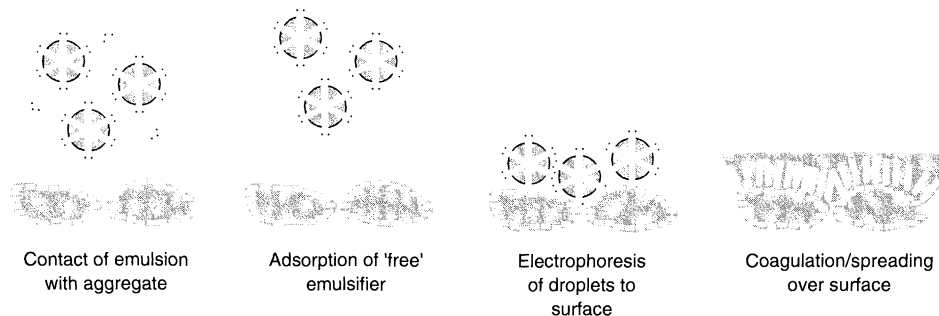
Bitumen emulsions for road use are classified into classes depending on their reactivity. *Rapid-setting* emulsions set quickly in contact with clean aggregates of low surface area, such as the chippings used in chipseals (surface dressings). *Medium-setting* emulsions set sufficiently less quickly so that they can be mixed with aggregates of low surface area such as those used in open-graded mixes (mixes with low fines content). *Slow-setting* emulsions will mix with aggregates of high surface area. The actual setting time in practice depends on environmental conditions such as temperature, humidity, the compaction of emulsion aggregate mixtures and the chemistry of the aggregate surface. Cationic emulsions are generally preferred because the surface of most aggregates is negatively charged so contact with the aggregate can initiate the setting process, and after curing the cationic emulsifiers act as adhesion promoters. Where anionic emulsions are used, cationic adhesion promoters are often included in the

Table 14.10. Recipes for some typical bitumen emulsions

Emulsion type	Emulsifier level ^a %	Emulsion pH	Typical use	Typical emulsifier ^b
Cationic rapid-setting	0.15–0.25	2–4	Spray seals	Tallow diamine C ₁₈ alkyl amidoamines
Cationic medium-setting	0.3–0.6	1.5–4	Open-graded mixes	Tallow diamine, tallow tetramine
Cationic slow-setting	0.8–2.0	2–5	Dense-graded mixes	Quaternary amines, ethoxylated tallow diamines, lignin amines

^aBased on total emulsion.

^bAs hydrochloride salt.

**Figure 14.35.** Possible stages in the setting of a cationic bitumen emulsion

formulation to improve the water resistance of the cured bitumen film.

The mechanism of emulsion setting is not yet fully understood, although some factors have been identified. Figure 14.35 shows the process thought to occur when a rapid-setting cationic emulsion comes in to contact with clean aggregates.

Not all of the emulsifier in an emulsion is associated with the bitumen droplets. The amount of “free” emulsifier decreases over time as more emulsifier is adsorbed on to the bitumen droplets during storage, a process related to the migration of polar materials in the bitumen droplet to the interface. The rate of setting is related to the concentration of free emulsifier which can adsorb on to the aggregate surface and reduce the charge.

Electrophoresis of the bitumen droplets to the aggregate surface depends both on the charge on the asphalt droplets and on the aggregate surface, as well as the size of the bitumen droplets – small particles mean faster-setting emulsions. The rise in pH resulting from the contact of emulsion with the aggregate surface or filler in the mixture, can result in a deprotonation of the cationic emulsifiers and consequent destabilization of the emulsion.

The choice and concentration of cationic emulsifier influences the setting rate. Emulsifiers most suitable for slow-setting emulsions tend to have large head-groups

and are used at higher concentrations, while emulsifiers used for rapid-setting emulsions have small head-groups. Because they are less sensitive to the pH increase which occurs when aggregate is mixed with emulsion, quaternary ammonium emulsifiers tend to give slow- or medium-setting emulsions.

The setting of cationic emulsions can be accelerated or slowed down in the field by the use of additives. To accelerate the setting process, alkaline materials can be added to the emulsion; to slow down the process, additional cationic surfactant (known as “dope”) may be added.

As well as the setting rate, a further important characteristic of the emulsion is its viscosity. The choice of emulsifier can influence the viscosity of the emulsion, through an influence on the particle size distribution, or on the extent of multiple-phase droplets that are formed.

Bitumen peptizers

Bitumen is a colloidal dispersion of high-molecular-weight polar asphaltenes in lower-molecular-weight relatively non-polar hydrocarbons. Asphaltenes can associate strongly and this leads to difficulties in emulsification. One solution is to add cationic surfactants, so-called peptizing agents, which help disperse the asphaltenes and improve the emulsion quality. Bitumen

ages by oxidation and the loss of lower-molecular-weight components, with the result being a stronger association of asphaltene components and a stiffening of the bitumen. Peptizing agents can slow down this stiffening effect.

11 CATIONIC SURFACTANTS IN VISCOSE/RAYON PRODUCTION (*Anders Cassel*)

Surfactants today are necessary process additives in the viscose/rayon industry. Their proper use gives better process control, costs and product quality. Such process surfactants display familiar functions in their applications in this industry. The surfactants used in viscose processing therefore act as phase-transfer catalysts, dispersants, emulsifiers, wetting agents, anti-foaming agents and finishing agents. As the chemical conditions in the viscose/rayon process stages vary so drastically, care must be taken to ensure that the surfactants introduced early in the process do not introduce unwanted functions in subsequent steps.

11.1 Mercerization, xanthogenation, dissolving and ripening

The surfactants used in the "alkaline stage" of the viscose/rayon process are classified, according to their functions or addition points, as reactivity (improving) additives, viscose process additives and modifiers. Chemically, such surfactants are normally linear or branched fatty alcohol ethoxylates or fatty amine ethoxylates. In Figure 14.36, a simplified block scheme of this stage of the viscose/rayon process is presented. Reactivity-improving additives are added to the process either to the pulp water slurry just before the pulp enters into the drying section or to the alkalization slurry (mercerization). Often, the surfactants are introduced by spraying them on to the wet pulp. The surfactants added this early on in the process must possess good solubility in the process water being used. This leads to a good distribution within the pulp material. The most desired effect of the reactivity additive appears later in the xanthogenation step. Here, a reactivity additive, at a typical dosage of 0.5–2 kg/ton cellulose improves the reactivity between carbon disulfide and the mercerized cellulose, thus leading to either the same or a better quality of the produced liquid viscose, but *with use of less* CS₂. The use of electron-beam treated pulp, in combination with suitable surfactants, also leads to improved reactivity.

Other typical effects of the *reactivity additives* are that the alkali celluloses are more easily shredded and become fluffier after shredding, the dissolving pulps have a more open structure and will be more reactive towards lye, and hornification of dried and stored pulp becomes less serious a problem.

A viscose process additive is a surfactant that disperses hydrophobic particles in the viscose, for example, insoluble resins or other insoluble hydrophobic material. The dosage used is 0.5–3 kg/ton cellulose. A modifier is an additive, not always a surfactant, that decreases the regeneration speed. This leads to viscose/rayon fibres with higher wet strengths when modifiers are used at dosages of 5–30 kg/ton cellulose.

11.2 Spinning, regeneration, washing and spin finishing

Figure 14.37, shows a block scheme of the viscose/rayon process from the spinning stage to production of the final viscose/rayon material. In this process, two types of surfactant process additives are introduced, i.e. spin bath additives and lubricant finishing additives.

A spin bath additive acts as a dispersant for the insoluble material formed in the spin bath during regeneration. Examples of insolubles formed from side reactions include solid sulfur and zinc sulfide, plus other solids such as resins from the pulp raw material. With the exception of the lauryl pyridinium chlorides (LPCs), in practice, all dispersing spin bath additives used today are ethoxylated fatty polyamines. The more nitrogens present and the longer the carbon chain, then the better is the dispersing property. Often, wetting and anti-foaming functions accompanying the dispersing function are required in a spin bath. If this is the case, then mixtures of surfactants which display all of these different functions are needed. As wetting agents, fatty amine ethoxylates can be utilized. Non-hydrolysable fatty polyamine spin bath additives are now available on the market. Major components in many lubricant finishing additives are ethoxylated fatty acids; the latter can be doped with surface-active quaternary ammonium compounds to improve the substantivity. Such ethoxylated fatty acids typically contain carbon chains of C_{16–18} or longer.

12 CATIONIC SURFACTANTS IN OILFIELDS (*James Gadberry*)

In the 1940s, Armour and Company first prepared fat-derived cationic surfactants and immediately began

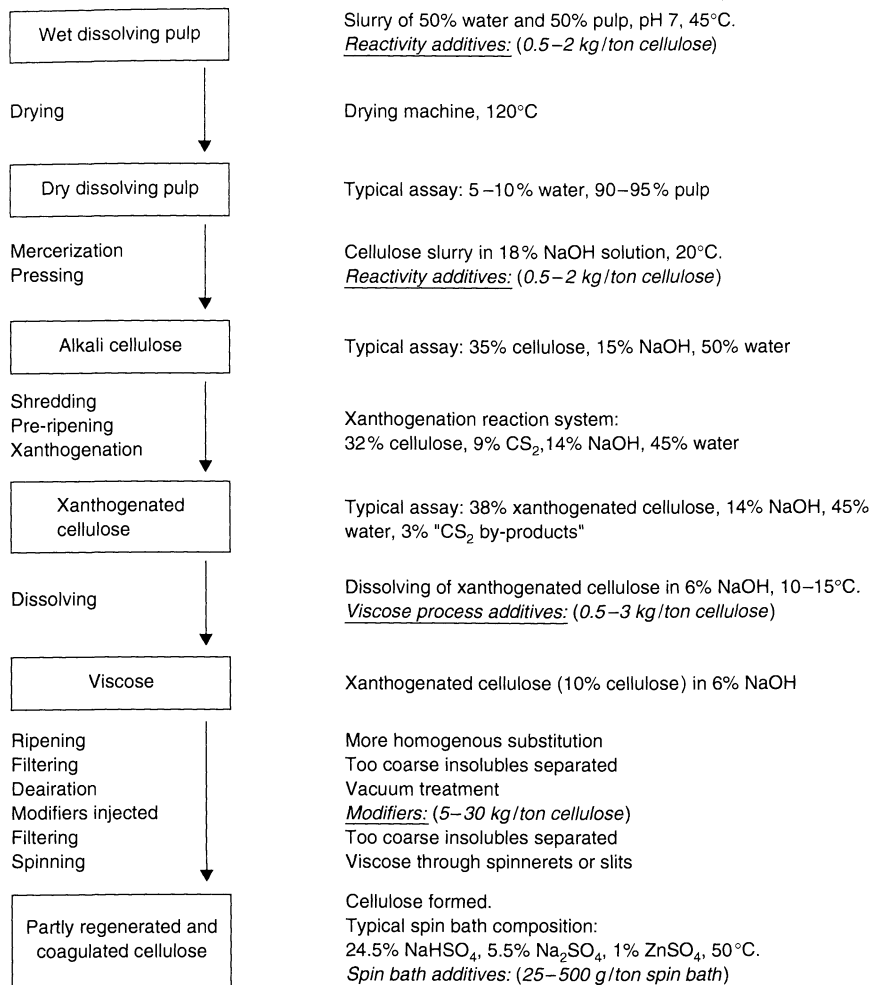


Figure 14.36. Block scheme of the viscose/rayon process, up to and including the spinner stage, showing the general process conditions and typical addition points for the surfactants

offering these products for a broad spectrum of applications within the petroleum industry. Since then, this class of products has been used in applications in the production, transportation and refining of petroleum. Most of the current uses of cationic surfactants in the petroleum industry are long established and mature in nature. In drilling and production, cationics have been used as silt suspension additives, acid inhibitors, wetting agents, emulsifiers, rheology control agents, corrosion inhibitors, scale inhibitors, anti-swelling agents and intermediates to other useful additives. For transportation and refining, cationic surfactants have been used as corrosion inhibitors, biocides, de-emulsifiers, anti-fouling agents and containment agents. Table 14.11

presents a general picture of the uses of cationic surfactants in oilfield applications (6).

12.1 Rheology

Cationic surfactants are used in a variety of rheological applications. Perhaps chief among these is the use of quaternary ammonium salts as reactive intermediates to the formation of organophilic clays that are used in drilling muds (see Section 14 below).

Another rheological application is in conformance control whereby the water flow is diverted due to fatty amine oxide induced gelation. This plugging of

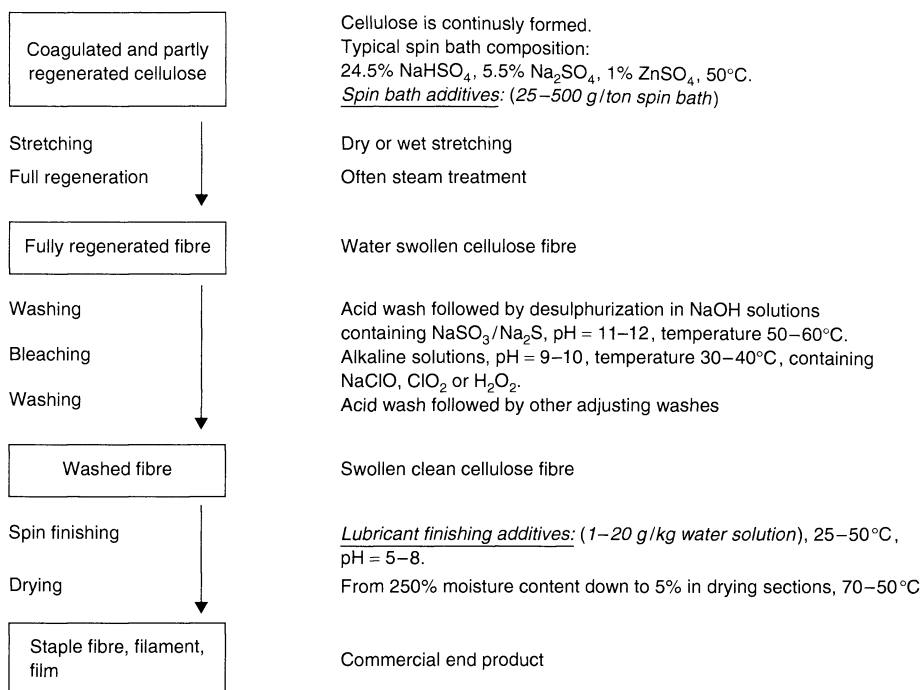


Figure 14.37. Block scheme of the viscose/rayon process, from the spinning stage to production of the commercial end product, showing the general process conditions and typical addition points for the surfactants

Table 14.11. Uses of Cationic (amine) surfactants in oilfield applications (6)

Application	Surfactant Class					
	Amines and diamines	Quaternary salts	Amine salts	Ethoxylated amines	Ethoxylated quaternary salts	Amine oxides
<i>Drilling and production</i>						
Anti-swelling/clay stabilization		◆		◆		
Foaming		◆				◆
Silt suspension		◆				◆
Wetting						◆
Emulsification				◆		◆
Fluid additives						
Rheology control				◆	◆	
Fracture fluids				◆	◆	
Corrosion inhibition	◆	◆	◆	◆		
Biocides	◆	◆		◆		
Demulsification		◆		◆		
<i>Transportation</i>						
Corrosion inhibition		◆	◆	◆		
Paraffin inhibition				◆		
<i>Refining</i>						
Anti-fouling	◆					
Corrosion inhibition	◆					

high-flow zones allows increased oil production by forcing injected water through areas of high oil content.

Control of rheology in acidizing operations is possible by using two-mole ethoxylated fatty amines. Used in the form of their acid salts, these surfactants give high gel strength during the digestion of carbonates in the formation, and then, as the electrolyte builds to higher levels, are self-breaking and allow flow again. Such salts are also useful in foamed systems. Salts of ethoxylated fatty amines have been reported to be effective thickening agents for acid or salt solutions used as oil well treatment fluids.

12.2 Corrosion inhibition

Fatty amines and diamines can be used for corrosion inhibition in oil-producing wells. Typically, these products are dispersed as salts of organic acids such as fatty acids or petroleum sulfonic acids. Fatty amines and diamines have also been used as corrosion inhibitors in the transportation and storage of petroleum products. Quaternary ammonium salts, including dialkyldimethylammonium, monoalkyltrimethylammonium and monoalkyldimethylbenzylammonium, are good corrosion inhibitors.

12.3 Other applications

Highly ethoxylated amines and diamines have been recommended for demulsification of crude oil. Combinations of quaternary ammonium salts and amines oxides are useful for foaming and silt suspension. Coco alkyltrimethylammonium chloride and bis(2-hydroxyethyl)coco alkylamine oxide comprise the preferred combinations. Quaternary ammonium salts, including coco alkyltrimethylammonium chloride, are useful for preparing foamed oil-in-water emulsions, which can dissolve paraffins and asphaltenes without formation damage. The pyrolyzed amine salts of humic acid have been used in filtrate control additives.

12.4 Recent trends and developments

12.4.1 Environmental

The coupling of the dramatic increase in offshore oil production in recent decades with changing legislation regarding the ecological impact of chemicals has put pressure on cationic surfactant producers to supply

alternative products. In some cases, this has caused dramatic changes in product selection. For example, coco alkyltrimethylammonium chloride, once the work-horse in acid foaming operations, is no longer recommended for offshore applications due to marine toxicity legislation. Such changes in product selection are driving research into exploring new molecules and chemistries.

12.4.2 Surfactant-based fracturing fluids

Although polymeric rheology control additives dominate the market for fracturing fluids, cationic surfactant-based systems have been introduced. Ethoxylated quaternary ammonium salts have been shown to afford viscoelastic aqueous fracturing fluids. The strength and temperature stability of the viscoelastic formulations depends upon the purity of the surfactant. These systems are claimed to break upon exposure to hydrocarbons, thereby affording clean-up behaviour superior to that available when using polymer-based fracture fluids.

12.4.3 Hydrate inhibitors

Simple monoalkyl quaternary ammonium salts have been shown to inhibit formation of gas hydrates of the type that block gas and oil pipelines and equipment. For the most part, in order to be effective the salts must have at least two C₄-C₆ alkyl groups on the quaternary head-group. Such head-groups appear to fit well within the nascent gas hydrate crystal and, by a mechanism that is not yet totally understood, inhibit further growth of such crystals.

Quaternary ammonium salts containing hydroxyl or ether functions in the shorter groups attached to the head-group are can also be used as hydrate inhibitors. Ethoxylated alkyldiamines are another class of cationic hydrate inhibitor that has been patented recently. In all of the above cases, cationic hydrate inhibitors appear to work best when used in combination with other additives.

12.4.4 Miscellaneous oilfield applications

Quaternary ammonium hydroxides are a recent development for use in scavenging mercaptans from hydrocarbons, such as from crude oil. In addition, a novel method for the preparation of quaternary ammonium hydroxides has been disclosed. A further invention claims the use of amine oxides for removal of sulfur compounds from hydrocarbon streams.

Primary alkylamines have been found to enhance the performance of compositions useful for dissolving aliphatic and paraffin deposits. In addition, primary alkylamines are useful for producing drilling fluids that are stable when acidic gases are present.

13 CATIONIC SURFACTANTS IN AGRICULTURAL FORMULATIONS (*Bodil Gustavsson*)

Many pesticides are insoluble in water and biologically inactive if they are not formulated with surfactants (adjuvants). Even water-soluble compounds may be inactive when applied as unformulated material (7). The technical rationale for incorporating adjuvants into pesticides includes improved wetting, rain fastness and increased penetration.

For example, glyphosate (*N*-(phosphono methyl) glycine) is a foliage acting herbicide with little selectivity, which is used for controlling undesirable vegetation. Surfactants are used to improve the efficiency of this herbicide. The most common surfactants used in glyphosate formulations as adjuvants are polyethoxy fatty amines, quaternary ammonium salts, nonylphenol ethoxylates, alkyl polyglucosides and amine oxides.

13.1 Adjuvants

Agrochemical adjuvants are widely used to improve agrochemical applications. Improvement can be interpreted as "better weed/disease control" or "reducing active ingredient per hectare", or even "reducing amount of water to spray per hectare". Claims related to the adjuvant function vary from "wetter", "spreader", "sticker", "penetrator" to "synergist".

The word adjuvant generally refers to ready-to-use "tank-mix" products, of which a specified amount (% vol of spray volume or ml/ha) is recommended for certain applications.

However, it is clear that the adjuvant function can be incorporated in pesticide formulations as well. For convenience, we refer in this context to "formulation-adjuvant".

Work has been carried out to determine the physical and chemical properties in relation to agrochemical formulations and especially their adjuvant effect on plant protection agents. Polyethoxy tallow amine was used as a model adjuvant for comparative purposes. The knowledge from extensive studies of physical and chemical properties shows that

the most important property of the adjuvant is the ability to penetrate through the cuticle of the leaf. The surfactants which exhibit the best results according to greenhouse tests, are surfactants which contain a nitrogen atom, e.g. amine surfactants such as polyethoxy fatty amines, amine oxides, quaternary ammonium salts and amphoteric. Ethoxylated fatty amines are used extensively as adjuvants with hydrophilic pesticides, particularly with glyphosate-based herbicides. In the free acid form, glyphosate has low water solubility, and because of this, commercial formulations contain a water-soluble salt of glyphosate. For example, in the Roundup® herbicide, glyphosate is present as the water-soluble monoisopropyl amine salt.

The basic physico-chemical properties of the fatty amine surfactants drive their utilities as adjuvants. Such molecules consist of a water-insoluble hydrophobic unit, in this case derived from tallow fatty acid. The water-soluble unit of the molecules consist of two chains of polymeric alkoxides, in these cases ethylene oxide and/or another alkylene oxide, such as propylene oxide. A nitrogen atom in the middle of the molecule connects the water-soluble and water-insoluble parts. Due to the electronic properties of nitrogen with respect to the carbon atom connectors which are usual in surfactants, the molecule has an overall cationic character, thus resulting in improved substantivity (adherence) to the leaf surface.

In an agrochemical spray formulation, the initial action of the surfactant relates to its influence on the air-droplet interface. In spray formulations where the surfactant is present for its adjuvant properties, the cationic is present at concentration above the critical micelle concentration (CMC). A typical CMC for an adjuvant surfactant is approximately 0.01 vol%. Typical adjuvant concentrations in agrochemical tank-mix sprays range from 0.05 to 0.5 vol%. Such concentrations are different from those of the surfactants used in the agrochemical formulations themselves, for instance as emulsifiers. The latter are generally present at approximately 1–6 vol% of the formulation and are diluted in the actual tank spray mixture to 0.001–0.006 vol%, which is usually below the CMC. The surfactant property is important because it influences wetting, spreading, coverage and droplet size, as well as spray equipment performance. All of these factors can, of course, be related to the surface-active properties of surfactants in general.

Once the spray particle lands on the surface of a leaf, there a new interface is created, i.e. the plant surface solid-droplet interface. It is well known that

surfactants can penetrate the plant (wax) cuticle fairly rapidly. For penetration, the micelle structures have to be broken up since only individual surfactant molecules can penetrate the plant cuticle as the micelle structures themselves are too large to penetrate. The penetration of surfactants influences both the water permeance of the plant cuticle, as well as the solute mobility in the cuticle, i.e. this process influences the rate of uptake of pesticides.

Additionally, surfactants in agrochemical formulations affect retention and resistance to rain of the active ingredient. These factors can be more related to the chemistry on which the surfactants is based. Due to the cationic character of (tertiary) amine-based surfactants, i.e. their substantive properties, they are known to give good retention, as well as rain-fastness. Surfactants affect the physical state of actives in the spray residue once the water has evaporated. They can contribute to keeping the active from crystallizing out of solution or from solidification by other mechanisms. Surfactants can affect the volatilization of actives, as they may react with the latter to form ion-pairs, salts or complexes. Depending on the solvent properties of the actives, surfactants will affect the equilibrium distribution of active between spray residue and cuticles. Referred to as the *K*-depression effect, surfactants affect the equilibrium partition coefficient of the solutes over the aqueous phase (spray-droplet-residue) and the plant cuticle. Surfactants also can change the transport properties of cuticles by increasing the diffusion coefficients of water and actives.

A significant number of studies of the effect of surfactants on the herbicidal activity of the monoisopropyl amine salt of glyphosate have been reported in the literature. Fatty amine ethoxylates having a hydrophilic-lipophilic balance (HLB) of 17, are generally the most effective in increasing the herbicidal activity of solutions of the Roundup® herbicide. In addition, in spray solutions containing ammonium sulfate, responses to the surfactants were different, with lipophilic surfactants, for example fatty amine ethoxylates having an HLB of 6, being usually observed to have greater effects. There is an additional observation that glyphosate acid is much more soluble in a solution of a tertiary amine from tallow (containing 15 moles of ethylene oxide per mole of amine) than it is in pure water.

The range of surfactants compatible with monoammonium glyphosate at, for example, a glyphosate concentration of 360 g a.e. (acid equivalent)/l and a surfactant concentration of 180 g/l, is much more

restricted than the range of surfactants compatible with mono(isopropyl ammonium) glyphosate at the same glyphosate and surfactant concentrations. At the illustrative concentrations given above, the surfactant MON® 0818 (of the Monsanto Company), based on polyoxyethylene tallow amine, shows excellent compatibility with mono(isopropylammonium) glyphosate, but is incompatible with monoammonium glyphosate, with this incompatibility resulting in immediate phase separation. Additional compatibilizing agents, such as octylamine hydrochloride, which are unnecessary in aqueous concentrate formulations of mono(isopropyl ammonium) glyphosate with a particular surfactant, may be required for acceptable storage stability in the case of the monoammonium glyphosate.

In general, lower-molecular-weight surfactants are preferred to higher-molecular-weight surfactants, because a given weight of the former provides a higher molecular concentration of surfactant than the same weight of the latter. Those surfactants where the number (or average number) of carbon atoms in the alkyl group or groups is from about 10 to about 20 are most preferred. The number of ethoxylate groups which can be present in effective agricultural adjuvants range from 1.5 to 12 with the most effective being in the range of 2 to about 10. Specific examples of preferred surfactant are ethoxylated derivatives of coco amine, tallow amine and oleyl amine, where in each case the total ethoxylation level is from 2 to about 8.

Other amine surfactants used in the adjuvant area include quaternary ammonium compounds. Many of these surfactants are commercially available, such as Ethoquad C/25, a polyoxyethylene alkylmethyl ammonium chloride with an average alkyl chain length of about 12 carbon atoms and an average of 15 oxyethylene units, available from Akzo Nobel Surface Chemistry AB. When this surfactant is used, a further unexpected advantage is that no additional solubilizing agent, such as a glycol, is necessary to prevent the surfactants from gelling when added to water. Optionally, however, compositions of this product can contain additional glycols such as poly(ethylene glycol) having a molecular weight of about 400 (PEG-400). Other optional additional ingredients include ammonium salts, for example ammonium sulfate, and active ingredients such as 2,4-dichlorophenoxyacetic acid, dicamba or aciflourfen. Ethoquad C/25 also has a very low toxicity to fish, is similar in herbicidal efficacy to the best commercial *N*-phosphonomethylglycine formulations and has excellent physical stability at low and high temperatures without the need for additional glycols as solubilizing agents.

14 CATIONIC SURFACTANTS IN ORGANOCLOYS (*Mike Hoey*)

The manufacture of organoclays consumes a large amount of quaternary ammonium salts each year. These organoclays are in turn used in industries as diverse as oilfield chemicals (drilling muds), lubricants (greases) and paints and inks (rheology modifiers). The value of organoclays lies in their ability to disperse, and interact, in organic liquids. This property is caused by the unique structure of the clay, coupled with the surface treatment of the quaternary ammonium salt.

The development of today's commercial organoclays can be traced back to the work by Ernest Hauser and John Jordan for the National Lead Company in 1946. Armour and Company developed a commercial process (1946) for manufacturing quaternary ammonium salts to supply National Lead for this use. Since this beginning, a wide variety of organoclays have been manufactured for different uses, although the standard organoclays are still made by using dimethyldi(hydrogenated tallow)ammonium chloride, dimethylbenzyl(hydrogenated tallow)ammonium chloride, and methylbenzyl(hydrogenated tallow)-ammonium chloride.

A description of the clay is necessary to discuss the resultant organoclay. An excellent discussion of clay mineralogy can be found in ref. (8). Clays, as referred to in this section, are aluminium and magnesium silicates, or smectites. These silicates consist of arrays of silicon-oxygen tetrahedra and aluminium or magnesium oxygen-hydroxyl octahedra. This octahedral layer is responsible for the classification of a mineral as being trioctahedral or dioctahedral. This comes down to the use in the unit cell of trivalent aluminium (dioctahedral) or divalent magnesium (trioctahedral). In addition to this, there can be substitution of atoms in both the octahedral and tetrahedral sheets. This replacement is known as isomorphous substitution. In these minerals of interest, such replacement involves an atom with a lower valence for an atom of higher valence (Al^{+3} for Si^{+4} , Mg^{+2} for Al^{+3} , Li^{+1} for Mg^{+2} , etc.). This gives the unit cell an excess of

negative charge that is compensated for by absorption of sodium or calcium atoms on the surface of the mineral. The amount of substitution, and the atoms involved, give minerals of different species, as shown in Table 14.12.

Most commercial organoclays are made from montmorillonite or hectorite. Clays are also referred to as bentonites. This is actually the name given to the ore from which the smectites are extracted.

The structure described above is the basis for the unusual performance of smectites. The most unique characteristic of smectites are their ability to swell in water. If they are dispersed, one can generate a gel in water or in a brine solution. This behaviour is caused by the shape and size of the smectite particles; a typical montmorillonite particle has dimensions of $1 \times 10 \times 20$ millimicrons. This small particle has a high surface area because it is so thin. Because of the unit cell structure described above, the "top" and "bottom" surfaces of the platelet will have a series of areas of net negative charge that will have positive cations adsorbed onto them. This surface charge is what causes the aggregated smectite platelets to "swell"; osmotic pressure brings water into the space between the particles and the overall aggregation to absorb water. This surface charge also allows the particles to interact and form ordered associated structures in water. Such associations are responsible for the gelling rheology observed for an aqueous smectite solution. The amount of charge on the surface is measured as the amount of exchangeable cations per unit volume, or the cation exchange capacity (CEC). The latter is usually expressed as the number of millequivalents per 100 g of dry clay.

In making an organoclay, one exchanges a quaternary ammonium cation for the inorganic cations absorbed on the surface of the smectite platelet. This simple ion-exchange has a rather dramatic effect upon the final product. The clay will go from being water-dispersible and hydrophilic to hydrophobic and will flocculate out of a water system. This organoclay will be dispersible in organic liquids and will also exhibit swelling and rheological modification behaviour, analogous to the behaviour of the smectite in water. The

Table 14.12. Different species of aluminium and magnesium silicates (smectites)

Principal substitution	Trioctahedral minerals	Dioctahedral minerals
Prototype (no substitutions)	Talc, Mg_3Si_4	Pyrophyllite, Al_2Si_4
Practically all octahedral	Hectorite, $(\text{Mg}_{3-x}\text{Li}_x)\text{Si}_4$	Montmorillonite, $(\text{Al}_{2-x}\text{Mg}_x)\text{Si}_4$
Predominantly octahedral	Saponite, $(\text{Mg}_{3-x}\text{Al}_x)(\text{Si}_{4-y}\text{Al}_y)$, sauconite, $(\text{Zn}_{3-x}\text{Al}_x)(\text{Si}_{4-y}\text{Al}_y)$	Volchonskoite, $(\text{Al}, \text{Cr})_2(\text{Si}_{4-y}\text{Al}_y)$
Predominantly tetrahedral	Vermiculite, $(\text{Mg}_{3-x}\text{Fe}_x)(\text{Si}_3\text{Al})$	Nontronite, $(\text{Al}, \text{Fe})_2(\text{Si}_{4-y}\text{Al}_y)$

adsorbed quaternary ammonium cation is responsible for this change in behaviour.

The preparation of organoclays is fairly standard. A slurry of purified smectites in water is made up and stirred to maintain good agitation. A quaternary ammonium salt is then added to this stirring slurry. After the exchange, the organoclay is filtered and dried. A number of process adjustments and improvements have been patented, mostly concerned with improving the efficiency or consistency of the finished product.

The organoclays are used by adding them to an organic liquid under shear. To improve the dispersability of the organoclay, a dispersant or polar activator will be added. This polar activator is usually a low-molecular-weight alcohol, diol, or ketone. Methanol, ethanol, propylene carbonate, hexylene glycol, neopentyl glycol and acetone have all been used. It is believed that these compounds function by helping to disperse the organoclay particles from each other, thus allowing the organic liquid to increase the separation. Dispersability is a critical function affecting the performance of an organoclay, and thus a considerable amount of work has been carried out concerning this concept.

The biggest difference involved in describing an organoclay is the type of quaternary ammonium salt(s) used to prepare it. Although most commercial products are made from three types of quaternaries, namely dimethyldi(hydrogenated tallow)ammonium chloride, dimethylbenzyl(hydrogenated allow)ammonium chloride, and methylbenzyl(di(hydrogenated tallow)ammonium chloride, many other quaternaries have been used and described in the patent literature.

Most of these patented materials were developed because the inventors were looking for a way to modify the performance of the organoclay from that of the "standard" commercial organoclays. One other avenue that has been explored is the use of a non-volatile (high flashpoint) diluent in manufacturing the quaternary ammonium salt that will be employed to make the organoclay. When the latter is produced, the diluent will co-precipitate with the quaternary on to the surface of the clay particles. The value of this process is described to be a reduction in waste, since the standard diluents (isopropanol and, ethanol) will not precipitate on to the surface and thus must be removed at some point in the organoclay manufacturing process.

Organoclays have been used in a number of different commercial applications. They are used to control the rheology of organic fluids in a number of areas. They are also used in oil-based drilling fluids. Such fluids have to lubricate the drill bit, carry cuttings up and out of the wellhole, and provide appropriate back pressure in

order to minimize damage to the formation being drilled. Organoclays have also been used as packer fluids in drilling. In areas that are subjected to extreme cold, the drilling process has to be insulated from the surrounding formation. If not, then the drilling process can thaw the formation, hence resulting in damage. A packer fluid is placed in the space between the formation and the drilling piping to insulate them from each other.

Organoclays are also used in printing inks for rheological control, in oil-based paints and in oil-continuous latex polymers. In addition, they are used to thicken nail polish and for fabric conditioning, where in the latter the organoclays provide a carrier for the (di(hydrogenated tallowalkyl)dimethylammonium chloride) (DHTDMAC) fabric softener, and provide additional softening due to the lubricity of the clays.

Organoclays are also used for applications other than rheological control. These materials are known to be able to adsorb organic molecules both from aqueous systems and from air. A few developments have taken advantage of this to develop systems that remove contaminants from water systems and air and also to remove ink from wastepaper. A additional use of an organoclay is to prevent skin irritation from such irritants as poison ivy. It is claimed that the organoclay can be applied from a lotion to form a barrier on the skin and adsorb the irritant organic molecule (urushiol for poison ivy). A similar application is the use of organoclays to prevent diaper rash. Once again, the organoclay is used to provide a barrier layer that also adsorbs the fecal proteolytic enzymes that cause such rashes.

Another new application for organoclays is in producing plastic nanocomposites. In such an application, the organoclay is dispersed into a polymer. If the dispersion is complete and uniform, then the resulting plastic material has certain unusual properties, including increased gas barrier properties, flame retardancy and increased tensile strength. Work is continuing in this area, which promises to be an interesting new use for organoclays.

15 CATIONIC SURFACTANTS IN MINING (*Jan-Olof Gustavsson*)

Cationic surfactants are an important class of flotation collectors. Flotation is a separation process for minerals which utilizes the difference in surface properties. The first step is to liberate the minerals by grinding the ore to an appropriate particle size, usually finer than 200 μm . Then the flotation collector is added, together with other flotation chemicals (dispersants, depressants, flocculants,

activators, etc.), to the aqueous mineral slurry. The flotation collector adsorbs to a specific hydrophilic mineral surface, thus transforming this surface to hydrophobic in character. By introducing air in to a flotation cell, very fine air bubbles are formed. The mineral particles with the adsorbed collector will be trapped by the air bubbles and form a froth layer on the surface. This froth is skimmed off and the minerals are concentrated. If the froth contains the valuable mineral, this is known as *direct* flotation. In those cases where the froth contains the waste minerals or tailings, it is called *reverse* flotation (the valuable mineral remains in the flotation cell).

Cationic flotation collectors can be divided in two main groups, i.e. primary alkyl amines and quaternary ammonium compounds. These collectors are used in the selective flotation of oxide minerals, mainly quartz and numerous silicates, and in potash flotation (9–11). Alkylmorpholine (with a ring structure containing tertiary-*N* and ether oxygen groups) is a special collector which adsorbs to halite (NaCl) and is used in the reverse flotation of potash. The alkyl amines used are typically mono- ($R-NH_2$) or diamine ($R-NHCH_2CH_2CH_2NH_2$) compounds. Etheramines ($R-OCH_2CH_2CH_2NH_2$) are also commonly used in iron ore flotation. With such compounds, the polar head of the cationic reagent forms an ionic bond with a negative site on the mineral surface. The mineral which is separated has the most negative surface potential (zeta potential) in the treated ore mixture. To enhance the solubility, the amine collectors are often used as salts of hydrochloric or acetic acid. The pH range used is wide, i.e. 2 to 11, depending on the type of minerals being treated. The actual flotation process itself is complex, containing many stages with different mechanisms. The hydrophobic part of the collector molecule is important, as it affects, for example, the solubility, adsorption, hydrophobicity and froth characteristics. Addition of other surfactants, oils and fatty acids is also common to achieve good flotation performance. In many cases, the cationic reagents are tailor-made for a certain ore or ore type to give an optimized performance regarding selectivity and efficiency, which improves the recoveries and grades achieved.

15.1 Flotation of oxide minerals

15.1.1 Silicates from calcite

Ground calcium carbonate (GCC) is important as a filler in plastics and paper, and in coatings for paper. Quartz and other silicate minerals often accompany the carbonate ore. These abrasive and discolouring minerals

have to be removed, which is very often performed by reversed flotation with cationic collectors. Dialkyl quaternary compounds, and in particular dicocodimethylammonium chloride, are widely used for this purpose.

15.1.2 Silicates from iron ore

Cationic flotation of silica is widely used to beneficiate low-grade iron ore. The removal of silica is carried out by using reverse flotation, with the silica being removed with the froth. The steel making industry has put greater emphasis on low-silica metallurgy, meaning that the need for reduction of silica is growing in iron ore mining. The iron ore consists of several types of iron oxides, mainly magnetic (magnetite) and non-magnetic (haematite). Two techniques are available to separate silica in addition to gravimetric methods, namely magnetic separation (high and low intensity) and flotation. Historically alkyl mono- and diamines have been used as flotation collectors, although etheramines and etherdiamines started to replace them in the 1970s. The etheramines, whose general structure is shown in Figure 14.38, were found to be more efficient collectors; one explanation for this is that they are more easily dispersed when compared with alkylamines. The etheramines also showed other advantages, such as less sensitivity to pH variations and greater tolerance towards fine particles (slime). The etheramines used today contain both straight chain and branched alkyl groups.

Straight carbon chains (C_{8-10}) are common as hydrophobic units in ethermonoamines, while branched carbon chains (C_{12-14}), such as isotridecyl, are common units in etherdiamines. The shorter ethermonoamines are recommended for very fine ground pulps, while the branched etherdiamines show good results for coarser particles.

It is common practice to add the etheramines, which are partly neutralised (5–30%) with acetic acid, direct to the mineral slurry. As in all flotation operations, the collector is sensitive to slime; in iron ore applications, and in particular for haematite, a lot of fine material is produced during the grinding process. The presence of slime will increase the collector consumption drastically, and give poor silica reduction and decrease the iron recovery. Therefore, a de-sliming stage is often used prior to flotation. In this, the iron oxide particles are “depressed” with starch or dextrin; alkalinized corn starch is also commonly used. The depressant is added in a conditioner formulation before the collector is added. The pH varies between 8 to 10.5 in haematite flotation, with 10.5 being the common pH used, while magnetite flotation often takes place at pH levels of 8 to 10.

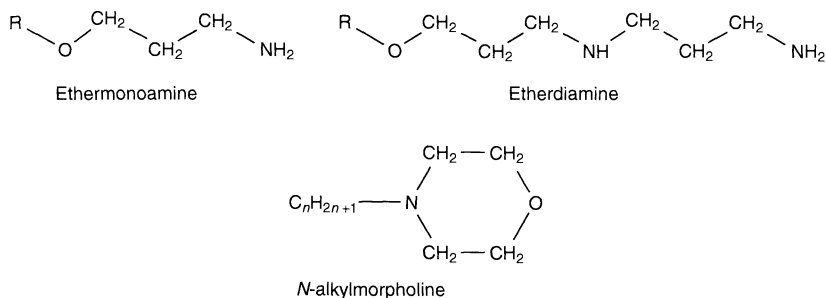


Figure 14.38. Structures of some cationic surfactants used in flotation

15.1.3 Feldspar from quartz

Feldspar is separated from quartz by using fatty mono- or diamines. The most commonly used are amines derived from fatty acids containing 8 to 18 carbon atoms, preferably C_{16-18} alkyl groups. The amine employed is widely used as its amine acetate, and it is also common to use blends with fatty acids. The flotation of feldspar from quartz is carried out at a very low pH. Sulfuric acid and hydrofluoric acid are used to adjust the pH to 2–3. Fluoride ions activate feldspar, which improves the recovery and grade of the feldspar product. In order to avoid the discharge of fluoride ions in wastewater and the handling of poisonous and corrosive hydrofluoric acids, a significant amount of effort has been made to develop a non-hydrofluoric-based process. Nevertheless, the most common process still used today is that involving fluoride activation. Sodium fluoride is often used instead of hydrofluoric acid, so as to decrease the risks of acid handling.

15.2 Potash

15.2.1 Flotation of sylvite

Sylvinite, a mixture of sylvite (KCl) and halite (NaCl), is the predominant source of potash deposits. The sylvite is separated from the gangue salts and clay minerals by direct flotation, using neutralized long-chain alkylamines, typically containing a C_{16-18} saturated alkyl group, with C_{18} being the major part. If the temperature is above 25°C , longer alkylamines (C_{20-24}) are often mixed with the C_{16-18} alkylamine to achieve a more efficient collector material. The amine ion is considered to fit in the crystal lattice by attaching itself to a potassium ion site. The adsorption is strong and the sylvite crystal becomes hydrophobic.

In the beneficiation of potash, the ore is first crushed and ground to an appropriate particle size. All wet operations must take place in saturated brine, since potash is readily water-soluble. The different solubility of the salts affects the composition of the brine at different temperatures, (see Table 14.13).

Compared to the other flotation systems, the material is much coarser in potash flotation, due to a large liberalization size of the crystals. The rather small difference in density between the mineral salt and the brine makes it possible to float much larger particles in the brine system as compared to water systems.

The potash contains clay minerals, often as slime. This clay represents a large surface area and adsorbs the alkylamine collector. This is detrimental to the potash flotation, and therefore several methods are used to dispose of the clay. Mechanical de-sliming using hydrocyclones and hydroseparators is common practice. Slime flotation is often used. In this, the clay minerals are separated in a pre-flotation step by using a polymer and a non-ionic surfactant, for example, polyacrylamide and ethoxylated fatty acid, respectively. An alternate way is to depress the clay minerals with polymers such as sodium carboxymethyl cellulose (CMC), potato starch and lignosulfonate.

The potash is often separated as a coarse and fine particle fraction by screening at 0.6–0.8 mm; the fractions are then treated separately. The concentration process is quite complex, including several classification

Table 14.13. The composition of brine at different temperatures

Temperature ($^\circ\text{C}$)	Saturated solution (wt%)		Density	Solid phase
	KCl	NaCl		
20	10.2	20.0	1.234	Na + K
40	13.2	19.7	1.236	Na + K

Table 14.14. Mineral flotation separation processes involving the use of cationic surfactants

Separation (of)	Cationic reagent	Trade name	pH	Remarks
<i>Oxide minerals</i>				
Silica from calcite	Quaternary ammonium compounds	Armoflote® 18, Lilafлот® 1590	8–9	
Silica from iron ore	Etheramines	Lilafлот® 810M, Lilafлот® 819M, Lilafлот® D817M	9–10.5	
Feldspar from quartz	Alkylamines, alkyldiamines, mixtures with fatty acid	Armac® T, Lilafлот® OT36, Armoflote® 820, Armoflote® 543	2–3	The feldspar is activated with fluoride in most cases
<i>Potash</i>				
KCl from potash	Alkylamines	Armeen® HT, Armoflote® 953, Armac® HT	7–8	The amine is often used together with frothers and “extender” oils
NaCl from carnallite	Alkylmorpholine	Armoflote® 619	5–6	

steps, flotation and regrinding, and may also differ between different mines. Flotation is generally carried in at least two stages, i.e. “rougher” and “cleaner” steps. The froth product from the first flotation (rougher) enters a second flotation step (cleaner) where the flotation is repeated and the sylvite product becomes concentrated. It is common practice to use additives in the flotation to improve the recovery of sylvite and increase the efficiency of the collector. Frothers such as pine oil or methylisobutyl carbinol (MIBC) are frequently used. Emulsions made of process oil mixed with collector and frother are often employed to improve the recovery of coarse-grained sylvite.

15.2.2 Flotation of halite

N-alkylmorpholine, whose structure is shown in Figure 14.38 is used as a collector for halite. The adsorption mechanism to halite is assumed to be a hydrogen-bond formation between the hydrated (Na^+) halite surface and the ether oxygen in the morpholine, and an ionic interaction between the morpholine tertiary nitrogen atom and a negatively charged chlorine ion at the halite surface. Reports in the literature also suggest the use of anionic surfactants such as fatty acids and alkyl phosphates as possible collectors for the flotation of halite; again, the adsorption mechanism is assumed to be by hydrogen-bond formation, as described above.

The reverse flotation of halite is preferable when KCl is in the form of carnallite ($\text{KCl}\cdot\text{MgCl}_2\cdot 6\text{H}_2\text{O}$). Traditional direct flotation of sylvite (KCl) with fatty amines will not work with carnallite ores. From carnallite, it is possible to produce pure KCl and MgCl_2 by using

hot- or cold-crystallization processes. Reverse flotation of halite (NaCl) can be utilized as a purification step in the cold-crystallization process. It is also possible to use alkylmorpholine in a reverse flotation of halite in processing sylvite, instead of the direct flotation of sylvite with fatty amines.

The flotation is sensitive to pH; according to the literature, optimal flotation is obtained between pH 4 and 7, with pH 4 being preferable. The effectiveness of the collector has an optimum at pH 4, and at higher pH values the collector dosage has to be increased to reach the same halite recovery performance. Increased collector dosage will affect the floatability of KCl, which increases at higher collector concentration, thus meaning increased losses. The alkyl group varies between C_{12} to C_{18} according to the literature, although most work reports the use of *N*-dodecylmorpholine as the collector surfactant. Table 14.14 presents a summary of mineral flotation techniques involving the use of cationic surfactants.

16 ACKNOWLEDGEMENTS

I would like to thank my administrative assistant, Ulrika Mårdud, for her untiring work in preparing the manuscript for this chapter.

17 REFERENCES

1. Dery, M., Quaternary ammonium compounds, in *Kirk Othmer Encyclopedia of Chemical Technology*, 4th Edn,

- Vol. 20, Kroschwitzand, J. I. and Howe-Gant, M. (Eds), Wiley, New York, 1996, pp. 739–767.
2. Kruger, G., Boltersdorf, D. and Overkempe, K., Esterquats, in *Novel Surfactants*, New York, Holmbeg, K. (Ed.), Marcel Dekker, New York, 1998, Ch. 4, pp. 115–138.
3. Conte, J. S. and Bender, G. W., *Softening/Debonding Agents*, Tappi Papermaking Chemical Processing Aids, Vol. 47, Tappi Press, Atlanta, GA, 1986.
4. *The Shell Bitumen Handbook*, Shell Bitumen, Chertsey, Surrey, UK, 1990.
5. *The Shell Bitumen Industrial Bitumen Handbook*, Shell Bitumen, Chertsey, Surrey, UK, 1995.
6. (a) *Witco Products for the Petroleum Industry*, Witco Corporation, New York, 1995; (b) *Chemicals for the Petroleum Industry*, Akzo Chemicals Inc., Chicago, IL, 1998.
7. Kudsk, P. and Streibig, C., *Herbicide Bioassays*, CRC Press, Boca Raton, FL, 1993
8. van Olphen, H. *An Introduction to Clay Colloid Chemistry*, Wiley, New York, 1963, pp. 59–69.
9. Leja, J., *Surface Chemistry of Froth Flotation*, Plenum Press, New York, 1982, pp. 301–306.
10. Fuerstenau, D. W. and Herrera-Urbina, R., Adsorption of cationic surfactants and the flotation of minerals, in *Cationic Surfactants Physical Chemistry*, Rubingh, D. N. and Holland, P. M. (Eds), Surfactant Science Series, Vol. 37, Marcel Dekker, New York, 1991, pp. 407–447.
11. Smith, R. W., Cationic and amphoteric collectors, in *Reagents in Mineral Technology*, Somasundaran, P. and Moudgil, B. M. (Eds), Surfactant Science Series, Vol. 27, Marcel Dekker, New York, 1988, pp. 219–256.

CHAPTER 15

Zwitterionic and Amphoteric Surfactants

David T. Floyd[†], Christoph Schunicht[‡] and Burghard Gruening[‡]

[†]*Degussa–Goldschmidt Care Specialties, Hopewell, VA, USA* [‡]*Degussa–Goldschmidt Care Specialties, Essen, Germany*

1	Introduction	349	6.1	Ecological evaluation	364
2	Chemistry of Zwitterionic Surfactants	350	6.2	Toxicological profile	364
	2.1 Carboxybetaines	350	6.3	Evaluation of toxicological results	364
	2.2 Special carboxybetaines	354	7	Application Properties	365
	2.3 Sulfo- and phosphobetaines	354		7.1 Alkali tolerance and chemical stability	365
3	Chemistry of Amphoteric Surfactants	355		7.2 Foaming and viscosity	366
	3.1 Aminoethylethanolamine-derived amphoteric	356	8	Applications	367
	3.2 Salt-free aminoethylethanolamine-derived amphoteric	359		8.1 Hard surface cleaners	367
	3.3 Other amphoteric	359		8.2 Laundry products	368
4	Analysis of Zwitterionic and Amphoteric Surfactants	361		8.3 Sanitizers and disinfectants	368
5	Physico-Chemical Properties	362		8.4 Personal care cleansers and shampoos	368
	5.1 Micelle formation	362		8.5 Cosmetics	368
	5.2 Surface tension	363		8.6 Oral care products	369
6	Ecological and Toxicological Properties of Zwitterionic and Amphoteric Surfactants	364		8.7 Pharmaceutical industry	369
				8.8 Other industrial applications	369
			9	References	369

1 INTRODUCTION

Zwitterionic and amphoteric surfactants are often regarded as a single group of surfactants using the general term amphoteric surfactants. Besides the similarities and general structural aspects that both types of surfactants have in common, there are also distinct differences to distinguish both product types. Historical, economical and chemical structural reasons contribute to placing both surfactant types together. Betaines and amphoteric acetates are the typical and most prominent representative examples of the zwitterionic and amphoteric surfactants (1–3). Both types are relatively new surfactants – the amphoteric acetates were first

proposed by Mannheimer (4) in the early 1950s. In the early 1960s, betaines were first introduced into the market. These surfactants experienced only a moderate growth and remained as relatively unimportant specialty surfactants until the 1980s, when a pronounced growth, especially for the zwitterionic betaines, began.

Zwitterionic surfactants contain at least one negative and one positive charge in the molecule at the same time, with both charges neutralizing each other internally under normal conditions. The molecules are overall neutral and do not move in an electric field. Zwitterionic compounds are also referred to as “inner salts”.

In general, the cationic moiety consists of a quaternary ammonium group, which retains its positive charge

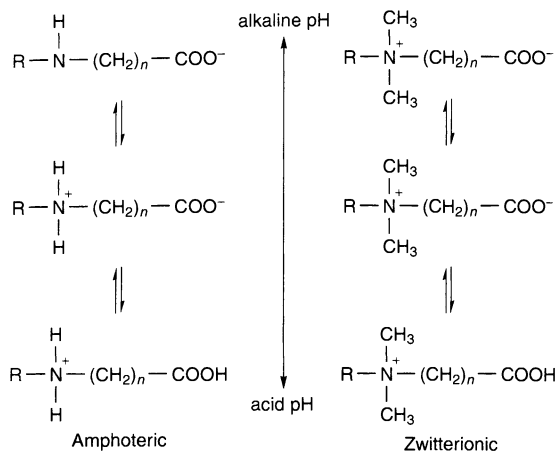


Figure 15.1. Amphoteric and zwitterionic behaviour at different pH values

over the entire pH range. The removal of this charge is only possible by degradation of the molecule. In most cases, the anionic moiety is a carboxylic group, although sulfonate and sulfate groups are also common. At strongly acidic pH values, this anionic moiety can be protonated. Consequently, most zwitterionic surfactants can exist, not only in a zwitterionic but also in a cationic form, which exhibits the typical behaviour of a cationic surfactant. However, an anionic behaviour cannot be achieved.

The term “amphoteric” (from *amphos*, meaning both) was first used for surfactants in the 1940s by H. Mannheimer (5). Amphoteric substances can have – like an amino acid – anionic, cationic or zwitterionic properties. These three forms exist in an equilibrium, depending on the pH range (Figure 15.1). At an acidic pH, the molecules will be protonated to form cations, while at an alkaline pH they will be deprotonated to form anionic species. Only in a mid-pH range can they exist as neutral molecules and demonstrate their zwitterionic character. This pH is called the isoelectric point. Amphoteric behaviour requires the presence of a secondary or tertiary amine group, which can be protonated easily.

The betaines, especially the coconut-oil-derived cocamidopropyl betaines, are the most important zwitterionic surfactants. The name “betaine” refers to trimethylglycine, which was first isolated from sugar beet (*beta vulgaris*). Cocoamphomonoacetate and cocoamphodiacetate are the most important types for the amphoteric surfactants. The structures and names for both product types are summarized in Table 15.1.

The main uses of betaines and amphotacetates are as secondary surfactants in the cosmetic field (6). The cocamidopropyl betaine and the coco-derived amphotacetates are incorporated in increasing amounts into modern formulations for shampoos and shower gels. These formulations are still mainly based on anionic surfactants such as lauryl sulfate or lauryl ether sulfate. These anionic surfactants can be referred to as primary surfactants. The zwitterionic and amphoteric surfactants interact with the anionic surfactants to form mixed micelles. The mildness, foaming and viscosity of the formulations are considerably improved. More recent uses for betaines are as modifiers in dish-washing liquids, household cleaners and wool-wash detergents. While the mildness of the formulation is important, the excellent lime soap tolerance of the betaines, combined with the overall improved cleaning performance, is of primary importance. Special betaines have been designed to meet demands such as low foam, extraordinary mildness or viscosity building. In technical applications, the hydrolytic stability of the surfactant is an important requirement. For this, alkyl betaine, carboxy or sulfo alkyl betaines are preferred.

2 CHEMISTRY OF ZWITTERIONIC SURFACTANTS

2.1 Carboxybetaines

Betaines are the most important secondary surfactants. The hydrophilic group in the important carboxybetaine is identical to that of the zwitterionic *N,N,N*-trimethylglycine, a betaine obtained from sugar beet (Figure 15.2). The term betaine is used synonymously for carboxybetaine, while other functional groups are always indicated, i.e. sulfobetaines. The positive charge is located at a quaternary nitrogen atom, and the negative charge at a carboxylic group linked closely to the quaternary nitrogen by a methylene group. It is important to note that the electron-attracting effect of the positive nitrogen atom strongly enhances the acidity of the carboxylic acid group, which results in an

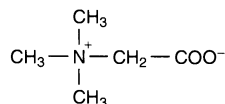


Figure 15.2. Structure of the natural betaine, *N,N,N*-trimethylglycine

Table 15.1. Structures and nomenclature of zwitterionic and amphoteric surfactants

Formula	Generic name	INCI name ^a	Chemical name
$\begin{array}{c} \text{CH}_3 \\ \\ \text{C}_{12}\text{H}_{25}-\text{N}^+-\text{CH}_2-\text{COO}^- \\ \\ \text{CH}_3 \end{array}$	Lauryl- betaine	Lauryl- betaine	2-Dodecyl(dimethyl)- ammonioacetate
$\begin{array}{c} \text{O} \\ \\ \text{C}_{11}\text{H}_{23}-\text{C}-\text{N}-(\text{CH}_2)_3-\text{N}^+(\text{CH}_3)_2-\text{CH}_2-\text{COO}^- \\ \qquad \\ \text{H} \qquad \text{CH}_3 \end{array}$	Laurylamido- propylbetaine	Lauramidopropyl- betaine	2-dimethyl(3-undecyl- carboxamidopropyl)- ammonioacetate
$\begin{array}{c} \text{O} \\ \\ \text{R}-\text{C}-\text{N}-(\text{CH}_2)_3-\text{N}^+(\text{CH}_3)_2-\text{CH}_2-\text{COO}^- \\ \qquad \\ \text{H} \qquad \text{CH}_3 \end{array}$ <p>(R-C=O derived from coconut oil)</p>	Cocoamido- propylbetaine	Cocamidopropyl- betaine	2-dimethyl(3-cocoyl- carboxamidopropyl)- ammonioacetate
$\begin{array}{c} \text{CH}_3 \\ \\ \text{C}_{16}\text{H}_{33}-\text{N}^+-\text{CH}_2-\text{SO}_3^- \\ \\ \text{CH}_3 \end{array}$	Cetylsulfo- betaine	-	3-hexadecyl- (dimethyl)ammonio- 1-propane sulfonate
$\begin{array}{c} \text{O} \\ \\ \text{R}-\text{C}-\text{N}-(\text{CH}_2)_3-\text{N}^+(\text{CH}_3)_2-\text{CH}_2-\text{CH}(\text{OH})-\text{CH}_2-\text{SO}_3^- \\ \qquad \qquad \\ \text{H} \qquad \text{CH}_3 \qquad \text{OH} \end{array}$ <p>(R-C=O derived from coconut oil)</p>	Cocoamido- propylhydroxy- sulfobetaine	Cocamidopropyl- hydroxysultaine	3-dimethyl(3-cocoyl- carboxamidopropyl)- ammonio-2-hydroxy-1- propane sulfonate
$\begin{array}{c} \text{O} \\ \\ \text{R}-\text{C}-\text{N}-(\text{CH}_2)_3-\text{N}^+(\text{CH}_3)_2-\text{CH}_2-\text{CH}(\text{OH})-\text{CH}_2-\text{O}-\text{P}(\text{OH})(\text{O})-\text{O}^- \\ \qquad \qquad \qquad \\ \text{H} \qquad \text{CH}_3 \qquad \text{OH} \qquad \text{O} \end{array}$ <p>(R-C=O derived from coconut oil)</p>	Cocoamido- propylhydroxy- phosphato- betaine	-	3-dimethyl(3-cocoyl- carboxamidopropyl)- ammonio-2-hydroxy-1- propane phosphate
$\begin{array}{c} \text{O} \\ \\ \text{R}-\text{C}-\text{N}-\text{CH}_2-\text{CH}_2-\text{N}(\text{H})-\text{CH}_2-\text{COO}^-\text{Na}^+ \\ \qquad \\ \text{H} \qquad \text{H}_2\text{C}-\text{CH}_2-\text{OH} \end{array}$ <p>(R-C=O derived from coconut oil)</p>	Cocoampho- monoacetate	Sodium coco- amphoacetate	Sodium 2-[2-hydroxyethyl (2-cocoylcarboxamido- ethyl) amino]acetate
$\begin{array}{c} \text{O} \\ \\ \text{R}-\text{C}-\text{N}-\text{CH}_2-\text{CH}_2-\text{N}(\text{H})-\text{CH}_2-\text{COO}^-\text{Na}^+ \\ \qquad \\ \text{H}_2\text{C}-\text{CH}_2-\text{OH} \end{array}$ <p>(R-C=O derived from coconut oil)</p>	Cocoampho- diacetate	Disodium- Cocoampho- diacetate	Disodium 2-carboxylato- methyl[2-(2-hydroxy- ethylcocoylcarboxamido- ethyl)amino]acetate
$\begin{array}{c} \text{C}_{12}\text{H}_{25}-\text{N}-\text{CH}_2-\text{CH}_2-\text{COOH} \\ \\ \text{H} \end{array}$	Laurylamino- propionic acid	Lauramino- propionic acid	3-Dodecylamino- propanoic acid

^aINCI, International Nomenclature of Cosmetic Ingredients.

acidity which is not comparable to that of acetic acid or fatty acids. The pK_a values of *N,N,N*-trimethylglycine and acetic acid are 2.351 and 4.762, respectively (7), and thus a pH of approximately 1 is needed to protonate a carboxybetaine into its cationic form. At higher pH values, a carboxybetaine is a neutral zwitterion. Betaines generally contain a fully quaternized nitrogen atom.

Replacing one methyl group in *N,N,N*-trimethylglycine by a long alkyl chain gives the simple structure of an alkyl betaine surfactant (Figure 15.3).

Alkyl betaines are synthesized by carboxymethylating a long alkyl chain tertiary amine with chloroacetic acid (MCA) or its sodium salt (Figure 15.4). The alkyl chain of these amines is mostly derived from natural sources such as coconut oil.

The reaction is carried out in aqueous solution. In order to drive the reaction to completion, the pH of the reaction mixture is controlled by addition of sodium

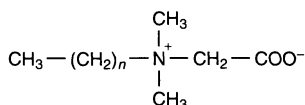


Figure 15.3. General structure of an alkyl betaine

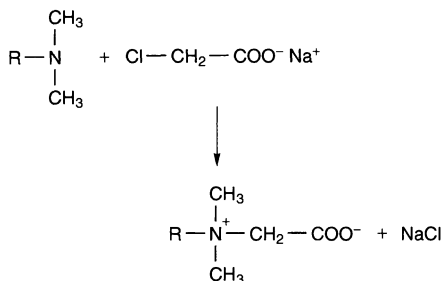


Figure 15.4. Synthesis of an alkyl betaine

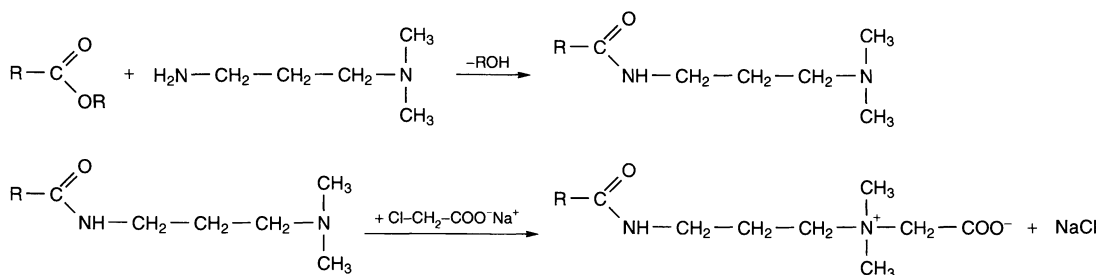


Figure 15.6. Synthesis of an alkylamido betaine

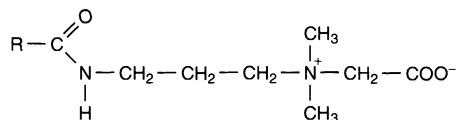


Figure 15.5. General structure of an alkylamido betaine

hydroxide. The pH is preferably kept in the range of 7 to 8 (8). The resulting surfactants are mostly aqueous solutions with approximately 30% active betaine and 5% sodium chloride as a by-product. In more recent years, the market focus has been less on the alkyl betaines and more on the alkylamido betaines. Because of performance advantages, innovations have concentrated on the alkylamido betaines. In Figure 15.5, the typical structure of an alkylamido betaine is shown.

The production of alkylamido betaines is usually accomplished in two steps. The first involves the formation of an alkylamidopropyl dimethylamine, which is then followed by a carboxymethylation step to form the final betaine (Figure 15.6).

In the amidoamine formation, 3-aminopropyl dimethylamine (DMAPA) is reacted with a fatty acid derivative. This may either be the fatty acid or its methyl or glycerin ester. In the latter case, this means a natural oil is used. To produce cocamidopropyl betaine (CAPB) the raw materials of choice are refined coconut or palm kernel oil, either in their unhydrogenated or hydrogenated forms. A typical fatty acid composition for cocamidopropyl betaine is given in Table 15.2.

If the oil is used as the starting raw material, glycerin will be formed as a by-product. Glycerin does not have a negative effect on most applications and in fact, may even be desired. A glycerin content of 2–3% is normal in CAPB solutions. If desired, some glycerin can be removed from the amidoamine by phase separation or distillation. Thus, a glycerin content of approximately 1% can be achieved. The use of fatty acids or their methyl esters will result in CAPBs which are glycerin

Table 15.2. Typical Fatty Acid Composition of cocamidopropyl betaine (CAPB)

Fatty acid ^a	Content ^b (wt%)
8	7
10	6
12	49
14	19
16	9
18	10

^aRepresented by the number of carbon atoms.^bApproximate values.

free. Any water or methanol produced is distilled off. Specialty betaines can be made which differ in their fatty acid distribution, such as a betaine which does not contain caprylic and capric acid derived parts.

All amidoamines contain a small amount of fatty acid, which is carried over to the second reaction step, i.e. the formation of the betaine. Depending on the source, the fatty acid is either residual unreacted fatty acid or it is formed by hydrolysis of a fatty acid ester, which takes place to a minor extent. The DMAPA, which is used in excess, is distilled off after completion of the reaction.

The betaine is formed in a carboxymethylation reaction starting with the amidoamine and chloroacetic acid or its sodium salt. The reaction is carried out in aqueous solution at a temperature of 80–100°C.

Similar to the carboxymethylation of tertiary fatty amines to alkyl betaines, the pH value in the carboxymethylation of alkylamidoamines needs to be controlled and kept between 7.5 to 10.5 (9). If the pH of the reaction medium is below approximately 7.5, the carboxymethylation will slow down due to the increasing protonation of the amine, while the undesired hydrolysis of chloroacetate will result in large amounts of glycolic acid. When the pH exceeds approximately 10.5, hydrolysis of the amide group may occur, which leads to undesired high contents of fatty acids and carboxymethylated amine derivatives, and finally to decomposition of the final product.

Alkylamido betaines are usually supplied as 30% aqueous solutions, containing several by-products, which may effect the physical properties or the toxicological profile of the betaine. Formerly, CAPB contained approximately 3% of the amidoamine because of an incomplete reaction. The amidoamine has some advantages, contributing to viscosity and providing some substantivity to hair and skin. The tertiary amine is an irritant and sensitization is suspected to be related to the level of the tertiary amine (10) or the dimethyl aminoamine (11). The content of amidoamine in modern

CAPBs is typically below 0.3%, which is normally achieved by controlling the reaction pH. The dimethyl aminoamine content is controlled to be below 15 ppm, which is regarded as safe. Sodium chloride is formed as the main by-product, and is present in most betaine solutions in concentrations of about 5%. Typically, the salt is left in the surfactant solution as it has no negative side effects for most applications. It is even desirable for the enhancement of viscosity in ready-to-use preparations such as shampoos.

In a side reaction, the sodium chloroacetate or chloroacetic acid is hydrolysed to glycolic acid; this side reaction is controlled by the pH of the reaction mixture. The glycolic acid content usually is below 0.1% but may be as high as 1%. There is little concern about the glycolic acid, as it is often added to personal care formulations.

The presence of monochloroacetic acid (MCA), and dichloroacetic acid (DCA), which is an impurity in MCA, is more critical because of their toxicological implications. While chloroacetic acid is almost completely consumed under proper reaction conditions, dichloroacetic acid takes no part in the carboxymethylation and its hydrolytic degradation is also very limited. Diverse methods have been developed to reduce the residual content of chloroacetic acids. One possibility is the reaction of such acids with sulfonating reagents such as sodium hydrogen sulfite, which leads to a sulfo-carboxy acid (12). A second method is the treatment of the cocamidopropyl betaine at alkaline pH in combination with ammonia or amino acids (13). A more simple way is the hydrolysis of mono- and dichloroacetic acid at elevated temperatures, i.e. > 120°C (14). Contents of mono- and dichloroacetic acid of < 5–10 ppm can be reached when using the latter methods.

Other research efforts have focused on increasing the concentration of the betaine solution as supplied. As previously mentioned, the usual concentration for commercial cocamidopropyl betaine is approximately 30% of active matter, comprising all surface-active compounds, or about 35% solids. At slightly higher concentrations, aqueous cocamidopropyl betaine solutions form high-viscous solutions or even solid gels. These gels often show the typical behaviour of “ringing” gels. The critical concentration depends strongly on the alkyl chain length of the fatty acid. The influence of the chain length on the flow behaviour of betaine solutions is shown in Figure 15.7.

Numerous attempts have been made to produce flowable, highly concentrated CAPB. A possible route is the use of additional components such as other surfactants (15), solvents such as 1,2-propylene glycol

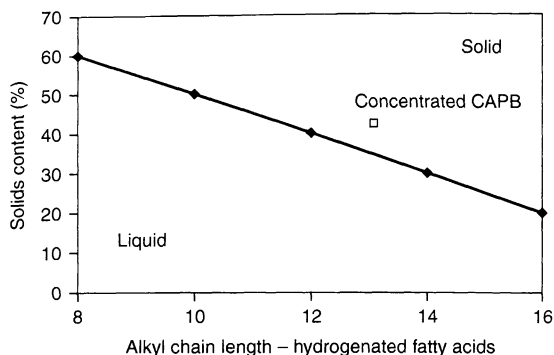


Figure 15.7. Flowability of aqueous solutions of alkylamido-propyl betaines (at 25°C)

or salts, i.e. sodium citrate (16), or the homologous trimethylglycine (17). A preferred way is the addition of free fatty acids (18). In this manner, the active matter concentrations of 38% can be reached. Fatty acids are brought into the reaction mixture as a by-product of the amidoamine; by using this procedure, no new compounds are added to the betaine. Highly concentrated betaines save on storage and transportation costs. They are microbiologically stable and require no preservation.

Highly concentrated betaines are produced by the spray drying of the aqueous betaine solution. This can result in products containing 80–85% active matter, 13–15% sodium chloride and 0.3–3.0% water. Another possibility for the production of a solid betaine is the use of a solvent in which the betaine is substantially insoluble. For this purpose, polar aprotic solvents such as esters or liquefied gas solvents can be used (19). The solid betaines have advantages in those applications where the water content is critical.

2.2 Special carboxybetaines

Powdered betaines are just one example of the advanced development of special carboxybetaines. For technical applications, chloride ions need to be excluded to avoid corrosion. Low-salt betaines can be produced by special membrane-separation processes. Another possibility is the use of non-aqueous solvents such as ethanol and the subsequent filtration and separation of the precipitated salt (20).

To modify the cocamidopropyl betaine for special foam and viscosity requirements, the fatty acid composition is often adjusted. Examples include betaines based on stripped coconut fatty acid with only a very small

fraction of caprylic and capric acid or betaines based on lauric acid only. It is noted that betaines based on caprylic and capric acid are practically non-irritating. They are interesting surfactants for extremely mild consumer products such as facial washes or baby shampoos (21). The C_{8–10} alkylamido betaine acts as a foam booster when combined with anionic surfactants. Interestingly, the surfactant itself is a low foamer, especially when it is used in low concentrations. For technical applications, such as in “cleaning in place” (CIP) liquids, where low foam is a requirement, this betaine is gaining increasing acceptance.

Undecylenic amidopropyl betaine combines the antimicrobial activity of the undecylenic moiety with surface-active properties. Since this betaine acts as a mild active, selectively against *Malassezia furfur*, it is an interesting raw material for the formulation of anti-dandruff shampoos (22).

Gemini betaines have been made on the basis of dimer acids (23). Such acids are produced by dimerization of unsaturated fatty acids such as oleic and linoleic acid and then purified by distillation. Dimer acids are a mixture of different dicarboxylic acids with an average chain length of 36 carbons (24).

Aqueous solutions of dimer amidopropyl betaine are highly viscous, and are typically non-flowable above a betaine actives concentration of 5 wt%. They display interesting rheological phenomena (25). To achieve higher concentrations for shipment of this Gemini betaine, mixtures with cocamidopropyl betaine can be made. On this basis, concentrations of 25 wt% active matter are achievable. Dimer amidopropyl betaine shows an increased substantivity, compared to cocamidopropyl betaine, on fibres and is a very effective irritancy mitigant in anionic-surfactant-based systems.

2.3 Sulfo- and phosphobetaines

Sulfobetaines are a product group with properties very similar to the carboxybetaines (26). They have found application in the technical and personal care areas, although their usage is limited compared to the carboxybetaines.

The acidity of the sulfonic group is slightly more pronounced than that of the carboxylic group in the carboxybetaines. This aspect does not differentiate the sulfobetaines distinctly from the carboxybetaines. The synthesis of sulfobetaines either starts with tertiary fatty amines or more commonly with fatty amidopropylamines and is in this respect similar to the synthesis of carboxybetaine. The sulfonic group can be introduced

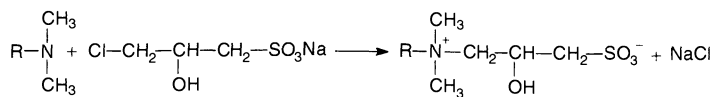


Figure 15.8. Preparation of a sulfobetaine using chlorosulfonate

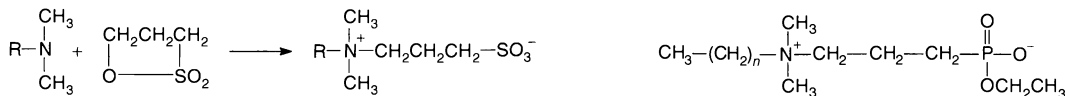


Figure 15.9. Preparation of a sulfobetaine using 1,3-propanesultone

in two ways. One way is the reaction with 1-chloro-2-hydroxypropane-3-sulfonate which results in hydroxysulfobetaines (Figure 15.8). The by-product of this reaction is sodium chloride.

An alternative route to sulfobetaines is the reaction of a tertiary amine with 1,3-propanesultone (Figure 15.9). This route leads to salt-free products. Since propanesultone is a highly carcinogenic chemical, the products must be checked carefully for residual sultone content. The production of these propylsulfobetaines is limited to a few specialized producers.

Sulfobetaines are typically produced as aqueous solutions containing approximately 30 wt% of the active matter. The fatty residue is similar to that of the common carboxybetaines coconut or lauryl material. Special alkyl compositions are possible, such as a hydroxypropyl sulfobetaine based on synthetic C₁₄₋₁₅ alkyl raw material.

A further class of betaines containing an anionic moiety based on a hetero atom are the phosphobetaines. This group can be divided into betaines with a C-P linkage and others with a C-O-P linkage. To the first group belong the phosphinate betaines and the phosphonate betaines (Figure 15.10 and 15.11, respectively).

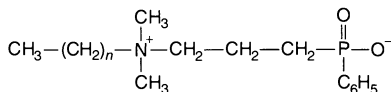


Figure 15.10. General structure of a phosphinate betaine

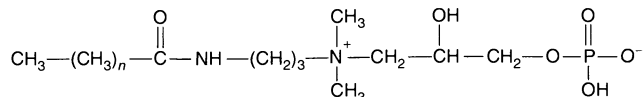


Figure 15.12. General structure of a phosphatobetaine

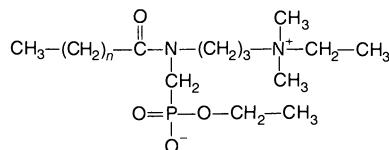


Figure 15.11. Two general structures of phosphonate betaines

The phosphobetaines can be prepared by the reaction of alkyldimethylamine with bromoalkylethylphenylphosphinate or bromoalkyldiethylphosphonate. The phosphorus reagents are prepared from diethylphenylphosphonite or triethylphosphite and a dibromalkane by an Arbusov reaction (27). Alternatively, phosphobetaines can be prepared by the reaction of an alkylamido-propyldimethylamine with a phosphoric acid ester and formaldehyde (28).

Phosphatobetaines (Figure 15.12) represent examples of betaines containing a C-O-P linkage. These betaines can be synthesized by the reaction of a chlorohydroxyalkylphosphate with an alkylamidopropyldimethylamine (29). A disadvantage of phosphatobetaines is their susceptibility to hydrolysis of the C-O-P linkage.

3 CHEMISTRY OF AMPHOTERIC SURFACTANTS

Amphoteric surfactants are often called amphoteric to distinguish them from betaines. They are characterized by a hydrophilic group in which the state of ionization depends on the pH, a behaviour which is typical of amino acids. At high pH values, the carboxyl group is

ionized, thus resulting in a negative charge, while at low pH values, the amino group is ionized, so resulting in a cationic charge. Between these extremes, there is a pH range in which the molecule is neutral. This pH range represents the isoelectric range depending on the alkalinity of the nitrogen atom and the acidity of the carboxylic function in the given structure.

3.1 Aminoethylethanolamine-derived amphoteric

A secondary surfactant group with increasing economical importance are the *N*-(2-aminoethyl)-2-aminoethanol (aminoethylethanolamine)-derived amphoteric. Because the intermediate in the synthesis of these surfactants is a substituted imidazoline, they are also classified as being imidazoline-derived. Historically, these mild surfactants have been the first to offer the possibility for the production of non-eye-stinging shampoos. Still today, aminoethylethanolamine-derived amphoteric are mainly used in personal care formulations where mild properties are desired, whereas industrial applications play only a minor role.

The intermediate in the synthesis of aminoethylethanolamine-derived amphoteric is a heterocyclic imidazoline with an unsaturated five-membered ring system containing an amine and an imine group (Figure 15.13).

Due to the availability of only limited analytical methods at the time of their market introduction, it was assumed that these surfactants also possessed the cyclic structure of the precursor (4). In later years, it turned out that they are more correctly described by an open-chain structure (30, 31). In contrast to the well-defined composition of amidopropyl betaines, aminoethylethanolamine-derived amphoteric often are complex mixtures of different types of compounds and impurities. The composition of the mixtures varies with the production parameters.

In particular, two groups of aminoethylethanolamine-derived amphoteric have found use in personal care formulations, i.e. the amphomonoacetates and amphodiacetates. The key structures of these mono- and dicarboxylic derivatives are given in Figure 15.14.

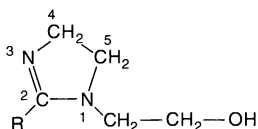


Figure 15.13. The imidazoline intermediate for aminoethylethanolamine-derived amphoteric

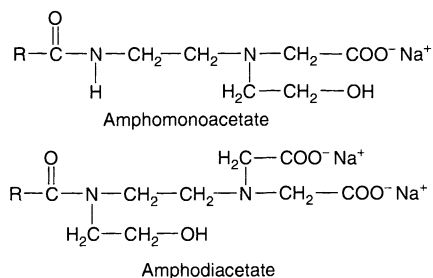


Figure 15.14. General (base) structures of amphomonoacetate and amphodiacetate

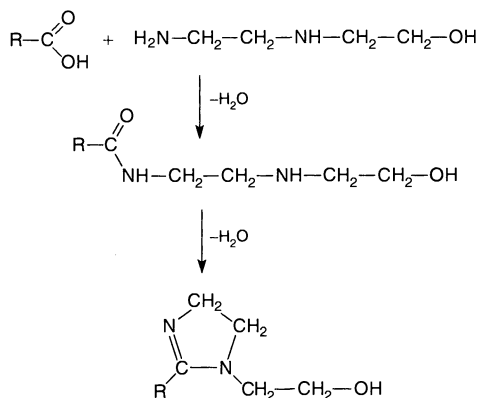


Figure 15.15. Preparation of the imidazoline intermediate

The synthesis of these surfactants involves several steps. The first step is the preparation of a substituted imidazoline, usually 1-(hydroxyethyl)-2-alkyl imidazoline, starting from fatty acids or fatty acid methyl esters and aminoethylethanolamine (AEEA) (Figure 15.15). For the production of betaines, the choice of fatty material is in most cases hydrogenated coco fatty acid. The distribution composition of fatty acid chain lengths, given above in Table 15.2, is typical also for cocoamphoacetates.

The reaction is carried out at temperatures of 140–200°C under moderate vacuum. The water formed in the course of the reaction is continuously distilled off. Under these conditions, the amide is first formed, followed by ring-closure to give the imidazoline. To obtain a complete conversion of the fatty acid to the amide, an excess of AEEA is used. This excess is needed to avoid the formation of a diamide (Figure 15.16). This by-product stems from the reaction of both the primary and the secondary amino group with fatty acid. The diamide tends to crystallize out and form

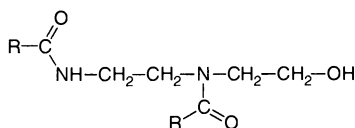


Figure 15.16. Structure of the diamide based on aminoethyl-ethanolamine (AEEA)

finely dispersed precipitates in the final formulation after an unpredictable storage time. This precipitate is, of course, detrimental to the product quality, and thus a low diamide content is a prerequisite for an amphotoacetate of good quality. Excess of AEEA can be removed at elevated temperatures and reduced pressures. A small amount of free fatty acid usually remains in the imidazoline.

In the next reaction step, the imidazoline is carboxymethylated with chloroacetic acid (MCA) or sodium monochloroacetate in alkaline aqueous solution. Depending on the reaction conditions, this step results in sodium amphotmonoacetate or sodium amphodiacetate.

For the production of amphomonoacetates (Figure 15.17), the imidazoline is hydrolysed under alkaline conditions by heating an aqueous solution for several hours at a temperature of 80–90°C before

carboxymethylation. Imidazolines are stable at low pH values except for very acidic conditions. They are easily hydrolysed at pH values above 7 – under these conditions, ring opening of the imidazoline takes place. In a following step, chloroacetic acid or its sodium salt is added to the mixture at a temperature of 60–90°C and the pH is kept in the range of 8.5–9.5 by using caustic soda. The hydrolysis may result in primary and secondary amide derivatives, depending on which bond is cleaved. If the 1,2-bond is hydrolysed, a primary amide is formed, while if the 2,3-bond is hydrolysed, a secondary amide is formed. Under aqueous alkaline conditions as described above, the formation of a primary amide derivative is favoured (Figure 15.17, Structure I). There is evidence that ring-opening occurs mainly at the 2,3-double bond, giving the secondary amide first (Figure 15.17, Structure II), followed by a rearrangement, i.e. a shift of the acyl group. Thus, the result is the same as if the 1,2-bond was hydrolysed (I). The primary amide derivative can react only with one mole of chloroacetic acid, giving amphomonoacetates as the main product of the reaction sequence (Path B).

The secondary amide derivative is of minor importance and is present in an amount of not more than 10% of the active matter in the mixture. This compound can

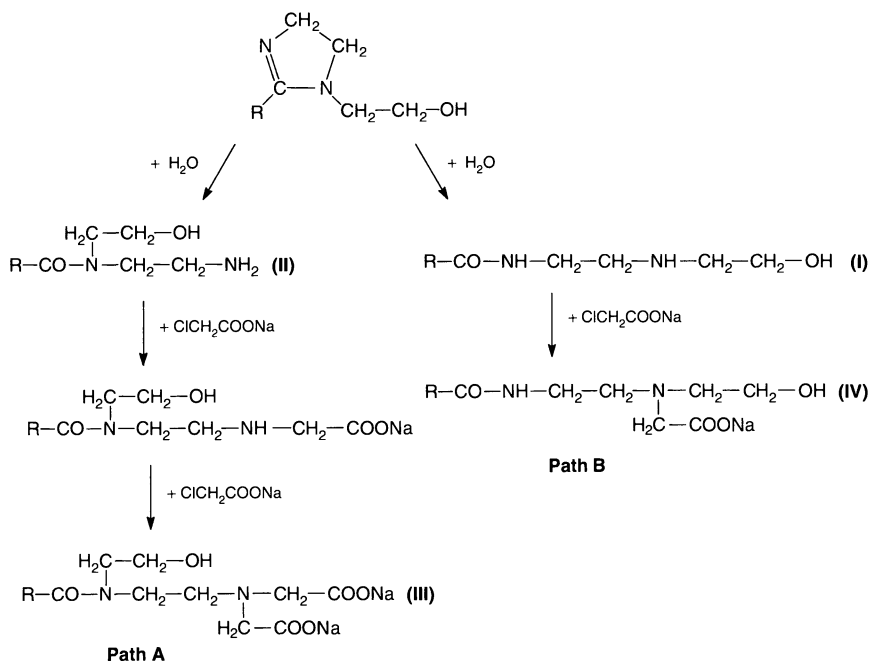


Figure 15.17. Synthesis of amphomonoacetates

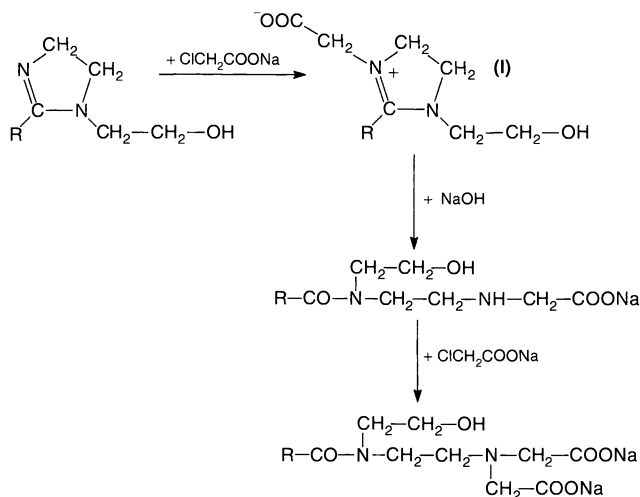


Figure 15.18. Synthesis of an amphodiacetate

react with two moles of chloroacetic acid, which leads to amphodiacetate as the product (Path A).

Commercial amphomonoacetates (the same is also true for commercial amphodiacetates) are always a mixture of amphomono- and amphodiacetates. The surfactant is obtained as an aqueous mixture containing ca. 30% of active matter, similar to cocamidopropyl betaine.

In order to obtain amphodiacetate as the main reaction product, the imidazoline is directly carboxyalkylated with an excess of chloroacetic acid or sodium chloroacetate for several hours at a temperature of 70–100°C and a pH of 8–10, which is maintained by the addition of caustic soda. In the next step, hydrolysis and further carboxyalkylation occurs under alkaline conditions. Once again, hydrolytic ring-opening occurs mainly at the 2,3-double bond and a product is formed which is identical with that formed via Path A in Figure 15.17 (Structure III). Further investigations are needed for clarification of the mechanism. Theoretically, an imidazoline betaine may be formed as an intermediate (Figure 15.18, Structure I).

Several other structures have been discussed or proposed for amphodiacetates (with some examples being shown in Figure 15.19). There is, however, no evidence for the existence of these types of molecules in amphodiacetate products.

Commercial amphodiacetates mainly consist of the surfactant corresponding to Structure III (Figure 15.17) and also, to a minor extent, an amphomonoacetate (Figure 15.17, Structure IV), which can clearly be identified. A complete analysis of amphodiacetates,

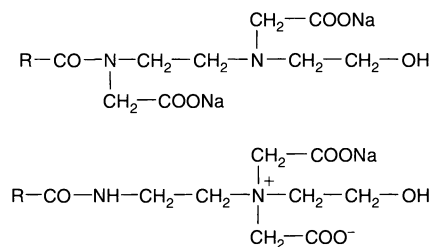


Figure 15.19. Proposed structures for amphodiacetates

however, is difficult and thus the commercial products can be regarded as “products by process”. Amphodiacetates can be delivered in a higher concentration when compared to the corresponding monoacetates and cocoamphodiacetate types. Amphodiacetates with up to 40% surfactant content are available on the market.

Since the chemistry of amphoacetates is related to a large extent to that of betaines, the by-products (apart from the amine) are almost identical. Sodium chloride is contained in a range of 6% for monoacetates, and up to 12% for diacetates. Glycolic acid, formed by hydrolysis from chloroacetic acid, is contained at 0.5–1.0% but may be as high as 4% in some grades of the surfactant. Dichloroacetic acid and residual monochloroacetic acid are found in similar concentrations as in betaines. Glycerin is not usually present, because the oil is not normally used as a raw material. However, a complete analysis of the product composition still remains to be carried out.

3.2 Salt-free aminoethylethanolamine-derived amphoteric

By reacting the imidazoline intermediate (Figure 15.13) with acrylic acid or methyl acrylate under aqueous alkaline conditions, amphomonopropionates are formed (Figure 15.20).

The acrylic acid derivative presumably adds, via a Michael Addition Reaction, to the nucleophilic nitrogen atom of the open-ring amidoamine, thus forming an amphopropionate. No salt is formed as a by-product. This reaction was first described in 1963, assuming a cyclic product structure which contained imidazoline (32). Later, it was shown that the reaction in aqueous medium results in a linear product (33).

In contrast to betaines, which can be made by carboxyalkylation of the precursor amidoamine with 3-bromopropionic acid and which are characterized by a permanent cationic group, these propionates are sufficiently stable and do not suffer noticeably from any

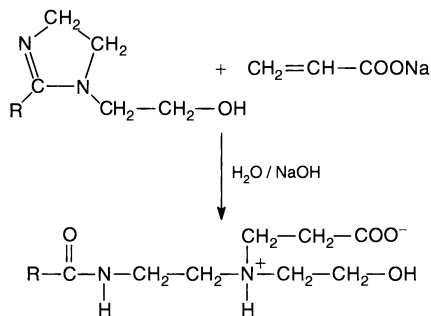


Figure 15.20. Synthesis of an aminoethylethanolamine-derived amphomonopropionate

reversibility of the reaction. However, the development of acrylate cannot be completely excluded.

Amphopropionates are used in personal care, as well as in technical applications, which require the absence of salt. These may be, for example, electrolyte-sensitive hair dye formulations or metal-working fluids. In addition, a special dicarboxylic amphoteric based on the addition of acrylic acid to an imidazoline has been described (34).

3.3 Other amphoteric

By carboxyalkylation of alkylamines, alkyletheramines or alkylpolyamines, either with chloroacetic acid or acrylic acid (or their derivatives), a multitude of special amphoteric surfactants can be achieved. An overview is given in Table 15.3.

The salt-free propionates have found versatile technical applications in metal-working fluids, and because of their excellent alkali stability, in alkaline cleaning compounds. The acetates are more suitable for use in personal care or general cleaning applications. Some acetates have anti-microbial properties and are used as disinfectants. Alkylaminopropionates and alkylaminodipropionates are synthesized by carboxyalkylation of fatty amines with methyl acrylate or acrylic acid, following the mechanism of the Michael (Addition) Reaction (Figure 15.21).

Whether a mono- or a diadduct is formed mainly depends on the stoichiometry. Unreacted acrylate can be removed by distillation. Finally, the methyl ester is hydrolysed in the presence of alkali at an elevated temperature under pressure, thus producing the sodium salt or the partial salt. The use of acrylic acid instead

Table 15.3. Amphoteric Surfactants Derived from Amine Derivatives

Formula	Chemical name
$\text{CH}_3-(\text{CH}_2)_{11}-\text{N} \begin{array}{l} \diagup \text{CH}_2-\text{CH}_2-\text{COONa} \\ \diagdown \text{CH}_2-\text{CH}_2-\text{COONa} \end{array}$	Disodium 3-(2-carboxylatoethyl)dodecylamino propanoate
$\text{CH}_3-(\text{CH}_2)_3-\underset{\text{CH}_2-\text{CH}_3}{\text{CH}}-\text{CH}_2-\text{O}-(\text{CH}_2)_3-\text{NH}-\text{CH}_2-\text{CH}_2-\text{COONa}$	Sodium 3-[3-(2-ethylhexyloxy)propylamino] propanoate
$\text{CH}_3-(\text{CH}_2)_{11}-\text{NH}-(\text{CH}_2)_2-\underset{\text{CH}_2-\text{COONa}}{\text{N}}-(\text{CH}_2)_2-\text{NH}-\text{CH}_2-\text{COONa}$	Disodium 2-[2-carboxylatomethylaminoethyl(2-dodecylaminoethyl)amino]acetate
$\text{CH}_3-(\text{CH}_2)_{17}-\underset{\text{NaOOC}-\text{CH}_2}{\text{N}}-(\text{CH}_2)_3-\underset{\text{CH}_2-\text{COONa}}{\text{N}}-(\text{CH}_2)_3-\text{NH}-\text{CH}_2-\text{COONa}$	Trisodium 2-[3-carboxylatomethylaminopropyl(3-carboxylatomethyloctadecylaminopropyl)-amino]acetate

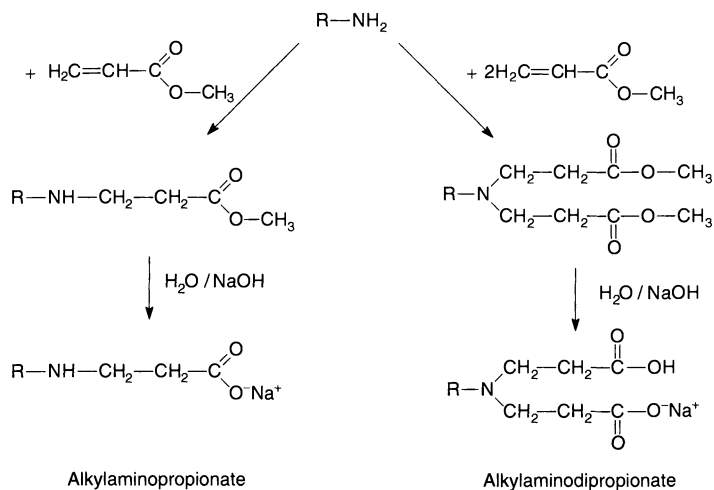


Figure 15.21. Syntheses of alkylaminopropionates and alkylaminodipropionates

of methyl acrylate directly leads to the product and saves the ester hydrolysis. This alternative, however, only results in the dipropionates. If equimolar amounts of amine and acrylic acid are used, a mixture of all three products, but mainly residual amine and the diadduct, are produced (1).

Amphopropionates have an isoelectric range at pH values of approximately 2.5–4.5. Within this range, their solubility is lowest and in some cases precipitates may form. Thus, corresponding alkyletheraminepropionates are made which can be used in a far wider range of applications (3).

Structurally related to the propionates are the aminoacetates. The latter are synthesized by the reaction of fatty amines with chloroacetic acid as the alkylation reagent. Depending on the amount of chloroacetic acid used, mono- and disubstituted amines can be produced in this way (Figure 15.22) (35).

Related to these compounds are alkyl polyamino carboxylates, which can be derived from fatty polyamines.

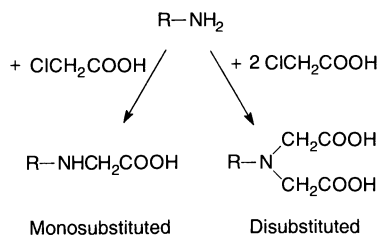


Figure 15.22. Syntheses of mono- and disubstituted amines by the reaction of fatty amines with chloroacetic acid

In these molecules, several amine groups and one or more carboxylic acid groups are combined to give highly functionalized surfactants. In particular, alkyl amino acetic acids prepared from polyamines have found interest since these amphoteric show microbicidal properties (36). An example is dodecyl propylene diamine acetic acid, which is derived from a diamine and chloroacetic acid by carboxymethylation (Figure 15.23).

Another amphoteric with efficient bactericidal and fungicidal properties is dodecyl diethylene triamine acetic acid, which is synthesized in a similar manner from the corresponding triamine (Figure 15.24).

An example of fully carboxymethylated alkyl polyamino amphoteric is the class of compounds introduced by E.G. Lomax (Figure 15.25) (37). These so-called “APACS”, which are mainly based on tallow, are prepared in the usual manner by carboxymethylation with monochloroacetic acid or by acrylation. Because of their mildness, they have found use in special personal care applications.

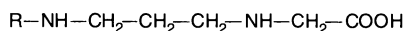


Figure 15.23. Structure of dodecyl propylene diamine acetic acid ($\text{R} = \text{CH}_3(\text{CH}_2)_{11}-$)

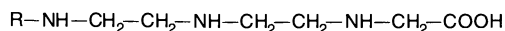


Figure 15.24. Structure of dodecyl diethylene triamine acetic acid ($\text{R} = \text{CH}_3(\text{CH}_2)_{11}-$)

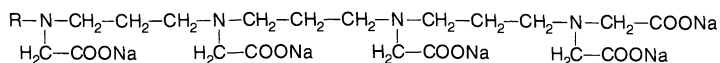


Figure 15.25. Structure of a fully carboxymethylated alkyl polyamino carboxylate (APAC)

4 ANALYSIS OF ZWITTERIONIC AND AMPHOTERIC SURFACTANTS

Since the analytical methods for the characterization of aminoethylethanolamine-derived amphoteric are in most cases very similar to those used for betaine analysis, the focus will be on the latter. Only small modifications need to be made for the determination of impurities and by-products in amphotoacetate solutions.

The analysis of the content of surfactant actives of betaine solutions is rather complicated. No direct titration method for the determination of the betaine concentration was available in the past, since all methods known have lead to incorrect results due to the presence of protonable by-products such as glycolic acid or free amidoamine (38). A modified titration method has been developed in recent years which gives more accurate results due to the choice of a special solvent mixture (39). The use of methanol and ethylene glycol monomethyl ether allows the almost selective titration of a betaine in its complex solution.

Despite these direct titration methods, the surfactant actives content is usually calculated indirectly by a subtraction method. For this, the water and sodium

chloride content is measured, since these substances represent two of the main components of a typical betaine solution. The water content can be determined very accurately by using a Karl Fischer titration. Another method, which gives a greater standard deviation, is the drying of a small sample of the mixture and the determination of the mass reduction. The sodium chloride content can be measured by the potentiometric titration of chloride with silver nitrate.

Another method for the quantification of the betaine or amphotoacetate content is proton nuclear magnetic resonance (^1H NMR) spectroscopy. In addition, NMR spectroscopy gives structural information and is suitable for the detection of unusual components in the solution. In Figure 15.26, the spectra of pure cocoamphomonoacetate and cocamidopropyl betaine are given.

The signal most suited in the ^1H NMR spectrum for the determination of the betaine content is that observed at 3.2 ppm. This signal is very specific and usually no other compound shows a signal at this position. Such a signal is produced by an overlap of the signal of the hydrogens which are part of the methyl groups attached to the quarternary nitrogen and that of the hydrogens of the methylene group next to the amide moiety.

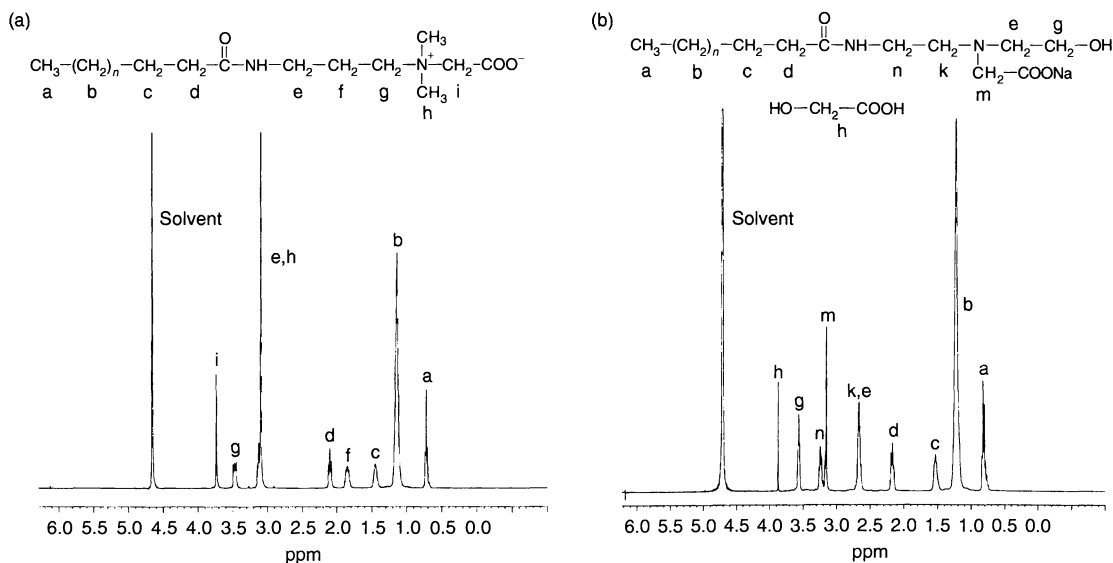


Figure 15.26. ^1H NMR spectra of (a) cocamidopropyl betaine and (b) cocoamphomonoacetate

In addition to the determination of the total amount of betaine, it is possible to analyse the fatty acid composition of the surfactant. Usually the chain length distribution is checked in the raw material before the reaction. In the product, this composition can be analysed by cleavage of the amide bond of the betaine in hydrochloric acid and subsequent conversion of the resulting free fatty acids into their methyl esters. The separation is accomplished by gas chromatography (GC).

The determination of the contents of monochloro- and dichloroacetic acids is of high priority due to the negative toxicological profile of these substances. One method makes use of the separation of these substances via GC. For this analysis, both compounds have to be converted into their corresponding methyl esters. The detection is accomplished by using an electron capture detector. The second method – High Pressure Liquid Chromatography (HPLC) separation – allows the direct determination of both organic acids without further modification of the substances. This method, which makes use of anion exchange columns, is advantageous since glycolic acid, a main by-product, can be detected simultaneously.

The amount of free fatty acid in the betaine solution can be measured by special GC techniques or reversed-phase HPLC. Free fatty acid amidoamine can be determined very accurately by HPLC using a ion-exchange column and a phosphate buffer solution as an eluent.

The amount of residual dimethylaminopropylamine (DMAPA) is usually determined directly after the first reaction step of the betaine synthesis, i.e. the preparation of amidoamine. After this has been reacted with phenyl isothiocyanate, it can be analysed by HPLC using a reversed-phase column. The quantitative determination of aminoethylethanolamine (AEEA) in aminoethylethanolamine-derived amphoterics cannot currently be accomplished in the final product. Residual amounts of this compound have to be measured in the imidazoline intermediate of the reaction sequence.

5 PHYSICO-CHEMICAL PROPERTIES

5.1 Micelle formation

For amphoteric surfactants, the critical micelle concentrations (CMCs) are often stated. However, most studies concerning the CMC have centred around betaines and the information extrapolated or applied to the other types of amphoteric surfactants.

Conductivity methods are often used to determine CMCs for surfactants. However, the conductivity of

betaines is negligible when compared to that of strong electrolytes (40), and therefore the conductivity method is generally not suitable for determining the critical micelle concentration. However, many other methods, for instance those based on surface tension, refractive index or dye solubilization, can be used.

One of the most detailed studies on the critical micelle concentrations of betaines is that of Beckett and Woodward⁴¹ who determined the CMCs of betaines with octyl to hexadecyl alkyl chains by surface tension, dye solubilization, iodine and refractive index methods. Due to the peculiar character of betaines, the conductivity method and octanol solubilization method were both unsuitable.

It was also determined that the critical micelle concentration, especially for betaines, but also for surfactants in general, decrease logarithmically as the number of carbon atoms in the alkyl chains increases. This was determined by Klevens (42) and is referred to as the Klevens equation, as follows:

$$\log(\text{cmc}) = A - (B \times N) \quad (15.1)$$

where N is the number of carbon atoms in the hydrophobic chain, A and B are empirical constants, and the cmc parameter is given in mol/l. The values of A and B can be obtained by using Beckett and Woodward's CMC results. For most surfactants, B is close to $\log 2$, while betaines have values which are closer to $\log 3$.

This would indicate that changes in the alkyl chain length have a greater effect on the CMC in betaines than in anionic or cationic surfactants. This was explained by the nature of the surface of micelles, probably formed by a network of alternate positive and negative charges that correspond to the positive charge at the nitrogen atom and the negative charge of the carboxylate. Hence, molecules of these substances attract each other on the surface of the micelle, while in anionic and cationic surfactants the polar groups repel one another. Consequently, changes in the alkyl chain length have a greater effect on molecular aggregation and lower the critical micelle concentration (41).

Since alkyl betaines may exist as either zwitterionic or cationic surfactants, depending on the pH, their critical micelle concentration shows a complicated behaviour. The CMCs of alkyl betaines are significantly higher in dilute acid solutions than in dilute alkaline solutions because at low pH the surfactant is at least partly in the cationic form (43–45). As the concentration of HCl increases, the amount of the cationic form in solution increases and the resulting CMC of the zwitterionic/cationic surfactant mixture increases because the value of the cationic form is higher than that of the

zwitterionic. However, increasing the concentration of HCl also increases the ionic strength of the solution, which tends to lower the CMC.

Chevalier *et al.* (44) studied the critical micelle concentrations of alkyl betaines for different members of the series as a function of the number of methylene groups between the quaternary nitrogens and the carboxylate groups. The CMC increases as the number of methylene groups increases from one to three, reaching a maximum value and then decreasing for higher numbers of methylene groups. This phenomenon was similarly observed for phosphinate betaines. This was explained as a competition between the increasing total hydrophobicity of the molecule as the number of methylene groups increases, which tends to lower the CMC and the increasing strength of the repulsive dipole-dipole interactions between the head-groups at the interface which occurs also as the number of methylene groups increases, tending to raise the CMC values. This increase in the strength of repulsion is due to an increase in the cationic character, because the methylene groups reduce the electronegative effect of the cationic centre on the carboxyl group, thus leading to reduced acidity and increased protonation.

Tables 15.4 and 15.5 present the CMC values determined for alkyldimethylammonioacetates and dodecyldimethylammonioalkylcarboxylates, respectively. For comparison, the following CMCs were recently derived for cocamidopropyl betaine:

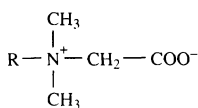
caprylic/capramidopropyl betaine, 5.8 mM

cocamidopropyl betaine, 0.041 mM

Among the many unique properties of zwitterionic surfactants, the strong interactions of their molecules

Table 15.4. Critical Micelle Concentrations (CMCs) of alkyldimethylammonio acetates

Alkyl chain	CMC (mM)	Reference
Decyl	23.3	46
Undecyl	7.2	46
Dodecyl	1.9	47
Tridecyl	0.795	48
Tetradecyl	0.11	47
Pentadecyl	0.056	48
Hexadecyl	0.02	43

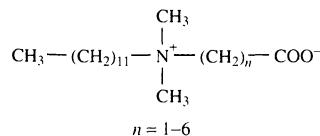


R = Alkyl chain

Table 15.5. Critical micelle concentrations (CMCs) of dodecyldimethylammonioalkyl carboxylates (43)

n	CMC ^a (mM)
1	2.4
2	5.3
3	6.0
4	6.5
5	5.1
6	3.8

^aIn 1.0 mM NaOH.



with other ionic surfactants, particularly anionics, is of prime interest because it drives many of their practical applications. It is not possible to cover in full detail the vast number of papers dealing with this subject. However, several studies on synergism in mixtures containing zwitterionic surfactants have been published by Rosen and co-workers. (49–51).

Jansson and co-workers (52–55) studied the interactions of amphoteric surfactants with other surfactants. They found that mixed micelles containing anionic surfactants are larger than those containing the corresponding cationic surfactants.

The thermodynamics of mixed micelle formation has been recently reported (56).

5.2 Surface tension

Surface tension measurements of betaines, especially of alkyldimethyl betaines, have been reported repeatedly. For alkyl betaines with increasing chain lengths of the alkyl group, the results for surface tensions above the CMC, given in Table 15.6, have been reported (41).

Measurements of commercial alkylamidopropyl betaines, in contrast to the values reported for the pure alkyl betaines, give significantly lower surface tensions at concentrations above the CMC (Table 15.7) (57).

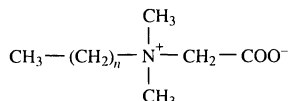
These results show that with commercial alkylamidopropyl betaines, characterized by fatty acid compositions (instead of one single fatty acid) and in cases containing by-products derived from the synthesis, very low surface tensions are achievable. This effect is certainly related to the known effects in surfactant mixtures, which usually show lower surface tensions than the pure products.

Table 15.6. Surface tension of alkyl betaines (41)

Number of methylene groups, <i>n</i>	Surface tension, γ^a (mN/m)	Concentration ^b (%(wt/vol))
7	34	3.5
9	33	0.5
10	37	0.2
11	36	0.05
13	35	0.005
15	33	0.001

^aDe Nuy ring method, $T = 23 \pm 1^\circ\text{C}$.

^bApproximate values.



6 ECOLOGICAL AND TOXICOLOGICAL PROPERTIES OF ZWITTERIONIC AND AMPHOTERIC SURFACTANTS

6.1 Ecological evaluation

A cocobetaine, a cocamidopropyl betaine, and also a cocoamphomonoacetate, were tested with regard to their environmental compatibility (54). These compounds proved to be readily biodegradable in the Organization for Economic Co-operation and Development (OECD) tests for ultimate biodegradation. As was

demonstrated in the metabolite test, their degradation to CO_2 , H_2O , inorganic salts and biomass occurs quantitatively and no recalcitrant metabolites were formed. It was confirmed that when sewerage treatment simulation tests were run, these classes of surfactants were easily eliminated from waste water. The aquatic toxicity (towards algae, daphnia and fish) of these substances is in the same order of magnitude as for other surface-active substances ranging from toxic to moderately toxic ($\text{EC}_{50}/\text{LC}_{50} > 1-100 \text{ mg/l}$). For waste water bacteria, these substances are slightly toxic.

6.2 Toxicological profile

Some typical properties of these classes of surfactants are presented in Table 15.8. All of these surfactants have been extensively tested by the manufacturers and by researchers, and their safety profiles are well accepted.

The zwitterionic and amphoteric surfactants have been comprehensively reviewed and reported on in detail (58, 59).

6.3 Evaluation of toxicological results

While the ecological data indicate a good tolerance to the environment, the toxicological findings seem to reveal deficits with regard to the skin and eye irritation

Table 15.7. Surface tension of various alkylamidopropyl betaines (57)

Betaine system	Surface tension, γ^a (mN/m)	Concentration ^b (% (wt/vol))
Cocamidopropyl betaine	30	0.01
Cocamidopropyl betaine + cocamidopropyldimethyl amine	27	0.01
Capryl-/caprylylamidopropyl betaine	24	0.2

^aDe Nuy ring method, $T = 25 \pm 1^\circ\text{C}$.

^bApproximate values.

Table 15.8. Toxicological properties of amphoteric surfactants

Surfactant	Acute toxicity	Irritation to skin ^a (rabbit)	Irritation to eye ^b (rabbit)	Sensitization (Magnusson-Kligman test)	Gene mutation (Ames test)	NOAEL ^c
Cocobetaine	None	Yes	Yes	None	None	> 250 mg/kg
Cocamidopropyl betaine	None	None	Yes	None	None	1000 mg/kg
Cocoamphomonoacetate	None	Moderately	Slightly	None	None	> 1000 mg/kg

^aConcentration of 25%.

^bConcentration of 20%.

^cOral toxicity: NOAEL, "No observed adverse effect level," is the maximum dose tolerated in cumulative toxicity studies.

values. These disadvantages, however, arise only at higher concentrations.

More important for a toxicological evaluation is the fact that amphoteric surfactants are usually combined with anionic surfactants, i.e. alkyl or alkyl ether sulfates. Such blends are assessed to be very mild to skin and mucous membranes (60, 61).

These synergistic effects play an important role with regard to the use of betaines and amphoteric surfactants in dermatologically compatible formulations. Results from the Draizetest (determination of the irritation capacity in the rabbit eye) clearly show the synergistic effect of sodium lauryl ether sulfate/betaine with respect to mucous membrane compatibility. The initial level of the dermatological irritation potential of the disodium cocoamphodiacetate is lower than that of the betaine. Depending on the ratio of alkyl ether sulfate/amphoteric surfactant or alkyl ether sulfate/betaine combinations, a minimum in the irritation potential can be achieved.

The observed synergism can be understood in the light of the work of Zeidler and Reese (62) who studied the swelling of the pig epidermis caused by surfactants when compared to the swelling effect of pure water. In contrast to anionic surfactants, betaines and amphoteric surfactants cause negative swelling of the skin relative to water. This may reduce penetration and irritation effects of the anionics.

Lang and Spengler (63) described a correlation between CMC values and irritancy values, i.e. the lower the CMC, then the lower the irritation of the surfactant system. These authors showed synergistic effects in systems of alkyl sulfate/cocamidopropyl betaine and alkyl ether sulfate/cocamidopropyl betaine. Similarly, modification of micelle composition was taken as an explanation of such synergies (64).

7 APPLICATION PROPERTIES

Zwitterionic and amphoteric surfactants are typically used as secondary surfactants. The existence of secondary surfactants obviously implies that there are primary surfactants. The latter are mostly the anionic alkyl sulfates and alkylether sulfates, but also include different types of sulfonates. These very often are the main components of a formulation and provide the basic properties of detergency, wetting and foaming. In modern formulations, however, their base properties are not sufficient and need to be improved by secondary surfactants. Improvement is especially needed with respect to mildness, but foaming and viscosity are also enhanced by the use of secondary surfactants. This is where zwitterionic

and amphoteric surfactants are used, especially cocamidopropyl betaine and the cocoamphoacetates.

Zwitterionic and amphoteric surfactants are unique in their excellent responses for the following:

- Irritation and toxicity
- Detoxification
- Biodegradability
- Chemical stability
- Foaming Power
- Viscosity Buildup
- Detergency
- Wetting
- Lime soap dispersion
- Emulsification
- Conditioning

These properties have been widely described and in more recent times scientifically reviewed (65, 66).

7.1 Alkali tolerance and chemical stability

Stability performance at acidic and alkaline pH extremes are a signature characteristic of amphoteric surfactants (67). One manufacturer determined the alkali tolerance by titrating a 1% active surfactant solution with increasing concentrations of sodium hydroxide until the solution changed from clear to hazy. The maximum level of sodium hydroxide was then measured as an "end point". According to this simple approach, alkylamphoacetates, alkylamphodipropionates, alkyl betaine, alkylamineoxide and alkylamidopropyl betaine all displayed good alkali tolerance. The NaOH end points were 40,37,21,17 and 10%, respectively, (68).

Commercial amphoteric surfactants such as dihydroxyethylalkyl glycinate (Figure 15.27) are considered excellent thickeners for strongly alkaline oven cleaners, as well as for acid toilet bowl cleaners.

Most betaine-derived surfactants are chemically stable in acid and alkaline media due to the properties of the quaternary nitrogen. Instability arises from other functional groups, as in amidobetaines, which although they are fairly stable, can suffer hydrolysis of the amido group (69). Apart from compounds having amido or

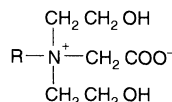


Figure 15.27. General structure of a dihydroxyethylalkyl glycinate

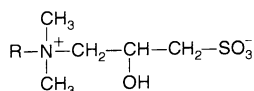


Figure 15.28. General structure of a hydroxysulfobetaine

ester groups, only betaine derivatives containing S–O–C and P–O–C bonds, such as sulfito, sulfato, phosphito and phosphato betaines, show a comparatively lower stability to hydrolysis. From this point of view, sulfobetaines, phosphinate and phosphonate betaines are superior.

Hydroxysulfobetaines (Figure 15.28) are soluble and stable in concentrated alkaline solutions. The results recorded over time demonstrated that all samples were stable (70, 71).

Obviously, betaine-type cleavable surfactants of the acetal type hydrolyse in acid media (72). The dodecyl derivative decomposes completely after 2 hours 40 minutes in a 2% HCl solution, after 24 hours at pH 1, and only after more than one week at pH 3.

7.2 Foaming and viscosity

Zwitterionic and amphoteric surfactants contribute to the overall generation of foam, foam stability and foam quantity. Regardless of the type of amphoteric, a generalization can be made concerning the hydrophobic “R” group: The total number of carbon atoms in the “R” group has a profound effect upon performance.

The typical chain length distribution from the coconut oil or coconut fatty acids gives the best overall performance response. The properties of different carbon chain length compositions are presented in Table 15.9.

Amphoteric surfactants have especially good foaming profiles in soft water. Betaines, in particular the amidopropyl types, are tolerant of hard water, followed closely by the tolerance of sulfobetaines and

Table 15.9. Contribution of carbon chain length contribution to function properties

Number of carbon atoms	Functional properties
8–10	Good foam stability, no viscosity improvement
12–16	Good foam stability, good viscosity building, some emollient properties, some conditioning
≥18	Reduced foam stability, good viscosity building

propionates. The amphotoacetates show some limited tolerance for hard water. Tests have been conducted for the effects of hard water or lime soap dispersability using the methods of Borghetty and Bergman (73, 74). The “APAC” amphoteric are also very efficient for lime soap dispersing. Table 15.10 presents the ranking of amphoteric for lime soap dispersability.

Secondary surfactants also play a role in the development of viscosity in surfactant systems or blends. Amidobetaines are efficient components in foam bath compositions because they are good thickeners and enhance foam properties. Beh and James (75) studied the foam stabilities of some bubble bath formulations and, after examining several surfactants, found that amidobetaines are the best stabilizing agents, with alkyl betaines being the next efficient. Domingo and Druguet (76) developed mathematical equations for the response surfaces of apparent viscosity, rheological behaviour and foaming power for a ternary mixture of surfactants. High apparent viscosities can be obtained either with alkanolamides or with the amidobetaines but the apparent density of foam is greatly increased as the amidobetaine content increases, and smaller bubbles are produced.

It is generally known that aqueous solutions of true amphoteric can be difficult to thicken. Viscosity control is best achieved by using either the amphoteric salts or by combining with anionic surfactants. The traditional thickening aids, the alkanolamides, are not particularly effective with amphoteric. Nonionic surfactants offer the best thickening support for amphoteric surfactants, especially those based on fatty acids or alcohols ethoxylated with 50–200 moles of ethylene oxide, but like all nonionics, they could exert a foam depressing effect if used at a higher level. When amphoteric surfactants are combined with anionic surfactants, the traditional alkanolamides are effective. The final pH adjustment can also make a difference to the viscosity of the product.

Amidopropyl betaines, when used as secondary surfactants in anionic surfactant systems, respond quickly with viscosity when salts or alkanolamides are added.

Table 15.10. Relative lime soap dispersability of amphoteric

Amphoteric type	Lime soap dispersability
Alkyl polyamine carboxylates	Excellent ↑ ↓ Fair
Amidopropyl Betaines	
Sulfoamidobetaines	
Sulfobetaines	
Sulfobetaines	
Alkyl betaines	
Propionates	
Amphotoacetates	Fair

Mixtures of cocamidopropyl betaine and sodium lauryl sulfate in molar ratios of 8:1 to 1:8 were investigated for their viscosity response at a total surfactant concentration of 0.83 mol/l and a NaCl content of ca. 0.5% (77). At the molar ratios of 8:1, 6:1, 4:1, and 1:8, a Newtonian flow behaviour was found, while in other regions the system shows pseudoplastic or plastic behaviour.

The viscosity responses of cocamidopropyl betaine and cocoamphomonoacetate cocoamphodiaceate in mixtures with sodium lauryl ether sulfate are very similar to each other and exhibit a maximum value around a 1:1 ratio (78).

We thus note that for most cleansing applications the zwitterionic and amphoteric surfactants are used as formulation modifiers, thus contributing their aforementioned properties to the final application formulation.

8 APPLICATIONS

Even though many applications for zwitterionic and amphoteric surfactants are well known and documented, new applications and refinements in the art continue to

be developed. A search of United States patents between 1991 and 1997 reveals a wide range of current consumer, pharmaceutical and industrial uses for zwitterionic and amphoteric surfactants. A review of over 500 patents yielded over 200 industry-specific-application patent references. Of these, approximately 31% referred to household, industrial and institutional markets, 22% pertained to personal care applications, 13% applied to oral care or pharmaceutical products and 33% could be categorized as industrial applications. Examples include metal working, mining, photographic processes, paper, textile treatments, etc. This list is not meant to be all encompassing. Undoubtedly, many additional references could probably be found if specific search criteria were assigned. It does, nevertheless, provide a good survey of the contemporary art. The results of this survey are presented in Table 15.11.

8.1 Hard surface cleaners

Hard surface cleaners, household, industrial and institutional detergents, and laundry detergents, continue to

Table 15.11. Result obtained from a survey of the USA patent literature, over the period 1991–1997, for applications of zwitterionic and amphoteric surfactants

Application	Zwitterionics	Amphoterics
<i>Consumer or Industrial and Institutional</i>		
Detergents, undifferentiated liquids	15	4
Hard surface cleaners	12	14
Light-duty liquids, including dishwashing	3	2
Fabric and laundry cleaners	5	5
Shampoos	3	7
Skin cleansers and gels	6	6
Hair treatment products and dyes	2	18
Cosmetic and skin products	2	9
Oral care and food	4	9
<i>Pharmaceutical and Clinical</i>	6	10
<i>Industrial and Agricultural</i>		
Agricultural products	1	0
Metallurgy	4	6
Photography	3	6
Inks	3	0
Magnetic recording devices	2	1
Corrosion inhibitors	1	1
Mining and well treatment	0	6
Paper	0	6
Flame retardants	0	3
Electronics	0	5
Latex and rubber	0	8
Leather and textile process	0	4
Cellulose processing	0	0
Waste treatment	0	3
Biocides	1	2
Fibreglass	0	1

account for a significant proportion of zwitterionic and amphoteric surfactant use.

For example, detergent compositions containing a alkylamidopropyl betaine in combination with at least one cosurfactant can offer excellent removal of grease soils and also provide superior filming and anti-streaking properties in hard surface cleaners (79). Similarly, short-chain amphocarboxylates, when incorporated into formulations that do not contain large amounts of builders, are also said to offer improved filming or anti-streaking properties and good cleaning in glass cleaner formulations (80).

A related application is the car wash market. Winkler describes the use of a cocodimethyl betaine as a mild foaming agent for car wash compounds dispensed in commercial equipment (81).

Performance criteria for light-duty liquid dish wash detergents include mildness, good foam, good detergency, and grease removal ability over a range of water hardness conditions. Erille, in a patent assigned to the Colgate-Palmolive has Company, has selected zwitterionic betaines and amine oxides as the cosurfactants of choice to ensure mildness in other dish detergent systems (82).

Other hard surface applications rely on amphoteric surfactants to enhance viscosity in highly acidic or alkaline formulations. Some liquid toilet bowl cleaners, for instance, are formulated within a pH range of 2–4 (83). Amphoteric surfactants have been demonstrated to provide good gellation and stability in compounds containing peracetic acid (84).

Likewise, thickened aqueous hypochlorite compositions rely on these surfactants to accomplish the same purpose at pH levels of 11 or higher (85). The desired viscosity for such formulations may range from 150 to 3000 cPa s. This would permit easy dispensing but provide good coating action necessary for cleaning toilet bowls, bathroom tiles and shower walls (86). Effective viscosity control is also necessary to suspend abrasives found in scouring cleansers. Finally, the choice of surfactant is an important factor in the preparation of “low solvent” hard surface cleaners. Such products are said to have more desirable fragrance profiles (87, 88).

8.2 Laundry products

Although not widely used in this area, amphoteric surfactants continue to be evaluated by mass market producers. Ilardi, in a patent assigned to the Lever Brothers Company, describes new fabric conditioning compounds, which provide effective softening and static

control, are derived from glycerol and betaine (89). Cao, in a patent assigned to the Colgate-Palmolive Company, reports that amphoteric surfactants such as sodium carboxymethyl tallow propylamine contribute to fabric cleansing and softening when incorporated into aqueous systems with polyethoxylated fatty alcohols, inorganic builders and bentonite (90). Colgate, as well as Procter & Gamble, have been developing systems using amphoteric surfactants in lipase-containing laundry detergents (91, 92).

8.3 Sanitizers and disinfectants

Owing to their compatibility with cationic biocides, amphoteric and zwitterionic surfactants continue to be used widely in the development and formulation of disinfectants and sanitizers for personal care, household, industrial and institutional markets. For instance, substituted imidazoline amphoteric surfactants, in combination with didecyldimethylammonium chloride, have been found to display unexpected synergistic irritation reduction compared to formulations with alkyldimethylbenzylammonium chlorides (93). Imidazoline derivatives and betaines are known to impart moderate cleansing without causing skin roughness, stickiness or irritating reactions with cationic disinfectants (94). Amphoteric surfactants are also suitable for use in antimicrobial medications requiring subcutaneous cutaneous or mucosal membrane administration (95).

8.4 Personal care cleansers and shampoos

Not surprisingly, there are many references citing the use of betaines and imidazoline-derived amphoteric surfactants in foaming systems. Examples include shampoos, hair tint treatments, permanent waves formulations, anti-dandruff preparations, hair revitalizing tonics, shower gels, facial cleansers, foam baths, etc. Performance claims include mildness, improved lathering, cleansing/oil removal, suspending, viscosity stabilizing and functional enhancement of actives such as hair dyes (96–102).

8.5 Cosmetics

Broad pH surfactant compatibility characteristics have contributed to greater usage of amphoteric surfactants in a variety of “leave-on” cosmetic and skin treatment

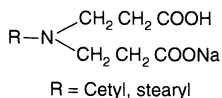


Figure 15.29. Structure of an amphoteric surfactant used to stabilize emulsions (from ref. (110))

products. These include *alpha*-hydroxy acid treatment creams, skin desquamation aids, cleansing gels and massage creams. Excellent skin feel and moisturization, coupled with long term stability of the active components are some requirements which must be met when developing such “new generation” beauty aids (103–108).

Amphoterics can also be used to stabilize emulsions by immobilizing the oil droplets in a network to retard or prevent coalescences (109). Chun (110), in a conference paper presented in 1978, proposed using an amphoteric surfactant (see Figure 15.29) in combination with a fatty amphophile, such as cetyl alcohol, to form a gel network (similar to that of liquid crystal formation) to further improve emulsion stability. A number of commercial skin preparations have used this technique to stabilize treatment lotions.

8.6 Oral care products

As the line between therapeutic cosmetics (cosmeceuticals) and drugs becomes more vague, the use of amphoteric surfactants in the development of products which are evaluated through clinical trials is likely to increase. This is especially true concerning the use of amphoteric surfactants in the oral care industry.

Toothpastes contain foaming agents which impart a pleasant feel to the mouth during use. This foam also helps create a suspension of abrasive ingredients, thereby improving cleaning efficacy. Sodium lauryl sulfate is typically used for this purpose (111). The use of betaine as a surfactant alternative to sodium lauryl sulfate is not yet widespread in the North American market. However, commercial products are now available internationally. Clinical studies describing the use of betaine in oral care applications have been published (112), and major producers, such as Procter & Gamble and Colgate have been awarded patents in this area.

Herlofson and Barkpoll, in an experimental toothpaste study involving twenty eight subjects, determined that sodium lauryl sulfate significantly increased the incidence of desquamation of oral mucosa when compared with cocamidopropyl betaine. Less toxic detergents, such as cocamidopropyl betaine, were therefore found to be desirable in oral care products (113).

Lukacovic, in a patent assigned to Procter and Gamble, describes the preparation of a toothpaste containing betaine surfactants such as cocamidopropyl betaine or laurylamidopropyl betaine. This composition is said to retard or stop the proliferation of plaque, which is detrimental to oral health (114).

Polefka, in a patent assigned to Colgate, utilized cocamidopropyl betaine as a cationic-compatible surfactant in the preparation of another anti-plaque composition utilizing bisbiguanide as an antimicrobial active (115). Similar plaque control claims are made by Michaels, who describes a composition based on a blend of C₁₀–C₁₈ alkyl *N*-sulfobetaine and C₁₀–C₁₈ alkyl *N,N*-dihydroxyethylamine oxide (116).

8.7 Pharmaceutical industry

The most recent patent references to amphoteric surfactants for the pharmaceutical industry involve the development of new diagnostic test methods. These include immunochemical assays and improved genetic diagnostic methods. In these applications, the selective use of amphoteric surfactants has been shown to enhance the sensitivity of detection (117–119).

8.8 Other industrial applications

The use of amphoteric surfactants in heavy industry is a broad topic encompassing such varied applications as oil well and mining fluids, fire fighting foams, printing inks, wastewater effluent recovery aids, leather softeners, electroplating bath additives and corrosion inhibitors (120–129). While these topics are beyond the scope of this present chapter, they are worth mentioning since developments involving amphoteric surfactants here will ultimately have an impact on their consumption and availability in consumer markets and elsewhere.

9 REFERENCES

1. Uphues, G., *Fett/Lipid*, **100**(11), 490–497 (1998), CA 130:26471.
2. Lomax, E. G. (Ed.), *Amphoteric Surfactants* 2nd Edn, *Surfactant, Science Series* 59, Marcel Dekker, New York (1996).
3. Bilbo, R. E. and Swenson, R. A., *Soap/Cosmetics/Chemical Specialties*, April 46–50 and 114–116 (1990).

4. Mannheimer, H. S., *US Patents 2 528 378* (1950), CA 45:2285; *US Patent 2 528 379* (1950), CA 45:2286; *US Patent 2 773 068* (1956), CA 51:39472.
5. Mannheimer, H. S., *Soap Chem. Spec.*, **34**(9), 56–58 and 206 (1958), CA 52:108540.
6. Rieger, M., *Cosmetics & Toiletries*, **103**, 59–72 (1988), CA 108:192569.
7. Laughlin, R. G., *Langmuir*, **7**, 842–847 (1991), CA 114:235841.
8. Morris, P., *GB Patent 1 185 111*, to The Procter & Gamble Company (1968), CA 73:5267.
9. Bade, V., *European Patent 20 907* to Th. Goldschmidt AG (1980), CA 94:174298.
10. de Groot, A. C., van der Walle, H. B. and Weyland, J. W., *Contact Dermatitis*, **33**, 419–422 (1995).
11. Angelini, G., Rigano, L., Foti, F., Grandolfo, M. and Grüning, B., *Contact Dermatitis*, **39**, 152–153 (1998), CA 130:91369.
12. Seitz, H. and Vybirol, R., *German Patent DE 4 232 157*, to Hoechst AG (31 March 1994), CA 121:60250.
13. Uphues, G., Ploog, U., Bischof, K., Kenar, K. and Sladek, P., *German Patent DE 3 939 264*, to Henkel KGaA (29 May 1991), CA 115:94849.
14. Foitzik, W., Grüning, B., Käseborn, D. and Weitemeyer, C., *German Patent DE 4 205 880*, to Th. Goldschmidt AG (2 Sept. 1993), CA 119:249585.
15. Hamann, I., Köhle, H.-J. and Wehner, W., *US Patent 5 464 565*, to Witco Surfactants GmbH (7 Nov. 1995), CA 123:147329.
16. Hamann, I., Köhle, H.-J. and Wehner, W., *European Patent EP 0 739 878*, to Witco Surfactants GmbH (30 Oct. 1996), CA 126:31649.
17. Armada, M., Rho, M., Behler, A., Bigorra, L., Herrmann, H., Pi Subirana, R., Seipel, W., Tesmann, H., Uphues, G. and Schmid, K. H., *German Patent DE 19 505 196*, to Henkel KGaA (2 May 1996), CA 125:61508.
18. Begoihn, U., Foitzik, W., Grüning, B., Käseborn, D. and Weitemeyer C., *German Patent DE 4 207 386*, to Th. Goldschmidt AG (13 Feb. 1997), CA 120:57225.
19. Perine, J. W., Smith K. R., Sauer J. D., and Borland J. E., *Patent WO 9 213 825*, to Ethyl Corporation (20 Aug. 1992), CA 117:69463.
20. Sakaguchi, N. and Obara, S., *Japanese Patent JP 63 012 333*, to Matsmoto Yushi-Seiyaku Company (19 Jan. 1988), CA 109:75756.
21. Grüning, B. and Weitemeyer, C., *US Patent 5 792 737*, to Th. Goldschmidt AG (11 Aug. 1998), CA 129:163136.
22. McGinley, K. J., Leydon, J. J., Marples, R. R., Path, M. R. C. and Kligman, A. M., *J. Invest. Dermatol.*, **64**, 401–405 (1975).
23. Grüning, B., *German Patent DE 4 227 391*, to Th. Goldschmidt AG (30 Sept. 1993), CA 120:110011.
24. Leonard, E. C. (Ed.), *The Dimer Acids: The Chemical and Physical Properties, Reactions and Applications*, Humko Sheffield Chemical, Memphis, TN (1975).
25. Fischer, P., Rehage, H. and Grüning B., *Tenside Surf. Det.*, **31**(2), 99–108 (1994), CA 120:301636.
26. *US Patent 3 280 179*, to Textilana Corporation (1966), CA 66:30267.
27. Chevalier, Y., Germanaud, L., Brunel, S., Storet, Y., Berthelon, B., Le Perchec, P. and Gallot, B., *Commun. Journ. Com. Esp. Deterg.*, **18**, 231–245 (1987), CA 110:179897.
28. Giersberg, J. and Kollmeier, H.-J., *German Patent DE 3 826 805*, to Th. Goldschmidt AG (1989), CA 112:235611.
29. O'Lenick, Jr, A. J. and Mayhew R. L., *US Patent 4 283 542*, to Mona Industries (1981), CA 94:67631.
30. Schwarz, G., Leenders P. and Ploog, U., *Fette Seifen Anstrichmittel*, **81**(4), 154–158 (1979).
31. Rieger, M., *Cosmetics & Toiletries*, **99**, 61–67 (1984), CA 100:212092.
32. Arndt, G. J., *British Patent 1 078 101* (1967).
33. Hein, H., Jaroschek H. J. and Melloh W., *Cosmetics & Toiletries*, **95**, 37–42 (1980), CA 94:67614.
34. Yasuda, Y., Tschuchihashi, K., and Nishimura, T., *German Patent DE 3 144 341*, to Kao Soap Company (1980); *Chem. Abstr.*, 97:110006.
35. Rosenblatt, W., Amino acid amphoteric, in *Amphoteric Surfactants*, 2nd Edn, Lomax E. G. (Ed.), Surfactant Science Series 59, Marcel Dekker, New York (1996), pp. 49–73.
36. Schmitz, A., *Fette Seifen Anstrichmittel*, **55**(1), 10–16 (1953).
37. Lomax, E. G., Alkyl Poly Amino Acid Amphoteric, in *Amphoteric Surfactants*, 2nd Edn, Lomax E. G. (Ed.), Surfactant Science Series 59, Marcel Dekker, New York (1996), pp. 237–251.
38. Leidreiter, H. I., Grüning, B. and Käseborn, D., Amphoteric Surfactants—Processing, Product Composition and Properties, *SÖFW-Journal*, **126**, 2–10 (2000).
39. Gerhards, R., Jussofie, I., Käseborn D., Keune, S. and Schulz, R., *Tenside Surf. Det.*, **33**, 8–14 (1996), CA 124:264041.
40. Barnhurst, J. D., *J. Org. Chem.*, **26**, 4520–4525 (1961).
41. Beckett, A. H. and Woodward, R. J., *J. Pharm. Pharmacol.*, **15**, 422–428 (1963).
42. Klevens, H. B., *J. Am. Oil Chem. Soc.*, **30**, 74–80 (1953).
43. Weers, J. G., Rathman, J. F., Axe, F. U., Crichlow, C. A., Foland, L. D., Scheuing, D. R., Wiersema, R. J. and Zielske, A. G., *Langmuir*, **7**, 854–857 (1991).
44. Chevalier, Y., Storet, Y., Pourchet, S. and Le Perchec, P., *Langmuir*, **7**, 848 (1991).
45. Chevalier, Y., Germanaud, L. and Le Perchec, P., *Colloid Polym. Sci.*, **266**, 441–443 (1988).
46. Swarbrick, J. and Daruwala, J., *J. Phys. Chem.*, **73**, 2627–2631 (1969).
47. Amin-Alami, A., Kamenka, N. and Partyka, S., *Thermochim. Acta*, **122**, 171–178 (1987).
48. Swarbrick, J. and Daruwala, J., *J. Phys. Chem.*, **74**, 1293–1299 (1970).
49. Rosen, M. J. and Zhu, B. Y., *J. Colloid Interface Sci.*, **99**, 427–428 (1984).
50. Rosen, M. J., *Langmuir*, **7**, 885–888 (1991).

51. Rosen, M. J., Zhu, Z. H. and Gao, T., *J. Colloid Interface Sci.*, **157**, 254–262. (1993).
52. Jansson, M. and Rymden, R., *J. Colloid Interface Sci.*, **119**, 185–191 (1987).
53. Jansson, M., Puyong, L. and Stilbs, P., *J. Phys. Chem.*, **91**, 5279–5285 (1987).
54. Jansson, M., Linse, P. and Rymden, R., *J. Phys. Chem.*, **92**, 6689–6691 (1988).
55. Puyong, L., Jansson, M. and Stilbs, P., *J. Colloid Interface Sci.*, **142**, 593–598 (1991).
56. Hall, D. G., Meares, P., Davidson C., Wyn-Jones, E. and Taylor, J., Thermodynamics of Mixed Micelles, ACS Symposium Series, Vol. 50, American Chemical Society, Washington, DC, 1992, pp. 128–135.
57. Personal Communication from the Technical Research Laboratories of Th. Goldschmidt AG, Kaseborn Germany, 1998.
58. Final Report on the Safety Assessment of Cocoamidopropyl Betaine, *J. Am. Coll. Toxicol.*, **10**, pp 33–52 (1991).
59. Final Report on the Safety Assessment of Cocoamphoacetate, Cocoamphopropionate, Cocoamphodiacetate, and Cocoamphodipropionate, *J. Am. Coll. Toxicol.*, **9**, pp. 121–124 (1990).
60. Klein, K. and Bator, O., *Drug Cosmetic Ind.*, 38–42 and 76–77 (December 1981).
61. Alexander, P., *Manufact. Chem.*, 54–57 (August 1985).
62. Zeidler, U. and Reese, G., *Arztliche Kosmetologie*, **13** 39–45 (1983).
63. Lang, G. and Spengler J., Surfactants in Cosmetic Formulations: Skin Irritancy and Physical Properties, in *Proceedings of the XIVth IFSCC Congress*, Barcelona, Spain, 1986, Vol. 1, pp. 25–37.
64. Lomax, E., *Cosmetics Toiletries*, Manufacturers and Suppliers Issue XI, 13–18 (1989).
65. Hein, H., Wehner, W. and Peschke, W., Properties of Secondary Surfactants, in *Proceedings of the 1984 World Surfactants Congress*, Vol. II, pp. 181–183.
66. Huttinger, R., Hladik, M., Marienfeld, G., and Schleger, H., Amphoteric Surfactants: Applications and Properties, in *Proceedings of the 1984 World Surfactants Congress*, Vol. IV, pp. 175–183.
67. Technical and Product Development Data, Miranol, Incorporated, Dayton, NJ, 1987.
68. Amphoterics, Betaines, Amine Oxides, Nonionics, McIntyre Corporation, Chicago, IL, 1988, pp. 6–8.
69. Micich, T. J., Linfield, W. M. and Weil, J. K., *J. Am. Oil Chem. Soc.*, **54**, 91–94 (1977).
70. *US Patent 4 913 841*, to Sherex Chemical Company Inc. (1990).
71. *US Patent 5 105 412*, to Sherex Chemical Company Inc. (1991).
72. Ono, D., Masuyama, A., Tanaka, T. and Okahara, M. *Tenside Surf. Det.*, **29**, 412–415 (1992).
73. Borghetty, H. C. and Bergman C. A., *J. Am. Chem. Soc.*, **37**, 88–95 (1950).
74. Palicka, J., in *Proceedings of the 3rd CESIO International Surfactants Congress and Exhibition*, London, 1992, Section D, pp. 300–309.
75. Beh, H. H. and James, K. C., *Cosmetics Toiletries*, **12**(11), 21–24 (1977).
76. Domingo, F. J. and Druguet, R. M., *Tenside Surf. Det.*, **18** (1981).
77. Dominguez, J. G., Balaguer, F., Parra, J. L. and Palejero, C. M., *Goldschmidt Informiert*, No. **55** (1981).
78. Leidreiter, H. I., Grüning, B., Käseborn D., *SÖFW-J.*, **126** (2000).
79. *US Patent 5 540 865*, to The Procter & Gamble Company (1996).
80. *US Patent 5 536 451*, to The Procter & Gamble Company (1996).
81. Winkler, III, J.A., *US Patent 5 534 199*, to (1996).
82. *US Patent 5 629 279*, to The Colgate-Palmolive Company (1997).
83. *US Patent 5 612 308*, to The Procter & Gamble Company (1997).
84. *US Patent 5 078 896*, to Akzo, AV (1992).
85. *US Patent 5 549 842*, to Rickett & Colman, Inc. (1996).
86. *US Patent 5 348 682*, to The Procter & Gamble Company (1994).
87. *US Patent 5 462 689*, to The Clorox Company (1995).
88. *US Patent 5 470 499*, to The Clorox Company (1995).
89. *US Patent 5 663 138*, to Lever Brothers Company (Division of Conopco, Inc.) (1997).
90. *US Patent 5 500 151*, to The Colgate-Palmolive Company (1996).
91. *US Patent 5 496 490*, to The Colgate-Palmolive Company (1996).
92. *US Patent 5 614 484*, to The Procter & Gamble Company (1997).
93. *US Patent 5 547 990*, to Lonza, Inc. (1996).
94. *US Patent 5 651 974*, to Shiseido Company, Ltd. (1997).
95. *US Patent 5 661 170*, to Woodward Laboratories, Inc. (1997).
96. *US Patent 5 156 836*, to Shiseido Company Ltd. (1992).
97. *US Patent 5 422 031*, to Kao Corporation (1995).
98. *US Patent 5 624 666*, to The Procter & Gamble Company (1997).
99. *US Patent 5 632 978*, to The Procter & Gamble Company (1997).
100. *US Patent 5 641 479*, to Richardson-Vicks, Inc. (1997).
101. *US Patent 5 151 210*, to The Procter & Gamble Company (1992).
102. *US Patent 5 609 168*, to Wella Aktiengesellschaft (1997).
103. *US Patent 5 420 106*, to Bristol-Myers Squibb Company (1995).
104. *US Patent 5 648 395*, to Tristrata Technology, Inc. (1997).
105. *US Patent 5 607 980*, to The Procter & Gamble Company (1997).
106. *US Patent 5 474 776*, to Kao Corporation (1995).
107. *US Patent 5 643 672*, to L’Oreal (1997).
108. *US Patent 5 120 716*, to Shiseido Company Ltd (1992).

109. Klein, K., *Cosmetics Toiletries*, **99**(12) 121–126 (1984).
110. Chun, H., Amphoteric surfactants as stabilizers for cosmetic type emulsions, in *Proceedings of the 1978 Annual Scientific Seminar of the Society of Cosmetic Chemists*, 1, December 1978.
111. Knowlton, J. L. and Pearce, S. E. M., *Handbook of Cosmetic Science and Technology*, 1st Edn, Elsevier Advanced Technology, Kidlington, Oxford, UK, 1993, pp. 243–253.
112. Herlofson, B. and Barkpoll, P., *Acta Odontol. Scand.*, **54**, 150–153 (1996).
113. Herlofson, B. and Barkpoll, P., *Eur. J. Oral Sci.*, **104**, 21–26 (1996).
114. *US Patent 5 578 294*, to The Procter & Gamble Company, (1996).
115. *US Patent 5 180 577*, to The Colgate-Palmolive Company (1993).
116. *US Patent 5 403 579*, to Research Associates, Inc. (1995).
117. *US Patent 5 545 539*, to The Genzyme Corporation (1996).
118. *US Patent 5 618 733*, to The Toa Medical Electronics Co., Ltd. (1997).
119. *US Patent 5 360 717*, to Behringwerke Aktiengesellschaft (1994).
120. *US Patent 5 593 952*, to Baker Hughes Inc. (1997).
121. *US Patent 5 614 473*, to Rhone-Poulenc Inc. (1997).
122. *US Patent 5 591 701*, to Clearwater, Inc. (1997).
123. *US Patent 5 603 733*, to Allied Colloids Ltd. (1997).
124. Tyler, R., Tinsley Jr, R., Hagar M., Wright, W. and Ferrell, G., *US Patent 5 585 028* (1996).
125. *US Patent 5 531 817*, to The Hewlett-Packard Company (1996).
126. *US Patent 5 523 000*, to Ecolab Inc. (1996).
127. *US Patent 5 122 186*, to BASF Corporation (1992).
128. *US Patent 5 167 866*, to W. R. Grace & Company (1992).
129. *US Patent 5 096 595*, to W. R. Grace & Company (1992).

CHAPTER 16

Polymeric Surfactants

Tharwat F. Tadros

Wokingham, Berkshire, UK

1	Introduction	373	4	Stabilization of Dispersions containing Polymeric Surfactants	381
2	Solution Properties of Polymeric Surfactants	374	4.1	Mixing interaction	382
2.1	Thermodynamic treatment	374	4.2	Elastic (volume restriction or entropic) interaction	382
2.2	Solubility parameters and cohesive energy density	375	4.3	Main criteria for effective steric stabilization	383
2.3	Size and shape of polymers in solution	376	5	References	384
3	Adsorption and Conformation of Polymeric Surfactants at Interfaces	377			

1 INTRODUCTION

The simplest types of polymeric surfactants are homopolymers, with only one repeat unit in a single sequential arrangement. Examples of homopolymers are poly(ethylene oxide) (PEO), poly(vinyl pyrrolidone) (PVP) and poly(acrylic acid) (PAA). Homopolymers have little surface activity at the air/liquid (A/L) and liquid/liquid (L/L) interface. However, they may adsorb at the solid/liquid (S/L) interface. The reduction in configurational entropy of the chain on approaching the solid surface (an unfavourable process) may be compensated by a sufficient adsorption energy. For high-molecular-weight materials, a significant proportion of the segments may reside in direct contact with the surface (in “trains”, see below). Even if the adsorption energy per segment, χ^s , is small ($< 0.1 kT$, where k is the Boltzmann constant and T is the absolute temperature), the total adsorption energy per chain may be sufficient to overcome the entropy loss. For example, for a chain with 1000 segments and 10% in direct contact with the surface, the adsorption energy per chain is $10 kT$ which is sufficient for adsorption to take

place. In this case, hydrophobic interactions or van der Waals forces are sufficient for adsorption. However, with many surfaces stronger interaction between the polymer segments and the particle surface may take place, e.g. adsorption of PEO on silica, whereby the interaction occurs through hydrogen bonding between the EO units and the silanol groups on the surface.

Due to the relatively weak adsorption of homopolymers at the L/L interface, and in some cases at the S/L interface, homopolymers are seldom used as emulsifiers or dispersants. For this purpose, the molecule is modified to include some specific units that have strong adsorption to the surface. A good example is partially hydrolysed poly(vinyl acetate), which is commercially referred to as poly(vinyl alcohol) (PVA). The polymer contains 4–12% acetate groups (i.e. 96–88% hydrolysed) and these groups impart an amphipathic character to the chain. The polymer becomes surface-active at the L/L interface and hence it can be used as an emulsifier. In addition, on a hydrophobic surface such as polystyrene, the acetate groups become preferentially adsorbed on the surface of the particles, thus leaving the PVA units dangling in solution as “loops” and “tails”. The latter provide the required steric stabilization.

The most convenient polymeric surfactants are those of the block (A–B and A–B–A) and graft (BA_n) type, whereby the B chain is chosen to be insoluble in the medium and having a strong affinity to the surface (strong “anchoring”), whereas the A chain is chosen to be highly soluble in the medium and strongly solvated by it to provide effective steric stabilization (see below). Examples of such block copolymers are those based on PEO and poly(propylene oxide) (PPO), i.e. PEO–PPO–PEO, which are commercially available with various proportions of PEO and PPO (“Pluronic” by BASF and “Synperonic PE” by UNIQEMA). The PPO chain adsorbs at a hydrophobic surface, leaving the PEO chains dangling in solution. With oil-in-water (O/W) emulsions, the situation is different since the PPO chains are not soluble in most organic solvents. Since the PPO chain is also insoluble in water, adsorption occurs by a process referred to as rejection anchoring, whereby the molecule is rejected from both phases to the interface. In this respect, these block copolymers are not the most suitable emulsifiers. A better block is that based on PEO–polystyrene (PS), whereby the PS chains ensure strong adsorption on a hydrophobic surface. Triblocks of PEO–PS–PEO are very useful as dispersants or emulsifiers, although these are not commercially available.

Another useful class of dispersants/emulsifiers are the graft copolymers consisting of one B chain and several A chains grafted on to the backbone. These graft copolymers are sometimes referred to as “comb” polymers. Examples of suitable B chains are poly(methyl methacrylate) (PMMA) or polystyrene, with A chains of PEO or PVP. The copolymer is usually prepared by grafting a macromonomer such as methoxy poly(ethylene oxide) methacrylate with poly(methyl methacrylate).

Block and graft copolymers exhibit surface activity since one of the blocks is soluble in one of the phases (e.g. oil) and the other is soluble in the other phase (e.g. water). Since block and graft copolymers are amphiphilic, they aggregate in solution to form micelles. However, most block and graft copolymers have low critical micelle concentrations (CMCs) and in most cases it is difficult to measure this parameter. In addition, the aggregation number of most block and graft copolymers is low and this requires sensitive techniques to measure them, e.g. time-average and dynamic light scattering. By measuring the intensity of scattered light (when using time-average measurements) as a function of concentration, one can extrapolate the results to zero concentration and obtain the molecular weight of the micelle. In dynamic light scattering, we can measure the

hydrodynamic radius of the micelle and this can give a rough estimate of the aggregation number.

2 SOLUTION PROPERTIES OF POLYMERIC SURFACTANTS

2.1 Thermodynamic treatment

The solution properties of blocks and grafts are complicated since the copolymer components A and B behave differently in different solvents. In order to simplify the analysis, one usually starts with a solvent in which both A and B are soluble. In this case, the solution properties approach those of a homopolymer, for which accurate theories exist, e.g. in the thermodynamic treatment of Flory and Huggins (1, 2). The latter considers the free energy of mixing of pure polymer with pure solvent, ΔG_{mix} , in terms of two contributions, i.e. the enthalpy of mixing, ΔH_{mix} , and the entropy of mixing, ΔS_{mix} , as follows:

$$\Delta G_{\text{mix}} = \Delta H_{\text{mix}} - T \Delta S_{\text{mix}} \quad (16.1)$$

A negative value of ΔG_{mix} indicates that the dissolution process will occur spontaneously. The term $T \Delta S_{\text{mix}}$ is generally positive, since there is an increase in disorder on mixing a polymer with a solvent (positive entropy). Thus, the sign of ΔG_{mix} depends on the sign of ΔH_{mix} . The latter is usually positive and hence the enthalpy term opposes the mixing of polymer and solvent. However, when there is interaction between the polymer and solvent molecules, e.g. through hydrogen bonding, the enthalpy of mixing is negative and hence dissolution of the polymer in the solvent is spontaneous. A good example is PEO in water, where the EO units will hydrogen-bond with the water molecules.

Assuming that the polymer chain adopts a configuration on a lattice (provided by the solvent molecules) and considering that the mixing is “random”, ΔS_{mix} is given by the following:

$$\Delta S_{\text{mix}} = -k(n_1 \ln \phi_1 + n_2 \ln \phi_2) \quad (16.2)$$

where n_1 is the number of solvent molecules with a volume fraction ϕ_1 , and n_2 is the number of solvent molecules with a volume fraction ϕ_2 .

The heat of mixing of polymer solutions, ΔH_{mix} , was calculated by Flory and Huggins (1, 2) who introduced the concept of contact energy as the cause of the heat of mixing of polymer solutions. In this treatment, the energy change on mixing is assumed to arise from the formation of new polymer–solvent

contacts, which replace some of the solvent–solvent and polymer–polymer contacts present in pure solvent and pure polymer, respectively. By assuming that the size of polymer segments to be similar to that of solvent molecules, Flory and Huggins (1, 2) introduced a dimensionless parameter χ , the Flory–Huggins (polymer–solvent) interaction parameter, given by the following:

$$\chi = \frac{\Delta H_{\text{mix}}}{kTn_1\phi_2} \quad (16.3)$$

or:

$$\Delta H_{\text{mix}} = n_1\phi_2\chi kT \quad (16.4)$$

The χ parameter can be used as a measure of the solvent power; it has a value < 0.5 when the polymer is in a good solvent, and a value > 0.5 when the polymer is in a poor solvent. The point where $\chi = 0.5$ is referred to as the θ -solvent point.

By combining equations (16.2) and (16.4), we obtain the following:

$$\Delta G_{\text{mix}} = kT(n_1 \ln \phi_1 + n_2 \ln \phi_2 + \chi n_1 \phi_2) \quad (16.5)$$

The mixing of a pure solvent with a polymer creates an osmotic pressure, π , which can be expressed in terms of the polymer concentration c_2 and its partial specific volume v_2 , as follows:

$$\pi/c_2 = RT[(1/M_2) + (v_2^2/V_1)(1/2 - \chi)c_2 + \dots] \quad (16.6)$$

The second term in equation (16.6) is known as the second virial coefficient, B_2 , i.e.

$$\pi/c_2 = RT[(1/M_2) + B_2c_2 + \dots] \quad (16.7)$$

where B_2 is given by the expression:

$$B_2 = (v_2^2/V_1)(1/2 - \chi) \quad (16.8)$$

Note that $B_2 = 0$ when $\chi = 0.5$, i.e. the polymer displays ideal mixing with the solvent (θ -point). Under these conditions, the polymer chains in solution have no attraction or repulsion and they adopt their unperturbed dimensions. B_2 is positive when $\chi < 0.5$ and mixing of the polymer with the solvent is non-ideal with a positive deviation (good solvent for the polymer). In this case, a plot of π/c_2 versus c_2 gives a line with a positive slope. When B_2 is negative, i.e. $\chi > 0.5$, mixing is non-ideal with a negative deviation (poor solvent for the polymer). In this case a plot of π/c_2 versus c_2 gives a line with negative slope. Under these conditions, the polymer may precipitate out.

Since the polymer solvency depends on temperature, one can also define a θ -temperature at which $\chi = 0.5$.

This concept was introduced by Flory and Krikbaum (3) who postulated the presence of an excluded volume for the polymer chain, i.e. the volume occupied by the polymer chain which exhibits long-range intramolecular interaction. These interactions were introduced as an enthalpic term κ_1 and an entropic term ψ_1 . The two terms become equal when $\Delta G_{\text{mix}} = 0$. The temperature at which these conditions prevail in a given solvent is the θ -temperature, given as follows:

$$\theta = \frac{\kappa_1 T}{\psi_1} \quad (16.9)$$

It is clear from equation (16.9) that when $T = \theta$, $\kappa_1 = \psi_1$. At the θ -temperature, the effects of excluded volume are eliminated and the polymer chain adopts its unperturbed conformation in dilute solutions.

The χ parameters can be expressed in terms of κ_1 and ψ_1 as follows:

$$[(1/2) - \chi] = \kappa_1 - \psi_1 \quad (16.10)$$

Alternatively one can write:

$$[(1/2) - \chi] = \psi_1[1 - (\theta/T)] \quad (16.11)$$

Several experimental results cannot be accounted for by the Flory–Huggins theory, such as the dependence of the χ parameter on polymer concentration and phase separation of many polymer solutions on heating, e.g. PEO.

The solution properties of copolymers are much more complicated (4). The two copolymer components A and B behave differently in different solvents. When the two components A and B are both soluble in the same solvent, they exhibit similar solution properties, e.g. a non-polar copolymer in a non-polar solvent. With branched copolymers of high monomer density (e.g. star-branched copolymers), the θ -temperature depends on the length of the arms and is in general lower than that of a linear polymer with the same molecular weight. Another complication arises from specific interaction with the solvent, e.g. hydrogen bonding between polymer molecules and solvent, e.g. PEO and PVA in water. Aggregation in solution (lack of complete solution) and formation of micelles may also present a problem in determining the solution properties of block and graft copolymers.

2.2 Solubility parameters and cohesive energy density

As is clear from the thermodynamic treatment discussed above, it is not easy to predict the solubility of a polymer in a given solvent, since this requires knowledge of

the χ parameter. A qualitative guide for predicting the solubility of a polymer in a solvent is to use the solubility parameter concept introduced by Hildebrand (5). The enthalpy of mixing of solute and solvent could be derived by using the heat of vaporization of a liquid in a binary mixture. The energy of vaporization of any material, ΔE^v , when divided by its molar volume, V , gives a measure of the strength of the internal forces between the molecules. This is termed the cohesive energy density (CED), given as follows:

$$CED = \frac{\Delta E^v}{V} \quad (16.12)$$

The CED is a measure of the "internal pressure" and its square root is defined as the solubility parameter δ . Thus, the enthalpy of mixing of polymer and solvent is given by the following expression:

$$\Delta H_{\text{mix}} = V_M(\delta_1 - \delta_2)^2 \chi_1 \chi_2 \quad (16.13)$$

or:

$$\delta = \left(\frac{\Delta H_M - RT}{V_M} \right)^{1/2} \quad (16.14)$$

Thus, one can calculate the solubility parameter from a knowledge of the heat of vaporization, ΔH_M , and the molar volume, V_M . This is straightforward for many solvents and values of δ have been tabulated by Barton (6). For polymers this is not easy since the heat of vaporization is not known and other methods have to be applied to determine the solubility parameter of various polymers. Several experimental methods such as the measurement of polymer swelling or intrinsic viscosity may be applied. Alternatively, δ may be calculated from a knowledge of the molar attraction constants, G , of the various functional groups in the polymer (7, 8). The values of G for the various groups are assumed to be additive:

$$\delta = \frac{\rho \Sigma G}{M} \quad (16.15)$$

It is usually found that polymers will dissolve in solvents having solubility parameters within about one unit of their own. The closer the values of δ between polymer and solvent, then the more soluble is the polymer.

2.3 Size and shape of polymers in solution

A knowledge of the conformation of the polymer chains in space is very important for its characterization. Once a polymer-solvent pair has been selected, the physical

properties of the resulting solution are controlled by how the polymer behaves among the solvent molecules. Of particular importance is the size, or hydrodynamic volume, of the polymer in solution. The polymer chain may be envisaged as a coil continuously changing its shape and hence its size as a result of thermal fluctuations. Two useful parameters can be employed for characterizing the conformation of the polymer in solution, namely the root-mean-square (rms) end-to-end length, $\langle r^2 \rangle^{1/2}$, which represents a configurational character with r being the distance from one end group to the other in a polymer chain molecule, and the radius of gyration, $\langle s^2 \rangle^{1/2}$, which is a measure of the effective size of a polymer molecule: The latter represents the rms distance of the elements of the chain from its centre of gravity.

For simple linear polymers, we have the following:

$$\langle s^2 \rangle^{1/2} = (\langle r^2 \rangle^{1/2}) / 6^{1/2} \quad (16.16)$$

It is convenient to express r and s in terms of two factors, i.e. an unperturbed dimension, r_0 or s_0 (i.e. in a θ -solvent) and an expansion factor α (which determines the polymer expansion as a result of the solvation of the polymer), as follows:

$$r = r_0 \alpha \quad (16.17)$$

$$s = s_0 \alpha \quad (16.18)$$

In a good solvent, α is greater than 1, and the greater the value of α , then the better the solvent.

The radius of gyration of a polymer molecule in solution can be determined from light scattering measurements. This is straightforward for homopolymers and for copolymers in solvents that are good for both components A and B. However, it is essential to use selective solvents, whereby the medium is a good solvent for one component, say A, and a poor solvent for the second component, B. In this case, one part of the amphipathic block or graft copolymer will separate as a distinct phase, while the other remains in solution. The insoluble portion of the amphipathic copolymer will aggregate reversibly to form micelles. It is believed that the micelles of block and graft copolymers are spherical. The critical micelle concentration of block and graft copolymers is usually very low.

Several methods may be used to obtain the micellar size and shape of block and graft copolymers, e.g. light scattering, small-angle X-ray scattering and small-angle neutron scattering. Dynamic light scattering (photon correlation spectroscopy (PCS)) can also be applied to obtain the hydrodynamic radius of the micelle. By measuring the intensity fluctuation of scattered light

by the micelles (which undergo Brownian diffusion), one can obtain the diffusion coefficient of the micelle, D , from which the hydrodynamic radius, R_h , can be obtained by using the Stokes–Einstein equation, as follows:

$$D = \frac{kT}{6\pi\eta R_h} \quad (16.19)$$

where η is the viscosity of the medium.

3 ADSORPTION AND CONFORMATION OF POLYMERIC SURFACTANTS AT INTERFACES

Understanding the adsorption and conformation of polymeric surfactants at interfaces is key to understanding how these molecules act as stabilizers for suspensions and emulsions. Most basic theories on polymer adsorption and conformation have been developed for the solid/liquid interface (9). The same concepts may be applied for the liquid/liquid interface, with some modifications whereby some part of the molecule may reside within the oil phase, rather than simply staying at the interface. Such modifications do not alter the basic concepts, particularly when one deals with the stabilization by these molecules.

The process of polymer adsorption involves a number of interactions that need to be carefully considered. Three main interactions are obvious, i.e. the surface/solvent, the chain/solvent and the chain/surface. For adsorption to take place, then unfavourable entropy loss when a polymer molecule approaches a surface must be compensated for by an energy of adsorption term. One usually describes the adsorption energy in terms of the value per segment in direct contact with the surface, χ^s . In addition, the polymer molecule must displace the solvent molecules at the surface. The interaction between the chain and the solvent, as determined by the Flory–Huggins interaction parameter χ , also plays a major role in polymer adsorption.

Apart from knowing the above interactions, one of the most fundamental considerations is the conformation of the polymer molecule at the interface. This is determined by the structure of the polymer molecule (whether this is a homopolymer, a block or a graft copolymer), its flexibility, molecular weight and the various environmental conditions such as solvency, temperature, addition of electrolyte, etc.

The simplest polymer conformation to consider is that of a homopolymer (which consists of identical segments such as PEO or PVP), whereby the molecule attaches itself with some segments (“trains”) leaving

loops and tails dangling in solution (10). This is illustrated in Figure 16.1(a). As mentioned above, for such a molecule to adsorb, the total adsorption energy per molecule (number of segments in trains $\times \chi^s$) must overcome the entropy loss. A minimum value of χ^s is required for adsorption and this value could be a fraction of kT , since a large number of segments may be attached to the surface. For example, with a polymer chain consisting of 1000 segments, with a fraction of 0.1 in trains and an adsorption energy per segment of $0.1kT$, the total adsorption energy per molecule is $10kT$, which in most cases is sufficient for adsorption to occur. However, with highly water-soluble polymers such as PEO, the adsorption energy per segment on a hydrophobic surface may be too small for adsorption to take place. In addition, even if adsorption occurs, the molecule becomes weakly adsorbed and hence it will not provide effective steric stabilization (see below).

In order to enhance the adsorption of a molecule on the surface, one may incorporate specific groups on a random basis on the chain. These groups will enhance the adsorption of the polymer and hence may provide effective stabilization. A good example is partially hydrolysed poly(vinyl acetate). The polymer chain contains random segments of vinyl acetate (which are hydrophobic in nature) and these will enhance the adsorption of the molecule on a hydrophobic surface such as polystyrene. The conformation of such molecule is shown in Figure 16.1(b). Clearly if all of the segments are made hydrophobic, the molecule will lie flat on the surface, as represented in Figure 16.1(c). Such molecules will not offer any steric stabilization.

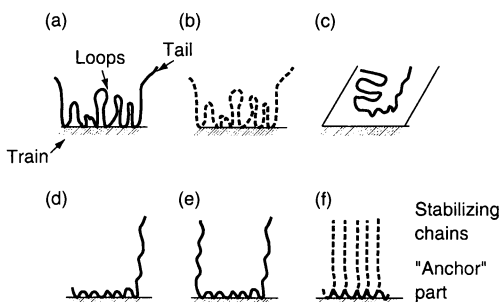


Figure 16.1. Various conformations of polymeric surfactants adsorbed on a plane surface: (a) random conformations of loops–trains–tails (homopolymer); (b) preferential adsorption of “short blocks”; (c) chain lying flat on the surface; (d) AB block copolymer with loop–train conformation of B and long tail of A; (e) ABA block copolymer, as in (d); (f) BA_n graft with backbone B forming small loops and several tails of A (“teeth”)

The most favourable structures for polymeric surfactants are those of the block and graft type, represented in Figures 16.1(d–f). In all of these cases, the chain B is chosen to be highly insoluble in the medium and hence it adsorbs on the surface with several attachment points (small loops) and this ensures strong adsorption (“anchor”) on the surface. The chain A is chosen to have little affinity to the surface and high affinity to the medium, i.e. strongly solvated by the molecules of the solvent and having a $\chi < 0.5$. This A chain provides the steric stabilization. The molecule shown in Figure 16.1(d) represents the case of an A–B block copolymer, that of Figure 16.1(e) represents the case of an A–B–A block copolymer, whereas that of Figure 16.1(f) is that of a graft copolymer BA_n .

Several theories describe the process of polymer adsorption, with these having been developed by using either the statistical mechanical approach or the quasi-lattice model. In the first approach, the polymer is considered to consist of three structure with different energy states, i.e. trains, loops and tails (11, 12). The structures close to the surface (trains) are adsorbed with an internal partition function which is determined by the short-range interaction forces between the segment and surface. As mentioned above, this can be described by an adsorption energy per segment, χ^s . The segments in the loops and tails are considered to have an internal partition function equivalent to that of the segments in the bulk solution. These segments in loops and tails are assigned a segment–solvent interaction parameter χ (the Flory–Huggins interaction parameter). By equating the chemical potential of the macromolecule in the adsorbed state with that in the bulk solution, the adsorption isotherm can be obtained. In the earlier theories, the case of an isolated chain on the surface (low coverage) was considered. This is clearly an unrealistic model, since even at low coverage the polymer concentration on the surface is sufficiently high for lateral interactions between the chains to take place. Later theories were modified to take into account such lateral interactions.

The quasi-lattice model was developed by Roe (13) and Scheutjens and Fleer (14) (SF theory). The basic analysis considered all chain conformations as step-weighted random walks on a quasi-crystalline lattice that extends in parallel layers from the surface. This is illustrated in Figure 16.2 which shows a possible conformation of a polymer molecule at a flat surface. The partition function was written in terms of the number of chain configurations that were treated as connected sequences of segments. In each layer parallel to the surface, random mixing between the segments and solvent molecules was assumed, i.e. by using

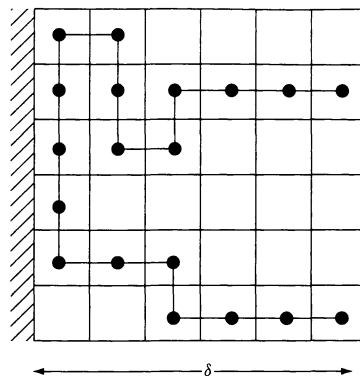


Figure 16.2. Possible conformation of a polymer molecule at an interface

Bragg–William or mean field approximations. Each step in the random walk was assigned a weighting factor, p_i , which was considered to consist of three factors, i.e. the adsorption energy χ^s , the configurational entropy of mixing, and the segment–solvent interaction parameter χ . The only layer that contains these three contributions is the first one, since the segments are directly attached to the surface with a segment–surface adsorption energy χ^s . All other layers far from the first layer contain only two factors (entropy of mixing and segment–solvent interaction). A summary of the prediction from the theory is given below.

Figure 16.3 shows typical adsorption isotherms plotted as surface coverage in equivalent monolayers, θ , versus the polymer volume fraction, ϕ_* , in the bulk solution (ϕ_* was taken to vary between 0 and 10^{-3} , which

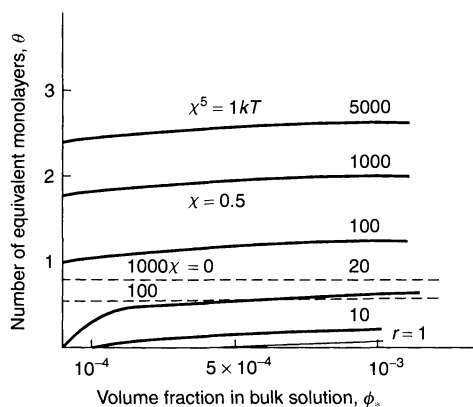


Figure 16.3. Adsorption isotherms for oligomers and polymers in the dilute region: (—), $\chi = 0.5$; (---), $\chi = 0$ ($\chi^s = 1kT$; hexagonal lattice)

is the normal experimental range). The results presented in Figure 16.3 show the effect of increasing the chain length r (from $r = 1$ representing a solute molecule with one segment, to $r = 5000$ which represents a very high-molecular-weight polymer). The effect of solvency was also considered by assigning the two extreme values of χ from 0 for an athermal solvent to 0.5 for a θ -solvent. The adsorption energy per segment, χ^s , was assigned the same value of $1kT$.

When $r = 1$, θ is very small and the adsorption increases linearly with the increase in ϕ_* (Henry's type isotherm). On the other hand, when $r = 10$ the isotherm deviates from such a straight line and approaches a Langmuirian type with a near-plateau value at high ϕ_* values. However, when $r > 20$, high affinity isotherms are obtained. In this case, the adsorption rises very steeply at low polymer concentrations and thereafter it reaches a pseudo-plateau region. The adsorption isotherms for chains with $r = 100$ and above are typical of those obtained experimentally for most polymers that are not too polydisperse (i.e. showing a steep rise followed by a nearly horizontal pseudo-plateau (which only increases by few percent per decade increase in ϕ_*).

In these dilute solutions, the effect of solvency is most clearly seen, with a poor solvent ($\chi = 0.5$) giving the highest adsorbed amounts. In a good solvent ($\chi = 0$), θ is much smaller (see the dashed lines in Figure 16.3) and it levels off for long chains to attain an adsorption plateau which is essentially independent of the molecular weight. It should be noted that in most real situations the χ value is somewhere between 0 and 0.5 (probably nearer the latter value).

Some general features of the adsorption isotherms over a wide concentration range can be illustrated by using logarithmic scales for both θ and ϕ_* which also highlights the behaviour in extremely dilute solutions. Such a presentation (15) is shown in Figure 16.4. The calculations show a linear Henry region followed by a pseudo-plateau region. A transition concentration, ϕ_*^c , can be defined by extrapolation of the two linear parts. It was found that ϕ_*^c decreases exponentially with increasing chain length and when $r = 50$, ϕ_*^c is so small (10^{-12}) that it does not appear within the log scale shown in Figure 16.4.

The presentation in Figure 16.4 answers the question of irreversibility versus reversibility of polymer adsorption. When $r > 50$, ϕ_*^c reaches such a low value that, experimentally when using low polymer concentrations, one cannot detect any polymer in solution. This means that on dilution of the system after complete adsorption, desorption is practically impossible, since one has to reach such low polymer concentrations in the bulk

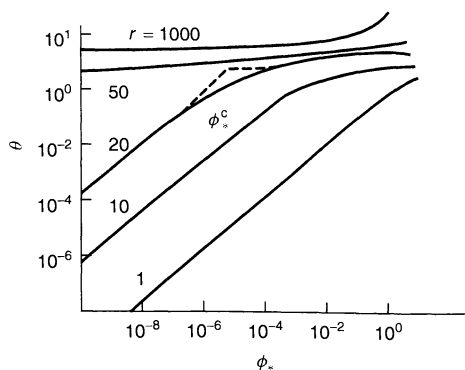


Figure 16.4. Log-log presentation of adsorption isotherms for various r values: $\chi^s = 1kT$; $\chi = 0.5$; hexagonal lattice

(10^{-12}). This lack of desorption under practical situations is one of the reasons for the effective stabilization produced by macromolecular surfactants for suspensions and emulsions.

According to the SF theory, the bound fraction of segments in trains, p (number of segments in direct contact to the surface relative to the total number of segments in the chain), is high at low polymer concentrations ($\phi_* < \phi_*^c$), approaching unity and relatively independent of the molecular weight when $r > 20$. With an increase in surface coverage and/or molecular weight, p decreases, thus indicating the formation of larger loops and tails.

The structure of the adsorbed layer (conformation of the polymer at the interface) is described in terms of the segment density distribution $\rho(z)$ which is simply the number of segments in each layer in the z -direction from the surface. Calculations by Scheutjens and Fleer (14) showed that for a chain with $r = 1000$, $\phi_* = 10^{-5}$ and $\chi = 0.5$, 38% of the segments are in trains, 55.5% in loops and 6.5% in tails. This theory demonstrates the importance of tails which dominate the total distribution in the outer region of the adsorbed layer.

It is clear from the above theories that for full characterization of polymer adsorption and configuration at the interface, one needs to measure the following values, i.e. the amount of polymer adsorbed per unit area of the surface, Γ (mol m^{-2}), the fraction of segments in direct contact with the surface (in trains), p , and the segment density distribution $\rho(z)$. Measurement of Γ and p as a function of polymer concentration is fairly straightforward. The parameter Γ can be directly determined by equilibrating a known amount of disperse phase (particles or droplets) of known surface area with polymer solutions with various concentrations, starting

from very small values. When the system reaches equilibrium (this may take hours or days depending on the polymer molecular weight), the particles of the disperse phase are removed by centrifugation and/or filtration. The equilibrium concentration of the supernatant liquid is determined by using a suitable analytical technique. If C_1 and C_2 are respectively the initial and equilibrium concentrations of the polymer (i.e. before and after adsorption), m is the mass of the disperse phase and A its surface area, then Γ is simply given by the following:

$$\Gamma = \frac{C_1 - C_2}{mA} \quad (16.20)$$

Figure 16.5 shows the adsorption isotherms at 25°C for PVA (containing 12% acetate groups) on polystyrene latex (16). The high-affinity isotherms for the polymers and the clear increase in amount of PVA adsorbed (mg m^{-2}) with increase in molecular weight are clearly shown. Indeed the amount of adsorption at the plateau value increased linearly with the square root of the molecular weight of the polymer, thus indicating a near-random-coil arrangement at the surface with few attached segments.

Figure 16.6 shows the adsorption isotherms (at 20°C) of two graft copolymers based on a poly(methyl methacrylate-methacrylic acid) backbone and PEO chains, namely Atlox 4913 and Hypermer CG-6(a) (17). The latter has a higher proportion of poly(methacrylic acid) and hence contains a lower PEG chain density than Atlox 4913. Two latex particles with diameters of 427 and 867 nm were used for these measurements. The adsorption isotherms are of a Langmuir type and the plateau value does not seem to depend on the particle size. However, the adsorption plateau value of Hypermer CG-6(a) (1.2 mg m^{-2}) is lower than that obtained when using Atlox 4913 (1.6 mg m^{-2}). This is due to the

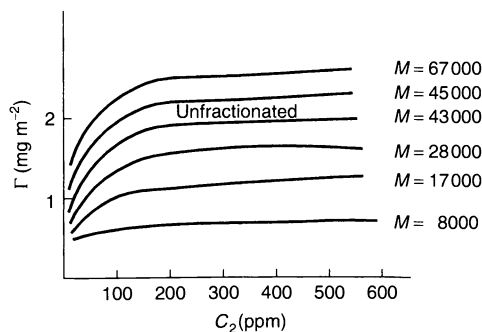


Figure 16.5. Adsorption isotherms of poly(vinyl alcohol) on a polystyrene latex at 25°C

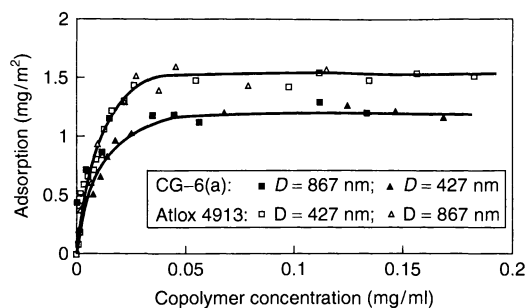


Figure 16.6. Adsorption isotherms of graft copolymers on a polystyrene latex at 20°C

lower PEO side-chain density with Hypermer CG-6(a) when compared with that of Atlox 4913.

The effect of temperature on the adsorption isotherms for both copolymers on the larger latex particles ($D = 867$) is shown in Figure 16.7. In both cases, adsorption increases with increase of temperature from 20 to 40°C. This is due to the reduction of solvency of the medium for the side chains with increasing temperature. Increase in the χ parameter (with increase of temperature) results in an increase in polymer adsorption.

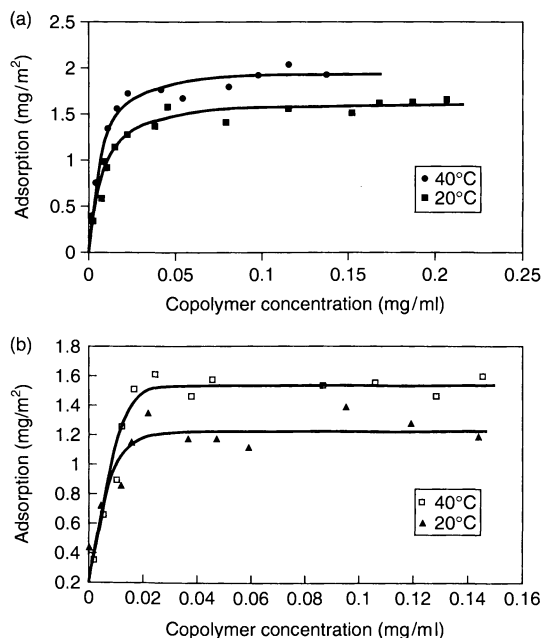


Figure 16.7. Adsorption isotherms for (a) Atlox 4913 and (b) Hypermer CG-6(a) on a polystyrene latex ($D = 867$ nm), measured at 20 and 40°C

The polymer-bound fraction p can be directly determined by using spectroscopic methods such as infrared (IR), electron spin resonance (ESR) and nuclear magnetic resonance (NMR) spectroscopy. The latter method depends on the reduction of the mobility of the segments that are in close contact with the surface. By using pulsed-gradient NMR spectroscopy, one can obtain the fraction of segments that are "immobilized" (near the surface) and hence one can obtain p (18, 19). An indirect method for the estimation of p is microcalorimetry. In this method, basically one compares the enthalpy of adsorption per molecule with the enthalpy of adsorption of one segment (20); this ratio gives the number of segments per molecule in direct contact with the surface and thus allows the calculation of p . The enthalpy of adsorption per segment is assumed to be equivalent to that for a small molecule with an equivalent structure.

The most difficult parameter to measure is the segment density distribution $\rho(z)$. The latter can be obtained from ellipsometry and attenuated total reflection (spectroscopy) but these methods require the use of a flat surface (21) and hence cannot be applied for the practical systems of particles. For the latter case, small-angle neutron scattering (spectroscopy) can be employed to obtain $\rho(z)$. The basic principle of this technique is to measure the scattering due to the adsorbed layer, when the scattering length density of the particle core is matched to that of the medium (the so-called "contrast-matching" method). For example, for polymer layers of PVA or PEO on polystyrene latex in water, one can use a deuterated latex in a medium of H_2O and D_2O (to contrast the scattering length density of the deuterated styrene with that of the medium) (22).

In view of the above difficulties in determining the segment density distribution, one usually determines the hydrodynamic thickness, δ_h , which gives a measure of the extension of the polymer layer from the surface. This value is important when discussing steric stabilization, as will be shown below. Several methods may be applied to obtain δ_h and these are all based on measuring the hydrodynamic radius of a particle containing the adsorbed layer, R_h . From a knowledge of the particle core radius R , one can obtain δ_h . For accurate measurements, the adsorbed layer thickness has to be greater than 10% of the core radius and hence one should use small particles for these measurements.

One of the simplest ways to obtain the hydrodynamic radius of a particle is to measure the relative viscosity of dilute dispersions, η_r , and then apply the Einstein equation to obtain the effective volume fraction of the particles, ϕ_{eff} . Assuming that the particles behave as hard spheres (when δ_h is small compared to the core radius

R) of non-interacting particles (which is the case at low volume fraction), we can write the following:

$$\eta_r = 1 + 2.5\phi_{\text{eff}} \quad (16.21)$$

From ϕ_{eff} and ϕ (the core volume fraction), δ_h can be calculated as follows:

$$\phi_{\text{eff}} = \phi \left(1 + \frac{\delta_h}{R} \right)^3 \quad (16.22)$$

To apply the above method, one should use a dispersion with monodisperse particles and so this limits its use for emulsions which are often polydisperse in nature.

Another method for determining δ_h is to apply dynamic light scattering, referred to as photon correlation spectroscopy (PCS). For this purpose, dilute monodisperse particles must be used. From measurements of the intensity fluctuations of scattered light by the particles as they undergo Brownian diffusion, one can obtain the diffusion coefficient D , which can be used to obtain the hydrodynamic radius by using the Stokes–Einstein equation (equation (20.19)). By measuring D for the particles, both with and without the polymer layer, one can obtain R_h and R , respectively. One should make sure that the bare particles are sufficiently stable; δ_h is then equal to $(R_h - R)$.

The dynamic light scattering method cannot be applied for emulsions since these cannot be prepared in a monodisperse form. However, by measuring the adsorbed layer thickness on a model monodisperse hydrophobic particle such as polystyrene, one can make the assumption that the layer thickness is similar to that obtained on an emulsion droplet.

4 STABILIZATION OF DISPERSIONS CONTAINING POLYMERIC SURFACTANTS

Solid/liquid (suspensions) and liquid/liquid (emulsions) dispersions can be prepared by using polymeric surfactants, which ensure their long-term physical stability, i.e. prevention of both flocculation and coalescence of the emulsions. The stabilization produced by polymers is usually referred to as steric stabilization, and arises from two main effects (23). First, an unfavourable mixing of the stabilizing polymer chains when these are in good solvent conditions – this is referred to as the mixing free energy G_{mix} (osmotic repulsion). Secondly, a reduction of the configurational entropy of the chains on significant overlap – this is referred to as the elastic free energy G_{el} (entropic or volume restriction repulsion). A summary of the two effects is given below.

4.1 Mixing interaction

When two particles containing an adsorbed or grafted polymer layer, with thickness δ_h , approach to a surface-to-surface distance of separation h which is less than $2\delta_h$, the polymer chains may undergo some penetration and/or compression. In both cases, there will be an increase in the segment density of the chains in the interaction zone. A schematic representation of this interaction is given in Figure 16.8 which shows the very simple case of two equal spheres, with an adsorbed layer of thickness δ (with uniform segment density), a polymer volume fraction ϕ_2 and an overlap zone of dV . Before overlap, the chemical potential of the solvent in the adsorbed layer is μ_i^α . In the overlap zone dV , the chemical potential of the solvent is μ_i^β which is lower than μ_i^α (i.e. the osmotic pressure in the overlap zone is higher than that in the layer before overlap). As a result, solvent will diffuse from the bulk, thus separating the particles (i.e. leading to strong repulsion). This condition is satisfied provided that the stabilizing polymer chains (A in a block or graft copolymer) are in good solvent conditions (i.e. $\chi < 0.5$).

The above mixing interaction can be calculated from a consideration of the free energy of mixing two polymer solutions, e.g. by using the Flory–Krigbaum theory (3), as follows:

$$\frac{G_{\text{mix}}}{kT} = \frac{4\pi}{3V_1} \phi_2^2 N_{\text{av}} \left(\frac{1}{2} - \chi \right) \left(\delta - \frac{h}{2} \right)^2 \times \left(3R + 2\delta + \frac{h}{2} \right) \quad (16.23)$$

It is clear from equation (16.23) that when the Flory–Huggins interaction parameter χ is less than 0.5, i.e. the stabilizing chains are in good solvent conditions,

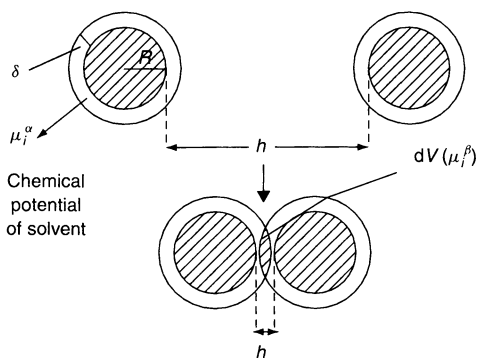


Figure 16.8. Schematic representation of the overlap of two polymer layers

G_{mix} is positive and the interaction is repulsive. The G_{mix} value increases very rapidly with a decrease in h when the latter is less than 2δ . This explains why graft copolymers, such as Atlox 4913 or Hypermer CG-6(a) are ideal for the stabilization of suspensions in aqueous media. For the stabilization of dispersions in non-aqueous media, such as water-in-oil (W/O) emulsions, the stabilizing chain has to be soluble in the oil phase (normally a hydrocarbon oil). In this case, poly(hydroxystearic acid) (PHS) chains are ideal. An ABA block of PHS–PEO–PHS (Arlacel P135, from UNIQEMA) is ideal for the stabilization of W/O emulsions.

Equation (16.23) also shows that when $\chi > 0.5$, i.e. the chains are in poor solvent conditions, G_{mix} is negative and the interaction becomes attractive. This explains the phenomenon of incipient flocculation which may occur when the medium become a poor solvent of the chains. This can occur if a non-solvent for the chains is added to the medium, on the addition of high salt concentrations to the aqueous medium (which is sufficient to “salt-out” the chain, or by increasing temperature (whereby the chains become less soluble at high temperature, e.g. PEO).

The condition $\chi = 0.5$ is referred to as the θ -point and denotes the onset of change of repulsion to attraction, i.e. the onset of flocculation. In many cases, there is good correlation between the θ -point and the flocculation point (e.g. the critical flocculation temperature).

4.2 Elastic (volume restriction or entropic) interaction

This arises from the loss of configurational entropy of the chains, particularly at significant overlap. This is schematically illustrated in Figure 16.9 for a simple case where the chain is represented by one rod with one attachment point that rotates freely on the surface when the surfaces are separated by an infinite distance. Under these conditions, the rod has a number of configuration Ω_∞ which is proportional to the volume

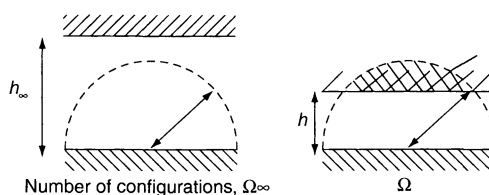


Figure 16.9. Schematic representation of the elastic interaction

of the hemisphere “swept out” by the rod on free rotation. When the two surfaces approach a distance h which is smaller than the radius of the hemisphere swept out by the rod, the volume available to the chains becomes smaller and this results in a reduction in the configurational entropy to a value Ω which is smaller than Ω_∞ . This results in strong repulsion and the effect is referred to as an elastic, volume restriction or entropic repulsion, given by the following:

$$G_{el} = 2v \ln \frac{\Omega}{\Omega_\infty} \quad (16.24)$$

where v is the number of chains per unit area of the surface. The parameter G_{el} is always positive (repulsive) and becomes very high on significant overlap of the chains.

Plots of G_{mix} , G_{el} and G_A (the van der Waals attraction) versus h are given in Figure 16.10, which also shows the variation of the net total interaction energy, G_T , given by the following:

$$G_T = G_{mix} + G_{el} + G_A = G_s + G_A \quad (16.25)$$

The mixing interaction, G_{mix} , increases very rapidly with a decrease in h when $h < 2\delta$ (and $\chi < 0.5$), while G_{el} also increases very rapidly with decrease of h on further overlap. The G_T-h curve shows a minimum (G_{min}) at $h \sim 2\delta$, but when $h < 2\delta$, G_T increases very rapidly with further decreases in h . The depth of the minimum depends on the particle size, the Hamaker constant (A) and the adsorbed layer thickness δ . For a given particle size with a Hamaker constant A , G_{min} decreases as δ increases. When δ reaches values of the order of 5–10 nm, G_{min} becomes quite small (particularly when the particle radius is small, say $< 1 \mu\text{m}$). In this case, the

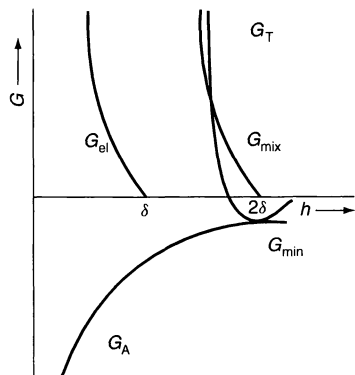


Figure 16.10. Schematic representation of the variation of G_{mix} , G_{el} , G_A and G_T with h

weak attraction that may occur at large separation distances may be overcome by Brownian diffusion and the dispersion approaches thermodynamic stability. This is particularly the case with dilute dispersions. However, with concentrated dispersions, the small energy minimum may be sufficient to cause some weak flocculation, although in practice this may not be a problem since the system can be redispersed by gently shaking. Indeed, such a phenomenon of weak flocculation is beneficial in some cases, for example, in the prevention of formation of hard sediments.

4.3 Main criteria for effective steric stabilization

From the above discussion, one can summarize the most important criteria for effective steric stabilization when using polymeric surfactants. First, there should be enough polymer to ensure complete coverage of the particle surface by the chains. This will prevent any attraction between the bare patches of the particles, while it also prevents any bridging flocculation (simultaneous adsorption of the chain on more than one particle).

The second and most important criterion for effective steric stabilization is to ensure strong adsorption of the chain to the particle surface (a strong “anchor” to the surface is essential). This prevents any displacement of the chains on close approach of the particles. This is particularly the case with concentrated dispersions, whereby the particles approach each other to close distances of separation. In order to ensure a strong “anchor” to the surface, one uses block and graft copolymers (A–B, A–B–A and BA_n). The chain B is chosen to be highly insoluble in the medium and should have strong affinity to the surface. Suitable examples of B chains for hydrophobic particles in aqueous media are polystyrene and poly(methyl methacrylate).

The third criterion for effective stabilization is to ensure that the stabilizing chain A remains in good solvent conditions under all practical situations, for example during storage (at different temperatures) and on application. For aqueous media, the most effective A chains are those based on PEO, PVA and PVP. Such chains are highly solvated by water and can also tolerate reasonable amounts of electrolytes.

The last criterion for effective steric stabilization is to have a sufficiently thick or grafted polymer layer to screen the van der Waals attraction. An adsorbed layer thickness in the region of 5–10 nm is usually sufficient in most cases, particularly when the dispersion particle size is not too high (a few μm). With graft copolymers, a molecular weight of the side chains of the order of

1000–2000 is usually adequate, since in this case the chains then become extended (forming a “brush”).

5 REFERENCES

1. Flory, P. J., *Principles of Polymer Chemistry*, Cornell University Press, New York, 1953.
2. Huggins, M., *J. Phys. Chem.*, **46**, 151 (1942).
3. Flory, P. J. and Krigbaum, W. R., *J. Chem. Phys.*, **18**, 1086 (1950).
4. Pirma, I., *Polymeric Surfactants*, Marcel Dekker, New York, 1992.
5. Hildebrand, J. H., *Solubility of Non-Electrolytes*, Reinhold, New York, 1936.
6. Barton, A. F. M. *Handbook of Solubility Parameters and Other Cohesive Parameters*, CRC Press, Boca Raton, FL, 1983.
7. Small, P. A., *J. Appl. Chem.*, **3**, 71 (1953).
8. Hoy, K. L., *J. Paint Technol.*, **42**, 76 (1970).
9. Fleer, G. J., Cohen Stuart, M. A., Scheutjens, J. M. H. M., Cosgrove, T. and Vincent, B., *Polymers at Interfaces*, Chapman Hall, London, 1993.
10. Tadros, Th. F., in *Polymer Colloids*, Buscall, R., Corner, T. and Stageman, J. (Eds), Elsevier Applied Sciences, London 1985.
11. Silberberg, A., *J. Chem. Phys.*, **48**, 2835 (1968).
12. Hoeve, C. A., *J. Polym. Sci.*, **30**, 361 (1970); *J. Polym. Sci.*, **34**, 1 (1971).
13. Roe, R. J., *J. Chem. Phys.*, **60**, 4192 (1974).
14. Scheutjens, J. M. M. and Fleer, G. J., *J. Phys. Chem.*, **83**, 1619 (1979); *J. Phys. Chem.*, **84**, 178 (1980).
15. Scheutjens, J. M. H. M. and Fleer, G. J., *Adv. Colloid Interface Sci.*, **16**, 341 (1982).
16. Garvey, M. J., Tadros, Th. F. and Vincent, B., *J. Colloid Interface Sci.*, **49**, 57 (1974).
17. Liang, W., Bognolo, G. and Tadros, Th. F., *Langmuir*, **11**, 2899 (1995).
18. Robb, I. and Smith, R., *Eur. Polym. J.*, **10**, 1005 (1974).
19. Barnett, K. G., Cosgrove, T., Vincent, B., Burgess, A. N., Crowley, T. L., Kims, J., Turner, J. D. and Tadros, Th. F., *Polymer*, **22**, 283 (1981).
20. Killmann, E., *Polymer*, **17**, 864 (1976).
21. Peyser, P. and Stromberg, R. R., *J. Phys. Chem.*, **71**, 2066 (1967).
22. Cosgrove, T., Crowley, T. L., Vincent, B., Barnett, K. G. and Tadros, Th. F., *Faraday Symp., Chem. Soc.*, **101** (1991).
23. Napper, D. H., *Polymeric Stabilisation of Dispersions*, Academic Press, London, 1983.

CHAPTER 17

Speciality Surfactants

Krister Holmberg

Chalmers University of Technology, Göteborg, Sweden

1	Gemini Surfactants	385	2.4	Concluding remarks	397
1.1	Introduction	385	3	Polymerizable Surfactants	397
1.2	Synthesis	386	3.1	Introduction	397
1.3	Micellization and behaviour at the air–water interface	388	3.2	Mode of surfactant polymerization	398
1.4	Micelle shape and effect on rheology of solutions of gemini surfactants	389	3.2.1	Homopolymerization versus copolymerization	398
1.5	Concluding remarks	390	3.2.2	Autoxidative versus non-autoxidative polymerization	398
2	Cleavable Surfactants	390	3.2.3	Position of polymerizable group	399
2.1	Introduction	390	3.3	Applications of polymerizable surfactants	400
2.2	Acid-labile surfactants	391	3.3.1	Emulsion polymerization	400
2.2.1	Cyclic acetals	391	3.3.2	Alkyd emulsions	402
2.2.2	Acyclic acetals	392	3.3.3	Surface modification	403
2.2.3	Ketals	393	3.4	Concluding remarks	404
2.2.4	Ortho esters	394	4	Bibliography	405
2.3	Alkali-labile surfactants	395			
2.3.1	Normal ester quats	395			
2.3.2	Betaine esters	396			

1 GEMINI SURFACTANTS

1.1 Introduction

The term “gemini surfactant” was coined by Menger in 1991. A gemini surfactant may be viewed as a surfactant dimer, i.e. two amphiphilic molecules connected by a spacer. Figure 17.1 shows the general structure. Gemini surfactants are also referred to as “twin surfactants”, “dimeric surfactants” or “bis-surfactants”.

The spacer chain, which can be hydrophilic or hydrophobic, rigid or flexible, should bind the two moieties together at, or in close proximity to, the head-groups. Connecting two surfactant moieties

towards the end of their hydrophobic tails results in a so-called “bolaform surfactant” and the physico-chemical properties of such species are not very interesting. Most geminis are composed of two identical halves, but unsymmetrical gemini surfactants have also been synthesized, either having different hydrophobic tail lengths, or different types of polar groups (“heterogemini surfactants”), or both. In recent years, “higher oligomers” of single surfactants, i.e. “tris-surfactants”, “tetrasurfactants”, etc. have also been synthesized. Little is known today about properties and usefulness of these species, however.

Gemini surfactants have not yet reached the market on a large scale. They are, however, attracting

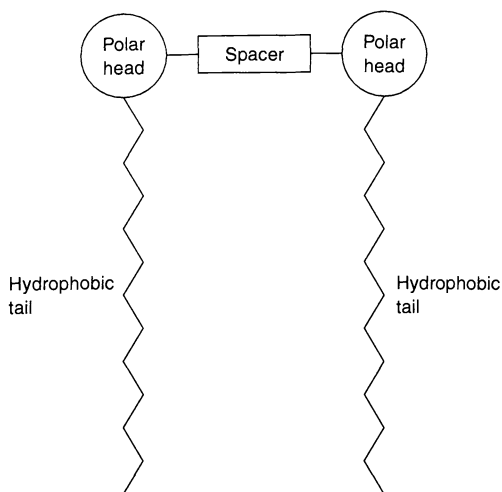


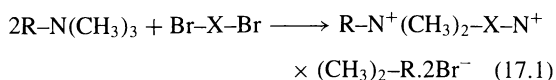
Figure 17.1. Schematic structure of gemini surfactants

considerable attention, both in industry and in academia. Some gemini surfactants, in particular symmetrical cationic ones, are made from readily available raw materials by a straightforward synthesis, as discussed below. Thus, they should not be regarded as just being research curiosities.

Figure 17.2 shows examples of gemini surfactants, which have been somewhat randomly taken from the literature. Compounds **1–3** are cationics differing in the type of spacer unit connecting the two ionic moieties. The spacer of Compound **1** is hydrophobic and flexible, that of Compound **2** is hydrophilic and flexible, while that of Compound **3** is hydrophobic and rigid. Compound **4** is a typical nonionic gemini and Compound **5** is an anionic one, based on the same backbone structure. Compounds **6** and **7**, finally, are examples of heterogemini surfactants.

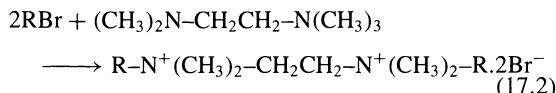
1.2 Synthesis

Cationic geminis such as Compounds **1–3** of Figure 17.2 are conveniently prepared by reacting an alkyldimethylamine with an α,ω -dihalo compound. Dibromo reagents are more reactive and are usually employed in laboratory synthesis, although the corresponding dichloro compounds may be preferred in large scale preparation:

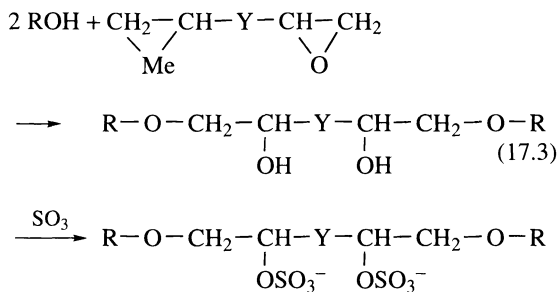


where R is an alkyl group of normal surfactant chain length such as $C_{12}H_{25}$. X can be an alkylene group to give a hydrophobic, flexible spacer, while it can be $CH_2CH(OH)CH_2$ or $CH_2(CH_2OCH_2)_nCH_2$ to give a hydrophilic flexible spacer, or it can be $CH_2-\Phi-CH_2$ to give a hydrophobic, rigid spacer (Φ denotes a phenyl ring, i.e. in this case C_6H_4).

For the specific (but important) case when X equals CH_2CH_2 in equation (17.1), the dihalo compound is not very reactive. The preferred synthesis route is then as follows:

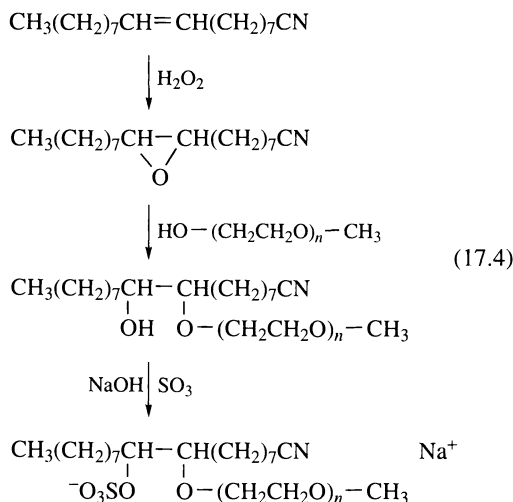


Anionic and nonionic geminis are often prepared by ring opening of a bisepoxide, giving a bishydroxyether intermediate. We show below a synthesis of a gemini surfactant with sulfates as the polar headgroups (Compound **5** of Figure 17.2):



where R is an alkyl group of normal surfactant chain length and Y is $-OCH_2CH_2O-$.

Below is shown the synthesis for the heterogemini surfactant Compound **7** of Figure 17.2:



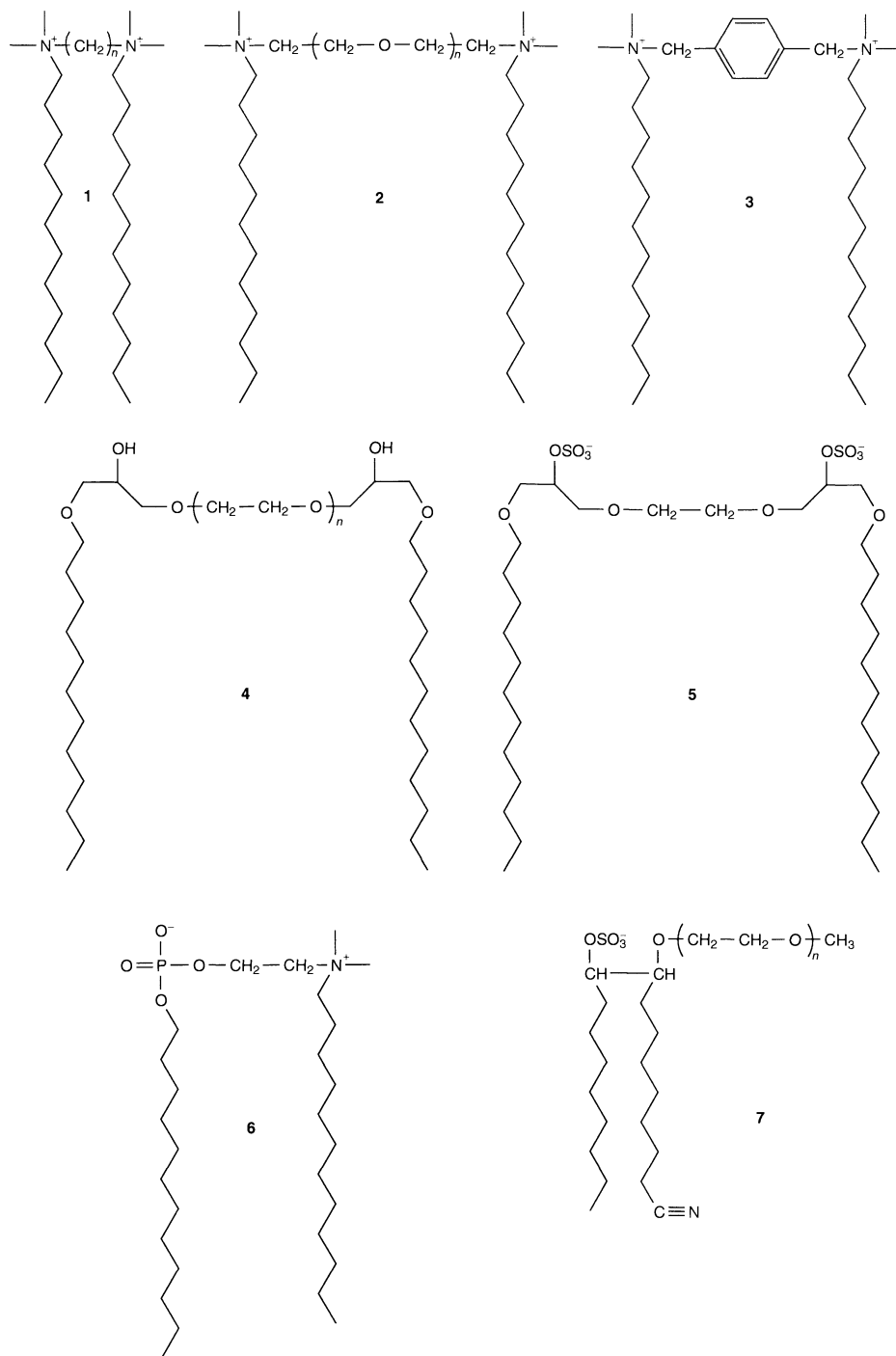


Figure 17.2. Structures of some gemini surfactants. Compounds 1–3 are cationics differing in the type of spacer unit, Compounds 4 and 5 are nonionic and anionic surfactants, respectively, based on the same backbone structure, while Compounds 6 and 7 are heterogemini surfactants, having non-equal polar head-groups

1.3 Micellization and behaviour at the air–water interface

A very striking feature of gemini surfactants is that they start to form micelles at a concentration more than one order of magnitude lower than that of the corresponding “monomer” surfactant. The low value of the critical micelle concentration (CMC) is an important property, implying, for instance, that geminis are very effective in solubilizing oily components. The efficiency of geminis, expressed as the C_{20} value, i.e. the surfactant concentration at which the surface tension (γ) is lowered by 20 mN/m, is also very high, again when compared with the monomeric species. The effectiveness of geminis, which is given by the value of the surface tension at the CMC (γ_{CMC}) is usually also somewhat better than for the corresponding monomeric surfactants. Figure 17.3 shows surface tension plots for a cationic gemini surfactant and for the corresponding monomeric amphiphile.

The dynamic surface tension is an important property, relevant to many practical, non-equilibrium processes such as emulsification and foaming. Dynamic surface tension is a measure of how fast, in the millisecond range, a surfactant decreases the surface tension from the value of pure water (around 70 mN/m) to values in the range of 30 mN/m. It has been found that the type of spacer governs the dynamic surface tension of geminis to a considerable degree, i.e. the longer and

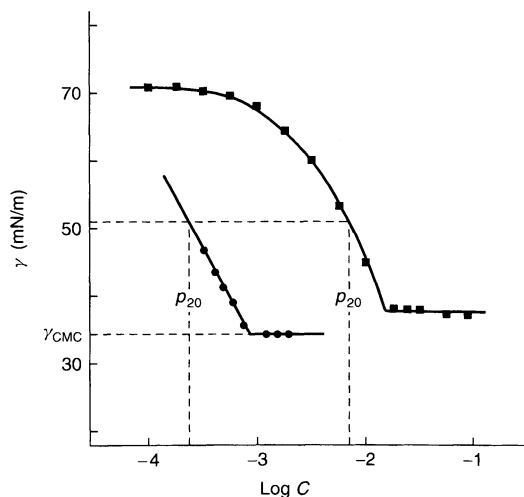


Figure 17.3. Surface tension versus log concentration plots of the gemini surfactant $C_{12}H_{25}N(CH_3)_2-(CH_2)_3-N(CH_3)_2C_{12}H_{25}^{2+}.2Br^-$ (●) and the monomeric surfactant $C_{12}H_{25}N(CH_3)_3^+.Br^-$ (■). (From R. Zana, Dimeric (gemini) surfactants, in *Novel Surfactants* (Ed. K. Holmberg), Surfactant Science Series 74, Marcel Dekker, New York, 1998)

the more flexible the spacer, then the better, i.e. the shorter, the time before the onset of surface tension reduction.

Geminis with flexible spacers, both hydrophilic and hydrophobic, generally show lower γ_{CMC} values than the corresponding surfactants with rigid spacers. This is probably due to a better packing of the former at the air–water interface (see below).

As mentioned above, geminis have remarkably low CMC values when compared with conventional surfactants of the same hydrocarbon chain length. CMC ratios as high as 80 between monomeric and dimeric species have been reported. Somewhat surprisingly, the CMC values are not very dependant on the polarity of the spacer. The values change with the length of the spacer, however, as is illustrated in Figure 17.4 for three series of cationic gemini surfactants, all having hydrophobic spacers. For all three series, there is a CMC maximum at a spacer length of 5–6 carbon atoms. This maximum has been attributed to changes of spacer conformation and its resulting effect on head-group hydration and alkyl chain orientation. When the spacer becomes long enough it is likely to twist in order to allow its middle portion to reside in the micelle interior, thus contributing to the hydrophobicity of the surfactant. For geminis with a hydrophilic spacer, such as oligo(ethylene glycol), the CMC values keep increasing with increasing spacer chain length.

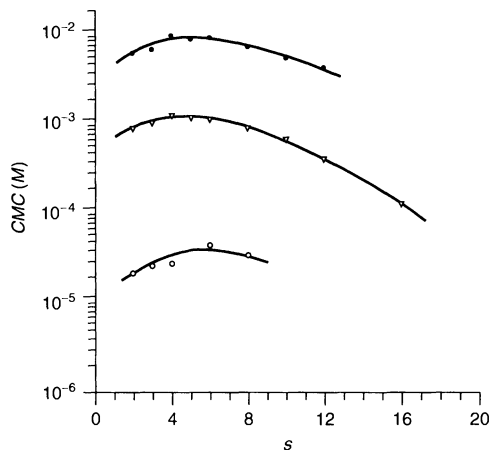


Figure 17.4. Variation of CMC against the number of methylene groups, s , in the spacer for three series of cationic gemini surfactants: (●) $C_{10}H_{21}N(CH_3)_2-(CH_2)_s-N(CH_3)_2C_{10}H_{21}^{2+}.2Br^-$; (∇) $C_{12}H_{25}N(CH_3)_2-(CH_2)_s-N(CH_3)_2C_{12}H_{25}^{2+}.2Br^-$; (○) $C_{16}H_{33}N(CH_3)_2-(CH_2)_s-N(CH_3)_2C_{16}H_{33}^{2+}.2Br^-$. (From R. Zana, Dimeric (gemini) surfactants, in *Novel Surfactants* (Ed. K. Holmberg), Surfactant Science Series 74, Marcel Dekker, New York, 1998)

The area occupied by a surfactant at the air–water interface can be obtained from the slope of the curve of surface tension, γ , versus the logarithm of surfactant concentration, $\ln C$, using the Gibbs equation, which can be expressed as follows:

$$\Gamma = - \left(\frac{1}{nRT} \right) \left(\frac{d\gamma}{d \ln C} \right) \quad (17.5)$$

where Γ is the surface excess concentration, n is 3 for ionic gemini surfactants, R is the gas constant and T is the absolute temperature. Figure 17.5 shows the variation of area per surfactant molecule at the surface with the spacer length for a series of cationic geminis. As can be seen, there is a pronounced maximum at 10–12 carbon atoms in the spacer. This maximum has been explained in terms of change of location of the hydrophobic spacer. At chain lengths below 10, the spacer lies more or less flat at the interface, thus occupying a larger and larger area as the number of methylene groups increases. Above around 12 carbon atoms, the spacer chain starts to fold, hence forming a loop into the air. This is analogous to the explanation of the relationship between *CMC* and the chain lengths of the hydrophobic spacers given above.

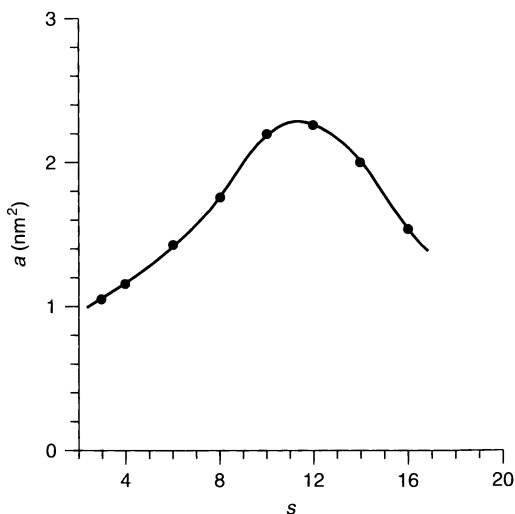


Figure 17.5. Variation of the area, a , per surfactant molecule at the air–water interface against the number of methylene groups, s , in the spacer for the series of gemini surfactants $C_{12}H_{25}N(CH_3)_2-(CH_2)_s-N(CH_3)_2C_{12}H_{25}^{2+} \cdot 2Br^-$. (From R. Zana, Dimeric (gemini) surfactants, in *Novel Surfactants* (Ed. K. Holmberg), Surfactant Science Series 74, Marcel Dekker, New York, 1998)

1.4 Micelle shape and effect on rheology of solutions of gemini surfactants

At low concentrations, i.e. just above the *CMC*, cationic geminis form spherical micelles just as their monomeric counterparts do. The aggregation number, i.e. the number of molecules that make up a micelle, for surfactants with 12 carbon atoms in the hydrophobic tails goes from around 40 for the species with two methylene groups as the spacer to around 25 for the surfactant with a ten-methylene spacer unit. The surfactants with short spacers (two, three and four methylene groups) show a very steep growth of the aggregation number with concentration, thus indicating a transition from spherical to elongated micelles, already at a very low surfactant concentration. The surfactants with longer spacer units show a much less pronounced micelle growth with increasing concentration, in this respect resembling the behaviour of the corresponding monomeric surfactants. The difference in the slopes of the plots of the aggregation numbers versus surfactant concentrations between geminis with short spacers and those with long spacers, schematically illustrated in Figure 17.6, can be explained as follows. When the spacer consists of four carbon atoms or less, the distance between the charged head-groups becomes shorter than the inter-head-group distance in conventional micelles. The surfactant packing in the micelles will therefore be different from the packing of the corresponding normal surfactant having the same hydrophobic tail. The gemini surfactant can be said to pack as if the polar head-group were smaller than it really is. This is the reason why the transition from spherical to rod-like aggregates occurs so readily; for geometrical reasons, surfactants with small

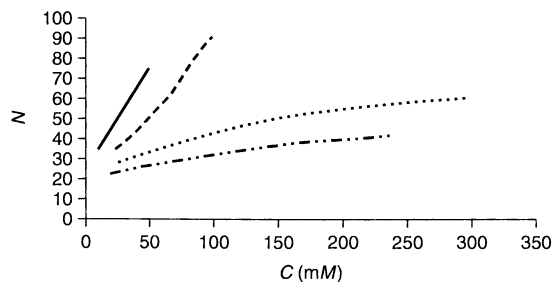


Figure 17.6. Variation of micelle aggregation number, N , with surfactant concentration, C , for cationic geminis with $C_{12}H_{25}$ hydrophobic tails and with different lengths of the spacer: (—) three methylene groups; (---) four methylene groups; (.....) five methylene groups. The monomeric analogue, didodecylidimethylammonium bromide, is shown as a reference (— · — · — ·). (Data taken from K. Esumi *et al.*, *Langmuir*, **13**, 2585 and 2803 (1997))

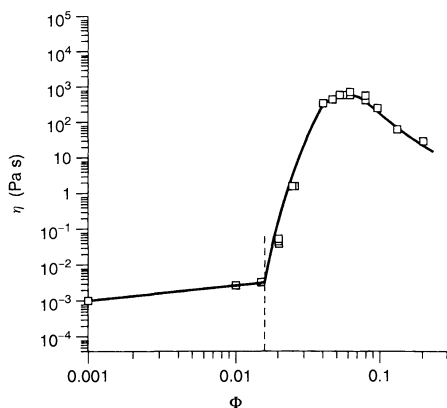


Figure 17.7. Variation of the zero shear viscosity, η , with the surfactant volume fraction, Φ , of solutions of the cationic gemini surfactant $C_{12}H_{25}N(CH_3)_2-(CH_2)_2-N(CH_3)_2C_{12}H_{25}^{2+}$, $2Br^-$ at $20^\circ C$. (From F. Kern *et al.*, *Langmuir*, **10**, 1714 (1994))

head-group areas prefer to arrange themselves in elongated structures. When the spacer length becomes equivalent or larger than the normal inter-head-group distance in micelles of cationic surfactants, the growth of the micelle with surfactant concentration for geminis is similar to that displayed for monomeric surfactants.

The shape of the micelles governs the solution viscosity of gemini surfactants. The cationic gemini surfactant with $C_{12}H_{25}$ hydrophobic tails and a two-methylene spacer unit exhibits a dramatic viscosity increase at about 2 wt% surfactant. As can be seen from Figure 17.7, the viscosity increases between six and seven orders of magnitude within a rather narrow concentration range. This is a much more pronounced viscosity increase with concentration than what one normally encounters with cationic surfactants and can be accounted for by the sharp transition from spherical to thread-like micelles characteristic of geminis with short spacer units. It can also be noted that thread-like micelles, and thus increased viscosity, can be induced by the use of an applied shear already at a concentration below that where they form under static conditions. The unusual rheological behaviour of gemini surfactants, which takes place at relatively low surfactant concentrations, can have important practical consequences.

1.5 Concluding remarks

This overview only covers isolated aspect of the interesting chemistry of gemini surfactants. This surfactant

class is subject to much evaluation work at present and one may foresee that the attractive features of these surfactants, such as high efficiency, low CMC and γ_{CMC} , and a very steep rise in viscosity with concentration, will find practical use. The high surfactant efficiency and the low CMC has triggered much effort into using gemini surfactants as solubilizers of various kinds. In model experiments, using hydrocarbons as the compounds to be solubilized, geminis have been found to be significantly better than conventional surfactants, both on molar and on weight basis. It may be that the tubular shape of the aggregates contributes to the excellent solubilization capacity of geminis.

Much effort is also devoted to exploit the specific geometry of gemini surfactants to create structures of well-defined geometry. Gemini surfactants form vesicles and liquid crystalline phases over broad concentration ranges, a property that can be taken advantage of for a variety of applications. One example of such work is the preparation of a mesoporous molecular sieve called MCM-48. This material is cubic in structure and is characterized by a three-dimensional pore system. It is made from a template of a cubic liquid crystal composed of cationic geminis with very long spacer units, typically 12 methylene groups. The liquid crystal is formed in a solution of tetraethylorthosilicate. The silicate is allowed to gel by a pH adjustment, hence solidifying the liquid crystalline structure. The surfactant is subsequently removed by a calcination procedure leaving a residue with a very high surface area and an extremely well-defined pore radius. The radius can be tailor-made by the choice of surfactant: the cationic gemini with $C_{16}H_{33}$ hydrophobic tails gives a pore radius of 12 Å, while that with $C_{18}H_{37}$ tails gives a pore radius of 13 Å. This kind of synthesis precision is valuable in materials technology, e.g. in the synthesis of carrier materials for heterogeneous catalysis.

2 CLEAVABLE SURFACTANTS

2.1 Introduction

By tradition, surfactants are stable species. Among the surfactant work-horses, e.g. anionics such as alkylbenzene sulfonates and alkyl sulfates, nonionics such as alcohol ethoxylates and alkylphenol ethoxylates, and cationics such as alkyl quats and dialkyl quats, only the alkyl sulfates are not chemically stable under normal conditions. Through the years the susceptibility of alkyl sulfates to acid-catalysed hydrolysis has been seen as a considerable problem, particularly well-known for the

most prominent member of the class, i.e. sodium dodecyl sulfate (SDS). The general attitude has been that weak bonds in a surfactant may cause handling and storage problems and should therefore be avoided.

In recent years, the attitude towards easily cleavable surfactants has been changed. Environmental concern has become one of the main driving forces for the development of new surfactants and the rate of biodegradation has become a major issue. One of the main approaches taken to produce readily biodegradable surfactants is to build into the structure a bond with limited stability. For practical reasons, the weak bond is usually the bridging unit between the polar head-group and the hydrophobic tail of the surfactant, which means that degradation immediately leads to destruction of the surface activity of the molecule, an event usually referred to as the primary degradation of the surfactant. Biodegradation then proceeds along various routes, depending on the type of primary degradation product. The ultimate decomposition of the surfactant, often expressed as the amount of carbon dioxide evolved during four weeks exposure to appropriate micro-organisms, counted as the per cent of the amount of carbon dioxide that could theoretically be produced, is the most important measure of biodegradation. It seems that for most surfactants containing easily cleavable bonds, the values for ultimate decomposition are also higher than for the corresponding surfactants lacking the weak bond. Thus, the strong trend towards more environmentally benign products favours the cleavable-surfactant approach on two accounts.

A second incentive for the development of cleavable surfactants is to avoid complications such as foaming or formation of unwanted, stable emulsions after use of a surfactant formulation. Cleavable surfactants present the potential for elimination of some of these problems. If the weak bond is present between the polar and the non-polar part of the molecule, cleavage will lead to one water-soluble and one water-insoluble product. Both moieties can usually be removed by standard work-up procedures. This approach has been of particular interest for surfactants used in preparative organic chemistry and in various biochemical applications.

A third use of surfactants with limited stability is to have the cleavage product impart a new function. For instance, a surfactant used in personal care formulations may decompose on application to form products beneficial to the skin. Surfactants that after cleavage impart a new function are sometimes referred to as "functional surfactants".

Finally, surfactants that, in a controlled way, break down into non-surfactant products may find use in

specialized applications, e.g. in the biomedical field. For instance, cleavable surfactants which form vesicles or microemulsions can be of interest for drug delivery, provided that the metabolites are non-toxic.

Most cleavable surfactants contain a hydrolysable bond. Chemical hydrolysis is either acid- or alkali-catalysed and many papers have discussed the surfactant breakdown in terms of either of these mechanisms. In the environment, bonds susceptible to hydrolysis are often degraded by enzymatic catalysis, but few papers dealing with cleavable surfactants have investigated such processes *in vitro*. Other approaches that have been taken include the incorporation of a bond that can be destroyed by UV irradiation or the use of an ozone-cleavable bond. This presentation is subdivided according to the type of weak linkage present in the surfactant.

2.2 Acid-labile surfactants

2.2.1 Cyclic acetals

Cyclic 1,3-dioxolane (five-membered ring) and 1,3-dioxane (six-membered ring) compounds, illustrated in Figure 17.8, were early examples of acid-labile surfactants. They are typically synthesized from a long-chain aldehyde by reaction with a diol or a higher polyol. Reaction with a vicinal diol gives the dioxolane, while 1,3-diols yield dioxanes.

If the diol contains an extra hydroxyl group, such as in glycerol, a hydroxy acetal is formed and the remaining hydroxyl group can subsequently be derivatized to give anionic or cationic surfactants, as illustrated in Figure 17.9. It is claimed that glycerol gives ring closure to dioxolane, yielding a free, primary hydroxyl

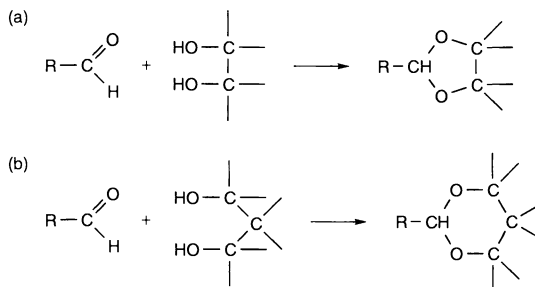


Figure 17.8. Preparation of (a) 1,3-dioxolane and (b) 1,3-dioxane surfactants from a long chain aldehyde and a 1,2- and a 1,3-diol, respectively. (From K. Holmberg, *Cleavable surfactants*, in *Novel Surfactants* (Ed. K. Holmberg), Surfactant Science Series 74, Marcel Dekker, New York, 1998)

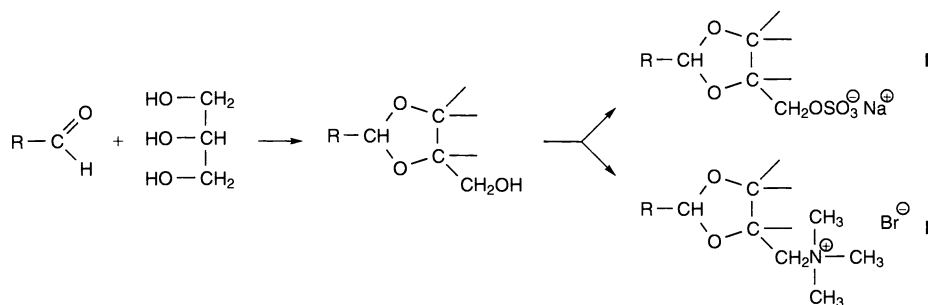


Figure 17.9. Examples of anionic (I) and cationic (II) 1,3-dioxolane surfactants

group, but it is likely that some dioxane with a free, secondary hydroxyl group is formed as well. This free hydroxyl group can be treated with SO_3 and then neutralized to give the sulfate, it can be reacted with propane sultone to give the sulfonate, or it can be substituted by bromine or chloride and then reacted with dimethylamine to give a tertiary amine as the polar group. Quaternization of the amine can be made in the usual manner, e.g. with methyl bromide. The remaining hydroxyl group may also be ethoxylated to give nonionic chemodegradable surfactants. The rate of decomposition in sewage plants of this class of nonionic surfactants is much higher than for normal ethoxylates.

Hydrolysis splits acetals into aldehydes, which are intermediates in the biochemical β -oxidation of hydrocarbon chains. Acid-catalysed hydrolysis of unsubstituted acetals is generally facile and occurs at a reasonable rate at pH 4–5 at room temperature. However, electron-withdrawing substituents, such as hydroxyl, ether oxygen and halogens, reduce the hydrolysis rate. Anionic acetal surfactants are more labile than cationic, a fact that can be ascribed to the locally high oxonium ion activity around such micelles. The same effect can be seen also for surfactants forming vesicular aggregates, again undoubtedly due to differences in the oxonium ion activity in the pseudo-phase surrounding the vesicle. Acetal surfactants are stable at neutral and high pH levels.

The 1,3-dioxolane ring has been found to correspond to approximately two oxyethylene units with regard to effect on the *CMC* and adsorption characteristics. Thus, surfactant type I in Figure 17.9 should resemble ether sulfates of the general formula $\text{R}(\text{OCH}_2\text{CH}_2)_2\text{OSO}_3\text{Na}$. This is interesting since the commercial alkyl ether sulfates contain two to three oxyethylene units.

2.2.2 Acyclic acetals

Alkyl glucosides, often somewhat erroneously referred to as alkyl polyglucosides or APGs, are cyclic compounds but since the ring does not involve the two geminal hydroxyl groups of the aldehyde hydrate, it is included here in the category of acyclic acetals. Alkyl glucosides are by far the most important type of acetal surfactant.

Alkyl glucosides are made either by direct condensation of glucose and a long-chain alcohol or by transesterification of a short-chain alkyl glucoside, such as ethyl glucoside, with a long chain alcohol, in both cases by using an acid catalyst (Figure 17.10). The procedure leads to some degree of sugar ring condensation, the extent of which can be governed by various means, e.g. the ratio of long-chain alcohol to sugar.

The alkyl glucoside surfactants break down into glucose and long-chain alcohol under acidic conditions. On the alkaline side, even at very high pH, they are

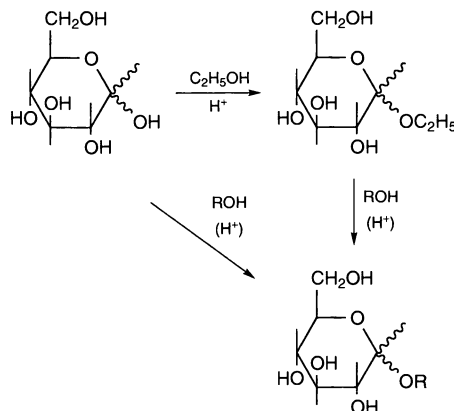


Figure 17.10. Two routes of preparation of alkyl glucosides (R is a long-chain alkyl)

stable to hydrolysis. Their cleavage profiles, along with their relatively straightforward synthesis routes, make these surfactants interesting candidates for various types of cleaning formulations.

Polyoxyethylene-based cleavable surfactants have been synthesized by reacting end-capped poly(ethylene glycol) (PEG) with a long-chain aldehyde, as shown in Figure 17.11. During acid hydrolysis, these compounds will revert to the original fatty aldehyde and end-capped PEG. Studies of the relationship between structure and hydrolytic reactivity have shown that the hydrolysis rate increases as the hydrophobe chain length decreases when the hydrophilic part was kept the same. This has been attributed to decreased hydrophobic shielding of the acetal linkage from oxonium ions. No effect on the hydrolysis rate was seen when the hydrophilic part was varied while the hydrophobic part was kept constant or when the structure of the hydrophobe was varied from linear to branched. Furthermore, the hydrolytic reactivity is higher for non-aggregated than for micellized surfactants.

Acetal surfactants have been found to resemble traditional surfactants in terms of their physico-chemical properties. However, it has been reported that the *CMC* values for acetal-containing surfactants are somewhat lower than those of the corresponding conventional surfactants. Furthermore, the efficiency of the surfactants, expressed as the concentration required to produce a 20 mN/m reduction in surface tension, was higher for the cleavable surfactants. Evidently, the acetal linkage connecting the hydrophobic tail and the polar head-group gives a contribution to the surfactant

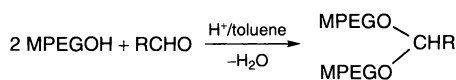


Figure 17.11. Preparation of a cleavable surfactant containing two polyoxyethylene chains (R is a long-chain alkyl)

hydrophobicity, thus resulting in higher adsorption efficiency at the air–water interface and increased tendency to aggregate into micelles.

2.2.3 Ketals

Surfactants containing ketal bonds can be prepared from a long-chain ketone and a diol in analogy with the reaction schemes given in Figures 17.8 and 17.9 for the preparation of acetal surfactants. Nonionic cleavable surfactants based on a long-chain carbonyl compound, glycerol and a polyoxyethylene chain have been commercialized. Both long-chain ketones and aldehydes can be used and they form cyclic ketals and acetals, respectively, upon condensation with glycerol, as discussed above for cyclic acetals. Ketones give primarily 4-hydroxymethyl-1,3-dioxolanes, whereas aldehydes give a mixture of 4-hydroxymethyl-1,3-dioxolanes and 5-hydroxy-1,3-dioxanes. The remaining hydroxyl function is alkoxyated in the presence of a conventional base catalyst.

Ketal-based surfactants have also been prepared in good yields from esters of keto acids by either of two routes, as shown in Figure 17.12. The biodegradation profiles of the dioxolane surfactants of Figure 17.12 are shown in Figure 17.13. As expected, the degradation rate is very dependent on the alkyl chain length. The process is markedly faster for the labile surfactants (and particularly for structure “a” which contains an extra ether oxygen) than for the conventional carboxylate surfactant of the same alkyl chain length used as the reference. Ketal surfactants are in general more labile than the corresponding acetal surfactants. As an example, a ketal surfactant kept at pH 3.5 was cleaved to the same extent as an acetal surfactant of similar structure kept at pH 3.0. The relative lability of the ketal linkage is due to the greater stability of the carbocation formed during ketal hydrolysis when compared to the

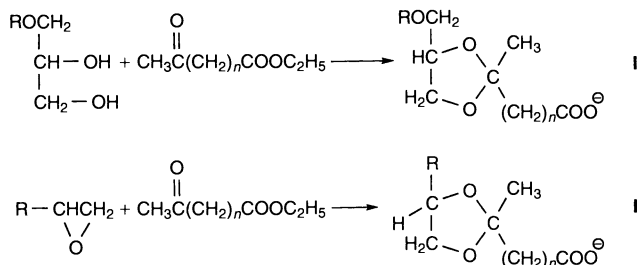


Figure 17.12. Preparation of anionic 1,3-dioxolane surfactants from ethyl esters of keto acids. (From A. Sokolowski *et al.*, *J. Am. Oil Chem. Soc.*, **69**, 633 (1992))

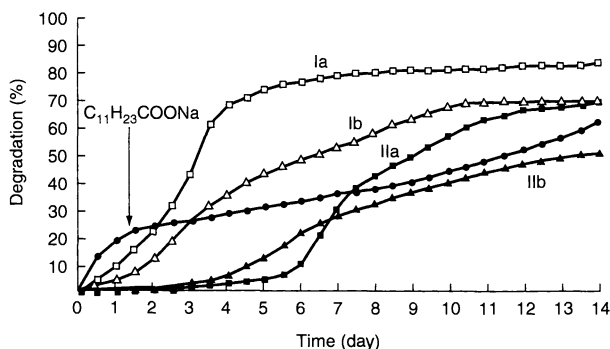


Figure 17.13. Rate of biodegradation versus time for four ketal surfactants with sodium dodecanoate as reference (I and II relate to the compounds of Figure 17.12): (a) $R = C_{12}H_{25}$, $n = 2$; (b) $R = C_{16}H_{33}$, $n = 2$. (From D. Ono, *et al.*, *J. Am. Oil Chem. Soc.*, **72**, 853 (1995))

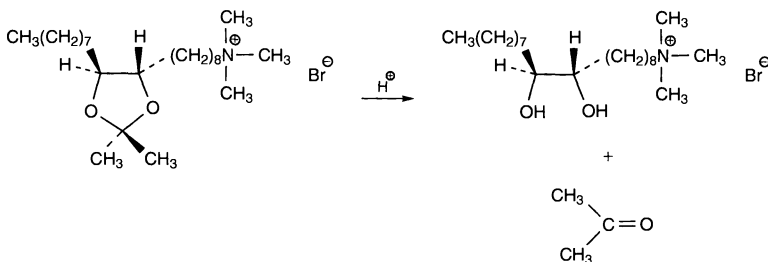


Figure 17.14. Acid-catalysed hydrolysis of a second-generation cleavable surfactant. (From D. A. Jaeger, *Supramol. Chem.*, **5**, 27 (1995))

carbocation formed during acetal hydrolysis. (It is noteworthy that biodegradation of an acetal surfactant has been found to be faster than for a ketal surfactant of very similar structure. Evidently, there is no strict correlation between the ease of biodegradation and the rate of chemical hydrolysis.)

The term “second-generation cleavable surfactant” has been introduced for labile surfactants which on cleavage give another surfactant together with a small water-soluble species. The daughter surfactant generally has a higher *CMC* than the parent surfactant. Figure 17.14 shows a typical example of a second-generation cleavable surfactant. The concept has been applied to a variety of structures, including phospholipid analogues and several applications of this specific type of cleavable surfactants have been proposed.

2.2.4 Ortho esters

Ortho esters are a new class of surfactants that have recently been described. Surfactant ortho esters are conveniently prepared by transesterification of a

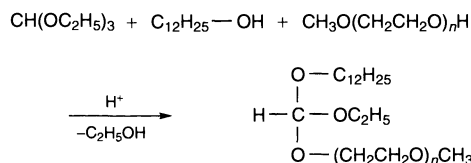


Figure 17.15. Synthesis and structure of an ortho-ester-based surfactant. (From P. -E. Hellberg *et al.*, *J. Surf. Det.*, **3**, 369 (2000))

low-molecular-weight ortho ester (such as triethylorthoformate) with fatty alcohol and poly(ethylene glycol) (PEG). An example of a typical structure and method of preparation are given in Figure 17.15. Due to the trifunctionality of the ortho ester, a distribution of species is obtained. Furthermore, if the reactant alcohol is difunctional, cross-linking will occur and a large network may be formed. Such compounds have been shown to be effective foam depressants and an example based on poly(propylene glycol) (PPG) and PEG is shown in Figure 17.16. By varying the number and types of substituents (fatty alcohol, alkyleneoxy group, end blocking,

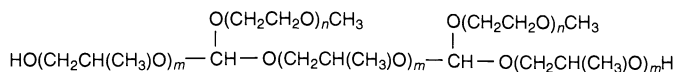


Figure 17.16. An ortho-ester-based block copolymer. (From P. -E. Hellberg *et al.*, *J. Surf. Det.*, **3**, 369 (2000))

etc.), the properties of the ortho-ester-based surfactant or block copolymer can be tailor-made for a specific field of application.

Hydrolysis of ortho esters occurs by a mechanism analogous to that of acetals and ketals and gives rise to one mole of formate and two moles of alcohols. Both formates and alcohols can be regarded as non-toxic substances and recent research has shown that surface-active formates (similar to surface-active alcohols and esters, but in contrast to surface-active aldehydes) have no or little dermatological effect, evaluated in terms of sensitizing capacity and irritancy. Ortho-ester-based surfactants undergo acid-catalysed cleavage much more readily than acetal-based surfactants under the same conditions. For instance, a water-soluble ortho ester based on octanol and monomethyl-PEG is hydrolysed to 50% in 2 h at pH 5. The structure of the surfactant has been found to influence the hydrolysis rate and, in general, a more hydrophilic surfactant has a higher decomposition rate.

Ortho-ester linkages can also be used to improve biodegradation properties in long-chain ethoxylates or block copolymers. It has been shown that a conventional PEG–PPG copolymer with a molecular weight of 2200 biodegrades to only 3% in 28 days. However, if an equivalent molecule is built up from PEG 350 and PPG 400, connected with ortho-ester links, it will reach 62% biodegradation within 28 days and thus be classified as “readily biodegradable”.

2.3 Alkali-labile surfactants

2.3.1 Normal ester quats

By the term “ester quat”, we refer to surface-active quaternary ammonium compounds which have the general formula $\text{R}_4\text{N}^+\text{X}^-$ and in which the long-chain alkyl moieties, R, are linked to the charged head-group by an ester bond and with X^- being a counterion. With “normal” ester quats, we mean surfactants based on esters between one or more fatty acids and a quaternized amino alcohol. Figure 17.17 shows examples of three different ester quats, all containing two long-chain and two short substituent on the nitrogen atom. This figure also shows the “parent”, non-cleavable quat. As can be seen, the

ester-containing surfactants contain two carbon atoms between the ester bond and the nitrogen which carries the positive charge. Cleavage of the ester bonds of surfactants **II–IV** yields a fatty acid soap in addition to a highly water-soluble quaternary ammonium di- or triol. These degradation products exhibit low fish toxicity and they are degraded further by established metabolic pathways. The overall ecological characteristics of ester-quats are much superior to those of traditional quats, such as that represented by compound **I** of Figure 17.17.

During the last decade, the dialkylester quats have to a large extent replaced the stable dialkyl quats as rinse-cycle softeners, which is the single largest application for quaternary ammonium compounds. The switch from stable dialkyl quats to dialkylester quats may represent the most dramatic change of product type in the history of surfactants, and is entirely environment-driven. Unlike stable quats, ester quats show excellent values for biodegradability and aquatic toxicity. Ester quats have also fully or partially replaced traditional quats in other applications of cationics, such as hair care products and various industrial formulations.

The cationic charge close to the ester bond renders normal ester quats unusually stable to acid and labile

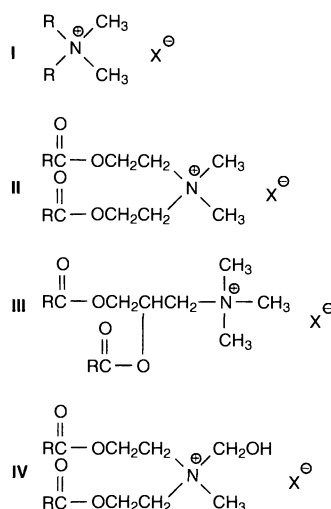


Figure 17.17. Structures of one conventional quaternary ammonium surfactant (**I**) and three ester quats (**II–IV**) (R is a long-chain alkyl, and X is Cl, Br or CH_3SO_4)

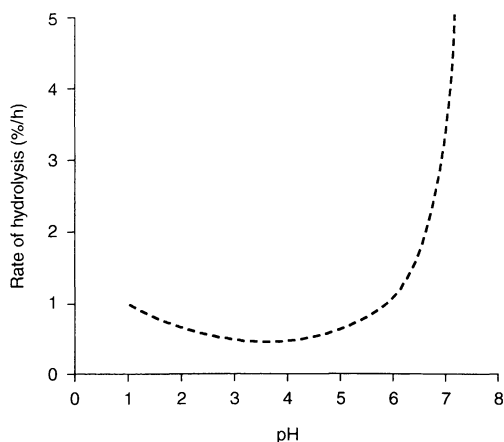


Figure 17.18. Influence of pH on the hydrolytic stability of the diacetylstere of bis(2-hydroxyethyl)ammonium chloride at 25°C. (From G. Krüger *et al.*, Esterquats, in *Novel Surfactants* (Ed. K. Holmberg), Surfactant Science Series 74, Marcel Dekker, New York, 1998)

to alkali. The strong pH dependence of the hydrolysis can be taken advantage of to induce rapid cleavage of the product. This phenomenon is even more pronounced for betaine esters and the mechanism of hydrolysis is discussed in some detail in the following section. Figure 17.18 illustrates the pH dependence of hydrolysis of an ester quat. As can be seen, the hydrolysis rate is at a minimum between pH 3 and 4 and accelerates strongly above pH 5–6. Evidently, formulations containing ester quats must be maintained at low pH.

2.3.2 Betaine esters

The rate of alkali-catalysed ester hydrolysis is influenced by adjacent electron-withdrawing or electron-donating groups. A quaternary ammonium group is strongly electron-withdrawing. The inductive effect will lead to a decreased electron density at the ester bond;

hence, alkaline hydrolysis, which starts by a nucleophilic attack by hydroxyl ions at the ester carbonyl carbon, will be favoured. Compounds **II–IV** of Figure 17.17 all have two carbon atoms between the ammonium nitrogen and the –O–oxygen of the ester bond. Such esters undergo alkaline hydrolysis at a faster rate than esters lacking the adjacent charge, although the difference is not very large. If, on the other hand, the charge is at the other side of the ester bond, the rate enhancement is much more pronounced. Such esters are extremely labile on the alkaline side, but very stable even under strongly acidic conditions. The large effect of the quaternary ammonium group on the alkaline and acid rates of hydrolysis is due to a stabilization/destabilization of the ground state, as illustrated in Figure 17.19. The charge repulsion, involving the carbonyl carbon atom and the positive charge at the nitrogen atom, is relieved by hydroxide ion attack, but augmented by protonation. The net result is that compared with an ester lacking the cationic charge, the rate of alkaline hydrolysis is increased 200-fold, whereas the rate of acid hydrolysis is decreased 2000-fold. For surface-active betaine esters based on long-chain fatty alcohols the rate of alkaline hydrolysis is further accelerated due to micellar catalysis. However, the presence of large, polarizable counterions, such as bromide, can completely outweigh the micellar catalysis.

The extreme pH dependence of surface-active betaine esters makes them interesting as cleavable cationic surfactants. The shelf life is long when stored under acidic conditions and the hydrolysis rate will then depend on the pH at which they are used. Single-chain surfactants of this type has been suggested as “temporary bactericides” for use in hygiene products, for disinfection in the food industry and in other instances where only a short-lived bactericidal action is wanted. The patent literature also contains examples of betaine esters containing two long-chain alkyl groups. Two examples are given in Figure 17.20.

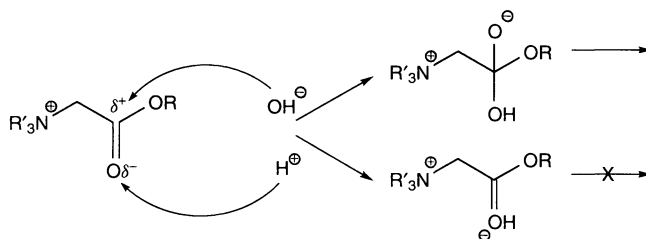


Figure 17.19. Mechanisms for acid- and base-catalysed hydrolysis of a betaine ester

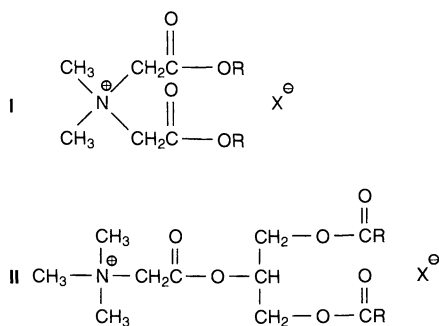


Figure 17.20. Structures of two surface-active betaine esters (R and X are the same as those in Figure 17.17)

2.4 Concluding remarks

Amphiphiles with an acid- or alkali-labile bond constitute the most widely explored routes to achieve cleavable surfactants. However, other approaches have also been taken. For instance, several types of surfactants with UV-labile bonds have been synthesized and evaluated. Photochemical cleavage yields non-surface-active species and the concept is attractive because it allows an extremely fast breakdown of the surfactant to occur.

An interesting use of photolabile surfactants is as emulsifiers in emulsion polymerization. The use of a photolabile emulsifier opens the possibility to control the latex coagulation process simply by exposing the dispersion to UV irradiation. The ionic head-group of the surfactant will be split off by photolysis, thus leading to aggregation of the latex particles. Such latexes could be of interest for coatings applications.

Another example of UV-labile amphiphiles relate to double-chain surfactants containing Co(III) as the complexing agent for two single chain surfactants based on ethylene diamine in the polar head-group. UV irradiation, or merely sunlight, causes reduction of Co(III) to Co(II). The latter gives a very labile complex and the double-chain surfactant immediately degrades into two single-chain moieties.

Ozone-cleavable surfactants have also been developed as examples of environmentally benign amphiphiles. These surfactants, which contain unsaturated bonds, break down easily during ozonization of water, which is a water purification process of growing importance. It is likely that other mechanisms of surfactant breakdown in the environment will be explored in the future in the design of new surfactants with good environmental characteristics.

3 POLYMERIZABLE SURFACTANTS

3.1 Introduction

In many instances, surfactant action is needed at some stage of an operation but unnecessary, or even unwanted, at some later stage. The problems with residual surfactant may be environmentally related, such as with slowly biodegradable surfactants in sewage plants. The problems may also be of a technical nature since the presence of surface-active agents in the final product may affect the product performance in a negative way.

The paint area is a good example where surfactants are needed at one stage but unwanted at a later stage. Surfactants are used in paints as emulsifiers for the binder, as dispersants for the pigment and to improve wetting of the substrate. In the dried paint film, the presence of surfactant frequently causes problems, however, since the surfactant acts as an external plasticizer in the film, thus imparting softness and flexibility. This could be taken advantage of, had the plasticizer been evenly distributed in the coating. However, due to its surface activity, the surfactant will migrate out of the bulk phase and concentrate at the interfaces. It has been shown that surfactant molecules preferably go to the film-air interface, where they align with their hydrophobic tails pointing towards the air. As an example, calculations from electron spectroscopy for chemical analysis (ESCA) spectra show that the dried film from a lacquer containing 1% surfactant may have an average surface surfactant concentration of 50% (Figure 17.21). The overall bulk concentration of surfactant is still approximately 1% since the modified surface region is a very thin layer compared to the thickness of the whole film. The surfactant surface layer constitutes a so-called weak boundary layer when a second coating is applied, thus leading to the frequently encountered problem of repaintability.

It is also known that during the drying of emulsion paints the surfactant may undergo phase separation,

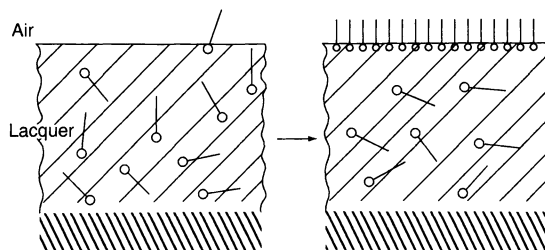


Figure 17.21. Migration of surfactant in a lacquer film leads to enrichment at the surface

forming lumps, tenths of microns wide, distributed throughout the film. Atomic force microscopy (AFM) studies have revealed that these surfactant lumps can extend far down into the film. On exposure to water, the surfactant is washed out of the film, the result being that deep cavities appear where the lumps had been. Such film defects are believed to be one of the causes of the poor water resistance of many latex paint films.

A way to overcome the problems associated with the presence of surfactant in the final product is to have the surfactant chemically bound to the latex particle or, alternatively, to make the surfactant polymerize during the setting or curing stage. In principle, the surfactant may either undergo homopolymerization or copolymerize with some other component of the system. In paints and lacquers, the obvious choice of co-reactant is the binder.

A completely different way to avoid the problem of residual surfactant in the end-product is to use cleavable surfactants, i.e. surfactants that spontaneously break down at some stage. This concept has been discussed above in Section 2.

3.2 Mode of surfactant polymerization

3.2.1 Homopolymerization versus copolymerization

In a formulation containing reactive surfactant, homopolymerization of the amphiphile may take place if the concentration is high enough. However, in most

technical formulations the surfactant concentration is too low to allow substantial homopolymerization in the bulk phase. A monolayer of surfactant, on the other hand, may homopolymerize when adsorbed at an interface, as will be shown below. The palisade layer may either form by adsorption from an aqueous solution or by migration through a film, as discussed above.

Copolymerization, on the other hand, may take place in a bulk phase. For copolymerization of a monomer, M_1 , and a surfactant, M_2 , to occur, the reactivity ratios should preferably be $r_1 \leq 1$ and $r_2 \leq 1$, where r_1 and r_2 are defined as $r_1 = k_{11}/k_{12}$ and $r_2 = k_{22}/k_{21}$, with k_{nm} being the rate constants for the four possible ways in which the monomer can add, shown as follows:



3.2.2 Autoxidative versus non-autoxidative polymerization

Autoxidation, i.e. oxygen-induced curing, may take place both during copolymerization in the bulk phase and during homopolymerization of a surface monolayer. Two surfactants capable of undergoing autoxidation are shown in Figure 17.22. Surfactants that can undergo

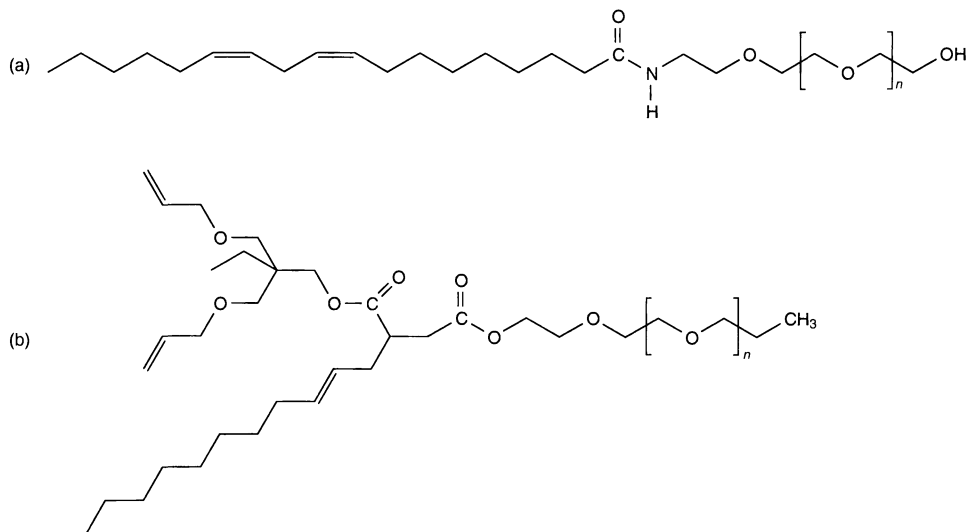


Figure 17.22. Two nonionic surfactants capable of autoxidation: (a) the ethoxylated monoethanolamide of linoleic acid; (b) the ethoxylated dodeceny succinic acid monoester of trimethylolpropanediallyl ether

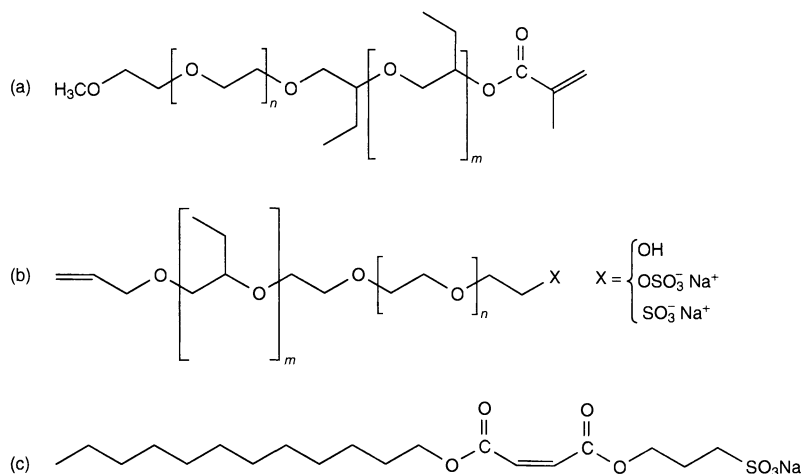


Figure 17.23. Examples of polymerizable surfactants: (a) A methacrylate ester of a methyl-capped block copolymer of ethylene oxide and butylene oxide; (b) an allyl-capped block copolymer of butylene oxide and ethylene oxide with varying end-groups; bottom; (c) monododecylmonosulfopropylmaleate

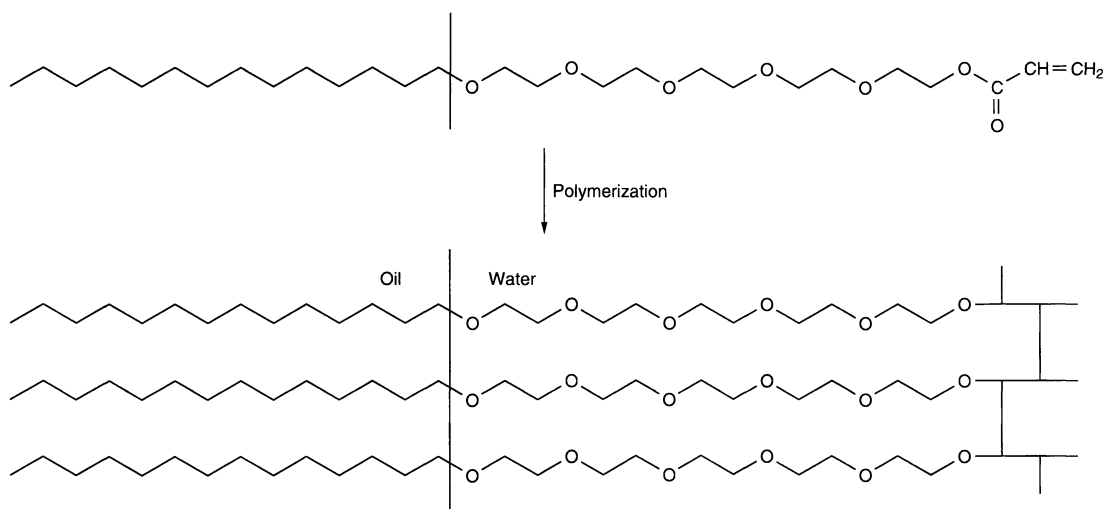


Figure 17.24. Schematic representation of a polymerizable nonionic surfactant with the reactive group in the hydrophilic part of the molecule

autoxidation are of particular interest in combination with alkyd resins. Autoxidation is normally catalysed by cobalt or manganese salts.

Non-autoxidative polymerization includes UV curing or thermally induced curing with the use of free-radical initiators, such as benzoyl peroxide or potassium persulfate. Similar to autoxidation, both bulk and surface curing may occur. Surfactants based on activated vinyl groups, such as acrylate and methacrylate esters, are typical examples of this class. Some examples of

surfactants capable of rapid UV curing are shown in Figure 17.23.

3.2.3 Position of polymerizable group

The reactive group may be present either in the polar, hydrophilic part or in the hydrophobic part of the surfactant molecule, as shown in Figures 17.24 and 17.25, respectively.

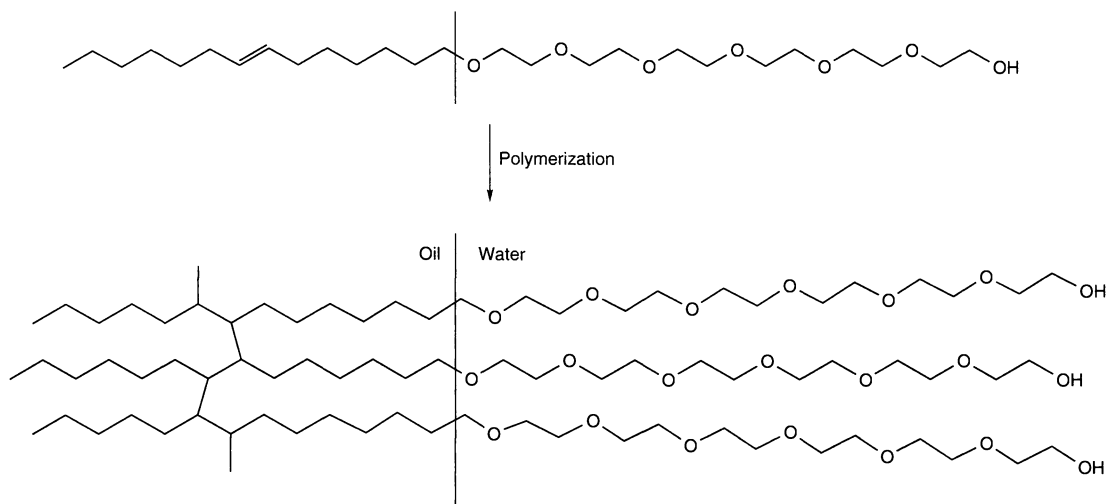


Figure 17.25. Schematic representation of a polymerizable nonionic surfactant with the reactive group in the hydrophobic part of the molecule

In liquid–liquid two-phase systems, the solubility characteristics of the initiator are important. The distribution of initiator between oil and water phases should be such that it is predominantly present in the phase where the polymerizable function is located. The polymerization depicted in Figure 17.24 is best served with a water-soluble initiator, whereas that of Figure 17.25 proceeds best with an oil-soluble one. In the most important application of polymerizable surfactants, that of emulsion polymerization (see below), water soluble initiators, such as potassium persulfate and hydrophilic azo compounds, are used.

In general, polymerization at the polar end of non-ionic surfactants, as illustrated in Figure 17.24, requires relatively severe conditions and often gives poor yields. When the same functional group is present in the hydrophobic tail, reactivity in a two-phase system is much higher. The poor reaction in the aqueous phase is probably due to the energetically unfavourable situation of two polyoxyethylene chains being forced close together to enable the new carbon–carbon link to form. Cross-linking of the polar groups should also be avoided if the surfactant after polymerization is expected to provide steric stabilization, for instance, in the stabilization of dispersed systems. The entropy term, which is the main driving force behind steric stabilization, will be reduced if the freedom of motion of the polar head-groups is restricted.

Cross-linking of the hydrophobic tails is also natural in those cases when the surfactant polymerizes when adsorbed at a hydrophobic surface. Adsorption at such

surfaces occurs with the surfactant hydrophobic chains come close together, an alignment that should facilitate formation of inter-chain bonds.

3.3 Applications of polymerizable surfactants

3.3.1 Emulsion polymerization

Polymerizable surfactants are of interest in emulsion polymerization, e.g. in the conversion of vinyl chloride to poly(vinyl chloride) (PVC) and of acrylates and vinyl acetate to lattices for coatings. Use of a reactive surfactant in vinyl chloride polymerization leads to PVC with improved shear stability. In lattices, polymerizable surfactants can bring about several advantages such as the following:

- improved stability against shear, freezing and dilution
- reduced foaming
- reduced problems with competitive adsorption (see below)
- improved adhesion properties of the film
- improved water and chemical resistance of the film

Competitive adsorption is a serious problem in many paint formulations, as well as in many other surfactant-containing formulations. A pigmented latex coating contains a variety of interfaces at which surfactants may adsorb, such as binder–water, pigment–water, substrate–water and air–water. In addition, the surfactant

molecules may assemble in micelles or form aggregates together with hydrophobic segments of the associative thickener which is normally present in today's latex paints. Since different surfactants are normally introduced into the system together with the individual components, e.g. emulsifier (often a mixture of an anionic and a nonionic surfactant) with the binder, pigment dispersant with the pigment, wetting agent added directly to the formulation, etc., the situation becomes very complex and competitive adsorption is a potential problem in all pigmented emulsion paints. The surface-active agent used as the binder emulsifier may desorb from the emulsion droplet and adsorb at the pigment surface. The pigment dispersing agent may go the other way. Such an exchange is known to occur and to cause problems in terms of instability and unwanted rheological behaviour.

Compounds of the types shown in Figure 17.23 are useful as reactive surfactants for latex preparation. Out of these, maleic acid derivatives are particularly interesting since they are unable to homopolymerize at ordinary temperature. The maleic-acid-based surfactant shown in this figure can be easily prepared by first reacting maleic anhydride with a fatty alcohol and subsequently treating the monoester formed with propane sultone (which is toxic and should be handled with great care). Extensive homopolymerization is unwanted since the resulting chains of oligomeric or polymeric surfactant will

constitute highly water-soluble segments on the surface of the latex particles. After drying, these will be distributed throughout the coating and may cause film defects. Instead, the reactive surfactant should preferably copolymerize, i.e. react only with latex monomers, in order to be evenly distributed on the particle surface. It is also important that the reactivity is not too high. If polymerization occurs too rapidly in the water phase, the surfactant-containing polymer may end up in the serum rather than on the particle surface. If the polymerizable surfactant is too rapidly consumed by polymerization in the emulsion droplets, the probability is high that the surfactant will be buried in the interior of the particle.

Polymerizable surfactants for lattices are sometimes referred to as "surfmers", with this name indicating that the surfactant can be seen as a special type of comonomer. Reactive surfactants can also be employed as initiators in which case they are called "inisurfs". Finally, they can be used as chain-transfer agents, i.e. to control the molecular weight of the latex polymer, in which case they are named "transurfs". Figure 17.26 shows representative examples of inisurfs and transurfs, along with structures of a conventional initiator and a conventional chain-transfer agent for emulsion polymerization. With the use of inisurfs of the type given in this figure, it is possible to prepare lattices of high-solids content without the use of extra surfactant.

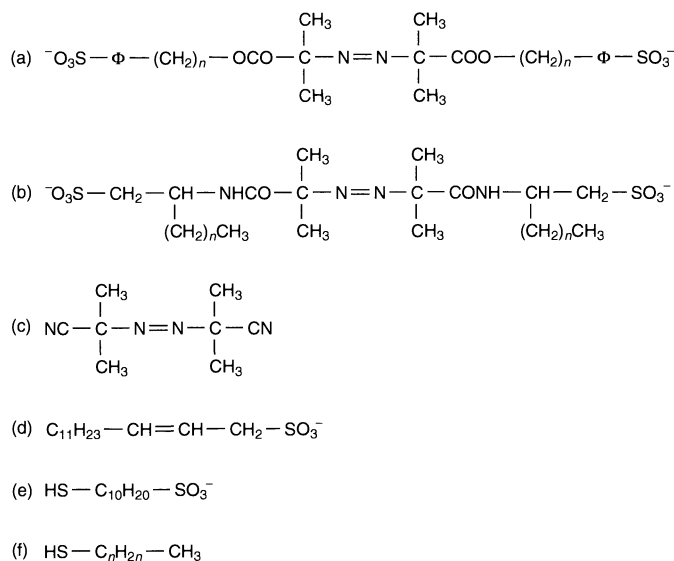


Figure 17.26. Structures of two inisurfs (a and b), i.e. polymerizable surfactants that also serve as polymerization initiators, and two transurfs (d and e), polymerizable surfactants with chain-transfer capability. One conventional initiator (c) and one conventional chain-transfer agent (f) are also given

with proper storage stability. It has been found that alkyd lacquer films containing this type of surfactant dry faster and become harder than films containing the same amount of a non-reactive nonionic surfactant with a similar hydrophilic–lipophilic balance (HLB) value.

3.3.3 Surface modification

Modification of solid surfaces can be achieved by an adsorbed layer of reactive surfactant on the surface, as illustrated in Figure 17.29. Provided the surfactant molecules are extensively cross-linked, such a thin surface film will be attached irreversibly. In this way, hydrophobic surfaces can be made hydrophilic or a specific functionality can be introduced.

For example, low-density polyethylene films can be hydrophilized with surfactants having one or two polymerizable groups, such as methacrylate or diacetylene derivatives. Adsorption can be made from buffer solution and the subsequent polymerization of the adsorbed monolayer achieved by UV irradiation. Particularly good results are often obtained with surfactants of the “twin-tail type”, i.e. having a hydrophobic part consisting of two hydrocarbon chains. This structure gives optimal packing on planar surfaces since such surfactants have a value of the critical packing parameter close to

unity. Proper alignment of the surfactants at the surface is believed to be vital for effective cross-linking to occur.

There is experimental evidence that surfactants that contain two polymerizable functions give better result in terms of permanent hydrophilization than surfactants containing only one reactive group. Most likely, surfactants with more than one polymerizable group give a cross-linked networks of higher molecular weight and such a surface layer will be completely water-insoluble and irreversibly attached to the surface.

Paint and lacquer films can also be surface-modified by migration of a dissolved surfactant to the film–air interface during the drying or curing stage. The principle is shown in Figure 17.30 for a UV-polymerizable surfactant.

As an example, a fluorocarbon surface layer can be obtained by dissolving a small amount (less than 1%) of a polymerizable fluorosurfactant in a lacquer and cross-linking the surfactant monolayer formed at the surface. Figure 17.31 shows two fluorocarbon surfactants, one polymerizable (a) and the other non-reactive (b), used in such an experiment. The surfactants were added to a poly(methyl methacrylate) (PMMA) lacquer. PMMA is more polar than the hydrocarbon part of the surfactant so the surfactant orients at the film–air interface with

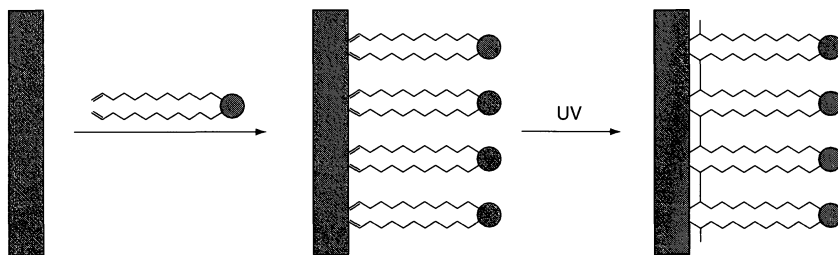


Figure 17.29. Schematic representation of surface modification using a UV-curable surfactant

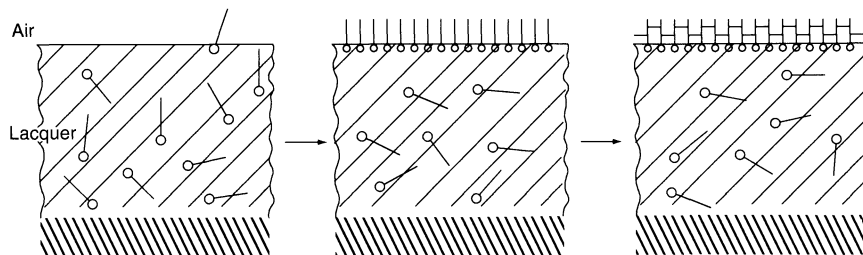


Figure 17.30. Schematic representation of surface modification of a lacquer film through migration of the surfactant to the film–air interface, followed by UV curing

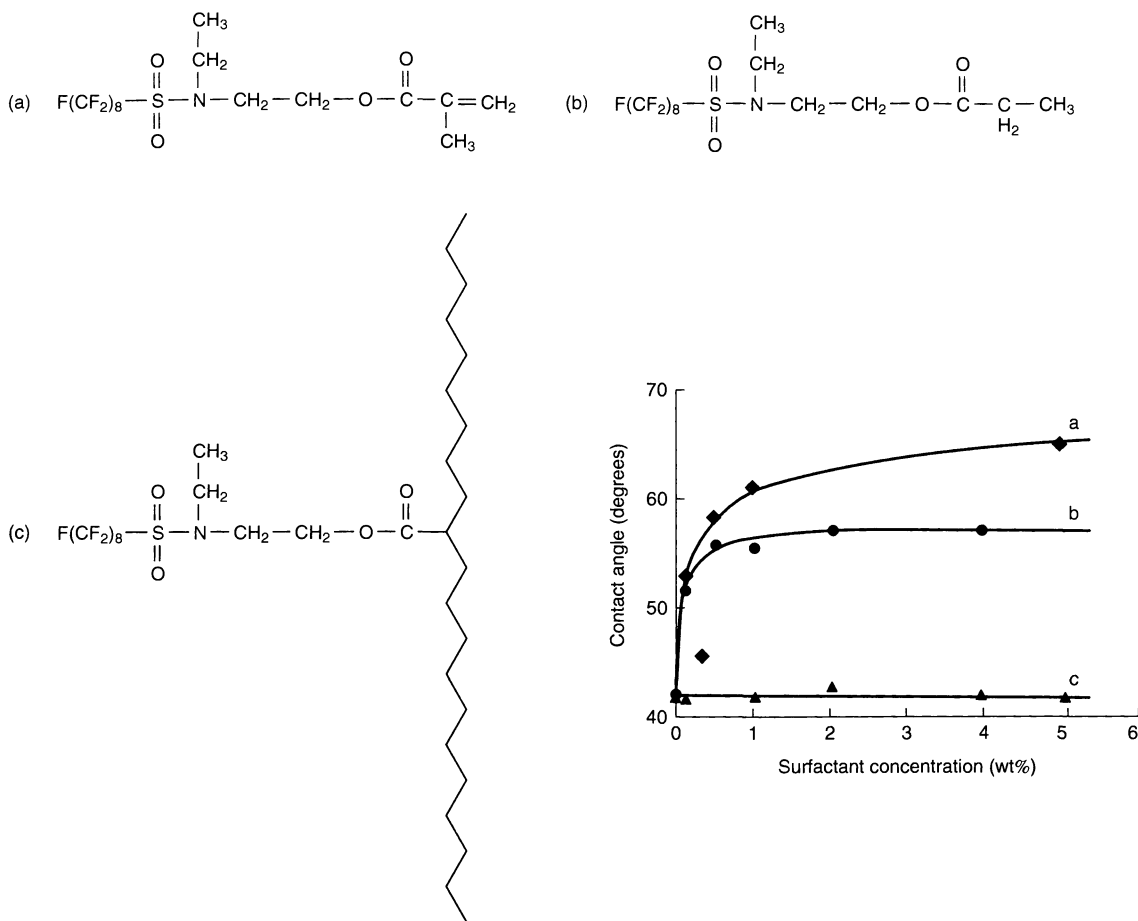


Figure 17.31. Modification of a PMMA lacquer film by surface-active fluorocarbons of similar structure: (a) a reactive surfactant containing a methacrylate group; (b) a non-reactive surfactant; (c) a surface-active polymer. (Redrawn from M. Torstensson *et al.*, *Macromolecules*, **23** 126 (1990))

its polar part in the lacquer and the fluorocarbon residue away from it, i.e. pointing into the air. ESCA revealed that a dense fluorocarbon layer formed at the surface. After curing the films were washed with solvent. Contact-angle measurements showed that the lacquer to which the methacrylate surfactant had been added had been properly and permanently hydrophobized. The non-reactive surfactant could be washed away from the surface, i.e. the hydrophobation was not permanent. A preformed polymer of the same type (Figure 17.31(c)) also gave a substantial and permanent increase in contact angle. Migration of the polymer to the surface was a slow process, however, and several days were required in order to attain an equilibrium surface composition.

3.4 Concluding remarks

The homopolymerization of reactive surfactants in the form of assemblies, such as micelles or liquid crystals, have been attempted as a way to freeze the structure and prepare various types of nano-sized materials. Polymerization of micelles has not been entirely successful, however. With both spherical and rod-like micelles, the polymerized aggregates were of much larger size than the original structures. With liquid crystals and, in particular, with vesicles, the result is more promising. Stable vesicles, of interest for drug administration, have been prepared by free-radical polymerization of preformed vesicles. Such vesicles need not be based entirely on polymerizable surfactants. Incorporation of

smaller amounts, i.e. 10–30%, of reactive species into a phospholipid-based formulation leads to vesicles with much improved stability.

Although considerable academic attention has been devoted to the homopolymerization of surfactant solutions, the main industrial interest in polymerizable surfactants lies in applications, such as those described above, where the surfactant is used in the normal way, i.e. as an additive in concentrations of a few percent or less. In such applications, polymerizable surfactants are likely to be of increasing importance in the future.

4 BIBLIOGRAPHY

1. Guyot, A., Polymerizable surfactants, in *Novel Surfactants*, Holmberg, K. (Ed.), Surfactant Science Series, Vol. 74, Marcel Dekker, New York, 1998.
2. Guyot, A. and Tauer, K., Reactive surfactants in emulsion polymerization, *Adv. Polym. Sci.*, **111**, 44–60 (1994).
3. Holmberg, K., Polymerizable surfactants, *Prog. Org. Coatings*, **20**, 325–337 (1992).
4. Holmberg, K., Cleavable surfactants, in *Novel Surfactants*, Holmberg, K. (Ed.), Surfactant Science Series, Vol. 74, Marcel Dekker, New York, 1998.
5. Holmberg, K., Cleavable surfactants, in *Reactions and Synthesis in Surfactant Systems*, Texter, J. (Ed.), Marcel Dekker, New York, 2001.
6. Jaeger, D. A., Cleavable surfactants, *Supramol. Chem.*, **5**, 27–30 (1995).
7. Menger, F. M. and Keiper, J. S., Gemini surfactants, *Angew. Chem. Int. Edn Engl.*, **39**, 1906–1920 (2000).
8. Rosen, M. J., Geminis: a new generation of surfactants, *Chemtech*, **23**, 30–33 (1993).
9. Zana, R., Dimeric (gemini) surfactants, in *Novel Surfactants*, Holmberg, K. (Ed.), Surfactant Science Series, Vol. 74, Marcel Dekker, New York, 1998.

CHAPTER 18

Hydrotropes

Anna Matero

YKI Institute for Surface Chemistry, Stockholm, Sweden

1	Introduction	407	4	Applications	415
2	Structure of Hydrotropic Compounds	408	4.1	Detergents/liquid cleaners	415
3	Function and Mechanism	409	4.2	Separation processes	416
3.1	Minimal hydrotropic concentration	409	4.2.1	Extractive separation	416
3.2	Association structures in hydrotropic solutions	409	4.2.2	Distillation	416
3.3	Comparisons between surfactants and hydrotropes	410	4.2.3	Crystallization	416
3.4	The influence of molecular structure on hydrotropic efficacy	411	4.3	Polymers and hydrotropes	417
3.5	Hydrotropes as coupling agents	412	4.4	Chemical reactions	417
			4.5	Preparation of vesicles	418
			4.6	Solubilization of pharmaceuticals	418
			5	References	419

1 INTRODUCTION

The term “hydrotrope” was first introduced by Neuberg in 1916 (1) to describe the power of anionic short-chain organic compounds to dissolve organic compounds such as carbohydrates, alcohols, aldehydes, ketones, hydrocarbons, esters, ethers, lipids, fats and oils in water. A number of organic and inorganic compounds were also tested by McKee in 1946 (2). This author found that many hydrotropic solutions precipitate the solute when diluting the system with water. This will ensure that the hydrotrope can be recovered after use, which can be recognized as an important feature for industrial applications. It was also noted that a high concentration of the hydrotrope is required to exhibit the hydrotropic action. The phenomenon of increased solubility of the organic compound by addition of the hydrotrope was attributed to a salting-in effect. Booth and Everson (1948–1950) found that the solubility of the solute was not linearly dependent on the hydrotrope concentration (3–5). They observed a sigmoidal behaviour for concentration

dependence and a drastic increase in the solubility of the solute in the hydrotropic solutions above a certain concentration. Lumb (1951) studied ternary systems with potassium *n*-butyrate or potassium *n*-octanoate, a normal primary alcohol and water (6). This author concluded that the hydrotropic behaviour of the lower alkanooates represented essentially the same phenomenon as solubilization, i.e. the presence of colloidal association structures. Further comparisons with surfactants were also made by Lawrence (1959) (7), Friberg and Rydhag (1970) (8) and Pearson and Smith (1974), (9) by performing phase behaviour studies on systems including hydrotropes. These studies showed that hydrotropic solubilization is an extension of surfactant solubilization.

Even though hydrotropes have not received the same attention as surfactants in the literature, reviews on the topic have been presented (see, for example, refs (10–13)). A number of mechanisms have been suggested in the literature as described above, although the exact mechanism is not yet fully understood. This present chapter will be dealing with hydrotropes from

a fundamental point of view by describing the structure and the function of the compounds. However, it was recognized at an early stage that hydrotropes may be very interesting for industrial applications, and so brief descriptions of a number of applications where hydrotropes have been found useful are included.

2 STRUCTURE OF HYDROTROPIC COMPOUNDS

The organic salts that Neuberg introduced as hydrotropes consist of an anionic group and a hydrophobic aromatic ring or ring system such as sodium benzoate. Later on, the definition was revised by Saleh and El-Khordagui (14) by including cationic and nonionic organic compounds. The following definition was made: "hydrotropic agents are freely soluble organic compounds which at a concentration sufficient to induce a stack-type aggregation, considerably enhance the aqueous solubility of organic substances, practically insoluble under normal conditions. These compounds may be anionic, cationic or neutral molecules".

Traditional hydrotropes are usually characterized by a short and bulky structure, such as sodium xylene sulfonate (SXS), sodium benzene sulfonate (SBS), sodium toluene sulfonate (STS), sodium toluene sulfonate (STS) and sodium cumene

sulfonate (SCS) (see Figure 18.1). The compounds are amphiphilic with a quite small polar part and a bulky non-polar part. Therefore, the hydrotrope will be soluble in both non-polar and polar solvents. In comparison with surfactants, hydrotropes have a less profound hydrophobic character and hence a higher solubility in water. The polar part will ensure a high solubility in water, while the non-polar part acts as the functional group. The term hydrotrope usually refers to organic compounds, although inorganic examples, such as alkali iodides, bicarbonates, oxalates and thiocyanates, have also been mentioned (2). However, this is quite uncommon and the definition of hydrotropes made by Saleh and El-Khordagui (14) will exclude such compounds. Their main effect is merely a salting-in phenomenon.

The diacid, 5-carboxy-4-hexyl-2-cyclohexene-1-yl octanoic acid, has a total chain length of 21 carbon atoms and the structure does not resemble the structure of traditional hydrotropes such as the short-chain aromatic sulfonates (see Figure 18.2). Despite the difference in structure, this diacid exhibits hydrotropic properties (15). However, it has been proven that the structure of the diacid when active as a hydrotrope will not be very different from the short and bulky conventional compounds. The conformation of the diacid within a lamellar liquid crystal is composed of a short loop where

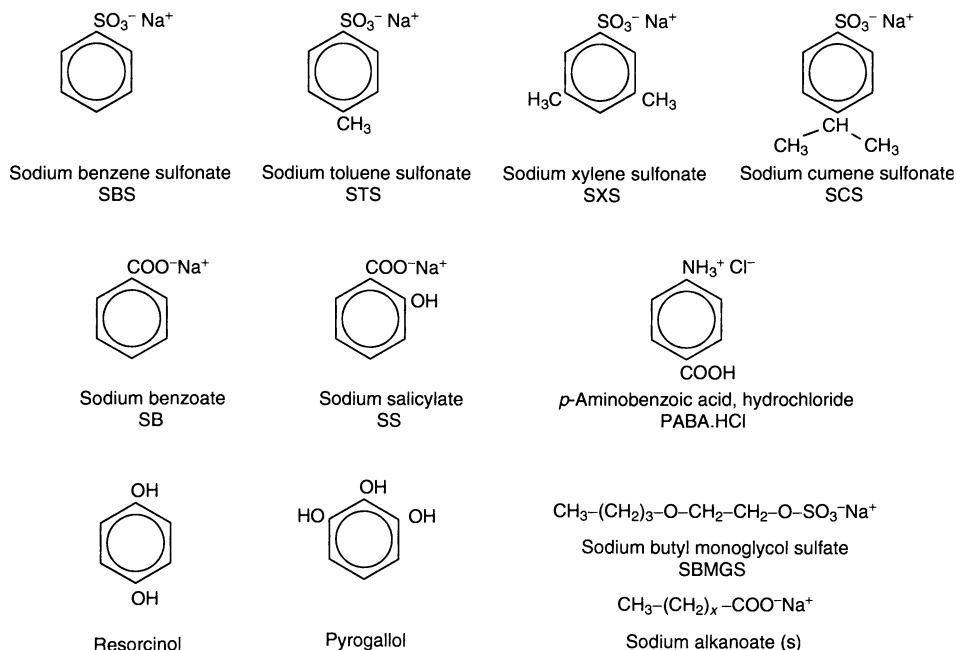
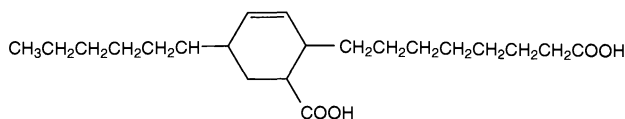
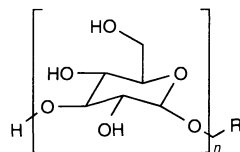


Figure 18.1. Some examples of traditional hydrotropes



Diacid (5-carboxy-4-hexyl-2-cyclohexene-1-yl octanoic acid)



Alkyl polyglucoside (s)

Figure 18.2. Two examples of alternative hydrotropes

the two polar carboxyl groups will be anchored at the surface and the short straight carbon chain is embedded in the hydrophobic part of the liquid crystal, which will result in a short and bulky structure. Because of the long carbon chain and the “double-hydrophilic” group, such substances have a more profound surfactant character than traditional hydrotropes.

Another class of compounds that may act as hydrotropes are sugar-based surfactants, such as alkyl polyglucosides (APGs) (see Figure 18.2) (16). These substances are nonionic surfactants, which are produced from renewable raw materials such as vegetable oils and sugar/starch. They have become important complements to ethoxylates due to their ecological, toxicological and technological properties. Alkyl polyglucosides are also characterized by a bulky structure, but in this case the hydrophilic group is bulky, while the hydrophobic alkyl chain is quite small.

3 FUNCTION AND MECHANISM

Two main functions of hydrotropes have been described in the literature, namely hydrotropes as (i) solubilizing agents, or (ii) coupling agents. Much of the literature has been focused on the first phenomenon, which is connected with the dramatic increase in the solubility of poorly water-soluble compounds in aqueous solutions over a specific hydrotrope concentration. The second function concerns the ability of hydrotropes to change a turbid solution into a transparent one when adding the hydrotropic compound. During the extensive study of hydrotropes to elucidate the exact mechanism, a number of important features regarding hydrotropes have been found, and these are described below.

3.1 Minimal hydrotropic concentration

A general observation is that a high amount of hydrotrope is needed in order for the molecule to exhibit hydrotropic activity, i.e. to facilitate a high solubility of the hydrophobic solute in water. The concentration of the hydrotrope needs to exceed a critical concentration (17), the so-called “minimal hydrotropic concentration” (MHC), to obtain a high solubility of the solute. This is illustrated in Figure 18.3 where the solubility of the dye fluorescein diacetate (FDA) in water was monitored as a function of hydrotrope concentration through the optical density (*OD*) values at the absorption band maximum (17). The solubility of FDA in solutions with three different hydrotropes, i.e. sodium *p*-toluene sulfonate (STS), sodium salicylate (SS) and sodium butyl monoglycol sulfate (SBMGS), does not vary linearly with the hydrotrope concentration. Instead, a sigmoidal behaviour is found, with the solubility increasing sharply above a specific concentration. A plateau is reached for even higher concentrations of the hydrotrope. The minimal hydrotropic concentration differs between the hydrotropes, i.e. about 0.2*M* for STS, 0.7*M* for SBMGS and 0.8*M* for SS. However, this study indicated that the MHC for a given hydrotrope will be the same for different solutes. This is presented in Figure 18.4 for the solubility of three solutes, perylene, FDA and ethyl-*p*-nitrobenzoate (EPNB) in an aqueous solution of sodium butyl monoglycol sulfate.

3.2 Association structures in hydrotropic solutions

The mechanism of hydrotropic action has been attributed to a salting-in effect, as well as to a phenomenon

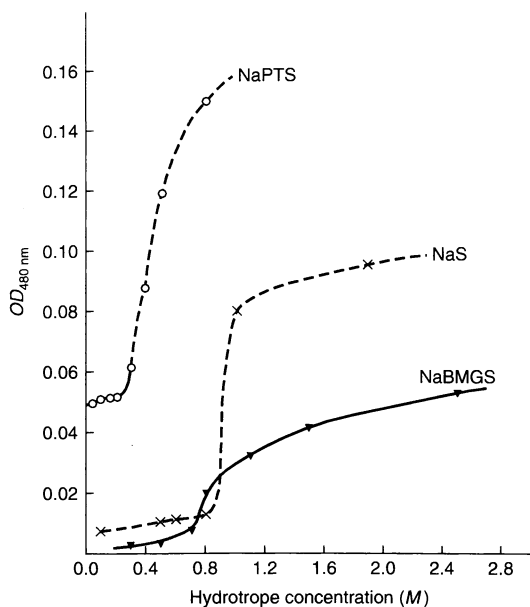


Figure 18.3. Solubility of the dye fluorescein diacetate (FDA) in aqueous hydrotropic solutions as a function of the hydrotrope concentration at room temperature. Three different hydrotropes, i.e. sodium *p*-toluene sulfonate (NaPTS), sodium salicylate (NaS) and sodium butyl monoglycol sulfate (NaBMGS) were studied. (Reprinted with permission from Balasubramanian, D. *et al.*, *J. Phys. Chem.*, **93**, 3865–3870 (1989). Copyright 2000 American Chemical Society)

similar to surfactant solubilization. The positive deviation from the linearity for the solubilization capacity as a function of the hydrotrope concentration indicates the importance of co-operative intermolecular interaction regarding the hydrotropes involved in the solubilization process. The effect of the hydrotrope sodium *p*-toluene sulfonate on perylene has been compared with a salting-in agent, guanidinium thiocyanate (GdSCN) and a phase-mixing agent, PEG-6000, (17). The solubility of perylene will increase monotonically with both GdSCN and PEG-6000, and not sigmoidal as is the case for STS. This indicates that different mechanisms are involved and hydrotrophy will differ from phenomena such as salting-in as well as cosolvency. The high values of the MHC and the gradual change in properties such as surface tension (see below) indicates that the self-aggregation might correspond to consecutive association such as dimerization, trimerization and so on, and not co-operative such as with micellar surfactants. The mechanism for aromatic hydrotropes has been attributed to the plane-to-plane stacking of the hydrophobic part of the molecule (14), thus requiring a planar aromatic

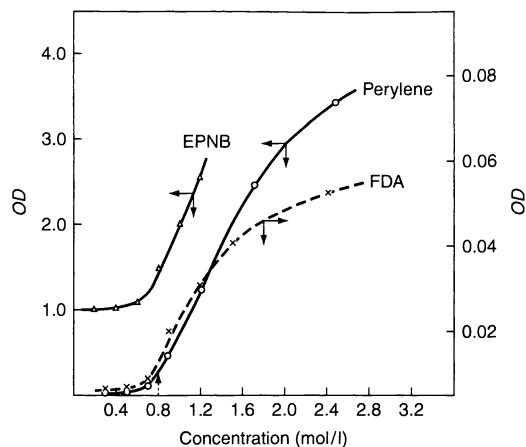


Figure 18.4. Solubility of perylene, fluorescein diacetate (FDA) and ethyl-*p*-nitrobenzoate (EPNB) in an aqueous solution of sodium butyl monoglycol sulfate (SBMGS); optical densities are given at their adsorption band maxima. (Reprinted with permission from Balasubramanian, D. *et al.*, *J. Phys. Chem.*, **93**, 3865–3870 (1989). Copyright 2000 American Chemical Society)

part. This has been employed to describe the differences observed for *p*-aminobenzoic acid-HCl (PABA-HCl), procaine-HCl and cinchocaine-HCl which have been used to increase the solubility of riboflavin (14). PABA-HCl and procaine-HCl were proven to exhibit hydrotropic activity, while cinchocaine-HCl did not perform as a hydrotropic agent. The side-chains in cinchocaine are likely to prevent a stack-type aggregation due to steric reasons, while the association is favourable for the planar molecules PABA and procaine.

3.3 Comparisons between surfactants and hydrotropes

Hydrotropes have been proven to be surface-active. The surface tensions for anionic hydrotropes such as sodium salicylate, sodium xylene sulfonate, sodium *p*-toluene sulfonate, sodium cumene sulfonate and sodium butyl monoglycol sulfate decrease as a function of the concentration in water, until a plateau is reached (17) (see Figure 18.5). The same behaviour is also observed for the nonionic hydrotropes resorcinol, catechol, and pyrogallol (18). This means that they exhibit the same behaviour as surfactants, even though the drop in surface tension is not as dramatic but more gradual for hydrotropes when compared to surfactants. The concentration for the onset of self-aggregation of the anionic hydrotropes in non-covalent assemblies determined from

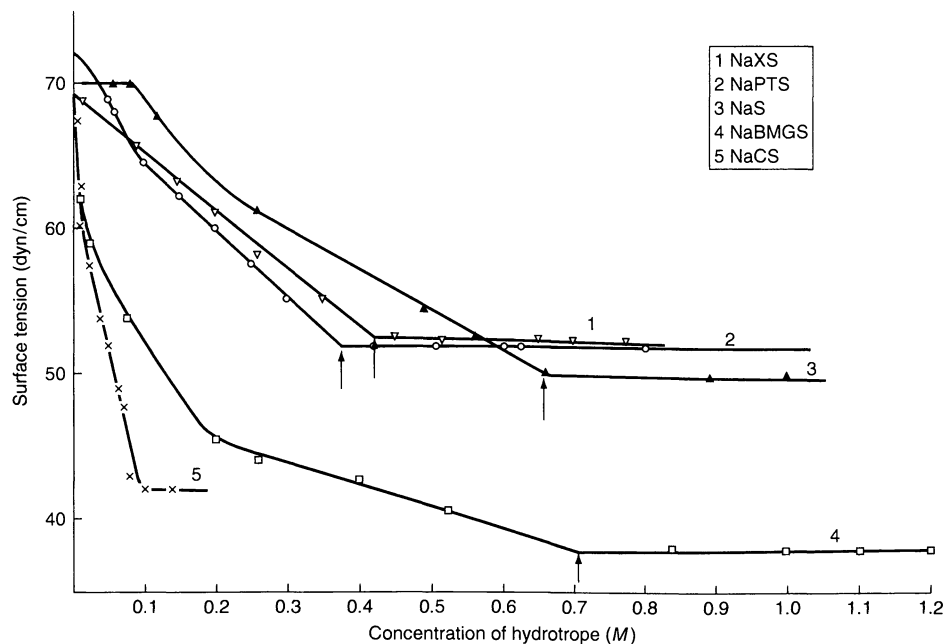


Figure 18.5. Surface tension as a function of the hydrotrope concentration at room temperature. (Reprinted with permission from Balasubramanian, D. *et al.*, *J. Phys. Chem.*, **93**, 3865–3870 (1989). Copyright 2000 American Chemical Society)

the surface tension measurements are quite close to the MHC values observed for these hydrotropes in solubilization processes. Hence, this will also suggest that association is important for hydrotropic solubilization of organic compounds in water. The micro-environmental features of hydrotrope assemblies have been studied (11, 17), and it was concluded that the micro-viscosity offered by hydrotropes such as sodium *p*-toluene sulfonate, sodium cumene sulfonate and sodium butyl monoglycol sulfate is in the same range as for ionic micelles, although slightly less polar in nature.

Even though hydrotropes exhibit a resemblance to surfactants, a number of differences are obvious. The amount of hydrotrope needed to facilitate solubilization of the solute in water is usually much higher than that needed for surfactants. The reason for this is that the shorter carbon chain of the hydrotrope will result in a higher concentration for self-association, which is a requirement for solubilization (12). In the case of hydrotropes, the maximum solubilization will usually be higher than for surfactants. This might be explained by the fact that the micellar solution of a surfactant will be transformed into an “inverse” micellar solution via the formation of a lamellar liquid crystalline structure and the solubilization of the solute in water will be

stopped when the lamellar liquid crystal appears. These structures will not occur when hydrotropes are used for solubilization. The fact that ordered structures are found in the case of surfactant solutions and not in hydrotrope solutions, where disordered structures and aggregates are formed, indicates that there is a difference in structural features and not in solubility (11). The solubility capacity of hydrotropes are also more selective and not as general as for surfactants in the sense that not all organic compounds will become more soluble in water by the addition of hydrotropes.

3.4 The influence of molecular structure on hydrotropic efficacy

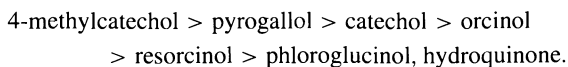
Hydrotropes do not perform so generally as surfactants do, i.e. the solubility will not increase for all organic compounds in hydrotropic solutions. The efficacy will also vary among the different hydrotropes, even though very small structural differences may be present. This has been reported for the solubilities in aqueous sodium *o*-, *m*- and *p*-xylene sulfonate solutions of solutes such as acetophenone, aniline, benzaldehyde, *o*-cresol, etc. It was found that the *meta* structure was more effective, particularly at lower temperatures since it had a higher water solubility (5). Another example is

the observation that the solubilizing effect is higher for sodium salicylate than for sodium benzoate with respect to cyclohexanol, thus indicating the importance of the presence of the hydroxyl group (19). The solubility of riboflavin in water could also be increased by changing the structure of the hydrotrope to become more hydrophobic (11), hence suggesting that hydrophobic interactions play a major role in the solubilization process.

Many of the polyhydroxybenzenes are efficient hydrotropes and these molecules offer a possibility for evaluating the influence of the molecular structure and the role of intermolecular interactions on the hydrotropic action (18). The molecules used to increase the solubility of fluorescein diacetate are presented in Table 18.1.

A positive deviation from linearity and a sigmoidal behaviour is observed for the hydrotropic activity as a function of the hydrotrope. The latter will only be active above a certain hydrotrope concentration (MHC). Among the dihydroxy isomers it was found that catechol is more effective than resorcinol, i.e. the *o*-isomer is more effective than the *m*-isomer. The water solubility of hydroquinone, the *p*-isomer, is very low and will reduce the hydrotropic function of the molecule. The amphiphilic nature of catechol and resorcinol is quite similar, which is obvious from surface tension measurements. They do also have similar MHC values (0.8M for catechol and 0.7M for resorcinol). The reason for the difference in the hydrotropic actions of catechol and resorcinol lies in their structures, which will determine the packing of the molecules as well as the organization of the functional group. It has been indicated that catechol is able to arrange itself in a more compact form than both resorcinol and hydroquinone. By comparing resorcinol and orcinol, as well as catechol and 4-methylcatechol, it was found that the introduction of a methyl group will improve the hydrotropic activity. Replacing one hydroxyl group with a methyl group will also result in an increased solubility of FDA. This is concluded by comparing the effects of

phloroglucinol and orcinol. Summarizing, the following order for hydrotropic activity was obtained:



The hydrotrope 4-methylcatechol has also been studied by using NMR spectroscopy, evaluating various aspects concerning self-association. A dramatic change in the ^1H NMR chemical shift for the ring protons, as well as for the methyl group protons, will occur at about the MHC and around the concentration where the surface tension levels off. Spin-lattice relaxation measurements also showed a restriction in the molecular motion above the MHC. Both of these observations are indicative of self-association of non-covalent assemblies. A gradual aggregation is suggested since the T_1 -value stays approximately stable as a function of the hydrotrope concentration until the MHC is reached, after which it decreases quite slowly.

The function of hydrotropes may vary in different systems. This has been observed in sun-screen microemulsions prepared with water, pentanol, sodium dodecyl sulfate (SDS) and a hydrotrope (13). Three different hydrotropes were tested, i.e. *p*-aminobenzoic acid (PABA), octyldimethyl-*p*-aminobenzoic acid (ODP) and 2-hydroxy-4-methoxy-5-sulfobenzophenone (HMSB). Their effects are presented in Table 18.2.

3.5 Hydrotropes as coupling agents

Hydrotropes are also known to behave as coupling agents, thus transforming a turbid solution into a homogeneous transparent system (13). This has been reported for systems consisting of water, sodium dodecyl sulfate (SDS), pentanol and *p*-xylene (20). The addition of a hydrotrope, i.e. sodium xylene sulfonate (SXS), has united the oil-in-water (o/w) and water-in-oil (w/o) regions by destabilizing and reducing the lamellar liquid crystal region and enlarging the bicontinuous region (see Figure 18.6). It has been stated that the hydrotrope

Table 18.1. Polyhydroxybenzenes used for hydrotropic studies (18)

"Common" name	Chemical name
Catechol	1,2-Dihydroxybenzene
Resorcinol	1,3-Dihydroxybenzene
Hydroquinone	1,4-Dihydroxybenzene
Pyrogallol	1,2,3-Trihydroxybenzene
Phloroglucinol	1,3,5-Trihydroxybenzene
4-Methylcatechol	4-Methyl-1,2-dihydroxybenzene
Orcinol	1-Methyl-3,5-dihydroxybenzene
2-Methylresorcinol	2-Methyl-1,3-dihydroxybenzene

Table 18.2. Function of three different sun-screen hydrotropes in microemulsion preparations

Hydrotrope	Function ^a
PABA	Stabilizes the o/w microemulsion
ODP	Stabilizes the w/o microemulsion
HMSB	Stabilizes both of the o/w and w/o parts

^ao/w, oil-in water.

^bw/o, water-in-oil.

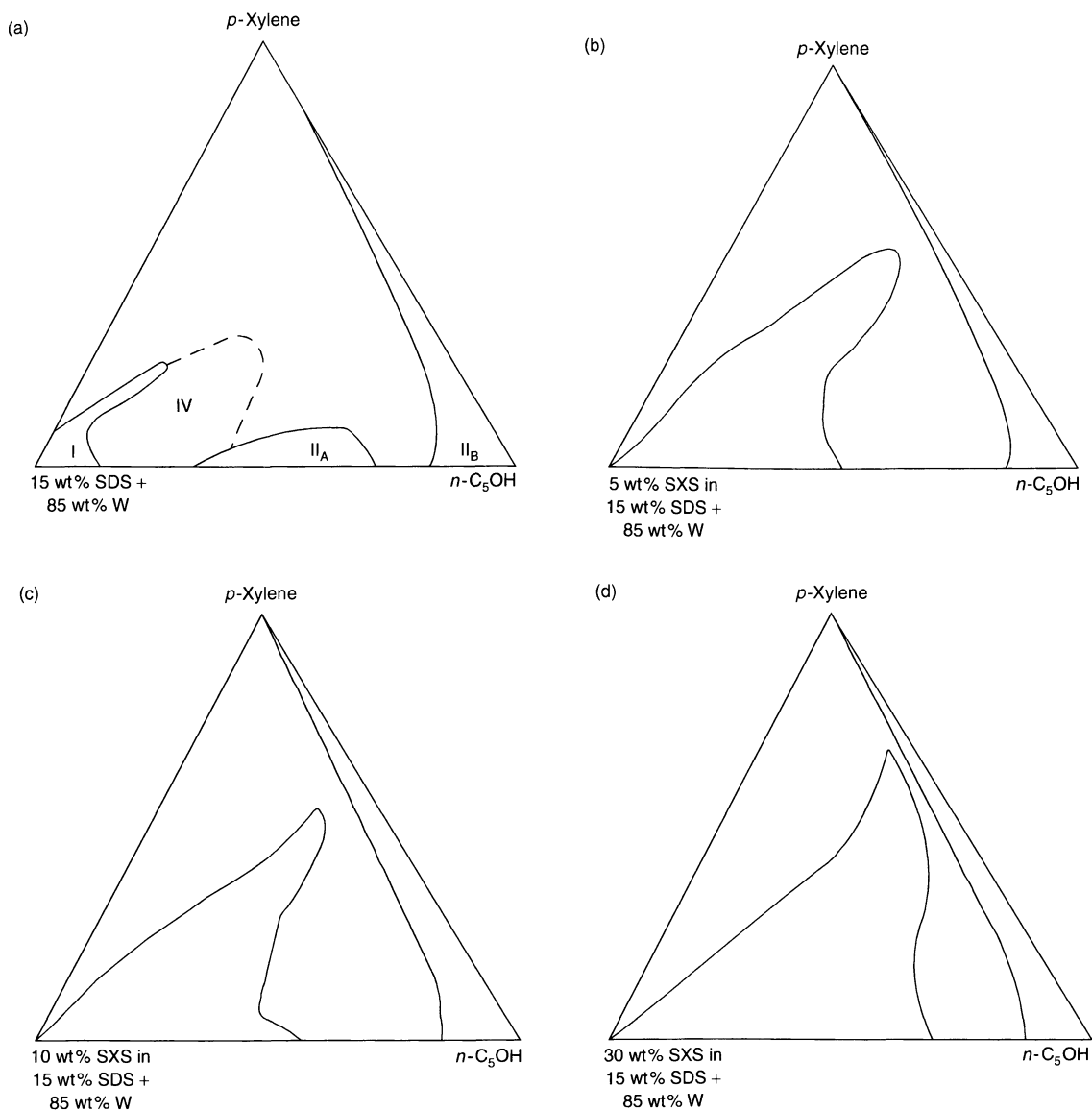


Figure 18.6. The effect of the hydrotrope sodium xylene sulfonate (SXS) on the phase behaviour for a system consisting of water (w), sodium dodecyl sulfate (SDS), pentanol ($n\text{-C}_5\text{OH}$) and p -xylene: I, o/w microemulsion; II_A, w/o microemulsion; II_B, C_5OH and p -xylene solution; IV multiphase region with lamellar liquid crystal. (Reprinted from Guo, R. *et al.*, *J. Disp. Sci. Tech.*, **17**, 493–507 (1996) p. 498–499, by courtesy of Marcel Dekker, Inc.)

will migrate into the ordered structure of liquid crystals, resulting in a disruption due to the mismatch in the structure between the surfactant and the shorter hydrotrope. This transition from a lamellar liquid crystal to a bicontinuous structure is likely to be due to the resemblance between the two structures. By mixing short-chain and long-chain amphiphiles, an enhanced disorder in the

liquid crystalline phase is obtained and hence a destabilization.

Alkyl polyglucosides (APGs) do also have the possibility to perform as coupling agents (16). Two different APGs with varying alkyl chain lengths have been evaluated as hydrotropes in a system with water, SDS and pentanol. The hydrotropes are described in Table 18.3.

Table 18.3. Alkyl polyglucosides used as coupling agents

Surfactant	Hydrophobic part	Degree of polymerization (dp)
SL4	C4	1
SL8	C8	ca. 1.9
SL10	C10	ca. 1.5
SL11	C11	ca. 1.5

The model system contains regions with an aqueous micellar solution, as well as regions with an inverse micellar solution. These regions are connected with a bicontinuous solution. A region of different types of lamellar liquid crystal phases is also present. The model hydrotrope, toluol-4-sulfonic acid, added to the water phase, resulted in an extension of the solubility region to higher surfactant concentrations, as well as a destabilized liquid crystalline phase, which almost disappears. The alkyl chain length of the APG SL4, is four and the compound is claimed to be a hydrotrope. Comparisons have been made with SL8, with an alkyl chain length of eight carbon atoms. It was found that SL4 with a

short (butyl) group was more effective as a coupling agent than the intermediate-chain-length (octyl) APG, SL8. SL4 enlarges the microemulsion region and destabilizes the liquid crystalline region, while SL8 has an opposite effect, stabilizing the liquid crystal and disconnecting the w/o and o/w regions. However, hydrotropes are also used to increase the cloud point of solutions with nonionic surfactants (see Section 4.1 below). In such an experiment, 1% of four different sugar-based surfactants (see Table 18.3) have been added to solutions containing 1% of three different nonionic surfactants, C₆EO₂, C₁₁EO₅, and C₁₃EO₆. The hydrotropic effect is small for short (butyl) and long (undecyl) hydrocarbon chains. The maximum in cloud point elevation is observed for intermediate chain lengths, (see Figure 18.7). The fact that the short-chain-length APG (SL4) is more effective as a coupling agent than the intermediate-chain-length APG (SL8) is in contrast to that found for the cloud point elevation. This means that the hydrotropic behaviour is dependent on the way it is assessed and that the cloud point elevation and breakdown of liquid crystalline structures are not governed by the same phenomenon.

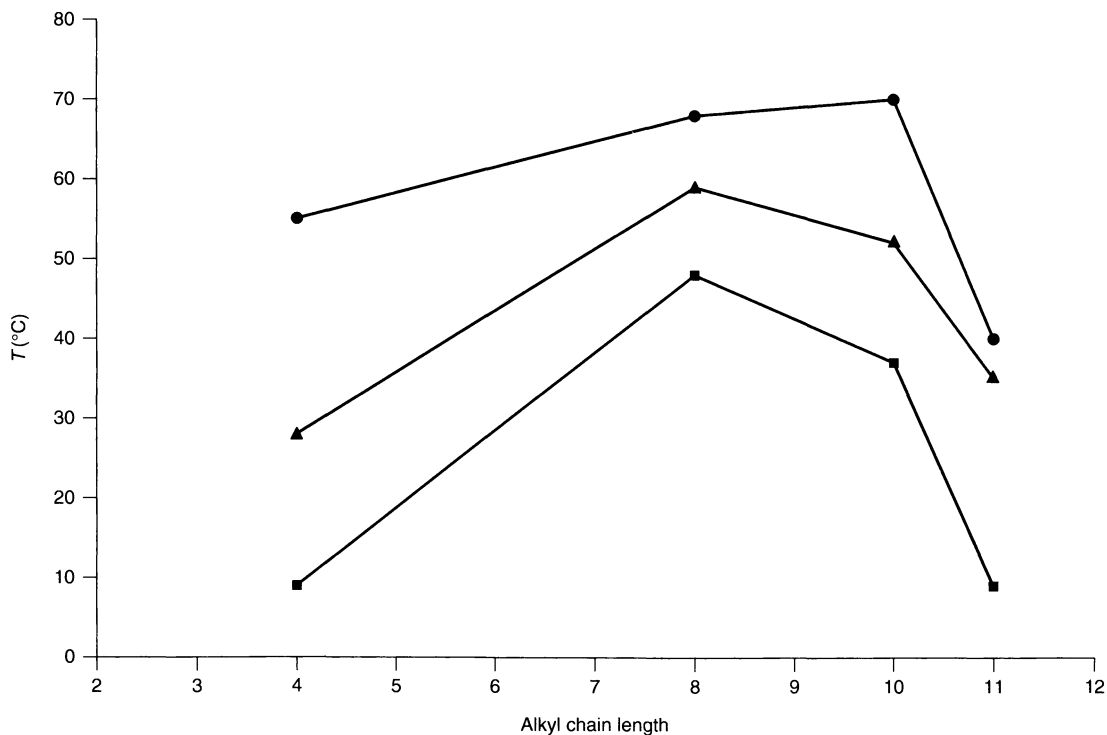


Figure 18.7. The cloud points for solutions with 1% nonionic surfactant and hydrotrope, respectively. The following surfactants have been used: (●) C₆EO₂; (▲) C₁₁EO₅; (■) C₁₃EO₆. (Redrawn from data from Matero *et al.*, *J. Surf. Det.*, **1**, 485–489 (1998), The American Oil Chemists' Society)

4 APPLICATIONS

The potential industrial use of hydrotropes was recognized in 1946 by McKee (2) due to the interesting characteristics that these materials displayed. By diluting a hydrotropic solution, the solute will precipitate and the hydrotrope can easily be recovered. The lack of flammability and (in general) no problems with emulsification, as might be the case for surfactants, are also properties which are valuable in industrial applications. The use of hydrotropes in various applications is described in refs (11) and (13).

4.1 Detergents/liquid cleaners

Surfactant solubilization in liquid cleaners may be limited due to a high concentration of the surfactant or a high amount of electrolytes present in the formulations. In order to enhance the solubility and to increase the cloud point for nonionic-based systems, hydrotropes are often added. This phenomenon has already been pointed out in Section 3.5 above, where the cloud points of solutions with nonionic surfactants were elevated upon the addition of alkyl polyglucosides (16). Hydrotropic activity can be evaluated by determining the amount of hydrotrope required to clarify a cloudy solution or the cloud point elevation obtained for a specific concentration of a hydrotrope. The efficacy of hydrotropes varies for different classes of compounds. This has been observed for short-chain alkylbenzene and alkylnaphthalene sulfonates when added to a number of detergent formulations (21). The alkylnaphthalene sulfonates were found to be more efficient than the alkylbenzene sulfonates in elevating the cloud point.

The hydrotrope may also assist in solubilizing components such as perfumes, colorants, bactericides, etc. that are added in small amounts. The reason for using hydrotropes is to obtain a clear and stable product, which is very important from a market appeal point of view. Sodium xylene sulfonate, sodium cumene sulfonate, sodium toluene sulfonate, urea and ethanol have been the most widely used hydrotropes in light-duty liquid detergents. Apart from resulting in a stable product, the hydrotropes should be nearly colourless and odourless. This is the case for sodium xylene sulfonate, sodium cumene sulfonate and ethanol. Isopropanol, propylene glycol and poly(ethylene glycol ethers) can also be found as hydrotropes in formulations.

Another important feature is that hydrotropes will prevent formation of gels in concentrates as well as in diluted systems (12). For concentrated products, the

aim is to obtain a stable product. In the case of diluted formulations, the hydrotrope will facilitate the removal of the dirt and contaminants by prevention of the formation of a viscous gel as well as by increasing the solubility of the hydrophobic dirt in the aqueous solution of the hydrotrope (12, 15).

The hydrotropic compound diacid referred to earlier (see Figure 18.2), which has a structure far from traditional hydrotropes, has been used as a solubilizing agent in formulations for laundry applications. This molecule has been proven to retard the formation of liquid crystalline structures in such a concentrated system, as well as in the diluted system used to model actual washing conditions (12). The hydrotrope in the diluted system with a hydrophobic solute, octanol, used as a model for the dirt, will also increase the solubility of the solute. This means that the diacid will facilitate the formulation and stability of products for cleaning as well as the cleaning action to remove contaminants. Systems containing the diacid have been characterized by a variety of techniques such as NMR spectroscopy to study the ordering of the hydrocarbon chains with and without the hydrotrope present by determining the quadrupolar coupling and the order parameter (22). The model system, octanol, water and surfactant, is a liquid crystalline sample. The addition of the diacid resulted in a decrease of the order parameter for the octanol molecule (see Figure 18.8). Hence, the organized structure will be affected and the liquid crystalline structure will be disordered. X-ray diffraction, used to study the interlayer spacing of the lamellar liquid crystal, showed that the organization of the diacid molecule active as a hydrotrope was quite close to the structural appearance of traditional short-chain hydrotropes (12, 15).

Rinse aids are usually based on nonionic surfactants. These compounds will provide the wetting properties as well as the defoaming action to enable higher water rinse velocities (23). Defoaming will occur above the cloud point and low cloud points are therefore wanted to reduce the energy consumption by using lower temperatures. Lower cloud points influence the stability of the products and hydrotropes are used to increase the stability of the final product. It is also important to determine how the hydrotrope will effect parameters such as dispersibility, cloud point and foaming. Examples of hydrotropes used in rinse aid formulations are alkylnaphthalene sulfonates and sulfosuccinate esters since these are regarded as the most effective, increasing the cloud points of solutions with nonionic surfactants without leading to excessive foaming. Propylene glycol, isopropanol and urea are

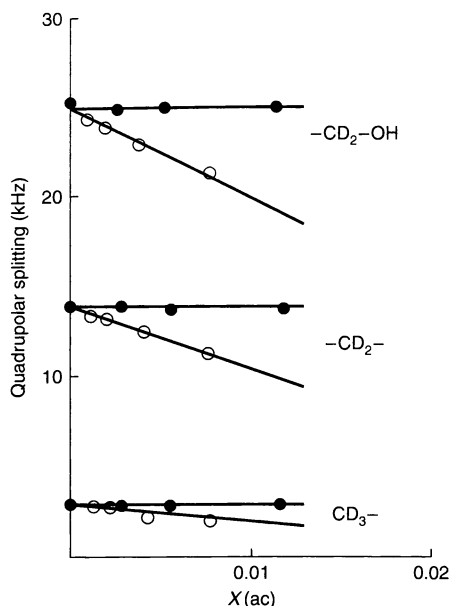


Figure 18.8. The quadrupolar splitting of octanol as a function of the molar fraction with added surfactant (●) or hydrotrope (○) diacid. (Redrawn from Friberg, S. E. *et al.*, *J. Colloid Interface Sci.*, **109**, 487–492 (1986))

also commonly found, while alcohols in general are not effective as solubilizers in such formulations.

4.2 Separation processes

A variety of isomeric or closely related mixtures of organic compounds are often found when manufacturing chemical and pharmaceutical products. However, it is usually necessary to separate these molecules in order to obtain the expected functionality of the products. Conventional methods such as distillation, extraction and crystallization might be difficult to use since the molecules to be separated might have very close chemical and physical properties. Hydrotropes are known to be selective in the solubilization of compounds and as mentioned earlier, do not perform so generally as surfactants. It has been found that the solubility enhancement in water by adding the hydrotrope sodium xylene sulfonate (SXS) will vary for different isomers such as *o*- and *p*-nitrochlorobenzene, as well as for *o*- and *p*-dichlorobenzene (24). In this case, the *o*-isomer is more soluble than the *p*-isomer. Higher solubilities have also been reported for aromatic compounds when compared to aliphatic and alicyclic compounds (24). This selective

Table 18.4. The effect of different parameters on the hydrotropic activity in extractive separation

Parameter	Effect
Nature of hydrotrope	The hydrophobicity will effect the aggregational behaviour and hence the solubilization of the solute
Hydrotrope concentration	The separation factor will increase with the concentration, with the selectivity being higher above the MHC
Nature of solvent	Extractions from inert solvents are more efficient than from polar solvents

solubilization provides the basis for using hydrotropes as separation agents. This behaviour has been especially useful for the separation of close-boiling mixtures.

4.2.1 Extractive separation

Separation of two compounds by using liquid–liquid extraction can be enhanced by using a hydrotropic water-phase (24). Since the hydrotrope is highly selective in the solubilization, the extraction percentage and hence the separation factor will be different for the two solutes (25). The yield and the separation factor will be influenced by a number of parameters (see Table 18.4).

4.2.2 Distillation

Addition of a hydrotrope to a mixture of compounds to be separated will modify the vapour–liquid equilibrium. The volatilities for the compounds will change differently due to a preferential association of one of the components with the hydrotrope. In this case, one of the components will have a higher solubility in the liquid phase and the other component will be enriched in the vapour phase (24, 26).

4.2.3 Crystallization

The phenomenon of hydrotrope can also be used for the separation of similar compounds and isomers by crystallization and precipitation of the selected component from their mixtures in the presence of a hydrotrope. The basis for this is the difference in the solubilities for the two compounds as a function of the temperature and the concentration of the hydrotrope. This has been used for the separation of *o*-chlorobenzoic acid and *p*-chlorobenzoic acid (27) using sodium butyl monoglycol

Table 18.5. Examples of systems used in separative processes

Compounds to be separated	Hydrotrope ^a	Technique	References
<i>p</i> -Cresol/2,6-xylene	ST, STS, SMS, SCyS, SPCS	Extractive separation	25
Phenol/ <i>o</i> -chlorophenol	ST, STS, SMS, SCyS, SPCS	Extractive separation	25
Xylenol/ <i>p</i> -cresol	<i>p</i> -Toluene sulfonic acid	Distillation	26
Phenol/ <i>o</i> -chlorophenol	<i>p</i> -Toluene sulfonic acid	Distillation	26
<i>o</i> -Chloronitrobenzene / <i>p</i> -chloronitrobenzene	Sodium butyl monoglycol sulfate	Crystallization	28
<i>o</i> -Chlorobenzoic acid/ <i>p</i> -chlorobenzoic acid	Sodium butyl monoglycol sulfate	Crystallization	27

^aST, sodium toluate; STS, sodium toluene sulfonate; SMS, sodium mesitylene sulfonate; SCyS, sodium cymene sulfonate; SPCS, sodium pseudo-cumene sulfonate.

sulfate as a hydrotrope. By adding the hydrotrope to the water phase, the absolute increase will be higher for *o*-chlorobenzoic acid than for *p*-chlorobenzoic acid, while the solubility of the *p*-isomer is lower than for the *o*-isomer in the hydrotropic solution. This difference in the solubility can be used for separation since one component will precipitate upon dilution with water. The initial composition, temperature, water addition flow-rate and the path followed during the process will influence which component will precipitate, as well as the size distribution of the crystals. The same behaviour is also expected and has in fact been reported for *o*- and *p*-chloronitrobenzenes due to different solubilities in the solution of sodium butyl monoglycol sulfate (28).

Table 18.5 gives an overview of different systems used in separative processes.

4.3 Polymers and hydrotropes

The amino acid proline, which has a high water solubility, will increase the solubility of a number of different hydrophobic substances such as pyrene, fluorescein diacetate (FDA), progesterone and estradiol. The increase in the solubility of FDA as a function of the proline concentration is sigmoidal in form, thus indicating the hydrotropic activity of proline (29). The efficacy regarding increasing the solubility is in the same range as for traditional hydrotropes such as sodium toluene sulfonate, sodium cumene sulfonate and sodium butyl monoglycol sulfate. It has been suggested that the stacking of the molecule might be more difficult for proline since the solubility curve is not as steep as that observed for hydrotropes in general. The polarity of the proline solution is not very different from water, which means that this amino acid does not offer a micro-environment which is as non-polar as found for other hydrotropes. This might, in fact, be regarded as an advantage for biopolymers, which need to contain their active conformations to retain their specific functions. Proline has been proven to increase the denaturation

temperature for the protein enzyme α -chymotrypsin, as well as for ribonuclease A. Due to this ability, proline is a protein-compatible hydrotrope. The 4-hydroxyproline compound will not exhibit hydrotropic activity, due to a limited solubility in water of the actual compound itself. The self-aggregation of 4-hydroxyproline may also be prevented by the presence of the hydroxyl group (13, 29).

4.4 Chemical reactions

Due to a low solubility of the hydrophobic reactant in the aqueous-phase and/or of the aqueous-phase reagent in the organic phase, the rates of many heterogeneous reactions are generally low. Since the hydrotrope will enhance the solubility of the organic compound in the aqueous phase, the employment of such compounds is very useful for increasing the rates for heterogeneous reactions (11, 13).

The solid-liquid alkaline hydrolysis of esters such as phenyl benzoate, ethyl *p*-nitrobenzoate and 2,4-dichlorophenylbenzoate has been studied in the presence of sodium *p*-toluene sulfonate, sodium xylene sulfonate and the sodium salts of phenol, *p*-chlorophenol, 2,4-dichlorophenol and 2,4,6-trichlorophenol. The solubilities of the esters in water is very low, but in the presence of the hydrotropes considerably higher reaction rates are obtained due to higher solubilities (30). The same behaviour was observed by using urea in the solid-liquid oximation of cyclododecanone where the reaction rate was increased. From studies of these types of reactions, the following observations were made (31):

- (i) Potassium salts were more effective than the sodium salts of different hydrotropes.
- (ii) Increasing the hydrophobicity of the hydrotrope by increasing the size of the bulky group attached to the benzene ring will enhance the hydrotropic intensification factor.

- (iii) The intensification factor will vary exponentially with the hydrotrope concentration.

Another example is the enhancement of the reaction rate for the Claisen–Schmidt condensation of benzaldehydes with acetophenone by using either sodium butyl monoglycol sulfate or the sodium salts of aromatic sulfonic acids as hydrotropes (32). Solvents such as *N*, *N*-dimethylformamide, tetrahydrofuran and alcohols are generally used in these preparations. However, by introducing hydrotrope solutions as the reactive media, the use of expensive organic solvents can be avoided.

4.5 Preparation of vesicles

Amphiphilic association structures such as micelles, microemulsion droplets, vesicles, etc. have a high potential in the biomedical, agricultural and chemical industries. Vesicles are characterized by a bilayer structure, where the bilayer, which is composed of surfactants, will separate two different water compartments, one forming the core and the other forming the external phase. They have proven to be useful in medical and personal care applications. Vesicles may, for example, be used as encapsulating agents for the controlled release of drugs in various formulations. Three examples of traditional procedures for preparing vesicles are as follows:

- mechanical agitation of lamellar liquid crystals
- evaporation of a volatile oil from an emulsion based on water, oil and the vesicle-forming compound
- solubilization of the vesicle-forming compound in surfactant micelles and thereafter dilution with water below the critical micelle concentration (CMC).

The disadvantage with the last method is that a high amount of micelle-forming surfactants, compared to the amount of vesicle-forming surfactants, is present. The micelle-forming surfactants will later on have to be removed by dialysis and the method is very time-consuming.

Aqueous solutions of hydrotropes have proven to be powerful systems for preparing vesicles. In this case, the vesicle-forming compound has been mixed with water and the hydrotrope, and dilution with water resulting in the vesicles (33). Vesicles formed by the nonionic surfactant Laureth 4 (Brij® 30) from an aqueous solution of sodium xylene sulfonate (SXS) were more stable and smaller than vesicles prepared from the suspension of the lamellar liquid crystal in water.

The preparation, structure and stability of vesicles have been thoroughly studied. However, it has been

difficult to investigate the kinetics for vesicle formation by preparing vesicles using the above traditional techniques. By using mechanical agitation, the size and the distribution is dependent on the added energy. The high ratio between the micelle-forming surfactant and the vesicle-forming compound indicates that the osmotic process will be time-consuming. Since a very low amount of hydrotropes is necessary in the procedure of vesicle formation, use of such compounds is considered to be a very interesting technique for these types of studies (34).

4.6 Solubilization of pharmaceuticals

The importance of using hydrotropes in pharmaceutical formulations was realized quite early on in the history of hydrotropes. They have to a high extent been used as solubilizing agents for preparing formulations of specific drugs since the low water solubility of the drug is usually the limiting factor in the formulation process (11, 13). Other methods to achieve stable drug formulations are to use cosolvent systems and micellar solubilization employing surfactants. However, problems with toxicity and precipitation of microcrystals have occurred (35) and hydrotropic solubilization offers new possibilities in the field to prepare safe, non-toxic systems of poorly water-soluble drugs. When the drug is kept solubilized in emulsions and suspensions, multiphase systems are achieved. In the case of hydrotropes, a homogenous phase is expected. Much of the literature regarding hydrotropes in the pharmaceutical area have dealt with the solubilization of drugs in aqueous-based formulations. A number of studies have also been performed to explore the mechanistic performance of the hydrotrope, in particular to elucidate complexation between the hydrotrope and the drug. Examples of drugs known to be poorly water-soluble which have been studied by using hydrotropes are riboflavin (vitamin B₂) (35), nifedipine (36), ketoprofen (37), flurbiprofen (38) and oxamniquine (39).

Nicotinamide, or vitamin B₃, characterized by a low toxicity, has been proven to solubilize a number of drugs, such as, for example, riboflavin (35) and nifedipine (36). A 36-fold increase of the solubility of riboflavin, which has a multi-aromatic ring system, at nicotinamide concentrations of about 2*M*, has been observed (35). It has been shown that complexation occurs between the riboflavin and the hydrotropic agents cytosine and caffeine, respectively (35). However, in the case of nicotinamide, no evidence for complexation between riboflavin and nicotinamide,

by performing fluorescence studies, could be found. Therefore, complexation could not explain the increased solubility of riboflavin in this case (35). The importance of self-association of the hydrotrope for the solubilizing process has been indicated for the system riboflavin and nicotinamide, since the solubilizing capacity of nicotinamide will decrease with temperature as the extent of self-association increases.

The aqueous solubility of ketoprofen (37) has been increased by using hydrotropes such as sodium benzoate, sodium-*m*-hydroxy benzoate, sodium *o*-hydroxy benzoate, sodium dihydroxy benzoate, sodium ascorbate and nicotinamide. Two different mechanisms have been proposed at low and high concentrations of hydrotropes, respectively. At low hydrotrope concentrations, it is assumed that a weak ionic interaction between the hydrotrope and the drug will occur, which is a result of the differences in electronegativity found for the two solutes. Other interactions such as hydrogen bonding may also be of importance. The proposed mechanism for enhanced solubilization at high hydrotrope concentrations, i.e. above the MHC, is the formation of molecular aggregation between the drug and the hydrotrope.

The effect of nicotinamide, sodium benzoate, sodium naphthoate, sodium nicotinate and sodium isonicotinate on the solubility of oxamniquine in water (39) has revealed the importance of the structure of the hydrotrope. Sodium naphthoate resulted in a higher solubility of the solute when compared to sodium benzoate. This indicates that an expansion of the ring system enhances solubility, a phenomenon that has also been found for chlorothiazide, phenacetin and allopurinol. The solubilizing capacity of the hydrotrope will also increase by replacing the benzene ring with a pyridine ring, which has been observed for the systems sodium nicotinate, sodium isonicotinate and sodium benzoate, where the benzoate showed the least increase in solubility of oxamniquine. Differential UV absorption studies indicated that molecular interactions occurred between the hydrotropes and oxamniquine since spectral changes were observed in the presence of the hydrotropes, thus suggesting that complexation is an important mechanism. This study revealed the formation of 1:1 complexes of oxamniquine with sodium naphthoate, sodium isonicotinate and nicotinamide, and 1:2 complexes with sodium nicotinate and sodium benzoate. A correlation was also found between the solubilizing powers of the hydrotropes and the stability constants for their complexes. Even though complex formation seemed to be responsible for the increased solubility of the drug, the effect of salting-in may also

play a role for the hydrotropes sodium nicotinate and sodium isonicotinate.

5 REFERENCES

1. Neuberg, C., Hydrotropische Erscheinungen, *Biochem. Z.*, **76**, 107–176 (1916).
2. McKee, R. H., Use of hydrotropic solutions in industry, *Ind. Eng. Chem. Ind. Ed.*, **38**, 382–384 (1946).
3. Booth, H. S. and Everson, H. E., Hydrotropic solubilities – Solubilities in 40 per cent sodium xylenesulfonate, *Ind. Eng. Chem.*, **40**, 1491–1493 (1948).
4. Booth, H. S. and Everson, H. E., Hydrotropic solubilities – Solubilities in aqueous sodium arylsulfonate solutions, *Ind. Eng. Chem.*, **41**, 2627–2628 (1949).
5. Booth, H. S. and Everson, H. E., Hydrotropic solubilities – Solubilities in aqueous sodium *o*-, *m*- and *p*-xylenesulfonate solutions, *Ind. Eng. Chem.*, **42**, 1536–1537 (1950).
6. Lumb, E. C., Phase equilibria in mixtures of alcohols with aqueous hydrotropic salt solutions, *Trans. Faraday Soc.*, **47**, 1049–1055 (1951).
7. Lawrence, A. S. C., The mechanism of detergency, *Nature (London)*, **183**, 1491–1494 (1959).
8. Friberg, S. and Rydhag, L., Löslichkeit und assoziationsverhältnisse hydrotroper substanzen, *Tenside Surf. Det.*, **7**, 80–83 (1970).
9. Pearson, J. T. and Smith, J. M., Effect of hydrotropic salts on the stability of liquid crystalline systems, *J. Pharm. Pharmacol.*, **26**, (Suppl.), 123–124 (1974).
10. Friberg, S. E. and Chiu, M., Hydrotropes, *J. Disp. Sci. Tech.*, **9**, 443–457 (1988–1989).
11. Balasubramanian, D. and Friberg, S. E., Hydrotropes – Recent developments, *Surf. Colloid Sci.*, **15**, 197–220 (1993).
12. Friberg, S. E. and Brancewicz, C., Hydrotropy, in *Liquid Detergents*, Lai, K.-Y. (Ed.), Surfactant Science Series, Vol. 67, Marcel Dekker, New York, 1997, pp. 21–33.
13. Friberg, S. E., Hydrotropes, *Curr. Opinion Colloid Interface Sci.*, **2**, 490–494 (1997).
14. Saleh, A. M. and El-Khordagui, L. K., Hydrotropic agents: a new definition, *Int. J. Pharm.*, **24**, 231–238 (1985).
15. Friberg, S. E., Diacid – a hydrotrope of unusual structure, *Spec. Publ. – R. Soc. Chem.*, **107** (Ind. Appl. Surfactants III), 227–241 (1992).
16. Matero, A., Mattsson, Å., and Svensson, M., Alkyl polyglucosides as hydrotropes, *J. Surf. Det.*, **1**, 485–489 (1998).
17. Balasubramanian, D., Srinivas, V., Gaikar, V. G. and Sharma, M. M., Aggregation behavior of hydrotropic compounds in aqueous solution, *J. Phys. Chem.*, **93**, 3865–3870 (1989).
18. Srinivas, V., Sundaram, C. S. and Balasubramanian, D., Molecular structure as a determinant of hydrotropic action: A study of polyhydroxybenzenes, *Ind. J. Chem.*, **30B**, 147–152 (1991).

19. Saleh, A. M., Badwan, A. A. and El-Khordagui, L. K., A study of hydrotropic salts, cyclohexanol and water systems, *Int. J. Pharm.*, **17**, 115–119 (1983).
20. Guo, R., Compo, M. E., Friberg, S. E. and Morris, K., The coupling action of a hydrotrope and surface transition from lamellar liquid crystal to bicontinuous microemulsion, *J. Disp. Sci. Technol.*, **17**, 493–507 (1996).
21. Burns, R. L., Hydrotropic properties of some short-chain alkylbenzene and alkyl-naphthalene sulfonates, *J. Surf. Det.*, **2**, 13–16 (1999).
22. Friberg, S. E., Rananavare, S. B. and Osborne, D. W., The mechanism of hydrotrope action of a dicarboxylic acid, *J. Colloid Interface. Sci.*, **109**, 487–492 (1986).
23. Otten, J. G. and Nestor, C. L., Anionic hydrotropes for industrial and institutional rinse aids, *J. Am. Oil Chem. Soc.*, **63**, 1078–1081 (1986).
24. Gaikar, V. G. and Sharma, M. M., Separations with hydrotropes, *Sep. Technol.*, **3**, 2–11 (1993).
25. Agarwal, M., and Gaikar, V. G., Extractive separations using hydrotropes, *Sep. Technol.*, **2**, 79–84 (1992).
26. Mahapatra, A., Gaikar, V. G. and Sharma, M. M., New strategies in extractive distillation: Use of aqueous solutions of hydrotropes and organic bases as solvent for organic acids, *Sep. Sci. Technol.*, **23**, 429–436 (1988).
27. Colonia, J. C., Dixit, A. B. and Tavare, N. S., Separation of chlorobenzoic acids through hydrotrophy, *Ind. Eng. Chem. Res.*, **37**, 1956–1969 (1998).
28. Geetha, K. K., Tavare, N. S. and Gaikar, V. G., Separation of *o*- and *p*- chloronitrobenzenes through hydrotrophy, *Chem. Eng. Commun.*, **102**, 211–224 (1991).
29. Srinivas, V. and Balasubramanian, D., Proline is a protein-compatible hydrotrope, *Langmuir*, **11**, 2830–2833 (1995).
30. Janakiraman, B. and Sharma, M. M., Enhancing rates of multiphase reactions through hydrotrophy, *Chem. Eng. Sci.*, **40**, 2156–2158 (1985).
31. Pandit, A. and Sharma, M. M., Intensification of heterogeneous reactions through hydrotrophy: alkaline hydrolysis of esters and oximation of cyclododecanone, *Chem. Eng. Sci.*, **42**, 2517–2523 (1987).
32. Sadvilkar, V. G., Samant, S. D. and Gaikar, V. G., Claisen–Schmidt reaction in a hydrotropic medium, *J. Chem. Tech. Biotechnol.*, **62**, 405–410 (1995).
33. Friberg, S. E., Yang, H., Fei, L., Sadasivan, S., Rasmussen D. H. and Aikens, P. A., Preparation of vesicles from hydrotrope solutions, *J. Disp. Sci. Technol.*, **19**, 19–30 (1998).
34. Campbell, S. E., Yang, H., Patel, R., Friberg, S. E. and Aikens, P. A., Kinetics of vesicle formation, *Colloid Polym. Sci.*, **275**, 303–306 (1997).
35. Coffman, R. E. and Kildsig, D. O., Hydrotropic solubilization – Mechanistic studies, *Pharm. Res.*, **3**, 1460–1463 (1996).
36. Suzuki, H. and Sunada, H., Mechanistic studies on hydrotropic solubilization of nifedipine in nicotinamide solution, *Chem. Pharm. Bull.*, **46**, 125–130 (1998).
37. Jain, N. K., Singhai, A. K. and Jain, S., Hydrotropic solubilization of ketoprofen, *Pharmazie*, **51**, 236–239 (1996).
38. Gupta, G. D., Jain, S. and Jain, N. K., Formulation of an aqueous injection of flurbiprofen, *Pharmazie*, **52**, 709–712 (1997).
39. Ammar, H. O. and Khalil, R. M., Effect of aromatic hydrotropes on the solubility of oxoamniquinone, *Pharmazie*, **51**, 490–493 (1996).

CHAPTER 19

Physico-Chemical Properties of Surfactants

Björn Lindman

Lund University, Lund, Sweden

1	Different Surfactant Systems	421	9	Micelle Size and Structure may Vary	431
2	Surfactants Start to Form Micelles at the <i>CMC</i>	422	10	A Geometrical Consideration of Chain Packing is Useful	432
3	The <i>CMC</i> Depends on the Chemical Structure	423	11	Kinetics of Micelle Formation	433
4	Temperature and Cosolutes Affect the <i>CMC</i>	425	12	Surfactants may Form Aggregates in Other Solvents than Water	434
5	The Solubility of Surfactants may be Strongly Temperature-Dependent	427	12.1	Polar solvents	434
6	Driving Forces of Micelle Formation and Thermodynamic Models	428	12.2	Non-polar solvents	434
6.1	Hydrophobic interactions	428	13	General Comments on Amphiphile Self-Assembly	435
6.2	Phase separation model	429	14	Micelle Type and Size Vary with Concentration	435
6.3	Mass action law model	429	15	Micellar Growth is Different for Different Systems	437
6.4	Multiple equilibrium model	429	16	Surfactant Phases are Built Up by Discrete or Infinite Self-Assemblies	439
7	The Association Process and Counterion Binding can be Monitored by NMR Spectroscopy	430	17	Nonionic Oxyethylene Surfactants Display Special Temperature Effects	440
8	Hydrophobic Compounds can be Solubilized in Micelles	431	18	Clouding is a Characteristic Feature of Polyoxyethylene-Based Surfactants	442
			19	Bibliography	442

1 DIFFERENT SURFACTANT SYSTEMS

Self-assembly of amphiphilic molecules, such as surfactants and polar lipids, leads to a range of different structures, of which a few are shown in Figure 19.1. Systems containing amphiphiles are best classified into homogeneous, or single-phase, systems and heterogeneous systems of two or more phases. The single-phase systems can in turn be divided into isotropic solutions,

solid phases and liquid crystalline phases. The solid crystalline phases have, as do crystals in general, both long-range and short-range order, but the degree of short-range order varies between different phases. Isotropic solution phases are characterized by disorder over both short and long distances, while liquid crystalline phases or mesophases have a short-range disorder but some distinct order over larger distances. In both isotropic solutions and liquid crystals, the state of the amphiphile alkyl chains can be denoted as “liquid-like”.

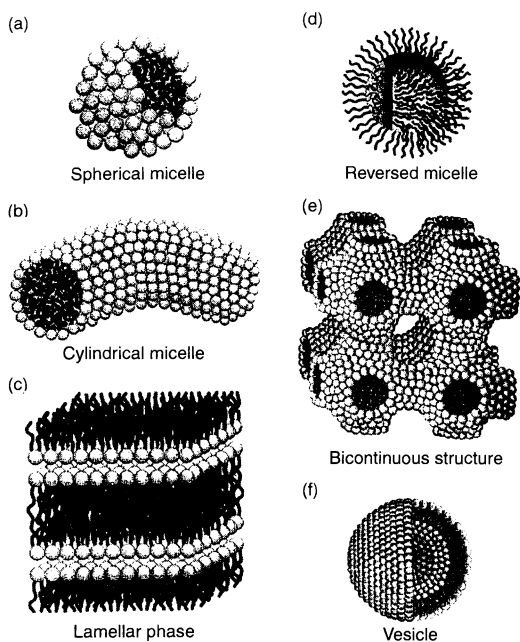


Figure 19.1. Surfactant self-assembly leads to a range of different structures of which a few are shown here. (a) Spherical micelles with an interior composed of the hydrocarbon chains and a surface of the polar head-groups (pictured as spheres) facing the water. Spherical micelles are characterized by a low surfactant number (critical packing parameter) and a strongly positive spontaneous curvature. The hydrocarbon core has a radius close to the length of the extended alkyl chain. (b) Cylindrical micelles with an interior composed of the hydrocarbon chains and a surface of the polar head-groups facing the water. The cross-section of the hydrocarbon core is similar to that of spherical micelles. The micellar length is highly variable so these micelles are polydisperse. (c) Surfactant bilayers which build up lamellar liquid crystals have, for surfactant–water systems, a hydrocarbon core with a thickness of ca. 80% of the length of two extended alkyl chains. (d) Reversed or inverted micelles have a water core surrounded by the surfactant polar head-groups. The alkyl chains, together with a non-polar solvent, make up the continuous medium. Like “normal” micelles, they can grow into cylinders. (e) A bicontinuous structure with the surfactant molecules aggregated into connected films characterized by two curvatures of opposite sign. The mean curvature is small (zero for a minimal surface structure). (f) Vesicles are built from bilayers similar to those of the lamellar phase and are characterized by two distinct water compartments, with one forming the core and one the external medium. Vesicles may have different shapes, and there are also reversed-type vesicles. (Redrawn from D. F. Evans and H. Wennerström, *The Colloidal Domain: Where Physics, Chemistry, Biology and Technology Meet*, VCH, New York, 1994, pp. 14–15)

In crystals, formed below the “chain melting temperature”, the state is more or less “solid-like”. The more

Table 19.1. Different amphiphile systems

<i>Homogeneous systems</i>	
Solid phases	
Many different structures	
Liquid crystalline phases	
Lamellar	
Hexagonal	
Reversed hexagonal	
Cubic: several structures are known, which can be grouped into water-continuous, hydrophobe-continuous and bicontinuous	
“Intermediate” and “deformed” phases, including “nematic lyotropic”	
Isotropic solution phases	
Dilute and concentrated micellar solutions	
Reversed micellar solutions	
Microemulsions	
<i>Heterogeneous systems</i>	
Emulsions	
Suspensions	
Vesicles, liposomes	
Foams	
Adsorbed surfactant layers and other surfactant films	
Gels	

important amphiphile systems can be arranged as shown in Table 19.1.

This present chapter describes micelle formation in isotropic solutions, while surfactant self-assembly into other structures is treated in other chapters in this volume, as well as surfactant self-assembly in the presence of polymer chains and solid surfaces.

2 SURFACTANTS START TO FORM MICELLES AT THE *CMC*

When measuring the different physico-chemical properties of aqueous solutions of a surfactant or lipid, which is polar enough to be water-soluble up to relatively high concentrations, we will encounter many peculiarities, as exemplified in Figure 19.2 for an ionic surfactant. At low concentrations, most properties are similar to those of a simple electrolyte. One notable exception is the surface tension, which decreases rapidly with the surfactant concentration. At some higher concentration, which is different for different surfactants, unusual changes are recorded. For example, the surface tension, and also the osmotic pressure, takes on an approximately constant value, while light scattering starts to increase and self-diffusion starts to decrease. All of these observations suggest and are consistent with a change-over from a solution containing single surfactant molecules or ions, “unimers”, to a situation where the surfactant more and more occurs in a self-assembled or self-associated state.

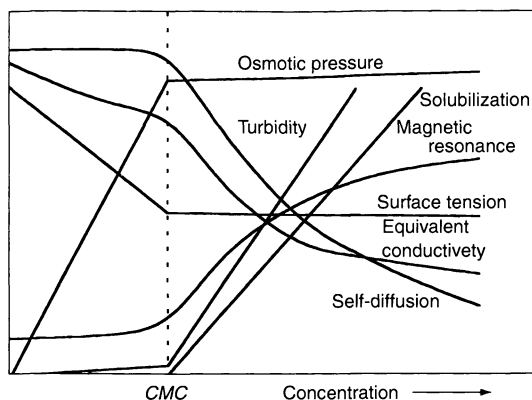


Figure 19.2. Schematic representation of the concentration dependence of some physical properties for solutions of a micelle-forming surfactant. (Redrawn from B. Lindman and H. Wennerström, *Topics in Current chemistry*, Vol. 87, Springer-Verlag, Berlin, 1980, p. 6)

We will examine in detail the structures formed as well as the underlying mechanisms, and will only note here two general features. The concentration for the onset of self-assembly is quite well defined and becomes more so the longer the alkyl chain of the surfactant. The first-formed aggregates are generally approximately spherical in shape. We call the aggregates “micelles”, and the concentration where they start to form the “critical micelle concentration” (*CMC*). An illustration of a micelle’s structure is given in Figure 19.3.

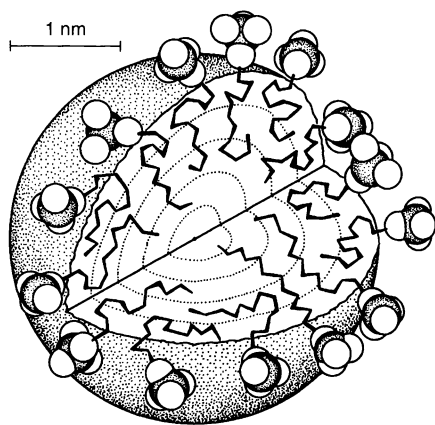


Figure 19.3. An illustration of a spherical micelle (for dodecyl sulfate), with a disordered hydrocarbon core and a rough surface, emphasizing the liquid-like character. (Redrawn from J. Israelachvili, *Intermolecular and Surface Forces, with Applications to Colloidal and Biological Systems*, Academic Press, London, 1985, p. 251)

The *CMC* is the single most important characteristic of a surfactant, useful *inter alia* in considerations of practical uses of surfactants. We will now consider how different factors influence the *CMC*, but let us first make a note on how to measure it. The two most common and generally applicable techniques are surface tension and, solubilization, i.e. the solubility of an otherwise insoluble compound. For an ionic amphiphile, the conductivity offers a convenient approach to obtain the *CMC*. However, as a very large number of physico-chemical properties are sensitive to surfactant micellization, there are numerous other possibilities, such as self-diffusion measurements and NMR and fluorescence spectroscopy. As we will see, the *CMC* is not an exactly defined quantity, which causes difficulties in its determination. For long-chain amphiphiles, an accurate determination is straightforward and different techniques will give the same results. However, for short-chain, weakly associating amphiphiles this is not the case and great care must be taken not only in the measurements but also in evaluating the *CMC* from experimental data.

3 THE *CMC* DEPENDS ON CHEMICAL STRUCTURE

A list of the *CMC* values of selected surfactants at 25°C is given in Table 19.2, while in Table 19.3 a list for nonionic surfactants is given. From these and other data, several general remarks about the variation of the *CMC* with the surfactant chemical structure can be made, as follows:

- (i) The *CMC* decreases strongly with increasing alkyl chain length of the surfactant (Figures 19.4 and 19.5). As a general rule, the *CMC* decreases by a factor of ca. 2 for ionics (without added salt) and by a factor of ca. 3 for nonionics on adding one methylene group to the alkyl chain (Table 19.4). Comparisons between the different classes of surfactants are best made at a fixed number of carbons in the alkyl chain length.
- (ii) The *CMCs* of nonionics are much lower than those of ionics. The relationship depends on alkyl chain length, although two orders of magnitude is a rough starting point.
- (iii) Besides the major difference between ionics and nonionics, the effects of the head-groups are moderate. Cationics typically have slightly higher *CMCs* than anionics. For nonionics of the oxyethylene variety, there is a moderate increase of the *CMC* as the polar head-group becomes larger.

Table 19.2. CMC values of some selected surfactants at 25°C

Surfactant	CMC ^a
Dodecylammonium chloride	$1.47 \times 10^{-2} M$
Dodecyltrimethylammonium chloride	$2.03 \times 10^{-2} M$
Decyltrimethylammonium bromide	$6.5 \times 10^{-2} m$
Dodecyltrimethylammonium bromide	$1.56 \times 10^{-2} m$
Hexadecyltrimethylammonium bromide	$9.2 \times 10^{-4} m$
Dodecylpyridinium chloride	$1.47 \times 10^{-2} M$
Sodium tetradecyl sulfate	$2.1 \times 10^{-3} M$
Sodium dodecyl sulfate	$8.3 \times 10^{-3} M$
Sodium decyl sulfate	$3.3 \times 10^{-2} M$
Sodium octyl sulfate	$1.33 \times 10^{-1} M$
Sodium octanoate	$4 \times 10^{-1} m$
Sodium nonanoate	$2.1 \times 10^{-1} m$
Sodium decanoate	$1.09 \times 10^{-1} m$
Sodium undecanoate	$5.6 \times 10^{-2} m$
Sodium dodecanoate	$2.78 \times 10^{-2} m$
Sodium <i>p</i> -octylbenzene sulfonate	$1.47 \times 10^{-2} m$
Sodium <i>p</i> -dodecylbenzene sulfonate	$1.20 \times 10^{-3} m$
Dimethyldodecylamineoxide	$2.1 \times 10^{-3} M$
CH ₃ (CH ₂) ₉ (OCH ₂ CH) ₆ OH	$9 \times 10^{-4} M$
CH ₃ (CH ₂) ₉ (OCH ₂ CH) ₉ OH	$1.3 \times 10^{-3} M$
CH ₃ (CH ₂) ₁₁ (OCH ₂ CH) ₆ OH	$8.7 \times 10^{-5} M$
CH ₃ (CH ₂) ₇ C ₆ H ₄ (CH ₂ CH ₂ O) ₆	$2.05 \times 10^{-4} M$
Potassium perfluorooctanoate	$2.88 \times 10^{-2} m$

^aIn moles/dm³ (*M*) or moles/kg H₂O (*m*).

Table 19.3. CMC values for some selected nonionic surfactants

Surfactant	CMC (μM)
C ₆ E ₃	10×10^4
C ₈ E ₄	8.5×10^3
C ₈ E ₅	9.2×10^3
C ₈ E ₆	9.9×10^3
C ₁₀ E ₅	9.0×10^2
C ₁₀ E ₆	9.5×10^2
C ₁₀ E ₈	10×10^2
C ₁₂ E ₅	6.5×10
C ₁₂ E ₆	6.8×10
C ₁₂ E ₇	6.9×10
C ₁₂ E ₈	7.1×10
C ₁₄ E ₈	9.0
C ₁₆ E ₉	2.1
C ₁₆ E ₁₂	2.3
C ₁₆ E ₂₁	3.9
C ₈ φE ₉	3.4×10^2
C ₈ φE ₁₀	3.4×10^2
C ₁₂ NO	2.2×10^3
β-D-C ₈ glucoside	2.5×10^4
β-D-C ₁₀ glucoside	2.2×10^3
β-D-C ₁₂ glucoside	1.9×10^2

(iv) The valency of the counterion is significant. While simple monovalent inorganic counterions

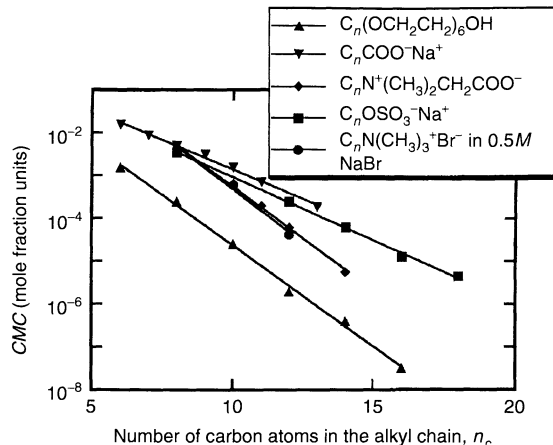


Figure 19.4. The logarithm of the CMC varies linearly with the number of carbon atoms in the alkyl chain of a surfactant. The slope is larger for a nonionic surfactant, or an ionic with added salt, than for an ionic surfactant without added electrolyte. (Redrawn from B. Lindman and H. Wennerström, *Topics in Current Chemistry*, Vol. 87, Springer-Verlag, Berlin, 1980, p. 8)

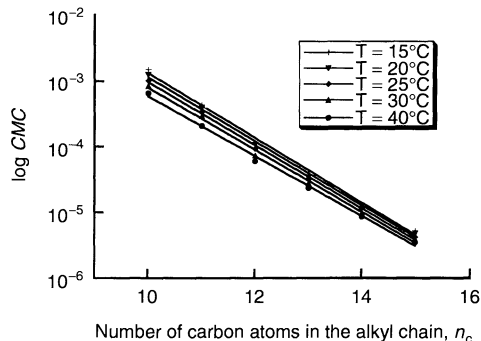


Figure 19.5. The logarithm of the CMC (molar concentration) versus the number of carbons in the alkyl chain for various octa(ethylene glycol)monoalkyl ethers at different temperatures. From top to bottom, the temperatures are 15.0, 20.0, 25.0 and 30.0 and 40.0°C. (Redrawn from K. Meguro, M. Ueno and K. Esumi, in *Nonionic Surfactants Physical Chemistry*, M. J. Schick (Ed.), Marcel Dekker, New York, 1987, p. 134)

give roughly the same CMC, increasing the valency to 2 gives a reduction of the CMC by roughly a factor of 4. Organic counterions reduce the CMC when compared to inorganic ones – the more so the larger the nonpolar part.

(v) While alkyl chain branching and double bonds, aromatic groups or some other polar character in the hydrophobic part produce sizeable

Table 19.4. The *CMC* decreases strongly with the alkyl chain length. The decrease follows, to a good approximation, the relationship $\log CMC = A - Bn_C$, where n_C is the number of carbons in the alkyl chain

Surfactant series	Temperature (°C)	A	B
Na carboxylates (soaps)	20	1.8(5)	0.30
K carboxylates (soaps)	25	1.9(2)	0.29
Na (K) <i>n</i> -alkyl 1-sulfates or -sulfonates	25	1.5(1)	0.30
Na <i>n</i> -alkane-1-sulfonates	40	1.5(9)	0.29
Na <i>n</i> -alkane-1-sulfonates	55	1.1(5)	0.26
Na <i>n</i> -alkane-1-sulfonates	60	1.4(2)	0.28
Na <i>n</i> -alkyl-1-sulfates	45	1.4(2)	0.30
Na <i>n</i> -alkyl-1-sulfates	60	1.3(5)	0.28
Na <i>n</i> -alkyl-2-sulfates	55	1.2(8)	0.27
Na <i>p</i> - <i>n</i> -alkylbenzene sulfonates	55	1.6(8)	0.29
Na <i>p</i> - <i>n</i> -alkylbenzene sulfonates	70	1.3(3)	0.27
<i>n</i> -Alkylammonium chlorides	25	1.2(5)	0.27
<i>n</i> -Alkylammonium chlorides	45	1.7(9)	0.30
<i>n</i> -Alkytrimethylammonium bromides	25	1.7(2)	0.30
<i>n</i> -Alkytrimethylammonium chlorides (in 0.1 M NaCl)	25	1.2(3)	0.33
<i>n</i> -Alkytrimethylammonium bromides	60	1.7(7)	0.29
<i>n</i> -Alkylpyridinium bromides	30	1.7(2)	0.31
<i>n</i> -C _n H _{2n+1} (OC ₂ H ₄) ₆ OH	25	1.8(2)	0.49

changes in the *CMC*, a dramatic lowering of the *CMC* (one or two orders of magnitude) results from perfluorination of the alkyl chain. Interestingly, partial fluorination may increase the *CMC*; for example, fluorination of the terminal methyl group roughly doubles the *CMC*. The anomalous behaviour of partially fluorinated surfactants is due to unfavourable interactions between the hydrocarbon and fluorocarbon groups.

4 TEMPERATURE AND COSOLUTES AFFECT THE *CMC*

It is a characteristic feature of ionic surfactant micellization that the *CMC* is, to a first approximation, independent of the temperature. The temperature-dependence of the *CMC* of sodium dodecyl sulfate (SDS), displayed in Figure 19.6, is a good illustration of this. The *CMC* varies in a non-monotonic way by ca. 10–20% over a wide range. The shallow minimum at around 25°C can be compared with a similar minimum in the solubility of hydrocarbons in water. Nonionic surfactants of the polyoxyethylene type deviate from this behaviour and show typically a monotonic, and much more pronounced, decrease in *CMC* with increasing temperature. As will be discussed briefly at the end of this chapter, this class of nonionics behaves differently from other surfactants with respect to temperature effects.

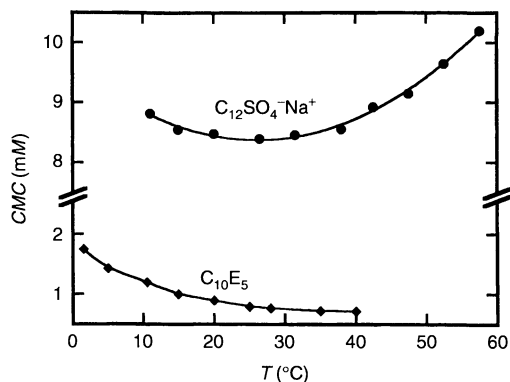


Figure 19.6. Temperature dependence of the *CMC* of sodium dodecyl sulfate (top) and penta(ethylene glycol)monodecyl ether. (Redrawn from P. H. Elworthy, A. T. Florence and C. B. Macfarlane, *Solubilisation by Surface-Active Agents*, Chapman & Hall, London, 1968)

Pressure has little influence on the *CMC*, even up to high values.

Turning next to the effect of cosolutes on the *CMC*, this is an important and broad issue that we will come back to later. A most important matter is the effect of added electrolyte on the *CMC*s of ionics. This is illustrated in Figure 19.7 for the simplest and generally most important case of adding a 1:1 inert electrolyte to a solution of a monovalent surfactant. The following features are noted:

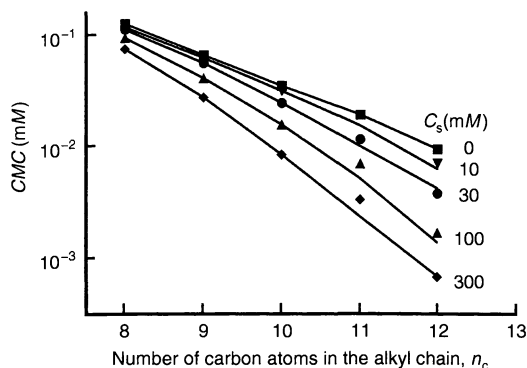


Figure 19.7. Effect of sodium chloride addition on the *CMC* of different sodium alkyl sulfates. The solid lines represent predictions from electrostatic theory (Poisson–Boltzmann equation), with c_s being the salt concentrations. (Redrawn from G. Gunnarsson, B. Jönsson and H. Wennerström, *J. Phys. Chem.*, **84** (1980) 3114)

- (i) Salt addition gives a dramatic lowering of the *CMC*, which may amount to an order of magnitude.
- (ii) The effect is moderate for short-chain surfactants but much larger for long-chain ones.
- (iii) As a consequence, at high salt levels the variation of the *CMC* with the number of carbons in the alkyl chain is much stronger than without added salt. The rate of change at high salt levels becomes similar to that of nonionics.
- (iv) The salt effects (as many other aspects of ionic surfactant self-assembly) can be quantitatively reproduced from a simple model of electrostatic interactions, via the Poisson–Boltzmann equation. Let us further add that:
- (v) The effect of added salt depends strongly on the valency of the ions, and in line with what was noted above, it is most sensitive to the valency of added counterions.

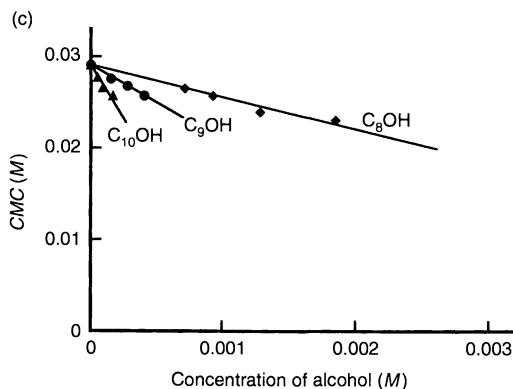
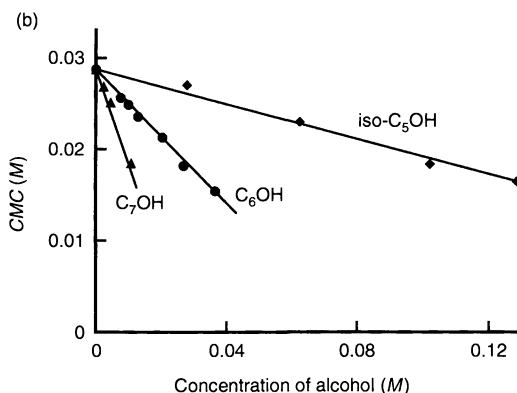
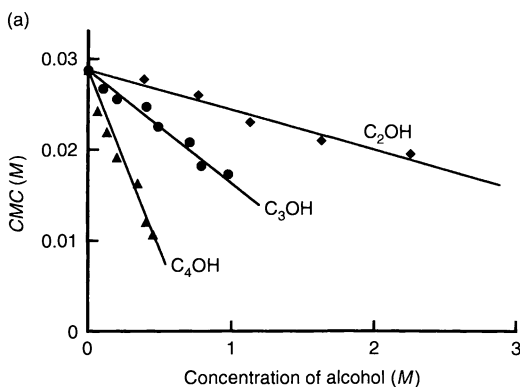


Figure 19.8. Addition of simple alcohols gives a lowering of the *CMC* (in this case for potassium dodecanoate) which is approximately linear with the cosolute concentration. The slope increases rapidly when the alcohol becomes less polar. (Redrawn from K. Shinoda, T. Nakagawa, B. -I. Tamamushi and T. Isemura, *Colloidal Surfactants: Some Physicochemical Properties*, Academic Press, London, 1963)

(vi) For nonionics, simple salts produce only small variations in the *CMC* with both increases and decreases possible.

Other low-molecular-weight cosolutes produce changes in the *CMC* to a very different extent depending on the cosolute polarity. Both increases and decreases in the *CMC* are possible. Small or moderate increases may result from the addition of highly water-soluble compounds, the reason being that water is the most effective solvent for surfactant self-assembly. More common and more interesting are the decreases in *CMC* observed for most uncharged cosolutes. The effect will depend on cosolute polarity and on any amphiphilic character it may have and is perhaps best illustrated by the addition of simple alcohols. As seen in Figure 19.8, alcohols lower the *CMC*, but to very different extents. The alcohols are less polar than water and are distributed between the bulk solution and the micelles. The more preference they have for the micelles, then the more they will stabilize them. A longer alkyl chain leads to a less favourable location in water and a more favourable one in the micelles. Here, it will act basically as any added nonionic amphiphile, such as a nonionic surfactant, in lowering the *CMC*.

5 THE SOLUBILITY OF SURFACTANTS MAY BE STRONGLY TEMPERATURE-DEPENDENT

There are many important and intriguing temperature effects in surfactant self-assembly. One, which is of great practical significance, is the dramatic temperature-dependent solubility notably displayed by many ionic surfactants. The solubility may be very low at low temperatures and then increases by orders of magnitude over a relatively narrow temperature range. The phenomenon is generally denoted as the “Krafft phenomenon”, with the temperature for the onset of the strongly increasing solubility being the “Krafft point” or “Krafft temperature”. The temperature-dependence of surfactant solubility in the region of the Krafft point is illustrated in Figure 19.9. The Krafft point may vary dramatically with subtle changes in the surfactant chemical structure, although some general remarks can be made for alkyl chain surfactants, as follows:

- (i) The Krafft point decreases strongly as the alkyl chain length increases. The decrease is not regular but displays an odd–even effect.
- (ii) The Krafft point is strongly dependent on the head-group and counterion. Salt addition typically

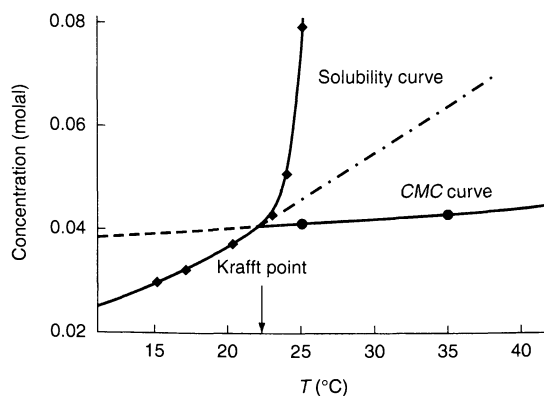


Figure 19.9. Temperature-dependence of surfactant solubility in the region of the Krafft point. (Redrawn from K. Shinoda, T. Nakagawa, B. -I. Tamamushi and T. Isemura, *Colloidal Surfactants: Some Physicochemical Properties*, Academic Press, London, 1963)

raises the Krafft point, while many other cosolutes decrease it. There are no general trends for the counterion dependence. Thus, for example, for alkali alkanooates the Krafft point increases as the atomic number of the counterion decreases, while the opposite trend is observed for alkali sulfates or sulfonates. For cationics, the Krafft point is typically higher for bromide than for chloride, and still higher for iodide. With divalent counterions, the Krafft point is typically often much higher.

The Krafft phenomenon is best discussed from the interplay between the temperature-dependence of the surfactant unimer solubility and the temperature dependence of the *CMC*. As we have learnt above, the latter temperature dependence is very weak and we can consider here that the *CMC* is, to a good approximation, independent of temperature. On the other hand, we expect the dissolution of the surfactant into the constituent solvated ions to increase markedly with temperature as seen for simple salts. If this solubility is below the *CMC*, no micelles can form and the total solubility is limited by the (low) unimer solubility. If, on the other hand, the unimer solubility reaches the *CMC*, micelles may form. It is a characteristic feature of micellization, as we will see later, that as the micelle concentration increases there is virtually no change in the free unimer activity (or concentration). This, together with a very high micelle solubility, explains why a quite small increase in unimer solubility (resulting here from a temperature increase) leads to a dramatic increase in the overall surfactant solubility.

The Krafft point is determined by the energy relationships between the solid crystalline state and the micellar solutions. It appears that the micellar solutions vary only weakly between different cases, like different counterions, while due to packing effects the solid crystalline state may change dramatically. Looking for an understanding of the Krafft phenomenon we have therefore to examine the packing effects and ionic interactions in the solid state.

If the solubility of a surfactant is very low it will clearly not be operative in various applications. Since a longer chain surfactant is generally more efficient, there is commonly a delicate compromise in the design of surfactants. Attempts to lower the Krafft point should mainly be directed towards the conditions in the solid state. Besides changing the counterion, which is not always possible, we should look into the packing conditions of the hydrophobic chains. The development of surfactants with a lower Krafft point is generally based on making the packing conditions in the solid state less favourable in one of the following ways:

- introduction of a methyl group, or some other chain branching, in the alkyl chain
- introduction of a double bond in the alkyl chain
- introduction of a polar segment, usually an oxyethylene group, between the alkyl chain and the ionic group.

These are also the common approaches to manufacturing surfactants compatible with hard water. Control of chain melting is also very important in biological systems, notably biological membranes, and is achieved by controlling the chain unsaturation.

6 DRIVING FORCES OF MICELLE FORMATION AND THERMODYNAMIC MODELS

6.1 Hydrophobic interactions

The most important characteristic of surfactants and polar lipids is the amphiphilicity. Water does not interact favourably with the hydrophobic groups and there is a driving force for expelling the latter from the aqueous environment. This may be achieved by a macroscopic phase separation or by hiding the non-polar groups in some other way. There are numerous other examples of hydrophobic effects and hydrophobic interactions, as illustrated in Figure 19.10. For a hydrocarbon in water there is a strong driving force for transfer to a hydrocarbon phase or to some other non-polar environment.

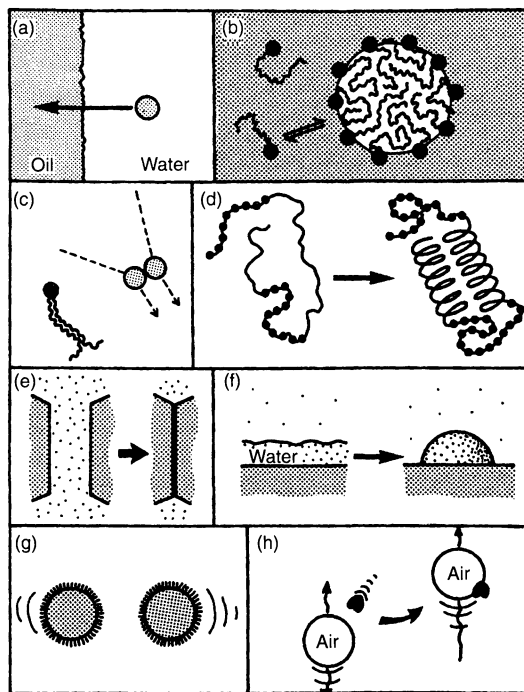


Figure 19.10. Illustrations of the effects of hydrophobic interactions, i. e. the tendency to eliminate contacts between water and nonpolar molecules or surfaces: (a) water and oil are immiscible, with a strong driving force to expel hydrocarbon molecules from water; (b) self-assembly of surfactant molecules; (c) other types of association of hydrocarbon chains; (d) folding of proteins; (e) strong adhesion between non-polar surfaces in water; (f) non-wetting of water on hydrophobic surfaces; (g) rapid coagulation of hydrophobic particles in water; (h) attachment of hydrophobic particles to air bubbles (mechanism of froth flotation). (Redrawn from J. Israelachvili, *Intermolecular and Surface Forces, with Applications to Colloidal and Biological Systems*, Academic Press, London, 2nd Edn, 1991)

When attaching a polar group to the hydrocarbon, an opposing force is created, which counteracts any phase separation. If the opposing force is weak, phase separation will still result. If it is very strong when compared to the hydrophobic effect, on the other hand, the amphiphile will occur as single molecules or as small aggregates, such as dimers. It is the common intermediate situation with a balance between hydrophobic and hydrophilic interactions that we are concerned with in surfactant self-assemblies.

The hydrophobic interaction increases with increasing alkyl chain length of an alkane or the hydrophobic group of a surfactant. Indeed, the decrease in solubility of an alkane with the number of carbons very much parallels the change in *CMC* that we discussed above.

We have noted that micellization (and surfactant self-assembly in general) is some intermediate between phase separation and simple complex formation and this is illustrated in the ways that micellization has been modelled in thermodynamic analyses. Micelle formation is generally discussed in terms of one of the following models.

6.2 Phase separation model

In this model, micelle formation is considered as being akin to a phase separation, with the micelles being the separated (pseudo-) phase, and the *CMC* the saturation concentration of surfactant in the unimeric state. Surfactant addition above the *CMC* consequently only affects the micelle concentration, but not the unimer concentration. In many physico-chemical investigations, we observe a number average over the different states that a surfactant molecule can occupy. The phase separation model is particularly simple for the interpretation of experimental observations. Below the *CMC*, we have only unimers and the average of a quantity Q is simply given as follows:

$$\langle Q \rangle = Q_{\text{aq}} \quad (19.1)$$

For a concentration above the *CMC*, we get, since $C_{\text{mic}} = C_{\text{tot}} - \text{CMC}$ and $C_{\text{aq}} = \text{CMC}$, the following:

$$\begin{aligned} \langle Q \rangle &= p_{\text{mic}} Q_{\text{mic}} + p_{\text{aq}} Q_{\text{aq}} \\ &= (1 - \text{CMC}/C_{\text{tot}}) Q_{\text{mic}} + (\text{CMC}/C_{\text{tot}}) Q_{\text{aq}} \end{aligned} \quad (19.2)$$

For concentrations sufficiently above the *CMC*, $\langle Q \rangle$ approaches Q_{mic} .

The phase separation model is simple to apply, illustrative and sufficient for many considerations. As we would expect, it becomes a better approximation the higher the aggregation number, i.e. the number of surfactant unimers in the micelle.

6.3 Mass action law model

Here, we assume a single micellar complex in equilibrium with the unimeric surfactant, as follows:



$$(A_n)/(A_1)^n = K \quad (19.4)$$

In this model, the aggregation number may be obtained from the variation in Q_{obs} around the *CMC*. The more

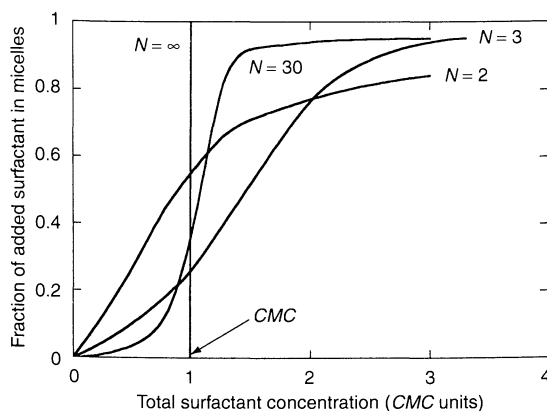
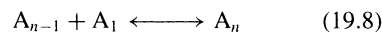
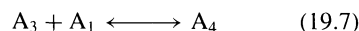
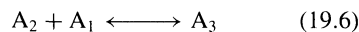
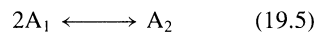


Figure 19.11. The fraction of added surfactant that goes to the micelles as a function of the total surfactant concentration for different aggregation numbers (N). (Redrawn from R. J. Hunter, *Foundations of Colloid Science*, Oxford University Press, Oxford, 1989, p. 576)

gradual the change, then the lower is the aggregation number and the more appropriate is the mass action law model with respect to the phase separation model. The fraction of added surfactant that goes to the micelles is plotted as a function of the total surfactant concentration for different aggregation numbers in Figure 19.11. For very high aggregation numbers, N , there is a close to stepwise change and the variation is in the limit the same as that predicted by the phase separation model.

In reality, micelles are not monodisperse, but there is a distribution of aggregation numbers, and micelles are formed in a stepwise process. This is taken into account in the following model.

6.4 Multiple equilibrium model



$$(A_n)/(A_{n-1}A_1) = K_n \quad (19.9)$$

As written, all of these treatments consider nonionic surfactants. To account for the association of the counterions to the micelles, we can add the relevant (stepwise if needed) equilibria for the counterions. This is normally not a reasonable approach though since the treatment in terms of equilibrium constants assumes short-range

interactions and the formation of well-defined complexes. The distribution of counterions is governed by electrostatic interactions which are long-range. It is, therefore, not possible to assign definite characteristics of “micellar-bound” counterions. This does not mean that counterion binding or association may not be a useful concept. However, we should be aware of the limitations and analyse findings in terms of the appropriate models.

7 THE ASSOCIATION PROCESS AND COUNTERION BINDING CAN BE MONITORED BY NMR SPECTROSCOPY

A complete characterization of the self-association of a surfactant would include giving the concentration of all of the different species as a function of the total surfactant concentration. We can not easily measure the concentration of micelles of all different aggregation numbers, but we can obtain some suitable averages. Let us consider the unimer concentration, the concentration of micellized surfactant, the concentration of bound and free counterions and the hydration of micelles. By using counterion- and surfactant-specific electrodes, we can obtain counterion and surfactant activities, which provide information on the distribution between micellar and unimeric states. Even more complete information is obtained if we measure the self-diffusion coefficients of surfactant molecules, micelles, counterions and water molecules. These can nowadays be obtained in a single fast experiment by using NMR methodology. A representative example is given in Figure 19.12 for the case of decylammonium dichloroacetate. The *CMC* is 26 mM. Self-diffusion coefficients constitute one example where the observed quantity is a weighted average over the different environments (micellar and unimeric) so that:

$$D_{\text{obs}} = p_{\text{mic}} D_{\text{mic}} + p_{\text{free}} D_{\text{free}} \quad (19.10)$$

or:

$$D_{\text{obs}} = (C_{\text{mic}} D_{\text{mic}} + C_{\text{free}} D_{\text{free}}) / C_{\text{tot}} \quad (19.11)$$

where D , p and C denote, respectively, the self-diffusion coefficient, the fraction of molecules in a given environment and the concentration; D_{free} is obtained from data below the *CMC* and D_{mic} , for example, from measurements on probe molecules confined to the micelles. In the study of Figure 19.12, a low (to avoid perturbation of the micellization) concentration of sparingly soluble tetramethylsilane (TMS) is used. Since

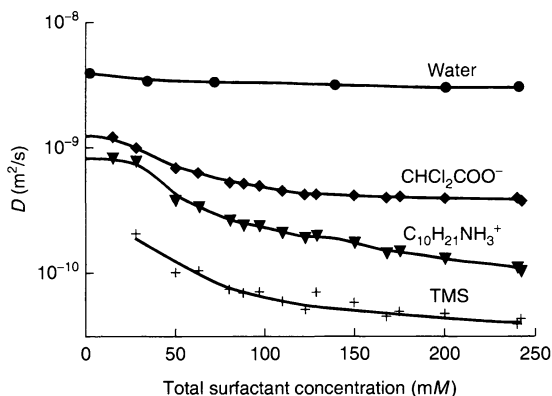


Figure 19.12. Dependence on the surfactant concentration of the self-diffusion coefficients of surfactant ions (decylammonium), counterions (dichloroacetate), water molecules and micelles (approximated by the diffusion of added tetramethylsilane (TMS)). (Redrawn from P. Stilbs and B. Lindman, *J. Phys. Chem.*, **85** (1981) 2587)

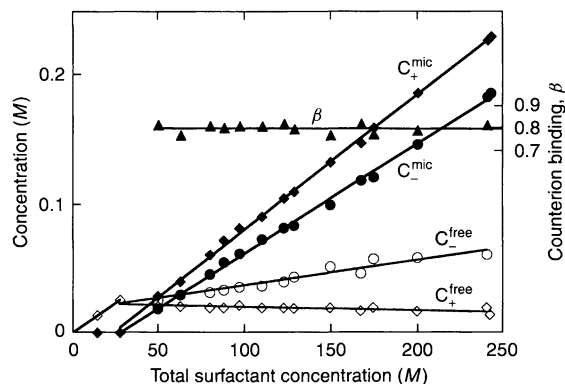


Figure 19.13. Concentrations of micellar and free unimeric surfactant ions (+) and counterions (−) as a function of the total surfactant (decylammonium dichloroacetate) concentration; β is the degree of counterion binding. (Redrawn from P. Stilbs and B. Lindman, *J. Phys. Chem.*, **85** (1981) 2587)

micelles are large entities, their D values are very much lower than those of single unimeric molecules.

As can be seen from Figure 19.12, the rate of self-diffusion is very different for the different molecules at concentrations well above the *CMC*. We can directly state that water molecules are least associated with the (slowly moving) micelles, while the TMS molecules are located in micelles to the largest extent. A quantitative analysis of the surfactant and counterion diffusion data gives the results presented in Figure 19.13. There are some important general features, generally applicable for ionic surfactants, which we should note, as follows:

- (i) To a good approximation, all surfactant molecules are in the unimeric state below the *CMC*.
- (ii) Above the *CMC*, the surfactant unimer concentration decreases and may reach values well below the *CMC*.
- (iii) The free counterion concentration increases at a lower rate above than below the *CMC*.
- (iv) If we normalize the micellar bound counterion concentration (C_{mic}^c) to the micellar surfactant concentration (C_{mic}^s), we obtain the degree of counterion binding, β , as follows:

$$\beta = C_{\text{mic}}^c / C_{\text{mic}}^s \quad (19.12)$$

It is an important result that β remains constant when we vary the micelle concentration over orders of magnitude.

The latter observation is often referred to as *counterion condensation*, meaning that counterion association is on a level which gives a certain critical effective charge density. The parameter β then remains approximately constant, even with large variations of the conditions, not only the micelle concentration but also the added salt and temperature. The counterion condensation phenomenon is common to all systems of high charge densities, including also polyelectrolytes and charged surfaces. It is very well understood from electrostatic theory.

8 HYDROPHOBIC COMPOUNDS CAN BE SOLUBILIZED IN MICELLES

TMS (Figure 19.12) is an example of a solubilized compound or a “solubilize”, i.e. a compound which becomes soluble due to the presence of micelles. Typically, the solubility stays very low until the *CMC* is reached, while above the *CMC* it increases rapidly and almost linearly with the surfactant concentration (Figure 19.14). Solubilization is one of the most important phenomena for surfactant solutions, with a direct bearing on, *inter alia*, detergency and the formulation of pharmaceuticals. In order to study the solubilization equilibria, and thus obtain information on the thermodynamics of solubilization, the mentioned self-diffusion technique is the most general and useful approach.

Surface tension measurements on impure surfactants provide an illustration of solubilization. If the surface tension is measured for sodium dodecyl sulfate solutions, one frequently obtains a minimum. On purification, this minimum is eliminated. The explanation is that SDS often contains some dodecanol (due to hydrolysis). The latter is more surface-active than SDS and

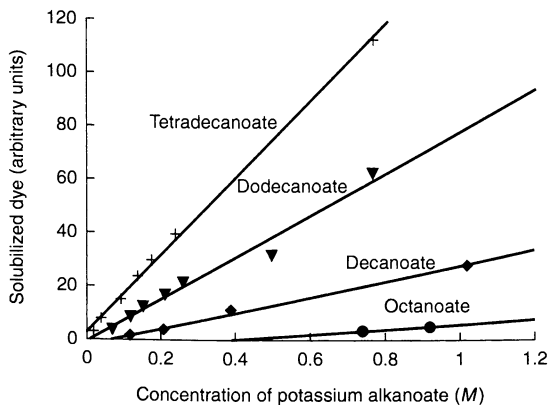


Figure 19.14. Amount of a dye solubilized in solutions of potassium alkanooates; from right to left, octanoate, decanoate, dodecanoate and tetradecanoate. (Redrawn from K. Shinoda, T. Nakagawa, B. -I. Tamamushi and T. Isemura, *Colloidal Surfactants: Some Physicochemical Properties*, Academic Press, London 1963, p. 26)

becomes concentrated at the air–water interface. However, as soon as micelles start to form there is another, more favourable, location for dodecanol, namely in the micelles. Dodecanol is removed from the surface by solubilization and the surface tension then increases.

9 MICELLE SIZE AND STRUCTURE MAY VARY

As a good approximation, micelles can, in a wide concentration range above the *CMC*, be viewed as microscopic liquid hydrocarbon droplets covered with the polar head-groups, which are in interaction with water. It appears that the radius of the micelle core constituted of the alkyl chains is close to the extended length of the alkyl chain, i. e. in the range of 1.5–3.0 nm. Why is this so?

The driving force of micelle formation is the elimination of the contact between the alkyl chains and water. The larger a spherical micelle, the more efficient this is since the volume-to-area ratio increases. Decreasing the micelle size always leads to an increased hydrocarbon–water contact. However, if the spherical micelle was made so large that no surfactant molecule could reach from the micelle surface to the centre, one would either have to create a void or some surfactant molecules would lose contact with the surface. Both of these options are unfavourable.

We should note that the fact that the micelle radius equals the length of an extended surfactant

molecule does not mean that the surfactant molecules are extended. Only one molecule needs to be extended (in an all-*trans* state) to fulfil the requirements mentioned and the majority of the surfactant molecules are in a disordered state with many *gauche*-conformations. From spectroscopic studies, the state of the alkyl chains in micelles has been characterized in detail. This state indeed is very close to that of the corresponding alkane in a neat liquid oil. The liquid-like state is clearly expressed by molecular dynamics. Thus, chain isomerism occurs on a time scale of a few tenths of picoseconds, only slightly slower than for liquid alkanes. Due to the constraint the attachment to the micelle surface involves, the motion is slightly anisotropic.

We emphasize that a micelle may for many purposes be considered as a microscopic droplet of oil. This explains the large solubilization capacity towards a broad range of non-polar and weakly polar substances. We note, however, that the locus of solubilization will be very different for different solubilizates. While a saturated hydrocarbon will be rather uniformly distributed over the micelle core, an aromatic compound, being slightly surface-active, will be concentrated to the interfacial region. An amphiphilic solubilizate, like a long-chain alcohol, tends to orient in the same way as the surfactant itself.

At the surface of the micelle we have the associated counterions, which in number amount to 50–80% of the surfactant ions, which as noted above is a number quite invariant to the conditions. Simple inorganic counterions are very loosely associated with the micelle. The counterions are very mobile and there is no specific complex formed with a definite counterion–head-group distance. Rather, the counterions are associated by long-range electrostatic interactions to the micelle as a whole. They remain hydrated to a great extent, and especially cations tend to keep their hydration shells.

Some water of hydration is thus accounted for by the associated counterions and, furthermore, the polar head-groups are extensively hydrated. On the other hand, water molecules are effectively excluded from the micelle core. There is, due to packing limitations, some inevitable exposure of the hydrocarbon chains at the micelle surface, but even a short step inwards, the probability of finding water molecules becomes extremely low.

The micelle size, as expressed by the radius of a spherical aggregate, may be obtained *inter alia* from various scattering experiments and from micelle self-diffusion. A related and equally important characteristic of a micelle is the micelle aggregation number, i. e. the number of surfactant molecules in one micelle. This is

best determined in fluorescence quenching experiments. To take an example, the aggregation number of SDS micelles at 25°C is 60–70. The aggregation number is quite well-defined, with only a narrow distribution. Micelles of all aggregation numbers exist in equilibrium but for aggregation numbers deviating markedly from the average the probability is very small. For this reason, the mass action law model offers a good description. In fact, as mentioned above, the analysis of experimental observations around the CMC using this model gives some information on the micelle aggregation numbers.

Based on the approximate validity of the mass action law model:

$$(A_n)/(A_1)^n = K \quad (19.13)$$

and the general relationship between the free energy change and the equilibrium constant:

$$\Delta G^0 = -RT \ln K \quad (19.14)$$

one can derive an approximate relationship for micelle formation as follows:

$$\Delta G^0 = RT \ln CMC \quad (19.15)$$

This is a convenient starting point for thermodynamic considerations.

10 A GEOMETRICAL CONSIDERATION OF CHAIN PACKING IS USEFUL

We came above to a simple characterization of the micelle core as a hydrocarbon droplet with a radius equalling the length of the extended alkyl chain of the surfactant. We noted also that, since the cross-sectional area per chain decreases radially towards the centre, only one chain can be fully extended while the others are more or less folded. The aggregation number, N , can be expressed as the ratio between the micellar core volume, V_{mic} , and the volume, v , of one chain as follows:

$$N = V_{mic}/v = (4/3)\pi R_{mic}^3/v \quad (19.16)$$

We can alternatively express the aggregation number as the ratio between the micellar area, A_{mic} , and the cross-sectional area, a , of one surfactant molecule:

$$N = A_{mic}/a = 4\pi R_{mic}^2/a \quad (19.17)$$

By putting these aggregation numbers equal, we obtain the following:

$$v/R_{mic}a = 1/3 \quad (19.18)$$

Table 19.5. Kinetic parameters of association and dissociation of alkyl sulfates from their micelles

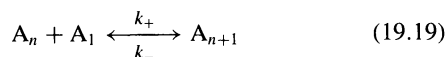
Surfactant	N	CMC (M)	k_+ (s^{-1})	k_- ($M^{-1} s^{-1}$)
NaC ₆ SO ₄	17	0.42	1.32×10^9	3.2×10^9
NaC ₇ SO ₄	22	0.22	7.3×10^8	3.3×10^9
NaC ₈ SO ₄	27	0.13	1.0×10^8	7.7×10^9
NaC ₉ SO ₄	33	6×10^{-2}	1.4×10^8	2.3×10^9
NaC ₁₁ SO ₄	52	1.6×10^{-2}	4×10^7	2.6×10^9
NaC ₁₂ SO ₄	64	8.2×10^{-3}	1×10^7	1.2×10^9
NaC ₁₄ SO ₄	80	2.05×10^{-3}	9.6×10^5	4.7×10^8

Since R_{mic} cannot exceed the extended length of the surfactant alkyl chain, $l_{max} = 1.5 + 1.265n_c$ we find that $v/l_{max}a$ is less than or equal to 1/3 for a spherical micelle.

The ratio $v/l_{max}a$, which gives a geometric characterization of a surfactant molecule, is very useful when discussing the type of structure formed by a given amphiphile. This is called the *critical packing parameter* (*CPP*) or the *surfactant number*.

11 KINETICS OF MICELLE FORMATION

We already noted that micelles are formed in a stepwise process, so the elementary step is the equilibrium between a unimer and a micellar aggregate.



The 'on' rate constant, k_+ , is diffusion-controlled and depends little on surfactant and micelle size (cf. Table 19.5). The 'off' rate constant, k_- , on the other hand, is strongly dependent on alkyl chain length, micelle size, etc. Because of the co-operativity in micelle formation there is a very deep minimum in the size distribution curve. This leads to a two-step approach to equilibrium after a perturbation. In a fast step, quasi-equilibrium is reached under the constraint of a constant total number of micelles. The redistribution of unimers between abundant micelles is a fast process. In order to reach a true equilibrium, the number of micelles must change. Because of the stepwise process, this also involves the very rare intermediate micelles. Therefore, this process is slow.

From fast kinetic measurements, two relaxation times are determined which characterize molecular processes in micellar solutions, i.e. τ_1 measures the rate at which surfactant molecules exchange between

micelles, while τ_2 measures the rate at which micelles form and disintegrate. Some examples of relaxation times are given in Table 19.6. As can be seen, τ_1 is of the order of 10 μs for SDS, while τ_2 is longer than a millisecond. Both relaxation processes become much slower as the surfactant alkyl chain length increases.

Since the slow relaxation process is critically dependent on the micelle size distribution, kinetic measurements can be used to determine the standard deviation of the distribution. As can be seen in Table 19.7, the distribution is relatively narrow for surfactants with longer alkyl chains.

Table 19.6. Relaxation times τ_1 and τ_2 for some sodium alkyl sulfates

Surfactant	Temperature ($^{\circ}C$)	Concentration (M)	τ_1 (μs)	τ_2 (ms)
NaC ₁₆ SO ₄	30	1×10^{-3}	760	350
NaC ₁₄ SO ₄	25	2.1×10^{-3}	320	41
	30	2.1×10^{-3}	245	19
	35	2.1×10^{-3}	155	7
	25	3×10^{-3}	125	34
NaC ₁₂ SO ₄	20	1×10^{-2}	15	1.8
	20	5×10^{-2}	-	50

Table 19.7. The CMC , the mean aggregation number N , and the standard deviation σ of the micelle size distribution for a series of sodium alkyl sulfates, as determined from kinetic measurements. (From E. A. G. Aniansson *et al.*, J. Phys. Chem., 80 (1976) 905)

Surfactant	Temperature ($^{\circ}C$)	CMC (M)	N	σ
NaC ₆ SO ₄	25	0.42	17	6
NaC ₈ SO ₄	25	0.22	22	10
NaC ₁₂ SO ₄	25	8.2×10^{-3}	64	13
NaC ₁₄ SO ₄	40	2.05×10^{-3}	80	16.5

12 SURFACTANTS MAY FORM AGGREGATES IN OTHER SOLVENTS THAN WATER

12.1 Polar solvents

In strongly polar solvents, like formamide and ethylene glycol, micelles are formed with qualitatively the same features as in water. As exemplified by surface tension studies in Figure 19.15, the *CMC* is much higher in formamide than in water, in this case 100 mM compared to 1 mM in water. It is a general feature, also exemplified by smaller micelle radii and aggregation numbers, that self-assembly is much less co-operative in

alternative polar solvents. As a consequence, the degree of counterion binding is also lower.

12.2 Non-polar solvents

For simple amphiphilic compounds, the association is of low co-operativity in non-polar solvents and leads typically only to smaller and polydisperse aggregates. An illustration is given in Figure 19.16. However, introduction of even quite small amounts of water can induce a co-operative self-assembly leading to reverse micelles.

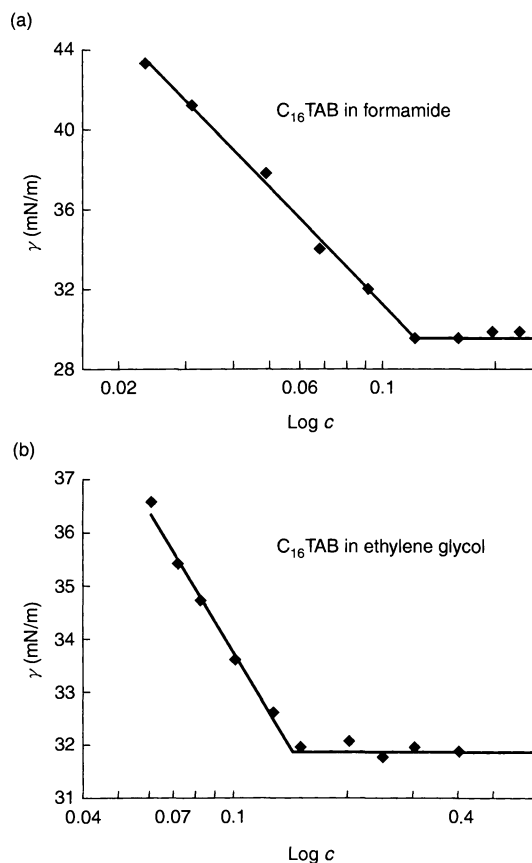


Figure 19.15. Surface tension, γ of hexadecyltrimethylammonium bromide, $C_{16}TABr$, in (a) formamide, and (b) ethylene glycol as a function of the logarithm of the surfactant concentration (M) at 60°C. (Redrawn from M. Sjöberg, *Surfactant Aggregation In Nonaqueous Polar Solvents*, *Doctoral Thesis*, Department of Physical Chemistry, The Royal Institute of Technology, Stockholm, Sweden (1992)

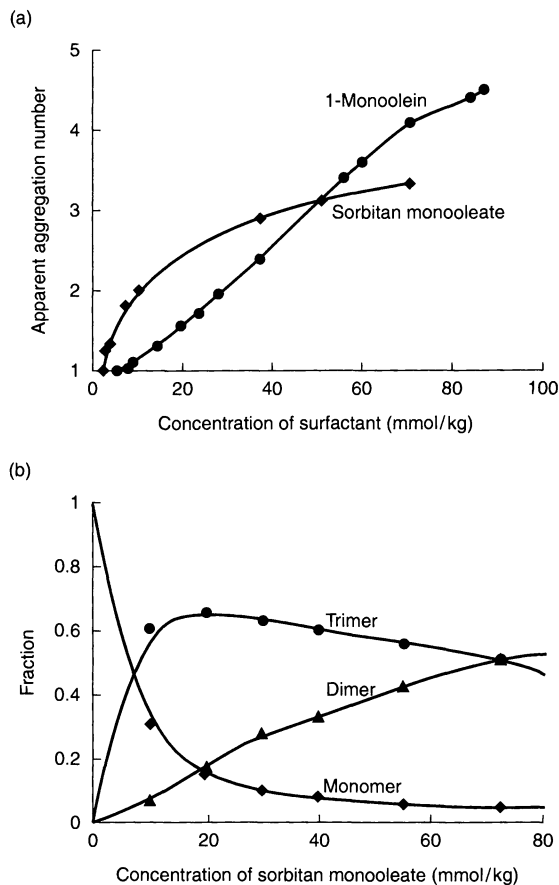


Figure 19.16. The aggregation numbers of amphiphiles in non-polar solvents are generally low. The plots in (a) show the average aggregation numbers of 1-monoolein and sorbitan monooleate in cyclohexane, while those in (b) show the fractions of surfactant as monomer, dimer and trimer of sorbitan monooleate in benzene as a function of surfactant concentration. (Redrawn from K. Konno and A. Kitahara, in *Nonionic Surfactants Physical Chemistry*, M. J. Schick (Ed.), Marcel Dekker, New York, 1987, pp. 195–196)

13 GENERAL COMMENTS ON AMPHIPHILE SELF-ASSEMBLY

In water (and other polar solvents), aggregation results from the insolubility of the non-polar parts in water. The packing of the hydrocarbon chains results from the drive to minimize contact with water. Aggregation is opposed by the hydrophilic interactions giving a repulsion between the polar head-groups on the micelle surface. The head-groups will arrange themselves to minimize the unfavourable repulsions.

The self-assembly of an amphiphile depends on the strength of the opposing force. It must be strong enough to compete with one alternative, which is macroscopic phase separation, but must also be limited in magnitude since otherwise the unimeric state will be the most stable one. Examples of head-groups giving too weak amphiphiles are hydroxyl, aldehyde, ketone and amine. For a long-chain alcohol, macroscopic phase separation results rather than micelle formation.

For ionic surfactants, the counterion dissociation plays a great role. Because of the counterions, macroscopic phase separation becomes entropically very unfavourable and there is a strong tendency to form small micelles.

Cosolutes may affect amphiphile self-assembly in many different ways. They can, for example, stabilize the micelles by reducing the polar interactions. For ionic surfactants, we can neutralize the charges by adding an oppositely charged surfactant, we can “screen” the repulsions between head-groups, or rather even out the uneven counterion distribution by adding electrolyte, or we can dilute the charges by introducing a nonionic amphiphile, such as a long-chain alcohol. In all cases, we observe a marked reduction in the *CMC*, and an increase in micelle size.

Self-assembly and micelle formation have, however, a broader significance than this. Mixed polymer-surfactant solutions have many applications and it has become more and more evident that an important role of the polymer chains in many systems is to promote micelle formation. A macromolecular cosolute will be much more effective in reducing the *CMC* than a low-molecular-weight one. This is discussed in some detail in Chapter 20.

Surfactant adsorption at hydrophilic solid surfaces is often pictured as leading to surfactant monolayers and bilayers (Figure 19.17) but it has become increasingly clear that also this process is best regarded as a process of surfactant self-assembly. In such cases, the picture of continuous surfactant layers must be replaced by one

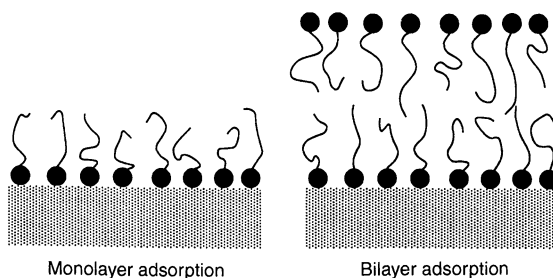


Figure 19.17. Conventional pictures of surfactant adsorption at hydrophilic solid surfaces involve monolayer and bilayer structures

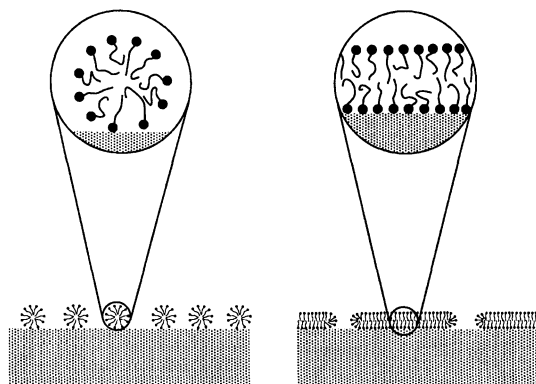


Figure 19.18. In the absence of strong specific interactions between a hydrophilic surface and the surfactant head-groups, surfactant molecules will self-assemble into discrete micelles at the surface

with discrete surfactant aggregates, i.e. surface micelles, as illustrated in Figure 19.18.

14 MICELLE TYPE AND SIZE VARY WITH CONCENTRATION

The spherical micelle discussed so far is but one possibility of an amphiphile self-assembly. The spherical micelle does not form at all for many amphiphiles, while for others it occurs only in a limited range of concentrations and temperatures. In general, we can distinguish between three types of behaviour of a surfactant or a polar lipid as the concentration is varied:

1. The surfactant has a high solubility in water and the physico-chemical properties (viscosity, scattering, spectroscopy, etc.) vary in a smooth fashion from the *CMC* region up to saturation. This suggests that there

are no major changes in micelle structure, and the micelles remain small and do not depart much from a spherical shape.

- The surfactant has a high solubility in water but as the concentration is increased there are quite dramatic changes in certain properties. This indicates that there are marked changes in the self-assembly structures.
- The surfactant has a low solubility and there is a phase separation at low concentrations.

The three cases are characterized by different ranges of existence of the isotropic solution phase. In either case the new phase formed above saturation may be:

- a liquid crystalline phase
- a solid phase of (hydrated) surfactant
- a second, more concentrated, surfactant solution.

Different phase structures give very different physico-chemical properties and, therefore, in any practical use of surfactants it is mandatory to have control over phase structure. The regions of existence of different phases and the equilibria between different phases are described by phase diagrams. These are significant, not only as a basis of applications, but also for our general understanding of surfactant self-assembly.

For a relatively short-chain surfactant, such as C_8 or C_{10} , one usually observes a slow and regular variation of relevant properties, and no phase separation, up to high concentrations, say 10–40 wt% (Figure 19.19). The viscosity, which is an important property for the uses of surfactants, varies smoothly and approximately as predicted for a dispersion of spherical particles up to high concentrations. By scattering experiments and by NMR spectroscopy, direct evidence is obtained for closely spherical aggregates up to the approach of phase separation. For some surfactants, it may be for only at micelle volume fractions of the order of 0.3 that appreciable deformations of the micelles are seen.

A frequently encountered behaviour for longer chain surfactants, say C_{14} or above, is that at low or intermediate concentrations the viscosity starts to increase rapidly with concentration. This is exemplified in a plot of the (zero-shear) viscosity versus concentration in Figure 19.20. Here, the micelles grow with increasing concentration, at first to short prolates or cylinders and then to long cylindrical or thread-like micelles (Figure 19.21).

A third, less common, behaviour is the growth to very long thread-like micelles even at very low concentrations, sometimes just above the *CMC*.

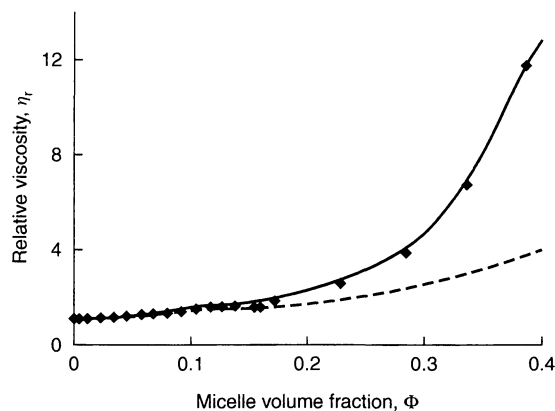


Figure 19.19. Relative viscosity as a function of micelle volume fraction for solutions of spherical micelles. The dashed and continuous curves give theoretical predictions for two models of spherical particles, in the latter case taking into account particle–particle interactions. The system exemplified is that of $C_{12}E_5$ micelles with equal weights of solubilized decane. (Redrawn from M. S. Leaver and U. Olsson, *Langmuir*, **10** (1994) 3449)

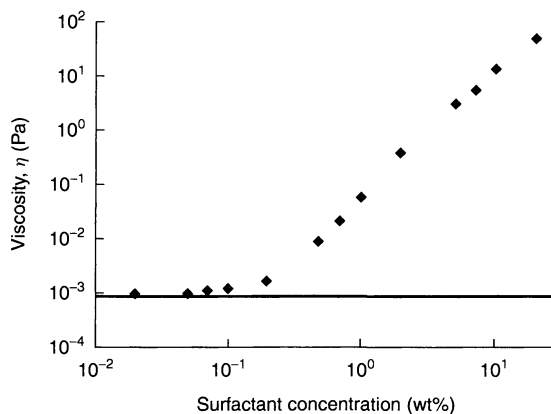


Figure 19.20. For surfactants forming large micelles, the viscosity starts to increase rapidly with surfactant concentration. The increase in zero shear viscosity is plotted as a function of surfactant concentration for $C_{16}E_6$. (By courtesy of U. Olsson, M. Malmsten and F. Tiberg)

The growth of micelles is generally a one-dimensional process leading to aggregates with a circular cross-section. The hydrophobic core has a radius which, as for the spherical micelles and for the same reasons, equals the length of the extended alkyl chain of the surfactant. The linear length of the rod-like micelles can vary over wide ranges, from well below 10 nanometres to many hundred of nanometres.

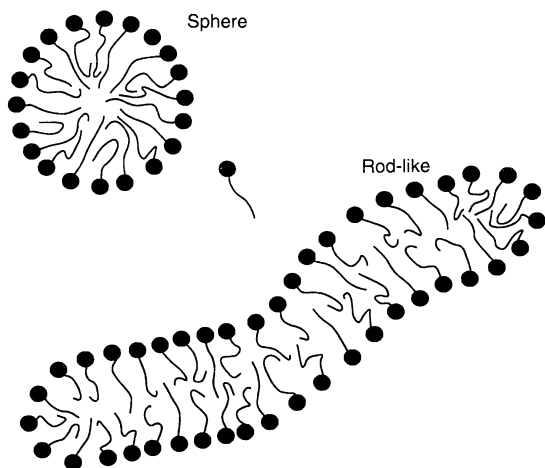


Figure 19.21. At higher concentrations the micelles often grow from spherical aggregates to long rod- or thread-like micelles

15 MICELLAR GROWTH IS DIFFERENT FOR DIFFERENT SYSTEMS

Micellar growth is a very common phenomenon and for ionic surfactants the following factors (some of which are exemplified in Figures 19.22 and 19.23) influence the growth:

- (i) The tendency to growth increases strongly with the alkyl chain length and there is no growth for shorter chains.
- (ii) Micellar growth is strongly dependent on temperature and is strongly promoted by a decrease in temperature. For example, for hexadecyltrimethylammonium bromide, there is micellar growth at 30°C but not at 50°C.
- (iii) While the *CMC* is only slightly dependent on the counterion within a given class, micellar growth displays a strong variation. The dependence of growth on counterion, however, is very different for different surfactant head-groups. For example, for hexadecyltrimethylammonium bromide, there is major micellar growth while there is no growth with chloride as the counterion. For alkali dodecyl sulfates, growth is insignificant with Li^+ as the counterion, moderate with Na^+ , but quite dramatic with K^+ or Cs^+ . With carboxylate as the head-group, the opposite variation along the series of alkali ions is observed.

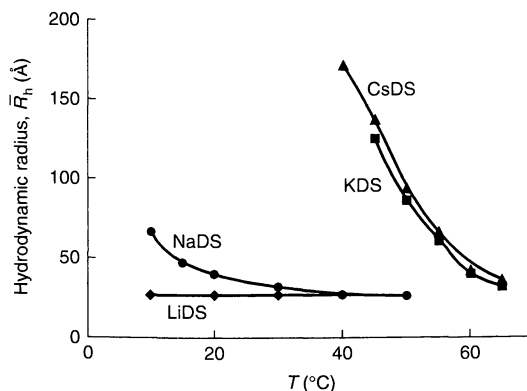


Figure 19.22. The size of alkali dodecyl sulfate (DS) micelles, here characterized by the hydrodynamic radius, decreases with increasing temperature and is very sensitive to the choice of counterion. The following concentrations are used: LiDS, 20 g/l + 1 M LiCl; NaDS, 20 g/l + 0.45 M NaCl; KDS, 5 g/l + 0.45 M KCl; CsDS 5 g/l + 0.45 M CsCl. As can be seen, KDS and CsDS give much more pronounced growth in spite of lower concentrations of surfactant. (Redrawn from P. J. Missel, N. A. Mazer, M. C. Carey and G. B. Benedek, in *Solution Behavior of Surfactants*, K. L. Mittal and E. J. Fendler (Eds.), Plenum Press, New York, 1982, Vol. 1, p. 373)

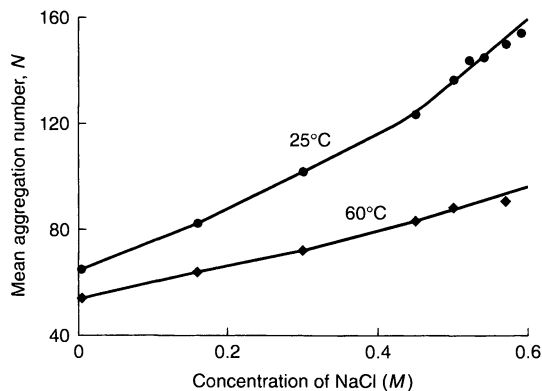


Figure 19.23. The aggregation number of sodium dodecyl sulfate (SDS) micelles increases with decreasing temperature and increasing salt concentration. (Redrawn from N. J. Turro and A. Yekta, *J. Am. Chem. Soc.*, **100** (1978) 5951)

Organic counterions may induce dramatic growth at low concentrations, as exemplified by salicylate in the presence of long-chain cation surfactants:

- (i) In the case of micellar growth, micellar size increases strongly with surfactant concentration.
- (ii) Large micelles are, in contrast to the small spherical micelles, very polydisperse.

(iii) Micelle size is very sensitive to cosolutes. Addition of salt promotes micelle growth, while solubilized molecules can have very different effects depending on the surfactant system involved. However, in general, non-polar solubilizes, like alkanes, which are located in the micellar core, tend to inhibit micellar growth, while alcohols or aromatic compounds, which are located in the outer part of the micelles, tend to strongly induce growth. For example, for hexadecyltrimethylammonium bromide there is no growth on adding cyclohexane, while hexanol and benzene both give dramatic growth.

For other classes of surfactants there are different characteristics of micellar growth. Nonionic surfactants of the polyoxyethylene type give growth with increasing concentration which is much more marked the shorter the polar group. With 4–6 oxyethylene units there is dramatic growth, while with 8 or more oxyethylenes there is negligible growth under all conditions. These surfactants show a micellar growth which is much more pronounced at a higher temperature, i. e. opposite to other classes of surfactants (see below).

Solutions of large micelles show many parallels with solutions of linear polymers and the micelles have been denoted as “living polymers”. Because of the polymer-like behaviour, concepts and theories developed for polymer solutions have been successfully applied. Differences from polymers, which complicate the comparison, include the strong dependence of the “degree of

polymerization” on the conditions (surfactant concentration, temperature, etc.) Furthermore, under certain conditions, such as very high concentrations, growth may lead to branched structures.

The large micelles can differ strongly in flexibility and may be referred to as rigid rods, semi-flexible or highly flexible. As for polymers, they can be characterized by a persistence length.

The flexibility of ionic micelles is strongly dependent on electrolyte addition. Thus, salt addition can induce a change from rigid rods to very flexible micelles.

In dilute solutions, where the micelles do not overlap they behave as independent entities (Figure 19.24). After the overlap volume fraction, ϕ^* , in the so-called semi-dilute concentration regime, the micelles are entangled and there is a transient network characterized by a correlation length; the latter is independent of micelle size and polydispersity; the overlap concentration of the system presented in Figure 19.20 is ca. 0.1%. The viscosity of solutions of long linear micelles can be analysed in terms of the motion of the micelles, for example by using the reptation model of polymer systems. In this model, the micelles creep “like a snake” through tubes in a porous structure given by the other micelles. The zero shear viscosity, η , depends on micelle size (aggregation number, N) and volume fraction, ϕ , according to the following:

$$\eta = a N^3 \phi^{3.75} \quad (19.20)$$

where a is a constant.

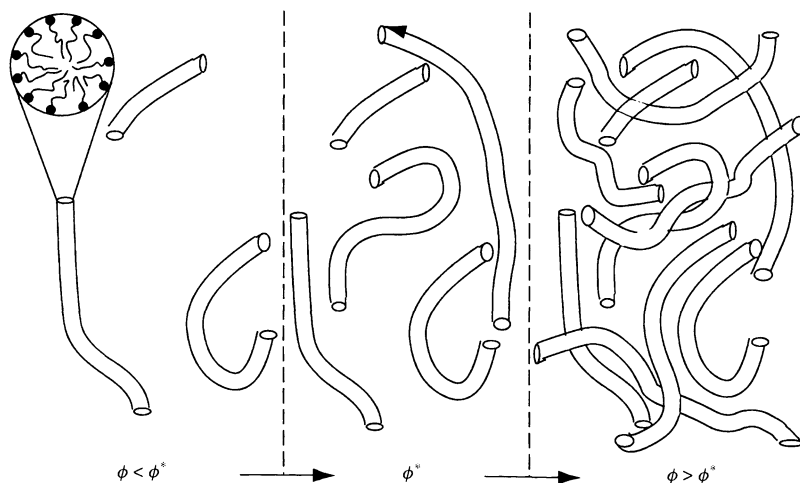


Figure 19.24. There is a close analogy between solutions of long micelles and polymer solutions, including transient networks. The figure illustrates the transition from dilute to semi-dilute solutions and the overlap concentration; ϕ^* is the overlap volume fraction

As also observed experimentally, the viscosity increases very strongly with both micelle size and surfactant concentration.

The linear growth of micelles is the strongly dominating type of growth. Disc-like or plate-like structures may also form, but these micelles are quite small and exist only over a narrow range of conditions (concentration, etc.). The linear growth can, as mentioned earlier, lead to branched structures, which at high enough concentrations may lead to the transition into a surfactant micellar structure which is completely connected so that the concept of distinct micelles loses its meaning (Figure 19.25). In such a case, we use the term bicontinuous structure, since the solutions are continuous not only in the solvent but also in the surfactant.

As we will see below, bicontinuous structures are very significant in many contexts of amphiphile self-assembly. Another type of bicontinuous structure in simple surfactant–water solutions is the “sponge phase”, formed also in quite dilute surfactant solutions (Figure 19.26). This structure forms for all classes of surfactants but in particular for nonionics. We will also mention that the structure of the sponge phase is related to that of many microemulsions.

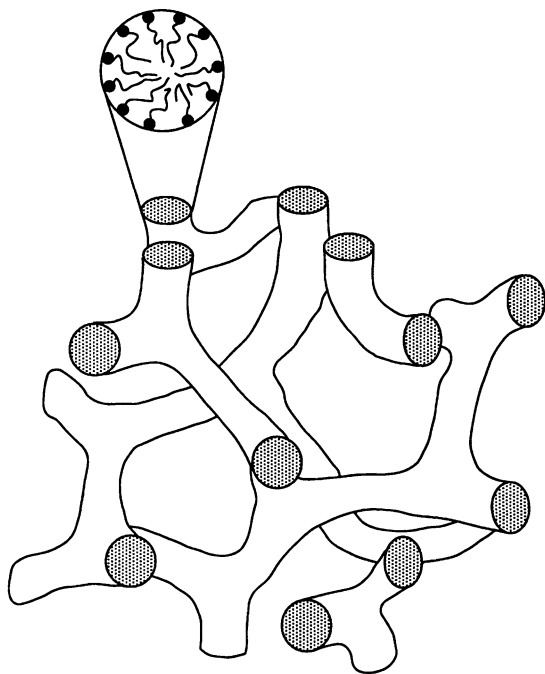


Figure 19.25. Representation of branched micelles

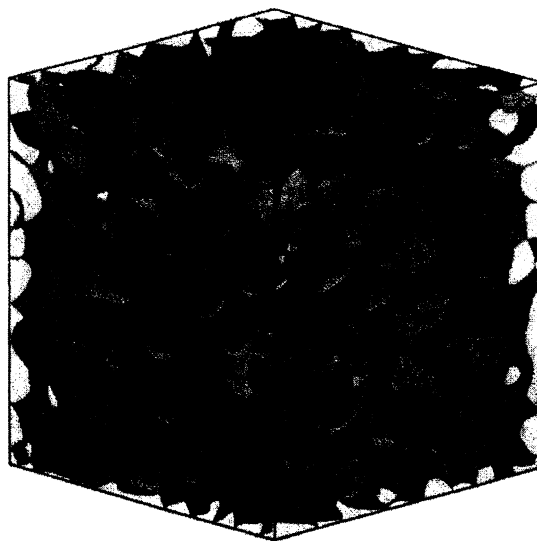


Figure 19.26. Representation of the sponge phase. For many surfactants, there is an isotropic solution phase where the surfactant forms a connected three-dimensional network. Since both water and the hydrophobic regions are connected over macroscopic distances, such structures are termed bicontinuous. (Redrawn from P. Pieruschka and S. Marcelja, *Langmuir*, 2 (1994) 345)

16 SURFACTANT PHASES ARE BUILT UP BY DISCRETE OR INFINITE SELF-ASSEMBLIES

Surfactant micelles and bilayers are the building blocks of most self-assembly structures and it is natural to dwell on the distinction between these and to give some further examples. As schematized in Figure 19.27 we

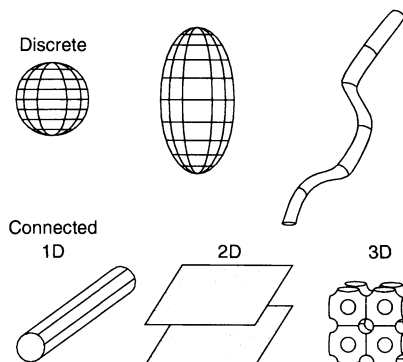


Figure 19.27. Amphiphile self-assembly structures can be divided into discrete micellar-type and connected forms. There may be connectivity in one, two or three dimensions

can divide phase structures in two groups, i.e. those which are built up of limited or discrete self-assemblies, which may be roughly characterized as spherical, prolate, oblate and cylindrical (more or less flexible), or infinite or unlimited self-assemblies. In the latter case, the surfactant aggregate is connected over macroscopic distances in one, two or three dimensions. The hexagonal phases are examples of one-dimensional continuity, the lamellar phase of two-dimensional continuity, while three-dimensional continuity is found for the bicontinuous cubic phases, for the “sponge” phase and for many microemulsions.

Phases built up of discrete aggregates include the normal and reversed micellar solutions, micellar-type microemulsions, and certain (micellar-type) normal and reversed cubic phases. However, discrete self-assemblies are also important in other contexts. Adsorbed surfactant layers at solid or liquid surfaces may involve micellar-type structures and the same applies to mixed polymer–surfactant solutions.

Other examples of bilayer structures already mentioned are the “sponge” phase and bicontinuous cubic phases. The sponge phase has been most studied for nonionic surfactants and is related to common microemulsions. Bilayers may also easily close on themselves to form discrete entities including unilamellar vesicles and multilamellar liposomes. Vesicles are of interest because of the division into inner and outer aqueous domains separated by the bilayer. Vesicles and liposomes are normally not thermodynamically stable (although there are exceptions) and tend to phase separate into a lamellar phase and a dilute aqueous solution. Lipid bilayers are important constituents of living organisms and form membranes, which act as barriers between different compartments. Certain surfactants and lipids may form reversed vesicles, i. e. vesicles with inner and outer oleic domains separated by a (reversed) amphiphile bilayer; the bilayer may or may not contain some water.

17 NONIONIC OXYETHYLENE SURFACTANTS DISPLAY SPECIAL TEMPERATURE EFFECTS

For ionic surfactants, the electrostatic interactions are, as seen above, decisive for the properties of simple and complex systems. Nonionic surfactants are controlled by very different hydrophilic interactions. The most important type of nonionic surfactants is that with an oligo(oxyethylene) group as the polar head. Denoting an oxyethylene group by E, simple nonionics can be

abbreviated as C_mE_n if we have an alkyl chain as the lipophilic part.

For typical ionic surfactants, as well as many other surfactants, the volume of the polar head-group is much smaller than that of the non-polar part. For the polyoxyethylene surfactants, the situation is different in that the volumes of the two parts are similar in size; typically, the polar part is larger than the non-polar one.

One conspicuous feature of a nonionic surfactant is the temperature-dependence of physico-chemical properties. The temperature dependence of the CMC (Figure 19.28) differs from that of ionics in two respects: it is markedly stronger and there is typically a monotonic decrease with increasing temperature rather than an increase at higher temperatures. A nonionic micelle (Figure 19.29) has a thick interfacial layer of polar head-groups rather than the quite sharp transition from the hydrophobic micellar interior to the aqueous bulk of ionics. We will see that changes in the intermolecular interactions in the polar layer account for the special temperature-dependent behaviour of nonionics.

The spherical micelle depicted in Figure 19.29 is typical for surfactants with long polyoxyethylene chains, in particular at low temperatures and concentrations. As for ionics, micellar growth may occur but the conditions are different for nonionics. In particular, the temperature-dependence of micelle size is opposite to that of ionics.

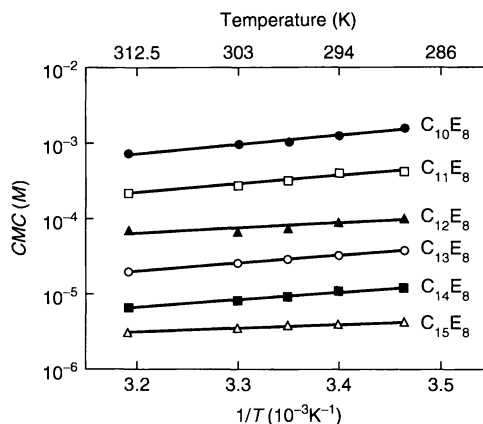


Figure 19.28. The logarithm of the CMC plotted against the inverse absolute temperature for nonionics with eight oxyethylenes in the head-group. From top to bottom, the numbers of carbon atoms in the alkyl chain are 10, 11, 12, 13, 14 and 15. (Redrawn from K. Meguro, M. Ueno and K. Esumi, *Nonionic Surfactants Physical Chemistry*, M. J. Schick (Ed.), Marcel Dekker, New York, 1987, p. 136)

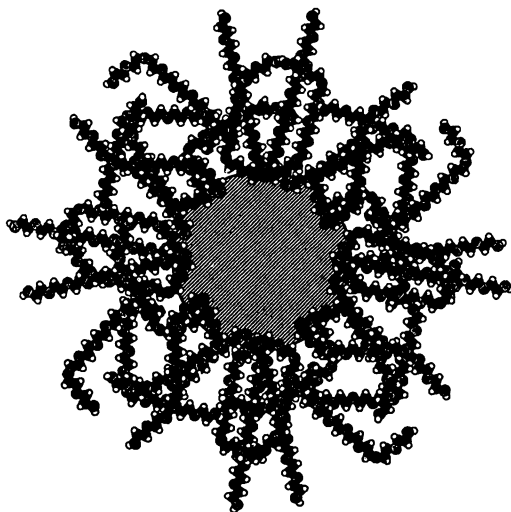


Figure 19.29. A schematic representation of a nonionic micelle. (Redrawn from M. Jonströmer, B. Jönsson and B. Lindman, *J. Phys. Chem.*, **95** (1991) 3293)

would give even less of such growth. For a short oxyethylene chain, illustrated here by $C_{12}E_5$, there is a dramatic growth with increasing temperature.

In general, we can summarize micellar size effects for nonionics as follows:

- (i) The polyoxyethylene chain length is the prime factor in determining growth. The shorter the chain, then the larger is the tendency to growth, with respect to both temperature and concentration.
- (ii) As with all types of surfactants, micellar growth is promoted by an increased alkyl chain length. For example, C_{16} surfactants give much stronger growth than C_{12} ones.
- (iii) Cosolutes influence growth differently than for ionics. Salting-out electrolytes tend to promote growth, while salting-in ones tend to inhibit growth. Ionic surfactants have a strong tendency for reducing growth, and even quite small amounts may inhibit growth.

Unusual temperature dependencies are ubiquitous for oxyethylene-containing systems. As indicated, there is a weakened interaction between the oxyethylene groups and the water solvent with increasing temperature. There is a smoothly decaying hydration with increasing temperature which is strikingly similar for quite dissimilar systems. In fact, the apparent number of hydration per oxyethylene group is sensitive to temperature, but closely the same for different systems.

A lower consolute curve is typical of phase diagrams of oxyethylene-based surfactants and polymers. This implies that the effective solute-solute interactions have a significant temperature-dependence and changes from repulsive to attractive with increasing temperature. In turn, this can reflect changes in either solute-solute, solute-solvent or solvent-solvent interactions, or a combination of these. All alternatives have been suggested and there is as yet no consensus about the dominating effect. However, a water-water interaction mechanism, relating to a temperature-dependent structuring of water around the oxyethylene groups, is less likely in view of analogous observations in solvents other than water. Hydrogen bonding between water molecules and the ether oxygens represent another model which has been analysed. Here, we describe a model based on temperature-dependent solute conformational effects which has a strong predictive power.

A polyoxyethylene chain may exist in a large number of conformations, which have different energies. The conformation of an oxyethylene group, which is *gauche(g)* around the C-C bond and *anti(a)* around

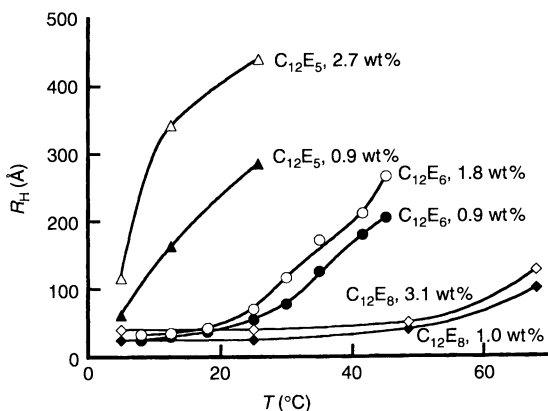


Figure 19.30. Nonionic micelles grow with increasing temperature for surfactants with short polar heads, while growth is weak or insignificant for larger head-groups. The size is characterized by the hydrodynamic radius, R_H . (Redrawn from B. Lindman and M. Jonströmer, *Springer Proceedings in Physics: Physics of Amphiphilic Layers*, J. Meunier, D. Langevin and N. Boccarda (Eds), Springer-Verlag, Berlin, 1987, p. 235)

The most significant features are illustrated in Figure 19.30, where the hydrodynamic radii of the micelles are given as a function of temperature for three relatively dilute surfactants. For a surfactant such as $C_{12}E_8$ there is insignificant or moderate growth up to high temperatures; a longer polyoxyethylene chain

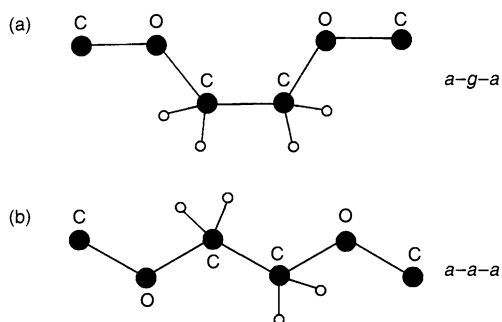


Figure 19.31. Different conformations of an oxyethylene group have different stabilities and polarities. The *anti-gauche-anti* conformation (a) has a lower energy and is more polar than the lower *anti-anti-anti* conformation (b)

the C–O bond (Figure 19.31) has the lowest energy of all conformers. This low energy conformation, which will dominate at low temperatures, has a large dipole moment. On the other hand, it has a low statistical weight. With increasing temperature, other conformations of higher statistical weight will become increasingly more important. These have smaller or no dipole moments, as in the *anti-anti-anti* conformation.

The conformational changes will consequently make the polyoxyethylene chains progressively less polar as the temperature is increased. Becoming less polar, they will interact less favourably with water, leading to reduced hydration, and more favourably among themselves, thus leading to a closer packing of head-groups in the surfactant self-assemblies, as well as to an increased tendency to separate into a more concentrated phase.

18 CLOUDING IS A CHARACTERISTIC FEATURE OF POLYOXYETHYLENE-BASED SURFACTANTS

A common observation for a solution of a nonionic surfactant is that on heating the solution may start to scatter light strongly in a well-defined temperature range. It becomes “cloudy”. This is a consequence of one feature of the phase diagram. The isotropic solution region is bordered towards higher temperatures by a lower consolute curve, above which there is a phase separation into one surfactant-rich and one surfactant-poor solution. Onset of phase separation is manifested by a cloudiness of the solutions. The minimum in a lower consolute curve represents a critical point. Approaching

this is accompanied by strong scattering of light due to critical fluctuations.

The clouding temperature or the cloud point depends strongly on the polyoxyethylene chain length but is less influenced by the hydrophobe size. Normally, the cloud point is recorded for a certain fixed solute concentration (say 1 wt%). The cloud point of $C_{12}E_8$ is around 80°C , while it is ca. 50 and 10°C for $C_{12}E_6$ and $C_{12}E_4$, respectively. For still shorter polyoxyethylene chains, the surfactant is insoluble even at the freezing temperature of water, so the cloud point is below 0°C .

Clouding is strongly dependent on cosolutes. Electrolytes may either increase or decrease the cloud point and may be termed “salting-in” or “salting-out”, respectively. This may be understood from the interaction between surfactant and cosolute. The effect is dominated by the anions. Some anions, such as SCN^- , show a preference for the surfactant relative to the bulk solvent and are enriched in the vicinity of the oxyethylene groups. Others, such as Cl^- , do not show such preference and are depleted in the vicinity of the oxyethylene groups. In the former case, increased solubility and an increased cloud point results, while the opposite is observed in the latter case. Very low concentrations of an ionic surfactant strongly increase solubility, and thus also the cloud point. This is due to the formation of mixed micelles. This results in charged aggregates which are much more difficult to concentrate in one of the phases due to the unfavourable electrostatic interactions arising from the entropy of the counterion distribution.

19 BIBLIOGRAPHY

1. Evans, D. F., Wennerström, H., *The Colloidal Domain, where Physics, Chemistry, Biology and Technology Meet*, 2nd Edn, Wiley-VCH, New York, 1999, Chs 1 and 4, pp. 1–47 and 153–216.
2. Friberg, S. E. and Lindman, B. (Eds), *Organized Solutions*, Surfactant Science Series, Vol. 44, Marcel Dekker, New York, 1992.
3. Israelachvili, J., *Intermolecular and Surface Forces*, Academic Press, San Diego, CA, 1991.
4. Jönsson, B., Lindman, B., Holmberg, K. and Kronberg, B., *Surfactants and Polymers in Aqueous Solution*, Wiley, Chichester, 1998, Chs 2–4, pp. 33–114.
5. Larsson, K., *Lipids – Molecular Organization, Physical Functions and Technical Applications*, The Oily Press, Alloway, NJ, 1994.
6. Laughlin, R. G., *The Aqueous Phase Behavior of Surfactants*, Academic Press, London, 1994.
7. Lindman, B. and Wennerström, H., *Micelles*, Topics in Current Chemistry, Vol. 87, Springer, Berlin, 1980.

8. Lindman, B., Söderman, O. and Wennerström, H., NMR of surfactant systems, in *Surfactant Solutions: New Methods of Investigation*, Zana, R. (Ed.), Marcel Dekker, New York, 1987, Ch. 6, pp. 295–358.
9. Lindman, B., Olsson, U. and Söderman, O., Surfactant solutions: Aggregation phenomena and microheterogeneity, in *Dynamics of Solutions and Fluid Mixtures by NMR*, Delpuech, J.-J. (Ed.), Wiley, Chichester, 1995, Ch. 6, pp. 345–396.
10. Olsson, U. and Wennerström, H., Globular and bicontinuous phases of nonionic surfactant films, *Adv. Colloid Interface Sci.*, **49**, 113–146 (1994).
11. Schick, M. J. (Ed.), *Nonionic Surfactants: Physical Chemistry*, Marcel Dekker, New York, 1987.
12. Shinoda, K., *Principles of Solution and Solubility*, Marcel Dekker, New York, 1978.
13. Tanford, C., *The Hydrophobic effect. Formation of Micelles and Biological Membranes*, Wiley, New York, 1980.

CHAPTER 20

Surfactant–Polymer Systems

Björn Lindman

Lund University, Lund, Sweden

1	Introduction	445	6.2	Introduction of charges	454
2	Polymers can Induce Surfactant Aggregation	445	6.3	Mixed ionic systems	454
3	Attractive Polymer–Surfactant Interactions Depend on both Polymer and Surfactant	447	7	Phase Behaviour of Polymer–Surfactant Mixtures in Relation to Polymer–Polymer and Surfactant–Surfactant Mixtures	456
4	Surfactant Association to Surface-Active Polymers can be Strong	449	8	Polyelectrolyte–Surfactant Systems Show a Complex Behaviour	458
5	The Interaction between a Surfactant and a Surface-Active Polymer is Analogous to Mixed Micelle Formation	451	9	Polymers may Change the Phase Behaviour of Infinite Surfactant Self-Assemblies	460
6	The Phase Behaviour of Polymer–Surfactant Mixtures Resembles that of Mixed Polymer Solutions	452	10	Surfactant Binding Strongly Affects Adsorbed Polymer Layers and the Swelling of Chemical Gels	462
	6.1 General aspects and nonionic systems	452	11	There are many Technical Applications of Polymer–Surfactant Mixtures	462
			12	Bibliography	463

1 INTRODUCTION

Surfactants and water-soluble polymers have very broad ranges of applications. By reviewing the compositions of various products we learn that in the large majority of cases one or more polymers are present together with one or more surfactants. In a typical situation they are employed to achieve different effects – colloidal stability, emulsification, flocculation, structuring and suspending properties, rheology control – but in some cases a synergistic effect is addressed. The combined occurrence of polymers and surfactants is found in such diverse areas as cosmetics, paints, detergents, foods, polymer synthesis and formulations of drugs and pesticides.

In this present chapter we will broadly investigate the interactions between different types of polymers,

in particular water-soluble homopolymers and graft copolymers, with the different classes of surfactants. It will be found that important starting points in a discussion are other mixed solute systems, in particular surfactant–surfactant and polymer–polymer mixed solutions.

2 POLYMERS CAN INDUCE SURFACTANT AGGREGATION

One of the most significant aspects of a surfactant is its ability to lower the interfacial tension between an aqueous solution and some other phase. In particular for an ionic surfactant this is modified by the presence of a polymer in the solution. As illustrated in Figure 20.1, the effect of a polymer on the surface tension of an aqueous solution is different for different surfactant

concentrations. At low concentrations, there may or may not be, depending on the surface activity of the polymer, a lowering of the surface tension. However, at some concentration there is a break in the surface tension curve and a more or less constant value is attained. There is then a concentration region, roughly proportional in extent to the polymer concentration, with a constant γ value. Finally, there is a decrease towards the value obtained in the absence of polymer.

We may interpret the concentration dependence of γ in the presence of a polymer as follows. At a certain concentration, often termed the critical association concentration (CAC) and denoted T_1 in Figure 20.1, there

is an onset of association of surfactant to the polymer. Because of this, there is no further increase in surfactant activity and thus no further lowering of γ . As the polymer is saturated with surfactant (at T_2'), the surfactant unimer concentration and the activity start to increase again and there is a lowering of γ until the unimer concentration reaches the critical micelle concentration (CMC) (at the concentration T_2), after which γ is constant and normal surfactant micelles start to form.

This picture is confirmed if the association of the surfactant is monitored directly (for example, by surfactant-selective electrodes, by equilibrium dialysis, by self-diffusion or by some spectroscopic technique). As illustrated by the binding isotherm given in Figure 20.2, there is at low surfactant concentrations no significant interaction. At the CAC , a strongly co-operative binding is indicated. At higher concentration, we see a plateau level, and then a further increase of the free surfactant concentration until the surfactant activity or unimer concentration joins the curve obtained in the absence of polymer. We note from Figure 20.2 the strong analogy with micelle formation and the interpretation of the binding isotherm in terms of a depression of the CMC .

Such a description is supported by solubilization studies, as illustrated in Figure 20.3. We note from this that the solubilization curves in the presence of polymer are shifted to lower surfactant concentrations but are otherwise essentially the same as those without polymer. From the break-points we can deduce the CMC/CAC values which decrease by the same factor as without polymer as the alkyl chain is lengthened.

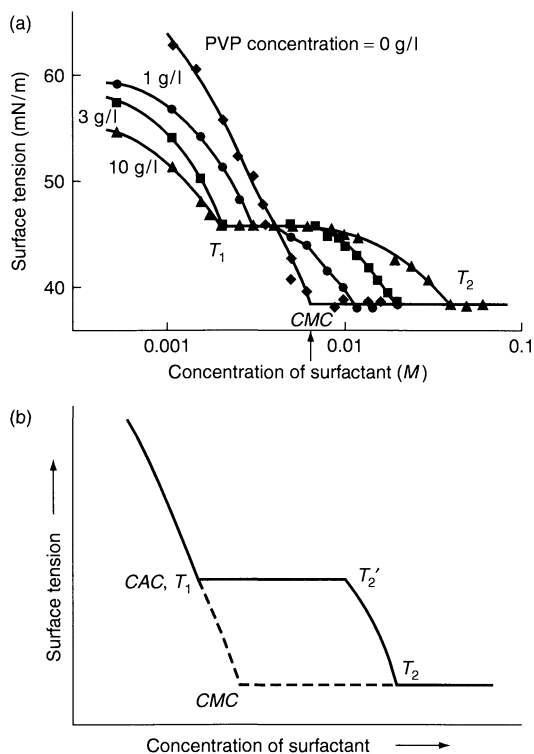


Figure 20.1. (a) Surface tensions of sodium dodecyl sulfate (SDS) solutions as a function of surfactant concentration in the presence of different concentrations of poly(vinyl pyrrolidone) (PVP). (b) A schematic plot for the case where the polymer itself does not influence γ . The concentrations T_1/CAC , T_2' and T_2 are used to identify the concentrations of changes in the surface tension. As discussed in the text these parameters characterize different aspects of the polymer-surfactant association. ((a) Redrawn from M. M. Breuer and I. D. Robb, *Chem. Ind.*, **530**, (1972)) and ((b) redrawn from E. D. Goddard, in *Interactions of Surfactants with Polymers and Proteins* E. D. Goddard and K. P. Ananthapadmanabhan (Eds), CRC Press, Boca Raton, FL, 1993, p. 139)

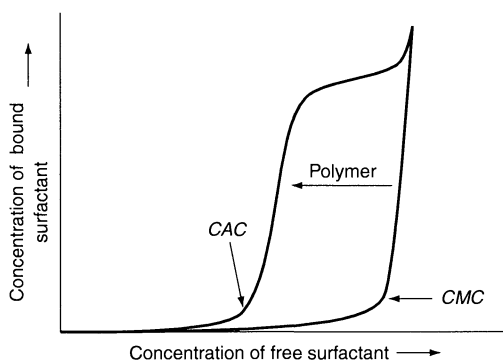


Figure 20.2. The binding isotherm of a surfactant to a polymer without distinct hydrophobic moieties, giving the concentration of bound surfactant as a function of the free surfactant concentration, can be interpreted as a lowering of the surfactant CMC by the polymer, or a strongly co-operative binding

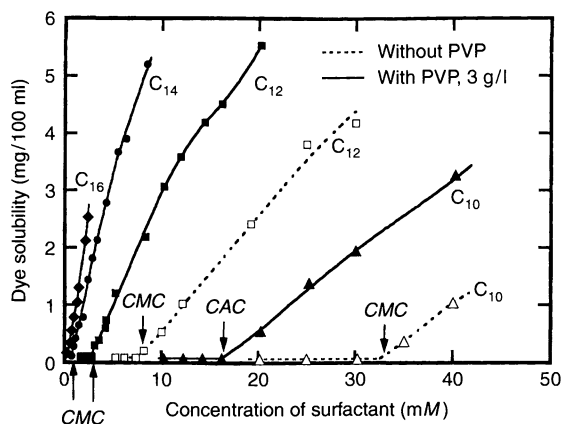


Figure 20.3. Solubilization experiments support the notion of a polymer-induced micellization. The amount of a dye, Orange OT, solubilized in mixtures of sodium alkyl sulfates of different chain lengths (C_{10} – C_{16}) and poly(vinyl pyrrolidone) (PVP) is given as a function of the surfactant concentration. (Redrawn from H. Lange, *Kolloid-Z. Z. Polym.*, **243** (1971) 101)

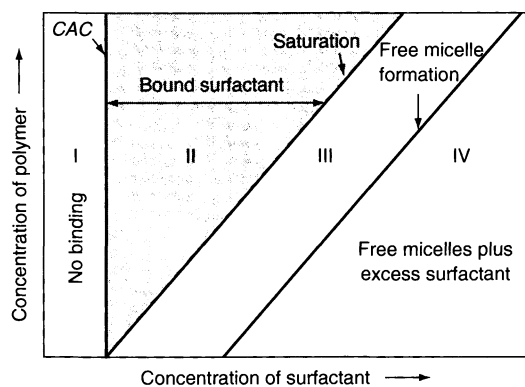


Figure 20.4. Association between a homopolymer and a surfactant in different concentration domains: (I) at low surfactant concentrations, there is no significant association at any polymer concentration; (II) above the CAC, association increases up to a particular surfactant concentration, which increases linearly with the polymer concentration; (III) association is saturated and the surfactant monomer concentration increases; (IV) There is a coexistence of surfactant aggregates at the polymer chains and free micelles. This picture is schematic but gives a good description for aqueous mixtures of an ionic surfactant and a nonionic homopolymer. (Redrawn from B. Cabane and R. Duplessix, *J. Phys. II (Paris)*, **43** (1982) 1529)

Experimental binding studies of mixed polymer-surfactant solutions can be summarized as follows (cf. Figure 20.4):

- (i) The CAC/CMC value is only weakly dependent on the polymer concentration over wide ranges.
- (ii) The CAC/CMC value is to a good approximation, independent of the polymer molecular weight down to low values. For very low molecular weights, the interaction is weakened.
- (iii) The plateau binding increases linearly with the polymer concentration.
- (iv) Anionic surfactants show a marked interaction with most homopolymers, while cationic surfactants show a weaker but still significant interaction. Nonionic and zwitterionic surfactants only rarely show a distinct interaction with homopolymers.

3 ATTRACTIVE POLYMER-SURFACTANT INTERACTIONS DEPEND ON BOTH POLYMER AND SURFACTANT

There are thus two alternative pictures of mixed polymer-surfactant solutions, one describing the interaction in terms of a (strongly co-operative) association or binding of the surfactant to the polymer, and one in terms of a micellization of surfactant on or in the vicinity of the polymer chain. Both descriptions are useful and are largely overlapping. However, we will see that for polymers with hydrophobic groups the binding approach is preferred, while for hydrophilic homopolymers the micelle formation picture has distinct advantages.

As regards the aggregate structure in these systems, the pearl-necklace model (Figure 20.5), with the surfactant forming discrete micellar-like clusters along the polymer chain, has received wide acceptance for the case of mixed solutions of ionic surfactants and homopolymers. The micelle sizes are similar with polymer present as without and aggregation numbers are typically similar or slightly lower than those of micelles forming in the absence of a polymer.

In the presence of a polymer, the surfactant chemical potential is lowered with respect to the situation without polymer (Figure 20.6). There are several interactions which can be responsible for surfactant binding or a polymer-induced micellization. We note that in many respects (variation with surfactant alkyl chain length, solubilization, micelle structure and dynamics) there is a close similarity to the micellization of the surfactant alone. The normal hydrophobic interaction between the alkyl chains must therefore still be a dominating contribution to the free energy of association. However, it is modified by mainly one of the following two factors.

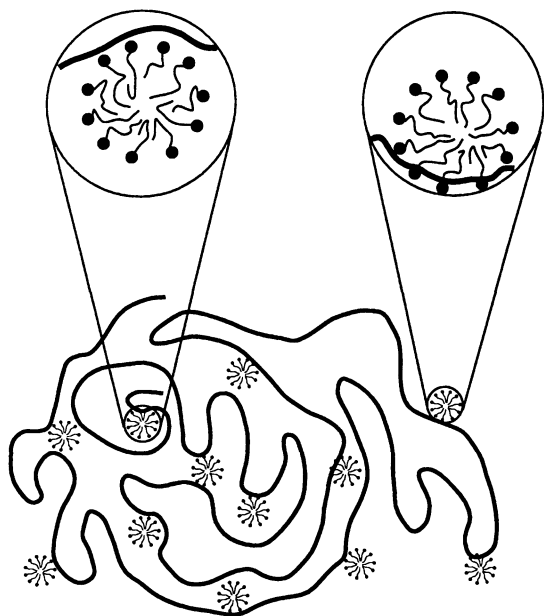


Figure 20.5. Pearl-necklace model of surfactant–polymer association

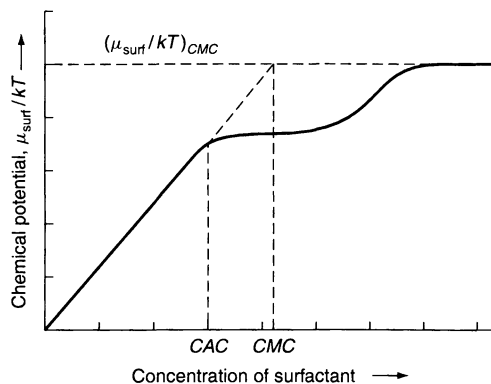


Figure 20.6. In the presence of a polymer, the chemical potential may be lowered leading to micelle formation at a lower concentration. The figure gives the chemical potential (μ) of the surfactant divided by kT as a function of surfactant concentration on a logarithmic scale. In the presence of polymer, the chemical potential is lowered and micelle formation on the polymer starts at a lower concentration (CAC) than in the absence of polymer (CMC). (Redrawn from D. F. Evans and H. Wennerström, *The Colloidal Domain: Where Physics, Chemistry, Biology and Technology Meet*, VCH, New York, 1994, p. 312)

For polymers which have hydrophobic portions or groups, there will be a hydrophobic attraction between

the polymer molecules and the surfactant molecules. Such interactions will be particularly strong for block copolymers, with hydrophobic and hydrophilic blocks, and with graft copolymers, where hydrophobic groups have been grafted on a hydrophilic polymer backbone. However, homopolymers can also have hydrophobic groups, strong as in poly(styrene sulfonate) or weak as in poly(ethylene glycol). The polarity of such groups can decrease with increasing temperature.

Electrostatic interactions are obvious if both surfactant and polymer are charged; then, in the case of opposite signs of the charges, we can expect a quite strong association. However, we must also take into account the repulsive interactions between charged polymer molecules or between charged surfactant molecules. In particular, we learnt in our discussion of ionic surfactant self-assembly that the entropy loss associated with the increased concentration of counterions at the aggregate surface compared to the bulk is highly unfavourable for self-assembly and explains, *inter alia*, why ionic surfactants have orders-of-magnitude higher $CMCs$ than nonionics.

A polymer may modify this entropy contribution in a number of different ways. If it is ionic and has a similar charge, then we have a simple and relatively moderate electrolyte effect. If its charge is opposite, and it acts as a multivalent counterion, then the interaction becomes very strong since an association between polymer and micelle leads to a release of the counterions of both the micelles and the polymer molecules; a very similar effect will be obtained in mixtures of two oppositely charged polymers. Indeed there is for such a case a lowering of the CMC by orders of magnitude.

In addition, nonionic cosolutes may decrease the CMC for ionics, as we learn elsewhere from the example of addition of different alcohols (see Chapter 19). If the cosolute is slightly amphiphilic, it will be located in the micelle surface, lower the charge density and hence decrease the entropic penalty in forming micelles. This is believed to be the mechanism behind the moderate depression of the CMC for ionic surfactants produced by poly(ethylene glycol) and several nonionic polysaccharides.

We note from these arguments that ionic surfactants would be expected to interact broadly with different types of water-soluble polymers. This is true, in particular, for anionics; the considerably weaker interaction of cationics is not well understood. Nonionic surfactants, on the other hand, should have little tendency to interact with hydrophilic homopolymers since no further stabilization of the micelles can be expected; we noted above that nonionic surfactants only exceptionally associate to

homopolymers. The situation will, of course, be different for polymers with hydrophobic parts to which nonionics will associate by hydrophobic interaction.

From this discussion, it is thus clear that a number of factors influence polymer-surfactant interactions. However, we can define three categories of surfactant binding to polymers, as follows:

1. Charged surfactants bind to oppositely charged polymers.
2. Charged surfactants generally bind to slightly hydrophobic nonionic polymers – exemplified by poly(ethylene glycol), poly(vinyl pyrrolidone) and nonionic cellulose ethers). Binding is considerably stronger for anionic than for cationic surfactants and decreases with increasing polarity of the polymer.
3. All surfactants tend to bind to hydrophobically modified polymers.

Hydrophobic interactions are important in all three cases but there are important differences. In case 1, the normal surfactant-surfactant hydrophobic interaction is very similar to what applies in the absence of polymer while the attractive polymer-surfactant interaction is due to electrostatics. In case 2, there is a weak hydrophobic polymer-surfactant attraction (and an even weaker polymer-polymer attraction) and a partial elimination of an unfavourable surfactant-surfactant electrostatic repulsion. In case 3, there are strong

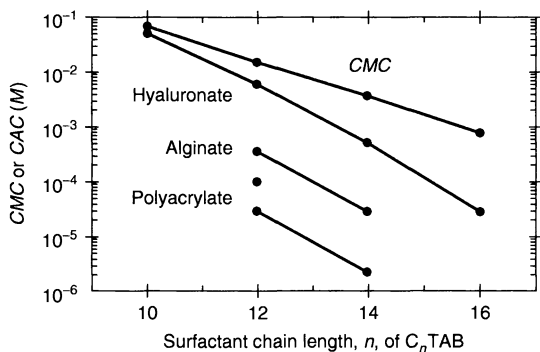


Figure 20.7. The lowering of the *CMC* of ionic surfactants in the presence of oppositely charged polymers increases with increasing charge density of the polymer and can amount to several orders of magnitude. The figure compares *CMC* and *CAC* data of alkyl trimethylammonium bromides in the presence of three polyanions, sodium hyaluronate (linear charge density ca. $1e/nm$), sodium alginate (ca. $2e/nm$) and sodium polyacrylate (ca. $3e/nm$). (By courtesy of Per Linse. Data from K. Hayakawa J. P. Kwate and J. C. T. Kwak, *Macromolecules*, **16**, (1983) 1642, and K. Thalberg and B. Lindman, *J. Phys. Chem.*, **93**, (1989) 1478

hydrophobic attractions between all species, i.e. polymer-polymer, polymer-surfactant and surfactant-surfactant. Categories 1 and 2 are best regarded as a polymer-induced surfactant self-assembly, i.e. fruitfully discussed in terms of a lowering of the *CMC*. For category 2, the *CMC* lowering is relatively small – a factor of 1–5 – while in case 1 it can, as illustrated in Figure 20.7, amount to several orders of magnitude for higher polymer charge densities. In category 3, which will now be examined in some detail, mixed surfactant micellization is a better analogue.

4 SURFACTANT ASSOCIATION TO SURFACE-ACTIVE POLYMERS CAN BE STRONG

The modification of water-soluble homopolymers by grafting a low amount of hydrophobic groups (of the order of 1% of the monomers reacted is a typical figure), such as alkyl chains, leads to amphiphilic polymers which have a tendency to self-associate by hydrophobic interaction. This weak aggregation (Figure 20.8) leads to an increase in viscosity and in other rheological characteristics, and hence the use of these “associative thickeners” as rheology modifiers in paints and other products.

An added surfactant will interact strongly with the hydrophobic groups of the polymer, so leading to a strengthened association between polymer chains and thus to an increased viscosity. We exemplify the behaviour with a hydrophobically modified nonionic cellulose ether (HM-EHEC) (Figure 20.9). As can be seen in Figure 20.10, sodium dodecyl sulfate increases the viscosity dramatically for HM-EHEC but very slightly for unmodified EHEC. At higher surfactant content, the viscosity effect is lost. As we will see later, we can best understand these systems in terms of a mixed micelle formation between the surfactant and the amphiphilic polymer. In order to have cross-linking, and thus a viscosity effect, there must be a sufficiently high number of polymer hydrophobes per micelle. At higher surfactant concentrations there will be only one polymer hydrophobe in a micelle and all of the cross-linking effect is lost.

These viscosity effects of the addition of surfactant to a solution of a hydrophobically modified water-soluble polymer are general, although the effect will be modified by other interactions such as electrostatic ones. As exemplified in Figure 20.11, addition of an oppositely charged surfactant to a solution of a hydrophobically

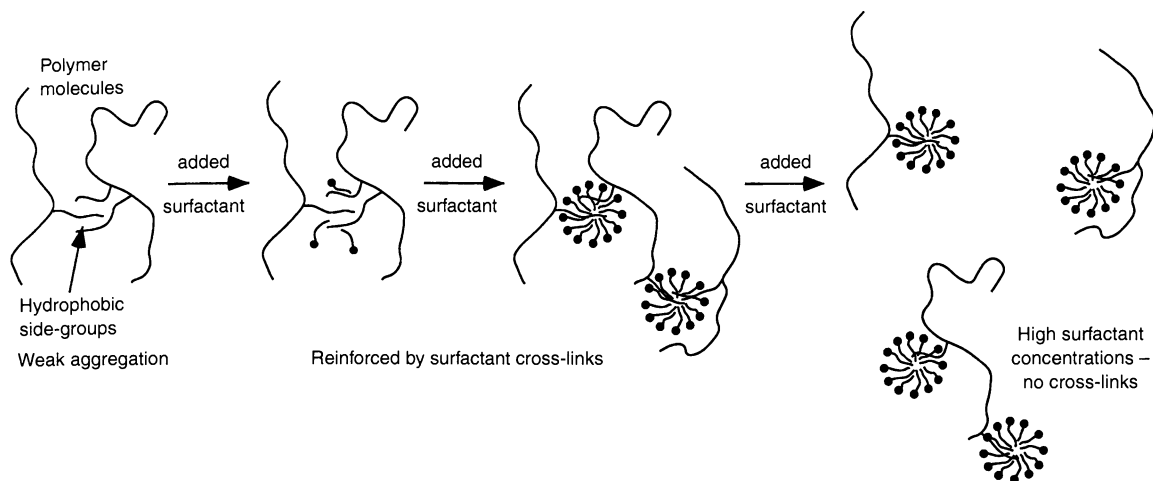


Figure 20.8. The self-association of a hydrophobically modified (HM) water-soluble polymer can be strengthened or weakened by a surfactant, depending on the stoichiometry

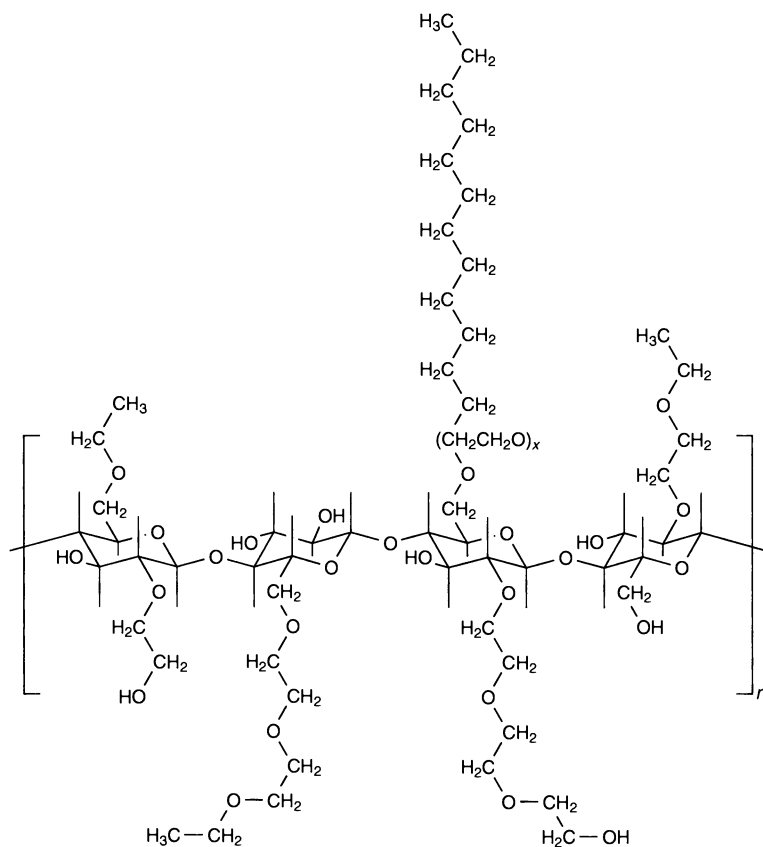


Figure 20.9. Cellulose can be modified by a relatively random substitution of hydroxyethyl and ethyl groups to give ethylhydroxyethyl cellulose (EHEC). In HM-EHEC, a low fraction of hydrophobic groups is inserted

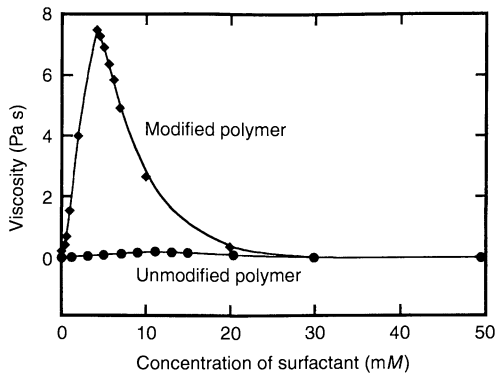


Figure 20.10. Addition of sodium dodecyl sulfate to a solution of a hydrophobically modified polymer (EHEC) gives a strong increase in viscosity at first and then a decrease to a low value. For the unmodified polymer, changes in viscosity are small. (By courtesy of K. Thuresson)

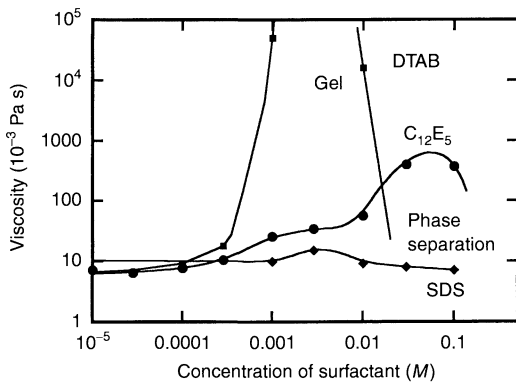


Figure 20.11. Addition of a surfactant to a solution of a hydrophobically modified polyelectrolyte (in this case hydrophobically modified polyacrylate) gives very different viscosity effects for different types of surfactants. The effect is much larger for an oppositely charged surfactant, dodecyltrimethylammonium bromide (DTAB), than it is for a nonionic ($C_{12}E_5$) or a similarly charged one, sodium dodecyl sulfate (SDS). (Redrawn from B. Magny, I. Iliopoulos, R. Audebert, L. Piculell and B. Lindman, *Progr. Colloid. Polym. Sci.*, **89** (1992) 118)

modified polyelectrolyte gives much larger viscosity effects than for a nonionic or a similarly charged surfactant; however, even in the latter case there are substantial effects especially if the hydrophobic grafts are larger.

In mixtures of surfactants and clouding polymers, which become less polar at increasing temperatures, thermoreversible gels may be formed. On increasing the temperature, gelation is induced and on cooling the gel

melts. Such an effect may also be obtained in mixtures of a nonionic surfactant and a hydrophobically modified water-soluble polymer, when there is an important temperature-induced micelle growth or a transition from micelles to vesicles or some other self-assembly structure.

5 THE INTERACTION BETWEEN A SURFACTANT AND A SURFACE-ACTIVE POLYMER IS ANALOGOUS TO MIXED MICELLE FORMATION

A hydrophobically modified water-soluble polymer (HM-polymer) can be viewed as a modified surfactant. It forms micelles, or hydrophobic microdomains, on its own at very low concentrations (intramolecularly, at infinite dilution) and these micelles can solubilize hydrophobic molecules. Furthermore, an HM-polymer and a surfactant in general have a strong tendency to form mixed micelles in a similar way as two surfactants. Two stoichiometries are important for HM-polymer-surfactant systems, i.e. the alkyl chain stoichiometry and the charge stoichiometry.

Since the mixed aggregates dominate, we have a low concentration of free surfactant and essentially no free micelles until the concentration of micelles exceeds the concentration of polymer hydrophobic groups. From this, we can understand the binding isotherm of a surfactant to an HM-polymer, as schematized in Figure 20.12. The binding isotherm of an ionic surfactant to a nonionic HM-polymer will be very similar to its binding

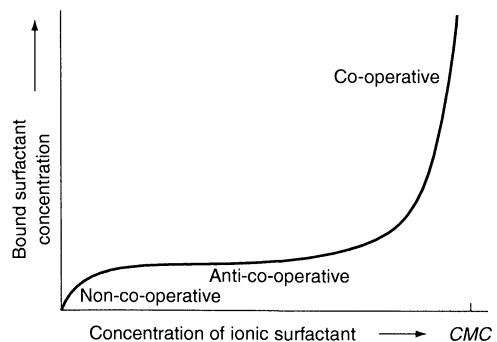


Figure 20.12. The binding isotherm (giving the concentration of bound surfactant as a function of the free surfactant concentration) for an ionic surfactant to a nonionic HM-polymer is similar to the binding to a nonionic micelle, i. e. with one non-co-operative (a), one anti-co-operative (b) and one co-operative (c) region. With the parent homopolymer, only the co-operative region is seen

to nonionic surfactant micelles. We can distinguish between three concentration regions. In the first region, there is a high affinity non-co-operative binding of individual ionic surfactant molecules to micelles of the nonionic surfactant or the HM-polymer. As the number of ionic surfactant molecules per micelle exceeds one, the binding becomes anti-co-operative since the binding of surfactant to a similarly charged micelle is unfavourable. Finally, as the free surfactant concentration equals the *CAC*, i. e. the *CMC* in the presence of the homopolymer, there is a self-association of the ionic surfactant into micelles at the polymer. This is seen as a co-operative binding region, which is the only binding seen for the corresponding polymer, which has no hydrophobic grafts.

The peak in the plot of viscosity vs. surfactant concentration in general occurs in the vicinity of the *CAC*. Here, the composition of the mixed HM-polymer–surfactant micelles changes strongly with concentration to become dominated by the surfactant; thus, the cross-linking effect is lost.

The significance of the surfactant micelle–polymer hydrophobe stoichiometry is nicely illustrated if the viscosity is presented as a function of the concentration of micelles (or hydrophobic microdomains), as determined by fluorescence quenching. In Figure 20.13 viscosity

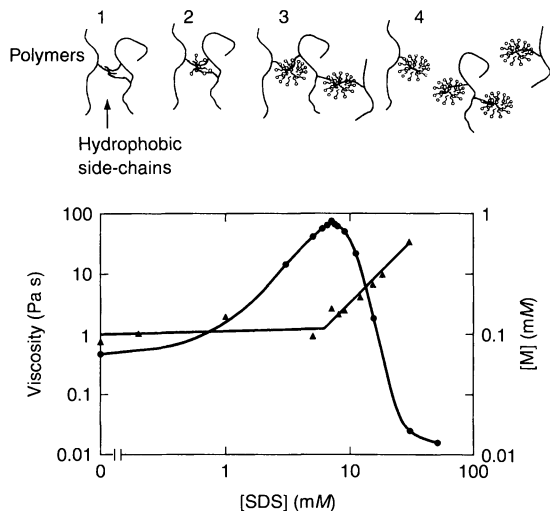


Figure 20.13. The viscosity of a solution of a hydrophobically modified water-soluble polymer and a surfactant compared to the concentration of micelles (determined by fluorescence quenching). The viscosity (filled circles) has a maximum when the micelle concentration starts to increase. The system illustrated is that of hydroxyethyl cellulose (1 wt%) and sodium dodecyl sulfate (SDS). (S. Nilsson, *Ph. D. Thesis*, Lund University, Sweden, 1999)

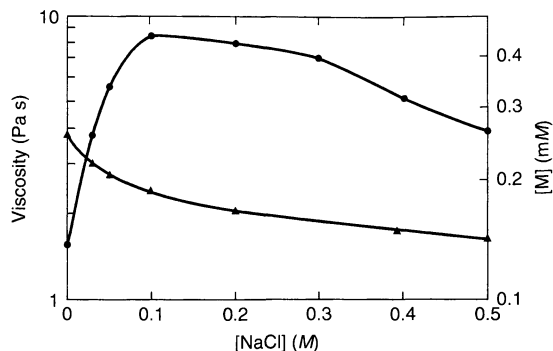


Figure 20.14. The viscosity (filled circles) of a solution of a hydrophobically modified water-soluble polymer and a surfactant increases as the concentration of micelles increases. The system illustrated is that of hydroxyethyl cellulose (1 wt%) and sodium dodecyl sulphate, upon the addition of an electrolyte (NaCl). (S. Nilsson, *Ph. D. Thesis*, Lund University, Sweden, 1999)

data and micelle concentrations are presented for a system of a nonionic cellulose ether and an anionic surfactant. The micelle concentration remains constant up to surfactant concentrations of the order of the *CMC*; in this concentration range, the viscosity increases by orders of magnitude. As the micelle concentration then increases, the viscosity drops very strongly, since the number of polymer hydrophobes per micelle decreases towards one. Such a strong dependence of rheological characteristics on surfactant concentration is problematic in many formulations but a simple remedy is to switch over to a surfactant system with micellar growth, thus eliminating or reducing the increase in micellar concentration. For an ionic system, micellar growth can be induced by the addition of an electrolyte, oppositely charged surfactant or some weakly polar solubilize. For the system discussed here, electrolyte addition induces micellar growth, and hence a decreased micellar concentration, and as expected, a major increase in viscosity (Figure 20.14).

6 THE PHASE BEHAVIOUR OF POLYMER–SURFACTANT MIXTURES RESEMBLES THAT OF MIXED POLYMER SOLUTIONS

6.1 General aspects and nonionic systems

For the case of mixed solutions of a surfactant and an HM-polymer, we can see a large tendency to association

between the two cosolutes. We also learnt above that many homopolymers facilitate micelle formation of an ionic surfactant. However, an associative interaction is by no means evident since for most polymer-surfactant pairs there is no net attractive interaction.

For two polymers in a common solvent, the entropic driving force of mixing is weak and we typically encounter a segregation into two solutions, with one rich in one polymer and one rich in the other; the tendency to phase separation increases strongly with the molecular weights of the polymers. In addition, since a micelle is characterized by a high molecular weight, we would expect segregative phase separation to be a common phenomenon (Figure 20.15).

For polymer solutions, we can distinguish between two types of phase separation, i.e. one segregative and one associative (Figure 20.16). If there is no attractive interaction, a segregative phase separation is obtained, while if there is a moderately strong attraction complete miscibility may result. In the case of strong attraction between the two polymers, we will have an associative phase separation, with one phase concentrated in both polymers and one dilute solution. The degree of phase separation will in both cases increase with the molecular weight of the polymers.

For a mixed polymer-surfactant system, the behaviour is completely analogous. One difference is that the "degree of polymerisation" of a micelle, unlike a polymer, is not fixed but may vary with the conditions (temperature, electrolyte concentration, etc.), as we

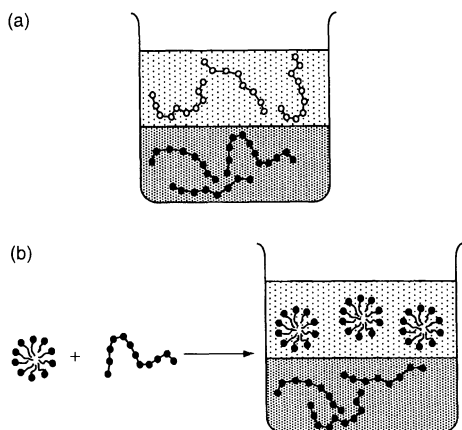


Figure 20.15. Because of the high molecular weight of a micelle we expect a mixed polymer-surfactant solution, in the absence of significant attractive interactions, to display the incompatibility typical of polymer mixtures (a), i. e. segregate into one polymer-rich and one micelle-rich solution (b)

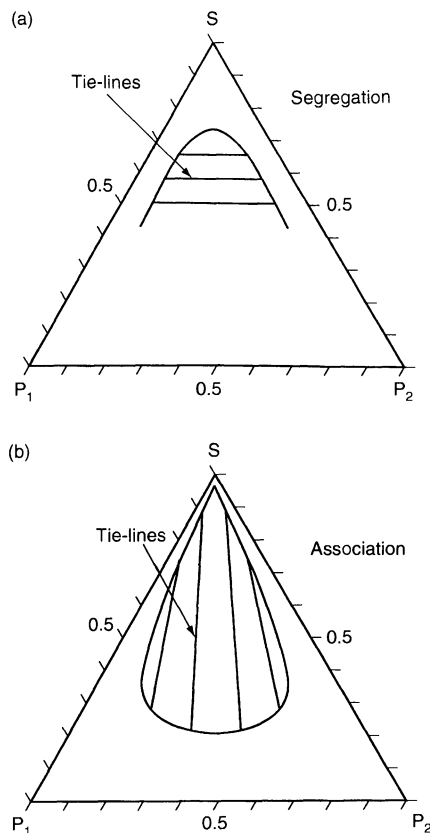


Figure 20.16. Ternary phase diagrams for two polymers (P_1 and P_2) in a common solvent (S) showing (a) segregation and (b) association. In the two-phase regions, tie-lines are given to show the compositions of co-existing solution phases. (Redrawn from L. Piculell and B. Lindman, *Adv. Colloid Interface Sci.*, **41** (1992) 149)

learnt elsewhere in our discussion of micellar growth (see Chapter 19).

In Figure 20.17, we compare a polymer-surfactant mixture, a nonionic polyoxyethylene surfactant and dextran, with a related polymer-polymer mixture, poly(ethylene glycol) and dextran. We can see that the two mixtures phase-separate in qualitatively the same way.

Upon changing the surfactant there are major changes in the phase diagram. Thus, $C_{12}E_5$ gives a much stronger segregation than $C_{12}E_8$ and with the former segregation increases strongly with increasing temperature. We note that this is exactly what we would expect from our discussion of micelle sizes for these surfactants (see Chapter 19). $C_{12}E_8$ forms small roughly spherical micelles at all temperatures, while $C_{12}E_5$

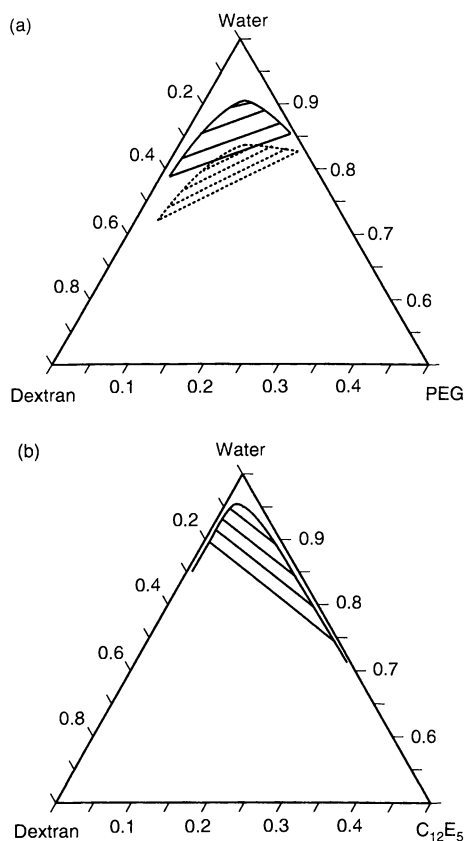


Figure 20.17. Phase diagrams of (a) aqueous mixtures of dextran (molecular weight 23 000) and poly(ethylene glycol) (PEG) (molecular weight 2300 (dashed curve) and 18 000 (continuous curve), compared with (b) a mixture of dextran (40 000) with $C_{12}E_5$. Above the curves, there is miscibility, while below the curves there is phase separation into two solutions. ((a) Redrawn from L. Piculell and B. Lindman, *Adv. Colloid Interface Sci.*, **41** (1992) 149, and (b) redrawn from L. Piculell, K. Bergfeldt and S. Gerdes, *J. Phys. Chem.*, **100** (1996) 3675)

forms large micelles which grow strongly with temperature.

The segregative phase separation is not the only one observed for mixtures of a nonionic polymer and a nonionic surfactant. For the case of a less polar polymer, the phase separation can be associative, especially at higher temperatures, due to hydrophobic association.

6.2 Introduction of charges

The introduction of charged groups in the solutes has a profound influence on phase-separation phenomena.

We have already learnt that polyelectrolytes are much more soluble than the corresponding uncharged polymer, which we attribute to the entropy of the counterion distribution: confining polymer molecules to part of the system costs little entropy due to the low number of entities. On the other hand, there is a large entropy loss on confining the (much more numerous) counterions. In mixed polymer systems, we see many consequences of the electrostatic interactions due to net charges. One is the low tendency to phase separation in a mixed solution of one nonionic and one ionic polymer; in the presence of added electrolyte, this inhibition of phase separation is largely eliminated and typical polymer incompatibility is observed.

Completely analogous effects are observed for mixed polymer–surfactant solutions. Even a very slight charging up of either the polymer (by introducing ionic groups) or the micelles (by adding ionic surfactant) strongly enhances polymer–surfactant miscibility. This is illustrated for the system of Figure 20.17(b) in Figure 20.18, where we also see that addition of electrolyte tends to eliminate these effects of the charges. When the polymer molecules are similarly charged, there is also a return towards the incompatibility of the parent nonionic mixture.

Ionic surfactants broadly tend to associate to nonionic polymers. The lower the polarity of the polymer, the stronger the association. For clouding polymers, which are on the limit of being water-soluble, the association is strong and leads to a strong increase of the cloud point. This decreased tendency to phase separation is illustrated in Figure 20.19, where we also see that quite low concentrations of electrolyte change the behaviour completely. As we have seen above, there is polymer-induced micellization in these cases and thus a formation of polymer–surfactant complexes. Because of the charging up of the polymer, its solubility increases, again as a result of the entropic penalty of confining the counterions to one phase. However, this is eliminated on addition of low concentrations of electrolyte and there is a dramatic lowering of the cloud point.

6.3 Mixed ionic systems

A mixture of two oppositely charged polyelectrolytes shows a strongly associative behaviour, as demonstrated by a strong tendency to phase separation. A mixture of a polyelectrolyte and an oppositely charged surfactant will also associate strongly. As exemplified in Figure 20.20, there is a lowering of the *CMC* by orders of magnitude for long-chain surfactants and, as shown in Figure 20.21,

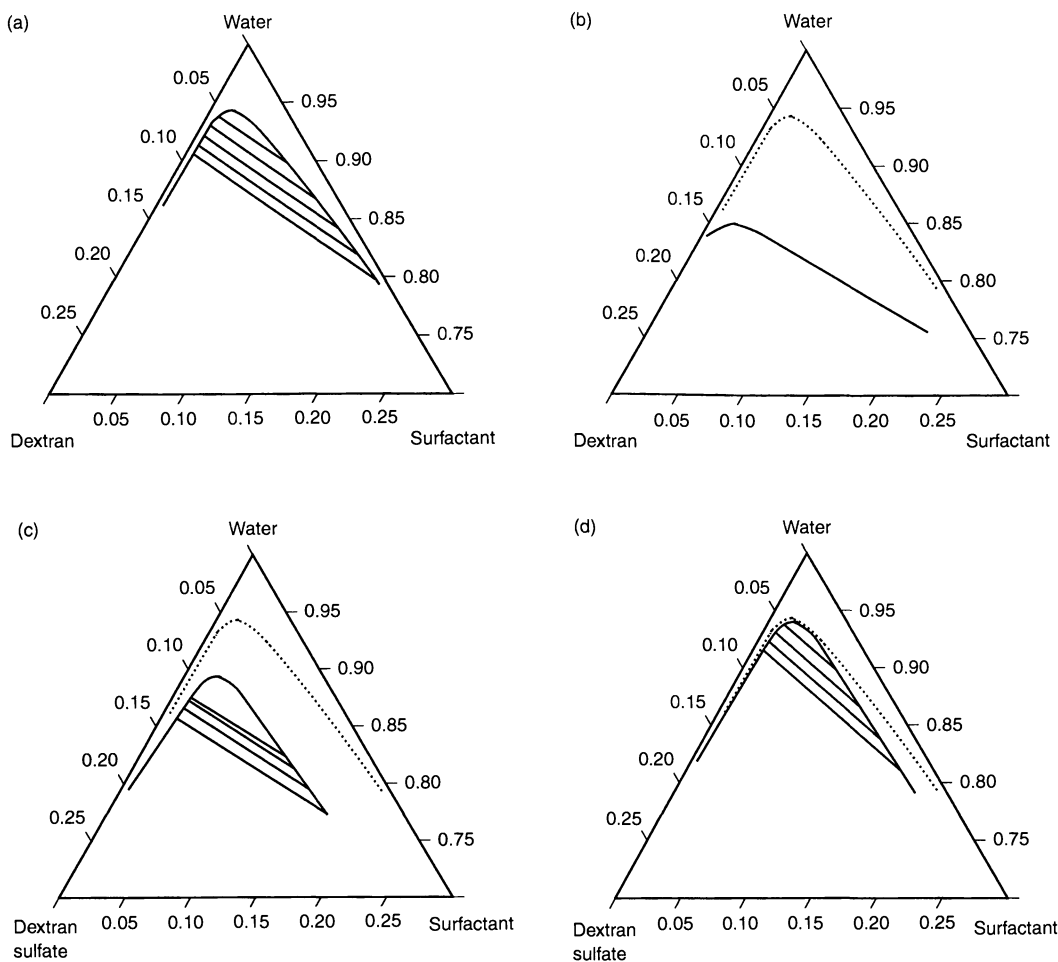


Figure 20.18. Effect of introducing charges in a mixture of a nonionic polymer and a nonionic surfactant, illustrated for the mixture of dextran and a polyoxyethylene surfactant (reference system in (a)). Both upon introducing a low fraction of ionic surfactant in the micelles (b) or a low amount of sulfate groups in dextran (c), the mutual miscibility is strongly enhanced. This can be eliminated either if electrolyte is added or if both the polymer molecules and the micelles are charged (d). Above the curves there is miscibility, while below there is phase separation into two solutions. The dashed curves give the miscibility limits for the reference system. (Redrawn from K. Bergfeldt and L. Piculell, *J. Phys. Chem.*, **100** (1996) 5935)

there is a strong associative phase separation. An aqueous mixture of a polyelectrolyte and an oppositely charged surfactant phase separates into one dilute phase and one, typically highly viscous, phase concentrated in both polymer and surfactant.

The extent of phase separation in the system shown in Figure 20.21 increases strongly with the surfactant alkyl chain length and polymer molecular weight. On addition of electrolyte, the phase separation is eliminated, but at higher electrolyte content there is a phase separation again. However, as we can see in Figure 20.22, it is of a different nature. This behaviour, which is

very similar to what we observe for mixtures of two oppositely charged polymers, can best be understood from a combination of polymer incompatibility and electrostatic effects. We note that the concentration of counterions is very high and, therefore, unlike that observed for the nonionic polymers, phase separation with a polyelectrolyte in one phase leads to confinement of the counterions and a very significant entropy loss. Therefore, polyelectrolytes are highly soluble when compared to the corresponding uncharged polymer. At high electrolyte concentrations, this entropy contribution is eliminated and phase separation will be similar

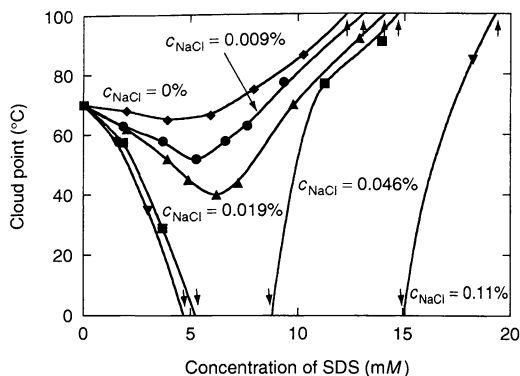


Figure 20.19. Addition of an ionic surfactant to a solution (0.9 wt%) of a clouding polymer (illustrated by ethylhydroxyethyl cellulose (EHEC)) raises the cloud point in the absence of added electrolyte but decreases it in the presence of (low amounts of) electrolyte. The change in the cloud point on addition of sodium dodecyl sulfate (SDS) is given in the absence of added electrolyte and in the presence of different concentrations of added NaCl; from top to bottom the curves refer to 0, 0.009, 0.019, 0.06 and 0.01 wt% of salt. (Redrawn from A. Carlsson, G. Karlström and B. Lindman, *Langmuir*, 2 (1986) 536)

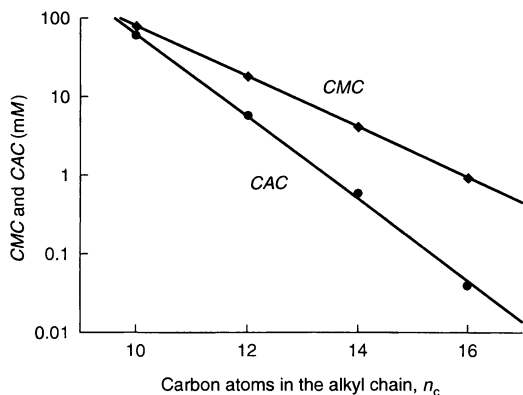


Figure 20.20. The CAC is typically orders of magnitude lower than the CMC for an ionic surfactant in the presence of an oppositely charged polymer, illustrated by plotting the logarithm of the CMC and the CAC of alkyltrimethylammonium bromides in the presence of an anionic polysaccharide, sodium hyaluronate, versus the number of carbons in the alkyl chain. (Redrawn from K. Thalberg and B. Lindman, *J. Phys. Chem.*, 93 (1989) 1478)

to that of uncharged polymer systems. In the case of Figure 20.22, we have an intrinsically segregating system, as can be seen from the phase diagram at high electrolyte concentrations.

The associative phase separation at low salt contents is also understood from the entropy of the counterion

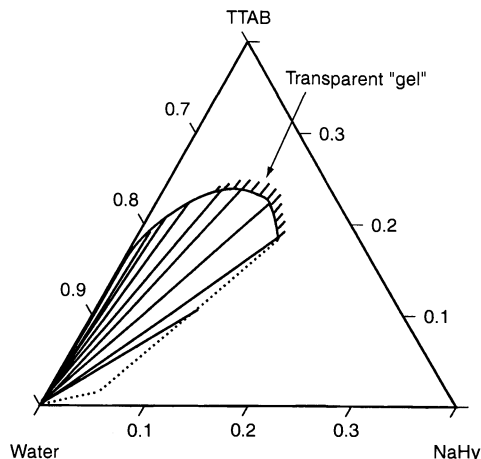


Figure 20.21. A mixture of an ionic surfactant and an oppositely charged polyelectrolyte typically gives an associative phase separation, as exemplified here by tetradecyltrimethylammonium bromide (TTAB) and sodium hyaluronate (NaHy). (Redrawn from B. Lindman and K. Thalberg, in *Interactions of Surfactants with Polymers and Proteins*, E. D. Goddard and K. P. Ananthapadmanabhan (Eds), CRC Press, Boca Raton, FL, 1993, p. 252)

distribution. The highly charged micelles and polyelectrolyte molecules are enriched with counterions at their surface due to the process of Coulomb attraction. On association, counterions of both cosolutes are transferred into the bulk with a concomitant entropy gain; therefore, the strong tendency to display associative phase separation in the absence of added salt.

Replacing the surfactant of this system with one which has a similar charge as the polymer, the entropic loss is essentially absent and a segregative phase separation is the rule, as illustrated in Figure 20.23. At high salt contents, phase separation is enhanced, which can be referred to the growth of sodium dodecyl sulfate micelles.

7 PHASE BEHAVIOUR OF POLYMER-SURFACTANT MIXTURES IN RELATION TO POLYMER-POLYMER AND SURFACTANT-SURFACTANT MIXTURES

We may summarize the phase behaviour of mixtures of polymer (P) and surfactant (S) depending on charge (superscript +, - or 0) as follows:

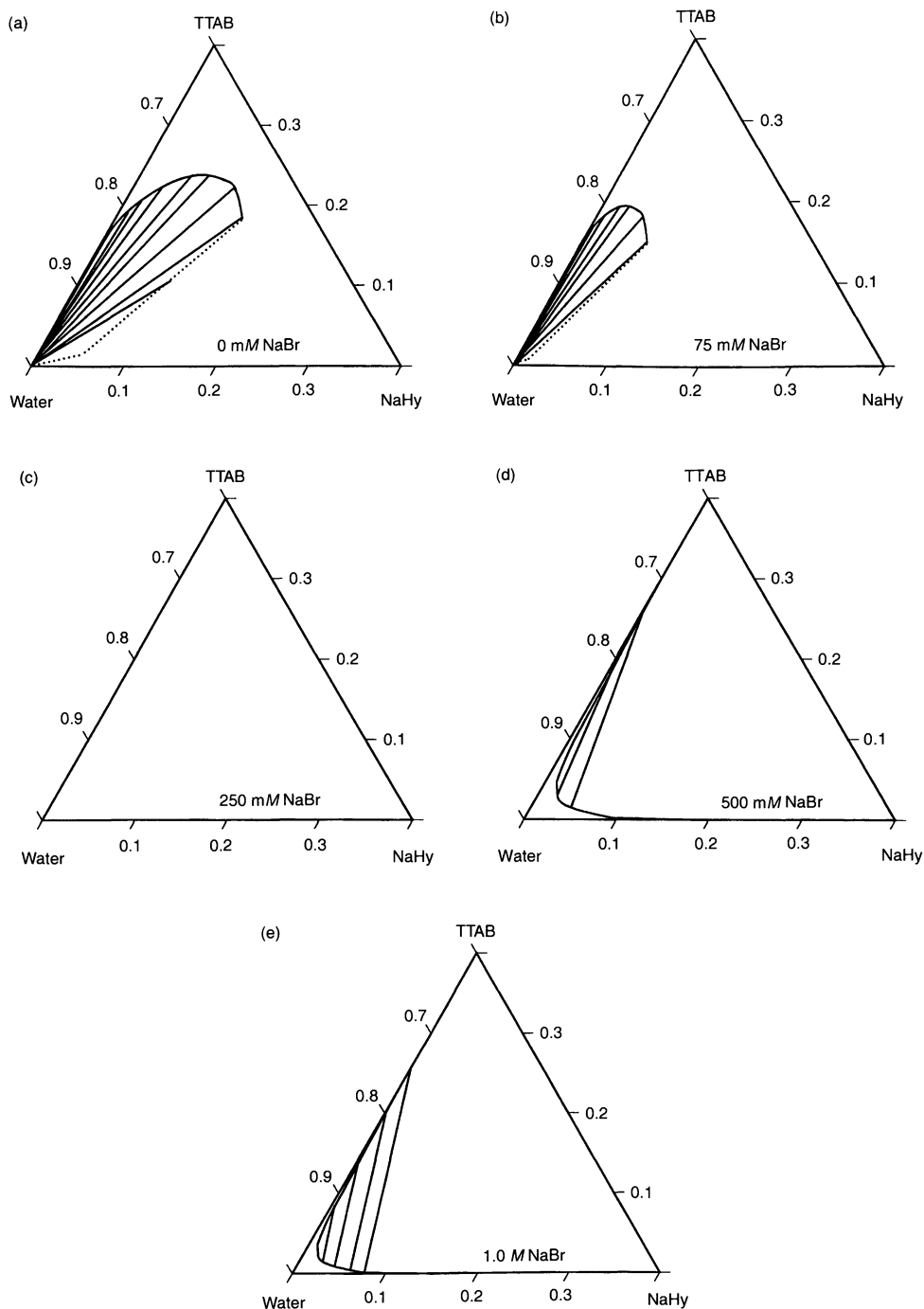


Figure 20.22. Phase separation in mixtures of a polyelectrolyte and an oppositely charged surfactant changes from associative (a,b), to no phase separation (c) and finally to segregative (d,e) as electrolyte is added. This example shows mixtures of a cationic surfactant, tetradecyltrimethylammonium bromide (TTAB), and an anionic polysaccharide, sodium hyaluronate (NaHy). (Redrawn from B. Lindman and K. Thalberg, in *Interactions of Surfactants with Polymers and Proteins* E. D. Goddard and K. P. Ananthapadmanabhan (Eds), CRC Press, Boca Raton, FL, 1993, p. 254)

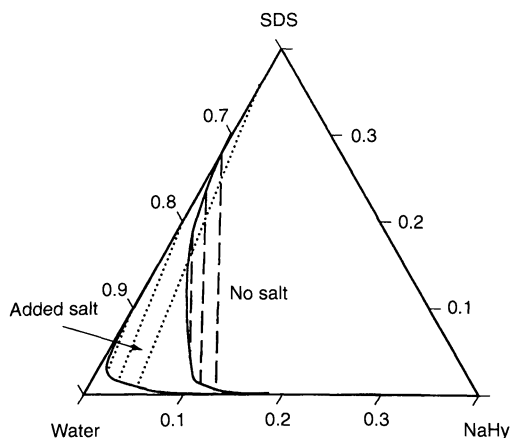


Figure 20.23. Phase separation in mixtures of a polyelectrolyte and a similarly charged surfactant is typically segregative and may be enhanced on salt addition if there is an electrolyte-induced micellar growth. This example refers to mixtures of sodium dodecyl sulfate (SDS) and an anionic polysaccharide, sodium hyaluronate (NaHy). (Redrawn from B. Lindman and K. Thalberg, in *Interactions of Surfactants with Polymers and Proteins* E. D. Goddard and K. P. Ananthapadmanabhan (Eds), CRC Press, Boca Raton, FL, 1993, p. 257)

P^+S^-, P^-S^+	Association without added electrolyte, miscibility at intermediate electrolyte, and segregation at high electrolyte concentration
P^-S^-, P^+S^+	Segregation
P^0S^0	Segregation; association may occur for less polar polymers, especially at higher temperature
P^0S^+, P^0S^-	Phase separation inhibited; association or segregation
P^+S^0, P^-S^0	May be induced by added salt

PS systems are closely analogous to PP systems. The degrees of polymerization of both polymer and surfactant aggregate determine the extent of phase separation. Since the micelle size is not fixed but may vary with the conditions, phase separation will be variable.

The phase behaviour of PS systems is also affected by specific interactions between the two cosolutes, similar to hydrophobic interactions in the case of HM-polymers. This may enhance phase separation for nonionic systems but decrease it for ionics. For a mixture of oppositely charged polymer and surfactant,

the formation of a concentrated phase with charge stoichiometric amounts of polymer and surfactant and a dilute phase containing any excess of either polymer or surfactant becomes unfavourable if the polymer is hydrophobically modified. The reason for this is the tendency of the polymer to associate hydrophobically with the micelles in the concentrated phase. Then, this phase will lose the charge stoichiometry and have a tendency to swell. Therefore, associative phase separation will occur only over a restricted concentration region for a mixture of a hydrophobically modified polyelectrolyte and an oppositely charged surfactant.

Mixing two surfactants, on the other hand, does not give rise to segregative phase separation. The reason in this case is the strong tendency to form mixed aggregates, which gives an important additional contribution to the entropy of mixing. It is common, however, for a mixture of two oppositely charged surfactants to observe an associative phase separation.

8 POLYELECTROLYTE-SURFACTANT SYSTEMS SHOW A COMPLEX BEHAVIOUR

Mixed solutions of a polyelectrolyte and an oppositely charged surfactant show some features that cannot be understood from the triangular representation of a phase diagram. For any system of a solvent and four ionic species, a three-dimensional representation of the phase diagram is needed. The pyramidal version illustrated in Figure 20.24, with water at the top and each of the possible electrolytes at the apices of the base, is very suitable for many purposes. In a simplified ternary representation, we can, with the exception of the conventional mixing plane of surfactant, polyelectrolyte and water, consider the alternative mixing plane of water, simple salt (the two inorganic counterions) and complex salt (polyion and surfactant ion).

A very significant observation, with a number of practical consequences, is that under certain conditions, dilution of a homogeneous solution of polyelectrolyte and surfactant can lead to separation of a concentrated phase enriched in both surfactant and polyelectrolyte; the more water is added, then the more concentrated is the polyion-surfactant phase and consequently there may be transitions from a

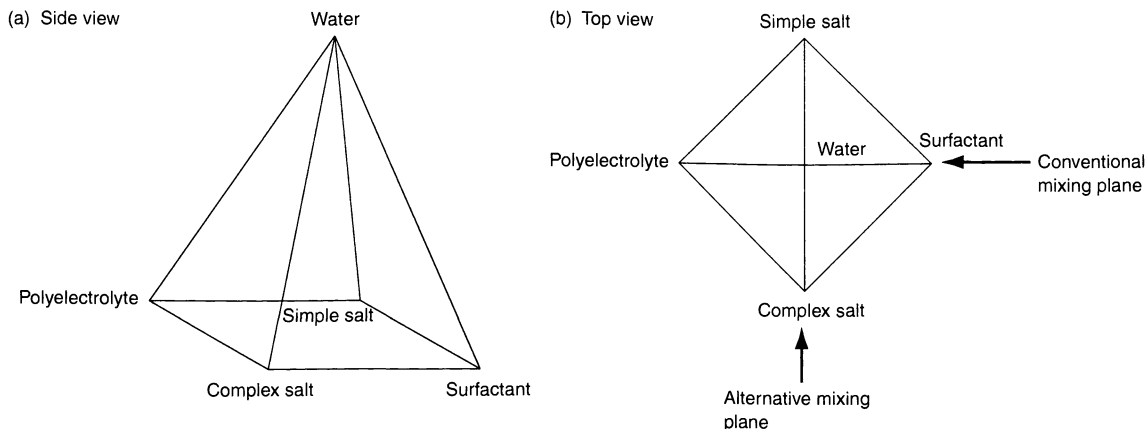


Figure 20.24. A mixed aqueous system of a polyelectrolyte and an oppositely charged surfactant is best represented by using a pyramidal phase diagram, with the four apices of the base corresponding to the four possible electrolytes. Important phenomena are better visualized in the alternative mixing plane than in the conventional mixing plane. (By courtesy of Lennart Piculell)

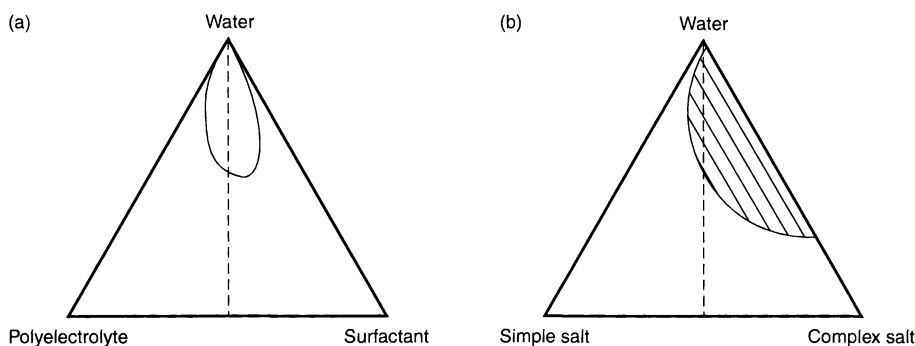


Figure 20.25. Schematic ternary phase diagrams of a mixed aqueous system of a polyelectrolyte and an oppositely charged surfactant in (a) the conventional and (b) alternative mixing planes. In the latter, it can be easily realized how the addition of water to a homogeneous mixed solution can lead to phase separation, with the concentrated phase becoming more and more concentrated as more water is added. (By courtesy of Lennart Piculell)

homogeneous solution to different liquid crystalline phases. This concentration on dilution can be easily understood by viewing the alternative mixing plane (Figure 20.25).

A polyelectrolyte has typically a very extended conformation due to the electrostatic repulsion between the different parts of the chain, as the counterion entropy demands a large volume. This can be dramatically changed on binding of an oppositely charged surfactant. We can illustrate this by using the case of DNA, characterized by a high rigidity and a very high molecular weight. Compaction of DNA from an extended

coil state to a compact globular state is a significant mechanism in promising routes of gene delivery to cells (Figure 20.26). Compaction can be effected by the binding of self-assembling cationic surfactants or lipids, or by positively charged surfaces, such as those of cationic vesicles; decompaction can be accomplished by the use of an anionic amphiphile. Because of its size, DNA compaction can be directly visualized by using fluorescence microscopy (Figure 20.27). An important observation relates to the strongly co-operative surfactant binding, thus leading to the coexistence of both coil and globular states of DNA.

Compaction of DNA

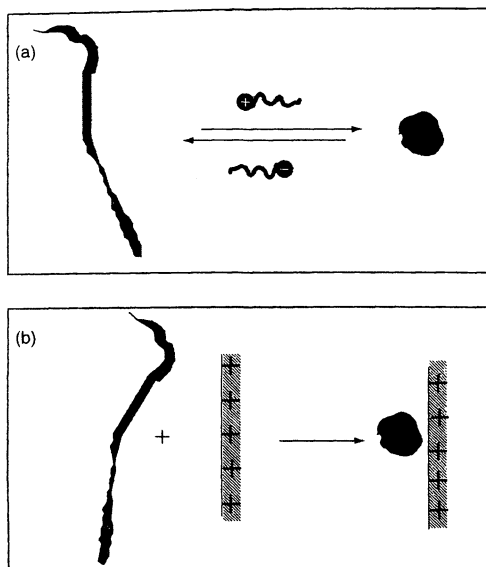


Figure 20.26. Upon the addition of a cationic surfactant the extended conformation of DNA can be transformed into a compact one, (a) while the same effect can also be induced by cationic surfaces (b) Such a compaction can be reversed by the addition of an anionic surfactant. (By courtesy of Maria Miguel)

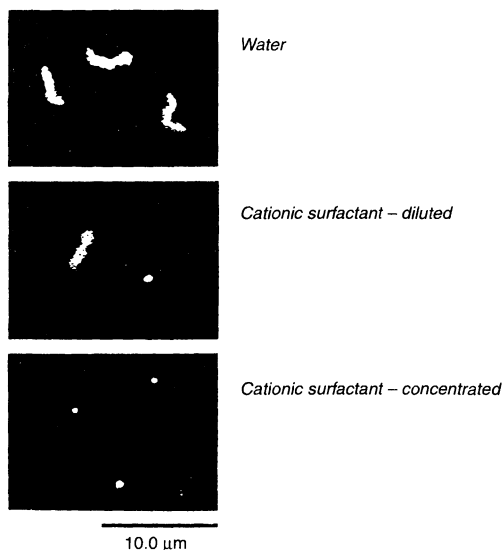


Figure 20.27. The compaction of DNA due to the addition of a cationic surfactant can easily be visualized by the use of fluorescence microscopy. At intermediate surfactant concentrations, there is a coexistence of coils and globules. (By courtesy of Maria Miguel)

9 POLYMERS MAY CHANGE THE PHASE BEHAVIOUR OF INFINITE SURFACTANT SELF-ASSEMBLIES

The larger the surfactant self-assembly aggregate, then the larger will be the tendency for phase separation of any kind. For polymers mixed with infinite surfactant aggregates, as in a bicontinuous microemulsion or a lamellar phase, weak repulsive and attractive interactions will have a profound influence on the phase behaviour. A bicontinuous microemulsion has oil and water domains, which are separated by a monolayer surfactant film, and which are connected over macroscopic distances; the structure is similar to that of the sponge phase, with the surfactant bilayer replaced by a monolayer and every second water channel replaced by an oil channel. In the phase diagram of a surfactant–oil–water system there is (under balanced conditions) a large three-phase region where the bicontinuous microemulsion is in equilibrium with the oil and water phases.

For the case of adding a polymer to a lamellar phase or a bicontinuous phase, where there is no net attraction between polymer and surfactant films, the polymer may enter the narrow water slits or channels only if it has a low molecular weight and a low radius of gyration (Figure 20.28). For a higher molecular weight,

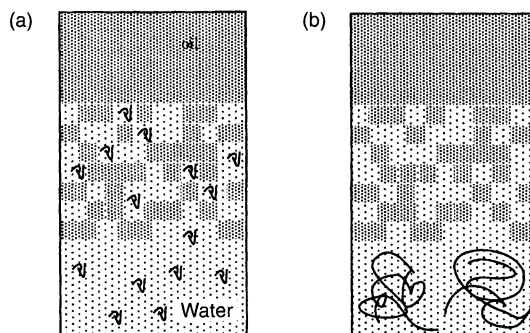


Figure 20.28. On addition of a water-soluble non-associating polymer to a system of a bicontinuous microemulsion in equilibrium with excess water and oil, the distribution of the polymer will be very different for different molecular weights. A low-molecular-weight polymer is soluble in the microemulsion phase (a), whereas coils that are larger than the pore size of the microstructure are insoluble in the microemulsion phase and confined to the excess water phase (b) (or excess oil phase in the case of an oil-soluble polymer). (Redrawn from A. Kabalnov, B. Lindman, U. Olsson, L. Piculell, K. Thuresson and H. Wennerström, *Colloid Polym. Sci.*, **274** (1996) 297)

it will stay outside (Figures 20.29 and 20.30) and thereby destabilize the surfactant phase. However, only a moderate hydrophobic modification of the polymer will induce an association to the surfactant films and increase the stability of the surfactant phase (Figure 20.31).

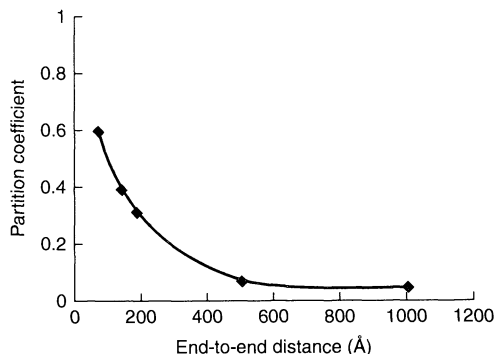


Figure 20.29. Dextran and nonionic surfactants tend to segregate. For a three-phase system of $C_{12}E_5$ microemulsions and dextran, the partitioning of the polymer into the bicontinuous microemulsion phase is high for low molecular weights but very low for high molecular weights. This is illustrated here by plotting the partition coefficient for dextran versus the unperturbed end-to-end distance. This microemulsion has a pore size of ca. 300 Å. (Redrawn from A. Kabalnov, B. Lindman, U. Olsson, L. Piculell, K. Thuresson and H. Wennerström, *Colloid Polym. Sci.*, **274** (1996) 297)

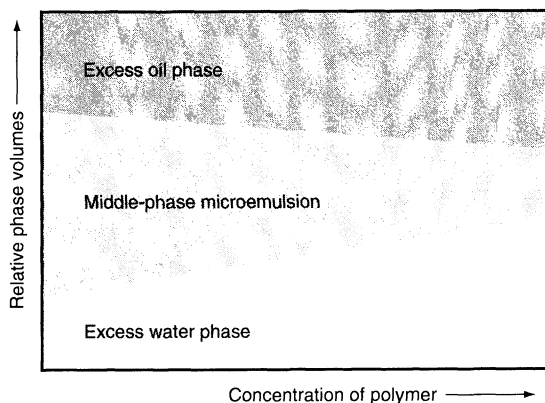


Figure 20.30. The partitioning of high-molecular-weight polymers into the lower aqueous phase of a three-phase system leads to a destabilization and decreased volume of the microemulsion phase. This is illustrated here by a schematic of the relative phase volumes as a function of the polymer concentration. (A corresponding effect is obtained on adding a high-molecular-weight oil-soluble polymer.) (Redrawn from A. Kabalnov, B. Lindman, U. Olsson, L. Piculell, K. Thuresson and H. Wennerström, *Colloid Polym. Sci.*, **274** (1996) 297)

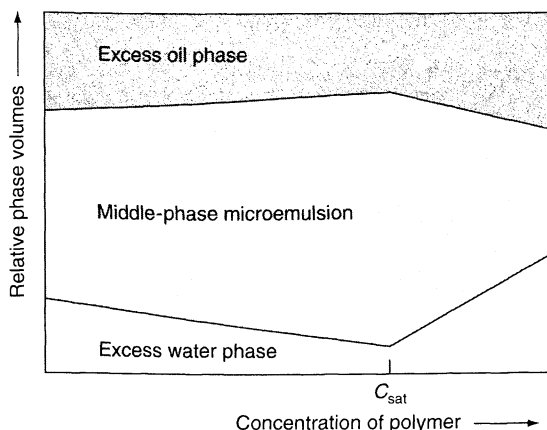


Figure 20.31. While a hydrophilic polymer enriches in the lower aqueous phase of a three-phase system and destabilizes the microemulsion phase, the corresponding hydrophobically modified polymer, which associates to the surfactant films, is incorporated in the microemulsions and stabilizes them. This is illustrated here by a schematic of the relative phase volumes as a function of the polymer concentration. The initial swelling of the middle phase is reversed at higher polymer concentrations when the middle phase has been saturated with polymer (C_{sat}). (Redrawn from A. Kabalnov, B. Lindman, U. Olsson, L. Piculell, K. Thuresson and H. Wennerström, *Colloid Polym. Sci.*, **274** (1996) 297)

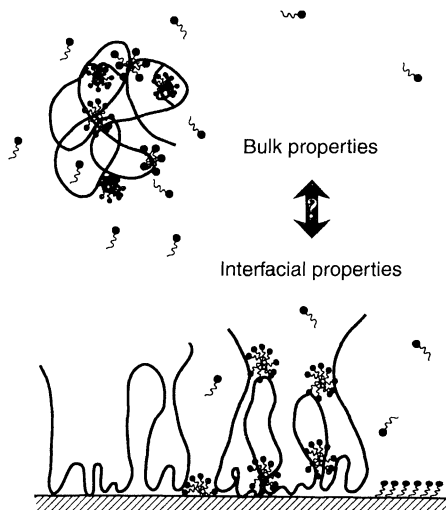


Figure 20.32. The interfacial behaviour of polymer-surfactant mixtures depends on several factors such as the bulk properties of complexes formed, the surfactant association to free and interfacial polymer chains and the affinity of the polymer and the surfactant for the interface. (By courtesy of Fredrik Joabsson)

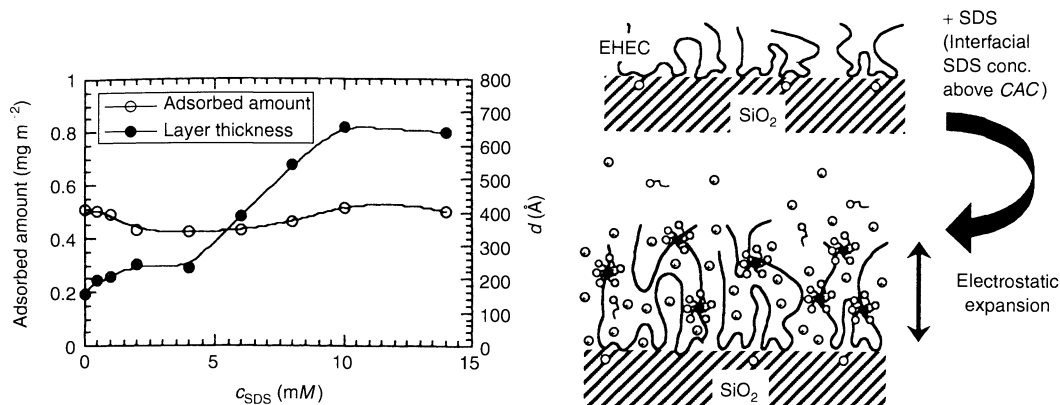


Figure 20.33. The extension of an adsorbed polymer layer can be strongly modified on the association of an ionic surfactant due to electrostatic interactions. On addition of an ionic surfactant (sodium dodecyl sulfate) (SDS) to an adsorbed layer of a nonionic cellulose ether (ethylhydroxyethyl cellulose) (EHEC) there is a dramatic increase in the thickness of the adsorbed layer (filled circles) while there is little change in the total adsorbed amount (open circles). (By courtesy of Fredrik Joabsson)

10 SURFACTANT BINDING STRONGLY AFFECTS ADSORBED POLYMER LAYERS AND THE SWELLING OF CHEMICAL GELS

Adsorption from a mixed polymer–surfactant solution or from surfactant interaction with an adsorbed polymer layer depends on many factors, including the surfactant association to the polymer chains, the interfacial behaviour of the mixed aggregates and the competitive adsorption between polymer and surfactant. As schematized in Figure 20.32, the desorption of a polymer from a surface can be due to a high bulk stability of the polymer–surfactant complex, as well as on a stronger and competitive adsorption of the surfactant. The binding of an ionic surfactant into the adsorbed layer of a nonionic polymer can dramatically change the adsorbed layer. As illustrated in Figure 20.33, there can be a dramatic swelling of the polymer layer due to electrostatic repulsions. This swelling is quite analogous to the effect that ionic surfactants have on the swelling of covalent gels of a nonionic polymer (Figure 20.34).

11 THERE ARE MANY TECHNICAL APPLICATIONS OF POLYMER–SURFACTANT MIXTURES

The use of a polymer and a surfactant in combination may be based on different effects such as controlling the

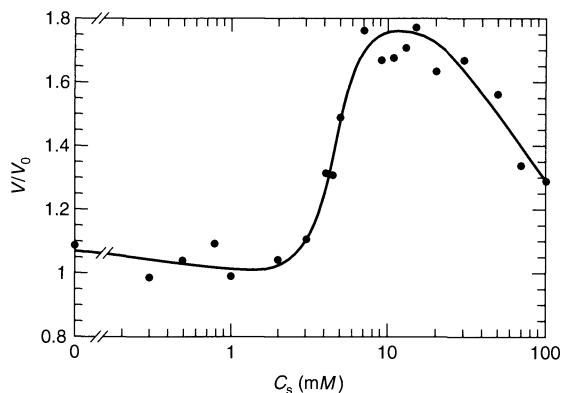


Figure 20.34. Swelling of covalent gels is mainly controlled by electrostatic interactions. Therefore, the binding of an ionic surfactant (exemplified by sodium dodecyl sulfate) into a nonionic polymer gel (cross-linked ethylhydroxyethyl cellulose) leads a large increase in the gel volume. Gel swelling starts in the vicinity of the CAC, where also the swelling of an adsorbed polymer layer takes place. (Redrawn from O. Rosén and L. Piculell, *Polym. Gels Networks*, **5** (1997) 185)

phase behaviour, controlling the interfacial properties or controlling the formation of networks due to association. The most important and well understood use of polymers and surfactants together is to achieve a suitable rheology, i. e. thickening and gelation effects. It is also possible to design systems, based on hydrophobically modified water-soluble polymers or homopolymers,

which respond to different external factors. One example of a responsive system is gelation which is induced on temperature increase.

Phase behaviour effects include the solubilization of water-insoluble polymers. One example is the depression of clouding (increase of cloud point) of a polymer solution, achieved by the addition of an ionic surfactant.

The polymer-induced micellization leads to a lowering of the surfactant unimer concentration and activity. This can be significant for the elimination of skin irritation caused by the surfactant.

The interfacial behaviour of surfactant-polymer mixtures, utilized for example in the stabilization of suspensions, depends on a complex interplay between different pair interactions. Addition of a polymer can either remove surfactant from a surface or enhance its adsorption, and vice versa, depending on the relative stability of the polymer-surfactant complexes in solution and at the interface.

12 BIBLIOGRAPHY

1. Goddard, E. D. and Ananthapadmanabhan, K. P., *Interactions of Surfactants with Polymers and Proteins*, CRC Press, Boca Raton, FL, 1993.
2. Hayakawa, K. and Kwak, J.C.T., Interaction between polymers and cationic surfactants, in *Cationic Surfactants: Physical Chemistry*, Rubingh, D. and Holland, P. M., (Eds), Marcel Dekker, New York, 1991, pp. 189-248.
3. Kabalnov, A., Lindman, B., Olsson, U., Piculell, L., Thuresson, K. and Wennerström, H., Microemulsions in amphiphilic and polymer-surfactant systems, *Colloid Polym. Sci.*, **274**, 297-308 (1996).
4. Kwak, J. C. T. (Ed.), *Polymer-Surfactants Systems*, Marcel Dekker, New York, 1998.
5. Piculell, L. and Lindman, B., Association and segregation in aqueous polymer/polymer, polymer/surfactant, and surfactant/surfactant mixtures: Similarities and differences, *Adv. Colloid Interface Sci.*, **41**, 149-178 (1992).
6. Piculell, L., Guillemet, F., Thuresson, K., Shubin, V. and Ericsson, O., Binding of surfactants to hydrophobically modified polymers, *Adv. Colloid Interface Sci.*, **63**, 1 (1996).

CHAPTER 21

Surfactant Liquid Crystals

Syed Hassan, William Rowe and Gordon J. T. Tiddy

UMIST, Manchester, UK

1	Introduction	465	8	Block Copolymer Nonionic Surfactants	491
2	Liquid Crystals	466	9	Zwitterionic Surfactants	493
3	Surfactant Solutions: Micelles	467	10	Ionic Surfactants	493
4	Liquid Crystal Structures	472	11	The Influence of Third Components: Cosurfactants, Mixed Surfactants, Oils, Hydrotropes, Electrolytes and Alternative Solvents	497
4.1	Lamellar phase (L_α)	472	11.1	Cosurfactants	497
4.2	Hexagonal phases (H_1 , H_2)	473	11.2	Mixed surfactants	498
4.3	Cubic phases	473	11.3	Oils	499
4.4	Nematic phases	475	11.4	Hydrotropes	500
4.5	Gel phases (L_β)	476	11.5	Electrolytes	500
4.6	Intermediate phases	477	11.6	Alternative solvents	501
5	Origins of the Formation of Surfactant Liquid Crystals – Water-Continuous Phases	479	12	Conclusions and the Future	502
6	Origins of the Formation of Surfactant Liquid Crystals – Reversed Phases	480	13	References	504
7	Phase Behaviour of Nonionic Surfactants	480			

1 INTRODUCTION

Surfactants have been used for over 1000 years in everyday applications, for example as emulsifiers in cleaning and in foods. They occur widely in nature, where as a *bilayer* they constitute a vital structural unit of biological membranes. Their functionality derives from the molecular structure, with a polar (hydrophilic) head-group, which conveys water-solubility, being attached to a non-polar (hydrophobic) tail, which drives the formation of self-assembled aggregates (micelles). Other chapters in this volume detail the wide variety of chemical structures that can form the polar groups (ionic, nonionic, zwitterionic, etc.) and tail structures.

The latter are limited to hydrocarbon, perfluorocarbon and polydimethylsiloxane chains. While the formation of micelles is well known, surfactants also form a wide variety of liquid crystalline phases in water which are much less familiar. Almost all surfactants that form micelles also form liquid crystals, while many do not form micelles but *do* form liquid crystals. Thus, liquid crystal formation by surfactants is more widespread than micelle formation. Indeed, an understanding and knowledge of liquid crystals can provide a comprehensive guide to the application of surfactants. This is because the size and shape of the surfactant molecules determine the structure of the self-assembled aggregates, which in turn, controls the liquid crystal

structures. The adsorption of surfactants at surfaces and interfaces, which determines surface/interfacial properties, also depends on the same factors, and hence all of these are closely related.

This review sets out to give a general description of such liquid crystal structures, and how these relate to surfactant chemical structures. Our objective is to enable the reader to control the liquid crystal properties for practical applications by selection of suitable single or mixed surfactants, also in the presence of other components such as polymers, electrolytes, organic constituents ("actives", flavours, perfumes, etc.). This is not a comprehensive review of all of the research being carried out on surfactant liquid crystals. The selection of references here is obviously idiosyncratic and opportunistic. However, this article does cover the main aspects of the subject, and indicates areas of weakness which require attention. We commence with a brief introduction to liquid crystals in general. Then, we will give a summary of the behaviour of micellar solutions because micelles can be regarded as the building blocks of surfactant liquid crystals that occur at still higher concentrations. Sections describing the various liquid crystal phases, the way that the mesophase type varies with surfactant chemical structure, and what happens with mixed surfactants follow this. We also include the effects of additives such as electrolytes and other solutes. Because of the enormous number of publications in this area, space considerations, and the limited time of the authors, it simply is not possible to document all of the available information here. While we make, in passing, some reference to experimental techniques, these are dealt with more fully in the chapter by Hyde (Chapter 39). Instead, it is our intention to give an introduction to the concepts and phenomena that underlie the formation of surfactant mesophases and to summarize the present knowledge of the area. As well as an up-to-date description, our objective is to provide sufficient information so that anyone with a practical problem concerning mesophase formation or structure can see the general context. This should allow them to find some indication of steps that may provide a solution. The article follows very closely, and relies heavily on, a contribution produced previously (1) for the "*Handbook of Liquid Crystals*", but is somewhat more up-to-date, and (we hope) contains fewer errors!

As a further comment, we draw attention to several books (2–13) which provide a good general introduction to the area of surfactants and colloid science. Most of the books have been published in the last few years and summarize recent research.

2 LIQUID CRYSTALS

For a pure substance we are familiar with three distinct states which change from one to another at a *first-order* phase transition, for example on heating: *crystal* \rightarrow *liquid* \rightarrow *gas*. These are all single-phase states, and their equilibrium with other phases is described by the Gibbs phase rule. In addition to these, there are various phase states with properties intermediate between liquids and crystals – unimaginatively termed liquid crystals or mesophases (the latter is often employed to describe some ill-defined "pasty", turbid gel, although we employ the word here as an alternative to liquid crystal!). Crystals have long-range order, with the molecules being rigid and located in precise, regular, repeating patterns, over dimensions of ten thousand molecular diameters or more. Liquids usually have very rapid molecular motion (rotation times of ca. 10^{-11} s) and are disordered, with molecular positions being almost random except for some loose correlation between neighbours. Crystals can support other objects without significant deformation, while liquids deform and flow under an applied stress. Liquid crystals have the properties of both types. There is some long-range order, and the molecules have molecular motion, usually anisotropic. Their rheological properties vary between a resemblance to "pig's excrement", and that of "gnat's urine"! While textbooks refer to liquid crystals as the fourth state of matter, in fact there are dozens of different liquid crystalline states, all with different degrees of molecular mobility and order. The overwhelming majority are separated from other phase states by a first-order phase transition. The transition *crystal* \rightarrow *liquid* on heating is accompanied by an endothermic transition enthalpy, reflecting the increase in molecular disorder (increased entropy) of the higher temperature state. Similarly, transitions to or from liquid phases involve enthalpy changes, but because the difference in molecular disorder is often small, the enthalpy changes are typically only ca. 10% (or less) of those normally encountered at a melting point.

Crystalline solids can be transformed into a liquid state either by increasing the temperature to the melting point or by dissolution in a solvent. Liquid crystals can be produced similarly, either on heating or dissolution. Those produced on heating are termed *thermotropic*, while those produced with a solvent are termed *lyotropic*. The former are usually organic compounds with a rigid polyaromatic moiety attached to a flexible alkyl chain. The liquid crystal order arises from the anisotropic molecular shape and a short-range, anisotropic intermolecular attraction. The latter generally occur with solutes where the solution species

(molecules or aggregates) have a much larger molecular size than the solvent, and the liquid crystal order arises from the repulsive interactions between solute entities at high concentration. The free energy change arising from the loss of entropy in forming an “ordered solution” (a liquid crystal) is less than the gain in free energy from dissolution of more solute. One immediate consequence of this is that lyotropic mesophases form more readily with pure, monodisperse solutes than with polydisperse materials. *Lyotropic* liquid crystals form frequently with polymers, particularly biological macromolecules. Protein crystals, formed by macromolecules having a narrow range of configurations and with no size or composition polydispersity, together with their requirement for the presence of typically 50% water (by volume), are a classic example of this. Rigid, high-molar-mass polymers, synthetic or natural, frequently form mesophases where the molecules are aligned parallel to each other. Surfactant monomers in solution are usually not large or rigid enough to give mesomorphic states, although the micelles are. Their mesophases are the subject of this review. Another class of materials that form multimolecular aggregates which then become ordered lyotropic liquid crystals at higher concentrations is comprised of polyaromatic compounds with polar substituents (14, 15). These self-associate through attractive intermolecular dispersion forces (π -stacking), *not* the hydrophobic effect. Once the aggregates have formed, their mesophases (termed *chromonic*) show a similar general behaviour to those of surfactants.

The occurrence of lyotropic liquid crystalline phases is usually documented with the aid of a phase diagram, numerous examples of which are given in this review. Phase diagrams are simply a “map” showing the physical state for a particular range of constituents over some variation of composition, temperature and/or pressure. Each separate phase is represented as an area on this map. The relationships between the various phases, particularly the transitions between them and the number of phases that can co-exist *at equilibrium*, are given by the Gibbs phase rule as follows:

$$P + F = C + 2 \quad (21.1)$$

where P is the number of phases, F the number of degrees of freedom and C the number of components. A knowledge of the phase rule is an invaluable asset in any attempt to investigate the behaviour of lyotropic mesophase systems, and indeed, for general investigations of any multi-component surfactant/polymer/additive... mixture. Non-equilibrium states can be recognized from discrepancies between observations and the number of phases allowed by

the phase rule. Much more frequently, such discrepancies suggest that the original data require re-evaluation. A good illustration of this is given in the review of phospholipid liquid crystals by Chernik (16), and the more general description of surfactants by Laughlin (4). It is extremely time-consuming and difficult to construct phase diagrams showing all aspects of the phase behaviour in consistency with the phase rule where multiple liquid crystals are present. Equilibrium phase states, particularly the compositions, are often very slow to form. Most authors concentrate on particular parts of the mesophase regions. Many of the diagrams presented here are not strictly consistent with the phase rule because the multiple phase regions are not shown, particularly when these are small. One of us (GJTT) suggests that *those without sin cast the first stone*.

3 SURFACTANT SOLUTIONS: MICELLES

Only a brief summary is given here, since other chapters in this volume discuss this in detail. When surfactants dissolve in water at low concentrations, they exist as monomers (ionic surfactants are dissociated). As the concentration is increased, aggregates termed *micelles* are formed. These appear at a well-defined concentration known as the “critical micelle concentration” (CMC). This is *not* a critical point in the sense of modern physics since micelle formation occurs over a *very narrow range* of concentrations. This range is so small that for almost all practical purposes it can be represented by a specific value, i.e. the CMC. For pure single surfactants below the CMC, all of the dissolved surfactant exists as monomers, while above the CMC all added surfactant forms micelles. With surfactant mixtures the phenomena is more complex because the components usually have different individual CMCs, but the same considerations apply (3).

Micelles are aggregates of at least 15–20 monomers, usually more. Typical surfactants such as sodium dodecyl sulfate (SDS) or octaethyleneglycoldodecyl ether ($C_{12}EO_8$) form micelles with aggregation numbers (q) in the range of about 50–100 or so, with the exact number varying with the temperature and concentration. The aggregation numbers can become very large – up to 10^4 or more, according to surfactant type, aggregate shape, temperature and surfactant concentration (see below).

Micelle formation arises from the *hydrophobic effect* (5, 17–21). This is the term used to describe the interaction between *non-polar* solutes and water. It is well known that non-polar solutes are almost insoluble

in water, with the limited degree of solubility decreasing rapidly with increasing solute size. A thermodynamic analysis of the process shows that the introduction of a hydrocarbon into water at ambient temperature is always associated with a decrease of entropy, and an enthalpy of about zero, thus resulting in a large and positive free energy (18–22). “Structuring” of water molecules in the neighbourhood of the alkane, akin to the formation of clathrate hydrates (23), is frequently cited as the origin of the entropy change. Unfortunately, attempts to locate the “clathrate structure”, for example, by self-diffusion measurements of water and organic solutes such as tetra-alkylammonium ions (24), have consistently failed to show that more than a single layer of water around the solute differs from bulk water – hardly evidence to support the “water structure” concept.

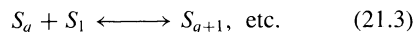
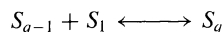
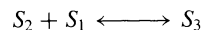
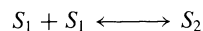
In a series of recent papers Kronberg and co-workers (18–20) have discussed this problem in detail. These authors view the hydrophobic effect as the result of two contributions, with one arising from the “ordering” of water molecules around the solute, and the second from the energy required to make a cavity in water large enough to accommodate the non-polar solute. The first contribution is associated with a negative entropy because ‘vicinal’ water molecules (next to a non-polar solute) have fewer conformations available than “free” water – they can not hydrogen bond to the solute. It also gives a negative enthalpy, presumably because ‘vicinal’ water molecules make stronger hydrogen bonds. The second and opposite contribution arises from the large energy required to form a cavity to accommodate the solute. This is large, due both to the high cohesion in water arising from hydrogen-bonding connectivity, and the small size of water molecules compared to, e.g. alkanes. An important consequence of this mechanism is that the magnitude of the hydrophobic effect is proportional to the AREA of hydrophobic contact between water and the solute. As will be seen below, by using this concept it is possible to estimate an approximate CMC for almost any novel surfactant, given that a few simple guidelines are followed.

Micelles can only form when the surfactant solubility is equal to or greater than the CMC. In general, this occurs only above a particular temperature known as the “Krafft point” (temperature). Below this temperature, the surfactant solubility increases slowly with increasing temperature because the surfactant dissolves as monomers. The limit to monomer solubility occurs when the chemical potential of the monomers is equal to that of the pure (usually crystalline) surfactant. Above this temperature, the solubility increases VERY rapidly

because the surfactant dissolves as micelles – the contribution of each micelle to the surfactant chemical potential being the same as that of a monomer. Micelle formation involves a dynamic equilibrium between monomers and aggregates, represented by the following equation (25–29):



where S_n represents an aggregate of n monomers. In fact, micelles form by a series of step-wise reactions from monomers, follows:



Clearly, there is a range of aggregate sizes present in solution, with an average value of q . However, the size distribution is usually narrow (say $\pm 10\%$), particularly for globular micelles. Although the micelle formation process involves dimers, trimers, etc., the actual concentration of these species is very, very small. Hence, once formed, micelles have a reasonably large, but finite, lifetime. For dilute solutions, using fast relaxation techniques, such as stopped flow, pressure/temperature jump and ultrasound relaxation (2), it is possible to measure both the exchange rate between monomers and micelles, and the rate of micelle formation/breakdown. Both of these processes are related to the CMC, becoming faster as the CMC increases. Typically, the monomer–micelle exchange rate is in the range 10^3 – 10^6 s^{-1} , while micelle breakdown/formation rates are ca. 10^{-1} – 10^2 s^{-1} (i.e. micelle lifetimes of 10^{-2} – 10 s). Note that from the kinetic analysis of fast relaxation studies an upper limit of $< 10^{-10}$ mol dm^{-3} can be placed on the concentration of dimers, trimers, etc. (i.e. aggregates with radii r much smaller than q) (28, 29). Figure 21.1 shows a schematic representation of a small globular micelle. The rapid, continuous exchange of monomers with bulk solution means that the micelle is a very mobile, disordered, aggregate. There is a continuous movement of molecules jumping part way in and out of the interface³⁰ (this has recently been termed “protrusion” (31, 32). In addition, diffusion around the micelle surface is rapid (self-diffusion coefficient (D) $\simeq 10^{-10}$ $\text{m}^2 \text{s}^{-1}$), as is the exchange between the various possible conformations of the alkyl chain (correlation time (τ_c) $\simeq 10^{-9}$ – 10^{-10} s). With an ionic surfactant, typically about 70–80% of counterions reside close (within ca. 10 \AA) to the micelle

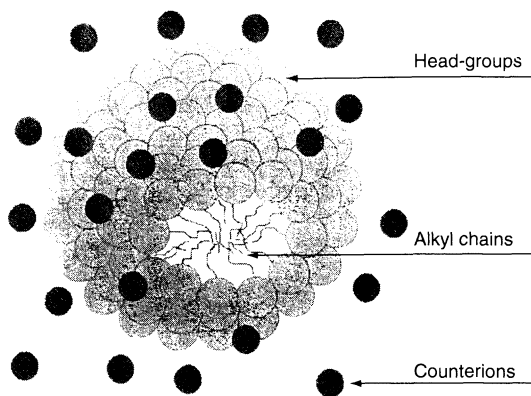


Figure 21.1. Schematic representation of micelles formed by ionic surfactants. Note that this is a “locally disordered” aggregate with almost free molecular mobility. The interior resembles a liquid hydrocarbon. About 70–80% of counterions reside close to the charged micelle surface (within ca. 2 nm). The micelle surface is rough, to at least ca. 0.2–0.3 nm

surface in a loosely “bound” state due to the very high surface charge density. The exchange between “bound” and free counterions occurs on a time scale of ca. 10^{-9} s. There also exists a single layer of “bound” water molecules associated with polar groups and ions. Again, the exchange between bound and free water occurs on a time-scale of 10^{-9} s(33).

We have discussed the formation of micelles at a “critical micelle concentration”, and the absence of significant concentrations of small aggregates. In fact, micelle formation occurs over a very narrow *range* of concentrations, with this *range* being too narrow to detect for all but the shortest chain (highest CMC) surfactants. The almost complete absence of small aggregates at concentrations above the CMC makes their occurrence *below* this highly unlikely. There are numerous claims in the literature of “pre-CMC” surfactant aggregates formed due to a contribution from the hydrophobic effect. To date, none of these have withstood a thorough examination of the evidence. Usually, the deviations from expected behaviour are due to the presence of impurities. Penfold and co-workers (34) have given a good illustration of how minor constituents can influence surfactant properties. Their recent study demonstrates (34) that doubts concerning the application of the Gibbs adsorption equation apply to the *systems* (i.e. the presence of impurities, which should be included in the equation) rather than the *thermodynamics*! In some cases, the impurities can cause the precipitation of a minor fraction of a liquid crystalline phase (see below) below the real CMC of the surfactant.

Arguably the most important parameter for any surfactant is the CMC value. This is because below this concentration the monomer level increases as more is dissolved, and hence the surfactant chemical potential (activity) also increases. Above the CMC, the monomer concentration and surfactant chemical potential are approximately constant, so surfactant absorption at interfaces and interfacial tensions show only small changes with composition under most conditions. For liquid crystal researchers, the CMC is the concentration at which the building blocks (micelles) of soluble surfactant mesophases appear. Moreover, with partially soluble surfactants it is the lowest concentration at which a liquid crystal dispersion in water appears. Fortunately there are well-established simple rules which describe how CMC values vary with chain length for linear, monoalkyl surfactants. From these, and a library of measured CMC values (35–38), it is possible to estimate the approximate CMC for branched alkyl chain and di- (or multi-) alkyl surfactants. Thus, most materials are covered. This includes the “gemini” surfactants, a “new” *fashionable* group where two conventional surfactant molecules are linked by a hydrophobic spacer of variable length (38).

The hydrophobic effect provides the major determinant of the CMC; its contribution is proportional to the area (a_h) of the non-polar chain removed from exposure to water when micelles form (see above) (18–20). (The hydrophobic contribution is given by a term in γa_h , where γ = oil/water interfacial tension.) This leads to a logarithmic relationship between the CMC and alkyl chain length for linear surfactants, as follows:

$$\log c_{mc} = An + B \quad (21.4)$$

where n is the alkyl chain number, and A and B are constants.

The second factor is the valency (s) of the head-group charge ($s = 0, 1, 2, \dots$, etc. for nonionic/zwitterionic, mono-ionic, di-ionic \dots , etc. species). According to the value of s , the constant A takes the values: $A = 0.5$ ($s = 0$), $A = 0.3$ ($s = 1$), and $A = 0.15\text{--}0.18$ ($s = 2$). Finally, the valency of the counterions is also important as this influences the value of B . Essentially, the CMC is reduced for multivalent counterions because fewer ions are required close to the micelle surface to (partially) balance the high surface charge density.

Lists of CMC values for various surfactants are given elsewhere in this volume (see Chapter 19). While there is some temperature-dependence of the CMC (17–20), with many materials showing a shallow minimum, the effect is small below 100°C. Equation (21.4) shows that for nonionic and zwitterionic surfactants the CMC

reduces by about a factor of 10 for the addition of two CH_2 groups to the alkyl chain, while for monovalent ionic surfactants the corresponding factor is 4. Branched and multi-chain surfactants can be treated by estimating the equivalent linear chain having the same area of hydrophobic contact with water. There is a free energy penalty for constraining the conformations of multi-chain surfactants at the micelle surface (39, 40) which leads to a higher than expected CMC. This effect is small – equivalent to the loss of ca. one CH_2 group (40).

For surfactants with other types of hydrophobic groups, the CMC values are less readily available because far fewer measurements have been made, especially on pure compounds. However, the oil/water interfacial tensions are 56 and 46 dyn/cm for fluorocarbon and polydimethylsiloxane oils respectively, compared to the value of 52 dyn/cm for hydrocarbon/water. Hence from the sizes of the hydrophobic groups (see Table 21.1 below), the magnitude of the hydrophobic effect, and hence their CMCs can be estimated. This clearly shows that the well-known lower CMCs for fluorocarbon surfactants compared to normal derivatives arise from the much larger size of fluorocarbons, rather than any magic structuring of water!

With mixed surfactants, the CMC of the mixed micelle varies according to the CMCs of the individual surfactants, and their proportions. Clearly, micelle composition varies with concentration since the micelles that form at lowest concentration are rich in the lowest-CMC surfactant, while the higher-CMC materials become more abundant in micelles as the overall concentration is increased. The detailed dependence of CMC values on mixed surfactant composition varies according to whether there are specific interactions between head-groups which lead to non-ideal mixing in the micelle. This applies particularly with mixtures of nonionic and ionic surfactants, and ionic surfactants of opposite charge. Various treatments are available to describe the behaviour (see Chapter 19), for example, as outlined in the text by Clint (3) (Chapters 5 and 6).

Given that micelles are present in solution above the CMC, the most important consideration for the liquid crystal phases is the micelle shape. There are three major types, namely spheres, rods and “discs”. They can be described by using the *packing constraint* concepts (5, 41, 42). These give a simple description of the relationship between micelle shape and molecular shape. The micelles are assumed to be smooth, with only the hydrophobic volume in the micelle interior. The main molecular parameters are the hydrophobic group volume, usually taken as being equal to the alkyl chain volume (v), the area that the molecule occupies at the

micelle surface (a) and the maximum length of the alkyl chain (taken as the all-*trans* length, l_t). For a spherical micelle having a hydrophobic volume (V) with radius r , a total surface area A and aggregation number q , we have the following relationships:

$$A = qa = 4\pi r^2$$

$$V = qv = \frac{4}{3}\pi r^3$$

and hence:

$$a = 3\frac{v}{r} \quad (21.5)$$

Ignoring end or edge effects for circular cylinders (radius = r) and bilayer/disc (thickness = $2r$) shapes, the equivalent relationship are as follows:

$$a = 2\frac{v}{r} \quad (\text{rod}) \quad (21.6)$$

$$a = \frac{v}{r} \quad (\text{disc}) \quad (21.7)$$

The value of r can not be larger than l_t , and hence there are limitations on the lowest value of a for a given shape:

$$a \geq 3\frac{v}{l_t} \quad (\text{sphere}); \quad a \geq 2\frac{v}{l_t} \quad (\text{rod}); \quad a \geq \frac{v}{l_t} \quad (\text{disc}) \quad (21.8)$$

Clearly, a surfactant with a given chain length can pack into spheres, rods or discs, according to the size of the head-group, with all three shapes being possible for the largest a values and only disc micelles for small a values. Entropy favours the formation of the smallest possible aggregate at the CMC – i.e. spheres over rods and rods over discs. The present authors are not aware of any exceptions to this generalization. Thus, large head-group surfactants form spherical micelles, smaller head-groups give rods, and still smaller head-groups give discs. (Because of the flexibility of alkyl chains there does not appear to be a lower limit on the values of r for conventional surfactants, and hence the maximum values for a are not known.)

It is a simple matter to estimate the volumes of hydrophobic groups from published density data for alkanes (normal and fluorinated) and polydimethylsiloxanes (5, 6, 43). One simply sums the group volumes (see Table 21.1). Similarly, the maximum length of the hydrophobic group can be calculated from known bond lengths. Thus, the maximum micelle radius and hence the limiting a values for the various aggregates can be calculated. Note that there are small differences between the parameters of Table 21.1 and those of other authors (5–7). These are unimportant since they result only in small differences in the calculated limits of the

Table 21.1. Molecular sizes of various hydrophobic groups (at 25°C)

Hydrophobic group	Fragment volumes (Å ³)			Bond length (Å)	
	$V(\text{CH}_3)$	$V(\text{CH}_2)$	$V(\text{CH})$	$L(\text{C}-\text{C}-\text{C})$	$L(\text{CH}_3)$
Alkane	54.2	27.0	~ 0	2.54	2.3
Fluorocarbon	$V(\text{CF}_3)$ 92.5	$V(\text{CF}_2)$ 36.0	–	$L(\text{C}-\text{C}-\text{C})$ 2.54	$L(\text{CF}_3)$ 2.8
Polydimethylsiloxane	$V \begin{pmatrix} \text{Me} \\ \\ \text{O}-\text{Si} \\ \\ \text{Me} \end{pmatrix}$	–	–	$L \begin{pmatrix} \text{Me} \\ \\ \text{O}-\text{Si} \\ \\ \text{Me} \end{pmatrix}$	–
	123	–	–	2.4	–
Hydrophobic group	Limiting a values (Å ²)				
	Sphere	Rod	Disc		
Alkane	68	46	23		
Fluorocarbon	102	68	34		
Polydimethylsiloxane	~ 160	~ 106	~ 53		

a values. Moreover, we recall the known roughness of the micelle surface (typically 2–3 Å), and hence we emphasize that this model gives only an approximate description.

An important consequence of the above model is that a simple increase in alkyl chain length should *not* alter the micelle shape because both chain length and volume increase by a constant increment. However, in practice it is often observed that short chain (e.g. C₁₂) surfactants form globular (“spherical”) micelles while higher-chain-length materials with the same head-group form long rod micelles. This probably arises from the influence of surface roughness on micelle shape and aggregation numbers.

Micelle size (aggregation number) varies according to the micelle shape and alkyl chain length. Spherical micelles always have low aggregation numbers, due to the micelle radius being limited by the all-*trans* alkyl chain length, and hence the surface area is limited. For rod and disc micelles, where the fraction of “end” or “edge” molecules plays a significant part in micelle size, it is useful to consider a thermodynamic description employed by Israelachvili and co-workers (7, 41, 42). In a solution of aggregates with a range of aggregation numbers at equilibrium, the chemical potential (μ) of all identical molecules is the same, whatever the aggregation number, as follows:

$$\mu_n = \mu_n^0 + \frac{kT}{n} \log \frac{X_n}{n} = \text{constant}, \quad n = 1, 2, 3, \dots, \text{etc.} \quad (21.9)$$

where μ_n is the mean chemical potential of a molecule in aggregates of aggregation number n , μ_n^0 is the standard

part of the chemical potential (i.e. the mean interaction-free energy per molecule) and X_n the concentration of molecules for the n -aggregates. Taking simple models for the interaction free energy within aggregates of various shapes, it can be shown that:

$$\mu_n^0 = \mu_{\text{infinity}}^0 + \frac{\alpha kT}{n^p} \quad (2.10)$$

where p takes the value 1/3, 1/2 or 1 for spheres, discs or rods, respectively. The monomer–monomer bond energy within an aggregate is described by αkT . Above the CMC, with $\alpha > 1$ (a reasonable assumption) and $p < 1$ (i.e. for spheres and discs), this approach leads to expressions which predict vanishingly low concentrations of aggregates having n values which are not small (say $n > 10$ –20). Thus, spherical and disc micelles remain small – or increase to “infinite” aggregation numbers – i.e. they phase-separate. Only rod micelles can have large aggregation numbers ($n > \text{ca. } 100$). In practice, this does appear to be generally true. In any case, we have already seen that spherical micelles are prevented from becoming large by the alkyl chain packing constraints. Hence, the major conclusion of this approach is that disc micelles either remain small – or grow to infinite size to form a lamellar liquid crystalline phase (see below).

In real surfactant systems, the interactions are much more complex than the simple picture used above. However, the general formalism still holds – but observed aggregation numbers for small micelles are often larger than expected for spheres, thus indicating globular shapes, while the micelles do *not* grow very large as is expected for rods. This is almost certainly due to micelle

surface roughness. A surface roughness of 1–2 C–C bonds allows the micelle radius to be slightly larger than the all-*trans* chain length – with a significant increase in n . The roughness also allows repulsive interactions between adjacent head-groups to be relaxed by the formation of a thick interfacial layer rather than a smooth surface. In addition, shape fluctuations can occur, which can also lead to aggregation numbers larger than those expected for spheres. However, if the alkyl chain length is long enough, the micelles that do have a rod shape become very long – up to $> 1000 \text{ \AA}$. This is not usually seen for common ionic surfactants because the longer chain homologues have high Krafft temperatures, and hence they are insoluble at normal temperatures.

4 LIQUID CRYSTAL STRUCTURES

There are six classes of liquid crystal phases, most of which now have well-established structures. These are the lamellar, hexagonal, cubic, nematic, gel and intermediate phases. All except the intermediate phases have been recognized for many years, and hence a *comprehensive* literature review is outside the scope of this present article. In all of the states except the gel phases, both surfactant and water have a liquid-like molecular mobility – i.e. short-range rotational and translational diffusion on a time-scale of 10^{-12} s . They differ in the long-range symmetry of the surfactant aggregates and in the curvature of the micelle surface. Except for the phases with flat aggregate surfaces, each class can occur with either the polar regions or the non-polar regions as the continuous medium, with the former being referred to as *normal*, while the latter are *reversed*. As will be seen later, the phases occurs in a particular composition sequence, thus occupying a specific region of the phase diagram. Each class of mesophases is usually labelled by a particular letter (see below) with the symbols having subscripts of “1” or “2” to distinguish between the *normal* or *reversed* forms. Unfortunately, there is no universally accepted nomenclature as is the case with thermotropic mesophases. Over the past few years, a number of new *intermediate* phases have become well-established; these have complex structures which further complicate the nomenclature. In a recent review, Holmes (45) has made the sensible suggestion that letters representing the phase structure be followed by its symmetry in parentheses. This removes any ambiguity. In this present review, we employ the system used in previous papers (44–46), with the Holmes modification. As with thermotropic mesophases, the most important

technique to identify the mesophase type is polarizing microscopy. The birefringent phases usually have typical textures, while cubic phases have none – however, they are very viscous!

4.1 Lamellar phase (L_α)

By far the most common surfactant mesophase is the lamellar phase (L_α) (44–52), also known as the “neat phase” from its occurrence during soap manufacture. In this phase, the surfactant molecules are arranged in bilayers frequently extending over large distances (a micron or more), which are separated by water layers (Figure 21.2). Its major repeating unit, the bilayer, forms the basic structural matrix of biological membranes (6–8). While the lamellar phase does not usually flow under gravity, it has a fairly low viscosity, with the material being easily shaken into a container. It is readily identified from its characteristic optical textures (Figure 21.3).

The surfactant bilayer thickness can vary from ca. 1.0–1.9 times the all-*trans* alkyl chain length (l_t) of the surfactant. With longer-chain surfactants, the maximum thickness is reduced to $< 1.7l_t$. Within this layer, the ‘fluid-like’ characteristic of the alkyl chains is shown by a diffuse wide-angle X-ray diffraction peak corresponding to a Bragg reflection of 4.5 \AA (49). The difference in layer thickness arises from differences in head-group areas and gives rise to differing degrees of disorder within the alkyl chain region. For bilayers of thickness $1.0 l_t$, the disorder is large. Alternative suggestions that these lamellar phases consist of “interdigitated monolayers” are incorrect. In contrast, the water layer thickness varies over a much larger range,

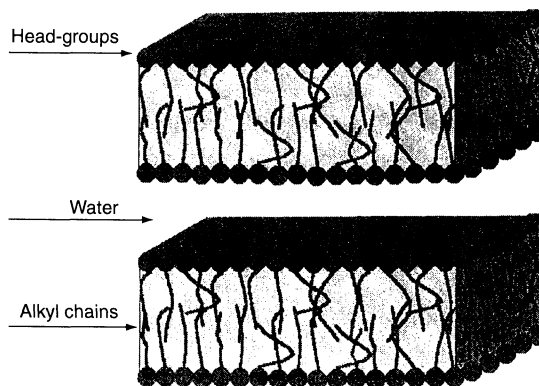


Figure 21.2. Schematic representation of a lamellar phase

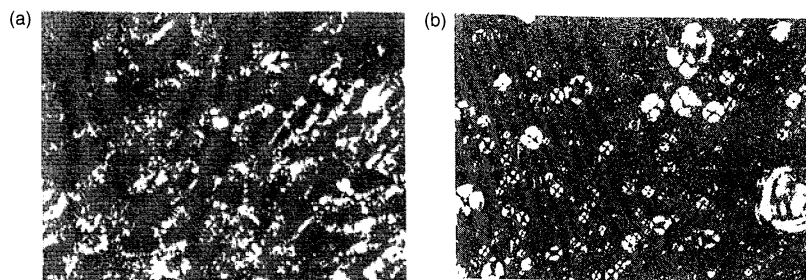


Figure 21.3. Typical optical textures of a lamellar phase, showing (a) oily streaks and (b) Maltese crosses

i.e. $> 8 \rightarrow 200 \mu\text{\AA}$. The water thickness is the same throughout the sample, except at very high water contents (47) where low energy fluctuations can occur. The minimum water content is often that required to hydrate the polar groups, but very low or zero water content can occur with surfactants that form thermotropic lamellar phases. Sharp reflections in the ratio $d:d/2:d/3,\dots$ etc. are observed in low-angle diffraction experiments (X-ray or neutron) due to the regular alternating layer structure with the repeat spacings being the sum of the water and the alkyl chain layer dimensions.

4.2 Hexagonal phases (H_1 , H_2)

The next most common mesophase type is the hexagonal phase (44–52). There are two distinct classes of hexagonal phase, with these being a “normal hexagonal” (H_1) phase, also known as the “middle phase” – again from the soap industry – and a “reversed hexagonal” (H_2) phase. The *normal* phase (H_1) is water-continuous, while the *reversed* (H_2) is alkyl-chain-continuous. They consist of indefinitely long circular aggregates packed on a hexagonal lattice (Figure 21.4).

The normal micelles have a diameter of 1.3–2.0 times the all-*trans* alkyl chain length, with a typical inter-micellar separation being in the region of 8 to 50 Å. The reversed micelles have a polar region diameter in the same range (8–50 Å), but values above 30 Å are rare. The alkyl chain regions are of order (1–1.5 l_t) in thickness, but note that the centre of three rods cannot be more than l_t from the micelle surface.

X-ray diffraction studies of both phases shows Bragg reflections in the ratio $1:1/\sqrt{3}:1/\sqrt{4}:1/\sqrt{7}:1/\sqrt{12},\dots$ etc., again with a diffuse reflection at 4.5 Å. Both phases are rather viscous, much more so than the L_α phase. It is usually not possible to shake a sample into a container by hand. The optical textures are similar for both types,

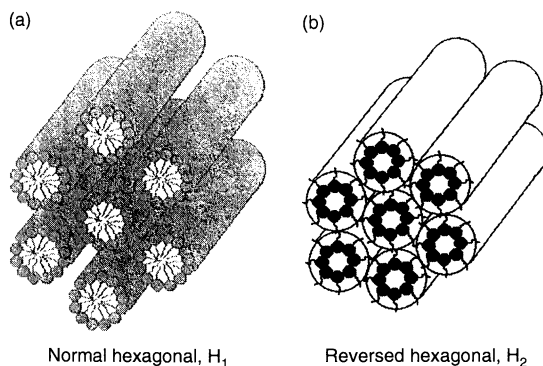


Figure 21.4. Schematic representations of (a) normal and (b) reversed hexagonal phases

again being distinctly different from those of the L_α phase (Figure 21.5).

4.3 Cubic phases

The cubic phases are also known as viscous isotropic phases – because they are! As the name implies, these phases have structures based around one of several possible cubic lattices, namely the primitive, face-centred and body-centred. There are two very distinct aggregate structures, i.e. one comprised of small micelles, normal or reversed, and one based on three-dimensional “bicontinuous” aggregates. The “normal” and “reversed” structures that occur for both make a total of four classes. It is still not certain exactly which structures can occur for the different classes, but the overall picture has become much clearer during the past few years (46, 49–57), with more and more structures being identified. The first set of structures comprised of small globular micelles is labelled “I”, while the second group, the “bicontinuous” three-dimensional (3-D) micellar network, is labelled “V”.

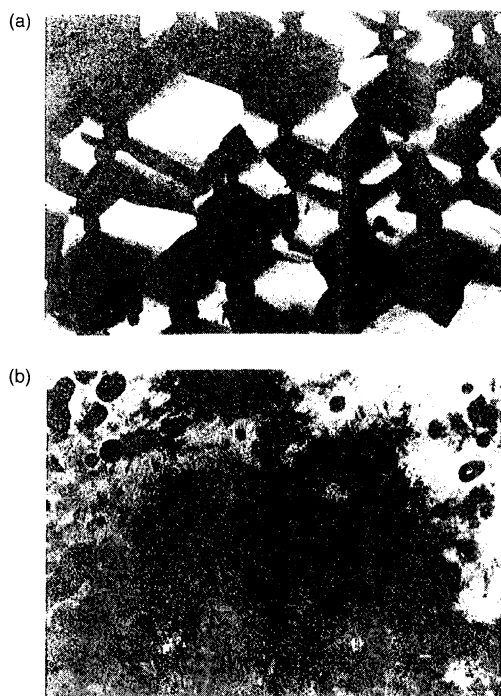


Figure 21.5. Typical optical textures of a hexagonal phase: (a) fan-like; (b) non-geometric

The simplest cubic structures are those of the I_1 type, where the surfactant aggregates are small globular micelles. For the water-continuous I_1 phases, primitive, body-centred and face-centred lattices (51) have all been proposed. In the non-ionic surfactant dodecaethyleneglycol-dodecyl ether [$C_{12}EO_{12}$]/water system (56), all three symmetries have been found, with the three different cubic phases having different compositions (see Figure 21.6). The micelles have diameters similar to those in normal solutions, with a separation similar to that found in the H_1 phase. For the $Im\bar{3}m$ and the $Fm\bar{3}m$ cubic lattices, only one micelle type, a quasi-spherical

structure, is proposed for the lattice (See Figure 21.6) (56, 59). However, the structure of the $Pm\bar{3}n$ phase has been the subject of much discussion (55–59). It is now thought that two slightly different micelles are present, with one being slightly larger than the other. Whether these micelles are short rods or flattened spheres is still a matter for debate. The short-rod model fits better with their position in the phase diagram (between L_1 and H_1). However, a model composed of two spherical micelles and six disc-shaped micelles has been proposed (59). It is this structure which is now thought by some to be the more accurate.

Reports of the reversed I_2 structure of globular aggregates packed in a cubic array are becoming more frequent as suitable surfactants are examined (56–59), despite previous doubts about their existence. A phase with $Fd\bar{3}m$ symmetry is now well established (58, 59). Here it appears that the micelles are spherical, but of two different sizes (Figure 21.7). For reversed micelles, the alkyl chain packing constraints no longer limit the micelle diameter, and hence the co-existence of two spherical micelles of different sizes is more plausible

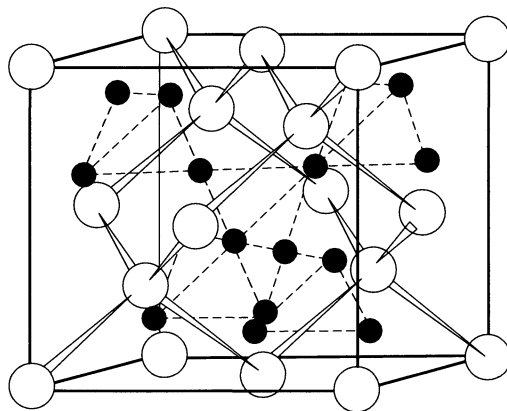


Figure 21.7. Schematic representation of the $Fd\bar{3}m$ I_2 phase (reproduced from ref. (42))

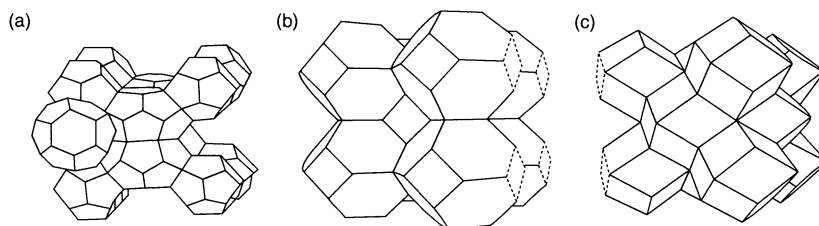


Figure 21.6. Polyhedral representations showing the micellar arrangements for the (a) $Pm\bar{3}n$, (b) $Im\bar{3}m$ and (c) I_1 cubic lattices (reproduced from ref. (56))

than with the I_1 phases, but again, there appear to be other distinct symmetries possible in the I_2 region. Branched-chain polyoxyethylene surfactants with short EO groups often show at least two I_2 regions by optical microscopy (58). It is likely that the confusion in this area will be resolved in the next few years as the surfactant structures necessary for both I_1 and I_2 phases are now clear; hence, we can obtain the phases with many more surfactant types.

The second set of cubic phases (V) has a "bicontinuous" aggregate structure, with three main space groups, $Pn3m$, $Im3m$ and $Ia3d$, all being well reported (51–54). The aggregates form a 3-D network extending throughout the sample. Their main feature is that within the structure there exists a surface (not the surfactant/water interface) where most points are saddle points, having radii of curvature of opposite sign at right angles. This surface can have a positive net curvature towards water (V_1) or towards oil (V_2). Their net curvature lies between that of hexagonal and lamellar phases, and this is the composition region where they often occur. The first report was of a body-centred lattice, $Ia3d$, (see Figure 21.8) by Luzzati (60), who proposed a structure of rod-like aggregates joined three-by-three to form two independent networks. However, it is now believed that these structures are better described by infinite periodic minimal surfaces (61).

There is a significance difference between the occurrence of the different symmetries between V_1 and V_2 . For the V_1 states, only the $Ia3d$ phase has been reported, although tens of different systems have been examined. For V_2 , all three forms have been observed, but usually only one or two are present.

The two classes of cubic phase, I and V, are distinguished from each other by their location in the phase diagram. The I phases occur at compositions between micellar solutions and hexagonal phases, while the V phases occur between hexagonal and lamellar phases. The factors that determine which particular

structure occurs within any set of I or V phases are not yet understood.

4.4 Nematic phases

Lyotropic nematic phases were first reported by Lawson and Flautt (62) for mixtures of C_8 and C_{10} alkyl sulfates, together with their corresponding alcohols in water. They are somewhat less common than the mesophases discussed so far. When they do form, they occur at the boundary between an isotropic micellar phase (L_1) and the hexagonal phase (L_1/H_1), or between L_1 and the lamellar phase (L_1/L_α). As their name implies, they have a similar micellar order to that of the molecules in a thermotropic nematic phase. This long-range micellar orientational and translational order is lower than in the other lyotropic phases described above. Like the thermotropic phases, they are of low viscosity and can be aligned in a magnetic field. It is possible to identify nematic phases optically because of their characteristic *schlieren* optical texture.

Lyotropic nematic phases are generally found for short-chain surfactants, and for both hydrocarbon or fluorocarbon derivatives (63, 64). Two different micelle shapes can occur (65) (See Figure 21.9). One type (N_c) is thought to be composed of small cylindrical micelles and is related to the hexagonal phase, while the other type of nematic (N_d) is composed of planar disc micelles and is related to the lamellar phase. Note that the "disc" micelles are likely to be "matchbox-" or "ruler-shaped", rather than the circular discs. Hence the "disc" nematic phase can have the director (the main axis) along the long axis of "ruler" micelles or along the shortest micelle dimension, as with "matchbox" micelles, while with N_c phases the director always lies along the rod axis.

As with thermotropic nematics, the addition of optically active species to lyotropic nematic phases gives lyotropic cholesteric phases. While details of their structures are not fully established, they appear to follow the

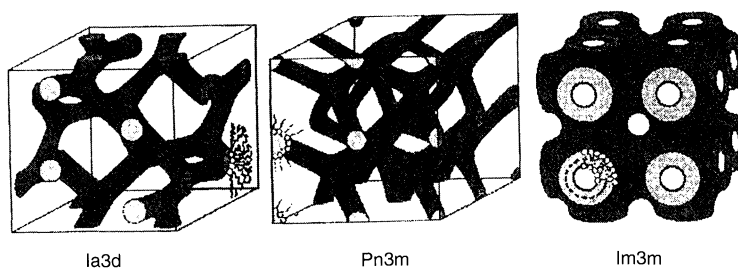


Figure 21.8. Schematic representations of cubic phases (reproduced from ref. (42))

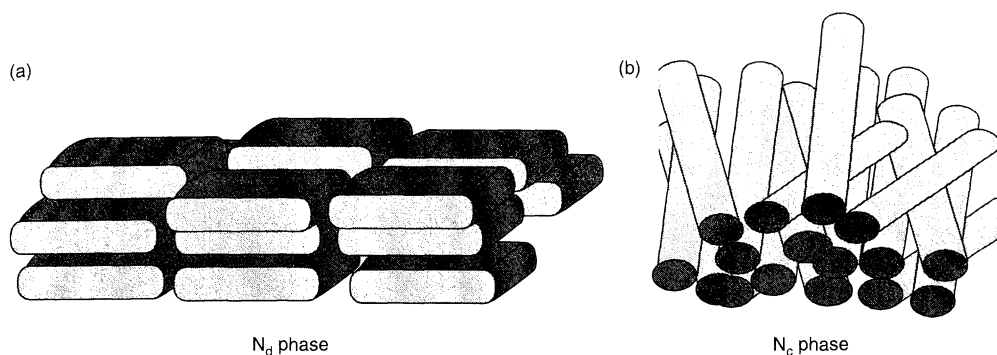


Figure 21.9. Schematic representations of (a) disc (N_d) and (b) rod (N_c) nematic phases

general pattern outlined above. The cholesteric “twist” would appear to derive from the packing of optically active molecules within the micelles, thus leading to a twisted micellar structure, rather than to the transmission of the anisotropic forces via solvent mediation. A recent report has shown evidence for the occurrence of cholesteric “blue” phases – a remarkable observation (66).

4.5 Gel phases (L_β)

The gel phase (L_β) closely resembles the lamellar phase (Figure 21.10) in that it is comprised of surfactant layers, but it differs in its very high viscosity. The term “gel” again originates from industry where these systems were observed to have a gel-like rheology. However, these states should not be confused with polymer gels or gels formed by hydrocolloid systems, since they are

single phases as defined by the phase rule, rather than being multi-phase systems like polymer and colloid gels.

There is a considerable complexity in the nomenclature employed for gel phases. Here, the label “ L_β ” is used because it is very common as a general abbreviation. In the literature, a number of additional symbols have been employed, such as P_β , L_c , and very recently (67, 68), $L_{\beta 1}$ and $L_{\beta F}$. These are used to distinguish different specific details of the structures, for example, differences in the direction of chain tilt (67, 68). Exactly how commonly some of these structures occur has yet to be established. The P_β phase, where a “ripple” can be seen in freeze-fracture electron microscopy, is certainly a distinct and widespread structure for pure lecithins.

Within the gel phase, the bilayers have rigid, mostly all-*trans* alkyl chains, as shown by a sharp, wide-angle X-ray spacing of about 4.2 Å and a large transition heat on melting, typically 25–75% of the crystalline surfactant melting transition. This indicates restricted chain motions, mostly limited to rotation about the long axis only. In contrast, the water (polar medium) is in a “liquid-like” state, with fast rotational and translational mobility. (*Since the structure contains both crystalline and liquid domains it is a true LIQUID CRYSTAL!*)

There are commonly reported to be three different structures of the gel phase, as shown in Figure 21.10. The first structure, with the bilayer normal to the liquid crystal axis, is the structure most commonly found in dialkyl lipid systems (69). Here, the alkyl layer thickness is found to be approximately twice the all-*trans* alkyl chain length of the surfactant. The second structure shown, i.e. the tilted bilayer, is found in systems where the polar head-group is larger than the width of the alkyl chain. This structure has been reported for monoglyceride systems (70). The third structure, the

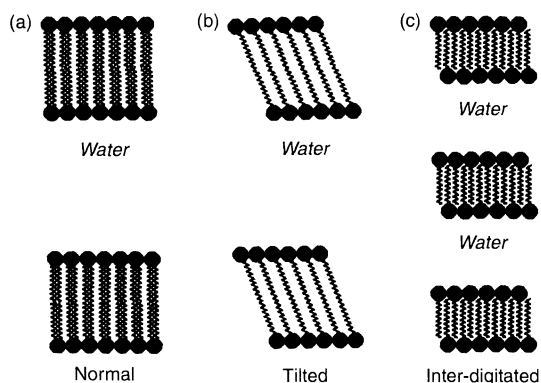


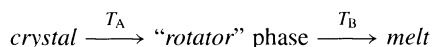
Figure 21.10. Schematic representations of the three possible gel phases: (a) normal; (b) tilted; (c) inter-digitated

inter-digitated form, is found with long chain monoalkyl systems such as potassium stearate (71).

While the occurrence of gel phases is commonly recognized for long-chain dialkyl surfactants, it is also a common occurrence for monoalkyl surfactants. Because of the lower packing order within the alkyl chain region than that found in normal crystals, different chain length derivatives (usually up to four carbons) can mix within the L_β phase. Additionally, different head-groups can also mix within the L_β phases. Indeed, L_β phases can occur for mixed systems where none is observed for the individual constituents. For example, sodium dodecyl sulfate (SDS) and dodecanol form a mixed gel phase where none is observed for SDS alone (72). (Note that dodecanol does form a stable L_β phase, termed the “ α -crystalline phase” with ca. 0.2 mol fraction of water (6, 73, 74).)

While L_β phases have been accepted for years, recently there has been debate about whether the state really does exist as a true thermodynamic equilibrium phase, based on very reasonable criticisms of deficiencies in their location on properly determined phase diagrams (75). However, in at least one case (the non-ionic surfactant trioxyethylenehexadecyl ether (76) the L_β phase in water melts at a higher temperature than the crystalline surfactant. It forms on mixing water and the liquid surfactant just above the crystalline surfactant melting point, thus giving clear proof that it is the equilibrium state.

In fact, as Small has discussed in detail (6), the stability of the L_β state is determined by the packing of the alkyl chains. Polyethylene does not melt to a liquid until 135–140°C (77). Long-chain alkanes do form stable “ α -crystalline” (rotator) phase where the alkyl chain packing and mobility is similar to that of the L_β phase. The melting of alkanes can be regarded as being partly driven by the mismatch between CH_2 and CH_3 sizes within the crystal (24 Å³ and (possibly) ca. 45 Å³, respectively) (6). Thus, the transition temperatures for the sequence:



increase with hydrocarbon chain length, with the minimum chain size required to form a rotator phase being ca. C_{22} . The value of T_B for an alkane of chain length $2n$ (see ref. (6) for values) represents an approximate upper temperature limit for the hydrated L_β phase of surfactants with chain length n because the head-groups pack less effectively in the structure than a CH_2 group. Usually, the L_β phases melt at a lower temperature than the limit T_B because the head-groups are more hydrated in

the molten phases than the L_β phase, and this free energy contribution is larger than the chain packing energy.

To date, the hydration of head-groups in the the L_β phase has always been found to be lower than that of the higher-temperature molten phases (usually lamellar). Hence, L_β phases do not swell in water to the same extent as the L_α phases. Moreover, the size (area) of the hydrated head-group determines which of the three structures occur (see Figure 21.10). The perpendicular bilayer requires a head-group area (a) of ca. 22 Å², while the tilted bilayer occurs with $a = 22\text{--}40$ Å², and the monolayer interdigitated structure with $a \geq 44$ Å². Hence, on increasing m in the series of polyoxyethylene surfactants $C_n\text{EO}_m$ ($n > 16$, $m = 0\text{--}3$), either singly or in mixtures, one expects to encounter all three phases. While the monolayer and perpendicular bilayer structures are known, the tilted phase has not been reported for this series.

In fact, a careful examination of properties such as the enthalpy of melting, high-angle X-ray data and phase behaviour for a series of closely related surfactants show that considerable anomalies exist in both the assumed alkyl chain packing structure and phase stability with the conventional picture. This area deserves and requires a systematic broad study to give a proper molecular-based understanding.

4.6 Intermediate phases

We have already described the occurrence of bicontinuous cubic phases having an aggregate curvature between those of the hexagonal and lamellar phases. Over the past 40 years, there have been sporadic reports of other structures with similar *intermediate* curvature. A number of these so-called “intermediate” phases have now been identified. They replace V_1 bicontinuous cubic phases for surfactants with longer or more rigid hydrophobic chains. It is likely that they replace V_2 phases under certain conditions, but this area has yet to receive the same systematic attention as given to the V_1 /intermediate phases. Unlike the V phases, intermediate phases are anisotropic in structure, and consequently birefringent; in addition, they often have a lower viscosity than the cubic phases, although most are still fairly viscous. There is a continuing discussion in the literature as to which structures are possible. Holmes (45) has given a recent review of the area. The observed or proposed structures divide topologically into three broad types according to symmetry, namely *rectangular ribbon* structures, layered *mesh* structures and *bicontinuous* structures which do not have cubic symmetry. Ribbon

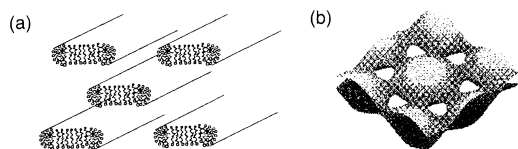


Figure 21.11. Schematic representations of (a) the centred rectangular phase and (b) the six-connected rhombohedral mesh phase

phases may be regarded as a distorted hexagonal phase (see Figure 21.11(a)). Mesh phases are distorted lamellar phases in which the continuous bilayers are broken by water-filled defects which may or may not be correlated from one layer to the next (Figure 21.11(b)). The bicontinuous phases are distorted cubic structures.

Phases with non-cubic structures were first identified by X-ray scattering from aqueous soap mixtures (78, 79) and anhydrous soap melts in a series of papers by Luzzati and Skoulios (79–83). In the first of these papers (78), the term intermediate was applied to a rectangular structure found in aqueous mixtures of potassium and sodium oleates and potassium laurate and palmitate. The structures found in the anhydrous soaps were reinterpreted as intermediate, tetragonal, rhombohedral and ribbon structures in the paper by Luzzati *et al.* (84) in 1968. It was not until the early 1980s that interest in these unusual phase structures was rekindled.

Ribbon phases have been the most comprehensively studied of the intermediate phases. They occur when the surfactant molecules aggregate to form long flat ribbons with an aspect ratio of ca. 0.5, located on two-dimensional lattices of oblique, rectangular (primitive or centred) or hexagonal symmetry. Hagslätt *et al.* (85) have investigated ribbon phases in a number of ternary systems, concluding that all of their ribbon phases index to a centred rectangular cell, *cm*. A “hexagon-rod” model of the ribbon cross-section was suggested in which the ribbon structure is controlled by the competition between the requirement for a constant water layer thickness around each ribbon, the surface area per molecule and the minimization of total surface area. Note that given the anisotropic nature of the interaction forces between the ribbons, the assumption of a constant water layer must be an approximation.

The first identification of intermediate *mesh*-phase structures was by Luzzati *et al.* (84) from the measurements by Spegt and Skoulios (80–83) in anhydrous soap melts. It was not until the work of Kékicheff and others (72, 86–91) on sodium dodecyl sulfate (SDS)/water and on lithium perfluorooctanoate (LiPFO)/water (92) that

intermediate mesh phases were recognized in aqueous surfactant water systems. More recently, mesh intermediate phase structures have been identified in a number of nonionic surfactants with long alkyl chains (93–95). These reveal a very rich intermediate behaviour. There are a number of possible mesh phase structures with both tetragonal and rhombohedral symmetry. These generate X-ray scattering patterns which, although they may show up to ten lines, must be indexed with care because a variety of structures may be possible.

Many intermediate phase regions are bounded by random mesh lamellar phases, i.e. ones that contain water-filled defects, so that the non-uniform curvature is retained although there is no longer any ordering of the defects within the bilayer and there are no correlations of defects between the bilayers. For example, they have been seen in the SDS/water and LiPFO/water systems, and as independently occurring phases in decylammonium chloride/ NH_4Cl /water (96, 97), and in caesium perfluorooctanoate/water (98–101). These phases are characterized by lamellar-like Bragg reflections in the ratio $1:1/2:1/3, \dots$ etc., but with an additional broad liquid-like reflection from the intra-lamellar defects.

While ribbon and mesh phases are now fairly well established, the bicontinuous non-cubic structures are still elusive. The identification of tetragonal or rhombohedral phases of a mesh or bicontinuous type is ambiguous because there usually is insufficient information to make a definitive identification. There are only a few examples where authors have identified a bicontinuous phase, usually because of its association with adjacent bicontinuous cubic phases (89, 102). Anderson and co-workers (103–105) propose that both rhombohedral and tetragonal bicontinuous structures of the type first proposed by Schoen (106) are not only possible but are the most likely intermediate phase structures with these symmetries. Hyde (107, 108) has considered the origin of intermediate phases in detail. Theoretically, doubts on the existence of non-cubic bicontinuous phases have been raised because periodic minimal surfaces with tetragonal or rhombohedral symmetries are expected to have a higher associated bending energy cost than their cubic phase counterparts. Hyde suggests that the phase transition from ribbons to the V_1 phase can be achieved by extra tunnels connecting the mesh layers in a rhombohedral mesh phase. All intermediate phase structures are characterized by a non-uniform interfacial curvature. The forces between the polar head-groups and those between the lipidic alkyl chains tend to impose a certain value for the interfacial curvature. This curvature may not be compatible with the molecular length. The

problem is resolved by either the system phase separating or by the formation of structures with non-uniform surface curvatures. However, it is still not clear why an increasing chain length or rigidity should favour the formation of these intriguing phases over bicontinuous cubic structures. Recall that the surfactant/water interface does not correspond to the V_1 minimal surface, and hence as the surfactant chain length increases, the distance from the minimal surface increases. It may be that the cubic minimal surface places constraints on chain packing which are less serious with anisotropic bicontinuous structures.

While the early reports of intermediate phases concerned systems with *reversed* curvature (83, 84), these were for surfactants where some residual short-range order in the polar groups was probably present. There are few definitive reports of fully molten intermediate phases with reversed curvatures. In fact, the pattern of how intermediate phases replace the normal bicontinuous cubic phase as the alkyl chain size increase only became recognized as systematic studies on homologous series were carried out (46, 76). Here, it has required a combination of microscopy, multi-nuclear NMR spectroscopy and X-ray diffraction to elucidate the structures. Such studies on reversed phases have yet to be carried out, particularly where *small* variations in alkyl chain structure are made.

The key factor in studies of the normal systems was a gradual increase of chain length. Conformational restrictions on the chains in normal aggregates appear to be responsible for the reduced stability of the V_1 phase for long-chain derivatives. With reversed structures, the presence of water in the aggregate cores allows conformational freedom. Hence, it is likely that reversed intermediate phases will be found for systems with low water contents and bulky head groups – inevitably with multiple alkyl chain compounds. Where the chains have identical lengths, such surfactants have high melting temperatures. Hence, multiple unequal chains are probably required to observe reversed intermediate phases.

5 ORIGINS OF THE FORMATION OF SURFACTANT LIQUID CRYSTALS – WATER-CONTINUOUS PHASES

As we have seen above, the I_1 , H_1 and L_α phases have structures based on ordered globular (spherical), rod and disc micelles. Intermediate and V_1 phases have an aggregate curvature between that of rods and discs. Hence, the mesophases formed, and their sequences, can

be described simply in terms of micelle shape at the CMC and the ‘effective’ volume fraction of micelles, which governs what happens to the micelle packing at high concentrations (46). The “effective” volume fraction includes the actual volume occupied by tails, head-groups and bound water. It also includes the affects of soft-core inter-micellar interactions (2, 7) such as repulsions due to overlap of head-group conformations (as with EO surfactants), electrostatics, hydration (solvation) forces, the specific adsorption/desorption of solutes such as ions, polarizable organics, and polymers. All of these are complex and a molecular description is well outside the scope of this present review. Fortunately, the general behaviour is usually close to that of an “effective hard-wall” particle. The major influence of the chemical structure details is to alter somewhat the concentration ranges of the mesophases, but not their sequences.

The micelle shape is determined by the molecular structure as described above (see equations (21.5–21.8) and Table 21.1). There is a critical volume fraction (concentration) above which random (disordered) solutions cannot occur for each of the shapes, i.e. spheres, rods and discs (bilayers). An ordered state (liquid crystal) must form at some higher concentrations if the surfactant is sufficiently soluble. Thus the general scheme is as follows:

Increase concentration

Micellar solution —→ *liquid crystals*

Spheres —→ *CUBIC liquid crystals (I_1)*

Rods —→ *HEXAGONAL*

liquid crystals (H_1)

Discs —→ *LAMELLAR*

liquid crystals (L_α)

In addition, for spherical and rod micelles, there is a maximum volume fraction for the packing in an ordered structure without a change of shape, these being ca. 0.74 for spheres and ca. 0.91 for rods (46). The lamellar bilayers can, of course, pack to fill all the available volume (1.0). When all of the available volume is occupied for a given shape, then more surfactant can only dissolve with a reduction of aggregate curvature to a shape with a higher packing limit. Hence the sequence of mesophases with increasing surfactant concentration is as follows:

Small Polar Group: *Disc (ruler-shaped) micelles*

—→ *Lamellar*

Medium Polar Group: *Rod micelles* \longrightarrow *Hexagonal*
 $\longrightarrow (V_1/\text{Intermediate}) \longrightarrow$ *Lamellar*

Large Polar Group: *Spherical micelles* \longrightarrow *Cubic*
 \longrightarrow *Hexagonal* $\longrightarrow (V_1/\text{Intermediate})$
 \longrightarrow *Lamellar*

Intermediate and V_1 cubic phases do not easily lend themselves to this simple treatment because of their more complex shapes; nevertheless, because their micellar curvature is between that of the H_1 and L_α phases, we expect them to occur at these concentrations – and they do! One final point, we have already mentioned that V_1 cubic phases are replaced by intermediate phases for long-chain surfactants. For some short-chain surfactants, particularly nonionic ones (e.g. EO derivatives or methyl phosphine oxides, C_n , $n < 12$), the V_1 phases do not occur and there is a direct H_1/L_α transition.

6 ORIGINS OF THE FORMATION OF SURFACTANT LIQUID CRYSTALS – REVERSED PHASES

The sequence in which reversed phases occur is much more complicated than that for the normal phases and is not yet understood in terms of surfactant molecular structures. The main reason is (probably) that there is no limitation on the radius of the inverse micelles such as that imposed by the length of the paraffin chain on normal micelles. Water could swell the micelles indefinitely (this does not happen because the size and shape of inverse micelles is controlled by limits on surfactant packing on a curved surface). Figure 21.12 (or something similar) is often employed to describe the general pattern of mesophase behaviour as a function of surfactant (water) concentration. In the description

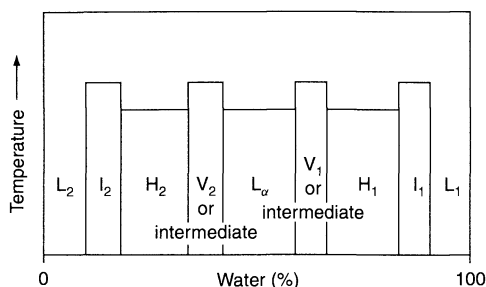


Figure 21.12. Schematic illustration of the mesophase sequence with increasing water concentration as a function of temperature (redrawn from ref. (51))

of the normal phases, it does not include explicitly the role of head-group size. In the description of the reversed phases, it is misleading in that there are few surfactants that exhibit more than two phases from the sequence I_2 , H_2 , V_2 and L_α at a given temperature. More seriously, the sequences observed on increasing water content are often L_α/V_2 or V_2/H_2 . The diagram does show phases that are likely to be neighbours, but even with this caution is required because it is not infrequent to observe a direct L_α/H_2 transition without an intervening V_2 phase. To date, reports of reversed intermediate phases are very rare.

7 PHASE BEHAVIOUR OF NONIONIC SURFACTANTS

In principle, the aggregation properties and mesophases of nonionic surfactants should be easier to understand than the behaviour of ionic surfactants because there are no long-range electrostatic forces. The intra- and intermicellar head-group interactions operate over a much shorter range than for ionic compounds, and so the head-groups can pack close together. Thus, the range of mesophase structures for monoalkyl surfactants can vary from those with highly curved aggregates, such as in I_1 and H_1 phases, to geometries with a smaller or negative curvature, as in the reversed phases (46, 109–111). The effective head-group volume is given by its actual size, together with about one hydration layer.

The most widely studied group of nonionic surfactants is that of the poly(ethylene oxide) alkyl ethers ($n\text{-}C_n\text{H}_{2n+1}(\text{OCH}_2\text{CH}_2)_x\text{OH}$; $C_n\text{EO}_x$) (46, 109–112). One reason for this is that it is possible to study the phase behaviour while systematically varying the length of either the hydrophobic alkyl chain or the hydrophilic ethylene oxide groups. Surfactants with large head-groups form cubic (I_1) and hexagonal (H_1) phases. With increasing temperature, the head-group dehydrates and reduces in effective size, often until the interfacial curvature becomes zero or even negative. This results in the formation of the lamellar (L_α) phase and a subsequent temperature increase (or further decrease in hydration and head-group size) can lead to the formation of reversed phases.

The variation of the phase behaviour with head-group size is illustrated with reference to the $C_{12}\text{EO}_x$ homologous series (46, 56, 113, 114), where $x = 2\text{--}6$, 8 and 12. The simplest phase behaviour is shown by $C_{12}\text{EO}_6$ (Figure 21.13), which has H_1 , V_1 and L_α phases and a region of partial miscibility or clouding ($W + L_1$). The cloud temperature (critical point) is defined as

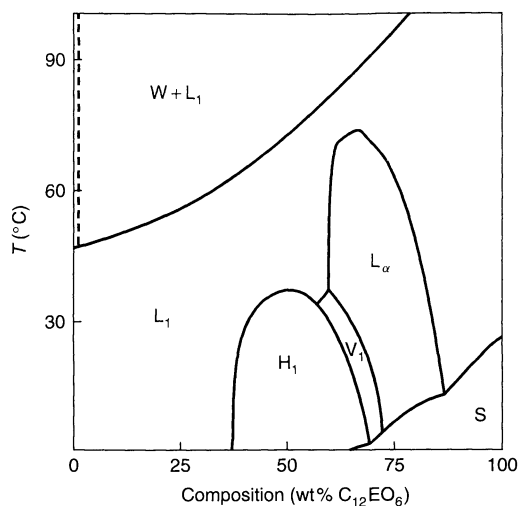


Figure 21.13. Phase diagram of the $C_{12}EO_6$ /water system (note that most of the two-phase regions are small and are not shown): L_1 , aqueous surfactant solution; W , very dilute surfactant solution; H_1 , normal hexagonal phase; V_1 , normal bicontinuous cubic phase; L_α , lamellar phase; S , indicates the presence of solid surfactant (reproduced from ref. (46) by permission of The Royal Society of Chemistry)

the lowest temperature at which the region of partial miscibility is seen. The maximum temperatures of the H_1 and V_1 phases are 37 and 38°C, respectively, while the L_α phase exists up to 73°C. Note that the pure surfactant forms a liquid, which is miscible with water over a certain composition/temperature range. The clouding region arises from the partial miscibility of the $C_{12}EO_6$ micellar solution with water above ca. 49°C. This is caused by a net inter-micellar attraction arising from EO–EO interactions between adjacent micelles. This is discussed further in ref. (114), and the references contained therein. While the clouding phenomenon is important for many micellar properties of these surfactants, its only influence on the mesophases is to determine the limit to which they can swell in water, i.e. it fixes the boundaries between mesophases and the dilute aqueous solution.

On increasing the EO size, an I_1 cubic phase is observed for $C_{12}EO_8$ between ~30 and 43 wt% surfactant on the dilute side of the large H_1 region (Figure 21.14). A V_1 cubic is seen over a narrow concentration range and the L_α phase is reduced to an even smaller concentration and temperature range. With a further increase in EO size to $C_{12}EO_{12}$, only I_1 and H_1 phases are observed with the cubic phase existence range increasing to ~35–53 wt% surfactant (Figure 21.15). Recently it has been shown that there are in fact three

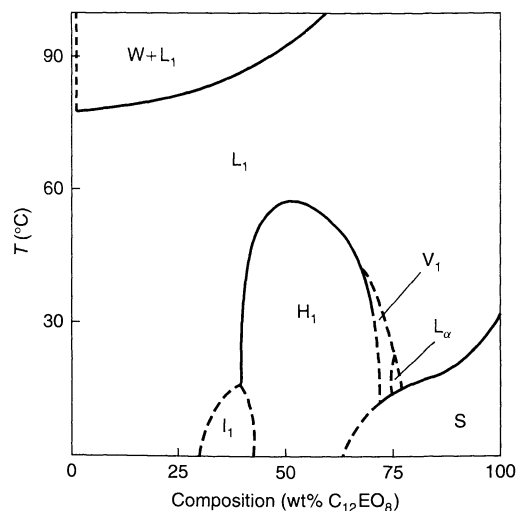


Figure 21.14. Phase diagram of the $C_{12}EO_8$ /water system: I_1 , close-packed spherical micelle cubic phase; other phases, etc. as for Figure 21.13 (reproduced from ref. (46) by permission of The Royal Society of Chemistry)

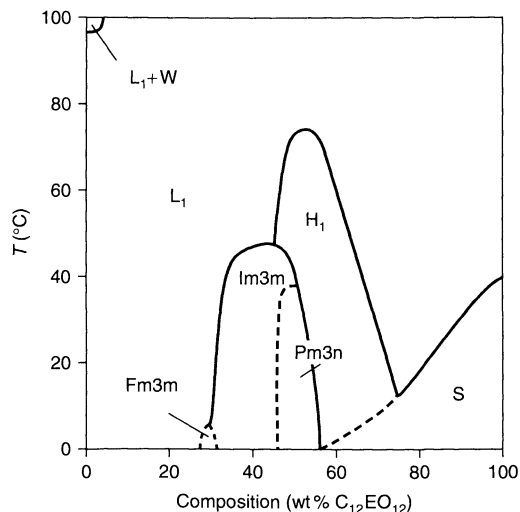


Figure 21.15. Phase diagram of the $C_{12}EO_{12}$ /water system: $Fm3m$, $Im3m$ and $Pm3n$ represent different I_1 cubic phases; other phases, etc. as for Figure 21.13 (Reprinted with permission from ref. (56). Copyright (1997) American Chemical Society)

distinct I_1 phases present (56). With increasing surfactant concentration, these have space groups $Fm3m$, $Im3m$ and $Pm3m$. As one might expect, the partial miscibility region shifts to higher temperatures as the EO size increases. With very long EO groups, the I_1

phase becomes even more dominant. However, eventually, increasing the EO size is expected to lead to "micelles" with small aggregation numbers and a tiny micelle core, which will not form ordered phases.

There is a distinct change in the behaviour as the number of ethylene oxide groups decreases below 6. For $C_{12}EO_5$ (113), H_1 , V_1 and L_α phases are all clearly observed (Figure 21.16), but with the H_1 and V_1 phases existing over much narrower concentration ranges and to lower temperatures than for $C_{12}EO_6$ (to 18.5 and 20°C, respectively). The L_α phase is formed over a much wider concentration range. Note that above the cloud point the lamellar phase co-exists with a dilute aqueous phase and just above this the L_3 , the so-called "sponge phase", occurs. This phase has received much attention from academic researchers, both because of its unique position in the phase diagram and because it is closely related to the occurrence of bicontinuous microemulsions (114–118). It is comprised of large aggregates having a net negative curvature (the opposite of normal micelles). The aggregates extend throughout the phase, and hence it is continuous in both the aqueous and surfactant regions, i.e. it is bicontinuous! In addition, the "aggregates" are extremely labile, and hence the L_3 phases have low viscosities but occasionally show shear birefringence at higher concentrations. Their formation can be slow, and so the establishment of exact phase

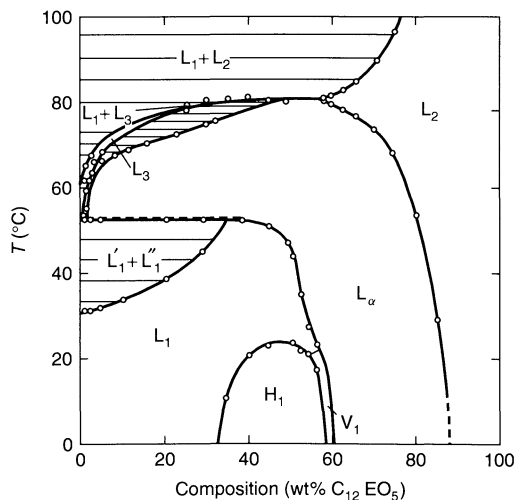


Figure 21.16. Phase diagram of the $C_{12}EO_5$ /water system: L'_1 and L''_1 , surfactant solutions; L_2 , liquid surfactant containing dissolved water, not fully miscible with water; L_3 , sponge phase, not fully miscible with water or surfactant; other phases, etc. as for Figure 21.13 (reproduced from ref. (113) by permission of The Royal Society of Chemistry)

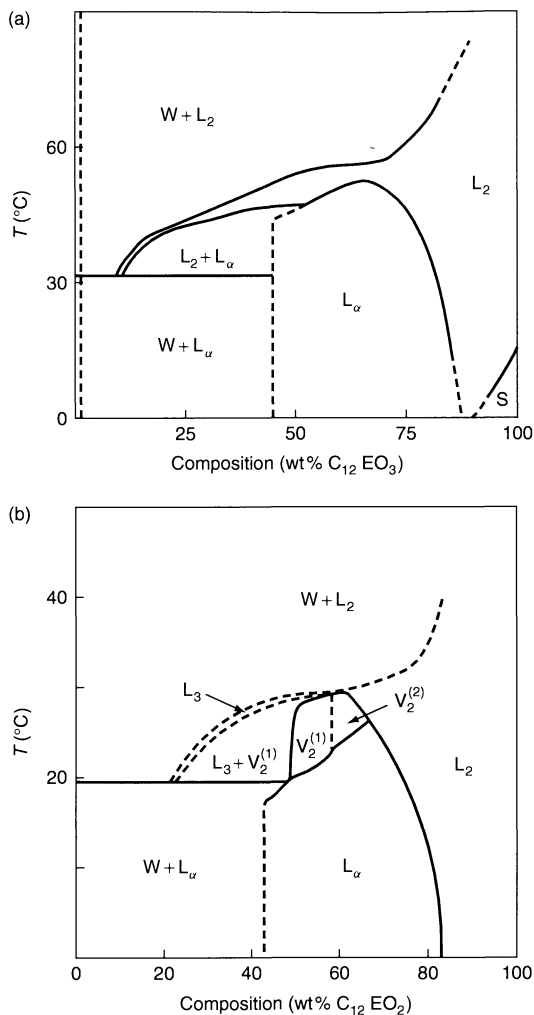


Figure 21.17. Phase diagrams of (a) the $C_{12}EO_3$ /water system (reproduced from ref. (46) permission of The Royal Society of Chemistry), and (b) the $C_{12}EO_2$ /water system (Reprinted with permission from ref. (120). Copyright (1997) American Chemical Society). Symbols used are as given for Figures 21.13 and 21.16

boundaries is sometimes tedious and time-consuming. In some of the earlier mesophase studies, it was not recognized just how slowly the L_3 forms under some conditions; hence the L_3 regions may be underestimated (e.g. see Figure 21.17 above). In fact, the surfactant aggregate structure is closely related to that of the reversed bicontinuous cubic phases which are frequently found on the phase diagram adjacent to the L_3 regions (e.g. $C_{12}EO_2$, see below). While there is a dramatic difference between the mesophase regions of $C_{12}EO_6$

and $C_{12}EO_5$, the difference arises just from the small difference in head-group size, and the existence of partial miscibility above the cloud temperature. Note the marked decrease in the miscibility of $C_{12}EO_5$ and water above 80°C . This is a common feature with these surfactants.

The phase behaviour of $C_{12}EO_4$ is very similar to that of $C_{12}EO_5$, with the L_α phase existing over a similar concentration range (25–80 wt%), but to a slightly lower temperature (68°C). Clouding occurs at 4°C and the H_1 phase exists only at temperatures below -2°C . The occurrence of a V_1 phase, however, cannot be definitely proved. An L_3 phase is observed at similar concentrations but ca. 10°C below that of $C_{12}EO_5$.

For $C_{12}EO_3$, no micellar phase occurs (Figure 21.17), at least above 0°C , while the only mesophase shown on the phase diagram is L_α . This exists over a concentration range of ~ 47 –85% surfactant and to a maximum temperature of 52°C . The L_3 phase is shown on the phase diagram as being continuous with L_2 . In many of these systems, it is difficult to observe the co-existence of the L_2 and L_3 phases at high concentrations because of the similar refractive index of the two phases. Laughlin has observed that L_3 and L_2 are NOT continuous in this system (119). In the above three systems, there are also a number of two-phase regions in which various phases co-exist with very dilute surfactant solution ($W + L_1$, $W + L_2$, $W + L_3$ and $W + L_\alpha$).

For $C_{12}EO_2$ (114), in addition to L_α and L_3 phases there are two V_2 reverse bicontinuous cubic phases which exist between the other two phases over a temperature range of 24 – 36°C (Figure 21.17(a)). X-ray diffraction studies (120) has shown the cubic phases to have space groups $Ia3d$ and $Pn3m$. Because of the reduced hydrophilicity of the head-group, no mesophases exist above 36°C . Note that these occur at higher water concentrations than the L_α phase over a small temperature region – so that addition of water promotes negative aggregate curvature. This is consistent with the view of L_3 as having aggregates with negative curvature, and is a common occurrence with many surfactants that form reversed phases. It underpins the general observations above that *there is not a similar regular phase sequence (L_α , V_2 , H_2 , etc.) with concentrations for the reversed structures as those that occur for normal mesophases.*

For the remaining members of the series, $C_{12}EO_1$ and $C_{12}EO_0$ (dodecanol), no mesophases occur – only separate water and amphiphile phases which show slight miscibility. With all of the C_{12} surfactants, no mesophase exists above 80°C , while the maximum mesophase “melting” temperature varies much less with EO size than the cloud temperatures.

A similar behaviour is observed for homologous series of surfactants of different alkyl chain lengths, for example, there are recent reports on $C_{10}EO_4$ – $C_{10}EO_7$ which show the same general pattern (121–123) (but note the reservations expressed in a recent review by Chernik (112) about “compound formation”). The mesophase regions extend to higher temperatures with increasing n . The effect of curvature increases with EO number, as expected. Thus, for all alkyl chain lengths ($n > 10$), I_1 cubic phases only exist for EO_x when $x > 8$ and extensive L_α regions occur for small EO groups ($x \leq 5$).

The influence of alkyl chain length can be illustrated by using C_nEO_6 surfactants (46). C_8EO_6 gives just an H_1 phase which melts at $\sim 12^\circ\text{C}$ (124, 125). $C_{10}EO_6$ shows a substantial area of H_1 phase but there is contention as to whether it additionally shows a low-temperature L_α phase (125, 126). No V_1 phase occurs with these two materials. The phase behaviour of $C_{12}EO_6$ is reported above. $C_{14}EO_6$ is very similar to $C_{12}EO_6$, except that the L_α phase has a significantly higher melting temperature (95°C , as opposed to 73°C). On increasing the chain length to C_{16} , there is a dramatic alteration in the phase behaviour similar to the difference between $C_{12}EO_6$ and $C_{12}EO_5$. The behaviour is even more complex because a monolayer inter-digitated gel (L_β) phase occurs below ca. 25°C . The H_1 and V_1 melting temperatures are slightly decreased (both 34°C , compared to 37 and 40°C for $C_{14}EO_6$) and the L_α melting temperature slightly increased (102°C). This is the first member of the C_nEO_6 series to show an $L_\alpha + W$ region and an L_3 phase (90 – $> 102^\circ\text{C}$). Moreover, with an increase in chain size to C_{16} , the bicontinuous cubic phase begins to be replaced by intermediate phases. In fact, $C_{16}EO_6$ exhibits several phases not in the original report, including a rod-micelle nematic phase, a random-mesh-lamellar phase and another intermediate phase, with the latter being metastable (127).

While the existence range of the nematic phase is small for $C_{16}EO_6$, with $C_{16}EO_8$ a low-viscosity, long rod-micelle nematic phase (N_c) has been observed (Figure 21.18) over a narrow concentration range at ~ 34 wt% surfactant over the temperature range 28 – 54°C between the H_1 and L_1 phases (128). Here the increase in EO size removes the intermediate phases and the $L_\alpha + W$ and L_3 regions, but a gel (L_β) phase is present at temperatures below the molten phases. For much longer chain surfactants, such as $C_{22}EO_6$ (hexaethylene glycol *cis*-13-docosenyl ether) (129) or “ $C_{30}EO_9$ ” (nonaethylene glycol mono(11-oxa-14,18,22,26-tetramethylheptacosyl ether) (95), the correlated defect mesh-phases replace

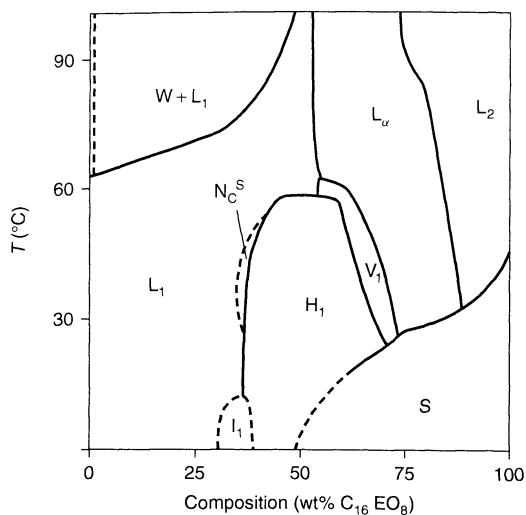


Figure 21.18. Phase diagram of the $C_{16}EO_8$ /water system: N_C^S , rod-nematic phase; other phases, etc. as for Figures 21.13, 21.16 and 21.17 (reproduced from ref. (128) by permission of The Royal Society of Chemistry)

the V_1 region. No gel phases are expected here because of the disrupted alkyl chain packing. Note that several general conclusions are illustrated by the above behaviour. First, an increasing surfactant chain length has little effect on the composition ranges of phases with positive curvature, with the major influence being to raise the upper temperature limit of the mesophases. Hence, very short-chain (C_n , $n < 8$) surfactants do not form mesophases at all. Moreover, N_C phases occur at the L_1/H_1 boundary for long-chain surfactants. This pattern of behaviour is true for all surfactant types. The reason why few N_C phases are reported in the literature is because such long-chain surfactants are usually insoluble. The “ C_{22} ” and “ C_{30} ” derivatives referred to above have their molecular packing in the crystal disrupted by the presence of methyl side-groups or unsaturation, both of which increase miscibility with water.

Conroy *et al.* (114) investigated the effect of replacing the terminal OH in three polyoxyethylene surfactants by OMe ($C_{12}EO_mOMe$, $m = 4, 6$ and 8). For $m = 4$, the L_α phase melts at 27°C for OMe (68°C for OH) and the L_3 phase is seen at lower temperatures (24 – 27° , as opposed to 51.5 – 70°C). For $m = 6$, the H_1 , V_1 and L_α phases all melt at lower temperatures for OMe (24 , 28 and 43 , as opposed to 37 , 38 and 73°C for OH). For $m = 8$, the V_1 and L_α phases are not seen for OMe and the I_1 and H_1 melting temperatures are reduced to 15 and 41°C , respectively, from 16 and 59°C for OH. This

shows the importance of the terminal OH of the EO groups, a factor which is often neglected.

Commercial polyoxyethylene surfactants contain a wide range of EO sizes, often with a reasonably defined alkyl chain. Bouwstra and co-workers (130) have studied a commercial sample of $C_9=C_9EO_{14}$ (i.e. a C_{18} chain with 9–10 *cis* double bonds and a polydisperse EO group). The latter exhibits phase behaviour similar to $C_{12}EO_8$, with I_1 , H_1 , V_1 and L_α phases. The H_1 phase exists between 35.6 and 74.8 wt% surfactant and up to 84°C . The other phases exist over narrower concentration ranges and to lower temperatures. Similar studies have also been reported by Kunieda and co-workers (131, 132) for a wide range of commercial oleoyl EO derivatives; again, the commercial actives behave like pure ones with a shorter EO size.

The commercial “Synperonic A” surfactants are a mixture of C_{13} (66%) and C_{15} (34%) alkyl chains while the hydrophilic chains are composed of polydisperse ethylene oxide groups. Investigations into the phase behaviour of the A7, A11 and A20 surfactants (containing an average of 7, 11 and 20 EO groups respectively) have been achieved by using a number of experimental techniques (133, 134). The A7 material shows H_1 and L_α phases, with the H_1 phases existing between 30 and 62 wt% surfactant up to a maximum of $\sim 30^\circ\text{C}$, while the L_α phases exist between 51 and 86 wt% surfactant to a temperature greater than 60°C . With an increase of EO size to the A11 compound, a small area of V_1 cubic phase appears between the H_1 and L_α phases, while the latter is greatly reduced in stability (73–83 wt%, with a maximum temperature of $\sim 35^\circ\text{C}$). The H_1 phase exists at slightly higher concentrations than for A7, and up to $\sim 64^\circ\text{C}$.

The phase behaviour of the A20 compound is radically different to the shorter-chain homologues, with only I_1 and H_1 phases being present. The I_1 phase exists between 24 and 62 wt% surfactant up to $\sim 70^\circ\text{C}$, and the H_1 between 60 and 81 wt% to over 80°C . Unlike the other two surfactants, the A20 compound shows no cloud point (below 100°C) at low surfactant concentrations.

Triton X-100[®] and X-114[®] are industrial *p*-tert-octylphenol polyoxyethylene surfactants with about 9.2 and 7.5 ethylene oxide groups per molecule, respectively. They are used in biochemical studies because of their ability to disrupt biological membranes without denaturing integral membrane proteins (135). TX-100 (136) forms an H_1 phase between 37 and 63% surfactant contact from 0– 28°C and an L_α phase between 65 and 78% up to 6°C . TX-114 (137) exhibits a larger area of L_α phase from 35 to 83% surfactant

content and from ~ -20 to 65°C , but does not form an H_1 phase.

Essentially, these studies allow two general conclusions to be made when comparing pure and commercial nonionic surfactants. First, the stability of the V_1 phase is much reduced in commercial materials. Secondly, a commercial surfactant of average formula C_nEO_m resembles a pure surfactant with a slightly smaller EO group such as C_nEO_{m-1} . (An example is given below in Section 11.2 on mixed surfactants). Thus, the surfactant molecules with different EO sizes mix together in the same aggregates, rather than the long and short EO components separating into phases with large and small aggregate curvatures, respectively. The small difference in hydrophilicity caused by changing the head-group size by one EO unit is responsible for this behaviour. With other commercial surfactants where the head-group is a small polymer of strongly hydrophilic residues, such as with alkyl polyglycerols, the difference in hydration and size between head-groups differing by 1–2 polymer units is very often sufficient to cause the co-existence of phases with different curvatures (e.g. $L_\alpha + H_1$) over a wide range of water contents. Obviously, this is only a rough guide for materials where the EO distribution follows some regular pattern. Mixed commercial nonionic surfactants can show marked deviations from that expected for the “average” EO size if the distribution of EO sizes is bimodal.

While studies on linear alkyl surfactants are common, in recent years branched-chain nonionic surfactants have been studied, as well as surfactants with novel head-groups and surfactant mixtures. The phase behaviour of a series of mid-chain-substituted surfactants with the general structure $\text{CH}_3(\text{CH}_2)_4\text{CHEO}_x(\text{CH}_2)_5\text{CH}_3$ where $x = 3, 4, 6, 8$ and 10 (denoted $s\text{-C}_{12}\text{EO}_x$) has been studied by optical microscopy using the penetration technique (138). These have much more bulky hydrophobic groups and show clear differences from the behaviour of the linear materials described above, as expected from the packing constraints. No liquid crystal phases are seen for $s\text{-C}_{12}\text{EO}_3$, as expected for a short-chain surfactant, just the co-existence of W and L_2 . For the other materials, mesophases are observed. With $s\text{-C}_{12}\text{EO}_4$, a V_2 reversed bicontinuous cubic and an L_α phase are seen, both of which melt at low temperature (8.0 and 0.5°C , respectively) in addition to L_2 and W . On increasing the EO size to that of $s\text{-C}_{12}\text{EO}_6$, L_α and L_3 phases are observed. The L_3 phase exists between 35.3 and 53°C on the lower-surfactant-concentration side of the L_α phase that exists up to 48.8°C . L_1 micellar solution is seen only below 5.9°C with a cloud temperature below 0°C .

The next compound, $s\text{-C}_{12}\text{EO}_8$ (Figure 21.19), shows similar phase behaviour to $s\text{-C}_{12}\text{EO}_6$ with the melting temperatures of the L_α and L_3 phases increased (to 63.5 and 66.7°C , respectively). A micellar solution with a cloud point at 19.2°C is present. Finally, $s\text{-C}_{12}\text{EO}_{10}$ (Figure 21.20) gives H_1 , V_1 and L_α phases on penetration at 0°C . The H_1 and V_1 phases melt to micellar solution at $< 10^\circ\text{C}$, while the L_α phase exists up to 74.2°C . An L_3 phase also exists between 69.0 and 79.0°C , with the cloud point being 46.4°C . Clearly, the pattern of behaviour resembles that of the linear surfactants, but an increase EO size is required to observe a particular phase sequence. It is initially surprising that mesophases do form with the small (maximum) hydrophobic chain of C_7 , where none are seen with simple linear surfactants of this chain length. This may indicate that the micelles are more monodisperse in size for dialkyl surfactants than for monoalkyl surfactants because local molecular “protrusion” of monomers out of the micelle is damped by the hydrophobic effect on two alkyl chains, rather than one. Thus, the micelle surface is smoother for dialkyl surfactants than for monoalkyl derivatives.

Another series of “branched” (dialkyl) nonionic surfactants has been studied (139) having the general formula $C_kC_n\text{GE}_8\text{M}$, where C_k and C_n denote different alkyl chains, with $k = 4$ for *n*-butyl (C_4) and *tert*-butyl (C_{4-t}) and $n = 10$ or 12 ; G denotes a glyceryl unit and

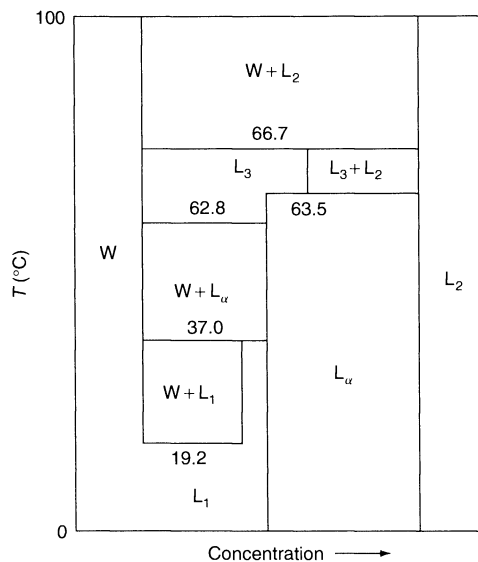


Figure 21.19. Schematic phase diagram of the $s\text{-C}_{12}\text{EO}_8$ /water system; symbols used for phases, etc. are as given for Figures 21.13 and 21.16 (reproduced from ref. (138) with permission from Elsevier Science)

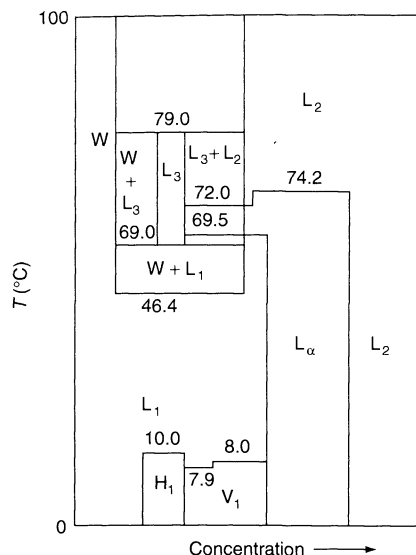


Figure 21.20. Schematic phase diagram of the $s\text{-C}_{12}\text{EO}_{10}$ /water system; symbols used for phases, etc. are as given for Figures 21.13 and 21.16 (reproduced from ref. (138) with permission from Elsevier Science)

E_8M denotes octaoxyethylene monomethyl ether. This work follows on from earlier work on similar compounds (140–142). The structural differences between *n*- and *tert*-butyl chains within the asymmetrical V -isomers leads to a different phase behaviour as expected by the packing constraints. Both C_{10} isomers show H_1 , V_1 and L_α phases, with the existence range and maximum temperature of the L_α much greater for the *n*-butyl compound (8–80 wt% surfactant, compared to 68–77 wt%, and 50.1°C compared to 11.6°C). The H_1 and V_1 phase ranges are similar for the two compounds, but with the V_1 phase existing to higher temperature for the *n*-butyl compound (Figure 21.21). This compound also shows a L_3 phase above the dilute L_α phase up to 50.1°C. The *n*-butyl isomer of C_{12} has very similar phase behaviour to the C_{10} compound with all of the phases existing to slightly higher temperatures.

Previously to the above work, Kratzat and Firnkellmann had investigated a homologous series of nonionic surfactants containing two hydrophilic chains (143), and having the general formula $\text{C}_n\text{G}(\text{E}_m\text{M})_2$, where C_n denotes the alkyl chain ($n = 10\text{--}16$), G = glycerol and E_mM = oligooxyethylene monomethyl ether ($m = 3\text{--}5$) (Figure 21.22). The compound $\text{C}_{10}\text{G}(\text{E}_4\text{M})_2$ exhibits no mesophases but has a cloud temperature of 54.2°C. The other compounds studied (for which $n = 12, 14$ and 16) all exhibit two I_1 cubic phases and a hexagonal phase

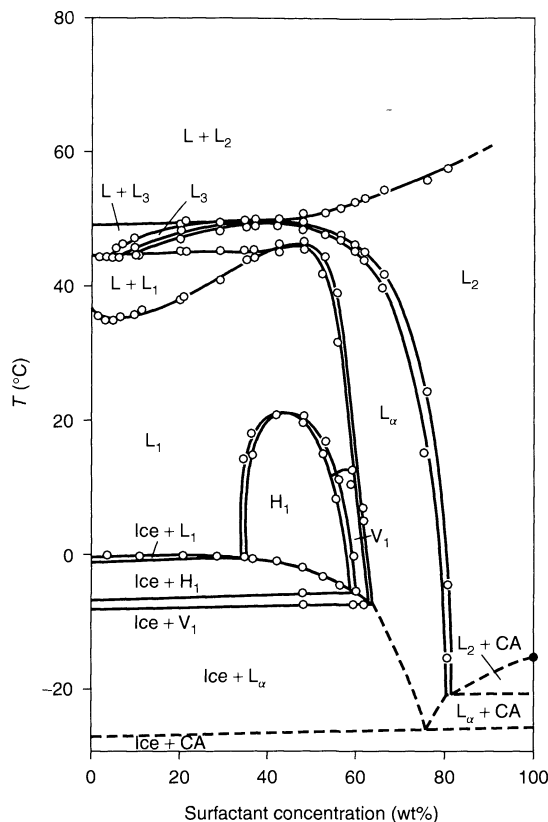


Figure 21.21. Phase diagram of the $(\text{C}_4)(\text{C}_{10})\text{GE}_8\text{M}$ /water system: L , very dilute surfactant solution; CA , indicates the presence of solid surfactant; other phases, etc. as for Figures 21.13 and 21.16 (reproduced from ref. (139) with permission of Academic Press)

(Figure 21.23). The temperature at which the phases melt increases with increasing length of alkyl chain (the melting temperatures of the H_1 phase in $\text{C}_n\text{G}(\text{E}_4\text{M})_2$ for $n = 12, 14$ and 16 are 2.1, 31.6 and 38.6°C, respectively). The cloud point is virtually unaffected. However, on increasing the length of the head-group, the cloud point increases (38.7, 53.0 and 61.8°C for $\text{C}_{14}\text{G}(\text{E}_m\text{M})_2$ where $m = 3, 4$ and 5, respectively).

All of these studies confirm that the pattern of phase behaviour shown for the conventional surfactants generally holds at least qualitatively, whatever the head-group or chain structure, provided that a proper consideration of the alkyl chain packing conditions is made.

A severe test of this is where the flexible alkyl chain is replaced by a rigid hydrophobic steroid skeleton. When sufficiently long ethoxy chains are attached to the cholesterol OH, a phase behaviour similar to more

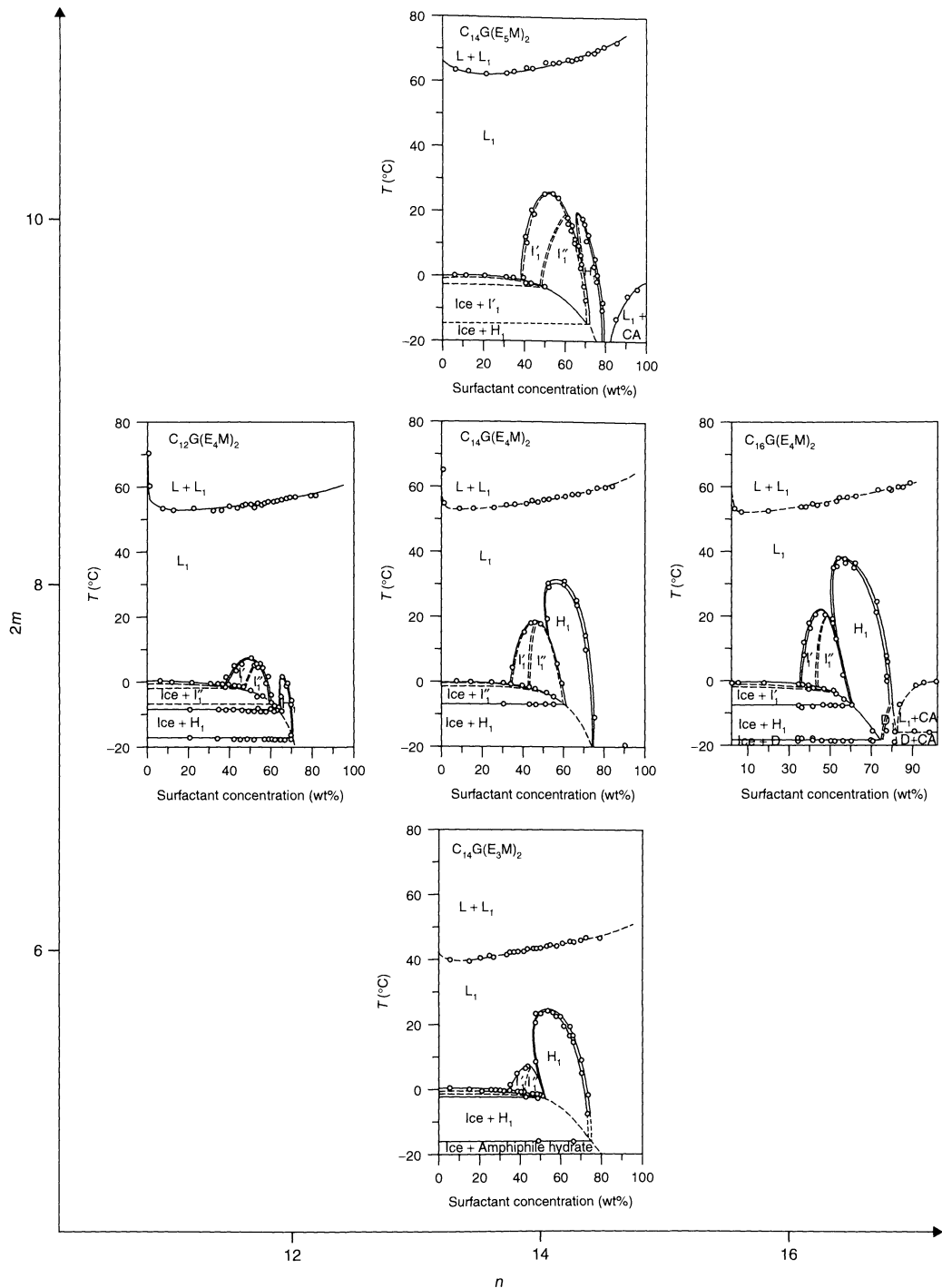


Figure 21.22. Phase diagrams of $C_n G(E_m M)_2$ /water systems, showing the dependence of phase behaviour on the alkyl chain length, n , and the number of oxyethylene units, $2m$, per surfactant material; D, lamellar phase; other phases, etc. as for Figures 21.13, 21.14 and 21.21 (reproduced from ref. (143) with permission from Taylor & Francis Ltd)

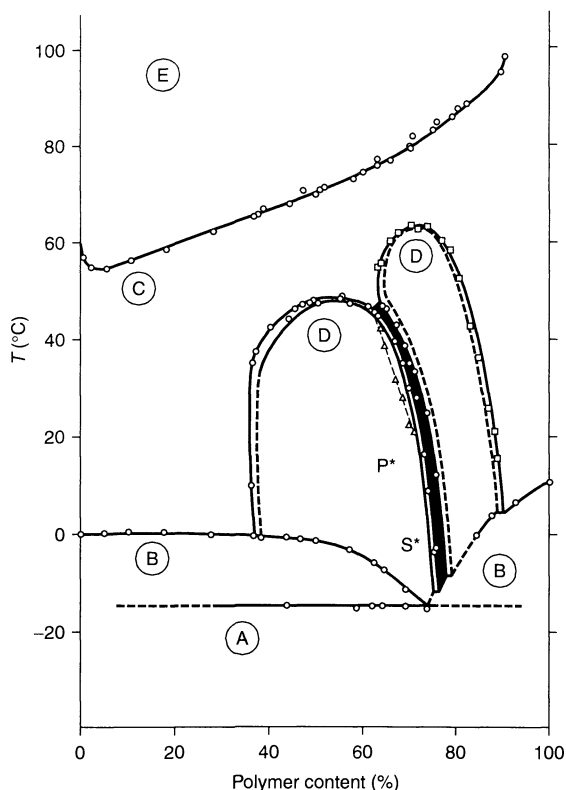


Figure 21.23. Phase diagram of the $P_{95}C_{10}EO_8$ /water system: A, heterogeneous mixed crystals; B, heterogeneous melt; C, homogeneous isotropic solution; D, homogeneous mesomorphic phase; E, heterogeneous isotropic liquids, miscibility gap with lower consolute point (reproduced from ref. (145) with permission of Springer-verlag GmbH & Co, KG)

common alkyl derivatives is observed (144). For a polydisperse EO_{13} chain, L_1 , H_1 , L_α and L_2 phases are seen, along with a region of clouding above 85°C . The H_1 phase exists between 18 and 60% surfactant content from at least room temperature to 65°C . The L_α phase exists from 35 to over 85% and to at least 100°C . When the EO length is increased to 35, no lamellar phase occurs, but an I_1 cubic phase is seen between 23 and 67% surfactant and to over 100°C . The H_1 phase is seen between 67 and 83% and up to $\sim 80^\circ\text{C}$. For a chain length of 50 ethoxy groups, only the I_1 phase is seen between 27 and 93% up to 100°C . Estimating the cholesterol length as being equivalent to ca. C_{15} , and a volume of ca. C_{20} , this is well in agreement with the packing behaviour of the normal surfactants. It might be thought that the bulky nature of the cholesterol moiety would prevent packing into spherical micelles, but this is clearly not the case.

An exciting development in recent years has been the systematic study of polymeric surfactants rather than the occasional studies reported previously. Polysurfactants can be made via polymerization of the chain termini (head-groups or tails) or from hydrophilic and hydrophobic blocks (called side-chain or block copolymer surfactants, respectively). Over the years, Finkelmann and Lühmann have reported the phase behaviour of a variety of non-ionic surfactants and the polymers formed from them. In the latter category, they report (145) on the liquid crystalline properties of side-chain polymers comprising a polyoxymethylsilyl backbone ("P" = $O-SiCH_3-$, average degree of polymerisation 95) with side chains of $(CH_2)_{10}C(O)O(CH_2CH_2O)_8CH_3$. These are produced by esterifying the polyglycol with 10-undecanoic acid, which forms the hydrophobic part of the amphiphilic molecule. In water (Figure 21.23), the polymer exhibits large regions of H_1 (36–75%, $-15 \rightarrow 49^\circ\text{C}$) and L_α (64–90%, $-5 \rightarrow 64^\circ\text{C}$) phases separated by a narrow band of V_1 phase ($-10 \rightarrow 45^\circ\text{C}$). A region of clouding is seen up to 90% polymer. The clouding temperature increases with concentration from a minimum of 53°C . The changes induced by polymerization are similar to those expected for increasing the alkyl chain size to ca. C_{14} , a rather small alteration. The high flexibility of the polyoxysilyl backbone is probably responsible for this. A more rigid backbone would lead to larger changes.

When the side-chain is modified to include a rigid rod-like biphenyl moiety, $((CH_2)_3-\theta-\theta-O-(CH_2CH_2O)_9CH_3)$ (146) and the degree of polymerization reduced to 55 ($P_{55}C_3BiE_9$), subtle differences are seen in the phase behaviour. H_1 (34–75%, $-2 \rightarrow 68^\circ\text{C}$) and L_α (60–95%, $20 \rightarrow > 100^\circ\text{C}$) phases are still seen but with no V_1 phase between them. Clouding is observed up to 58% polymer between 66 and 82°C . Above this, a bi-phasic $L_1 + L_\alpha$ region is seen to $\sim 80\%$.

The phase behaviour of related polymers and monomers containing the rigid biphenyl moiety was studied in a later paper (147). The phase behaviour of the monomeric surfactants is generally comparable with that of common nonionic surfactants (especially methyl-capped ethylene oxide alkyl ethers). They exhibit I_1 (sometimes two), H_1 and L_α phases, as well as clouding. The polymers, which have an average degree of polymerization of 55, nearly all exhibit H_1 and L_α phases, whereas the I_1 phase is seen only in one ($P_{55}C_3BiE_{11}$). One major difference between the polymer and monomer phase behaviour is the appearance of a nematic phase (N_c) built up of rod-like micelles in a number of the polymers. This is seen over a narrow concentration range between the L_1

and H_1 phases, melting at temperatures below the H_1 phase. The phase behaviour of oligomers of $P_rC_3BiE_9$ for $r = 3-6$ and 13.4 has also been reported. H_1 and L_α phases are seen for all of these, but the I_1 phase is not seen for $r = 13.4$ (or $r = 55$, i.e. the polymer). The nematic phase is seen for $r = 6$ ($<50.0-52.2^\circ\text{C}$), $r = 13.4$ ($38.6-58.2$) and $r = 55$ ($34.8-58.2^\circ\text{C}$).

Lümann and Finkelmann also made the first published report of a nematic phase in a binary nonionic/water system (148). This was formed by disc-shaped micelles of the surfactant $\text{H}_2\text{C}=\text{CH}-\text{CH}_2-\text{O}-\phi-\phi-\text{O}-\text{CH}_2-\text{COO}(\text{CH}_2\text{CH}_2)_7\text{CH}_3$, being observed between the L_1 and L_α phases in a narrow band of 34–38% surfactant between 7.5 and 23.4°C (Figure 21.24). The L_α phase exists up to ~72% surfactant (and to ~80% in a bi-phasic region with water). Clouding is seen over a wide concentration range (up to >90% surfactant) with a lower critical temperature of 33.2°C.

Polyhydroxy surfactants have recently received some attention as alternatives to EO materials. Polyhydroxy

compounds are more strongly hydrated than those containing EO groups, and hence the mesophases exist to high temperatures. In addition, the intermolecular hydrogen bonding results in the occurrence of thermotropic mesophases to above 100°C. An up-to-date summary of their surfactant properties has been published recently (149). Generally, one requires at least a hydrophilicity of ca. $2 \times \text{OH}$ groups for surfactant properties, although di or trihydroxy compounds form lamellar or reversed phases only. Very common examples of this type of compounds are the monoglycerides. While their formation of lamellar and inverse cubic phases have been known for many years (50–52), only recently has a definitive phase diagram of monoolein, one of the commonest, been published (150, 151). Major problems can occur with the slow establishment of phase equilibria, particularly where V_2 phases are involved, as is illustrated by comparing the phase diagram in ref. (149) with an earlier version (152). Chernik has given sound warnings of the problems involved (16).

For water-continuous phases, a larger polyhydroxy group is required. An easily synthesized class of materials is the alkyl glucamides with five OH groups. Unfortunately, single-chain materials have high Krafft temperatures. Lower Krafft boundaries occur with surfactants possessing two fairly short n -alkyl chains and two glucamide head-groups (153). These have the general formula $(\text{C}_n\text{H}_{2n+1})_2\text{C}[\text{CH}_2\text{NHCO}(\text{CHOH})_4\text{CH}_2\text{OH}]_2$ with $n = 5-9$ (abbreviated to di-(C_n -Glu). Di-(C_5 -Glu) shows H_1 , V_1 and L_α phases on penetration at ~5°. The H_1 and V_1 phases melt above 80° with the L_α remaining to >100°C. Di-(C_6 -Glu) shows the same sequence of phases as above, with the H_1 phase first seen at 56 wt% surfactant (co-existing with an L_1 micellar solution). A single H_1 region exists between 62 and 71 wt% surfactant and the V_1 region between 71 and 75 wt%. Both phases melt between 70 and 85°C. The L_α phase exists at higher concentrations and to >90°C.

Di-(C_7 -Glu) also has a bi-phasic H_1/L_1 phase forming at 62 wt% surfactant and existing to ~60°C. The H_1 phase melts over a range from 62–80°C. Between the H_1 and L_α phases is another bi-phasic region between 71 and 75 wt%. This, and the L_α phase exist to >90°C. A two-phase loop occurs at low surfactant concentrations and temperatures (<8 wt% and <50°C). The authors believe this to be the first observation of an upper critical solution temperature for a nonionic surfactant. The shape of the upper consolute loop is *extremely unusual*, suggesting remarkable changes in micellar interactions, or perhaps the presence of impurities! One would be pleased to see these observations verified by

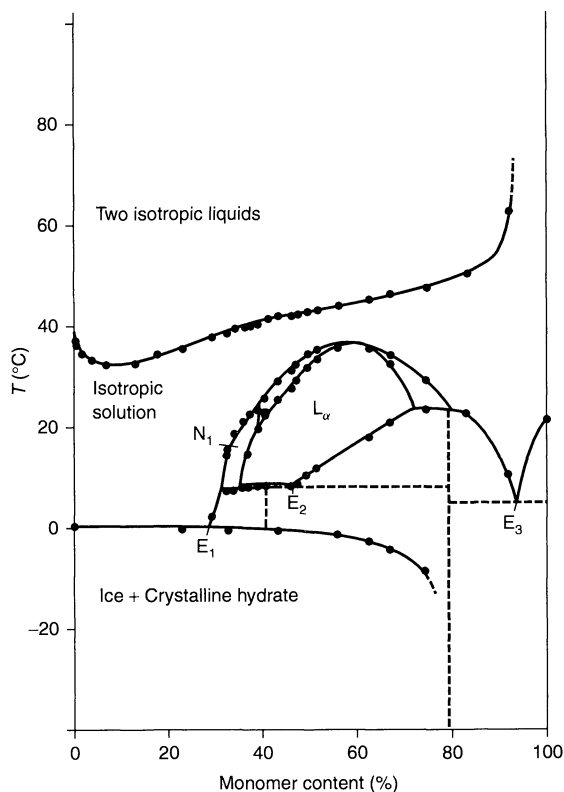


Figure 21.24. Phase diagram of the $\text{H}_2\text{C}=\text{CHCH}_2\text{O}\phi\phi\text{EO}_7/\text{water}$ system; N_1 , disc-nematic phase; E_1 , E_2 and E_3 , eutectic points; other phases, etc. as for Figure 21.13 (reproduced from ref. (148))

other groups. Di-(C₈-Glu) shows only an L_α phase but with a wide miscibility gap to a dilute aqueous solution. This is not a remarkable behaviour.

Seddon and co-workers have studied the lyotropic (and thermotropic) phase behaviour of *n*-octyl-1-*O*-β-D-glucopyranoside (G) and its thio derivative, *n*-octyl-1-*S*-β-D-glucopyranoside (154). Both form L₁ micellar solutions, and V₁ (1a3d) and L_α phases in water with the β-*O*-G also forming an H₁ phase. For β-*O*-G, the L_α phase exists from 80 to 100% surfactant and to over 120°C, V₁ exists between 73 and 80% and up to ~60°C, while H₁ has a limited region between 64 and 73%, up to 35°C. All melt to give micellar solutions. The L_α phase of β-thio-*O*-G also exists up to 100% surfactant (from 75%) and to ~135°C. The V₁ phase exists between 72 and 90% surfactant (i.e. it melts to give the lamellar phase above 75%). The temperature at which it melts varies from 0° at 90% to 65°C at 75%. In a later paper, the mesophases of a series of these surfactants were described (155). The behaviour of β-*O*-G in water has also been reported independently (156), with H₁, V₁ and L_α phases being shown over very similar concentration and temperature ranges. In further work, these latter authors also record (157) the co-existence of two micellar phases for the C₁₀ derivative, an important observation which merits further work (149).

Hall *et al.* studied a series of 1-(alkanoylmethylamino) 1-deoxy-D-glucitols (C₈-C₁₂, C₁₈=) (158). These are also called *N*-methyl glucamides, with the presence of the *N*-methyl group increasing solubility compared to the glucamides referred to above. They form both thermotropic and lyotropic mesophases. Schematic phase diagrams were produced for all of the compounds by using the phase penetration technique with a complete phase diagram being produced for the C₁₀ compound (Figure 21.25). The C₈ derivative (C₈G) forms an H₁ phase when contacted with water. This exists between 0 and 39°C, melting to a micellar L₁ phase. C₉G forms an extensive range of mesophases, e.g. H₁ (15–69°C), V₁ (36–56°C) and L_α (44–76°C). All of these melt to an L₁ phase. C₁₀G observes the same phase sequence as C₉G. The H₁ phase forms between 42 and 75% surfactant (from 30–81°C), the V₁ phase between 67 and 79% (42–80°C) and the L_α phase between 75 and 100% (46–> 100°C). C₁₁G exhibits an H₁ phase between 33 and 86°C, and V₁ and L_α phases from 39.5 and 49°C, respectively, to > 100°C. Similarly, C₁₂G, exhibit phases of H₁ (45.5–75°C), V₁ and L_α (50 and 56°C, respectively, to > 100°C). The phase behaviour for C₁₈=G is much simpler, exhibiting only an L_α phase from 22 to > 100°C.

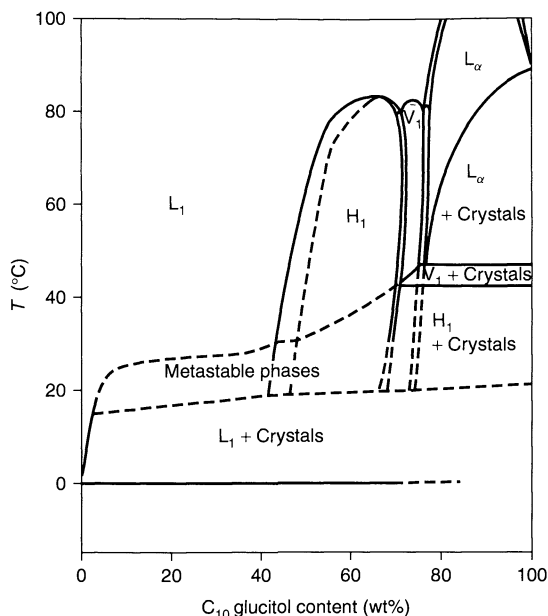


Figure 21.25. Phase diagram of the C₁₀ glucitol/water system: symbols used for phases, etc. are as given for Figure 21.13 (reproduced from ref. (158) with permission from Taylor & Francis Ltd)

Raaijmakers *et al.* studied the mesogenic properties of some 3-*O*-alkyl derivatives of D-glucitol and D-mannitol (159). Phase penetration scans have shown that the C_{10–16} glucitol derivatives and the C₁₂ mannitol derivative all exhibit lyomesophases. The 3-*O*-decyl-D-glucitol (C₁₀G) material gives an H₁ phase on penetration at room temperature, and on heating, a V₁ phase at 34°C and an L_α phase at 46°C. The solid bulk melts to L_α at 55°C and all phases exist to at least 98°C. C₁₂G gives an I₁ phase at 36°C, plus H₁ (37°C), V₁ (40°C) and L_α (46°C), with the solid melting to L_α at 65°C. All phases exist to > 100°C, with the exception of the H₁ which melts to an I₁ phase at 62°C. C₁₄G gives only V₁ and L_α phases from 48 to > 100°C. Below T_{pen} , the L_α phase cools to give an L_β gel phase, a transition which is reversible on reheating. C₁₆G gives an L_α phase from 52 to > 100°C. A reversible L_α-L_β transition is observed on cooling at 44°C. The pattern of phase formation in 3-*O*-dodecyl-D-mannitol (C₁₂M) is similar to C₁₂G with all transition temperatures approximately 20°C higher, apart from the melting temperature of the solid (97°C).

Finkelmann and Schafheutle have studied monomeric and polymeric amphiphiles containing a monosaccharide head-group (160). The monomer, *N*-D(-)-gluco-*N*-methyl-(12-acryloyloxy)dodecane-1-amide, exhibits L₁

(> 52°) and L_α phases (65–88%, 57–87°C), with a bi-phasic region separating the two. The polymer, poly[(*N*-D(-)-gluco-*N*-methyl-(12-acryloyloxy)dodecane-1-amide)] again exhibits L_1 and L_α phases, but these are formed at -0.1°C. The lamellar phase exists between 37 and 100% polymer, and up to 184.8°C. It is separated from the L_1 phase by a narrow bi-phasic region. There is a region of clouding ($L_1 + L_2$) reaching from ~ 0 to 31% polymer, with a lower critical temperature of 17.9°C at 4.6% and an upper critical temperature of 105.5°C at 9.6% polymer.

Most of the above studies involve changes in alkyl chain size, with no alteration of the head-group. In a very important early study, Sagitani and co-workers reported the behaviour of pure alkyl polyglycerol [$C_{12}O(CH_2CHOHCH_2O)_nOH$] surfactants with an ether-linked C_{12} alkyl chain, with $n = 1-4$ (161). The compounds with $n = 1$, and 2 give just a lamellar phase to over 120°C, while with $n = 4$, a micellar solution and a hexagonal phase occur. For $n = 3$, there is a cloud point at ca. 53°C, with both micellar solution and lamellar phase being present. The shape of the L_1/L_α phase boundary indicates the presence of an H_1 phase below the cloud point, i.e. remarkably similar behaviour to $C_{12}EO_6$, as these authors point out. In fact, poly-OH compounds do resemble EO nonionics, but with a very much reduced influence of temperature.

Much attention has been given recently to commercial polyglucoside surfactants (alkyl polyglucosides (APGs)) (162, 163), where the average number of "poly"-glucoside units (degree of polymerization (DP)) falls within 1–3. From the above studies, one expects short-chain derivatives with DP = ca. 1 to form L_1 , H_1 and L_α phases, while the low stability of the H_1 phase suggests that long-chain compounds will form L_α dispersions. Compounds with DP = 2 will give H_1 and L_α phases, while with DP = 3 or more the I_1 cubics will appear. Multi-phase co-existence is likely, along with the occurrence of metastable, sticky, viscous phases at high concentrations.

8 BLOCK COPOLYMER NONIONIC SURFACTANTS

Block copolymer surfactants show a qualitatively similar phase behaviour with temperature to conventional materials. However, solubility requires the presence of branched chains and/or ether links to reduce the occurrence of crystalline polymer with a high melting point. It must be emphasized that commercial polymeric surfactants are polydisperse in both alkyl chain and EO blocks,

and hence a range of molecular weights and head-group sizes will be present. This will certainly modify the behaviour compared to pure low-molar-mass surfactants, but should not qualitatively change it. It could lead to the occurrence of multi-phase regions, such as H_1 and L_α , or cubic regions, rather than single phases and "intermediate" structures that might occur with very monodisperse polymers.

Alexandridis *et al.* (164) have studied a number of block copolymers of ethylene oxide (EO), propylene oxide (-OCH₂CHCH₃- (PO)) and butylene oxide (-OCH₂CH(CH₂CH₃)- (BO)) in water and in ternary systems with *p*-xylene. The poly(propylene oxide) and poly(butylene oxide) blocks represent the hydrophilic portions in such systems. Obviously, the short methyl and ethyl branches will need to be included in any packing constraints considerations.

The phase behaviours of three ethylene oxide/propylene oxide ABA copolymers, (EO)₆(PO)₃₄(EO)₆ (L62), (EO)₁₃(PO)₃₀(EO)₁₃ (L64) and (EO)₃₇(PO)₅₈(EO)₃₇ (P105) have been investigated (164). The number of mesophases formed increases with the poly(ethylene oxide) content (Figure 21.26). L62 exhibits only a L_α phase, between 51 and 76% polymer, and from < 20 up to 65°C. Two-phase regions of lamellar phase with both L_1 and L_2 solution phases exist, with the former first seen at < 30% polymer. L64 has a small region of H_1 phase between 46 and 54% polymer; this forms at 22°C and melts at 46°C. The L_α phase exists between 48 and 82% polymer, from below 10 to 85°C. Again, the two-phase regions are fairly wide. P105 exhibits an I_1 cubic phase between 26 and 44% polymer, melting at 60°C. The H_1 (47–67%) and L_α (67–88%) are separated by a two-phase region and exist to > 85°C. Note that simple AB block copolymers are expected to resemble even more closely the conventional surfactants. (The ABA blocks are likely to assume a "U"-type conformation for the hydrophobic block.)

The ternary system of L64/P105/water was also studied (165) (Figure 21.27). At 25°C, a lamellar phase is formed along the L64–water axis between 61 and 79% polymer, and between 73 and 87% polymer on the P105–water axis, and extends all the way from one axis to the other. Upon increasing the water concentration, the hexagonal phase is formed. This extends between 52–55% on the L64–water axis and 47–67% on the P105–water axis. Additionally, there is an I_1 cubic phase between 28 and 43% P105, and a narrow melted V_1 phase between 58 and 59% L64 between the H_1 and L_α regions.

The L64/water (D_2O)/*p*-xylene ternary system exhibits L_1 , L_2 (containing a high *p*-xylene-to-water

is dominated by two- and three- phase regions. The L_α phase is formed along the polymer–water axis at polymer concentrations between 61 and 79%, and can accommodate up to 25% *p*-xylene. The H_1 phase is formed between the L_1 and L_α phases at polymer concentrations of between 43 and 56%; 3–4% xylene is actually required for this phase to form. The H_2 phase is formed between the L_α and L_2 phases, at polymer concentrations of between 48 and 73% polymer, with the water concentration varying in the range 13–18%. The V_2 phase forms in a narrow concentration range of 65–68% polymer. It is thought to have a space group of Ia3d.

For the $(EO)_{17}(BO)_{10}/D_2O/p$ -xylene system, Alexandridis *et al.* claimed the first occurrence, to their knowledge, of a reversed-micellar cubic phase in a “typical” ternary amphiphile/water/oil system (168), before studying and reporting the system in more detail (169). These authors report six mesophases and two solution phases at 25°C. On increasing the polymer concentration along the polymer–water axis the phase sequence L_1 (< 22% polymer), I_1 (23–37% polymer), H_1 (42–54% polymer) and L_α (62–84% polymer) is observed. At even higher concentrations, a polymer-rich paste-like phase is seen. The L_α phase is the most extensive of the mesophases and can accommodate up to 16% xylene. The I_1 phase most likely has the Im3m space group. Along the polymer–xylene axis, the same sequence of structures (sphere → cylinder → plane) is seen for the reversed-phases. The L_2 phase exists below 75% polymer, the I_2 between 47 and 62% polymer, the H_2 between 45 and 84% polymer, and the V_2 at ~80% polymer between the H_2 and L_α phases. The I_2 phase has the Fd3m space group, while the V_2 phase has the Ia3d group. Note that all of the reverse mesophases require the presence of water to form (whereas the normal mesophases can form without xylene).

A comparison of the phase behaviour of PEO/PPO and PEO/PBO copolymers in butanol/water was recently reported (170). (Note that in this paper, poly(butylene oxide) is referred to as polytetrahydrofuran.) “Pluronic F127”, $E_{100}P_{70}E_{100}$, exhibits L_1 , L_2 , I_1 , H_1 and L_α phases. The L_1 phase exists along the polymer–water axis up to 20% polymer, accommodating up to 10% butanol. The I_1 cubic phase supercedes the L_1 phase and exists up to 65% polymer. Its ability to solubilize butanol decreases with increasing polymer concentration. The H_1 phase is formed at above ~20% polymer, although at least 15% butanol is required for it to form. A maximum of ~23% butanol can be accommodated in the H_1 phase. As the polymer concentration is increased, the butanol concentration required to form the H_1 phase decreases,

and between 70 and 80% polymer no butanol is required. The L_α phase is stable in the 20–30% polymer and 25–30% butanol ranges. A large L_2 region extends from the butanol-rich corner down to 20% butanol. Note that when butanol is replaced by hexanol, the L_1 and L_2 regions are reduced and the I_1 phase is still observed, along with a birefringent phase that was not investigated.

$E_{100}B_{27}E_{100}$ is of a similar molecular weight to $E_{100}P_{70}E_{100}$, but with a more hydrophobic middle block. Only a single one-phase region is observed, extending from the water-rich corner over a middle region to the butanol-rich corner. No liquid crystalline phases are observed. The $E_{17}B_{27}E_{17}$ /butanol/water system also shows only a single one-phase region and no mesophases.

9 ZWITTERIONIC SURFACTANTS

Zwitterionic surfactants broadly resemble nonionic materials, but because two bulky charged groups are usually involved, the head-groups are large. An exception is dimethyldodecylamine oxide (171) which has a compact head-group. This surfactant forms H_1 , V_1 and L_α phases. The H_1 phases (termed the “middle phase” in this paper) exists between 35 and 65% surfactant and from < 20°C to > 105°C. The V_1 (viscous isotropic) phase has a narrow range of existence (65–70% surfactant) and melts at a slightly higher temperature than the H_1 phase. The L_α (neat) phase exists between 70 and 80% surfactant at 20°, and up to 95% surfactant at 90°C. This melts at > 140°C. The C_{14} compound exhibits a similar phase behaviour (172), but also has a nematic phase (N_D) between 31 and 35% surfactant, up to 60°C.

A more typical surfactant is dodecyldimethylammonio propane sulphonate (173). This forms an I_1 cubic phase between 49.5 and 63% surfactant from ~20°C up to ~85°C. A hexagonal phase (65–87% surfactant) forms at a slightly higher temperature but exists up to > 160°C. A lamellar phase is seen at very high concentrations and above 170°C. Below this is a hydrated solid surfactant phase which when viewed under a polarizing microscope has the optical appearance of a gel phase.

10 IONIC SURFACTANTS

Ionic surfactants have been studied over a much longer period than nonionic materials, although the long-range electrostatic interactions and the insolubility of long-chain materials have resulted in the general picture

of mesophase behaviour emerging only rather slowly. Typical surfactants with a single-charge ionic group usually give small globular micelles and H_1 as the low-concentration mesophase. As the chain length increases (and if solubility allows), then long rod-micelles form and a rod nematic phase can occur at the L_1/H_1 boundary. Occasionally, if the counterion is highly dissociated, an I_1 phase can occur as the first mesophase. Otherwise, two charged groups are required for I_1 formation. At higher concentrations, the sequence $H_1/V_1/L_\alpha$ changes to H_1 /Intermediate/ L_α (or a combination of the two) as the alkyl chain size increases. In this region, there can be long-lived metastable phases that are difficult to work with and prevent the easy determination of equilibrium boundaries.

Sodium dodecyl sulfate (SDS) is a very commonly used surfactant, and yet for many years its mesophase behaviour was not studied in detail. One reason for this is the number of phases to be dealt with. Besides the lamellar and hexagonal phases, there are a number of

intermediate phases existing over narrow concentration ranges (88). The complete phase diagram was reported by Kékicheff *et al* (72) (Figure 21.28). (Note that in this paper, the hexagonal phase is represented by the symbol H_α .) Between the H_α and L_α phases, the authors identify four intermediate phases, with bi-phasic regions separating most of the single-phase regions. The H_α phase is first seen at 37% (with L_1) and at 40% in a single-phase region at 25.7°C. A two-dimensional monoclinic phase (M_α) exists with the H_α phase from 57–59% up to 58°C. Note that this is the only mesophase region that doesn't exist up to $\sim 100^\circ\text{C}$. On increasing the surfactant concentration between 59 and 69%, the phase sequence is M_α (40.1°C), $M_\alpha + R_\alpha$ (rhombohedral), R_α (43.0°C), Q_α (cubic, 47.8°C), $Q_\alpha + T_\alpha$ (tetragonal), T_α (48.5°C), $T_\alpha + L_\alpha$, and L_α (49.8°C). The L_α phase exists up to 87% surfactant, above which it co-exists with a crystal phase. Despite the extensive work involved in this diagram, there still remain questions to answer. For example, the

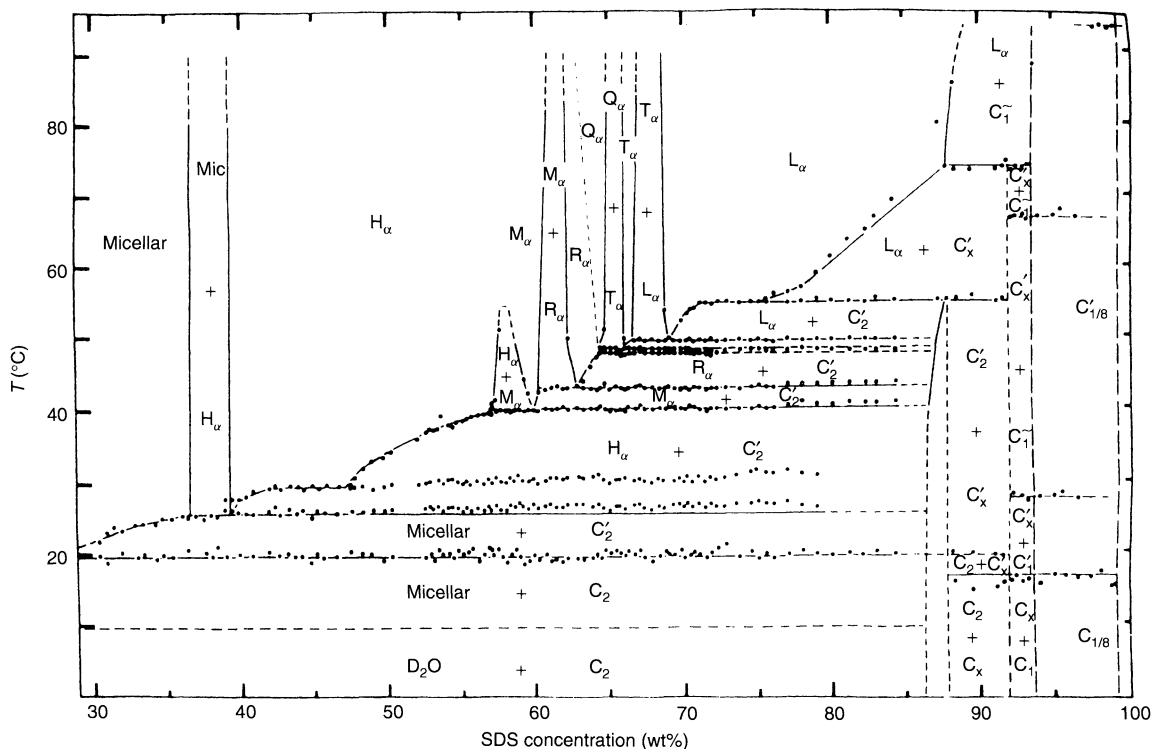


Figure 21.28. Phase diagram of the SDS/water system: H_α , hexagonal phase; M_α , two-dimensional monoclinic phase; R_α , rhombohedral phase; Q_α , cubic phase; T_α , tetragonal phase; C , C' and C'' , refer to different polymorphic varieties for the same SDS hydrate; other phases, etc. as for Figure 21.13 (Reprinted with permission from ref. (189). Copyright (1996) American Chemical Society)

disappearance of the $H_\alpha + M_\alpha$ two-phase region is difficult to understand. Note that this system typifies those where equilibration between different states is expected to be slow (as mentioned above).

Another system showing an intermediate phase between the H_1 and L_α phase is that of caesium tetradeconoate–water (174). The phase behaviour between 24 and 80°C was studied in detail (Figure 21.29). The H_1 phase is first seen in a two-phase region with an L_1 micellar phase at 33% surfactant and in a single-phase region between 37 and 67%. Above 65°C, the H_α phase is replaced by a two-phase $H_\alpha + V_1$ region. However, below this temperature, a ribbon phase (R) is formed. The most likely structure of this phase is rod-like aggregates with an elliptic cross-section. At 24°C, the R phase exists from 62–72% surfactant, with the concentration range decreasing with increasing temperature. Below 39°C, a bi-phasic R + L_α region exists between 72 and 75% surfactant, while between 39 and 65°C the two phase region is R + V_1 . The V_1 region is very narrow (~2% surfactant) and is bordered by a two-phase $V_1 + L_\alpha$ region up to 75% surfactant. The lamellar phase exists to over 90% surfactant. That the sequence of phases can be very complex and varies with chain size is illustrated by the “penetration scan” table reported by Rendall *et al.* (175). Here, the “intermediate” phase types have not been identified, but the general pattern and complexity of behaviour is clear. One should also caution that minor levels of surface-active impurities are likely to have a marked influence on the cubic/intermediate phases, particularly if the

impurities are uncharged cosurfactants (often likely to be present from the chemical synthesis).

One of the first major surveys into the phase behaviour of cationic surfactants was reported by Blackmore and Tiddy who undertook penetration scans on a variety of surfactants with a range of alkyl chain sizes, including the NH_3^+ , NMe_3^+ , NEt_3^+ , NPr_3^+ and NBu_3^+ series (176). Previous studies had mostly been limited to alkylammonium and alkylmethylammonium salts (44, 177, 178). These show a qualitatively similar pattern of behaviour to that of the anionic systems, with the sequence $H_1/V_1/L_\alpha$ for short-chain derivatives being replaced by H_1 /Intermediate/ L_α for long-chain compounds. For the intermediate chain lengths, V_1 phases replace the intermediate structures as the temperature increases.

Surfactants containing divalent head-groups have received little attention. Hagslätt *et al.* have investigated a number of these (179). Dodecyl-1,3-propylenebis(ammonium chloride) (DoPDAC) has a head-group consisting of two protonated amine groups separated by a propylene group (179). The surfactant shows conventional phase behaviour in water (D_2O) (Figure 21.30), forming L_1 , I_1 cubic (denoted as I_1'), H_1 hexagonal (denoted as E), V_1 cubic (denoted as I_1'') and L_α lamellar (denoted as D) phases. The I_1 cubic phase forms at 30% surfactant at ~30°C and exists up to ~150°C. The hexagonal phase is seen at 42% surfactant from 38 to > 160°C. Between 65 and 72% surfactant, the H_1 phase melts to the V_1 cubic phase (which forms above

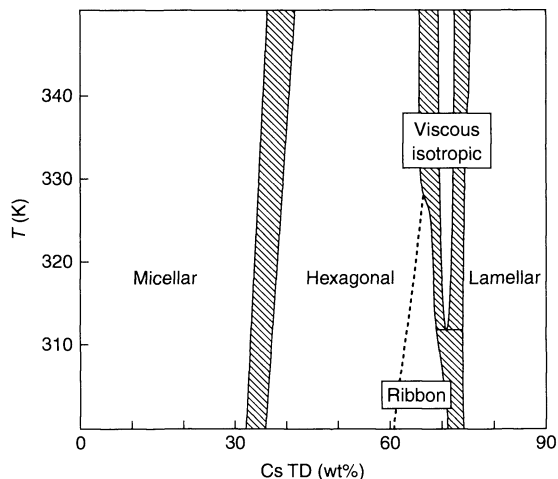


Figure 21.29. Phase diagram of the caesium tetradeconoate (CsTD)/water system (reproduced from ref. (174) with permission of Academic Press)

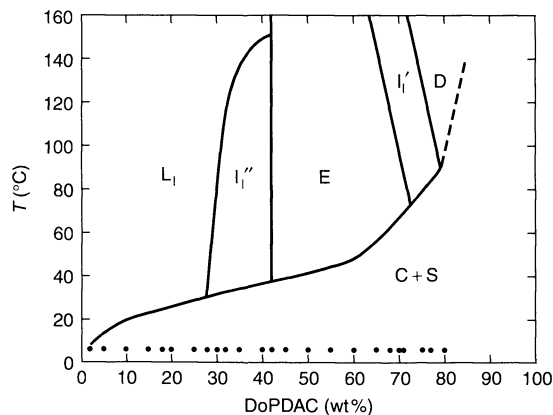


Figure 21.30. Phase diagram of the dodecyl-1,3-propylenebis(ammonium chloride) (DoPDAC)/water system: C+S, indicates the presence of solid surfactant; other phases, etc. as for Figures 21.13, 21.14, 21.23 and 21.26 (Reprinted with permission from ref. (179). Copyright (1991) American Chemical Society)

$\sim 75^\circ\text{C}$). Similarly, above 72% surfactant the V_1 phase melts to an L_α lamellar phase. At 79%, surfactant the L_α phase forms at 90°C . Note that the Krafft boundary has a rather large slope. Usually for monovalent surfactants, the Krafft boundary is flat or has only a small slope (50).

These workers also studied the ternary phase diagram of the divalent surfactant dipotassium dodecylphosphate (K_2DoP), the monovalent surfactant potassium tetradeconoate (KTD) and D_2O (180). At 25°C , K_2DoP exhibits L_1 (0–37% surfactant), I_1 (37–67%) and H_1 (67–75%) phases, plus a two-phase liquid crystal/hydrated surfactant crystal (75–100%). In the ternary system, the I_1 cubic phase is seen between 20 and 60% K_2DoP . Up to 30% KTD can be incorporated into the phase at lower concentrations of K_2DoP . On decreasing the percentage of D_2O along the D_2O –KTD axis, hexagonal (E), ribbon (R), intermediate (possibly orthorhombic) and lamellar (D) phases are seen. The hexagonal phase exists right down to the K_2DoP – D_2O axis (70–75% K_2DoP), whereas the maximum K_2DoP concentrations for the ribbon, intermediate and lamellar phases are 45, 24 and 22%, respectively.

Amphitropic (also referred to as amphotropic) surfactants are compounds containing both lyotropic (e.g. quaternary ammonium head-groups) and thermotropic (e.g. oxycyanobiphenyl (OCB) groups, moieties (181). Fuller and co-workers have reported on two such compounds. The first of these, 10-(4'-cyano-4-biphenyloxy)decyltriethylammonium bromide, exhibits only an L_α phase (182, 183) from 22 to $>90\%$ surfactant with a temperature range of 33 – 100°C . The second compound, N,N' -bis[5-(4'-cyano-4-biphenyloxy)pentyl]-(N,N,N',N' -tetramethylhexanediammonium dibromide (5-6-5 OCB), exhibits two L_α phases with a re-entrant L'_1 micellar phase between them (Figure 21.31). The low-concentration lamellar phase (L_α) exists between 18 and 64% surfactant, up to 65°C . Between 35 and 47% surfactant, the melting temperature of the L_α phase decreases from 65 to 50°C with increasing surfactant concentration. At this concentration, the high-concentration phase (L'_α) appears and exists to $>80\%$ surfactant and $>90^\circ\text{C}$. Note that the absence of H_1 and V_1 phases is due to the difficulty of packing the bulky oxycyanobiphenyl group into spherical or rod-like micelle interiors. The influence of a range of added electrolytes on the lamellar phase of the first surfactant was studied (184) in order to induce the co-existence of two lamellar phases. This experiment failed, although a wide co-existence region of micellar and lamellar phases was observed. This indicated that the two lamellar phases arises from the specific adsorption of counterions. In further work (185), it was demonstrated that the addition of thermotropic mesogens

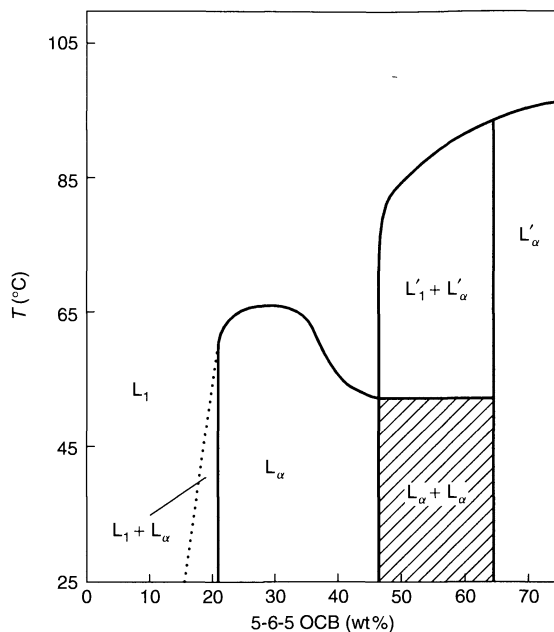


Figure 21.31. Phase diagram of the '5-6-5 OCB'/water system; symbols used for phases, etc. as for Figure 21.13 (reproduced from ref. (181) with permission from Taylor & Francis Ltd)

stabilized the lamellar phase, thus suggesting a route to obtain *true amphitropic mesophases!*

The second of the above compounds is an example of a so-called "gemini" surfactant. Recently, there has been considerable interest in these surfactants, which are double-headed cationic compounds where two alkyldimethyl quaternary ammonium groups per molecule are linked by a hydrocarbon spacer chain. (These are denoted as n - m - n surfactants, where n is the length of the terminal alkyl chains and m the length of the spacer chain.) In the second paper (183), Fuller *et al.* reported the phase behaviour of further m - n - m OCB surfactants and some straight-chain 15 - n - 15 surfactants ($n = 1, 2, 3$ and 6). Note that these compounds have terminal hydrophobic chains of the same length as the oxycyanobiphenyl compounds. The m - n - m OCB surfactants all give just a lamellar phase from $<18^\circ$ – $>100^\circ\text{C}$. Penetration scans on the 15 - n - 15 surfactants show that they all exhibit H_1 , V_1 and L_α phases to $>100^\circ\text{C}$. Additionally, a nematic phase is seen for $m = 1$ and 2 , and intermediate phases for $m = 1, 2$ and 3 .

Zana and co-workers have investigated various properties of a series of gemini surfactants, including their thermotropic and lyotropic phase behaviours.

These authors report that the 12-4-12 and 12-8-12 compounds form hexagonal and lamellar phases in water (186, 187). For the latter compound, the H_1 phase exists between ~ 55 and 78% surfactant and the L_α phase between 82 and 97% surfactant. The phase behaviour of a wide range of gemini surfactants ($n = 12-18$, $m = 2-20$) has now been studied and a wide range of phases observed (188). Generally, the phases are qualitatively in accord with packing constraint expectations, where the spacer group is included in the hydrophobic volume. However, unusual partial miscibility regions involving hexagonal, lamellar or concentrated surfactant solutions in co-existence with dilute solutions are also observed.

Pérez *et al* (189) have studied a series of novel gemini surfactants with guanidyl head-groups (from the amino acid arginine); such compounds are referred to as “bis(Args)”. They are made up of two symmetrical N^α -acyl-L-arginine residues of 10 ($C_n(\text{CA})_2$) or 12 ($C_n(\text{LA})_2$) carbon atoms linked by covalent bonds to an α,ω -alkenediamine spacer chain of varying length, n ($n = 3, 6$ and 9). In the $C_3(\text{LA})_2$ and $C_6(\text{LA})_2$ /water systems, an H_1 phase is seen at very low surfactant concentrations (lower than 5%) between 4 and 20°C. Penetration scans have shown that in $C_9(\text{LA})_2$, the H_1 phase is replaced by an L_α phase.

11 THE INFLUENCE OF THIRD COMPONENTS: COSURFACTANTS, MIXED SURFACTANTS, OILS, HYDROTROPES, ELECTROLYTES AND ALTERNATIVE SOLVENTS

There is a vast body of data concerning the influence of third components on surfactant liquid crystals. Because of the potentially great complexity of the inherent mesophase behaviour, this array of data can appear to be enormously difficult to rationalize. However, if we consider the simple concepts described above (micelle formation, micelle shape/packing constraints, volume fractions and the nature of intermicellar interactions), then a reasonably simplified picture emerges, at least for the water-continuous phases. This present section does not attempt to be comprehensive – it simply reports selected examples of behaviour to illustrate the general concepts. The simplest way to show the changes in mesophase behaviour is to employ ternary phase diagrams. The reader should recall that the important factors are (i) *the behaviour as a function of surfactant/additive ratio*, and (ii) *the volume*

fraction of surfactant plus amphiphile (where present) for mesophase formation.

11.1 Cosurfactants

Cosurfactants are “surfactants” that are insufficiently hydrophilic to form micelles or mesophases with water alone, but can have dramatic effects when mixed with normal surfactants. Examples of such materials are alcohols, fatty acids and long-chain aldehydes. Depending on the strength of the polar group hydration, there is greater or smaller incorporation of the cosurfactant into mesophases. The extent to which the polar group resides at the micelle surface also has a profound effect on the mesophases. Weakly polar groups, such as methyl esters, can occupy both the micelle interior and reside with the ester group at the surface. They could be classified as “polar oils”. Thus, cosurfactants span the range of properties from oils to surfactants. In order to illustrate the effects, we show the behaviour of a simple surfactant, sodium octanoate, with various additives taken from the extensive body of research produced by Per Ekwall, Kristofer Fontell and their co-workers (50, 190). Sodium octanoate forms only a hexagonal phase at room temperature, but with V_1 cubic and lamellar phases occurring at higher temperatures. Figures 21.32–21.34 show the ternary phase behaviours of sodium octanoate with decanol, octyl aldehyde (octanal) and methyl octanoate, respectively.

All three additives have roughly the same alkyl chain length and volume as sodium octanoate (decanol is just a bit bigger). Data for the phase behaviour of octanol/sodium octanoate/water are available, although the decanol system has received the most attention by far! We see that decanol mixes in the system to form a large lamellar region, and even an inverse-hexagonal phase. This is because the alcohol group always resides at the water/alkyl chain surface. Its contribution to the micelle area is ca. 12 \AA^2 , and since sodium octanoate has a head-group size of ca. 58 \AA^2 in the mesophases, packing constraint calculations suggest a hexagonal/lamellar transition at a sodium octanoate/decanol weight ratio of 7:3, in excellent agreement with the phase diagram. (A theoretical calculation of this type of phase behaviour has been described by Wennerström and Jönsson (191).) The other two additives are dissolved much more extensively within the hexagonal region, presumably because they occupy the micelle interior to some extent. Octanal can reside at the micelle surface to some degree because it forms a lamellar phase which is in equilibrium with L_1 , and hence disc

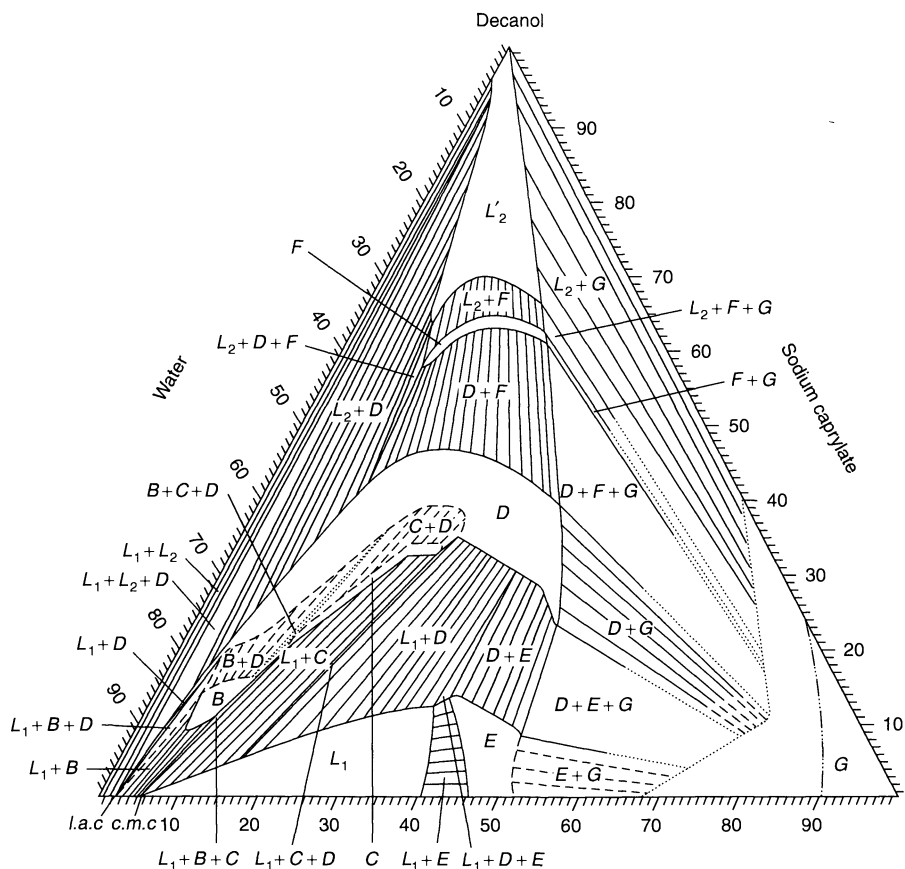


Figure 21.32. Phase diagram of the sodium octanoate (caprylate)/decanol/water system: B, 'mucous woven' lamellar phase; C, tetragonal phase; F, reversed-phase; G, isotropic phase; other phases, etc. as for Figures 21.13, 21.16, 21.22 and 21.26 (reproduced from ref. (50) with permission of Academic Press)

micelles can occur. Methyl octanoate mainly resides in the micelle interior, and thus the lamellar phase does not have a boundary with L_1 . The fact that the lamellar phase appears rather than a V_1 cubic phase is a general observation. *Both intermediate and bicontinuous cubic phases are much less frequently encountered in multicomponent systems than in binary surfactant/water mixtures.*

11.2 Mixed surfactants

The behaviour of mixed surfactants (at least in water-rich regions) can be understood by considering the nature of interactions between the head-groups and various packing constraints. A simple example is that of the commercial nonionic surfactants reported by

Bouwstra *et al.* (192). These authors compared the phase behaviour of technical-grade $C_{12}EO_{<7>}$ and pure $C_{12}EO_6$. The ternary phase behaviour with water and decane were studied and compared. Both exhibited I_1 , H_1 and L_1 phases, but only $C_{12}EO_6$ gives a very small region of a V_1 cubic phase. Note that the I_1 phase is not seen in the binary $C_{12}EO_6$ /water system (46). In addition, their X-ray data indicated that the H_1 phase in $C_{12}EO_6$ is composed of infinite long rods, whereas short interrupted rods were reported for the hexagonal phase of $C_{12}EO_{<7>}$.

Where ionic surfactants are involved, like charges show only small changes in phase structures, but overall solubility can be greatly increased because surfactants do not generally form mixed crystals, and hence each increases the solubility of the other. For surfactants with opposite charges, usually the mixed salt

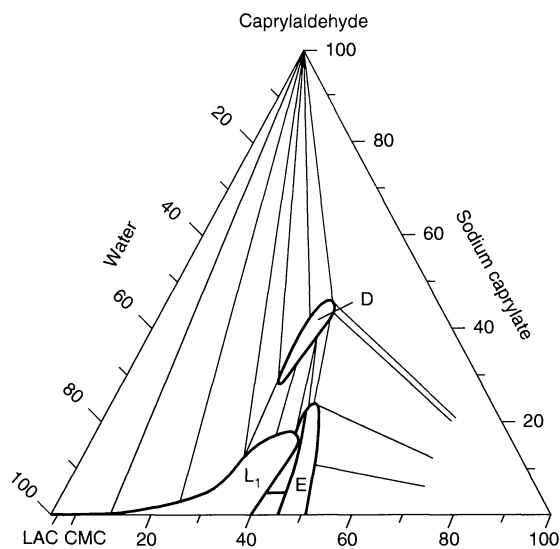


Figure 21.33. Phase diagram of the sodium octanoate (caprylate)/octanol (caprylaldehyde)/water system; symbols used for phases, etc. as for Figures 21.13, 21.16 and 21.22 (reproduced from ref. (50) with permission of Academic Press)

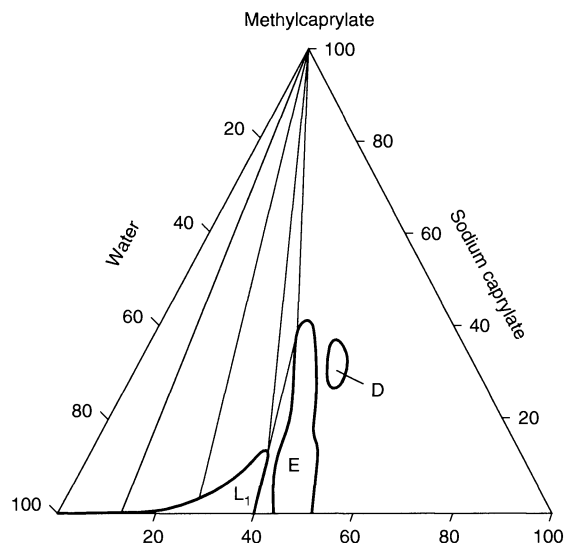


Figure 21.34. Phase diagram of the sodium octanoate (caprylate)/methyl octanoate methyl caprylate/water system; symbols used for phases, etc. as for Figures 21.13, 21.22 and 21.26 (reproduced from ref. (50) with permission of Academic Press)

is insoluble. Where solubility does occur, the average head-group size is much reduced because of the neutralized electrostatic repulsions. Typically, cationic and

anionic surfactants, which alone form hexagonal or I_1 cubic phases, form lamellar phases at low concentrations in 1:1 mixtures (193). Obviously, with dialkyl surfactants more complex behaviour can occur.

11.3 Oils

Oils are solubilized into the interior of micelles where they allow the micelle to swell to a larger radius, hence giving rise to cubic (I_1) and hexagonal (H_1) phases at smaller a -values than for the surfactant alone. Polar oils can also reside at the micelle surface to some extent, thus reducing micelle curvature and inducing the occurrence of lamellar and inverse phases. This behaviour is typified by the behaviour of the commercial non-ionic surfactant nonylphenol-(probably branched)-decaethylene oxide (EMU-09) with and p -xylene and hexadecane (50) (see Figures 21.35 and 21.36, respectively).

These figures show that the hexadecane induces the formation of an I_1 cubic phase, whereas the much more polarizable p -xylene, which can reside at the chain/water interface, induces a lamellar phase. As expected with the increase in micelle diameter, all of the

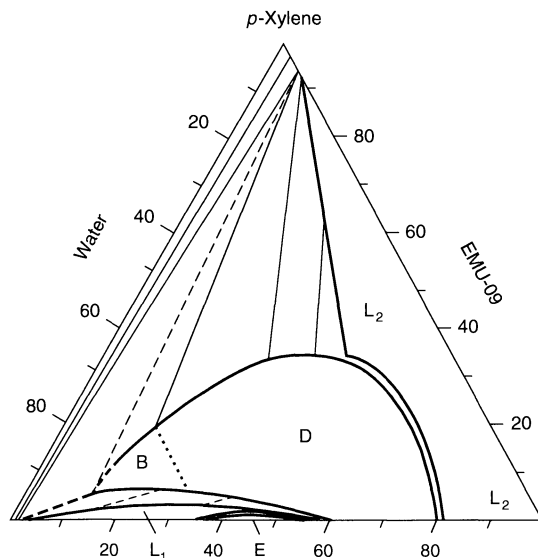


Figure 21.35. Phase diagram of the commercial nonionic surfactant, nonylphenol-(probably branched)-decaethylene oxide (EMU-09)/ p -xylene/water system; symbols used for phases, etc. as for Figures 21.13, 21.16, 21.22 and 21.28 (reproduced from ref. (50) with permission of Academic Press)

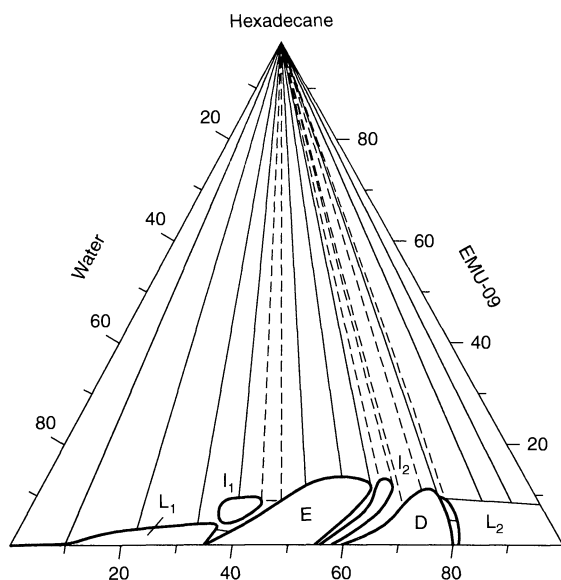


Figure 21.36. Phase diagram of the commercial nonionic surfactant, nonylphenol-(probably branched)-decaethylene oxide (EMU-09)/hexadecane/water system; symbols used for phases, etc. as for Figure 21.13, 21.16, 21.22 and 21.26 (reproduced from ref. (50) with permission of Academic Press)

phases have their boundaries shifted to higher volume fractions with hexadecane addition.

For surfactants having small polar groups and bulky chains, there can be extensive effects with the addition of oils. Alone with water, the surfactants form reversed micelles and/or reversed mesophases. Large volumes of oil can be incorporated into these systems because of the possibility of swelling the alkyl chain regions in these oil-continuous phases (L_2 , H_2 and V_2). While extensive research has been carried out in this area, it appears to be much more complex than for the water-continuous phases. Each different surfactant type can show individual behaviour according to the curvature properties of the surfactant layer.

11.4 Hydrotropes

Hydrotropes are small, highly water-soluble additives that increase markedly the solubility of other components, including surfactants, in water. They are employed very widely in industry. In fact, they only work when the “insoluble” phase is a mesophase with high molecular mobility (e.g. a polymer coacervate

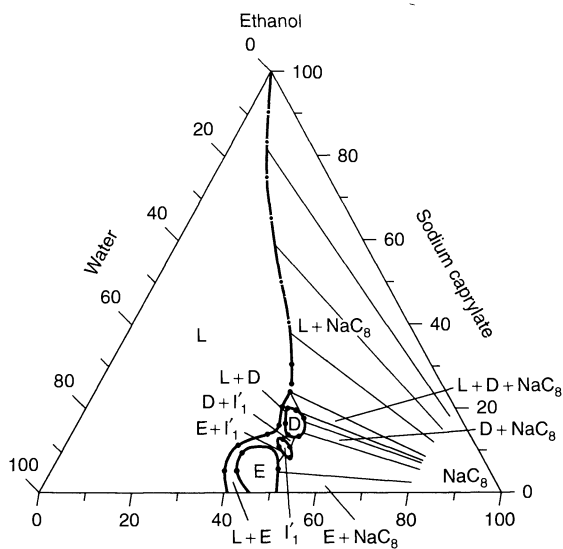


Figure 21.37. Phase diagram of the sodium octanoate (caprylate)/ethanol/water system; symbols used for phases, etc. as for Figures 21.14, 21.21, 21.22 and 21.26 (reproduced from ref. (50) with permission of Academic Press)

or surfactant mesophase). These include weakly self-associating electrolytes such as sodium xylene sulfonate and short-chain alcohols. Their influence can be illustrated by the effect of ethanol on the hexagonal mesophase of sodium octanoate (Figure 21.37).

Ethanol “solubilizes” the hexagonal phase, shifting the boundary from ca. 40 to ca. 45%, although it initially stabilizes it. There is almost no increase in the maximum solubility of crystalline surfactant. Where *mesophases* occur over a wider concentration range (say, 10–40%) then hydrotropes can sharply increase the isotropic solution range by removing the mesophase.

11.5 Electrolytes

The influence of electrolytes divides into two areas, i.e. the influence on nonionic (uncharged) surfactants and that on ionic materials. For nonionic surfactants, the effects are either “salting-out” or “salting-in”, in line with observations from the Hoffmeister series of electrolyte effects on protein precipitation. While there has been much discussion over the past 50 years on the molecular mechanism involved, including many words on the “structure” of water, Ninham and Yaminsky have recently shown in a *landmark* paper that the phenomena can be explained by dispersion interactions (194).

Essentially, electrolytes that are adsorbed to surfactants increase their solubility, and hence mesophases dissolve. Those that are desorbed from the aggregates raise the chemical potential and decrease the solubility. Like hydrotropes, large effects are seen only with mesophase or "coacervate" precipitates. For ionic surfactants, there are two additional effects. Where a counterion that produces an insoluble surfactant salt is present then any mesophases are removed by an increase of the Krafft temperature. In addition, the well-known common-ion effect raises the Krafft temperatures. Furthermore, electrolytes have a marked influence on the CMC values, reducing the relatively high values of ionic surfactants to the low values of zwitterionic derivatives. This happens typically when the added electrolyte level is of the same order as the CMC range (ca. 1–300% of the CMC without electrolyte). Otherwise, where solubility is maintained at high electrolyte levels, one observes salting-in or salting-out effects. These can be illustrated by the phase behaviour of sodium soaps with water (Figure 21.38) (195).

Added electrolyte induces co-existence between a dilute aqueous phase and micellar solutions (similar to a nonionic surfactant cloud temperature) and then changes the hexagonal phase to the lamellar phase. Clearly, the ionic surfactant mesophase dissolves in water because of electrostatic repulsions. High-salt levels negate the electrostatic repulsions, changing the behaviour to that of a moderately polar surfactant (e.g. $C_{12}EO_3$). Salting-in electrolytes, such as sodium thiocyanate, are likely to

cause the lamellar phase to swell to much higher water levels. If the adsorption of thiocyanate ions is sufficient, it is possible that micelles will form again at very high levels. This behaviour merits further study.

11.6 Alternative solvents

Over recent years, the question of whether or not surfactants form aggregates similar to micelles, which then form mesophases in other polar solvents, has received considerable attention (196–219). The solvents concerned are polar liquids such as glycerol, ethylene glycol, formamide or ethyl ammonium nitrate (a molten electrolyte at ambient temperature). The answer is YES, but the thermodynamics of the aggregation process is somewhat different. Figures 21.39 and 21.40 show measurements of the EMF from a surfactant-specific electrode in hexadecylpyridinium bromide solutions where water and ethylene glycol are solvents.

These results clearly show that aggregates form over a very narrow concentration range in ethylene glycol, similar to micelle formation. However, the aggregation concentration is higher by two orders of magnitude – simply because the "solvophobic" effect is much smaller than the hydrophobic effect. In fact, a useful "rule of thumb" is that a surfactant with a C_{16} chain in the alternative solvents resembles a C_{12} surfactant in water. It seems that at least a C_{10} or C_{12} chain is required for micelle-like aggregation in these solvents.

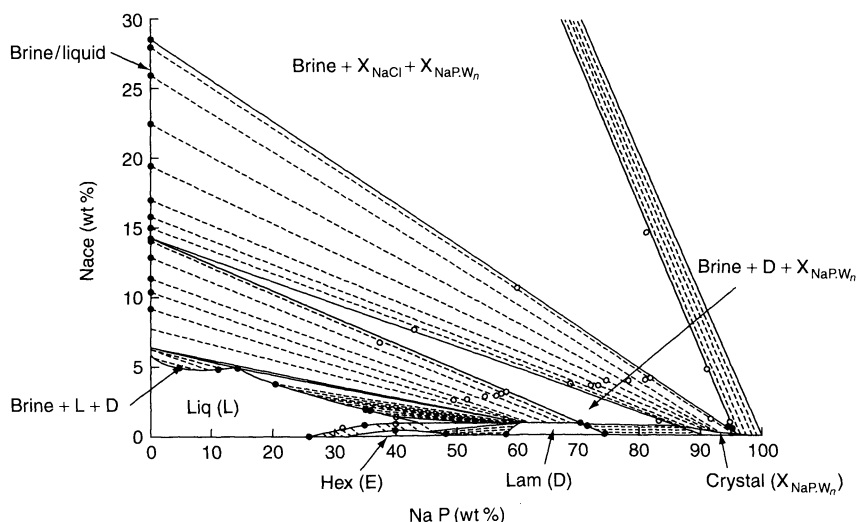


Figure 21.38. Phase diagram of the sodium palmitate (NaP)/sodium chloride/water system at 90°C (reproduced from ref. (195) with permission of Academic Press)

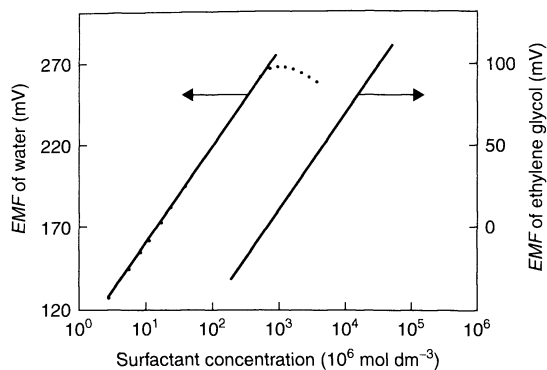


Figure 21.39. EMF from a surfactant-specific (cetylpyridinium bromide) electrode as a function of concentration for solutions in water and ethylene glycol (cf. Figure 21.40) (reproduced from ref. (196) by permission of The Royal Society of Chemistry)

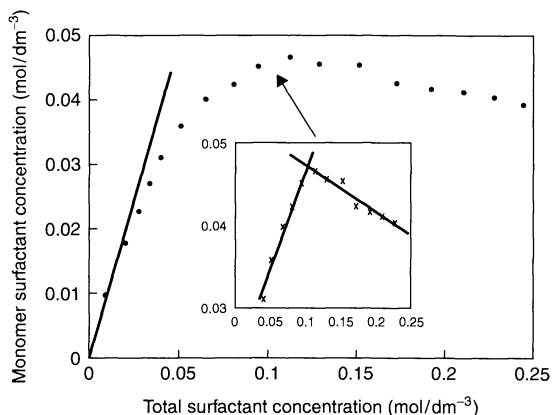


Figure 21.40. The monomer concentration of cetylpyridinium bromide as a function of total concentration (cf. Figure 21.39) (reproduced from ref. (196) by permission of The Royal Society of Chemistry)

The mesophase behaviour is remarkably similar to that in water, again with a C_{16} chain derivative in the solvent resembling that of a C_{12} surfactant in water. There are, of course, detailed differences. Thus, cubic phases are stabilized over the intermediate phases (as expected for shorter-chain surfactants). Polyoxyethylenes are not miscible with glycerol, so they form no mesophases. In the main though, given the large differences between the nature of the polar solvents and water (molecular size, symmetry, polarity, hydrogen-bonding ability, conformational freedom, influence on electrostatics, etc.), this similarity is remarkable. Table 21.2 shows the

mesophase behaviour of octadecylpyridinium bromide in a range of solvents.

The phase sequence and types are all remarkably similar. Only formamide shows a real difference, with I_1 cubic phases being observed. Even so, these *are* formed by shorter-chain derivatives (the chloride salts) in water, so their occurrence with the longer-chain bromide is different – but *not that much!* The phase diagrams (Figure 21.41) show clearly that in ethylammonium nitrate as solvent the boundaries are shifted to much higher concentrations, again resembling a shorter-chain surfactant.

12 CONCLUSIONS AND THE FUTURE

It is clear that a framework based on packing constraints, surfactant chemical type, and water (solvent)–surfactant interactions now exists, so that the pattern of solvent-continuous surfactant mesophases can be rationalized for a wide range of materials, both for water and other polar solvents. Moreover, many data exist on the influence of additives, which can be seen to fit into the general picture. While no mention of theoretical computer modelling has been made here, this is an area that is evolving rapidly at present. Both molecular and mesoscopic models are under development that should enable semi-quantitative computer predictions of phase behaviour to be made within the next few years. These should be able to shed light on remaining problems such as the structures of intermediate and gel phases. However, further experimental work *is* still required on the structures of intermediate phases and gel phases. In addition, the knowledge of mesophase glasses and particularly other semi-solid mesophases is at a rather primitive level. For example, we have not discussed at all the mesophases where the head-groups are partially crystalline and chains are molten (220). These swell in oil, in a type of behaviour that is analogous to that of L_β phases that swell in water. Moreover, the general framework can now be employed to rationalize surfactant mesophase behaviour with more complex additives such as well-defined biomolecules (e.g. proteins), as well as synthetic polymers of all types. Membrane protein crystals (where the protein hydrophobic region is covered by surfactant) certainly fall into this class. Lyotropic liquid crystals have recently been investigated as suitable media for membrane protein crystallization (221). Such studies will certainly grow in the immediate future.

Table 21.2. Phase penetration data of anhydrous octadecylpyridinium bromide, showing the temperature ranges of the mesophases (217). The sequence of columns indicates the order of the phases with increasing surfactant concentration: the first temperature given is T_{pen} ; the second indicates the upper temperature limit of the mesophase

Solvent ^a	Temperature/range (°C)					
	I_1	L_1^b	H_1^c	L_1^{nd}	V_1^c	$L_\alpha^{c,e}$
Water	–	–	43–100+	–	54–100+	59–100+
EG	–	–	44–108	99	54–106	56–150+
GLY	–	–	31–150+	–	48–150+	48–150+
FA	48–61	57	50–100+	–	61–100+	61–100+
EAN	–	–	49–120+	–	74–120+	73–120+

^aEG, ethylene glycol; GLY, ●●●; FA, ●●●; EAN, ethyl ammonium nitrate.

^b L_1^b , indicates L_1 intrusion between the I_1 and H_1 phases.

^c $+/-$, indicates that the mesophase is stable above the temperature given (the temperature limit).

^d L_1^{nd} , indicates L_1 intrusion between the H_1 and V_1 phases.

^eThe anhydrous surfactant forms the L_α phase at 74–75°C.

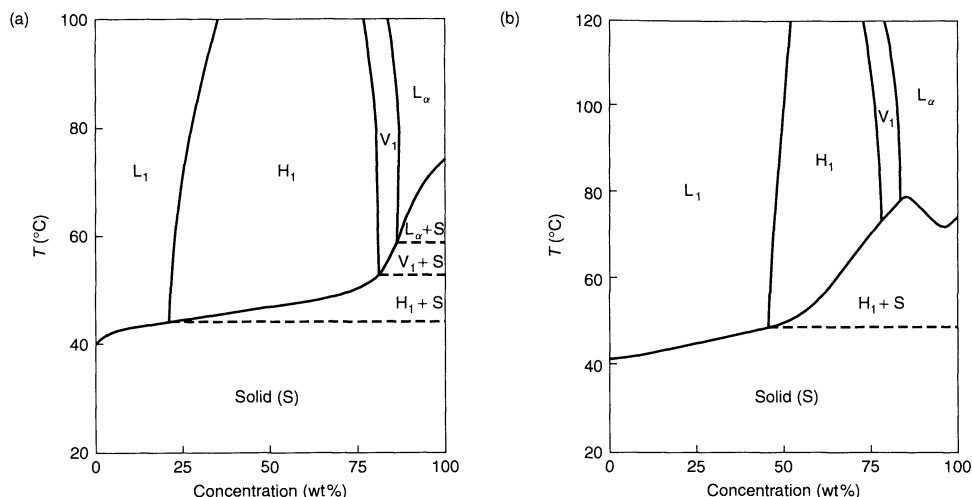


Figure 21.41. Phase diagrams of (a) octadecylpyridinium bromide/water and (b) octadecylpyridinium bromide/ethylammonium nitrate; Symbols used as for Figure 21.13 (reprinted from ref. (217) by courtesy of Marcel Dekker, Inc.)

It is now timely to consider problems where mesophase kinetics are important. Mesophase formation is involved in the applications of many specialist formulated products, including detergents. Recent advances in instrumental techniques allow the initial events that occur on mixing surfactant and water to be monitored, for example by using synchrotron X-ray diffraction and a fast-mixing cell (222). To develop a proper understanding of the behaviour will require a consideration of diffusion processes in labile anisotropic media – an exciting opportunity for computational modelling.

Rheology is perhaps the most important user property of surfactant mesophases, since almost every product is

pumped, poured and stirred. Recent developments mean that it is now possible to make X-ray, neutron, optical microscopy and other measurements on flowing systems to relate macroscopic orientation/morphology to rheological properties at the same time as molecular/aggregate reorientation is also studied (223). This offers the exciting prospect that in future not only will it be possible to formulate products for control of the mesophase structure through an understanding of ideas such as packing constraints, etc., but rheological properties and dissolution rates will be controlled to deliver optimum benefit to customers. The future developments offer exciting intellectual challenges which will have an important scientific impact as well as being of widespread practical use.

13 REFERENCES

1. Fairhurst, C., Fuller, S., Gray, J., Holmes, M. C. and Tiddy, G. J. T., Lyotropic surfactant liquid crystals, in *Handbook of Liquid Crystals*, Vol. 3, Demus, D., Goodby, J., Gray, G. W., Spiess, H. W. and Vill, V. (Eds), Wiley-VCH, New York, 1998, pp. 341–392.
2. Evans, D. F. and Wennerström, H., *The Colloid Domain where Physics, Chemistry, Biology and Technology Meet*, VCH, New York, 1994.
3. Clint, J. H., *Surfactant Aggregation*, Blackie, Glasgow, 1990.
4. Laughlin, R. G., *The Aqueous Phase Behaviour of Surfactants*, Academic Press, London, 1994.
5. Tanford, C., *The Hydrophobic effect: Formation of Micelles and Biological Membranes*, Wiley-Interscience, New York, 1980.
6. Small, D. M., *The Handbook of Lipid Research – The Physical Chemistry of Lipids*, Plenum Press, New York, 1988.
7. Israelachvilli, J., *Intermolecular and Surface Forces*, Israelachvilli, J., Academic Press, London, 1992.
8. Lipowsky, R. and Sackmann, E. (Eds), *Handbook of Biological Physics*, Vol. 1, *Structure and Dynamics of Membranes. Generic and Specific Interactions*, Elsevier, Amsterdam, 1995.
9. Lipowsky, R. and Sackmann, E. (Eds), *Handbook of Biological Physics*, Vol. 2 *Structure and Dynamics of Membranes. Generic and Specific Interactions*, Elsevier, Amsterdam, 1995.
10. Cevc, G. (Ed.), *Phospholipids Handbook*, Marcel Dekker, New York, 1993.
11. Tsujii, K., *Surface Activity: Principles, Phenomena and Applications*, Academic Press, New York, 1999.
12. Jönsson, B., Lindman, B., Holmberg, K. and Kronberg, B., *Surfactants and Polymers in Aqueous Solution*, Wiley, Chichester, 1998.
13. Stokes, R. J. and Fennell Evans, D., *Fundamentals of Interfacial Engineering*, Wiley-VCH, New York, 1996.
14. Lydon, J. E., in *Handbook of Liquid Crystals*, Vol. 2b, Demus, D., Goodby, J., Grecy, G.W., Spiess, H.-W. and Vill, V. (Eds), Wiley-VCH, Weinheim, 1998, pp. 981–1007.
15. Lydon, J. E., *Curr. Opinion Colloid Interface Sci.*, **3**, 458–466 (1998).
16. Chernik, G. C., *Adv. Colloid Interface Sci.*, **61**, 65–129 (1995).
17. Evans, D. F., *Langmuir*, **4**, 31257–1261 (1988).
18. Costas, M., Kronberg, B. and Silveston, R., *J. Chem. Soc., Faraday Trans. 1*, **90**, 1513–1522 (1994).
19. Kronberg, B., Costas, M. and Silveston, R., *Pure Appl. Chem.*, **67**, 897–902 (1995).
20. Kronberg, B., Costas, M., Silveston, R., *J. Disp. Sci. Technol.*, **15**, 333–351 (1994).
21. Shinoda, K. and Fujihara, M., *Bull. Chem. Soc. Jpn*, **41**, 2162 (1968).
22. Shinoda, K., *J. Phys. Chem.*, **81**, 1300 (1977).
23. Glew, D. N., *J. Phys. Chem.*, **66**, 605 (1962).
24. Eriksson, P., Lindblom, G., Burnell, E., Tiddy, G. J. T., *J. Chem. Soc., Faraday Trans. 1*, **84**, 3129–3139 (1988).
25. Aniansson, E. A. G., Wall, S. N., Almgren, M., Hoffmann, H., Kielmann, I., Ulbicht, W., Zana, R., Lang, J. and Tondre, C., *J. Phys. Chem.*, **80**, 905 (1976).
26. Elvingson, C. and Wall, S., *J. Colloid Interface Sci.*, **121**, 414–424 (1981).
27. Palepu, R., Hall, D. G. and Wyn-Jones, E., *J. Chem. Soc., Faraday Trans. 1*, **86**, 1535–1538 (1990).
28. Bloor, D. M. and Wyn-Jones, E., Department of Chemistry, Salford University, Salford, UK, unpublished data.
29. Gharabi, H., Takisawa, N., Brown, P., Thomason, M. A., Painter, D. M., Bloor, D. M., Hall, D. G. and Wyn-Jones, E., *J. Chem. Soc., Faraday Trans. 1*, **87**, 707–710 (1991).
30. Aniansson, E. A. G., *J. Phys. Chem.*, **82**, 2805 (1978).
31. Israelachvilli, J. and Wennerström, H., *Langmuir*, **6**, 873–876 (1990).
32. Israelachvilli, J. and Wennerström, H., *J. Phys. Chem.*, **96**, 520–531 (1992).
33. Tiddy, G. J. T., Walsh, M. F. and Wyn-Jones, E., *J. Chem. Soc., Faraday Trans. 1*, **78**, 389–401 (1982).
34. Li, Z. X., Lee, E. M., Thomas, R. K. and Penfold, J., *J. Colloid Interface Sci.*, **187**, 492–497 (1997).
35. Mukerjee, P. and Mysels, K. J. *Critical Micelle Concentrations of Aqueous Surfactant Systems*, Report NSRDS-NBS 36 National Bureau of Standards, 1971.
36. Degiorgio, V., in *Physics of Amphiphiles: Micelles, Vesicles and Microemulsions* Degiorgio, V. and Corti, M., (Eds), NHPC, 1985.
37. Tausk, R. J. M., Physical Chemical Studies of Short-Chain Lecithin Homologues, *Ph. D. Thesis*, State University, Utrecht, The Netherlands, 1974.
38. Rosen, M. J., *Chemtech.*, **23**(3), 16–27 (1993).
39. Goon, P., Das, S., Clemett, C. J., Tiddy, G. J. T. and Kumar, V. V., *Langmuir*, **13**, 5577–5582 (1997).
40. Madden, T. J., Unilever Research Port Sunlight Laboratory, Personal Communication, 1990.
41. Mitchell, D. J., Ninham, B. W. and Israelachvilli, J., *J. Chem. Soc., Faraday Trans. 1*, **72**, 1525 (1976).
42. Mitchell, D. J., Ninham, B. W. and Israelachvilli, J., *Biochim. Biophys. Acta*, **470**, 605 (1977).
43. Lide, D.R. (Ed.) *CRC Handbook of Chemistry and Physics*, 69th Edn, CRC Press, Boca Raton, FL, 1988.
44. Tiddy, G. J. T., Concentrated surfactant systems, in *Modern Trends of Colloid Science in Chemistry and Biology*, Eicke, H. F. (Ed.), Birkhauser, Basel, 1985, pp. 148–161.
45. Holmes, M. C., *Curr. Opinion Colloid Interface Sci.*, **3**, 485–492 (1988).
46. Mitchell, D. J., Tiddy, G. J. T., Waring, L., Bostock, T. and McDonald, M. P., *J. Chem. Soc., Faraday Trans. 1*, **79**, 975–1000 (1983).
47. Tiddy, G. J. T., *Phys. Rep.*, **57** (1980).
48. Winsor, P. A., *Chem. Rev.*, **68**, 1–46 (1968).
49. Luzzati, V., *Biological Membranes. Physical Fact and Function*, Academic Press, New York, 1968.

50. Ekwall, P., in *Advances in Liquid Crystals*, Vol. 1, Brown, G. H. (Ed.), Academic Press, New York, 1975.
51. Seddon, J. M., *Biochim. Biophys. Acta*, **1031**, 1–69 (1990).
52. Seddon, J. M. and Templer, R. H., *Structure and Dynamics of Membranes: From Cells to Vesicles*, Hoff, A. J. (Ed.), Elsevier, Amsterdam, 1995, ch. 3, pp. 97–160.
53. Lindblom, G. and Rilfors, L., *Biochim. Biophys. Acta*, **998**, 221–256 (1989).
54. Fontell, K., Fox, K. K. and Hanser, E., *Mol. Cryst. Liq. Cryst. Lett.*, **1**, 9 (1989).
55. Charvolin, J. and Sadoc, J. F., *J. Phys. (Paris)*, **49**, 521–526 (1988).
56. Sakya, P., Seddon, J. M., Templer, R. H., Mirkin, R. J. and Tiddy, G. J. T., *Langmuir*, **13**, 3706–3714 (1997).
57. Gulik, A., Delacroix, H., Kischner, G. and Luzzatti, V., *J. Phys. II, France*, **5**, 445–464 (1995).
58. Tiddy, G. J. T., Seddon, J. M. and Walsh, J., UMIST, Manchester, UK, unpublished data.
59. Seddon, J. M., Bartle, E. A. and Mingins, J., *J. Phys., Condensed Matter*, **2**, Supplement A (1990).
60. Luzzatti, V. and Spegt, P. A., *Nature (London)*, **215**, 707 (1967).
61. Scriven, L. E., *Nature (London)*, **263**, 123 (1976).
62. Lawson, K. D. and Flautt, T. J., *J. Am. Chem. Soc.*, **89**, 5489 (1967).
63. Forrest, B. J. and Reeves, L. W., *Chem. Rev.* **81**, 1–14 (1981).
64. Boden, N., Jackson, P. H., McMullen, K. and Holmes, M. C., *Chem. Phys. Lett.*, **65**, 476 (1979).
65. Luhmann, B., Finkelmann, H. and Rehage, G., *Makromol. Chem. phys.*, **186**, 1059–1073 (1985).
66. Radley, K., *Liq. Cryst.*, **18**, 151–155 (1995).
67. Smith, G. S., Sirota, E. B., Safinya, C. R., Plano, R. J. and Clark, N. A., *J. Chem. Phys.*, **92**, 4519–4529 (1990).
68. Katsaras, J., *J. Phys. Chem.*, **99**, 4141–4147 (1995).
69. Chapman, D., Williams, R. M. and Labroke, B. D., *Chem. Phys. Lipids*, **1**, 445 (1967).
70. Larsson, K., *Z. Phys. Chem.*, **56**, 173 (1967).
71. Vincent, J. M. and Skoulios, A. E., *Acta Crystallogr.*, **20**, 432 (1966).
72. Kékicheff, P., Grabielle-Madellmont, C. and Ollivan, M., *J. Colloid Interface Sci.*, **131**, 112–132 (1989).
73. Lawrence, A. S. C. and McDonald, M. P. *Liq. Cryst.*, **1**, 205 (1966).
74. Lawrence, A. S. C., *Mol. Cryst. Liq. Cryst.*, **7**, 1 (1969).
75. Laughlin, R. C., Paper presented to the SIS Conference, Jerusalem, Israel, 1996.
76. Adam, C. D., Durrant, J. A., Lowry, M. R. and Tiddy, G. J. T., *J. Chem Soc., Faraday Trans 1*, **80**, 789–801 (1984).
77. Mandelkern, L., in *Comprehensive Polymer Science*, Vol. 2, Booth, C. and Price, C. (Eds), Pergamon, Oxford, 1989.
78. Luzzati, V., Mustacchi, H., Skoulios, A. and Husson, F., *Acta Crystallogr.*, **13**, 660 (1960).
79. Husson, F., Mustacchi, H. and Luzzati, V., *Acta Crystallogr.* **13**, 668 (1960).
80. Skoulios, A. and Luzzati, V., *Acta Crystallogr.*, **14**, 278 (1961).
81. Skoulios, A., *Acta Crystallogr.*, **14**, 419 (1961).
82. Spegt, P. A. and Skoulios, A., *Acta Crystallogr.*, **16**, 301 (1963).
83. Spegt, P. A. and Skoulios, A., *Acta Crystallogr.*, **17**, 198 (1964).
84. Luzzati, V., Tardieu, A. and Gulik-Krzywicki, T., *Nature (London)*, **217**, 1028 (1968).
85. Hagslätt, H., Söderman, O. and Jönsson, B., *Liq. Cryst.*, **12**, 667–688 (1992).
86. Söderman, O., Lindblom, G., Johansson, L. B.-A. and Fontell, K., *Mol. Cryst. Liq. Cryst.*, **59**, 121 (1980).
87. Leigh, I. D., McDonald, M. P., Wood, R. M., Tiddy, G. J. T. and Trevethan, M. A., *J. Chem. Soc., Faraday Trans. 1*, **77**, 2867–2876 (1981).
88. Kékicheff, P. and Cabane, B., *J. Phys.*, **48**, 1571–1583 (1987).
89. Kékicheff, P. and Cabane, B., *Acta Crystallogr., Sect. B*, **44**, 395–406 (1988).
90. Kékicheff, P., *J. Colloid Interface Sci.*, **131**, 133–152 (1989).
91. Quist, P., Fontell, K. and Halle, B., *Liq. Cryst.*, **16**, 235–256 (1994).
92. Kékicheff, P. and Tiddy, G. J. T., *J. Phys. Chem.*, **93**, 2520–2526 (1989).
93. Fairhurst, C. E., Holmes, M. C. and Leaver, M. S., *Langmuir*, **13**, 4964–4975 (1997).
94. Fairhurst, C. E., Holmes, M. C. and Leaver, M. S., *Langmuir*, **12**, 6336–6340 (1996).
95. Burgoyne, J., Holmes, M. C. and Tiddy, G. J. T., *J. Phys. Chem.*, **99**, 6054–6063 (1995).
96. Holmes, M. C. and Charvolin, J., *J. Phys. Chem.*, **88**, 810–818 (1984).
97. Holmes, M. C., Charvolin, J. and Reynolds, D. J., *Liq. Cryst.*, **3**, 1147–1155 (1988).
98. Holmes, M. C., Sotta, P., Hendriks, Y. and Deloche, B., *J. Phys. II*, **3**, 1735–1746 (1993).
99. Holmes, M. C., Smith, A. M. and Leaver, M. S., *J. Phys. II*, **3**, 1357–1370 (1993).
100. Leaver, M. S. and Holmes, M. C., *J. Phys. II*, **3**, 105–120 (1993).
101. Holmes, M. C., Leaver, M. S. and Smith, A. M., *Langmuir*, **11**, 356–365 (1995).
102. Auvray, X., Perche, T., Anthore, R., Petipas, C., Rico, I. and Lattes, A., *Langmuir*, **7**, 2385–2393 (1991).
103. Anderson, D. M. and Ström, P., Polymer association structures, in *Microemulsions and Liquid Crystals*, El-Nokaly, M. A. (Ed.), ACS Symposium Series, 384, American Chemical Society, Washington, DC, 1989, pp. 204.
104. Anderson, D. M., *Colloq. Phys.*, **51**, C7–1 (1990).
105. Anderson, D. M., Davis, H. T., Scriven, L. E. and Nitsche, J. C. C., in *Advances in Chemical Physics*, Vol. LXXVII, Prigogine, I. and Rice, S. A. (Eds), Wiley, New York, 1990, pp. 337.
106. Schoen, A. H., *Infinite Periodic Minimal Surfaces without Self Intersections*, NASA Technical Note D-5541, NASA, Washington, DC, 1970.

107. Hyde, S. T., *Pure Appl. Chem.*, **64**, 1617–1622 (1992).
108. Hyde, S. T., *Colloq. Phys.*, **51**, C7-209 (1990).
109. Lindman, B., in *Surfactants*, Tadros, Th. F. (Ed.), Academic Press, London, 1984.
110. Degiorgio, V. and Conti, M., in *Proceedings of the International School of Physics "Enrico Fermi"*, Italy, 1985 Italian Physical Society, Italy, 1985.
111. Sjöblom, J., Stenius, P. and Danielsson, I., in *Nonionic Surfactants*, Schick, M. J. (Ed.), Marcel Dekker, New York, 1987, Ch. 7.
112. Chernik, G. G., *Curr. Opinion Colloid Interface Sci.*, **4**, 381–402 (1999).
113. Strey, R., Schomäker, R., Roux, D., Nallet, F. and Olsson, U., *J. Chem. Soc., Faraday Trans.*, **86**, 2253–2261 (1990).
114. Conroy, J. P., Hall, C., Leng, C. A., Rendall, K., Tiddy, G. J. T., Walsh, J. and Lindblom, G., *Prog. Colloid Polym. Sci.*, **82**, 253–262 (1990).
115. Binks, B. P., in *Annual Reports, Section C*, Vol. 92, The Royal Society of Chemistry, Cambridge, UK, 1996.
116. Kellay, H., Binks, B. P., Hendriks, Y., Lee, L. T. and Meunier, J., *Adv. Colloid Interface Sci.*, **49**, 85–112 (1994).
117. Leaver, M. S., Olsson, U., Wennerström, H., Strey, R. and Wurz, U., *J. Chem. Soc., Faraday Trans.*, **91**, 4369–4274 (1995).
118. Olsson, U. and Wennerström, H., *Adv. Colloid Interface Sci.*, **49**, 113–146 (1994).
119. Laughlin, R. G., Procter & Gamble, Cincinnati, OH, Personal Communication, 1996.
120. Funari, S. S. and Rapp, G., *J. Phys. Chem., B*, **101**, 732–739 (1997).
121. Nibu, Y., Suemori, T. and Inoue, T., *J. Colloid Interface Sci.*, **191**, 256–263 (1997).
122. Nibu, Y. and Inoue, T., *J. Colloid Interface Sci.*, **205**, 231–240 (1998).
123. Nibu, Y. and Inoue, T., *J. Colloid Interface Sci.*, **205**, 305–315 (1998).
124. Marland, J. S. and Mulley, B. A., *J. Pharm. Pharmacol.*, **23**, 561 (1971).
125. Mulley, B. A. and Metcalf, A. D., *J. Colloid Sci.*, **19**, 501 (1964).
126. Clunie, J. S., Corkill, J. M., Goodman, J. F., Symons, P. C. and Tate, J. R., *Trans. Faraday Soc.*, **63**, 2839 (1967).
127. Funari, S. S., Holmes, M. C. and Tiddy, G. J. T., *J. Phys. Chem.*, **98**, 3015–3023 (1994).
128. Corcoran, J., Fuller, S., Rahman, A., Shinde, N. N., Tiddy, G. J. T. and Attard, G. S., *J. Mater. Chem.*, **2**, 695–702 (1992).
129. Funari, S. S., Holmes, M. C. and Tiddy, G. J. T., *J. Phys. Chem.*, **96**, 11029–11038 (1992).
130. Jousma, H., Bouwstra, J. A., Spiess, F. and Junginger, H. E., *Colloid Polym. Sci.*, **265**, 830–837 (1987).
131. Shigeta, K., Suzuki, M. and Kunieda, H., *Prog. Colloid Polym. Sci.*, **106**, 49 (1997).
132. Kunieda, H., Shigeta, K., Ozawa, K. and Suzuki, M., *J. Phys. Chem. B*, **101**, 7952–7957 (1997).
133. Dimitrova, G. T., Tadros, Th. F. and Luckham, P. F., *Langmuir*, **11**, 1101–1111 (1995).
134. Dimitrova, G. T., Tadros, Th. F., Luckham, P. F. and Kipps, M. R., *Langmuir*, **12**, 315–318 (1996).
135. Tanford, C. and Reynolds, J. A., *Biochim. Biophys. Acta*, **457**, 133 (1976).
136. Beyer, K., *J. Colloid Interface Sci.*, **86**, 73–89 (1982).
137. Heusch, R. and Kopp, F., *Ber. Bunsenges. Phys. Chem.*, **91**, 806–811 (1987).
138. Thompson, L., Walsh, J. M. and Tiddy, G. J. T., *Colloid Surf. A*, **106**, 223–235 (1996).
139. Kratzat, K. and Finkelmann, H., *J. Colloid Interface Sci.*, **181**, 542–550 (1996).
140. Kratzat, K. and Finkelmann, H., *Colloid Polym. Sci.*, **272**, 400–408 (1994).
141. Kratzat, K., Schmidt, C., Finkelmann, H., *J. Colloid Interface Sci.*, **163**, 190–198 (1994).
142. Kratzat, K., Stubenrauch, C. and Finkelmann, H., *Colloid Polym. Sci.*, **273**, 257–262 (1995).
143. Kratzat, K. and Finkelmann, H., *Liq. Cryst.*, **13**, 691–699 (1993).
144. Söderlund, H., Sjöblom, J. and Wärmheim, T., *J. Disp. Sci. Technol.*, **10**, 131 (1989).
145. Finkelmann, H., Lühmann, B. and Rehage, G., *Colloid Polym. Sci.*, **260**, 56–65 (1982).
146. Finkelmann, H., Lühmann, B. and Rehage, G., *Angew. Makromol. Chem.*, **123**, 217–227 (1984).
147. Lühmann, B. and Finkelmann, H., *Colloid Polym. Sci.*, **265**, 506–516 (1987).
148. Lühmann, B. and Finkelmann, H., *Colloid Polym. Sci.*, **264**, 189–192 (1986).
149. Söderman, O. and Johansson, I., *Curr. Opinion Colloid Interface Sci.*, **4**, 391–401 (1999).
150. Qui, H. and Caffrey, M., *Biomaterials*, **21**, 223–234 (2000).
151. LIPIDAG database [Website: www.ldb.chemistry.ohio-state.edu].
152. Briggs, J., Chung, H. and Caffrey, M., *J. Phys. II*, **6**, 723–751 (1996).
153. Eastoe, J., Rogueda, P., Howe, A. M., Pitt, A. R. and Heenan, R. K., *Langmuir*, **12**, 2701–2705 (1996).
154. Sakya, P., Seddon, J. M. and Templer, R. H., *J. Phys. II*, **4**, 1311–1331 (1994).
155. Sakya, P., Seddon, J. M. and Vill, V., *Liq. Cryst.*, **23**, 409–424 (1997).
156. Nilsson, F., Södermann, O. and Johansson, I., *Langmuir*, **12**, 902–908 (1996).
157. Nilsson, F., Södermann, O. and Reimer, J., *Langmuir*, **14**, 6396–6402 (1998).
158. Hall, C., Tiddy, G. J. T. and Pfannemüller, B., *Liq. Cryst.*, **9**, 527–537 (1991).
159. Raaijmakers, H. W. C., Arnouts, E. G., Zwanenburg, B., Chittenden, G. J. F. and van Doren, H. A., *Rec Trav. Chim. Pays-Bas*, **114**, 301–310 (1995).
160. Finkelmann, H. and Schafheutle, M. A., *Colloid Polym. Sci.*, **264**, 786–790 (1986).
161. Sagitani, H., Hayashi, Y. and Ochiai, M., *J. Am. Oil Chem. Soc.*, **66**, 146–151 (1989).

162. Balzer, D., *Langmuir*, **9**, 3375–3384 (1993).
163. Platz, G., Thunig, C., Policke, J., Kirchhoff, W. and Nickel, D., *Colloid Surf. A*, **88**, 113–122 (1994); Platz, G., Policke, J., Thunig, C., Hofman, R., Nickel, D. and Vonrybinski, W., *Langmuir*, **11**, 4250–4255 (1995).
164. Alexandridis, P., Zhou, D. and Khan, A., *Langmuir*, **12**, 2690–2700 (1996).
165. Zhou, D., Alexandridis, P. and Khan, A., *J. Colloid Interface Sci.*, **183**, 339–350 (1996).
166. Alexandridis, P., Olsson, U. and Lindman, B., *Macromolecules*, **28**, 7700–7710 (1995).
167. Alexandridis, P., Olsson, U. and Lindman, B., *J. Phys. Chem.*, **100**, 280–288 (1996).
168. Alexandridis, P., Olsson, U. and Lindman, B., *Langmuir*, **12**, 1419–1422 (1996).
169. Alexandridis, P., Olsson, U. and Lindman, B., *Langmuir*, **13**, 23–34 (1997).
170. Holmqvist, P., Alexandridis, P. and Lindman, B., *Langmuir*, **13**, 2471–2479 (1997).
171. Lutton, E. S., *J. Am. Oil Chem. Soc.*, **43**, 28 (1966).
172. Hoffmann, H., Oetter, G. and Schwandner, B., *Prog. Colloid Polym. Sci.*, **73**, 95 (1987).
173. La Mesa, C., Sesta, B., Bonicelli, M. G. and Ceccaroni, G. F., *Langmuir*, **6**, 728–731 (1990).
174. Blackburn, J. C. and Kilpatrick, P. K., *J. Colloid Interface Sci.*, **149**, 450–471 (1992).
175. Rendall, K., Tiddy, G. J. T. and Trevethan, M. A., *J. Chem. Soc., Faraday Trans. 1*, **79**, 637 (1983).
176. Blackmore, E. S. and Tiddy, G. J. T., *J. Chem. Soc., Faraday Trans. 2*, **84**, 1115–1127 (1988).
177. Khan, A., Fontell, K. and Lindblom, G., *J. Phys. Chem.*, **86**, 383–386 (1982).
178. Laughlin, R. G., in *Cationic Surfactants*, Rubingh, D. N. and Holland, P. M. (Eds), Surfactant Science Series, Vol. 37, Marcel Dekker, New York, 1990.
179. Hagslätt, H., Söderman, O., Jönsson, B. and Johansson, L. B.-A., *J. Phys. Chem.*, **95**, 1703–1710 (1991).
180. Hagslätt, H., Söderman, O. and Jönsson, B., *Langmuir*, **10**, 2177–2187 (1994).
181. Fuller, S., Hopwood, J., Rehman, A., Shinde, N. N., Tiddy, G. J. T., Attard, G. S., Howell, O. and Sproston, S., *Liq. Cryst.*, **12**, 521–529 (1992).
182. Fuller, S., Lyotropic and thermotropic behaviour of amphitropic systems, *Ph.D. Thesis*, University of Salford, UK, 1995.
183. Fuller, S., Shinde, N. N., Tiddy, G. J. T., Attard, G. S. and Howell, O., *Langmuir*, **12**, 1117–1123 (1996).
184. Attard, G. S., Fuller, S., Howell, O. and Tiddy, G. J. T., *J. Phys. Chem. B*, **103**, 10426–10436 (2000).
185. Attard, G. S., Fuller, S., Howell, O. and Tiddy, G. J. T., *Langmuir*, **17** (2001).
186. Alami, E., Levy, H., Zana, R. and Skoulios, A., *Langmuir*, **9**, 940–944 (1993).
187. Zana, R. and Talmon, Y., *Nature (London)*, **362**, 228–230 (1993).
188. Fuller, S., Tiddy, G. J. T. and Zana, R., Department of Chemical Engineering, UMIST, Manchester, UK, unpublished data, 1996.
189. Pérez, L., Torres, J. L., Manresa, A., Solans, C. and Infante, M. R., *Langmuir*, **12**, 5296–5301 (1996).
190. Hagslätt, H. and Fontell, K., *J. Colloid Interface Sci.*, **165**, 431–444 (1994).
191. Wennerström, H. and Jönsson, B., *J. Phys. Chem.*, **91**, 338–352 (1987).
192. Bouwstra, J. A., Jousma, H., van der Meulen, M. M., Vijverberg, C. C., Gooris, G. S., Spies, F. and Juninger, H. E., *Colloid Polym. Sci.*, **267**, 531–538 (1989).
193. Barker, C. A., Saul, D., Tiddy, G. J. T., Wheeler, B. A. and Willis, E., *J. Chem. Soc., Faraday Trans. 1*, **70**, 154–162 (1974).
194. Ninham, B. W. and Yaminski, V., *Langmuir*, **13**, 2097–2108 (1997).
195. Laughlin, R. G., *The Aqueous Phase Behaviour of Surfactants*, Academic Press, London, 1994, p. 378.
196. Gharabi, H., Palepu, R., Tiddy, G. J. T., Hall, D. G. and Wyn-Jones, E., *J. Chem. Soc., Chem. Commun.*, 115–116 (1990).
197. Evans, D. F., Yamauchi, A., Roman, R. and Casassa, E. Z., *J. Colloid Interface Sci.*, **88**, 89–96 (1982).
198. Evans, D. F., Yamauchi, A., Wei, G. and Bloomfield, A., *J. Phys. Chem.*, **87**, 3537–3541 (1983).
199. Binani-Limbele, W. and Zana, R., *Colloid Polym. Sci.*, **267**, 440–447 (1989).
200. Sjöberg, M., Henriksson, U. and Wärnheim, T., *Langmuir*, **6**, 1205–1211 (1990).
201. Jonströmer, M., Sjöberg, M. and Wärnheim, T., *J. Phys. Chem.*, **94**, 7549–7555 (1990).
202. Ricco, I. and Lattes, A., *J. Phys. Chem.*, **90**, 5870–5872 (1986).
203. Couper, A., Gladden, G. P. and Ingram, B. T., *Faraday Discuss. Chem. Soc.*, **59**, 63 (1975).
204. Ray, A., *J. Am. Chem. Soc.*, **91**, 6511 (1969).
205. Fletcher, P. D. I. and Gilbert, P. J., *J. Chem. Soc., Faraday Trans. 1*, **85**, 147–156 (1989).
206. Moucharafieh, N. and Friberg, S. E., *Mol. Cryst. Liq. Cryst.*, **49**, 231 (1979).
207. El Nokaly, M. A., Ford, L. D., Friberg, S. E. and Larsen, D. W., *J. Colloid Interface Sci.*, **84**, 228–234 (1981).
208. Ganzui, L., El Nokaly, M. A. and Friberg, S. E., *Mol. Cryst. Liq. Cryst.*, **72**, 183–188 (1982).
209. Friberg, S. E., Laing, P., Lockwood, K. and Tadros, M., *J. Phys. Chem.*, **88**, 1045–1046 (1984).
210. Friberg, S. E., Solans, C. and Ganzuo, L., *Mol. Cryst. Liq. Cryst.*, **109**, 159–168 (1984).
211. Evans, D. F., Kaler, E. W. and Benton, W. J., *J. Phys. Chem.*, **87**, 533–535 (1983).
212. Balmajdoub, A., Marchal, J. P., Canet, D. and Rico, I., Lattes, A., *Nouv. J. Chim.*, **11**, 415–418 (1987).
213. Wärnheim, T. and Jönsson, A., *J. Colloid. Interface Sci.*, **125**, 627–633 (1988).
214. Auvray, X., Petipas, C., Anthore, R., Rico, I. and Lattes, A., *J. Phys. Chem.*, **93**, 7458–7464 (1989).
215. Lin, Z., Davies, H. T. and Scriven, L. E., *Langmuir*, **12**, 5489–5493 (1996).

216. Bleasdale, T. A., Tiddy, G. J. T. and Wyn-Jones, E., *J. Phys. Chem.*, **95**, 5385–5386 (1991).
217. Bleasdale, T. A. and Tiddy, G. J. T., in *Organized Solutions*, Friberg, S. E. and Lindman, B. (Eds), Marcel Dekker, New York, 1992, pp. 125–141.
218. Auvray, X., Petipas, C., Rico, I. and Lattes, A., *Liq. Cryst.*, **17**, 109–126 (1994).
219. Dörfler, H. D., *Z. Phys. Chem.*, **187**, 135–151 (1994).
220. Harrison, W. J., McDonald, M. P. and Tiddy, G. J. T., *J. Phys. Chem.*, **95**, 4136–4140 (1991).
221. Caffrey, M., *Curr. Opinion Struct. Biol.*, **10**, 486–497 (2000).
222. CLCR Synchrotron Radiation Department, *Daresbury Laboratory Annual Report*, HMSO, London, 1995–1996.
223. Terry, A. E., Odell, J. A., Nicol, R. J., Tiddy, G. J. T. and Wilson, J. E., *J. Phys. Chem.*, **103**, 11218–11226 (1999).

CHAPTER 22

Environmental Aspects of Surfactants

Lothar Huber

München, Germany

Lutz Nitschke

Ebersberg, Germany

1	Introduction	509	5.5	Bioaccumulation and biomagnification	520
2	Use and Environmental Relevance of Surfactants in Different Fields of Application	510	5.6	Behaviour of surfactants in sewage sludge, soil and plants	520
2.1	Detergents and cleaning agents	511	6	Anionic Surfactants	520
2.2	Cosmetics and pharmaceuticals	511	6.1	General remarks	520
2.3	Textile industry	511	6.2	Biodegradability	521
2.4	Mining and oil production/refining	512	6.3	Aquatic toxicity	524
2.5	Metal processing industry	512	7	Nonionic Surfactants	525
2.6	Dyes, varnishes and plastics	512	7.1	General remarks	525
2.7	Food industries	512	7.2	Biodegradability	527
2.8	Leather and fur industry	512	7.3	Aquatic toxicity	529
2.9	Pulp and paper production	512	8	Cationic Surfactants	529
3	Environmental Legislation	512	8.1	General remarks	529
4	Analysis of Surfactants in the Environment	513	8.2	Biodegradability	531
5	Criteria for Ecological Assessment and Biological Testing Procedures	514	8.3	Aquatic toxicity	531
5.1	Biological degradation	515	9	Amphoteric Surfactants	532
5.2	Mechanical, chemical and physico-chemical elimination	517	9.1	General remarks	532
5.3	Aquatic toxicity	518	9.2	Biodegradation	532
5.4	Formation of hazardous metabolites	519	9.3	Aquatic toxicity	534
			10	Environmental Behaviour under Real Conditions and Risk Assessment	534
			11	References	535

1 INTRODUCTION

The world-wide extensive use of surfactants in various areas of application (emulsifiers, detergents, cosmetics, industrial cleaners, textile and food industries,

etc.) leads to a considerable discharge of these compounds into the environment. These substances are introduced into the aquatic system mainly by the waste-water path via waste-water treatment plants or by direct discharge. On account of these first exten-

sive application of a synthetic anionic surfactant in household detergents (tetrapropylenebenzene sulfonate) in Central Europe in the 1950s and 1960s, with the consequence of a strong formation of foam in waste water-treatment plants and rivers, it became evident that surfactants have strong environmental impacts. The need for legal regulations was very rapidly realized in several European countries and North America. Regulation of the biodegradation of surfactants was the primary aim. Initially, anionic and nonionic surfactants became the focus of attention because of their extensive use and their partially low biodegradability. Legal regulations generally defined the minimum requirements for biodegradability. At the same time, a great international effort was made to develop chemical methods for analysis and biological test procedures to assess the degree of degradation. It can be assumed that surfactants were the initiators of the ecological assessment of chemicals.

2 USE AND ENVIRONMENTAL RELEVANCE OF SURFACTANTS IN DIFFERENT FIELDS OF APPLICATION

Surfactants with different chemical structures and specific properties are used world-wide in different fields of application. Figure 22.1 represents an overview of the percentage of the applied amounts in the relevant fields. The main share (42%) is used for washing and

Table 22.1. Production and consumption of surfactants in Western Europe according to Comité Européen des Agents de Surface et de leurs Intermédiaires Organiques (CESIO) (in 1000 t – as 100% active)

Surfactant	Production		Total market	
	1996	1997	1996	1997
<i>ANIONICS</i>				
Alkylbenzene sulfonates (LASs ^a)	400	420	390	390
Alkane sulfonates	77	70	74	60
Alcohol sulfates	111	115	103	108
Alcohol ether sulfates	229	254	210	240
Other anionics	82	80	87	72
<i>Total Anionics</i>	<i>899</i>	<i>939</i>	<i>864</i>	<i>870</i>
<i>Soaps</i>	<i>550</i>	<i>550</i>	<i>550</i>	<i>550</i>
<i>NONIONICS</i>				
All ethoxylates	844	879	800	807
Other nonionics	224	236	200	196
<i>Total nonionics</i>	<i>1068</i>	<i>1115</i>	<i>1000</i>	<i>1003</i>
<i>CATIONICS</i>				
	170	174	145	149
<i>AMPHOTERICS</i>				
	43	60	40	56
<i>GRAND TOTAL</i>	<i>2730</i>	<i>2838</i>	<i>2599</i>	<i>2628</i>

^aLASs, linear alkylbenzene sulfonates.

cleaning purposes. This is followed by the textile industry with 16%, and cosmetics and mining/oil-recovery and -refining (each 7%). Table 22.1 shows the production and consumption of surfactants in Western Europe. Figure 22.2 reflects the surfactant production in the Federal Republic of Germany, including developments from 1978 to 1996 where a shift from anionic compounds to

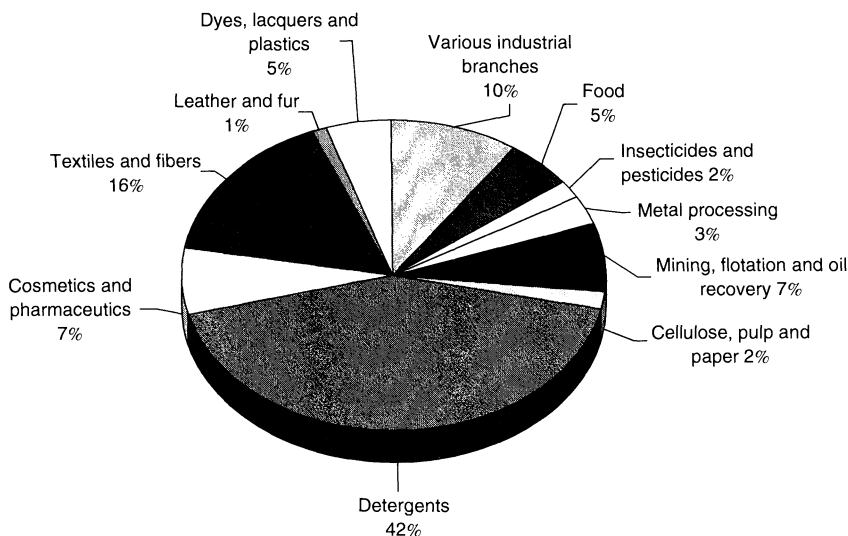


Figure 22.1. Percentage of surfactant amounts in different fields of application in Western Europe

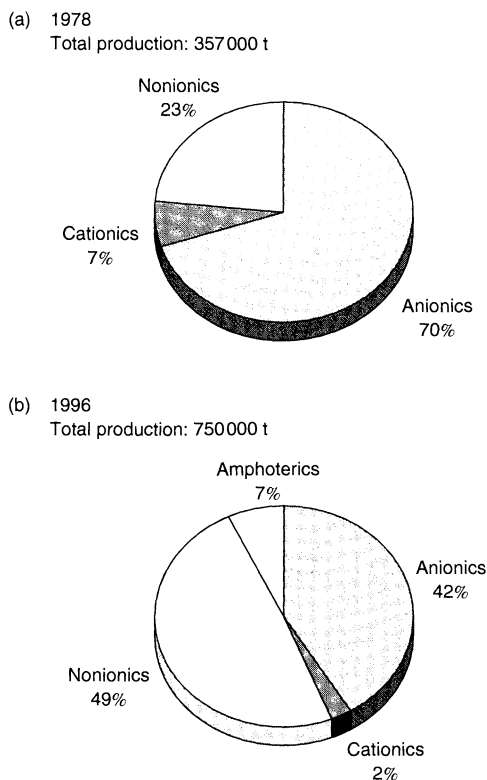


Figure 22.2. Production of surfactants in the Federal Republic of Germany for (a) 1978, and (b) 1996

nonionics is clearly visible. The rise in total production from 357 000 t/a to 750 000 t/a is also a clear indication of the growing importance of these compounds (Figure 22.2). Based on this large production and consumption figures, a direct ecological relevance of these compounds can be derived. The main portion of the surfactants after their proper use is discharged into the environment via the waste-water path. In most fields of application, surfactants are not changed in their chemical structure so that their characteristic property, i.e. surface-activity, is maintained. To a certain degree, a direct or an indirect terrestrial disposal of surfactants also takes place. The different fields of application of these compounds are described in some detail in the following sections.

2.1 Detergents and cleaning agents

By far the largest consumption of surfactants world-wide is for washing and cleaning purposes. This application

represents a share of 42% of the total consumption. Household detergents have different application profiles (e.g. heavy duty detergents, special detergents, liquid detergents, etc.) and therefore also different formulations for the surfactant components. The most important ingredients of detergents are the surfactants, where the linear alkylbenzene sulfonates (LASs) still have a dominant position. Generally, these compounds are used in combination with nonionic fatty alcohol polyglycol ethers.

Surfactants have another central importance and function in the overwhelming majority of household, commercial and industrial cleaning agents. In the case of commercial and industrial cleaners, the following applications can be mentioned:

- Cleaning of hard surfaces
- Car washing
- Cleaning of buildings
- Bottle cleaning

In addition, for household purposes many surfactant-containing preparations are used in dishwashing.

2.2 Cosmetics and pharmaceuticals

As shown in Figure 22.1, 7% of total surfactants are used in cosmetics and pharmaceuticals, especially in personal care products such as shampoos, bath preparations or toothpastes. Surfactants are important in their function as emulsifiers in creams and lotions. A great variety of anionic, nonionic, cationic and also amphoteric surfactants are used here.

2.3 Textile industry

Another important field of surfactant application is as auxiliaries in the textile industry, where mainly for washing, wetting, bleaching, dyeing and finishing procedures, anionic, nonionic and cationic formulations are used to a considerable extent and where generally the used chemicals are directly or indirectly discharged into the environment. The range of surfactant types used in auxiliaries and finishing agents is very high; just to mention a few, these include:

- Combinations of nonionic ethoxylated products
- Sulfosuccinates
- Polyglycol ether phosphates
- Fatty acid polyglycol ethers
- Fatty acid sarcosinates

- Betaines
- Aryl sulfonates
- Quaternary ammonium compounds

In this field, it is difficult to differentiate between the specific effects of surfactants which are not only restricted to washing.

2.4 Mining and oil production/refining

Considerable amounts of surfactants are used for ore and mineral flotation in mining activities. These act as collectors and foamers. Today, surfactants are also indispensable in coal-mining, too, where they are used in flotation, binding of coal dust, and coal transport through pipelines.

Surfactants are of great importance as auxiliaries for the production and processing of crude oil and gas (emulsifiers, agents for foaming and defoaming, lubricants, bactericides, corrosion inhibitors, de-emulsifiers, etc.). In particular, tertiary oil production represents a broad field for such applications.

2.5 Metal processing industry

Surfactants play an important role in the processing of metals. They are used in many treatment steps as emulsifiers, surface-active agents, lubricants, cleaning agents and corrosion inhibitors.

2.6 Dyes, varnishes and plastics

Surfactants are used in the so-called flush process in the dye and varnish industry. Organic and inorganic pigments are transferred from an aqueous medium into an oily medium in this procedure. In addition, surfactants disperse pigments in dyestuffs, emulsify pigments in emulsion dyestuffs and stabilize the formulations of dyes and varnishes.

Surfactants are also used as dispersing agents for dyestuffs in the plastics industry. Furthermore, they are used to a large extent as emulsifiers for emulsion polymerization e.g. poly(vinyl chloride) (PVC).

2.7 Food industries

Independent of a natural content of surface-active substances in food (e.g. phosphorus lipids, glucolipids,

proteins, etc.), synthetic surfactants are used in considerable amounts in this field where emulsifiers for fats and oils are most important. The fat processing industry is included here, where with surfactants, renetting processes play a major role.

2.8 Leather and fur industry

Surfactants are important auxiliaries in practically all processes in the production of leather and fur from the raw to the finished product.

2.9 Pulp and paper production

Considerable amounts of surfactants are used as auxiliaries in pulp and paper production, for instance in waste-paper recycling, flotation, adjustment of the absorptive capacity of paper, and finishing.

3 ENVIRONMENTAL LEGISLATION

As early as 1961, the first legal actions by different European governments were taken to control the environmental impacts from the use of surfactants and detergents. The general aim was to establish a standard for the biological degradability based on the background that considerable volumes of these compounds are discharged into the environment. In the same year in Germany, a law on surfactants in washing and cleaning products was published, comprising regulations (1962) on the biological degradability of anionic surfactants. A minimum degradation rate of 80% was stipulated here. This was analytically based on the "methylene blue active substances" (MBAS) test which defines primary degradation. Already in 1968, under the patronage of the European Council, an agreement on detergents was elaborated. On a supranational level (European Economic Community (EEC) – European Working Group (EWG)), a first guideline was issued with the aim to harmonize the different regulations for detergents in the member states of the EEC (73/404/EWG). Consecutive guidelines, i.e. 73/405/EWG, 82/242/EWG, 82/243/EWG, and 86/94/EWG, were based on this first version. According to the latest status, these require a 90% degradation of all surfactants. Additionally, the EEC Directive has also laid down principles for the environmental risk assessment of new chemicals. As part of this assessment, the measured or calculated environmental concentrations, the "Predicted

Environmental Concentrations" (PECs), are compared with those concentrations of the chemicals that have no negative effects towards representative organisms ("Predicted No-Effect Concentrations" (PNECs)). This is a tiered process in which each step requires more refined data and represents an increased relevance to real-world systems.

Concurrent to these legal actions, adequate methods for measuring biodegradability were developed, including various analytical procedures. The most important tests specified by the detergent legislation are the following:

- The Organization for Economic Co-operation and Development (OECD) Screening Test
- The OECD Confirmatory Test

The same relates to the analytical methods, where for anionic, nonionic and cationic surfactants, various colorimetric procedures (MBAS, "bismuth active substance(s)" (BiAS), and "disulfine blue active substance(s)" (DSBAS)) were introduced. Since these methods analyse only the loss of surface-activity or primary degradation, other analytical approaches have been employed in the last 10 years in order to characterize the total or ultimate degradation. These include methods such as high performance liquid chromatography (HPLC), gas chromatography (GC) GC/mass spectrometry (MS), and the measurement of total organic carbon (TOC) and chemical oxygen demand (COD).

4 ANALYSIS OF SURFACTANTS IN THE ENVIRONMENT

A large share of surfactants is discharged after their application via sewer systems to waste-water treatment plants. In spite of the high biodegradability of modern surfactants, considerable amounts of surfactants are still introduced into the aquatic environment, especially in places where there is no adequate waste-water treatment. The large amount of surfactants which are specifically used in detergents causes surface water pollution in the µg/l-range. Table 22.2 shows a simple estimation for the situation in Germany today for the main type of detergent surfactant i.e. linear alkylbenzene sulfonates, (LASs). This estimation is a very simple approach to the real situation, for example, the small share of direct discharges to surface water or a further biodegradation in rivers are disregarded. However, the estimated LAS concentrations correspond well to an extensive monitoring study (1, 2) and to a recently

Table 22.2. Estimation of LAS concentrations in river waters in Germany

Aspect/feature	Value	LAS concentration
Population	80 000 000	–
Water consumption per person per day	200 l/d	–
LAS consumption per year	39 000 t/a	–
Raw waste water	–	6.7 mg/l
Elimination in sewage treatment plants with nitrification and denitrification	99–99.6%	–
Effluents of sewage treatment plants	–	27–67 µg/l
Dilution in rivers	6–10	–
Rivers and surface waters	–	2–10 µg/l

carried out monitoring programme in the Bavarian Main–Danube region where LAS concentrations from 0.9 to 11.4 mg/l (average 5.4 mg/l) were measured in influents of waste-water treatment plants and from <2 to 13 µg/l in the Main and Danube receiving waters.

With respect to these data and an insufficient elimination in waste-water treatment plants at that time, measurements of the surfactant concentration in the aquatic environment were begun. Rather early on, for example, extensive data have been received since the beginning of the 1960s from the River Rhine (3).

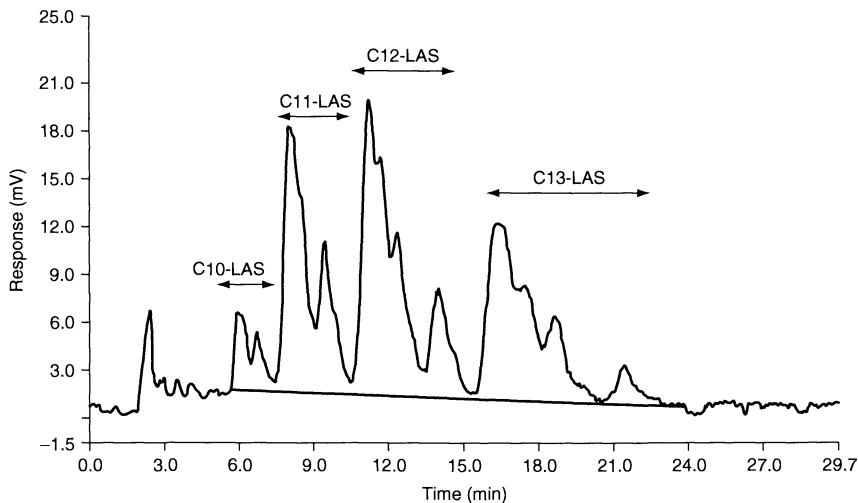
However, determination of surfactants in the environment was difficult up to the 1980s because of the lack of analytical methods which allow a selective determination of single surfactant species. The term "Surfactant" indicates only the physical property of decreasing the surface tension. Generally, we can distinguish between four groups of surfactants depending on their charge. Special analytical procedures were developed to determine all surfactants of each group as a "sum" parameter. Some of these were internationally standardized, as shown in Table 22.3. As mentioned above, the use of these methods provides no specific information about the surfactant species, homologous or isomeric compounds or metabolites. In addition, there are some further disadvantages to these methods as follows:

- Vulnerability to interfering substances
- Use of a halogenated solvent
- Lower detection limit in real samples is not better than 0.1 mg/l

The use of chromatographic methods, especially high performance liquid chromatography (HPLC), solves these problems and yields more information about the

Table 22.3. Analytical methods to determine surfactants depending on their charge as the sum parameter

Surfactant group	Analytical method	International standard
Anionic	Measurement of the methylene blue index, MBAS (methylene blue active substance(s))	ISO 7875-1 (1984) EN 903 (1994)
Nonionic	Determination of the bismuth active substance(s) (BiAS) using the Dragendorff reagent	ISO 7875-2 (1984)
Cationic	Determination of the disulfine blue active substance(s) (DSBAS)	—
Amphoteric	Orange II method	—

**Figure 22.3.** Reversed-phase HPLC chromatogram of an LAS surfactant

surfactants and their metabolites in the environment. Figure 22.3 shows, as an example, an HPLC chromatogram of an LAS surfactant. This figure demonstrates the advantages of chromatographic methods in surfactant analysis. Homologues of the LAS with different alkyl chain lengths are chromatographically well resolved, which thus allows the quantitative determination of the single homologues. This situation is illustrated in Figure 22.3 where the labelled main peak groups in the chromatogram are LAS molecules with different alkyl chain lengths. The fine resolution within these main peak groups indicates the presence of isomeric LAS compounds.

A sample pre-treatment by solid phase extraction (SPE), followed by HPLC using the sensitive fluorescence detection method, allows the determination of the LAS surfactant up to the concentration of about 2 µg/l in environmental samples, i.e. in surface waters.

The separate determination of homologous and isomeric compounds is absolutely necessary in order to assess the aquatic toxicity of a surfactant because biodegradability and aquatic toxicity are strongly

dependent on the composition of the surfactant. It should be noted here that commercial surfactants are mixtures of many homologous and isomeric substances.

Many articles dealing with the determination of surfactants and their metabolites in surface waters, sewage treatment processes, biodegradation tests, soils, etc. have been published during the last 10 to 15 years. Some surveys refer to the original literature (e.g. see the review by Kloster (4)).

Generally, it must be mentioned that the determination of surfactants in environmental samples sometimes requires extensive isolation and pre-concentration procedures.

5 CRITERIA FOR ECOLOGICAL ASSESSMENT AND BIOLOGICAL TESTING PROCEDURES

The evaluation of the environmental compatibility of chemical substances and preparations is today based on several mainly ecological criteria. When considering

surfactants, such criteria are listed according to their importance as follows:

- (i) Primary and total biological degradation in the aquatic and terrestrial environment.
- (ii) Acute and chronic aquatic and terrestrial toxicity, especially against bacteria, algae, crustaceans (daphnia), fish, worms and groups of organisms.
- (iii) Bioaccumulation and biomagnification in the single organism or in the food chain in water and soil.
- (iv) Formation of ecologically hazardous degradation products and metabolites in the course of biological degradation processes.
- (v) Elimination by mechanical, chemical or physico-chemical processes, e.g. sorption, photolysis or hydrolysis, in waste-water treatment plants or surface water.
- (vi) Causation of unwanted physico-chemical effects in waste-water treatment processes and surface water, e.g. foaming or negative impacts on aeration in the activated sludge process.

5.1 Biological degradation

Biological degradation, which means the biological transformation of an organic molecule by enzymatic breakdown to carbon dioxide and water, is one of the most important ecological criteria for an ecological appraisal and ranking of surfactants. This is especially true for surfactants which normally have the additional property of a higher toxicity. A specific differentiation between primary and total degradation is typically made for surfactants. The degree of biological degradation is not an absolute dimension. It is strongly defined by the testing method and also the type of analytical evaluation (biochemical oxygen demand (BOD), TOC, COD, formation of CO_2 , etc.). The end-products which are postulated for total or ultimate degradation are CO_2 , H_2O and inorganic ions such as SO_4^{2-} and NO_3^- . However, it is also acceptable to understand total degradation respective elimination not only as a catabolic process but also as an anabolic process where surfactants are transformed into biomass and finally removed as surplus sludge from a waste-water treatment plant. Initiated by environmental problems with surfactants, a large number of test methods were developed to determine the biological degradation of organic substances. A quantification of the degree of biodegradability depends on the test method. Most of the tests are carried out under aerobic conditions. All of these tests are generally influenced by the following important factors and parameters (5, 6):

- (i) The concentration of test material must be high enough for the analytical methods chosen or available.
- (ii) The concentration must be sufficiently low in the case of toxic substances (e.g. cationic surfactants) or when real environmental concentrations have to be simulated (surface waters).
- (iii) Physico-chemical properties of the test substances, such as water solubility, volatility and absorption behaviour, which influence their bioavailability and abiotic elimination from water.
- (iv) Composition and concentration of inorganic and also organic nutrients in the test medium, especially nitrogen and phosphorus, but also trace elements, and a sufficient buffer capacity of the total substrate.
- (v) Presence and absence of other carbon-containing biodegradable substances in the same medium for cometabolic competing or otherwise modifying processes.
- (vi) Conditions and properties of the test systems such as volume, shape configuration of the test vessel, temperature, mode of mixing or shaking and oxygen supply, especially in simulation tests which approach the conditions of modern waste-water treatment plants. Sludge loading, sludge age, return sludge volume, oxygen concentration and settling time are very important parameters in this context.
- (vii) Duration of the test.

It is quite obvious that test conditions within the same test method must be standardized on an international basis in order to obtain comparable results. Such requirements have only been partially realized up until now. Especially with anaerobic testing, there is still a situation where the number of available and generally accepted tests is very small and further developments and agreements are necessary for the simulation of anaerobic digestion in waste-water treatment plants. It cannot be ignored that this treatment step also decides the fate of a considerable amount of surfactants in our environment.

Other factors which are very important but have not yet been standardized are the composition and quality of the inoculum. Composition relates to the species of bacteria and other micro-organisms, including the bio-coenotic aspect which will degrade the surfactant under consideration. The quality of the inoculum is mainly described by its status of adaptation and acclimatization and therefore by the enzymatic activities and capabilities of the microbial cell. The inoculum can usually only be defined in terms of its origin and metabolic history.

Biodegradation tests are used to predict the biodegradation behaviour of a test material in natural or technical

environments. Each test method should simulate such an environment to a certain degree.

The biodegradability of substances and waste-water constituents not only depends on the molecular structure of the test material but also on important additional factors such as the following:

- Concentration of the test material
- Availability in inorganic nutrients and additional organic material for cometabolic processes
- Possible toxic effects of the test material under test conditions
- Conditions and physical chemical properties and bioavailability of the test material

just to mention some aspects.

In particular, processes of adaption or acclimatization are very complex and the biological phenomena which contribute to this may include the following:

- (i) Regulation of enzymes in competent micro-organisms through introduction by substrate(s) and/or de-repression by removal of repressing substances. These processes are fast; for example, enzyme induction or de-repression may take minutes or even days.
- (ii) Growth of existing competent species from initially low numbers, possibly limited by adverse effects such as predation by protozoa or viral infection.
- (iii) Genetic mutation – at typical spontaneous mutation rates, new genotypes may emerge with better capacities for breakdown.
- (iv) Association of appropriate organisms into consor-tial arrangements.
- (v) Gene transfer, for instance, on plasmids.

A considerable number of standardized OECD and International Organization for Standardization (ISO) methods for measuring the biodegradability of surfactants are available. Table 22.4 gives an overview of such methods. ISO 7827 and OECD 301 A are used to determine the ultimate biodegradability in the aquatic environment. This is achieved via the measurement of dissolved organic carbon (DOC) at an incubation period of 28 days. The widely used Zahn–Wellens Test (OECD 302 B) is also a static method but works with a substantially higher biomass and substrate concentration (50–400 mg/l). This corresponds more to the situation in a real waste-water treatment plant.

Table 22.5 describes a set of standard conditions for aerobic batch tests which are generally applied (5).

Table 22.4. ISO Standards and OECD Guidelines for biodegradation tests

Test method	OECD Guideline	ISO Standard
DOC Die-Away Test	301 A	7 827
CO ₂ Evolution Test	301 B	9 439
Modified MITI Test (I)	301 C	–
Closed Bottle Test	301 D	10 707
Modified OECD Screening Test	301 E	7 827
Manometric Respirometry Test	301 F	9 408
Modified SCAS Test	302 A	9 887
Zahn–Wellens/EMPA Test	302 B	9 888
Modified MITI Test (II)	302 C	–
Aerobic Sewage Treatment: Coupled Units Test	303	11 733
Inherent Biodegradability in Soil	304	–
Biodegradability in Seawater	306	–
Test Guidance for Poorly Water-soluble Substances	–	10 634
Anaerobic Degradation Test	–	11 734
Two-phase Closed Bottle Test	–	10 708
Biodegradation Test at Low Concentrations	–	14 592
CO ₂ Test in Sealed Vessels	–	14 593

The ISO 11 733 and OECD 303 are continuous flow tests involving laboratory activated-sludge plants which closely correspond to technical waste-water treatment plants. During the last five years, these tests have been developed further in Germany. Corresponding to modern waste-water treatment processes, these new laboratory activated-sludge plants are also designed to simulate nitrification and pre-denitrification. BOD₅ sludge loading and sludge retention times (SRTs) are the decisive design parameters. The so-called Modified OECD Confirmatory Test works with a sludge age of 8–10 days which ensures nitrification and reflects the status of waste-water treatment plants in many countries today.

Complete degradation of surfactants is accomplished by mixed cultures of micro-organisms, mainly bacteria constructed on the basis of synergistic and commensal-istic relationships. However, degradation of a surfactant by one member of a commensalistic consortium may lead to the formation of more toxic or also non-toxic metabolites. Under practical conditions in waste-water treatment plants, this can be avoided by the application of a low sludge loading corresponding to high sludge retention times (SRTs) in the biological reactor. The present development in the design and construction of waste-water treatment plants with nitrification and denitrification clearly favours a very high degradation of surfactants (90–99%), especially when biological nitrification and denitrification is applied on a large scale. Under these improved conditions, even hard to

Table 22.5. Standard conditions for aerobic batch tests

Test mixtures contain test compound, inorganic test medium and inoculum

The organic test compound is the source of carbon and energy

The concentration of the test compound must be high enough for the analytical procedure and not inhibitory to the test micro-organisms under test conditions. Frequently used test concentrations are, e.g. 20 mg/l DOC for ISO 7827 and ISO 9439 and 100 mg/l for ISO 9408

A standardized defined inorganic test medium is used with sufficient buffering capacity to maintain a pH value of about 7 throughout the test

As inoculum, unadapted mixed micro-organisms are used, e.g. from a municipal activated sludge plant at a concentration of 30 mg/l dry solids

Degradation of the test compound is usually determined in at least two parallel vessels, and the following controls are required:

- blank control (only inoculum)
- reference substance

and optionally:

- inhibition control (test compound and reference substance)
- abiotic elimination control (no inoculum, addition of biocide to prevent microbial growth, etc.)
- adsorption control (inoculum, addition of biocide, etc.)

The test mixture is aerated, mixed (by shaking) and incubated at a constant test temperature in the range of 20–25 °C.

The test duration is normally 28 days, with at least three to four samplings, per week to obtain about 15 values for the degradation curve

All aerobic batch tests are predominantly used to determine the ultimate biodegradability (mineralization) of a test compound. Therefore, the summary parameters, DOC (e.g. for ISO 7827), BOD (e.g. for ISO 9408) or CO₂ evolution (e.g. for ISO 9439), are used for analysis.

Additionally and optionally, the primary biodegradability of the test compound can be determined by a specific analysis

From the measured data, the biodegradation is calculated for every sampling day, e.g. DOC compared to the concentration at the start of the test, BOD as a percentage of ThOD and CO₂ as a percentage of ThCO₂. From these values, a degradation curve is drawn and the biodegradation degree of the test compound is indicated as the mean value of the plateau phase

degrade surfactants such as tetrapropylenebenzene sulfonate (TPBS) can be degraded by up to more than 90%.

Anaerobic biodegradation refers to the microbial degradation of organic substances in the absence of free oxygen (O₂). While O₂ serves as the electron acceptor in aerobic biodegradation processes, forming H₂O as the final product, degradation processes under anaerobic or anoxic conditions depend on alternative acceptors such as nitrate, sulfate or carbonate, yielding as final products molecular nitrogen (N₂), hydrogen sulfide (H₂S) and/or ammonia (NH₃) and methane (CH₄), respectively (7).

Anaerobic degradation is a multistep process which can be carried out by different bacterial groups and consortia. With polymeric substances like proteins or carbohydrates, this involves as a first step hydrolysis to monomeric compounds. Then in a subsequent step, the decomposition to soluble acids, alcohols, molecular hydrogen (H₂) and carbon dioxide is effected. Especially with surfactants of the sulfonate type, such as LASs, it has been shown that desulfonation reactions

take place (8). Desulfonation with assimilation of the sulfur moiety by strictly anaerobic bacteria was followed by the reduction of the sulfonate as a source of electrons and carbon under anaerobic nitrate-respiring conditions. Up until now, there is no clear evidence that such mechanisms would also occur at significant rates under real-world conditions, e.g. anaerobic digesters or denitrification stages in waste-water treatment plants.

5.2 Mechanical, chemical and physico-chemical elimination

Surfactants can also be removed from waste-water by mechanical, chemical and physico-chemical processes at waste-water treatment plants and in surface waters. If there are no undesired secondary effects during waste-water treatment and in sludge disposal, this way of elimination is, from the environmental point of view, of equal value to biodegradation. In this context, sorption

effects on sewage sludge particles are important. At the same time, precipitation effects in sewer systems and at the mechanical stage of a waste-water treatment plant can play an important role with surfactants such as LASs which are sensitive to water hardness. By the formation of insoluble calcium salts, a higher elimination can take place. In this way, certain surfactants are already removed in the mechanical stage. From there, they are immediately transferred to the anaerobic digestion stage, where for LASs no further degradation can be expected. Photolytic and hydrolytic degradation mechanisms for cationic compounds also have to be regarded, especially in surface waters.

5.3 Aquatic toxicity

In particular for the assessment of ecological risks with surfactants, aquatic toxicity is of outstanding importance since this is the most deleterious effect such a compound can exert on the environment (9–11).

Orally administered surfactants have only a low toxicity against higher organisms but they generally show a rather high toxicity in surface waters against algae, crustaceans, fish and many other water organisms in the freshwater and marine environments. With anionic surfactants, these effects on fish are mainly caused by damaging the gills. With nonionic compounds, narcotic effects on the central nervous system are a way of attack. Since surfactants have a high affinity to proteins, they can also influence enzymatic activities and in this way can cause disorders in metabolism. In the ecological assessment of surfactants today, acute and

chronic toxicity must be equally regarded with the restriction that the amount of data on chronic toxicity is still limited.

The acute toxicity test which is mostly used describes the adverse biological effect or effects which occur within a short period of time after a short-term exposure. The results are often expressed as the LC₅₀ or EC₅₀ (median lethal or median effect concentration) values which are statistically derived concentrations which over a defined period of exposure in an acute toxicity test are expected to cause death or effects in 50% of the organism in a given period (24, 48 or 96 h).

The major application of LC₅₀/EC₅₀ values is for the classification of substances according to their toxicities. There are a multitude of laws and regulations worldwide which are based to some degree on these numerical values. The complete hazard evaluation of a substance must include an examination of its lethal concentration, as well as all other aspects of its acute toxicity. It should be understood that the use of LC₅₀/EC₅₀ (0, 100) for classification is based more on expediency and regulatory demands than on science. It must equally be recognized that the LC₅₀/EC₅₀ (0, 100) values have become an integral part of most regulatory systems.

The LC₅₀/EC₅₀ values are statistically derived from biological data and thus are inherently variable values. They cannot be considered to be constants and therefore their accuracies cannot be determined. There are several international standards (ISO) for testing the aquatic toxicity with freshwater organisms. Table 22.6 gives an overview on these methods and the corresponding OECD guidelines for the testing of chemicals. For a

Table 22.6. International standards (ISO) for testing the aquatic toxicity with freshwater organisms and the corresponding OECD Guidelines for the testing of chemicals

Test organism	Title (ISO)	ISO	OECD Guideline
Fish	Determination of the acute lethal toxicity of substances to a freshwater fish (<i>Brachydanio rerio</i> Hamilton-Buchanan (Teleostei, Cyprinidea))	7346-1,-2,-3 (1996)	203
Fish	Determination of the prolonged toxicity of substances to freshwater fish – Method for evaluating the effects of substances on the growth rate of rainbow trout (<i>Oncorhynchus mykiss</i> Walbaum (Teleostei, Salmonidae))	10 229 (1994)	204
Fish (embryo)	Determination of toxicity to embryos and larvae of freshwater fish	12 890 (1999)	
Daphnia	Determination of the inhibition of the mobility of <i>Daphnia magna</i> Straus (Cladocera, Crustacea) – Acute toxicity test	6341 (1996)	202
Algae	Freshwater algal growth inhibition test with <i>Scenedesmus subspicatus</i> and <i>Selenastrum capricornutum</i>	8692 (1989)	201
Algae	<i>Pseudomonas putida</i> growth inhibition test (<i>Pseudomonas</i> cell multiplication inhibition test)	10 712 (1995)	–
Algae	Guidelines for algal growth inhibition tests with poorly soluble materials, volatile compounds, metals and waste-water	14 442 (1999)	–
Luminescent bacteria	Determination of the inhibitory effect of water samples on the light emission of <i>Vibrio fischeri</i> (Luminescent bacteria test)	11 348-1,-2,-3 (1998)	–

general description and evaluation of acute ecotoxicity the following ranking is generally accepted:

< 1 mg/l,	very toxic
1–10 mg/l,	toxic
10–100 mg/l,	slightly toxic
> 100 mg/l,	non toxic

A growing importance is dedicated to chronic toxicity, which describes the harmful properties of a substance which are demonstrated only after a long-term exposure in relation to the live span of the test organism. This is usually expressed by either the “LOEC” or “NOEC” values.

The LOEC (lowest observed effect concentration), or threshold level of observed effects, is the lowest test concentration at which a substance is observed to have a statistically significant and unequivocal effect on the test species. The NOEC (no observed effect concentration) is the highest tested concentration below the LOEC where the stated effect was not observed. A chronic toxicity test may include more than one generation of the test organism.

A knowledge of chronic and sub-acute toxic effects is the basis of a risk-assessment procedure which is closer to natural conditions. It is decisive to know what concentration of surfactant causes no observable effects any more. For the quantitative description of a chronic exposure situation, the NOEC value is used. By the eventual use of additional safety factors a so-called PNEC (predicted no effect concentration) value can be derived. The latter describes a situation where in the environment no deleterious effects should be expected any more. Aquatic toxicity and biological degradation are closely connected with each other insofar as a

good and rapid biological degradation in a waste-water treatment plant prevents a transfer of a toxicity potential into a recipient.

Another important definition and terminology is the so-called “application factor”, which is applied for converting data from one exposure period or end point to another, e.g. from an acute EC₅₀ (measured) to a chronic NOEC (predicted). For surfactants, application factors from 10 to 1000 are generally used when missing data for chronic toxicity have to be derived from acute toxicity tests. The stringency of the acute test influences the dimension of the application factor.

5.4 Formation of hazardous metabolites

The criterion for the formation of hazardous metabolites describes a behaviour where mainly biological degradation produces more toxic intermediates than the original compound.

This problem is essentially restricted to the alkylphenol ethoxylates (APEOs). Here, during biological degradation lower ethoxylated compounds, with one or two EO units, and nonylphenol are formed which are more toxic and additionally display undesired effects on the endocrine system. The opposite, for instance, is true for degradation products from LASs such as sulfophenolic fatty acids which display a highly reduced aquatic toxicity.

Metabolite formation with surfactants has also been shown in fish without any identifying harmful effects (Table 22.7).

Table 22.7. Surfactant metabolism in fish

Substance	Species	Matrix	Metabolite
Sodium lauryl sulfate	<i>Carassius auratus</i>	Bile	Principal metabolite: butyric acid-4-sulfate ^a Minor metabolites: C ₁₀ , C ₈ and C ₆ intermediates ^b
Linear alkylbenzene sulfonates	<i>Pimephales promelas</i>	Water	Principle metabolite: butyric acid-4-sulfate ^a
		Bile	98% of ¹⁴ C recovered as metabolites ^b
		Gills	25–75% of ¹⁴ C as metabolites ^b
		Kidney	75–85% of ¹⁴ C as metabolites ^b Principal metabolites (4) including 3-phenyl-butyric acid ^a Minor metabolites (10) ^b
Diocetyl sodium sulfosuccinate	<i>Oncorhynchus mykiss</i>	Bile	Principal metabolites (2): 85% of ¹⁴ C recovered ^b Parent substance: 14% of ¹⁴ C recovered ^b
Sodium dodecyl tri(oxyethylene)ether	<i>Cyprinus carpio</i>	Bile	Majority of ¹⁴ C recovered as metabolites ^b
Sodium dodecyl tetra(oxyethylene)ether	<i>Cyprinus carpio</i>	Bile	> 95% of recovered ¹⁴ C as metabolites ^b
		Gills	> 85% of recovered ¹⁴ C as metabolites ^b
		Kidney	> 90% of recovered ¹⁴ C as metabolites ^b
		Liver	> 85% of recovered ¹⁴ C as metabolites ^b
		Blood	> 80% of recovered ¹⁴ C as metabolites ^b

^ametabolite identified by using GC-MS.

^bidentity of metabolite(s) not known.

5.5 Bioaccumulation and biomagnification

Bioconcentration is usually defined as the net result of the uptake, distribution and elimination of a substance in an organism due to water-borne exposure, whereas *bioaccumulation* includes all routes of exposure (i.e. air, water, soil, food, etc.). *Biomagnification* is defined as the accumulation and transfer of substances via the food web.

The bioaccumulation of a substance into an organism is not an adverse effect hazard in itself. Bioconcentration and bioaccumulation may lead to an increase in body burden which may cause toxic effects due to direct and/or indirect exposure. Bioaccumulative substances characterized by high persistence and toxicity, negligible metabolism and a log K_{ow} between 5 and 8 may represent a concern when widely dispersed in the environment. The potential of a substance to bioaccumulate is primarily related to its lipophilicity. A surrogate measure of this quality is the *n*-octanol – water partition coefficient (K_{ow}), which is correlated with bioconcentration potential. Therefore, K_{ow} values are normally used as predictors in quantitative structure – activity relationships (QSARs) for bioconcentration factors (BCFs) of organic non-polar substances.

It has to be considered that when biotransformation of a substance by the organism occurs, elimination may significantly increase this reducing bioconcentration.

A number of test guidelines for the experimental determination of bioconcentrations in fish have been documented and adopted, with the most generally applied being the OECD test guidelines and the ASTM standard guide. However, there are no internationally recognized guidelines on the experimental determination of bioaccumulation and biomagnification. Generally, substances with high solubilities, such as surfactants, are less likely to partition into lipids and hence have a low bioconcentration potential. Linking surface activity with bioconcentration has not been well studied.

With regard to bioconcentration, it is important that surfactants are characterized by combining a lipophilic and a hydrophilic moiety in the same molecule. This is true for all four classes, namely anionic, nonionic, cationic and amphoteric surfactants. Although these classes possess quite different hydrophilic groups, the lipophilic part usually consists of an alkyl chain or alkyl chains of different lengths. There is some evidence that the lipophilic groups of surfactants are metabolized after uptake by aquatic invertebrate species (*Daphnia* and *Chironomus*) and fish.

Laboratory studies carried out with ^{14}C -labelled LASs indicated that the BCFs of LAS 11.6 and 11.7 ranged from 50 to 70. Concentrations in fish (300 $\mu\text{g}/\text{kg}$) measured in the Tokyo Bay area in the Pacific Ocean is related to local discharges. Surface water concentrations averaged around 10 $\mu\text{g}/\text{l}$ (Field BCF = 30).

It can be concluded that LASs do not represent a significant hazard for toxicity due to bioaccumulation.

5.6 Behaviour of surfactants in sewage sludge, soil and plants

In the last 10 years, accumulation processes of surfactants on sewage sludge, in soil and in plants have been investigated with the following main areas of focus:

- Aerobic and anaerobic degradation behaviour in soil (pilot and monitoring studies), including the identification of metabolites
- Transport of surfactants in soil and groundwater
- Uptake by plants and general bioavailability in soil
- Influence on the behaviour of other sewage sludge and soil components (polyaromatic hydrocarbons and other hazardous compounds)

In several studies, it was found that a real risk could not be recognized.

6 ANIONIC SURFACTANTS

6.1 General remarks

Anionic surfactants are used to a great extent in the industrial sector as well as in the household and personal care sector. In this context, sulfonates and sulfates are especially important. Apart from soaps, the most important mass produced compounds are:

- Linear alkylbenzene sulfonates
- Fatty alcohol sulfates
- Fatty alcohol ether sulfates
- Paraffin sulfonates
- α -olefin sulfonates
- Petroleum sulfonates

while of minor importance are:

- α -sulfo fatty acid esters
- Sulfosuccinic acids
- Alkyl esters
- Acyl oxyalkane sulfonates

- Acyl aminosulfonates (taurides)
- Sarcosinates
- Alkyl phosphates

which are mainly used in cosmetics and in cleaning formulations.

Anionic surfactants also comprise most of the so-called *bio-surfactants*. These fulfil important physiological functions in nature. To a lesser degree, they also have commercial applications.

Low production costs, technical application properties, high water solubility, and cold-resistance of solutions are the reasons which determine the high importance of this surfactant group, which has the consumption amounts in the Federal Republic of Germany as shown earlier in Figure 22.2.

All large-scale produced surfactants are not pure chemical substances, but mixtures of isomeric and homologous compounds. This is especially true for most of the anionic surfactants. Isomerism can be related to the alkyl chain length, the location of alkyl branching, the kind of branching, or the number of ethoxylate groups in ethylene oxide adducts. The occurrence of single isomeric and homologous compounds follows statistical frequency distribution patterns which results in a more or less high content of the main component. It can be observed that purer fractions are increasingly being introduced into the market. The distribution of homologues and isomers strongly influences biodegradation and aquatic toxicity characteristics.

Soaps also belong to the group of anionic surfactants. These are alkali salts (mainly Na and K) from medium- to long-chain saturated and unsaturated fatty acids (C₁₂–C₂₂). Based on their chemical structure and their electrochemical behaviour, they belong to anionic surfactants of the carboxylate type. The consumption of soaps is 105 000 t/a in Germany, which corresponds to a raw waste-water concentration of around 24 mg/l.

6.2 Biodegradability

The introduction and use of tetrapropylenebenzene sulfonate (TPBS) in household detergents in the 1950s directed, for the first time, public attention to the ecological behaviour of a chemical compound produced in large volumes. The poor biodegradability of TPBS in waste-water treatment plants at that time and a general poor status of such biological treatment plants resulted in serious foam problems in these plants and surface waters and in high concentrations in recipients.

Linear alkylbenzene sulfonates (LASs) are primarily attacked via a hydroxylation of the alkyl chain from

the methyl group, followed by β -oxidation. The ultimate biodegradation to CO₂, H₂O and SO₄²⁻ requires many different enzyme systems. For this reason, several taxonomically different bacteria are involved in the mineralization of LASs. Generally it can be stated that the microbial degradation of an LAS is well elucidated. Figure 22.4 shows the main degradation path of an LAS, which is the degradation of the alkyl chain followed by ring fission and desulfonation. At the same time, it can be concluded that no stable or harmful metabolites are formed during these different degradation steps.

According to several studies, the biodegradation of primary alkane sulfonates begins with a desulfonation step, followed by a final β -oxidation of the alkyl chain. The biodegradation of alkyl sulfates starts with the splitting off of the sulfate group, which is catalysed by sulfatases. The resulting alcohol is oxidized via the aldehyde to the corresponding carbon acid, followed by a final metabolization via β -oxidation (Figure 22.5). The initial attack on alkane sulfonates depends on the presence of molecular oxygen and NADH (reduced nicotinamide – adenine dinucleotide), indicating mono-oxygenase activity. A hydrolysis of the α -carbon of alkane sulfonate by this mono-oxygenase yields the labile 1-hydroxy-*n*-alkane sulfonate, which then hydrolyses to give the corresponding alkanals. The oxidation of the alkanals leads to the production of homologous carbon acids. The carbon acids, in turn, are further metabolized by β -oxidation.

Quantitative data on the biological degradation of anionic surfactants can be found in Table 22.8. Pilot studies carried out with LASs in the Netherlands, Germany, Italy, Spain and the UK show mean removals of 99.2% in activated sludge plants in these countries where a high standard in waste-water treatment exists.

An additional extensive field study by Association Internationale de la Savonnerie, de la Détergence et des produits d'Entretien (A.I.S.E.) and Comité Européen des Agents de Surface et de leurs Intermediaires Organiques (CESIO) (*Environmental Risk Assessment of Detergent Chemicals*) (13) in 1995 provides substantial measuring data on the elimination of commercially important surfactants, i.e. alcohol ethoxylates (AEs), alkyle ether sulfates (AESs), alkyl sulfonates (ASs) and linear alkylbenzene sulfonates (LASs), in seven modern waste-water treatment plants in The Netherlands. Table 22.9 summarizes the key monitoring data for these surfactants.

The results indicate that on average all surfactants were removed by more than 99% during activated sludge treatment. The removal of surfactants was always higher than the elimination of organic material, expressed as the

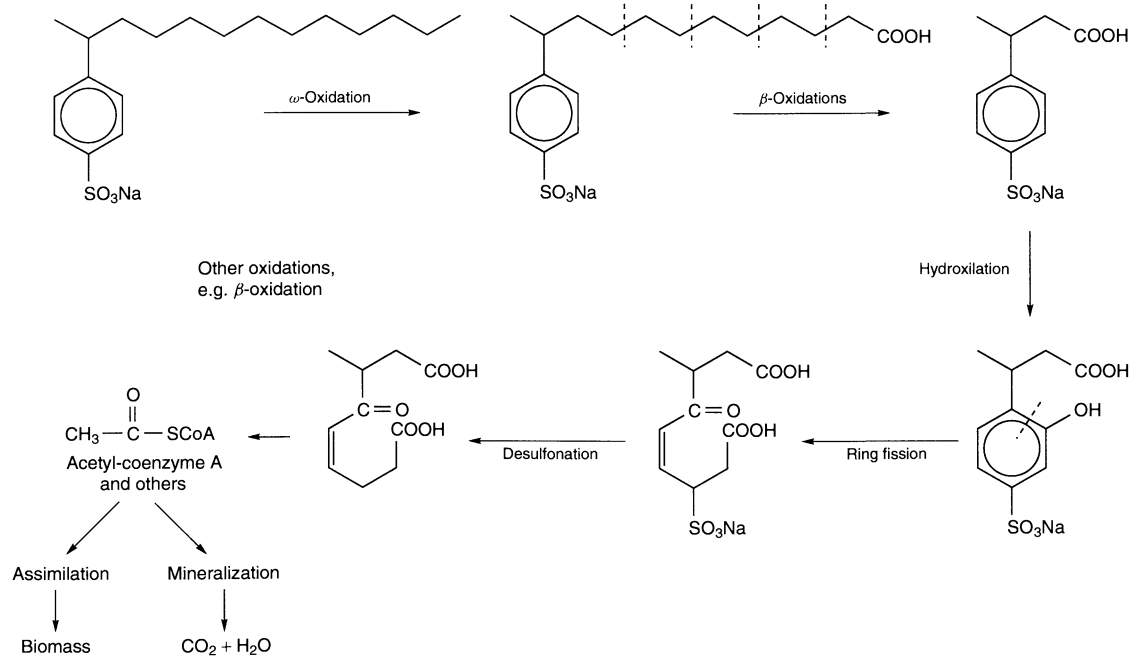


Figure 22.4. Main degradation pathways of linear alkylbenzene sulfonates (from *Fond der Chemischen Industrie*, Folien serie "Tenside", Frankfurt/Main, Germany, 1992)

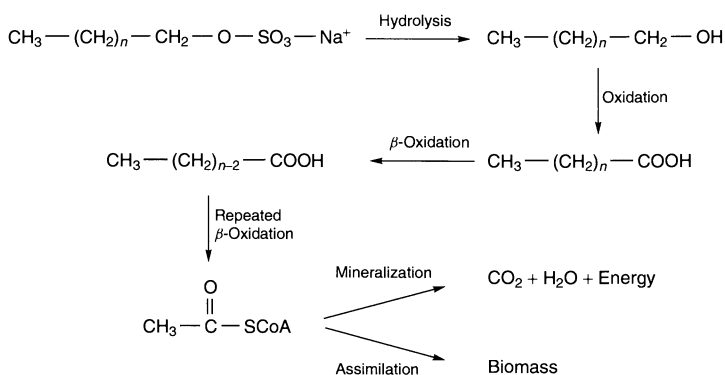


Figure 22.5. Biodegradation of alkyl sulfates (from ref. (12) with kind permission from Kluwer Academic Publishers)

BOD. The measured effluent concentrations were in the low $\mu\text{g/l}$ range and therefore not acutely toxic to aquatic organisms (14).

Surfactants containing perfluoroalkyl groups (fluorinated surfactants) play an important role in different manufacturing processes (metal working, the photo industry, etc.). They are generally considered as being very stable compounds because the enzymatic cleavage of the carbon-fluorine bond is very hard to achieve. This is confirmed by the behaviour of perfluorooctane

sulfonic acid which was degraded neither under aerobic nor under anaerobic conditions (15).

Generally, soaps are readily biodegradable up to a concentration of 1000 mg/l. Soaps with shorter alkyl chains are faster degraded. In addition, they do not inhibit the biodegradation of other organic substance contained in domestic waste-water. Soaps are readily biodegradable under anaerobic conditions. Non-soluble calcium soaps show the same behaviour if the particle size is small enough.

Table 22.8. Data obtained for the biodegradability of anionic surfactants

Surfactant	Removal of MBAS ^a		Ultimate degradation				
	OECD Screening Test (%)	OECD Confirmatory Test (%)	Screening Tests			Coupled Units Test	
			Removal (%)	Parameter ^b	Test	Removal (%)	Parameter
LAS (C ₁₀₋₁₃ : Ø C _{11,6}); MW 348	95	93-97	73-84	C	MOST	73 ± 6	C
			55-65	BODT	CB	74 ± 11	C
			45-76	CO ₂	Sturm	93 ^c	C
Secondary alkane sulfonate (C ₁₃ -C ₁₈)	96	97-98	88-96	C	MOST	96 ± 3	C
			63-95	BODT	CB	93 ± 5	C
			56-91	CO ₂	Sturm	83 ± 13	C
Alcohol sulfate (C ₁₂ -C ₁₈ -FA-, C _{12/14} FA-oxo-alcohol sulfate)	99	98-99	88-96	C	MOST	97 ± 7	C
			63-95	BODT	CB	94-99 ^d	C
			64-96	CO ₂	Sturm		
Alcohol ether sulfate (C _{12/14} FA + 2EO sulfate, C _{12/15} oxo-alcohol + 3EO sulfate)	98-99	96	96-100	C	MOST	67 ± 6	C
			58-100	BODT	CB	68 ± 3	C
			65-83	CO ₂	Sturm	89 ± 6	C
						99 ± 8	C
Sulfosuccinic ester, Dioctyl sulfosuccinate	97	96	50	BODT	CB	49 ± 13	C
α-Olefinsulfonate (C ₁₄ -C ₁₈)	99	98	85	C	MOST	70 ± 5	C
			85	BODT	CB	78 ± 3	C
			65-80	CO ₂	Sturm		
α-Methyl ether sulfonate	99	95	76	BODT	CB	98 ± 6	C
			42-57	CO ₂	Sturm		

^aMethylene blue active substance(s).

^bBODT, BOD₃₀ related to the theoretical BOD (%).

^cMOST, Modified OECD Screening Test; CB, Closed Bottle Test; Sturm-Test.

^dWithout sludge exchange.

Table 22.9. Summary of the key monitoring data for surfactants obtained by field studies in waste-water treatment plants in The Netherlands

Surfactant	Influent range (mg/l)	Influent average (mg/l)	Effluent range (µg/l)	Effluent average (µg/l)	Removal range (%)	Removal average (%)
BOD ^a	134-285	221	2000-4300	3200	96.4-99.2	98.1
LASs	3.4-8.9	5.2	19-71	39	98.0-99.6	99.2
AE (C ₁₂₋₁₅)	1.6-4.7	3.0	2.2-13	6.2	99.6-99.9	99.8
AES (C ₁₂₋₁₅)	1.2-6.0	3.2	3.0-12	6.5	99.3-99.9	99.6
AS (C ₁₂₋₁₅)	0.1-1.3	0.6	1.2-12	5.7	99.0-99.6	99.2
Soap	1.4-4.5	2.8	91-365	174	97.7-99.6	99.1

^aElimination of organic material, expressed as the BOD.

^bIn units of µg/l.

An important abiotic elimination process of LASs during waste-water treatment is chemical precipitation in sewer systems and in mechanical sedimentation tanks of waste-water treatment plants by alkaline-earth ions. As a result of this, a possible aerobic degradation of those surfactants sensitive to water hardness during the biological treatment (activated sludge, trickling filter, etc.) is prevented. Together with the primary sludge water, insoluble precipitates reach the anaerobic digester

where no further anaerobic degradation takes place. In this way, LASs contained in digested sludge can possibly contaminate soil. Non-sulfonated anionic surfactants are biodegradable under anaerobic conditions.

According to a review by AISE and CESIO on the fate and biodegradation of commercial surfactants, which was completed in 1999, the following statements on the anaerobic biodegradation behaviour of anionic surfactants can be made:

- Sulfonated anionic surfactants (LAS, SAS and MES) – poorly biodegradable
- Sulfated anionic surfactants – well biodegradable
- Fatty acids and soaps – well biodegradable

6.3 Aquatic toxicity

Seen as a whole, there are many data available on the aquatic toxicity of anionic surfactants, mainly for acute

toxicity. In a status report by the German “Hauptausschuß Detergentien” which was published in 1988, data, mainly on acute toxicity, were presented for seven different surfactants (Table 22.10).

Since LAS surfactants are still widely used as work-horses in household detergent formulations, most data are available for this compounds, and also with special regard to the effects of alkyl chain length on aquatic toxicity. In optimizing detergency and ecology,

Table 22.10. Data obtained for the aquatic toxicity of anionic surfactants

Surfactant	Fish toxicity, LC ₅₀ (mg/l)	Daphnia toxicity, EC ₅₀ (mg/l)	Toxicity data for other species (mg/l)	Remarks
LAS (C ₁₀₋₁₃ ; Ø C _{11,6}) MW 348 (common in Germany)	Golden orphee, 3.2–4.9 Zebra fish, 7.8 Rainbow trout, 5.6 Goldfish, 9.2 Fathead minnow, 4.1 (Ø 3–10)	8.9–14	Algae (cell multiplication inhibition), 10–300	Toxic long-chain isomers are degraded faster than less toxic short-chain isomers. After waste-water treatment, the mixture of isomers is 10-fold less toxic than the original substance. The first metabolic degradation step already leads to total detoxification. The reliable assessment of toxicity by considering the composition is not possible
Alkyl chain > C _{11,6} (not used in Germany)	Toxicity ca. 1 mg/l or < 1 mg/l			
Secondary alkane sulfonate (C ₁₃ –C ₁₈)	3–24	8.7–13.5	–	
Alcohol sulfate (C ₁₂ –C ₁₈ -FA-, C _{12/15} FA- oxoalcohol sulfate)	3–20	5–70	Algae (growth), 60	
Alcohol ether sulfate (C _{12/14} FA + 2EO sulfate, C _{12/15} oxo-alcohol + 3EO sulfate)	1.4–20	1–50	Algae (growth), 65	
Sulfosuccinic ester, Dioctyl sulfosuccinate	39	33	–	Pure carbon chains from C ₁₂ to C ₁₈ are considerably less toxic (daphnia)
α-Olefin sulfonate (C ₁₄ –C ₁₈)	2–20	5–50	Algae (growth), 10–100	Often other names for the same substance: C ₁₄ –C ₁₆
α-methyl ether sulfonate	0.5–5	acute, 7–40 chronic (NOEC), 0.2–0.6	Algae (growth), 3.0 Bacteria, <i>Ps.</i> <i>putida</i> (growth), EC ₁₀ of 220	

a C_{11,6}-LAS is preferred; the LC₅₀ value for fish is in the range of 3–10 mg/l. Long-chain LASs are more toxic (< 1 mg/l). Daphnids are, by a factor of two less sensitive than fish. The α -olefin sulfonates display an acute toxicity between 2 and 20 mg/l, again with longer-chain compounds being more toxic.

Sulfosuccinates have a rather good ecological profile, with acute toxicities of about 33–39 mg/l.

The aquatic toxicity of primary alkyl sulfates with a chain length range from C₁₂ to C₁₈ generally lies between 3 and 20 mg/l. The toxicity to daphnids is lower by a factor from 2 to 3.

Alkyl ether sulfates (C₁₂–C₁₄, C₁₆–C₁₈, 1–4 EO) have a similar toxic profile. Compounds with a higher number of EO units are less toxic.

According to Figure 22.6, the toxicity of alkane sulfonates is a function of chain length. For three important groups of water organisms (fish, daphnia and algae), alkane sulfonates become more toxic with growing chain length.

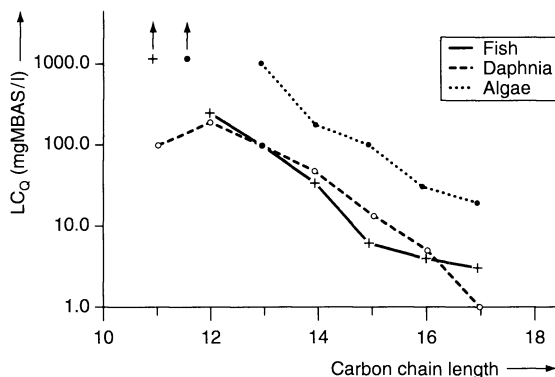


Figure 22.6. Toxicity of alkane sulfonates as a function of chain length (from ref. (17))

Table 22.11. Aquatic toxicity of soaps against daphnia (test duration of 24 h)

Substance	Test criteria	Concentration (mg/l)
Sodium oleate	EC ₅₀	4.2
	EC ₀	1.6
	EC ₁₀₀	15
Sodium laurate	EC ₅₀	48
	EC ₀	15
	EC ₁₀₀	125
Tallow soap	EC ₅₀	40
	EC ₀	30
	EC ₁₀₀	50
Palm kernel soap	EC ₅₀	25
	EC ₀	6.3
	EC ₁₀₀	50

Table 22.12. Aquatic toxicity of soaps against algae (in mg/l) after 72 h exposure time

Substance	EC ₅₀ (bio mass)	EC ₁₀ (bio mass)	EC ₅₀ (growth rate)	EC ₁₀ (growth rate)
Sodium tallow soap	190	70	280	104
Sodium palm kernel soap	140	60	195	102
Sodium oleate	58	10	95	34
Sodium laurate	53	9	160	17
Sodium behenate	230	30	500	79

Data for acute aquatic toxicity against daphnia are found in Table 22.11, with a clear indication that also soaps as surface-active compounds display a toxicity similar to synthetic surfactants. The aquatic toxicity of soaps depends considerably on the water hardness.

Table 22.12 presents data obtaining for the aquatic toxicity of soaps, as determined by the algae cell multiplication inhibition test (DIN 38412 L9).

Chronic and sub-lethal toxicities of anionic surfactants to aquatic animals (invertebrates and vertebrates) generally occur at concentrations equal to greater than 0.1 mg/l. Table 22.13 gives an overview of the reported chronic toxicities to invertebrates, including freshwater and marine organisms.

Table 22.14 presents chronic toxicities of surfactants to fish, mainly restricted to various blends and homologous of LASs. Additional information comes from Table 22.15, where other anionic surfactants were tested, leading to similar results (18).

7 NONIONIC SURFACTANTS

7.1 General remarks

The use of nonionic surfactants has reached more than 50% of the total market in Western Europe today (Table 22.1), with a rather pronounced rise in the last few years. For this reason the ecological behaviour of nonionic surfactants is very important.

According to production figures the following ranking of nonionic surfactants can be made:

- Fatty alcohol ethoxylates (fatty alcohol polyglycol ethers)
- Alkylphenol ethoxylates (alkylphenol polyglycol ethers)
- Fatty acid esters
- Fatty acid amides

Table 22.13. Chronic toxicities of surfactants to invertebrates

Surfactant	First-effect concentration (mg/l)	Test species	Test duration ^a	Effect ^a
C _{11,8} -LAS	1.7–3.4	<i>Daphnia magna</i>	21 d	Survival, reproduction
LAS	> 10.0	<i>Daphnia magna</i>	21 d	Reproduction
C _{11,8} -LAS	1.18 (NOEC)	<i>Daphnia magna</i>	21 d	Reproduction
C ₁₃ -LAS	0.57 (NOEC)			
AES	0.27 (NOEC)			
AS	0.25	Flatworms: <i>Dugesia gonocephala</i> and <i>Notoplana humilis</i>	30 d	Regeneration
LAS	0.2–0.4	<i>Gammarus pseudolimnaeus</i>	6–15 weeks	Growth, reproduction
	0.4–1.0	<i>Campeloma decisum</i> (snail)		
	> 4.4	<i>Physa integra</i> (snail)		
LAS	0.05–0.10	Oyster (<i>Crassostrea virginica</i>)	10 d	Larval growth, egg development
C _{11,8} -LAS	< 0.32, 0.89	<i>Ceriodaphnia dubia</i>	7 d	Reproduction
LAS (C ₁₀ –C ₁₄ homologues)	0.1–9.8 (NOEC range)	<i>Daphnia magna</i>	ND	Reproduction
C _{11,7} -LAS	3.0 (NOEC)	<i>Ceriodaphnia</i> sp.	ND	Reproduction
C _{13,1} -LAS	0.04 (NOEC)	Mysid shrimp (<i>Mysidopsis bahia</i>)	ND	ND
C _{11,4} -LAS	0.4 (NOEC)			
ABS	0.55–5.8	Clams (<i>Mercenaria mercenaria</i>)	14 d	Larval growth and development
	0.14–1.63	Oyster (<i>C. virginica</i>)		
AS	0.47–1.46	<i>M. mercenaria</i>	14 d	Larval growth and development
	0.37–1.46	<i>C. virginica</i>		
LAS	0.05	Mussel (<i>Mytilus edulis</i>)	10 d	Fertilization, larval growth

^aND, not defined.**Table 22.14.** Chronic toxicities of surfactants to fish (Reproduced with permission of Hanser Verlag, Munich)

Surfactant	First-effect concentration (mg/l)	Test species	Test duration	Effect
C _{11,8} LAS	0.90 (NOEC)	Fathead minnow	28 d	Hatching, growth, larval survival
C ₁₃ -LAS	0.15 (NOEC)			
AES	0.10 (NOEC)			
C _{11,2} -LAS	5.1–8.4	Fathead minnow	Complete life cycle, partial life cycle	Hatching, growth, larval survival
C _{11,7} -LAS	0.48–0.49			
C _{13,3} -LAS	0.11–0.25			
LAS	0.63–1.2	Fathead minnow	28 weeks	Survival
C ₁₀ -LAS	14.0–28.0	Fathead minnow	28 d	Survival, hatching
C ₁₁ -LAS	7.2–14.5			
C ₁₂ -LAS	1.08–2.45			
C ₁₃ -LAS	0.12–0.28			
C ₁₄ -LA	0.05–0.10			
LAS	3.2 (NOEC)	<i>Poecilia reticulata</i>	28 d	Immobility
LAS	0.05–0.50	Marine flatfish (<i>Limanda yokohamae</i> , <i>Paralichthys ovaliceus</i>)	30 d	Hatching
LAS	2.0–5.0	Fathead minnow	30 d	–
LAS	0.25–1.10	Tilapia mossambica	90 d	Fecundity, maturity
LAS	4–10	Bluegill	6 d	Fertilization, hatching
LAS	0.5–1.1	Fathead minnow	30 d	Standing crop
	< 0.3	White sucker		
	0.5–1.2	Northern pike		
	2.3–5.8	Smallmouth bass		

Table 22.15. NOEC and LOEC values of SAS and AE2S for fish and daphnia (12)^a

Surfactant	Fish (<i>Oncorhynchus mykiss</i>)		<i>Daphnia magna</i>	
	NOEC	LOEC	NOEC	LOEC
SAS	0.85	2.87	0.37	1.16
AE2S	0.1	0.27	0.72	2.16

^aAll values in units of mg/l, measured after 28 d.

- Fatty acid alkanol amides
- Carbohydrate surfactants (e.g. alkyl polyglycosides)

Furthermore, many ethoxylated and/or propoxylated compounds and amines are used in many applications and can be introduced into the environment via generally known pathways. Especially from the ecological point of view, the application of some groups of

nonionic surfactants has changed dramatically over the past few years. The use of alkylphenol ethoxylates has been reduced due to the formation of toxic metabolites (especially nonylphenol with its endocrine effects). For example, in Germany from 1986 there has existed a voluntary self-obligation by detergent producers that they will no longer use alkylphenol ethoxylates in detergents. On the other hand, surfactants which are based on renewable materials have increased considerably (e.g. alkyl polyglycosides).

7.2 Biodegradability

The important group of fatty alcohol ethoxylates is readily biodegradable (Table 22.16). The ultimate degradation measured by Coupled Units Tests ranges between 93 and 96%. The mineralization determined in a

Table 22.16. Data obtained for the biodegradability of nonionic surfactants

Surfactant	Removal of BiAS ^a		Ultimate degradation				
	OECD Screening Test (%)	OECD Confirmatory Test (%)	Screening Tests			Coupled Units Test	
			Removal (%)	Parameter ^b	Test ^c	Removal (%)	Parameter
Fatty alcohol ethoxylate							
C _{16/18} -FA + 5EO	96		65–75	BODT	CB		
C _{12–18} -FA + (10–14) EO	98–99	93–98	69–86	BODT	CB	95 ± 3	C
C _{16/18} -FA + 30EO	99	98	94	C	MOST	96 ± 4	C
C _{16/18} -FA + 25EO			27	BODT	CB	93 ± 6	C
C _{16/18} -FA + 25EO						75 ^d	C
Oxoalcohol ethoxylate							
C _{9/11} + 7EO		86				36 ± 9	C
C _{13/15} + (3–12)EO		95	75	C	MOST		
C _{14/15} + (9–20)EO		83–93	65–75	CO ₂	Sturm		
Nonylphenol ethoxylate							
NP-5/6EO	85	91–93				91 ± 5	C
NP-7EO						71 ^d	C
NP-9/10EO	≈ 80	87–97	8–17	C	MOST	90 ± 3	C
			5–10	BODT	CB	71 ^d	COD
			40	CO ₂	Sturm	77 ± 8	C
NP-20EO	80	85–90				70 ± 8	C
NP-25EO		85				50 ± 16	C
Fatty amine ethoxylate							
C _{16/18} -amine + 10EO	16	97–98				33 ± 9	C (6 h)
						6 ± 12	C
C _{16/18} -amine + 12EO	88		33	BODT	CB		
+ 20EO						70 ± 5	C
+ 2EO			85	CO ₂	Sturm		

(continued overleaf)

Table 22.16. (continued)

Surfactant	Removal of BiAS ^a		Ultimate degradation				
	OECD Screening Test (%)	OECD Confirmatory Test (%)	Screening Tests			Coupled Units Test	
			Removal (%)	Parameter ^b	Test ^c	Removal (%)	Parameter
Fatty acid polyglycol ester							
C ₁₂₋₁₈ (saturated and unsaturated)	95-99	92-96	60-80 100	BODT C	CB MOST	71 ± 4 71 ± 4 85 ^d 71 ± 4 85 ^d	C C C C C
+ 5-29EO oleic acid + 5EO							
Alcohol EO/PO adducts							
FA+(2-5)EO + 4PO	90	93-97	52 52 52	C BODT CO ₂	MOST CB Sturm	60 ± 18	C (6 h)
C _{12/18} -FA + 2.5EO + 6PO	97	87	43 36	C BODT	MOST CB	37 ± 14	COD
C _{12/18} -FA + 2.5EO + 6PO	95		69 83	C BODT	MOST CB		
C _{12/18} -oxoalcohol + 6EO + 2PO		76				17 ^d	COD
EO/PO block polymer:							
20% EO: MW 2500	32	7	8 0-10	C BODT	MOST CB	2 ± 4	COD
End-capped C _{12/14} -FA + 9EO- <i>n</i> -butylester	98		80	BODT	CB	88 ± 10	C (6 h)
Alkylolamide							
C _{12/14} -ethanol -amide+4EO	no BiAS	no BiAS	47	BODT	CB		
C _{12/14} -ethanol -amide+10EO			35	BODT	CB		
C _{12/14} -diethanolamide			74	C	MOST	61 ^d	C
Glucose amide					Modified		
C _{12/14} -GA			86-89	CO ₂	Sturm		
Alkyl polyglycoside		no BiAS					
C _{8/10} -APG			88	C	MOST		
C _{12/14} -APG			56-82	C	MOST	89 ± 2	C

^aBiAS, bismuth active substance(s).

^bBODT, BOD₃₀ related to the theoretical BOD(%).

^cMOST, Modified OECD Screening Test; CB, Closed Bottle Test; Sturm-Test.

^dWithout sludge exchange.

catabolic test was 99 ± 3%. These high degradation values indicate that no poorly degradable metabolites are formed.

Two mechanisms for the initial attack of fatty alcohol ethoxylates by micro-organisms are described. First, the fission of the surfactant molecule into the alkyl and the ethoxylate chain, followed by an independent degradation of both components, or secondly, an attack at both ends of the molecule at the same time. The

degradation of alkylphenol ethoxylates is effected by shortening the polyethoxylate chain.

Several metabolites are formed during the aerobic and anaerobic biodegradation of alkylphenol ethoxylates (APEOs). Significant amounts are found of alkylphenol, mono- and diethoxylated alkylphenols and the equivalent carboxylates, i.e. alkylphenoxyacetic acid and alkylphenoxyethoxyacetic acid. A simplified scheme, according to Thiele *et al.* (19), of the biodegradation

Table 22.17. Acute aquatic toxicity of nonionic surfactants

Surfactant	EC ₅₀	Criterion	Concentration (mg/l)
Alkyl ethoxylate (C _{12/15} -(3-10)EO)	<i>Brachydanio rerio</i>	LC ₅₀	1.2-2.3
	<i>Daphnia magna</i>	EC ₅₀	0.41-4.17
	Luminescent bacteria	EC ₅₀	1.5
Alkyl ethoxylate (C ₁₃ -7EO, branched)	Fathead minnow	LC ₅₀	4.0
	<i>Daphnia magna</i>	EC ₅₀	9.0
	Luminescent bacteria	EC ₅₀	8.1
Alcohol EO/PO adducts C _{10/12} -4EO + 6PO	<i>Daphnia</i> species	EC ₀	2.2
	<i>Daphnia</i> species	EC ₀	17.3
Nonylphenol ethoxylate (9EO)	Fathead minnow	LC ₅₀	4.5
	<i>Daphnia magna</i>	EC ₅₀	12.9
	Luminescent bacteria	EC ₅₀	60
Alkyl polyglycoside	<i>Brachydanio rerio</i>	LC ₅₀	3.0
	<i>Daphnia</i>	EC ₅₀	7.0
	Algae	EC ₅₀	6.0
Glucose C _{12/14} amide	<i>Brachydanio rerio</i>	LC ₅₀	7.5
	<i>Daphnia</i>	EC ₅₀	18
	Algae	EC ₅₀	12.6

Table 22.18. Chronic aquatic toxicity of nonionic surfactants

Surfactant	Organism	Test and Criterion	Concentration (mg/L)
Alkylphenol ethoxylate	<i>Daphnia</i>	21 d, reproduction (NOEC)	0.24
	Fathead minnow	28 d, growth, hatching, larval survival (NOEC)	0.18-0.32
Fatty alcohol ethoxylate (C ₁₂₋₁₈ +9EO)	Rainbow trout	28 d (OECD 204) (NOEC)	0.25
	<i>Daphnia</i>	21 d (OECD 202) (NOEC)	2.9
	Algae	72 h (EG 92/69) (NOEC)	0.2
Alcohol EO/PO adducts C ₁₂₋₁₈ -2EO+4PO	Algae	96 h (NOEC)	0.6
	Biocenosis	(NOEC)	0.15
C ₁₂₋₁₈ -2EO+4PO Fatty acid C ₁₂₋₁₈ diethanol amide	Rainbow trout	28 d (OECD 204) (NOEC)	0.26
	<i>Daphnia</i>	21 d (OECD 202) (NOEC)	0.07
	Algae	72 h (EG 92/69) (NOEC)	0.32
Alkyl polyglycoside (C _{12/14} -APG)	Fish	Chronic, growth (NOEC)	1.6
	<i>Daphnia</i>	Chronic, reproduction (NOEC)	1.0
	Algae	Chronic, cell multiplication (NOEC)	2.0

- Salts of amine oxides
- Sulfonium salts

Until the beginning of the 1990s, di-tallow dimethylammonium chloride (DTDMAC) (see Figure 22.8) was the most important fabric-softening agent, but due to its poor biodegradability DTDMAC has been almost completely replaced by so-called "esterquats". The latter are quaternary ammonium compounds with ester linkages in their aliphatic chains, i.e. esterquats can undergo hydrolysis and therefore they are more easily biodegradable than DTDMAC. This introduction of ester linkages in aliphatic chains was also used to improved the

biodegradability of other groups of cationic surfactants (e.g. imidazolium salts). Today, commercially important cationic surfactants with ester linkages in their aliphatic chains include the following:

- Esterquat (commercial name)
- Diethylester dimethylammonium chloride (DEED-MAC)
- Diesterquaternary (DEQ)
- Di-tallow imidazolinester (DTIE)

The structures of these surfactants are shown in Figure 22.8.

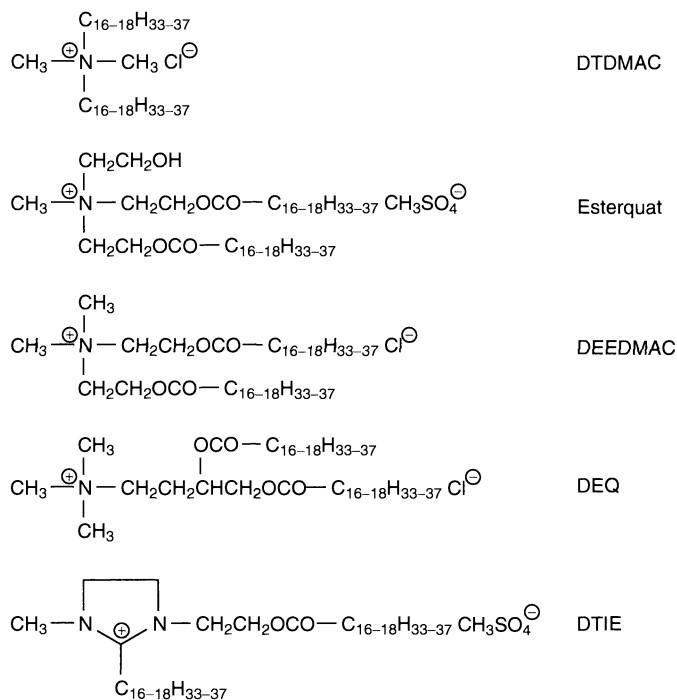


Figure 22.8. Chemical structures of commercial fabric softeners

8.2 Biodegradability

The ecological behaviour of cationic surfactants is basically determined by their basic physico-chemical property, i.e. the strong adsorption on surfaces, e.g. on clay minerals or activated sludge, thus leading to their elimination in water treatment plants and water courses. Although physico-chemical processes are primarily effective in the elimination of cationic surfactants of the quaternary-ammonium-ion type in waste-water treatment, there are indications on the basis of experiments that these substances are aerobically biodegradable.

Two mechanisms for the first step of biodegradation of alkylmethylammonium salts are described. The first of these is oxidation of the methyl groups at the far end of the alkyl chain end a stepwise shortening of the latter. The second is a fission of the bond between the nitrogen atom and the alkyl chain, followed by the oxidation of the alkyl chain to the carbon acid which is further metabolized through β -oxidation. It was proven in laboratory tests that alkylmethylammonium compounds are subjected to a primary degradation with an approximate half-life of 2.5 h. The ultimate degradation requires 28–40 h half-life.

However, alkylmethylammonium-type cationic surfactants are primarily very poorly biodegradable under anaerobic conditions and an ultimate biodegradation does not take place.

As described above, esterquats differ structurally from DTDMACs by the presence of ester linkages in the alkyl chains. These linkages allow a rapid and complete biodegradation of esterquats. For example, DEEDMACs reached about 80% CO₂ evolution in the modified Sturm test. With respect to the other criteria, DEEDMACs can be classified as readily biodegradable. In addition, a rapid and high anaerobic biodegradability of DEEDMACs was found (22). Similar results were reported from biodegradation tests with esterquats, DEQs and DTIEs. There was almost a complete mineralization and stable metabolites were not formed.

8.3 Aquatic toxicity

Several data for the acute and chronic toxicities of cationic surfactants with different aquatic organisms are shown in Table 22.19.

The aquatic toxicity of DTDMACs is generally higher than the aquatic toxicity of anionic and nonionic

Table 22.19. Aquatic toxicity of cationic surfactants

Surfactant	Organism	Test and Criterion	Concentration (mg/l)
DTDMAC	Fish	LC ₅₀	1–6
	Daphnia	EC ₅₀	0.1–1.0
	Fathead minnow	Early-life-stage (NOEC)	0.23
	Daphnia	Reproduction (NOEC)	0.38
Esterquat	Algae	NOEC	0.71
	Trout	LC ₅₀	3.0
	Daphnia	EC ₅₀	78.3
	Algae	EC ₁₀	1.4
DEEDMAC	Biocenosis	NOEC	0.15
	Algae	EC ₅₀ , 96 h, growth inhibition (OECD 201)	2.9
	<i>Daphnia magna</i>	LC ₅₀ , 24 h (OECD 202)	14.8
	<i>Brachydanio rerio</i>	LC ₅₀ , 96 h (OECD 203)	5.2
DEQ	<i>Daphnia magna</i>	21 d, growth (NOEC)	1.0
	Fathead minnow	35 d, growth (NOEC)	0.68
	Trout	LC ₅₀	7.0
	Daphnia	EC ₅₀	7.7
DTIE	Algae	EC ₅₀	1.8
	Daphnia	NOEC	1.0
	<i>Brachydanio rerio</i>	LC ₅₀ , 48 h	5–6
	Daphnia	EC ₅₀ , 48 h	0.4
	<i>Brachydanio rerio</i>	28 d (NOEC)	0.5–0.6
	Daphnia	28 d (NOEC)	0.25

surfactants, while the toxicity of esterquats is similar to that of commonly used anionic and nonionic surfactants.

Of far-reaching consequence from the toxicological aspect is the fact that neutral salts are formed with the anionic surfactants which are present in excess in domestic waste-water, thus leading to a considerable decrease in toxicity (23).

9 AMPHOTERIC SURFACTANTS

9.1 General remarks

Amphoteric surfactants have a special application profile which favours their use mainly in cosmetics. In recent years, they have also found increasing application in the development of dishwashing agents or household cleaners. Compared to the amounts produced world-wide of anionic and nonionic surfactants, the volume of amphoteric is still relatively small. For cosmetic products, their consumption in Europe in 1992 was about 15 000 t. The main carbon chain includes the C₈–C₁₈ range. The zwitterionic character of amphoteric strongly influences their particular behaviour, i.e. both anionic and cationic

units are found in the molecules. Figure 22.9 shows the two most important types of amphoteric, i.e. betaines and “true” amphoteric, and the structural dependence on the pH range. Real amphoteric surfactants form salts in both alkaline (anion) and acid (cation) environments. Between the two structures, there is a status of compensation designated as the “isoelectric range” (24).

Table 22.20 presents a list of commercially available amphoteric substances.

9.2 Biodegradation

According to Table 22.21, commercially used amphoteric surfactants are readily biodegradable under stringent OECD tests on ultimate biodegradation and therefore pose no risk for the environment if biological treatment is applied. In addition, anaerobic degradation values of 54 to 56% indicate that decomposition of these compounds is easily achieved under the rather stringent conditions of the European Center for Ecotoxicology and Toxicology of Chemicals (ECETOC) test.

In particular, coco betaine and cocoamphoacetate have been extensively tested with regard to their

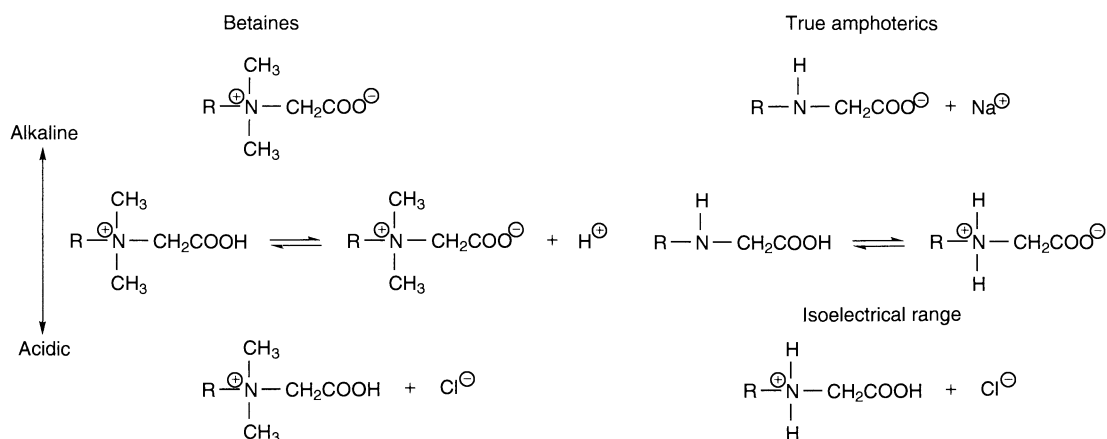


Figure 22.9. Dependence of amphoteric surfactants on pH range (from ref. (24) with permission from Wiley-VCH)

Table 22.20. Some commercially available amphoteric surfactants

Chemical designation	Fat basis	Amine basis	INCI designation ^a
<i>Betaines</i>			
Cocoalkyldimethyl betaine	Tertiary amine	Not applicable	COCO BETAINE
Lauryl, myristyl dimethyl betaine	Tertiary amine	Not applicable	LAURYL BETAINE
Cocoamidopropyl <i>N,N</i> -dimethyl betaine	Fatty acid, coconut oil	Dimethylamino-propylamine	COCAMIDOPROPYL BETAINE
Lauroylamidopropyl <i>N,N</i> -dimethyl-hydroxypropyl betaine	Fatty acid, coconut oil	Dimethylamino-propylamine	LAURYL HYDROXSULTAINE
<i>True amphoterics</i>			
Cocoamidoethyl hydroxyethyl glycinate	Fatty acid	Aminoethyl-ethanolamine	SODIUM COCOAMPHO-DIACETATE
Cocoamidoethyl hydroxyethyl <i>N</i> -carboxy glycinate	Fatty acid	Aminoethyl-ethanolamine	DISODIUM COCOAMPHO-DIACETATE

^aInternational Nomenclature of Cosmetic Ingredients.

Table 22.21. Data obtained for the biodegradability of amphoteric surfactants

Surfactant	Test method	Parameter	Value(%)
Cocamidopropyl betaine	Modified OECD Screening Test (OECD 301 E)	DOC	100
	Zahn-Wellens Test (OECD 302 B)	DOC	97-100
	Coupled Units Test (OECD 303 A)	DOC	97 ± 4
	Anaerobic Degradation Test (ECETOC)	CO ₂ and methane formation	56 ± 17
Disodium cocoampho-diacetate	Modified OECD Screening Test (OECD 301 E)	DOC	80-96
	Zahn-Wellens Test (OECD 302 B)	DOC	61-88
	Coupled Units Test (OECD 303 A)	DOC	74 ± 4
	Anaerobic Degradation Test (ECETOC)	CO ₂ and methane formation	54 ± 17

Table 22.22. Aquatic toxicity of amphoteric surfactants

Surfactant	Organism	Test and Criterion	Concentration (mg/l)
Cocamidopropyl betaine	<i>Brachydanio rerio</i>	LC ₅₀ , acute (OECD 203)	6.7
	Daphnia	EC ₅₀ , acute (OECD 202)	3.7
	Algae	Chronic (NOEC)	0.96
	Rainbow trout	Chronic (NOEC)	0.16
	Daphnia	Chronic (NOEC)	0.9
Disodium cocoamphodiacetate	Golden orphe	LC ₅₀ , acute (OECD 203)	27
	Daphnia	EC ₅₀ , acute (OECD 202)	520

environmental compatibility. It was demonstrated that no recalcitrant metabolites are formed.

9.3 Aquatic toxicity

Under the aspects of acute and chronic aquatic toxicities, amphoteric surfactants display a behaviour which is quite similar to the other groups of surfactants, with disodium cocoamphodiacetate being less toxic against fish and daphnids than cocamidopropyl betaine, according to the data presented in Table 22.22. All NOEC values are below 1 mg/l, with daphnia and algae having a lower sensitivity than fish.

10 ENVIRONMENTAL BEHAVIOUR UNDER REAL CONDITIONS AND RISK ASSESSMENT

While laboratory studies are very useful in predicting the fate of chemicals *in vitro*, a thorough assessment requires that their fate under real-world environmental conditions is also examined. This means that surfactants also have to be observed in surface waters such as lakes and rivers. The use of laboratory data only to describe and assess risks in the real environment usually leads to considerable problems, mostly in overestimating the hazards. Therefore, it is necessary to perform field studies, particularly in critical stretches of water with high pollution. In its simplest form, this can be river monitoring programmes, where at selected sampling points actual surfactant concentrations are measured at certain time intervals. A typical example is the monitoring of MBASs in the River Neckar (Germany) over a time period of 19 years. It can be recognized from this that there is a considerable reduction in surfactant concentration from 1965 to 1983. This is largely due to an improved sewage treatment situation along the river. Monitoring should take precedence over the theoretically predicted PEC and must be considered as an integral part of risk

assessment. More extensive monitoring programmes for surfactants (LASs, AESs and FAEOs) have been performed in The Netherlands and Germany in order to obtain reliable data on the real concentrations.

When considering the fate of residual concentrations of surfactants which are discharged into receiving waters after biological treatment, it is important to know what additional elimination can be achieved in flowing or stagnant waters. It is generally accepted that biological degradation in this context again plays a major role, while not ignoring the fact that physico-chemical effects are also effective, e.g. photolytic decomposition with some cationic surfactants. Degradation of organic compounds in surface waters is generally characterized by half-life expectancy ($t_{0.5}$ (h)). Data for some important surfactants for real-river situations are presented in Table 22.23. It can be seen from this table that a rather short time interval (0.2–2.4 h) is needed to achieve an additional 50% reduction of surfactant concentrations.

With a total consumption of about 17 million tons, the ecological safeguarding of surfactants is of central importance world-wide. Figure 22.10 outlines some important aspects of the environmental acceptability of surfactants, which do not only include biodegradability and environmental toxicity but also eco-balances and safety in application. Eco-balances describe the whole life cycle of a surfactant under ecological aspects from production, use and disposal. These different aspects can be summarized in an extended risk assessment exercise. Risk in this context represents the likelihood that a hazard will be realized i.e. that due to exposure an adverse effect may occur in some recipients (e.g. a

Table 22.23. Some half-life periods of surfactants in rivers

Surfactant	River $t_{0.5}$ (h) ^a
C ₁₀₋₁₃ -alkylbenzene sulfonate	0.2–2.4
sec-C ₁₄₋₁₇ -alkyl sulfonate	0.8
C ₁₂₋₁₄ -alkyl polyglycol (2EO) ether sulfate	0.7–2.0
C ₁₂₋₁₄ -alkyl sulfate	0.3

^aRelated to the maximum flow rate of 1 m/h.

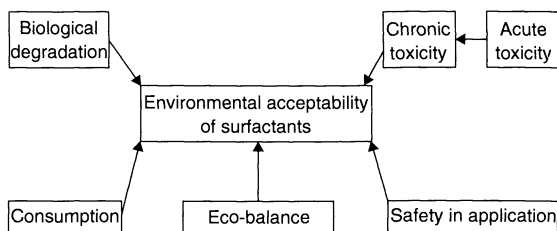


Figure 22.10. Important aspects of the environmental acceptability of surfactants

river). Risk assessment, again in this context, is the process that evaluates the likelihood that adverse ecological effects may occur, are occurring, or have occurred upon exposure to one or more chemical agent (surfactant(s)). Fundamental to the definition of risk assessment is the recognition that risk requires two elements:

- (i) The inherent ability of a chemical to cause adverse effects e.g. aquatic toxicity:
- (ii) The exposure or interaction of the chemical with an ecological component or partner (e.g. fish, crustacean, etc.) at sufficient intensity and duration to elicit the harmfulness or effect(s).

The ratio of the Predicted Environmental Concentration (PEC) to the Predicted No-Effect Concentration (PNEC) is used as a measure of this risk.

The assessment of risk normally requires an evaluation of the intrinsic physico-chemical properties, i.e. biodegradability and toxicity, of the chemical. The risk assessment for surfactants is usually based on biodegradability and aquatic toxicity data. Generally in environmental exposure assessment, the concentration of a substance in the different environmental compartments is estimated from the amount of the substance released from domestic and industrial use. The PEC can therefore be calculated from a knowledge of the quantity of the substance that will be discharged (e.g. via waste-waters) into the environment and the distribution and degradation processes (e.g. waste-water treatment plant).

Improvements for current environmental risk assessment models come from new approaches such as GREAT-ER (Geography-Referenced Exposure Assessment Tool for European Rivers) which will allow us to generate better and more reliable exposure concentrations. This uses a GIS (Geographic Information System) to produce a simple and clear visualization of predicted chemical concentrations and water quality along a river by colour coding. GREAT-ER has already been implemented for a variety of river basins in the UK, Germany, Italy and Belgium (25).

11 REFERENCES

1. Schöberl, P., Klotz, H., Spilker, R. and Nitschke, L., Alkylbenzolsulfonat (LAS) – monitoring, *Tenside Surf. Det.*, **31**, 243–252 (1994).
2. Schöberl, P., Alkylbenzolsulfonat (LAS) – monitoring, *Tenside Surf. Det.*, **32**, 25–35 (1995).
3. Gerike, P., Winkler, K. Schneider, W. and Jakob, W., Residual LAS in German rivers, *Tenside Surf. Det.*, **26**, 136–140 (1989).
4. Kloster, G., Analytical methods for surfactants and complexing agents at concentrations relevant to environmental occurrence, in *Detergents in the Environment* Schwuger, M. J. (Ed.), Surfactant Science Series, Vol. 65, Marcel Dekker, New York, 1997, pp. 65–126.
5. Pagga, U., Testing biodegradability with standardized methods, *Chemosphere*, **35**, 2953–2968 (1997).
6. SETAC, Biodegradation kinetics: generation and use of data for regulatory decision making, SETAC Workshop, Port Sunlight, UK, 1996.
7. Salanitro, J. P. and Diaz, L. A., Anaerobic biodegradation testing of surfactants, *Chemosphere*, **30**, 813–830 (1995).
8. Kertesz, M. A., Kölbener, P., Stockinger, H., Beil, S. and Cook, A. M., Desulfonation of linear alkylbenzenesulfonate surfactants and related compounds by bacteria, *Appl. Environ. Microbiol.*, **60**, 2296–2303 (1994).
9. Lewis, M. A., Chronic toxicities of surfactants and detergent builders to algae: a review and risk assessment, *Ecotox. Environ. Safe*, **20**, 123–140 (1990).
10. Lewis, M. A., Chronic and sublethal toxicities of surfactants to aquatic animals: a review and risk assessment, *Water Res.*, **25**, 101–113 (1991).
11. Lewis, M. A., The Effects of mixtures and other modifying factors on the toxicities of surfactants to freshwater and marine life, *Water Res.*, **26**, 1013–1023 (1992).
12. van Ginkel, C. G., Complete degradation of xenobiotic surfactants by consortia of aerobic microorganisms, *Biodegradation*, **7**, 151–164 (1996).
13. AISE/CESIO, Environmental risk assessment of detergent chemicals, in *Proceedings of AISE/CESIO*, Limelette III Workshop, Limelette, 25–29 Nov., 1995.
14. Matthijs, E., Holt, M. S., Kiewiet, A. and Rijs, G. B. J., Environmental monitoring for linear alkylbenzene sulfonate (LAS), alcohol ethoxylate (AE), alcohol ethoxy sulfate (AES), alcohol sulfate (AS) and soap, *Environ. Sci. Techn.* (2000).
15. Remde, A. and Debus, R., Biodegradability of fluorinated surfactants under aerobic and anaerobic conditions, *Chemosphere*, **32**, 1563–1574 (1996).
16. Schöberl, P., Bock, K. J. and Huber, L., Ökologisch relevante Daten von Tensiden in Wasch- und Reinigungsmitteln, *Tenside Surf. Det.*, **25**, 86–98 (1988).
17. Falbe J. (Ed.), *Surfactants in Consumer Products*, Springer-Verlag, Heidelberg, 1997.

18. Scholz, N., Ecotoxicology of surfactants, *Tenside Surf. Det.*, **34**, 229–232 (1997).
19. Thiele, B., Günther, K. and Schwuger, M. J., Alkylphenol ethoxylates: trace analysis and environmental behavior, *Chem. Rev.*, **97**, 3247–3272 (1997).
20. Steber, J., Guhl, W., Stelter, N. and Schröder, R. F., Alkylpolyglycosides – ecological evaluation of a new generation of nonionic surfactants, *Tenside Surf. Det.*, **32**, 515–521 (1995).
21. Stalmans, M., Matthies, E., Weeg, E. and Morris, S., The environmental properties of glucose amide – a new non-ionic surfactant, *SÖFW-J.*, **119**, 794–808 (1993).
22. Giolando, S. T., Rapaport, R. A., Larson, R. J., Federle, T. W., Stalmans, M. and Masscheleyn, P., Environmental fate and effects of DEEDMAC: a new rapidly biodegradable cationic surfactant for use in fabric softeners, *Chemosphere*, **30**, 1067–1083 (1995).
23. Huber, L., Ecological behaviour of cationic surfactants from fabric softeners in the aquatic environment, *J. Am. Oil. Chem. Soc.*, **61**, 377–382 (1984).
24. Uphues, G., Chemistry of amphoteric surfactants, *Fett-Lipid*, **100**, 490–497 (1998).
25. Schröder, F. R., Das GREAT-ER Projekt, *Henkel Referate*, **35**, 58–62 (1999).

CHAPTER 23

Molecular Dynamics Computer Simulations of Surfactants

Hubert Kuhn and Heinz Rehage

University of Essen, Essen, Germany

1	Introduction	537	4.1	C ₁₂ E ₅ at the air/water interface	541
2	Surfactants Adsorbed at Surfaces and Interfaces	537	4.2	Orientation of C ₁₂ E ₅ at the water/oil interface	543
3	The Molecular Dynamics Method	539	5	Molecular Dynamics Computer Simulation of Micelles	544
3.1	The force field	539	6	The Dissipative Particle Dynamics Simulation Method	546
3.2	The functional form of the AMBER force field	539	7	Limits and Restrictions of the Molecular Dynamics Technique for Surfactant Simulations	547
3.3	The energy cut-off and periodic boundary conditions	540	8	References	550
3.4	The molecular dynamics procedure	540			
4	Molecular Dynamics Computer Simulations of Surfactant Monolayers at Air/Water and Oil/Water Interfaces	541			

1 INTRODUCTION

Due to the rapid development of modern high-performance computers as fast parallel machines, molecular dynamics computer simulations has nowadays an enormous potential to give new insights into the structure, function and dynamics of surfactant aggregates. It seems realistic, therefore, to expect that these methods will be more extensively applied in the future. About 10 years ago, molecular dynamics, in combination with force fields, were first developed for new applications in biochemistry and biophysics. In this research area, advanced computer simulation methods tend to be a useful and powerful tool for the prediction of protein and lipid structures. In principal, all of these methods can also be applied in order to calculate the aggregation and adsorption processes of surface-active molecules. This field of research is growing rapidly at present, and it thus seems interesting to give an actual

overview concerning this special simulation technique. As fluid interfaces have many applications in science and industry, we shall therefore give some insight into recent results obtained from various modelling studies of surfactant monolayers. We shall briefly discuss the molecular dynamics method and then switch to advanced modelling strategies developed for the bulk phase of micellar systems, i.e. the “Dissipative Particle Dynamics Method”, which has been developed in order to predict the phase behavior of surfactant/water and surfactant/water/oil systems. This is followed by a brief discussion about the restrictions and limits of the molecular dynamics simulation method.

2 SURFACTANTS ADSORBED AT SURFACES AND INTERFACES

Monomolecular films are two-dimensional layers of amphiphilic molecules adsorbed at a fluid interface. It

18. Scholz, N., Ecotoxicology of surfactants, *Tenside Surf. Det.*, **34**, 229–232 (1997).
19. Thiele, B., Günther, K. and Schwuger, M. J., Alkylphenol ethoxylates: trace analysis and environmental behavior, *Chem. Rev.*, **97**, 3247–3272 (1997).
20. Steber, J., Guhl, W., Stelter, N. and Schröder, R. F., Alkylpolyglycosides – ecological evaluation of a new generation of nonionic surfactants, *Tenside Surf. Det.*, **32**, 515–521 (1995).
21. Stalmans, M., Matthies, E., Weeg, E. and Morris, S., The environmental properties of glucose amide – a new non-ionic surfactant, *SÖFW-J.*, **119**, 794–808 (1993).
22. Giolando, S. T., Rapaport, R. A., Larson, R. J., Federle, T. W., Stalmans, M. and Masscheleyn, P., Environmental fate and effects of DEEDMAC: a new rapidly biodegradable cationic surfactant for use in fabric softeners, *Chemosphere*, **30**, 1067–1083 (1995).
23. Huber, L., Ecological behaviour of cationic surfactants from fabric softeners in the aquatic environment, *J. Am. Oil. Chem. Soc.*, **61**, 377–382 (1984).
24. Uphues, G., Chemistry of amphoteric surfactants, *Fett-Lipid*, **100**, 490–497 (1998).
25. Schröder, F. R., Das GREAT-ER Projekt, *Henkel Referate*, **35**, 58–62 (1999).

CHAPTER 23

Molecular Dynamics Computer Simulations of Surfactants

Hubert Kuhn and Heinz Rehage

University of Essen, Essen, Germany

1	Introduction	537	4.1	$C_{12}E_5$ at the air/water interface	541
2	Surfactants Adsorbed at Surfaces and Interfaces	537	4.2	Orientation of $C_{12}E_5$ at the water/oil interface	543
3	The Molecular Dynamics Method	539	5	Molecular Dynamics Computer Simulation of Micelles	544
3.1	The force field	539	6	The Dissipative Particle Dynamics Simulation Method	546
3.2	The functional form of the AMBER force field	539	7	Limits and Restrictions of the Molecular Dynamics Technique for Surfactant Simulations	547
3.3	The energy cut-off and periodic boundary conditions	540	8	References	550
3.4	The molecular dynamics procedure	540			
4	Molecular Dynamics Computer Simulations of Surfactant Monolayers at Air/Water and Oil/Water Interfaces	541			

1 INTRODUCTION

Due to the rapid development of modern high-performance computers as fast parallel machines, molecular dynamics computer simulations has nowadays an enormous potential to give new insights into the structure, function and dynamics of surfactant aggregates. It seems realistic, therefore, to expect that these methods will be more extensively applied in the future. About 10 years ago, molecular dynamics, in combination with force fields, were first developed for new applications in biochemistry and biophysics. In this research area, advanced computer simulation methods tend to be a useful and powerful tool for the prediction of protein and lipid structures. In principal, all of these methods can also be applied in order to calculate the aggregation and adsorption processes of surface-active molecules. This field of research is growing rapidly at present, and it thus seems interesting to give an actual

overview concerning this special simulation technique. As fluid interfaces have many applications in science and industry, we shall therefore give some insight into recent results obtained from various modelling studies of surfactant monolayers. We shall briefly discuss the molecular dynamics method and then switch to advanced modelling strategies developed for the bulk phase of micellar systems, i.e. the "Dissipative Particle Dynamics Method", which has been developed in order to predict the phase behavior of surfactant/water and surfactant/water/oil systems. This is followed by a brief discussion about the restrictions and limits of the molecular dynamics simulation method.

2 SURFACTANTS ADSORBED AT SURFACES AND INTERFACES

Monomolecular films are two-dimensional layers of amphiphilic molecules adsorbed at a fluid interface. It

is well known that in emulsions, microemulsions or foams, these surfactant monolayers determine the properties, and hence the technical applications of these systems. Surfactant films are, therefore, the subject of intensive research activities and investigations. The current interest is focused on film formation processes at the air/water or air/oil interface and also on Langmuir–Blodgett films which are adsorbed on the surface of solids. It turns out that the understanding of the phase behaviour of the surfactants adsorbed in the monolayer is crucial for the prediction of film properties.

It is common knowledge that the shape of the Π/A isotherm depends on the structure and phase behaviour of the investigated monomolecular film. In this context, Π denotes the surface pressure and A is the area occupied by one surfactant molecule. In the case of insoluble surfactants, a gas phase is observed in the highly dilute concentration regime. If the surface pressure is increased, then transitions to condensed phases will occur. The latter might be liquid-expanded or liquid-condensed structures. A solid phase appears in the regime of high surface pressure values. Under these conditions, the surfactants are densely packed. Further increasing of the surface pressure results in a collapse of the monomolecular film structure. In the case of water-soluble surface-active compounds, the situation is more complicated and amphiphilic molecules can be dissolved in the bulk phase during compression of the monolayer. In both structures, the monomolecular film is composed of only one single layer of amphiphilic molecules. On this molecular length scale, the film structure can be characterized by molecular parameters. It turns out that the formation of different condensed phases can be well described by the orientation of the hydrophobic and hydrophilic chains with respect to the water surface. This property is often denoted as the *tilt angle*.

The molecular tilt angle depends on the surfactant concentration at the interface. In the regime of infinitely small surfactant concentrations, the molecules tend to lay almost flat on the surface. This corresponds to tilt angles of about 90° measured with respect to the surface normal vector. During film compression, the phase transitions towards liquid-expanded and liquid-condensed phases can be characterized by decreasing tilt angles.

In order to gain more insight into the molecular structure of surfactant monolayers, experimental methods such as fluorescence microscopy, light scattering, small-angle X-ray scattering and neutron diffraction were employed. By using Brewster-angle microscopy techniques or fluorescence microscopy the domain structures in surfactant monolayers can be visualized. A

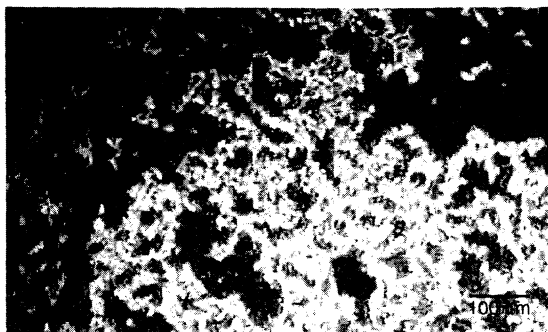


Figure 23.1. Network-like superstructure of a surfactant film of cetyltrimethylammonium bromide ($c = 6 \times 10^{-7}$ mol/l). The cross-linking process between the molecules was induced by adding multivalent counterions such as cerium sulfate ($c = 10^{-3}$ mol/l). The Brewster-angle image was obtained during the adsorption process of the amphiphilic molecules and represents the situation near the sol–gel transition, where the first “infinite” large clusters were formed. Black zones represent the pure water surface, while clear areas correspond to the presence of surfactant clusters

typical example is given in Figure 23.1, which shows a network-like superstructure of an adsorbed film of cetyltrimethylammonium bromide spread on an aqueous solution of $\text{Ce}(\text{SO}_4)_2$. On close inspection, it becomes clear that the surfactant molecules of this sample tend to form large clusters of fractal geometry. Each of the aggregates observed in Figure 23.1, contain large amounts (i.e. billions) of molecules and up until now it has not been possible to treat such large systems by using computer simulations. This problem leads to the restriction of building up simple model systems, which can still represent the major properties of the investigated surfactant films.

Due to the rapid development of computer performance in the last few years, the molecular dynamics simulation method can now be used in order to get more detailed information on the phase behaviour of surfactant molecules at the air/water interface, provided that the number of molecules does not exceed a certain threshold value. With these computer simulation methods, it is possible to directly calculate molecular parameters such as the average tilt angle of the surfactant molecules adsorbed in the monolayer.

Due to the fact that the computer time for calculating the atomic interactions generally increases with approximately the square of the number of investigated atoms, one still needs simple systems consisting of a relatively small number of molecules. Whereas chemists usually work with molar quantities, molecular dynamics

computer simulations are still limited to some thousand interacting atoms. However even in this case, one already needs the technology of parallel computers in order to reduce the simulation time down to days or weeks. By using these advanced techniques, it is possible nowadays to explore the dynamic features of the investigated systems on time-scales of several nanoseconds. The basic processes of such calculations is summarized in the following section.

3 THE MOLECULAR DYNAMICS METHOD

It is not the aim of this present section to discuss the methods and procedures in great detail. We therefore refer to an excellent review book which deals particularly with the molecular dynamics simulation technique as applied to liquids (1).

3.1 The force field

For molecular dynamics calculations, it is first necessary to determine the interactions between atoms. The principal result of such a calculation depends strongly on the force field. The latter is in fact an empirical fit of the potential energy surface of the molecular system. Such treatment represents the functional forms and parameters of the potential energy of a given molecular configuration. These theories are developed to explain a wide range of experimental parameters. Force fields, commonly used for describing molecular structures employ bond distances, bond angles and torsions to calculate the part of the potential energy surface belonging to the intramolecular interactions. Interatomic distances between non-bonded atoms are input variables into functions for calculating the van der Waals and electrostatic interactions.

The calculation of the potential energy, along with its first derivatives with respect to the atomic coordinates, is the crucial and necessary input into the dynamics simulation procedure. The nature of the force field, its applicability to the system and the ability to predict particular properties determine the quality of the results.

In the last decade, special force fields have been developed for polymers, proteins, biomacromolecules, small organic molecules, carbohydrates and inorganic compounds. Up until now, force field developments and refinements are still an active part of scientific research. The functional forms range from simple quadratic to Morse functions, Fourier expansions, and

Lennard–Jones potentials. Because it is not our intention to review all advantages and applications of these different functional forms and parameter sets, we shall focus our explanations to the well-known AMBER force field (2, 3). This parameter set is widely used, and has already been successfully applied to molecular dynamics simulations of various surfactant systems.

3.2 The functional form of the AMBER force field

Basically, this method has been specially used for proteins and DNA, but nowadays it has also been accepted for advanced calculations of other types of molecules such as polymers, surfactants and small organic molecules. The general procedure used by AMBER to calculate the potential energy is given by the following equation:

$$\begin{aligned}
 E_{\text{pot}} = & \sum_b K_b (b - b_0)^2 + \sum_{\theta} H_{\theta} (\theta - \theta_0)^2 \\
 & (1) \qquad \qquad \qquad (2) \\
 & + \sum_{\phi} \frac{V_n}{2} [1 + \cos (n\phi - \phi_0)] \\
 & (3) \\
 & + \sum_{i < j} \varepsilon \left[\left(\frac{r^*}{r_{ij}} \right)^{12} - 2 \left(\frac{r^*}{r_{ij}} \right)^6 \right] \\
 & (4) \\
 & + \sum_{i < j} \frac{q_i q_j}{E_0 r_{ij}} + \sum_{i < j} \left[\frac{C_{ij}}{r_{ij}^{12}} - \frac{D_{ij}}{r_{ij}^{10}} \right] \\
 & (5) \qquad \qquad \qquad (6) \qquad \qquad (23.1)
 \end{aligned}$$

A pictorial presentation of the functional terms is presented in Figure 23.2. The first three terms describe the

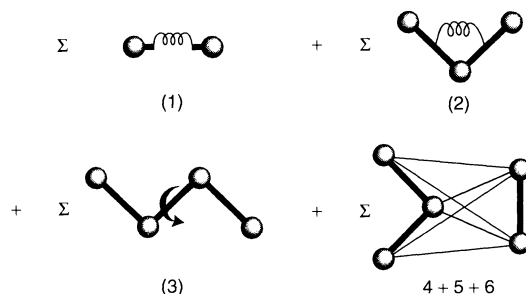


Figure 23.2. Pictorial representation of the functional terms used in the AMBER force field model

potential energy of the bond lengths b , bond angles θ and dihedrals ϕ , while b_0 , θ_0 and ϕ_0 denote the corresponding equilibrium values. The interactions between non-bonded atoms are represented by terms (4), (5) and (6). Term (4) accounts for the van der Waals interactions and includes the parameters ε and r^* . Electrostatic interactions are calculated by using the Coulomb equation (term (5)), where q_i and q_j are the partial charges on atoms i and j , respectively. E_0 denotes the permittivity, while E_0 is a constant and describes a macroscopic property. Therefore, in all atomistic simulations, E_0 is set to unity. However, in the AMBER force field a distance-dependent dielectric function $E_0 = f(r)$ can be used. The energetic contributions of hydrogen bonds are often treated by using a modified 12–10 Lennard–Jones potential function. This term includes typical parameters such as C_{ij} and D_{ij} (term (6)).

In molecular dynamics simulations, it is useful to include specific parameters describing the influence of intra- and intermolecular interactions of water molecules. These parameter sets represent water models such as SPC, SPC/E, ST2, TIP3P and TIP4P. Such models were successfully used for the prediction of thermodynamic data of liquid water. If a special water model is chosen in combination with the AMBER force field for calculation of the potential energy according to equation (23.1), term (6) is omitted.

AMBER belongs to the group of classical force fields (Class I), in which the molecular motions are treated by changing bond angles and torsions. The analogy of vibrating atoms connected by springs to describe interatomic interactions is also included into these force fields. Certainly, such classical models have limitations, but many experimental properties such as vibration frequencies, sublimation energies or crystal and liquid structures can be reproduced by using classical force fields. More sophisticated or second (Class II) force fields such as CFF91 include additional functional terms (cross-terms). These new parameters were introduced to take into account the coupling between different atomic vibrations (e.g. bond distance and bond-angle bending). It was shown that Class II force fields are more accurate than Class I force fields such as AMBER.

3.3 The energy cut-off and periodic boundary conditions

In order to reduce the computation time for calculation of the non-bonded interactions, it is inevitable to truncate the range of intermolecular van der Waals and electrostatic interactions. In practice, periodic simulation

boxes with boundary conditions and cut-offs of the non-bonded electrostatic and van der Waals energies were introduced.

The van der Waals interaction potential is relatively short-range and “dies” out at r^{-6} . At $r = 0.8–1.0$ nm, the energy and the resulting forces are quite small. Truncation of the van der Waals potential to zero at about $r = 1.0$ nm is, thus, a reasonable approximation. Conversely, the Coulomb interactions disappear at r^{-1} . Generally, at considerable distances the electrostatic energy is not negligible. This holds especially for ionic systems. Therefore, the energy cut-off procedure is often not suitable for calculations of ionic surfactant systems and an appropriate treatment of the non-bonded contributions to the electrostatic energy is crucial. The Ewald and the Cell Multipole techniques are convenient methods which perform a rather precise calculation of the long-range Coulombic forces.

In simulations of nonionic systems, the construction of neutral charged groups appeared to be a reasonable approximation. When considering a molecular dynamics simulation of the surfactant molecule $C_{12}E_5$ (monododecylpentaethylene glycol) with the AMBER force field, the CH_3 , CH_2 , CH_2-O-CH_2 and CH_2-OH groups can be defined as neutral charged groups. This means that the sum of the atomic partial charge in each of these groups totals zero. In a neutral charge group, one atom is designated as a switching atom. In the CH_3 and CH_2 groups, the carbons are switching atoms, while in the CH_2-O-CH_2 and CH_2-OH charge groups, the oxygens are switching atoms. If the switching atom is in the range of the energy cut-off, then all atoms included in the charge group are also used for the calculation of the electrostatic energy. This procedure ensures that artificial dipole splits are avoided and the interactions between neutral charge groups are dominated by dipole interactions which decrease with r^{-3} . Then, the dipole–dipole interactions mainly contribute to the Coulomb energy. The charge group approximation is sufficient to obtain reliable interatomic Coulomb interaction energies for neutral surfactant molecules with small dipole moments, such as $C_{12}E_5$.

3.4 The molecular dynamics procedure

A molecular dynamics simulation describes the phase space region defined by atomic positions and velocities. Consequently, this method allows the calculation of thermal motion. On close inspection, one obtains information on conformations, thermodynamic properties and dynamic features of surfactant and solvent molecules. A

typical result of a molecular dynamics simulation consists of a trajectory, which is defined as a set of positions and velocities of atoms as a function of time. This trajectory can be systematically analysed and this leads to investigations of conformational changes, structural relaxations or diffusion processes.

Frequently, molecular dynamics simulations are performed at conditions of constant pressure or temperature. In constant volume simulations, the volume of the simulation box is thought to be constant, although the pressure is changing. Simulations under these conditions represent only a rough estimate and the results must be verified by comparison with corresponding experiments. It turns out that in the simulation the values of T and P often have a crucial influence on the course of the computer simulation.

In cases of constant temperature and constant volume simulations, an initial Boltzmann distribution of velocities representing a well-defined start temperature is assigned to each atom. After a certain heating period, the atoms move under their "own" forces. The displacement of the molecules at a specific time step Δt is calculated from Newton's law of motion, as follows:

$$F = m \frac{d^2 r}{dt^2} \quad (23.2)$$

Actually, the problem with this is the numerical integration of equation (23.2) to obtain the trajectory, or in other words, the $r(t)$ function for each atom. In molecular dynamics simulation programs, a widely used integrator algorithm is the "Verlet leap-frog integrator method". A key parameter in the numerical integration procedure is the time step Δt . To make the best use of the computer time, a large time step is desirable. However, if Δt is too large, then instability and inaccuracy in the integration process occur. The time step is assigned to the highest frequency motion in the system. Normally, this is the C-H vibration in surfactant molecules, whose period is of the order of 1 femtosecond. Therefore, Δt should be set to at least 1 fs when C-H bond vibrations are taken into account.

Molecular dynamics simulations are usually carried out in two stages. After an initial equilibration process, a data collection period then follows. The duration of each stage depends on the system, under investigation as well as on its properties.

In a molecular dynamics simulation, it is necessary to reach a system state in which the relevant properties do not change with proceeding simulation time. There are different ways to judge whether a system has equilibrated. One method is to plot the various thermodynamic quantities, such as energy, temperature or pressure, versus time. Very often, the kinetic and potential energy

terms of the system can be analysed. These equilibration tests are necessary, but indeed not sufficient, since a sudden conformational change can occur after a long period of time. Another way to check equilibration is to start the calculation with different initial configurations and a different initial atomic velocity distribution. Unfortunately, convergence to similar conformations is not a proof for equilibration but merely an indicator that equilibrium has occurred.

In the following section, we will discuss some examples of molecular dynamics simulations of surfactants at liquid interfaces and in aqueous solution.

4 MOLECULAR DYNAMICS COMPUTER SIMULATIONS OF SURFACTANT MONOLAYERS AT AIR/WATER AND OIL/WATER INTERFACES

4.1 $C_{12}E_5$ at the air/water interface

A number of molecular dynamics (MD) simulations of surfactant monolayers have been published during the last decade. In these studies, the water surface was often modelled as a flat, amorphous plane. Due to severe computer power restrictions, there have been only a few attempts in which the surface was modelled in all atomic details. Monolayers of trimethylammonium chloride at the air/water interface and the properties of tetradecyltrimethylammonium bromide monolayers have been simulated. In addition to these computer experiments, the structures of phenol, *p*-*n*-pentylphenol and *N,N'*-diethyl-*p*-nitroaniline adsorbed on water have been investigated by MD simulations. Recently, molecular dynamics simulations of sodium dodecyl sulfate at the water/vapour and the water/ CCl_4 interfaces in regimes of small surface concentrations have been performed (4).

A microscopic part of a monolayer consisting of monododecylpentaethylene glycol surfactants ($C_{12}E_5$) adsorbed at the water surface was simulated with the AMBER force field and the SPC water parameter set (5). The temperature T was set to 298 K, while the number of molecules, N , was composed of 36 surfactant and 1575 water molecules arranged in a cubic box with periodic boundary conditions. The area per surfactant molecule (A) corresponded to a value of $A = 0.55 \text{ nm}^2$, which is somewhat larger than the critical micelle concentration (CMC) of $C_{12}E_5$ ($A = 0.50 \pm 0.03 \text{ nm}^2$).

During a 500 ps simulation, the system was allowed to equilibrate to a constant total energy. The final

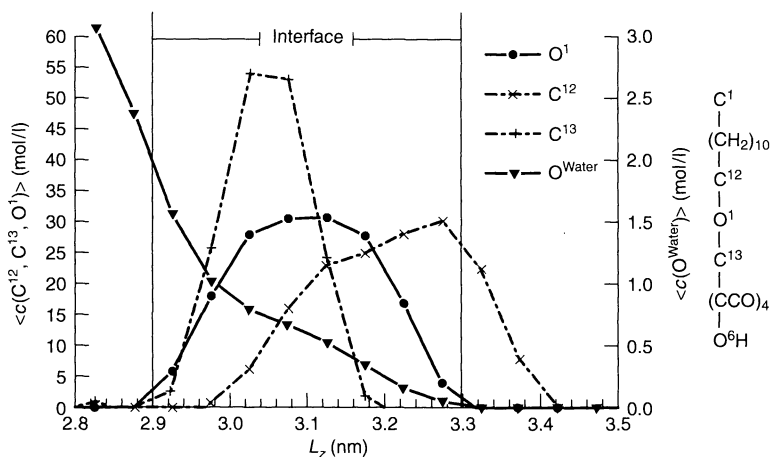


Figure 23.3. Average concentration profiles of O^1 , C^{12} , C^{13} and O^{Water} atoms in the direction of the water surface normal L_z

data collection was performed for an additional 500 ps molecular dynamics simulation run.

The evaluation of structural properties such as orientation angles and layer thicknesses requires an appropriate definition of the water surface. In Figure 23.3 the average concentration profiles in the z -direction for water oxygen atoms, O^{Water} , and the C^{12} , C^{13} and O^1 atoms of the surfactant molecules are summarized. The average water oxygen concentration decreases to zero at 3.3 nm, while at $L_z = 2.9$ nm, $\langle c_z \rangle$ is about half that of the water bulk density. No water molecules evaporated in the gas phase beyond the L_z value of 3.3 nm. Analogous to the Gibbs Dividing Plane, the water surface was defined by a plane lying between $L_z = 2.9$ –3.3 nm. Additionally, some interesting points are revealed from the average atomic concentrations shown in Figure 23.3. The O^1 oxygen atoms participate at the water surface since these atoms tend to be concentrated in the interface region. In addition, the C^{13} atoms are mainly located in the interface region. The C^{12} atom is also partially in contact with water molecules at the interface. The interaction between C^{12} and water is less distinctive. The peak of this curve is very close to that point where the water concentration decays to zero.

The orientations of the hydrophobic alkyl chains and the hydrophilic glycol chains within the monolayer are of foremost interest since molecular orientation is a strong indicator for the phase state of the surfactant monolayer. In Figure 23.4, a method is presented for calculating the average tilt angle of the specific C_{12} and E_5 chains. In the E_5 chains, vectors were constructed from the distance between the first oxygen atom O^1 and the terminal hydrogen atom connected to O^6 . In the

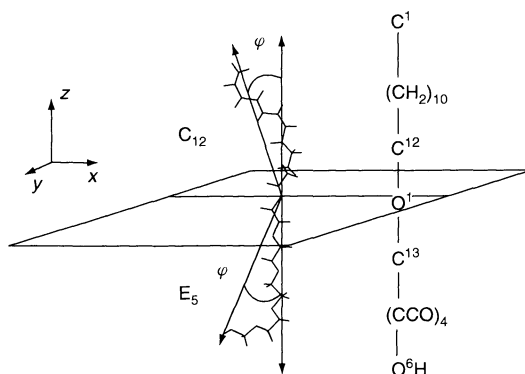


Figure 23.4. Definitions of the tilt angles between the water surface normal and the E_5 and C_{12} chains. Vectors are defined between C^{12} and C^1 and between O^1 and O^6 respectively

C_{12} chains, the vectors between C^{12} and the hydrogens connected to C^1 were used for the calculation of tilt angles. The average tilt angle (φ) was calculated from angles between these vector definitions and the normal of the water surface.

From the molecular dynamics simulations, it became evident that the C_{12} chains are tilted away with respect to the surface normal with an average tilt angle of about 43 ± 3 degrees. The calculation results predict an almost parallel orientation of the E_5 chains with respect to the surface normal, with a tilt angle value of about 11 ± 0.5 degrees. The molecular orientation and chain ordering become obvious from the molecular structure of the surfactants adsorbed on the water surface, as displayed in Figure 23.5. It is easy to see the different

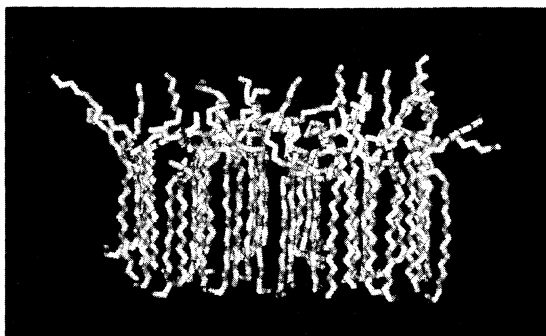


Figure 23.5. A representative molecular structure of the $C_{12}E_5$ surfactant molecules adsorbed on the water surface. The surfactant structures are extracted from the trajectory at a simulation time of 900 ps. The water molecules are not shown

orientations of the C_{12} and E_5 chains. It can also be recognized that the alkyl chains are more fluid-like. The molecular dynamics simulation results agree very well with those obtained from neutron reflection experiments. Additionally, some other important molecular properties have been investigated with molecular dynamics simulations. These include the following:

- Analysis of the chain conformations
- Mobility of the alkyl and glycol ether chains
- The lateral structure of the glycol ether chains

From the analysis of the molecular structure, from the conformation distribution and from the calculation of the mean square displacements in different chain sections, a high degree of flexibility of the terminal groups in the C_{12} and E_5 chains became evident. In comparison to E_5 , the hydrophobic C_{12} chains are considerably less ordered and are, in fact, not densely packed. From comparisons with molecular dynamics simulations of long-chain surfactants adsorbed on the air/water surface in the same surfactant concentration regime, it can be concluded that the molecular orientation of the C_{12} chain is similar to that for surfactants with linear hydrophobic chains and small polar head-groups. It was found that the monolayer tilts of single-chain surfactants varied from 10 to 36 degrees with increasing area/molecule values. Other simulations of long-chain surfactants revealed that the mean tilt angle varied from 40 to 60 degrees. In *n*-hexadecyltrimethylammonium chloride monolayers, the average tilt angle was found to be of the order of 40 degrees. Generally, the simulations of long-chain model surfactants showed that an increase of the molecular area causes an increase of the average tilt angle. The result of the enhanced C_{12} chain end

flexibility was also observed. It was found that most of the *gauche* conformations occurred around bonds near the hydrophobic chain ends.

There seems to be a difference in the diffusion behaviour between surfactants with small headgroups and surfactants with long hydrophilic glycol ether chains. In a previous simulation, the diffusion constant of *n*-hexadecyltrimethylammonium chloride in the monolayer was calculated to 1.9×10^{-6} – 4.8×10^{-6} cm^2/s . The diffusion constant increases with increasing molecular area, to a maximum of 1.6×10^{-5} cm^2/s . Conversely, the alkyl glycol ether headgroups are strongly anchored at the water surface, with the effect of a restricted mobility. This discrepancy can be explained by a network of hydrogen bonds which tends to “freeze” the monolayer structure. This result was supported by calculations of pair distribution functions between E_5 oxygen atoms arranged in a common layer (5).

4.2 Orientation of $C_{12}E_5$ at the water/oil interface

Now, we will focus our attention to the molecular structure of $C_{12}E_5$ at the octane/water interface. In a molecular dynamics simulation, octane molecules were used to build an appropriate model for the oil phase (6). The computer simulation provides new insights into two-dimensional monolayers at the water/oil interface. By using the neutron reflection method, the structure of $C_{12}E_5$ on the water surface, with and without added dodecane, was recently investigated. It was found that the C_{12} chains change to an almost perpendicular orientation to the surface upon incorporation of dodecane into the $C_{12}E_5$ layer.

In the MD simulation, the octane/water system consisted of 36 $C_{12}E_5$ surfactant, 1392 water and 143 octane molecules, and the simulation was performed at constant pressure of 10^5 Pa and a constant temperature of 298 K (6). In the equilibrium state, octane molecules penetrate into the hydrophobic monododecyl layer, which was also investigated by neutron reflection studies of the interactions between $C_{12}E_5$ and dodecane. From average concentration profiles of specified atoms in the *z*-direction of the simulation box, this penetration phenomenon becomes obvious (Figure 23.6). In Figure 23.6, the average concentration profiles of the carbon atoms of the C_{12} chain, the carbon atoms of octane molecules and the oxygen water atoms are plotted. The essential result is, that from 3.0 nm the C_{12} and octane concentrations coincide. This effect leads

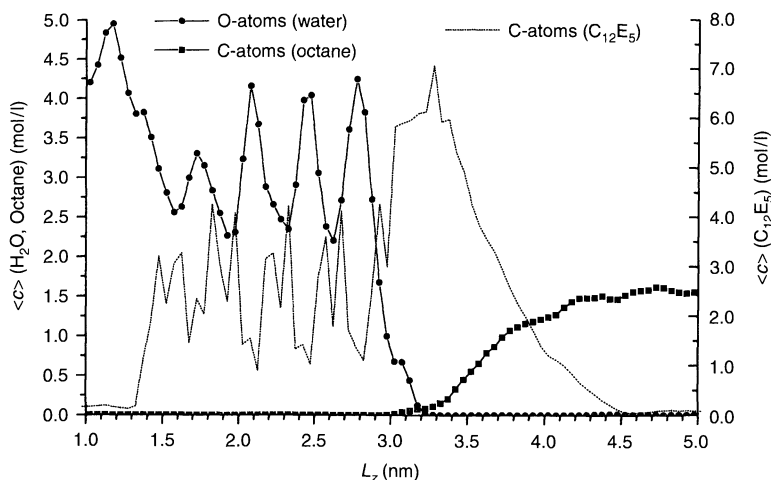


Figure 23.6. Average concentration profiles of O^{water} , carbon atoms of the C_{12} chain and carbon atoms of octane molecules in the z -direction of the simulation box representing the water surface normal

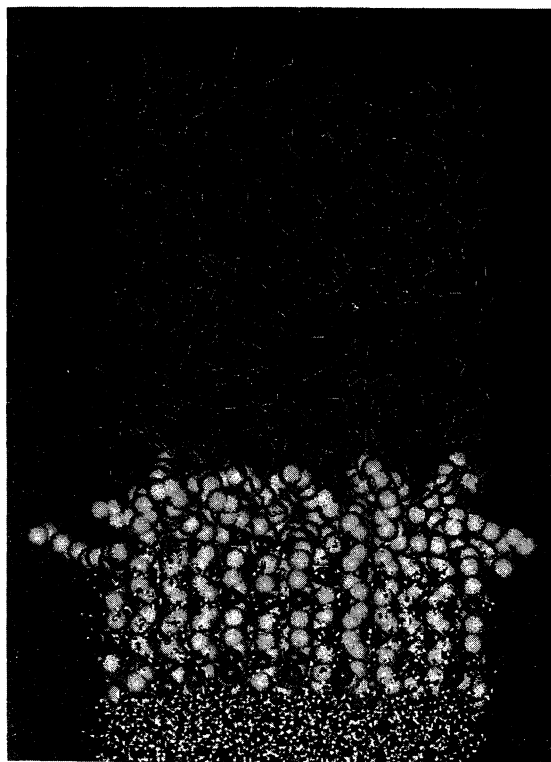


Figure 23.7. The molecular structure of $C_{12}E_5$ surfactant molecules adsorbed at the oil/water interface

to the conclusion that octane molecules penetrate into the C_{12} layer. Furthermore, the octane and water phases

are in contact. The observed oil penetration results in an increase of the surface area per surfactant molecule, which was also observed experimentally. The molecular film at the water/octane interface is depicted in Figure 23.7.

An analysis of the surfactant tilt angles revealed that no significant difference appears between the molecular orientations of the hydrophobic C_{12} chain at the air/water and the oil/water interface. This result is in discrepancy with experimental investigations of the interaction of $C_{12}E_5$ and dodecane. Neutron reflection measurements suggest an more upright arrangement of the C_{12} chains if dodecane penetrates into the C_{12} layer.

5 MOLECULAR DYNAMICS COMPUTER SIMULATION OF MICELLES

The results of molecular dynamics simulations which were performed to get more information on the physical properties of sodium octanoate micelles are discussed next. From the results thus reported, it was possible to obtain some typical properties of the micelle.

It is well known that water-soluble surfactants tend to form various types of aggregates at threshold values above the CMC. This aggregation process is the result of two competing factors. The hydrophobic chains try to avoid the energetically unfavourable contact with water. This can be achieved by forming various types of defined aggregates (micelles). These particles are stabilized by van der Waals attractions between the

non-polar paraffin chains. Conversely, there is often a strong repulsion between the polar head-groups. The actual shape and size of the micelles is controlled by the competition between these different forces. In aqueous solution, the polar head-groups are oriented towards the water phase and hydration forces also tend to stabilize this structure. Depending on the surfactant system, the polar head-centres can consist of cationic, anionic, amphoteric or nonionic groups.

Very often, micelles have a spherical shape and consist of 30–80 monomers. The aggregates can vary their size and shape continuously due to the exchange of monomers. Some important parameters which can influence the micellar structure are the surfactant concentration, the lengths of the paraffin chains, the salt content (ionic strengths), the temperature, the pH values and the pressure.

Some computer simulations of micelles on a molecular level have already been performed with molecular dynamics calculations. The models used in these simulations are based on different approximation levels. In simulations in which solvent molecules were omitted, the solvation shell was simulated by a sphere, and the interactions between the atoms and the sphere was calculated by Lennard–Jones-type potential functions. In more advanced simulations, the solvent molecules were especially considered and specific water models like SPC were used.

At first glance these models reflect the situation in a real physical micellar solution rather crudely, although the previously performed calculations have already been successful in gaining important information on micellar structures. In recent times, the models have been refined in the way that all interactions between all water and surfactant atoms were included in the simulations. This holds for hydrogen bonds, electrostatic Coulomb forces and van der Waals interactions.

Previously, the sodium dodecyl sulfate (SDS) surfactant system was also investigated with a 200 ps molecular dynamics computer simulation in the NVT-ensemble (7). In this computer simulation, the parameters of the atomic interaction potential functions were taken from the CHARMM force field. The calculations showed that the SDS micelle remains spherical with a radius of gyration in good agreement with the experimental results. Remarkable motions of the head-groups were observed and the *trans* to *gauche* populations are equivalent for the micelle and the analogous hydrocarbon, liquid dodecane. Recently, atomic-level studies of AOT reverse micelles and molecular dynamics simulations of the structure and dynamics of a dodecylphosphocholine micelle in aqueous solution have been published (8, 9).

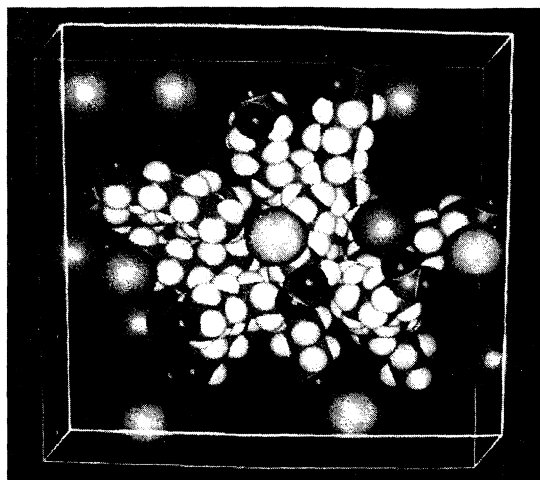


Figure 23.8. Average molecular structure of the sodium octanoate micelle after the simulation time between 250 and 300 ps. The water molecules surrounding the micelle are not shown

The simulations of the sodium octanoate micelle were based on the AMBER force field with a simulation period of 300 ps (10). The aggregate was surrounded by 870 water molecules and the simulation was performed at a temperature of 300 K and a pressure of 10^5 Pa.

Figure 23.8 shows a representative molecular structure of the surfactants forming the micelle. The micellar structure was obtained from averaging of the atomic Cartesian coordinates from the trajectory in the time interval between 250 and 300 ps. From Figure 23.8, it becomes evident that the micelle attains a roughly spherical shape. This holds at least for the investigated time regime. The polar head-groups are located on the micellar surface and are in direct contact with water molecules. The alkyl chains are directed into the hydrophobic core and the micelle itself is surrounded by sodium counterions. From the calculated trajectory, some important micellar properties has been investigated. Briefly summarized, these are as follows:

- Conformations of the hydrophobic alkyl chains
- Micellar radius
- Structure of the solvents around the carboxylate head-groups
- Water penetration into the micelles
- The micellar shape
- The surface charge of the micelle
- Sodium counterion distribution and solvation shells around the micelle
- Diffusion of solvent molecules within the micelle and at the micellar surface

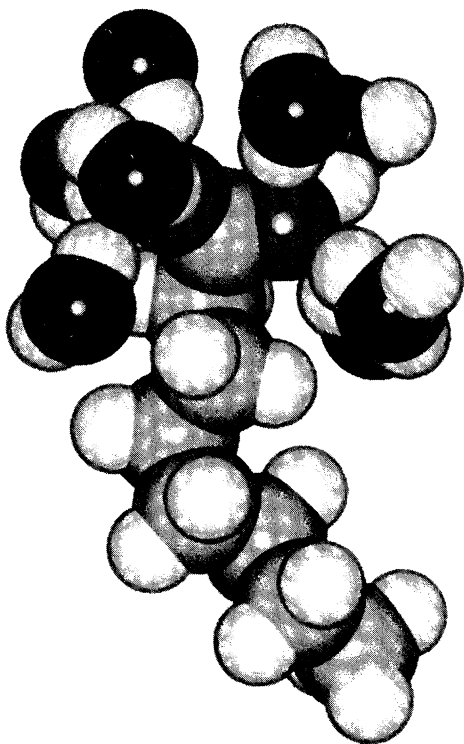


Figure 23.9. Molecular structure of one monomer of the micellar aggregate with the nearest neighbour water molecules

From the results thus produced, it was possible to obtain some typical properties of the micelle. It turned out that the average radius of the micelle coincides pretty well with that found from the experimental results of small-angle neutron scattering experiments. It was also possible to determine the actual conformations of surfactant monomers both outside and inside the micelle. These data are in general agreement with nuclear magnetic resonance studies and with Raman scattering experiments. On close inspection it was found that the micelle attains a slightly ellipsoidal shape. An average distance of 255 pm between the anionic polar head-groups and water molecules was obtained. This value agrees well with Heteronuclear Overhauser Effect measurements. In the first solvation shell, each head-group is surrounded by 10 water molecules, and eight of these tend to form hydrogen bonds to such polar groups (Figure 23.9). Furthermore, a second and third hydration shell could be observed. The average hydrogen-bond length corresponds to 175 pm and is slightly shorter than the observed hydrogen bonds between pure water molecules in the bulk phase. A complete dissociation

of the sodium counterions from the anionic polar-head groups was observed, and the distribution of sodium counterions and water molecules around the polar head-groups could be deduced. The first hydration shell, in the range of 200–280 pm, consists only of water molecules, resulting in a micellar surface charge of $15e$. Sodium counterions dissociate in the second and third hydration layers and are themselves surrounded with solvation shells. The diffusion of water molecules belonging to the first hydration layer of the sodium octanoate micelle is decreased by a factor of approximately 2 due to the formation of hydrogen bonds to the head-group oxygens.

Large numbers of water molecules are located in a globular shell with a diameter of 0.9–1.3 nm, which corresponds to the surface of the micelle. The internal core region between 500–900 pm also contains water, but only 10% of the total amount. Some molecules can even penetrate into the vicinity of the centre of the micelle, but this process rarely occurs. On the grounds of the thermal motion, hollow spaces, pores and channels are continuously formed and destroyed in which occasionally some water molecules are able to penetrate. This is, of course, a dynamic process with time-constants of only a few picoseconds. In contrast to the micellar systems consisting of sodium dodecyl sulfate surfactants (7), in sodium octanoate a significant amount of water penetration occurs. This process is certainly related to the aggregation number and the lengths of the paraffin chains. A sodium dodecyl sulfate micelle has a more compact structure and packing of the paraffin chains seems to be more effective. In this case, there are only a few solvent-accessible sites, and water penetration is, therefore, reduced. This situation changes, however, if micelles with small aggregation numbers, such as sodium octanoate micelles, are considered. Due to less distinctive hydrophobic forces, the micellar core is not very stable, and these aggregates are characterized by large thermal fluctuations.

6 THE DISSIPATIVE PARTICLE DYNAMICS SIMULATION METHOD

In concentrated solutions, surfactants and amphiphilic polymers tend to form mesophases such as nematic, lamellar, hexagonal or cubic structures. The characterization of these phases is very important for various technical applications. At present, phase diagrams of amphiphilic molecules in aqueous solution cannot be calculated by using the atomic-level MD technique. In order to improve this situation, some years ago a new simulation technique was introduced (11–13),

derived from molecular dynamics simulations and lattice gas automata, that effectively opens up the mesoscopic length and time regimes in complex fluids to simulation. This new theoretical approach is called “Dissipative Particle Dynamics” (DPD).

In the DPD methodology, small regions of fluid material are represented by fundamental particles called “beads”. These particles are not directly comparable to the atoms or molecules familiar from MD simulations since all degrees of freedom smaller than a bead radius are assumed to have been integrated out. Hence, coarse-grained interactions between beads can be calculated. There are three types of short-ranged forces between pairs of beads. A harmonic conservative interaction is given in the following equation:

$$F^C = \begin{cases} a_{ij}(1 - r_{ij})\hat{r}_{ij} & r_{ij} < 1, \\ 0 & r_{ij} > 1 \end{cases} \quad (23.3)$$

where \hat{r}_{ij} denotes the distance vector between particles i and j .

The dissipative force (Equation (23.4)) deals with the viscous drag between moving beads (i.e. fluid elements), as follows:

$$F_{ij}^D = \begin{cases} -\gamma\omega^D(r_{ij})(\hat{r}_{ij}v_{ij})\hat{r}_{ij} & r_{ij} < 1 \\ 0 & r_{ij} > 1 \end{cases} \quad (23.4)$$

where $\omega^D(r_{ij})$ is a short-range weight function, and v_{ij} is the bead velocity. Because of the form chosen for the dissipative force, this conserves the total momenta of each pair of particles, and hence also of the system.

A random force (equation (23.5)) ensures the maintaining of the energy input into the system in opposition to the dissipation:

$$F_{ij}^R = \begin{cases} \sigma\omega^R(r_{ij})\zeta_{ij}\hat{r}_{ij} & r_{ij} < 1 \\ 0 & r_{ij} > 1 \end{cases} \quad (23.5)$$

where $\zeta_{ij}(t)$ is a delta-correlated stochastic variable, and all forces are treated with a fixed cut-off radius.

The crucial advantage of Dissipative Particle Dynamics is the correspondence to the Gibbs Canonical NVT ensemble. It can be shown that the system evolves to a steady state by a suitable choice of the relative magnitudes of the forces acting on the particles.

The bead dynamics is realized by the integration of the equations of motion for the beads. A trajectory is generated through the system’s phase space. All thermodynamic observables (e.g. density fields, order parameters, correlation functions, stress tensor, etc.) can be constructed from suitable averages. An immense advantage over conventional molecular dynamics and Brownian dynamics is that all forces are “soft”, thus allowing

the use of a much larger time-step and correspondingly shorter simulation times.

Surfactants may be constructed out of the beads in a DPD simulation, hence allowing the investigation of the morphologies of the molecules. The interactions of a surfactant with other surfactants and the solvent occur via the conservative, dissipative and random forces between their component beads. Typically, the beads making up a surfactant are bound to each other with harmonic forces.

The mesoscale morphologies resulting from a DPD simulation can be analysed by means of a three-dimensional display of the beads making up the system by drawing density slices through the simulation box or by a display of the iso-density surfaces. The latter can be compared directly with experimental observations, e.g. from electron microscopy. This method allows the chemical engineer to assess the effects of changes to the molecular composition of a formulation on the microstructure and hence the expected macroscopic properties. With a combination of MD and DPD simulations, one can achieve a more detailed insight into the phase behaviour of surfactants and polymer amphiphiles in aqueous solution.

Two examples of DPD simulations of the $C_{12}E_5$ surfactant in aqueous solution at different concentrations are given in Figures 23.10 and 23.11. The measured phase diagrams for $C_{12}E_5$ in water located in the lower parts of Figures 23.10 and 23.11 were obtained from ref. (14). The precise simulation, and hence the prediction of phase behaviour of the nonionic surfactant $C_{12}E_5$, becomes obvious from an examination of these figures.

7 LIMITS AND RESTRICTIONS OF THE MOLECULAR DYNAMICS TECHNIQUE FOR SURFACTANT SIMULATIONS

The most accurate method of calculating the dynamical behaviour of surfactants is to integrate the equations of motion of all of the atoms in the system. It is obvious that the molecular dynamics calculations described in this chapter give only a rough estimate of the real situation. Such MD techniques require computer processor speeds and memory capacities that currently limit their applicability to a few nanoseconds of molecular motion. This is inadequate for many chemical processes of surfactants which occur on the microsecond (or longer) time-scales. Effects which are dependent on molecular diffusion cannot be investigated due to the

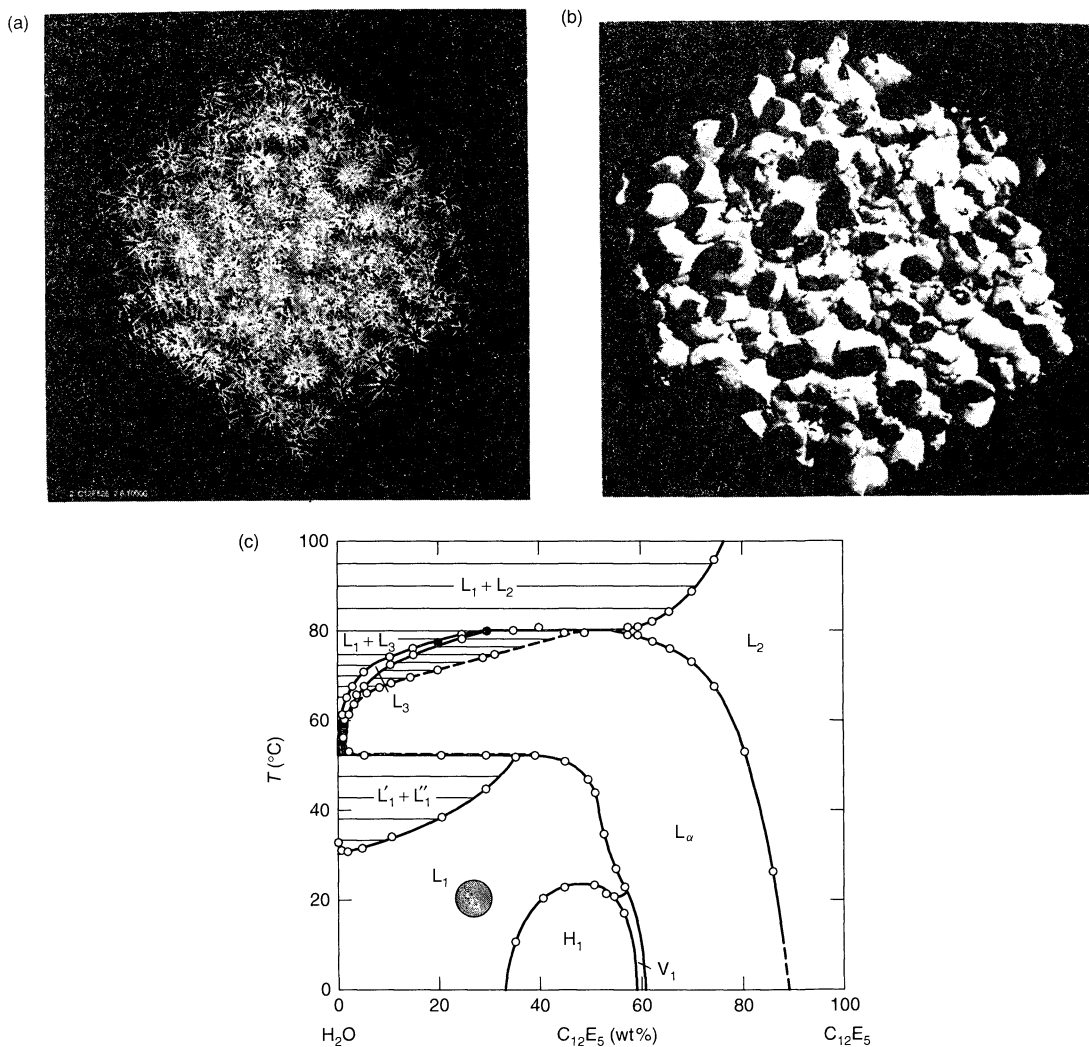


Figure 23.10. DPD simulation of C₁₂E₅ in water at a concentration of 25%, showing (a) a stick and (b) a C₁₂-iso-density presentation; L₁ corresponds to a micellar phase

relatively long-time scales involved, i.e. in the range of microseconds.

The accuracy of the simulation results depends on a suitable choice of the parameters in the potential functions. On account of equation (23.1), an essential restraint of the calculation method is the pair-wise addition of atomic forces. Although effective pair potentials are used, three-body terms and interactions of higher order are neglected. Consequently, the major many-body contributions to the induced dipole interactions in aqueous ionic systems are not modelled accurately. A further simplification is a common application of

fixed atomic partial charges. Conformational changes of the surfactants, or the presence of an external field by dynamic solvent molecules, influence the charge distribution in the surfactant monomers. Therefore, induced polarization effects are often not taken into account. The atomic interaction potential functions of bond vibrations, as well as bond angle and dihedral deformations, are based on classical instead of quantum mechanics. This is sometimes not sufficient to calculate precisely the intramolecular interactions.

Referring to the MD simulations of micelles and monomolecular films, it should be pointed out that

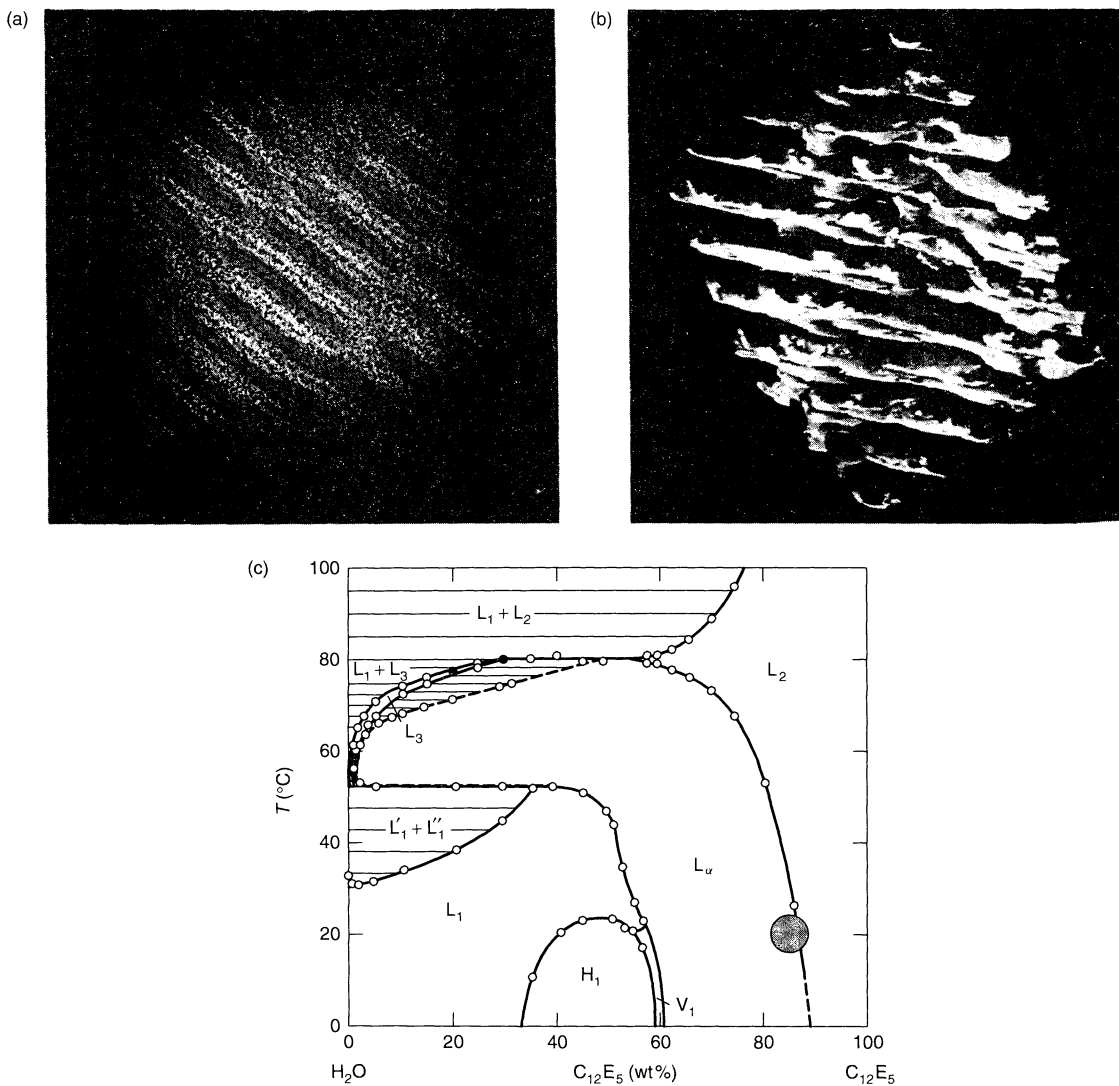


Figure 23.11. DPD simulation of $C_{12}E_5$ in water at a concentration of 90%, showing (a) a stick and (b) a C_{12} -iso-density presentation; L_α corresponds to a lamellar phase

the equilibrium state is related to isolated structures. This means that the interactions of the micelle and the monolayer with free monomers in solution or with different aggregates are also not taken into account.

Despite the restrictions of the molecular dynamics simulation technique, some important features of micellar structures have already been observed and reasonable results which coincide rather well with experimental data have been obtained. Nevertheless, in order to examine the dynamic of aggregation processes it is necessary to enlarge the simulation time drastically. A

general rule states that “computer power is currently increasing by a factor of 10 each six years”. This should lead to interesting consequences with respect to the molecular dynamics simulations of surfactant systems.

However, the dissipative particle dynamics simulation technique tries to avoid the major drawback of the classical MD method which often provides far more detail of the small-scale fluctuational motion of atoms than is necessary for an understanding of many physical processes of surfactants. With DPD, the mesoscopic length and time regimes in complex fluids are accessible

via computer simulations. DPD achieves this goal by retaining the principle of integrating the equations of motion for a system, while integrating out the smallest spatial degrees of freedom first. The fast motion of the atoms in a system is averaged over and the remaining structure is represented by a set of "beads", of given mass and size, that interacts via soft potentials with other beads. These approximations open the way to simulations of the phase behaviour of surfactants in aqueous solution and in emulsions.

8 REFERENCES

1. Allen, M. P. and Tildesley, D. J., *Computer Simulation of Liquids*, Clarendon Press, Oxford, 1987.
2. Weiner, S. J., Kollmann, P. A., Case, D. A., Cha Singh, U., Ghio, C., Alagona, G., Profeta, S. and Weiner, P., A new force field for molecular mechanical simulation of nucleic acids and proteins, *J. Am. Chem. Soc.*, **106**, 765–784 (1984).
3. Weiner, S. J., Kollmann, P. A., Nguyen, D. T. and Case, D. A., An all atom force field for simulations of proteins and nucleic acids, *J. Comput. Chem.*, **7**, 230–252 (1986).
4. Schweighofer, K. J., Essmann, U. and Berkowitz, M., Simulation of sodium dodecyl sulfate at the water–vapor and water–carbon tetrachloride interfaces at low surface coverage, *J. Phys. Chem., B*, **101**, 3793–3799 (1997).
5. Kuhn, H. and Rehage, H., Molecular dynamics computer simulations of surfactant monolayers: monododecyl pentaethylene glycol at the surface between air and water, *J. Phys. Chem., B*, **103**, 8493–8501 (1999).
6. Kuhn, H. and Rehage, H., Molecular orientation of monododecyl pentaethylene glycol at the water/air and water/oil interface. A molecular dynamics computer simulation study, *Colloid Polym. Sci.*, **278**, 114–118 (2000).
7. MacKerell, A. D., Molecular dynamics simulation analysis of a sodium dodecyl sulfate micelle in aqueous solution: decreased fluidity of the micelle hydrocarbon interior, *J. Phys. Chem.*, **99**, 1846–1855 (1995).
8. Derecskei, B., Derecskei-Kovacs, A. and Schelly, Z. A., Atomic-level molecular modeling of AOT reverse micelles. 1. The AOT molecule in water and carbon tetrachloride, *Langmuir*, **15**, 1981–1992 (1999).
9. Wymore, T., Gao, X. F. and Wong, T. C., Molecular dynamics simulation of the structure and dynamics of a dodecylphosphocholine micelle in aqueous solution, *J. Mol. Struct.*, **485–486**, 195–210 (1999).
10. Kuhn, H. and Rehage, H., The molecular structure of sodium octanoate micelles studied by molecular dynamics computer experiments, *Ber. Bunsenges. Phys. Chem.*, **101**, 1485–1492 (1997).
11. Hoogerbrugge, P. J. and Koelman, J. M. V. A., Simulating microscopic hydrodynamics phenomena with dissipative particle dynamics, *Europhys. Lett.*, **19**, 155–160 (1992).
12. Espanol, P. and Warren, P. B., Statistical mechanics of dissipative particle dynamics, *Europhys. Lett.*, **30**, 191–196 (1995).
13. Groot, R. D. and Warren, P. B., Dissipative particle dynamics: bridging the gap between atomistic and mesoscopic simulation, *J. Chem. Phys.*, **107**, 4423–4435 (1997).
14. Mitchell, D. J., Tiddy, G. J. T., Waring, L., Bostock, T. and McDonald, M. P., Phase behaviour of polyoxyethylene surfactants with water, *J. Chem. Soc., Faraday Trans. 1*, **79**, 975–1000 (1983).

Index – Volume 1

- α -crystalline phase 477
- α -olefinesulfonates 276–277
- α -sulfo fatty acid methylesters 277–278
- ab initio* polymerizations 194–195
- absorbency 138–139, 154–158, 159–162
- acetals 391–393
- acid fracturing 263
- acid–base interactions 233
- additives, phase behaviour 497–502
- adhesion 157–158, 334–336
- adjuvants 341–342
- adsorbable organic halogen (AOX)-containing substances 284
- adsorption
 - adsorbed films 252, 253
 - adsorber dyes 101–103
 - adsorption isotherms 167–168, 379–380
 - competitive 105–107
 - detergency 58–61
 - experimental techniques 237, 381
 - paper manufacture 132–136
 - polymeric surfactants 377–384
 - sensitizing dyes 98
 - surfactants 232–238, 240–241
- AEEA *see* aminoethylethanolamine
- aerobic batch tests 516–517
- aerosols 15
- AFM *see* atomic force microscopy
- agglomeration 79, 114, 206–208, 239
- aggregate, roads 334
- aggregation 79, 186, 188, 445–447
 - see also* coagulation; coalescence; flocculation
- agriculture 73–83, 341–342
- agrochemicals 80–83
- AKD *see* alkyl ketene dimer
- alcohol ethoxylates 301–302
- alcohols
 - nonionic hydrophobes 294–296
- algicides 318–321
- alkane sulfonates 282–285
- alkanolamides 306–307
- alkenyl succinic anhydride (ASA) 141, 143–144
- alkyd emulsions 113, 402–403
- alkyl chain length 484–488
- alkyl ketene dimer (AKD) 141, 142–144, 158
- alkyl *N*-methylglucamides 305
- alkyl quaternary ammonium salts 311–312, 314, 315–316, 318, 329–330
- alkylamines 328
- alkylbenzene sulfonates 278–282
- alkylene oxides 296
- alkylether carboxylates 275–276
- alkylether sulfates 275, 524–525
- alkylglucosides 392–393
- alkylphenol ethoxylates (APEOs) 302–303, 528–529
- alkylphenols 296
- alkylpolyglucosides 409
- alkylpolyglycosides (APGs) 304, 529
- alkylsulfates 273–275, 524–525
- AMBER force field 539–540, 541, 545
- amidopropylamines 327
- amine ethoxylates 307
- amine oxides 305–306, 324, 325–327
- amines 297
- aminoethylethanolamine (AEEA) 356–359
- amorphous dispersions 91
- amphipathic structure 232–233, 376
- amphiphiles
 - see also* hydrophobes; surfactants
 - drugs 4, 7
- amphitropic mesophases 496
- amphoacetates 349–350, 356–359
- amphoteric surfactants 294, 323, 349–350, 351, 355–372, 532–534
 - see also* zwitterionic surfactants
- anaerobic testing 515, 517
- anchoring 140, 205, 374, 377–378, 383
- anion-active sequestrants 291
- anionic surfactants 271–292, 520–525
- antifoamers 71, 263
- antisetling agents 79–80
- antistat layers 86–87
- antithixotropy 209
- AOX *see* adsorbable organic halogen-containing substances
- APEOs *see* alkylphenol ethoxylates
- APGs *see* alkylpolyglycosides
- aquatic toxicity 518–519, 524–525, 529, 531–532, 534
- aqueous dispersions 39
- aqueous injection moulding 216
- ASA *see* alkenyl succinic anhydride
- asphalt *see* bitumen
- asphaltic emulsions 265
- assessment criteria 514–520
- associative phase separation 453, 456–458
- associative thickeners 105–107, 449
- atomic force microscopy (AFM)
 - dispersions 242
 - latices 109–110
 - paper 127, 149, 165, 166
 - surfactant migration 398
- autophobicity 142
- autoxidation 398–399

- bactericides 318–321
 barrier coatings 152–154
 batch polymerizations 194–195
 batch tests 516–517
 Bendtsen test 165
 BET *see* Brunauer–Emmett–Teller
 betaines 349–355, 363–364, 396–397, 533
 BiAS *see* Bismuth active substances
 bicontinuous phases
 aggregates 473, 475, 477–478
 liquid crystals 473, 475, 477–478, 482
 microemulsions 460–462, 482
 ringing gels 353
 bilayers
 binder burnout 216–217
 binder–emulsion preparation 107–110
 binders 111–113, 116, 149
 Bingham solids 208–209
 bio-surfactants 521
 bioaccumulation 515, 520
 bioadhesion 14
 bioavailability 8–9
 biocides 318–321, 333–334, 360
 biodegradability
 amphoteric surfactants 532–534
 anionic surfactants 279, 521–524
 cationic surfactants 531
 cleavable surfactants 391, 394, 395
 drug delivery systems 26–30
 legislation 512–513
 nonionic surfactants 527–529
 surfactants 509–510, 515–517
 biomagnification 515, 520
 biostatic activity 319–320
 bis-surfactants *see* Gemini surfactants
 bismuth active substances (BiAS) 513, 527
 bitumen 265, 334–337
 bleaching 125
 block copolymers
 adsorption 374, 377–384
 drug delivery 8, 11, 13, 15–16, 21–25
 nonionic surfactants 303–304, 491–493
 blood substitute formulations 9
 blooming 116
 boundary conditions 227, 540
 Bragg–William approximations 378
 Brewster-angle microscopy 538
 bridging
 floculation 136–137, 205
 brightening 125
 Bristow wheel 160
 Brønsted acidity 231–232
 Brunauer–Emmett–Teller (BET) isotherm 167–168
 bubble formation 255, 274
 see also foams
 builders 54, 61, 65, 288

 CAC *see* critical association concentration
 calcium, detergency 61–65
 calcium carbonate 147
 cancer therapy 9–10
 capillary phenomena
 condensation 161–162
 dynamics 159–160
 carbohydrates 300–301
 carboxybetaines 350–354
 carrier effect 64
 casting 203, 212–213, 215–216
 cationic surfactants 309–348, 460, 529–532
 centrifugal casting 212
 ceramics 201–218
 chain length 297, 302
 chain lubricants *see* conveyor lubricants
 chain scission 217
 chain–chain interactions 236
 charge regulated surfaces 227–228
 charge-stabilized particles 136–137
 CHARMM force fields 545
 chelating agents 332
 chemical flooding 259–262
 chemical interactions 236
 chemical pulping 125
 chemically heterogeneous dispersions 40–42
 chemically homogeneous dispersions 40
 chemisorption 248
 clathrate hydrates 468
 clean-up, oil spills 264
 cleansing *see* detergency
 cleavable surfactants 291, 390–397
 clouding
 detergency 69
 hydrotropes 321–322, 414, 415
 liquid crystals 480–481
 nonionic surfactants 485–488
 oxyethylene surfactants 442
 surfactant–polymer systems 454–456, 463
 CMC *see* critical micelle concentration
 coalescence 106
 coatings 29–30, 146–154
 cobinders 148–149
 cobuilders 64–65
 cold isostatic pressing 214
 collectors, flotation 246–249
 colloidal processing 203
 colloidal silver 91, 92
 columnar mesophases
 see also rod-like micelles
 commercial processes *see* manufacture
 commercial surfactants 484, 492
 comminution 180–184, 190–191, 193
 compaction of DNA 460
 competitive adsorption 105–107, 109
 complexation 61–65, 96
 compression rheology 211–212
 computer simulation 537–550
 concentration effects 435–437
 concentration profiles 542, 544
 condensation 184–185, 190–191
 conditioning 327–328
 conductivity 87
 conformation 377–381, 543, 545
 consolidation 41, 124–125, 212–216, 239, 240
 constant charge surfaces 227
 constant potential surfaces 227
 consulate point 488
 contact angles

- see also* Young equation
 crude oil 254, 255
 conveyor lubricants 332–334
 cooperative binding 447, 451–452
 copolymers
 adhesion 86
 adsorption 374, 377–384
 drug delivery 8, 11, 13, 15–16, 21–25
 nonionic surfactants 303–304, 491–493
 pigment dispersion 119
 corrosion inhibition 263–264, 288, 307, 340
 cosmetics 327–328, 368–369, 511
 cosolutes 425–427, 435, 438, 442, 448
 cosurfactants 497–498
 Couette flow technique 183
 Coulombic forces 540
 counterions 274, 431, 468–469
 coupled units tests 527–528
 coupler dispersions 99–101
 coupling agents 409, 412–414
 CPP *see* critical packing parameter
 cracking process 265–266
 cratering, paints 121
 creaming, emulsions 186
 critical association concentration (CAC) 446–447, 452, 456
 critical micelle concentration (CMC)
 see also micelles
 amphoterics 362–363
 competitive adsorption 106–107
 detergency 55–56
 Gemini surfactants 388–389, 390
 micellization 253, 467–472
 surfactant–polymer systems 446–447
 surfactants 237, 388–390, 422–427
 critical packing parameter (CPP) 45, 422, 432–433
 critical solution temperature 189–190
 critical surface tension 120–121
 Cross equation 209
 ‘cross-talk’ 87, 92
 crude oil 252, 254, 255, 265–266
 cryoporometry 169–170
 crystal growth 79
 see also Ostwald ripening
 crystallization 416–417
 cubic phases
 drug delivery 12, 20
 multicomponent systems 492, 494, 498–499
 phase behaviour 481
 structure 472, 473–475
 curtain coating 88
 cyclic acetals 391–392
 cyclodextrin solutions 16–17

 Darcy’s law 152
 deagglomeration 206–208
 Debye–Hückel equation 131
 DEEDMAC *see* diethylester dimethylammonium chloride
 defects 202
 defoamers 263
 see also antifoamers; foam breaking
 deformation 146
 degradation products 515
 denaturation temperature 46

 deoxyribonucleic acid (DNA) 12–13, 460
 DEQs *see* diesterquaternaries
 destabilization 40–42
 detergency 53–72
 alkyl sulfates 274
 amphoterics 365, 366–367
 anionic surfactants 279–282
 betaines 350
 cationic surfactants 310, 314–318, 321–327
 cleavable surfactants 395
 environmental issues 511, 513, 521
 fabric softeners 314–318
 hydrotropes 415–416
 mesophases 503
 nonionic surfactants 302, 303, 305
 sulfosuccinates 289
 developer scavengers 87–88
 dewatering 152
 di-tallow dimethylammonium chloride (DTDMAC) 530–532
 di-tallow imidazolinester (DTIE) 530–532
 dialkyldimethyl quaternary ammonium salts 311–312, 314, 315, 318
 diesterquaternaries (DEQs) 530–532
 diethylene triamine quaternary ammonium salts 315–316
 diethylester dimethylammonium chloride (DEEDMAC) 530–532
 differential scanning calorimetry (DSC) 170
 dimeric surfactants *see* Gemini surfactants
 direct casting 215–216
 direct coagulation casting 215
 direct flotation 345
 disc-nematic phases 489
 disinfection 318–319, 368
 dispersants 116–119, 147–148, 288, 291
 dispersions
 absorber dyes 101–102
 agriculture 79
 aqueous 39
 ceramics 206–208
 chemically heterogeneous 40–42
 chemically homogeneous 40
 coupler 99–101
 drug delivery 8–15
 emulsions 99–100
 mixed micellization 100
 nanocrystalline 100–101
 natural systems 175–176
 oil-continuous 39
 paint pigments 113–119
 particle processing 238–243
 photography 91–92
 stabilization 381–384
 disproportionation 41
 dissipative particle dynamics (DPD) simulation method 537, 546–547, 548
 dissociation 221
 distillation 416
 disulfine blue active substances (DSBAS) 513
 DLVO theory 130–132
 DNA *see* deoxyribonucleic acid
 dodecyl-1,3-propylenebis(ammonium chloride) (DoPDAC) 495
 DoPDAC *see* dodecyl-1,3-propylenebis(ammonium chloride)

- double-chain surfactants
see also lipids
- DPD *see* dissipative particle dynamics
- drained casting 212–213
- drilling mud 259
- droplet size
 agrochemical sprays 80–83
 comminution 181–183
 monomer emulsions 191
 Ostwald ripening 186–187
 polymerization techniques 195–198
 surfactant role 111–113
- drugs (pharmaceutical) 3–6, 8–23
- dry pressing 214
- dry strength, paper 145
- drying, ceramics 216–217
- DSBAS *see* disulfine blue active substances
- DSC *see* differential scanning calorimetry
- DTDMAC *see* di-tallow dimethylammonium chloride
- DTIE *see* di-tallow imidazolinester
- dynamic swelling 185, 191
- EC₅₀ tests 518–519, 524–525, 530, 532
- edge penetration 161
- EDTA *see* ethylenediaminetetraacetic acid
- EEC *see* European Economic Community Directives
- elastic interaction 382–383
- electrical behaviour
 conductivity 233–236
- electrical double-layer 222–223
see also zeta potential
- electroacoustic sonic amplitude (ESA) 102–103
- electrokinetic potential *see* zeta potential
- electrokinetics 102–103
see also electroosmosis; electrophoresis; sedimentation potential; streaming potential
- electrolytes
 detergency 59, 60, 72
 foaming 72
 micellization 425–427
 phase behaviour 500–501
 surface charge 221–222
 surfactant–polymer systems 454–460
- electron spectroscopy for chemical analysis (ESCA) 51, 109, 111–113, 162–163, 397
- electronic properties 87
- electroosmosis 225
- electrophoresis 97, 102–103, 224, 336
- electrophoretic deposition (EPD) 213–214
- electrostatics
 air 50
 double-layers 204–205
 liquids 42
 patch aggregation 136, 137
 responsive systems 25–26
 stabilization 108
 surface charge 226–229
 surfactant–polymer systems 448
- electrosteric stabilization 206
- elongational rheology 153
- emulsifiable concentrates 73, 74–76
- emulsification
 comminution 179, 180–184
 condensation 179, 184–185
 emulsifiers 179–180
 foodstuffs 42, 45, 47
 paints 105, 107–110
 photography 91, 99–100
 photolability 397
 spontaneous 185
- emulsion concentrates 76–78
- emulsion polymerization 107–110, 175–200, 288, 290–291, 400–402
- emulsions
see also emulsification; microemulsions
 alkyd 113
 bitumen 335–336
 drug delivery 8–9
 foodstuffs 40–41
 miniemulsions 176, 177, 195–196
 monomer 191–196
 multiple 73
 nanoemulsions 77
 petroleum industry 256–259, 262, 263
 photography 85–86, 87–89
 radical polymerization 196–198
 separation 265–266
 spontaneous 74–76
 stability 186–190
 suspoemulsions 73
- encapsulation 28, 418
see also microencapsulation
- enhanced oil recovery (EOR) 259, 262–263
- entropic interactions 382–383
- environmental issues
see also biodegradability
 amphoteric surfactants 364, 365, 532–534
 analytical techniques 513–514
 anionic surfactants 279–280, 284, 520–525
 aquatic toxicity 524–525, 529, 531–532, 534
 assessment criteria 514–520
 cationic surfactants 321, 332, 340, 529–532
 ethoxylated surfactants 107, 117
 eutrophication 61, 116
 industry 510–512
 legislation 512–513
 nonionic surfactants 303, 305, 525–529
 oil industry 264–265, 340
 risk assessment 534–535
 softening agents 332
 zwitterionic surfactants 364, 365
- EOR *see* enhanced oil recovery
- EPD *see* electrophoretic deposition
- equivalence points 96–97
- ESA *see* electroacoustic sonic amplitude
- ESCA *see* electron spectroscopy for chemical analysis
- ester quaternary ammonium salts 316–317, 329–330, 395–397
- ethoxylated amines 327, 328–329
- ethoxylated quaternary ammonium salts 329–330
- ethoxylated surfactants 107
- ethoxymer distribution 299–300, 302
- ethylene oxide 298–300, 303–304
- ethylenediaminetetraacetic acid (EDTA) 332
- European Economic Community (EEC) Directives 512–513
- European Working Group (EWG) 512–513
- eutrophication 61, 116

- EWG *see* European Working Group
 extenders 114
 extraction 416
 extrusion coating 88
 extrusion molding 214
- fabric softeners 314–318
 fatty acids 277–278, 352–353
 fatty alcohols 273, 275
 fatty amines 318
 fatty nitriles 311
 Feldspar, flotation 346
 fibre collapse point 129
 fibre lignin content 125–127
 fibre properties, paper 125–128, 129
 fillers, paper 129
 films
 see also foams
 morphology 109–110
 filter dyes 101–103
 first-effect concentrations 526
 fixation, emulsions 196–198
 flexibility 438
 flocculation
 ceramics 205, 209–211, 213
 emulsion concentrates 76, 77
 foodstuffs 43, 44
 nanoparticles 135
 paper 129–130, 135–138, 141–142, 151
 pigment dispersion 114
 polymeric surfactants 381–382, 383
 selective 243–245
 Flory–Huggins theory 229–230, 374–375
 Flory–Krigbaum theory 382
 flotation 246–249, 289, 344–347
 fluidization 265
 fluorosurfactants 122, 291
 foams
 see also films
 amphoterics 365, 366–367
 anionic surfactants 274, 275, 280
 bubble formation 255, 274
 cationic surfactants 325
 detergency 71–72
 foodstuffs 41–42
 petroleum industry 254–256, 262–263
 stabilizers 306
 foodstuffs 39–52
 cationic surfactants 332–334
 environmental issues 512
 nonionic surfactants 297, 307–308
 force fields 539–541
 fracturing fluids 340
 free energy
 see also interfacial tension; surface tension
 free rosin distributions 140
 free volume theory 230
 functionality tests 46
 fungicides 318–321
- gas adsorption 167–168
 gas chromatography (GC) 362
- GC *see* gas chromatography
 gel phases
 betaines 353
 ceramics 215
 drug delivery 21–23, 29
 structure 476–477
 surfactant–polymer systems 455–456, 462–463
 gelatin 86, 97
 gemini surfactants 314, 354, 385–390, 469, 496–497
 gene therapy 11–12
 Geography-Referenced Exposure Assessment Tool for European Rivers (GREAT-ER) 535
 Gibbs equations
 adsorption 75, 76–77, 252, 389
 phase rule 466, 467
 Gibbs–Helmholtz equation 177
 Gibbs–Marangoni effect 255
 Gibbs–Thompson equation 169–170
 glucamides 327
 Gouy–Chapman model 222–223
 graft copolymers 374, 377–384
 granules 214
 GREAT-ER *see* Geography-Referenced Exposure Assessment Tool for European Rivers
 Griffith equation 201
 grinding, dispersion 114
- hair care 327–328, 354, 368
 hard surface cleaning 321–326, 367–368
 heat treatment 245
 heat-developable materials 90
 heavy metal ions 288–289
 Helmholtz model 222
 hemimicelles 236, 237, 238
 heterogeneity 40–42, 155–156, 202–203
 heteronuclear Overhauser effect 546
 heterophase polymerizations 181, 184, 185, 190
 hexagonal phases 473, 479, 481, 492
 high performance liquid chromatography (HPLC) 362, 513–514
 HLB *see* hydrophilic–lipophilic balance
 homogeneity 540
 homopolymers 373–374
 HPLC *see* high performance liquid chromatography
 hydrate inhibitors 340
 hydration interactions 42–43
 hydrogen bonding 230, 244, 489
 hydrolysis 100, 143–144, 391–397
 hydrophiles 298–301
 hydrophilic–lipophilic balance (HLB)
 anionic surfactants 275
 cationic surfactants 310
 emulsions 180, 257–258
 lipids 44–45, 48
 paint pigments 117
 spontaneous emulsification 74
 hydrophobic effect 467–469
 hydrophobicity
 interactions 233, 428–429, 449, 452
 lipids 12–13
 micelles 294–297
 modification 447–452, 461

- hydrophobizing *see* sizing
hydrotropes 321–323, 407–420, 500
- IEP *see* isoelectronic point
image analysis 164–166
immunization 28
in situ particle size measurement 239
in situ-forming carrier systems 20
inclusion complexes 17
industrial syntheses *see* manufacture
infrared (IR) spectroscopy 163
inisurfs 401–402
initiators 194, 400
injection molding 214
inner salts 350
insulin adsorption 5
interfacial polymerization 73
interfacial tension
 oil recovery 261
 polymers 178
 spontaneous emulsification 74–76
intermediate phases 477–479
internal sizing 138–145
International Organization for Standardization (ISO) 516,
 517
interpenetration 241–242
inverse micellar solutions 411
inverse phases 499
inverse polymerization 180
ion adsorption 220
ion dissolution 220–221
ion exchange 61–65, 233
ion pairing 233
ionic strength 226, 240
ionic surfactants 493–497
ionization 221
IR *see* infrared spectroscopy
isoelectronic point (IEP) 46, 96–97, 224, 225–226,
 246–248
isomorphous substitutions 221
- kaolin 147
Kelvin equation 161, 168
ketals 393–394
kinetics 433–434
Klevens equation 362
Kolmogorov length 181
Kozeny-Carman relationship 152
Krafft point 45, 427–428, 468, 489
Krafft temperature *see* Krafft point
Krieger–Dougherty equation 151, 210
- lamellar phases
 see also liquid crystals
 hydrotropes 411, 412–414
 micelle self-assembly 253
 phase behaviour 481
 structure 471, 472–473
 vesicles 418
Langmuir equation 58
Langmuir–Blodgett (LB) films
 computer simulation 538
- Laplace equations 168
laser-focusing techniques 165
LASs *see* linear alkylbenzene sulfonates
lateral interactions 236
lateral structure 543
latex 105–122
lattices 221, 401–402
LB *see* Langmuir–Blodgett
LC₄₅₀ tests 518–519, 524–525, 530, 532
legislation 512–513
Lial process 295
lidocaine 7, 8
ligand complexation 96
light scattering
 paper 129
light sensitivity 101
lignin content 125–127
ligninsulfonates 292
limited coalescence 103–104
linear alkylbenzene sulfonates (LASs) 511, 513, 521,
 523–526
linearized Poisson–Boltzmann distribution 228
lipids 12–13, 44–46
liposomes 9–12
liquid bridges 44, 50
liquid crystals
 agrochemical sprays 83
 chemical structure 465–508
 concentration effects 436
 drug delivery 12, 20–21
 foodstuffs 45
 formation 256
 hydrotropes 408–409, 411, 412–414, 415
 lamellar 411, 412–414, 418, 471, 472–473, 481
 lyotropic 466–467
 nematic 475–476, 483–484, 489
 phase behaviour 466, 472–502
 surfactants 66–67, 70
 vesicles 418
liquid soaps 273
liquid transport 162
liquid/liquid interface 65–67
LOEC *see* lowest observed effect concentration
loops 231, 377–379
lowest observed effect concentration (LOEC) 519, 527
lyotropic liquid crystals 466–467
lyotropic nematic phases 475
- macroemulsions 176, 177
macromolecules 15
Maltese cross textures 473
manufacturing processes
 amphoterics 356–360
 anionic surfactants 273–279, 282–284, 286–288, 290
 betaines 352–353, 355
 block copolymers 303
 cationic surfactants 311–314
 Gemini surfactants 386
 Lial process 295
 nonionic surfactants 294–297, 298–300, 302–308
 OXO process 274, 295
 Shell Higher Olefin Process 295

- Williamson synthesis 275, 276
 Ziegler process 279, 294–295
- mass action models 429
- matte beads 87, 103–104
- MBAS *see* methylene blue active substances
- MD *see* molecular dynamics
- mean field approximations 378
- mechanical pulping 125
- membrane emulsification 183
- mercerization 337, 338, 339
- mercury porosimetry 168–170
- mesh mesophases 477–478, 494
- mesogenic properties 490
- mesophases
 additives 497–502
 hydrogen bonding 489
 liquid crystals 465–508
 lyotropic liquid crystals 466–467
 meshes 477–478
 ringing gels 353
- metabolites 515, 519
- metals
 processing 512
- methyl ester ethoxylates 307–308
- methylene blue active substances (MBAS) 512, 513
- MHC *see* minimal hydrotropic concentration
- micelles
see also critical micelle concentration; rod-like micelles
 agrochemical sprays 83
 amphoteric 362–363
 cationic surfactants 324
 computer simulation 544–546
 concentration effects 435–437
 coupler dispersions 100
 detergency 55–56, 59
 drug delivery 15–16
 Gemini surfactants 388–390
 hemimicelles 236, 237, 238
 inverse solutions 411
 kinetics 433–434
 liquid crystals 465–466, 467–472
 mixed 100, 442, 451–452
 molecular dynamics 544–546
 nonionic 440–442
 phase behaviour 481
 polymeric surfactants 376
 self-assembly 252–254
 solvent effects 434
 sponge phase 439–440
 structure 421–423, 431–432, 437–441, 467–472
 surfactant adsorption 236–237
 temperature effects 440–442
 thermodynamic models 428–430
- Michael addition reactions 359–360
- microemulsions
see also emulsions
 agriculture 73
 bicontinuous 460–462, 482
 condensation 184–185
 detergency 68–70
 drugs 7, 17
 emulsion polymerization 176
 formation 253, 258–259
 hydrotropes 412, 414
 surfactant–polymer systems 460–462
- microencapsulation 73–74
- microorganisms 319–320
- migration, films 397
- mineral flotation 246–249, 344–347
- miniemulsions 176, 177, 195–196
- minimal hydrotropic concentration (MHC) 409, 412
- mining 344–347, 512
- mixed micelles 100, 442, 451–452
- mixed surfactants 498–499
- mobility 543
- modelling, Langmuir–Blodgett films 537–550
- molecular dynamics (MD) 537–550
- molecular recognition 244
- monolayers 541–544
- monomer emulsions 191–196
- multiple emulsions 73
- multiple equilibrium model 429–430
- nanocrystalline dispersions 91, 100–101
- nanoemulsions 77
- nanoparticles 135
- nanoparticulate semiconductors 87
- NaPA *see* sodium polyacrylate
- necking, ceramics 207
- nematic liquid crystals 475–476, 483–484, 489
- neutralization flocculation 137
- nitrogen-containing polymers 327
- NMR *see* nuclear magnetic resonance spectroscopy
- no observed effect concentration (NOEC) 284, 519, 526–527, 530, 532
- nonionic hydrophiles 298–301
- nonionic hydrophobes 294–297
- nonionic micelles 440–442
- nonionic surfactants 293–308
 block copolymers 491–493
 environmental issues 525–529
 phase behaviour 480–491
- nonpolar solvents 434
- nuclear magnetic resonance (NMR) spectroscopy
 amphoteric 361–362
 hydrotropes 412
 micellization 430–431
 porosity 170
- nucleation 95
- OECD *see* Organization for Economic Co-operation and Development
- oil ganglia 259, 261
- oil industry *see* petroleum industry
- oil-continuous dispersions 39
- oils 499–500
- oily streaks 473
- oligopeptides 4–5
- optical density 409–410
- optical textures 472–473, 474
- oral care 369
- oral drug administration 8–9, 13, 18, 28
- Organization for Economic Co-operation and Development (OECD) tests 513, 518, 520, 523, 527–528, 533–534
- organoclay 343–344

- ortho esters 394–395
osmosis 211–212
Ostwald ripening
 dynamic swelling 191
 emulsion concentrates 77–78, 79
 emulsions 185–188, 191
 foams 41
 photography 95–96
overcoating 87
OXO process 274, 295
oxyethylene surfactants 440–442
- π -stacking 467
packing density 211
paints 105–122, 397, 403–404
paper 123–173
 absorbency 154–158, 159–162
 cationic surfactants 331–332
 environmental issues 512
 formation 128–138
 internal sizing 138–145
 polymer adsorption 132–136
 porosity 167–171
 surface properties 155–156, 158–159, 162–166
 surface treatment 146–154
 wettability 154–159
paraphenylenediamines 89, 90, 93
parenteral drug administration 9–10, 19–20
Parker–Print–Surf (PPS) test 165
particle size 239
particulates 48–51, 91–92, 94–99
patch flocculation 136, 137
PB *see* Poisson–Boltzman theory
PCS *see* photon correlation spectroscopy
pearl-necklace model 447–448
PEC *see* predicted environmental concentrations
PEGs *see* poly(ethylene glycol)s
penetration
 capillary 160–162
 drug delivery 11
 molecular dynamics 544, 545
PEO *see* poly(ethylene oxide)
PEO–PPO–PEO block copolymers 11, 13, 15–16, 21–25
peptization 334, 336–337
perfluorocarbon fluids 179
personal care 327–330, 344, 354, 364–369
petrol sulfonates 278
petroleum industry 251–267, 295–296, 337–341, 343–344, 512
Peyer's patches 28
PGSE NMR *see* pulsed gradient spin-echo nuclear magnetic resonance
pH effects
 amphoterics 350
 betaine esters 396
 ceramics 204–205, 215
 dispersions 240
 drug delivery 25–26
 effects on sizing 141–142
 selective flocculation 245
 surface charge 221–222
 thickener stability 323–324
 zeta potential 225–226, 248–249
 zwitterions 350, 352–353
pharmacy 3–38, 369, 418–419, 511
phase behaviour
 amphiphilic drugs 7, 8
 computer simulations 547–550
 hydrotropes 412–414, 500
 in situ-forming carrier systems 20
 inversion 44, 186, 189–190, 258
 ionic surfactants 493–497
 liquid crystals 466, 472–502
 micelles 481
 nonionic surfactants 480–491
 separation 43, 186, 429
 surfactant–polymer systems 452–463
 surfactants 67–71, 480–497
 zwitterions 493
phase rule 466, 467
phosphated alcohols 285–287
phosphobetaines 354–355
phosphoric acid esters 285–289
photography 85–104, 176, 192–193
photolability 397
photon correlation spectroscopy (PCS) 381
physico-chemical processes 421–443, 515, 517–518
Pickering stabilizers 192–193
picture framing 121
pigments 108–109, 113–119, 147
plasticity 208
plastics 91, 512
PNEC *see* predicted no-effect concentrations
Poisson–Boltzmann (PB) theory 205, 226–228
polar solvents 434
polarizing microscopy 75, 472
polyamines 333
polycarboxylates 64–65
polydispersity index 19
polyelectrolytes 116–119, 132–136, 147–148
poly(ethylene oxide) (PEO) 5–6
polyglucoside surfactants 489–491
polyhydroxy surfactants 489
polyhydroxybenzenes 412
polymerization
 binder-emulsion preparation 107–110
 emulsions 107–110, 175–200, 288, 290–291, 400–402
 inverse 180
 radical 176, 196–198
 surfactants 107–110, 397–405
 suspensions 103–104, 176, 192–193
polymers
 adsorption 132–136, 229–232, 241
 bridging mechanism 136–137
 drug delivery 13–14, 23, 27–29
 electronically conducting 87
 nitrogen-containing 327
 particle interactions 43, 205–206
 surfactant–polymer systems 445–463
 surfactants 373–384
polyoxyethylene surfactants 287–288, 486–487, 502
polyphosphated alcohols 285–287
polysaccharides 44, 46–48
porosimetry, mercury 168–170
porosity 167–171
post-emulsified binders 111–113

- potash, flotation 347
 powders 50–51, 202–203
 PPS *see* Parker–Print–Surf test
 predicted environmental concentrations (PEC) 512–513, 535
 predicted no-effect concentrations (PNEC) 513, 519, 535
 pressure filtration 203
 proline 417
 propionates 359–360
 propylene oxide 300, 303–304
 protein crystals 467
 proteins 5, 46
 pulping 125
 pyrolysis 217
- quasi-lattice model 378
 quaternary ammonium salts
 agricultural adjuvants 341–342
 biocides 318–321
 cleavable surfactants 395–397
 cosmetics 316–317, 329–330
 detergency 314–318, 327
 environmental issues 530–532
 manufacture 311–314
 mineral flotation 345, 347
 oilfields 338–340
 organoclays 343–344
 paper 331
 thickeners 323
 quinonediimines 89, 93–94
- radical polymerization 176, 196–198
 Raman spectroscopy 163
 rayon 337, 338, 339
 refractive index 114
 RES *see* reticuloendothelial system
 responsive drug delivery 24–26
 retention, paper 129–130, 141–142
 reticuloendothelial system (RES) 9
 reverse flotation 345
 reversed phases
 liquid crystals 472–473, 480, 499
 Rhebinder effect 79
 rheology
 associative thickeners 449
 ceramics 208–212
 dispersions 239–240
 elongational 153
 foams 254
 foodstuffs 41
 liquid crystals 466
 mesophases 503
 modifiers 148–149, 343
 paper coatings 149–152
 surfactants 338–340, 389–390
 rheopexy 209
 rhombohedral mesh phases 477–478, 494
 ribbon phases 477–478, 495
 ringing gels 353
 rinse-added softeners 317
 risk assessment 534–535
 road construction 334–337
 rod-like micelles
 cationic surfactants 324
 concentration 437
 flexibility 438
 rolling-up mechanism 59, 65–67
 rosins 140–142
 rotator phase 477
- salting-in 407, 409–410, 500
 scanning electron microscopy (SEM) 127, 170–171
schlieren nematic texture 475
 SDS *see* sodium dodecyl sulfate
 secondary ion mass spectrometry (SIMS) 163
 secondary surfactants 365, 367
 sedimentation 186
 sedimentation potential 225
 seed particles 194
 segregative phase separation 453, 456–458
 selective flocculation 243–245
 self-emulsifiable oils 73
 SEM *see* scanning electron microscopy
 sensitization (paper) 97–98, 137
 separation 59, 416–417
 sequestration 288–289, 291
 sewage treatment *see* waste-water treatment
 SFA *see* surface force apparatus
 SFF *see* solid freeform fabrication
 shear behaviour 149–152, 208–210
 Shell Higher Olefin Process (SHOP) 295
 SHOP *see* Shell Higher Olefin Process
 short-chain sulfonates 291
 short-oil alkyds 113
 silicates, flotation 345
 silicone surfactants 122, 291–292
 silver halides 87–88, 90–92, 94–99
 SIMS *see* secondary ion mass spectrometry
 sizing 125, 138–145, 152–153
 skin care
 amphoteric 364–365, 366–367, 368
 betaines 354
 cationic surfactants 327–328, 344
 organoclays 344
 slide hopper coating 88
 slip casting, ceramics 203, 212
 SLNs *see* solid lipid nanoparticles
 slurries 176
 smectites, organoclays 343–344
 soaps 272–273, 280
 sodium dodecyl sulfate (SDS) 494
 sodium polyacrylate (NaPA) 147–149
 solid formulations, agriculture 73–74
 solid freeform fabrication (SFF) 216
 solid lipid nanoparticles (SLNs) 12–13
 solid loading, ceramics 210–211
 solid/liquid interfaces 58–61
 solubility 46, 178, 375–376
 solubilization
 capacity 69
 hydrotropes 409–412, 415, 418–419
 micelles 431, 432
 surfactant–polymer systems 447
 solvation shells 545
 solvents
 foodstuffs 43

- micellization 434
- multicomponent systems 501–502
- paints 119
- speciality surfactants 121–122, 385–405
- spin finishing 337, 338, 339
- sponge phases
 - block copolymers 492–493
 - liquid crystals 482
 - micelles 439–440
- spontaneous emulsification 74–76, 185
- sprays, agriculture 80–83
- stabilization
 - aggregation 188
 - coupler dispersions 99–100
 - dispersions 381–384
 - electrostatic 108
 - foams 306
 - foodstuffs 40–42
 - microemulsions 412, 414
 - Ostwald ripening 186–187
 - paper manufacture 130
 - steric 9, 205, 377, 381–384
 - suspension polymerization 192–193
 - suspensions 209–210, 212, 213
- starches, co-binders 149
- static cling 317
- steady shear 149–152
- stereolithography 216
- steric effects
 - stabilization 9, 205, 377, 381–384
- Stern plane 224–225, 235
- Stern–Graham model 223
- stiff gels, ceramics 215
- Stokes–Einstein equation 377
- streaming potential 224–225
- stress-craze inhibitors 333–334
- structural viscous liquids
 - see also* shear behaviour
- stylus contact method 165
- subbing layers 85
- sulfobetaines 354–355
- sulfochlorination 282–284
- sulfosuccinates 289–291, 524–525
- sulfoxidation 284
- supersaturation 184
- support base, photography 85
- surface charge
 - aqueous media 220–229
 - flotation 246–249
 - molecular dynamics 545
 - selective flocculation 243–244
- surface tension
 - agrochemical sprays 80–83
 - betaines 363–364
 - detergency 54–58
 - Gemini surfactants 388
 - paints 120–121
 - perfluorocarbon fluids 179
 - polymers 178
 - surfactant–polymer systems 445–446
- surfaces
 - see also* surface charge; surface tension
 - activity 4–6, 44–48, 73, 105
 - modification 403–404
 - morphology 125
 - reactions 247–249
 - roughness 155–156, 158–159, 163–166
 - treatment 125, 138–145, 146–154, 245
- surfactant affinity difference 258
- surfactant number *see* critical packing parameter
- surfactant systems, drug effects 6–8
- surfactant–polymer flooding 259–262
- surfactant–polymer systems 445–463
- surfactants
 - see also* zwitterionic surfactants
 - adsorption 232–238, 240–241
 - agriculture 73
 - amphipathic structure 232–233, 376
 - amphoteric 294, 323, 349–350, 351, 355–372, 532–534
 - anionic 271–292, 520–525
 - antifoaming agents 71–72
 - cationic 309–348, 529–532
 - cleavable 291, 390–397
 - commercial 484, 492
 - computer simulation 537–550
 - corrosion inhibition 263–264
 - cosurfactants 497–498
 - detergency 54–55, 58–61, 65–71
 - dispersions 240–241
 - droplet size 111–113
 - environmental issues 509–536
 - ethoxylated 107
 - experimental techniques 237
 - foams 254–256
 - Gemini 314, 354, 385–390, 469, 496–497
 - hydrophilic–lipophilic balance 180, 275, 310
 - hydrotropes 500
 - ionic 493–497
 - liquid crystals 465–508
 - mixed 498–499
 - molecular dynamics 537–550
 - nonionic 293–308, 480–493, 525–529
 - oil spill clean-up 264–265
 - paints 105–110
 - petroleum industry 252–256, 259–265
 - phase behaviour 67–71, 480–493
 - physico-chemical properties 421–443
 - polymeric 373–384
 - polymerizable 107–110, 397–405
 - secondary 365, 367
 - self-assembly 252–254
 - speciality 121–122, 385–405
 - surfactant–polymer systems 445–463
 - swelling 190
 - usage trends 510–511
 - UV-curable 403–404
- surfmers (polymerizable surfactants) 107–110, 397–405
- suspension polymerization 103–104, 176, 192–193
- suspensions
 - agriculture 78–80
 - ceramics 203, 205, 208–212
 - consolidation 212–216
 - foodstuffs 41
- suspoemulsions 73
- swelling
 - agents 184
 - drug delivery systems 25
 - emulsions 190–191

- heterophase polymerizations 190
- radical polymerization 197
- surfactant–polymer systems 462–463
- syntheses *see* manufacturing processes
- synthetic sizing agents 140
- tails 231, 377–379
- targeted drug administration 10–11
- temperature effects
 - drug delivery 24–25
 - micelles 425–428, 437, 440–442
 - oxyethylene surfactants 440–442
- tetrapropylenebenzene sulfonate (TPS) 279
- textiles 511–512
- thermodynamics
 - drug delivery 15–23
 - emulsions 176–179
 - micellization 428–430
 - polymer adsorption 229–230
 - polymeric surfactants 374–375
- thermoporosimetry 169–170
- thermotropic liquid crystals 466
- thickening 148–149, 323–325
- thixotropy 209, 210
- threshold effect 64, 288
- tilt angles 538, 542
- titania (titanium dioxide) 114
- toothpastes 369
- topical drug administration 11, 18–19
- topography, paper 163–166
- toxicology
 - amphoterics 364–365
 - aquatic 518–519, 524–525, 529, 531–532, 534
 - surfactants 515
- TPS *see* tetrapropylenebenzene sulfonate
- train formation 231, 377–379
- transport of liquids 162
- transurfs 401
- triglycerides 41, 296, 297
- twin surfactants *see* Gemini surfactants
- Ultra Turrax system 183
- ultrasound 182–183
- ultraviolet (UV) curable surfactants 403–404
- vaccination, oral 28
- van der Waals interactions
 - ceramics 203–204, 205, 207
 - DLVO theory 131–132
 - emulsion concentrates 76
 - liquids 42–43
 - molecular dynamics 539–540
 - pigment dispersion 115
 - powder systems 50
- vapour transport 161
- vesicles
 - hydrotropes 418
- viscoelasticity
 - ceramics 210
 - paper coatings 151–152
 - thickeners 325
- viscose 337, 338, 339
- viscosity
 - see also* thickening
 - amphoteric surfactants 365, 366–368
 - ceramics 209–211
 - dispersions 240
 - Gemini surfactants 390
 - micelle concentration 436
 - surfactant–polymer systems 449, 452
 - volume restriction interaction 382–383
- Washburn equation 159–161
- washing *see* detergency
- waste-water treatment 510, 515, 517, 520, 529
- water
 - see also* aqueous systems
 - bridges 50
 - flooding 261
 - hardness 61–65, 272–273, 288, 314
 - water-borne paints 116–119
 - water-continuous phases 479–480
 - Wenzel's equation 155
 - wet strength, paper 145–146
- wetting
 - agriculture 73, 78–79, 81–83
 - amphoterics 365
 - anionic surfactants 285, 288
 - cationic surfactants 325–326
 - counterions 274
 - crude oil 254, 255
 - detergency 54–58
 - foodstuffs 48–49
 - paints 119–121
 - paper 127–128, 142, 144, 154–159
 - pigment dispersion 114
 - sulfosuccinates 289, 290
- wicking 161
- Williamson synthesis 275, 276
- Winsor's *R* ratio 258
- wood preservatives 318, 320–321
- X-ray photoelectron spectroscopy (XPS) 144–145, 162–163
- xanthogenation 337, 338, 339
- XPS *see* X-ray photoelectron spectroscopy
- Young equation
 - agriculture 78–79
 - detergents 56
 - petroleum 254
- zeolites 61–65
- zeta potential
 - experimental techniques 237–238
 - flotation 248–249
 - manipulation 225–226
 - measurement 224–225
 - surfactant adsorption 235, 237–238
- Ziegler process 279, 294–295
- Zisman plots 120–121
- zwitterionic surfactants
 - characterization 361–372
 - chemistry 349–355
 - emulsions 257
 - paints 118
 - phase behaviour 493

Index – Volume 2

- absorption, molecular 243–244
- ACRPAC *see* analysis of capillary rise profile around a cylinder
- adhering bubble methods 253–254
- adhesion 125–126, 389–390
- ADSA *see* axisymmetric drop shape analysis
- adsorption
 - electrokinetics 371
 - measurement 435–444
 - thin-liquid films 416
- advancing contact angles 129–130
- Aerosol OT *see* sodium bis(2-ethylhexyl)sulfosuccinate
- aerosols 9
- AFM *see* atomic force microscopy
- ageing effects 154–155
- aggregation 15–19
 - see also* coagulation; coalescence; flocculation
- AKD *see* alkyl ketene dimer
- alcohols
 - bilayer solubilization 172
 - foaming 24
 - microemulsions 63, 64–66, 69
- alkane thiols 99–116
- alkyldimethylaminioxides (DMAOs) 196–199, 201–202, 208–210, 213
- amino acids 175–177
- Amonton friction 391
- amphiphiles
 - domain morphology 303–304, 306
 - Langmuir–Blodgett films 80–81
 - liquid crystals 300
 - microemulsions 57–58
- amphoteric surfactants
 - see also* zwitterionic surfactants
- analysis of capillary rise profile around a cylinder (ACRPAC) 268
- anionic surfactants 147
- antifoamers 143–157
- antipercolation threshold 181–182
- AOT *see* sodium bis(2-ethylhexyl) sulfosuccinate
- APGs *see* alkylpolyglycosides
- aqueous polymer solutions 400–402
- aqueous systems 143–156, 190–199
- atomic force microscopy (AFM)
 - surface forces 384–388, 390–391, 395, 397, 399–400
 - thin-liquid films 415
- attenuated total reflection (ATR) spectroscopy 101, 102
- autopoiesis 50–52
- axisymmetric drop shape analysis (ADSA) 253–254, 255–263, 264, 265–266
- azobenzene chromophore 91
- back-scatter technique 37, 39
- Berthelot's (geometric mean) combining rule 127
- BET *see* Brunauer–Emmett–Teller
- bicontinuous phases
 - characterization 352
 - domain morphology 302, 303, 306, 310–315, 316–317
 - mesophases 302, 303, 306, 310–315, 316–321
 - microemulsions 351–352
 - phase prisms 340–342
 - ringing gels 204
- Bikerman test 32–33
- bilayers 149–150, 171–173, 199–204, 211–212
 - see also* membranes, vesicles
- binary solutions 160, 162–173
- binary surfactant–water systems 166–169
- Bingham solids 190, 204
- biologically active molecules 106–109, 111–113
- birefringence 195, 206
- black films 28–29, 30, 426, 427, 431–433
- block copolymers
 - rheology 204–205
- blue laser diodes 87–89
- Boltzmann distribution law 4
- Boltzmann equation 373
- Bragg diffraction 301
- Bragg reflections 330
- brewing industry 155–156
- bridging
 - antifoaming agents 146, 149, 151
 - ceramics 430
 - measurement 402, 405
- Brownian motion 3, 13, 16, 20, 365
- Brunauer–Emmett–Teller (BET) isotherm 436
- bubble formation 418
 - see also* foams
- bubble methods
 - contact angle 253–254
 - dynamic surface tension 227–229, 232–236
 - equilibrium surface tension 217, 221–223, 235
- cadmium arachidate 82
- calcium myristate 327
- capillary phenomena
 - condensation 390
 - contact angle measurement 252, 264–266, 268, 272–274
 - penetration 120, 136–140
 - pressures 421–423, 431
 - rise 217, 218–219
- carbohydrates 17–19
- Cassie–Baxter equation 132

- cathetometers 265
 CBFs *see* common black films
 cell attachment 107, 111–113
 cell opening 41
 cell-surface interactions 17–18
 cellular foams 37
 cement foams 42
 centrifugation 358, 365, 367, 417
 chain length 245, 248
 champagne foams 416
 channel defects 319
 chemisorption 100–101
 chiral mesophases 316
 chirality 50–51
 cholesterics 299–300
 chromatographic retention 442–443
 clays 3, 8–9
 clouding
 cloud point defoamers 148
 curvature 338
 CMC *see* critical micelle concentration
 coagulation 15–19
 cobblestone model 383, 391
 cohesion 125–126
 cohesion energy 269–270
 collective diffusion 346–347, 350–351
 columnar mesophases 308–310
 see also rod-like micelles
 command surfaces 91–92
 commercial processes *see* manufacture
 commercial surfactants 63–64
 comminution 4–5
 common black films (CBFs) 427, 431–433
 competing microstructures 336–337
 competitive adsorption 429
 composite surfaces 131–132
 compressible fluids 68
 computers 89–90, 92–95
 concentration effects 287–288, 347, 380
 concrete foams 42
 condensation 4, 5–6
 condensed phases 189–190
 conductivity 213, 242, 335, 438
 contact angles
 see also Young equation
 definitions 133–134
 hysteresis 129, 130–133
 measurement 251–280
 particle/water interface 150
 temperature dependence 269, 276–277
 thin-liquid films 422
 wetting 119–140
 contamination, films 423
 copolymers
 rheology 204–205
 copper myristate 326
 cosurfactants 63, 64, 65–66
 Coulombic wells 430
 counterions 246
 Cox–Merz rule 211
 critical micelle concentration (CMC)
 see also micelles
 foams 25–26, 28, 29
 influencing factors 241, 245–246
 measurement 239–249
 micellization 190–191
 non-aqueous media 246–248
 self-diffusion NMR 286
 surface forces 398–399
 surface tension 438–439
 surfactants 162–166
 critical surface tension 126–127
 cryo-transmission electron microscopy (Cryo-TEM) 193,
 196, 198, 335, 358
 crystal growth
 cubic phases
 domain morphology 311–314
 rheology 204–205
 self-diffusion 353–355
 thermotropic behaviour 209
 cumulant analysis 366
 curvature 70–72, 160–161, 169, 301–321, 336–338, 345
 cylindrical electrophoresis chambers 376–377
 cylindrical micelles 193–194, 199

 data processing 89–90, 92–95
 DDAB *see* didodecyltrimethylammonium bromide
 de-wetting 146, 149
 Debye screening length 393–395
 Debye–Hückel equation 424
 defects 317–319
 defoamers 143, 154–155
 see also antifoamers; foam breaking
 deformation 388
 density fluctuations 431, 432–433
 deoxyribonucleic acid (DNA) 84, 85
 depletion method 436
 Derjaguin–Muller–Toporov (DMT) theory 389, 391
 detergency
 deuterium labelling 289–290
 diameter axisymmetric drop shape analysis (ADSA-D) *see*
 axisymmetric drop shape analysis
 didodecyltrimethylammonium bromide (DDAB) 181–184
 dielectric relaxation 11
 diffusion coefficient 244
 dilation 190, 206, 235, 237
 dimensional analysis 274
 1,2-dimyristoyl-*syn*-glycero-3-phosphatidylcholine (DMPC)
 50, 51–52
Discovery space shuttle 236
 disjoining pressure 417, 424–430, 431
 Disorder–Open–Connected–Cylinder (DOC) model 181,
 182–184
 dispersions
 emulsions 55–56
 methodology 4–5
 monolayer-protected metal clusters 113–114
 solid 3–20
 solubilization 159
 thin-liquid films 416, 425–426
 DLS *see* dynamic light scattering
 DLVO theory 13–15, 17, 29
 DMAOs *see* alkyltrimethylaminooxides
 DMPC *see* 1,2-dimyristoyl-*syn*-glycero-3-phosphatidylcholine
 DMT *see* Derjaguin–Muller–Toporov theory
 DNA *see* deoxyribonucleic acid
 DOC *see* Disorder–Open–Connected–Cylinder model

- DODAB surfactant 48, 49
domain morphology 301–321
double-chain surfactants 160
double-layers 11–14
drag reduction 210
drop methods
 contact angle 253–254, 255–263, 264
 dynamic surface tension 230–236
 equilibrium surface tension 217, 220–223, 235
droplet microemulsions 344–352
droplet sedimentation 271–272
dry wetting 122–123
Du Noüy ring method 217, 220
Dupré equation 125–126
dye micellization 243
dye solubilization 242–243, 247–248
dynamic light scattering (DLS) 242, 247, 294–296, 357, 365–369
dynamic surface forces 388–389
dynamic surface tension 218, 225–238, 439–440
- eddy currents 284–285
EFF *see* emulsion ferrofluid techniques
EHEC *see* ethyl(hydroxyethyl)cellulose
Einstein relationship 350
elasticity 206
electrical behaviour
 colloidal dispersions 9–13
 conductivity 213, 242, 335, 438
 dispersion 5
electrical double-layer 373–374
 see also zeta potential
electroacoustic sonic amplitude (ESA) 379
electrokinetic potential *see* zeta potential
electrokinetics 371–382
 see also electroosmosis; electrophoresis; sedimentation potential; streaming potential
electrolytes
 antifoaming agents 154
 critical micelle concentration 246
 electrostatic double-layers 393–397
electron microscopy (EM) 335–336
electronic properties 83–84, 92–95
electrooptics 89–90
electroosmosis 371–372, 375–379
electrophoresis 371–372, 375–379
electrostatics
 colloidal dispersions 13–15
 double-layers 424–425
 solubilization 165, 185
ellipsoids of revolution 322–323
ellipsometry 443–444
EM *see* electron microscopy
emulsification
 failure 339, 344, 351–352
emulsion ferrofluid (EFF) techniques 417
emulsion films 30–31
emulsions
 see also emulsification; microemulsions
 antifoaming agents 152–154
 characterization 55–56
 definition 4
 formation 74
 thin-liquid films 417
 encapsulation
 end-functionalization 105–109
 engulfment (particle behaviour) 275
 entropic interactions 426–427
 environmental issues
 EON *see* equivalent ethoxy number
 equation of state 127–128, 252–253, 270, 274
 equilibrium contact angles 129–130
 equilibrium films 28–29
 equilibrium phases 56
 equilibrium surface tension 217–224
 equivalent ethoxy number (EON) 161
 ESA *see* electroacoustic sonic amplitude
 ether oils 67
 ethoxylated alcohols 55–63, 69–70, 71–73
 ethyl(hydroxyethyl)cellulose (EHEC) 401–402
 Euclidean solids 190
 EWG *see* European Working Group
 excess solubilization 178–180
- fatty acids 49–52, 82
ferromagnetic colloids 7
Fick's law 16, 17
films
 see also foams
 film pressure concept 122–123
 film-dimpling 423
 flotation 269
 stratification 427
 thin-liquid 415–433
 wetting 122–123
fish-cuts, phase prisms 340
flexible surface model 336
flip-flop (transverse diffusion) 47, 50
flocculation
 colloidal dispersions 15–16
 definition 15–16
fluorescence quenching 281, 290–292
foam breaking 143–157
foams 23–43
 bubble formation 418
 characterization 415–416, 433
 film rupture mechanisms 26
 foaming agents 40–41
 industrial materials 37–43
 micellar structural forces 427–428
 preparation 24–25, 40–43
 stability 25–37
foodstuffs
 foam breaking 155–156
 foams 24–27, 43
force methods 217–221
fractional amino acid transfer 176–177
fragmentation fractal dimension 360
free energy 121–134
 see also interfacial tension; surface tension
freeze-fracture technique 335, 353
frequency doubling 88–89
frictional forces 390–392
fringes of equal chromatic order (FECO) interferometry 384
froth 25
funnel-shaped test 33–34

- gas-filled polymer foams 38, 40
gel phases
 definition 4
 domain morphology 307–308
 foam stabilization 27
 rheology 204
 vesicle bilayers 46–47
gel-like networks 430
genus concept 304–306, 314
geometric mean combining rule 127
Gibbs elasticity 27–28, 235
Gibbs equations
 adsorption 242
 solubilization 164
Gibbs free energy 122
Gibbs triangle 57–60
Gibbs–Marangoni effect 27–28
Girifalco–Good–Fowkes–Young equation 129
globules 304, 306, 310, 316
gold 3, 4, 6, 99–116
goniometer–telescopes 254, 260–262, 263
goniometry 357, 368
Gouy–Chapman model 373–374, 375
Gouy–Chapman–Stern–Grahame model 380
granules 269–277
grazing incidence X-ray diffraction 80, 82
Guinier approximation 362
- haematite 7
Hagen–Poiseuille equation 272
Hamaker theory 392
hard-sphere radius 346
head space measurement 35
head-group overlap 426–427
heat of immersion 269
Helfrich forces 429
Helmholtz free energy 122
Helmholtz–Smoluchowski equation 374–375
heterogeneity 130
hexagonal mesophases 308–309
hexagonal phases 167, 308–309
hexamethyldisiloxane (HMDSO) 380–381
HLB *see* hydrophilic–lipophilic balance
HMDSO *see* hexamethyldisiloxane
homogeneity 314, 321–323, 330
honeycombs 316
Hookean solids 190, 194
Hooke's law 387
hydration interactions 394
hydrocarbon radius 345–346, 348
hydrodynamic forces 375, 380–382, 388–389, 417
hydrodynamic radius 334, 346, 347, 368–369
hydrolysis 6–7
hydrophilic–lipophilic balance (HLB)
 microemulsions 61, 63, 69
 solubilization 161, 167
hydrophobic effect 240
hydrophobicity
 foams 151–152
 interactions 430
 micelles 162
hyperpolarizability 87–88
hysteresis 268, 401
- image analysis 35, 36
immersional wetting 126
indifferent adsorption 429
indifferent ions 10
industrial materials 37–43
infrared (IR) spectroscopy 101–102, 105–106
inhomogeneous surfaces 129–130, 135–136
integrated circuits 93–95
intensity-weighted distribution 362, 366
interfacial curvature 301–321
interfacial tension
 definition 121
 measurement 218–223, 225–226, 230–232, 235, 258–260
 microemulsions 70, 72–73
 sedimentation volume 269–270
 wetting thermodynamics 127–129
interference microscopy 263–264
interferometry 384–385
intermediate phases 316–317
ionic surfactants 64–66, 165–166
ionization 371
- Johnson–Kendall–Roberts (JKR) theory 388, 389–390, 391
Jönsson model 165–166
- kaolinite 8–9
kinetics 55
Krafft point 245
Krafft temperature *see* Krafft point
kugelschaum, foaming 24–25
- LAC *see* limiting association concentration
lamellae lifetime measurement 37
lamellae profiles 422
lamellar phases
 see also liquid crystals
 bilayer solubilization 171–173
 domain morphology 307, 308, 316
 phase prisms 340–341
 rheology 199–204
 rigid interface solubilization 185
 shear behaviour 211–214
 smectics 300, 307, 315
lamellar structural forces 428–429
laminar flow 18
Langmuir–Blodgett (LB) films 79–98
 command surfaces 91–92
 deposition 80–83, 85
 historic perspective 99
 molecular electronics 92–95
 nanoparticles 83–84
 nonlinear optical devices 85–90
 sensors 90–91
 surface forces 392, 396, 403–404
lanthanum myristate 329
lanthanum palmitate 329
Laplace equations 121, 252, 272, 421, 422
laser light 86–89
latex 8
LB *see* Langmuir–Blodgett
lead myristate 328

- life, origins 50
- Lifshitz theory 390, 392, 425–426
- light scattering
see also goniometry; static light scattering
 CMC determination 242, 247
 droplet microemulsions 349
 dynamic 242, 247, 294–296, 357, 365–369
 micelle size/shape 281, 294–296
 microemulsions 335
 particle size 357–370
 small-angle 357, 362, 364–365
 thin-liquid films 417
- limiting association concentration (LAC) 165
- lindane 178–184
- line tension approach 123–124
- liposomes 45, 49–50
- liquid crystals
 foam stabilization 29–30
 Langmuir–Blodgett films 82, 91
 lyotropic 299–338
 nematic 82, 299–300
 smectics 300, 307, 315
 solids/melts 299–301
 solubilization 166–169, 173
 vesicle bilayers 46–47
- liquid magnets 7
- LOEC *see* lowest observed effect concentration
- low shear viscosity 349–350
- lyotropic liquid crystals 299–338
- MAC *see* maximum additive concentration
- magnetic properties
 colloids 246
 Langmuir–Blodgett films 84
 liquids 7
- Maltese cross textures 308
- Marangoni flow 27–28, 146, 230
- MASIF *see* measurement and analysis of surface interactions and forces
- mass action models 163–164
- mass-weighted distributions 359
- maximum additive concentration (MAC) 163, 166, 170–171
- maximum bubble methods 217, 223, 227–229, 440
- Maxwell model 194–195
- measurement and analysis of surface interactions and forces (MASIF) 384–388, 406
- melts, liquid crystals 299–301
- membranes 46, 49–52, 171–173
- meniscus formation 136–137
- meniscus height 82–83
- meniscus radii 421
- mesh mesophases 302, 305–306, 315–316
- mesomorphism 300, 302
- mesophases
 bicontinuous 302, 303, 306, 310–315, 316–317
 columns 308–310
 cubic 311–314
 gels 307–308
 hexagonal 308–309
 lamellar 307, 308, 316
 lyotropic liquid crystals 299–338
 meshes 302, 305–306, 315–316
 molten 318–319
 morphology 301–321
 polycontinuous 316–317
 ribbons 309–310
 ringing gels 204
 smectics 300, 307, 315
- metals
 clusters 113–114
 foams 41–42
 ion hydrolysis 6–7
 nanoparticles 83–84, 113–114
- micelles
see also critical micelle concentration; rod-like micelles
 antifoaming agents 148
 aqueous solutions 190–192
 cylindrical 193–194, 199
 foam films 427–428
 non-aqueous media 246–248
 reversed 169–171, 174–177, 181–184
 self-assembly 239–241
 self-reproduction 50
 size/shape measurement 281–297
 solubilization 162–169
 stability 148
 structure 162
 vesicle comparison 45
- Michelson optics 264
- microcellular plastic foams 40
- microdomains 173
- microemulsions 55–77
see also emulsions
 antifoaming agents 152–153, 154
 applications 73–74
 bicontinuous 351–352
 characterization 333–356, 364
 definitions 56
 Disorder–Open–Connected–Cylinder model 181
 domain morphology 302, 317–319
 droplet 344–352
 formation 56, 68–70
 interfacial tensions 70, 72–73
 ionic surfactants 64–66
 mesophases 300
 microstructures 70–72, 342–344
 mixed surfactants 63–64, 66–67
 nonionic surfactants 57–64, 66–67
 phase behaviour 57–70, 178, 338–342, 344–345
 relaxation NMR 290
 reversed 9
 scattering techniques 293
 soft surfactant systems 174–181
 solubilization 169–171, 173, 174–185
 stiff surfactant systems 181–185
- microinterferometry 419–420
- microparticle electrophoresis chambers 375
- micropipets 417
- microscopic study 34–35
- microstructures 342–344
- middle mesophases 308–309
- Mie theory 362–365
- mixed films 30
- MLVs *see* multi-lamellar vesicles
- mobility 375–377
- moist wetting 122–123
- molal volume 244

- molecular absorption 243–244
 molecular dimensions 323–332
 molecular electronics 92–95
 molten mesophases 318–319
 monodisperse particles 6
 monolayer-protected clusters (MPC) 113–114
 monolayers 80–82, 99–116, 146, 147
 morphology 301–321
 motorized syringe methods 258
 multi-lamellar vesicles (MLVs) 45–46
- nanoassembly computers 93–95
 nanoparticles 83–84, 113–114
 Navier–Stokes equation 371–372, 374
 NBFs *see* Newton black films
 neat mesophases (smectics) 300, 307, 315
 nematic liquid crystals 82, 299–300
 neutron scattering *see* small-angle neutron scattering
 Newton black films (NBFs) 29, 30, 426, 427
 Newtonian liquids 190, 192–194
 NLO *see* nonlinear optical
 nonaqueous media 67, 246–248
 noninteracting micelles 191–192
 noninteractive adsorption 429
 nonionic surfactants
 microemulsions 57–64, 66–67
 solubilization 166–169
 nonlinear optical (NLO) devices 85–90
 non-Newtonian fluids 19–20
 nonpolar solvents 67, 246–248
 nonpolar surfaces 396–398
 nonwetting surfaces 121
 nuclear magnetic resonance (NMR) spectroscopy
 calibration 283–284
 intermediate mesophases 316
 micelle shape/size 281–290
 microemulsions 334–335, 347, 349
 pulsed gradient spin-echo 282, 284–286, 288–289
 relaxation 281–282, 289–290, 334–335, 347
 self-diffusion 281–289, 302, 334
 nucleation 5–6, 416, 431
 null ellipsometry 443
 number-weighted distributions 359
- o/w see* oil-in-water
 oblate ellipsoids of revolution 322–323
 oblate micelles 286–287
 oil-in-water (o/w) microemulsions 55–74, 177–181, 184–185
 oil-swollen lamellar phases 185
 oils 145, 147, 148–149, 151–154
 oligoethylene oxide surfactants 337–338
 open-cell structures 41
 optical fibre probes 35, 38
 optical storage devices 87
 ordered phases 307–317
 organic monolayers 79–98, 99–116
 origins of life 50
 orthokinetic coagulation 18–19
 oscillating jet method 229–230
 oscillatory force profiles 399–400
- osmometry 244, 247
 osmosis 349, 417
 oversize fraction 359
- palisade layer 162
 paper
 foam breaking 143, 145
 parachute morphology 49
 partial molal volume 244
 partial wetting 121
 particle size 357–370
 particle suspension layer stability 271–272
 particulates 150–152, 153
 Pascalian liquids 190
 patterned self-assembling monolayers 109–113
 PB *see* Poisson–Boltzman theory
 PEGs *see* poly(ethylene glycol)s
 pendant drop method 217, 221–222, 233
 penetration
 capillary 120, 136–140
 surfactant aggregates 166–168
 PEO–PPO–PEO block copolymers 168, 204–205
 peptization 3
 Percus–Yevick approximation 205
 peristaltic forces 426
 Perrin black films *see* Newton black films
 PGSE NMR *see* pulsed gradient spin-echo nuclear magnetic resonance
- pH effects
 electrokinetics 372, 376–377, 380
 fatty acid vesicles 49
 particle mobility 376–377
 zeta potential 380–381
 phase behaviour
 foam stabilization 31
 inversion 61, 338
 microemulsions 57–70, 178, 338–342, 344–345
 separation 40
 transition temperature 46–47, 50–52
 phase prisms 339–342
 phospholipid bilayers 45, 46–47, 49–52
 photochromism 91–92
 photomicroscopy 275–276
 photonic devices 85–90
 plasma polymerization 380–381
 plastics 37–38, 40–41
 plate methods 236–237
 point of zero charge (PZC) 9–10
 Poiseuille approximation 227
 Poisson–Boltzmann (PB) theory 12–13, 202–203, 373–374, 393–396, 424
 polar interactions 129
 polar layer 162
 polar surfaces 394–396, 398–399
 polarization (optical) 86, 367
 polarized attenuated total reflection infrared spectroscopy 101, 102
 polycontinuous mesophases 316–317
 polydimethylsiloxanes 145
 polydispersity 18, 199–202
 polydispersity index 359, 363–364
 polyederschäum, foaming 24–25

- polyelectrolytes 402–404, 429
 poly(ethylene glycol)s (PEGs) 106–107, 381–382
 polymerization
 plasma 380–381
 vesicles 49
 polymers
 foam stabilization 26
 latex dispersions 8
 microemulsion additives 67–68, 69
 patterned self-assembling monolayers 111
 plastic foams 37–38, 40–41, 42
 wetting 126–127
 polyurethane foam 38, 41, 42
 porosity 120, 136–140, 269–277
 porous disc holders 418
 potentiometry 438
 powders 136, 138–140, 269–277
 prebiological phases 50
 precursor films 135
 pressure drop technique 35–36
 pressure effects 62, 68, 69, 246
 pressure methods 217, 223, 227–229, 234–236
 probing aggregation 368–369
 profile axisymmetric drop shape analysis (ADSA-P) *see*
 axisymmetric drop shape analysis
 prolate ellipsoids of revolution 322–323
 prolate micelles 286–287
 proteins 106–109, 401
 protolysis 9–10
 protrusion 397, 427
 pseudo-binary phase diagrams 178–179
 pseudo-emulsions 30–31, 152–154
 pseudo-phase model 163, 173
 pulsed gradient spin-echo nuclear magnetic resonance (PGSE
 NMR) 282, 284–286, 288–289
 puncture defects 319
 PZC *see* point of zero charge
- quasi-equilibrium 400
 Quemada function 349, 351
- radius of gyration 295
 Rayleigh limit 349, 361–362
 Rayleigh–Debye–Gans (RDG) approximation 362, 363, 368
 reaction rates, vesicles 50
 receding contact angles 129–130, 150
 rectangular electrophoresis chambers 377–378
 reflected-light interferometry 419
 reflected-light video microscopy 419
 refractive index 242, 420, 437
 rejection (particle behaviour) 275
 relaxation, NMR 281–282, 289–290, 334–335, 347
 repulsion forces 429
 restricted equilibrium 400
 reversed phases
 micelles 169–171, 174–177, 181–184
 microemulsions 9
- rheology
 colloidal dispersions 19–20
 dilatational 237
 surfactants 189–214
 rheopexy 190, 206
 ribbon phases 309–310
 ring methods 236–237
 ringing gels 204
 robust beer foams 416
 rod-like micelles
 birefringence 195, 206
 domain morphology 304, 306, 308–310
 rheology 193–199
 shear behaviour 206–210
 Ross–Miles pour test 34
 rotor mixers 34, 35
 rough surfaces 129–130
 rupture, films 431
Saccharomyces cerevisiae (yeast) 112
- SALS *see* small-angle light scattering
 salts, microemulsions 62, 64–66, 69
 SAMs *see* self-assembling monolayers
 SANS *see* small-angle neutron scattering
 SAXS *see* small-angle X-ray scattering
 Scheludko cells 418
 Schulze–Hardy rule 17
 SDS *see* sodium dodecyl sulfate
 secondary black films *see* Newton black films
 sedimentation 358, 365
 sedimentation potential 371, 379
 sedimentation volume 269–271, 273
 self-assembling monolayers (SAMs) 99–116
 self-diffusion
 cubic phases 353–355
 droplet microemulsions 350–351
 microemulsions 342–344, 346–347
 NMR 281–289, 302, 334
 sponge phases 352–355
 self-reproduction 50–52
 semiconductors 83–84, 93–95
 sensors, Langmuir–Blodgett films 90–91
 serum replacement method 440–442
 sessile drop methods 217, 221–222, 253–254, 257–258
 SFA *see* surface force apparatus
 shape methods 217, 221–223, 232–234
 shape parameters, mesophases 331, 332
 shear behaviour 205–214, 349–350
 shear moduli 202–204
 shear planes 374–375
 Shinoda-cuts, phase prisms 340
 Siegert relation 295, 365
 silica, colloidal 7–8
 single-lamellar vesicles (SLVs) 45–46
 single-particle counting 358
 single-phase fluids 159
 ‘slip-stick’ patterns 260–261
 SLS *see* static light scattering
 SLVs *see* single-lamellar vesicles
 small-angle light scattering (SALS) 357, 362, 364–365
 small-angle neutron scattering (SANS)
 mesophases 301, 316
 micelles 281, 292–294
 microemulsions 71–72, 335, 347–349, 358
 rheology 205, 206, 211–212

- small-angle X-ray scattering (SAXS)
 mesophases 301, 316
 micelles 281, 292–294
 microemulsions 335, 358
 rheology 211
- 'Smart' surfaces 91–92
- smectics 300, 307, 315
- soaps 440
- sodium bis(2-ethylhexyl) sulfosuccinate (AOT) 65–67, 248, 364, 366–367
- sodium chloride 62, 64–66
- sodium dodecyl sulfate (SDS) 241, 426, 427
- soft surfactant systems 174–181
- sol, definition 4
- solid dispersions
 aggregation processes 15–19
 electrical properties 9–13
 rheology 19–20
 stability 5, 9, 13, 15
 synthesis 4–9
- solidification fronts 274–277
- 'solloids' 397
- solubilization
 antifoaming agents 147–148
 binary solutions 160, 162–173
 definition 159
 Jönsson model 165–166
 limit 345
 micelles 162–165
 organic compounds 246
 soft surfactant systems 174–181
 steric effects 166–169
 stiff surfactant systems 181–184
 ternary systems 173–184
 water-in-oil microemulsions 169–171, 174–177, 181–184
- solutions, spreading behaviour 136
- solvents
 diffusion 288
 exchange model 172
 surface forces 404–407
- space partitioners 316–317
- Sparge tube technique 32–33
- spatial fluctuations 431–432
- specific surface area 360
- spinning drop method 217, 222–223
- spinodal decomposition 416, 431
- sponge phases
 characterization 352–355
 domain morphology 302, 305–306, 316, 317–319
 liquid crystals 300
 phase prisms 340–342
- spontaneous curvature 70–72, 160–161, 169
- SPR *see* surface plasmon resonance
- spreading 124–126, 134–136, 146, 149–150
- spring deflection 385–387
- SSFQ *see* steady-state fluorescence quenching
- stabilization
 common black films 431–433
 foams 25–37
 micelles 148
 thin-liquid films 416–417, 426, 430
- stalagmometers 230–231
- static light scattering (SLS)
 CMC determination 242, 247
 micelle shape/size 294–296
 microemulsions 349
 particle size 357, 360–365, 368–369
- steady-state fluorescence quenching (SSFQ) 281, 290–292
- steric effects
 forces 397, 405, 424, 426–427
 solubilization 166–169
- 'sticky' contacts 208, 210
- stiff surfactant systems 181–185
- Stokes–Einstein equation 230–231, 347, 366
- stratification 29, 30
- streaming potential 371–372, 379
- stretching (antifoaming agents) 146, 149
- strontium myristate 325
- structural inversion 342–344
- structural viscous liquids 190
see also shear behaviour
- sugars 171–172
- supercritical fluids 68
- superlattices 83
- superspreaders 149–150
- suprafluid liquids 190
- supramolecular forces 427–430
- supramolecular structuring 424
- surface charge
 electrokinetics 371–382
- surface force apparatus (SFA) 384–385, 390–391, 415, 428
- surface plasmon resonance (SPR) 102, 103
- surface tension
 CMC determination 241–242
 component approach 128–129
 contaminant detection 163
 definition 121
 dynamic 225–238
 equilibrium 217–224
 film flotation 269
 gradients 150
 measurement 217–224, 225–238, 438–442
 sedimentation volume 273
 solidification fronts 274–277
 wetting 126–127
- surfaces
see also surface charge; surface tension
 conduction 11–13
 depletion 429
 genus concept 304–306, 314
 geometry 387–388
 separation measurement 385–387
 surface–surface interactions 383–414
 viscosity 27, 147
- surfactant films 336, 354
- surfactant monolayer model 173
- surfactants
see also zwitterionic surfactants
 adsorption 436–444
 anionic 147
 antifoaming agents 147, 149
 aqueous solutions 190–191
 commercial 63–64

- concentration measurement 436–444
 cosurfactants 63, 64, 65–66
 emulsions 55
 ionic 64–66
 microemulsions 55–74
 nonionic 57–64, 66–67, 166–169
 rheology 189–214
 shear behaviour 205–214
 solubilization 159–186
 structure 245
 surface forces 397–404
 thin-liquid films 415–417
 vesicles 45, 48
 suspension layer stability 271–272
 suspensions
 definition 4
 swelling
 domain morphology 319–321, 323
 exponents 331
 surfactant aggregates 166–168
 syneresis 3
 synergistic effects 151–152, 429

 Tanford's formulae 303
 Tanner's law 134
 temperature effects
 contact angle 269, 276–277
 critical micelle concentration 246
 liquid crystals 300
 microemulsions 60–70, 71–72
 nuclear magnetic resonance 284
 vesicle phase transition 46–47, 50–52
 tensiometry 217–224, 225–238
 ternary systems 160–161, 173–185
 TFB *see* thin-film balance
 thermodynamics
 microemulsions 56
 vesicles 48–49
 wetting 120, 121–134
 thermoplastic foams 40
 thermotropic liquid crystals 300
 thin-film balance (TFB) method 36, 39, 417–424
 thin-liquid films 415–430, 431–433
 thixotropy 190
 three-phase contact lines 259–260, 265–266
 time-resolved fluorescence quenching (TRFQ) 281, 290–292
 titration, soaps 440
 topology 301, 314, 316–321
 transition (particle behaviour) 275–276
 transverse diffusion (flip-flop) 47, 50
 TRFQ *see* time-resolved fluorescence quenching
 Triton X-*n* solutions 228
 turbulent flow 18–19

 ultracentrifugation 367
 ultrasound 155–156, 244
 ultraviolet (UV) spectroscopy 437–438
 undersize fractions 359
 undulation forces 426

 unilamellar vesicles *see* single-lamellar vesicles

 van der Waals interactions
 colloidal dispersions 13–15, 16–17
 measurement 392
 sedimentation 269, 272
 thin-liquid films 424
 wetting thermodynamics 127, 128
 vapour phase methods 9
 vapour pressure osmometry 244, 247
 vesicles
 antifoaming agents 149–150
 autopoiesis 50–52
 bilayer solubilization 171–173
 fatty acids 49–50
 formation 47–49
 phase structure/transition 46–47
 polymerization 49
 rheology 200–204, 211–213
 viscoelasticity
 measurement 388–389
 rheology 190, 193–198
 viscosity
 antifoaming agents 147
 CMC determination 244
 colloidal dispersions 19–20
 dilatational 235
 foam stabilization 26, 27
 microemulsions 335
 rheology 192–199
 shear behaviour 206–207, 211
 visible spectroscopy 437–438
 volatility of liquids 122–123
 volume fraction 345–346, 349–350

 w/o *see* water-in-oil
 Washburn equation 138–139, 272
 water
 see also aqueous systems
 solubilization 169–171
 water-in-oil (w/o) microemulsions 169–171, 174–177, 181–184
 waveguide format 88, 89
 Weaver–Bertucci equation 143–144
 wedge model 180–181
 wetting 119–142
 capillary penetration 136–140
 imperfect solid surfaces 129–134
 Langmuir–Blodgett films 82–83, 91–92
 porous surfaces 138–140
 solid surfaces 126–129
 spreading 124–126, 134–136
 tension 126
 thermodynamics 120, 121–134
 thin-liquid films 431
 wicking 120, 132
 Wilhelmy plate method 217–218, 219–220, 267–269
 Winsor equilibria, emulsification failure 161, 178, 351–352

 X-ray photoelectron spectroscopy (XPS) 105–106

X-ray reflectivity 427

X-ray scattering *see* small-angle X-ray scattering

XPS *see* X-ray photoelectron spectroscopy

yeast (*Saccharomyces cerevisiae*) 112

Young equation

background 120, 133–134, 252

modification 122–131

porous solids 74, 138–139

Young–Laplace equation 219, 222–223

zeta potential

electrokinetics 374, 380–381

Zimm plots 295

zirconium myristate 327

zwitterionic surfactants

critical micelle concentration 245

rheology 196–199, 201–202, 208–210, 213

Cumulative Index

- α -crystalline phase V1 477
 α -olefinesulfonates V1 276–277
 α -sulfo fatty acid methylesters V1 277–278
ab initio polymerizations V1 194–195
absorbency V1 138–139, V1 154–158, V1 159–162
absorption, molecular V2 243–244
acetals V1 391–393
acid fracturing V1 263
acid–base interactions V1 233
ACRPAC *see* analysis of capillary rise profile around a cylinder
additives, phase behaviour V1 497–502
adhering bubble methods V2 253–254
adhesion V1 157–158, V1 334–336, V2 125–126, V2 389–390
adjuvants V1 341–342
ADSA *see* axisymmetric drop shape analysis
adsorbable organic halogen (AOX)-containing substances V1 284
adsorption
 adsorbed films V1 252, V1 253
 adsorber dyes V1 101–103
 adsorption isotherms V1 167–168, V1 379–380
 competitive V1 105–107
 detergency V1 58–61
 electrokinetics V2 371
 experimental techniques V1 237, V1 381
 measurement V2 435–444
 paper manufacture V1 132–136
 polymeric surfactants V1 377–384
 sensitizing dyes V1 98
 surfactants V1 232–238, V1 240–241
 thin-liquid films V2 416
advancing contact angles V2 129–130
AEEA *see* aminoethylethanolamine
aerobic batch tests V1 516–517
Aerosol OT *see* sodium bis(2-ethylhexyl)sulfosuccinate
aerosols V1 15, V2 9
AFM *see* atomic force microscopy
ageing effects V2 154–155
agglomeration V1 79, V1 114, V1 206–208, V1 239
aggregate, roads V1 334
aggregation V1 79, V1 186, V1 188, V1 445–447, V2 15–19
 see also coagulation; coalescence; flocculation
agriculture V1 73–83, V1 341–342
agrochemicals V1 80–83
AKD *see* alkyl ketene dimer
alcohol ethoxylates V1 301–302
alcohols
 bilayer solubilization V2 172
 foaming V2 24
 microemulsions V2 63, V2 64–66, V2 69
 nonionic hydrophobes V1 294–296
algicides V1 318–321
alkane sulfonates V1 282–285
alkane thiols V2 99–116
alkanolamides V1 306–307
alkenyl succinic anhydride (ASA) V1 141, V1 143–144
alkyd emulsions V1 113, V1 402–403
alkyl chain length V1 484–488
alkyl ketene dimer (AKD) V1 141, V1 142–144, V1 158
alkyl *N*-methylglucamides V1 305
alkyl quaternary ammonium salts V1 311–312, V1 314, V1 315–316, V1 318, V1 329–330
alkylamines V1 328
alkylbenzene sulfonates V1 278–282
alkyldimethylaminioxides (DMAOs) V2 196–199, V2 201–202, V2 208–210, V2 213
alkylene oxides V1 296
alkylether carboxylates V1 275–276
alkylether sulfates V1 275, V1 524–525
alkylglucosides V1 392–393
alkylphenol ethoxylates (APEOs) V1 302–303, V1 528–529
alkylphenols V1 296
alkylpolyglucosides V1 409
alkylpolyglycosides (APGs) V1 304, V1 529
alkylsulfates V1 273–275, V1 524–525
AMBER force field V1 539–540, V1 541, V1 545
amidopropylamines V1 327
amine ethoxylates V1 307
amine oxides V1 305–306, V1 324, V1 325–327
amines V1 297
amino acids V2 175–177
aminoethylethanolamine (AEEA) V1 356–359
Amonton friction V2 391
amorphous dispersions V1 91
amphipathic structure V1 232–233, V1 376
amphiphiles
 see also hydrophobes; surfactants
 domain morphology V2 303–304, V2 306
 drugs V1 4, V1 7
 Langmuir–Blodgett films V2 80–81
 liquid crystals V2 300
 microemulsions V2 57–58
amphitropic mesophases V1 496
amphoacetates V1 349–350, V1 356–359
amphoteric surfactants V1 294, V1 323, V1 349–350, V1 351, V1 355–372, V1 532–534
 see also zwitterionic surfactants
anaerobic testing V1 515, V1 517

- analysis of capillary rise profile around a cylinder (ACRPAC) V2 268
- anchoring V1 140, V1 205, V1 374, V1 377–378, V1 383
- anion-active sequestrants V1 291
- anionic surfactants V1 271–292, V1 520–525, V2 147
- antifoamers V1 71, V1 263, V2 143–157
- antipercolation threshold V2 181–182
- antisetling agents V1 79–80
- antistat layers V1 86–87
- antithixotropy V1 209
- AOT *see* sodium bis(2-ethylhexyl) sulfosuccinate
- AOX *see* adsorbable organic halogen-containing substances
- APEOs *see* alkylphenol ethoxylates
- APGs *see* alkylpolyglycosides
- aquatic toxicity V1 518–519, V1 524–525, V1 529, V1 531–532, V1 534
- aqueous dispersions V1 39
- aqueous injection moulding V1 216
- aqueous polymer solutions V2 400–402
- aqueous systems V2 143–156, V2 190–199
- ASA *see* alkenyl succinic anhydride
- asphalt *see* bitumen
- asphaltic emulsions V1 265
- assessment criteria V1 514–520
- associative phase separation V1 453, V1 456–458
- associative thickeners V1 105–107, V1 449
- atomic force microscopy (AFM)
- dispersions V1 242
 - latices V1 109–110
 - paper V1 127, V1 149, V1 165, V1 166
 - surface forces V2 384–388, V2 390–391, V2 395, V2 397, V2 399–400
 - surfactant migration V1 398
 - thin-liquid films V2 415
- attenuated total reflection (ATR) spectroscopy V2 101, V2 102
- autophobicity V1 142
- autopoiesis V2 50–52
- autoxidation V1 398–399
- axisymmetric drop shape analysis (ADSA) V2 253–254, V2 255–263, V2 264, V2 265–266
- azobenzene chromophore V2 91
- back-scatter technique V2 37, V2 39
- bactericides V1 318–321
- barrier coatings V1 152–154
- batch polymerizations V1 194–195
- batch tests V1 516–517
- Bendtsen test V1 165
- Berthelot's (geometric mean) combining rule V2 127
- BET *see* Brunauer–Emmett–Teller
- betaines V1 349–355, V1 363–364, V1 396–397, V1 533
- BiAS *see* Bismuth active substances
- bicontinuous phases
- aggregates V1 473, V1 475, V1 477–478
 - characterization V2 352
 - domain morphology V2 302, V2 303, V2 306, V2 310–315, V2 316–317
 - liquid crystals V1 473, V1 475, V1 477–478, V1 482
 - mesophases V2 302, V2 303, V2 306, V2 310–315, V2 316–321
 - microemulsions V1 460–462, V1 482, V2 351–352
 - phase prisms V2 340–342
- ringing gels V1 353, V2 204
- Bikerman test V2 32–33
- bilayers V2 149–150, V2 171–173, V2 199–204, V2 211–212
- see also* membranes, vesicles
- binary solutions V2 160, V2 162–173
- binary surfactant–water systems V2 166–169
- binder burnout V1 216–217
- binder–emulsion preparation V1 107–110
- binders V1 111–113, V1 116, V1 149
- Bingham solids V1 208–209, V2 190, V2 204
- bio-surfactants V1 521
- bioaccumulation V1 515, V1 520
- bioadhesion V1 14
- bioavailability V1 8–9
- biocides V1 318–321, V1 333–334, V1 360
- biodegradability
- amphoteric surfactants V1 532–534
 - anionic surfactants V1 279, V1 521–524
 - cationic surfactants V1 531
 - cleavable surfactants V1 391, V1 394, V1 395
 - drug delivery systems V1 26–30
 - legislation V1 512–513
 - nonionic surfactants V1 527–529
 - surfactants V1 509–510, V1 515–517
- biologically active molecules V2 106–109, V2 111–113
- biomagnification V1 515, V1 520
- biostatic activity V1 319–320
- birefringence V2 195, V2 206
- bis-surfactants *see* Gemini surfactants
- bismuth active substances (BiAS) V1 513, V1 527
- bitumen V1 265, V1 334–337
- black films V2 28–29, V2 30, V2 426, V2 427, V2 431–433
- bleaching V1 125
- block copolymers
- adsorption V1 374, V1 377–384
 - drug delivery V1 8, V1 11, V1 13, V1 15–16, V1 21–25
 - nonionic surfactants V1 303–304, V1 491–493
 - rheology V2 204–205
- blood substitute formulations V1 9
- blooming V1 116
- blue laser diodes V2 87–89
- Boltzmann distribution law V2 4
- Boltzmann equation V2 373
- boundary conditions V1 227, V1 540
- Bragg diffraction V2 301
- Bragg reflections V2 330
- Bragg–William approximations V1 378
- brewing industry V2 155–156
- Brewster-angle microscopy V1 538
- bridging
- antifoaming agents V2 146, V2 149, V2 151
 - ceramics V2 430
 - flocculation V1 136–137, V1 205
 - measurement V2 402, V2 405
- brightening V1 125
- Bristow wheel V1 160
- Brønsted acidity V1 231–232
- Brownian motion V2 3, V2 13, V2 16, V2 20, V2 365
- Brunauer–Emmett–Teller (BET) isotherm V1 167–168, V2 436
- bubble formation V1 255, V1 274, V2 418
- see also* foams

- bubble methods
 contact angle **V2** 253–254
 dynamic surface tension **V2** 227–229, **V2** 232–236
 equilibrium surface tension **V2** 217, **V2** 221–223, **V2** 235
 builders **V1** 54, **V1** 61, **V1** 65, **V1** 288
- CAC *see* critical association concentration
 cadmium arachidate **V2** 82
 calcium, detergency **V1** 61–65
 calcium carbonate **V1** 147
 calcium myristate **V2** 327
 cancer therapy **V1** 9–10
 capillary phenomena
 condensation **V1** 161–162, **V2** 390
 contact angle measurement **V2** 252, **V2** 264–266, **V2** 268, **V2** 272–274
 dynamics **V1** 159–160
 penetration **V2** 120, **V2** 136–140
 pressures **V2** 421–423, **V2** 431
 rise **V2** 217, **V2** 218–219
 carbohydrates **V1** 300–301, **V2** 17–19
 carboxybetaines **V1** 350–354
 carrier effect **V1** 64
 Cassie–Baxter equation **V2** 132
 casting **V1** 203, **V1** 212–213, **V1** 215–216
 cathetometers **V2** 265
 cationic surfactants **V1** 309–348, **V1** 460, **V1** 529–532
 CBFs *see* common black films
 cell attachment **V2** 107, **V2** 111–113
 cell opening **V2** 41
 cell-surface interactions **V2** 17–18
 cellular foams **V2** 37
 cement foams **V2** 42
 centrifugal casting **V1** 212
 centrifugation **V2** 358, **V2** 365, **V2** 367, **V2** 417
 ceramics **V1** 201–218
 chain length **V1** 297, **V1** 302, **V2** 245, **V2** 248
 chain lubricants *see* conveyor lubricants
 chain scission **V1** 217
 chain–chain interactions **V1** 236
 champagne foams **V2** 416
 channel defects **V2** 319
 charge regulated surfaces **V1** 227–228
 charge-stabilized particles **V1** 136–137
 CHARMM force fields **V1** 545
 chelating agents **V1** 332
 chemical flooding **V1** 259–262
 chemical interactions **V1** 236
 chemical pulping **V1** 125
 chemically heterogeneous dispersions **V1** 40–42
 chemically homogeneous dispersions **V1** 40
 chemisorption **V1** 248, **V2** 100–101
 chiral mesophases **V2** 316
 chirality **V2** 50–51
 cholesterics **V2** 299–300
 chromatographic retention **V2** 442–443
 clathrate hydrates **V1** 468
 clays **V2** 3, **V2** 8–9
 clean-up, oil spills **V1** 264
 cleansing *see* detergency
 cleavable surfactants **V1** 291, **V1** 390–397
 clouding
 cloud point defoamers **V2** 148
 curvature **V2** 338
 detergency **V1** 69
 hydrotropes **V1** 321–322, **V1** 414, **V1** 415
 liquid crystals **V1** 480–481
 nonionic surfactants **V1** 485–488
 oxyethylene surfactants **V1** 442
 surfactant–polymer systems **V1** 454–456, **V1** 463
 CMC *see* critical micelle concentration
 coagulation **V2** 15–19
 coalescence **V1** 106
 coatings **V1** 29–30, **V1** 146–154
 cobblestone model **V2** 383, **V2** 391
 cobinders **V1** 148–149
 cobuilders **V1** 64–65
 cohesion **V2** 125–126
 cohesion energy **V2** 269–270
 cold isostatic pressing **V1** 214
 collective diffusion **V2** 346–347, **V2** 350–351
 collectors, flotation **V1** 246–249
 colloidal processing **V1** 203
 colloidal silver **V1** 91, **V1** 92
 columnar mesophases **V2** 308–310
 see also rod-like micelles
 command surfaces **V2** 91–92
 commercial processes *see* manufacture
 commercial surfactants **V1** 484, **V1** 492, **V2** 63–64
 comminution **V1** 180–184, **V1** 190–191, **V1** 193, **V2** 4–5
 common black films (CBFs) **V2** 427, **V2** 431–433
 compaction of DNA **V1** 460
 competing microstructures **V2** 336–337
 competitive adsorption **V1** 105–107, **V1** 109, **V2** 429
 complexation **V1** 61–65, **V1** 96
 composite surfaces **V2** 131–132
 compressible fluids **V2** 68
 compression rheology **V1** 211–212
 computer simulation **V1** 537–550
 computers **V2** 89–90, **V2** 92–95
 concentration effects **V1** 435–437, **V2** 287–288, **V2** 347, **V2** 380
 concentration profiles **V1** 542, **V1** 544
 concrete foams **V2** 42
 condensation **V1** 184–185, **V1** 190–191, **V2** 4, **V2** 5–6
 condensed phases **V2** 189–190
 conditioning **V1** 327–328
 conductivity **V1** 87, **V2** 213, **V2** 242, **V2** 335, **V2** 438
 conformation **V1** 377–381, **V1** 543, **V1** 545
 consolidation **V1** 41, **V1** 124–125, **V1** 212–216, **V1** 239, **V1** 240
 constant charge surfaces **V1** 227
 constant potential surfaces **V1** 227
 consulate point **V1** 488
 contact angles
 see also Young equation
 crude oil **V1** 254, **V1** 255
 definitions **V2** 133–134
 hysteresis **V2** 129, **V2** 130–133
 measurement **V2** 251–280
 particle/water interface **V2** 150
 temperature dependence **V2** 269, **V2** 276–277
 thin-liquid films **V2** 422
 wetting **V2** 119–140
 contamination, films **V2** 423
 conveyor lubricants **V1** 332–334
 cooperative binding **V1** 447, **V1** 451–452

- copolymers
 adhesion **V1 86**
 adsorption **V1 374, V1 377–384**
 drug delivery **V1 8, V1 11, V1 13, V1 15–16, V1 21–25**
 nonionic surfactants **V1 303–304, V1 491–493**
 pigment dispersion **V1 119**
 rheology **V2 204–205**
 copper myristate **V2 326**
 corrosion inhibition **V1 263–264, V1 288, V1 307, V1 340**
 cosmetics **V1 327–328, V1 368–369, V1 511**
 cosolutes **V1 425–427, V1 435, V1 438, V1 442, V1 448**
 cosurfactants **V1 497–498, V2 63, V2 64, V2 65–66**
 Couette flow technique **V1 183**
 Coulombic forces **V1 540**
 Coulombic wells **V2 430**
 counterions **V1 274, V1 431, V1 468–469, V2 246**
 coupled units tests **V1 527–528**
 coupler dispersions **V1 99–101**
 coupling agents **V1 409, V1 412–414**
 Cox–Merz rule **V2 211**
 CPP *see* critical packing parameter
 cracking process **V1 265–266**
 cratering, paints **V1 121**
 creaming, emulsions **V1 186**
 critical association concentration (CAC) **V1 446–447, V1 452, V1 456**
 critical micelle concentration (CMC)
 see also micelles
 amphoterics **V1 362–363**
 competitive adsorption **V1 106–107**
 detergency **V1 55–56**
 foams **V2 25–26, V2 28, V2 29**
 Gemini surfactants **V1 388–389, V1 390**
 influencing factors **V2 241, V2 245–246**
 measurement **V2 239–249**
 micellization **V1 253, V1 467–472, V2 190–191**
 non-aqueous media **V2 246–248**
 self-diffusion NMR **V2 286**
 surface forces **V2 398–399**
 surface tension **V2 438–439**
 surfactant–polymer systems **V1 446–447**
 surfactants **V1 237, V1 388–390, V1 422–427, V2 162–166**
 critical packing parameter (CPP) **V1 45, V1 422, V1 432–433**
 critical solution temperature **V1 189–190**
 critical surface tension **V1 120–121, V2 126–127**
 Cross equation **V1 209**
 ‘cross-talk’ **V1 87, V1 92**
 crude oil **V1 252, V1 254, V1 255, V1 265–266**
 cryo-transmission electron microscopy (Cryo-TEM) **V2 193, V2 196, V2 198, V2 335, V2 358**
 cryoporometry **V1 169–170**
 crystal growth **V1 79**
 see also Ostwald ripening
 crystallization **V1 416–417**
 cubic phases
 domain morphology **V2 311–314**
 drug delivery **V1 12, V1 20**
 multicomponent systems **V1 492, V1 494, V1 498–499**
 phase behaviour **V1 481**
 rheology **V2 204–205**
 self-diffusion **V2 353–355**
 structure **V1 472, V1 473–475**
 thermotropic behaviour **V2 209**
 cumulant analysis **V2 366**
 curtain coating **V1 88**
 curvature **V2 70–72, V2 160–161, V2 169, V2 301–321, V2 336–338, V2 345**
 cyclic acetals **V1 391–392**
 cyclodextrin solutions **V1 16–17**
 cylindrical electrophoresis chambers **V2 376–377**
 cylindrical micelles **V2 193–194, V2 199**

 Darcy’s law **V1 152**
 data processing **V2 89–90, V2 92–95**
 DDAB *see* didodecyldimethylammonium bromide
 de-wetting **V2 146, V2 149**
 deagglomeration **V1 206–208**
 Debye screening length **V2 393–395**
 Debye–Hückel equation **V1 131, V2 424**
 DEEDMAC *see* diethylester dimethylammonium chloride
 defects **V1 202, V2 317–319**
 defoamers **V1 263, V2 143, V2 154–155**
 see also antifoamers; foam breaking
 deformation **V1 146, V2 388**
 degradation products **V1 515**
 denaturation temperature **V1 46**
 density fluctuations **V2 431, V2 432–433**
 deoxyribonucleic acid (DNA) **V1 12–13, V1 460, V2 84, V2 85**
 depletion method **V2 436**
 DEQs *see* diesterquaternaries
 Derjaguin–Muller–Toporov (DMT) theory **V2 389, V2 391**
 destabilization **V1 40–42**
 detergency **V1 53–72**
 alkyl sulfates **V1 274**
 amphoterics **V1 365, V1 366–367**
 anionic surfactants **V1 279–282**
 betaines **V1 350**
 cationic surfactants **V1 310, V1 314–318, V1 321–327**
 cleavable surfactants **V1 395**
 environmental issues **V1 511, V1 513, V1 521**
 fabric softeners **V1 314–318**
 hydrotropes **V1 415–416**
 mesophases **V1 503**
 nonionic surfactants **V1 302, V1 303, V1 305**
 sulfosuccinates **V1 289**
 deuterium labelling **V2 289–290**
 developer scavengers **V1 87–88**
 dewatering **V1 152**
 di-tallow dimethylammonium chloride (DTDMAC) **V1 530–532**
 di-tallow imidazolinester (DTIE) **V1 530–532**
 dialkyldimethyl quaternary ammonium salts **V1 311–312, V1 314, V1 315, V1 318**
 diameter axisymmetric drop shape analysis (ADSA-D) *see* axisymmetric drop shape analysis
 didodecyldimethylammonium bromide (DDAB) **V2 181–184**
 dielectric relaxation **V2 11**
 diesterquaternaries (DEQs) **V1 530–532**
 diethylene triamine quaternary ammonium salts **V1 315–316**
 diethylester dimethylammonium chloride (DEEDMAC) **V1 530–532**
 differential scanning calorimetry (DSC) **V1 170**

- diffusion coefficient V2 244
dilation V2 190, V2 206, V2 235, V2 237
dimensional analysis V2 274
dimeric surfactants *see* Gemini surfactants
1,2-dimyristoyl-*syn*-glycero-3-phosphatidylcholine (DMPC)
V2 50, V2 51–52
direct casting V1 215–216
direct coagulation casting V1 215
direct flotation V1 345
disc-nematic phases V1 489
Discovery space shuttle V2 236
disinfection V1 318–319, V1 368
disjoining pressure V2 417, V2 424–430, V2 431
Disorder–Open–Connected–Cylinder (DOC) model V2
181, V2 182–184
dispersants V1 116–119, V1 147–148, V1 288, V1 291
dispersions
absorber dyes V1 101–102
agriculture V1 79
aqueous V1 39
ceramics V1 206–208
chemically heterogeneous V1 40–42
chemically homogeneous V1 40
coupler V1 99–101
drug delivery V1 8–15
emulsions V1 99–100, V2 55–56
methodology V2 4–5
mixed micellization V1 100
monolayer-protected metal clusters V2 113–114
nanocrystalline V1 100–101
natural systems V1 175–176
oil-continuous V1 39
paint pigments V1 113–119
particle processing V1 238–243
photography V1 91–92
solid V2 3–20
solubilization V2 159
stabilization V1 381–384
thin-liquid films V2 416, V2 425–426
disproportionation V1 41
dissipative particle dynamics (DPD) simulation method V1
537, V1 546–547, V1 548
dissociation V1 221
distillation V1 416
disulfine blue active substances (DSBAS) V1 513
DLS *see* dynamic light scattering
DLVO theory V1 130–132, V2 13–15, V2 17, V2 29
DMAOs *see* alkyldimethylaminioxides
DMPC *see* 1,2-dimyristoyl-*syn*-glycero-3-phosphatidylcholine
DMT *see* Derjaguin–Muller–Toporov theory
DNA *see* deoxyribonucleic acid
DOC *see* Disorder–Open–Connected–Cylinder model
DODAB surfactant V2 48, V2 49
dodecyl-1,3-propylenebis(ammonium chloride) (DoPDAC)
V1 495
domain morphology V2 301–321
DoPDAC *see* dodecyl-1,3-propylenebis(ammonium chloride)
double-chain surfactants V2 160
see also lipids
double-layers V2 11–14
DPD *see* dissipative particle dynamics
drag reduction V2 210
drained casting V1 212–213
drilling mud V1 259
drop methods
contact angle V2 253–254, V2 255–263, V2 264
dynamic surface tension V2 230–236
equilibrium surface tension V2 217, V2 220–223, V2 235
droplet microemulsions V2 344–352
droplet sedimentation V2 271–272
droplet size
agrochemical sprays V1 80–83
comminution V1 181–183
monomer emulsions V1 191
Ostwald ripening V1 186–187
polymerization techniques V1 195–198
surfactant role V1 111–113
drugs (pharmaceutical) V1 3–6, V1 8–23
dry pressing V1 214
dry strength, paper V1 145
dry wetting V2 122–123
drying, ceramics V1 216–217
DSBAS *see* disulfine blue active substances
DSC *see* differential scanning calorimetry
DTDMAC *see* di-tallow dimethylammonium chloride
DTIE *see* di-tallow imidazoliner
Du Noüy ring method V2 217, V2 220
Dupré equation V2 125–126
dye micellization V2 243
dye solubilization V2 242–243, V2 247–248
dynamic light scattering (DLS) V2 242, V2 247, V2
294–296, V2 357, V2 365–369
dynamic surface forces V2 388–389
dynamic surface tension V2 218, V2 225–238, V2 439–440
dynamic swelling V1 185, V1 191
EC₅₀ tests V1 518–519, V1 524–525, V1 530, V1 532
eddy currents V2 284–285
edge penetration V1 161
EDTA *see* ethylenediaminetetraacetic acid
EEC *see* European Economic Community Directives
EFF *see* emulsion ferrofluid techniques
EHEC *see* ethyl(hydroxyethyl)cellulose
Einstein relationship V2 350
elastic interaction V1 382–383
elasticity V2 206
electrical behaviour
colloidal dispersions V2 9–13
conductivity V1 233–236, V2 213, V2 242, V2 335, V2
438
dispersion V2 5
electrical double-layer V1 222–223, V2 373–374
see also zeta potential
electroacoustic sonic amplitude (ESA) V1 102–103, V2 379
electrokinetic potential *see* zeta potential
electrokinetics V1 102–103, V2 371–382
see also electroosmosis; electrophoresis; sedimentation
potential; streaming potential
electrolytes
antifoaming agents V2 154
critical micelle concentration V2 246
detergency V1 59, V1 60, V1 72
electrostatic double-layers V2 393–397
foaming V1 72
micellization V1 425–427
phase behaviour V1 500–501

- electrolytes (*Continued*)
 surface charge V1 221–222
 surfactant–polymer systems V1 454–460
- electron microscopy (EM) V2 335–336
- electron spectroscopy for chemical analysis (ESCA) V1 51,
 V1 109, V1 111–113, V1 162–163, V1 397
- electronic properties V1 87, V2 83–84, V2 92–95
- electrooptics V2 89–90
- electroosmosis V1 225, V2 371–372, V2 375–379
- electrophoresis V1 97, V1 102–103, V1 224, V1 336, V2
 371–372, V2 375–379
- electrophoretic deposition (EPD) V1 213–214
- electrostatics
 air V1 50
 colloidal dispersions V2 13–15
 double-layers V1 204–205, V2 424–425
 liquids V1 42
 patch aggregation V1 136, V1 137
 responsive systems V1 25–26
 solubilization V2 165, V2 185
 stabilization V1 108
 surface charge V1 226–229
 surfactant–polymer systems V1 448
- electrosteric stabilization V1 206
- ellipsoids of revolution V2 322–323
- ellipsometry V2 443–444
- elongational rheology V1 153
- EM *see* electron microscopy
- emulsifiable concentrates V1 73, V1 74–76
- emulsification
 comminution V1 179, V1 180–184
 condensation V1 179, V1 184–185
 emulsifiers V1 179–180
 failure V2 339, V2 344, V2 351–352
 foodstuffs V1 42, V1 45, V1 47
 paints V1 105, V1 107–110
 photography V1 91, V1 99–100
 photolability V1 397
 spontaneous V1 185
- emulsion concentrates V1 76–78
- emulsion ferrofluid (EFF) techniques V2 417
- emulsion films V2 30–31
- emulsion polymerization V1 107–110, V1 175–200, V1
 288, V1 290–291, V1 400–402
- emulsions
see also emulsification; microemulsions
 alkyd V1 113
 antifoaming agents V2 152–154
 bitumen V1 335–336
 characterization V2 55–56
 definition V2 4
 drug delivery V1 8–9
 foodstuffs V1 40–41
 formation V2 74
 miniemulsions V1 176, V1 177, V1 195–196
 monomer V1 191–196
 multiple V1 73
 nanoemulsions V1 77
 petroleum industry V1 256–259, V1 262, V1 263
 photography V1 85–86, V1 87–89
 radical polymerization V1 196–198
 separation V1 265–266
 spontaneous V1 74–76
 stability V1 186–190
 suspoemulsions V1 73
 thin-liquid films V2 417
- encapsulation V1 28, V1 418
see also microencapsulation
- end-functionalization V2 105–109
- engulfment (particle behaviour) V2 275
- enhanced oil recovery (EOR) V1 259, V1 262–263
- entropic interactions V1 382–383, V2 426–427
- environmental issues
see also biodegradability
 amphoteric surfactants V1 364, V1 365, V1 532–534
 analytical techniques V1 513–514
 anionic surfactants V1 279–280, V1 284, V1 520–525
 aquatic toxicity V1 524–525, V1 529, V1 531–532, V1
 534
 assessment criteria V1 514–520
 cationic surfactants V1 321, V1 332, V1 340, V1
 529–532
 ethoxylated surfactants V1 107, V1 117
 eutrophication V1 61, V1 116
 industry V1 510–512
 legislation V1 512–513
 nonionic surfactants V1 303, V1 305, V1 525–529
 oil industry V1 264–265, V1 340
 risk assessment V1 534–535
 softening agents V1 332
 zwitterionic surfactants V1 364, V1 365
- EON *see* equivalent ethoxy number
- EOR *see* enhanced oil recovery
- EPD *see* electrophoretic deposition
- equation of state V2 127–128, V2 252–253, V2 270, V2
 274
- equilibrium contact angles V2 129–130
- equilibrium films V2 28–29
- equilibrium phases V2 56
- equilibrium surface tension V2 217–224
- equivalence points V1 96–97
- equivalent ethoxy number (EON) V2 161
- ESA *see* electroacoustic sonic amplitude
- ESCA *see* electron spectroscopy for chemical analysis
- ester quaternary ammonium salts V1 316–317, V1
 329–330, V1 395–397
- ether oils V2 67
- ethoxylated alcohols V2 55–63, V2 69–70, V2 71–73
- ethoxylated amines V1 327, V1 328–329
- ethoxylated quaternary ammonium salts V1 329–330
- ethoxylated surfactants V1 107
- ethoxymer distribution V1 299–300, V1 302
- ethylene oxide V1 298–300, V1 303–304
- ethylenediaminetetraacetic acid (EDTA) V1 332
- ethyl(hydroxyethyl)cellulose (EHEC) V2 401–402
- Euclidean solids V2 190
- European Economic Community (EEC) Directives V1
 512–513
- European Working Group (EWG) V1 512–513
- eutrophication V1 61, V1 116
- EWG *see* European Working Group
- excess solubilization V2 178–180
- extenders V1 114
- extraction V1 416
- extrusion coating V1 88
- extrusion molding V1 214

- fabric softeners **V1** 314–318
 fatty acids **V1** 277–278, **V1** 352–353, **V2** 49–52, **V2** 82
 fatty alcohols **V1** 273, **V1** 275
 fatty amines **V1** 318
 fatty nitriles **V1** 311
 Feldspar, flotation **V1** 346
 ferromagnetic colloids **V2** 7
 fibre collapse point **V1** 129
 fibre lignin content **V1** 125–127
 fibre properties, paper **V1** 125–128, **V1** 129
 Fick's law **V2** 16, **V2** 17
 fillers, paper **V1** 129
 films
 see also foams
 film pressure concept **V2** 122–123
 film-dimpling **V2** 423
 flotation **V2** 269
 morphology **V1** 109–110
 stratification **V2** 427
 thin-liquid **V2** 415–433
 wetting **V2** 122–123
 filter dyes **V1** 101–103
 first-effect concentrations **V1** 526
 fish-cuts, phase prisms **V2** 340
 fixation, emulsions **V1** 196–198
 flexibility **V1** 438
 flexible surface model **V2** 336
 flip-flop (transverse diffusion) **V2** 47, **V2** 50
 flocculation
 ceramics **V1** 205, **V1** 209–211, **V1** 213
 colloidal dispersions **V2** 15–16
 definition **V2** 15–16
 emulsion concentrates **V1** 76, **V1** 77
 foodstuffs **V1** 43, **V1** 44
 nanoparticles **V1** 135
 paper **V1** 129–130, **V1** 135–138, **V1** 141–142, **V1** 151
 pigment dispersion **V1** 114
 polymeric surfactants **V1** 381–382, **V1** 383
 selective **V1** 243–245
 Flory–Huggins theory **V1** 229–230, **V1** 374–375
 Flory–Krigbaum theory **V1** 382
 flotation **V1** 246–249, **V1** 289, **V1** 344–347
 fluidization **V1** 265
 fluorescence quenching **V2** 281, **V2** 290–292
 fluorosurfactants **V1** 122, **V1** 291
 foam breaking **V2** 143–157
 foams **V2** 23–43
 see also films
 amphoterics **V1** 365, **V1** 366–367
 anionic surfactants **V1** 274, **V1** 275, **V1** 280
 bubble formation **V1** 255, **V1** 274, **V2** 418
 cationic surfactants **V1** 325
 characterization **V2** 415–416, **V2** 433
 detergency **V1** 71–72
 film rupture mechanisms **V2** 26
 foaming agents **V2** 40–41
 foodstuffs **V1** 41–42
 industrial materials **V2** 37–43
 micellar structural forces **V2** 427–428
 petroleum industry **V1** 254–256, **V1** 262–263
 preparation **V2** 24–25, **V2** 40–43
 stability **V2** 25–37
 stabilizers **V1** 306
 foodstuffs **V1** 39–52
 cationic surfactants **V1** 332–334
 environmental issues **V1** 512
 foam breaking **V2** 155–156
 foams **V2** 24–27, **V2** 43
 nonionic surfactants **V1** 297, **V1** 307–308
 force fields **V1** 539–541
 force methods **V2** 217–221
 fractional amino acid transfer **V2** 176–177
 fracturing fluids **V1** 340
 fragmentation fractal dimension **V2** 360
 free energy **V2** 121–134
 see also interfacial tension; surface tension
 free rosin distributions **V1** 140
 free volume theory **V1** 230
 freeze-fracture technique **V2** 335, **V2** 353
 frequency doubling **V2** 88–89
 frictional forces **V2** 390–392
 fringes of equal chromatic order (FECO) interferometry **V2** 384
 froth **V2** 25
 functionality tests **V1** 46
 fungicides **V1** 318–321
 funnel-shaped test **V2** 33–34
 gas adsorption **V1** 167–168
 gas chromatography (GC) **V1** 362
 gas-filled polymer foams **V2** 38, **V2** 40
 GC *see* gas chromatography
 gel phases
 betaines **V1** 353
 ceramics **V1** 215
 definition **V2** 4
 domain morphology **V2** 307–308
 drug delivery **V1** 21–23, **V1** 29
 foam stabilization **V2** 27
 rheology **V2** 204
 structure **V1** 476–477
 surfactant–polymer systems **V1** 455–456, **V1** 462–463
 vesicle bilayers **V2** 46–47
 gel-like networks **V2** 430
 gelatin **V1** 86, **V1** 97
 gemini surfactants **V1** 314, **V1** 354, **V1** 385–390, **V1** 469, **V1** 496–497
 gene therapy **V1** 11–12
 genus concept **V2** 304–306, **V2** 314
 Geography-Referenced Exposure Assessment Tool for European Rivers (GREAT-ER) **V1** 535
 geometric mean combining rule **V2** 127
 Gibbs elasticity **V2** 27–28, **V2** 235
 Gibbs equations
 adsorption **V1** 75, **V1** 76–77, **V1** 252, **V1** 389, **V2** 242
 phase rule **V1** 466, **V1** 467
 solubilization **V2** 164
 Gibbs free energy **V2** 122
 Gibbs triangle **V2** 57–60
 Gibbs–Helmholtz equation **V1** 177
 Gibbs–Marangoni effect **V1** 255, **V2** 27–28
 Gibbs–Thompson equation **V1** 169–170
 Girifalco–Good–Fowkes–Young equation **V2** 129
 globules **V2** 304, **V2** 306, **V2** 310, **V2** 316
 glucamides **V1** 327
 gold **V2** 3, **V2** 4, **V2** 6, **V2** 99–116
 goniometer–telescopes **V2** 254, **V2** 260–262, **V2** 263

- goniometry V2 357, V2 368
 Gouy–Chapman model V1 222–223, V2 373–374, V2 375
 Gouy–Chapman–Stern–Grahame model V2 380
 graft copolymers V1 374, V1 377–384
 granules V1 214, V2 269–277
 grazing incidence X-ray diffraction V2 80, V2 82
 GREAT-ER *see* Geography-Referenced Exposure Assessment
 Tool for European Rivers
 Griffith equation V1 201
 grinding, dispersion V1 114
 Guinier approximation V2 362
- haematite V2 7
 Hagen–Poiseuille equation V2 272
 hair care V1 327–328, V1 354, V1 368
 Hamaker theory V2 392
 hard surface cleaning V1 321–326, V1 367–368
 hard-sphere radius V2 346
 head space measurement V2 35
 head-group overlap V2 426–427
 heat of immersion V2 269
 heat treatment V1 245
 heat-developable materials V1 90
 heavy metal ions V1 288–289
 Helfrich forces V2 429
 Helmholtz free energy V2 122
 Helmholtz model V1 222
 Helmholtz–Smoluchowski equation V2 374–375
 hemimicelles V1 236, V1 237, V1 238
 heterogeneity V1 40–42, V1 155–156, V1 202–203, V2 130
 heteronuclear Overhauser effect V1 546
 heterophase polymerizations V1 181, V1 184, V1 185, V1 190
 hexagonal mesophases V2 308–309
 hexagonal phases V1 473, V1 479, V1 481, V1 492, V2 167, V2 308–309
 hexamethyldisiloxane (HMDSO) V2 380–381
 high performance liquid chromatography (HPLC) V1 362, V1 513–514
 HLB *see* hydrophilic–lipophilic balance
 HMDSO *see* hexamethyldisiloxane
 homogeneity V1 540, V2 314, V2 321–323, V2 330
 homopolymers V1 373–374
 honeycombs V2 316
 Hookean solids V2 190, V2 194
 Hooke's law V2 387
 HPLC *see* high performance liquid chromatography
 hydrate inhibitors V1 340
 hydration interactions V1 42–43, V2 394
 hydrocarbon radius V2 345–346, V2 348
 hydrodynamic forces V2 375, V2 380–382, V2 388–389, V2 417
 hydrodynamic radius V2 334, V2 346, V2 347, V2 368–369
 hydrogen bonding V1 230, V1 244, V1 489
 hydrolysis V1 100, V1 143–144, V1 391–397, V2 6–7
 hydrophiles V1 298–301
 hydrophilic–lipophilic balance (HLB)
 anionic surfactants V1 275
 cationic surfactants V1 310
 emulsions V1 180, V1 257–258
 lipids V1 44–45, V1 48
 microemulsions V2 61, V2 63, V2 69
- paint pigments V1 117
 solubilization V2 161, V2 167
 spontaneous emulsification V1 74
 hydrophobic effect V1 467–469, V2 240
 hydrophobicity
 foams V2 151–152
 interactions V1 233, V1 428–429, V1 449, V1 452, V2 430
 lipids V1 12–13
 micelles V1 294–297, V2 162
 modification V1 447–452, V1 461
 hydrophobizing *see* sizing
 hydrotropes V1 321–323, V1 407–420, V1 500
 hyperpolarizability V2 87–88
 hysteresis V2 268, V2 401
- IEP *see* isoelectronic point
 image analysis V1 164–166, V2 35, V2 36
 immersional wetting V2 126
 immunization V1 28
in situ particle size measurement V1 239
in situ-forming carrier systems V1 20
 inclusion complexes V1 17
 indifferent adsorption V2 429
 indifferent ions V2 10
 industrial materials V2 37–43
 industrial syntheses *see* manufacture
 infrared (IR) spectroscopy V1 163, V2 101–102, V2 105–106
 inhomogeneous surfaces V2 129–130, V2 135–136
 insurfs V1 401–402
 initiators V1 194, V1 400
 injection molding V1 214
 inner salts V1 350
 insulin adsorption V1 5
 integrated circuits V2 93–95
 intensity-weighted distribution V2 362, V2 366
 interfacial curvature V2 301–321
 interfacial polymerization V1 73
 interfacial tension
 definition V2 121
 measurement V2 218–223, V2 225–226, V2 230–232, V2 235, V2 258–260
 microemulsions V2 70, V2 72–73
 oil recovery V1 261
 polymers V1 178
 sedimentation volume V2 269–270
 spontaneous emulsification V1 74–76
 wetting thermodynamics V2 127–129
 interference microscopy V2 263–264
 interferometry V2 384–385
 intermediate phases V1 477–479, V2 316–317
 internal sizing V1 138–145
 International Organization for Standardization (ISO) V1 516, V1 517
 interpenetration V1 241–242
 inverse micellar solutions V1 411
 inverse phases V1 499
 inverse polymerization V1 180
 ion adsorption V1 220
 ion dissolution V1 220–221
 ion exchange V1 61–65, V1 233
 ion pairing V1 233

- ionic strength **V1** 226, **V1** 240
 ionic surfactants **V1** 493–497, **V2** 64–66, **V2** 165–166
 ionization **V1** 221, **V2** 371
 IR *see* infrared spectroscopy
 isoelectronic point (IEP) **V1** 46, **V1** 96–97, **V1** 224, **V1** 225–226, **V1** 246–248
 isomorphous substitutions **V1** 221
- Johnson–Kendall–Roberts (JKR) theory **V2** 388, **V2** 389–390, **V2** 391
 Jönsson model **V2** 165–166
- kaolin **V1** 147
 kaolinite **V2** 8–9
 Kelvin equation **V1** 161, **V1** 168
 ketals **V1** 393–394
 kinetics **V1** 433–434, **V2** 55
 Kleven equation **V1** 362
 Kolmogorov length **V1** 181
 Kozeny–Carman relationship **V1** 152
 Krafft point **V1** 45, **V1** 427–428, **V1** 468, **V1** 489, **V2** 245
 Krafft temperature *see* Krafft point
 Krieger–Dougherty equation **V1** 151, **V1** 210
 kugelschaum, foaming **V2** 24–25
- LAC *see* limiting association concentration
 lamellae lifetime measurement **V2** 37
 lamellae profiles **V2** 422
 lamellar phases
 see also liquid crystals
 bilayer solubilization **V2** 171–173
 domain morphology **V2** 307, **V2** 308, **V2** 316
 hydrotropes **V1** 411, **V1** 412–414
 micelle self-assembly **V1** 253
 phase behaviour **V1** 481
 phase prisms **V2** 340–341
 rheology **V2** 199–204
 rigid interface solubilization **V2** 185
 shear behaviour **V2** 211–214
 smectics **V2** 300, **V2** 307, **V2** 315
 structure **V1** 471, **V1** 472–473
 vesicles **V1** 418
 lamellar structural forces **V2** 428–429
 laminar flow **V2** 18
 Langmuir equation **V1** 58
 Langmuir–Blodgett (LB) films **V2** 79–98
 command surfaces **V2** 91–92
 computer simulation **V1** 538
 deposition **V2** 80–83, **V2** 85
 historic perspective **V2** 99
 molecular electronics **V2** 92–95
 nanoparticles **V2** 83–84
 nonlinear optical devices **V2** 85–90
 sensors **V2** 90–91
 surface forces **V2** 392, **V2** 396, **V2** 403–404
 lanthanum myristate **V2** 329
 lanthanum palmitate **V2** 329
 Laplace equations **V1** 168, **V2** 121, **V2** 252, **V2** 272, **V2** 421, **V2** 422
 laser light **V2** 86–89
 laser-focusing techniques **V1** 165
- LASs *see* linear alkylbenzene sulfonates
 lateral interactions **V1** 236
 lateral structure **V1** 543
 latex **V1** 105–122, **V2** 8
 lattices **V1** 221, **V1** 401–402
 LB *see* Langmuir–Blodgett
 LC₄₅₀ tests **V1** 518–519, **V1** 524–525, **V1** 530, **V1** 532
 lead myristate **V2** 328
 legislation **V1** 512–513
 Lial process **V1** 295
 lidocaine **V1** 7, **V1** 8
 life, origins **V2** 50
 Lifshitz theory **V2** 390, **V2** 392, **V2** 425–426
 ligand complexation **V1** 96
 light scattering
 see also goniometry; static light scattering
 CMC determination **V2** 242, **V2** 247
 droplet microemulsions **V2** 349
 dynamic **V2** 242, **V2** 247, **V2** 294–296, **V2** 357, **V2** 365–369
 micelle size/shape **V2** 281, **V2** 294–296
 microemulsions **V2** 335
 paper **V1** 129
 particle size **V2** 357–370
 small-angle **V2** 357, **V2** 362, **V2** 364–365
 thin-liquid films **V2** 417
 light sensitivity **V1** 101
 lignin content **V1** 125–127
 ligninsulfonates **V1** 292
 limited coalescence **V1** 103–104
 limiting association concentration (LAC) **V2** 165
 lindane **V2** 178–184
 line tension approach **V2** 123–124
 linear alkylbenzene sulfonates (LASs) **V1** 511, **V1** 513, **V1** 521, **V1** 523–526
 linearized Poisson–Boltzmann distribution **V1** 228
 lipids **V1** 12–13, **V1** 44–46
 liposomes **V1** 9–12, **V2** 45, **V2** 49–50
 liquid bridges **V1** 44, **V1** 50
 liquid crystals
 agrochemical sprays **V1** 83
 chemical structure **V1** 465–508
 concentration effects **V1** 436
 drug delivery **V1** 12, **V1** 20–21
 foam stabilization **V2** 29–30
 foodstuffs **V1** 45
 formation **V1** 256
 hydrotropes **V1** 408–409, **V1** 411, **V1** 412–414, **V1** 415
 lamellar **V1** 411, **V1** 412–414, **V1** 418, **V1** 471, **V1** 472–473, **V1** 481
 Langmuir–Blodgett films **V2** 82, **V2** 91
 lyotropic **V1** 466–467, **V2** 299–338
 nematic **V1** 475–476, **V1** 483–484, **V1** 489, **V2** 82, **V2** 299–300
 phase behaviour **V1** 466, **V1** 472–502
 smectics **V2** 300, **V2** 307, **V2** 315
 solids/melts **V2** 299–301
 solubilization **V2** 166–169, **V2** 173
 surfactants **V1** 66–67, **V1** 70
 vesicle bilayers **V2** 46–47
 vesicles **V1** 418
 liquid magnets **V2** 7
 liquid soaps **V1** 273
 liquid transport **V1** 162

- liquid/liquid interface **V1 65–67**
 LOEC *see* lowest observed effect concentration
 loops **V1 231, V1 377–379**
 low shear viscosity **V2 349–350**
 lowest observed effect concentration (LOEC) **V1 519, V1 527**
 lyotropic liquid crystals **V1 466–467, V2 299–338**
 lyotropic nematic phases **V1 475**
- MAC *see* maximum additive concentration
 macroemulsions **V1 176, V1 177**
 macromolecules **V1 15**
 magnetic properties
 colloids **V2 246**
 Langmuir–Blodgett films **V2 84**
 liquids **V2 7**
- Maltese cross textures **V1 473, V2 308**
 manufacturing processes
 amphoterics **V1 356–360**
 anionic surfactants **V1 273–279, V1 282–284, V1 286–288, V1 290**
 betaines **V1 352–353, V1 355**
 block copolymers **V1 303**
 cationic surfactants **V1 311–314**
 Gemini surfactants **V1 386**
 Lial process **V1 295**
 nonionic surfactants **V1 294–297, V1 298–300, V1 302–308**
 OXO process **V1 274, V1 295**
 Shell Higher Olefin Process **V1 295**
 Williamson synthesis **V1 275, V1 276**
 Ziegler process **V1 279, V1 294–295**
- Marangoni flow **V2 27–28, V2 146, V2 230**
 MASIF *see* measurement and analysis of surface interactions and forces
 mass action models **V1 429, V2 163–164**
 mass-weighted distributions **V2 359**
 matte beads **V1 87, V1 103–104**
 maximum additive concentration (MAC) **V2 163, V2 166, V2 170–171**
 maximum bubble methods **V2 217, V2 223, V2 227–229, V2 440**
- Maxwell model **V2 194–195**
 MBAS *see* methylene blue active substances
 MD *see* molecular dynamics
 mean field approximations **V1 378**
 measurement and analysis of surface interactions and forces (MASIF) **V2 384–388, V2 406**
 mechanical pulping **V1 125**
 melts, liquid crystals **V2 299–301**
 membrane emulsification **V1 183**
 membranes **V2 46, V2 49–52, V2 171–173**
 meniscus formation **V2 136–137**
 meniscus height **V2 82–83**
 meniscus radii **V2 421**
 mercerization **V1 337, V1 338, V1 339**
 mercury porosimetry **V1 168–170**
 mesh mesophases **V1 477–478, V1 494, V2 302, V2 305–306, V2 315–316**
 mesogenic properties **V1 490**
 mesomorphism **V2 300, V2 302**
 mesophases
 additives **V1 497–502**
- bicontinuous **V2 302, V2 303, V2 306, V2 310–315, V2 316–317**
 columns **V2 308–310**
 cubic **V2 311–314**
 gels **V2 307–308**
 hexagonal **V2 308–309**
 hydrogen bonding **V1 489**
 lamellar **V2 307, V2 308, V2 316**
 liquid crystals **V1 465–508**
 lyotropic liquid crystals **V1 466–467, V2 299–338**
 meshes **V1 477–478, V2 302, V2 305–306, V2 315–316**
 molten **V2 318–319**
 morphology **V2 301–321**
 polycontinuous **V2 316–317**
 ribbons **V2 309–310**
 ringing gels **V1 353, V2 204**
 smectics **V2 300, V2 307, V2 315**
- metabolites **V1 515, V1 519**
 metals
 clusters **V2 113–114**
 foams **V2 41–42**
 ion hydrolysis **V2 6–7**
 nanoparticles **V2 83–84, V2 113–114**
 processing **V1 512**
- methyl ester ethoxylates **V1 307–308**
 methylene blue active substances (MBAS) **V1 512, V1 513**
 MHC *see* minimal hydrotropic concentration
 micelles
 see also critical micelle concentration; rod-like micelles
 agrochemical sprays **V1 83**
 amphoterics **V1 362–363**
 antifoaming agents **V2 148**
 aqueous solutions **V2 190–192**
 cationic surfactants **V1 324**
 computer simulation **V1 544–546**
 concentration effects **V1 435–437**
 coupler dispersions **V1 100**
 cylindrical **V2 193–194, V2 199**
 detergency **V1 55–56, V1 59**
 drug delivery **V1 15–16**
 foam films **V2 427–428**
 Gemini surfactants **V1 388–390**
 hemimicelles **V1 236, V1 237, V1 238**
 inverse solutions **V1 411**
 kinetics **V1 433–434**
 liquid crystals **V1 465–466, V1 467–472**
 mixed **V1 100, V1 442, V1 451–452**
 molecular dynamics **V1 544–546**
 non-aqueous media **V2 246–248**
 nonionic **V1 440–442**
 phase behaviour **V1 481**
 polymeric surfactants **V1 376**
 reversed **V2 169–171, V2 174–177, V2 181–184**
 self-assembly **V1 252–254, V2 239–241**
 self-reproduction **V2 50**
 size/shape measurement **V2 281–297**
 solubilization **V2 162–169**
 solvent effects **V1 434**
 sponge phase **V1 439–440**
 stability **V2 148**
 structure **V1 421–423, V1 431–432, V1 437–441, V1 467–472, V2 162**
 surfactant adsorption **V1 236–237**
 temperature effects **V1 440–442**

- thermodynamic models **V1** 428–430
 vesicle comparison **V2** 45
 Michael addition reactions **V1** 359–360
 Michelson optics **V2** 264
 microcellular plastic foams **V2** 40
 microdomains **V2** 173
 microemulsions **V2** 55–77
 see also emulsions
 agriculture **V1** 73
 antifoaming agents **V2** 152–153, **V2** 154
 applications **V2** 73–74
 bicontinuous **V1** 460–462, **V1** 482, **V2** 351–352
 characterization **V2** 333–356, **V2** 364
 condensation **V1** 184–185
 definitions **V2** 56
 detergency **V1** 68–70
 Disorder–Open–Connected–Cylinder model **V2** 181
 domain morphology **V2** 302, **V2** 317–319
 droplet **V2** 344–352
 drugs **V1** 7, **V1** 17
 emulsion polymerization **V1** 176
 formation **V1** 253, **V1** 258–259, **V2** 56, **V2** 68–70
 hydrotropes **V1** 412, **V1** 414
 interfacial tensions **V2** 70, **V2** 72–73
 ionic surfactants **V2** 64–66
 mesophases **V2** 300
 microstructures **V2** 70–72, **V2** 342–344
 mixed surfactants **V2** 63–64, **V2** 66–67
 nonionic surfactants **V2** 57–64, **V2** 66–67
 phase behaviour **V2** 57–70, **V2** 178, **V2** 338–342, **V2** 344–345
 relaxation NMR **V2** 290
 reversed **V2** 9
 scattering techniques **V2** 293
 soft surfactant systems **V2** 174–181
 solubilization **V2** 169–171, **V2** 173, **V2** 174–185
 stiff surfactant systems **V2** 181–185
 surfactant–polymer systems **V1** 460–462
 microencapsulation **V1** 73–74
 microinterferometry **V2** 419–420
 microorganisms **V1** 319–320
 microparticle electrophoresis chambers **V2** 375
 micropipets **V2** 417
 microscopic study **V2** 34–35
 microstructures **V2** 342–344
 middle mesophases **V2** 308–309
 Mie theory **V2** 362–365
 migration, films **V1** 397
 mineral flotation **V1** 246–249, **V1** 344–347
 miniemulsions **V1** 176, **V1** 177, **V1** 195–196
 minimal hydrotropic concentration (MHC) **V1** 409, **V1** 412
 mining **V1** 344–347, **V1** 512
 mixed films **V2** 30
 mixed micelles **V1** 100, **V1** 442, **V1** 451–452
 mixed surfactants **V1** 498–499
 MLVs *see* multi-lamellar vesicles
 mobility **V1** 543, **V2** 375–377
 modelling, Langmuir–Blodgett films **V1** 537–550
 moist wetting **V2** 122–123
 molal volume **V2** 244
 molecular absorption **V2** 243–244
 molecular dimensions **V2** 323–332
 molecular dynamics (MD) **V1** 537–550
 molecular electronics **V2** 92–95
 molecular recognition **V1** 244
 molten mesophases **V2** 318–319
 monodisperse particles **V2** 6
 monolayer-protected clusters (MPC) **V2** 113–114
 monolayers **V1** 541–544, **V2** 80–82, **V2** 99–116, **V2** 146, **V2** 147
 monomer emulsions **V1** 191–196
 morphology **V2** 301–321
 motorized syringe methods **V2** 258
 multi-lamellar vesicles (MLVs) **V2** 45–46
 multiple emulsions **V1** 73
 multiple equilibrium model **V1** 429–430

 nanoassembly computers **V2** 93–95
 nanocrystalline dispersions **V1** 91, **V1** 100–101
 nanoemulsions **V1** 77
 nanoparticles **V1** 135, **V2** 83–84, **V2** 113–114
 nanoparticulate semiconductors **V1** 87
 NaPA *see* sodium polyacrylate
 Navier–Stokes equation **V2** 371–372, **V2** 374
 NBFs *see* Newton black films
 neat mesophases (smectics) **V2** 300, **V2** 307, **V2** 315
 necking, ceramics **V1** 207
 nematic liquid crystals **V1** 475–476, **V1** 483–484, **V1** 489, **V2** 82, **V2** 299–300
 neutralization flocculation **V1** 137
 neutron scattering *see* small-angle neutron scattering
 Newton black films (NBFs) **V2** 29, **V2** 30, **V2** 426, **V2** 427
 Newtonian liquids **V2** 190, **V2** 192–194
 nitrogen-containing polymers **V1** 327
 NLO *see* nonlinear optical
 NMR *see* nuclear magnetic resonance spectroscopy
 no observed effect concentration (NOEC) **V1** 284, **V1** 519, **V1** 526–527, **V1** 530, **V1** 532
 nonaqueous media **V2** 67, **V2** 246–248
 noninteracting micelles **V2** 191–192
 noninteractive adsorption **V2** 429
 nonionic hydrophiles **V1** 298–301
 nonionic hydrophobes **V1** 294–297
 nonionic micelles **V1** 440–442
 nonionic surfactants **V1** 293–308
 block copolymers **V1** 491–493
 environmental issues **V1** 525–529
 microemulsions **V2** 57–64, **V2** 66–67
 phase behaviour **V1** 480–491
 solubilization **V2** 166–169
 nonlinear optical (NLO) devices **V2** 85–90
 non-Newtonian fluids **V2** 19–20
 nonpolar solvents **V1** 434, **V2** 67, **V2** 246–248
 nonpolar surfaces **V2** 396–398
 nonwetting surfaces **V2** 121
 nuclear magnetic resonance (NMR) spectroscopy
 amphoterics **V1** 361–362
 calibration **V2** 283–284
 hydrotropes **V1** 412
 intermediate mesophases **V2** 316
 micelle shape/size **V2** 281–290
 micellization **V1** 430–431
 microemulsions **V2** 334–335, **V2** 347, **V2** 349
 porosity **V1** 170
 pulsed gradient spin-echo **V2** 282, **V2** 284–286, **V2** 288–289

- nuclear magnetic resonance (NMR) spectroscopy (*Continued*)
 relaxation V2 281–282, V2 289–290, V2 334–335, V2 347
 self-diffusion V2 281–289, V2 302, V2 334
 nucleation V1 95, V2 5–6, V2 416, V2 431
 null ellipsometry V2 443
 number-weighted distributions V2 359
- o/w see oil-in-water*
 oblate ellipsoids of revolution V2 322–323
 oblate micelles V2 286–287
 OECD *see* Organization for Economic Co-operation and Development
 oil ganglia V1 259, V1 261
 oil industry *see* petroleum industry
 oil-continuous dispersions V1 39
 oil-in-water (*o/w*) microemulsions V2 55–74, V2 177–181, V2 184–185
 oil-swollen lamellar phases V2 185
 oils V1 499–500, V2 145, V2 147, V2 148–149, V2 151–154
 oily streaks V1 473
 oligoethylene oxide surfactants V2 337–338
 oligopeptides V1 4–5
 open-cell structures V2 41
 optical density V1 409–410
 optical fibre probes V2 35, V2 38
 optical storage devices V2 87
 optical textures V1 472–473, V1 474
 oral care V1 369
 oral drug administration V1 8–9, V1 13, V1 18, V1 28
 ordered phases V2 307–317
 organic monolayers V2 79–98, V2 99–116
 Organization for Economic Co-operation and Development (OECD) tests V1 513, V1 518, V1 520, V1 523, V1 527–528, V1 533–534
 organoclays V1 343–344
 origins of life V2 50
 ortho esters V1 394–395
 orthokinetic coagulation V2 18–19
 oscillating jet method V2 229–230
 oscillatory force profiles V2 399–400
 osmometry V2 244, V2 247
 osmosis V1 211–212, V2 349, V2 417
 Ostwald ripening
 dynamic swelling V1 191
 emulsion concentrates V1 77–78, V1 79
 emulsions V1 185–188, V1 191
 foams V1 41
 photography V1 95–96
 overcoating V1 87
 oversize fraction V2 359
 OXO process V1 274, V1 295
 oxyethylene surfactants V1 440–442
- π -stacking V1 467
 packing density V1 211
 paints V1 105–122, V1 397, V1 403–404
 palisade layer V2 162
 paper V1 123–173
 absorbency V1 154–158, V1 159–162
 cationic surfactants V1 331–332
 environmental issues V1 512
 foam breaking V2 143, V2 145
 formation V1 128–138
 internal sizing V1 138–145
 polymer adsorption V1 132–136
 porosity V1 167–171
 surface properties V1 155–156, V1 158–159, V1 162–166
 surface treatment V1 146–154
 wettability V1 154–159
 parachute morphology V2 49
 paraphenylenediamines V1 89, V1 90, V1 93
 parenteral drug administration V1 9–10, V1 19–20
 Parker-Print-Surf (PPS) test V1 165
 partial molal volume V2 244
 partial wetting V2 121
 particle size V1 239, V2 357–370
 particle suspension layer stability V2 271–272
 particulates V1 48–51, V1 91–92, V1 94–99, V2 150–152, V2 153
 Pascalian liquids V2 190
 patch flocculation V1 136, V1 137
 patterned self-assembling monolayers V2 109–113
 PB *see* Poisson-Boltzman theory
 PCS *see* photon correlation spectroscopy
 pearl-necklace model V1 447–448
 PEC *see* predicted environmental concentrations
 PEGs *see* poly(ethylene glycol)s
 pendant drop method V2 217, V2 221–222, V2 233
 penetration
 capillary V1 160–162, V2 120, V2 136–140
 drug delivery V1 11
 molecular dynamics V1 544, V1 545
 surfactant aggregates V2 166–168
 PEO *see* poly(ethylene oxide)
 PEO-PPO-PEO block copolymers V1 11, V1 13, V1 15–16, V1 21–25, V2 168, V2 204–205
 peptization V1 334, V1 336–337, V2 3
 Percus-Yevick approximation V2 205
 perfluorocarbon fluids V1 179
 peristaltic forces V2 426
 Perrin black films *see* Newton black films
 personal care V1 327–330, V1 344, V1 354, V1 364–369
 petrol sulfonates V1 278
 petroleum industry V1 251–267, V1 295–296, V1 337–341, V1 343–344, V1 512
 Peyer's patches V1 28
 PGSE NMR *see* pulsed gradient spin-echo nuclear magnetic resonance
 pH effects
 amphoterics V1 350
 betaine esters V1 396
 ceramics V1 204–205, V1 215
 dispersions V1 240
 drug delivery V1 25–26
 effects on sizing V1 141–142
 electrokinetics V2 372, V2 376–377, V2 380
 fatty acid vesicles V2 49
 particle mobility V2 376–377
 selective flocculation V1 245
 surface charge V1 221–222
 thickener stability V1 323–324
 zeta potential V1 225–226, V1 248–249, V2 380–381
 zwitterions V1 350, V1 352–353

- pharmacy V1 3–38, V1 369, V1 418–419, V1 511
- phase behaviour
- amphiphilic drugs V1 7, V1 8
 - computer simulations V1 547–550
 - foam stabilization V2 31
 - hydrotropes V1 412–414, V1 500
 - in situ*-forming carrier systems V1 20
 - inversion V1 44, V1 186, V1 189–190, V1 258, V2 61, V2 338
 - ionic surfactants V1 493–497
 - liquid crystals V1 466, V1 472–502
 - micelles V1 481
 - microemulsions V2 57–70, V2 178, V2 338–342, V2 344–345
 - nonionic surfactants V1 480–491
 - separation V1 43, V1 186, V1 429, V2 40
 - surfactant–polymer systems V1 452–463
 - surfactants V1 67–71, V1 480–497
 - transition temperature V2 46–47, V2 50–52
 - zwitterions V1 493
- phase prisms V2 339–342
- phase rule V1 466, V1 467
- phosphated alcohols V1 285–287
- phosphobetaines V1 354–355
- phospholipid bilayers V2 45, V2 46–47, V2 49–52
- phosphoric acid esters V1 285–289
- photochromism V2 91–92
- photography V1 85–104, V1 176, V1 192–193
- photolability V1 397
- photomicroscopy V2 275–276
- photon correlation spectroscopy (PCS) V1 381
- photonic devices V2 85–90
- physico-chemical processes V1 421–443, V1 515, V1 517–518
- Pickering stabilizers V1 192–193
- picture framing V1 121
- pigments V1 108–109, V1 113–119, V1 147
- plasma polymerization V2 380–381
- plasticity V1 208
- plastics V1 91, V1 512, V2 37–38, V2 40–41
- plate methods V2 236–237
- PNEC *see* predicted no-effect concentrations
- point of zero charge (PZC) V2 9–10
- Poiseuille approximation V2 227
- Poisson–Boltzmann (PB) theory V1 205, V1 226–228, V2 12–13, V2 202–203, V2 373–374, V2 393–396, V2 424
- polar interactions V2 129
- polar layer V2 162
- polar solvents V1 434
- polar surfaces V2 394–396, V2 398–399
- polarization (optical) V2 86, V2 367
- polarized attenuated total reflection infrared spectroscopy V2 101, V2 102
- polarizing microscopy V1 75, V1 472
- polyamines V1 333
- polycarboxylates V1 64–65
- polycontinuous mesophases V2 316–317
- polydimethylsiloxanes V2 145
- polydispersity V2 18, V2 199–202
- polydispersity index V1 19, V2 359, V2 363–364
- polyederschaum, foaming V2 24–25
- polyelectrolytes V1 116–119, V1 132–136, V1 147–148, V2 402–404, V2 429
- poly(ethylene glycol)s (PEGs) V2 106–107, V2 381–382
- poly(ethylene oxide) (PEO) V1 5–6
- polyglucoside surfactants V1 489–491
- polyhydroxy surfactants V1 489
- polyhydroxybenzenes V1 412
- polymerization
- binder-emulsion preparation V1 107–110
 - emulsions V1 107–110, V1 175–200, V1 288, V1 290–291, V1 400–402
 - inverse V1 180
 - plasma V2 380–381
 - radical V1 176, V1 196–198
 - surfactants V1 107–110, V1 397–405
 - suspensions V1 103–104, V1 176, V1 192–193
 - vesicles V2 49
- polymers
- adsorption V1 132–136, V1 229–232, V1 241
 - bridging mechanism V1 136–137
 - drug delivery V1 13–14, V1 23, V1 27–29
 - electronically conducting V1 87
 - foam stabilization V2 26
 - latex dispersions V2 8
 - microemulsion additives V2 67–68, V2 69
 - nitrogen-containing V1 327
 - particle interactions V1 43, V1 205–206
 - patterned self-assembling monolayers V2 111
 - plastic foams V2 37–38, V2 40–41, V2 42
 - surfactant–polymer systems V1 445–463
 - surfactants V1 373–384
 - wetting V2 126–127
- polyoxyethylene surfactants V1 287–288, V1 486–487, V1 502
- polyphosphated alcohols V1 285–287
- polysaccharides V1 44, V1 46–48
- polyurethane foam V2 38, V2 41, V2 42
- porosimetry, mercury V1 168–170
- porosity V1 167–171, V2 120, V2 136–140, V2 269–277
- porous disc holders V2 418
- post-emulsified binders V1 111–113
- potash, flotation V1 347
- potentiometry V2 438
- powders V1 50–51, V1 202–203, V2 136, V2 138–140, V2 269–277
- PPS *see* Parker–Print–Surf test
- prebiological phases V2 50
- precursor films V2 135
- predicted environmental concentrations (PEC) V1 512–513, V1 535
- predicted no-effect concentrations (PNEC) V1 513, V1 519, V1 535
- pressure drop technique V2 35–36
- pressure effects V2 62, V2 68, V2 69, V2 246
- pressure filtration V1 203
- pressure methods V2 217, V2 223, V2 227–229, V2 234–236
- probing aggregation V2 368–369
- profile axisymmetric drop shape analysis (ADSA-P) *see* axisymmetric drop shape analysis
- prolate ellipsoids of revolution V2 322–323
- prolate micelles V2 286–287
- proline V1 417
- propionates V1 359–360
- propylene oxide V1 300, V1 303–304
- protein crystals V1 467

- proteins **V1** 5, **V1** 46, **V2** 106–109, **V2** 401
 protolysis **V2** 9–10
 protrusion **V2** 397, **V2** 427
 pseudo-binary phase diagrams **V2** 178–179
 pseudo-emulsions **V2** 30–31, **V2** 152–154
 pseudo-phase model **V2** 163, **V2** 173
 pulping **V1** 125
 pulsed gradient spin-echo nuclear magnetic resonance (PGSE NMR) **V2** 282, **V2** 284–286, **V2** 288–289
 puncture defects **V2** 319
 pyrolysis **V1** 217
 PZC *see* point of zero charge
- quasi-equilibrium **V2** 400
 quasi-lattice model **V1** 378
 quaternary ammonium salts
 agricultural adjuvants **V1** 341–342
 biocides **V1** 318–321
 cleavable surfactants **V1** 395–397
 cosmetics **V1** 316–317, **V1** 329–330
 detergency **V1** 314–318, **V1** 327
 environmental issues **V1** 530–532
 manufacture **V1** 311–314
 mineral flotation **V1** 345, **V1** 347
 oilfields **V1** 338–340
 organoclays **V1** 343–344
 paper **V1** 331
 thickeners **V1** 323
 Quemada function **V2** 349, **V2** 351
 quinonediimines **V1** 89, **V1** 93–94
- radical polymerization **V1** 176, **V1** 196–198
 radius of gyration **V2** 295
 Raman spectroscopy **V1** 163
 Rayleigh limit **V2** 349, **V2** 361–362
 Rayleigh–Debye–Gans (RDG) approximation **V2** 362, **V2** 363, **V2** 368
 rayon **V1** 337, **V1** 338, **V1** 339
 reaction rates, vesicles **V2** 50
 receding contact angles **V2** 129–130, **V2** 150
 rectangular electrophoresis chambers **V2** 377–378
 reflected-light interferometry **V2** 419
 reflected-light video microscopy **V2** 419
 refractive index **V1** 114, **V2** 242, **V2** 420, **V2** 437
 rejection (particle behaviour) **V2** 275
 relaxation, NMR **V2** 281–282, **V2** 289–290, **V2** 334–335, **V2** 347
 repulsion forces **V2** 429
 RES *see* reticuloendothelial system
 responsive drug delivery **V1** 24–26
 restricted equilibrium **V2** 400
 retention, paper **V1** 129–130, **V1** 141–142
 reticuloendothelial system (RES) **V1** 9
 reverse flotation **V1** 345
 reversed phases
 liquid crystals **V1** 472–473, **V1** 480, **V1** 499
 micelles **V2** 169–171, **V2** 174–177, **V2** 181–184
 microemulsions **V2** 9
 Rhebinder effect **V1** 79
 rheology
 associative thickeners **V1** 449
 ceramics **V1** 208–212
 colloidal dispersions **V2** 19–20
 dilatational **V2** 237
 dispersions **V1** 239–240
 elongational **V1** 153
 foams **V1** 254
 foodstuffs **V1** 41
 liquid crystals **V1** 466
 mesophases **V1** 503
 modifiers **V1** 148–149, **V1** 343
 paper coatings **V1** 149–152
 surfactants **V1** 338–340, **V1** 389–390, **V2** 189–214
 rheopexy **V1** 209, **V2** 190, **V2** 206
 rhombohedral mesh phases **V1** 477–478, **V1** 494
 ribbon phases **V1** 477–478, **V1** 495, **V2** 309–310
 ring methods **V2** 236–237
 ringing gels **V1** 353, **V2** 204
 rinse-added softeners **V1** 317
 risk assessment **V1** 534–535
 road construction **V1** 334–337
 robust beer foams **V2** 416
 rod-like micelles
 birefringence **V2** 195, **V2** 206
 cationic surfactants **V1** 324
 concentration **V1** 437
 domain morphology **V2** 304, **V2** 306, **V2** 308–310
 flexibility **V1** 438
 rheology **V2** 193–199
 shear behaviour **V2** 206–210
 rolling-up mechanism **V1** 59, **V1** 65–67
 rosins **V1** 140–142
 Ross–Miles pour test **V2** 34
 rotator phase **V1** 477
 rotor mixers **V2** 34, **V2** 35
 rough surfaces **V2** 129–130
 rupture, films **V2** 431
- Saccharomyces cerevisiae* (yeast) **V2** 112
 SALS *see* small-angle light scattering
 salting-in **V1** 407, **V1** 409–410, **V1** 500
 salts, microemulsions **V2** 62, **V2** 64–66, **V2** 69
 SAMs *see* self-assembling monolayers
 SANS *see* small-angle neutron scattering
 SAXS *see* small-angle X-ray scattering
 scanning electron microscopy (SEM) **V1** 127, **V1** 170–171
 Scheludko cells **V2** 418
schlieren nematic texture **V1** 475
 Schulze–Hardy rule **V2** 17
 SDS *see* sodium dodecyl sulfate
 secondary black films *see* Newton black films
 secondary ion mass spectrometry (SIMS) **V1** 163
 secondary surfactants **V1** 365, **V1** 367
 sedimentation **V1** 186, **V2** 358, **V2** 365
 sedimentation potential **V1** 225, **V2** 371, **V2** 379
 sedimentation volume **V2** 269–271, **V2** 273
 seed particles **V1** 194
 segregative phase separation **V1** 453, **V1** 456–458
 selective flocculation **V1** 243–245
 self-assembling monolayers (SAMs) **V2** 99–116
 self-diffusion
 cubic phases **V2** 353–355
 droplet microemulsions **V2** 350–351
 microemulsions **V2** 342–344, **V2** 346–347

- NMR V2 281–289, V2 302, V2 334
 sponge phases V2 352–355
 self-emulsifiable oils V1 73
 self-reproduction V2 50–52
 SEM *see* scanning electron microscopy
 semiconductors V2 83–84, V2 93–95
 sensitization (paper) V1 97–98, V1 137
 sensors, Langmuir–Blodgett films V2 90–91
 separation V1 59, V1 416–417
 sequestration V1 288–289, V1 291
 serum replacement method V2 440–442
 sessile drop methods V2 217, V2 221–222, V2 253–254, V2 257–258
 sewage treatment *see* waste-water treatment
 SFA *see* surface force apparatus
 SFF *see* solid freeform fabrication
 shape methods V2 217, V2 221–223, V2 232–234
 shape parameters, mesophases V2 331, V2 332
 shear behaviour V1 149–152, V1 208–210, V2 205–214, V2 349–350
 shear moduli V2 202–204
 shear planes V2 374–375
 Shell Higher Olefin Process (SHOP) V1 295
 Shinoda-cuts, phase prisms V2 340
 SHOP *see* Shell Higher Olefin Process
 short-chain sulfonates V1 291
 short-oil alkyds V1 113
 Siegert relation V2 295, V2 365
 silica, colloidal V2 7–8
 silicates, flotation V1 345
 silicone surfactants V1 122, V1 291–292
 silver halides V1 87–88, V1 90–92, V1 94–99
 SIMS *see* secondary ion mass spectrometry
 single-lamellar vesicles (SLVs) V2 45–46
 single-particle counting V2 358
 single-phase fluids V2 159
 sizing V1 125, V1 138–145, V1 152–153
 skin care
 amphoterics V1 364–365, V1 366–367, V1 368
 betaines V1 354
 cationic surfactants V1 327–328, V1 344
 organoclays V1 344
 slide hopper coating V1 88
 slip casting, ceramics V1 203, V1 212
 ‘slip-stick’ patterns V2 260–261
 SLNs *see* solid lipid nanoparticles
 SLS *see* static light scattering
 slurries V1 176
 SLVs *see* single-lamellar vesicles
 small-angle light scattering (SALS) V2 357, V2 362, V2 364–365
 small-angle neutron scattering (SANS)
 mesophases V2 301, V2 316
 micelles V2 281, V2 292–294
 microemulsions V2 71–72, V2 335, V2 347–349, V2 358
 rheology V2 205, V2 206, V2 211–212
 small-angle X-ray scattering (SAXS)
 mesophases V2 301, V2 316
 micelles V2 281, V2 292–294
 microemulsions V2 335, V2 358
 rheology V2 211
 ‘Smart’ surfaces V2 91–92
 smectics V2 300, V2 307, V2 315
 smectites, organoclays V1 343–344
 soaps V1 272–273, V1 280, V2 440
 sodium bis(2-ethylhexyl) sulfosuccinate (AOT) V2 65–67, V2 248, V2 364, V2 366–367
 sodium chloride V2 62, V2 64–66
 sodium dodecyl sulfate (SDS) V1 494, V2 241, V2 426, V2 427
 sodium polyacrylate (NaPA) V1 147–149
 soft surfactant systems V2 174–181
 sol, definition V2 4
 solid dispersions
 aggregation processes V2 15–19
 electrical properties V2 9–13
 rheology V2 19–20
 stability V2 5, V2 9, V2 13, V2 15
 synthesis V2 4–9
 solid formulations, agriculture V1 73–74
 solid freeform fabrication (SFF) V1 216
 solid lipid nanoparticles (SLNs) V1 12–13
 solid loading, ceramics V1 210–211
 solid/liquid interfaces V1 58–61
 solidification fronts V2 274–277
 ‘solloids’ V2 397
 solubility V1 46, V1 178, V1 375–376
 solubilization
 antifoaming agents V2 147–148
 binary solutions V2 160, V2 162–173
 capacity V1 69
 definition V2 159
 hydrotropes V1 409–412, V1 415, V1 418–419
 Jönsson model V2 165–166
 limit V2 345
 micelles V1 431, V1 432, V2 162–165
 organic compounds V2 246
 soft surfactant systems V2 174–181
 steric effects V2 166–169
 stiff surfactant systems V2 181–184
 surfactant–polymer systems V1 447
 ternary systems V2 173–184
 water-in-oil microemulsions V2 169–171, V2 174–177, V2 181–184
 solutions, spreading behaviour V2 136
 solvation shells V1 545
 solvents
 diffusion V2 288
 exchange model V2 172
 foodstuffs V1 43
 micellization V1 434
 multicomponent systems V1 501–502
 paints V1 119
 surface forces V2 404–407
 space partitioners V2 316–317
 Sparge tube technique V2 32–33
 spatial fluctuations V2 431–432
 speciality surfactants V1 121–122, V1 385–405
 specific surface area V2 360
 spin finishing V1 337, V1 338, V1 339
 spinning drop method V2 217, V2 222–223
 spinodal decomposition V2 416, V2 431
 sponge phases
 block copolymers V1 492–493
 characterization V2 352–355
 domain morphology V2 302, V2 305–306, V2 316, V2 317–319
 liquid crystals V1 482, V2 300

- sponge phases (*Continued*)
 micelles **V1** 439–440
 phase prisms **V2** 340–342
- spontaneous curvature **V2** 70–72, **V2** 160–161, **V2** 169
- spontaneous emulsification **V1** 74–76, **V1** 185
- SPR *see* surface plasmon resonance
- sprays, agriculture **V1** 80–83
- spreading **V2** 124–126, **V2** 134–136, **V2** 146, **V2** 149–150
- spring deflection **V2** 385–387
- SSFQ *see* steady-state fluorescence quenching
- stabilization
 aggregation **V1** 188
 common black films **V2** 431–433
 coupler dispersions **V1** 99–100
 dispersions **V1** 381–384
 electrostatic **V1** 108
 foams **V1** 306, **V2** 25–37
 foodstuffs **V1** 40–42
 micelles **V2** 148
 microemulsions **V1** 412, **V1** 414
 Ostwald ripening **V1** 186–187
 paper manufacture **V1** 130
 steric **V1** 9, **V1** 205, **V1** 377, **V1** 381–384
 suspension polymerization **V1** 192–193
 suspensions **V1** 209–210, **V1** 212, **V1** 213
 thin-liquid films **V2** 416–417, **V2** 426, **V2** 430
- stalagmometers **V2** 230–231
- starches, co-binders **V1** 149
- static cling **V1** 317
- static light scattering (SLS)
 CMC determination **V2** 242, **V2** 247
 micelle shape/size **V2** 294–296
 microemulsions **V2** 349
 particle size **V2** 357, **V2** 360–365, **V2** 368–369
- steady shear **V1** 149–152
- steady-state fluorescence quenching (SSFQ) **V2** 281, **V2** 290–292
- stereolithography **V1** 216
- steric effects
 forces **V2** 397, **V2** 405, **V2** 424, **V2** 426–427
 solubilization **V2** 166–169
 stabilization **V1** 9, **V1** 205, **V1** 377, **V1** 381–384
- Stern plane **V1** 224–225, **V1** 235
- Stern–Graham model **V1** 223
- ‘sticky’ contacts **V2** 208, **V2** 210
- stiff gels, ceramics **V1** 215
- stiff surfactant systems **V2** 181–185
- Stokes–Einstein equation **V1** 377, **V2** 230–231, **V2** 347, **V2** 366
- stratification **V2** 29, **V2** 30
- streaming potential **V1** 224–225, **V2** 371–372, **V2** 379
- stress-craze inhibitors **V1** 333–334
- stretching (antifoaming agents) **V2** 146, **V2** 149
- strontium myristate **V2** 325
- structural inversion **V2** 342–344
- structural viscous liquids **V2** 190
see also shear behaviour
- stylus contact method **V1** 165
- subbing layers **V1** 85
- sugars **V2** 171–172
- sulfobetaines **V1** 354–355
- sulfochlorination **V1** 282–284
- sulfosuccinates **V1** 289–291, **V1** 524–525
- sulfoxidation **V1** 284
- supercritical fluids **V2** 68
- superlattices **V2** 83
- supersaturation **V1** 184
- superspreaders **V2** 149–150
- support base, photography **V1** 85
- suprafluid liquids **V2** 190
- supramolecular forces **V2** 427–430
- supramolecular structuring **V2** 424
- surface charge
 aqueous media **V1** 220–229
 electrokinetics **V2** 371–382
 flotation **V1** 246–249
 molecular dynamics **V1** 545
 selective flocculation **V1** 243–244
- surface force apparatus (SFA) **V2** 384–385, **V2** 390–391, **V2** 415, **V2** 428
- surface plasmon resonance (SPR) **V2** 102, **V2** 103
- surface tension
 agrochemical sprays **V1** 80–83
 betaines **V1** 363–364
 CMC determination **V2** 241–242
 component approach **V2** 128–129
 contaminant detection **V2** 163
 definition **V2** 121
 detergency **V1** 54–58
 dynamic **V2** 225–238
 equilibrium **V2** 217–224
 film flotation **V2** 269
 Gemini surfactants **V1** 388
 gradients **V2** 150
 measurement **V2** 217–224, **V2** 225–238, **V2** 438–442
 paints **V1** 120–121
 perfluorocarbon fluids **V1** 179
 polymers **V1** 178
 sedimentation volume **V2** 273
 solidification fronts **V2** 274–277
 surfactant–polymer systems **V1** 445–446
 wetting **V2** 126–127
- surfaces
see also surface charge; surface tension
 activity **V1** 4–6, **V1** 44–48, **V1** 73, **V1** 105
 conduction **V2** 11–13
 depletion **V2** 429
 genus concept **V2** 304–306, **V2** 314
 geometry **V2** 387–388
 modification **V1** 403–404
 morphology **V1** 125
 reactions **V1** 247–249
 roughness **V1** 155–156, **V1** 158–159, **V1** 163–166
 separation measurement **V2** 385–387
 surface–surface interactions **V2** 383–414
 treatment **V1** 125, **V1** 138–145, **V1** 146–154, **V1** 245
 viscosity **V2** 27, **V2** 147
- surfactant affinity difference **V1** 258
- surfactant films **V2** 336, **V2** 354
- surfactant monolayer model **V2** 173
- surfactant number *see* critical packing parameter
- surfactant systems, drug effects **V1** 6–8
- surfactant–polymer flooding **V1** 259–262
- surfactant–polymer systems **V1** 445–463
- surfactants
see also zwitterionic surfactants
 adsorption **V1** 232–238, **V1** 240–241, **V2** 436–444
 agriculture **V1** 73

- amphipathic structure **V1** 232–233, **V1** 376
 amphoteric **V1** 294, **V1** 323, **V1** 349–350, **V1** 351, **V1** 355–372, **V1** 532–534
 anionic **V1** 271–292, **V1** 520–525, **V2** 147
 antifoaming agents **V1** 71–72, **V2** 147, **V2** 149
 aqueous solutions **V2** 190–191
 cationic **V1** 309–348, **V1** 529–532
 cleavable **V1** 291, **V1** 390–397
 commercial **V1** 484, **V1** 492, **V2** 63–64
 computer simulation **V1** 537–550
 concentration measurement **V2** 436–444
 corrosion inhibition **V1** 263–264
 cosurfactants **V1** 497–498, **V2** 63, **V2** 64, **V2** 65–66
 detergency **V1** 54–55, **V1** 58–61, **V1** 65–71
 dispersions **V1** 240–241
 droplet size **V1** 111–113
 emulsions **V2** 55
 environmental issues **V1** 509–536
 ethoxylated **V1** 107
 experimental techniques **V1** 237
 foams **V1** 254–256
 Gemini **V1** 314, **V1** 354, **V1** 385–390, **V1** 469, **V1** 496–497
 hydrophilic–lipophilic balance **V1** 180, **V1** 275, **V1** 310
 hydrotropes **V1** 500
 ionic **V1** 493–497, **V2** 64–66
 liquid crystals **V1** 465–508
 microemulsions **V2** 55–74
 mixed **V1** 498–499
 molecular dynamics **V1** 537–550
 nonionic **V1** 293–308, **V1** 480–493, **V1** 525–529, **V2** 57–64, **V2** 66–67, **V2** 166–169
 oil spill clean-up **V1** 264–265
 paints **V1** 105–110
 petroleum industry **V1** 252–256, **V1** 259–265
 phase behaviour **V1** 67–71, **V1** 480–493
 physico-chemical properties **V1** 421–443
 polymeric **V1** 373–384
 polymerizable **V1** 107–110, **V1** 397–405
 rheology **V2** 189–214
 secondary **V1** 365, **V1** 367
 self-assembly **V1** 252–254
 shear behaviour **V2** 205–214
 solubilization **V2** 159–186
 speciality **V1** 121–122, **V1** 385–405
 structure **V2** 245
 surface forces **V2** 397–404
 surfactant–polymer systems **V1** 445–463
 swelling **V1** 190
 thin-liquid films **V2** 415–417
 usage trends **V1** 510–511
 UV-curable **V1** 403–404
 vesicles **V2** 45, **V2** 48
 surfmers (polymerizable surfactants) **V1** 107–110, **V1** 397–405
 suspension layer stability **V2** 271–272
 suspension polymerization **V1** 103–104, **V1** 176, **V1** 192–193
 suspensions
 agriculture **V1** 78–80
 ceramics **V1** 203, **V1** 205, **V1** 208–212
 consolidation **V1** 212–216
 definition **V2** 4
 foodstuffs **V1** 41
 suspoemulsions **V1** 73
 swelling
 agents **V1** 184
 domain morphology **V2** 319–321, **V2** 323
 drug delivery systems **V1** 25
 emulsions **V1** 190–191
 exponents **V2** 331
 heterophase polymerizations **V1** 190
 radical polymerization **V1** 197
 surfactant aggregates **V2** 166–168
 surfactant–polymer systems **V1** 462–463
 syneresis **V2** 3
 synergistic effects **V2** 151–152, **V2** 429
 syntheses *see* manufacturing processes
 synthetic sizing agents **V1** 140
 tails **V1** 231, **V1** 377–379
 Tanford's formulae **V2** 303
 Tanner's law **V2** 134
 targeted drug administration **V1** 10–11
 temperature effects
 contact angle **V2** 269, **V2** 276–277
 critical micelle concentration **V2** 246
 drug delivery **V1** 24–25
 liquid crystals **V2** 300
 micelles **V1** 425–428, **V1** 437, **V1** 440–442
 microemulsions **V2** 60–70, **V2** 71–72
 nuclear magnetic resonance **V2** 284
 oxyethylene surfactants **V1** 440–442
 vesicle phase transition **V2** 46–47, **V2** 50–52
 tensiometry **V2** 217–224, **V2** 225–238
 ternary systems **V2** 160–161, **V2** 173–185
 tetrapropylenebenzene sulfonate (TPS) **V1** 279
 textiles **V1** 511–512
 TFB *see* thin-film balance
 thermodynamics
 drug delivery **V1** 15–23
 emulsions **V1** 176–179
 micellization **V1** 428–430
 microemulsions **V2** 56
 polymer adsorption **V1** 229–230
 polymeric surfactants **V1** 374–375
 vesicles **V2** 48–49
 wetting **V2** 120, **V2** 121–134
 thermoplastic foams **V2** 40
 thermoporosimetry **V1** 169–170
 thermotropic liquid crystals **V1** 466, **V2** 300
 thickening **V1** 148–149, **V1** 323–325
 thin-film balance (TFB) method **V2** 36, **V2** 39, **V2** 417–424
 thin-liquid films **V2** 415–430, **V2** 431–433
 thixotropy **V1** 209, **V1** 210, **V2** 190
 three-phase contact lines **V2** 259–260, **V2** 265–266
 threshold effect **V1** 64, **V1** 288
 tilt angles **V1** 538, **V1** 542
 time-resolved fluorescence quenching (TRFQ) **V2** 281, **V2** 290–292
 titania (titanium dioxide) **V1** 114
 titration, soaps **V2** 440
 toothpastes **V1** 369
 topical drug administration **V1** 11, **V1** 18–19
 topography, paper **V1** 163–166
 topology **V2** 301, **V2** 314, **V2** 316–321

- toxicology
 amphoterics V1 364–365
 aquatic V1 518–519, V1 524–525, V1 529, V1 531–532, V1 534
 surfactants V1 515
TPS *see* tetrapropylenebenzene sulfonate
train formation V1 231, V1 377–379
transition (particle behaviour) V2 275–276
transport of liquids V1 162
transurfs V1 401
transverse diffusion (flip-flop) V2 47, V2 50
TRFQ *see* time-resolved fluorescence quenching
triglycerides V1 41, V1 296, V1 297
Triton X-*n* solutions V2 228
turbulent flow V2 18–19
twin surfactants *see* Gemini surfactants
- Ultra Turrax system V1 183
ultracentrifugation V2 367
ultrasound V1 182–183, V2 155–156, V2 244
ultraviolet (UV) curable surfactants V1 403–404
ultraviolet (UV) spectroscopy V2 437–438
undersize fractions V2 359
undulation forces V2 426
unilamellar vesicles *see* single-lamellar vesicles
- vaccination, oral V1 28
van der Waals interactions
 ceramics V1 203–204, V1 205, V1 207
 colloidal dispersions V2 13–15, V2 16–17
 DLVO theory V1 131–132
 emulsion concentrates V1 76
 liquids V1 42–43
 measurement V2 392
 molecular dynamics V1 539–540
 pigment dispersion V1 115
 powder systems V1 50
 sedimentation V2 269, V2 272
 thin-liquid films V2 424
 wetting thermodynamics V2 127, V2 128
vapour phase methods V2 9
vapour pressure osmometry V2 244, V2 247
vapour transport V1 161
vesicles
 antifoaming agents V2 149–150
 autopoiesis V2 50–52
 bilayer solubilization V2 171–173
 fatty acids V2 49–50
 formation V2 47–49
 hydrotropes V1 418
 phase structure/transition V2 46–47
 polymerization V2 49
 rheology V2 200–204, V2 211–213
viscoelasticity
 ceramics V1 210
 measurement V2 388–389
 paper coatings V1 151–152
 rheology V2 190, V2 193–198
 thickeners V1 325
viscose V1 337, V1 338, V1 339
viscosity
 see also thickening
 amphoteric surfactants V1 365, V1 366–368
 antifoaming agents V2 147
 ceramics V1 209–211
 CMC determination V2 244
 colloidal dispersions V2 19–20
 dilatational V2 235
 dispersions V1 240
 foam stabilization V2 26, V2 27
 Gemini surfactants V1 390
 micelle concentration V1 436
 microemulsions V2 335
 rheology V2 192–199
 shear behaviour V2 206–207, V2 211
 surfactant–polymer systems V1 449, V1 452
 visible spectroscopy V2 437–438
 volatility of liquids V2 122–123
 volume fraction V2 345–346, V2 349–350
 volume restriction interaction V1 382–383
- w/o *see* water-in-oil
Washburn equation V1 159–161, V2 138–139, V2 272
washing *see* detergency
waste-water treatment V1 510, V1 515, V1 517, V1 520, V1 529
water
 see also aqueous systems
 bridges V1 50
 flooding V1 261
 hardness V1 61–65, V1 272–273, V1 288, V1 314
 solubilization V2 169–171
water-borne paints V1 116–119
water-continuous phases V1 479–480
water-in-oil (w/o) microemulsions V2 169–171, V2 174–177, V2 181–184
waveguide format V2 88, V2 89
Weaver–Bertucci equation V2 143–144
wedge model V2 180–181
Wenzel's equation V1 155
wet strength, paper V1 145–146
wetting V2 119–142
 agriculture V1 73, V1 78–79, V1 81–83
 amphoterics V1 365
 anionic surfactants V1 285, V1 288
 capillary penetration V2 136–140
 cationic surfactants V1 325–326
 counterions V1 274
 crude oil V1 254, V1 255
 detergency V1 54–58
 foodstuffs V1 48–49
 imperfect solid surfaces V2 129–134
 Langmuir–Blodgett films V2 82–83, V2 91–92
 paints V1 119–121
 paper V1 127–128, V1 142, V1 144, V1 154–159
 pigment dispersion V1 114
 porous surfaces V2 138–140
 solid surfaces V2 126–129
 spreading V2 124–126, V2 134–136
 sulfosuccinates V1 289, V1 290
 tension V2 126
 thermodynamics V2 120, V2 121–134
 thin-liquid films V2 431
wicking V1 161, V2 120, V2 132

- Wilhelmy plate method V2 217–218, V2 219–220, V2 267–269
- Williamson synthesis V1 275, V1 276
- Winsor equilibria, emulsification failure V2 161, V2 178, V2 351–352
- Winsor's *R* ratio V1 258
- wood preservatives V1 318, V1 320–321
- X-ray photoelectron spectroscopy (XPS) V1 144–145, V1 162–163, V2 105–106
- X-ray reflectivity V2 427
- X-ray scattering *see* small-angle X-ray scattering
- xanthogenesis V1 337, V1 338, V1 339
- XPS *see* X-ray photoelectron spectroscopy
- yeast (*Saccharomyces cerevisiae*) V2 112
- Young equation
- agriculture V1 78–79
 - background V2 120, V2 133–134, V2 252
 - detergents V1 56
 - modification V2 122–131
 - petroleum V1 254
 - porous solids V2 74, V2 138–139
- Young–Laplace equation V2 219, V2 222–223
- zeolites V1 61–65
- zeta potential
- electrokinetics V2 374, V2 380–381
 - experimental techniques V1 237–238
 - flotation V1 248–249
 - manipulation V1 225–226
 - measurement V1 224–225
 - surfactant adsorption V1 235, V1 237–238
- Ziegler process V1 279, V1 294–295
- Zimm plots V2 295
- zirconium myristate V2 327
- Zisman plots V1 120–121
- zwitterionic surfactants
- characterization V1 361–372
 - chemistry V1 349–355
 - critical micelle concentration V2 245
 - emulsions V1 257
 - paints V1 118
 - phase behaviour V1 493
 - rheology V2 196–199, V2 201–202, V2 208–210, V2 213